WATER FOR HUMAN NEEDS

Proceedings of the
Second World Congress on Water Resources

VOLUME V

TECHNOLOGY AND ECOLOGY

333.9106
W.C.W.R.
V.5

READING ROOM

G.K.V.K. Library

U.A.S. UNIVERSITY LIBRARY
BANGALORE
G.K.V.K., CAMPUS

Proceedings of the
SECOND WORLD CONGRESS ON WATER RESOURCES
New Delhi, India 12-16 December 1975

WATER FOR HUMAN NEEDS

VOLUME V

TECHNOLOGY AND ECOLOGY

Organised by the
International Water Resources Association

Hosted by the
Indian Committee for IWRA
Central Board of Irrigation and Power

Published by
C. V. J. VARMA
Executive Secretary, Indian Committee for IWRA
Central Board of Irrigation and Power
Kasturba Gandhi Marg, New Delhi 110001, India

G.K.V.K. Library

U. A. S. BANGALORE
UNIVERSITY LIBRARY

14SEP1979

ACC. NO. 83482

CL. NO. .....

FOREWORD

Water resources development is essential for the economic and social progress of mankind. Rapid population growth and ever-increasing living standards have resulted in a sharp rise in human requirements of water, necessitating expeditious development of the available water resources, and their proper management. The time is perhaps not too far when suitable technologies may have to be evolved for augmenting water resources to cater to the needs of areas with inadequate water supplies. Some of the present concepts of water resources management also require modification in order to deal more effectively with the problems of socio-economic growth. There is a continual need to evolve newer technologies and social innovations to solve water problems. This calls for a concerted international effort.

The International Water Resources Association organises biennially World Congresses to facilitate inter-disciplinary exchange of information and experiences on the problems met with in different countries in the optimal and economic development and utilisation of water resources. 'Water for Human Needs' is the theme of the Association's Second World Congress on Water Resources, New Delhi, 12-16 December 1975.

There has been an excellent response to the call for papers for the Congress. About 600 papers by experts from 43 countries were received for consideration. However in view of certain constraints, it has been possible to include only 261 papers in the Congress programme. These papers have been grouped under :

Water for Human Needs : Energy
Food
Health
General

In the 'General' group, the papers deal with various aspects of water resources planning, development, management, technology, ecology and education, and meteorology.

The papers contain valuable data and information, present several new concepts and methodologies, and detail experiences. These have been compiled and printed as Proceedings of the Congress in the following five volumes :

Volume I	Energy and Food
II	Health and Planning
III	Development and Meteorology
IV	Management and Education
V	Technology and Ecology

The discussions at the Congress will be published in Volume VI.

The Indian Committee of the International Water Resources Association is thankful to the authors for their useful contributions. It also owes its grateful thanks to the members of the Technical Programme Committee for their review of papers.

C. V. J. VARMA
Organising Secretary
Second World Congress on Water Resources

CONGRESS OFFICIALS

Presidents

Dr. Ven Te Chow
President, IWRA
Professor of Hydraulic Engineering
University of Illinois at Urbana-Champaign
Urbana, Illinois, U.S.A.

Dr. K. L. Rao
Vice-President, IWRA
Member of Parliament
New Delhi, India.

Vice-Presidents

Dr. William S. Butcher
Director
Office of Water Research and Technology
U.S. Department of the Interior
Washington, D.C., U.S.A.

Prof. Dr. Zdzisław Kaczmarek
International Institute for Applied Systems Analysis
Schloss Laxenburg
Austria.

Dr. Koichi Aki
Professor
Faculty of Engineering
Kanto Gukuin University
Yokohama, Japan.

Prof. Dr. E. Mosonyi
Direktor der Versuchsanatalt
für Wasserbau und Kulturtechnik und des
Theodor-Rehbock-Flussbaulaboratoriums
Universität Karlsruhe
Karlsruhe, Federal Republic of Germany.

Mr. Y. K. Murthy
Chairman
Indian Committee for IWRA
Chairman
Central Water Commission and
Ex-Officio Secretary to the
Government of India
New Delhi, India.

Mr. N. Tata Rao
Chairman
Andhra Pradesh State Electricity Board
Hyderabad, India.

Mr. N. C. Saksena
President
Central Board of Irrigation and Power
Secretary to Government of Uttar Pradesh
Irrigation Department
Lucknow, India.

Ing. Renato João Baptista Della Togna
Superintendente
Departamento de Aguas e Energia Elétrica
São Paulo, Brazil.

Dr. J. Toran
Honorary President
International Commission on Large Dams
Madrid, Spain.

Dr. Iraj Vahidi
Minister of Energy
Tehran, Iran.

Prof. A. Volker
Department of Water Management
'Rijkswaterstaat'
The Hague, The Netherlands.

Organising Secretary

Mr. C. V. J. Varma
Secretary
Central Board of Irrigation and Power
New Delhi, India.

INTERNATIONAL ADVISORY BOARD

Dr. Ven Te Chow
President, IWRA
Professor of Hydraulic Engineering
University of Illinois at Urbana-Champaign
Urbana, Illinois, U.S.A.

Mrs. Srimoerni Doelhomid
Lecturer
University of Indonesia
Indonesian Institute for Science
Jakarta, Indonesia.

Dr. D. Hariri
Director General
Center of Research and Laboratories
Ministry of Water and Power
Tehran, Iran.

Mr. Frank O. C. Hodges
Chartered Civil Engineer
Bournemouth, Britain.

Mr. Milan Jermar
Chief Engineer
Czech Ministry of Forest and Water Management
Prague, Czechoslovakia.

Dr. Gabor M. Karadi
Secretary General, IWRA
Professor of Civil Engineering
University of Wisconsin, Milwaukee
Wisconsin, U.S.A.

Mr. André Leclerc
Head, Divisions of Hydraulics and Environmental
Engineering, Ecole Polytechnique
Montreal, Quebec, Canada.

Dr. José M. M. Mendiluce
Director
Centro de Estudios Hidrograficos
Madrid, Spain.

Prof. L. J. Mostertman
Director of the International Courses
in Hydraulic and Sanitary Engineering
University of Technology
Delft, The Netherlands.

Dr. Subin Pinkayan
Associate Professor
Water Resources Engineering
Asian Institute of Technology
Bangkok, Thailand.

Mr. J. Piquemal
Directeur Scientifique
Institut de Mécanique des Fluides de Toulouse
Toulouse, France.

Dr. Herbert C. Preul
Professor of Civil and Sanitary Engineering
University of Cincinnati
Cincinnati, Ohio, U.S.A.

Ing. Renato João Baptista Della Togna
Superintendente
Departamento de Aguas e Energia Elétrica
São Paulo, Brazil.

Mr. C. V. J. Varma
Secretary
Central Board of Irrigation and Power
New Delhi, India.

TECHNICAL PROGRAMME COMMITTEE

Dr. S. P. Garg
Member
Ganga Flood Control Commission
Patna, India.

Mr. J. K. Jain
Chief Engineer and
Member
Central Ground Water Board
Ministry of Agriculture and Irrigation
New Delhi, India.

Dr. P. Koteswaram
Director General
India Meteorological Department
New Delhi, India.

Prof. V. C. Kulandaiswamy
Director of Technical Education
Madras, India.

Mr. Y. K. Murthy
Chairman
Central Water Commission and
Ex-Officio Secretary to the
Government of India
New Delhi, India.

Mr. J. P. Naegamvala
Chairman
Bhakra Management Board
Chandigarh, India.

Prof. J. V. Rao
Head
Department of Civil Engineering
Indian Institute of Technology
Kharagpur, India.

Mr. N. Tata Rao
Chairman
Andhra Pradesh State Electricity Board
Hyderabad, India.

Dr. T. S. M. Rao
Professor and Head
Department of Electrical Engineering
University of Roorkee
Roorkee, India.

Mr. C. V. J. Varma
Secretary
Central Board of Irrigation and Power
New Delhi, India.

CONTENTS

PAGE

FOREWORD ... (*i*)

CONGRESS OFFICIALS ... (*iii*)

CONGRESS PAPERS :

WATER FOR HUMAN NEEDS: GENERAL (TECHNOLOGY)

(1) Simulation of Unit Hydrograph by Isochrone Method for Water Resources Planning in Thailand—*Wiroj Sangvaree* ... 1

(2) On the Statistical Characteristics of Streamflow for Water Management Calculations—*G. L. Grigolia and A. N. Kilasonia* ... 7

(3) Mathematical Models of Streamflow for Water Power (Water Management) Calculations—*G. G. Svanidze* ... 17

(4) A Mathematical Model for Basin Runoff—*V. C. Kulandaiswamy and T. Babu Rao* ... 25

(5) Transformation of the Processes in the Linear Hydrological Systems—*Witold G. Strupczewski, Renata J. Kiczko, Zbigniew W. Kundzewicz, Jaroslaw J. Napiórkowski and Henryk T. Mitosek, Jr.* ... 33

(6) Decoupled Stochastic Models for Multisite Streamflows—*S. Ramaseshan and M. Krishnasami* ... 45

(7) Stochastic Modelling for Flood Flows—*H. D. Sharma, S. V. Singh and S. R. Jindal* ... 51

(8) Some Stochastic Runoff Models—*I. Kontur* ... 61

(9) Streamflow Synthesis of Ungauged Area—*Thaipuck Thammongkol* ... 73

(10) Influence of Probability Analysis on Selection of Design Flood—*E. Mosonyi, H. Eggers and D. Koberg* ... 83

(11) An Improved Estimation of Surface Water Resources—*M. B. Szalay* ... 93

(12) Urbanization—Its Effects upon Base Flow—*Paul MacRoberts* ... 99

(13) A Simple Runoff Model Utilizing Soil Moisture Parameters—*Vijay P. Singh and W. Trevor Dickinson* ... 111

(14) A Distributed and Deterministic Catchment Model using Finite Elements —*J. K. White and A. W. Jayawardena* ... 117

(15) An Approach to Flood Stage Forecasting—*S. Chander, G. Jagmohan Das and S. C. Padhi* ... 125

(16) Flood Routing through Non-linear Reservoirs—A Quasi-linear Approach—*P. Ramakrishna Rao, S. Chander and Y. K. Murthy* ... 131

(17) Influence of Chance Constraints on the Efficiency of a Reservoir operated according to a Linear Decision Rule—*G. A. Schultz and E. J. Plate* ... 139

(18) The Approximate Probability Density Function of Range and Adjusted Range—*Prathet Sutabutr* ... 147

(19) A Method for Computing Storage Capacity of a Reservoir Serving Irrigation, Considering the Demand as a Probability Process—*L. Kotov, G. Krafti and A. Popov* ... 155

(20) The Rapid Emptying of Water Reservoir Systems—*D. L. Vischer and M. Spreafico* ... 161

(21) Reservoir Models—*S. P. Chee* ... 171

(22) Dynamic Programming as Applied to Substantiation of a Reliable Water Supply in Integrated Water Management Systems—*A. L. Velikanov and D. N. Korobova* ... 177

(23) Response of Alluvial Channels to River Regulation—*R. D. Hey* ... 183

(24) Economy through Hydraulic Designs in Water Utilisation Projects—*C. V. Gole, P. C. Saxena, C. P. Venkatraman, V. N. Diwanji and V. Ramanathan* ... 189

(25) Potential of Conventional and Nuclear Techniques in Water Resources Evaluation in India—*Umesh Chandra, K. Balu and M. P. S. Ramani* ... 203

(26) Nuclear Techniques for Water Resources Technology—*Jagdish Bahadur* ... 213

(27) Time Series Analysis and its Application to Water Resources—*Sun-Fu Shih* ... 223

(28) Non-Linear Modelling of the Water Resources Systems—*Jagat N. Sharma* ... 237

(29) Integration of Filtration Equations and Parameter Optimization Techniques—*A. C. Payatakes, R. M. Turian and C. Tien* ... 241

(30) Combined Water Quality and Flow Monitoring Stations Employing New Techniques—*S. J. Gillam-Smith* ... 253

(31) The Potential Impact of Satellite Data-Relay Systems on the Operation of Hydrologic Data Programs—*D. W. Moody and D. M. Preble* ... 261

(32) Remote Sensing in Hydrogeological Mapping (with Special Respect to India and Canada)—*G. Ozoray* ... 275

(33) The Role of Direct Analogue Computers in the Solution of Water Resources Problems—*K. V. Ramana Murthy* ... 283

(34) Flow in a Leaky Aquifer with Time-Dependent Drawdown in the Well—*Robert Y. S. Lai* ... 291

(35) Least Cost Design of Water Distribution Networks—*R. G. Cembrowicz* ... 299

(36) Water Conveyance Capacity of Channels with an Ice Cover—*S. P. Chee* ... 313

(37) Inflatable Dams for Irrigation Projects—*H. O. Anwar* ... 317

(38) Uniformly Discharging Outlets for Irrigation Systems—*A. S. Ramamurthy, K. Subramanya and L. Carballada* ... 323

(39) Air Photo-Interpretation of Hydromorphology of Asan Basin, Doon Valley, India—*S. K. Sharma and S. C. Sharma* ... 327

(40) Some Considerations Concerning the Sorption Capacity of Several Radionuclides of the Black Sea Water in Sediments on the Black Sea Bottom—*Valentina Voljin, E. Zamfir and Mihaela Blidaru* ... 335

WATER FOR HUMAN NEEDS : GENERAL (ECOLOGY)

(1) Environmental Aspects of River Development in Tropical Asia with Particular Reference to the Mekong Basin—*V. R. Pantulu* ... 349

(2) Water Resources Ecology—*S. H. C. de Silva* ... 361

(3) Ecological Aspects of Water Resources Management—Study of a Case—*Ernest H. Razvan* ... 373

(4) Water Pollution Control during Dam and Tunnel Construction—*John C. Peters* ... 381

(5) The Ecological Effects of Thermal Discharge from Power Plants—*R. V. Harmsworth and C. H. Wahtola, Jr.* ... 389

(6) Environmental Impact of Water Resources Utilization—*Anand Prakash* ... 405

(7) Hydrodynamic Aspects in Environmental and Ecological Enhancement—*Daniel M. Dubois* ... 413

(8) Importance of Flushing Rate Calculations for Estimating Productivity of Tropical Reservoirs—*A. M. Beeton* ... 421

(9) Eutrophication Studies in a Planned Community—*Calvin H. Ward and Joe M. King* ... 425

(10) Coastal Zone Climatological Studies of the Laurentian Great Lakes *C. R. Murthy and J. O. Blanton* ... 431

(11) Monomixis in Kainji Lake, Nigeria—*H. A. Adeniji* ... 449

(12) Urban Development with Environmental Protection—*Walter Fox* ... 455

(13) Belgian Mathematical Model and Data Acquisition System for Monitoring, Prediction and Control of Marine Resources Quality—*Jacques C. J. Nihoul, François C. Ronday and Georges Pichot* ... 467

(14) Use of the Computer to Control Land Subsidence—*Giuseppe Gambolati* ... 485

AUTHORS' PHOTOGRAPHS ... 495

IWRA EXECUTIVE BOARD ... 505

GEOGRAPHICAL AREA COMMITTEES ... 507

The papers contained in these Proceedings have been judged solely on the basis of their technical merit, and no attempt has been made to edit or grammatically restructure any of the contributions. The statements and opinions expressed by the authors are their own and not necessarily of the International Water Resources Association.

WATER FOR HUMAN NEEDS : GENERAL

(TECHNOLOGY)

Simulation of Unit Hydrograph by Isochrone Method for Water Resources Planning in Thailand

WIROJ SANGVAREE
Chief of Hydrometeorology Division, Meteorological Department
Bangkok, Thailand.

SYNOPSIS

A first attempt to simulate unit hydrographs of the river basins in Thailand by the isochrone method was presented. Two river basins (drainage areas of 809 and 4,074 sq km), located in the central and western parts of Thailand, were selected for this study. The 1-day unit hydrographs of the two basins were firstly developed from the available daily rainfall and streamflow data by the conventional methods. Laterly the instantaneous unit hydrographs for both basins were simulated by the basin-areas routing or the isochrone method and were converted to the 1-day unit hydrographs for comparisons. The results of study indicated the 1-day unit hydrographs developed by the two methods were similar and close to each other for both basins.

1. Introduction

Attempts to develop general method for synthesizing unit hydrographs for ungaged watersheds had led to the use of runoff-routing or area-routing procedure (1). Rainfall excess or surface runoff was routed through basin storage to produce surface runoff hydrograph which is usually the portion of a hydrograph excluding base flow. Conceptually, this method or the isochrone method (2) has the advantage of allowing expression of the differing areal distribution of rainfall and infiltration characteristics over the drainage area.

A relatively small number of the streams in Thailand are gaged. Accordingly, enough streamflow (or river flow) data is not always available for planning of water resources development project, especially for remote area where streamflow measurement is lacking. Therefore, there exists problem, which takes the form of assessing the flood hydrograph by indirect methods like synthetic unit hydrographs, transposition of flood hydrographs, etc., derived from flood data observed elsewhere.

The main objective of this study is to investigate the method of simulation of unit hydrographs by isochrone method for river basins in Thailand. The study is also aimed to derive the unit hydrographs, which will be useful for future water resources development planning, as well as for the trial flood forecastings program of the selected basins.

2. Descriptions of Selected River Basins

Due to limiting time, only two river basins as shown in Figures 1 & 2, were selected for this study. Kang Sida basin having drainage area of 809 sq km, is located on the upper end of the Pasak River basin. Thong Pha Phum basin with drainage area of 4,074 sq km, is situated on the upper end of Khwae Noi River basin. Both basins are predominantly covered by tropical rainforests and only small percentages of areas along the river banks are in cultivations.

3. Isochrone Method and Routing Equations

The shape of hydrograph from a basin is dependent on the travel time through the basin and on the shape and storage characteristics of the basin. Considering excess rainfall (or runoff) to be inflow and the hydrograph to be outflow, the problem is analogous to storage routing. Inflow may be lagged by dividing the basin area into sub-areas by isochrones of travel time from the outlet (Figure 1). The area between isochrones is then measured and a time-area diagram is drawn.

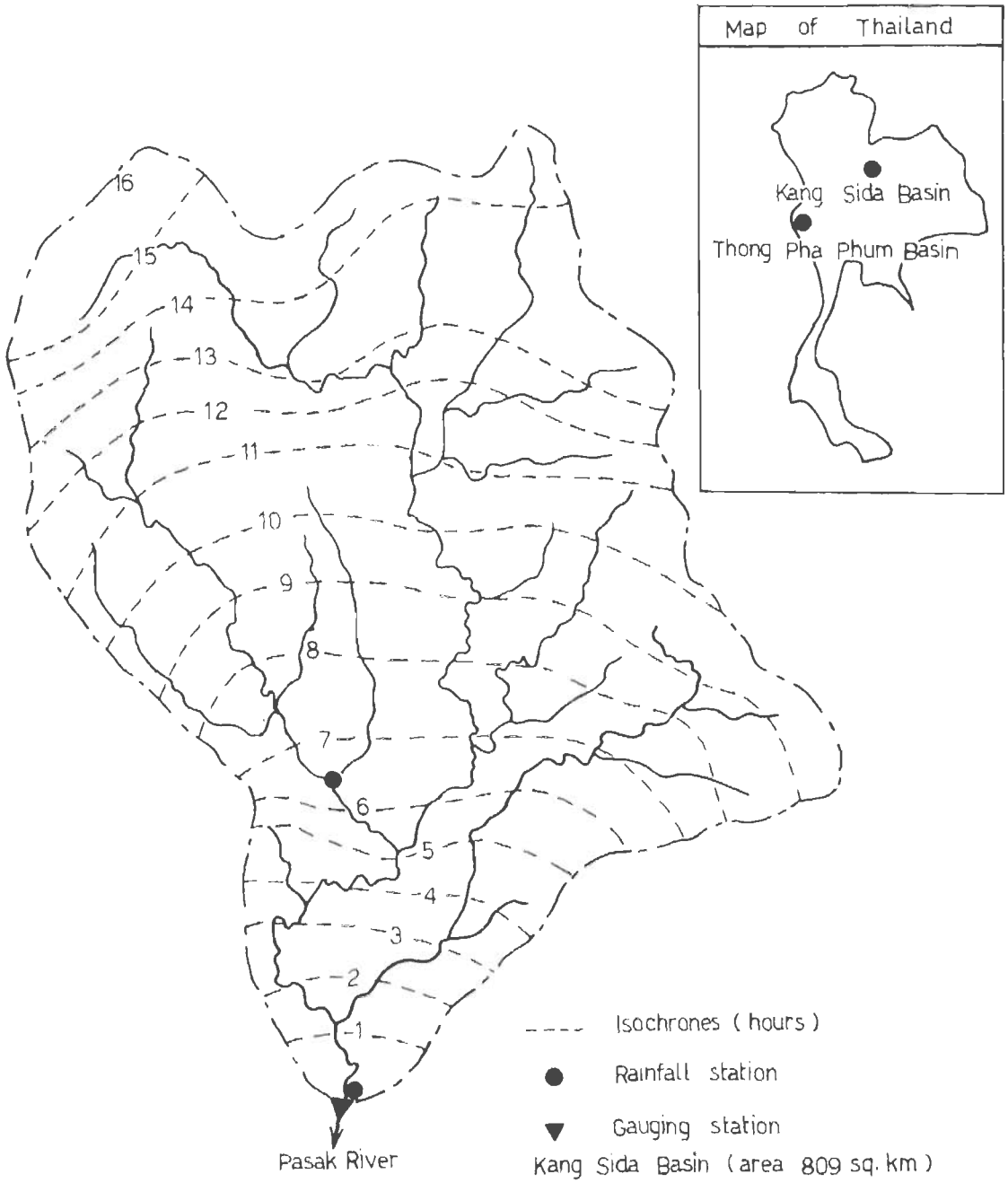

FIGURE 1 : Isochrones and river channel systems of Kang Sida basin and approximate locations of the selected basins.

Routing the time-area diagram by the Muskingum method yields the outflow hydrograph after adjustment for units. The resulting hydrograph is called an instantaneous unit hydrograph and can be converted to a unit hydrograph for any duration.

The difference between inflow (I_t) to the reservoir or the river channel reach and the outflow (Q_t) is the rate of change of storage, which is an expression of continuity,

$$I_t - Q_t = \frac{d S_t}{dt} \qquad \ldots(1)$$

A linear reservoir is a fictitious reservoir in which the storage (S) is directly proportional to the outflow,

$$S_t = KQ_t \qquad \ldots(2)$$

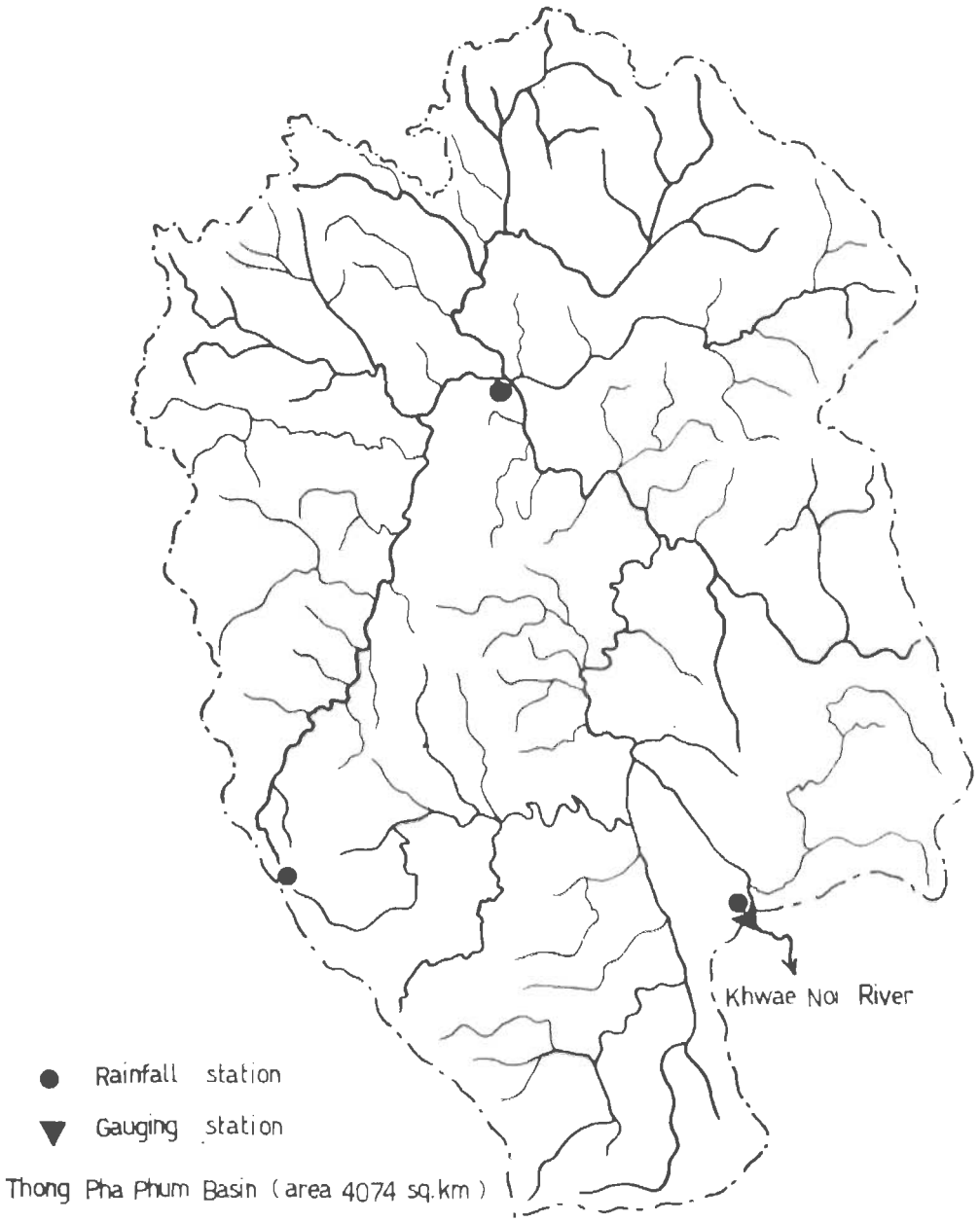

FIGURE 2 : Drainage area and river-channel systems of Thong Pha Phum basin.

For a river channel reach, Muskingum[3] assumes,

$$S_t = K\,[x\,I_t+(1-x)\,Q_t] \qquad ...(3)$$

The storage constant K has the dimension of time and depends on units of flow and storage, the constant x expresses the effect of inflow and outflow in determining storage. For a simple reservoir, where inflow has no effect $x=0$, and Equation (3) becomes Equation (2).

Using subscripts 1 and 2 to represent the beginning and end of the routing period ($\triangle t$) respectively, Equation (1) and Equation (2) can be combined and converted to :

$$Q_2 = C_0\,I_2+C_1\,I_1+C_2\,Q_1 \qquad ...(4)$$

where, $C_0 = (Kx-0{\cdot}5\,\triangle t)/(K-Kx+0{\cdot}5\,\triangle t)$ ...(5)

$C_1 = (Kx+0{\cdot}5\,\triangle t)/(K-Kx+0{\cdot}5\,\triangle t)$ ...(6)

and $C = (K-Kx-0{\cdot}5\,\triangle t)/(K-Kx+0{\cdot}5\,\triangle t)$ ...(7)

With K, x and $\triangle t$ established, values C_0, C_1 and C_2 can be computed from Equations (5) to (7). The routing operation is simply a solution of Equation (4) with Q_2 of one routing period becoming Q_1 of the succeeding period.

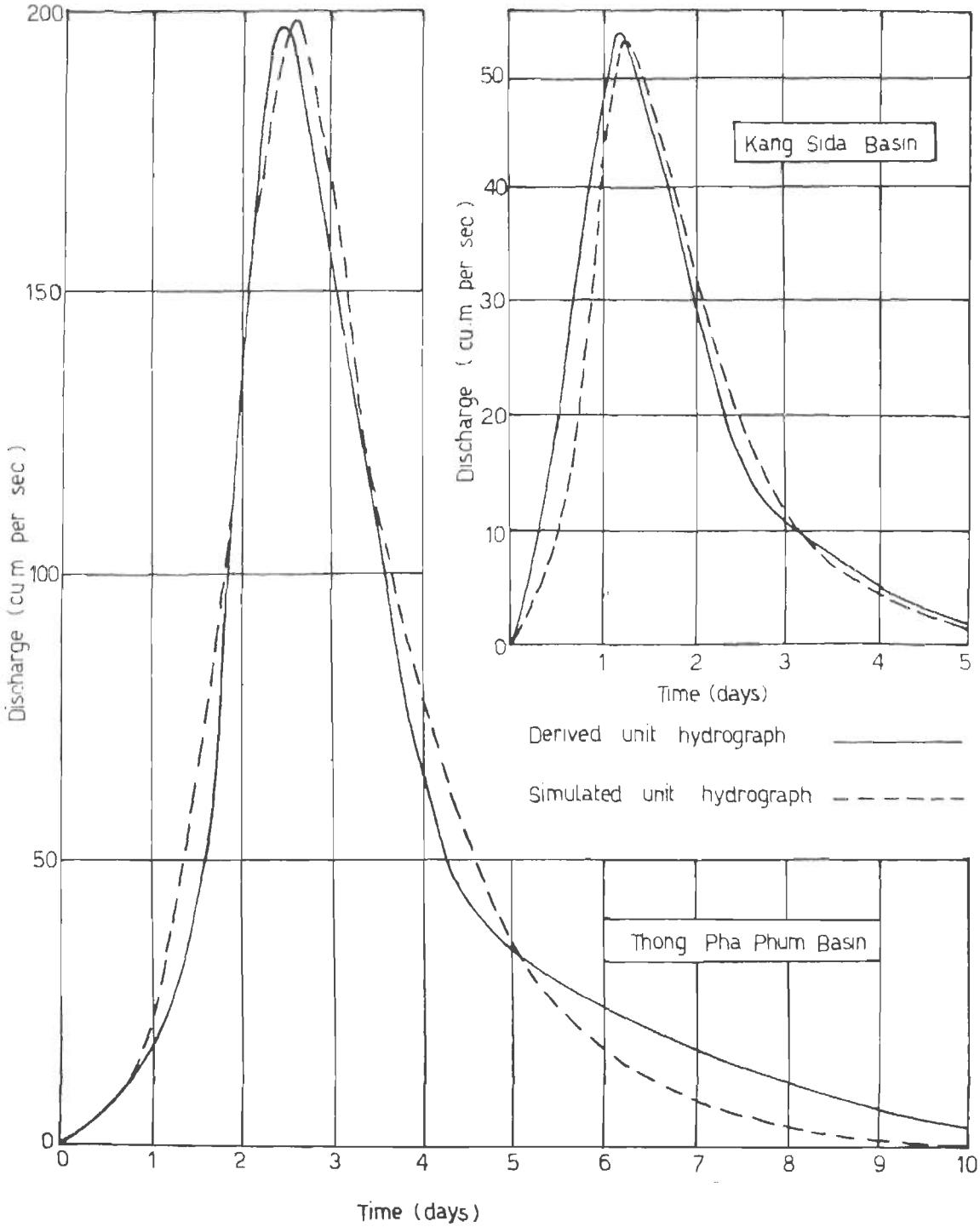

FIGURE 3 : Comparisons of the 1-day unit hydrographs resulted from this study.

4. Derivation of Unit Hydrographs

The available streamflow data of the selected basins are published in the form of mean daily flows. Accordingly the daily streamflow and rainfall data of three years of record were taken to derive 1-day unit hydrographs for each basin.

Eight suitable hydrographs were chosen for each basin to perform hydrograph separation, and their associated daily basin rainfalls were computed by Thiessen method. Using the ϕ-index method, the effective rainfall (direct-runoff) was initially determined and adjusted by assuming exponential infiltration losses.

For the direct-runoff hydrograph of a simple storm, the unit hydrograph (total runoff of 10 mm) was determined by the assumption of proportional ordinates. The method of successive approximations was used to obtain unit hydrograph resulted from a complex storm. The details of derivations had been published in Ref. (2) to (4).

The average 1-day unit hydrographs of both basins obtained from this study were shown in Figure 3. The solid-line graphs represent the instantaneous discharges, which were drawn to fit the mean daily flows of the 1-day unit hydrographs by trials

5. Simulation of Unit Hydrographs

The basin lag (T_1) and storage constant (K) for each basin were firstly estimated from the time interval between cessation of rainfall and point of contraflexure on the recession limb, and the slope of hydrograph at this point. The isochrones were drawn on the basin area map by dividing the length of main stream, extended to the basin boundary, into appropriate equal parts, and establishing additional point on each tributary by stepping off the same lengths along the tributary streams. The basin-area-time diagram was obtained by planimetering the areas between successive isochrones (which was not shown here).

Using the routing equations and procedures as described in Section 3, the instantaneous unit hydrograph for each basin was simulated. It was laterly converted to 1-day unit hydrograph by S-curve analysis. Details of simulating procedures of this method had been published in Ref. (1) & (3).

The simulated 1-day unit hydrographs for both basins were shown in Figure 3, which demonstrated the similarity and closeness of the simulated and derived unit hydrographs for each basin.

6. Conclusions

The following conclusions may be drawn from this study :

(1) The unit hydrographs simulated by the isochrone method are similar and close to the unit hydrographs derived by the conventional methods for both basins. This result is, therefore, a fine confirmation of the use of isochrone method for simulation of unit hydrographs.

(2) The basin-storage characteristic of Kang Sida basin may be represented by the reservoir-storage type ($x = 0$), with parameters $T_1 = 16$ hours and $K = 24$ hours.

(3) For Thong Pha Phum basin, the basin-storage model is of channel-storage type ($x = 0{\cdot}23$), with parameters $T_1 = 40$ hours and $K = 40$ hours.

Results of this study indicate the following areas warrant future study :

(1) Basins of wide range of geographic conditions in Thailand should be investigated by the similar approach.

(2) Relationships between the basin-storage-model parameters and the basin-physiographic factors should also be investigated.

Such studies might increase the physical understanding of the basin-storage-model parameters, and possibly be useful for synthesizing unit hydrographs for ungaged basin in Thailand.

7. References

(1) CLARK, C.O. : "Storage and the Unit Hydrograph." ASCE Trans., 1945.

(2) WORLD METEOROLOGICAL ORGANIZATION : "Guide to Hydrometeorological Practices." WMO-No. 168. TP. 82, 1970.

(3) JOHNSTONE, D. and CROSS, W.P. : "Elements of Applied Hydrology." The Ronald Press Co., 1949.

(4) LINSLEY, R.K., KOHLER, M.A. and PAULHUS, J.L.H. : "Hydrology for Engineers." McGraw-Hill Book Co., Inc., 1958.

On the Statistical Characteristics of Streamflow for Water Management Calculations

G. L. GRIGOLIA
Cand. Eng., docent

A. N. KILASONIA
Cand. Eng., docent

Hydrologic Department, Tbilisi State University, Tbilisi, USSR.

SYNOPSIS

The authors suggest to describe the streamflow process using Johnson distribution limited at both ends. The methods of determination of the probability distribution limits have been developed on the basis of numerous calculations of the actually observed data. The best agreement between these and the historical data has been achieved by changing the date of beginning of the hydrologic year. As opposed to other probability distribution laws, in this case no certain relation between the skewness and variation coefficient values is needed. The experimental calculations have lead to the conclusion that changing the starting date of the hydrologic year it is possible to change considerably the annual flow values of the statistical parameters—the skewness coefficient and the correlation coefficient between the adjacent streamflows, these changes being insignificant only in some particular cases, i.e., when the streamflow is regulated and the periodicity of its fluctuations is relatively regular in the rivers of the arid zones.

The stochastic nature of the streamflow processes should be taken into consideration in the design and optimal control of water resources systems, one of the main problems being the choice of the most suitable probability distribution law to describe the streamflow process.

The recent studies have shown that the probability distributions of the annual runoff variables are limited from above, while their inferior limit is a positive number different from zero ([1]). However, setting of those limits appeared to be a very difficult task, thus causing the use of the distribution laws covering the domain between zero and the infinity.

In Ref. (2) the authors suggest to describe the fluctuations of the annual runoff values with the help of Johnson S_B-distribution limited at both ends. The frequency distribution is as follows ([3]) :

$$f(x) = \frac{1}{\sqrt{2\pi}\,\sigma_\tau}\,\frac{b-a}{(x-a)(b-x)}$$

$$\exp\left\{-\frac{1}{2\sigma_\tau^2}\left[\ln\left(\frac{x-a}{b-x}\right)-m_\tau\right]^2\right\} \qquad \ldots(1)$$

where, b and a are the superior and inferior limits of the S_B-distribution, while m_τ and σ_τ are the mathematical expectation and the root-men-square deviation of the normally distributed continuous value τ, respectively.

Proceeding to the discrete random variable such as the annual runoff we find that the sequence

$$\tau_i = \ln\left(\frac{x_i-a}{b-x_i}\right), \qquad \ldots(2)$$

where, $x_i = \frac{Q_i}{\overline{Q}} = \frac{W_i}{\overline{W}}$ are the observed values of the modular coefficient of the mean annual discharges (Q_i) or the annual volumes (W_i), will have a normal distribution.

The graphical and statistical tests for many rivers of the world have shown that most of them can be quite well described using Johnson S_B-distribution ([4]). One of the

advantages of this S_β-distribution is that it possesses quite varied forms, the plotting of the corresponding function being relatively easy and sufficiently good for the statistical simulation of the synthetic hydrologic series of a long duration ([2]).

However, the most complicated problem with the S_β-distribution is the estimation of its superior (b) and inferior (a) limits. Further we suggest a number of ways of selecting these limits.

In the first approximation the limits of the S_β-distribution can be set by means of the graphs suggested by G.P. Kalinin ([1]), which present the data of 175 rivers. We have added more data of 155 rivers on the same graphs (Figure 1). It is clear from the figure that only few of the rivers under study are not seen in the defined areas. Besides, the superior and inferior limits of the S_β-distribution can be estimated by a graphical method of choosing these parameters considering the conditions of straightening the guarantee curve

$$P\left(\frac{x_m-a}{b-x_m}\right)=\frac{m-0.3}{n+0,4}\ 100\% \qquad \ldots(3)$$

on the probability paper of the log-normal distribution. Different values of a and b are preset for each river and the guarantee curves of the sequence $Z_i=\frac{x_i-a}{b-x_i}$ are plotted on the probability paper. The chosen combination of a and b should ensure the guarantee curve Z_i to be a straight line or, at least, close to it. Figure 2 presents the guarantee curves Z_i for the River Bzib' at the village of Jirkhva with different combinations of a and b. The analysis of these curves shows that the guarantee curve Z_i is closer to the straight line with $a=0.4$ and $b=10.0$.

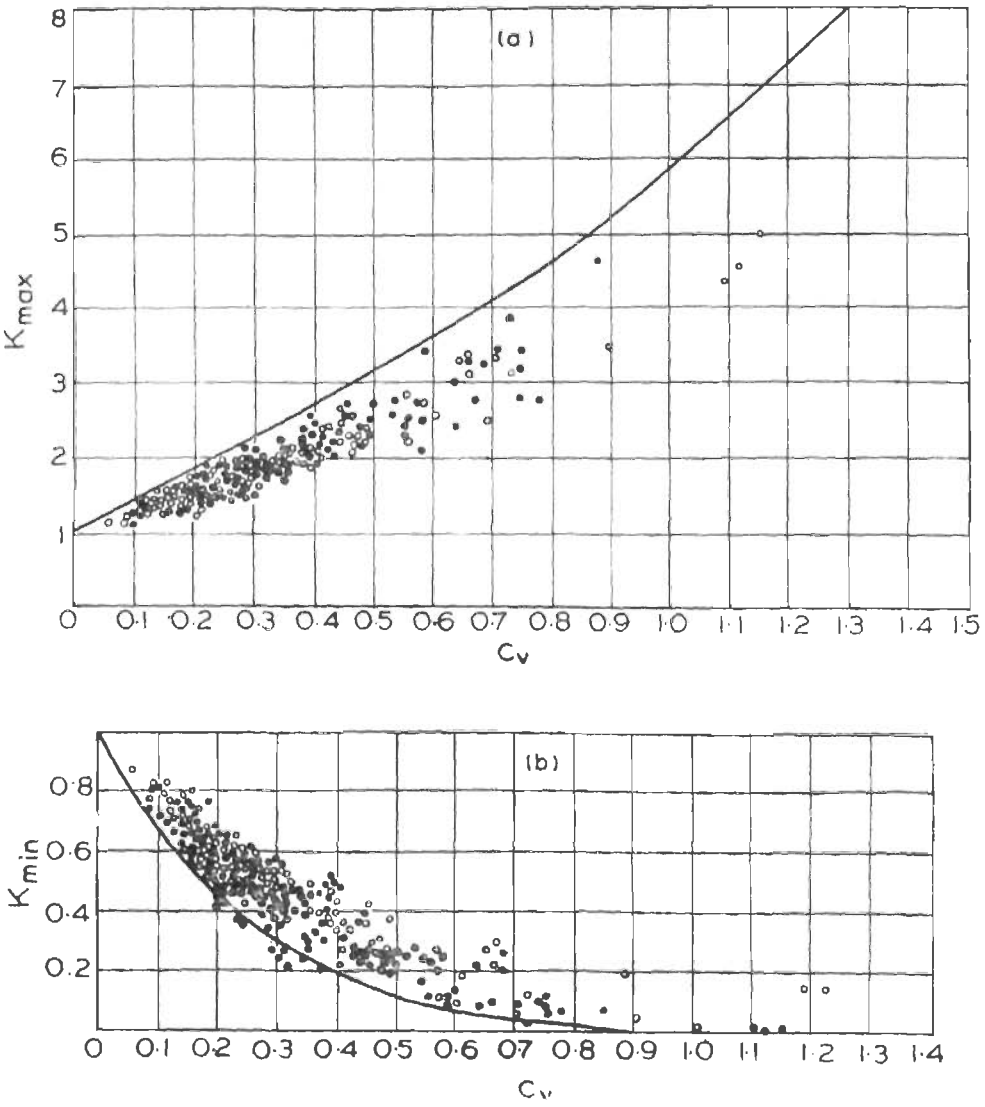

FIGURE 1 : Relation of maximal (a) and minimal (b) observed coefficients of the annual streamflow to the variation coefficient.

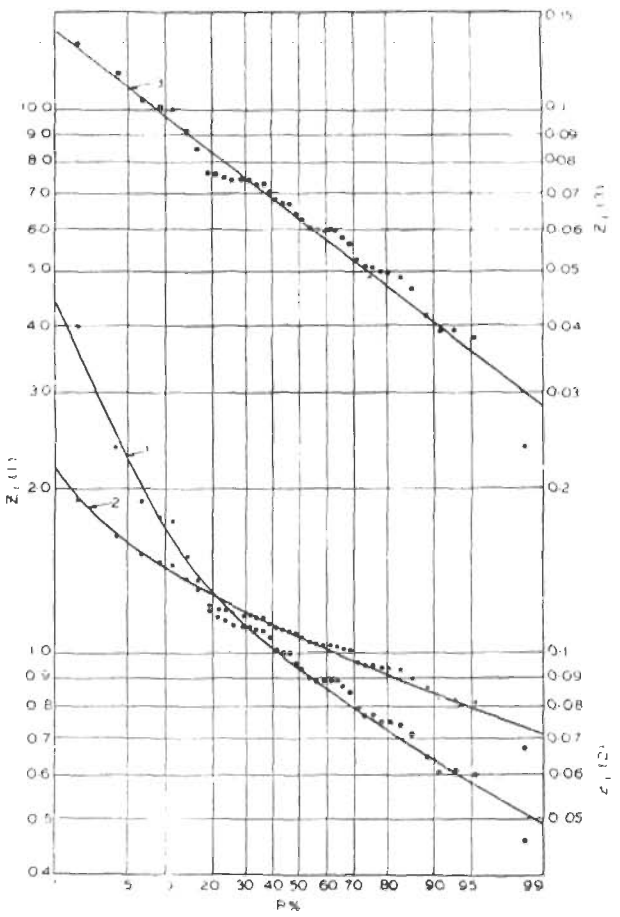

FIGURE 2 : Empirical guarantee curves $Z = \frac{x_i - a}{b - x_i}$ for the River Bzib' at Jirkhva with different a and b on the probability paper of the log-normal distribution : 1—a=0, b=2; 2—a=0, b=10; 3—a=0.4, b=10.

The selection of a and b is possible by another graphical method. As Ref. (2) shows the guarantee curve's ordinates of the S_B-distribution are easily calculated when the values of its parameters m_τ, σ_τ, a and b are known. The parameters m_τ and σ_τ can be estimated for different a and b by means of expressions

$$m_\tau = \frac{\sum_{i=1}^{n} ln\left(\frac{x_i - a}{b - x_i}\right)}{n};$$

$$\sigma_\tau = \sqrt{\frac{\sum_{i=1}^{n}\left[ln\left(\frac{x_i - a}{b - x_i}\right) - m_\tau\right]^2}{n-1}} \qquad ...(4)$$

or by an easier approximate method based on the use of quantiles and relations

$$m_\tau = \frac{\gamma}{\delta} \quad \text{and} \quad \sigma_\tau = \frac{1}{\gamma} \qquad ...(5)$$

while γ and δ are found by making the two percentiles calculated from the observed data equal to the respective percentiles of the rated normal distribution

$$\eta_i = \frac{ln\left(\frac{x_i - a}{b - x_i} - m_\tau\right)}{\sigma_\tau} \qquad ...(6)$$

and by solving the two obtained equations in respect to γ and δ. The corresponding equations for the calculated γ and δ are[3]

$$\delta = \frac{\eta_{1-\alpha'} - \eta_\alpha}{ln\left[\frac{(x_{1-\alpha'} - a)\ (b - x_\alpha)}{(x_\alpha - a)\ (b - x_{1-\alpha'})}\right]}$$

$$\gamma = \eta_{1-\alpha'} - \delta\ ln\left(\frac{x_{1-\alpha'} - a}{b - x_{1-\alpha'}}\right) \qquad ...(7)$$

where, η_α and $\eta_{1-\alpha'}$ are the α.100th and the $(1-\alpha')$.100th percentiles of the rated normal distribution, and x_α and $x_{1-\alpha'}$ are the corresponding empirical percentiles, i.e., x_α is the $\tau\ (n+1)$ ordered value in the observed series. The choice of the concrete percentiles is somewhat random. Usually, the 5th and the 95th or the 9th and 91st percentiles are assumed.

The parameters m_τ and σ_τ are quite simply defined by formulae (5) & (7) for different values of a and b and the definition can be made manually. After that the analytical curves of Johnson S_B-distribution are plotted for different combinations of a and b. The equation

$$x_p = \frac{b\, e^{\sigma_\tau \eta_p} + m_\tau + a}{e^{\sigma_\tau \eta_p + m_\tau} + 1}, \qquad ...(8)$$

where, $\eta_p = \phi\ (p)$ is the quantile value of the rated normal distribution with the parameters (0,1) [5] is used to fit the analytical curve. The values chosen for a and b as the S_B-distribution limits must provide the best agreement between the analytical curve and the empirical distribution of the historical data.

The values of γ and δ (for the 9th and 91st percentiles) were defined with different a and b and the analytical guarantee curves of the S_B-distribution for the m_τ-and σ_τ-values have been fitted for the River Bzib' at Jirkhva (Figures 3 & 4). As those figures show, the asymmetry of the distribution curve depends on the change of the superior and inferior limits of the distribution. It has been as well established that as the limits grow, the asymmetry of the theoretic curve increases.

This result can be used to choose the limits of the S_B-distribution by the Monte Carlo method. Long

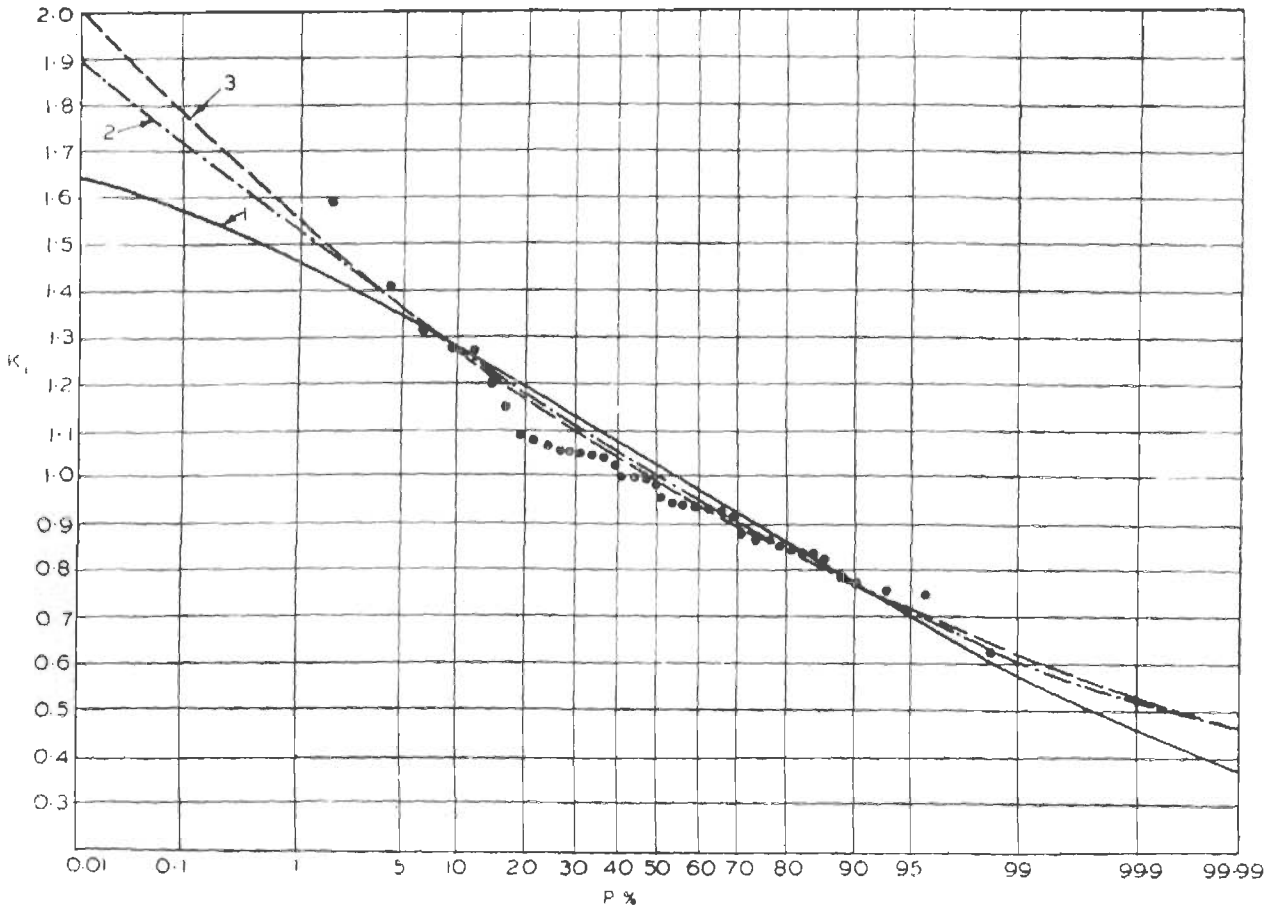

FIGURE 3 : Empirical and analytical guarantee curves of the annual streamflow for the River Bzib' at Jirkhva : 1—a = 0, b = 2; 2—a = 0, b = 4; 3—a = 0, b = 10.

synthetic hydrologic series with Johnson S_B -probability distribution laws and with different combinations of a and b are simulated for each certain river with preset main statistical parameters. In the first approximation the values of a and b can be assumed as in graphs of Figure 1. The parameters of the synthetic hydrologic series for these a and b are compared with those of the historical series. If the skewness coefficient of the simulated series does not coincide with the C_s of the historical series, the values of a and b should be changed and a new synthetic series should be simulated. It should be kept in mind that, as a and b grow, the skewness coefficient of the simulated series grows too, and vice versa, as a and b reduce, the C_s-value drops. Having made these calculations four-five times one can choose such limits of the S_B -distribution for which the parameters of the historical and simulated series agree sufficiently well.

The calculations have shown that when the synthetic hydrologic series are simulated, the change of the S_B -distribution limits affects the values of the skewness coefficient, rather than the flow norm ($\bar{Q}$), the variation coefficient (C_v) and the correlation coefficient (r_1). Figure 5 shows the effect of changing the limits of the S_B -distribution on the skewness coefficient value of the simulated hydrologic series ($n = 2{,}000$ years) for the River Bzib' ($n = 40$, $\bar{Q} = 96{\cdot}4$ m^3/sec, $C_v = 0{\cdot}19$, $C_s = 0{\cdot}95$, $r = 0{\cdot}16$). The other parameters of the simulated series seemed to change very negligibly.

The superior and inferior limits of the S_B -distribution can be set with the help of the χ^2-criterion's minimal value([4]) in the following way : the statistical criterion χ^2 is used to test the agreement between the historical data and the S_B -distribution for different combinations of a and b, and to pick out such values for which is minimal. The χ^2-test considers the fact that the annual streamflow variables are not independent random values, i.e., they are correlated. Therefore, using the N-hypothesis and the method of orthogonalization of the correlated random values([6]), we can obtain the uncorrelated normal sequence

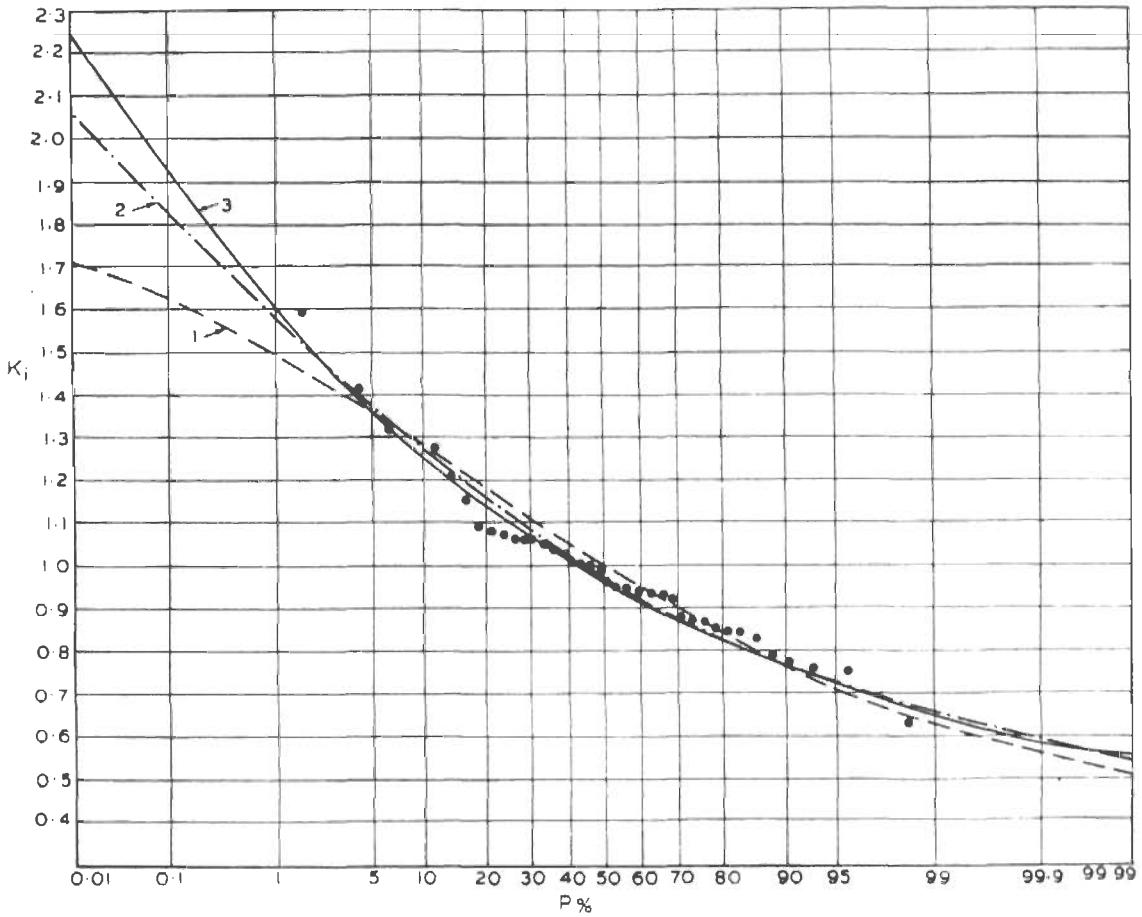

FIGURE 4 : Empirical and analytical guarantee curves of the annual streamflow for the River Bzib' at Jirkhva : 1—a – 0.4, b – 2; 2—a 0.4, b 4; 3—a 0.4, b 10.

$$\zeta_i^k = \frac{\eta_i - m_\tau + \sum_{j=1}^{k-1} \frac{\Lambda_{kk-j}}{\Lambda_{kk}} (\eta_j - m_\tau)}{\sqrt{\frac{\Lambda_k}{\Lambda_{kk}}}\,\sigma_\tau} \qquad \ldots(9)$$

from the observed values of the modular coefficient x_i, and check the agreement between the sequence ζ_i^k and the normal distribution law.

The calculations made for several rivers have shown that the χ^2-values depend on the values of the superior and inferior limits of the S_B -distribution. Figure 6 shows the dependence of the χ^2-value on the value of a and b for the River Bzib' at Jirkhva. This graph indicates that some combinations of a and b give a large value of χ^2 (e.g., $a = 0$, $b = 1{\cdot}61$, $\chi^2 = 20{\cdot}1$), therefore, the hypothesis of applicability of the S_B -distribution is rejected, while other combinations give the minimal values of χ^2 (e.g., $a = 0{\cdot}5$, $b = 3{\cdot}11$—$10{\cdot}11$, $\chi^2 = 0{\cdot}6$) and the hypothesis is accepted.

It has already been pointed out that when the S_B -distribution is used to describe the fluctuations of the annual streamflow values, the change of the superior and inferior limits causes changes mostly in the skewness coefficient and, subsequently, in the relation C_s/C_v. This means that opposite to other laws of distribution used now-a-days in hydrology, which assume a rigid relation between C_s and C_v (e.g., $C_s = 2\,C_v$ for Pearson Type III law; $C_s = 3\,C_v + C_v^3$ for the log-normal law, etc.), in Johnson distribution S_B, the relation variates within a wide range, depending on the assumed a and b ($0 \leqslant a \leqslant x_{min},\ x_{max} \leqslant b \leqslant \infty$). Therefore, this distribution is somehow, universal for the description of the streamflow process.

This conclusion is very important, especially if we consider the recent studies(7) which have shown that some hydrologic characteristics of the annual runoff depend significantly on the date of beginning of the year. Figure 7 presents the plot of change of the parameters of the annual runoff of the River Severnaya Dvina according to the beginning of the year. The graph shows that the mean long-term discharge does

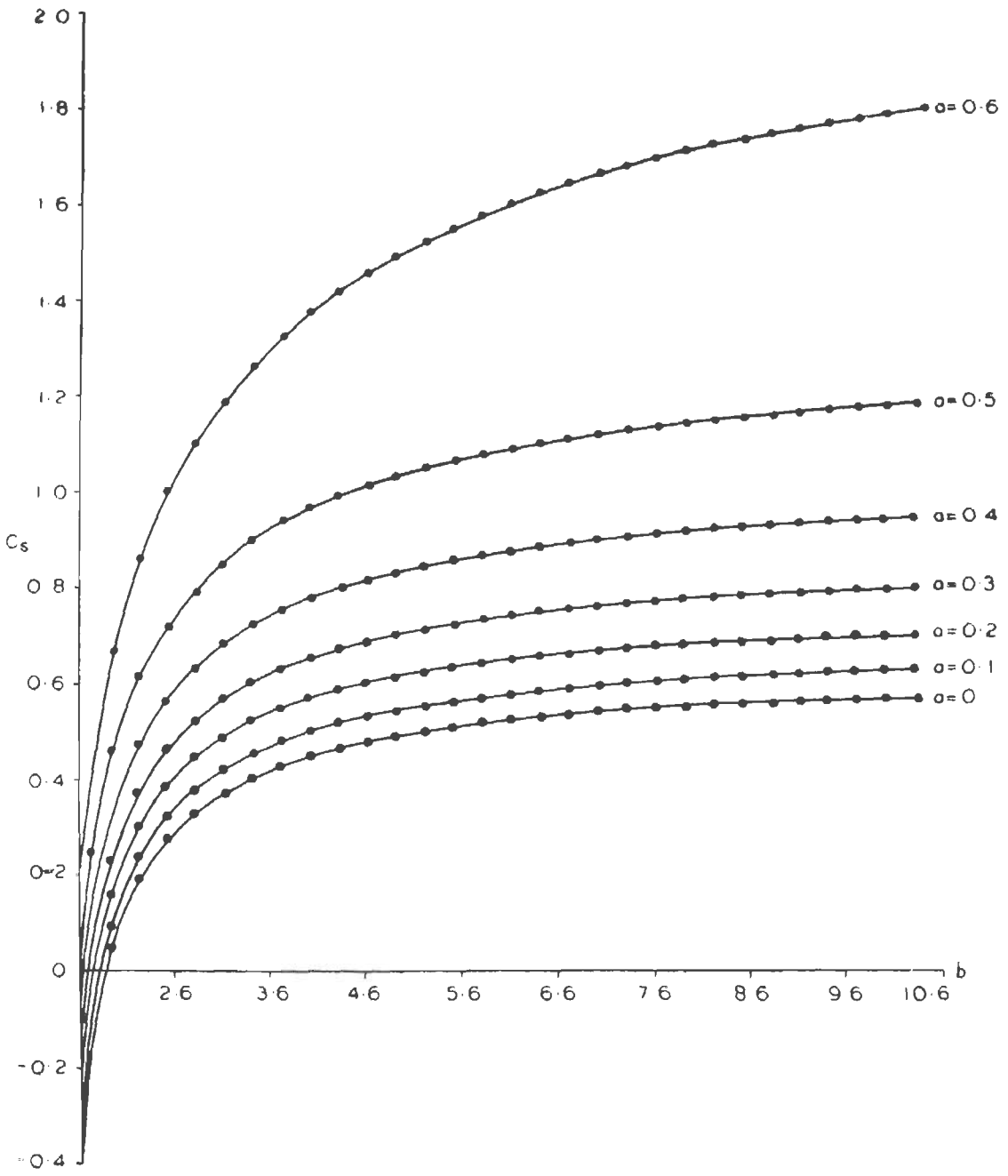

FIGURE 5 · Relation of the skewness coefficient change for the River Bzib' synthetic series to the limits (a and b) of Johnson S_B -distribution.

not depend on the starting date of the hydrologic year; the variation coefficient C_v fluctuates within very narrow limits, and the correlation coefficient between the adjacent members of the annual flow, r_1, and the skewness coefficient C_s change considerably with the change of the starting date of the year.

The character of the change of the correlation coefficient between the adjacent streamflows, and that of the variation coefficient is well reflected in the decrease of r_1 and the increase of C_v during floods. This phenomenon can be explained physically as due to the shift of the date of beginning of the flood, on the one hand,

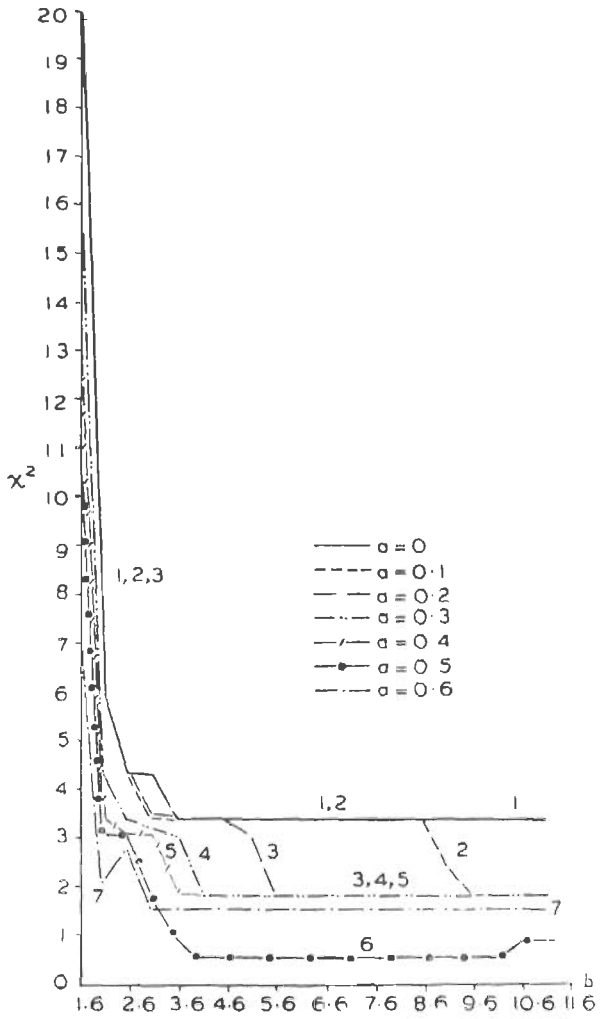

FIGURE 6 : Relation of the χ^2-criterion change to the limits of Johnson S_B -distribution.

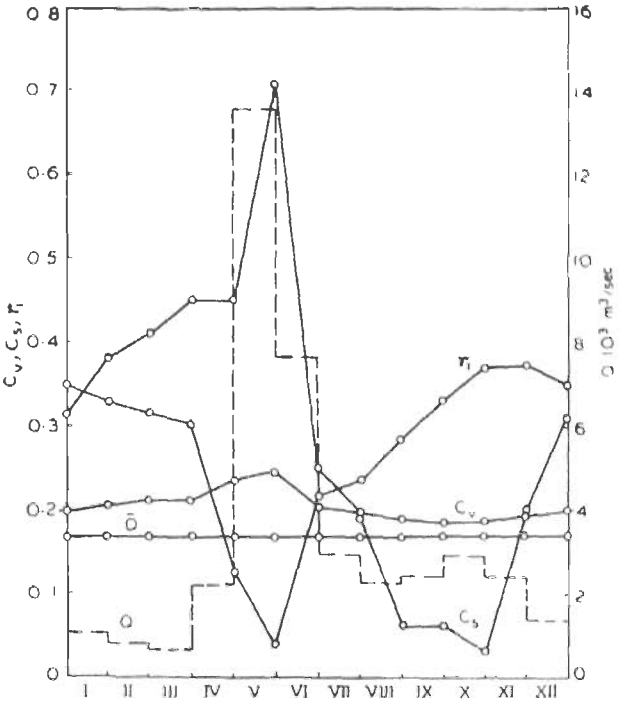

FIGURE 7 : Relation of the annual flow parameters for the River Severnaya Dvina at Ust Pinega to the beginning of the hydrologic year.

and to the various durations of the latter in the long-term case, thus causing the widespreading of the rises and drops of the hydrograph waveline of the flood and, consequently, the weakening of connections. The connections are broken up with the beginning of the flood, and the correlation coefficient which had been more or less stable, drops at once and becomes unreliable, its original value being restored only after complete ceasing of the processes caused by the flood in the within-the-year streamflow regime. Therefore, the stochastic relations between these two sections can be considered as broken up.

The theoretical analysis confirms as well the general dependence of the correlation function on the date of sectioning. Only in two particular cases this dependence seems to be insignificant: (1) in the wide sense of stationarity of the studied process, and (2) when almost all of its realizations present a periodic function with the periods of 1 year. The first case involves rivers with regimes more or less regular in the course of a year. The second case involves reverse of the arid zones.

As some extreme values of the monthly streamflow transfer from one group of annual averaging to another, the asymmetry of the streamflow annual volumes series changes. Sometimes these transfers cause sharp changes of the extreme values of the annual flow, which in their turn give rise to the changes in the flow distribution asymmetry.

Figure 8 gives a good example of a significant change of the series asymmetry with two different segmentations of the same hydrograph. These graphs show that with different segmentations of the hydrograph the annual streamflow values change as a rule very negligibly, and the series asymmetry changes only in the maximal ($p<5$—10 percent), and minimal ($p>90$—95 percent) annual streamflow values. For example, for the River Severnaya Dvina at Ust Pinega the transfer of the segmentation date from 1 December to 1 July resulted in the increase of the maximal mean annual discharge by 800 m^3/sec, with $p=0.6$ percent, which makes 25 km^3/year.

Therefore, it is suggested that the hydrologic series of the annual flow volumes could be often reduced to a random sequence with a preset law of distribution by changing the date of segmentation of the hydrograph.

Let us discuss some examples of the effect of shifting the beginning of the hydrologic year on the type of the distribution curves of the annual flow volumes.

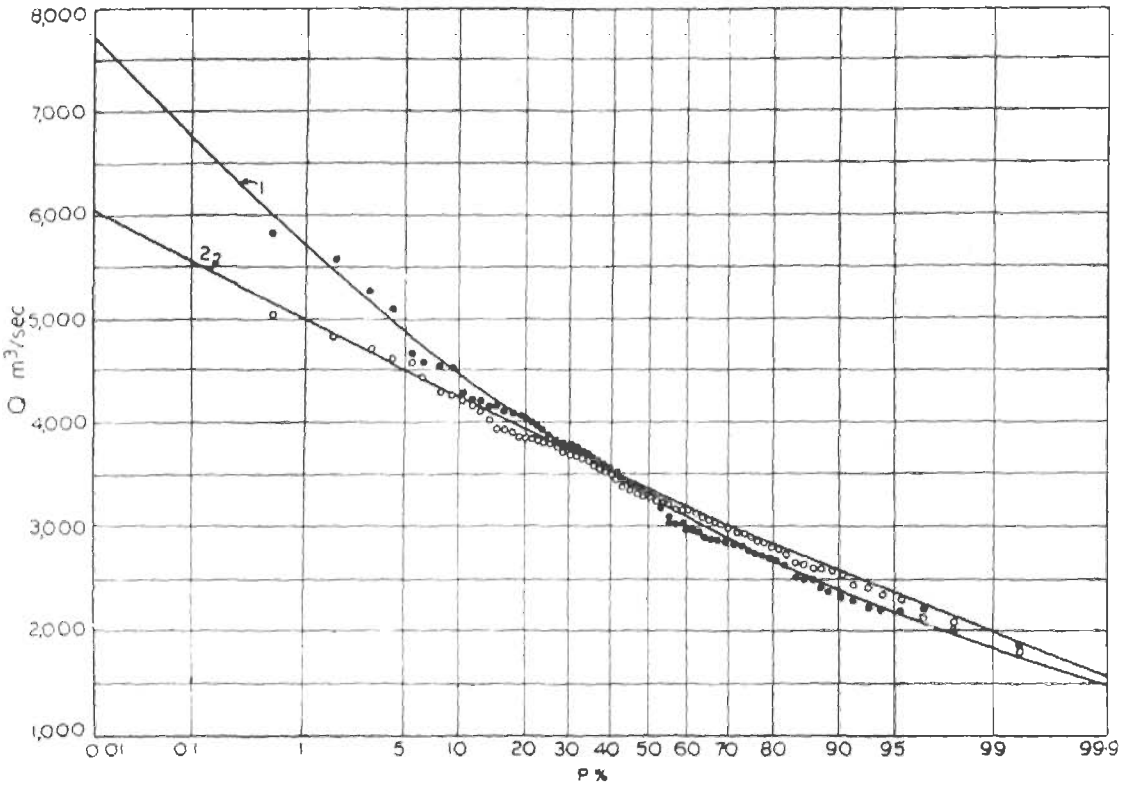

FIGURE 8 : Empirical and analytical guarantee curves with different starting dates of the year : 1—1.06 (C_v=0.24; C_s=0.7; r_1=0.04); 2—1.12 (C_v=0.19; C_s=0.2 ; r_1=0.37), for the River Severnaya Dvina at Ust Pinega.

Comparisons are made with the help of χ^2 and the graphs $\beta_1 O \beta_2$.

The χ^2-criterion was used to test the agreement between the fluctuations of the annual flow values and the log-normal distribution law with different starting dates of the hydrologic year for some rivers of Georgia. The χ^2 -values change according to the beginning of the year (Figure 9), e. g., with the beginning date on 1 February the χ^2 was 1.2 for the River Inguri, confirming the assumed hypothesis, while with the beginning date on 1 April the χ^2 was 8.2, thus rejecting the log-normal law. Similar results were obtained for the other rivers (Figure 9), indicating that the probability distribution law describing the annual streamflow fluctuations can change according to the different starting dates of the hydrologic year.

Graphs $\beta_1 O \beta_2$ (Figure 10) were used for a similar test but with more extensive data.

The graphs show quite clearly the dependence of the distribution changes on the different dates of beginning of the hydrologic year. The point (b_1, b_2) is plotted on the graph $\beta_1 O \beta_2$ for each historical series with different beginning dates of the year and, depending on the arc where the point falls, an adequate probability distribution law is established

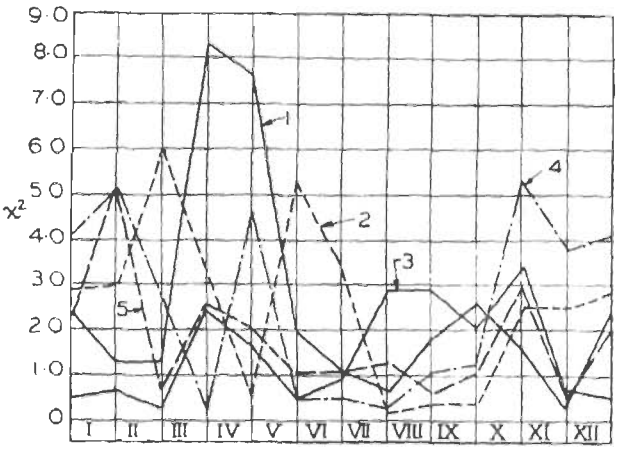

FIGURE 9 : Relation of the χ^2-criterion change to the beginning of the year : 1—The River Inguri: 2—The River Alazani ; 3—The River Aragvi, 4—The River Kura, 5—The River Rioni.

$$\left(b_1 = \frac{m_3^2}{m_2^3} \text{ and } b_2 = \frac{m_4^2}{m_3^3} \right)$$

where, m_2, m_3, m_4 are the values of the 2nd, the 3rd and the 4th central moments, respectively. Calculations were made with different beginning dates of the hydrologic years (1.01, 1.02, ..., 1.12) for 40 rivers of the

USSR, the number of years of observation being more than 50.

The values of b_1 and b_2 change considerably almost in all the studied cases according to the beginning of the hydrologic year. The points (b_1, b_2) which define the best suitable distribution law on the graphs, move. Most part of these transfers occur inside the domain of the S_B -distribution. These calculations have as well confirmed the above idea that in some cases the law of distribution of the annual streamflow volumes changes depending on the different dates of beginning of the year. For example, point (the Yenisei) in Figure 10 is properly described by the S_B -distribution when the beginning of the year in on 1 June and by Johnson S_U -distribution when the date is 1 July. This condition can be used to reduce the hydrologic series of the annual flow volumes to the random sequences with preset distribution.

If some points occur outside the limits of the S_B -distribution, then changing the beginning of the year one may change b_1 and b_2 so that the respective point should fall within the area of this distribution. In the present case all the 12 points outside the S_B -distribution limits were brought inside its area by changing the starting date of the year (the rest 28 points for all of the starting dates of the year remaining within the limits are not shown in the graph—see Figure 10). However, one should keep in mind that the beginning of the year should not fall in the period of flood, because in this case some years might include the runoffs of two floods, partially or completely, while the flood runoff in the adjacent years will be absent.

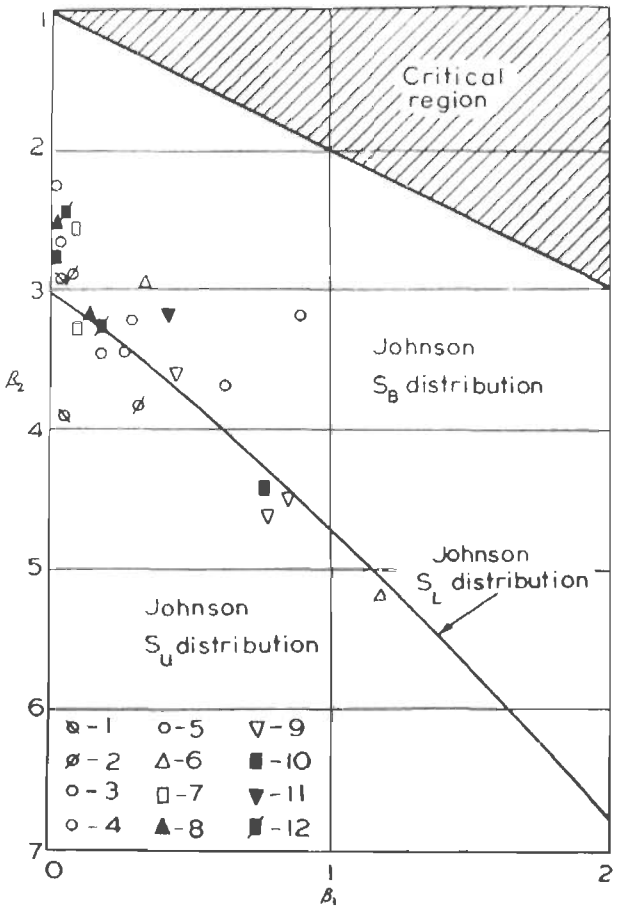

FIGURE 10: Relation of the change of the probability distribution laws to the beginning of the year.

All the above said leads to the conclusion that the fluctuations of the annual flow values for any beginning of the hydrologic year are in most cases well described by the S_B -distribution; while if some streamflows do not agree with this distribution, they can be reduced to the S_B -distribution by changing the beginning of the year.

The great variety of the relation C_s/C_v depending on the limits a and b makes it possible to use Johnson S_B -distribution to describe the streamflow monthly fluctuations. Extention of the probability distribution law to all of the months had formerly been regarded as difficult owing to the wide range of variations of the C_s/C_v-relation, e.g., for the monthly discharge of the River Bzib', $C_s/C_v=0.17$ in the 4th month, and $C_s/C_v=4.0$ in the 8th month. Of course, it is more difficult to make such a generalization for the monthly discharges of different rivers, therefore, very often simplifications were assumed and the variations of the runoff monthly values were described using Pearson Type III Law, the log-normal law or even the normal law, resulting eventually in too great errors.

Description of fluctuation of the monthly flow, considering the within-the-year irregularity, by Johnson S_B -distribution seemed to be sufficient (8), proving thus the advantages of the S_B -distribution over the other types of distribution.

References

(1) KALININ, G. P.: "The Problems of Global Hydrology." In Russian, "Gidrometeoizdat", Leningrad, 1968.

(2) SVANIDZE, G. G. and GRIGOLIA, G.L.: "The use of Johnson Distribution in the Streamflow Calculations." In Russian, J. "Vodnye Resursy" No. 6, 1974.

(3) KHAN, G. and SHAPIRO, S.: "Statistical Models in the Engineering Problems." In Russian, "Mir", Moscow, 1969.

(4) GRIGOLIA, G. L.; "Problems of Statistical Modelling of Hydrologic Series by Monte Carlo Method in the Water Resources Calculations." Synopsis of Thesis, in Russian, 1972.

(5) ALEKSEEV, G. A.: "Objective Methods of Straightening and Standardization of Correlations." In Russian, "Gidrometeoizdat", Leningrad, 1971.

G.R.V.K. Library

UNIVERSITY OF AGRICULTURAL SCIENCES
UNIVERSITY LIBRARY
BANGALORE 560024.

83482

(6) SVANIDZE, G. G. and TORONJADZE, A. P. et al : "Methods of Constructing the Mathematical Model Describing the Streamflow Process with the Analysis of the Assumed Statistical Hypothesis." In Russian, Trans. Ac. Sc. Georgian SSR, V. 53, No. 1, 1969.

(7) SVANIDZE, G. G. and KILASONIA, A.N. : "Relation between the beginning of the Hydrologic Year and the Statistical Parameters of the Streamflow and the required Capacity of the Reservoir." In Russian, J. "Meteorologia i Gidrologia", No. 1, 1969.

(8) TSERETELI, Z.I. and GRIGOLIA, G. L. : "Statistical Simulation of Hydrologic Series Considering the Within-the-Year Flow Distribution for the Water Power Calculations." In Russian, Tekhnicheskaya Informacia, Energetika, No. 1, Tbilisi, 1974.

Mathematical Models of Streamflow for Water Power (Water Management) Calculations

G. G. SVANIDZE
Professor & Head
Hydrologic Department, Tbilisi State University, Tbilisi, USSR.

SYNOPSIS

Special calculations required for the construction of power plants, irrigation plants, water supply systems, flood control reservoirs and more complex hydraulic units should be based on the statistical simulation of the runoff process with the help of the computer.

This report deals with several most efficient mathematical models, taking into consideration the within-the-year distribution of runoff, and discusses the methods of simulation, viz., the fragments method, the method of direct simulation, and the method of reducing the non-stationary flow process to the stationary random sequence. The dynamics of the system's operation regime in time is considered by simulating an ensemble of short runoff realizations and by constructing conditional distribution functions of the respective output probabilistic characteristics.

1. Introduction

Calculations required for the design of special or multipurpose water resource units are usually made by the chronological method which implies the water balance calculations made using the historical hydrologic series with monthly or decade averaging intervals. The results of these calculations are used to find such important parameters as the effective storage capacity and the height of the dam, the installed capacity of the power plant and the power generation, the water outflows for irrigation and water supply, the rate of free discharge losses, etc.

The chronological method has a number of advantages such as its plainness and clearness, its relations with the other regulating reservoirs, water consumers and water users, etc. Its main disadvantage, on the other hand, is its inherent false presumption that the historical series will be exactly repeated in future. It is only the main statistical regularities of the flow that are preserved in reality with completely different water content order in various years and seasons. It should be, therefore, noted that regardless of its popularity and extensive use in practice, the chronological method has become old fashioned and does not meet the requirements of the modern level of mathematical methods and computational means. It should be replaced by the probabilistic methods of calculation in case of a long-term (seasonal-annual and many-years) regulation.

Any streamflow is a probabilistic process and the methods of its description and calculation should be based on an adequate mathematical tool, such as the theory of random functions. In the regulation problems the streamflow is an input process which is subject to specific non-linear operations and is divided into several output processes during its transformation. As the analytical solution of this problem is possible only in the simplest cases, preference should be given to the direct statistical methods of solution, in particular, to the Monte Carlo method. With this in view, the input process is simulated statistically as synthetic hydrologic series which are let pass through the control operator; the selected balance calculations serve to construct the output realizations of the process just as in the chronological method. After the statistical processing of these realizations, one can plot the distribution functions of the system's characteristics sought for.

Therefore, it is necessary to find an adequate flow model and to simulate synthetic hydrologic series of a long duration or to simulate a number of short series (depending on the stationarity of the general conditions of the flow regulation regime), using the Monte Carlo method.

Fifteen years have passed since the first research work on the simulation of synthetic hydrologic series have appeared[1][11]; and about thirty different models have been created since then, which are discussed and classified in Ref. (16). If we try to pick out only those methods which enable the simulation of hydrologic series with the consideration of within-the-year flow distribution, we shall be able to classify them into three groups :

(*i*) the composition methods with the two-fold and multiple sampling;

(*ii*) the direct method, i.e., the method of direct simulation of monthly, decade and other water discharges; and

(*iii*) the method of reducing the non-stationary run-off process to the stationary random sequence.

The description of the three models and their respective simulation methods are given below—one for each group. These models were suggested several years ago, but during the subsequent period they have been thoroughly tested and improved. By now they have become more or less adjusted.

2. The Fragments Method

The fragments method is one of the composition methods suggested by the author[7][9] to simulate the hydrologic series taking into account the within-the-year distribution of the streamflow. The method has become widely used and seems to be the most rational of all the existing new methods of modelling[10].

The essence of the method is the two-fold sampling-first of the mean annual flow (Q_i) and then of the fragment $q_i(t)$ of the historical within-the-year irregularity of the flow distribution according to the calculated averaging interval (month, decade, five days, day). Multiplying the mean annual water discharge Q_i, say, by the mean monthly ordinates of the fragment one can get a new hydrograph with the monthly distributions of water discharges. A sequence of such synthetic hydrographs with preset correlations will yield a long (n = 1,000—10,000 years) hydrologic series or, if necessary, an ensemble of short series for some calculation period (5—50 years).

The order of the simulation process is as follows: The fragments are made according to all the observed years (m) by means of dividing the water discharges in each interval of the year under study by the respective mean annual water discharge. Figure 1 presents the fragments with continuous (a, a') and discrete time with the decade (b, b') and monthly (c, c') averaging intervals. Mean monthly discharges are usually used for the water power plants, while mean monthly or decade discharges are used for the irrigation systems. The division of all the functions of the observed hydrograph by a constant value (mean annual water discharge) does not affect the hydrograph's form and preserves all the within-the-year stochastic relations in the same state as they are in the historical series. These relations are considerably complicated and their nature still remains obscure, though in other flow models (see below) they are conditionally assumed as linear ones. In this aspect this method does not need any additional hypothesis because the relations remain in their natural state, which is the advantage of this method.

A series of the mean annual water discharges Q_i can be simulated by one of the existing methods, e.g., by the unified method[15]—by the first order or the higher order Markov chain, by the individual (for one unit) or aggregate (for a system of units) simulation method.

With the sequence of Q_i (i = 1, 2,..., n) and m fragments $q_j(t)$ available, the above method is used to construct a hydrologic series (Figure 2). With a set of fragments according to the number of the observed years (m) in case of n-years series, n various hydrographs are obtained with an extremely low probability of recurrence of similar hydrographs $\left(\frac{1}{m \cdot n}\right)$. There is no need to prove that this diversity of the hydrographs with a sufficient reliability might cover the possible future behaviour of the flow. If the year's water content and the pattern of the hydrograph, i.e., the nature of the within-the-year flow distribution, are not correlated, then the sequence of the fragments is established by means of a random sampling by the urn model with the returning ball. Otherwise the mentioned correlation can be accounted for quite easily in the following order: the fragments of the years with high, medium and low water content are placed in different urns and are picked out for each Q_i only from the respective urn according to the Q_i's value (i.e., the water content). Being so simple as not to cause any complications of the algorithm and the program, this method is introduced into the computer's standard program.

The method of fragments has been tested by numerous experimental calculations on the computer which have evidenced the rightfulness of the calculation pattern and principles underlying the method. At present, summing up the obtained results for the overall evaluation of the method we could recommend it for a more extensive use in practice for the hydropower and water management calculations.

3. The Method of Direct Simulation

A synthetic hydrologic series can be generated considering the within-the-year streamflow distribution using the Monte Carlo method by plotting corresponding functions of transition and by direct simulation of

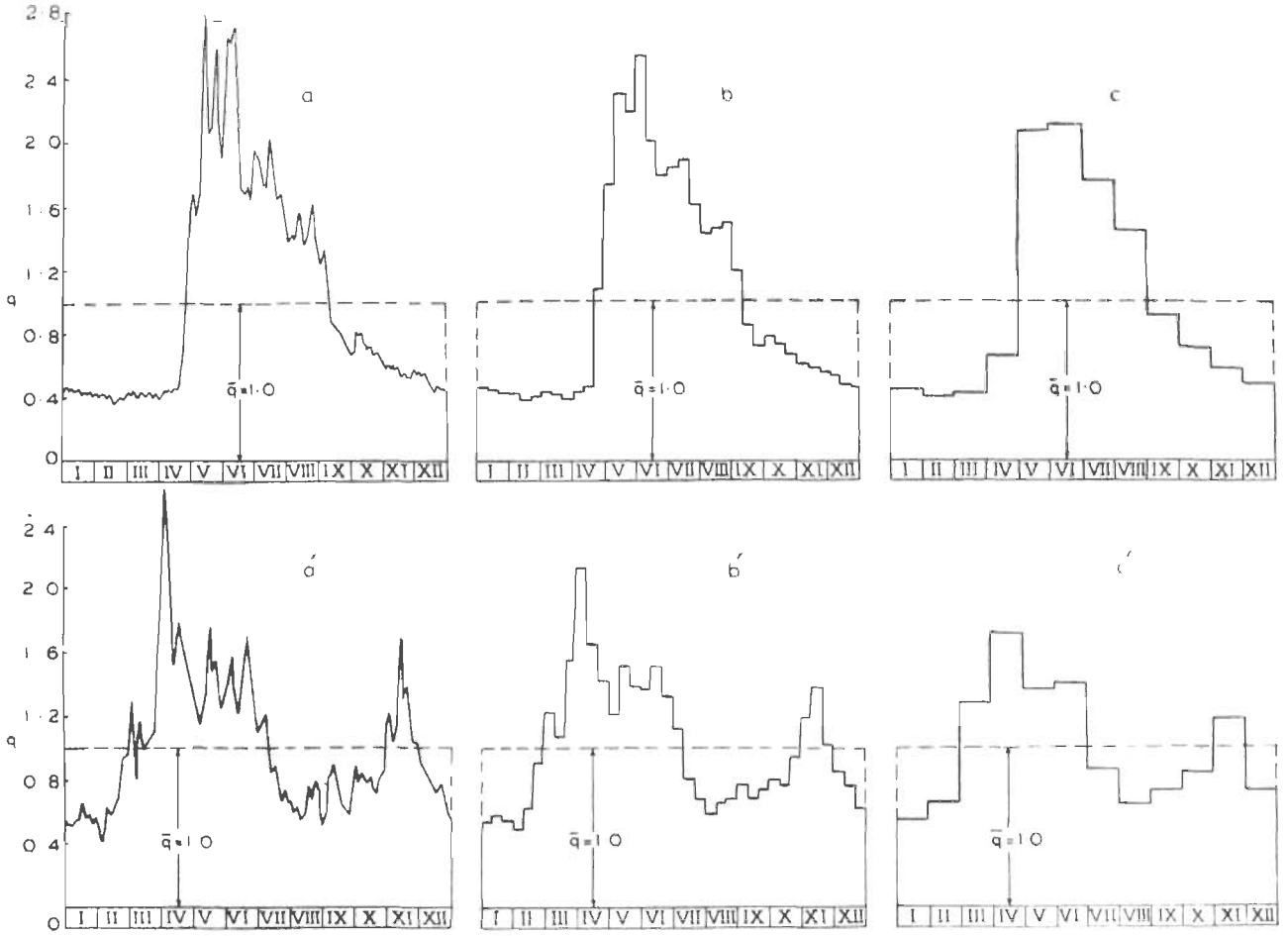

FIGURE 1 : Fragments : a and a'—with continuous time; b and b'— with the monthly and c and c'—with the monthly averaging intervals (for the Rivers Terek and Kura).

the mean interval water discharges according to the data of the water discharges in the previous time intervals. Such direct method of modelling by the first-order Markov chain was proposed in Ref. (1). Later such methods were given in Ref. (11) & (12) though with a bit different initial assumptions. Still, later a number of writers suggested to use the higher-order Markov chain, providing thus various reasonings in respect to the choice of the chain's length [(2) (3) (4) (5) and others]. The individual parts of the method being thus improved, it has grown quite well adjusted and fit for more extensive use in the simulation of hydrologic series designed for the water power and water management calculations.

The method of direct simulation, as it is described in Ref. (4) & (5) implies the following :

Let the streamflow be a periodic Markov process with one year period. For the multivariate distribution of the mean monthly water discharges, assume the *N*-hypothesis of normality of the multivariate distribution if the corresponding one-dimensional distributions are normal(3). For example, in the case of some asymmetric process $\xi(t)$ with the time dependent one-dimensional distribution function $F(x, t)$, the use of the *N*-hypothesis means that the process

$$\eta(t) = \phi^{-1}[F\{\xi(t)\}],$$

where, ϕ^{-1} is a function reverse to the function

$$\phi(x) = \frac{1}{\sqrt{2\pi}} \int_{-\infty}^{x} e^{-\frac{z^2}{2}} dz$$

is a normal process. Thus, the simulation of the streamflow process can be reduced to the simulation of a normal process with the parameters (O, σ^2). Considering the above said, the autoregressive discrete runoff model can be presented as a recurrence expression

$$x_{nT+n} = a^{(k)}_{m,1}\, x_{nT+m-1} + a^{(k)}_{m,2}\, x_{nT+m-2} + \ldots + a^{(k)}_{m,k}\, x_{nT+m-k} + \sigma_{m,k}\, \zeta_{nT+m} \quad \ldots(1)$$

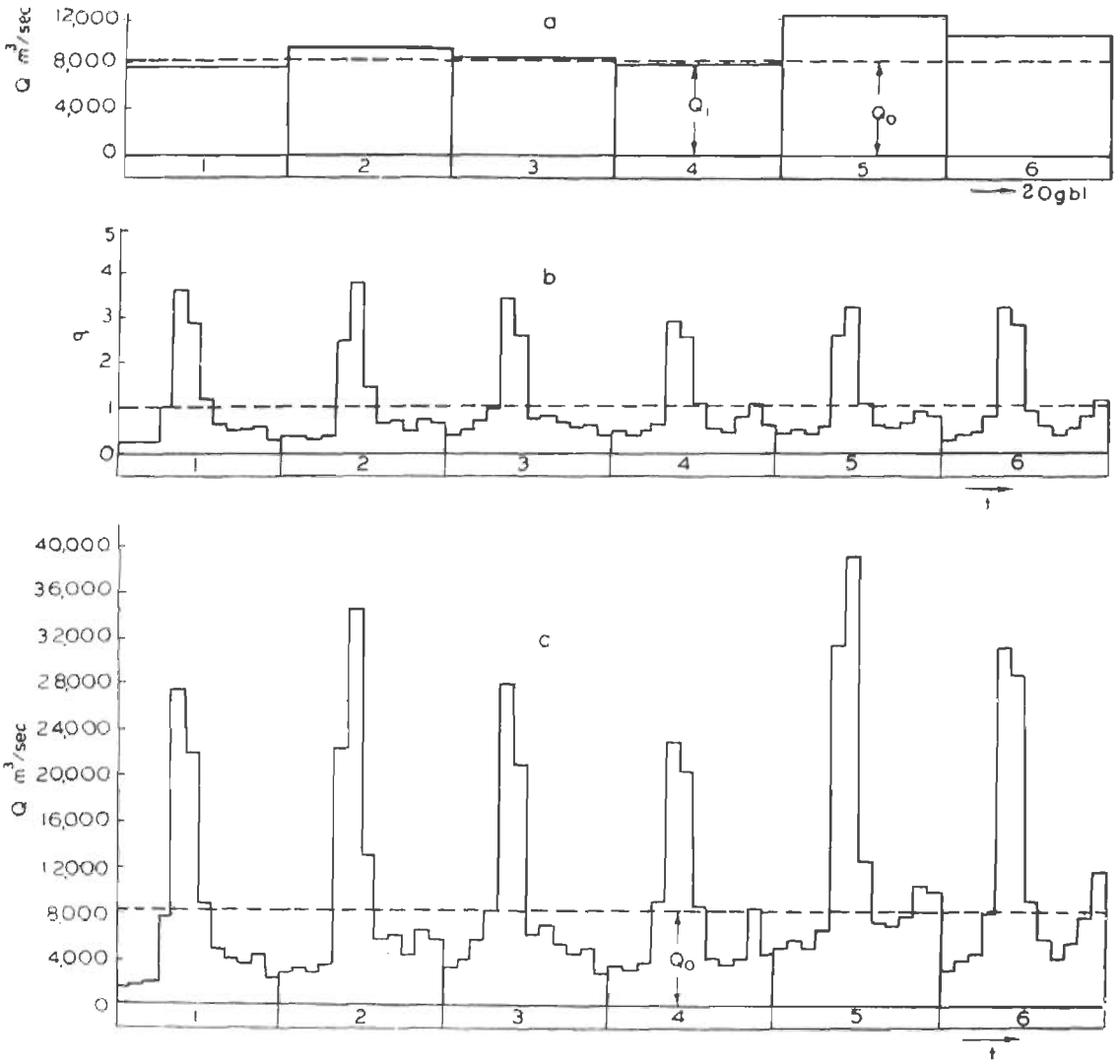

FIGURE 2 : The order of simulation of a hydrologic series by the fragments method: a—the first sampling (of mean annual water discharges Q_i); b—the second sampling [of fragments $q_j(t)$]; c—the hydrologic series (for the River Volga).

where, $a^{(k)}_{m,i}$, $i = 1, 2, \ldots, k$ are the regression coefficients corresponding to the length k; T is a period (assume $T = 12$); n is the number of periods; m is the months; $\sigma_{m,k}$ is the root-mean-square deviation of the sequence $x_{n,\,m-i}$ from its linear prediction; $\xi_{n,m}$ is the sequence of independent normally distributed random values with the parameters (0, 1).

As the value k is unknown before hand, it is to be found, the values of the regression coefficients and $\sigma_{m,k}$ change with the change of k. The problem consists in the finding of such k with which $\sigma_{m,k}$ either does not decrease at all or decreases but insignificantly.

It is necessary to establish the recalculation pattern of the regression coefficients. Let $R_{m,i}$ be the covariation between the values of the process in the intervals m and $m-i$. Then

$$R_{m,i} = \frac{1}{N-1}\sum_{n=0}^{N-1} x_{nT+m}\; x_{nT+m-i} \qquad \ldots(2)$$

where, N is the number of the years of observation.

Calculation of the unknown regression coefficients by the method of converting the covariation matrix is sufficiently difficult. It would be quite appropriate to use here the following generalization of Derbin's well-known recurrence formulae[13] designed for the recalculation of the regression coefficients and the residual depressions in the case of the periodic process[4] :

$$a_{m,i}^{(k)} = a_{m,i}^{(k)} - a_{m,k}^{(k)} \; b_{m,i}^{(k-1)}, \quad i=1,2,\ldots,k-1, \quad \ldots(3)$$

$$b_{m,i}^{(k)} = b_{m-1,i-1}^{(k-1)} - b_{m,i}^{(k)} \; a_{m-1,i-1}^{(k-1)}, \; i=2,3,\ldots,k, \quad \ldots(4)$$

$$a_{m,k}^{(k)} = \frac{R_{m,k} - \sum_{i=1}^{k-1} R_{m-i,k-i} \; a_{m,i}^{(k-1)}}{R_{m-1,o} - \sum_{i=1}^{k-1} R_{m-i,k-i} \; b_{m,i}^{(k-1)}}, \quad \ldots(5)$$

$$b_{m,1}^{(k)} = \frac{R_{m-1,k} - \sum_{i=1}^{k-1} R_{m-1,i} \; b_{m-1,i}^{(k-1)}}{R_{m-1,o} - \sum_{i=1}^{k-1} R_{m-1,i} \; a_{m-1,i}^{(k-1)}} \quad \ldots(6)$$

For the evaluation of $\sigma_{m,k}$ the recurrence expression is the following :

$$\sigma_{m,k}^{2} = \sigma_{m,k-1}^{2} \left(1 - a_{m,k}^{(k)} \; b_{m+1,1}^{(k)} \right) \quad \ldots(7)$$

Therefore, in the case of the periodic process the two-dimensional sequence $a_{m,i}^{(k)}$ and $b_{m,i}^{(k)}$ is required to calculate the values of $a_{m,i}^{(k)}$. It is clear that the initial values of the coefficients (for $k=0$) are equal to zero, i. e.,

$$a_{m,i}^{(o)} = b_{m,i}^{(o)} = 0 \quad \ldots(8)$$

Having found the values of the regression coefficient $a_{m,i}^{(k-1)}$, i=1, 2,..., k−1 and the values of the additional parameters $b_{m,i}^{(k-1)}$, $i=1, 2,\ldots, k-1$, the unknown parameters of the flow can be found by means of Equations (5) & (6), and then (3) & (4).

The choice of the coherency length is realized by means of the dispersion minimum criterion. The calculation should be ceased when the relation $\frac{\sigma_{m,k}}{\sigma_{m,k-1}}$ becomes close to 1 and it is possible to assume that the true coherency length is $k-1$.

Keeping in mind the wide applicability of the modern computers, it seems quite logical that the inter-series stochastic relations should be accounted together with all the preceding 11 months. This will make the program a little simpler because it is not necessary to look for the optimal value of K in each individual case.

Figure 3 presents a case of comparison of the correlation function of the observed series of the mean

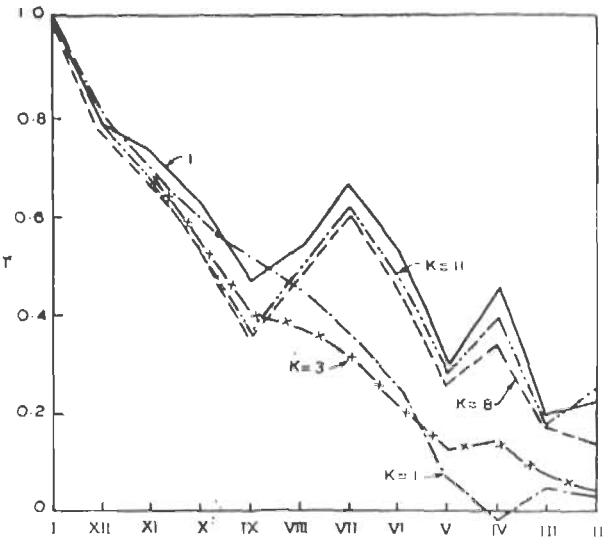

FIGURE 3 : Comparison of the correlation function of the January water discharges and the water discharges of the preceding months of the series observed (1), with the correlation function of series simulated by the Markov chain pattern for k 1, 3, 8 and 11 (for River Naryn).

January water discharges with the water discharges for k preceding months for the River Naryn (Uch-Kurgan), and the correlation functions of the series simulated in accordance with the relation (1) for different coherency lengths ($k=1$, 3, 8 and 11). As the graph shows, the greater the number of lags in the Markov chain, the better the results ; and with $k=11$ the agreement between the correlation functions of the initial and the simulated series is sufficiently good.

4. The Method of Simulation Based on the T-Transformation

The T-transformation, i. e., reducing the observed long-term hydrograph to the stationary model "T" can be described in brief as follows ([6]) ([14]) ([17]).

The streamflow process is assumed as a random non-stationary continuous periodic process whose mathematical expectation is estimated by plotting the average (the so-called "fictitious") annual hydrograph, to which the average long-term flow W (norm) corresponds. Further, the year is divided into a given number ($N=10-20$) of intervals $\triangle_j$ ($j=1,2,\ldots, N$) along the time axis, so that within their limits the mean value of the flow is constant (Figure 4), i. e.,

$$S_j = \frac{\overline{W}}{N} = \bar{S}$$

Then, with the whole observed series for m years, the actual observed flow values are determined ξ_i ($i=1, 2, \ldots, N-n$) in the strictly preset chronological limits of the interval $\triangle_j$. The resulting sequence is assumed as a stationary one in its wide sense. And this clearly

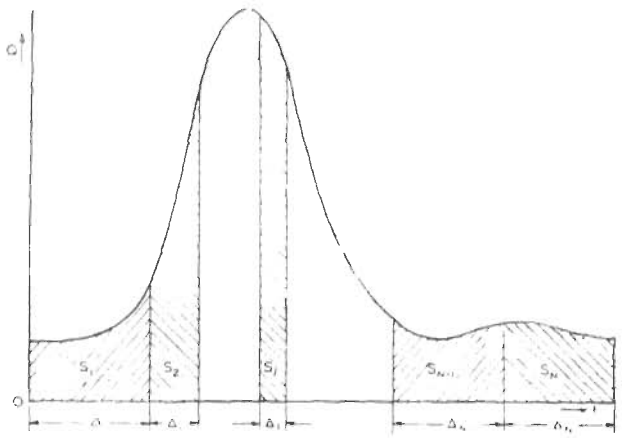

FIGURE 4 : Division of the averaged (fictitious) hydrograph into N-intervals within which the averaged flow volumes are equal.

means that in the known confident limits the mathematical expectation of the sequence remains constant, while the correlation function depends only on the distance between two arguments.

Since there may be a great many of sequences with equal mathematical expectations and correlation functions as an additional condition ensuring a suitable transient distribution function, we assume the ξ_i-sequence as related to the N-class process.

If the ξ_i-sequence is the first-order Markov chain subject, say, to the lognormal law and belongs to the N-class processes, then the sequence

$$\eta_i = \frac{ln(\xi_i - a) - m}{\sigma} \qquad ...(9)$$

should form a simple Markov chain of normally distributed random values with the parameters (0, 1) and the correlation coefficient ρ between the adjacent members of the series. In the case of Johnson distribution S_B we obtain

$$\eta_i = \frac{ln\left(\frac{\xi_i - a}{b - \xi_i}\right) - m}{\sigma} \qquad ...(10)$$

Therefore, the new sequence

$$\zeta_{i+1} = \frac{\eta_{i+1} - \rho\eta_i}{\sqrt{1-\rho^2}} \qquad ...(11)$$

should also be normally distributed with the parameters (0, 1), the values being independent owing to the orthonormalization.

Here m and σ are the estimates of the mathematical expectation and the standard, respectively, and a and b are the minimal and maximal values of ξ_i.

Thus, eventually the whole problem reduces to the testing of normality of the orthonormal sequence ζ_{i+1} with the help of some criterion (e. g., χ^2). Hence, follows the rule of simulation by the unified method designed both for individual and aggregate modelling ([15]).

In fact, referring to Ref. (3), we could write the recurrence relation

$$\eta_{i+1} = \rho\eta_i - \sqrt{1-\rho^2}\ \zeta_{i+1} \qquad ...(12)$$

which is used to determine η_{i+1} with the η_i known. After that the corresponding value of ξ_{i+1} can be found. With the lognormal distribution

$$\xi_{i+1} = e^{\sigma\eta_{i+1} + m} + a, \qquad ...(13)$$

and with Johnson distribution

$$\xi_{i+1} = \frac{b\, e^{\sigma\eta_{i+1} + m} + a}{e^{\sigma\eta_{i+1} + m} + 1} \qquad ...(14)$$

Similar expressions are obtained for the higher order one-dimensional Markov chain and for the multivariate case ([15]).

The chronological boundaries of the $\triangle_i$ intervals are set in different ways, the simplest and quite efficient one being the use of the integral curve $W(t) = \sum_{k=1}^{12} W_k$, where, W_k is the mean monthly volume of water for the whole observation period. In the same boundaries the water volumes are subsequently determined by the integral curves of individual years.

The discussed method of the T-transformation has been tested for several rivers in different physical and geographical environments : the Kura (Tbilisi), the Inguri (Jvari), the Neva (Novosaratovka), the Laba (Dachin), the Nile (Aswan). In all these cases the obtained irregularly discrete T-model of the streamflow was sufficiently close to the stationary random sequence.

Despite the different appearances of the observed hydrograph and its respective T-model, they are quite identical as far as the deficits distribution is concerned, which is the most important condition in the storage capacity calculations. Figure 5 compares the deficits for the initial series of mean monthly discharges (d_i) and the deficits according to the T-model (d_i') with different outflows (α = 0.7, 0.9, 1.0) for the River Kura at Tbilisi. The agreement between the data is quite good in the most interesting region with the 5—30 percent deficits guarantee level, to which 70—95 percent outflow guarantee level approximately corresponds. This slight discrepancy might have been caused by the different numbers of intervals (10 intervals of the T-model against 12 months of the initial series).

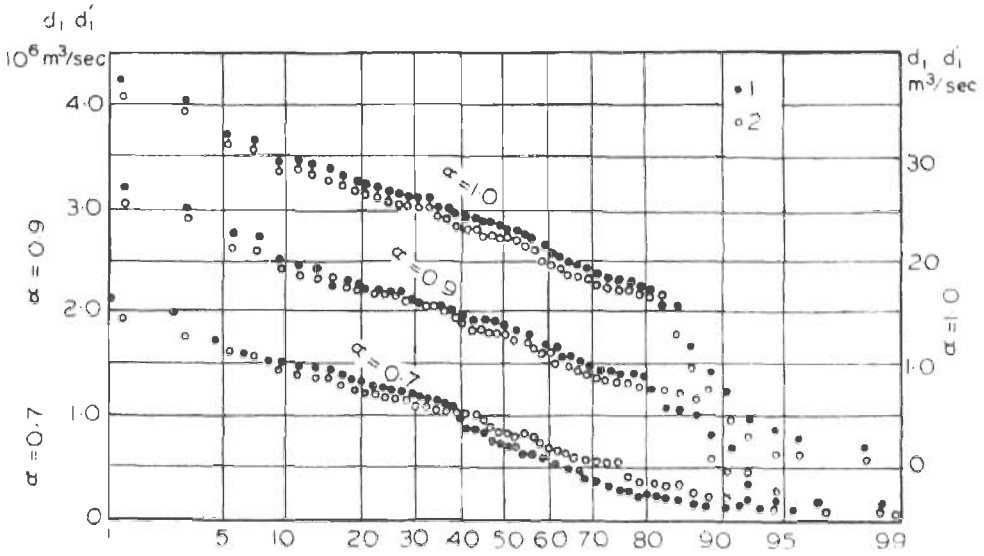

FIGURE 5 : **Comparison of water deficits with various outflow values α : 1— for the initial series; 2—for the model T (for the River Kura).**

5. Conclusion

Johnson S_B-distribution can be recommended as the one-dimensional function of distribution ([8]). This distribution limited at both ends is a universal one and covers almost the whole range of changes of the statistical characteristics of the distribution laws used now-a-days in hydrology. The S_B-distribution turned out to be applicable to the mean annual water discharges for the overwhelming majority of 200 rivers under study in different parts of the world ([8]). It can be as well used for the T-model of the flow. The superior and inferior limits of the distribution should be set by means of the χ^2-criterion.

The above simulation methods for the stationary random sequence of modular coefficients (ξ_i) or of the absolute values of the flow (Q_i) can be used to create both unconditional and conditional flow realizations. The first are used in the cases ("A") of the stationary regulation process, i.e., with the flow and water consumption conditions remaining steady; the second ones are used in the cases ("B") of the non-stationary regulation process, i.e., the dynamical regime. The difference between the simulation approaches is that in the case "A" one long series (1,000 or more years) is generated, while in the case "B" the water inflow for the future limited period ($n = 5-10-50$ years) is assumed as a conditioned random process, and an ensemble of short hydrologic series is generated. Statistical processing of the results on the computer gives the probability distribution function of the output characteristics.

The case "B" makes it possible to use the deterministic methods of optimization of the system's operation regime (according to a given hydrograph) for the probabilistic solution of the problem. With L realizations available (L-several hundreds) the water storage control can be carried out by each realization, provided there is a one-valued forecast for the future n_1-years period of operation. This condition is assumed with a very slight probability $(1/L)$*, since the one-valued forecast is practically impossible. Thus, if the inflow rate is known, the optimal regulation plan is easy to make. Having developed an adequate policy of regulation and programmed it, the calculation can be repeated on the computer L-times for n_1-years. Further, the same program is used to process statistically the data for certain time intervals (one year, or three-five years), and to plot the corresponding conditioned distribution functions of the output processes, such as the power generation, and the available power of the water power plants, the target outflows for irrigation and water supply, filling of the water reservoirs, free discharges, etc., which is indeed the ultimate object of all the hydropower and water management calculations.

6. References

(1) SVANIDZE, G.G. : "*Simulation of the Theoretic* Hydrologic Series by the Monte Carlo Method." Proc. Ac. Sc. GSSR, 1961, Vol. 26, No. 5 (In Russian).

(2) ALEKSANDROVSKI, A.Y. and REZNIKOVSKI, A. Sh. : "On the Statistical Simulation of Streamflow Considering the within-the-year Distribution." J. "Vodnye Resursi", 1972, No. 23.

(3) KARTVELISHVILI, N.A. : "The Streamflow Control". Leningrad. Gidrometeoizdat, 1970 (In Russian).

(4) TSERETELI, Z.I. and CHITASHVILI, R.J.: "About One Streamflow Model for Water Power Calculations." Proc. Ac. Sc. GSSR, 1973, Vol. 71, No. 3 (In Russian).

* For example, if L 500, then the statistical probability of each realization is $\frac{1}{500}$ 0.002 0.2 percent.

(5) SVANIDZE, G.G.; GRIGOLIA, G.L.; TSERETELI, Z.I. and CHITASHVILI R.J. : "The Method of Direct Simulation of Hydrologic Series". Considering the within-the-year Flow Distribution by the Higher-Order Markov Chain. J. "Vodnye Resursi", 1975, No. 5.

(6) SVANIDZE, G.G.; TORONJADZE, A.Ph.; EDIBERIDZE, M.G.; CHITASHVILI, R.J. and PIRANASHVILI, Z.A.: "Methods of Construction of Mathematical Model Describing the Streamflow Process with the Analysis of the Assumed Stochastic Hypotheses." Proc. Ac. Sc. GSSR, 1969, Vol. 53, No. 1 (In Russian.)

(7) SVANIDZE, G.G. : "Basic Calculations for the Streamflow Regulation by the Monte Carlo Method." Tbilisi. Metsniereba, 1964 (In Russian).

(8) SVANIDZE, G.G. and GRIGOLIA, G.L. : "The Use of Johnson Distribution for the Streamflow Calculations." J. "Vodnye Resursi", 1974, No. 6.

(9) SVANIDZE, G.G.: "Simulation of Hydrologic Series with Consideration of the within-the-year Flow Distribution (the Fragments Method)." Report at the Hydrologic Conference in Czechoslovakia, Bratislava, 1962 (J. Vodni hospodarstvi, 1963, No. 6).

(10) REZNIKOVSKI, A. Sh. and RUBINSTEIN, M.I. : "Power Plants Reservoirs Regime Control." Moscow. "Energia", 1974 (In Russian).

(11) FIERING, M.B.: "Queueing Theory and Simulation in Reservoir Design." J. Hydraulics Division, Proceedings of the ASCE, HY6, November 1961.

(12) MAASS, A.; HUFSCHMIDT, M.M.; DORFMAN R.; THOMAS, H.A.; MARGLIN, S.A. and FAIR G.M. : "Design of Water Resource Systems." Harvard University Press, Cambridge, Massachusetts, 1962.

(13) DERBIN, J. : "Estimation of Parameters in Time Series Regression Models." J. of the Royal Statistical Society, Series B, 1960.

(14) SVANIDZE, G.G. : "Use of Digital Computers for Mathematical Modelling of Hydrologic Processes." Symposium on the Use of Analog and Digital Computers in Hydrology. USA, Tucson, Arizona, 1968, Vol. 1.

(15) SVANIDZE, G.G.: "Mathematical Models of the Process of Runoff in Calculating Storage Reservoirs." International Symposium of Application of Mathematical Models in Hydrology, Warsaw, 1971.

(16) SVANIDZE, G.G. and REZNIKOVSKI, A. Sh. : "Stochastic Methods of Modelling for Designing Water Economy Systems." Proc. XY Congress of the International Association for Hydraulic Research, Turkey, Istanbul, 1973.

(17) SVANIDZE, G.G. : "Preparation of Hydrologic Data for Optimization of the Water Resource Systems." Proc. of the XYI Congress of the IAHR, Brazil, Sao Paulo, 1975.

UAS LIBRARY GKVK
83482

A Mathematical Model for Basin Runoff

V.C. KULANDAISWAMY
Director of Technical Education
Tamil Nadu, Madras (India).

T. BABU RAO
Lecturer in Applied Mechanics and Hydraulics Department
Karnataka Regional Engineering College
Suratkal (S. K.), Karnataka (India).

SYNOPSIS

Treating the drainage basin as a hydrologic system, Kulandaiswamy proposed a general model for the conversion of rainfall excess into surface runoff(7). *Two simplified versions of the above model have been investigated for the dependance of their coefficients on storm characteristics. A new method for the estimation of abstractions has been used in this study. From a study of 227 storms over 19 basins it is found that the coefficients in the models correlate fairly well with storm characteristics. Results obtained by applying the models to 96 storms over 9 basins are discussed. Based on this investigation, a 5-coefficient runoff model is recommended for application to natural drainage basins when a computer facility is available and simpler version, a 3-coefficient model is recommended, when computations have to be made using a desk calculator or slide rule.*

1. Introduction

The determination of runoff due to a known precipitation under given antecedent conditions is a major problem facing hydrologists. The problem is so complex that its complete solution is almost impossible for the present. Since the introduction of unit hydrograph theory, many models have been proposed for rainfall-runoff relationship. If the degree of theoretical sophistication is a measure of achievement, then the contributions are many and significant. But, if the degree of understanding of the parameters in the mathematical relationship describing surface runoff process is the yardstick, the progress made is not very commendable. In this study, two models are investigated for the dependance of their parameters on the storm characteristics.

Using Systems approach Kulandaiswamy proposed a general model for the conversion of rainfall excess into surface runoff. He also investigated a series of simplified versions of the above model and their solutions(7). Two of the simplified versions, a 5-coefficient model and a 3-coefficient model have been taken up for a detailed investigation in this study for the dependance of their coefficients on storm characteristics. A new method for the determination of abstraction rate curve has been used for obtaining rainfall excess. An exponential function has been used for baseflow. The component models are integrated to obtain the runoff from rainfall. All the component models used in this investigation have been reviewed for the sake of completeness. Results are discussed.

2. Description of the Model

The entire hydrologic cycle can be thought of, as a major system with a number of sub-systems. In such a system, the land area will be a constituent sub-system. Since the present study is concerned only with the precipitation occurring over a basin and the way it is disposed of, the basin becomes in this case, a main system with its own components. The investigation of rainfall-runoff relationship consists mainly of three components :

(*i*) Estimation of abstractions and consequent rainfall excess,

(*ii*) Conversion of rainfall excess into surface runoff, and

(*iii*) Determination of baseflow contribution.

The combination of surface runoff with baseflow gives runoff. A block diagram representing the basin system that converts rainfall into abstractions and

runoff, is given in Figure 1. The operators Φ_1' and Φ_1'', Φ_2 and Φ_3 in the figure represent the operations performed by the components to convert rainfall (R) into abstractions (R_L); baseflow (q_b) and surface runoff (q). The surface runoff is added to baseflow to get runoff, $Q(t)$. The following equations can be readily written for the model shown in Figure 1.

$$R_L = R_{L_1} + R_{L_2} \quad ...(1)$$

$$= \Phi_1' R + \Phi_1'' R \quad ...(2)$$

$$i = R - R_L \quad ...(3)$$

$$= R - \Phi_1' R - \Phi_1'' R \quad ...(4)$$

$$Q(t) = \Phi_3 [R - \Phi_1' R \quad \Phi_1'' R] + \Phi_2 [\Phi_1' R] \quad ...(5)$$

In the above equations, R_{L_1} is the rate of infiltration abstraction, R_{L_2} is the rate of evaporation abstraction, Φ_1' is the operator that converts rainfall into infiltration abstraction and Φ_1'' is the operator that converts rainfall into evaporation abstraction. The depression storage ultimately is depleted partly by infiltration and partly by evaporation. The intercepted water ultimately evaporates and gets depleted from the intercepting surfaces. For all practical purposes, it would be adequate if losses due to infiltration and evaporation are considered. Among the abstractions again, infiltration constitutes the major component during the period of precipitation. The evaporation during the period of precipitation can be treated as negligible. Hence, the estimation of total abstractions during precipitation, by and large, amounts to the determination of infiltration abstraction. Now Equation (5) can be written in the following form :

$$Q(t) = \Phi_3 [R - \Phi_1' R] + \Phi_2 [\Phi_1' R] \quad ...(6)$$

where, $\Phi_1' R$ represents the infiltration rate, which as per the assumption above, includes all other abstractions. In Equation (6), the first term $\Phi_3 [R - \Phi_1' R]$ indicates the surface runoff and the second term $\Phi_2 [\Phi_1' R]$ indicates the baseflow. Thus, the runoff is assumed to consist of two components, namely, surface runoff and baseflow :

$$Q(t) = q(t) + q_b(t) \quad ...(7)$$

where, $q(t)$ is the surface runoff and $q_b(t)$ is the baseflow at any time t.

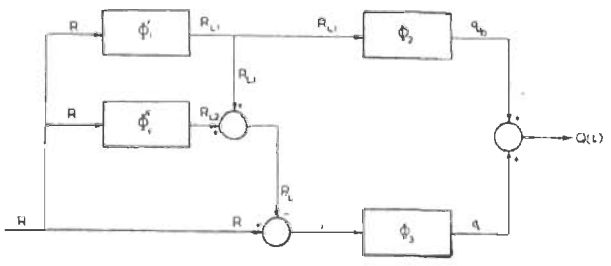

FIGURE 1 : Block diagram representation of a basin system.

A Method for the Determination of Abstraction Rate Curve

The abstractions are estimated using a new method, in which both rainfall characteristics and basin characteristics are quantified[2][9][10] and studied in detail and based on this investigation, total abstractions F_v is expressed as follows (Figure 2) :

$$F_v = R_v f(\theta) \quad ...(8)$$

where, $$\theta = \frac{I_{ap} \cdot T_g}{R_v} \quad ...(9)$$

in which T_g is the time to the centre of area of rainfall diagram, i.e., hyetograph (Figure 2), R_v is the volume of rainfall and I_{ap} is the antecedent precipitation index, given by :

$$I_{ap} = \sum_{n=1}^{30} \frac{P_n}{n} \quad ...(10)$$

where, P_n is the rainfall during 24-hour period, recorded on the n^{th} day preceding the storm for which runoff is being calculated. The plots of F_v/R_v versus θ are made for 6 basins (Basin Nos. 9, 10, 11, 13, 14 & 15 in Table 1) using 126 major and minor storms. One of them for Deep River Watershed-W1 is presented in Figure 3. From the given data, the value of θ is computed using Equations (9) & (10). The dimensionless

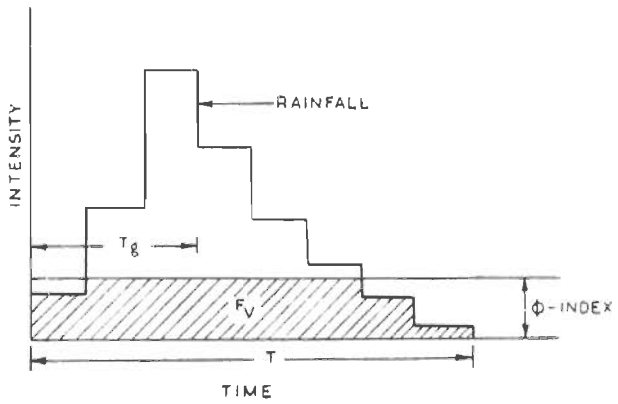

FIGURE 2 : Schematic representation of ϕ-index.

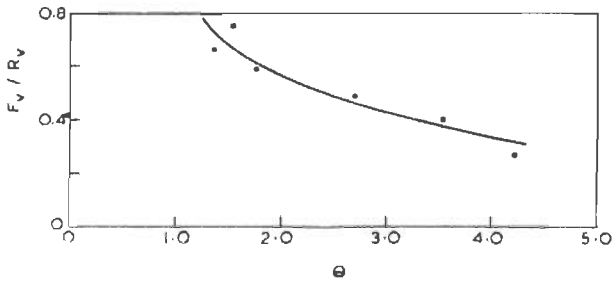

FIGURE 3 : Deep River Watershed-W1; graph of F_v/R_v versus θ.

value of F_v/R_v is read against the value of θ from the plot of F_v/R_v versus θ. As R_v is known, F_v can be computed. The value of average abstraction rate, i.e., ϕ-index is computed by a trial procedure[2][10], and it is indicated in Figure 4 for the storm of February 1939 in Deep River Watershed-W1.

To obtain the abstraction rate curve (f-curve) during a storm over a basin, the method has been applied to : (*i*) a 5-coefficient storage equation [Equation (12)] and a 5-coefficient surface runoff model [Equation (14)], and (*ii*) a 3-coefficient storage equation [Equation (13)] and a 3-coefficient surface runoff model [Equation (15)]. For 96 storms in 9 basins (Basin Nos. 4, 8, 9, 10, 11, 14, 15, 16 & 19 in Table I), the abstraction rate curves are drawn. The details of the methods are discussed in Ref. (2), (8) & (10). The plots of f-curve made, using (*i*) and (*ii*) for the storm of 26 February 1939 in Deep River Watershed-W1 are presented in Figures 4 & 5 respectively. Subtracting abstraction rate from the rainfall gives the volume of rainfall excess.

Conversion of Rainfall Excess to Surface Runoff

Starting with the general functional relationship between storage, S, inflow, $i(t)$, and outflow, $q(t)$, Kulandaiswamy [4][5][7] proposed a general storage equation as follows :

$$S = \sum_{n=0}^{N} a_n \frac{dq^n}{dt^n} + \sum_{m=0}^{M} b_m \frac{d^m}{dt^m} \qquad \ldots(11)$$

where, a_n' S and b_m' S are coefficients depending upon q and/or i, m and n are variables and M and N are numbers of terms in summation operations. Differential equations were formed and solutions for unit impulse input and unit step input were obtained for the following simplified cases of general storage equation by Kulandaiswamy. It was also recommended that the storage equations be preferred in the order in which they are given below [7] :

(1) $S = a_0 q + a_1 \frac{dq}{dt} + a_2 \frac{d^2q}{dt^2} + b_0 i + b_1 \frac{di}{dt}$

(2) $S = a_0 q + a_1 \frac{dq}{dt} + b_0 i + b_1 \frac{di}{dt}$

(3) $S = a_0 q + a_1 \frac{dq}{dt} + a_2 \frac{d^2q}{dt^2} + b_0 i$

(4) $S = a_0 q + a_1 \frac{dq}{dt} + a_2 \frac{d^2q}{dt^2}$

(5) $S = a_0 q + a_1 \frac{dq}{dt} + b_0 i$

(6) $S = a_0 q + a_1 \frac{dq}{dt}$

In the present investigation, the following two cases are considered for a detailed study of the variation of 'a' and 'b' coefficients with storm characteristics :

CASE 1 : $S = a_0 q + a_1 \frac{dq}{dt} + a_2 \frac{d^2q}{dt^2} + b_0 i + b_1 \frac{di}{dt}$ ...(12)

CASE 2 : $S = a_0 q + a_1 \frac{dq}{dt} + b_0 i$ ...(13)

These two equations when substituted in the equation of continuity, viz., $i - q = \frac{ds}{dt}$ will result in the following equations :

CASE 1 : $q(t) = \frac{1 - b_0 D - b_1 D^2}{a_2 D^3 + a_1 D^2 + a_0 D + 1} i(t)$ ...(14)

CASE 2 : $q(t) = \frac{1 - b_0 D}{a_1 D^2 + a_0 D + 1} i(t)$ ...(15)

where, D is the differential operator $\frac{d}{dt}$.

From a detailed investigation [2] [10] of the coefficients a_0, a_1, a_2, b_0 and b_1 in the above models made with storm characteristics using 17 basins with 205 major and minor

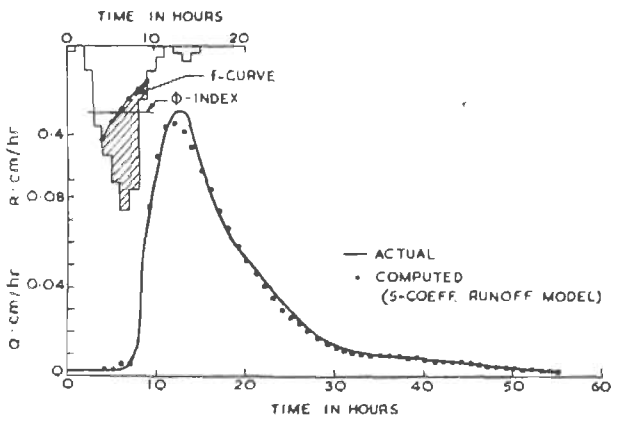

FIGURE 4 : Deep River Watershed-W1; storm of 26 February 1939.

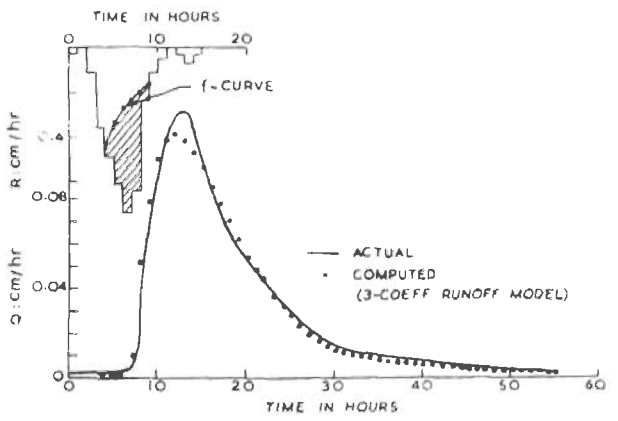

FIGURE 5 : Deep River Watershed-W1 ; storm of 26 February 1939.

storms (Basin Nos. 1 to 12, 14 to 16, 17 & 18 in Table I), the coefficients are expressed as a function of a parameter, η

$$\eta = R_{ev} \frac{t_r}{t_e} \qquad ...(16)$$

while, R_{ev} in Equation (16) represents the volume of rainfall excess, t_r/t_e represents the pattern of rainfall excess, t_r is the time to the centre of area of the rainfall excess from the beginning of rainfall excess and t_e is the duration of rainfall excess. Plots of the coefficients a_0, a_1, a_2, b_0 and b_1 in Equations (12) & (14) and a_0, a_1 and b_0 in Equations (13) & (15) against the parameter η are made for the above 17 basins and they are discussed in Ref. (2) & (10) in detail. These plots for Deep River Watershed-W1 are given in Figure 6. The solutions of Equations (14) & (15) (5-coefficient surface runoff model and 3-coefficient surface runoff model) are obtained as follows (7) :

5-Coefficient Surface Runoff Model

The characteristic polynomial in Equation (14) is of third degree and has three roots. Assuming that the system is stable, the following four cases are possible, depending on the nature of the roots.

Let the roots be m, n and p.

CASE 1 : All the roots are real and unequal

$$m \neq n \neq p$$

The *IUH* for this case is given by

$$U(t) = -mnp\,[Ae^{mt} + Be^{nt} + Ce^{pt}] \qquad ...(17a)$$

where,
$$A = \frac{-b_1 m^2 - b_0 m + 1}{m^2 - m(n+p) + np} \qquad ...(17b)$$

$$B = \frac{-b_1 n^2 - b_0 n + 1}{n^2 - n(m+p) + mp} \qquad ...(17c)$$

and
$$C = \frac{-b_1 p^2 - b_0 p + 1}{p^2 - p\,(m+n) + mn} \qquad ...(17d)$$

CASE 2 : All the roots are real and two of them are equal.

Let $n = p$

The *IUH* for this case is

$$U(t) = mn^2\,[Ae^{mt} + Be^{nt} + Cte^{nt}] \qquad ...(18a)$$

where,
$$C = \frac{-b_1 n^2 - b_0 n + 1}{n - m} \qquad ...(18b)$$

$$B = \frac{b_0 n + C\,(n - 2m) - 2}{n^2 - mn} \qquad ...(18c)$$

$$A = -b_1 - B \qquad ...(18d)$$

CASE 3 : All the roots are real and equal

$$m = n = p$$

For this case *IUH* can be stated as

$$U(t) = (A + Bt + Ct^2)\, e^{mt} \qquad ...(19a)$$

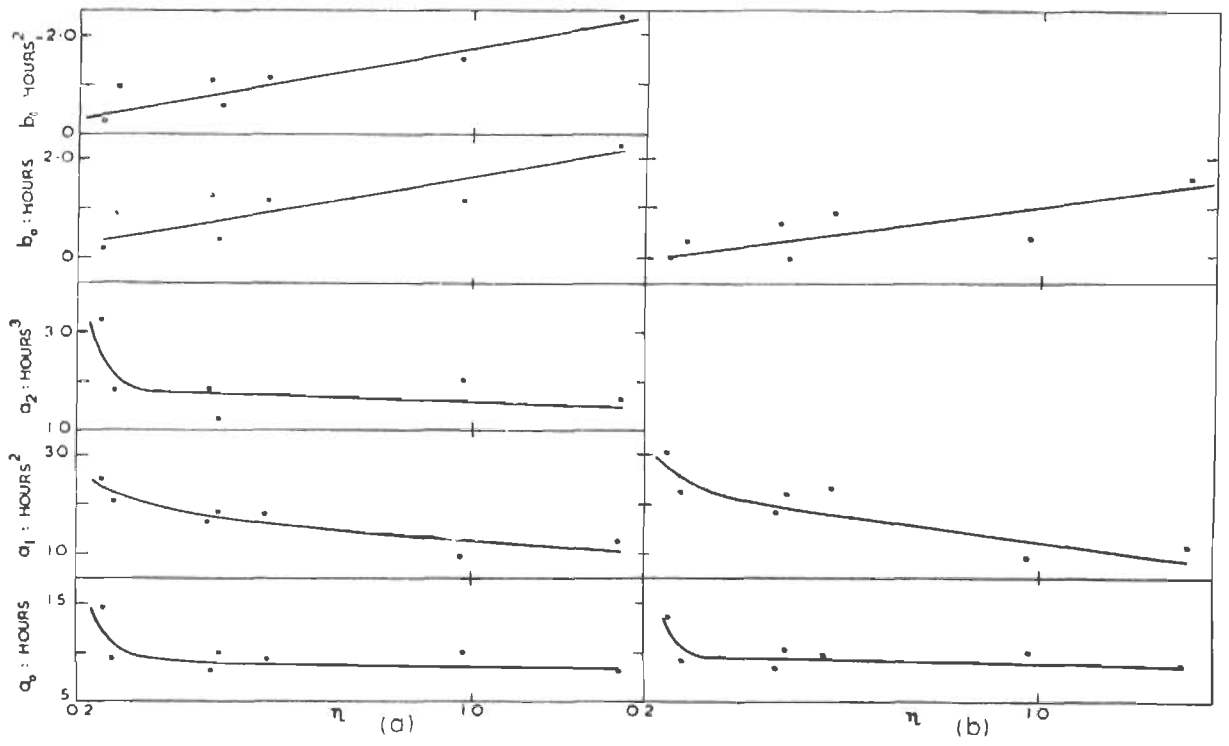

FIGURE 6 : Deep River Watershed-W1 : (a) graph of a_0, a_1, a_2, b_0, b_1 versus η ; (b) graph of a_0, a_1, b_0 versus η.

where, $A = -b_1 m^3$ ...(19*b*)

$B = -b_0 m^3 - 2b_1 m^4$ ...(19*c*)

and $C = \frac{1}{2}(m^3 - b_0 m^4 - b_1 m^5)$ ...(19*d*)

CASE 4 : One root is real and two roots are complex conjugates

Let $n = r + jw$ and $p = r - jw$

where, $j = \sqrt{-1}$

The *IUH* in this case is given by

$$U(t) = -m(r^2+w^2)\left[Ae^{mt} + e^{rt}\left(B \operatorname{Cos} wt + \frac{C+Br}{w} \operatorname{Sin} wt\right)\right] \quad ...(20a)$$

where, $A = \dfrac{-b_1 m^2 - b_0 m + 1}{m^2 - 2rm + (r^2+w^2)}$ ...(20*b*)

$B = -b_1 - A$ ...(20*c*)

and $C = -b_0 - b_1 m + A(2r - m)$ ...(20*d*)

The computation of surface runoff, $q(t)$, using instantaneous unit hydrograph obtained in the foregoing can be stated in the form of convolution integral :

$$q(t) = \int_0^{t' \leq t_e} U(t-\tau)\, i(\tau)\, d\tau \quad ...(21)$$

In the above equation, τ is the time variable and $t' = t$ when $t \leqslant t_e$ and $t' = t_e$ for $t > t_e$.

3-Coefficient Surface Runoff Model

The characteristics polynomial in Equation (15) is of the second degree and it has two roots. Depending upon the nature of the roots, different expressions for *IUH* are obtained. Let the roots be m and n.

CASE 1 : Both the roots are real and unequal

$m \neq n$

The *IUH* for this case is given by

$$U(t) = \frac{1}{a_1}\left[Ae^{mt} - Be^{nt}\right] \quad ...(22a)$$

where, $A = \dfrac{-b_0 m + 1}{m - n}$ ...(22*b*)

$B = \dfrac{-b_0 m + 1}{m - n}$ ...(22*c*)

CASE 2 : The roots are equal

$m = n$

In this case the *IUH* can be stated as

$$U(t) = \frac{1}{a_1}\left[-b_0 e^{mt} + (1 - b_0)\, te^{mt}\right] \quad ...(23)$$

CASE 3 : The roots are complex conjugates

Let $m = r + jw$ and $n = r - jw$

where, $j = \sqrt{-1}$

The *IUH* for this case is

$$U(t) = \frac{e^{rt}}{a_1}\left[-b_0 \operatorname{Cos} wt + \frac{1 - b_0 r}{w} \operatorname{Sin} wt\right] \quad ...(24)$$

Using the instantaneous unit hydrograph obtained above and convolution integral, i.e., Equation (21), the surface runoff, $q(t)$ is obtained.

Baseflow

From a study of the review of work done on baseflow[2][10], it is found that a satisfactory method has not yet been determined for baseflow separation. In the light of the present state of knowledge of baseflow hydrograph during the period of surface runoff, one has to depend on a study of the baseflow characteristics, obtained from dry weather flow, when the stream consists of baseflow only. An exponential function of the form given in the following equation fitted for the depletion curves of baseflow, yields satisfactory results:

$$q_b = q_i\, e^{-kt} \quad ...(25)$$

where, q_b is the baseflow at time t ; q_i is the initial baseflow, k is the recession constant and e is the Napierian logarithmic base. The value of k determined for some of the basins studied are given in Table 1. The following simple model based on Equation (25) is used in the present study for the baseflow hydrograph during the existence of surface runoff and thereafter :

$$\begin{aligned} q_b &= q_i\, e^{-kt} \quad 0 < t \leqslant t_p \\ &= q_{bp} \quad t_p < t \leqslant t_s \\ &= q_{op}\, e^{-kt} \quad t > t_s \end{aligned} \quad ...(26)$$

where, q_{bp} is the baseflow at time t_p, and t_s is the time where surface runoff ends.

3. Application to actual Basins

The aforementioned runoff models have been applied to 96 storms in 9 basins (Basin Nos. 4, 8, 9, 10, 11, 14, 15, 16 & 19 listed in Table 1). The successive steps involved are discussed below :

Runoff Model with 5-Coefficient System Function

(*a*) *Input Data Needed*

The following information about the basin must be available for predicting the runoff using the 5-coefficient runoff model for a given storm :

(*i*) A graph of F_r/R_r versus θ

(*ii*) Graphs connecting a_0, a_1, a_2, b_0 and b_1 with γ_i

(*iii*) Value of the constant k

(*iv*) Value of the delay time T, where, delay time is considered necessary ([7]).

These graphs can be plotted and the value of T can be determined by analysing the available rainfall excess and surface runoff data. The value of k can be

TABLE I
Details of Basins.

Sl. No.	Drainage basin	Area	No. of recording rain-gauges	No. of storms	Baseflow recession constant	Source of data
1	2	3	4	5	6	7
1.	Oxford, Mississippi Watershed-WC 2, North Mississippi Branch Experiment Station, Holly Springs, Mississippi	0·587 ha	1	11	—	U.S Deptt. of Agr., Washington D.C.
2.	Riesel (Waco) Watershed-Y4, Texas	32·34 ha	2	7	—	U.S. Deptt. of Agr., Washington D.C.
3.	Riesel (Waco) Watershed-W1, Texas	71·00 ha	4	10	—	U.S. Deptt of Agr., Washington D.C.
4.	Hastings, Nebraska Watershed-3	194·7 ha	6	11	—	U.S. Deptt. of Agr., Washington D.C.
5.	Safford, Arizona Watershed-WII	276·0 ha	2	8	—	U.S. Deptt. of Agr., Washington D.C.
6.	Riesel (Waco) Watershed-D, Texas	449·2 ha	4	8	—	U.S. Deptt. of Agr., Washington D.C.
7.	Hastings, Nebraska Watershed-8	844·2 ha	8	9	—	U.S. Deptt. of Agr., Washington D.C.
8.	Coshocton Watershed-97, Ohio	17·9 sq km	5	4	0·0554	U.S. Deptt. of Agr., Washington D.C.
9.	Beech River Basin near Lexington, Tenneessee	41·2 sq km	1	33	0·0014	Tenneessee Valley Authority, Knoxville, Tenneessee, U.S.A.
10.	North Creek Basin near Jacksboreo, Texas	56·2 sq km	2	13	0·0785	USGS through Colorado State University, U.S.A.
11.	West Fork, Deep River Watershed-W1. High Point, North Corolina	83·2 sq km	2	9	0·0204	U.S. Deptt. of Agr., Washington D.C.
12.	Farm Creek, Illinois River, East Peoria, Illinois	152·7 sq km	2	6	—	Deptt. of Public Works, Illinois
13.	Vero Beach Watershed-W1, Indian River Farms Drainage District Indian River Country, Florida	202·0 sq km	5	21	0·0119	U.S. Deptt. of Agr., Washington D.C.
14.	Chestuee Creek Basin, Dentiville	296·0 sq km	5	53	0·0015	Tenneessee Valley Auhority, Knoxville, Tenneessee, U.S.A.
15.	Mississippi Watershed-34, Oxford	304·0 sq km	29	7	0·0064	U.S. Deptt. of Agr., Washington D.C.
16.	Wills Creek Basin, Potamac River, Cumberland, Md.	543·0 sq km	4	5	0·0179	U.S. Army Corps of Engrs, Washington D.C.
17.	Ash Brook, United Kingdom	620·0 sq km	—	1	—	Proc. Int. Ass. Sci. Hydr. General Assembly of Toronto, No. 45, 1958, pp. 114-118
18.	N. Br. Potamac River, near Cumberland, Md.	2237·0 sq km	6	5	—	U.S. Army Corps of Engrs., Washington D.C.
19.	Little Red River, White River, Heber Springs, Ark	2852·5 sq km	4	6	—	U.S. Army Corps of Engrs., Washington D.C.

computed by studying the baseflow characteristics during the period of dry weather flow. Having obtained the above information, the runoff for any known storm real or hypothetical over the basin can be predicted as follows (Figure 4):

(b) Computation Procedure

STEP 1 : (*i*) For a given storm, the values of T_E and R_v are computed. Antecedent precipitation index, I_{ap} in Equation (10) is computed using the antecedent rainfall. From these values θ is computed using Equation (9). (*ii*) The value of F_v/R_v is read from the plot of F_v/R_v versus θ and F_v is computed as R_v is known. (*iii*) The value of average abstraction rate ϕ-index is computed by a trial procedure.

STEP 2 : Abstraction rate curve is drawn, using the method based on 5-coefficient storage equation as sub-routine for abstraction rate.

STEP 3 : Rainfall excess volume, R_{ev} is determined by subtracting abstractions from rainfall. The ratio, t_r/t_e is calculated from rainfall excess diagram and the parameter η is computed in Equation (16).

STEP 4 : The value of coefficients a_0, a_1, a_2, b_0 and b_1 are read from the graphs or tables of a_0 versus η, a_1 versus η, a_2 versus η, b_0 versus η and b_1 versus η.

STEP 5 : The three roots of the characteristic polynomial in Equation (14) are evaluated and the instantaneous unit hydrograph is obtained using the appropriate one, among the Equations (17) (18) (19) & (20).

STEP 6 : A delay time of T hours is used, if necessary in certain basins and surface runoff is computed using Equation (21).

STEP 7 : Baseflow is computed using Equation (26).

STEP 8 : The total runoff, $Q(t)$ is obtained by adding surface runoff to baseflow [Equation (7)].

Runoff Model with 3-Coefficient System Function

The model proposed above, with the 5-coefficient system function will involve tedious computations. These computations can be done with ease if a digital computer is available. Where calculations are to be made with the help of a desk calculator or slide rule, a simpler model will be more convenient. Investigations have shown that a simpler runoff model with a 3-coefficient system function is quite satisfactory. The procedure for the use of this simpler form of the model is explained as follows :

(a) Input Data Needed

The information needed is essentially the same as in the case of 5-coefficient runoff model, except that the graphs are needed only for three coefficients, namely, a_0, a_1 and b_0 which are to be computed separately, though the procedure is same as in the case of determination of five coefficients.

(b) Computation Procedure

The procedure is the same as that for 5-coefficient model (Figure 5) except that the 3-coefficient storage equation is to be used for determining abstraction rate curve and the corresponding characteristic polynomials are to be used [Equations (15) (22) (23) & (24)].

4. Results

For this investigation of the 5-coefficient and 3-coefficient runoff models for rainfall-runoff relationship, 96 storms in 9 basins (Basin Nos. 4, 8, 9, 10, 11, 14, 15, 16 & 19 in Table 1) are used. The results obtained for these storms for total runoff, $Q(t)$ for given rainfall and antecedent conditions are as follows :

5-Coefficient Model

It is seen that the error in the computed value of peak flow of runoff, Q_p using 5-coefficient runoff model, is less than 10 percent for 93 percent of the storms, 10 to 15 percent for 2 percent of the storms, 15 percent and above for the remaining 5 percent of the storms.

It is seen that the error in the computed value of time of peak flow, t_p is less than 10 percent for 81 percent of the storms, 10 to 15 percent for 12 percent of the storms, 15 percent and above for the remaining 7 percent of the storms.

For all the storms studied using 5-coefficient runoff model, the correlation coefficient varies between 0.9309 and 0.9998.

3-Coefficient Model

It is seen that the error in the computed value of Q_p using 3-coefficient runoff model, is less than 10 percent for 84 percent of the storms, 10 to 15 percent for 11 percent of the storms, 15 percent and above for the remaining 5 percent of the storms.

It is seen that the error in the computed value of t_p is less than 10 percent for 67 percent of the storms, 10 to 15 percent for 19 percent of the storms and 15 percent and above for the remaining 14 percent of the storms.

For all the storms studied using 3-coefficient runoff model, the correlation coefficient varies between 0.9123 and 0.9995.

In the models described above, the advantage of linear system is availed of, though non-linearity is taken into account indirectly by a variation of the coefficients with storm characteristics. Another advantage is that a trial procedure used in the earlier method ([5])([7]) is eliminated in the present method in obtaining the coefficients.

5. Conclusions and Recommendations

From the foregoing investigation of runoff models

the following conclusions and recommendations are made :

The runoff predictions made by using 5-coefficient runoff model and 3-coefficient runoff model are satisfactory. But the runoff predictions made by using 5-coefficient runoff model are more satisfactory when compared with the results obtained by using the 3-coefficient runoff model.

As the best results are obtained using the 5-coefficient runoff model, this model is recommended for practical use where a computer facility is available. The 3-coefficient runoff model is simple and hand computations can be made quickly. The results obtained by using this model are also very good. Therefore, the 3-coefficient runoff model is recommended where a computer is not available, and the computations have to be made using a desk calculator or slide rule.

6. Acknowledgements

This paper is essentially an abridgement of a thesis submitted to the University of Madras, by Dr. T. Babu Rao in partial fulfilment of the requirements for the degree of Doctor of Philosophy. The work upon which this paper is based was done during 1970-73 in the Hydraulics and Water Resources Department, College of Engineering, Madras-25, under a grant from University Grants Commission, New Delhi. The financial assistance received from U. G. C. for this project is gratefully acknowledged. Thanks are also due to the authorities of the Computer Centre, College of Engineering, Madras-25, for the facilities made available for the use of I. B. M. 1620 Model II Electronic Digital Computer System.

7. References

(1) AMOROCHO, J. and HART, W. E. : "Critique of Current Methods in Hydrologic Systems Investigation". Wat. Res. Res., Vol. 45, No. 2, June 1964, pp. 307-321.

(2) BABU RAO, T. : "A Mathematical Model for Basin Runoff". Ph. D. Thesis, University of Madras, India, 1973.

(3) BLANK, D. and DELLEUR, J. W. : "A Programme for Estimating Runoff from Indiana Watersheds, Part I—Linear System Analysis in Surface Hydrology and its Application to Indiana Watersheds". Tech. Rep. No. 4, Water Resources Research Centre, Purdue University, Lafayette, Indiana, August 1968.

(4) CHOW, V.T. : "Runoff". Hand Book of Applied Hydrology, Section 14, McGraw-Hill Book Co., New York, 1964.

(5) CHOW, V. T. and KULANDAISWAMY, V. C. : "A General Hydrologic System Model". Jour. of the Hyd. Div., Proc. Am. Soc. Civ. Engrs., Vol. 97, No. HY6, June 1971, pp. 791-804.

(6) CLARK, C. O. : "Storage and the Unit Hydrograph". Trans. Am. Soc. Civ. Engrs., Vol. 110, 1945, pp. 1419-1446.

(7) KULANDAISWAMY, V. C. : "A Basic Study of the Rainfall Excess—Surface Runoff Relationship in a Basin System". Ph. D. Thesis, University of Illinois, Urbana, Illinois, 1964.

(8) KULANDAISWAMY, V.C. and BABU RAO, T. : "An Analytical Approach to the Determination of Infiltration Rate". Jour. of Inst. of Civ. Engrs. (London), October 1969, pp. 137-145.

(9) KULANDAISWAMY, V.C. and BABU RAO, T. : "A Method for the Prediction of ϕ-Index". Irrigation and Power Jour., April 1971, pp. 135-140.

(10) KULANDAISWAMY, V.C. and BABU RAO, T. : "A Mathematical Model for Basin Runoff". Report 10, U. G. C. Project, Hydraulics and Water Resources Department, College of Engineering, Madras 600025, 1974.

Transformation of the Processes in the Linear Hydrological Systems

WITOLD G. STRUPCZEWSKI
Asstt. Professor

RENATA J. KICZKO
Asstt. Research Fellow

ZBIGNIEW W. KUNDZEWICZ
Asstt. Research Fellow

JAROSLAW J. NAPIORKOWSKI
Asstt. Research Fellow

Institute of Geophysics, Polish Academy of Science, Warsaw, Poland

HENRYK T. MITOSEK, JR.
Senior Lecturer

Institute of Environment Engineering, Technical University of Warsaw, Warsaw, Poland.

SYNOPSIS

Aim of the Paper

Mathematical models describing water systems are formed in empirical way. Because of a big choice of the models it seems that some theoretical works concerning the transformation of random processes in hydrologic systems may be useful.

Scope of the Paper

Transformation of the stochastic processes (White noise, Markov noise) in linear systems (serial and parallel two-river systems with common input) will be considered. Successively Nash, Muskingum, Diskin models will be taken as system models. Auto and crosscorrelation functions and power spectrum for the runoff process will be determined theoretically. The stochastic nature of storage is also analyzed. The results will be illustrated with plots. We shall also deal with time averaged processes. The above discussion may be extended onto the other linear and non-linear systems.

1. Introduction

The development of researches on satisfactory (optimal if possible) exploitation of water resources has created the need of extension of mathematical analysis of hydrologic data. In the last decade the field of researches moved from the applications of theory of random variables into the theory of random functions. The knowledge of the space-time stochastic structure of the hydrologic processes is necessary for modelling of water-economical systems. The problem of adequate choice of hypotheses and computing errors becomes more significant comparing to the problems existing in the case of the choice of the type of distribution and estimation of its parameters. Statistics is not a magic tool that enables obtaining satisfactory results from uncertain data, small sample sizes and short time series. Due to this fact the generalization and transfer of experience worked out on different watersheds relating to the structure of the outflow process, types of the distribution or possibility of utilizing the longer time series for the extrapolation and estimation of shorter series parameters are important. These attempts, however, are based on some new hypotheses that can be rejected basing on short random samples. The problem of proof of assumed hypotheses basing on our ideas of physical properties of investigated hydrologic systems is said to exist.

When modelling the hydrologic systems, the first common assumption is linearity. This assumption becomes sufficiently valid for the most of engineering and research works. Although the non-linear system modelling is already extensively developed it seems that due to the need of simplicity linear systems must be used in the stochastic hydrology applications. The choice of combination of inputs and outputs in hydrologic systems is very big and it results from some physical reasons. We shall draw our attention to the investigation of the structure of the river outflow process and of the water resources under the assumption of conceptual watershed models. We shall determine the relation between the structure and parameters of the outflow process. These results would be difficult to obtain experimentally because of the fact that these models approximate real hydrologic system and on the other hand hydrometeorological measurement instruments add some error to the actual signal that contributes to the noise produced by the system itself. The corrolaries resulting from the integration of conceptual models and the hydrologic processes can be helpful in acceptation of the hypotheses about the structure of the outflow process. When the watershed system operators are known, the results of transformation of the process may be applied to the prediction of the structure and parameters of the outflow process.

However, continuous processes are not commonly used for hydrologic applications. The time series are created from the average values for the same equal periods (an hour, a day). In the paragraph 6 we shall consider the relation between the averaging time and the structure of the process.

The prolongation of the observation series by utilizing the longer observation series from another station and the prediction of the volume levels based on water-level relations is of great practical importance. Both these actions are based on utilizing the correlative relation between the corresponding (in the sense of maximum correlation) observations in two space points. In both cases the procedure is the same as in the case of incomplete random sample two-dimensional normal variable. The similarity of inflow processes and watershed operators is the most important factor determining the power of this relation.

For the case of two river cross-section water levels these factors are transformating properties of the river sector and the ratio of an upstream inflow and lateral inflow. We shall analyze the accuracy of such relations basing on the conceptual linear models. To avoid repeating tedious algebraic calculations we do not present procedures leading to the final results. It was done in Ref. (5).

2. Some General Remarks

According to many papers [e. g., Kisiel (2), Yevjevich (3), Dooge (1),...] the action of hydrologic system can be represented by

$$Y(t) = H_d\,[X_d\,(t)] + H_s\,[X_s(t)] \qquad \ldots(2.1)$$

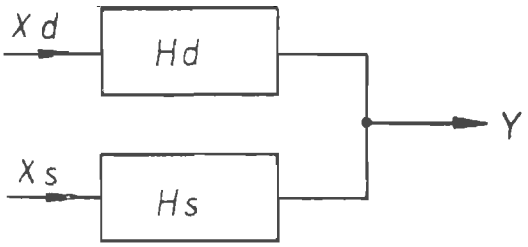

FIGURE 1.

where,

$X_d(t)$ = deterministic input signal

$X_s(t)$ = random noise input signal

H_d = linear model operator transforming the deterministic component of the input signal

H_s = linear model operator transforming the random component of the input signal

$Y(t)$ = output signal.

When analyzing the deterministic component of the input signal, it is most commonly represented by means of a sum of three components :

—linear or quasi-linear trend representing slowly varied tendency observed in the system due to the human activity influence on the physical conditions

—jump component representing short-lasting changes of the input process mean

—periodic component resulting from the periodicity of the precipitation, outflow, etc.

The first two components usually have relatively very small values what makes them very difficult to identify. Gathered empirical material does not allow to determine them quantitatively.

Let us assume the system to be linear, deterministic and time invariant. Then the responses of the model to each deterministic input component can be considered separately according to the principle of superposition. The operator transforms linear trend into output signal, tending asymptotically to a linear function. The nature of a periodic (harmonic) signal is not affected by the transformation by the linear operator (change of the signal amplitude and phase shift occurs).

The separation of the deterministic component of the input signal from the stochastic component enables the assumption of zero mean of the stochastic signal. That is the necessary condition for the weak stationarity. Moreover, we shall assume the stationarity of the dispersion and covariance of the process $X_s(t)$ throughout our paper. As a subject of the analysis we shall consider the structure of the random component transformed by some selected linear watershed models (Nash,

Diskin, Muskingum models). Throughout the paper the inflow to the system is assumed to be the input signal and the outflow is considered as the output signal.

The most general hydrologic model investigated by Kulandaiswamy, that covers all the models considered in this paper, has the form

$$\sum_{i=0}^{p} a_i (X, Y, t) \frac{d^i Y(t)}{dt^i} = \sum_{i=0}^{q} b_i (X, Y, t) \frac{d^i x(t-\tau)}{dt^i} \quad ...(2.2)$$

Assuming the coefficients a_i (X, Y, t) and b_i (X, Y, t) constant and selecting adequate p and q, we obtain linear models more suitable for analysis. In this paper we deal with the models being special cases of Kulandaiswamy's general model.

3. Transformation of Stochastic Processes in the Nash's Model

The model that we analyze in this paragraph is the Nash's conceptual model consisting of n equal linear reservoirs. Cascade of n linear reservoirs having different time constants (storage coefficients) will be called generalized Nash's model (Figure 2).

Its transfer function can be evaluated with the help of Laplace transformation techniques as

$$H(s) = \frac{1}{\bigcap_{i=1}^{N} K_i (S+1/K_i)} \quad K_i \neq K_j, \; i \neq j \quad ...(3.1)$$

where, s = complex variable.

After transformation to the time domain we obtain the kernel function (instantaneous unit hydrograph) :

$$h(t) = \sum_{i=1}^{N} \alpha_i e^{-t/K_i} \quad ...(3.2)$$

where,

$$\alpha_i = \frac{1}{\bigcap_{\substack{n=1 \\ n \neq i}}^{N} (1+K_n/K_i)} \quad ...(3.3)$$

For the Nash's model of $N+1$ linear reservoirs with the same storage coefficients $K = K = ... = K = K$ the kernel function is given by:

$$h(t) = \frac{1}{\Gamma(N) K^N} t^{N-1} e^{-t/K} \quad ...(3.4)$$

where, $\Gamma(N)$ denotes the gamma function.

Let us consider a single linear reservoir (Nash's model for $N = 1$). Its outflow is given by

$$y(t) = \int_{-\infty}^{+\infty} x(\alpha) h(t-\alpha) d\alpha \quad ...(3.5)$$

where,

$x(t), y(t)$ = stochastic processes

$h(t-\alpha)$ = kernel function, $h(t) = 1/K. \exp(-t/K)$ for $t \geqslant 0$

Let us apply White noise input to the model of a single linear reservoir. The autocovariance of the input process is given by

$$R_{xx}(\tau) = C . \delta(\tau) \quad ...(3.6)$$

$\delta(\tau)$ = Dirac delta function

Stochastic properties of the output are described by means of the following formulae

Crosscovariance

$$R_{yx}(\tau) = \int_{-\infty}^{\infty} R_x (\tau-\alpha). h(\alpha) d\alpha = \frac{C}{K} . e^{-\tau/K}, \; \tau \geqslant 0 \quad ...(3.7)$$

Autocovariance

$$R_{yy}(\tau) = \int_{-\infty}^{+\infty} R_{yx} (\tau+\alpha). h(\alpha) d\alpha = \frac{C}{2K} . e^{-\tau/K} \quad ...(3.8)$$

Obtained results enable us to say, that White noise passed through the single linear reservoir model is transformed into simple Markov noise(2).

In stochastic hydrology it is often convenient to assume that inflows form simple Markov processes. Let us apply now to the model of a single reservoir stationary and normal Markov noise of the autocovariance function given by

$$R_{xx}(\tau) = D^2_x e^{-c(\tau)} \quad ...(3.9)$$

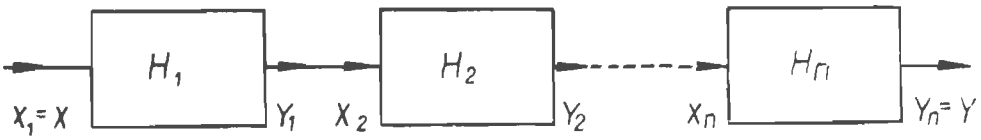

FIGURE 2.

Proceeding similarly as in the case of White noise input we have obtained the following formulae

Crosscovariance

$$R_{yx}(\tau) = \frac{D^2_x}{cK-1}\left(\frac{2cK}{cK+1}\, e^{-\tau/K} - e^{-c\tau}\right), \qquad \tau \geqslant 0 \qquad \ldots(3.10)$$

Autocovariance

$$R_{yy}(\tau) = \frac{D^2_x}{C^2K^2-1}\left(C.K.e^{-\tau/K} - e^{-c\tau}\right) \qquad \ldots(3.11)$$

It will be shown further that the above statement has the form similar to the output autocovariance function obtained for the generalized Nash's model consisting of two reservoirs when applying White noise input. Dividing Equation (3.11) by R_{yy} (0) we get autocorelation function

$$\rho_{yy}(\tau) = \frac{c.K\,(e^{-\tau/K} - e^{-c\tau})}{c.K-1} \qquad \ldots(3.12)$$

We shall consider now the Nash's model consisting of n similar reservoirs having the same storage coefficients K. The kernel function for this case is given by Equation (3.4).

For the White noise input we have obtained the following relations

Crosscovariance

$$R_{yx}(\tau) = \frac{C}{K^n\,\Gamma(n)}\, \tau^{n-1}\, e^{-\tau/K} \qquad \ldots(3.13)$$

Autocovariance

$$R_{yy}(\tau) = \frac{C}{K^n\,\Gamma(n)\,2^n}\, e^{-\tau/K} \sum_{j=0}^{n-1} \frac{\tau^{n-j-1}.K^j.(n+j-1)!}{(n-j-1)!\;\; j!.2^j} \qquad \ldots(3.14)$$

For $n=1$ the above formulae are consistent with these worked out for a single reservoir

For $n=2$

$$R_{yy}(\tau) = \frac{C}{4K^2}\, e^{-\tau/K}\,[\tau + K] \qquad \ldots(3.15)$$

and so on.

For the simple, stationary and normal Markov process on the input of the above model we have obtained the formulae

Crosscovariance

$$R_{yx}(\tau) = D^2_x \left\{ \frac{1}{(1-\alpha K)^n} n e^{-\alpha\tau} + e^{-\tau/K} \sum_{h=0}^{n-1} \left[\frac{1}{(1+\alpha K)^{n-h}} - \frac{1}{(1-\alpha K)^{n-h}} \right] \frac{\tau^h}{h!\,K^h} \right.$$

$$\text{dla } \tau \geqslant 0 \qquad \ldots(3.16)$$

Autocovariance

$$R_{yy}(\tau) = \frac{D^2_x}{\Gamma(n)} \left\{ \frac{\Gamma(n).e^{-\alpha\tau}}{(1-\alpha K)^n (1+\alpha K)^n} + \frac{1}{2^n}\, e^{-\tau/K} \sum_{h=0}^{n-1} \sum_{j=0}^{h} \frac{[(1-\alpha K)^{n-h} - (1+\alpha K)^{n-h}]\,(n+j-1)!\;\; K^{j-h}}{(1-\alpha K)^{n-h}\,(1+\alpha)^{n-h}\; j!\;(h-j)!\;\; 2^j}\, \tau^{h-j} \right\}$$

$$\ldots(3.17)$$

The autocovariance functions described by Equations (3.14—3.17) are plotted in Figures 3 & 4.

We shall analyze now the generalized Nash's model consisting of n linear reservoirs having different storage coefficients. Its kernel function is described by Equations (3.2-3.3).

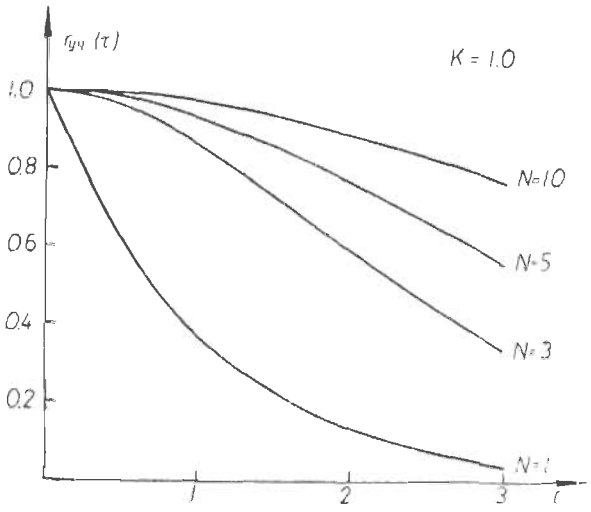

FIGURE 3 : Autocovariance function for Nash model with White noise on the input.

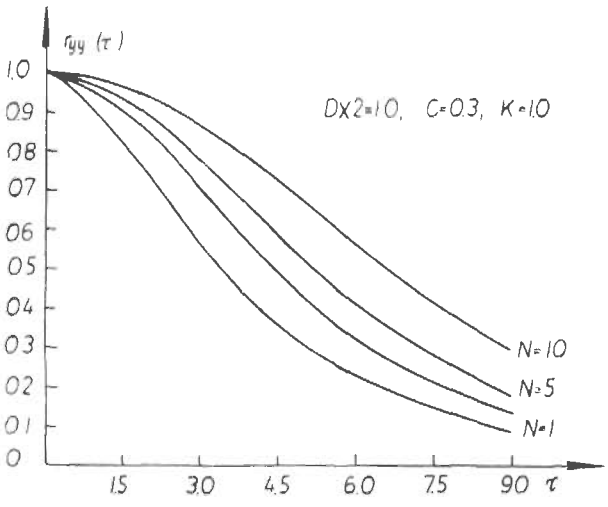

FIGURE 4 : Autocovariance function for Nash model with Markov process on the input.

When applying White noise to the input the following relations can be obtained

Crosscovariance

$$R_{yx}(\tau)=C.\sum_{i=1}^{n}\alpha\, i\, e^{-\tau/Ki} \qquad \tau\geqslant 0 \quad \ldots(3.18)$$

Autocovariance

$$R_{yy}(\tau)=C.\sum_{i=1}^{n} e^{-\tau/Ki}.\left(\alpha i^2.\frac{Ki^2}{2}+\sum_{j=1}^{N}\frac{-1}{1/Ki+1/K_j}\right) \quad \ldots(3.19)$$

Denoting

$$A_i=\left(\alpha_i\,\frac{2Ki}{2}+C.\sum_{j=1}^{N}\frac{-1}{1/Ki+1/K_j}\right) \quad \ldots(3.20)$$

we get

$$R_{yy}(\tau)=\sum_{i=1}^{n} e^{-\tau/Ki}.A_i \quad \ldots(3.21)$$

where, A_i depends on α_i and K_i, $i=1,\ldots,n$

The above equation can be considered as the autocovariance function for n-th order autoregressive process. It is easy to see that transformation of White noise in a Nash's model of n reservoirs is qualitatively equivalent to transformation of $(n-1)$th order autoregression scheme by a single storage reservoir. Both situations yield n-th order autoregression scheme of the output process. The above result means that the order of autoregression scheme of an input stochastic process increases by 1 after transformation in a single linear reservoir.

4. Crosscorrelation of the Processes on the Outputs of two Nash's Models

We shall consider two linear systems described by means of the kernel functions $h_1(t)$, $h_2(t)$ (see Figure 5).

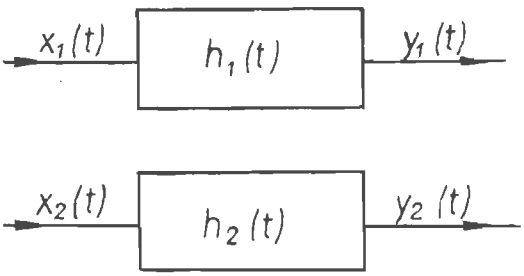

FIGURE 5.

Each of the subsystems consists of the Nash's model of linear reservoirs having the same storage coefficients. The crosscorrelation function on the input of the system is assumed to be known. The power spectrum of the input signal is given by

$$S_{x_1x_2}(\omega)=\int_{-\infty}^{+\infty}R_{x_1x_2}(\tau)e^{-j\omega\tau}\,d\tau=S_{x_2x_1}{}^{*}(\omega) \quad \ldots(4.1)$$

The crosscovariance function of the output processes from the both subsystems is most interesting from the practical point of view. This function can be obtained by integrating the cross power spectrum of the output signal

$$R_{y_1y_2}(\tau)=\frac{1}{2\pi}\int_{-\infty}^{+\infty}S_{y_1y_2}(\omega)\,e^{j\omega\tau}\,d\omega \quad \ldots(4.2)$$

If the frequency intervals where the transfer functions have non-zero values do not overlap, the value of output power spectrum $S_{y_1y_2}(\omega)=0$ for all frequencies, what means that for all $x_1(t)$, $x_2(t)$, are orthogonal. The output cross power spectrum is generally expressed in the form

$$S_{y_1y_2}(\omega)=S_{x_1x_2}(\omega)\,H_1(j\omega)H_2{}^{*}(j\omega) \quad \ldots(4.3)$$

Let us assume that $S_{x_1x_2}=A$ (White noise input) After integrating we have obtained

$$R_{y_1y_2}(\tau)=\frac{A\tau^{2n-1}}{KL^n(n-1)!}\,e^{-\tau/K}\sum_{p=0}^{n-1}\frac{(n+p-1)!}{p!(n-p-1)!\,Z^{n+p}} \quad \ldots(4.4)$$

For zero time-lag the above expression has the form :

$$R_{y_1y_2}(0)=A\,\frac{(2n-2)!}{[(n-1)!]^2}\,\frac{(KL)^{n-1}}{(K+L)^{2n-1}} \quad \ldots(4.5)$$

When assuming the linear dependence of the storage coefficients of both cascades the following autocorrelation function can be obtained

$$r_{y_1y_2}\left(\frac{\tau}{K}\right)=\frac{(n-1)!}{(2n-2)!}\,\frac{2^{2n-1}}{e^{\tau/K}}\sum_{p=0}^{n-1}\frac{(n+p-1)!}{p!(n-p-1)!}\cdot\frac{m^{p+1/2}}{(m+1)^{n+p}}\left(\frac{\tau}{K}\right)^{n-p}$$

for $\tau\geqslant 0$ $\quad \ldots(4.6)$

This function has its maximum value for zero time-lag

$$\max_{\tau/K} r_{y_1y_2}\left(\frac{\tau}{K}\right)=r_{y_1y_2}(0)=2^{2n-1}\left(\frac{\sqrt{m}}{1+m}\right)^{2n-1} \quad \ldots(4.7)$$

The specific case of the above relations, obtained for the common input $x_1=x_2$ is of vast interest for hydrologic applications. With the exception of high frequencies in the power spectrum, not transferred by the system, all the processes contributing to the inflow are strongly spatially correlated. Thus usually it can

be assumed that two adjacent watersheds have common input processes. Then the structure and parameters of the outflow process of one watershed can be determined basing on the inflow process and on the knowledge of both system operators. It is worth considering because the realizations of outflow process can be obtained in much easier way and more accurately than of an input stochastic process.

Let us assume common inflow process and consider two forms of these processes. When the inflow signal has the form of White noise, the crosscovariance function of the output signal is given by

$$R_{y_1y_2}(\tau)=\frac{A}{K^nL^m\Gamma(n)}\ e^{-\tau/K}\times$$

$$\sum_{j=0}^{n-1}\frac{(m+j-i)!}{(n-j-1)!\,j!}\,\tau^{n-j-1}\cdot\left(\frac{K+L}{KL}\right)^{-m-j} \qquad ...(4.8)$$

where, K, n and l, m represent the storage coefficient and the number of reservoirs respectively for both subsystems (see Figure 6).

The simple Markov noise applied to the common input yields the formula:

$$R_{y_1y_2}(\tau)=\frac{D^2_x\cdot e^{-C\tau}}{(1+CL)^m(1-CK)^n}-\frac{D^2_x\cdot e^{-\tau/K}}{(1+CL)^m(1-CK)^n}$$

$$\sum_{h=0}^{n-1}\frac{(1-CK)^h}{h!}\cdot\frac{\tau^h}{K^n}+\frac{D^2_x\cdot e^{-\tau/K}}{(1-CL)^m(1+CK)^n}\cdot$$

$$\sum_{h=0}^{n-1}\frac{(1+CK)^n}{h!}\cdot\frac{\tau^h}{K^n}+\frac{D^2_x\cdot e^{-\tau/K}}{\Gamma(n)\cdot K^n}\times$$

$$\sum_{h=0}^{n-1}\sum_{j=0}^{h}\sum_{i=0}^{n+j-1}\frac{[(1-CL)^{m-h}-(1+CL)^{m-h}]}{(1+CL)^{m-h}(1-CL)^{m-h}}\times$$

$$\frac{(n+j-1)!\ \tau^{h-j+i}\cdot(-1)^{h-i}}{L^h(h-j)!\,j!\,i!\left(\frac{K+L}{K.L}\right)^{n+j-i}} \qquad ...(4.9)$$

The above expression is illustrated in Figure 7.

The other model close to these previously analyzed is Diskin linear model (Figure 8).

The crosscorrelation of the output processes of both subsystems is given by

$$R_{y_1y_2}(\tau)=\int_{-\infty}^{+\infty}\int_{-\infty}^{+\infty}R_{x_1x_2}(\tau-\alpha+\beta)\,h_1(\alpha)h_2(\beta)\,d\alpha d\beta \qquad ...(4.10)$$

Let us apply to the input the normal, stationary Markov process. Then

$$R_{x_1x_2}(\tau)=E\{\alpha X(t)-\beta X(t-\tau)\}=\alpha\beta R_x(\tau)=\alpha\beta D^2_x e^{-C|\tau|} \qquad ...(4.11)$$

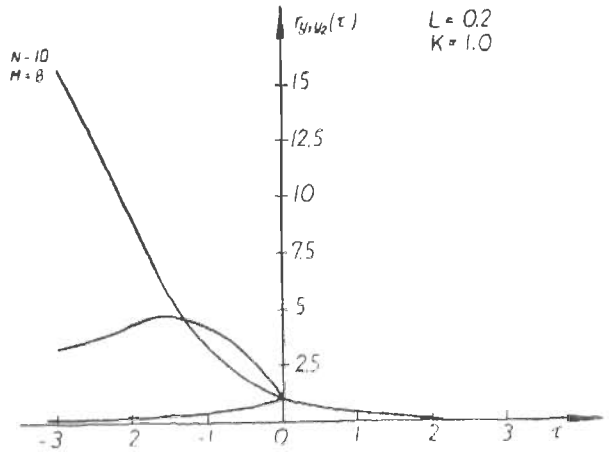

FIGURE 6.

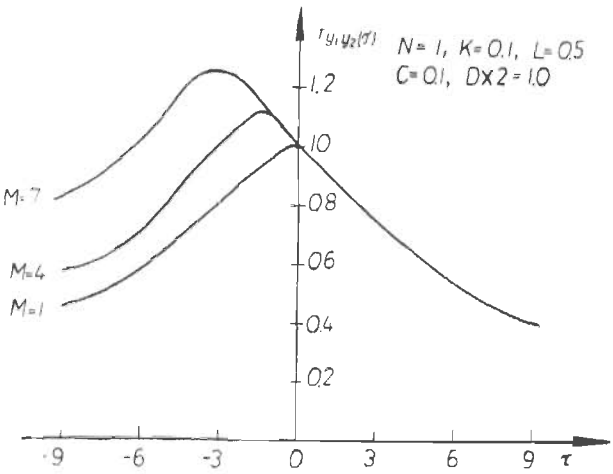

FIGURE 7.

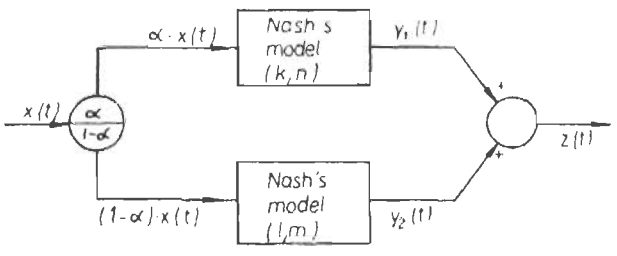

FIGURE 8.

The autocovariance function of the process on the combined output $[z(t)]$ is the most interesting from the practical point of view.

$$R_z(\tau)=E\{[Y_1(t)+Y_2(t)]\,[Y_1(t-\tau)+Y_2(t-\tau)]$$
$$=R_{y_1y_1}(\tau)+R_{y_1y_2}(\tau)+R_{y_2y_1}(\tau)+R_{y_2y_2}(\tau) \qquad ...(4.12)$$

where,

$$R_{x_1y_2}(\tau) = \int_{-\infty}^{+\infty} R_{x_1x_2}(\tau+\beta)\, h_2(\beta)\, d\beta \qquad \ldots(4.13)$$

$$R_{y_1y_2}(\tau) = \int_{-\infty}^{+\infty} R_{x_1y_2}(\tau-\alpha)\, h_1(\alpha)\, d\alpha$$

The above relations are illustrated in Figures 9 & 10.

5. Transformation of Stochastic Processes in Muskingum Model

Muskingum model is a special case of general conceptual hydrologic model (2.2), described by :

$$X(t) = y(t) + \frac{d\,W(t)}{dt} \qquad \ldots(5.1)$$

where,

$W(t) = Kx(t) + Ly(t)$ —storage

$x(t)$ —input to the system (inflow)

$y(t)$ —output (discharge)

Transfer function for that model, using Laplace transformation is expressed by

$$H(s) = \frac{1-Ks}{Ls+1} \qquad \ldots(5.2)$$

When returning to the time domain we get the expression for the kernel function of the model :

$$h(t) = \frac{L+K}{L^2}\, e^{-t/L} - \frac{K}{L}\,\delta(t) \qquad \ldots(5.3)$$

where, $\delta(t)$ denotes Dirac delta function.

With White noise on the input (Equation 3.6) we obtain the following autocovariance function

$$R_{yy}(\tau) = D^2_x \left[\frac{(L+K)^2}{2L^3}\, e^{-\tau/L} - \frac{(L+K)K}{L^3}\, 2ch\left(\frac{\tau}{L}\right) + \frac{K^2}{L^2}\,\delta(\tau) \right] \qquad \ldots(5.4)$$

For the simple Markov noise input crosscovariance function can be expressed as

$$R_{yx}(\tau) = \left\{ D^2_x \left\{ \frac{L+K}{L(\alpha L-1)} \left[\frac{2\alpha L}{\alpha L+1}\, e^{-\tau/L} - e^{-\alpha\tau} \right] - \frac{K}{L}\, e^{-\alpha\tau} \right\} \tau \geqslant 0 \qquad \ldots(5.5)$$

Autocovariance function of the output has the form

$$R_{yy}(\tau) = \frac{D^2_x}{\alpha^2 L^2 - 1} \left[\frac{\alpha(L^2-K^2)}{L}\, e^{-\tau/L} + (\alpha^2 K^2 - 1)\, e^{-\alpha\tau} \right] \qquad (5.6)$$

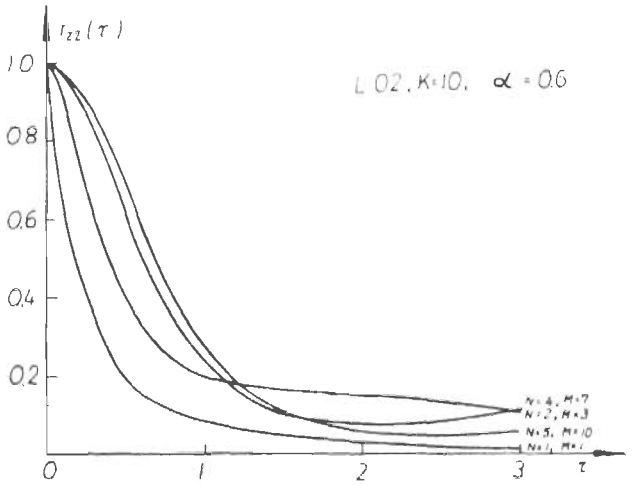

FIGURE 9 : Autocovariance function. White noise on the input.

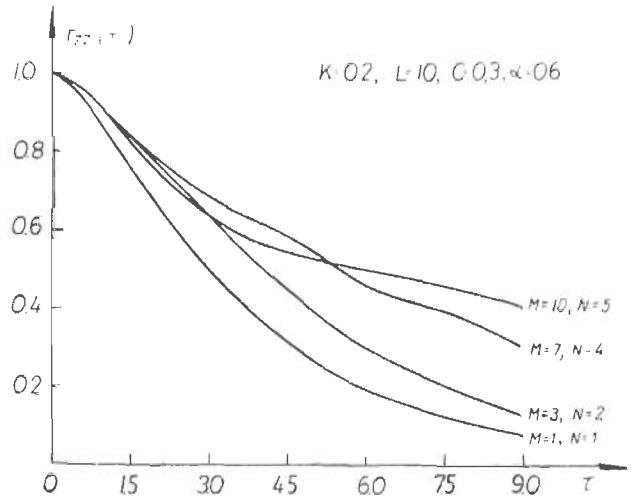

FIGURE 10 : Autocovariance function. Markov process on the input.

6. Process of Storage

In the preceding paragraphs we have considered outflow as the system output. Here we shall briefly analyze some relations for storage in linear reservoirs. It should be noted that by terms "outflow" and "storage" we mean the stochastic component of outflow or storage.

The storage equation for each included in the Nash model linear reservoir is given by

$$S_i = k_i\, y_i \qquad i = 1, 2, \ldots, n \qquad \ldots(6.1)$$

The total system storage for the Nash model having the same storage coefficients may be described as

$$S = \sum_{i=1}^{n} S_i = k \sum_{i=1}^{n} y_i \qquad \ldots(6.2)$$

Let $y : (t)$ be a stationary process in the wide sense, then $S(t)$ is also a stationary process in the wide sense with the autocovariance function

$$R_{ss}(\tau) = E[S(t+\tau)\, S(t)] = k^2 \sum_{i,\,j=1}^{n} R_{y_i y_j}(\tau) \quad \ldots(6.3)$$

and from the other side

$$S = \frac{d\,S(t)}{dt} = x(t) - y(t) \quad \ldots(6.4)$$

$$\dot{S}(t+\tau)\cdot\dot{S}(t) = x(t+\tau)\,x(t) - x(t+\tau)\,y(t) - y(t+\tau)\,x(t) + y(t+\tau)\,y(t) \quad \ldots(6.5)$$

It yields

$$R_{\dot{s}\dot{s}}(\tau) = R_{xx}(\tau) + R_{yy}(\tau) - R_{xy}(\tau) - R_{yx}(\tau) \quad \ldots(6.6)$$

Thus the autocovariance function can be calculated by double integrating of the above formula.

If the input process has the form of White noise, we obtain the following formula for the output process autocovariance function

$$R_{ss}(\tau) = \frac{A}{K^n\,\Gamma(n)}\, e^{-\tau/K} \sum_{p=0}^{n-1} a_p\, \tau^{n-p-1} \quad \ldots(6.7)$$

where,

$$a_p = \begin{cases} +[d_p + (n-p)\,a_{p-1}]\,k & p \neq 0 \\ +d_0\,K & p = 0 \end{cases} \quad \ldots(6.7a)$$

$$d_p = \begin{cases} -[C_p - (n-p)\,d_{p-1}]\,k & p \neq 0 \\ -C_0\,K & p = 0 \end{cases} \quad \ldots(6.7b)$$

For $n = 1$ the White noise input yields the storage in the form of simple Markov process. Hence for the case of a single linear reservoir retention is proportional to the outflow.

So its autoregression model has the same order as that of the outflow from the reservoir. Following the reasoning from the end of paragraph 3 it can be proved that the input stochastic process of n-th order of autoregression scheme gives the storage stochastic process of $(n+1)$ th order for a single linear reservoir.

7. Analysis of Time averaged Processes

Continuous time processes are rarely used in hydrologic system analysis. Discrete time sequences are usually formed by means of time averaging of continuous real processes.

In this part of the paper properties of the stochastic process transferred through the linear model of the part of a watershed (Nash model consisting of n linear reservoirs with the same time constants k) and time averaged will be analyzed.

The influence of averaging period length on the properties of the processes will be also described.

Let us consider two stationary stochastic processes $y_1(t)$ and $y_2(t)$ having zero means.

We shall form the following integrals :

$$S = \frac{1}{2T}\int_{-T}^{T} y_1(t)\, dt \quad \ldots(7.1)$$

and

$$V = \frac{1}{2T}\int_{-T}^{T} y_2(t)\, dt \quad \ldots(7.2)$$

Assuming their existence in Riemann sense for each process realization, s and v become random variables with the following properties [see Ref. (3)] :

$$E(s) = \frac{1}{2T}\int_{-T}^{T} E\{y_1(t)\}\, dt = 0 \quad \ldots(7.3)$$

$$R_{ss}(0) = \frac{1}{4T^2}\int_{-T}^{T}\int_{-T}^{T} R_{y_1}(t_1, t_2)\, dt_1\, dt_2 = \frac{1}{2T^2}\int_{0}^{2T} (2T-\tau)\, R_{y_1}(\tau)\, d\tau \quad \ldots(7.4)$$

$$R_{sv}(0) = \frac{1}{4T^2}\int_{-T}^{T}\int_{-T}^{T} R_{y_1 y_2}(t_1, t_2)\, dt_1\, dt_2 = \frac{1}{4T^2}\int_{-T}^{T} (2T - |\tau|)\, R_{y_1 y_2}(\tau)\, d\tau \quad \ldots(7.5)$$

In the hydrologic practice time sequences usually describe the runoff phenomena on different watersheds. The relations between them can be used to obtain missing data.

That gives autocovariance and crosscovariance functions expressed as follows :

$$R_{ss}(a) = \frac{1}{4T^2}\int_{(2a-1)T}^{(2a+1)T}\int_{-T}^{T} R_{yy}(t_1, t_2)\, dt_1\, dt_2 = \frac{1}{4T^2}\int_{-2T}^{2T} (2T - |\tau|)\, R_{yy}\, (2aT+\tau)\, d\tau \quad \ldots(7.6)$$

where, $a \in (0, \infty)$

$$R_{sv}(a) = \frac{1}{4T^2}\int_{-2T}^{2T} (2T - |\tau|)\, R_{y_1 y_2}\, (2aT+\tau)\, d\tau \quad \ldots(7.7)$$

We shall illustrate now the properties of stochastic process transferred through the linear model of the part of a watershed and time averaged.

Let us consider the input in the form of White noise, process being very simple for the analysis and of some importance for the hydrologic applications. The mean value of the time averaged output process equals zero, as it results from Equation (7.3).

The variance of the averaged output process can be evaluated from Equation (7.4), substituting Equation (3.14) as the autocovariance function of the continuous output process. After some rearranging we get :

$$E\{s^2\} = \frac{2A}{(n-1)!\,Kb^2}\sum_{p=0}^{n-1}\frac{(n+1-p)!}{p!\,2^{n+p}}\left\{(b-n+p)\left[1-e^{-b}\sum_{g=0}^{n-p-1}b^g\frac{1}{g!}\right]+e^{-b}\frac{b^{n-p}}{(n-p-1)!}\right\} \qquad \ldots(7.8)$$

where, $b = 2T/K$

Crosscorrelation function of the random synchronic sequences under the same averaging period is the most interesting from the practical point of view. Assuming, that both systems consist of Nash's model of the same number of reservoirs and applying common input in the form of White noise the crosscorrelation function for $\tau = 0$ is given by :

$$r_{sv}(b, c) = \frac{\frac{A}{2T}\left\{\left(\frac{b}{c}+1\right)^{-n}\sum_{p=0}^{n-1}\left(\frac{c}{b}+1\right)^{-p}\cdot f(b, n, p)+\left(\frac{c}{b}+1\right)^{-n}\sum_{p=0}^{n-1}\left(\frac{b}{c}+1\right)^{-p}\cdot f(c, n, p)\right\}}{\sqrt{\left[\frac{A}{T}\sum_{p=0}^{n-1}\frac{1}{2^{n+p}}\,f(b, n, p)\right]}\sqrt{\left[\frac{A}{T}\sum_{p=0}^{n-1}\frac{1}{2^{n+p}}\,f(c, n, p)\right]}} \qquad \ldots(7.9)$$

where,

$$f(x, n, p) = \frac{1}{\Gamma(n-1)!}\,\frac{(n+p-1)!}{p!}\left\{(x-n+p)\left[1-e^{-x}\sum_{g=0}^{n-p-1}\frac{x^g}{g!}\right]+\frac{x^{n-p}\,e^{-x}}{(n-p-1)!}\right\} \qquad \ldots(7.10)$$

and b, c have the same meaning as b in Equation (7.8), for the both systems. Results obtained for the case of one reservoir in each system are easy for the interpretation.

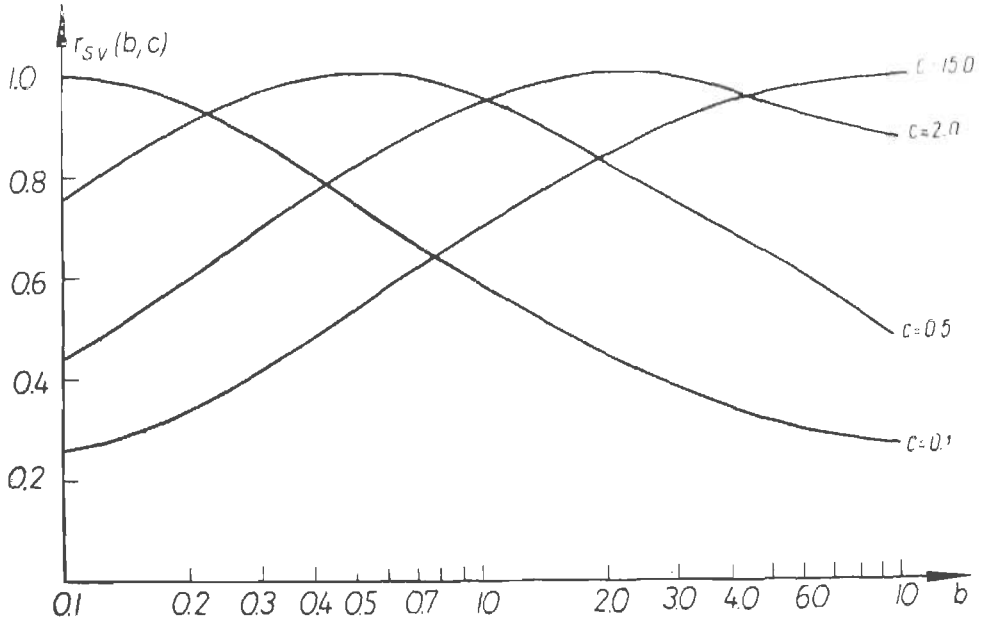

FIGURE 11.

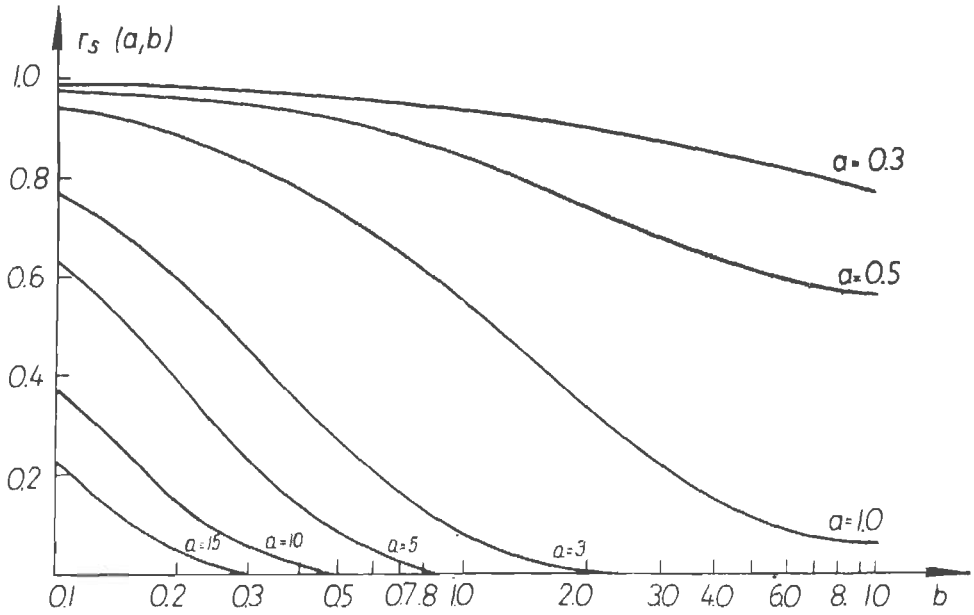

FIGURE 12.

The crosscorrelation function for $\tau = 0$ is given by :

$$r_{si}(0) = \frac{bc\sqrt{bc}\left(\frac{b+e^{-b}-1}{b^2}+\frac{c+e^{-c}+1}{c^2}\right)}{\sqrt{(b+e^{-b}-1)(c+e^{-c}-1)}} \quad ...(7.11)$$

This is illustrated in Figure 11.

The properties of the integral sequences (7.6-7.7) are illustrated by the autocorrelation function for one linear reservoir with White noise on the input :

$$r_s(a, b) = \begin{cases} \dfrac{b(1-a)-e^{-ab}+e^{-b}\,ch(ab)}{b+e^{-b}-1} & \text{for } 0 \leqslant a \leqslant 1 \\ \dfrac{ch\,b-1}{b+e^{-b}-1}\,e^{-ab} & \text{for } a \geqslant 1 \end{cases} \quad ...(7.12)$$

This leads to the conclusion that the time averaging of the processes on the output of the linear, supplied with White noise reservoir in equal unjoint intervals gives the Markov sequence for $a = 1, 2, 3, \ldots$. It is easy to notice from the formula Equation (7.12) for the case of $a \geqslant 1$. Figure 12 shows the relation between the autocorrelation function, index of the integral sequence a and the normalised period $b = 2T/K$.

8. Concluding Remarks

The usage of information concerning water resource stochastic properties in water-economic projects needs the developing of the methods enabling the utilization of longer informational sequences in short series. In hydrologic model systems there exists noise caused by the lack of the information concerning all input signals. Considering of random properties of watershed operator complicates the analytic determination of transformed stochastic process. Thus in this case and in the case of non-linear watershed model it is better to simulate the work of the system supplied with artificially generated process. In the paper there were found the relations between conceptual watershed models and stochastic models. The transfer of stochastic processes (White noise, Markov noise) through the conceptual models was examined in view of second order statistical moments. It was found that continuous processes when transferred through the linear reservoir cascade model preserve the autoregressive scheme character on the output. Each reservoir increases the order of the autoregressive scheme by one. There were also discussed some aspects of time averaging of output processes.

Human activity changes the watershed. The researches on the physical interpretation of watershed system parameters are being developed. It would enable the determination of changes in the watershed system operator caused by the men activity in the landscape. Although it is known that there is no need of many year observations to identify the stationary watershed system. It is supposed that the meteorological process, responsible for supplying the watershed (in the paper water supply was defined as the volume of water participation in mass transfer, here—the process responsible for the supplying that is precipitation, temperature, moisture) is not very sensitive on the human activity changes. Hence the random process transformation in the hydrologic systems will give the possibility of obtaining the runoff process characteristics under the new conditions.

9. References

(1) DOOGE, J.C.I. : "Mathematical Models of Hydrologic Systems." International Symposium on Modelling Techniques in Water Resources Systems, Proceedings, 1/1972/171-189. (Department of Environment, Ottawa).

(2) KISIEL, C.: "Time Series Analysis of Hydrologic Data." Advances in Hydroscience, Vol. 5-1969.

(3) PAPOULIS, A. : "Probability, Random Variables, and Stochastic Processes." McGraw-Hill, Inc. 1965.

(4) QUIMPO, R.G. : "Stochastic Hydrologic Systems." Final Report, Washington, D.C., Feb. 1973.

(5) STRUPCZEWSKI, S. W. ; MITOSEK, H. T., and NAPIÓRKOWSKI, J.J. : "Transformation of Processes in Linear Hydrologic Models." Unpublished Paper.

(6) VEN TE CHOW and KULANDAISWAMY, V.C. : "General Hydrologic System Model." J. Hydr. Div. Proc., ASCLE, June 1971.

(7) VEN TE CHOW : "Handbook of Applied Hydrology." McGraw-Hill, New York, 1964.

(8) YEVJEVICH, V. : "Stochastic Processes in Hydrology." Water Resources Publications, Colorado, 1972.

Decoupled Stochastic Models for Multisite Streamflows

S. RAMASESHAN
Associate Professor
Department of Civil Engineering
Indian Institute of Technology
Kanpur (India).

M. KRISHNASAMI
Reader in Civil Engineering
Annamalai University
Annamalainagar, Tamil Nadu (India).
(Presently Ph. D. Student, Indian Institute of Technology, Kanpur)

SYNOPSIS

In order to optimally design and operate multibasin and multireservoir systems, it is necessary to take into account the space-time correlation of inflows. Currently available models (1975) are based on small or long memory and they generally consider the variability in space and time simultaneously. It seems possible to decouple the variability of multisite streamflows into: (i) the within-the-station variation; (ii) the among-the-station variation; and (iii) the pure random variation at a given site. Decoupling makes it possible to use more complicated models and also the advances made in univariate modelling.

The following steps are suggested: (i) Normalisation of streamflows by logarithmic, square root or other appropriate transformation; (ii) Standardisation to have stationarity in the mean and variance; (iii) Fitting of a univariate model at each site to separate the persistence and serially independent random components; (iv) Fitting of a multivariate model for the random components at the several sites; and (v) By reversing the steps, a multivariate coupled model can be derived.

The procedure is illustrated with an example from India. The decoupled model indicates the variability of streamflows due to autoregression, cross-correlation and random components at each site. It can be used for flow forecasting, data generation and optimal design and control.

Introduction

The design and operation of a water resources system should be based on a clear understanding of the processes affecting them which in turn depends on proper analysis and interpretation of data. Particularly important are the streamflow data which exhibit complex stochastic characteristics. These include : (*i*) a non-stationary behaviour in terms of the seasonal variation of the mean, standard deviation, serial dependence, etc.; (*ii*) trends due to natural or human influences; (*iii*) periodic or cyclic components; (*iv*) autoregression or persistence within the time series ; (*v*) moving average component or external correlation between random components at the site; and (*vi*) correlation in space or among the time series. Generally factors (*i*) to (*v*) are studied in the univariate modelling of the time series of streamflow at a site and factor (*vi*) is studied in the multivariate modelling of several time series. Knowing the dependence or independence of streamflows in a multiple reservoir system, it is possible to design and operate the system by taking advantage of the dependence or independence. Multivariate modelling involves the representation in mathematical terms of the streamflow variability at each site and among the sites. Though the variables considered in this paper are streamflows,

the procedure developed can be used also for any set of related multivariate time series.

Multivariate Modelling in Hydrology

Multivariate time series models in hydrology belong generally to one of the following categories :

Small Lag Models

Fiering[1] proposed a principal component model for multiple time series. Torranin[2] suggested canonical correlation for application in multivariate hydrologic modelling. Matalas[3] proposed a general first order autoregressive multivariate model as follows :

$$\{x(j+1)\} = [A]\{x(j)\}+[B_0]\{\eta(j+1)\} \qquad ...(1)$$

where, $\{x(j)\}$ is a vector of n variables, say streamflows at n sites, at time j; $\{\eta(j)\}$ is a vector n independent variables at time j each with mean zero and unit variance; and $[A]$ and $[B_0]$ are $n \times n$ coefficient matrices. This model has been extensively used for modelling streamflows[3][4][5][6][7][8][9][13]. The components of $\{x(j)\}$ may also represent different processes at the same site at time j or different processes at different sites at time j. The Hydrologic Engineering Centre[10] uses a multivariate regression relationship which can be considered as a special case of Matalas model.

A higher order model has also been proposed as follows :

$$\{x(j+1)\} = [A_1]\{x(j)\}+\ldots\ldots$$
$$+[A_m]\{x(j+1-m)\}+[B_0]\{\eta(j+1)\} \qquad ...(2)$$

The model of Pentland and Cuthbert[12] is a modification of Beard's[11] model and it can be considered as a special case of Equation (2).

Long Lag Models

Hurst empirically analysed large number of natural data series and found that the n-year range R_n was proportional to the k-th power of the standard deviation of the variable where, $k \neq 0{\cdot}5$. Theoretically autoregressive models can be shown to have $k = 0{\cdot}5$. Since Hurst effect (i.e., $k \neq 0{\cdot}5$) was consistently shown by several natural processes, Mandelbrot and Wallis[14] proposed a so called "Fractional Gaussian Noise" model which has a long memory and long, though small, serial dependence. Matalas and Wallis[15] have proposed a multivariate fractional noise model. Mejia et al[16] have proposed a multivariate broken line model which also preserves the Hurst effect and which is an approximation of the fractional noise model.

Decoupling in Multivariate Models

A general (m, l) order autoregressive moving average multivariate model of the following form may be considered :

$$\{x(j+1)\} = [A_1]\{x(j)\}+\ldots\ldots+[A_m]\{x(j+1-m)\}$$
$$+[B_0]\{\eta(j+1)\}+\ldots\ldots+[B_l]\{\eta(j+1-l)\} \qquad ...(3)$$

where, $[B_1],\ldots\ldots,[B_l]$ are matrices of moving average coefficients and others have been defined earlier. Equation (3) can be considered as an extension of Equation (2). and of the univariate autoregressive moving average (ARMA) model for the multivariate case. With adequate data, it is mathematically possible to estimate the order (m, l) of the process and also determine the coefficients which are elements of $[A]$ and $[B]$ matrices. However, because of the large number of coefficients to be estimated, the results will be very much data dependent, unstable and furthermore they will be of questionable reliability.

Multivariate time series modelling is complicated by the fact that the variability of multisite streamflows may be attributed to :

(1) the within-the-station variation, say in terms of autoregressive, moving average and the serially independent random components at each site, and

(2) the among-the-station variations in terms of the cross-correlation between the streamflows at different sites and the internally and externally independent pure random components at each site. Univariate models in hydrology deal with the within-the-station variations and generally multivariate models consider both the above factors simultaneously. It seems possible to decouple the variability due to these two factors so that the within-the-station variability can be first estimated to determine the serially independent random component at each site and then use a multivariate model to explain the among-the-station variability and the interstation cross-correlation. This approach seems to be very advantageous because of the following factors : (*i*) The expertise developed in the past two decades in univariate time series modelling can be beneficially used. (*ii*) Since serially independent random normally distributed variates are used in the multivariate model, a better performance of the model can be expected than with serially correlated data. (*iii*) Since the parameters are estimated in stages, the number of parameters in each stage is comparable to that of univariate and multivariate models respectively and the problem of simultaneously estimating all parameters [as in the case of Equation (3)] is avoided. (*iv*) Where data lengths vary from station-to-station, all the available data can be used in the estimation of parameters and decoupling eliminates errors and bias that may be present in simultaneous estimation of parameters. (*v*) Decoupling of spatial and temporal variations has been suggested recently by Mejia and Iturbe[18] and Yevjevich and Karplus[19]. Rather than using simple spectral and correlation procedures to represent spatial variability, the use of multivariate models is suggested in this paper. (*vi*) The decoupled multivariate model is hence a very

powerful tool in representing complex multiple interrelated time series.

Proposed Methodology

The mathematical modelling of decoupled multisite streamflow sequences involve the following steps :

(*i*) Normalisation of streamflows at each station by logarithmic, square root or other transformations as appropriate.

(*ii*) Standardisation of streamflows at each site to have stationarity in the mean and standard deviation by suitable procedures [1][4][7][8].

(*iii*) Fitting a univariate model at each site to separate the persistence and serially independent random components. Suitable models include those of Beard [11], Arima[17], Thomas-Fiering[20], etc. It is proposed to consider only short lag models in this study. For example, let the ARMA model of order (p, q) be represented as follows :

$$\{x(j+1)\} = [R_1]\{x(j)\} + \ldots + [R_p]\{x(j+1-p)\} + [Q_0]\{\eta(j+1)\} + \ldots + [Q_q]\{\eta(j+1-q)\} \quad \ldots(4)$$

where, $\{\eta(j)\}$ is the vector of serially independent variates at time j ; and $[R_i]$ and (Q_i) are diagonal matrices of autoregressive and moving average coefficients. Further the univariate models may be stationary or, because of seasonal variations in serial correlation, non-stationary. After the univariate models are fitted, the serially independent random components at each site can be separated and tested for their randomness, distribution and parameters.

(*iv*) Let $\{\epsilon(j)\}$ be the vector of pure random components at time j which are free from serial and cross-correlation. Then $\{\eta(j)\}$ can be related to $\{\epsilon(j)\}$ by a (m, l) order multivariate ARMA model as given by Equation (3). In this study, the simpler Matalas model [Equation (2)] is used as follows :

$$\{\eta(j)\} = [C]\{\eta(j-1)\} + [D]\{\epsilon(j)\} \quad \ldots(5)$$

where, $[C]$ and $[D]$ are coefficient matrices. Depending on data, these may be stationary or, because of seasonal variations in cross-correlation structure, non-stationary.

(*v*) By reversing the steps, the coupled multivariate model can be derived.

Case Study

Data Used and Preliminary Analysis

Concurrent streamflow records for a duration of 25 years for 3 tributaries of a river in North India were used in this study. Non-concurrent records could have been used as in some earlier studies [5] [21]. Two sets of data, viz., the monthly series and the ten daily series were used. The data series were normalised by logarithmic transformation. They were then standardised to have zero mean and unit variance for all periods of the year by standard procedures [4]. The normalised standardised data series represent $\{x(j)\}$ and were used in subsequent steps.

Univariate Modelling

Box and Jenkins [17] have suggested procedures for fitting ARMA models to the univariate time series. The correlogram and partial correlation coefficients were calculated for each series. They are shown for monthly streamflow at station 1 respectively in Figures 1 & 2. From the results, autoregressive models of order 1 and 3 were identified respectively for the monthly and 10 daily series. The parameters were estimated by non-linear least squares algorithm[17] and are shown in Table 1. It may be noted from Table 1 that for the 10 daily data series the residual variance decreased only marginally when the order of the model was increased from 1 to 3, and so in this case also a first order model was considered satisfactory. The residual random components were calculated and tested for independence by correlation (Figure 1) and spectral analysis. They were also tested for normality. In all the three cases, they were found to be serially independent normal variables.

TABLE 1

Non-linear least squares estimates of parameters for univariate AR model.

Station No.	Order	Initial estimate	Final estimate	Std. error	Residual variance
MONTHLY FLOWS					
1	1	0.52	0.5176	0.0495	0.733
2	1	0.57	0.5714	0.0475	0.675
3	1	0.56	0.5593	0.0479	0.691
TEN DAILY FLOWS					
1	1	0.62	0.6219	0.026	0.6174
	2	0.534 0.139	0.5352 0.1397	0.033 0.033	0.6033
	3	0.522 0.092 0.088	0.524 0.0972 0.0796	0.033 0.0375 0.033	0.6002
2	1	0.67	0.6739	0.025	0.5467
	2	0.632 0.056	0.6322 0.0592	0.033 0.033	0.5455
	3	0.624 −0.034 0.143	0.6265 0.0223 0.1285	0.033 0.039 0.033	0.5371
3	1	0.67	0.6723	0.025	0.5481
	2	0.608 0.093	0.615 0.086	0.033 0.033	0.5448
	3	0.599 0.033 0.099	0.605 0.021 0.107	0.033 0.039 0.033	0.5392

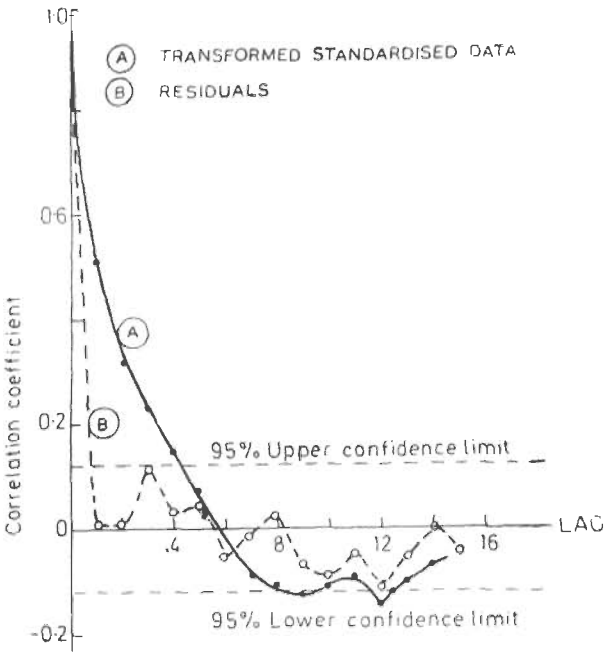

FIGURE 1 : Serial correlogram of flows at station 1 (monthly series)

Each of the random component series was tested for seasonal effects in serial correlation. It was found that correlation between adjacent periods was very significant though the correlation was positive for some periods and negative for others. This result derives from the fact that serial correlation is negligible in monsoon period and is large in winter months. The non-linear least squares estimate is an average over the seasons and so the residuals still preserve the seasonal variation in serial correlation. The AR model was hence rejected. A non-stationary (first order) Thomas-Fiering model (or AR model) was used and the resulting random components did not exhibit the seasonal variation in serial correlation. The results are not indicated in this paper. The residuals from the non-stationary Thomas-Fiering model constitute the $\{\eta(j)\}$ and were used in the next step, viz., multivariate modelling.

Multivariate Modelling

The multivariate model used in this study is the first order autoregressive model given by Equation (4). Using standard procedures [3][4] and assuming $[D]$ to be a lower triangular matrix, the elements of the matrices, $[C]$ and $[D]$ were determined. The results are given in Table II. The pure random components at each station were estimated and tested for randomness and normality. The cross-correlation between the pure random components at any two sites were calculated. The cross-correlation coefficient between the monthly data series at stations 1 and 2 are shown in Figure 3 for both the standardised normalised series and the pure random components. It may be seen that the pure random components are not significantly cross-correlated at 95 percent confidence level. The study is being continued to investigate whether a seasonal multivariate model is necessary or the stationary model is sufficient to represent the data series used.

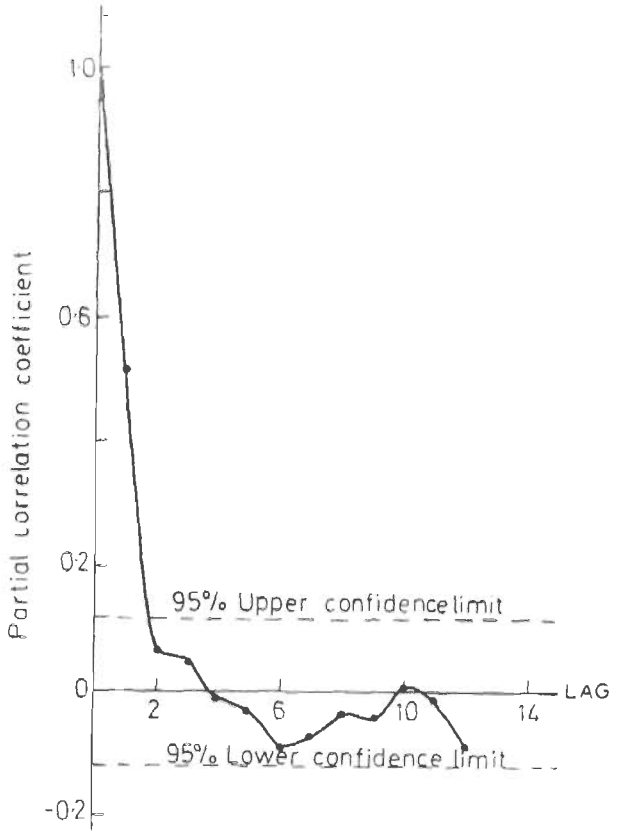

FIGURE 2 : Partial correlation coefficients at station 1 (transformed standardised monthly data series).

TABLE II

Parameters of the multivariate model Equation (5).

MONTHLY FLOWS

$$[C] = \begin{bmatrix} -0.015 & -0.022 & -0.006 \\ 0.034 & -0.017 & 0.003 \\ -0.029 & 0.005 & 0.005 \end{bmatrix}$$

$$[D] = \begin{bmatrix} 0.859 & 0.0 & 0.0 \\ 0.531 & 0.624 & 0.0 \\ 0.447 & 0.285 & 0.637 \end{bmatrix}$$

TEN DAILY FLOWS

$$[C] = \begin{bmatrix} -0.102 & 0.067 & 0.017 \\ 0.044 & 0.027 & 0.056 \\ 0.048 & 0.094 & 0.118 \end{bmatrix}$$

$$[D] = \begin{bmatrix} 0.776 & 0.0 & 0.0 \\ 0.480 & 0.560 & 0.0 \\ 0.360 & 0.234 & 0.592 \end{bmatrix}$$

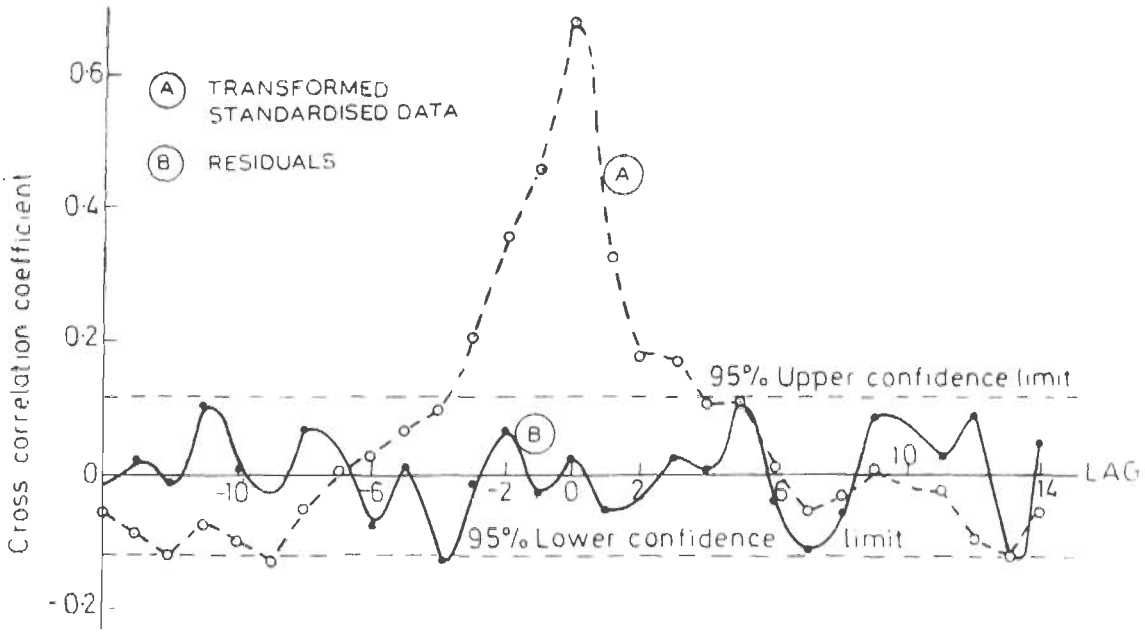

FIGURE 3 : Cross-correlogram between flows in stations 1 and 2 (monthly series)

Coupled Multivariate Model

By substituting the multivariate relationship of Equation (5) in the univariate relationship of Equation (4) the coupled multivariate relationship can be derived and it is as follows :

$$\{x(j+1)\} = [R_1]\{x(j)\}+\ldots+[R_p]\{x(j+1-p)\} +[Q_o][C]\{\eta(j)\}+\ldots+[Q_q][C]\{\eta(j-q)\} +[Q_o][D]\{\epsilon(j+1)\}+\ldots+[Q_q][D]\{\epsilon(j+1-q)\} \quad \ldots(6)$$

In the right hand side of Equation (6), the first p terms represent the autoregressive component; the next q terms represent the cross-correlated moving average terms among the serially independent random components; and the last q terms the cross-correlation between the pure random components. For the case studied, $p=1$; $q=1$ and $[Q_o]=[I]$, the identity matrix and so Equation (6) reduces to

$$\{x(j+1)\}=[R]\{x(j)\}+[C]\{\eta(j)\}+[D]\{\epsilon(j+1)\} \quad \ldots(7)$$

They can in turn be transformed back to the streamflow series by reversing steps (*ii*) and (*i*).

Uses of Decoupled Model

The decoupled multivariate model can be used in modelling and analysis of multivariate time series. Depending on the variance due to each component, the significance of auto and cross-correlation can be determined. It can be used in forecasting multivariate interrelated processes and in data generation. The generated data can be used in turn in optimal design and control of multi-reservoir systems.

Conclusions

On the basis of this study, the following conclusions can be made :

(1) Multiple streamflow series can be represented by a decoupled multivariate model which considers separately but in sequence the within-the-series correlation in each series and the among-the-series correlation.

(2) The delinking of the variabilities facilitates the use of well proven univariate models and the estimation of the parameters by standard procedures. The resulting multivariate model is also well behaved.

(3) The relatively simpler models in the two main stages can then be recoupled and transformed back to yield a complex multivariate model.

(4) The variability of the multivariate process in terms of the components gives a better understanding of the process.

(5) The results can be used in forecasting, data generation, and in turn in optimal design and control or operation of multi-reservoir systems.

Acknowledgment

The study reported is part of the Ph. D. thesis research of the junior author under the guidance of the senior author at the Indian Institute of Technology, Kanpur, India. The IBM 7044-1401 computer system at I.I.T., Kanpur has been used in this study.

References

(1) FIERING, M.B.: "Multivariate Techniques for Synthetic Hydrology". Proc. ASCE, Jour. Hydraulics Division, Vol. 90, No. HY 5, 1964, pp. 43-60.

(2) TORRANIN, P.: "Applicability of Canonical Correlation in Hydrology". Hydrology Paper No. 58, Colorado State University, November 1972.

(3) MATALAS, N.C.: "Mathematical Assessment of Synthetic Hydrology". Water Resources Research, Vol. 3, No. 4, 1967, pp. 937-945.

(4) YOUNG, G. K. and PISANO, W. C. : "Operational Hydrology using Residuals". Proc. ASCE, Jour. Hydraulics Division, Vol. 94, No. HY 4, July 1968, pp. 909-923.

(5) CROSBY, D. S. and MADDOCK, T. III : "Estimating Coefficients of a Flow Generator for Monotone Samples of Data". Water Resources Research, Vol. 6, No. 4, 1970, pp. 1079-1086.

(6) JEAN FROST and CLARKE, R.T. : "Use of Cross-correlation between Hydrologic Time Series to Improve Estimates of Lag One Autoregressive Parameters". Water Resources Research, Vol. 9, No. 4, August, 1973.

(7) VALENCIA, D. and SCHAAKE, J.C. JR.: "Disaggregation Process in Stochastic Hydrology". Paper presented at 53rd Annual Meeting, AGU, Washington, D.C., April 17-21, 1972.

(8) MC'MAHON, T. A. et al : "Single and Multisite Operational Hydrology". Nordic Hydrology, Vol. 3, No. 4, 1972.

(9) MEJIA, J. M. et al : "Multivariate Generation of Mixtures of Normal and Lognormal Variables". Water Resources Research, Vol. 10, No. 4, August 1974, pp. 671-693.

(10) PENTLAND, R. L. and CUTHBERT, D.R. : "Operational Hydrology for Ungaged Streams by the Grid Square Technique". Water Resources Research, Vol. 7, No. 2, April 1971, pp. 283-291.

(11) BEARD, L.R. : "Use of Interrelated Records to Simulate Streamflow". Proc. ASCE, Jour. Hydraulics Division, Vol. 91, No. HY 5, 1965.

(12) PENTLAND, R. L. and CUTHBERT, D. R.: "Multisite Flow Generator". Water Resources Research, Vol. 9, No. 2, April 1973, pp. 470-473.

(13) SLACK, J. R. : "I would if I could (Self Denial) by Conditional Models". Water Resources Research, Vol. 9, No. 1, February 1973, pp. 247-249.

(14) MANDELBROT, B. B. and WALLIS, J. R. : "Noah, Joseph and Operational Hydrology". Water Resources Research, Vol. 4, No. 5, October 1968, pp. 909-918.

(15) MATALAS, N. C. and WALLIS, J. R. : "Statistical Properties of Multivariate Fractional Noise Processes". Water Resources Research, Vol. 7, No. 6, 1971, pp. 1460-1468.

(16) MEJIA, J. M. et al : "Streamflow Simulation 3. Broken Line Process and Operational Hydrology". Water Resources Research, Vol. 10, No. 2, April 1974, pp. 242-245.

(17) BOX, G.E.P. and JENKINS, G. M. : "Time Series Analysis, Forecasting and Control". Holden Day Publishing Co., New York, 1970.

(18) MEJIA, J. M. and ITURBE, I. R. : "On the Synthesis of Random Field Sampling from the Spectrum, An Application to the Generation of Hydrologic Spatial Processes". Water Resources Research, Vol. 10, No. 4, August 1974, pp. 705-711.

(19) YEVJEVICH, V. and KARPLUS, A. K. : "Area-Time Structure of the Monthly Precipitation Process". Hydrology Paper No. 64, Colorado State University, August 1973.

(20) FIERING, M. B. : "Streamflow Synthesis". Harvard University Press, 1967.

(21) FIERING, M. B. : "Schemes for Handling Inconsistent Matrices". Water Resources Research, Vol. 4, No. 2, 1968, pp. 291-297.

Stochastic Modelling for Flood Flows

H. D. SHARMA
Director

S. V. SINGH
Research Officer

S. R. JINDAL
Statistical Officer

Irrigation Research Institute, Roorkee, U.P. (India).

SYNOPSIS

Following the theory of the extremes of a random number of random variables, a stochastic model is presented for the interpretation, analysis and prediction of the largest peak discharge above a given base level. The model for the distribution of the magnitude of flood peaks has been applied to 87 years' data for the Ganga River at Hardwar. A comparison of results with those obtained by Gumbel's method indicates that the introduced model fits the data better. Estimation of design flood has also been worked out for various recurrence intervals by this method.

1. Introduction

1.1 The estimation of flood flows or the maximum probable flood has been made in the past with the aid of a number of empirical formulae. These generally contain one or two parameters which are supposed to take cognizance of the entire set of variables affecting the flood flows.

1.2 In later studies, the estimation of flood flows was based on the use of formulae which gave the magnitude of the expected flood with a specified level of probability. Although the element of probability was introduced in these formulae, such as, modified California, modern California, Foster, Gumbel, Powell and Ven Te Chow, they are still not realistic because they are deterministic and do not consider the element of time. The latter is possible only by the stochastic (time dependent probabilistic) approach.

1.3 Work in the field of stochastic hydrology has been introduced in the United States of America by Yevdjevich, Ven Te Chow and others. But no general formula or procedure has been laid down for the estimation of the flood to be expected with a specified level of probability, based on the stochastic approach, nor has any numerical solution been presented for varying hydrologic situations. The paper presents a new approach based on stochastic properties of floods in which use is made of some recent developments in the theory of extremes.

2. Stochastic Approach

2.1 In the old or existing concept of only one peak flood in a year, it has been stated by Langbein(1), "Only the greatest flood in each year is used. An objection most frequently encountered with respect to the use of annual floods is that it uses only one flood in each year. Infrequently, the second highest flood in a given year, which the above rule (i.e., annual floods) omits may outrank many annual floods". An annual flood need not be an inundation and might even be a drought. An objection frequently taken to the conventional concept is that the flood level often does not exceed a certain stage, say the bankfull stage. During dry years, highest annual peak discharges may be quite small and may not constitute a flood.

2.2 In the new concept presented, the data on flood peaks are used above a given base level, to derive the distribution of the largest flood or peak flow in a given time interval (o, t). The magnitudes of these peaks are considered as a series of random variables. This replaces the existing concept of taking only one flood for a particular year irrespective of its magnitude.

2.3 In this manner, a sequence of random variables, $\xi_1, \xi_2, \xi_3, \ldots\ldots, \xi_n$, which are exceedances of flood flows above a base flow, is obtained as the series of floods. Both the number of flood peaks in each subsequent time interval (o, t), say with the year as the interval, and the time when a peak flow occurs are random variables.

The problem may thus be treated as an offshoot of the classical theory of extreme values(2). According to the latter, the number of observations n is always specified, the largest and smallest values being functions of n. In many practical investigations, particularly in flood control problems, it is pertinent to assess the maximum probable or expected peak in a given interval of time. Following the theory of a random number of random variables, the number of observations in the interval (o, t) is a random variable so that the extremes considered in the time interval (o, t) are functions of t. The series of floods, according to this concept, constitutes partial duration series.

2.4 Coming to the practical application of the concept, it may be pointed out that the design flood pertaining to an engineering structure is pertinent only when it exceeds a certain critical magnitude, which is termed as the base level. Flows below this base may be justifiably excluded because of their insignificant role with respect to the safety of the structure.

2.5 The base flow Q_b may be defined, as stated above, as the magnitude of the discharge above which water flows above the banks of a river at a specified point. In other words, Q_b may be taken to be equal to the bankfull discharge of the river at the particular point.

2.6 If Q_i is the flood peak which has occurred in the time interval (o, t), then the flood exceedance x_i in this interval may be defined as :

$$x_i = Q_i - Q_b \qquad \ldots(1)$$

where, Q_b denotes the base flow which is equal to the bankfull discharge of the river.

2.7 The number $n(t)$ of flood exceedances in an interval of time (o, t) as well as the magnitudes $x(t)$ of these exceedances are time dependent random variables. The time T_i of occurrence of these exceedances are also random variables. The time T_i is associated with the random variables x_i (for all $i = 1, 2, 3, \ldots\ldots, n$).

3. Distribution of the Magnitudes of Exceedances

3.1 Using the results obtained by Todorovic(3) and Emir Zelenhasic(4), the distribution function, $F_t(x)$, of the largest exceedance in a given interval of time (o, t) can be obtained as :

$$F_t(x) = \sum_{i=1}^{\infty} [\{H(x)\}^i . P(E_i^t)] \qquad \ldots(2)$$

in which, $H(x)$ is the distribution function of all exceedances in a given interval of time (o, t), and $P(E_i^t)$ is the probability of occurrence of, i, exceedances during the interval of time (o, t) which have been derived by standard mathematical methods and are given below :

$$H(x) = 1 - e^{-\beta x} \qquad \ldots(3)$$

and

$$P(E_i^t) = (\lambda . t)^i \exp.(-\lambda . t)/i \qquad \ldots(4)$$

where, $1/\beta$ is a scale parameter and λ is the mean number of exceedances in a unit time.

3.2 The distribution function $P(E_i^t)$ as given in Equation (4) is a time dependent Poissonian process. The other distribution function $H(x)$ of exceedances is a two parameter gamma probability distribution function. Two probability laws have played an important role in connection with the magnitude of flood peaks. These are the gamma and the exponential probability laws(4). Because the exponential distribution is a particular case of the gamma distribution, the family of (two parameter) gamma distributions is used in the sequel as the common distributions of exceedances. Therefore, the family of gamma distributions in combination with time dependent Poissonian process has been used in Equation (2) for the determination of the theoretical distribution of the largest exceedance. Substitution of Equations (3) & (4) in Equation (2) gives :

$$F_t(x) = \exp.[-\lambda . t . e^{-\beta x}] \qquad \ldots(5)$$

For a particular exceedance x_T for an interval of T years, Equation (5) may be rewritten as :

$$F(x_T) = \exp.[-\lambda . T . e^{-\beta x_T}] \qquad \ldots(6)$$

4. Estimation of Design Flood

4.1 Let x_T denote the magnitude of the flood exceedance whose expected recurrence interval is T years such that :

$$x_T \geqslant 0 \text{ and } T \geqslant 0$$

then $F(x_T)$ will represent the probability of occurrence of an exceedance x_T and may be taken as below :

$$F(x_T) = \frac{1}{\lambda . T} \qquad \ldots(7)$$

λ being the mean number of exceedance in one year.

Substitution of Equation (7) in Equation (6) gives :

$$\frac{1}{\lambda . T} = \exp.\left[\lambda . T . e^{-\beta x_T}\right] \qquad \ldots(8)$$

Solving Equation (8) for x_T we get the following mathematical model :

$$x_T = \frac{1}{\beta}[ln(\lambda . T) - ln\{ln(\lambda . T)\}] \qquad \ldots(9)$$

where, β and λ are constants for a particular series of data.

Therefore, the design flood y_T may be obtained as below :

$$y_T = Q_b + x_T \qquad \ldots(10)$$

Q_b being bankfull discharge of the river.

4.2 Substituting the expression for x_T from Equation (9), the stochastic model for the estimation of the design flood works out to :

$$y_T = Q_b + \frac{1}{\beta}\,[ln\,(\lambda\,.\,T) - ln\,\{ln\,(\lambda\,.\,T)\}] \qquad \ldots(11)$$

5. Analysis of Data

5.1 *Distribution of Magnitude of Exceedances*

5.1.1 The application of the above method has been made to study the distribution of the magnitude of exceedances for the Ganga River at Hardwar. Flood data, in the form of partial duration series, cover a period of 87 years, from 1885-1971. The base flow, Q_b, for this series is taken to be equal to 4,333 m³/sec as this is accepted as the bankfull discharge in the design of the weir at Bhimgoda. A series of 175 flood peak exceedances, in the course of 87 years, was obtained from the data which worked out to two flood peaks per year on an average. The data may be seen in Table I.

5.1.2 It is observed from the data given in Table I that the majority of the flood exceedances for the Ganga River at Hardwar occurred during 11 June to 28 October each year. Table II gives the number of recorded exceedances during this period which have been represented in Figure 1.

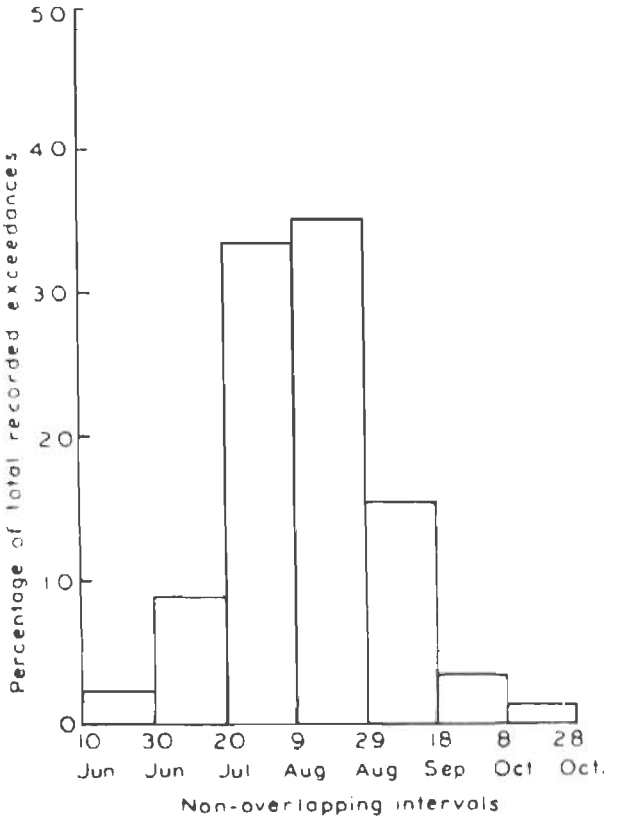

FIGURE 1 : Occurrence of exceedance during seven non-overlapping intervals of flood year considered (Ganga River at Hardwar).

5.1.3 The estimation of the value of the parameter β was made as per Table III by using Equation (3) which worked out to 4.05×10^{-4}, and with this estimated value of β the general distribution of the magnitudes of exceedances was obtained as beolw :

$$H(x) = 1 - \exp.(-4.05 \times 10^{-4}.x) \qquad \ldots(12)$$
$$x \geqslant 0$$

where, x is in m³/sec.

5.1.4 The observed frequency distribution and the corresponding fitted simple general exponential distribution function have been calculated, vide Table IV and plotted in Figure 2. It can be seen from Figure 2 that the simple exponential distribution function gives very good fit in the case of the observed frequency distribution.

5.1.5 The double exponential distribution of the flood exceedances with a year as the time interval has now been obtained as follows :

5.1.6 The value of the parameter λ which is the average number of exceedances per year, has been worked out as (175/87)=2.01. On substitution of the value in Equation (5), the frequency distribution becomes :

$$F(x) = \exp.\,[-2.01\{\exp.\,(-4.05 \times 10^{-4}.x)\}] \qquad \ldots(13)$$
$$x \geqslant 0$$

where, x is the flood exceedance over the bankfull discharge, which is a double exponential distribution. Values of this double exponential frequency distribution have been calculated as in Table V and have been plotted in Figure 3.

5.1.7 Chi-square test was applied for testing the quality of fit. The estimated value of χ^2 was 6.927, whereas the critical value of χ^2 at 5 percent level of significance is 7.815. This test shows close conformity between the fitted and the observed distributions of the largest magnitudes of exceedances.

5.1.8 The results of the method developed in this study have been compared with the method used by Gumbel. The mean and standard deviation of the maximum annual discharges for the 87 years considered have been worked out as $Q_a = \bar{x} = 6635.63$ m³/sec and $\sigma(Q_a) = s = 3130.8$ m³/sec. The data of annual peak discharges may be seen in Table VI.

TABLE 1

Flood peaks and magnitudes of flood peak exceedances (Base of partial duration series (Q_b) 4,333 m^3/sec).

Sl. No.	Year	Date	Flood peaks (Q) m^3/sec	Flood peak exceedances (x)=Q—Q_b m^3/sec
1	2	3	4	5
1.	1885	July 16	5,814	1,481
2.		Aug. 9	7,241	2,908
3.	1886	July 15	4,665	332
4.		July 22	4,848	515
5.		July 27	4,369	36
6.		Aug. 5	9,163	4,831
7.		Sept. 2	6,018	1,685
8.	1887	Aug. 2	5,882	1,549
9.		Aug. 22	7,407	3,074
10.	1888	July 22	5,417	1,084
11.		July 27	5,034	701
12.		July 31	4,909	576
13.		Aug. 2	4,848	515
14.		Sept. 3	5,417	1,084
15.		Sept. 20	6,870	2,537
16.	1889	June 25	5,680	1,347
17.		July 7	7,936	3,603
18.		July 17	4,848	515
19.		July 29	8,827	4,494
20.		Aug. 3	7,546	3,213
21.		Aug. 15	9,855	5,522
22.		Aug. 29	7,857	3,524
23.		Sept. 9	4,971	638
24.	1890	July 19	5,814	1,481
25.		July 30	11,887	7,554
26.		Aug. 7	6,508	2,175
27.		Aug. 19	9,249	4,916
28.		Aug. 31	5,417	1,084
29.	1891	July 26	4,786	453
30.		Aug. 14	8,827	4,494
31.	1892	July 26	4,605	272
32.		Aug. 15	5,747	1,414
33.		Aug. 25	7,546	3,213
34.		Sept. 3	4,971	608
35.	1893	June 29	5,287	955
36.		July 26	5,482	1,149
37.		Aug. 4	6,087	1,754
38.		Aug. 10	6,870	2,537
39.		Sept. 5	8,498	4,165
40.		Oct. 19	5,128	795

TABLE 1 (*Contd.*)

1	2	3	4	5
41.	1894	July 8	5,160	827
42.		July 21	6,018	1,685
43.		July 27	9,767	5,434
44.		July 30	13,179	8,846
45.		Aug. 6	10,032	5,699
46.		Aug. 12	9,680	5,347
47.		Aug. 26	16,757	12,424
48.		Sept. 6	7,376	3,043
49.	1895	July 2	5,747	1,414
50.		Aug. 13	9,680	5,347
51.		Sept. 8	5,034	701
52.	1896	Aug. 10	14,336	10,003
53.	1897	July 22	7,623	3,290
54.		Aug. 5	7,407	3,074
55.		Aug. 23	8,174	3,841
56.		Sept. 3	4,427	94
57.	1898	July 10	5,814	1,481
58.		July 24	5,882	1,549
59.		Aug. 12	8,953	4,620
60.		Aug. 18	7,241	2,908
61.		Sept. 7	6,366	2,033
62.	1899	July 23	7,546	3,213
63.	1900	July 17	4,486	153
64.		Aug. 11	6,651	2,318
65.		Aug. 26	5,097	764
66.		Sept. 6	5,950	1,617
67.		Sept. 12	4,786	453
68.	1901	July 19	4,427	94
69.		Aug. 8	7,700	3,367
70.		Aug. 24	11,409	7,076
71.	1902	Aug. 3	9,163	4,830
72.		Sept. 14	4,848	515
73.	1903	Aug. 14	7,407	3,074
74.		Aug. 27	6,296	1,963
75.	1904	July 29	8,579	4,246
76.		Aug. 3	7,092	2,759
77.		Aug. 12	7,091	2,758
78.		Aug. 21	7,017	2,684
79.	1905	Aug. 13	9,362	5,029
80.	1906	July 28	7,092	2,759
81.		Aug. 3	6,870	2,537
82.		Aug. 19	5,950	1,617
83.		Sept. 16	6,226	1,893
84.	1907	July 30	7,546	3,213
85.		Aug. 3	7,241	2,908

TABLE 1 (*Contd.*)

1	2	3	4	5
86.	1908	July 13	6,651	2,318
87.		Aug. 2	11,504	7,171
88.		Aug. 21	5,949	1,616
89.		Aug. 29	6,018	1,685
90.	1909	July 16	6,870	2,537
91.		July 21	8,335	4,002
92.		Aug. 12	7,407	3,074
93.		Aug. 20	6,724	2,391
94.		Aug. 27	5,949	1,616
95.	1910	June 15	4,605	272
96.		July 28	10,121	5,788
97.		Aug. 3	7,469	3,136
98.		Aug. 13	11,887	7,554
99.		Aug. 18	7,091	2,759
100.		Sept. 11	6,156	1,823
101.		Oct. 3	15,077	10,744
102.	1911	Aug. 18	6,943	2,610
103.		Sept. 13	4,369	36
104.	1912	Aug. 16	7,700	3,367
105.		Sept. 2	8,335	4,002
106.	1914	July 2	5,417	1,084
107.		July 28	6,018	1,685
108.		Sept. 19	9,249	4,916
109.	1915	Aug. 2	6,579	2,246
110.		Aug. 13	7,407	3,074
111.		Aug. 29	4,725	392
112.	1916	Aug. 26	4,725	392
113.	1917	July 11	8,416	4,083
114.		July 25	6,870	2,537
115.		Aug. 5	5,352	1,019
116.		Aug. 23	4,909	576
117.		Sept. 9	5,482	1,149
118.	1918	Aug. 22	4,665	332
119.	1919	July 13	6,296	1,963
120.		Sept. 7	5,160	827
121.	1920	July 23	4,848	515
122.		Aug. 14	8,174	3,841
123.	1921	June 26	5,680	1,347
124.		Aug. 4	7,623	3,290
125.		Aug. 18	9,079	4,746
126.		Sept. 9	6,508	2,175
127.		Sept. 15	5,950	1,617
128.	1922	July 20	5,814	1,481
129.		Aug. 17	7,407	3,074
130.		Sept. 3	5,034	701
131.	1923	Aug. 5	5,482	1,149

TABLE 1 (*Concld.*)

1	2	3	4	5
132.	1924	July 27	5,160	827
133.		Aug. 3	6,087	1,754
134.		Aug. 19	5,097	764
135.		Sept. 5	4,848	515
136.		Sept. 29	19,136	14,803
137.	1925	July 21	5,160	827
138.		Aug. 12	9,670	5,347
139.	1927	Aug. 5	7,236	2,903
140.		Aug. 20	7,241	2,908
141.	1929	Aug. 15	4,545	212
142.	1930	July 27	5,443	1,110
143.		Aug. 21	5,997	1,664
144.	1932	Aug. 14	5,532	1,199
145.		Aug. 24	6,155	1,822
146.	1933	July 25	4,692	359
147.		Aug. 15	5,267	934
148.	1934	Aug. 21	6,193	1,860
149.	1935	Aug. 4	5,289	956
150.	1942	July 24	4,887	554
151.		Aug. 9	6,650	2,317
152.	1943	Aug. 22	4,442	109
153.	1945	Aug. 19	4,836	503
154.		Sept. 3	5,101	768
155.	1946	July 28	4,629	296
156.	1947	Sept. 27	4,345	12
157.	1948	Aug. 25	4,890	557
158.	1950	July 26	4,562	229
159.		Aug. 18	5,899	1,566
160.	1951	Aug. 22	4,458	125
161.		Sept. 15	4,339	6
162.	1953	Aug. 13	5,470	1,137
163.	1954	Aug. 20	5,978	1,645
164.	1955	Oct. 5	4,644	311
165.	1956	Oct. 11	6,381	2,048
166.	1957	Sept. 15	4,548	215
167.	1959	Aug. 3	4,493	160
168.	1961	Aug. 17	4,855	522
169.	1962	July 28	5,760	1,427
170.	1963	Aug. 21	5,574	1,241
171.		Sept. 17	9,192	4,859
172.	1966	July 26	4,741	408
173.	1967	Aug. 27	5,919	1,586
174.	1969	Aug. 20	4,546	213
175.	1971	Aug. [illegible]	4,542	209

TABLE II

Percentage of number of exceedances (within 20 days period) with respect to the total number of exceedances during 87 years from 1885 to 1971.

Sl. No.	Period	Number of exceedances	Percentage of total number of recorded exceedances
1	2	3	4
1.	June 11—June 30	4	2.286
2.	July 1—July 20	16	9.143
3.	July 21—Aug. 9	59	33.714
4.	Aug. 10—Aug. 29	61	34.857
5.	Aug. 30—Sept. 18	27	15.429
6.	Sept. 19—Oct. 8	6	3.429
7.	Oct. 9—Oct. 28	2	1.143
	Total	175	

Note :

(1) Total number of exceedances in the period of 87 years (1885 to 1971) = 175.

(2) Average number of exceedances per year, $\lambda = \frac{175}{87} = 2.01$.

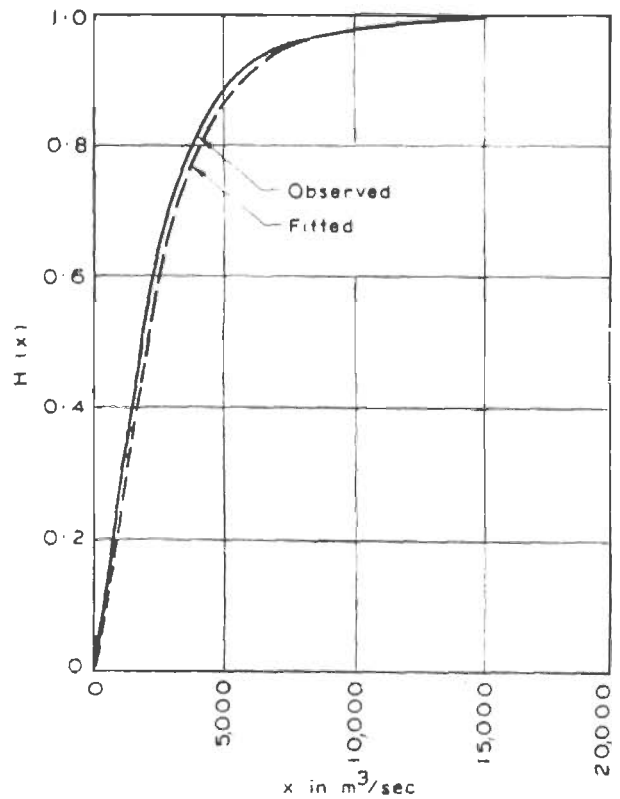

FIGURE 2 : Fitted simple exponential distribution H(x) and observed frequency distribution magnitudes (ξk) of exceedances during one year. (Ganga River at Hardwar).

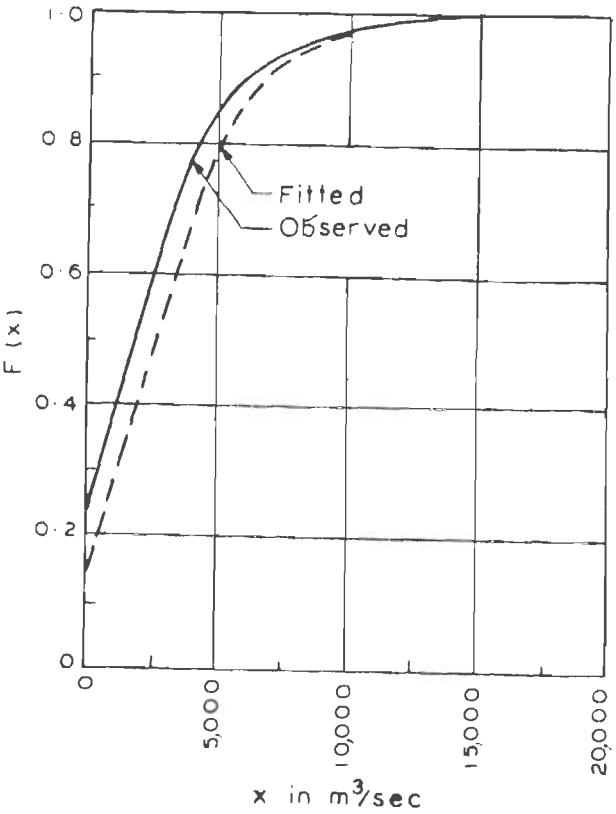

FIGURE 3 : Double exponential distribution and observed frequency distribution of largest exceedance using a one year interval (Ganga River at Hardwar).

5.1.9 The two parameters in the double exponential function have been estimated by Gumbel's method for 87 annual flood peak discharges. The double exponential distribution function for this case using Gumbel's estimate has been worked out as follows :

$$F(Y) = \exp.\{-\exp.(-Y)\} \qquad ...(14)$$

where, Y = reduced variate as given by Gumbel.

$= y_n + (x - \bar{x})\, \sigma y_n / s$

y_N = mean of reduced variate taken from Gumbel's table[5]

$= 0.55815$ for $N = 87$

σy_N = standard deviation of reduced variate taken from Gumbel's table

$= 1.1987$ for $N = 87$

$\bar{x}$ = mean of the series of annual peak discharges

$= 6635.63$

TABLE III

Estimation of the parameter β.

Sl. No.	Magnitude of flood peak exceedance m³/sec		Observed frequency	Cumulative frequency (C.F.)	$H(x)=\frac{(C.F.)}{175}$	$1-H(x)$	$\beta \quad \frac{-ln\{1-H(x)\}}{x}$
	Class Interval	Variable (x)					
1	2	3	4	5	6	7	8
1.	Below— 2,500	2,500	107	107	0.6114	0.3886	3.362×10^{-4}
2.	2,500— 5,000	5,000	51	158	0.9029	0.0971	4.649×10^{-4}
3.	5,000— 7,500	7,500	10	168	0.9600	0.0400	4.282×10^{-4}
4.	7,500—10,000	10,000	3	171	0.9771	0.0229	3.762×10^{-4}
5.	10,000—12,500	12,500	3	174	0.9443	0.0057	4.119×10^{-4}
6.	12,500—15,000	15,000	1	175	1.0000	0.0000	—

$\hat{\beta}$ = The average value of $\beta = 4.05\times10^{-4}$

TABLE IV

Estimation of theoretical values of H(x) for Ganga River at Hardwar.

Sl. No.	x m³/sec	$\frac{-\beta x}{2.30259}$	$1-H(x)$	$H(x)$ Estimated	$H(x)$ Observed	Remarks
1	2	3	4	5	6	7
1.	2,500	—0.448	0.35645	0.64355	0.6114	$1-(H)x=$ Antilog $\left\{\frac{-\beta x}{2.30259}\right\}$
2.	5,000	—0.896	0.12706	0.87294	0.9029	
3.	7,500	—1.344	0.04529	0.95471	0.9600	
4.	10,000	—1.792	0.016144	0.983856	0.9771	
5.	12,500	—2.240	0.00575	0.99425	0.9943	Estimate of $\beta=$
6.	15,000	—2.688	0.00205	0.99795	1.0000	$\hat{\beta}=4.05\times10^{-4}$

TABLE V

Estimation of observed and fitted values of F (x) for the magnitudes of exceedances of Ganga River at Hardwar.

Sl. No.	x m³/sec	Observed frequency f_o	Cumulative frequency (C.F.)	Observed value of $F(x)=F_o(x)$	$\beta.x$	exp.$(-\beta.x)$	2.01 x exp. $(-\beta.x)$	Estimated value of $F(x)$ $F_e(x)$	Remarks
1	2	3	4	5	6	7	8	9	10
1.	0	19	19	0.21839	0.00	1.00000	2.01000	0.13534	Estimated value
2.	2,500	31	50	0.57471	1.03	0.35738	0.72000	0.48714	$F_e(x)=$
3.	5,000	26	76	0.87356	2.10	0.12146	0.24000	0.78663	$e^{-2.01}\exp.(\beta x)$
4.	7,500	6	82	0.94253	3.10	0.04505	0.09000	0.91398	
5.	10,000	1	83	0.95402	4.10	0.01657	0.03000	0.97050	
6.	12,500	3	86	0.98851	5.20	0.00552	0.01100	0.98901	
7.	15,000	1	87	1.00000	6.20	0.00203	0.00408	0.99587	

TABLE VI

Annual peak discharges for Ganga River at Hardwar for the period 1885 to 1971.

Sl. No.	Year	Annual peak discharge (x) m³/sec	Sl. No.	Year	Annual peak discharge (x) m³/sec
1	2	3	1	2	3
1.	1885	7,241	45.	1929	4,545
2.	1886	9,164	46.	1930	5,998
3.	1887	7,407	47.	1931	3,470
4.	1888	6,870	48.	1932	6,155
5.	1889	9,855	49.	1933	5,267
6.	1890	11,887	50.	1934	6,193
7.	1891	8,827	51.	1935	5,289
8.	1892	7,546	52.	1936	3,320
9.	1893	8,498	53.	1937	3,232
10.	1894	16,757	54.	1938	3,525
11.	1895	9,680	55.	1939	2,341
12.	1896	14,336	56.	1940	2,429
13.	1897	8,174	57.	1941	3,154
14.	1898	8,953	58.	1942	6,650
15.	1899	7,546	59.	1943	4,442
16.	1900	6,652	60.	1944	4,229
17.	1901	11,409	61.	1945	5,101
18.	1902	9,164	62.	1946	4,629
19.	1903	7,404	63.	1947	4,345
20.	1904	8,579	64.	1948	4,890
21.	1905	9,362	65.	1949	3,619
22.	1906	7,092	66.	1950	5,899
23.	1907	7,546	67.	1951	4,458
24.	1908	11,504	68.	1952	3,919
25.	1909	8,335	69.	1953	5,470
26.	1910	15,077	70.	1954	5,978
27.	1911	6,943	71.	1955	4,644
28.	1912	8,335	72.	1956	6,381
29.	1913	3,579	73.	1957	4,548
30.	1914	9,299	74.	1958	4,056
31.	1915	7,407	75.	1959	4,493
32.	1916	4,726	76.	1960	3,884
33.	1917	8,416	77.	1961	4,855
34.	1918	4,668	78.	1962	5,760
35.	1919	6,296	79.	1963	9,192
36.	1920	8,174	80.	1964	3,024
37.	1921	9,079	81.	1965	2,509
38.	1922	7,407	82.	1966	4,741
39.	1923	5,482	83.	1967	5,919
40.	1924	19,136	84.	1968	3,798
41.	1925	9,680	85.	1969	4,546
42.	1926	3,698	86.	1970	3,842
43.	1927	7,241	87.	1971	4,542
44.	1928	3,698			

s = standard deviation of annual peak discharges

= 3130.8

Then the frequency distribution function will become :

$$F(x) = \exp.\left[-\exp.\left\{-x.\frac{\sigma y_N}{s} + \left(\bar{x}.\frac{\sigma y_N}{s} - \bar{y}_N\right)\right\}\right] \quad \ldots(15)$$

On substituting the above values of $\bar{x}$, s, $\bar{y}_N$ and σy_N, we get the double exponential distribution function for this case using Gumbel's estimate as below :

$$F(x) = \exp.\{-7.24843 \exp.(-3.83\times10^{-3}.x)\} \quad \ldots(16)$$
$$x \geqslant 0$$

where, x is the magnitude of the annual peak discharge.

5.1.10 Values of fitted Gumbel's $F(x)$ function and the corresponding observed frequency distribution of maximum annual peak discharges for the Ganga River have been calculated and are shown in Figure 4.

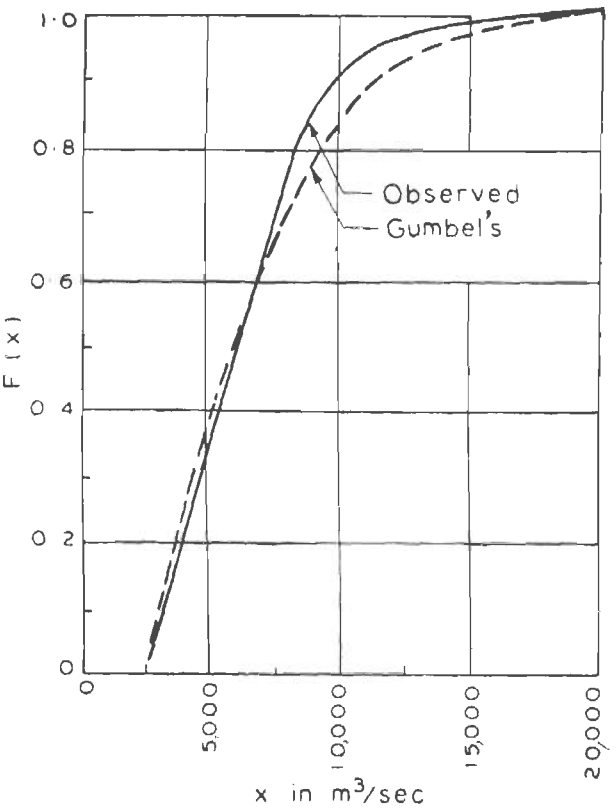

FIGURE 4 : Double exponential distribution function F(x) with parameters estimated by Gumbel's method and corresponding observed frequency distribution of peak discharge (Ganga River at Hardwar).

5.1.11 It has been found that for the Gumbel's estimates of the two parameters the chi-square is $\chi^2 = 8.906$, which is larger for the same number of class intervals than the chi-square obtained by the estimates of the new method used in this study with $\chi^2 = 6.927$.

5.1.12 Accordingly, for this example the method of estimates or parameters in the double exponential distribution function gives better conformity by the observed distribution than Gumbel's method of estimates.

5.2 *Estimation of Design Flood*

5.2.1 Estimation of the design flood equation for the Ganga River at Hardwar has been worked out as below :

$$y_T = 4333 + \frac{(10)^4}{4.05}[ln(2.01\,T) - ln\{ln(2.01\,T)\}] \quad ...(17)$$

TABLE VII

Comparison of results of the estimation of design flood for varying recurrence intervals for the Ganga River at Hardwar using different probability methods.

Return period in years	Gumbel's method m³/sec	Powell's method m³/sec	Ven Te Chow's method m³/sec	Stochastic model approach m³/sec
1	2	3	4	5
50	15,250	14,486	14,819	11,938
100	17,001	16,038	16,430	13,296
200	19,400	18 617	18,668	14,728
500	21,700	20,648	20,975	16,605
1,000	23,146	22,154	22,738	18,103

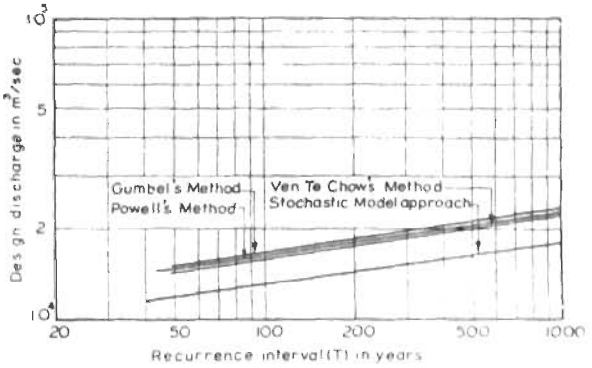

FIGURE 5 : Design flood with recurrence interval.

5.2.2 It is found that by the use of the stochastic model, 1,000-year design flood works out to 18,103 m³/sec against the observed figure of 19,136 m³/sec for which the recurrence interval has been estimated as 1,500 years.

5.2.3 Table VII gives a comparison of results of estimation of floods for varying recurrence intervals ranging from 50 to 1,000 years worked out by other probability methods, viz., Gumbel, Powell and Ven Te Chow. These have also been plotted in Figure 5. It is seen that the estimation of flood by the stochastic model approach gives values close to other methods, although slightly lower.

5.2.4 Estimation of design flood for a recurrence interval of 1,000 years has also been worked out by using the stochastic model approach when the period of record is taken as 25, 30, 40, 50, 60, 70 & 80 years. The results are shown in Table VIII, which also gives corresponding

TABLE VIII

Estimation of design flood by the use of stochastic model and by Gumbel's method when the period of record is varied.

Sl. No.	Period of record	Length of interval in years	λ	$\hat{\beta}$	Magnitude of design flood for a recurrence interval of 1,000 years	
					By stochastic model in m³/sec	By Gumbel's method in m³/sec
1	2	3	4	5	6	7
1.	1910–1934	25	2.016	3.815×10^{-4}	18,958	24,035
2.	1910–1939	30	1.833	3.848×10^{-4}	18,622	26,603
3.	1910–1949	40	1.575	4.094×10^{-4}	17,440	24,008
4.	1910–1959	50	1.460	4.368×10^{-4}	16,467	21,922
5.	1910–1969	60	1.350	4.514×10^{-4}	15,926	20,822
6.	1901–1970	70	1.514	4.345×10^{-4}	16,593	21,573
7.	1892–1971	80	1.800	4.045×10^{-4}	17,886	23,191
8.	1885–1971	87	2.010	4.050×10^{-4}	18,103	23,146

values estimated by Gumbel's method. It is found that with lesser period of record the design flood varies within a range of $\pm$ 9 percent of that for 87 years period, whereas by Gumbel's method the variation is of the order of $\pm$ 15 percent. The new stochastic model approach can, therefore, be used with greater reliability to estimate the design flood for large recurrence interval with inadequate data.

6. Conclusions

6.1 Equations have been derived for the determination of the theoretical distribution of the largest exceedance and also for the estimation of the design flood.

6.2 Data for the Ganga River at Hardwar for a period of 87 years, viz., 1885-1971, have been analysed for the determination of the distribution function of the largest exceedance for one year time interval. The results indicate that the stochastic model fits the data better than the distribution obtained by Gumbel's method.

6.3 Data for the Ganga River has also been analysed for the estimation of the design flood. It is found that by the use of the stochastic model, 1,000-year design flood for the Ganga River at Hardwar works out to 18,103 m^3/sec against the observed maximum figure of 19,136 m^3/sec, for which the recurrence interval has been estimated as 1,500 years.

6.4 A comparison of the results of estimation of design flood for varying recurrence intervals ranging from 50 to 1,000 years has been made with other probability methods, viz , Gumbel, Powell and Ven Te Chow. It is seen that the estimation of flood by the stochastic model approach gives values close to other methods, although slightly lower.

6.5 The new stochastic model has also been used for the estimation of design flood with lesser period of record and has been found to yield values within a range of $\pm$ 9 percent of those obtained with 87 years data as compared to a variation of $\pm$ 15 percent obtained by Gumbel's method.

7. Acknowledgments

Messrs. Ramjeet and D.C. Mittal, Research Supervisors, Basic Research Division, Irrigation Research Institute, Roorkee gave useful help in the compilation of tables and figures and collection of pertinent information. This is gratefully acknowledged.

8. References

(1) LANGBEIN, W.B. (1949) : "Annual Floods and the Partial duration Flood Series". Transactions, American Geophysical Union, Vol. 30, No. 6, December.

(2) GUMBEL, E.J. (1945) : "Floods Estimated by Probability Method". Engineering News-Record, June 14.

(3) TODOROVIC, P. (1970) : "On Some Problems Involving Random Number of Random Variables". Annals of Mathematical Statistics, Vol. 41, No. 3.

(4) EMIR ZELENHASIC (1970) : "Theoretical Probability Distributions for Flood Peaks". Hydrology Paper No. 42, Colorado State University, Fort Collins, Colorado.

(5) GUMBEL, E.J. (1958) : "Statistics of Extremes". Columbia University Press, New York.

Some Stochastic Runoff Models

I. KONTUR
Assistant

Budapest Technical University
Budapest, Hungary.

SYNOPSIS

To study the runoff of catchments lots of models are available. In this paper a family of stochastic models is presented. The basic concept is that the time of travel—or in other words—the necessary time for a water particle to move in a given distance, is a probabilistic variable. Since isotop techniques have been introduced and generally used in hydrology, the particle concept was again recovered in order to determine via experiments the track of water particles. The description of hydrologic systems or water-balances as wandering models is derived from the particle concept. The method of state space is only one further step in differentiating the state of various particles, concluding in the transition probability matrix. Finally, using the method of least squares for parameter determination stochastic analyses of time series can be executed. In our study, the novelty of the concept of modelling is emphasized.

The Runoff as Γ Distribution

Let the catchment be divided into N different $\triangle F_i$ areas. Let the amount of water the $M_i = h(i) \triangle F_i$ start of from a $\triangle F_i$ area at $t = 0$ time, where $h(i)$ is the height of precipitation in area i. Let the distance be L_i, the distance from area i to section A, the section in question. Distance L_i is divided into r_i intervals. These are :

$$l_1^{(i)}, l_2^{(i)}, \ldots, l_j^{(i)}, \ldots, l_r^{(i)}$$

(Figure 1), respectively.

As mentioned above, times of travel follow the exponential distribution. The conditions of validity of this statement must be analysed in details. The interval of travel at the end of the section for a unit or M_i amount of water should be chosen rather small that the time of arrival at the end of the section for a unit or M_i amount of water should be exponentially distributed.

For the model two velocities must be given, the average and the maximum.

Knowing the maximum velocity and the l_j length of the reach the minimum time of travel can be calculated. The "fastest" water particle (moving with the greatest speed) reaches the end of the j^{th} section by this time; that is the first water particles starting at time $t = 0$ will reach the end of the next section at $t = t_0$. The density function of the exponential distribution, or what is equal, the hydrograph derived from M_i amount of water after one section :

$$f(t) = M_i \cdot \lambda \cdot e^{-\lambda(t-t_0)} \qquad \ldots(1)$$

where, λ is the average time of travel. It is well-known that the sum of independent probability variables of an

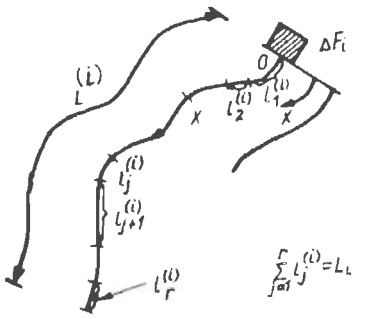

FIGURE 1 : Runoff length of the subcatchment area.

exponential distribution compose a Γ distribution. The M_i volume absolving section r_i will be an r_i order gamma-distribution and the runoff hydrograph will take the following form :

$$Q(t, i) = M_i \frac{\lambda^{r_i} \left[t - T_0^{(i)} \right]^{r_i - 1}}{(r_i - 1)!} e^{-\lambda \left[t - T_0^{(i)} \right]} \quad \ldots(2)$$

where, $T_0^{(i)}$ is the shortest time of travel from area ΔF_i to section A. The average time of travel for each section has been taken implicitly as if λ was the same; this is the reason of the simple form of Equation (2). Some further simplifications can be made if λ is chosen as one.

The complete discharge in section A can be obtained by summing up subdischarges.

The result naturally is equal to the well-known formula of Nash : the difference is only in the starting concepts.

It is worth to study what can be told about the distribution of velocities assuming exponential distribution for the times of travel. Transformation of the density-distribution can be seen in Figure 2. Let the distance l_j be constant, then the following density function, based on the transformation of the probability variables can be obtained :

$$g_j(v_1) = \frac{l_j \lambda_j}{\left(v_{max}^{(j)} - v_1 \right)} \exp \left\{ -\lambda_j l_j \frac{v_1}{v_{max}^{(j)\,2} - v_1 \cdot v_{max}^{(j)}} \right\} \quad \ldots(3)$$

where,

$v_1 = v_{max} - v$;

v = actual velocity;

$v_{max}^{(j)}$ = the greatest velocity in the section;

λ_j = the reciprocal of the average time of travel for the section.

The distribution function is defined in interval $0 \leqslant v_1 \leqslant v_{max}$. Introducing the value of average velocity, v_j is written instead if $l_j . \lambda_j$ and by using expression $v_1 = v_{max} - v$ distribution of velocities can be characterized by the maximum and the average velocity :

$$g_j(v) = \frac{v_j}{v} \exp \left\{ -v_j \frac{v_{max}^{(j)} - v}{v \cdot v_{max}^{(j)}} \right\} \quad \ldots(4)$$

A graphical solution of the transformation can be seen in Figure 2. To model the complete catchment, the discharges, arriving from the subcatchments, must

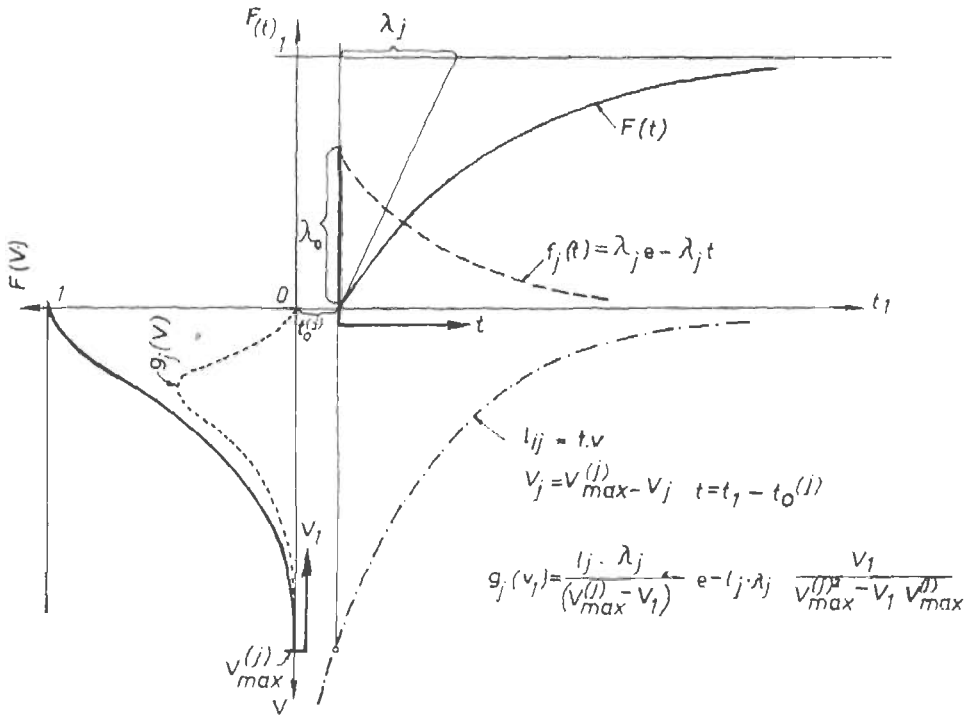

FIGURE 2 : Graphical drafting distribution function of runoff velocities.

be summed up. The division of the catchment area into $\triangle F_1, \triangle F_2, \ldots, \triangle F_i, \ldots, \triangle F_N$ subareas can be seen in Figure 3. Evidently the sum of subareas must give the complete catchment :

$$F = \sum_{i=1}^{N} \triangle F_i \qquad \ldots(5)$$

Moreover, stretch $L^{(i)}$ between the i^{th} subcatchment and section A, is made up of a number of substretches :

$$L^{(i)} = \sum_{j=1}^{r_i} l_{i,j} \qquad i = 1, 2, \ldots, N$$

Due to the effect of a unit impulse (precipitation), starting time $t_1 = 0$ from area $\triangle F_i$, a hydrograph is developing characterized by parameters λ_i and r_i in section A, in a time moment $t_1 = T_0^{(i)}$.

It is reasonable to take the time of travel as constant. So the length of stretches will be different and the number of stretches would vary along section $L^{(i)}$.

It must be mentioned that r_i is not an integer in general, and in such cases the not complete Γ function is used. The discharge from area i—choosing the reciprocal of the average time of travel as unit—along an elementary stretch is :

$$Q^{(i)}(t) = h(i) \cdot \triangle F_i \frac{t^{r_i-1} \cdot e^{-t}}{(r_i-1)!} \qquad \ldots(7)$$

where,

$h(i)$ = the precipitation for area i;

r_i = the number of stretches along distance $L^{(i)}$;

t = relative time coordinate, $t_1 = T_0^{(i)} + t$.

In engineering practice, particularly when the method of parallel runoff lines is applied, the average runoff velocity is a well-proved concept. To the average speed and to distance $L^{(i)}$ an average runoff time can be attached and let it be : τ_i. The expected value of the distribution function is $\bar{t}_i = r_i/\lambda_i$, but by setting λ_i to 1, $\bar{t}_i = r_i$. Among the three time values—$\bar{t}_i$; $T_0^{(i)}$, the minimum runoff time and τ_i, the average time of travel—the following relation exists :

$$\tau_1 - T_0^{(i)} = \bar{t}_i = r_i; \quad \text{when, } \lambda = 1 \qquad \ldots(8)$$

A further simplification is to write the relation between the minimum time of travel and the average

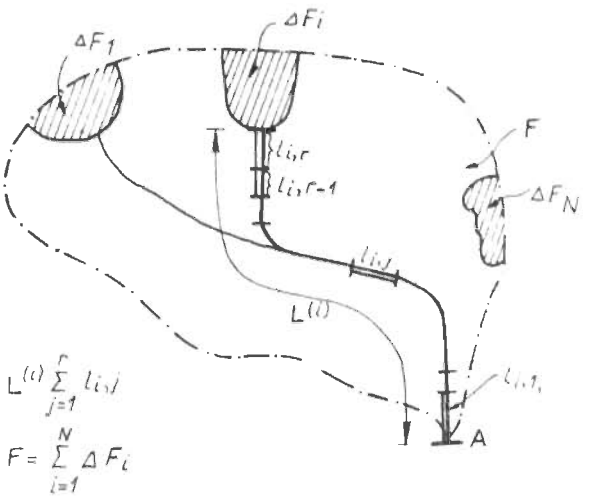

FIGURE 3 : Dividing the catchment into subcatchments.

time of travel as follows :

$$\tau_i - T_0^{(i)} = k.T_0^{(i)} \qquad \ldots(9)$$

where, k is a constant characterizing the catchment. The average time of travel can be obtained by multiplying the minimum time of travel by $(1+k)$: $\tau_i = (1+k) T_0^{(i)}$. The flood wave arriving from a greater distance would be the flatter which is in good accord with practical experiences.

The hydrograph of an area divided into four subcatchments is sketched in Figure 4. In this theoretical example λ was set to 1, k to 0.333 and the values of the $h(i) \cdot \triangle F_i$ were set as follows :

$$T_0^{(1)} = 6; \quad h(1) \triangle F_1 = 1$$

$$T_0^{(2)} = 12; \quad h(2) \triangle F_2 = 2$$

$$T_0^{(3)} = 15; \quad h(3) \triangle F_3 = 1$$

$$T_0^{(4)} = 24; \quad h(4) \triangle F_4 = 2$$

When plotting this figure, the well-known circumstances—that the medion of the Γ density function is at $\bar{t}_i = r_i$, its maximum at $t_{max}^{(i)} = r_i - 1$ and the influexion points are at $t_{inf}^{(i)} = r_i - 1 \pm \sqrt{r_i - 1}$, have been exploited. The superposition of sub-flood waves resulted in the total flood wave.

Runoff Modelling by Random Walk Models

Let a catchment be defined by a closed S boundary

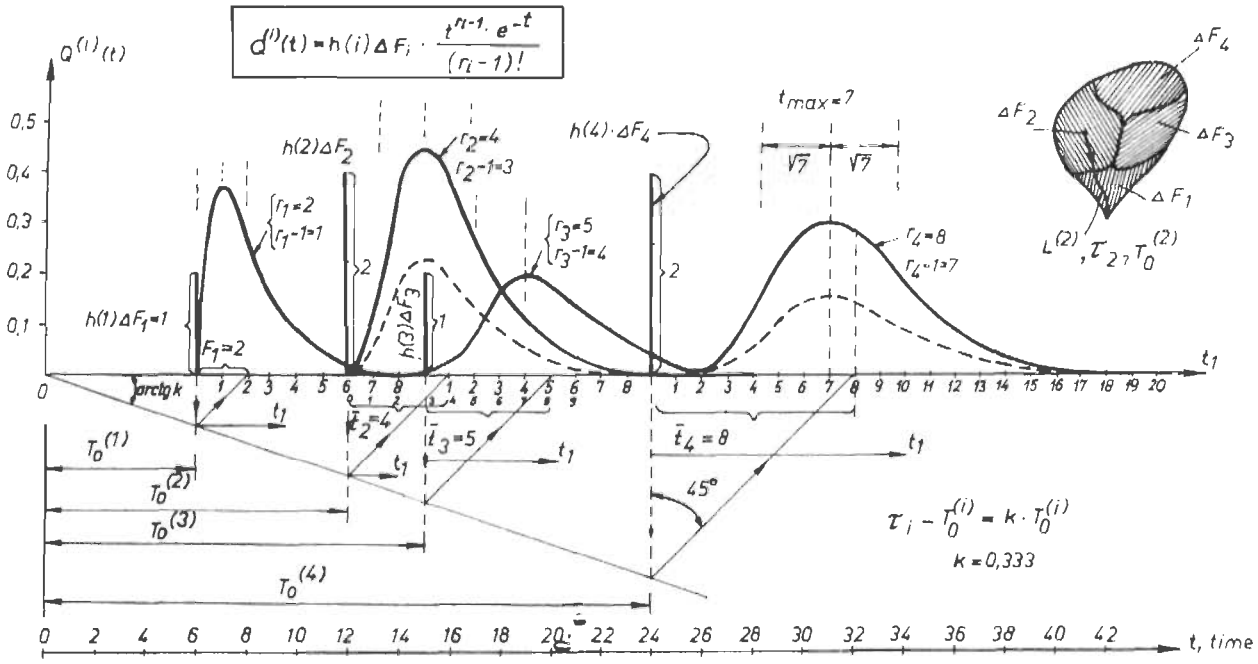

FIGURE 4 : Summation of the subcatchment's flood waves based on the Gamma-model.

(Figure 5). Inside S a system is created, which is connected to the atmosphere and to its geological environment. These are the main connections of the catchment plus the most interesting, the outflow section. These segments are S_1, S_2 and S_3.

In Figure 6, the catchment is briefly shown with its three connection-segments. For the sake of further simplification let S_2 be assumed to be a stream surface thus subsurface inflow and outflow are zero. Thus only segments S_1 and S_3 are of importance, in this case.

When a catchment is considered as a system, the random walk-probability model is as follows. Let the following logical experiment be considered. This will help for a better understanding of this new method of

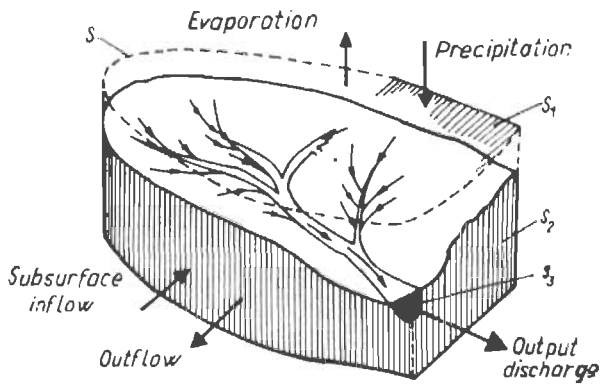

FIGURE 5 : General model for catchments.

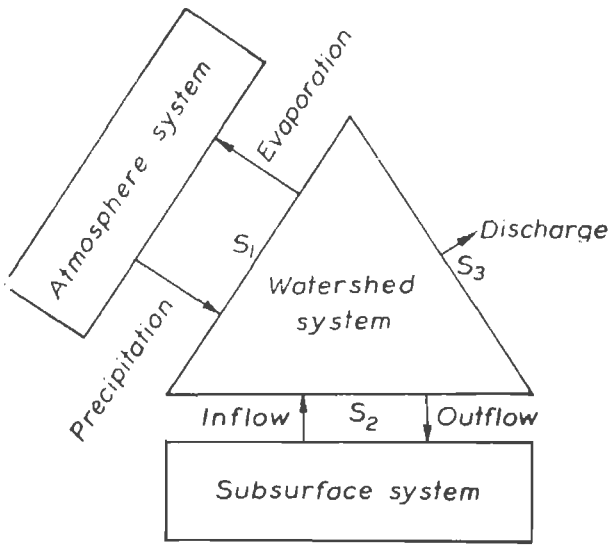

FIGURE 6 : Connection of the catchment system with the atmosphere and the subcatchment system.

thinking. Let some precipitation be fallen in the catchment and one particle enter the system at control section S_1. Follow the way of this particle, not inside the system but through the control sections. Note the time of travel of the particle from section S_1 to S_1 or S_3 (S_2 is excluded from the investigation by our assumptions). Observations should be registered. Let a great number of experiments be executed and a statistical evaluation made from the results. Let $p_A(t)$ denote the

probability of evaporation of the particle at $t = 0$ time instant (i.e., when it leaves the S_1 control segment), and $p_C(t)$ the probability of emerging at control section S_3 at time instant t, i.e., when t has gone. From $t = 0$ to t time instant the probabilities for evaporation and runoff are :

$$P_A(t) = \int_0^t p_A^{(s)} \, . \, ds \qquad \ldots(10)$$

and

$$P_C(t) = \int_0^t p_C^{(s)} \, . \, ds \qquad \ldots(11)$$

The probability of remaining inside the system is $P_B(t)$ and this has the meaning that entering the system at section S_1 at $t = 0$ the particle has not crossed neither S_1 nor S_3. The system and the two control segments form a complete events, system, therefore,

$$P_A(t) + P_B(t) + P_C(t) = 1 \qquad \ldots(12)$$

For the sake of demonstration graphs of $P_A(t)$, $P_B(t)$ and $P_C(t)$ shown in Figure 7 have been set up. $P_C(t)$ is the runoff discharge wave which was chosen to be the gamma density function according to the previous section. Thus $P_C(t)$ is a volume curve.

$P_A(t \to \infty)$ means the percentile ratio of evaporation, $P_C(t \to \infty)$ the percentile ratio of runoff projected for a longer time period (season, years). Assumption $P_B(t \to \infty) \simeq 0$ can be taken, as if all precipitation having fallen onto the catchment would runoff or evaporate at some time.

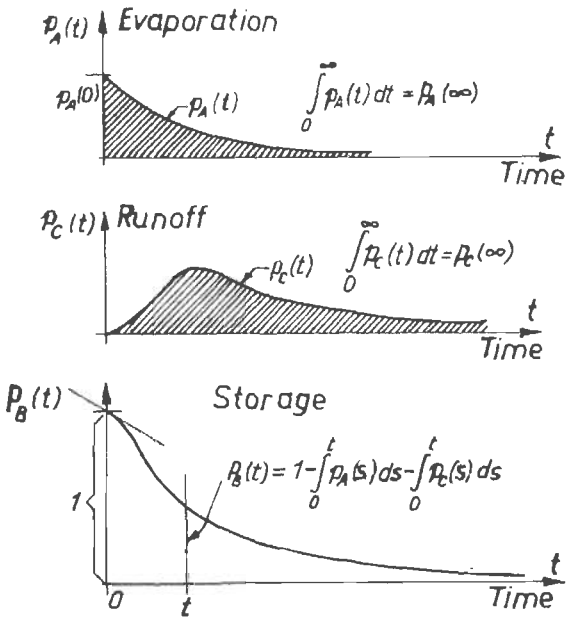

FIGURE 7 : Probabilities for evaporation, runoff and storage.

The random walk solution is much more easy to imagine looking at Figure 8. The particle entering at a $t = 0$ time instant makes a random walk (it does not mean the real motion of the particle). During the random walk sections S_1 or S_3 can be reached by the particle, it leaves for the atmosphere (I) or moves off at the outflow section (II), respectively. Having left, it cannot return—this is a preliminary assumption—and the walls are neither considered to be reflecting surfaces.

The continuous time-axis is divided into 1, 2, ..., i, j, discrete time instants in Figure 8, i.e., a random walk step can be made in these instants.

The state space approach can be obtained by further developing the random walk model as this will be shown in Section 5. On the other hand the random walk model can be restricted to single runoff events and in this way the extension of the gamma model described in Section 3 is obtained, what is a further step compared to Nash's concepts.

Taking Evaporation and Infiltration into Consideration

In the previous section the probability random walk model was presented in general. Now let distance L_i described in Section 2 be considered. Water moves down each $l_j^{(i)}$ distance, in a $\lambda = 1$ average time. Restrict our discussion to length $l_j^{(i)}$ and let it be the complete system in question. At the beginning of $l_j^{(i)}$, $M_i^{(j-1)}$ amount of water enters the system ($M_i^{(j-1)}$ is the number of the particles). Along $l_j^{(i)}$ the particle may evaporate with a probability $P_A(t = \lambda)$ and infiltrate with a $P_B(t = \lambda)$ probability so the particle reaches the end of distance $l_j^{(i)}$ with a probability of $P_C(t = \lambda) = 1 - P_A - P_B$. Therefore, only $P_C(t = \lambda)$. $M_j^{(j-1)}$ from $M_i^{(j-1)}$ will reach the beginning of the next section; the remainder will be evaporated or infiltrated.

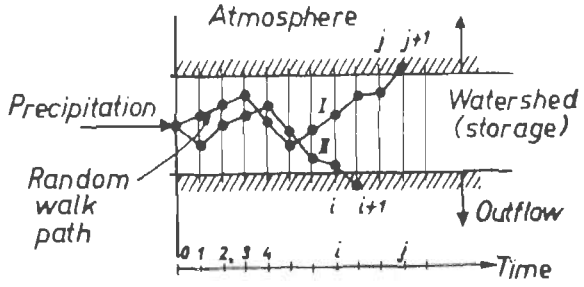

FIGURE 8 : Random walk of the particle in the catchment system.

Let the following notations be introduced: $s = P_C(t = \lambda)$, and $q = P_B(t = \lambda)$. From M_i amount of water starting from area $\triangle F_i$, only

$$M_i^{(j)} = s^j M_i \qquad ...(13)$$

will reach the end of distance $l_j^{(i)}$. Hence reduction of the amount of water will increase exponentially (for $s<1$) when the number of investigated sections is increased. This shows well that *specific discharge decreases when the catchment area increases*; which is in good accordance with real observations.

The volume of the flood wave—as mentioned above—(the number of particles passing on) is decreasing and instead of M_i in Formula 2, $s^r i$. M_i must be substituted. The shape of the flood wave is still the gamma-distribution, for all ordinates are reduced by the same probability.

The subsurface runoff is as follows: from M_i amount of water starting from area $\triangle F_{ij}\, K_{ij} = q \,.\, s^{j-1}\, M_i$ amount infiltrates along distance $l_j^{(i)}$. This will reach section A below the ground surface in a distance L_{ij} (Figure 9).

Subsurface infiltration is also a stochastic process and the model for surface runoff can be utilized for modelling subsurface infiltration. Subsurface runoff composes also a gamma-distribution with $(j-1+m)$ parameters. The average time of infiltration was assumed to be equal to λ^* for each l_k^* distance and this was equal to the average time of travel for surface runoff, $\lambda^* = \lambda$, i.e., the division of distance L_{ij}^* should satisfy condition $\lambda^* = \lambda$. The number of lengths is m in this case. This must be interpreted such as the time of arrival of the particles starting from area $\triangle t_i$ and moving until the j^{th} distance on the surface, and afterwards beneath the surface will compose at section A a Γ distribution and this can be taken as the discharge hydrograph, $Q_{ij}^*(t)$.

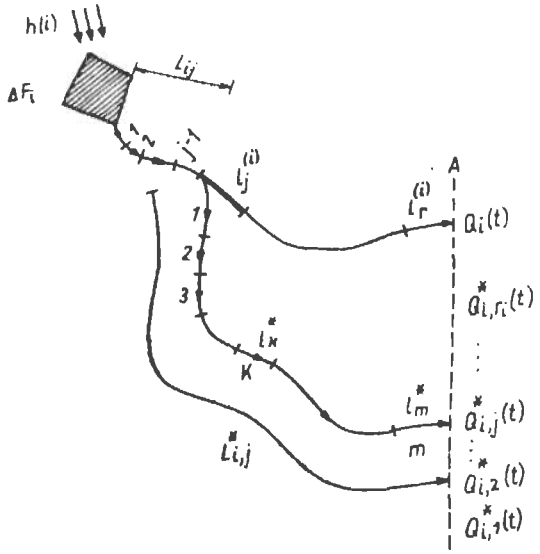

FIGURE 9 : Surface and subsurface streamlines.

From distances $j = 1, 2, \ldots, r_i$ subsurface flood waves will arrive,

$$Q_{i,1}^*(t),\ Q_{i,2}^*(t), \ldots, Q_{i,r_i}^*(t)$$

and their sum with the surface hydrograph $Q_i(t)$ compose a complete flood wave at section A from precipitation $h(i)$ of $\triangle F_i$.

To separate surface and subsurface runoff a theoretical example is shown in Figure 10, with evaporation and infiltration in each distance. Data of this example are : $\lambda = 1$, the probability of evaporation in a unit time is $p=0.1$, the probability of infiltration is $q=0.2$, the probability of passing on is $s=1-p-q=0.7$, the ratio of runoff velocities is $k=2$ [Equation (9)].

The ratio of average runoff velocities on the surface and beneath it was taken to be $\bar{v}/\bar{v}^* = 5$, while the maximum subsurface velocity was a fifth of the maximum surface velocity $\bar{v}_{max}^* = 1/5\ \bar{v}_{max}$. From area $\triangle F_i$ a unit amount of water [$M = h(i)\ \triangle F_i = 1$] was emitted. Concluded from the above that the ratio of surface runoff is 1. $s^i = 0.7^4 = 0.24$. The amount of subsurface water is composed of the total infiltration along the four lengths. The percents of M_i for each distance from up to down are 20, 14, 9.8 and 6.85 respectively. The number of distances from up to down was 20, 15, 10, 5 when λ was equal to 1. Surface and subsurface sub-flood waves can be seen in section B of Figure 10. The summation of the flood waves is in section C. The evaporation for the total runoff length was about 26 percent.

The example shows clearly, that if the subsurface velocity is chosen high a secondary maximum is generated by the subsurface runoff.

The model described previously can be attacked because evaporation and infiltration were not similar along the runoff length. Water on agricultural fields, or in forests is accumulated first in surface depressions, then in little ditches, afterwards in river beds. The described Γ model, combined with evaporation and infiltration is rather convenient to characterize runoff conditions of such valleys.

Let a valley side—a unit wide—be divided into r number of l_j lengths (Figure 11), where the average

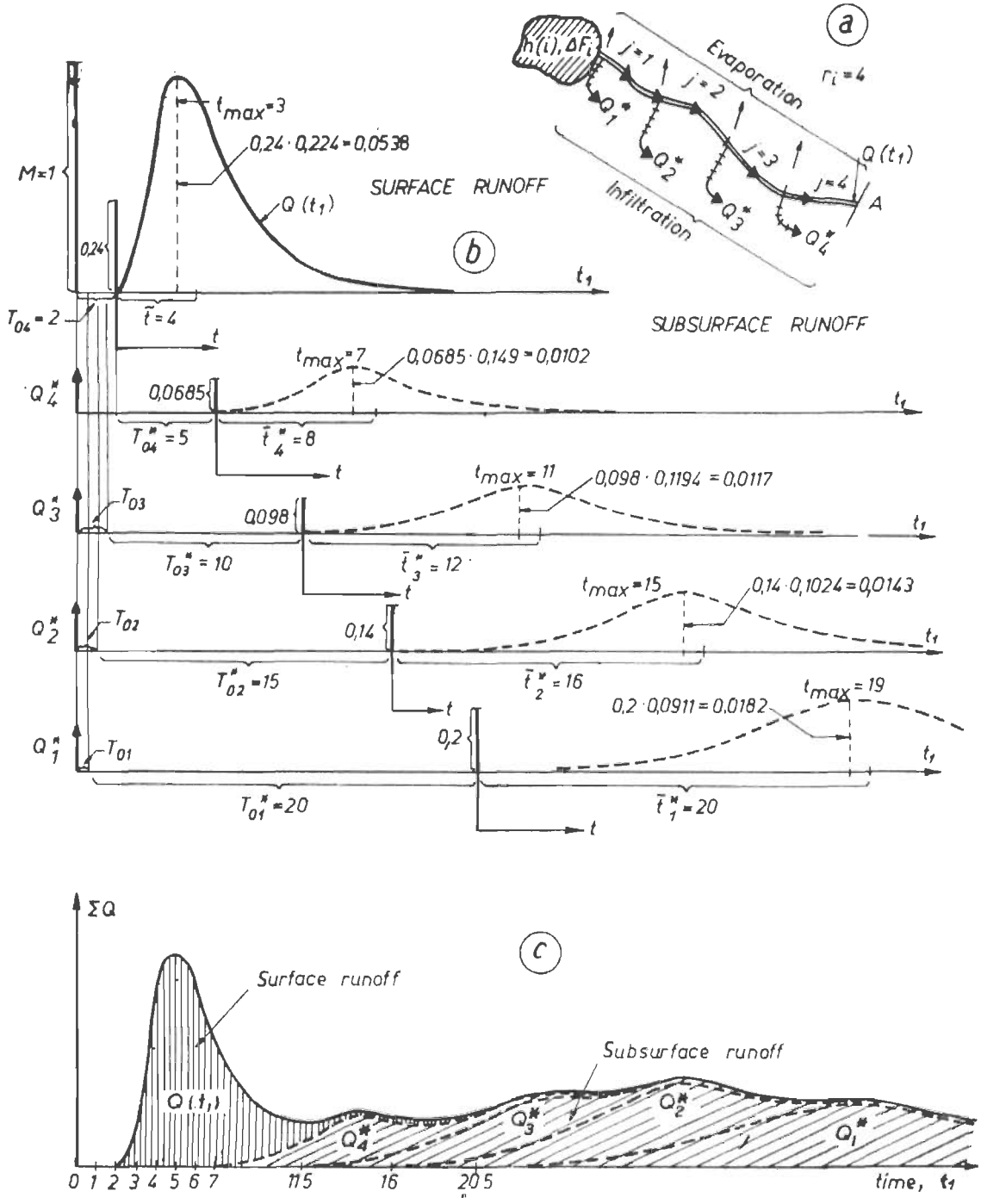

FIGURE 10 : An example for presenting the hydrographs of surface and subsurface flood waves.

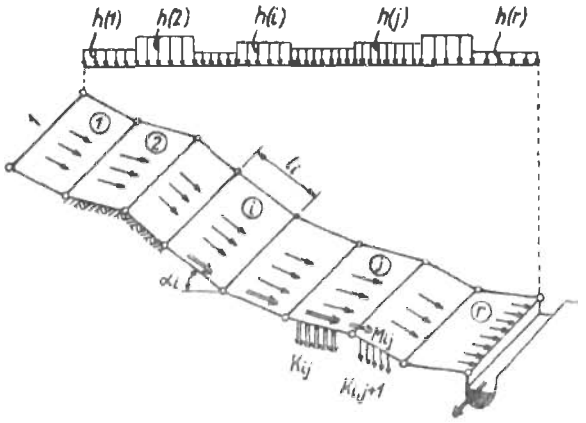

FIGURE 11 : Schematic diagram of an inhomogeneous slope.

time of travel for each l_j length is equal to λ [$\lambda_1 = \lambda_2 = \ldots \lambda_j$]. But let the probabilities for s and q be different:

$s_1, s_2, \ldots, s_j, \ldots$, and $q_1, q_2, \ldots, q_j, \ldots, q_r$

and the $s_j + q_j \leqslant 1$ condition should also be fulfilled for each j.

The M_i amount of water arriving from the i^{th} length $M_i = h(i)$. $l_i \cos \alpha_i$ gives the following runoff and the infiltration for the j^{th} length

$$M_{ij} = \prod_{k=1}^{i} s_k \, M_i \qquad \ldots(14)$$

$$K_{ij} = q_j \prod_{k=1}^{j-1} s_k \, M_i \qquad \ldots(15)$$

(π is the symbol for production). (Naturally, $i < j$ has been assumed). The flood wave of the surface runoff is again a Γ distribution with $(j-i)$ parameters. At the foot of the slope the Γ distributions with $(r-i)$ parameters must be summed to obtain the total flood wave.

State Space Approach for the Description of Runoff Conditions of Catchments

The mathematical description of stream networks for a catchment are well-known. The graph-theory is a rather good aid in this sense. Geometric interpretation of a catchment is characteristic for runoff. The graphs are not only convenient as geometric interpretations, but the inherence of runoff sequence can also be modelled by them. Simulation of surface and subsurface runoff based on probability theory was shown in the previous sections. The theory of graphs can be here regarded as an additional tool. The next step is to follow the way of a water particle appearing in the catchment as precipitation by a random-walk model. On the other hand, the methods of general systems theory have been proved rather efficient in the field of applied hydrology. The state space approach represents additional possibilities in this field. Moreover, relations of the graph theory offer good visual interpretation. In addition, the knowledge of graphs (matrix representation, the state matrices and the state graphs) is essential.

The essence of the method to be introduced is the following : the particle precipitating in the catchment can be found in different states in certain t_1, t,..., etc., instants, where the states can be referred to the location of the particle, e.g., the particle is in the river bed under the surface (has evaporated into the atmosphere) has passed through the outflow cross-section, etc. The states are presented as vertices. The edges of the graph are representing the transitions from one state to another.

Mathematical Background

Let the states of the system be expressed by the vector $\underline{s}(t)$ at a t time instant. The value of vector $\underline{s}$ is $[1 \times \bar{N}]$. Let the system have l number of input channels affected by $u_1^{(t)}, u_2^{(t)}, \ldots, u_l^{(t)}$ inputs at a t time moment. Vector $\underline{u}(t)$ should contain these in a $[1 \times l]$ length. Let the system have m number of output channels, the signals of each at a t time moment should be $y_1(t), y_2(t), \ldots, y_m(t)$, respectively. They are assembled into vector $\underline{y}(t)$ of $[1 \times m]$ length. Transition into state $\underline{s}(t+1)$ from state $\underline{s}(t)$ based on vector $\underline{u}(t)$ must be examined in details. Without any restriction, the values of t can be taken as equidistant periods, i.e., to have the $\underline{s}(t) - \underline{s}(t+1)$ transition it is sufficient to apply discrete summation.

Let the realisation of the state be treated first : in a general matrix form

$$\underline{s}(t+1) = \underline{\underline{A}}\,\underline{s}(t) + \underline{\underline{B}}\,\underline{u}(t) \qquad \ldots(16)$$

where, $\underline{s}(t+1)$ is the state vector and where $\underline{\underline{A}}$ is $[n \times n]$ and $\underline{\underline{B}}$ is $[n \times l]$; elaborating:

$$\begin{bmatrix} s_1(t+1) \\ s_2(t+1) \\ \vdots \\ s_i(t+1) \\ \vdots \\ s_n(t+1) \end{bmatrix} = \begin{bmatrix} a_{11}a_{12}\ldots a_{1n} \\ a_{21}a_{22}\ldots a_{2n} \\ \\ \underline{\underline{A}} \\ \\ a_{n1}a_{n2}\ldots a_{nn} \end{bmatrix} \cdot \begin{bmatrix} s_1(t) \\ s_2(t) \\ \vdots \\ s_j(t) \\ \vdots \\ s_n(t) \end{bmatrix} + \begin{bmatrix} b_{11}b_{12}\ldots b_{1l} \\ b_{21}b_{22}\ldots b_{2l} \\ \\ \underline{\underline{B}} \\ \\ b_{n1}b_{n2}\ldots b_{nl} \end{bmatrix} \cdot \begin{bmatrix} u_1(t) \\ u_2(t) \\ \vdots \\ u_j(t) \\ \vdots \\ u_l(t) \end{bmatrix} \qquad \ldots(17)$$

It is much more convenient for computational purposes to use :

$$s_i(t+1) = \sum_{j=1}^{n} a_{ij} a_j(t) + \sum_{j=1}^{l} b_{ij} u_j(t) \qquad \ldots(18)$$

The above expression is not new, and the first part of it shows clearly the utilisation of the probability transition matrix for the description of transitions from one state to another.

The $\underline{\underline{A}}$ matrix can be interpreted as a transition probability matrix. Naturally, in this case either $\underline{\underline{B}} = 0$ or $\underline{u}(t) = \underline{O}$, or both. In certain cases the output, for example the discharge in a section, can be interpreted as a state. More exactly, one of the elements of the list referring to the states of the system will be the outflow which is also characteristic for the system. *By this transcription of (Equation 16) the classical unit hydrograph method can be obtained.* The second part of (Equation 16) will express the above assuming $\underline{\underline{A}} = \underline{O}$. [In the case of real physical systems the assumption of $\underline{s}(t = 0) = 0$ is rather seldom]. Or if $n = 0$, the classical convolution equation can be obtained.

It can be seen that Equations (16), (17) & (18) describe a time invariant linear system, and can be treated as its subcases.

The discussion of non-linear systems would exceed the frames of this paper and it is not touched for this. However, with a simple contribution the time variant description of the system can be obtained, when $\underline{\underline{A}}$ and $\underline{\underline{B}}$ the so-called *characterizing matrices* are taken to be time variant, i.e., $\underline{\underline{A}}(t)$ and $\underline{\underline{B}}(t)$ are applied, in which $a_{ij}(t)$ and $b_{ij}(t)$ pivot elements are used. After these (18) takes:

$$s_i(t+1) = \sum_{j=1}^{n} a_{ij}(t)\, s_j(t) + \sum_{j=1}^{1} b_{ij}(t) u_j(t) \quad \ldots(19)$$

Abandoning one or another part of this expression *the time variant state probability model* or *the time variant unit hydrograph approach* can be obtained. Referring to our model state $s_i(t)$ is taken as the amount of water being at point i of the area in a (t) time instant. The relation of the i^{th} point and others is presented by the stream graph. More exactly, this means, that it was determined to what places water can move from place i which was assumed to be a vertex. In general all points can be in connection with each point, so n^2 stream arches can be imagined but lots of these have no reality, or in other words, the probability of streaming along that arch is zero, and just for the sake of homogeneous interpretation the probability of the amount of water passing through is also zero.

In the water network of the catchment the relation between excess rainfall and runoff is characterized by a system, which is distinguished by its states time by time ($t = 0, 1, 2, \ldots$). More exactly, let the states be the water amounts at each vertex, i.e., the storage.

Let a_{ij} amount of water flow through arch (ij) from i to j in a Δt time increment if the stored amount of water was unity. When Δt is set to 1 then $s_i(t)$ amount of water is in vertex i in a t time moment and $a_{ij} . s_i(t)$ would flow to vertex j, where, $s_j(t)$ is increased by it to $s_{ij} . s_j(t)$ and in $t+1$ time increment this amount will be $s_j(t+1) = s_j(t) + a_{ij} s_i(t)$. This is the situation with vertices i and j and to obtain a complete $s_j(t+1)$, all effects must be integrated. Besides to compute $s_j(t+1)$, water particles moving toward several other vertices must be considered as well.

Edges of the graph can be determined in advance and due to the nature of free concentration of water, the channel network of a catchment can always be transformed to such a *tree*.

Only these variations have been examined so for : only converging were considered during this investigation. An essential part of the computations is that the amount of water passing through at a vertex (or subarea) is proportional to the stored amount of water, it is the p^{th} part of it, and p is : $0 \leqslant p \leqslant 1$. From the stored amount at vertex i (precipitation + concentration) an amount $s_i(t)$ with probability P would stream to other areas, the percent of leaving the area i is $p_{ij_1} + p_{ij_2} + \ldots + p_{ij_m}$ and the percent of remaining in that area is

$$1 - p_{ij_1} + \ldots + p_{ij_m} = p_{ii}.$$

It can be concluded by physical reflections and by probability theory that :

$$p_{ii} + p_{ij_1} + p_{ij_2} + \ldots + p_{ij_m} = 1 \quad \ldots(20)$$

The p numbers will characterize the runoff conditions of the catchment, i.e., the probabilities of transit streaming. These p numbers will be the a_{ij} pivots of matrix $\underline{\underline{A}}$ and as mentioned before, more of these will be impossible arches for streaming. The structure of matrix $\underline{\underline{A}}$ is such that in its main diagonal $p_{ii} - s$ are located, i.e., the probability of not moving and the sum of the row elements is 1, e.g., a first order stochastic matrix.

An Example for Runoff Simulation

The examined graph can be seen in Figure 12. 13 vertices—states—were assumed where particles may be standing. The transition of one state to another is

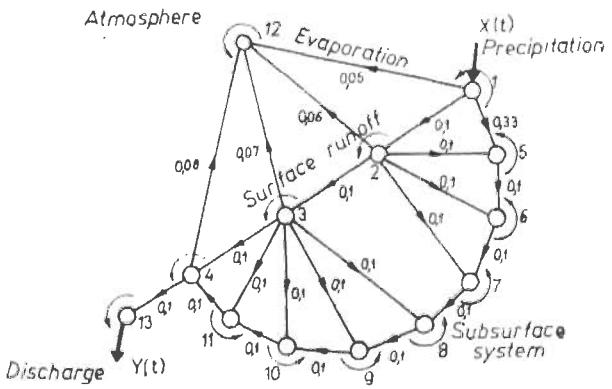

FIGURE 12 : A graph scheme to model the catchment.

represented by the edges. On these edges the probabilities of transition are indicated. Vertices 1, 2, 3, 4 are states for surface runoff in several parts of the catchment. Vertices 5, 6, 7, 8, 9 and 10 stand for states of residence of the particle under the surface. Vertex 12 represents the water evaporated into the atmosphere. Vertex 13 sums the complete volume of surface water. This can be taken as the change of the amount of water located in vertex 4.

Matrix representation of the state graph shown in Figure 12 is the matrix $\underline{\underline{A}}$ [Equations (16), (17), (18)]. It is a state-transition probability matrix at the same time. The used transition probabilities—to give an example—are only approximations to physical reality, but do not refer to a real catchment.

For the simulation of change of states and the amount of water flowing down at vertex 4 an ALGOL program was set up for an ODRA 1204 computer. This makes possible to calculate any other transition-probability matrix as well. The computer time for 13 vertices and 25-30 time increments did not exceed 1 minute. Some further simplifications are included in the model. To switch over from one state to another is proportional to the amount of water that has been flown through a vertex. It must be mentioned that this rough approximation may be refined if a well constructed state graph is set up. (For example, the circuit defined by vertices 2, 6, 7, 9, 2 and 8 is a feed-back loop).

In Figure 13 time variations of water amount crossing vertices 1, 2, 3 and 4 are presented in two versions. First flood waves (I) caused by a precipitation of 100 units, then by 100 units and again after 5 time units by 50 units (II) are shown.

Besides precipitation subsurface storage as an initial state at $t = 0$ was an input as well. The variation of subsurface water resources at vertices 5, 6, 7 and 10 is presented for case I in Figure 14.

In Figure 15 the total amount of water at vertex 13, coming from the catchment and the total amount of water evaporated at vertex 12 has been plotted.

A general description of runoff conditions by state graphs is rather flexible.

The mathematical bases are properly elaborated; the relation between the transition probability matrix and

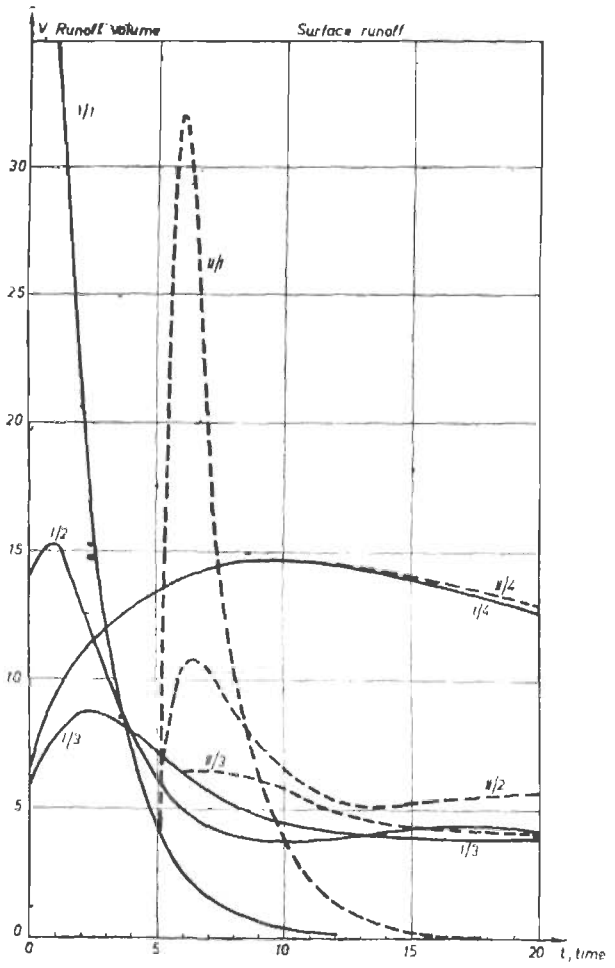

FIGURE 13 : Surface runoff for a given example.

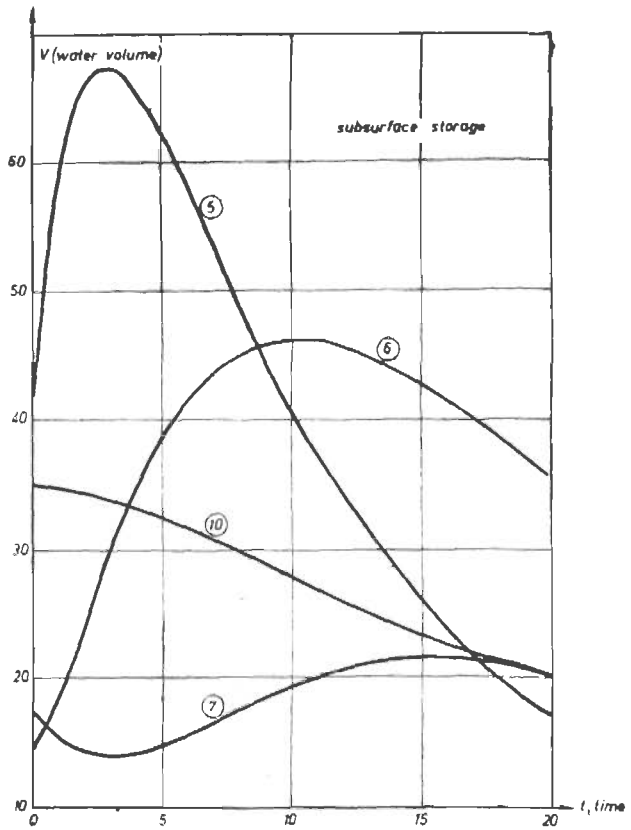

FIGURE 14 : Variation of subsurface resources.

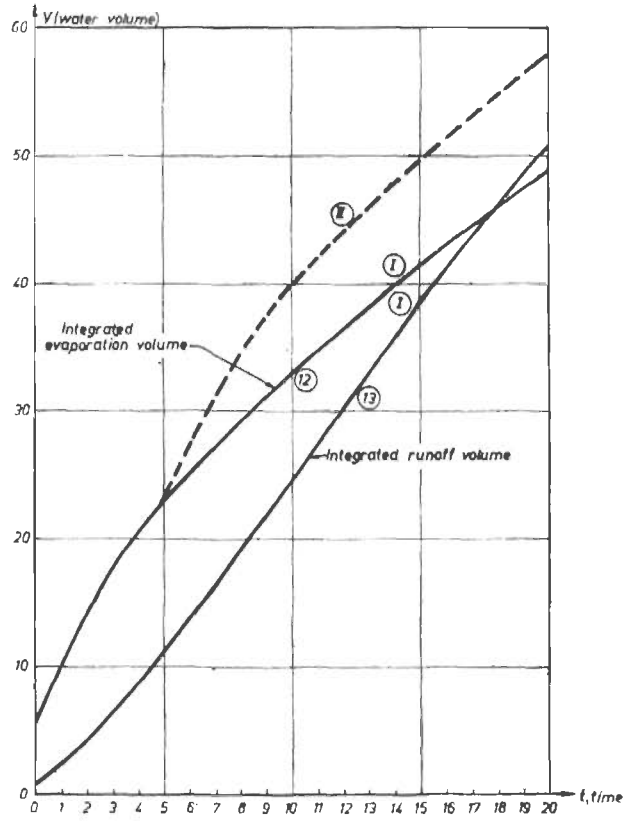

FIGURE 15 : Time series of evaporated and infiltrated water volumes.

the graph scheme, describing the wandering of the particle is a good example to show the complete harmony of stochastic and deterministic (physical) models. Moreover, space invariance, subsurface runoff and evaporation is considered as well, by the model.

Time invariant models can be obtained by non-stationary transition probability matrices. Finally, only the possibilities of using the method were discussed in this paper. Fitting it to natural hydrological processes is the task of further research.

Summary

Theoretical models of various approaches have been presented for catchment modelling. The cascade model can be obtained on a probability basis too (Section 2). A random-walk model of the particle was shown in Section 3. Uniting the random-walk model and the probability model the surface and subsurface runoff can be handled simultaneously. Subsurface runoff is approximated also by a probability model in this case (Section 4). The general state space approach has been shown in Section 5 and a convenient method is given for flexible, computer oriented simulation of the catchment.

In this paper the possibilities of a general system analysis have been discussed. Probability models set up by considering physical processes indicate harmony among the different approaches.

References

(1) DOOGE, J.C.I. : "A General Theory of Unit Hydrographs." J. of Geophys. Res., Vol. 64, No. 2, 1959, pp. 241-256.

(2) JAZWINSKI, A.H. : "Stochastic Processes and Filtering Theory." Academic Press, New York, London, 1970, pp. 1-376.

(3) KAUFMANN, A. : "Des points et des flèches...la théorie des graphes." Dunod, Paris, 1969.

(4) NASH, J.E. : "A Unit Hydrograph Study, with particular Reference to British Catchments." Proc. Inst. Civ. Eng., Vol. 17, 1960, pp. 249-271.

(5) QUIMPO, R.G. : "Structural Relation Between Parametric and Stochastic Hydrology Models." Proc. Int. Symp. Math. Models in Hydrol., Warsow, 1971, pp. 301-312.

(6) ZOCH, T.R. : "On the Relation between Rainfall and Streamflow." Monthly Weather Review 1934-37, Vol. 62, No. 9, pp. 315-322; Vol. 64, No. 4, pp. 105-121; Vol. 65, No. 4, pp. 135-147.

Streamflow Synthesis of Ungauged Area

THAIPUCK THAMMONGKOL
Hydrologist
Mekong Secretariat, Bangkok, Thailand.

SYNOPSIS

The study deals with the estimation of river flows from an ungauged area. Estimation of runoff from ungauged areas is one of the major problems encountered in water resource management, and one that commonly has to be faced in forecasting reservoir inflow and river flow at downstream points. This is especially true in developing countries, where hydrologic measuring stations are sparse. In the present study, the SSARR (Streamflow Synthesis and Reservoir Regulation) hydrologic model was used to simulate the flows from the sector of the Mekong basin between Luang Prabang and Pa Mong, a catchment area of 31,000 sq km. Four rainfall stations, two on the edge of the basin and two within the basin, were used in the study. For the purpose of the present exercise, flow values synthesized from rainfall data were compared with the estimated actual flow, obtained in this case from the records of the Luang Prabang and Pa Mong mainstream measuring stations, to test the validity of the method, its shortcomings and ways of improving the technique.

Introduction

In the hydrologic study of a water resource development project, one common problem faced by hydrologists and engineers is insufficient streamflow data. This is true particularly in developing countries where streamflow data are scarce or even not available at all for some areas, especially small basins or tributaries. Fortunately, rainfall data are available, in most cases, with reasonable length of record, and this provides a means of estimating river flows.

The purpose of this study is to demonstrate one possible way of simulating streamflow from rainfall data for an ungauged area. This can be very useful, for example, in flood forecasting and in estimating reservoir inflows for water resources management. Furthermore, once the basin parameters have been established, a unit hydrograph could then be derived for this particular basin.

The Study Area

The study area, part of the lower Mekong basin, lies between Luang Prabang and the site of the proposed Pa Mong Dam, about 20 km upstream from Vientiane (Figure 1). There are only two streamflow measuring stations, located at the upper and lower end (at Luang Prabang and the Pa Mong Dam site) of this catchment area, the boundaries of which are shown with a dotted line in Figure 1. This area, 31,000 sq km, of which approximately 75 percent is in Laos and 25 percent in Thailand, contributes a not inconsiderable part of the Mekong mainstream flow at Pa Mong. The area is mostly mountainous with a range of elevation from 160 m up to 2,100 m above mean sea level. The length of the Mekong in this Luang Prabang-Pa Mong reach is 410 km.

Basic Data

Streamflow Data

(1) Mekong at Luang Prabang (1950 to date)
(2) Mekong at Pa Mong Dam site (1967 to date)
(3) Mekong at Vientiane (1913 to date)

Rainfall Data

Of the 16 rainfall stations in the area four were

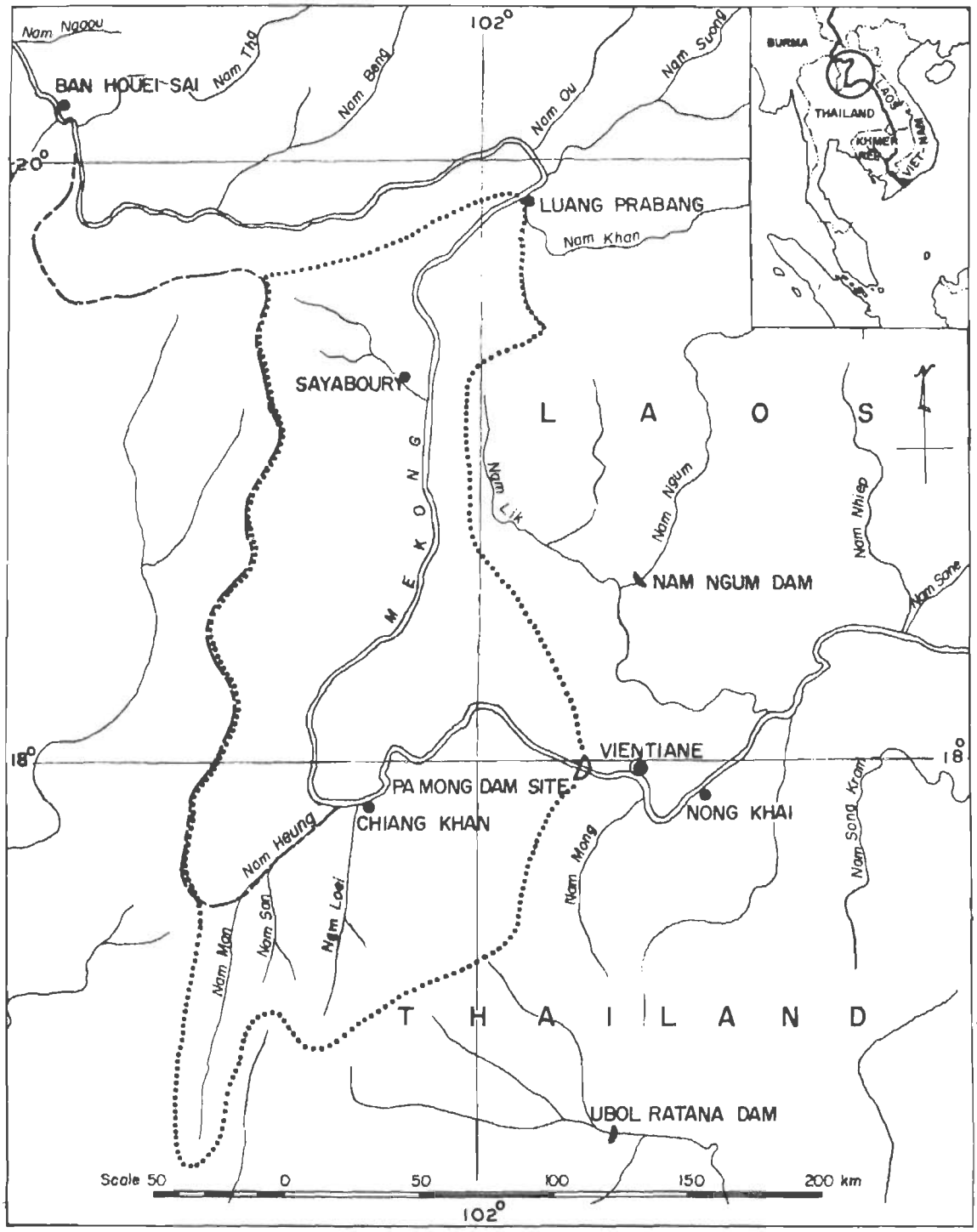

FIGURE 1 : Location map.

selected :

(1) Luang Prabang (1920 to date)

(2) Sayaboury (1963 to date)

(3) Chiang Khan (1913 to date)

(4) Vientiane (1920 to date)

Streamflow Simulation

The Hydrologic Model

During the past two decades a number of hydrologic models have been developed to simulate streamflow from rainfall data, ranging from the most general to those imitating special aspects of the river system. The SSARR model, (Streamflow Synthesis and Reservoir Regulation) is one such model, developed by the North Pacific Division of the U.S. Corps of Engineers in 1957, to synthesize all the various hydrologic and hydraulic process of a river system. The model was developed on a general basis so it can be used for almost any configuration of basins, sub-basins, channel reaches, lakes and reservoirs. In the SSARR watershed model, the various aspects of water balance of the drainage basin, such as rainfall, soil moisture, surface storage, subsurface storage and ground water storage, are taken into consideration.

Streamflow Simulation

The flow at the site of the proposed Pa Mong Dam was considered as having two components : the routed flow from above Luang Prabang and the added flow from the ungauged area between Luang Prabang and Pa Mong, the so-called Pa Mong local, which was computed from rainfall.

Due to the limited time available, only five years of data (1969-1973) were used in the calibration of the basin parameters. Pa Mong data were used instead of Vientiane data to avoid the complicated overbank flow problem, even though the length of records is much greater for the latter station. The river and basin configuration is shown in Figure 2.

Channel Routing

The temporal rate of change of streamflow in a river reach is evaluated by successive routings through increments. Outflow from each increment is used as inflow to the next downstream increment. The routing equation originally used with the SSARR programme is expressed as

$$Ts = \frac{KTS}{Q^n}$$

in which, Ts=Time of storage per increment per hour

KTS=a constant

Q=discharge in m^3/sec

n=a coefficient.

In general, the derivation of the routing parameters should begin with the above formula and assumed values taken from a channel with similar characteristics.

In the case of the Mekong, the routing parameters were originally developed based on the above equation, as shown in Figure 3. However, experience has shown that the variable time of storage curve in relation to discharge adapted from the equation type curve is more suitable and practical to the Mekong's channel characteristics. Therefore, this flexible curve was developed and used in the study as shown in Figure 3.

Local Watershed Flow

The local flow from the Luang Prabang-Pa Mong catchment (the so-called Pa Mong local) was derived by synthesizing the flow from rainfall over the basin. Steps of computation are as follows :

(1) Evaluate the weighed rainfall over the basin, taking into account the time distribution of rainfall.

(2) Evaluate the moisture input or the amount of rainfall contributing to runoff, from the relationship of SMI (Soil Moisture Index), rainfall intensity and the percent runoff, (in other words the runoff is determined from the basin rainfall

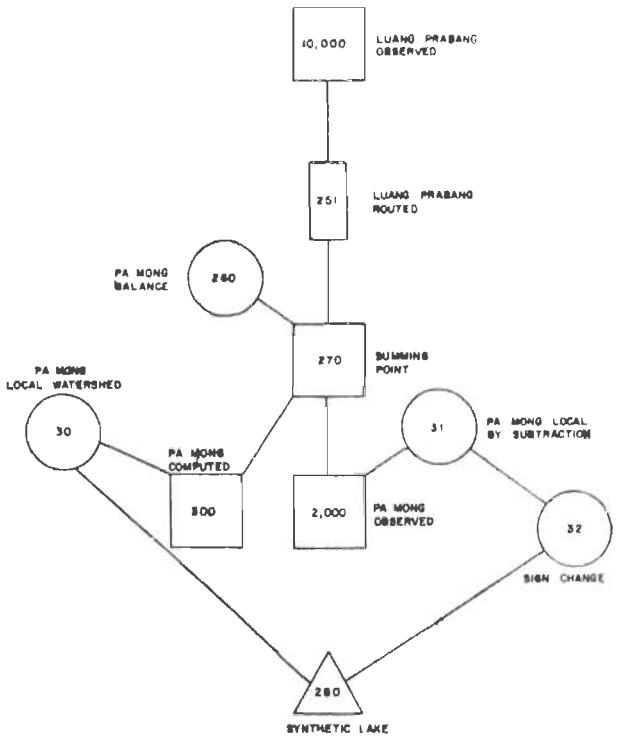

FIGURE 2 : Configuration—Luang Prabang-Pa Mong reach.

minus losses to evapotranspiration, deep percolation and soil moisture replenishment).

(3) Divide runoff into surface, sub-surface and baseflow components.

(4) Route each component of flow separately through successive increments of reservoir-type storage. The number of increments or phases of each component is specified in the basin characteristics.

(5) Compute the final outflow or the local flow from the sub-basin by adding each component of flow.

The computed Pa Mong local flow was compared with the estimated actual flow which is derived directly by subtracting the Luang Prabang routed flow from the Pa Mong flow. The computed flow was then adjusted to match with the estimated actual one by changing parameters or coefficients of the basin such as the weighed rainfall, the SMI curves, the evapotranspiration, the correlation between the surface, sub-surface and baseflow, and the routing characteristics of each component. In practice, the assumed coefficients taken from those of the similar basin were used in the first computation. The basin parameters were then gradually refined until the differences between the computed and observed flows were at the minimum.

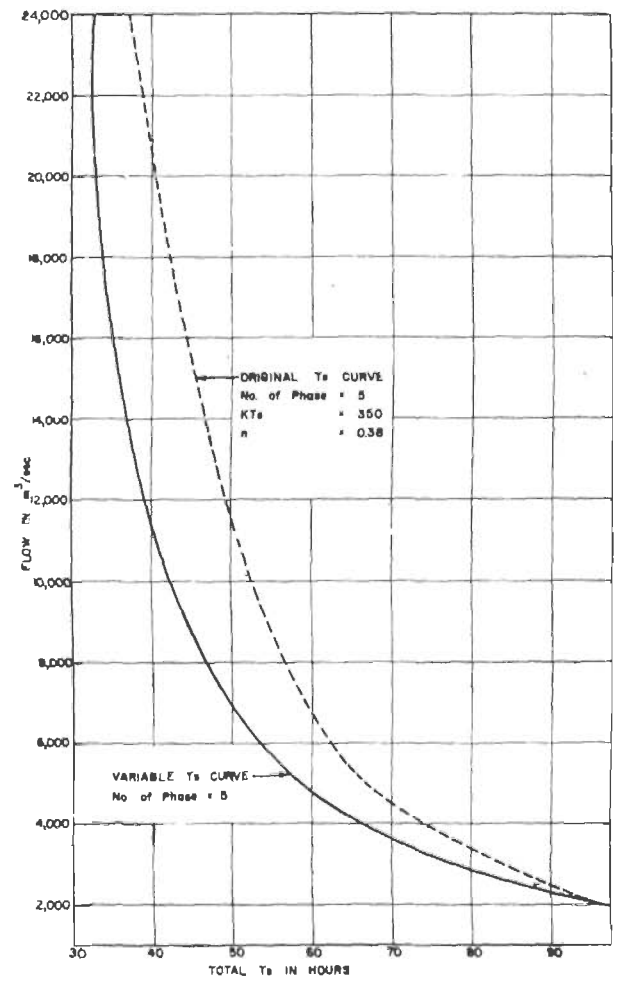

FIGURE 3 : Variable Ts curve—Luang Prabang-Pa Mong reach.

Results

Results were presented as plotted hydrographs from the computer printout as shown in Figures 4, 5 & 6. In each plotting, the streamflow synthesized from rainfall was plotted against the actual Pa Mong local flow, from April through the season of high flows to December. The rainfall input and the deviation of the computed volume from the actual volume of flow from the sub-basin were also included. On the same sheet, the computed discharge at Pa Mong, resulting from the estimated local flow, was also plotted against the observed Pa Mong discharge.

It was noted that the computed local flows from rainfall are in good agreement with those of the actual locals for 1970 and 1973 both in time of occurrence and magnitude of flow. Results for 1969, 1971 and 1972 are rated as only fair. In terms of volume, however, the results are encouraging in that the errors are consistently less than 10 percent, as shown below :

Year	Pa Mong local flow in $10^6 m^3$		Difference from actual flow	
	Computed	Actual	$10^6 m^3$	%
1969	16,200	16,700	−500	−3.0
1970	24,000	23,700	+300	+1.3
1971	15,300	16,100	−800	−5.0
1972	10,500	10,600	−100	−0.9
1973	18,200	17,500	+700	+4.0

The derived watershed parameters are, therefore, considered as reasonable. The obtained parameters are as follows :

Areal Distribution of Rainfall

Station	weight	% weight
Luang Prabang	100	18
Sayaboury	130	24
Chiang Khan	170	31
Vientiane	150	27

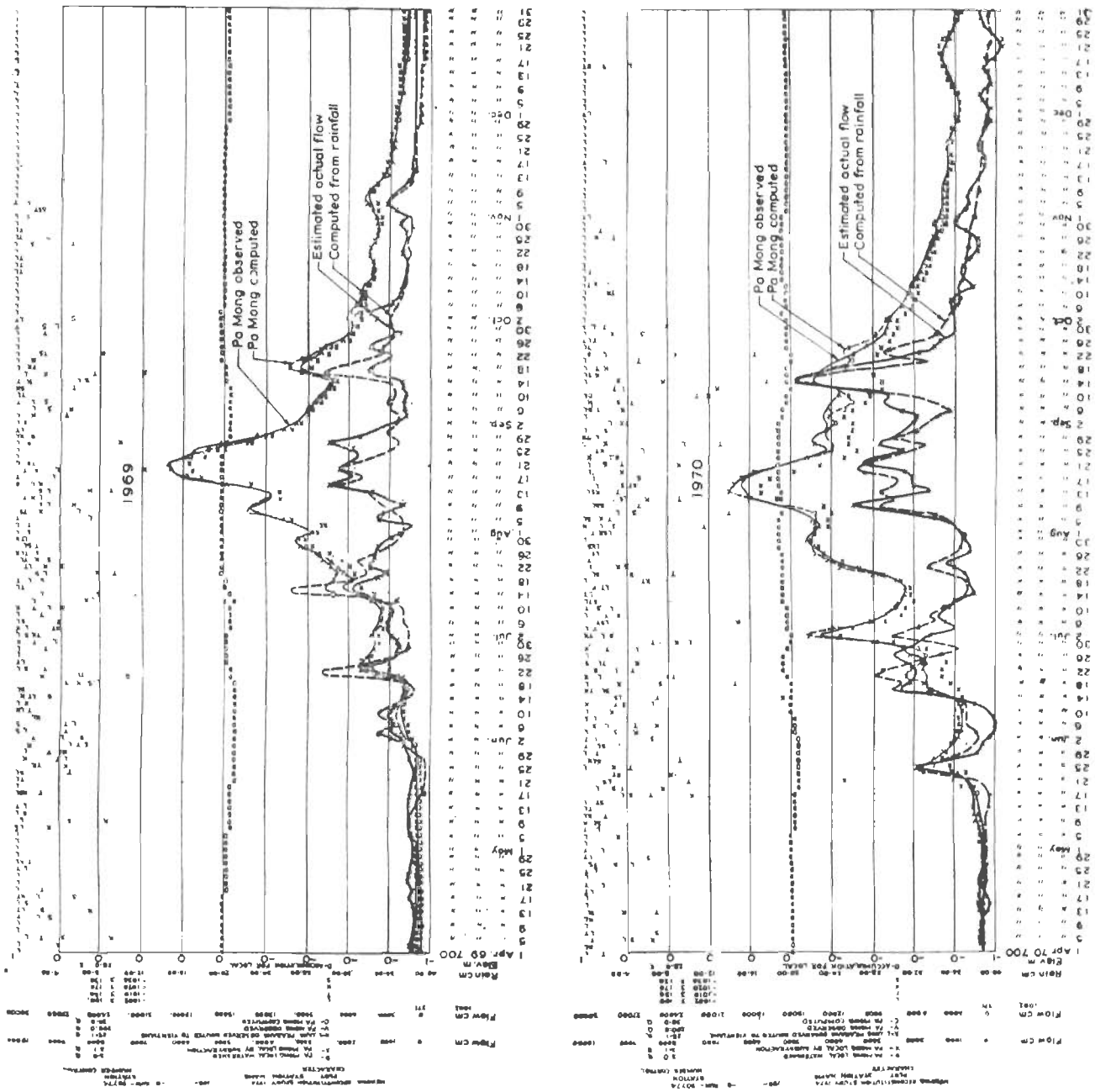

FIGURE 4 : Streamflow synthesis of Luang Prabang-Pa Mong sub-basin, Lower Mekong basin for 1969 and 1970.

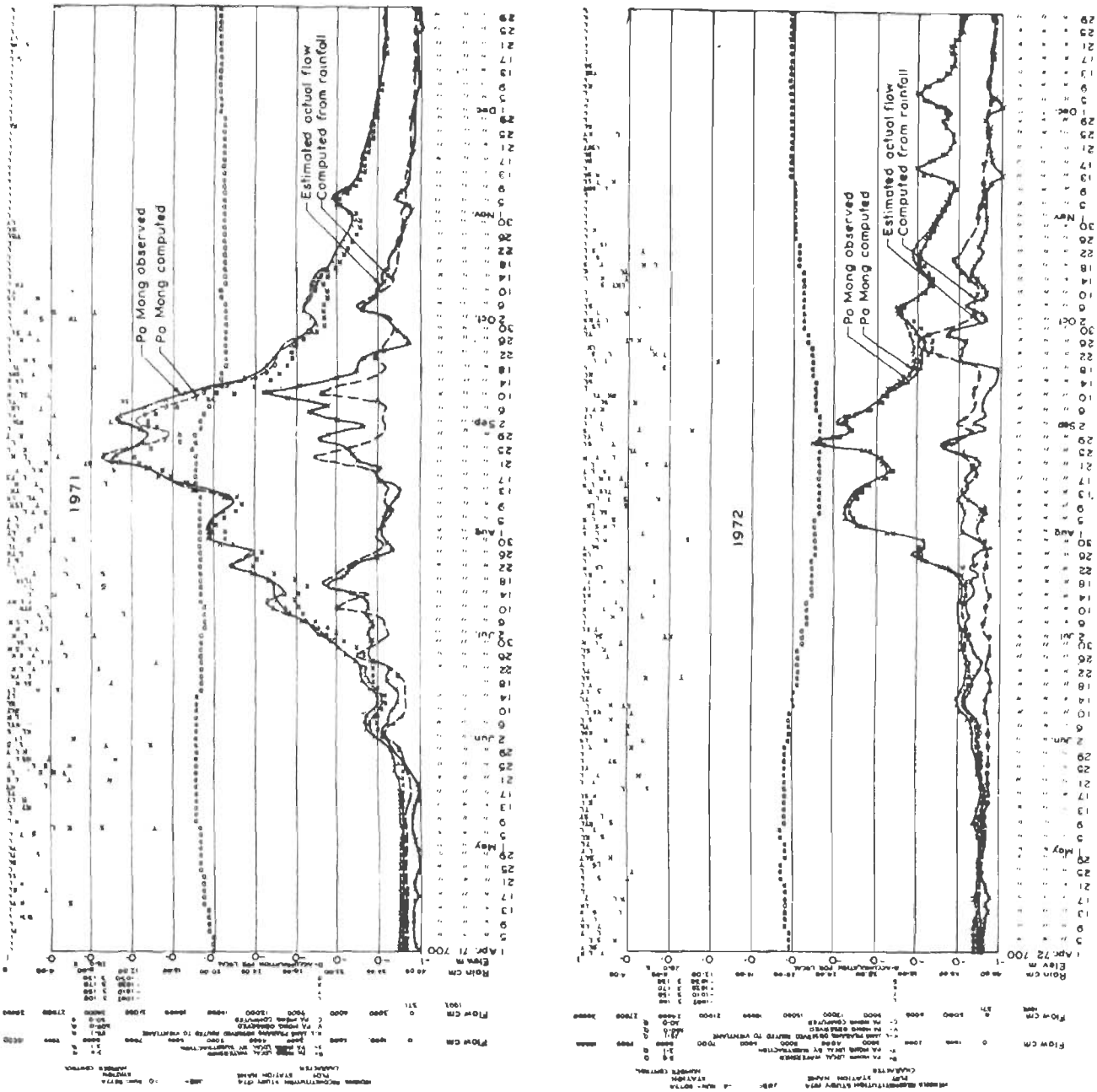

FIGURE 5 : Streamflow synthesis of Luang Prabang-Pa Mong sub-basin, Lower Mekong basin for 1971 and 1972.

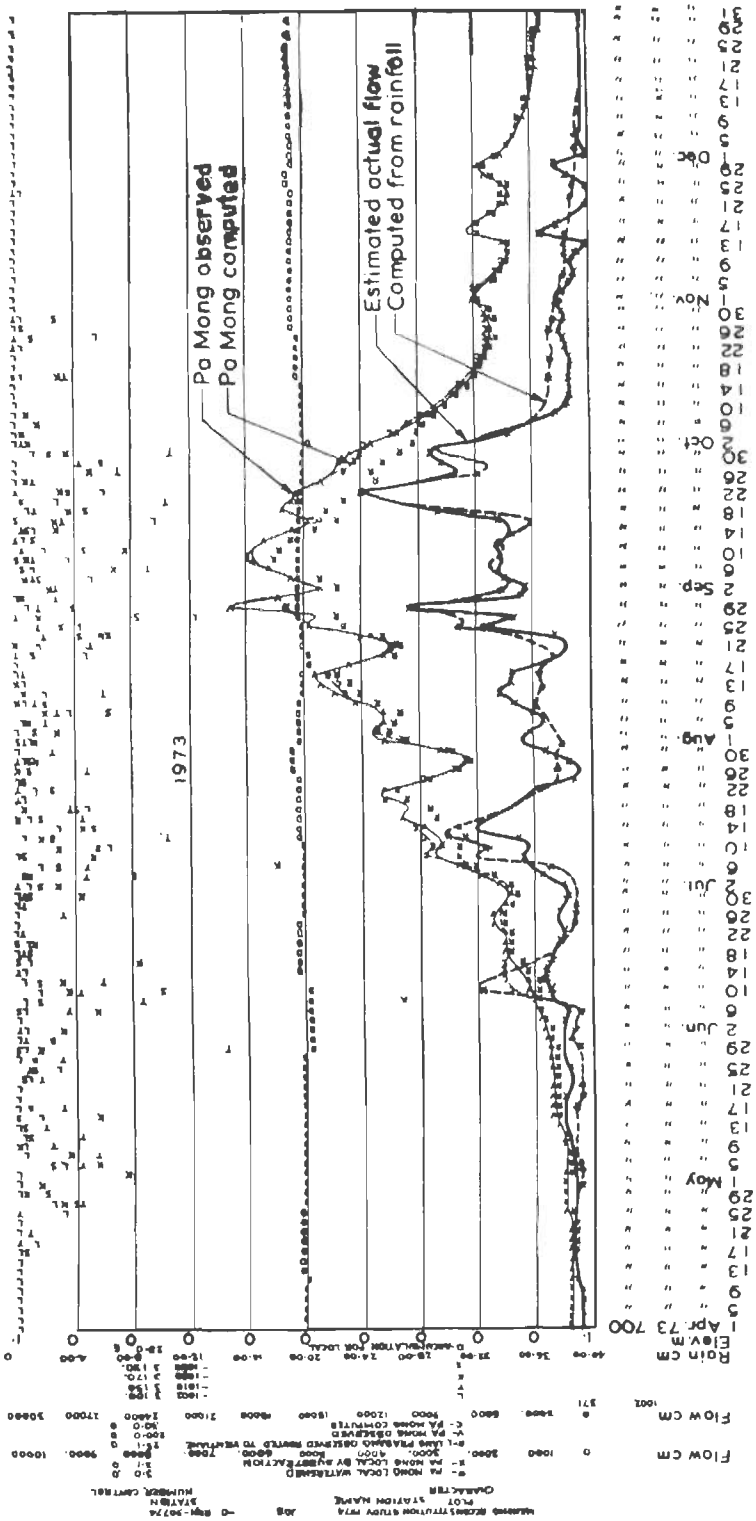

FIGURE 6 : Streamflow synthesis of Luang Prabang-Pa Mong sub-basin, Lower Mekong basin for 1973.

Soil Moisture Index

I = 0.05		I = 0.10		I = 0.50		I = 1.0		I = 5.0	
SMI	ROP	SMI	ROP	SMI	ROP	SMI	ROP	SMI	ROP
0	0	0	2	0	6	0	6	0	14
10	4	5	10	10	32	5	30	5	60
20	14	10	19	15	45	10	54	20	80
30	22	20	36	25	57	20	64	43	100
40	25	30	46	45	66	30	74	999	100
999	35	999	70	999	85	70	98		
						999	100		

I = rainfall intensity in cm/h
SMI = soil moisture index in cm
ROP = % runoff

Evapotranspiration Index

Month	ETI
1	0.30
2	0.32
3	0.45
4	0.50
5	0.52
6	0.47
7	0.48
8	0.46
9	0.42
10	0.40
11	0.33
12	0.29

ETI = evapotranspiration index in cm/day

Evapotranspiration Reduction

Rainfall cm/day	KE %
0	100
1	76
2	58
3	45
4	34
5	26
6	20
7	15
8	12
9	11
999	0

KE = evapotranspiration reduction.

Baseflow Infiltration Index

BII	BFP
0	80
0.3	55
0.6	37
1.0	20
999	20

BII = baseflow infiltration index in cm
BFP = % baseflow.

Surface-Subsurface Separation

Input cm/h	Surface component cm/h
0	0
0.01	0.001
0.1	0.01666
0.2	0.04666
0.3	0.09
0.4	0.14666
0.5	0.21666
0.6	0.3
50.6	50.3

Routing of Surface, Subsurface and Baseflow

Component	No. of phase	Time of storage (h)
Surface	4	13
Subsurface	4	26
Baseflow	5	500

Conclusions

(1) Synthesis of streamflow from rainfall data of the ungauged area is feasible, using the SSARR hydrologic model.

(2) Once reasonably good watershed parameters have been established, they are undoubtedly useful for predicting outflow from any ungauged areas, in connection with reservoir operation, flood forecasting and other hydrologic studies.

(3) A more accurate result could possibly be obtained by sub-dividing the study area into several hydrologically homogeneous sub-areas and employing more rainfall data.

References

(1) NELSON, M.L. and ROCKWOOD, D.M. : "Computer Application to System Analysis, Lower Mekong River." U.S. Army Engineer Division, North Pacific, Portland, Oregon, October 1964.

(2) THAIPUCK, T. : "Study of Evaporation Losses from Proposed Pa Mong Reservoir." Unpublished U.S. Bureau of Reclamation Report, Pa Mong Project, Bangkok, Thailand, July 1967.

(3) ANDERSON, J.A. : "Runoff Evaluation and Streamflow Simulation by Computer." U.S. Engineer Division, North Pacific, Portland, Oregon, December 1969.

(4) SCHERMERHORN, V.P. and KUEHL, D.W.: "Application of the SSARR Model to a Basin without Discharge Record." Unpublished manuscript, presented at the ASCE Specialty Conference, Minneapolis, August 1970.

(5) ROCKWOOD, D.M. and KUEHL, D.W. : "Evaluation Report for Mekong River Basin-wide Flood Forecasting, 1971 Flood Season." U.S. Army Engineer Division, North Pacific, Portland, Oregon, December 1971.

(6) KUEHL, D.W. : "Optimization of the SSARR Coefficients, River and Flood Forecasting, Lower Mekong River." National Weather Service, NOAA, Portland, Oregon, June 1974.

Influence of Probability Analysis on Selection of Design Flood

E. MOSONYI
Professor of Civil Engineering

H. EGGERS
Senior Research Engineer

D. KOBERG
Mathematician

Technical University of Karlsruhe, Karlsruhe, Federal Republic of Germany.

SYNOPSIS

In the current practice design flood is selected mainly on an empirical basis, viz., in most cases with reference to historical flood events. This routine, however, should be changed in every case by using flood probability analyses and, if possible, procedures of risk- and decision-theory. It occurs seldom that the elegant method of a true economic optimization can be applied.

In the entire chain of calculation in many cases the weakest part is the determination of the flood discharge in function of its exceedance probability, since diverse assumptions on probability distribution to simulate nature the best, result in values of very different magnitude.

Examples for discrepancies which may come into being due to uncertainties in the selection of probability distribution will be presented.

Introduction

Comprehensive studies on flood probability have been carried out by the Research Institute for Hydraulic Structures and Water Resources, University of Karlsruhe, during the last years. Peak discharges at more than 200 gauging stations were analysed by using 16 types of distribution functions with diverse methods of estimation of the parameters. Various test procedures (tests of fit and alternative tests) have been applied in order to compare the frequency distribution of observed peak discharges with the theoretical functions.

In this report the results of the study will be presented by answering the question: How great discrepancies in the magnitude of discharge may pertain to the same value of exceedance probability, originated by the application of diverse distribution functions? Thus the influence of selection of the distribution function on the design flood discharge (HQ_T), defined by the recurrence interval (T), can be established.

Data and Mathematics

The evaluation extended to such series of annual peak discharges only, which fulfilled the condition that the Kolmogoroff-Smirnov test analysis justified a significant value of 95 percent (i.e., an error probability of 5 percent) when comparing observed and theoretical frequency distributions. Thus the test of fit was not sufficient to promote decision on selection of a distribution function.

Only series having positive skewness have been considered here. This restriction was based upon a physical aspect. Namely the Pearson-type-III distribution, has a finite limitation in the range of high discharge values when the skewness is negative. Although it is believed that flood discharges must have a physical upmost value, still it is utmost doubtful that the true physical limit would be equal to that of the probabilistic frequency curve.

In order to avoid errors caused by sudden discharge

changes occurring in small creeks gauging stations were abandoned where the mean annual runoff is less than 20 m³/sec. Most series cover a period as long as 30 years and the drainage areas have a size from 100 to 100 000 km².

On basis of conditions mentioned in Table I, 37 flood series have been examined, which satisfied the 5 percent limit criterion of the Kolmogoroff-Smirnov-Test for all the following six distribution functions:

(1) *Log-Normal Distribution (LN)*

$$F(x)=\frac{1}{\sigma_{ln}\sqrt{2\pi}}\int_0^x \frac{1}{x}\cdot\exp\left(-\frac{(ln\ x-\mu\ ln)^2}{2\,\sigma^2_{ln}}\right)dx$$

(2) *Gumbel Distribution (GU)*

$$F(x)=\exp\left[-\exp\{-m(x-b)\}\right]$$

$$b=\mu-\gamma/m \quad m=\frac{\pi}{\sqrt{6}}\cdot\frac{1}{\sigma}\left(\gamma=\text{Euler-Number}\right)$$

(3) *Gamma Distribution (GA)*

$$F(x)=\frac{b^{a+1}}{\Gamma(a+1)}\int_0^x x^a\cdot\exp(-bx)\,dx$$

$$a=(\mu/\sigma)^2-1 \qquad b=\mu/\sigma^2$$

(4) *Log-Gamma Distribution (LGA)*

(5) *Pearson-Type-III Distribution (P 3)*

$$F(x)=\frac{b^{a+1}}{\Gamma(a+1)}\int_d^x (x-d)^a\cdot\exp\left[-b(x-d)\right]dx$$

$$a=4/CS^2-1\,;\ b=\frac{2}{\sigma\cdot CS} \quad d=\mu-\frac{2\sigma}{CS}$$

(6) *Log-Pearson-Type-III Distribution (LP 3)*

The equations describing the logarithmic distribution are formally the same as the above ones, only the boundary of integration have to correspondingly be changed and the integrand has to be multiplied by $1/x$.

The parameters of the above six distribution functions have been estimated by means of the Momentum Method, since this procedure of estimation is very handy and suits the current practice. Thus the first, second and third momentum present the three main parameters :

$$\text{Mean} \quad : \mu\cong\bar{x}=\frac{1}{N}\sum x_i$$

$$\text{Variance} \quad : \sigma^2\simeq S^2=\frac{1}{N-1}\sum(x_i-\bar{x})^2$$

$$\text{Skewness} \quad : \quad CS=\frac{N}{(N-1)(N-2)\sigma^3}\sum(x_i-\bar{x})^3$$

where, x_i denotes a recorded flood peak and N denotes the number of observations. In order to obtain the parameters of the logarithmic distributions (μ_{ln}, σ_{ln}, CS_{ln}), the x_i values have to be substituted by the $ln(x_i)$ ones.

Flood discharges (HQ_T) pertaining to recurrence intervals of $T = 100$, 1 000, 5 000 and 10 000 years have been calculated for each gauging station. (Recurrence intervals of from 100 to 1 000 years are very often selected as criteria for the design flood when planning spillways or flood levees). Tables III (*a*) & III (*b*) show results of calculations.

Results

In order to characterize the range of differences resulting due to possible application of diverse distribution functions the following dimensionless numbers have been selected :

$$R^*_T=\frac{max\,HQ_T-min\,HQ_T}{min\,HQ_T}\cdot 100\ (\%)$$

$$\bar{R}_T=\frac{max\,HQ_T-min\,HQ_T}{\bar{HQ}}\cdot 100\ (\%)$$

where every number refers to one gauge and one T value only. $\bar{HQ}$ in the second formula denotes the mean of observed flood discharges [Thus 37 times 4 = 148 numerical values are at disposal for both R^*_T and $\bar{R}_T$. On Tables III (*a*) to III (*d*) the $max\ HQ_T$ and $min\ HQ_T$ are signed by thick figures and by brackets respectively].

Eventually from all 37 values pertaining to *one* T recurrence interval, the minimum and the maximum are selected, furthermore the means of them is composed. These three numbers are shown in Figure 1 at every four values of the recurrence interval.

For example, let us select the 1 000-year probability flood. According to the figure the average range of difference due to selection of the frequency distribution attains 42 percent in comparison with the minimum value of HQ_T found from the analysis. In extreme case the discrepancy between maximum and minimum values of HQ_{1000} may reach a magnitude as high as the minimum value of HQ_T itself.

Figure 2 demonstrates a similar diagram when the range of discrepancy is related to the mean value of recorded flood discharges. Let us have a look again at the T_{1000} flood event. The discrepancy varies between 30 and 280 percent and its average value amounts to ca. 120 percent.

The data pertaining to the 37 gauging stations can be classified according to the magnitude of the skewness, viz., in two separate cases :

(*A*) Skewness is positive for both true discharges and logarithms of discharges : ($CS > 0$ and $CS_{ln} > 0$). Gauging station Nos. 1 to 21.

TABLE 1

List of Gauging Stations.

Sl. No.	Gauge	River/ Creek	A	N	$\overline{HQ}$	CS	CS_{ln}
1.	Schweighausen	Jagst	268	30	52	2,23	0,369
2.	Weilheim	Ammer	601	30	164	1,79	0,386
3.	Porta	Weser	19162	30	836	1,64	0,474
4.	Seebruck	Alz	1388	30	143	1,63	0,622
5.	Dantelbachm	Donau	77053	64	4140	1,62	0,496
6.	Jülich	Rur	1344	25	1034	1,47	0,146
7.	Nürnberg	Pegnitz	1192	30	59	1,42	0,315
8.	Hofkirchen	Donau	47496	121	1800	1,40	0,310
9.	Stein-Krems	Donau	96055	140	5200	1,39	0,463
10.	Schmerold	Mangfall	222	30	46	1,34	0,424
11.	Forbach	Murg	230	30	177	1,33	0,291
12.	Rheinfelden	Rhein	34550	100	2590	1,32	0,276
13.	Opladen	Wupper	606	30	124	1,21	0,148
14.	Hann. Münden	Weser	12440	69	620	1,21	0,136
15.	Zell	Wiese	209	30	94	1,08	0,090
16.	Letzter Heller	Werra	5487	30	272	1,06	0,334
17.	Landsberg	Lech	2295	25	430	1,02	0,183
18.	Ilsank	R. Ache	121	30	36	0,849	0,201
19.	Ingolstadt	Donau	20001	121	1070	0,801	0,186
20.	Aunkofen	Amper	3043	30	143	0,753	0,047
21.	Kempten	Iller	953	30	370	0,651	0,086
22.	Abtsgemünd	Lein	247	30	72	1,50	—0,398
23.	Bayreuth	R. Main	333	30	56	1,25	—0,114
24.	Zerkall	Rur	787	30	66	1,23	—0,327
25.	Oberwolfach	Wolfach	126	57	67	0,936	—0,277
26.	Lohmar	Agger	788	30	175	0,742	—0,425
27.	Pettstadt	Regnitz	7005	30	325	0,676	—0,279
28.	Eberfingen	Wutach	536	30	100	0,595	—0,370
29.	Grasdorf	Vechte	708	30	49	0,568	—0,360
30.	Plochingen	Neckar	4002	30	406	0,390	—0,622
31.	Steinheim	Murr	432	30	87	0,371	—0,350
32.	Lochbrücke	Schussen	792	30	87	0,266	—0,319
33.	Brenneckerbrügg	Aller	1639	34	40	0,217	—0,381
34.	Worms	Rhein	68936	39	3160	0,214	—0,483
35.	Kalkofen	Lahn	5308	30	373	0,183	—0,545
36.	Oppenweiler	Murr	180	30	82	0,177	—0,485
37.	Kaub	Rhein	103729	35	4000	0,042	—0,603

A = Catchment area in square kilometres

N = Number of observations

$\overline{HQ}$ = Mean annual flood discharge in cubic metres per second

CS = Coefficient of skewness

CS_{ln} = Coefficient of skewness of the logarithms.

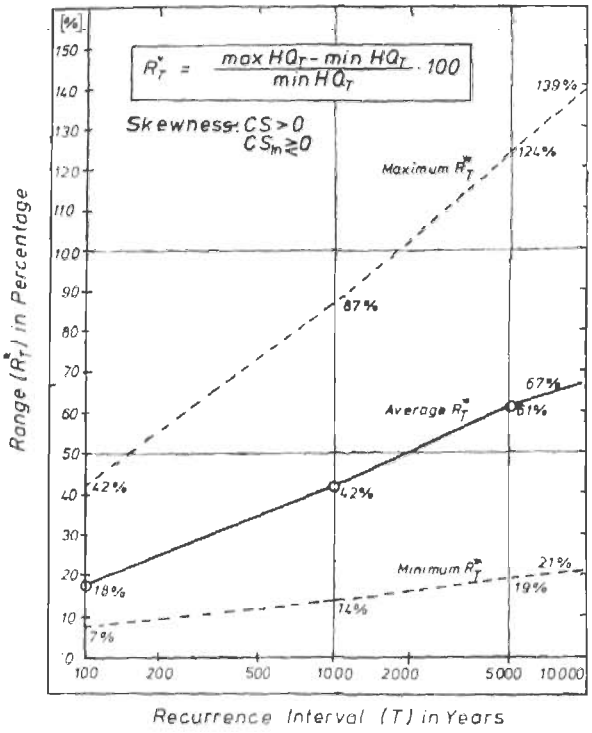

FIGURE 1 : Relation between the range (R^*_T) and its recurrence interval (T).

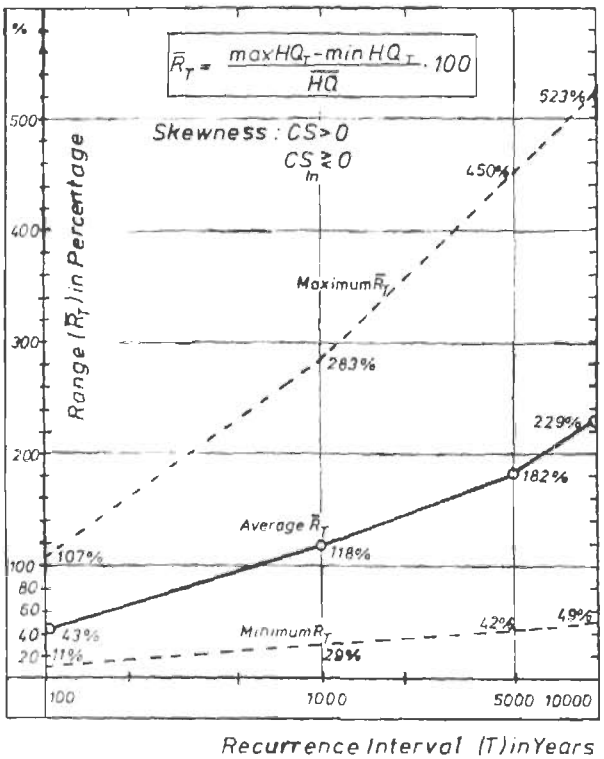

FIGURE 2 : Relation between the range ($\overline{R}_T$) and its recurrence interval (T).

(*B*) Skewness is positive for the true discharges and negative for the logarithms of the discharges : ($CS > 0$ and $CS_{ln} < 0$). Gauging station Nos. 22 to 37.

Table II illustrates the results of this analysis. The influence of the change in the sign of the skewness seemed to be remarkable, since the average discrepancy in the frame-work of our investigation showed that in case *B* it was almost the double of that in case *A*.

Conclusion

The authors of this paper tried to present a comparative analysis concerning the application of diverse distribution functions for flood probabilities. The results of their study can be grouped into two types of comments : specific remarks and general recommendations.

It is evident that detailed results obtained from the specific inventory of discharge data having been at disposal must not be generalized without criticism. It would be dangerous to jump to conclusions on basis of an investigation of 37 gauging stations only. Still some qualitative aspects and tendencies can be observed which may be of interest both for the researcher and the practical engineer. Firstly, the presumption of the authors seemed to be justified that a logarithmic transformation of the data (i.e., by applying logarithmic distribution functions) the flood discharges pertaining to a selected recurrence interval always exceed those which are computed on basis of the observed discharge values. The only exceptions—found by the authors—were the cases when, using Pearsons-III-distribution, the

TABLE II

Influence of the skewness on the range (R_T).

Range in (%)	Recurrence interval T (years)							
	100		1 000		5 000		10 000	
	CS_{ln}		CS_{ln}		CS_{ln}		CS_{ln}	
	pos.	neg.	pos.	neg.	pos.	neg.	pos.	neg.
max R^*_T	21	42	49	87	72	124	83	139
mean R^*_T	12	26	31	57	46	80	51	88
min R^*_T	7	14	14	25	19	32	21	36
max $\overline{R}_T$	55	107	171	283	293	450	354	523
mean $\overline{R}_T$	28	61	92	153	156	216	190	280
min $\overline{R}_T$	11	24	29	48	42	68	49	77

TABLE III (a)

Flood discharges (HQ_T in m^3/sec) of a recurrence interval of T = 100 years (Computed on basis of various *probability functions*).

Gauge No.	Probability-Function						R_T^* (%)	$\overline{R}_T$ (%)
	LN	*GU*	*GA*	*LGA*	*P3*	*LP3*		
1	(124)	128	125	130	**143**	136	14	37
2	441	440	(434)	461	471	**493**	14	36
3	2115	2130	(2080)	2166	2243	**2412**	16	40
4	(287)	305	289	292	318	**326**	13	27
5	(7363)	7860	7385	7392	**8169**	8044	11	20
6	294	280	(274)	307	290	**301**	12	25
7	175	(165)	(165)	189	170	**193**	17	48
8	3743	3871	(3680)	3808	3968	**4027**	9	19
9	9638	10216	(9622)	9717	10422	**10462**	11	16
10	109	109	(106)	114	111	**121**	14	33
11	493	471	(464)	518	479	**536**	16	40
12	4449	4699	(4404)	4471	**4755**	4659	8	14
13	324	310	(301)	**339**	311	344	13	31
14	1511	1478	(1426)	1561	1483	**1563**	10	22
15	282	253	(250)	**302**	(250)	284	21	55
16	727	697	(681)	756	687	**790**	16	40
17	1018	979	(944)	1041	960	**1055**	12	26
18	75	75	(71)	**77**	72	**77**	9	17
19	2056	2071	(1985)	2085	2026	**2134**	8	14
20	333	320	305	**343**	(304)	329	13	27
21	663	**678**	(636)	666	644	666	7	11
22	199	181	176	**211**	188	(170)	24	57
23	174	153	(151)	190	154	163	26	70
24	194	169	(165)	**209**	170	168	27	67
25	205	176	173	**225**	(171)	182	32	81
26	383	364	345	**391**	347	(337)	14	31
27	1090	873	862	**1161**	(816)	945	18	107
28	310	254	248	**333**	(235)	262	42	98
29	122	110	105	**128**	(101)	107	26	53
30	1046	915	875	**1087**	(829)	846	31	64
31	210	190	181	**218**	(173)	186	26	52
32	183	174	175	**187**	(157)	167	19	35
33	97	87	83	**102**	(77)	85	33	63
34	6085	5921	5559	**6111**	(5345)	5424	14	24
35	892	797	757	**913**	(706)	747	29	56
36	220	186	**179**	**232**	(164)	183	42	83
37	8204	7740	7282	**8248**	(6783)	7013	22	37
						Mean	18	43

TABLE III (b)

Flood discharges (HQ_T in m^3/sec) of a recurrence interval of T = 1 000 years (Computed on basis of various probability functions)

Gauge No.	Probability-Function						R_T^* (%)	$\bar{R}_T$ (%)
	LN	*GU*	*GA*	*LGA*	*P3*	*LP3*		
1	170	172	(160)	187	203	**206**	29	89
2	633	598	(571)	696	659	**800**	40	140
3	2964	2872	(2698)	3119	3074	**3901**	45	144
4	367	397	(356)	381	421	**480**	35	87
5	9001	9994	(8786)	8925	10537	**10782**	23	48
6	421	379	(357)	**466**	393	448	31	100
7	261	226	(220)	310	233	**322**	46	173
8	4855	5060	(4542)	4963	5169	**5627**	24	60
9	11937	13091	(11558)	11943	13323	**14390**	25	55
10	149	146	(135)	165	147	**187**	39	113
11	720	639	(610)	800	645	**860**	41	141
12	5363	5906	(5168)	5343	**5934**	5887	15	30
13	460	416	(388)	**506**	410	491	30	95
14	2084	1970	(1813)	2221	1940	**2224**	23	66
15	423	344	(330)	**491**	(330)	427	49	171
16	1042	941	(885)	1130	897	**1270**	44	142
17	1410	1304	(1198)	1482	1235	**1565**	31	85
18	97	(87)	(87)	104	89	**105**	21	50
19	2586	2702	(2387)	2642	2474	**2782**	17	37
20	450	421	380	**480**	(378)	420	27	71
21	812	**855**	(749)	817	766	816	14	29
22	287	244	228	**327**	254	(215)	52	156
23	264	208	(199)	**317**	206	225	59	211
24	289	228	(215)	**339**	225	223	58	188
25	309	238	226	**372**	(221)	248	68	225
26	505	473	421	**529**	426	(401)	32	73
27	1705	1188	1136	**1954**	(1036)	1320	87	283
28	469	343	322	**546**	(294)	346	86	252
29	169	145	131	**189**	(125)	134	51	131
30	1468	1207	1094	**1588**	(998)	(998)	59	145
31	288	250	225	**313**	(207)	213	51	122
32	238	225	199	**251**	(185)	201	36	76
33	133	114	103	**148**	(91)	105	63	143
34	7648	7504	6587	**7654**	(6144)	6203	25	48
35	1216	1041	932	**1278**	(825)	882	55	121
36	314	247	224	**351**	(193)	226	82	193
37	10556	9885	8711	**10565**	(7550)	7950	40	75
						Mean	42	118

TABLE III (c)

Flood discharges (HQ_T in m^3/sec) of a recurrence interval of T = 5 000 years (Computed on basis of various probability functions).

Gauge No.	Probability-Function						R^*_T (%)	$\bar{R}_T$ (%)
	LN	*GU*	*GA*	*LGA*	*P3*	*LP3*		
1	205	203	(184)	233	246	**268**	46	162
2	783	708	(663)	887	789	**1084**	64	257
3	3616	3390	(3108)	3810	3646	**5291**	70	261
4	425	462	(399)	443	492	**616**	54	152
5	10131	11483	(9684)	9953	12993	**12993**	34	80
6	521	447	(412)	**597**	463	559	45	170
7	331	269	(257)	420	275	**442**	72	314
8	5659	5890	(5103)	5579	5993	**6929**	36	101
9	13577	15096	(12805)	13083	15298	**17505**	37	90
10	180	171	(154)	206	172	**246**	60	200
11	899	757	(707)	1036	757	**1152**	63	251
12	5987	6748	(5654)	5682	6733	**6804**	20	44
13	565	490	(446)	**639**	476	609	43	156
14	2519	2313	(2069)	2697	2248	**2701**	31	102
15	537	408	(383)	**658**	(383)	513	72	293
16	1287	1111	(1020)	1422	1038	**1695**	66	248
17	1708	1530	(1366)	1799	1418	**1885**	38	121
18	113	113	(97)	124	101	**125**	29	78
19	2961	3117	(2646)	2961	2767	**3241**	23	56
20	538	491	430	**580**	(426)	455	36	108
21	915	**978**	(821)	905	844	897	19	42
22	357	287	262	**424**	299	(245)	73	249
23	337	246	(231)	**436**	242	291	89	366
24	366	269	(248)	**452**	263	259	82	309
25	394	282	261	**509**	(254)	294	100	381
26	594	548	471	**629**	477	(439)	43	87
27	2220	1407	1319	**2639**	(1178)	1725	124	450
28	599	404	371	**737**	(332)	402	122	405
29	205	170	149	**236**	(140)	151	69	196
30	1793	1410	1238	**1976**	1105	(1081)	83	215
31	347	291	254	**386**	(228)	260	69	182
32	278	260	221	**295**	(200)	222	48	109
33	160	133	116	**184**	(99)	117	86	213
34	**8750**	8609	7245	8417	6615	6645	32	68
35	1459	1210	1046	**1537**	(894)	959	72	172
36	387	288	254	**448**	(210)	250	113	290
37	**12245**	11383	9629	11740	(7817)	8452	57	111
						Mean	61	182

TABLE III (d)

Flood discharges (HQ_T in m^3/sec) of a recurrence interval of T 10 000 years (Computed on basis of various probability functions).

Gauge No.	Probability-Function						R_T^* (%)	$\bar{R}_T$ (%)
	LN	*GU*	*GA*	*LGA*	*P3*	*LP3*		
1	220	216	(194)	252	264	**298**	54	200
2	852	755	(700)	968	843	**1226**	75	321
3	3913	3613	(3277)	4082	3886	**5987**	83	324
4	450	490	(416)	463	522	**681**	64	185
5	10619	12124	10049	(9768)	12851	**14011**	43	102
6	567	477	(434)	**654**	492	605	51	202
7	364	287	(273)	475	293	**503**	84	390
8	6015	6247	(5332)	5781	6336	**7536**	41	122
9	14281	15960	(13313)	13519	16121	**18949**	42	108
10	193	182	(162)	223	182	**275**	70	246
11	982	808	(748)	1145	804	**1301**	74	312
12	6255	7110	(5851)	6776	7066	**7210**	23	52
13	613	522	(470)	**699**	504	656	49	185
14	2716	2461	(2174)	2869	2375	**2891**	34	116
15	591	435	(405)	**738**	(405)	533	82	354
16	1399	1184	(1076)	1546	1096	**1904**	77	304
17	1843	1628	(1436)	1919	1493	**2054**	43	144
18	120	120	(101)	132	106	**134**	33	92
19	3124	3296	(2752)	3061	2888	**3431**	25	63
20	577	521	450	**624**	(446)	459	40	124
21	960	**1031**	(850)	921	876	918	21	49
22	389	306	276	**467**	318	(256)	82	293
23	372	263	(245)	**496**	256	315	102	448
24	402	287	(262)	**505**	278	275	93	368
25	434	300	275	**570**	(268)	313	113	451
26	634	581	491	**670**	499	(454)	48	123
27	2465	1502	1305	**2936**	(1236)	1698	138	523
28	660	431	391	**830**	(347)	424	139	483
29	221	180	156	**258**	(146)	158	77	229
30	1941	1498	1297	**2193**	1148	(1112)	97	266
31	374	390	266	**414**	(236)	271	75	205
32	296	275	231	**313**	(207)	231	51	122
33	172	141	121	**201**	(102)	122	97	248
34	**9231**	9084	7513	8662	(6785)	6813	36	77
35	1569	1283	1093	**1629**	(921)	988	77	190
36	420	307	266	**490**	(218)	260	25	332
37	**12990**	12026	10004	11988	(7947)	8637	64	126
						Mean	67	224

skewness of the logarithmic distribution turned out negative (Gauge Nos. 21—37).

A further interesting observation has been made with the group of events characterized by positive values of both skewness factors : CS and CS_{ln} (Gauging station Nos. 1—21). In this group, namely, the Two-Parameter-Gamma distribution gave the minimum discharge values, while the Log-Pearson-III-distribution was mostly responsible for the maxima. Within the region where the behaviour of the logarithmic distribution was marked by a negative skewness, however, the minimum was represented by the Pearson-III-distribution, and the maximum was almost in all cases connected with the application of the Log-Gamma-distribution.

Finally, the authors would like to give a few general recommendations concerning the application of probability theory for selection of the design flood:

(1) If no standardization or official recommendation on probability calculation procedure exists and an individual analysis is required, special care should be taken for the selection of the distribution function.

(2) In several cases a reliable selection can be achieved by a preliminary test only, which may give hints about a separation of possible distribution functions, viz., into recommendable and non-recommendable ones.

(3) When after such a test of fit more than one functions remain as recommendable ones, still the question is open, which of them should be applied. Nevertheless, according to experiences, including those reported in this paper, certain knowledge can be gathered about discrepancies originating from the use of diverse distribution functions. This knowledge renders possible to valuate the safety when comparison one method with another.

(4) The authors would like to emphasize strongly the fact that a simple declaration on the exceedance frequency or *recurrence interval of a design flood* in several cases does *not say anything* if full information on the *distribution function is not simultaneously presented.*

For example, a weir or a spillway has been dimensioned for a barrage to be located at gauging station No. 9 and it is required to consider the 1 000-year flood as design flood. According to Table III (*b*) this is 14 390 m³/sec (corresponding to Log-Pearson-III-distribution). An other planner may say that he provides for a higher safety when selecting the 10 000-year flood. Since the latter based his calculation upon the Gamma type distribution, his design flood discharge is 13 313 m³/sec only, i.e., less than the first one. Such almost delusive actions have to be eliminated from a responsible engineering practice.

An Improved Estimation of Surface Water Resources

M. B. SZALAY
Associate Professor of Hydraulics
Budapest Technical University, Budapest, Hungary.

SYNOPSIS

First, it is shown that—as a matter of common place experience—the descending limb of flood waves has always a longer duration than the rising one. This fact, together with the use of stage-discharge curves, and utterly disregarding the effect of the hydraulic gradient entails an overrating of available surface water resources.

In order to overcome this difficulty, a simple geometrical method of calculating hydraulic gradients from gauge readings is adopted.

Next, it will be shown that the hydraulic gradient of rivers at steady flow is a function of the river stage too.

Finally, the improved value of discharge is obtained by applying a correction upon the discharge read from the rating curve.

Introduction

The stage-discharge curve (rating curve) is a rather poor tool of calculating river runoff but mostly, it is the only aid to be resorted to.

The inadequacy of the rating curve lies in the fact that besides of being a function of the river stage, the discharge is a function of the hydraulic gradient as well. Unfortunately, the influence of the latter is usually neglected by the simple reason of being unknown. In this context, two facts should be pointed out :

(1) As it is well-known, hydraulic gradient and discharge are lower at the same stage if the river is falling than if it is rising.

(2) The same discharge may runoff at a much higher stage and lesser hydraulic gradient if influenced by the simultaneous flood of a nearby tributary, than without such influence it may happen. The disregard of the hydraulic gradient may thus induce heavy errors in such cases.

With regard to the above reasons, efforts should be made in order to enable the introduction of hydraulic gradients into calculations, improving thus the estimation of surface water resources.

A daily measurement of the hydraulic gradient must be discarded as a requirement lacking reality. Thus, preference has to be given to geometrical methods based upon gauge readings. Such methods have the additional advantage of a retrospective use.

The Frequency of Rising and Falling Stages

By maintaining the assumption that discharge values yielded by the stage-discharge curve are correct only if the river stage attained one of its relative minima or maxima then it will become obvious that discharges pertaining to falling stages are less than indicated by the rating curve and inversely, discharges occurring during the rising stages are higher than those yielded by the curve.

The errors thus committed in determining momentary discharges are, however, not neutralizing each other in the long run, since the frequency of falling stages is appreciably higher than that of rising ones. This in turn, results in a regular error of overrating annual runoff, or water resources in general. The error may

become quite considerable as it will be pointed out later on.

In order to have an idea of the frequency of rising and falling river stages, the reader is referred to Table I where the results of such an investigations are summarized. The daily river stages at 6 stations were processed over the 7-year period of 1965-1971. As shown by the example, the annual frequency of rising water is roughly equal to, or less than, 40 percent of all days. The only exception, Tokaj with its 45.6 percent has not a natural river regime. Being in the backwater of the Tiszalök barrage, the fluctuation of stages is much restricted, and manipulations with the movable weir are a source of further unnatural features.

At river stations further upstream, where individual flood waves rise and recede separately, the frequency of rising stages is lower (e.g., Vásárosnamény) than more downstream where the next flood wave is superimposed upon the preceding one before the recession of the latter (Szolnok, Szeged).

The Hydraulic Gradient

Despite the clarity and simplicity of the concept of hydraulic gradient in theoretical hydraulics, it becomes a vague notion as soon as it is applied to fluvial hydraulics. The water surface of a sinuous river is a very complicate three-dimensional configuration, the shape of which is determined simultaneously by gravity, centrifugal and Coriolis force, wall friction and other forces acting. Transversal gradients and secondary currents still contribute to further confusions of the phenomenon. Therefore, the practical definition of the hydraulic gradient should be a matter of proper convention.

In the present paper, the hydraulic gradient (surface slope) is considered as the differential quotient $S = dy/dx$ of a plane curve. This curve is obtained if the cylindrical vertical surface containing the main streamline of the river surface is flattened out into a vertical plane. The curve itself is defined practically by a number of points corresponding to simultaneous stages at river gauges, and by the distance between these gauges measured along the main streamline. It is also assumed that these distances are independent of actually prevailing river stages, which is not always the case.

The plane curve of the water surface obtained in the above way is to be substituted expediently through polynomial curves of the second or third-degree.

A second-degree approximation has the advantage of requiring three simultaneous gauge readings only, which makes calculations very simple. On the other hand, if the surface curve has an inflexion, which is occurring at least twice during each flood wave, a second-degree curve cannot be fitted to the line of the water surface. This is the reason for introducing third-degree approximations as well.

TABLE I

Number of days with rising river stages and their percentage for some Hungarian gauging stations. Average of the years 1965 to 1971.

River and gauging station		Jan.	Feb.	Mar.	Apr.	May	Jun	July	Aug.	Sep.	Oct.	Nov.	Dec.	Year
Danube, Budapest	days	13,4	12,6	14,3	13,3	13,0	14,4	12,3	10,3	8,1	7,6	13,3	11,9	144,4
	%	43,3	44,6	46,2	44,4	42,0	48,0	39,7	33,3	27,0	24,6	44,3	38,4	39,5
Danube, Mohács	days	12,9	12,1	13,6	14,7	13,3	13,7	11,7	11,6	7,7	6,9	13,7	12,7	144,6
	%	41,7	42,8	44,0	49,0	43,0	45,6	37,8	37,5	25,6	22,4	45,6	41,0	39,6
Tisza, Vásárosnamény	days	11,9	12,1	10,4	12,1	10,4	8,3	9,4	10,0	6,7	8,3	10,4	10,0	121,6
	%	38,5	42,8	33,6	40,3	33,6	27,6	30,4	32,3	22,3	26,9	34,6	32,3	33,5
Tisza, Tokaj*	days	13,9	14,0	13,3	14,0	12,3	13,3	13,9	13,6	13,0	14,6	15,0	14,9	166,6
	%	44,9	49,6	43,0	46,7	39,7	44,3	44,9	44,0	43,3	47,0	50,0	48,1	45,6
Tisza, Szolnok	days	11,4	14,1	15,1	12,3	8,3	12,9	9,9	13,3	10,1	11,0	15,4	13,9	148,7
	%	36,8	50,0	48,8	41,0	26,9	43,0	32,0	43,0	33,6	35,5	51,2	44,9	40,7
Tisza, Szeged	days	12,6	14,4	15,3	15,4	9,9	12,3	10,9	9,4	11,7	9,9	16,7	13,6	150,7
	%	40,7	51,0	49,4	51,2	32,0	41,0	35,3	30,4	39,0	32,0	55,6	44,0	41,3

*The river regime at Tokaj is highly affected by Tiszalök River barrage, a few kilometres downstream.

Formulae of Second-degree Approximation

If a Lagrange polynomial passing three points of the river surface (Figure 1, top) is differentiated, one will obtain the following formulae of the hydraulic gradients S_0, S_1 and S_2, valid for the sections 0, 1 and 2, respectively :

$$S_0 = \frac{l_{01}+l_{02}}{l_{01}\,l_{02}}\,y_0 + \frac{l_{02}}{l_{01}\,l_{12}}\,y_1 + \frac{l_{01}}{l_{02}\,l_{12}}\,y_2 \qquad \ldots(1)$$

$$S_1 = \frac{l_{12}}{l_{01}\,l_{02}}\,y_0 - \frac{l_{12}-l_{01}}{l_{01}\,l_{12}}\,y_1 - \frac{l_{01}}{l_{02}\,l_{12}}\,y_2 \qquad \ldots(2)$$

$$S_2 = -\frac{l_{12}}{l_{01}\,l_{02}}\,y_0 + \frac{l_{02}}{l_{01}\,l_{12}}\,y_1 - \frac{l_{02}+l_{12}}{l_{02}\,l_{12}}\,y_2 \qquad \ldots(3)$$

Needless to say that among these three equations, Equation (2) is considered as the most accurate one. Equations (1) & (3) are to be used only if in the section to be investigated there is a discontinuity of the water surface, e.g., a river barrage.

Formulae of Third-degree Approximation

By using the notations of (Figure 1, bottom), the differentiation of the Lagrange polynomial of third-degree will yield the hydraulic gradients S_0 to S_3 for every one of the four gauge sections involved. Equations (5) & (6) should be considered as more accurate than Equations (4) & (7), the latter ones being at end sections of the river reach considered.

$$S_0 = \frac{l_{01}\,l_{03}+l_{02}\,l_{03}+l_{01}\,l_{02}}{l_{01}\,l_{02}\,l_{03}}\,y_0 - \frac{l_{02}\,l_{03}}{l_{01}\,l_{12}\,l_{13}}\,y_1 + \frac{l_{01}\,l_{03}}{l_{02}\,l_{12}\,l_{23}}\,y_2 - \frac{l_{01}\,l_{02}}{l_{03}\,l_{13}\,l_{23}}\,y_3 \qquad \ldots(4)$$

$$S_1 = \frac{l_{12}\,l_{13}}{l_{01}\,l_{02}\,l_{03}}\,y_0 - \frac{l_{12}\,l_{13}-l_{01}\,l_{13}-l_{01}\,l_{12}}{l_{01}\,l_{12}\,l_{13}}\,y_1 - \frac{l_{01}\,l_{13}}{l_{02}\,l_{12}\,l_{23}}\,y_2 + \frac{l_{01}\,l_{12}}{l_{03}\,l_{13}\,l_{23}}\,y_3 \qquad \ldots(5)$$

$$S_2 = -\frac{l_{12}\,l_{23}}{l_{01}\,l_{02}\,l_{03}}\,y_0 + \frac{l_{02}\,l_{23}}{l_{01}\,l_{12}\,l_{13}}\,y_1 + \frac{l_{02}\,l_{12}-l_{02}\,l_{23}-l_{12}\,l_{23}}{l_{02}\,l_{12}\,l_{23}}\,y_2 - \frac{l_{02}\,l_{12}}{l_{03}\,l_{13}\,l_{23}}\,y_3 \qquad \ldots(6)$$

$$S_3 = \frac{l_{13}\,l_{23}}{l_{01}\,l_{02}\,l_{03}}\,y_0 - \frac{l_{03}\,l_{23}}{l_{01}\,l_{12}\,l_{13}}\,y_1 + \frac{l_{03}\,l_{13}}{l_{02}\,l_{12}\,l_{23}}\,y_2 - \frac{l_{03}\,l_{13}+l_{03}\,l_{23}+l_{13}\,l_{23}}{l_{03}\,l_{13}\,l_{23}}\,y_3 \qquad \ldots(7)$$

For convenience, any of the Equations (1) to (7) may be rewritten in the form :

$$S_i = A_i h_1 + B_i h_2 + \ldots + D_i h_n + E_i \qquad \ldots(8)$$

where, $h_j = y_j - Y_j$

with y_j = the elevation of the water surface in the section j

Y_j = the elevation of the gauge zero in the same section

h_j = the gauge reading above zero or below zero

$$E_i = A_i Y_1 + B_i Y_2 + \ldots + D_i Y_n \qquad \ldots(9)$$

With aid of the *station Equation* (8), hydraulic gradients may be calculated as far back as gauge readings of the stations involved are available. It is also advisable to eliminate random fluctuations of gradients thus obtained, by smoothing the diagram. Thus, e.g., the smoothed weighted average $\bar{S}_n$ of the n-th day may be calculated as

$$\bar{S}_n = (S_{n-2}+2S_{n-1}+4S_n+2S_{n+1}+S_{n+2})/10 \qquad \ldots(10)$$

The whole process can easily be computerized.

Figure 2 shows an example of third-degree approximation at Dunaújváros (River Danube). One may perceive on this figure that maxima and minima of river stage are always slightly lagging behind those of the hydraulic gradient. It is also apparent that the gradient

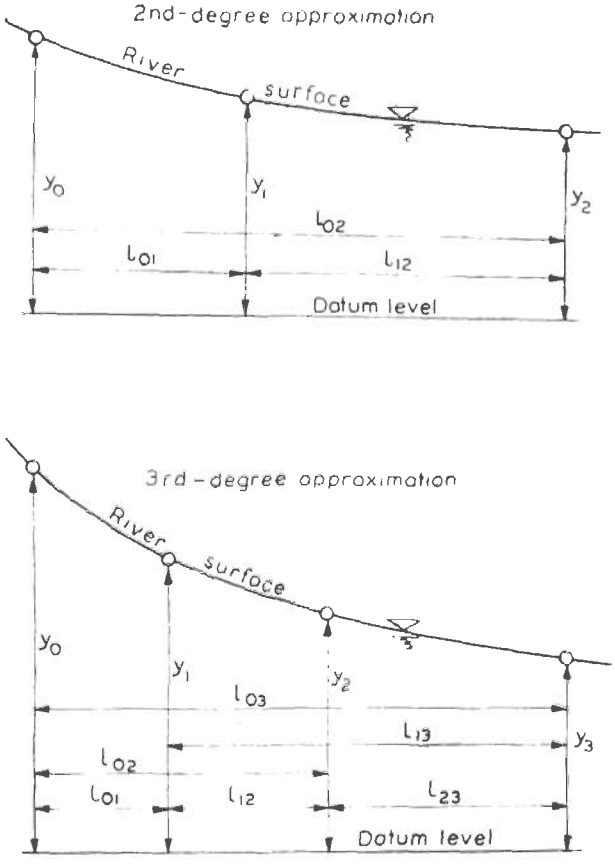

FIGURE 1 : Notations for Lagrange polynomials.

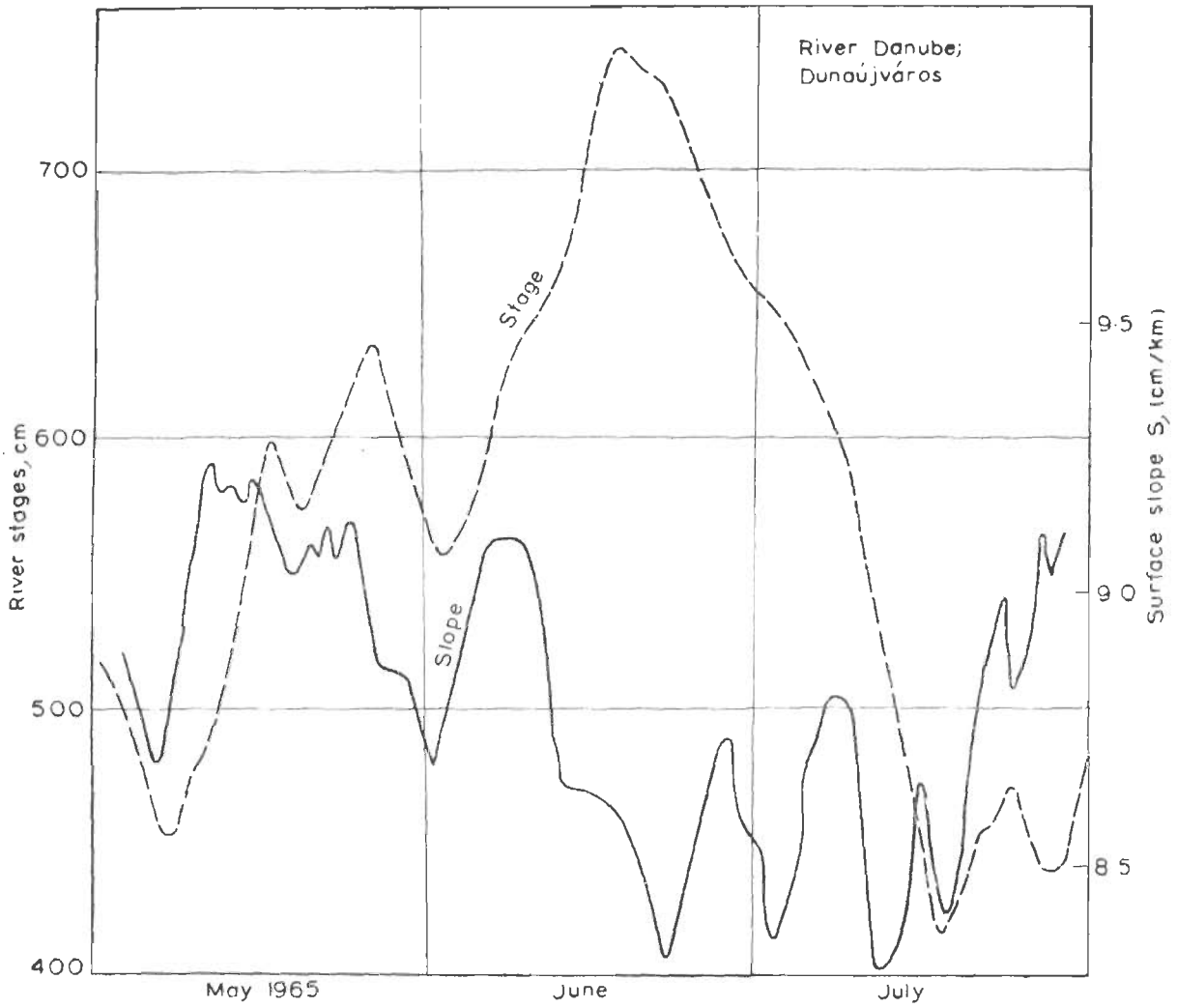

FIGURE 2 : Flood stage hydrograph and surface slope.

is very sensitive against the superposition of flood waves, otherwise hardly perceptible on the stage hydrograph.

On the Stage-discharge Curve

Without a further investigation one is inclined to believe that stage-discharge curves with a validity restricted to steady flow are also characterized by a certain average constant value of the hydraulic gradient. A more thorough investigation into the problem shows, however, that this is by far not the case.

Again in connection with Dunaújváros, river stages pertaining to discharges of 500, 1,000, ..., 8,000 cu m/sec were read from the stage-discharge curves of Dunaújváros and the neighbouring river gauges. Next, hydraulic gradients pertaining to these discharges of steady flow were calculated by using the above suggested method, and finally, the gradients thus obtained have been plotted against the corresponding stages at Dunaújváros. Results are shown in Figure 3. The curve obtained has a rather unexpected shape. Most probably, this is accounted for by the fact that floods with a stage higher than 450 cm begin to overflow the river banks.

Correction of Discharge Values

With regard to the above facts it is proposed to calculate the corrected values of actual discharge by means of the following formula :

$$Q_c = Q_s \sqrt{S_c/S_s} \qquad ...(11)$$

where,

Q_c = the corrected value of discharge

Q_s = the discharge read from the stage-discharge curve

S_c = hydraulic gradient calculated according to one of Equations (1) to (7)

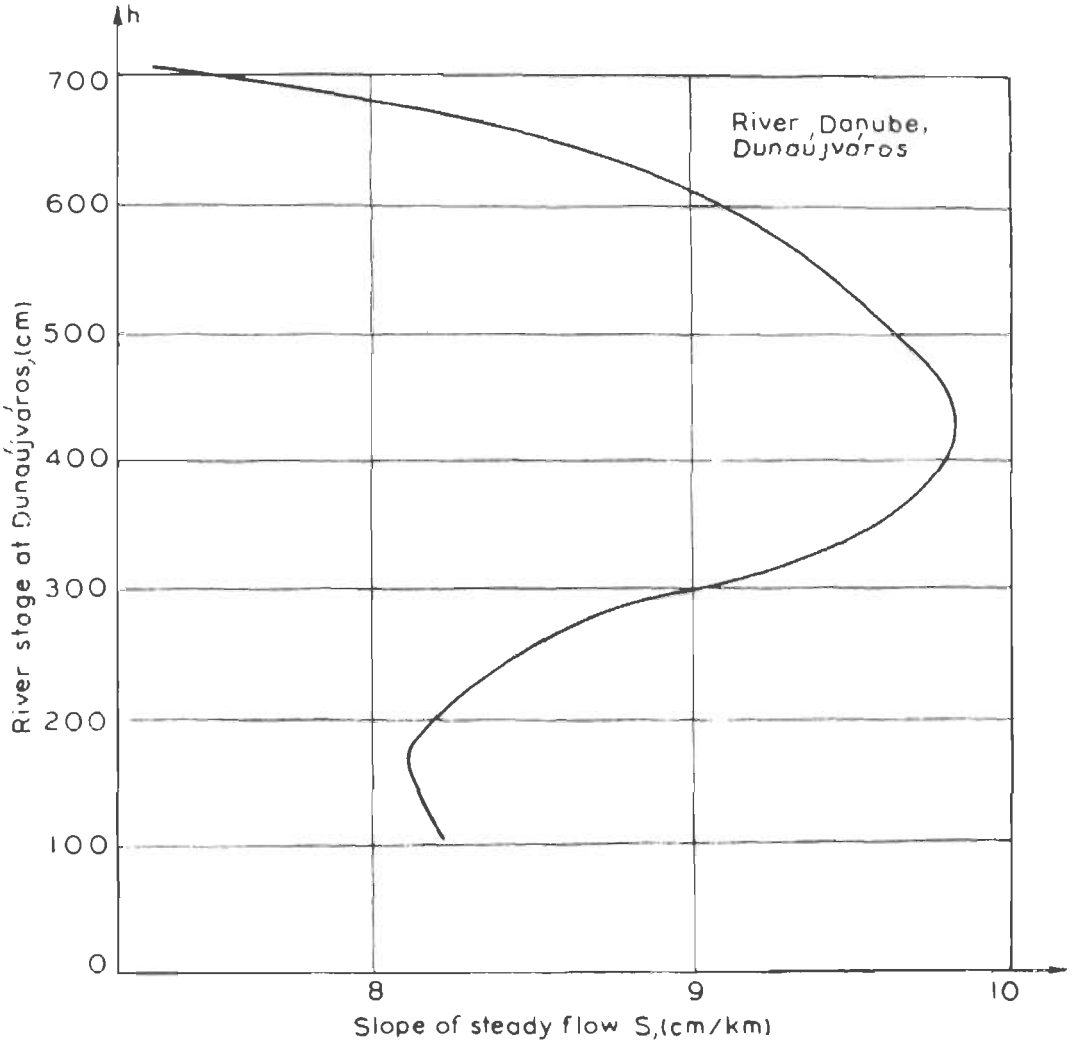

FIGURE 3 : Steady-flow surface slope versus river stage.

S_s = hydraulic gradient read from a curve constructed like that of Figure 3, as a function of momentary river stage.

By having adopted the described method to data of May 1965, the total monthly runoff thus calculated was less by 229 million cu m than if it were determined from the stage-discharge curve.

In this particular case, the percentual deviation was only—1.6 percent. But this reach of the Danube is practically devoid of tributaries, which is rather exceptional in river hydrology.

In other cases however, like at Station Szeged of the Tisza River, a few kilometres upstream of the mouth of River Maros, certain heavy flood peaks turned out to carry about 30 percent less of water than if calculated already conventionally from the stage-discharge curve. This is far beyond the permissible limit of errors in estimating surface water resources. *Reaches above the confluence of rivers are particularly sensitive to the taking or not taking into account of the hydraulic gradient.*

Conclusions

(1) The use of the stage-discharge curve is bound to give rise to considerable errors in river runoff if the hydraulic gradient is not taken into account.

(2) These errors mean an underrating of runoff during the rising period, but an overrating thereof during the falling-stage period. It is shown that only 33 to 40 percent of daily stages are rising ones and hence, the overall result will be an overrating of surface water resources.

(3) Relatively simple geometrical considerations allow for taking the hydraulic gradient into account. Formulae derived through the differentiation of Lagrange polynomials have been established for the purpose of calculating

actual values of the hydraulic gradient, by using sets of simultaneous gauge readings. The method is apt to a retrospective use if gauge readings are available.

(4) In order to utilize the calculated gradients in corrections of discharge it is indispensable to know, what gradients belong to the various river stages in the steady state of flow. A simple method of finding these gradients has been advised.

(5) In unfavourable conditions, the overrating of runoff may attain values as high as 30 percent.

(6) The method may find another use in flood routing where it enables the employment of more accurate discharge inputs at the upstream end of the river reach computed.

References

(1) SZALAY, M B. : "Bestimmung des Spiegelgefälles aus Pegelablesungen". Beiträge zur Konferenz für Wasservorhersage, Budapest, 1961.

(2) SZALAY, M.B. : "Metodo per aumentare la precisione nella determinazione di portate giornalieri dei fiumi". Atti del X. Convegno di Idraulica e Costruzioni Idrauliche, Cagliari, 1967.

Urbanization—Its Effects upon Base Flow

PAUL MACROBERTS
Water Resources Engineer
Black & Veatch Consulting Engineers, Kansas City, Missouri, U.S.A.

SYNOPSIS

The recently concluded water quality management study conducted by Black & Veatch Consulting Engineers, for the Denver Regional Council of Governments produced findings which indicate that urbanization may materially effect base flow regimes. Historical streamflow records for the Cherry Creek watershed located in Denver, Colorado (U.S.A.) show annual yield to be considerably higher than would be expected from natural precipitation conditions. Detailed computer analyses of the hydrologic responses of this watershed substantiated that natural rainfall-runoff was not sufficient to account for the elevated water yields. A discussion of the various analyses is presented with supporting illustrations.

Introduction

Urbanization has long been thought to affect various streamflow characteristics, particularly the volume and peak flow rate of storm runoff. Numerous articles have discussed this cause and effect relationship. It has repeatedly been documented that increases in flood peak flow rates have the effect of reducing the volume of water available for infiltration into ground water horizons and are, therefore, instrumental in reducing base flows.

A recent hydrologic analysis performed in conjunction with an extensive water quality management study conducted by Black & Veatch for the Denver metropolitan area in Colorado strongly indicates that, in at least one drainage basin, urbanization and accompanying land use changes may be responsible for a general increase in the base flow. This particular watershed, Cherry Creek, behaves contrary to catchment areas discussed in the literature, in that its base flows are not reduced with increasing urbanized area.

This paper discusses in detail the analytical procedures utilized in the moisture budget analyses, presents conclusions derived from the hydrologic analyses, and illustrates conclusively that urbanization in semi-arid regions, rather than causing decreased base flows, as is generally thought, may be responsible for increases in base flow.

Description of Study Area

General

The Denver metropolitan area is located in the west-central region of the United States at about Latitude N 39° 15′ and Longitude W 105° 00′. It is composed of numerous independently governed suburban communities, each of which generally exhibits the features of larger cities, i.e., central shopping areas, municipal wastewater treatment facilities, sewers (storm and sanitary, or combined), schools, etc. The metropolitan area encompasses about 750 sq miles (1,945 sq km) along the eastern foot-hills of the rocky mountains, and is situated along both banks of the South Platte River and its numerous tributary streams, one of which is the reservoir-controlled Cherry Creek. Figure 1 presents location information.

The Cherry Creek watershed covers about 409 sq miles (1,059 sq km) of relatively flat, sandy, dry land located east of the City of Denver proper. Situated at about river mile 11 are the federally owned and operated Cherry Creek flood control dam and reservoir, which control runoff from about 385 sq miles (997 sq km) of rather sparsely populated land and protect 24 sq

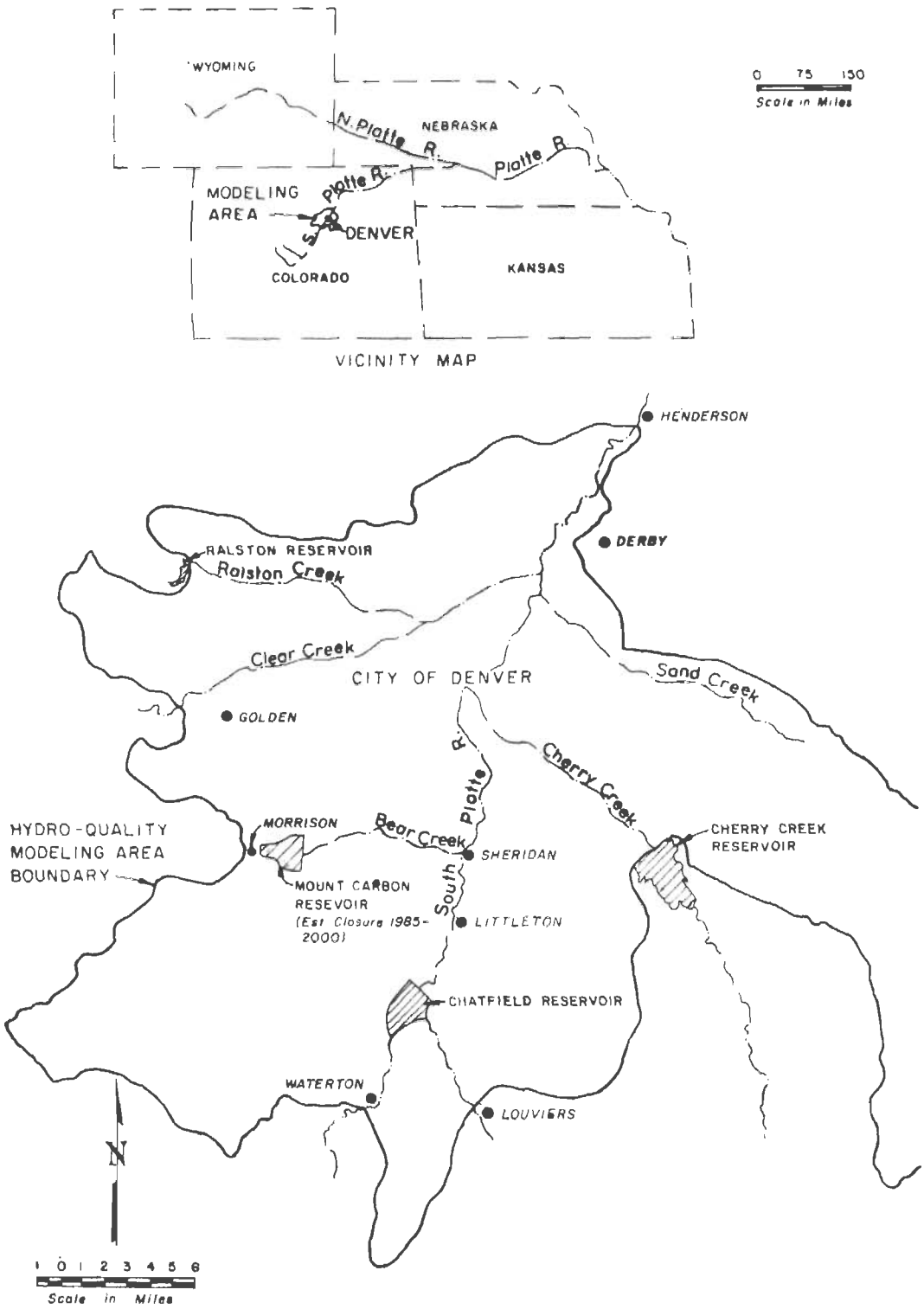

FIGURE 1 : Hydro-quality modelling area and vicinity map.

miles (62 sq km) of primarily urbanized land in the Cherry Creek watershed.

Topography

The general topography of the controlled portion of the Cherry Creek watershed is one of relatively little relief, having a mean elevation of about 5,425 ft (1,654 m) above mean sea level. Elevation extremes vary from about 5,700 ft (1,740 m) to about 5,200 ft (1,580 m). No extreme elevation changes are found in the area.

Geology

Surface soils in the Cherry Creek study area consist primarily of various gradations of sand. Erosion processes and resulting deposition are clearly evident. Some wind erosion has taken place.

Precipitation

Precipitation varies across the watershed; for the period from 1941 to 1970 it averaged about 15 in. (38 cm) per year. The area can be classified as semi-arid. About 45 percent of the annual precipitation occurs during the months of April through June. Scattered thunderstorms and massive frontal systems, to a large degree brought about by orographic mechanisms, generate most of the precipitation. Areal distributions are reflective of the orographic influence.

Mean annual snowfall is about 60 in. (152 cm). General temperature conditions are such that continuous snow cover beyond a two or three week period is rare.

Temperature

Average temperatures range from a high of 73°F (23°C) in July to a low of about 31°F (0°C) in January. The mean annual temperature is 51°F (10°C), and extremes rarely exceed 100°F (38°C) or drop below 0°F (−18°C) for extended time periods.

Computer Model

Simulation of streamflow conditions for given historical precipitation patterns, wastewater loadings and flow diversions was conducted for the Cherry Creek watershed. Analyses were then made of resulting stream conditions to assess the influence of the various affecting parameters. The model used for this study was written by Hydrocomp International, Palo Alto, California, U.S.A., and requires a large, high-speed IBM digital computer.

The algorithms incorporated into the program for quantity studies were divided into three sub-programs or modules: (A) Library; (B) Lands; and (C) Channels. They are briefly described in the following:

(A) *Library Module* : The library module operates primarily with basic data storage and retrieval. Its main function is to provide the user with high-speed capabilities for managing the voluminous hydrometeorological data required in the application of the model.

(B) *Lands Module* : The lands module contains the first series of algorithms used for simulation of the hydrologic cycle. This module defines the land phase of the hydrologic cycle by utilizing approximated areal parameters and the hydro-meteorological data series. It simulates the hydrologic responses of the land surface.

Provisions have been made in this module to simulate the processes controlling the various components of runoff (overland flow, base flow) by accounting for losses or gains in ground water zones and in moisture content of snowpacks.

(C) *Channels Module* : This module is designed to utilize the channel inflow data generated by the lands module and to route it through the defined channel system. The routing procedure used in the Hydrocomp model is based on the "kinematic wave" theory and utilizes actual or estimated dimensions and roughness coefficients for the channel system. Figure 2 presents a schematic flow chart of the simulation program.

Calibration

The purpose of model calibration was to adapt the computer program to the hydrologic, meteorologic and physiographic characteristics of the watershed. During the process which essentially entailed the adjustment and fitting of various parameters and constants used by the program, historically observed and synthetically developed hourly data on precipitation, evaporation, temperature, cloud cover and wind, and information on physical characteristics such as soils, land usage and imperviousness were utilized to compute the moisture budget for the Cherry Creek watershed on an hourly time interval. Cognizance was taken of multi-faceted interrelationships believed to be relevant in the rainfall-runoff cycle. The following are some of the parameters considered in the simulation process :

(1) Impervious area
(2) Interceptor storage
(3) Soil moisture content
(4) Evaporation rate
(5) Infiltration rate
(6) Interflow rate
(7) Length of overland flow
(8) Overland flow range
(9) Manning's "*n*" coefficient for overland flow
(10) Interflow recession rate
(11) Ground water recession rate
(12) Radiation
(13) Forest cover
(14) Ground water storage.

Results of calculations made during the calibration process showed that recorded inputs and recorded

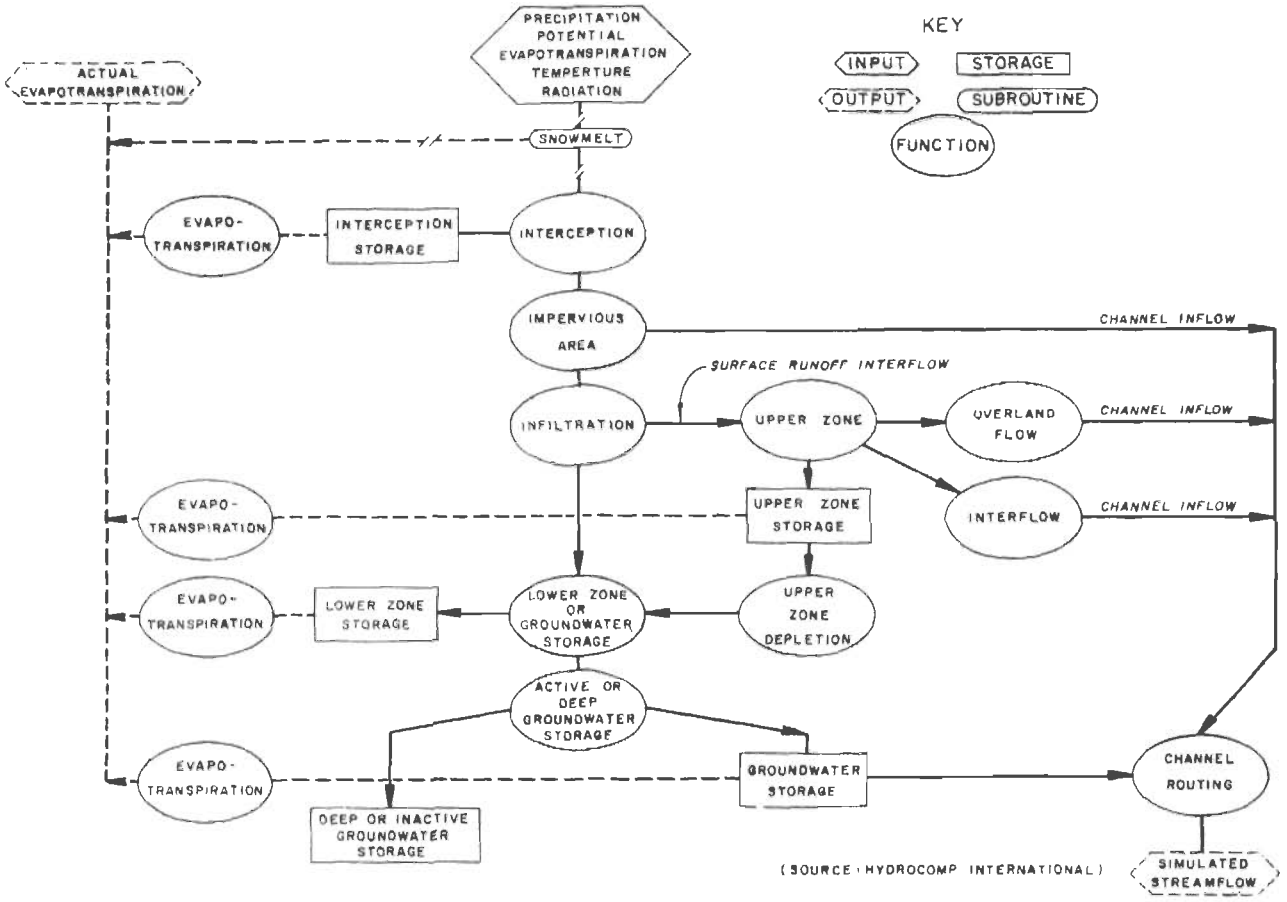

FIGURE 2 : Flowchart for lands and channel in the Hydrocomp simulation program.

abstractions did not result in a mass balance for the Cherry Creek area. The average annual runoff measured at the official stream gauge for the trial period was about 6.9 in. (17.5 cm), while the simulated annual runoff was only about 2.1 in. (5.34 cm), which represents a deviation of about 70 percent from the observed value. This indicated that not all water inputs were properly being accounted for.

It was initially thought that programming errors were responsible for the deviation between historical and simulated runoffs. Detailed reviews of the modelling logic and validation of mathematical algorithms were made, and it was concluded that there were no errors which would account for the significant variation.

It was then concluded that the land surface response mechanisms were partially or wholly responsible for the discrepancy. The relative magnitudes of land-related parameters were further analyzed by simulation of rainfall-runoff responses from the undeveloped areas of the upper Cherry Creek watershed. This clearly showed that the land parameters used for urbanized areas yielded too much flow in the rural regions. It became, therefore, obvious that water from sources other than natural precipitation was being introduced into the stream network in the urbanized areas of the watershed. The Cherry Creek watershed has no surface water diversion and only one very small, fairly well-documented wastewater treatment plant discharging to the river, apart from the previously mentioned flood control reservoir. Since all of these factors, when combined, had only a small effect upon the streamflow, it was not considered possible that errors in their measurement would result in the significant deviation between observed and simulated streamflow.

Irrigation

Considering these findings, it became apparent that the observed sustained water flows evident in the stream were largely the result of return flows from irrigation of crops and lawns. Reviews of historical hydrographs from the study area indicated that recession constants were similar to those commonly found in irrigation situations. The seasonal irrigation in the watershed builds up a substantial ground water reservoir which,

when interfaced with the Cherry Creek channel or with storm sewers, provides a low, steady base flow during periods of no irrigation.

Field observations following an extended period of no measurable precipitation showed that major gains in streamflow occurred in the more densely populated lower reaches of the basin where lawn irrigation is widespread. This, coupled with a review of the 1965 through 1970 water consumption curves for the area, indicated that the effects of lawn sprinkling above other basic, domestic water requirements extend from April through October. Observed hydrographs further substantiated this by their generally increased base flow contributions during the corresponding time period.

In order to substantiate the premise that irrigation contributes to the watershed's base flow, it was necessary to develop a series of algorithms to represent irrigation applications in the Hydrocomp computer program. To make the application of irrigation water most realistic, a target value of total moisture required to sustain lawns and crops was established for each month. Each day during the month was then checked sequentially to determine if the daily portion of the monthly requirement was met by natural precipitation. When necessary, irrigation water was applied to bring the moisture up to target level. Precipitation in excess of the required daily amount was carried forward to satisfy subsequent daily demands.

The application of this artificially determined irrigation moisture was determined to vary between two basic uses, crop irrigation and lawn irrigation. The irrigation application rates thus determined reflected this breakdown, and for the Cherry Creek basin, lawn irrigation constituted the greater percentage. Because of differing rates, it was decided that areas under each category of irrigation should be determined in addition to the amount of impervious and pervious land in each area. Residential areas in the Cherry Creek basin were assumed to be 60 percent irrigated and were distributed within the watershed by the proportion of land tributary to each defined reach. By means of this approach it was possible to account for artificially applied moisture in a manner similar to the irrigation practices used by the residents of the region.

Application Rates

The actual lawn and crop irrigation application rates for the watershed were established from historical water department records and State water district records. The lawn irrigation target was established by graphically separating lawn irrigation from the monthly domestic uses. The volume of water thus determined was divided by the estimated land area under irrigation, supplied by the water department, thus resulting in an average monthly irrigation application rate. The resulting rates, added to the average monthly precipitation, gave the total monthly moisture lawn target values listed below:

Estimated monthly lawn irrigation requirements.

Month	Monthly target requirement	
	(inches)	(centimetres)
April	2.96	7.5
May	5.10	13.0
June	5.66	14.4
July	5.90	15.0
August	5.43	13.8
September	3.62	9.2
October	2.27	5.8
Total for season	30.94	78.7

Crop irrigation requirements were computed in a similar fashion, except that "headgate" requirements, as documented in the State's irrigation water districts records, were utilized in place of the domestic water consumption records. The crop moisture target values thus established are listed below:

Estimated monthly crop irrigation requirements.

Month	Monthly target requirement	
	(inches)	(centimetres)
April	3.75	9.5
May	4.74	12.0
June	7.46	18.9
July	9.15	23.2
August	8.60	21.8
September	5.45	13.8
October	2.90	7.4
Total for season	42.05	106.6

The total amount of irrigation water placed into the model were computed by respective monthly requirements. Irrigation applications were assumed to be made daily during a three-hour period commencing at 12:00 noon. It was thought that the decision whether or not to irrigate is fairly random, and that the ultimate application would be determined as a function of the target

values by charting accumulated moisture against the requirements to meet the monthly target. Monthly carryovers were made up to the end of the irrigation season at which point the only moisture being applied to the land surface was that generated naturally.

Calibration runs were subsequently made utilizing the irrigation algorithms and historical hydro-meteorological data for the five-water-year period, October 1965—September 1970. The results thus generated, analyzed by the three methods discussed below, were found to be within defined limits of accuracy.

Model Verification

Verification of the numerical results generated by the computer model was achieved by utilizing the following :

(1) Mass Curves

(2) Flow Duration Curves

(3) Hydrograph Comparisons

(4) Basin Climatic Indices.

Each analysis was performed on the data generated by the model for the five-water-year calibration period.

Mass Curves

Generally utilized in other types of analyses such as reservoir studies, they were used during this work to graphically compare monthly and seasonal variations between model-generated values and historically recorded values as a measure of the model's capability for reconstituting historical cyclic patterns.

Figure 3 presents the final calibrated mass curve for the Cherry Creek Basin. As can be noted from this figure, there are certain differences between historical and simulated values of accumulated streamflow. The pattern of the divergence indicates that exact reproduction of historical records was not achieved but, more importantly, that the timing of seasonal variations is fairly well reproduced. It should be pointed out that, even though irrigation applications were made according to the procedure discussed above, the simulated total mass was still lower than the observed value. It was found that the model did not correctly account for some isolated daily peaks in streamflow, and thus underestimated total mass.

Flow Duration Curves

The daily duration distribution of streamflow is a good indicator of how well the model is able to compute streamflows of the same order of magnitude and frequency of occurrence. Duration curves were used in conjunction with mass curves during the parameter adjustment period of the study.

Figure 4 presents the historical and simulated daily flow duration curves for Cherry Creek. The duration analysis indicates that the simulated records contain more occurrences in the low flow range than were noted in the historical data. Attempts were made to reduce the divergence in the low flow range by adjusting the irrigation algorithms for Cherry Creek. They proved unsuccessful because it was not possible to discretely define the behavioural patterns of individual irrigators. It was, therefore, concluded that it would be best to simply note the divergence and to take it into consideration in the water quality analysis. The flow duration curve in Figure 4 serves to illustrate that base flows in urban areas remained higher in the historical record even though large irrigation applications were made through the irrigation algorithm, thus further substantiating that urbanization affects base flow in the manner cited.

Hydrograph Comparisons

Time sequence plots of generated and historical streamflow values are probably the best indicators of how well the model is capable of reproducing the hydrologic responses taking place in the Cherry Creek Basin. Figures 5 through 8 present a partial selection of such plots. They illustrate that historical base flows are higher than simulated flows, even though significant moisture contributions were made artificially through the irrigation algorithm.

Basin Climatic Indices

The magnitude of streamflow resulting in the Cherry Creek watershed from normal precipitation was determined by an independent empirical approach developed only recently and discussed before the International Symposium on Design of Water Projects for Areas of Inadequate Data in Madrid, Spain, in June 1973([1]).

Utilizing this approach, streamflows were computed for the watershed assuming that man's activities which have an effect on runoff and flow regimes, e.g., irrigation, construction of impervious areas, etc., could be effectively accounted for through appropriate adjustments of the calculation procedure.

The drainage area selected for study contained about 15 percent of near impervious surface with an assumed runoff coefficient of 0.90, and about 30 percent of urban lawns. As previously noted, the lawn area is heavily irrigated at about 30 in. (76.2 cm) per year; annual rainfall is about 15 in. (38 cm).

Utilizing Thornthwaite's Basin Climatic Index (BCI) equation as discussed by R.L. Smith, Professor of Civil Engineering, University of Kansas, Lawrence, Kansas, the BCI value under normal rainfall was computed to be 32, and an adjusted index of approximately 90 was computed in order to compensate for irrigation. The estimate of annual stream yield, with and without man-

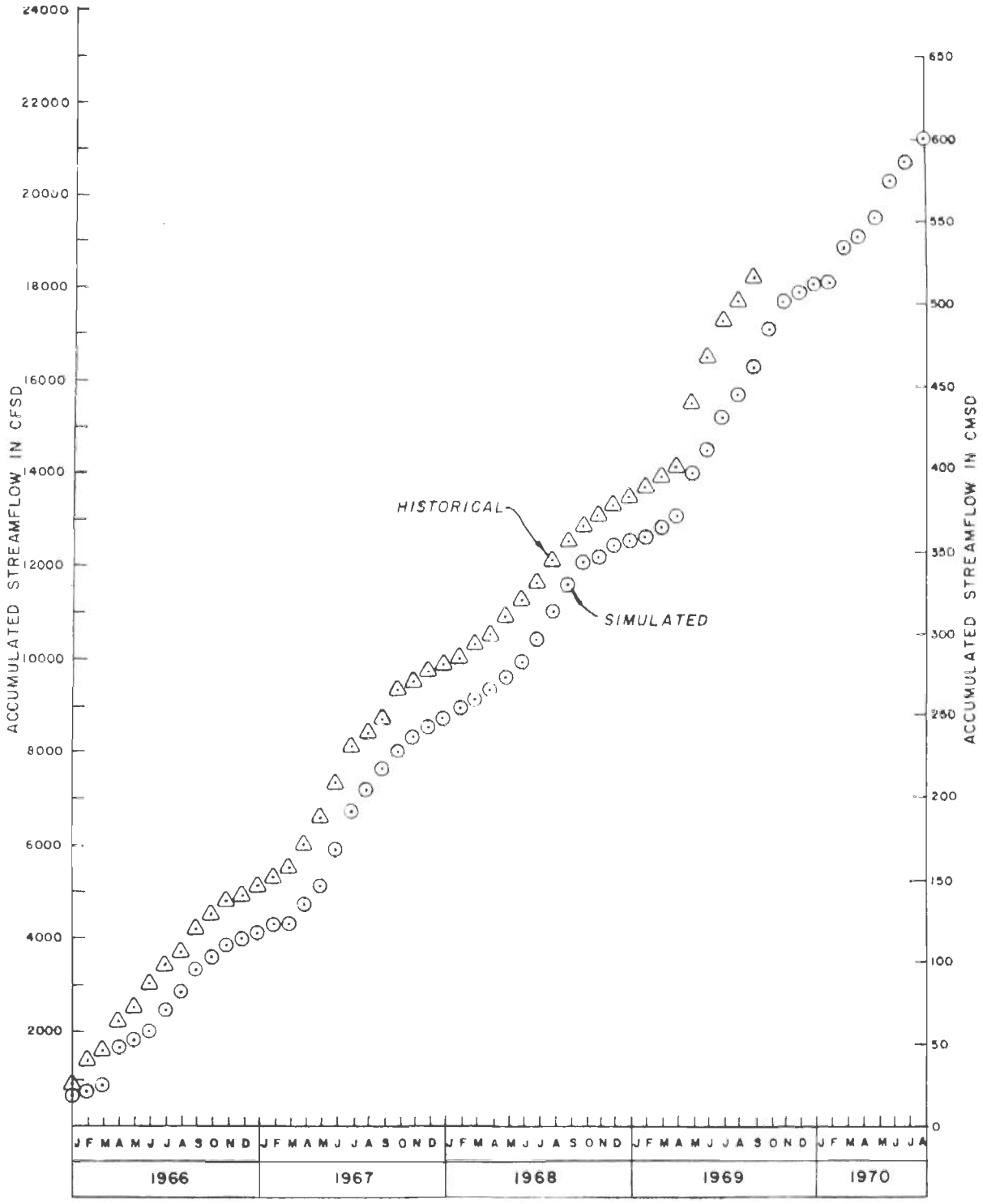

FIGURE 3 : Mass curve comparison, Denver, Colorado—Cherry Creek.

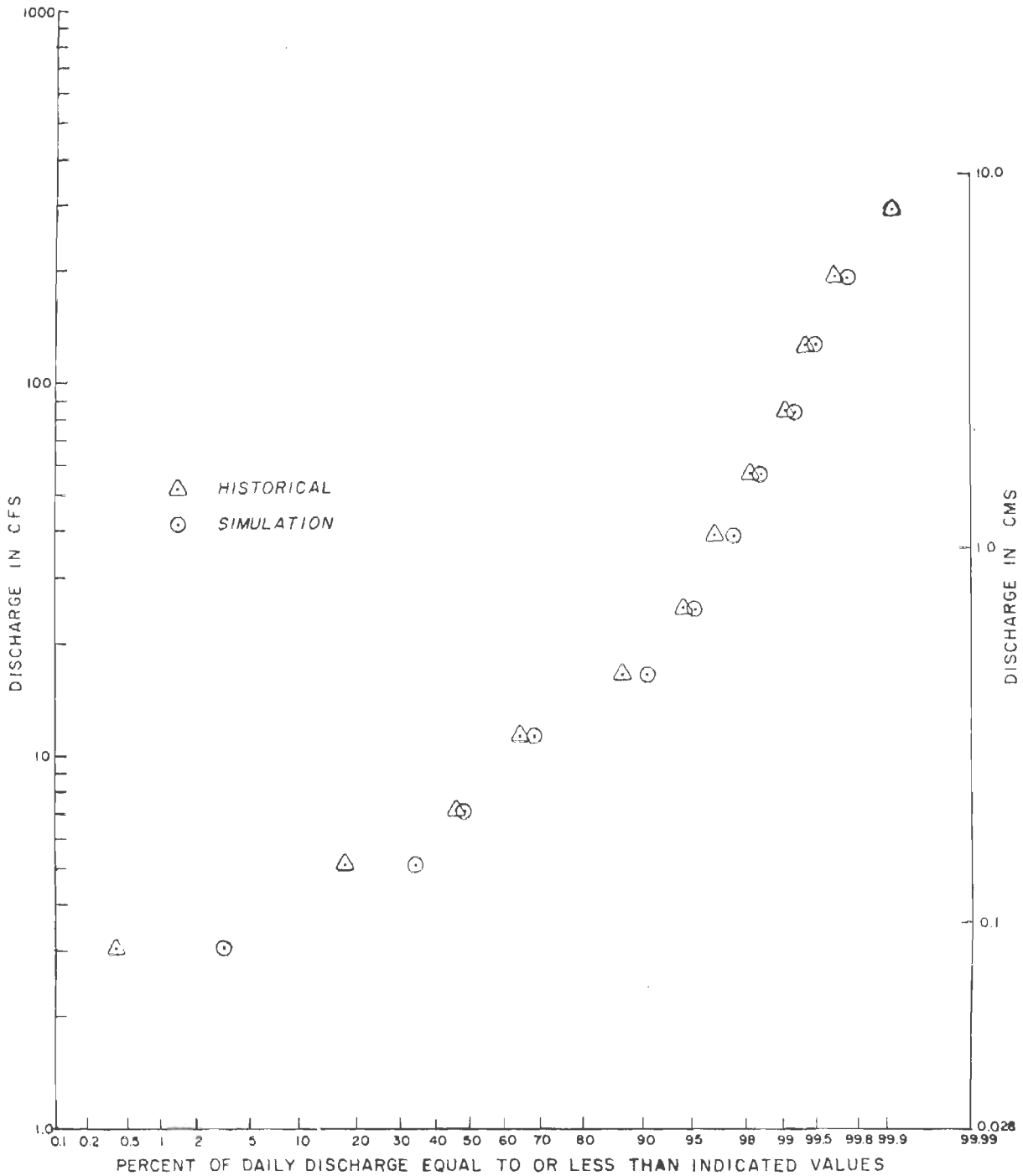

FIGURE 4 : Flow duration curve comparison Cherry Creek, Denver, Colorado daily duration.

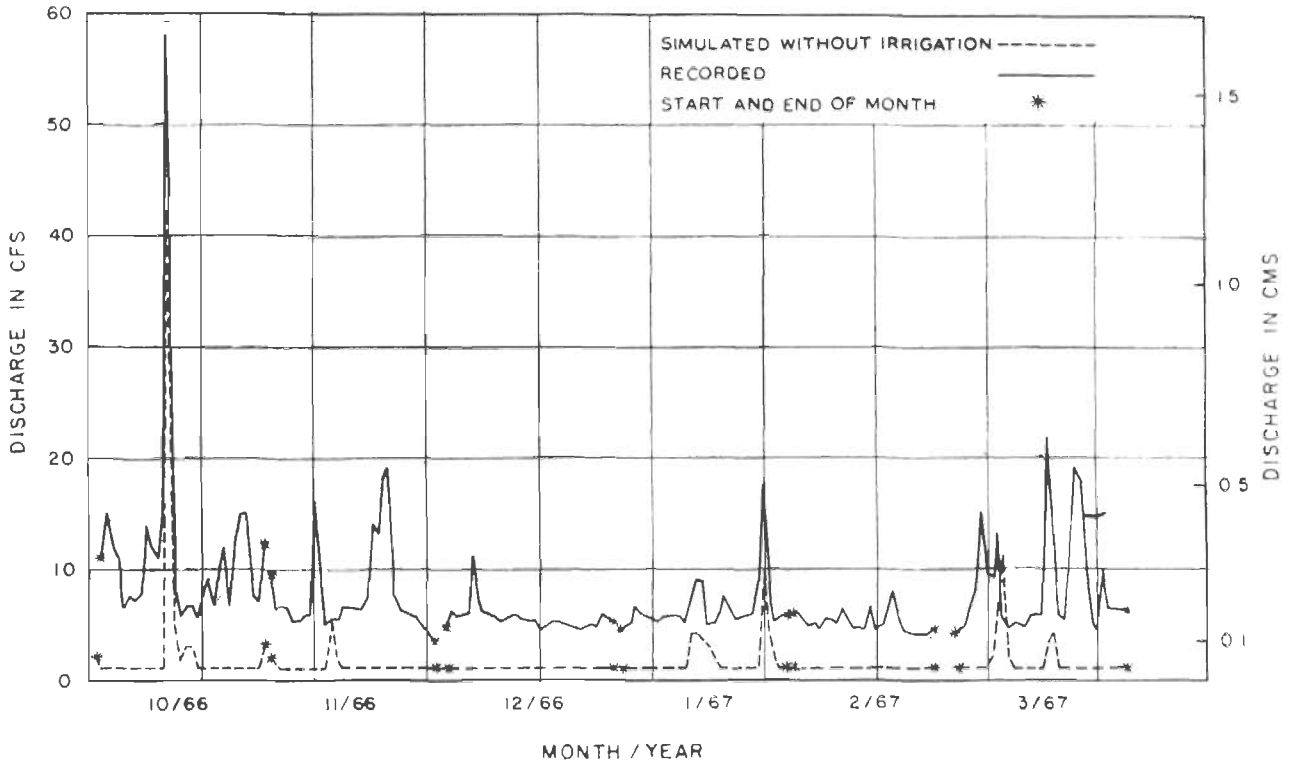

FIGURE 5 : Historical and simulated hydrographs, Cherry Creek at Denver.

induced influences taken into account, is summarized below:

	Percent area	Moisture applied (cm/yr)	C^*	Weighted runoff (cm/yr)
Natural conditions	100	38	0.025	0.95
Modified conditions				
Natural	55	38	0.025	0.52
Impervious	15	38	0.900	5.13
Irrigated	30	117	0.325	11.40
Total annual yield for modified conditions				17.05

* Runoff coefficient from BCI versus Runoff/Rainfall curves developed by R.L. Smith, June 1973.

The observed mean annual streamflow for this watershed over the test period was about 17.5 cm.

The above numerical example illustrates that the streamflow of the Cherry Creek watershed is strongly influenced by irrigation waters. Many areas are affected in an opposite manner by urbanization, i.e., areas of recharge are reduced, thus diminishing base flow contributions. The Cherry Creek watershed is one example where this is not the case.

Conclusions

In summary, it has been found that urbanization may have an unexpected influence upon the base flow regime of a watershed, namely, that base flow increase rather than decrease with expanding urbanization. Through the use of a complex hydrologic computer program and an unrelated procedure for the determination of water yields, it has been shown conclusively that in one semi-arid metropolitan area of the United States, man's endeavours to maintain esthetically pleasing surroundings have appreciably altered the base flow regime. Further exploration and utilization of the concepts discussed above to appraise other areas of the world for similar conditions are recommended.

Acknowledgements

The author wishes to express his gratitude to the

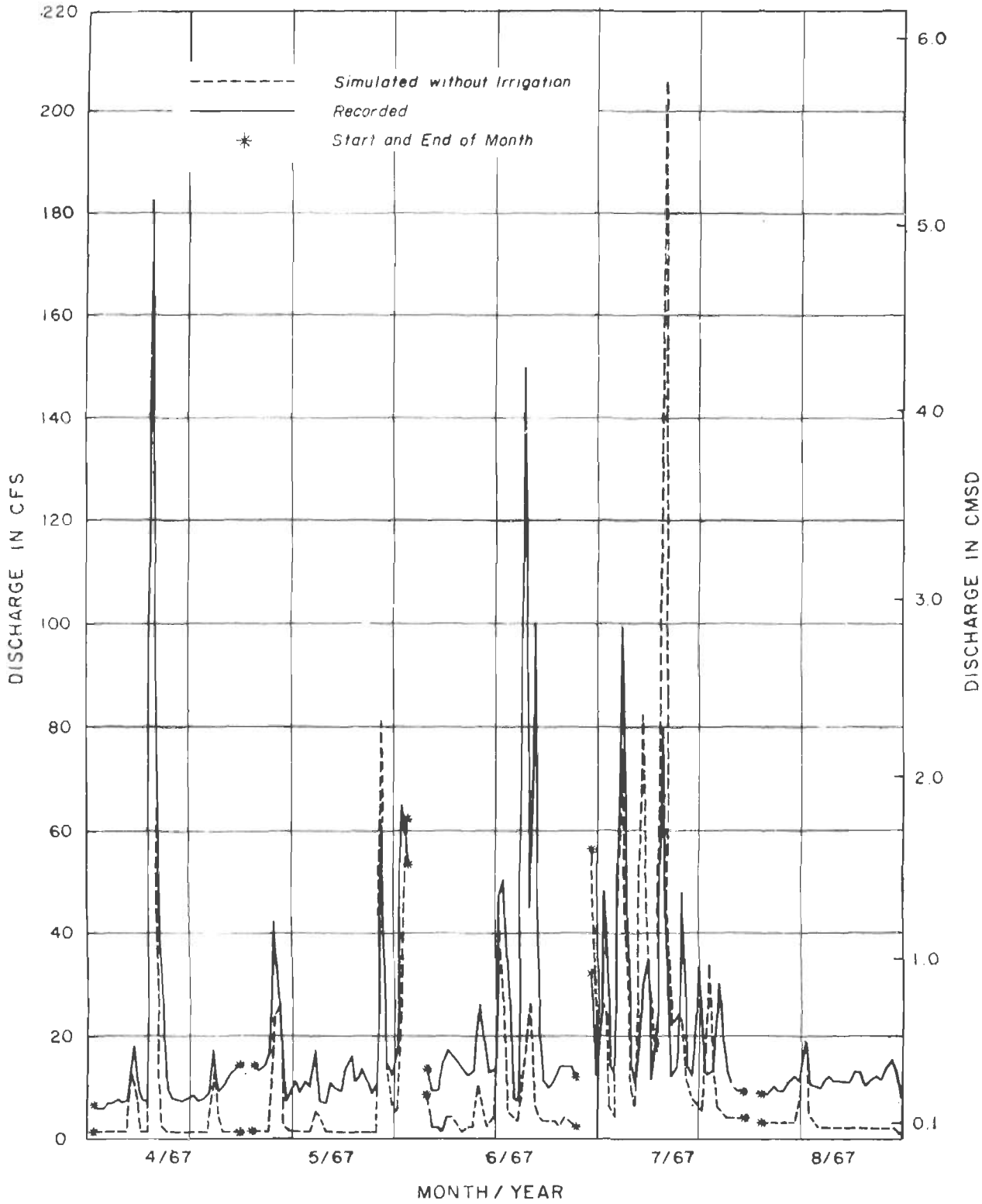

FIGURE 6 : Historical and simulated hydrographs, Cherry Creek at Denver.

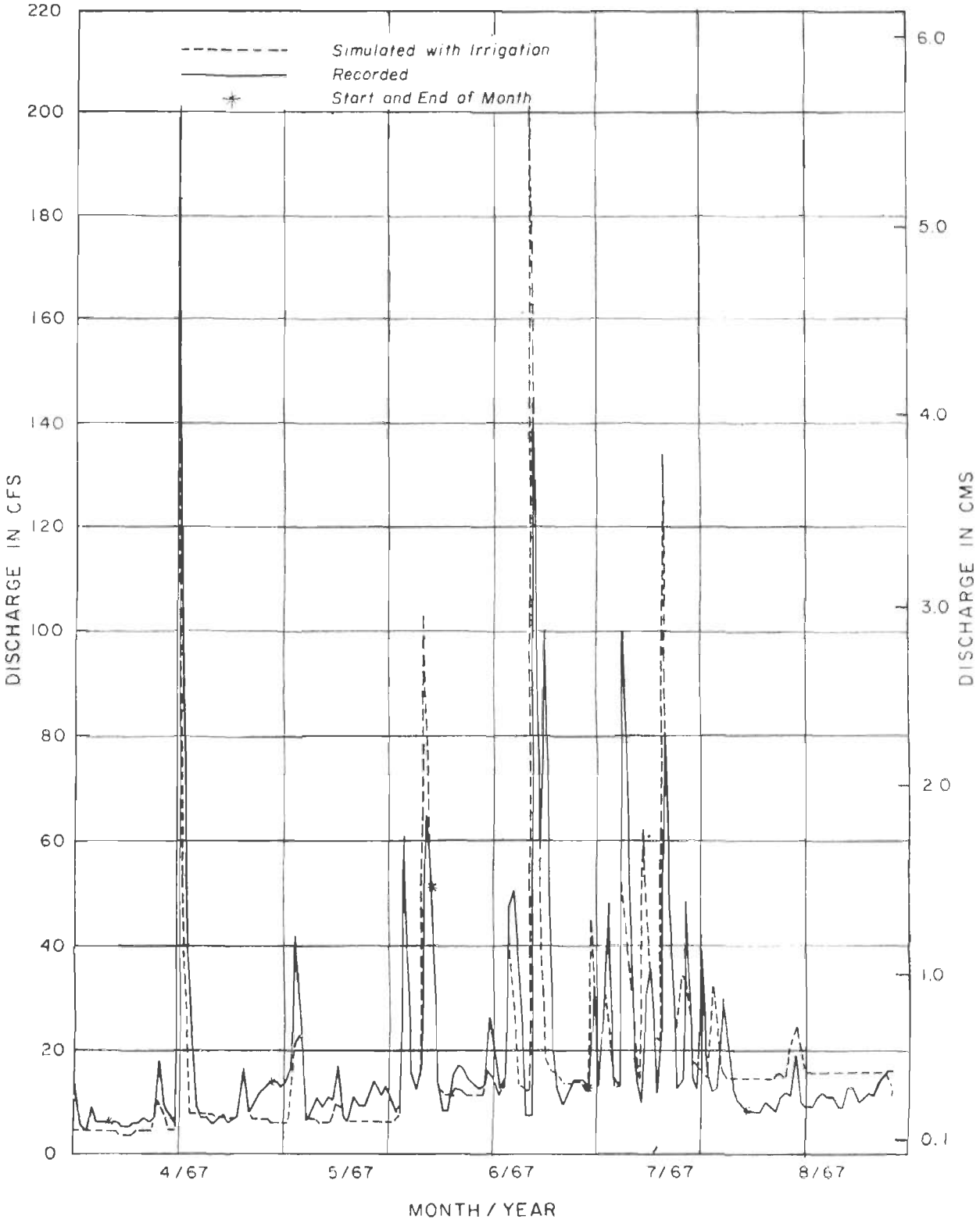

FIGURE 7 : Historical and simulated hydrographs, Cherry Creek at Denver.

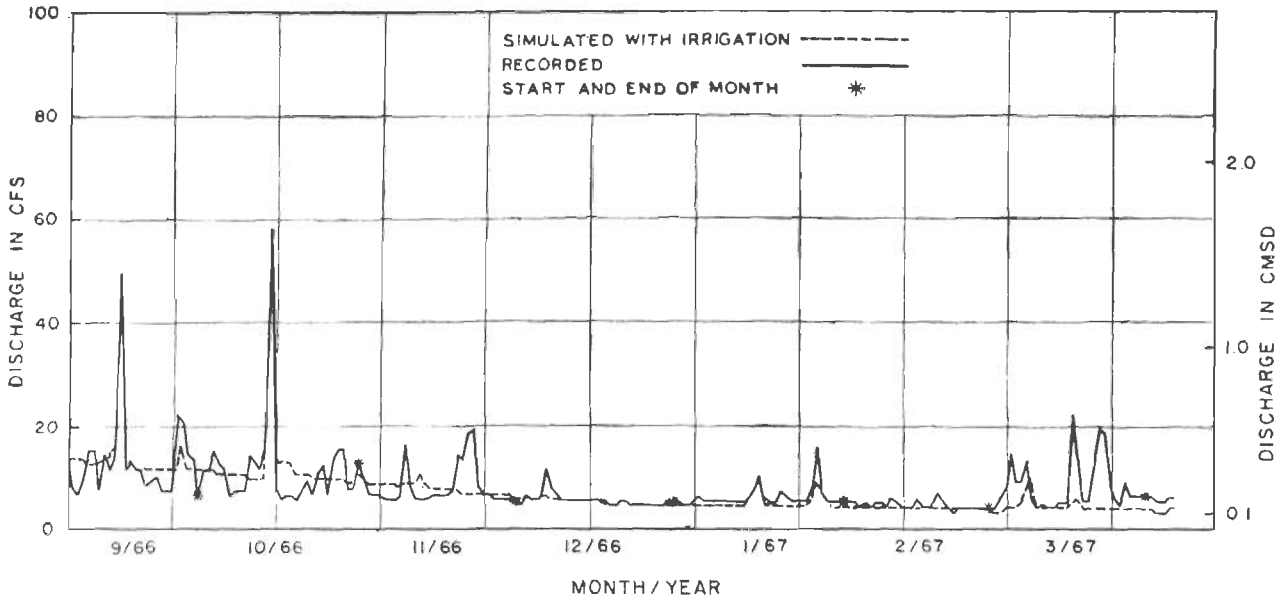

FIGURE 8 : Historical and simulated hydrographs, Cherry Creek at Denver.

Denver Regional Council of Governments for the permission to use information developed during the recently completed water quality management study. In addition, the author is indebted to Black & Veatch and Black & Veatch International, for giving him the opportunity to present these findings before the Second World Congress on Water Resources sponsored by the International Water Resources Association. Special thanks are extended to Mr. V. Phillip Soice, Black & Veatch, Denver for contributions made during this study.

References

(1) SMITH, ROBERT L., Deane Ackers Professor of Civil Engineering, University of Kansas, Lawrence, Kansas, U.S.A. : "Utilizing Climatic Data to Appraise Potential Water Yields," presented at the International Symposium on Design of Water Projects for Areas of Inadequate Data, Madrid, Spain, June 1973.

(2) BLACK & VEATCH, Consulting Engineers, Hydroquality Model Report, Denver Regional Council of Governments, Water Quality Management Program, Project No. IGA-00034, Volume 2, May 1974.

(3) HYDROCOMP INTERNATIONAL, Operations Manual, Second Edition, 15 July 1969.

A Simple Runoff Model Utilizing Soil Moisture Parameters

VIJAY P. SINGH
Assistant Professor of Hydrology
New Mexico Institute of Mining and Technology
Socorro, New Mexico, 87801, U.S.A.

W. TREVOR DICKINSON
Associate Professor of Hydrology
School of Engineering, University of Guelph
Guelph, Ontario, Canada

SYNOPSIS

It is contended that soil moisture storage characteristics in the upper horizons of the soil profile are important parameters affecting the runoff generation on small agricultural watersheds. A simple runoff model has been developed, utilizing parameters of soil moisture storage. These parameters are obtained from an independent soil moisture model. The runoff model is applied to predict runoff on a small agricultural watershed in the Southern Ontario Region of Canada. The model parameters are optimized by an iterative algorithm utilizing an objective function based on the minimization of the sum of squares of deviations between observed and predicted runoff. Agreement between observed and predicted runoff is found to be satisfactory, and sources of discrepancies in the predictive performance of the model are briefly indicated.

Introduction

The development of a runoff prediction model for agricultural watersheds is vital for the solution of many water resource problems, including the design of surface water control facilities, the economic appraisal of flood prevention programs, the study of the effects of existing and proposed watershed projects, and the evaluation of the effects of changes in land management. Given the direct runoff, design hydrographs can be developed using the methods of hydrograph synthesis. The use of available long-term rainfall data, in conjunction with a rainfall-runoff prediction model, permits the determination of various runoff probabilities and long-term sediment yields when given a relationship between direct runoff and sediment.

It is recognized that there are a number of runoff models in hydrology today. Some of them are very elaborate [Crawford and Linsley (1966) ; Dawdy et al (1970); Holtan and Lopez (1973) ; Singh (1974)], while others are simple. Most of these models require specialized computer programming skill and an extensive amount of data for their calibration. Both these facilities are often lacking in some developing countries. This predicament makes advanced modelling technology practically useless in such situations, at least for some time to come. Simple procedures, amenable to hand or desk calculators and having a fewer number of parameters, might be desirable for the solution of many problems.

The objective of this study was to develop a simple surface runoff model that utilized the parameters of soil moisture storage determined from an independent soil moisture model.

The Soil Moisture Model

The soil moisture model is only briefly described here. For a more complete discussion, see the reference by Singh and Dickinson (1975). The model accounts for the movement of moisture into and out of the upper 30 in. of soil profile, and for the moisture stored within the profile. The distributed nature of the model, as shown in Figure 1, incorporates five zones of storage derived from field observations of soil characteristics. The choice of the number of zones is made such that each

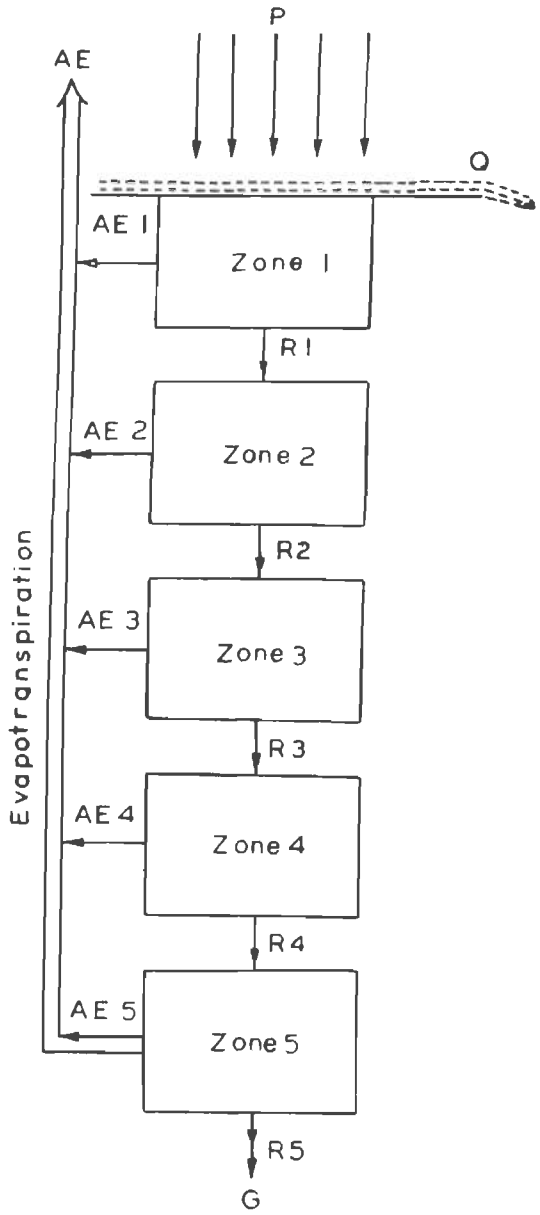

FIGURE 1 : Soil moisture model.

zone is homogeneous and isotropic. The potential evapotranspiration (*PE*) is taken as a possible maximum of actual evapotranspiration (*AE*). The simultaneous withdrawal of soil moisture is allowed to occur from different zones permeated by roots, at rates dependent upon the rate of *PE* and the available soil moisture.

The wetting of the zones takes place from the uppermost zone to the lowermost, each filling to capacity before discharging to the next lower zone. When all zones have attained their maximum values of moisture content, additional rain is treated as runoff [surface runoff (Q)+ground water (G) or $R5$]. If surface runoff is known, the residual (R) will be treated as ground water runoff. During the wetting phase, evapotranspiration takes place at potential rates.

The drying of the zones is caused by both evapotranspiration and vertical drainage during saturated conditions, and by evapotranspiration alone during unsaturated conditions. The evapotranspiration is distributed over the zones for the simultaneous extraction of soil moisture from them. This distribution is in correspondence with the extraction coefficients assigned to the zones which are considered to be a function of plant root development, soil characteristics, and climatological factors. The actual evapotranspiration (*AE*) is considered to be a function of potential evapotranspiration and available soil moisture in each zone under consideration. This functional relationship is assumed to be linear when soil moisture is equal to or greater than 80 percent of its maximum, and non-linear below this moisture level. It must be noted that evapotranspiration takes place from the zones at different rates at the same time.

Employing these basic concepts, the model monitors and integrates soil moisture in relation to time and space, given daily rainfall, daily evaporation, and daily surface runoff. This integrated effect is easily exhibited by a consideration of the hydrologic continuity equation.

The Runoff Model

The runoff model estimates surface runoff utilizing antecedent soil moisture deficiency (d) which is obtained independently from the soil moisture model described above. Two natural, agricultural watersheds designated as *W*-1, and Speedvale, were selected in the Guelph region of Southern Ontario, Canada. Both watersheds are small, *W*-1 being 20 acres and Speedvale 623 acres in extent. The model was calibrated on watershed *W*-1 and tested on the Speedvale basin. A description of these watersheds is briefly given by Singh and Dickinson (1975). A more complete discussion is presented by Singh (1970).

Concepts basic to the runoff model are considered below.

Antecedent Soil Moisture Index (ASMI)

The antecedent soil moisture index is considered as an index of watershed parameters affecting runoff. It is expressed in terms of antecedent soil moisture deficiency (d) which is obtained independently using the soil moisture model [Singh (1970); Singh (1971); Singh and Dickinson (1975)]. The moisture deficiency existing prior to the occurrence of rainfall, is the amount of moisture necessary to bring available moisture in the upper profile to its field capacity.

Retained Rainfall (RR)

A certain portion of rainfall is retained by the vegetation and the depressions in the ground surface before

runoff commences. This part of rainfall is a lumping of so-called interception loss with the depressional storage and is designated here as retained rainfall. Hence, the retained rainfall is the amount of rainfall necessary to satisfy the initial loss before the occurrence of surface runoff. It is difficult to estimate retained rainfall without having some knowledge with respect to the stage of development of the vegetative canopy and the surface conditions on the watershed. For simplicity, it was assumed to be a function of antecedent soil moisture deficiency (d), and was approximated by a cubic polynomial. To determine the polynomial, a number of rainfall episodes which did not produce any surface runoff, and which were small in magnitude, were selected and analyzed using the soil moisture model. The operation of soil moisture model yielded antecedent soil moisture deficiency for all such events. The following relationship was developed :

$$RR = 0.1036 + 0.2775d - 0.0365d^2 - 0.00093d^3$$

Based on the work of Kohler (1963), and incorporating the above concepts, the following non-linear functional relationship for surface runoff was hypothesized :

$$Q = A\left[\{(R - RR)^n + d^n\}^{1/n} - d\right]$$

where, Q = surface runoff, R = rainfall, RR = retained rainfall, d = antecedent soil moisture deficiency, and n and A are watershed coefficients. This relationship takes cognizance of the following facts and hypotheses :

(1) Surface runoff can occur before the entire soil moisture deficiency is satisfied.

(2) Recharge, i.e., rainfall minus retained rainfall and surface runoff, approaches the antecedent soil moisture deficiency as rainfall continues (see Figure 2).

(3) The antecedent soil moisture index ($ASMI$) is used as an index of the watershed parameters affecting runoff.

The above functional relationship is shown graphically in Figure 3, where antecedent soil moisture is the amount of moisture available in the upper 30 in. of soil profile, prior to the occurrence of rainfall. This also illustrates the role of soil moisture in the runoff process.

The coefficients A and n depend on watershed characteristics. The coefficient A appears to account for losses such as depression storage not accounted for by retained rainfall. The coefficient n depends on antecedent soil moisture deficiency (d) and is assumed to be linearly related to it [Kohler, 1963], i.e., $n = a + bd$ where, a is the intercept of the line and b the slope of the line.

Parameter Estimation

The model has three parameters A, n and b. The following objective function was utilized in estimating these parameters :

$$min \sum_{j=1}^{n} \{Q_o(j) - Q_e(j)\}^2$$

Subject to the constraints : $o < A \leqslant 1$, $n \geqslant o$, $\neq 1$; where, $Q_o(j)$ is observed surface runoff for the j^{th} event, $Q_e(j)$ is estimated surface runoff for the j^{th} event and N is the number of events in the optimization set. An iterative optimization algorithm was developed to minimize the objective function. First, the surface runoff events for a few years were noted on the watershed W-1; and antecedent soil moisture deficiency was computed for all such events, using the soil moisture model. Initial estimates were then made of the values of the

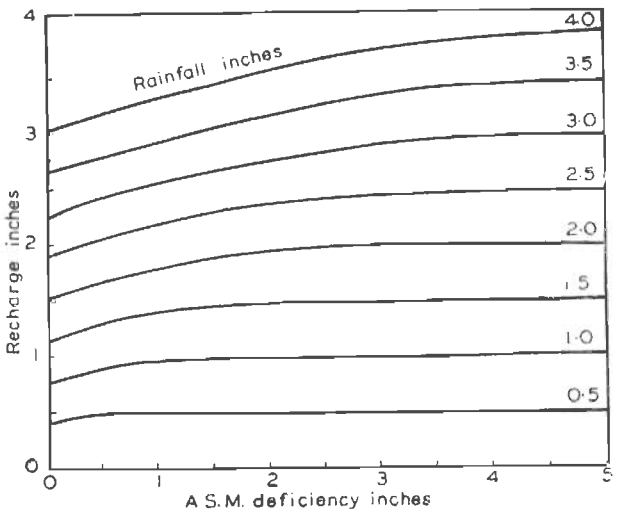

FIGURE 2 : Rainfall-recharge relation.

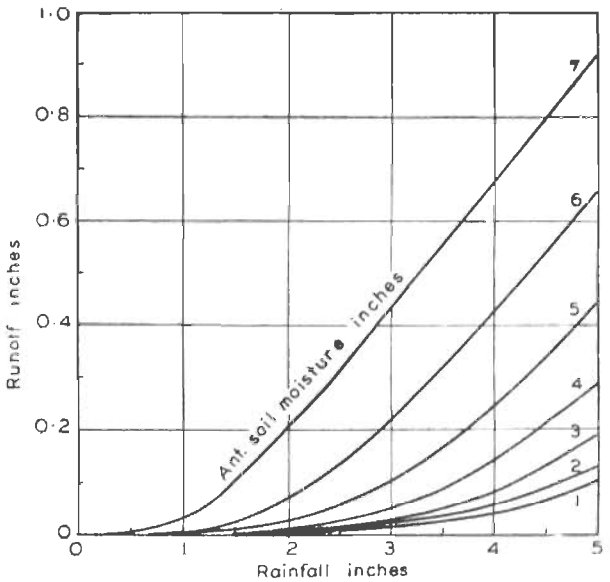

FIGURE 3 : Rainfall-surface runoff relation.

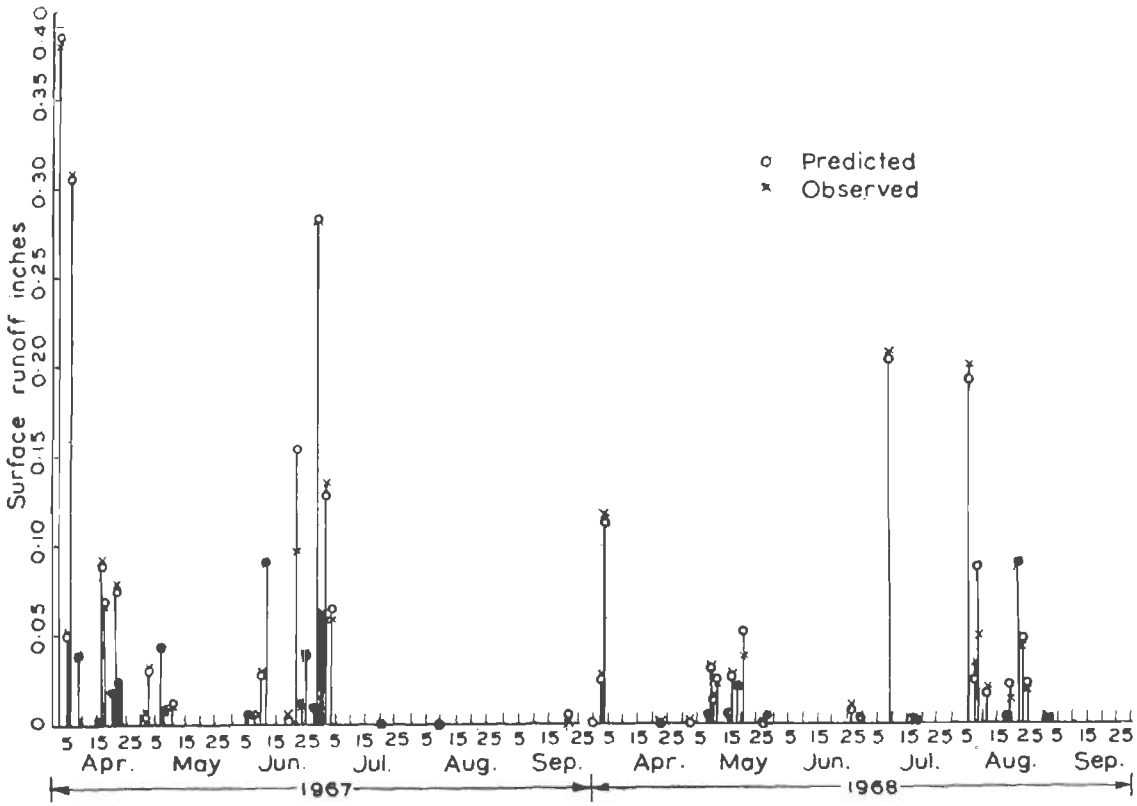

FIGURE 4 : Comparison of observed and predicted runoff for Speedvale watershed.

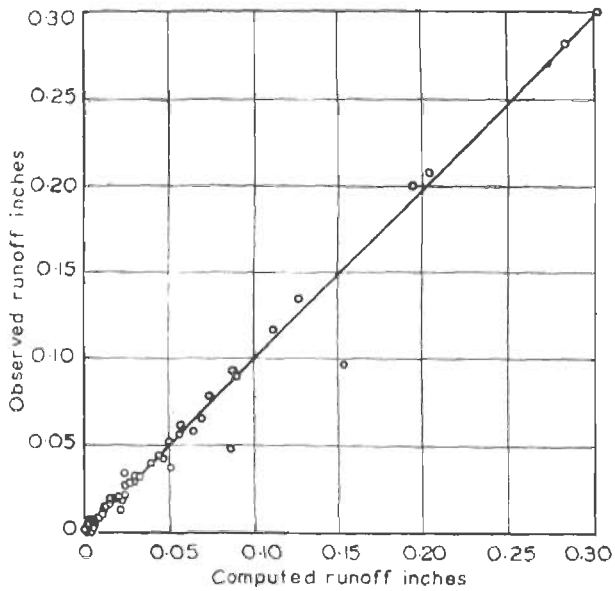

FIGURE 5 : Comparison of observed and predicted runoff for Speedvale watershed.

parameters a, b and A. Surface runoff computations were then made and compared with the corresponding observations. Depending upon their mutual comparability and compatibility, the parameter values were incremented by small amounts and the process of comparison repeated. At the same time, the sensitivity of surface runoff to the various parameters was noted. This process of computation and comparison was repeated until a minimum of the objective function was achieved. The optimum values of the parameters were found to be $A = 0.25$, $a = 2.5$, $b = 0.25$.

Initial Conditions

The following information is required to initiate the operation of the model :

(1) Initial estimates for the parameters.

(2) Soil moisture information prior to the occurrence of rainfall.

(3) Parameters of the soil moisture model.

Operation and Application

Daily estimates of rainfall and evapotranspiration are used to operate the soil moisture model which estimates soil moisture in the upper horizons of the soil profile, and ground water. Utilizing soil moisture deficiency, the runoff model estimates surface runoff.

Having optimized the parameters on watershed W-1, the model was tested on the Speedvale watershed for several rainfall-runoff events, utilizing the parameters determined above. The predicted flows were then

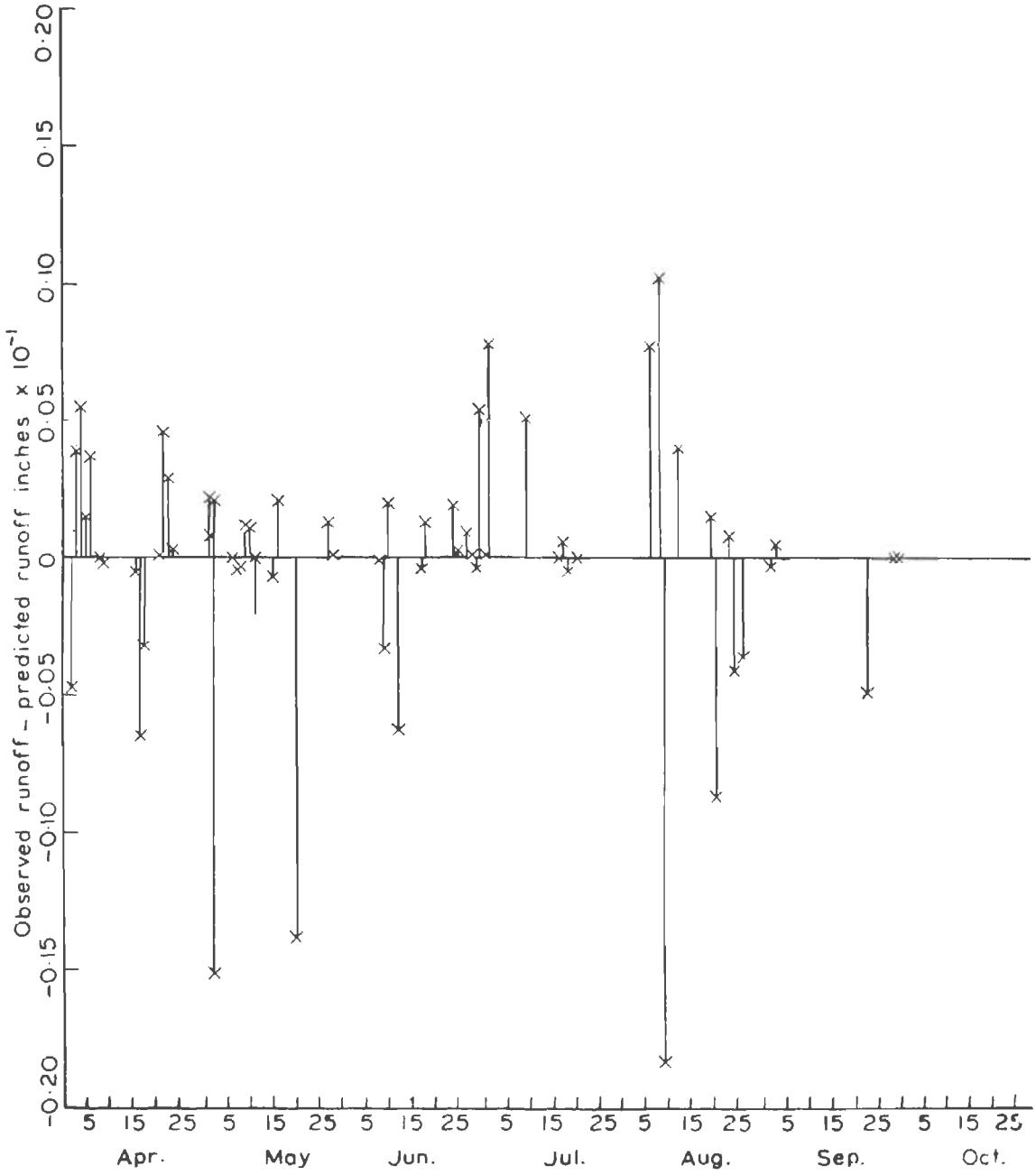

FIGURE 6 : Difference between observed and predicted runoff for the years 1967 and 1968 on Speedvale watershed.

compared with the actual events recorded on the Speedvale watershed as shown in Figures 4—6. These figures illustrate well the agreement between observed and computed runoff. There are a number of instances, however, where no runoff is observed although the model estimates its occurrence, and also the agreement is not as good. Discrepancies are attributable to four main sources of error:

(1) Errors due to the assumptions in the model.
(2) Errors in the data used to calibrate the model.
(3) Errors in the data used to test the model.
(4) Error due to transposition from watershed *W*-1 to Speedvale.

The assumption of antecedent soil moisture deficiency as an index of watershed parameters affecting runoff, is not entirely valid. There are certainly other factors such as rainfall intensity, rainfall duration, watershed shape, size, stream pattern, surface characteristics that affect runoff. Also, there are errors in the assumption associated with retained rainfall. The effect of this inadequacy is seen in several cases in Figure 6, i.e., 2 May 1967; 25 June 1968. This might lead to either overestimation or underestimation.

The calibration and test data possess some element of error, but in comparison to the other sources of error these sources of error are of little consequence. The model does not adequately account for the presence of surface storage in the watershed. Under conditions of relatively large volumes of surface storage, the model tends to predict the occurrence of small runoff events when, in fact, none may have been observed. This inadequacy may be further enhanced by transposition errors.

From Figures 4 & 6, it is apparent that underestimation or overestimation of runoff by the model does not follow any particular trend. This implies that the errors incurred by the model are not systematic in nature. From these figures, it is seen that the relative error which is the difference of observed and computed runoff divided by observed runoff, is generally high when runoff event is small. Thus, by itself, the range of relative error is not a good index for testing models.

Conclusion

The soil moisture storage characteristics in the upper profile are useful parameters to include in an empirical runoff model. Such parameters are easily obtainable, and do not require specialized computing facilities or extensive amount of data. In solving water management problems where these facilities are lacking, simple empirically developed models may prove to be useful. The simple model presented in the paper illustrates this point.

References

(1) CRAWFORD, N.H. and LINSLEY, R.K.: "Digital Simulation in Hydrology: Stanford Watershed Model IV." Technical Report No. 39, July 1966, Stanford University Department of Civil Engineering, Stanford, California.

(2) DAWDY, D.R. et al : "A Rainfall-Runoff Simulation Model for Estimation of Flood Peaks for Small Drainage Basins—A Progress Report." USGS Open File Report, 1970, Colorado State University, Fort Collins, Colorado.

(3) HOLTAN, H.N. and LOPEZ, N.C. : "USDAHL-73 Revised Model of Watershed Hydrology." Plant Physiology Institute Report No. 1, 1973, USDA-ARS, Beltsville, Maryland.

(4) KOHLER, M.A. : "Rainfall-Runoff Models." IASH Publication No. 63, August 1963, pp. 473-491.

(5) KOHLER, M.A. : "Simulation of Daily Catchment Water Balance." Proceedings of Symposium on Water Resources use and Land Management, September 1963, Australia, pp. 312-328.

(6) SINGH, V.P. : "Estimation of Soil Moisture and Surface Runoff for Small Agricultural Watersheds." Unpublished M.S. Thesis, May 1970, School of Engineering, University of Guelph, Canada.

(7) SINGH, V.P. : "Soil Moisture Models (A Review)." Paper Presented at ASAE Annual Meeting at Washington State University, July 1971, Pullman, Washington.

(8) SINGH, V.P. : "A Non-linear Kinematic Wave Model of Surface Runoff." Ph. D. Dissertation, May 1974, Colorado State University, Fort Collins, Colorado.

(9) SINGH, V.P. and DICKINSON, W.T. : "An Analytical Method to Determine Daily Soil Moisture." For Presentation at 2nd World Congress on Water Resources, December 1975, New Delhi, India.

A Distributed and Deterministic Catchment Model using Finite Elements

J. K. WHITE
Lecturer in Civil Engineering
University of London King's College
London (U. K.).

A. W. JAYAWARDENA
Research Assistant in Hydrology
University of London King's College
London (U. K.).

SYNOPSIS

A catchment model is described which is both distributed and deterministic. Use is made of the finite element method to provide the framework within which the model is constructed. The configuration of the model consists of an assembly of simple one-dimensional strip catchments which are orthogonal to the contours of the catchment. The constitutive equations of the model are either the kinematic wave equation for the overland and streamflows, or the diffusion equation for the throughflow component in the upper zones. The ground water flow component of the catchment is not modelled because this was outside the scope of the present study, but there is no reason why this could not be incorporated in an extended model. Apart from the immediate objective of simulating the runoff at any desired point within the catchment, this method of modelling has the potential for study of sediment and pollutant transport processes in catchments. Also the effects of change in land use patterns on the runoff mechanism is another area of application.

Introduction

The processes which determine the nature of the movement of water in the gathering grounds or catchment areas of streams and rivers have attracted the attention of hydrologists, geomorphologists and water resource engineers for more than three centuries. In recent times these processes have become better understood and in certain instances they have been successfully manipulated to produce improved water supplies. The development and control of catchments is often assisted by the availability of a mathematical model which simulates on a computer the movement of water through the catchment.

The complex topography and inhomogeneity of catchments has often led hydrologists to simulate the runoff mechanism using a "black box" approach (1) (2) (3). In this type of model, the distributed characteristics of the catchment are lumped together and only the external response to a given input is simulated. A more helpful model, from the point of view of planning Water Resource Systems, would be one that simulated hydrologic processes within a catchment as well as behaviour on the boundaries. Furthermore, recent developments in hydrology place more emphasis upon the mathematical formulation of the basic physical and chemical processes in the hydrological cycle, and this creates the need for a model that has a framework within which these formulations can be placed. This calls for the development of deterministic models capable of predicting the distributed response of a catchment to a given input. Although the development of a distributed and deterministic model of a real catchment involves the processing of a large number of physical parameters and variables, the rapid development of the computer is operate. It is, therefore, often necessary to make some simplifications to the catchment geometry and some assumptions about the pattern of flow.

Some hydrodynamical models, for example, simplify the catchment into two overland flow planes and one channel reach only (6) (7). In this study, the simplification that is made is to divide the catchment into sub-catchments which take the form of strips, and these in

turn are divided up into elements. The strip catchments are modelled independently and then assembled to obtain the overall catchment response.

In a strip catchment the flow is assumed to be taking place in directions orthogonal to the equipotential lines. For surface drainage systems, equipotential lines are identical with the topographical contours and, therefore, the catchment may be represented as a set of contour lines and a set of flow lines which are orthogonal to each other. Figure 1 shows this for the Plynlimon Catchment. In a natural catchment, as can be seen in Figure 1, the topographical contours are of irregular patterns and are unevenly spaced. When sub-divided into strips this results in an assembly of irregularly shaped strips, so that the approach to modelling the flow within an individual strip must be sufficiently general to accommodate this and permit the same calculation to be carried out for strips of any shape. A typical strip catchment, sub-divided into elements, is shown in Figure 2.

The flow along these strips is considered to be one-dimensional, by assuming that the flow is always orthogonal to the topographical contours. This of course does not mean that the flow has to be assumed to be unidirectional, as the constitutive equations may be framed with reference to a curvilinear axis along a strip.

This process of breaking up the catchment into an assembly of strip catchments has the typical advantages

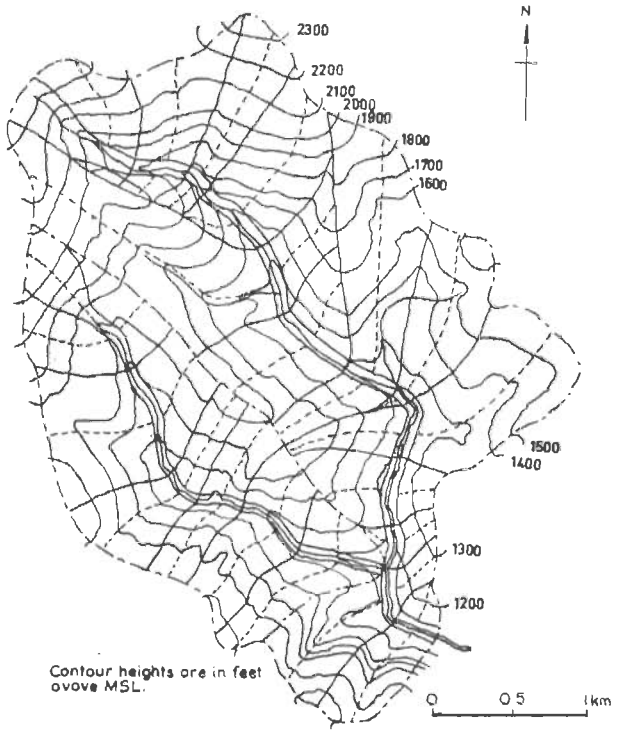

FIGURE 1 : Plynlimon Wye catchment divided into one-dimensional sub-catchments.

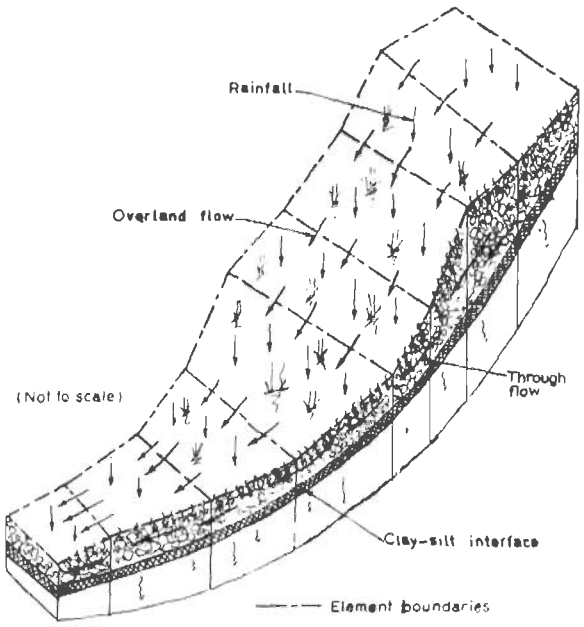

FIGURE 2 : Strip catchment sub-divided into elements.

of constructing with a modular system. The description of the catchment for computing purposes becomes a routine, the actual numerical operations carried out on each module are the same, the behaviour of any particular module within the catchment may be monitored with ease, and changes in the catchment parameters may be made by simple exchange of modules. Overland flow, throughflow and streamflow are all modelled using this modular approach.

The disadvantage is that numerical inaccuracy is inevitable. This occurs when any continuum is sub-divided into elements for analysis, and the proposed method is no exception.

Flow Models

In view of the fact that distributed models of ground water flow have received a great deal of attention in the past and have been developed to a much higher degree of sophistication than surfaceflow models, this study has been confined to modelling the surfaceflow components of the hydrological cycle. There are three of these components, overland flow, throughflow and streamflow, and the constitutive equations used for them are described in separate sections below.

Overland Flow

Overland flow is defined as the flow of precipitated water in excess of infiltration and evaporation. If it is imagined to flow down a slope in the form of a thin sheet, the following equations based on the conservation of mass and momentum define the flow in a

one-dimensional domain such as a strip catchment, when the Coriolis term is omitted :

$$\frac{\partial q}{\partial x} + \frac{\partial h}{\partial t} = Q \qquad \ldots(1)$$

$$\frac{\partial h}{\partial x} + \frac{u}{g}\frac{\partial u}{\partial x} + \frac{1}{g}\frac{\partial u}{\partial t} + \frac{Qu}{gh} = S_o - S_f \qquad \ldots(2)$$

where, q = discharge/unit width,

h = depth of flow,

Q = lateral inflow/unit area,

u = velocity of flow,

g = acceleration due to gravity,

S_o = bed slope of the flow plane,

S_f = friction slope,

x = distance down the plane, and

t = time.

For hillside slopes it is often adequate to approximate the momentum equation, Equation (2), by ignoring the inertia terms, the lateral inflow term and the depth gradient term. This can be justified by an order of magnitude analysis of the different terms. The momentum equation then reduces to a statement that the friction slope is equal to the bed slope which implies that,

$$q = \alpha h^m \qquad \ldots(3)$$

where for laminar flow $\alpha = \frac{gS_o}{3\nu}$, $m = 3$

and for turbulent flow $\alpha = \frac{\sqrt{S_o}}{n}$, $m = 5/3$

ν is the kinematic viscosity and 'n' is Manning's roughness coefficient ([8]) ([9]).

When Equation (3) is substituted into Equation (1) this becomes the familiar kinematic wave Equation (10).

Numerical solutions for Equations (1) & (2) have been obtained by several investigators for flow over simple planes ([11]) ([12]) ([13]). For natural surfaces where the flow pattern is very complex and is more likely to be composed of a system of rivulet and vein flows in the root zone, rather than be in the form of sheet flow, Horton's experiments indicate that $m = 2$, ([14]). In the present study overland flow, when encountered, is modelled in strip catchments using $m = 2$ and $\alpha = \frac{\sqrt{S_o}}{n}$ in Equation (3), with x becoming the distance along the curvilinear axis of the strip, and h becoming the average depth of flow.

Throughflow

The overland flow theory seems to fail in most humid forested areas where the infiltration rates are usually in excess of the normal rainfall rates. Although the exact mechanism which causes flow in such areas is not completely understood, it can be thought of as a combination of saturated and unsaturated sub-surface flow in the upper zones, the relative importance of the two types depending upon the type of soil. The experiments of Whipkey and Weyman ([15]) ([16]), have revealed that in these areas the sub-surface flow within the layers of soils immediately below the ground surface is the major component of streamflow. This slow saturated sub-surface flow is known as throughflow.

For the present study, the saturated phase is the appropriate model but the unsaturated phase may be significant for other types of soils.

The proposed constitutive equations, given below, are the continuity equation and a diffusion equation, implying that throughflow is a diffusive process ([17]) :

$$\frac{\partial q}{\partial x} + S\frac{\partial h}{\partial t} = Q' \qquad \ldots(4)$$

$$q = -Kh\frac{\partial \phi}{\partial x} \qquad \ldots(5)$$

where,

h = depth of saturated region,

S = porosity of soil or saturated volumetric soil moisture content,

K = hydraulic conductivity of the soil in the direction of a strip,

ϕ = total potential ($h+z$),

z = gravitational potential, and

Q' = recharge rate per unit area due to rainfall.

In practice $\frac{\partial h}{\partial x} \ll \frac{\partial z}{\partial x}$ and the approximation $-\frac{\partial \phi}{\partial x} = S_o$ may be made.

Streamflow

The streams in hillside catchments are quite often not well defined waterways. Therefore, the same equations that govern overland flow may be assumed to govern the streamflow. This assumption is not valid for channel reaches of very mild slopes such as estuaries or for very steep hillside streams. An advantage in using the kinematic wave approximation is that the solution scheme does not require a downstream boundary condition. The channel reaches, in addition to local precipitation, receive lateral inflow from overland slopes either as surface or sub-surface flow.

Method of Solution

For overland flow on a strip catchment, Figure 2, Equations (1) & (3) may be combined to obtain,

$$\frac{\partial}{\partial x}\left[\frac{w\sqrt{S_o}}{n}h^2\right] + w\frac{\partial h}{\partial t} = Qw \qquad \ldots(6)$$

Similarly for throughflow Equations (4) & (5) may

be combined to obtain,

$$\frac{\partial}{\partial x}(KS_o wh) + Sw\frac{\partial h}{\partial t} = Q'w \qquad ...(7)$$

In Equations (6) & (7) 'w' indicates the width of a strip at any point, and is included to account for variations in width along a strip catchment.

The application of the finite element method of solution of differential equations which describe field phenomena, such as Equations (6) & (7), results in the determination of values of the solution at points around the boundary of the individual elements of the assembly. The complete solution is determined by the interpolation between these points so that the accuracy of solution is related to the density of the elements. The method is similar to the finite difference method, but it is easier to use in that the shape of the elements is more flexible and, therefore, it is more adaptable to fields with complex geometries. In both methods the solution is obtained by solving a matrix equation for the unknown variables. In the case of constitutive equations containing time as an independent variable it is possible to solve the space domain by the finite element method and the time domain by the finite difference method.

For the solution in using linear interpolation functions, the matrix equations are of the form,

$$|HH|\ |h^2| + |HIJ|\ |h_i h_j| + |D|\left|\frac{\partial h}{\partial t}\right| - |D|\ |Q| = 0 \qquad ...(8)$$

for overland flow and,

$$|H|\ |h| + |C|\left|\frac{\partial h}{\partial t}\right| - |D|\ |Q'| = 0 \qquad ...(9)$$

for throughflow.

When combined with the solution in time the matrix Equations (8) & (9) become

$$|A|\ |h| = |B| \qquad ...(10)$$

Initial conditions are assumed and the finite difference method outlined in the Appendix is used.

The matrices $|H|$, $|HH|$, $|HIJ|$, $|C|$, $|D|$, $|A|$ and $|B|$ are defined in the Appendix.

For overland flow the matrix $|A|$ is a function of $|h|$ and Equation (10) is non-linear. An iterative method based on the Newton-Raphson technique is then used to obtain a solution.

Once the values of h have been obtained these may be converted to values of flow using Equation (3) or (5) as appropriate. Thus for each time interval of the computation the flows throughout each strip catchment are determined in turn taking into account the fact that some of these flows contribute to the inflow of other strips, such as those which model well defined drainage paths or streams.

Application to Plynlimon Catchment

The Plynlimon Catchment

Plynlimon is located in North Wales, Great Britain, between the approximate latitudes 52° 25′ and 52° 28′ *N* and the approximate longitudes 3° 36′ and 3° 45′ *W*. This is an experimental catchment set up by the Institute of Hydrology to identify hydrological differences between two adjacent upland catchments with different vegetative cover. The two adjacent ones are the headwaters of the River Wye which has a catchment area of 1,055 ha and the River Severn which has a catchment area of 870 ha. The Wye Catchment which will be used as an example in this study is mainly a peat covered catchment. A typical soil profile consists of 10-15 cm of peat above 5-10 cm of clay/silt horizon overlying 50 cm of loose, shaly mudstone flakes which grade into the bedrock ([18]). The vaguely known properties of peat suggest that the main drainage process in this catchment is throughflow above the clay/silt interface, and this is assumed in this example. However, for higher rainfall intensities, a combination of overland flow and saturated sub-surface flow may exist. Unsaturated flow through different layers of soil is ignored for this study.

Storm Hydrograph Simulation

Due to lack of adequate physical data, model parameters had to be estimated using available information from other sources ([19]) as guidelines. In view of the fact that the physical characteristics of the catchment are approximately uniformly distributed, all model parameters were assumed to be uniform over the entire catchment. This method of modelling, however, readily accommodates non-uniform parameters when necessary. The following values were found to give reasonably good simulated hydrographs, when compared with the recorded streamflow from three winter storms, Figures 3, 4 & 5 :

Hydraulic Conductivity (K)	0.1 m/sec
Porosity (saturated volumetric soil moisture content, S)	0.75
Mannings 'n'	2.02

The hydraulic conductivity may appear to be quite high when compared with that for an ordinary soil. But in Plynlimon, the presence of a network of sub-surface soil pipe formation may explain this rather high value. Although these values have not been experimentally verified, they seem to fall within the ranges of values quoted by others ([19]) ([20]), for similarly textured surfaces.

Measured values of storm losses such as interception, depression storage, evaporation, and deep percolation were not available for this study. Therefore, an estimation of losses based upon a short-term water budget analysis was used for determining the amount of precipitation producing direct runoff, and this was found to be about 25 percent of the recorded precipitation. A time span equal to twice the duration of the storm was

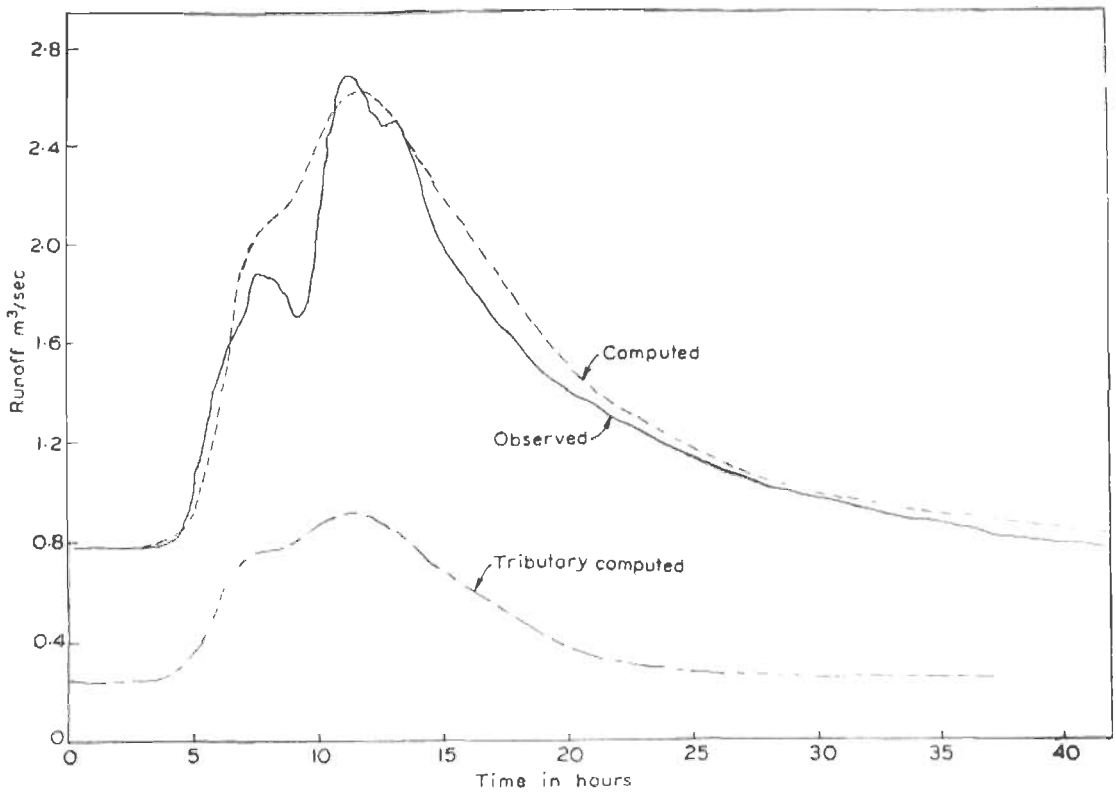

FIGURE 3 : Flood hydrographs for the storm on 22 November 1971.

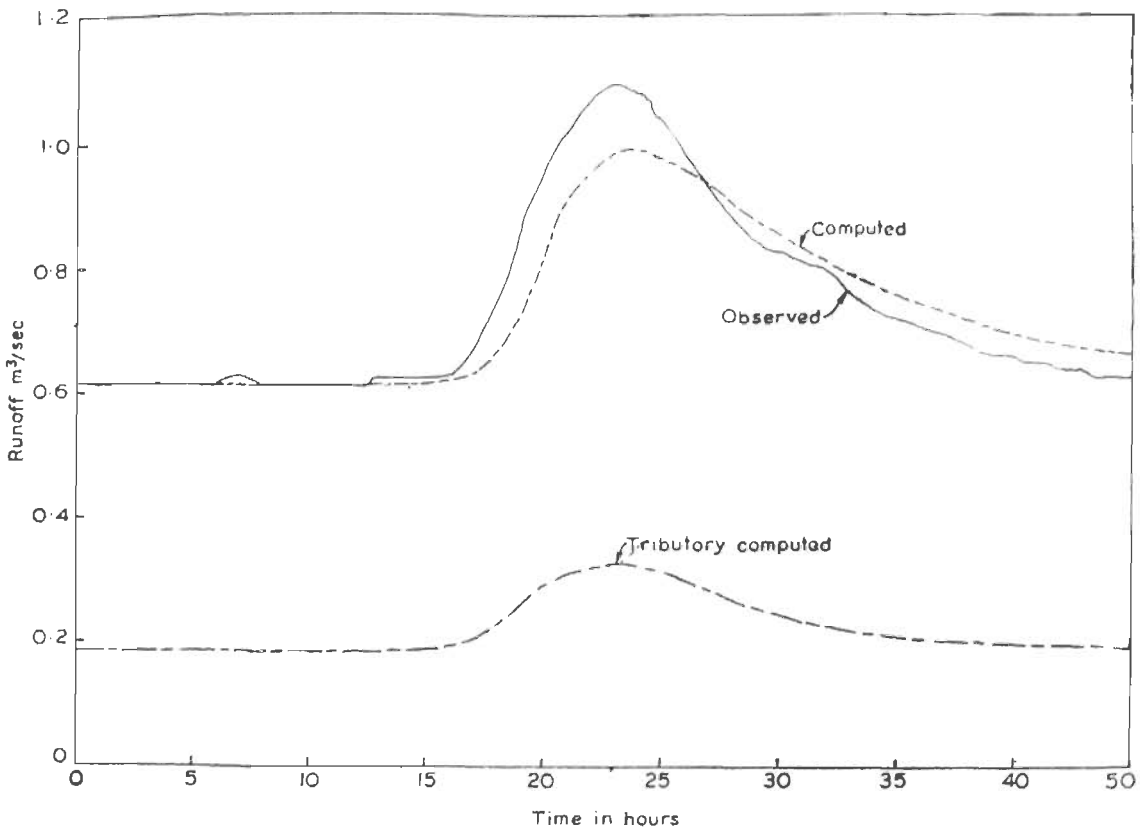

FIGURE 4 : Flood hydrographs for the storm on 25 November 1971.

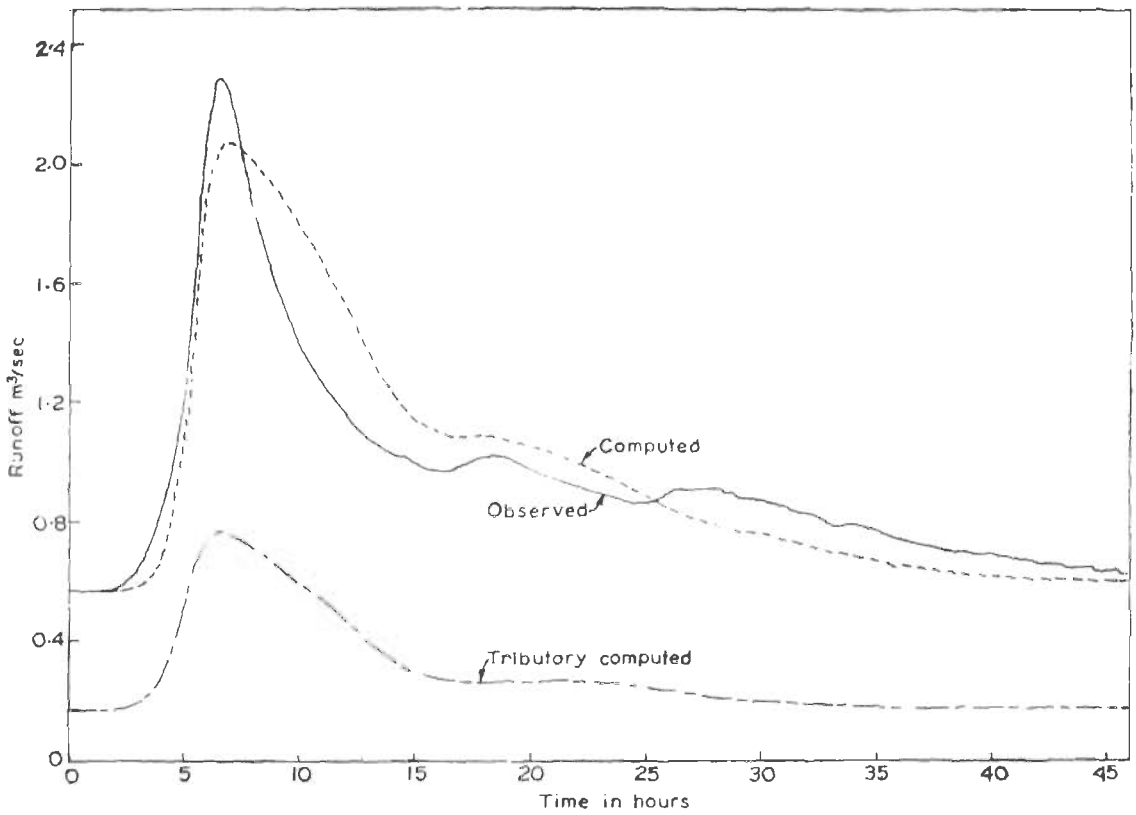

FIGURE 5 : Flood hydrographs for the storm on 27 November 1971.

found to be reasonable for the short-term water budget analysis, because, most of the winter storm flows reach a steady state during this time. Baseflow, which is the contribution from ground water was assumed to be constant during this span which at the most was about 3 days. As indicated before, the most valuable potential of a distributed model is its capability to simulate the internal behaviour of the catchment. This method can simulate the flow at any point in the catchment with no additional effort or resources. Although at this stage, there is no verification for the internal results, due to lack of recorded information, the contribution from a sub-catchment of 318 ha in area, which drains through a tributary of the Wye is indicated in Figures 3, 4 & 5.

For these examples the catchment area of 1,055 ha was sub-divided into 40 strip catchments and 350 elements, that is an average of 3 ha per element or 7·4 acres per element. The computation was carried out on a CDC 7600 computer which took 17 seconds of computing time to process a 45 hour storm and a further 5 seconds to plot the results on a microfilm plotter. Thus computing time for a catchment of this size with an element density of 3 ha per element is about 0·5 seconds per hour of storm. The time interval in the calculation was 15 minutes.

Conclusion

The design of a distributed catchment model by a method of assembling strip catchments has been demonstrated to work successfully as an input-output model for three storms on a particular catchment, even though the mechanism of flow and the characteristic parameters of the catchment have been greatly simplified. Although this is not sufficient evidence to make any great claims for its immediate usefulness, the foundations have been laid for the development of the model to simulate catchment storage effects and ground water flow as well as surface flow. If further tests confirm the general application of this approach, then the potential exists for the model to simulate sediment transport and water borne pollution processes within catchments, as well as the simulation of the effects of changes in land use and of the introduction of water resources systems on the catchment hydrology.

Acknowledgements

This study is part of a research project sponsored by the Natural Environment Research Council of Great Britain. Their generous financial assistance is gratefully acknowledged. The authors also wish to acknowledge the Institute of Hydrology for their co-operation in

making the rainfall and runoff data available for the project.

References

(1) SHERMAN, L.K. : "Streamflow from Rainfall by the Unit-graph Method". Eng. News-Record, Vol. 108, 7 April 1932, pp. 501-505.

(2) NASH, N.E. : "Determining Runoff from Rainfall". Proc. Inst. of Civil Engrs., Vol. 10, June 1958, pp. 163-184.

(3) SUGAWARA, M. and MARUYAMA, F. : "A Method of Revision of the River Discharge by Means of a Rainfall Model". Symposia Darcy, Intern. Assoc. Sci. Hydrology, Pub. 42, Vol. 3, 1956, pp. 71-76.

(4) WHITE, J.K. : "A Finite Element Deterministic Catchment Model". Numerical Methods in Fluid Dynamics, Pentech Press, Edited by Brebbia, C.A. and Connor, J.J., 1973, pp. 533-543.

(5) TAYLOR, C. et al : "A Finite Element Approach to Watershed Runoff". Journal of Hydrology, Vol. 21, 1974, pp. 231-246.

(6a) WOODING, R.A. : "A Hydraulic Model for the Catchment Stream. Problem 1, Kinematic Wave Theory". Journal of Hydrology, Vol. 3, 1965, pp. 254-267.

(6b) WOODING, R.A. : "A Hydraulic Model for the Catchment Stream, Problem 2, Numerical Solutions". Journal of Hydrology, Vol. 3, 1965, pp. 268-282.

(7) CHOW, V.T and BEN-ZVI, A. : "Hydrodynamic Modelling of Two-Dimensional Watershed Flow". Journal of the Hydraulics Division, A.S.C.E., Nov. 1973, pp. 2023-2040.

(8) VENNARD, J.K. : "Elementary Fluid Mechanics". 4th Edition, John Wiley & Sons, Inc., New York, N.Y., 1960, pp. 356-357.

(9) CHOW, V.T. : "Open Channel Hydraulics". International Student Edition, McGraw-Hill Book Company, Inc., Kogaku-Sha Company Ltd., Tokyo, 1969, pp. 98-100.

(10) LIGHTHILL, M.J. and WHITHAM, G.B. : "On Kinematic Waves. I. Flood Movement in Long Rivers". Proc. of the Royal Society of London, Vol. 229, May 1955, pp. 281-316.

(11) MORGALI, J.R. : "Computer Analysis of Overland Flow". Journal of the Hydraulics Division, A.S.C.E., May 1965, pp. 81-100.

(12) ABDEL-RAZAQ, A.Y. et al : "A Solution to the Surface Runoff Problem". Journal of the Hydraulics Division, A.S.C.E., Nov. 1967, pp. 335-352.

(13) CHEN, C. and CHOW, V.T. : "Formulation of Mathematical Watershed-Flow Model". Journal of the Engineering Mechanics Division, A.S.C.E., June 1971, pp. 809-828.

(14) HORTON, R.E. : "The Interpretation and Application of Runoff Plot Experiments with Reference to Soil Erosion Problems". Proc. Soil Sci. Soc. of America, Vol. 3, 1938, pp. 340-349.

(15) WHIPKEY, R.Z. : "Sub-surface Stormflow from Forested Slopes". Bulletin Intern. Assoc. of Scientific Hydrology, Vol. 10, No. 3, 1965, pp. 74-85.

(16) WEYMAN, D.R. : "Throughflow on Hillslopes and its Relation to the Stream Hydrograph". Bull. Inter. Assoc. of Scientific Hydrology, Vol. 15, No. 3, 1970, pp. 25-33.

(17) KIRKBY, M.J. and CHORLEY, R.J. : "Throughflow Overland Flow and Erosion". Bull. of the Inter. Assoc. of Scientific Hydrology, Vol. 12, 1967, pp. 5-21.

(18) Institute of Hydrology, "Research 1972-73" Wallingford, Berkshire, England, 1972. p. 20.

(19) MACFARLANE, I.C (Ed) : "Muskeg Engineering Handbook". Univ. of Toronto Press, 1969, p. 297.

(20) Reference (9) pp. 109-123.

(21) ZIENKIEWICZ, O.C. : "The Finite Element Method in Engineering Science". 2nd edition, McGraw Hill, London, 1971, p. 521.

(22) DESAI, C.S. and ABEL, J.F. : "Introduction to the Finite Element Method—A Numerical Method for Engineering Analysis". Van Nostrand Reinhold Co., New York, N.Y., 1972, p. 477.

APPENDIX

The Finite Element Method

Finite Element Method is a numerical technique used for solving partial differential equations. The theory, applications and limitations are well documented elsewhere([21]) ([22]) and, therefore, no attempt is made to elaborate on the method in this paper. However, some points relevant to this work are briefly outlined in the following paragraph.

Basically, there are two approaches to the problem of formulating a scheme for a discrete solution of a field problem defined over a continuum namely, the variational method and the method of weighted residuals. The latter is adopted for this study since the former has some mathematical limitations to the types of equations that can be solved. Galerkin's method, which is used below is a special case of the method of weighted residuals where the 'interpolation functions' are made equal to the 'weighting functions'. A local co-ordinate system is required for the implementation of the technique and it is best to use the Natural Co-ordinate System, which permits the specification of a point within an element by a set of dimensionless numbers whose magnitude never exceed unity. This system is shown below :

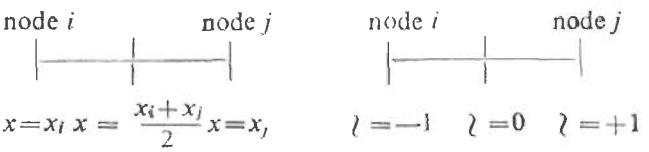

Global Co-ordinate System Local Co-ordinate System

With this system, for a one-dimensional element with linear functional variation, the interpolation functions N_i and N_j can be shown to be

$$N_i = \tfrac{1}{2}(1-\zeta)$$

$$N_j = \tfrac{1}{2}(1+\zeta)$$

Where, ξ is the local co-ordinate given by

$$\frac{2}{L}\left(x-\frac{x_i+x_j}{2}\right)$$

and L is the length of the element.

Overland Flow

Applying Galerkin's method to Equation (6) the following pair of equations can be obtained :

$$\int_e \left[\frac{\sqrt{S_o}}{n}\left(2h\frac{\partial h}{\partial x}+h^2\frac{\partial w}{\partial x}\right)+w\frac{\partial h}{\partial t}-Qw\right]N_i\,dx=0$$

$$\int_e \left[\frac{\sqrt{S_o}}{n}\left(2h\frac{\partial h}{\partial x}+h^2\frac{\partial w}{\partial x}\right)+w\frac{\partial h}{\partial t}-Qw\right]N_j\,dx=0$$

the integration is being carried out over the element between points i and j in the strip catchment.

With some mathematical manipulation it is possible to show that the above two equations are equivalent to the following matrix equation

$$\frac{1}{12}\frac{\sqrt{S_o}}{n}\begin{bmatrix}9w_i+w_j, & w_i+3w_j\\ -3w_i-w_j, & -w_i+9w_j\end{bmatrix}\begin{bmatrix}h_i^2\\ h_j^2\end{bmatrix}$$
$$+\frac{1}{6}\frac{\sqrt{S_o}}{n}\begin{bmatrix}w_i+w_j\\ -w_i-w_j\end{bmatrix}\begin{bmatrix}h_i\,h_j\\ h_i\,h_j\end{bmatrix}$$
$$+\frac{L}{12}\begin{bmatrix}3w_i+w_j, & w_i+w_j\\ w_i+w_j, & w_i+3w_j\end{bmatrix}\begin{bmatrix}\frac{\partial h_i}{\partial t}\\ \frac{\partial h_j}{\partial t}\end{bmatrix}$$
$$-\frac{L}{12}\begin{bmatrix}3w_i+w_j, & w_i+w_j\\ w_i+w_j, & w_i+3w_j\end{bmatrix}\begin{bmatrix}Q_i\\ Q_j\end{bmatrix}=0 \quad ...(11)$$

This is of the form

$$|\,HH\,|\;|\,h^2\,|+|\,HIJ\,|\;|\,h_i\,h_j\,|+|\,D\,|\;|\,\partial h/\partial t\,|-|\,D\,|\;|\,Q\,|=0 \quad ...(12)$$

Throughflow

On the same basis, Equation (7) can be written as :

$$\int_e \left[KS_o\left(h\frac{\partial w}{\partial x}+w\frac{\partial h}{\partial x}\right)+S_w\frac{\partial h}{\partial t}-Q'w\right]N_i\,dx=0$$

$$\int_e \left[KS_o\left(h\frac{\partial w}{\partial x}+w\frac{\partial h}{\partial x}\right)+S_w\frac{\partial h}{\partial t}-Q'w\right]N_j\,dx=0$$

which can be simplified to the following matrix equation :

$$\frac{KS_o}{6}\begin{bmatrix}-4w_i+w_j, & w_i+2w_j\\ -2w_i-w_j, & -w_i+4w_j\end{bmatrix}\begin{bmatrix}h_i\\ h_j\end{bmatrix}$$
$$+\frac{SL}{12}\begin{bmatrix}3w_i+w_j, & w_i+w_j\\ w_i+w_j, & w_i+3w_j\end{bmatrix}\begin{bmatrix}\partial h_i/\partial t\\ \partial h_j/\partial t\end{bmatrix}$$
$$-\frac{L}{12}\begin{bmatrix}3w_i+w_j, & w_i+w_j\\ w_i+w_j, & w_i+3w_j\end{bmatrix}\begin{bmatrix}Q_i'\\ Q_j'\end{bmatrix}=0 \quad ...(13)$$

This is of the form

$$|\,H\,|\;|\,h\,|+|\,C\,|\;\left|\frac{\partial h}{\partial t}\right|-|\,D\,|\;|\,Q'\,|=0 \quad ...(14)$$

Solution in Time Domain

Initial conditions are assumed and a finite difference scheme based upon the following approximation is used to march the solution forward in time :

$$|\,h\,|_{t_2}=|\,h\,|_{t_1}+\left[\frac{\left|\frac{\partial h}{\partial t}\right|_{t_2}+\left|\frac{\partial h}{\partial t}\right|_{t_1}}{2}\right]\Delta T \quad ...(15)$$

the suffixes denote times 1 and 2.

With this approximation substituted in Equation (12), for overland flow, the following matrix equation can be obtained :

$$|\,HH\,|\;|\,h^2\,|_{t_2}+|\,HIJ\,|\;|\,h_i\,h_j\,|_{t_2}+\frac{2\,|\,D\,|}{\Delta T}\;|\,h\,|_{t_2}$$
$$+|\,HH\,|\;|\,h^2\,|_{t_1}+|\,HIJ\,|\;|\,h_i\,h_j\,|_{t_1}$$
$$-\frac{2\,|\,D\,|}{\Delta T}\;|\,h\,|_{t_1}-|\,D\,|\left[|\,Q\,|_{t_1}+|\,Q\,|_{t_2}\right]=0 \quad ...(16)$$

which could be further factorised to obtain the final matrix equation which is of the form

$$|\,A\,|\;|\,h\,|_{t_2}+|\,B\,|=0 \quad ...(17)$$

Similarly, for throughflow the resulting equation is of the form

$$|\,A\,|\;|\,h\,|+|\,B\,|=0 \quad ...(18)$$

These element matrices are then assembled to obtain the global matrix for the strip before the solution is carried out. In the case of overland flow, $|\,A\,|$ contains the unknown $|\,h\,|_{t_2}$, thereby making it non-linear.

An Approach to Flood Stage Forecasting

S. CHANDER
Professor
Civil Engineering Department
Indian Institute of Technology, New Delhi (India)

G. JAGMOHAN DAS
Lecturer
Civil Engineering Department
Nagarjunasagar College of Engineering, Hyderabad (India)

S. C. PADHI
Senior Research Scholar
Civil Engineering Department, Indian Institute of Technology, New Delhi (India).

SYNOPSIS

A model of a linear channel and a linear reservoir in series has been adapted for predicting flood stage hydrographs at a downstream section of a river reach knowing the flood stage hydrographs at an upstream section. The technique developed requires the use of only stage data. The method is designed to suit conditions obtaining in India, where discharge data on most of the river sections are not normally available.

The method utilises the Muskingum equation for routing the flood through the river reach. Approximating the unknown stage-discharge curves of the upstream and downstream sections of the river reach to a series of straight lines, it has been found possible to formulate a set of algebraic equations relating the gauges at the upstream and downstream sections. Multiple regression technique has been used for estimating the parameters which are functions of the unknown slope ratios of the stage-discharge curves and coefficients of the Muskingum routing equation. The set of algebraic equations with the estimated parameters has been used for prediction purposes.

A 195 km reach of the River Yamuna between Kalanaur and Delhi bridges has been chosen for checking the validity of the analysis. The predicted and the observed flood stages are compared and are found to be satisfactory.

Introduction

Conceptual models have been developed ([1]) for forecasting discharge hydrographs of the River Yamuna at Delhi, knowing the flood hydrographs at Kalanaur bridge, 195 km upstream of Delhi. These models consist of a linear reservoir and a linear channel in series. The linear reservoir in these models ([1]) has two storage-discharge relations one for rising or constant discharge portion of the Kalanaur hydrograph and the other for falling portion of the Kalanaur hydrograph. The storage is considered to be directly proportional to discharge at Delhi for the rising and for the constant discharge portion of the Kalanaur hydrograph and is given by the Muskingum equation for the falling portion of the Kalanaur hydrograph. This variable storage-discharge relation was found particularly useful in representing the long reach of the river and yielded hydrographs which are physically realizable. However, this method cannot be used on rivers where discharge hydrographs are not available at upstream reaches, owing to the difficulties, administrative and financial, at the time of high floods. This necessitates further research in developing methods which use only the stage data.

In the present paper, an attempt has been made in this direction and the proposed method has been used to predict the stage hydrographs at Delhi using the stage data at Kalanaur Bridge.

The Model

A linear reservoir attenuates the peak of an inflow hydrograph and a linear channel translates the inflow hydrograph in time, which are representative of the physical action performed by the catchment. Hence, a model of a linear reservoir connected in series with a linear channel is selected in this study.

A linear channel is defined by the delay time or the time of travel, T, of the flood wave, and is approximately determined with the help of the time to peaks of some flood events at the upstream and the downstream stations of a river reach.

A linear reservoir is defined by its storage-discharge relation. For this purpose, the Muskingum Equation (1) has been considered :

$$S = K[x.I+(1-x).Q] \qquad ...(1)$$

where,

S = channel storage in the reach,

I = inflow discharge entering at the upstream station,

Q = outflow discharge leaving at the downstream station,

x = a coefficient expressing the relative influence of discharge at the upstream and downstream stations on the variation in the channel storage, and

K = a parameter with units of time.

The continuity equation can be written in the finite difference form as shown below :

$$\frac{(I_1+I_2)}{2}-\frac{(Q_1+Q_2)}{2}=\frac{(S_2-S_1)}{\triangle t} \qquad ...(2)$$

where, the subscripts 1 and 2 denote the values of I, Q and S at the beginning and end of the time interval, $\triangle t$.

Inserting the values of S from Equation (1) in Equation (2) :

$$Q_2 = C_1Q_1 + C_2I_1 + C_3I_2 \qquad ...(3)$$

where,

$$C_1 = \frac{K-K.x-0.5\triangle t}{K-K.x+0.5\triangle t} \qquad ...(4)$$

$$C_2 = \frac{K.x+0.5\triangle t}{K-K.x+0.5\triangle t} \qquad ...(5)$$

$$C_3 = \frac{-K.x+0.5\triangle t}{K-K.x+0.5\triangle t} \qquad ...(6)$$

and $C_1 + C_2 + C_3 = 1$ ...(7)

For different discharges of the downstream station, Equation (3) can be written as :

$$\begin{aligned} Q_2 &= C_1Q_1 + C_2I_1 + C_3I_2 \\ Q_3 &= C_1Q_2 + C_2I_2 + C_3I_3 \\ Q_4 &= C_1Q_3 + C_2I_3 + C_3I_4 \\ &\cdots\cdots\cdots\cdots \\ Q_n &= C_1Q_{n-1} + C_2I_{n-1} + C_3I_n \end{aligned} \qquad ...(8)$$

Taking the difference of the successive discharges, the following set of equations are obtained :

$$(Q_3-Q_2) = C_1(Q_2-Q_1) + C_2(I_2-I_1) + C_3(I_3-I_2) \qquad ...(9)$$

$$(Q_4-Q_3) = C_1(Q_3-Q_2) + C_2(I_3-I_2) + C_3(I_4-I_3)$$

$$\cdots\cdots\cdots\cdots$$

$$Q_n-Q_{n-1} = C_1(Q_{n-1}-Q_{n-2}) + C_2(I_{n-1}-I_{n-2}) + C_3(I_n-I_{n-1})$$

A general stage-discharge curve, as shown in Figure 1, may be assumed for each of the two stations. These curves are used only to derive the final set of equations and are divided into (say) three linear ranges as shown in Figure 1. Let the slopes of the 3 linear ranges be denoted by $1/U_1$, $1/U_2$ and $1/U_3$ for the upstream station, and $1/D_1$, $1/D_2$ and $1/D_3$ for the downstream station. Let G_1, G_2, G_3 and G_4,... refer to the stages of the downstream hydrograph and H_1, H_2, H_3,... refer to the stages of the upstream hydrograph and the corresponding linear ranges of the stage-discharge curves in which these stages lie be as indicated in Table I.

TABLE I

	Range of stages	The linear range in which they lie
Downstream Section	G_1, G_2; G_4, G_5;...	One
Downstream Section	G_2, G_3, G_4;	Two
Upstream Section	H_1, H_2, H_3; H_5, H_6;...	One
Upstream Section	H_3, H_4;	Two

The following relations can be established using the definition of slope and the information contained in Table I :

$$1/D_1 = (G_2-G_1)/(Q_2-Q_1)$$

$$1/D_2 = (G_3-G_2)/(Q_3-Q_2)$$

$$1/D_2 = (G_4-G_3)/(Q_4-Q_3)$$

and $1/U_1 = (H_2-H_1)/(I_2-I_1)$

$$1/U_1 = (H_3-H_2)/(I_3-I_2)$$

$$1/U_2 = (H_4-H_3)/(I_4-I_3)$$

Substituting these relations in Equation (9) the following

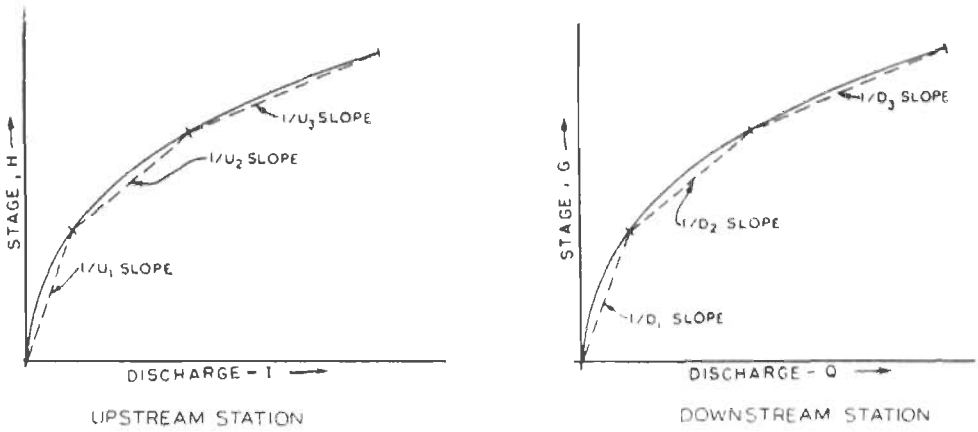

FIGURE 1 : Assumed stage-discharge curves and their conversion into 3 linear parts.

set of equations are obtained :

$$(G_3-G_2) = C_1(D_1/D_2)\,(G_2-G_1) + C_2(U_1/D_2)\,(H_2-H_1) + C_3(U_1/D_2)\,(H_3-H_2)$$

$$(G_4-G_3) = C_1(D_2/D_2)\,(G_3-G_1) + C_2(U_1/D_2)\,(H_3-H_2) + C_3(U_2/D_2)\,(H_4-H_3) \quad \ldots(10)$$

.....

The set of Equations (10) can be written in a general form as :

$$(G_{i+2}-G_{i+1}) = C_1\,\frac{D_{(Gi+1,\ Gi)}}{D_{(Gi+2,Gi+1)}}\,(G_{i+1}-G_i) + C_2\,\frac{U_{(Hi+1,\ Hi)}}{D_{(Gi+2,\ Gi+1)}}(H_{i+1}-H_i) + C_3\,\frac{U_{(Hi+2,\ Hi+1)}}{D_{(Gi+2,\ Gi+1)}}\,(H_{i+2}-H_{i+1}) \quad \ldots(11)$$

where,

G_i = i^{th} gauge reading at downstream section;

H_i = i^{th} gauge reading at upstream section ;

$U_{(Hi+1,\ Hi)}$ = reciprocal of the slope of the stage-discharge curve at the upstream section between the gauges, H_{i+1} and H_i, and

$D_{(Gi+2,\ Gi+1)}$ = reciprocal of the slope of the stage-discharge curve at the downstream section between the gauges, G_{i+2} and G_{i+1}.

In the above set of equations, the first parameter, viz.,

$$C_1\,\frac{D_{(Gi+1,\ Gi)}}{D_{(Gi+2,Gi+1)}}$$

is assumed to be equal to C_1 in this study, as the slope ratio is nearly one. The number of parameters in the above set of Equations (11) will depend upon the number of linear ranges of the stage-discharge curves in which the observed gauges lie. With two linear ranges of the stage-discharge curves at each of the two stations as indicated in Table I, the maximum number of parameters in the set of Equations (11) would be 9; they are :

$$C_1, [(C_2\,.\,\frac{U_m}{D_n},\ C_3\,.\,\frac{U_m}{D_n},\ m = 1, 2),\ n = 1, 2]$$

Similarly, it can be shown that with three linear ranges, the maximum number of parameters will be 19 ; with one linear range, they will be 3, and with N-linear ranges, they will be $(2N^2+1)$.

Estimation of Parameters

To achieve computational efficiency and to facilitate understanding of the method, let the stage-discharge curves at each of the stations be approximated to a single linear range, so that the number of unknown parameters reduce to three in the set of Equations (11). They are C_1 or x_1, C_2. U_1/D_1 or x_2, and C_3. U_1/D_1 or x_3. Let the difference of gauges such as $(G_{i+1}-G_i)$ be represented as g_i and $(H_{i+1}-H_i)$ as h_i. The set of Equations (11) now become :

$$\begin{aligned} g_2 &= g_1x_1 + h_1x_2 + h_2x_3 \\ g_3 &= g_2x_1 + h_2x_2 + h_3x_3 \\ g_4 &= g_3x_1 + h_3x_2 + h_4x_3 \\ g_5 &= g_4x_1 + h_4x_2 + h_5x_3 \\ &\ldots\ldots \end{aligned} \quad \ldots(12)$$

It is seen that each of the values on the L.H.S. of the set of Equations (12), requires the calculation of the previous step. This reduces the time of forecast considerably. To increase this time, the differences g_2, g_3..... on the R.H.S. of set of Equations (12) are eliminated by substituting their values in terms of g_1 and the set of Equations (12) are rewritten as under :

$$\begin{aligned} g_2 &= g_1x_1 + h_1x_2 + h_2x_3 \\ g_3 &= x_1(g_1x_1 + h_1x_2 + h_2x_3) + h_2x_2 + h_3x_3 \\ &= g_1x_1^2 + h_1x_1x_2 + h_2x_1x_3 + h_2x_2 + h_3x_3 \end{aligned}$$

Similarly,

$$g_4 = g_1x_1^3 + h_1x_1^2x_2 + h_2x_1^2x_3 + h_2x_1x_2 + h_3x_1x_3 + h_3x_2 + h_4x_3 \quad ...(13)$$

$$g_5 = g_1x_1^4 + h_1x_1^3x_2 + h_2x_1^3x_3 + h_2x_1^2x_2 + h_3x_1^2x_3 + h_3x_1x_2 + h_4x_1x_3 + h_4x_2 + h_5x_3$$

.....

All the successive steps given in Equations (13) are added cumulatively with a view to eliminate the error, if any, in the starting value of the stage difference of the downstream hydrograph and also to minimise the cumulative errors between the observed and calculated values of differences in gauges at the end of each step at the time of estimation of the parameters.

After rearranging the terms, the set of equations now takes the form $Y = A\,x_2 + B\,x_3$ as under :

$$g_2 - g_1x_1 = (h_1)\,x_2 + (h_2)x_3 \quad ...(14)$$

$$(g_2 + g_3) - g_1(x_1 + x_1^2) = (h_1x_1 + h_1 + h_2)x_2 + (h_2x_1 + h_2 + h_3)x_3$$

.....

Examining the above equations, it may be noted that these are non-linear in x_1. By choosing a suitable value for x_1, they become linear and the number of parameters are reduced to two.

For n gauge readings at each of the stations, the number of Equations (14) would be $(n-2)$. But the number of praameters are only 2. The equations are thus over-determined and are solved for x_2 and x_3, using multiple regression analysis.

Case Study

A 195 km reach of the River Yamuna between Kalanaur and Delhi bridges has been chosen for testing the validity of the above mentioned analysis. Five flood events listed in Table II have been analysed.

The Kalanaur flood gauges were shifted forward by time 'T' given in column 6 of Table II and a set of Equations (14) were formulated for each flood. The value of the parameter x_1 in these equations has been fixed at 0.65 for the rising or constant gauge portion and 0.7 for the falling gauge portion of the Kalanaur hydrograph on the basis of previous studies [1][2].

The regression coefficients x_2 and x_3 in Equations (14) are estimated using multiple regression technique. The total and partial correlation coefficients, standard errors and confidence limits of the regression coefficients are tabulated in Table III.

All the floods at Delhi listed in Table II are predicted using the values of parameters x_2 and x_3 in the set of Equations (13). The observed and predicted values of the peak gauges are shown in Table IV. The predicted gauge hydrographs of two typical floods have been compared with the observed hydrographs in Figures 2 and 3.

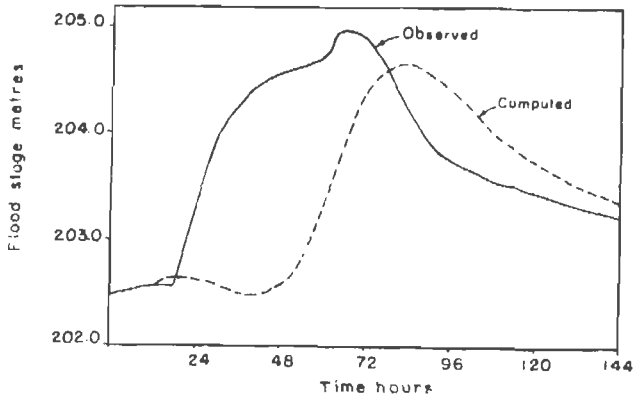

FIGURE 2 : Gauge hydrograph at Delhi (September 1972).

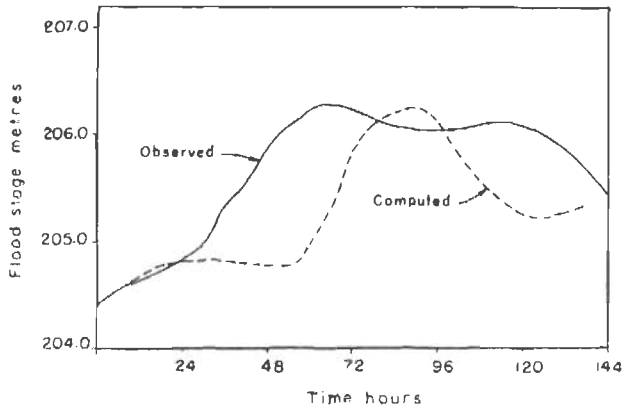

FIGURE 3 : Gauge hydrograph at Delhi (August 1971).

Comments

The analysis described herein uses the difference in gauges in formulating the equations connecting upstream and downstream gauge hydrographs. These equations do not change as long as the shape of the stage-discharge curves do not change appreciably. Under these conditions any change in bed because of silting or scouring will not effect the model.

The gauge discharge curves at Delhi and Kalanaur have been approximated by a single line. This is a gross approximation and has produced wide variations in the observed and predicted peaks. However, it may be noted that one of the lowest and the highest peak (Table IV) have been predicted well. These facts and the random variations in observed and predicted peak gauges show that the model is valid and requires further study to reduce these variations.

Equation (7) is a necessary condition for satisfying the continuity equation. This condition superimposes

TABLE II

Particulars of floods used in the analysis.

Flood No.	Year of flood	Date of flood at Delhi	Peak gauge observed at Delhi (m)	Peak gauge observed at Kalanaur (m)	Value of the parameter 'T' of the linear channel (hr)
1	2	3	4	5	6
1.	1970	4 August 0.30 a.m. to 10 August 6.30 p.m.	204.7	266.6	42
2.	1971	7 August 12.30 p.m. to 13 August 6.30 p.m.	206.29	267.31	54
3.	1972	7 July 6.30 p.m. to 12 July 12.30 p.m.	204.4	266.49	24
4.	1972	15 September 6.30 p.m. to 25 September 6.30 p.m.	204.96	266.84	30
5.	1974	4 August 0.30 a.m. to 10 August 6.30 p.m.	205.15	267.1	42

TABLE III

Some of the statistical properties of the model.

No.	Properties	Values
1.	Value of the regression coefficient x_2	0.4955
2.	Value of the regression coefficient x_3	0.0463
3.	Standard error of x_2	0·05701
4.	Standard error of x_3	0.05806
5.	95 percent confidence limits for x_2	0.4955 $\pm$0·11287
6.	95 percent confidence limits for x_3	0.0463 $\pm$0·11495
7.	Total correlation coefficient	0.837
8.	Partial correlation coefficients between x_2 and Y	0.7923
	between x_3 and Y	0.7623
9.	Standard deviation in Y	0.3535
10.	Total No. of regression equations	170

a constraint on the sum of the parameters x_2 and x_3 :

Since $C_1+C_2+C_3 = 1$ ...(7)

$$C_2 \cdot U_1/D_1+C_3 \cdot U_1/D_1 = (1-C_1)\, U_1/D_1 \quad ...(15)$$

or $$x_2+x_3 = (1-C_1)\, U_1/D_1 \quad ...(16)$$

The R.H.S. of Equation (16) has been assumed to be constant in this study ; therefore, the sum of the parameters must be maintained in predicting the hydrographs. For this reason, the extreme values of the parameters as determined for the 95 percent confidence range have not been used for prediction purposes as the sum of parameters will not be maintained in these cases.

TABLE IV

Comparison of peak gauges.

Flood No. from Table II	Observed peak gauge at Delhi (m)	Predicted peak gauge at Delhi using the model (m)	Difference between the observed and predicted peak gauge
1	204.70	204.53	—0.17
2	206.29	206.23	- 0.06
3	204.40	204.79	+ 0.39
4	204.96	204.65	—0.31
5	205.15	205.60	+0.45

The parameter 'T' plays an important role in estimating the regression coefficients. A little variation in 'T' results in change in the values of these coefficients though the sum of the parameters is more or less maintained. Sometimes the value of the parameter x_2 turns out to be negative which is in contradiction with Equation (5). In order to avoid this contradiction, the Delhi gauge hydrograph was shifted by 'T' hours such that the rising limb of the hydrograph coincides with the rising limb of Kalanaur hydrograph. This reduces the time of forecast to 24 hours for a flood with the peak gauge of 204·40 and 54 hours for a flood with peak gauge of 206·29. The higher value of 'T' has been obtained for the highest flood, as the river is in spate at the time and spills on to flood plain, thereby reducing the mean velocity of travel of the flood wave resulting in increased value of 'T'.

The rising and falling limbs of the observed and predicted hydrographs in Figure 2 show a reasonably good correspondence. The same model has been used to predict one of the highest recorded floods of 1971. The observed and computed hydrographs have been shown in Figure 3. There is close correspondence between the observed and predicted gauges uptil the first peak. However, the second successive peak could not

be predicted. This is due to the fact that there was heavy rain in the intervening catchment, which has not been taken into account while formulating the model.

Conclusions

It is shown that a simple model of a linear channel in combination with a linear reservoir can be adapted for predicting flood stage hydrographs. It is seen that in spite of gross approximation of linear stage discharge curves both at Kalanaur and Delhi bridges, it has been possible to predict reasonably some of the floods. The model is promising and needs further study to reduce the effect of approximations regarding the linearizing of the stage-discharge curves in the case study.

References

(1) CHANDER, S. : "Conceptual Models for Flood Forecasting on the River Yamuna." Unpublished Report C.F.F.D., Central Water and Power Commission, New Delhi, September 1971.

(2) DAS, G. JAGMOHAN : "Development of Models for Flood Forecasting purposes using only Flood Stages Data". I.I.T., Delhi (India), M. Tech. Thesis, 1973.

Flood Routing through Non-linear Reservoirs A Quasi-linear Approach

P. RAMAKRISHNA RAO
Deputy Director (Flood Estimation)
Central Water Commission and Sr. Research Scholar
Indian Institute of Technology, New Delhi

S. CHANDER
Professor
Civil Engineering Department
Indian Institute of Technology, New Delhi

Y. K. MURTHY
Chairman
Central Water Commission and Ex-officio Secretary to the
Government of India, New Delhi (India).

SYNOPSIS

A procedure for flood routing through a non-linear reservoir is presented in this paper. The procedure enables the extension of the applicability of the principle of superposition to non-linear reservoirs also. A new concept of linearised input has been introduced. It has been shown that the process of transformation of input into outflow by non-linear reservoirs can be decomposed into two elements with memory, a non-linear lag-one element and a linear time-lag element. The method is shown to be simpler than, but as accurate as, the fourth order Runge-Kutta method of numerical integration. An illustrative example is given to demonstrate the use of the method developed.

1. Introduction

Flood forecasting is one of the most important aspects in reservoir planning and management. It involves the prediction of the flood hydrograph at a section on the stream from the known flood hydrograph at an upstream section. The theoretical analysis of the movement of flood waves through a reservoir or a river reach is quite complex and involves the solution of continuity and dynamic equations under ill-defined system characteristics. However, for practical applications, procedures based on simplified assumptions have been developed. These are referred to as flood routing procedures.

The routing procedures are based on the relationship between discharge and storage. Two methods are available for evolving this relationship. One is to arrive at the relationship knowing the stage-discharge curve and the volume of storage at different levels from detailed topographic surveys. The other is to use the records of the past floods and deduce the relationship; this relationship is utilised assuming that it will not change substantially in time and will be valid for future flood events also.

If the storage-discharge relationship is linear, the convolution operation involving lagging and summing the Unit Hydrograph ordinates multiplied by the associated inflow volumes and the method of routing the inflow hydrograph through the reservoir are mathematically identical (Overton, 1970) as the principle of superposition is valid. A procedure following a quasi-linear approach for flood routing through a non-linear reservoir is attempted here so as to enable the extension of the applicability of the principle of superposition to non-linear reservoirs also.

Rao (1975), while modelling the non-linear behaviour of drainage basins, has shown that the response of drainage basins to rainfall inputs can be simulated by a network of non-linear reservoirs with appropriate parameters and observed that the important properties of the outflow hydrographs, viz., lag, peak and weighted mean discharge, can be predicted through a single non-

linear reservoir which has the same recession parameters as for the basin. Thus, this procedure for flood routing through single non-linear reservoir would be useful in the application to the natural drainage basins also.

2. Functional Relationship of a Reservoir

Consider a reservoir of constant area, A, with a rectangular spillway. Then, one has :

Discharge over the spillway, $Q = \frac{2}{3}C_d\sqrt{2g}.\ L.\ h^{3/2}$ ...(1)

and the storage in the reservoir, $S = A.h$ ...(2)

where, L = effective length of spillway; h is the head causing flow; C_d is coefficient of discharge; and g is the gravitational acceleration.

Eliminating h from Equations (1) & (2),

$$S = \frac{A}{(\frac{2}{3}C_d\sqrt{2g}.\ L)^{2/3}}\ Q^{2/3} \qquad ...(3)$$

Thus, the storage-discharge relation can be written in the form :

$$S = CQ^B \qquad ...(4)$$

where, B and C are the parameters of the reservoir. B is a function of the type of spillway and C is a function of the area of the reservoir, type of spillway, length or area of spillway and B. The reservoir is termed as non-linear if the Equation (4) is non-linear.

3. Differential Equation for a Reservoir

A non-linear reservoir of storage-discharge relationship given by Equation (4) is chosen. The continuity equation of the reservoir is :

$$I - Q = \frac{dS}{dt} \qquad ...(5)$$

Differentiating Equation (4) and substituting the value of dS/dt in Equation (5), the differential equation for the reservoir will be :

$$CBQ^{B-1}\ \frac{dQ}{dt} = I - Q \qquad ...(6)$$

To find the equation for output, Q, Equation (6) is to be solved.

3.1 *Operational Approach*

For instantaneous input of volume, V, it can be shown that the outflow, Q_t, at any time, t, is given by :

$$Q_t^{B-1} = Q_0^{B-1} + \frac{1-B}{CB}\,t \qquad ...(7)$$

where, Q_0 is the outflow at time, $t = 0$ and is given by :

$$Q_0 = (V/C)^{1/B}$$

For any input, other than instantaneous input, solution of Equation (6) cannot be accomplished for all values of B and variations in input. This difficulty is overcome by solving Equation (6) over a time in which the input can be considered as constant. Assuming I to be constant over a time period and separating the variables, Equation (6) gives :

$$\frac{B}{I}\cdot\frac{(Q/I)^{B-1}}{1-Q/I}\cdot dQ = \frac{dt}{C}\ .I^{1-B} + \text{constant} \qquad ...(8)$$

The solution of Equation (8) is obtained by expanding $(1-Q/I)^{-1}$ by Binomial series for different initial conditions. The solution obtained is so complex that application to practical problems is cumbersome requiring the use of specially prepared tables (Chander, 1965, 1970). Alternatively, the differential Equation (6) has to be solved by the use of numerical integration methods (e.g., Runge-Kutta method) on digital computers.

This approach, which involves the solution of differential or integro-differential equations describing the mechanisms involved in the system's operation, is termed as "operational" approach.

3.2 *Functional Approach*

An alternative approach is to represent a system by functionals; the typical example is the convolution integral :

$$Q_t = \int_0^t H_{(\tau)}\cdot I_{(t-\tau)}\cdot d\tau \qquad ...(9)$$

The functional approach has the advantage over the operational approach in that, in some cases, it is possible to determine the system response function, $H_{(\tau)}$, without the fore-knowledge of the inner mechanism of the system.

The convolution integral is capable of representing, under the frame-work of functional approach, a linear system only. In the case of non-linear systems, the functional approach involves the representation of the systems by the summation of a first term identical to the convolution integral and series of similar terms, which are multi-dimensional generalisations of the convolution integral, forming a functional series :

$$Q_t = \int_0^t H_{1(t-\tau_1)}\cdot I_{(t-\tau_1)}\cdot d\tau_1 + \int_0^t\int_0^t H_{2(\tau_1,\tau_2)}\cdot I_{(t-\tau_1)}\cdot I_{(t-\tau_2)}\cdot d\tau_1\cdot d\tau_2 + \int_0^t\cdots\int_0^t H_{n(\tau_1,\ldots,\tau_n)}\cdot I_{(t-\tau_1)}\ldots I_{(t-\tau_n)}\cdot d\tau_1\ldots d\tau_n \qquad ...(10)$$

This functional series can be viewed (Amorocho, 1969) as a conceptual model of a number of reservoirs in

parallel, all receiving the same input and producing independent outputs (Figure 1). The output from the first reservoir is obtained by the convolution of the input function with a fixed kernel function. The output from the second reservoir is obtained by a convolution integral containing the input and a variable kernel function which is obtained by the convolution of the input and some fixed kernel function. Similarly, the outputs from other reservoirs are obtained and the final output is the sum of all outputs from the reservoirs in parallel.

The determination of the non-linear responses in Equation (10) is far more complex than in the case with the linear systems. The methods evolved for non-linear systems in electronics require the selection of particular types of input functions and measurement of the corresponding outputs. Amorocho (1961, 1969) has attempted to model hydrologic systems for a chosen type of input functions. A more general model for hydrologic systems with arbitrary inputs was proposed by Jacoby (1962, 1966). This model involves the decomposition of the system into two types of basic elements, viz., linear elements with memory and non-linear elements with no-memory. In mathematical terms, Jacoby's approximation of a non-linear system is given by :

$$\underline{H}[I] \simeq \sum_{n=1}^{r}\left[\sum_{l=1}^{m}\prod_{i=1}^{n}\left(\sum_{m=0}^{\infty} b_{l,i,m} * l_m\,[I']\right)\right] \quad \ldots(11)$$

where,

l_m denotes linear systems with memory of a special class, known as "Laguerre Systems", operating on the input I'.

$b_{l,i,m}$ denotes the first-order no-memory systems into which the output of the Laguerre Systems is cascaded.

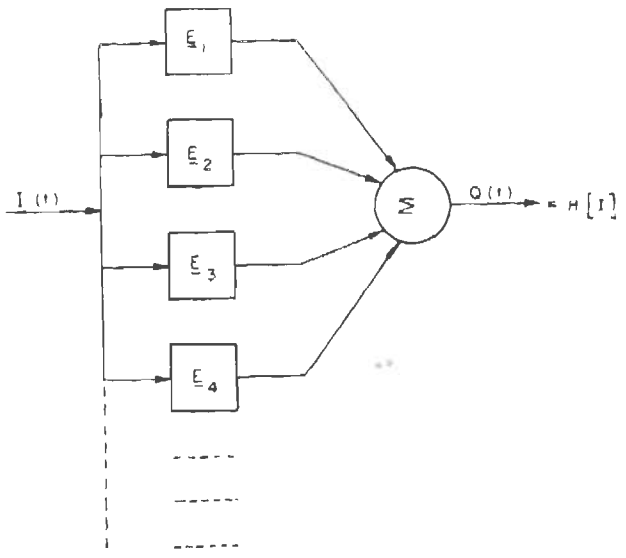

FIGURE 1 : Functional series representation of a non-linear system H (Amorocho, 1969).

r is the order of the polynomial system.

l, i, m & n are indices to denote each one of the elements of the combination.

A flow diagram representation of Equation (11) is given in Figure 2 for the case of the second order polynomial system.

4. Linearised Input Concept

The methods based on operational and functional approaches described above are complex. The numerical integration in the case of operational approach and the expansion into functional series in the functional approach are resorted to, as the principle of superposition is not applicable in the case of non-linear systems. The principle of superposition is simple for application to practical problems and is always preferred. In this study, an attempt has been made to extend the application of this principle even in the case of non-linear systems. This has been accomplished by modifying the input, I, in such a way that the output given by the convolution integral, Equation (9), matches with that given by the solution of differential Equation (6).

When a non-linear reservoir of storage-discharge relationship given by Equation (4) is fed with an input of uniform intensity, I, for a period, T, it is assumed that the transformation of input into output by the non-linear reservoir can be resolved into two phases, viz. :

Phase 1 : Input is modified as per the non-linear relationship :

$$\int_0^t \frac{I_{mt}\,.\,dt}{V} = \left(\frac{I\,.\,t}{V}\right)^{1/b} \text{ for } 0 \leqslant t \leqslant T \quad \ldots(12)$$

where,

I_{mt} = intensity of modified input at time, t ;

V = total input volume = $I.T$; and

b = a coefficient to be determined.

Equation (12) can be re-written as

$$\int_0^t I_{mt}\,dt = V(I.t/I.T)^{1/b} = V(t/T)^{1/b}$$

Differentiating, $I_{mt} = \dfrac{d}{dt}\left[V\,(t/T)^{1/b}\right]$ ...(13)

Phase 2 : The modified input, I_{mt}, is transformed into output by linear process of convolution. Convolving the modified input with the instantaneous unit response, *IUH*, the output is determined as under :

$$Q_t = \int_0^t I_{mt}\,H_{(t-\tau)}\,d\tau$$

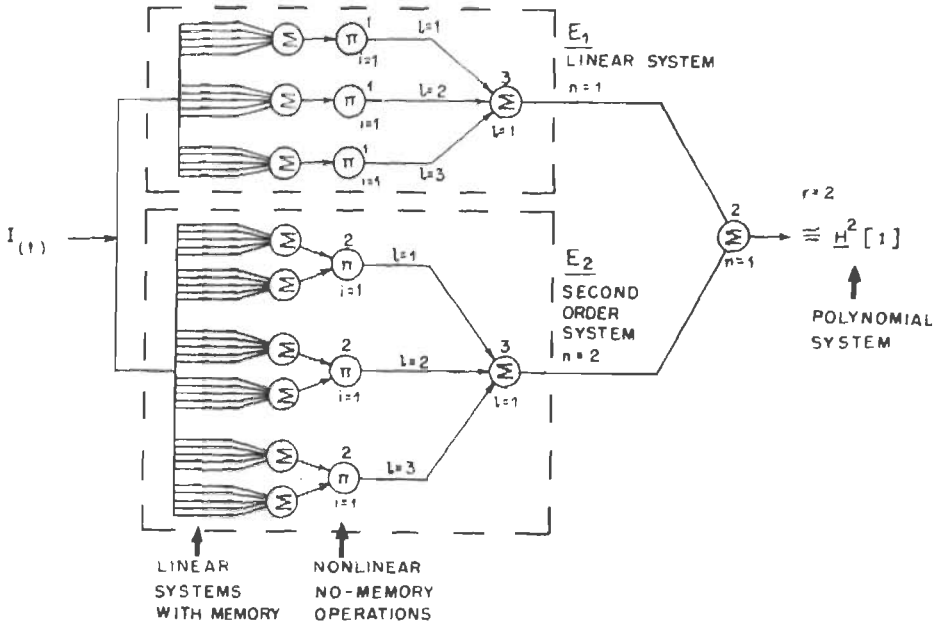

FIGURE 2 : Complex cascade equivalence of a second-order polynomial system (Jacoby, 1966).

in which

$$H_{(t-\tau)} = \frac{1}{V}\left[\frac{1-B}{CB}\left(t-\tau+\frac{CB}{1-B}Q_0^{B-1}\right)\right]^{1/(B-1)}$$

from Equation (7)

and $I_{mt}\,d\tau = \frac{V}{T^{1/b}}\,d(\tau^{1/b})$ from Equation (13)

Therefore,

$$Q_t = \int_0^t \left[\frac{1-B}{CB}\left(t+\frac{CB}{1-B}\,Q_0^{B-1}-\tau\right)\right]^{1/(B-1)} d(\tau/T)^{1/b}$$

which can be simplified as :

$$Q_t = Q_0\left(\frac{t}{T}\right)^{1/b}\left[1-\frac{x}{1+b}+\frac{(2-B)\,x^2}{(1+b)\,(1+2b)}-\cdots\right] \quad \ldots(14)$$

where, $X = \frac{Q_0}{I}\cdot\frac{t}{T}\cdot\frac{b}{B}$; $Q_0 = (I.T/C)^{1/B}$ and

$$0 \leqslant t \leqslant T$$

Equation (14) involves summation of infinite terms in the series. The series converges provided the ratio of the absolute values of $(n+1)^{th}$ term and the n^{th} term is less than 1. It can be shown that the series converges if :

$$\frac{Q_0}{I}\cdot\frac{t}{T} < \left|\frac{B}{1-B}\cdot\frac{B}{b}\right|$$

Since the maximum value of $\frac{Q_0}{I}\cdot\frac{t}{T}$ is equal to $\frac{Q_0}{I}$ when $t = T$, the condition for convergence is :

$$\frac{Q_0}{I} < \left|\frac{B}{1-B}\cdot\frac{B}{b}\right| \quad \ldots(15)$$

It can be seen that, when compared with Jacoby's method of decomposition (Figure 2), this approach consists of decomposition of the system into two elements with memory :

(*i*) Non-linear lag-one element ; and

(*ii*) Linear time-lag element.

5. Estimation of b-Value

Value of b in Equations (12) and (14) is determined by mathematical experimentation. For various values of input intensity, I, and duration, T, and for different values of B and C, Equation (6) is solved for Q_t using fourth order Runge-Kutta method on digital computer. Knowing the output, Q_t and *IUH* given by Equation (7), the modified input, I_{mt}, is determined by matrix inversion method. A log-log plot of

$$\int_0^t I_{mt}\,dt \text{ versus } \int_0^t I.dt$$

has shown a linear relationship, the slope of the line giving the value of b. The value of b is found to be equal to B for all practical purposes, provided the duration of input, T, is small such that :

$$\frac{Q_0}{I} < \left|\frac{B}{1-B}\right| \quad \ldots(16)$$

The above condition is same as the condition for convergence of the series, Equation (15).

Substituting $(I.T/C)^{1/B}$ for Q_0 and re-arranging,

$$T < \left| C.\left(\frac{B}{1-B}\right)^{B}.I^{B-1}\right| \qquad ...(17)$$

6. Application

The method can be conveniently applied for short duration inputs, without appreciable error, in one step for computing output hydrographs. In the case of inputs of long duration, the output hydrographs are to be computed by considering the input in steps satisfying the condition given by Equation (16). To illustrate the accuracy of the method, typical results are presented in this section.

6.1 *Input of Short Duration*

Input of 60 mm volume but of various temporal distributions for a duration of 2 hours is fed to a reservoir of area of 1,800 ha with B-value = 2/3 and C-value = 70,000 m sec$^{2/3}$ units.

$$\text{Average input rate, } I = 1{,}800\times10^{4}\times\frac{60}{1{,}000}\times\frac{1}{2\times3{,}600} = 150 \text{ m}^3/\text{sec}$$

It is seen that the condition given by Equation (17) is satisfied :

$$\because\ C\left(\frac{B}{1-B}\right)^{B}I^{B-1} = 70{,}000\left(\frac{2/3}{1/3}\right)^{2/3}/(150)^{1/3}$$
$$= 20{,}910 \text{ sec} = 5.81 \text{ hrs}$$

which is greater than T = 2 hrs.

The input distributions, their modified shapes as per Equation (12) are shown in Figure 3. The output hydrographs obtained by convolving the modified inputs of 0.2 hour duration with 0.2 hour Unit Hydrograph, which is assumed to be same as *IUH* lagged by 0.1 hour, are compared with those obtained by Runge-Kutta method. The output hydrographs obtained from both the methods for the same input distribution match extremely well (Figure 4).

6.2 *Inputs of Long Duration*

Consider a non-linear reservoir continuously fed with varying input. Divide the varying input into equal area step inputs, each of short duration, T. The duration, T, called the routing period, must be chosen sufficiently short, so that :

(*i*) the condition given by Equation (17) is satisfied and also,

(*ii*) the variation of input and output during the routing period can be assumed to be linear, without appreciable error.

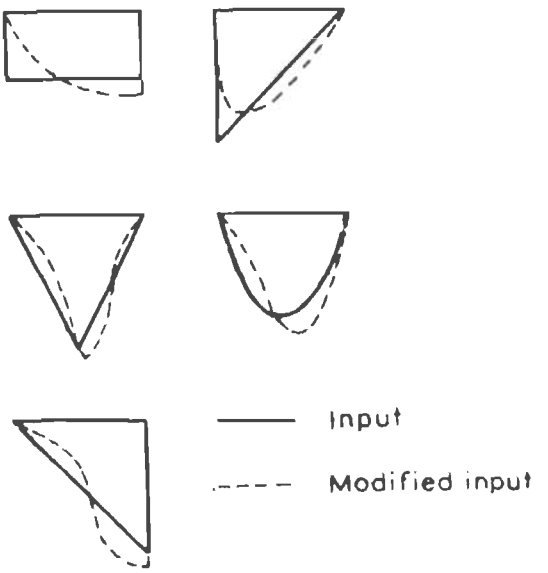

FIGURE 3 : Input distributions and their modified shapes.

Let, I_1, I_2 be the intensities of input

Q_1, Q_2 be the rates of output, and

S_1, S_2 be the storages

where, the subscripts 1 and 2 denote the values at the beginning and end of the routing period, T.

Average intensity of input, I, will be $(I_1 + I_2)/2$. Considering S_1 as instantaneous input at the beginning of the period, total volume of input, V, will be equal to $S_1 + IT$. Output ordinates for an instantaneous input of V can be computed utilising Equation (7) as under :

$$U_{(0,\,0)} = (V/C)^{1/B} \qquad ...(18)$$

$$U_{(0,\,T/2)} = \left[\ U^{B-1}_{(0,\,0)} + \left(\frac{1-B}{BC}\right)\frac{T}{2}\ \right]^{1/(B-1)} \qquad ...(19)$$

$$U_{(0,\,T)} = \left[\ U^{B-1}_{(0,0)} + \frac{1-B}{BC}T\ \right]^{1/(B-1)} \qquad ...(20)$$

For small values of T, it can be safely assumed that

$$U_{(T,\,T)} = U_{(0,\,T/2)}$$

Using the linearised input concept, the modified input as ratio of the total input during the routing period will be :

(*i*) $(S_1/V)^{1/B}$ instantaneous input at the beginning of the routing period

(*ii*) $1-(S_1/V)^{1/B}$ step input of duration, T.

The output ordinates are then given by the linear process of convolution :

$$Q_1 = (S_1/V)^{1/B}.U_{(0,\,0)}$$
$$= (S_1/C)^{1/B} \qquad ...(21)$$

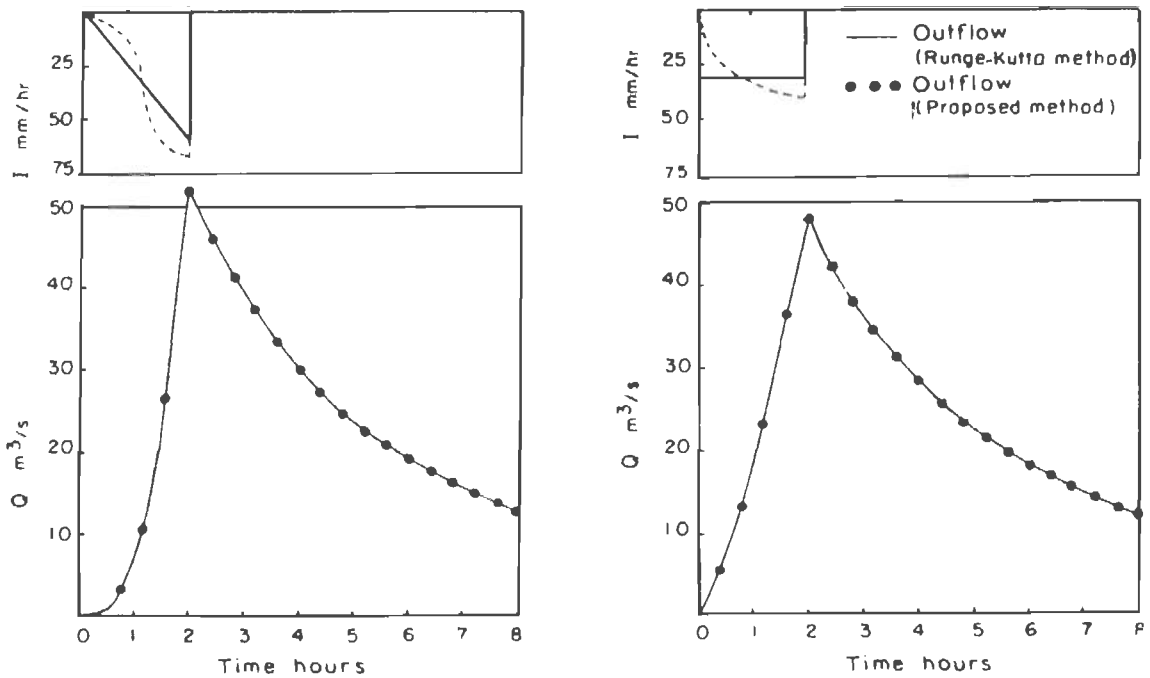

FIGURE 4 : Outflow from a non-linear reservoir for different inputs.

$$Q_2 = (S_1/V)^{1/B} \cdot U_{(O,T)} + [1-(S_1/V)^{1/B}] \cdot U_{(T,T)} \quad \ldots(22)$$

Storage, S_2, at the end of the routing period, T, is given by :

$$S_2 = S_1 + IT - (Q_1+Q_2)\,T/2 \quad \ldots(23)$$

The storage, S_2, is now taken as the initial storage, S_1 and the computation is repeated for determining the next output ordinate.

The use of the method is illustrated by an example.

EXAMPLE : A lake having steep banks and surface area of 2 km² discharges into steep channel which is approximately rectangular in section, with a width of 7.50 m. Initially, conditions are steady with a flow of 30 m³/sec passing through the lake, then a freshet comes down the river feeding the lake, giving rise to the following inflow hydrograph :

Time (hrs)	0	3	6	9	12	15	18	21	24
Inflow (m³/sec)	30.0	35.7	47.0	61.2	76.2	85.2	88.0	86.7	82.1
Time (hrs)	27	30	33	36	39	42	45	48	51
Inflow (m³/sec)	75.3	66.8	58.3	49.8	42.2	35.7	31.4	30.0	3.00

The outflow hydrograph is to be predicted.

SOLUTION

For a rectangular spillway of length, L and head causing flow, h, and the constant of discharge,

$$\tfrac{2}{3} C_d \sqrt{2g} = 3.09 \text{ ft}^{1/2}/\text{sec} = 1.7 \text{ m}^{1/2}/\text{sec}.$$

$$Q = 1.7\, L\, h^{3/2} = 12.75\, h^{3/2} \text{ m}^3/\text{sec} \quad \ldots(i)$$

For the lake of area (A) of 2 km², the storage (S) is given by:

$$S = Ah = 2.0 \times 10^6 \times h \text{ m}^3 \quad \ldots(ii)$$

Eliminating h from Equation (i) and (ii)

$$S = 0.366 \times 10^6 \times Q^{2/3} \text{ m}^3 \quad \ldots(iii)$$

Comparing with Equation (4), the lake parameters are

$$C = 366{,}000 \text{ m sec}^{2/3}$$

$$B = 2/3$$

Initial storage, S_1, in the lake is given by

$$S_1 = 366{,}000\ (30)^{2/3}$$

$$= 3.562 \times 10^6 \text{ m}^3$$

Assuming that the average input rate, $I = 60$ m³/sec Equation (16) stipulates that :

$$\left(\frac{S_1 + I \,.\, T_{max}}{C}\right)^{1/B} < \frac{B}{1-B} \cdot I$$

i.e.,

$$\frac{3.562 \times 10^6 + 60 \times T_{max} \times 3600}{0.366 \times 10^6} < (2 \times 60)^{3/2}$$

TABLE 1

Routing through a non-linear reservoir.

Time t (hrs)	Inflow I_t (m^3/s)	Average Inflow (I) (m^3/s)	Storage S_t (10^6 m^3)	Storage $S_t + IT$ (10^6 m^3)	$\left(\frac{S_t}{S_t+IT}\right)^{1/B}$	$U_{(0,T)}$ (m^3/s)	$U_{(0,T/2)}$ (m^3/s)	Outflow, Q_t (m^3/s)	
								Proposed method	Runge-Kutta method
1	2	3	4	5	6	7	8	9	10
0	30·0							30·000	30 000
3	35 7	32·85	3·562	3·888	0·8663	30 08	32 25	30·368	30 367
6	47 0	41·35	3·673	4·009	0 8377	31 42	33·72	31·795	31·794
9	61 2	54 10	3·898	4 258	0·8014	34 24	36 83	34·756	34 754
12	76·2	68 70	4·240	4 640	0·7700	38·72	41 76	39 416	39 414
15	85·2	80·60	4·653	5·110	0 7557	44 41	48·08	45 310	45 304
18	88·0	86·60	5·065	5·588	0 7598	50·42	54 78	51·470	51·456
21	86·7	87·35	5·423	6 009	0 7740	55·89	60 89	57·017	56 994
24	82·1	84 35	5·695	6 334	0 7922	60·21	65·75	61·361	61·329
27	75·3	78·70	5·867	6·545	0 8117	63·06	68 96	64 169	64 131
30	66·8	71·05	5·935	6·634	0 8316	64·28	70 33	65·298	65 257
33	58 3	62·55	5·908	6 610	0·8507	63·96	69 97	64 854	64 815
36	49 8	54·05	5 800	6 491	0 8682	62·34	68·14	63 101	63 069
39	42·2	46·00	5·631	6 297	0 8840	59·72	65 20	60·354	60·331
42	35·7	38·95	5 418	6·051	0·8976	56·45	61·52	56·966	56 954
45	31·4	33·55	5·184	5 780	0·9075	52·90	57 55	53 328	53 326
48	30·0	30·70	4 959	5·516	0·9112	49 50	53 76	49 882	49 890
51	30·0	30·00	4·760	5 283	0 9094	46 56	50 47	46·912	46 928
54	30 0	30·00	4 591	5·084	0·9059	44 09	47 72	44 431	44 451
57	30·0	30·00	4·446	4 915	0 9028	42 02	45 42	42 347	42 369
60	30·0	30·00	4·322	4 770	0·8999	40·27	43 48	40 589	40·612
63	30·0	30·00	4 216	4 646	0·8972	38·79	41 84	39 100	39 123
66	30·0	30·00	4·124	4·540	0·8949	37·53	40 45	37·834	37·857
69	30·0	30·00	4·046	4 448	0 8928	36·45	39 26	36·755	36 777
72	30·0	30·00	3 978	4 370	0 8909	35·54	38 35	35·832	35 853
		30·00	3·919	4 302	0·8892	34 75	37 38		

where, T_{max} is the maximum routing period in hours. Simplifying,

$$T_{max} = 25 \text{ hrs approximately.}$$

As the time to peak of the inflow hydrograph is 18 hours, routing period of 3 hours is chosen and the calculations for arriving at the outflow ordinates by the proposed method are tabulated in Table 1. Outflow ordinates are also computed by solving the differential Equation (11) directly, using the fourth order Runge-Kutta method of numerical integration, assuming that the input is constant and is equal to the average input during the routing period. The results are shown in Col. 10 of Table 1. It is seen that the outflow ordinates obtained by the proposed method match extremely well with those given by the Runge-Kutta method. The inflow and outflow hydrographs are shown in Figure 5.

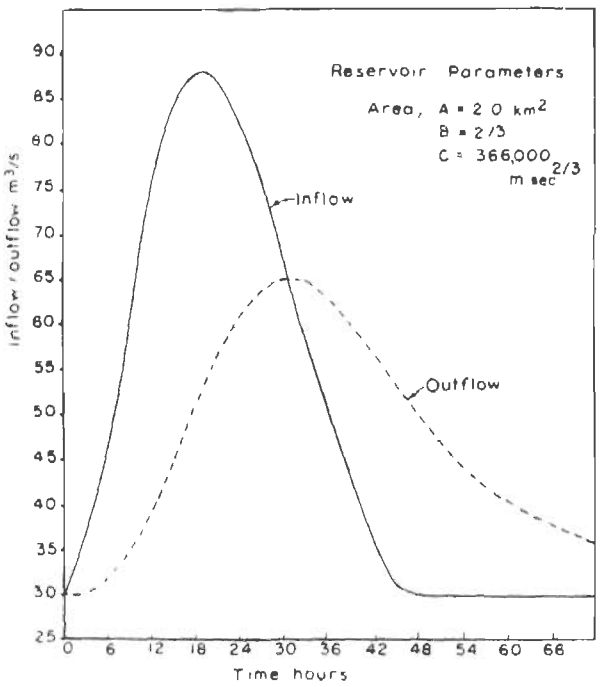

FIGURE 5 : Routing through non-linear reservoir.

7. Conclusion

The proposed method of routing through non-linear reservoir based on the linearised input concept is as accurate as the Fourth Order Runge-Kutta method. The proposed method is simpler and can be adopted as routine design practice in field offices, where accessibility to sophisticated electronic computers is extremely limited.

8. Symbols

Symbols used in this paper are defined where they first appear and those that are used more than once are given below for convenient reference :

A = Area of reservoir

B = Index of non-linearity (parameter) of reservoir

b = Exponent (parameter)

C = Storage-delay parameter of reservoir

C_d = Coefficient of discharge

g = Gravitational acceleration

h = Head causing flow over spillway

$H_{(\cdot)}$ = Kernel (response) function or Instantaneous Unit Hydrograph, *IUH*

$I, I_1, I_2, \ldots I_t$ = Input rate

I_{mt} = Modified input rate

$Q, Q_1, Q_2, \ldots Q_t$ = Outflow rate

$S, S_1, S_2, \ldots S_t$ = Storage in the reservoir

T = Routing period/Duration of step input

t = Time variable

τ, τ_1, τ_2 = Time variables

$U_{(0, t)}$ = Output at time, t, for instantaneous input of volume, V

$U_{(T, t)}$ = Output at time, t, for step input of duration, T and volume, V.

V = Volume of input.

9. References

(1) AMOROCHO, J. and ORLOB, G.T. : "Non-linear Analysis of Hydrologic Systems." University of California, Berkeley, Water Res. Centre Contr. 40, 1961, pp. 1-147.

(2) AMOROCHO, J. : "Deterministic Non-linear Hydrologic Models." Proc. First Int. Seminar for Hydrology Professors, Urbana, Illinois, 1969, pp. 420-469.

(3) CHANDER, S. : "Computed Hydrographs of Catchments." University Manchester (U.K.), Ph.D. Thesis, 1965.

(4) CHANDER, S. : "Flood Routing—Using Dimensionless Parameters." Jnl. Irrigation & Power, CBI&P, India, Oct. 1970, pp. 395-400.

(5) JACOBY, S.L.S. : "Analysis of some Non-linear Hydraulic Systems." University of California, Berkeley, Ph.D. Thesis, 1962.

(6) JACOBY, S.L.S. : "A Mathematical Model for Non-linear Hydrologic Systems." Jnl. Geophys. Res., Vol. 71 (20), 1966, pp. 4811-4824.

(7) OVERTON, D.E. : "Route or Convolute ?" Water Resources Research, Am. Geophys. Union, Vol. 6 (1), 1970, pp. 43-52.

(8) RAMAKRISHNA RAO, P. : "Modelling of Non-linear Behaviour of Drainage Basins." IIT Delhi, India, Ph.D. Thesis, 1975, under the Research Supervision of S. Chander and Y.K. Murthy.

Influence of Chance Constraints on the Efficiency of a Reservoir operated according to a Linear Decision Rule

G. A. SCHULTZ
Associate Professor

E. J. PLATE
Professor

Institut Wasserbau III, University of Karlsruhe, 75 Karlsruhe, Germany.

SYNOPSIS

Questions of optimum design and operation of reservoirs may be treated by use of mathematical programming techniques, which require an objective function and constraints. The aim of this paper is, to give some information about finding the minimum required reservoir capacity in a design problem if the normally used deterministic constraints are replaced by chance constraints. Before the design can be dealt with, it is necessary to specify the reservoir operation rule. In this paper it is assumed that a linear decision rule (LDR) is acceptable. Therefore, the optimization problem can be solved by linear programming.

For a reservoir to be designed in the "Black Forest" mountains deterministic constraints were first formulated for guaranteeing minimum release, maximum release, minimum reservoir content and flood storage on a monthly basis. The resulting values of minimum required storage capacity were rather large. The next step consisted in replacing the deterministic constraints by chance constraints, i.e., the new formulation allows to violate the constraints with a given, rather small probability of occurrence. If this probability is chosen to be 10 percent the computed values of reservoir capacity became considerably smaller than those of the deterministic case.

If, furthermore, the conventional LDR is replaced by another LDR, which releases part of the inflow in the same month it occurs, a further reduction of required reservoir capacity may be achieved.

Introduction

Optimum design as well as operation of reservoirs applying mathematical programming algorithms is based on an objective function (O.F.) and on constraints. The O.F. may be deterministic like the minimization of required storage capacity for fulfilment of certain demand requirements in a design problem, or like the maximization of target outputs in a reservoir operation problem. O.F. may, however, be stochastic like maximization of the expected value of the benefit/cost ratio. In this paper only deterministic O.F.s will be considered.

The constraints may also be deterministic or stochastic. One type of stochastic constraints, which is called "chance constraints" form the major part of the investigations in this paper.

Deterministic constraints are formulated in a rigid way, e.g.,

$$S \leqslant k \qquad \ldots(1)$$

which means that the reservoir content S has always to be equal or smaller than the reservoir capacity k.

Very common constraints are

(*a*) $A_t \geqslant AM$ ...(2)

which requires that in each time increment the reservoir release A_t must be equal or larger than a certain minimum release AM, and

(*b*) $S_t \geqslant S_{min}$ ...(3)

which requires the reservoir content S_t always to be equal or larger than a given minimum storage S_{min}. This last constraint is often demanded by people concerned with the environmental aspects of the design problem, in order to avoid that the lake is empty or at a too low level for recreational purposes. If, however, such a constraint is violated only very seldom, i.e., with a certain rather small probability of occurrence this will do almost no harm to the environment and may be tolerated.

Later the constraints of Equations (2) & (3) will be formulated in this way on the basis of probability theory, whereby these constraints will be changed from the deterministic type into chance constraints.

It is the aim of this paper to estimate quantitatively the benefit of changing deterministic constraints into chance constraints in a real world example.

The Problem

The problem for which this comparison will be carried out is the design of a water supply reservoir (i.e., the finding of required storage capacity) on a river in the "Black Forest" in Southern Germany. This problem is of current interest, since presently preliminary investigation are being carried out by the authors for the design of a system of four water supply reservoirs in the upper Danube River catchment, which is partly situated in the "Black Forest" mountains.

The Method

While the actual design of the four Danube reservoirs is based on simulation techniques, the study presented in this paper applies on optimization method. Since the main interest here lies upon the influence of chance constraints on the reservoir efficiency or the required reservoir capacity, the type of the mathematical programming technique is not important.

It was assumed, therefore, that a linear decision rule (LDR) is acceptable. The pros and cons of the LDR have been discussed in great detail in the literature [1] [2] [3] [4] [5] [6]. Therefore, this rule will not be discussed here, although it can be seen from the results, that it itself is a strong constraint on the possible performance of the reservoir. It will even be shown, that an almost "useless" reservoir operated according to a LDR requires sometimes a rather large storage capacity. Here the LDR is used only, for the reason that it allows application of Linear Programming and is thus a convenient vehicle to show the influence of chance constraints on reservoir performance.

Mathematical Formulation on the Design Problem

A reservoir has to be designed, which will be operated according to certain requirements formulated by constraints. The optimization consists in finding the minimum reservoir size k which meets the constraints.

Thus the objective function is

$$\text{O.F.} = k = \min !$$

Deterministic Constraints

The constraints are formulated similar to an example given in (1). The time increment chosen is one month.

(1) Reservation of flood storage :

$$k - S_t \geqslant V_i \qquad ...(4)$$

The index t indicates the sequence of months (e.g., $t = 1,...240$ if the time series consists of 20 years) and the index i indicates the month of the year, thus $i = 1, ...12$.

k = required reservoir capacity

S_t = reservoir content in month t

V_i = flood storage to be provided in the i^{th} month of the year

(2) Minimum reservoir content S_{min}

$$S_t \geqslant S_{min} \qquad ...(3)$$

(3) Minimum release AM_i

$$A_t \geqslant AM_i \qquad ...(2)$$

(4) Maximum release AN_i

$$A_t \leqslant AN_i \qquad ...(5)$$

AN_i = maximum permissible release in the i^{th} month of the year.

According to the linear decision rule as introduced by Revelle et al[1] the release is

$$A_t = S_{t-1} - E_i \qquad ...(6)$$

E_i is the decision variable, forming a vector of 12 values. Continuity requires

$$S_t = S_{t-1} - A_t + I_t \qquad ...(7)$$

I_t = reservoir inflow in month t.

Inserting A_t of Equation (6) into Equation (7) yields

$$S_t = E_i + I_t \qquad ...(8)$$

Inserting Equation (8) for S_{t-1} into Equation (6) yields

$$A_t = I_{t-1} + E_{i-1} - E_i \qquad ...(9)$$

Inserting Equations (8) & (9) into Equations (2), (3), (4) & (5) yields

$$k - E_i \geqslant V_i + I_t \qquad ...(4a)$$

$$E_i \geqslant S_{min} - I_t \qquad ...(3a)$$

$$E_{i-1} - E_i \geqslant AM_i - I_{t-1} \qquad ...(2a)$$

$$E_{i-1} - E_i \leqslant AN_i - I_{t-1} \qquad ...(5a)$$

In our case 45 years of observed data for the Kinzig River in the "Black Forest" are available.

$$1 \leqslant t \leqslant 540 \quad (= 45 \times 12).$$

This means that Equations $(2a) \div (5a)$ exist 540 times each, yielding 2,160 constraints with 14 unknowns, i.e., the storage capacity k, 12 values of E_t and the initial storage content S_o.

In Appendix-I it is shown, how these 2,160 constraints may be reduced to $4 \times 12 = 48$ constraints [Equations $(2a) \div (5a)$] plus 2 constraints. The additional 2 constraints deal with initial conditions and are given in Appendix-I, Equations (I.1) & (I.2).

Summarizing the mathematical problem formulation in a deterministic way we can state : a supply reservoir has to be designed, which has to fulfil certain requirements at minimum construction costs. This leads to the objective function

$$\text{O.F.} = k - \min !$$

and to 50 deterministic constraints given in Equations $(2b) \div (5b)$, Equations (I.1) & (I.2), all given in Appendix-I. The solution of this problem will be found by applying linear programming, in this case by the simplex algorithm.

Results of the Deterministic Design Problem

For a potential reservoir site near the village of Schwaibach on the Kinzig River in the "Black Forest", Southern Germany, the alternatives listed in Table I have been computed for a reservoir operated according to the linear decision rule :

$$A_t = S_{t-1} - E_t \qquad \ldots(6)$$

The values of V_i, S_{min}, AM_i, and AN_i were chosen to be the same for all months.

Some of the results given in Table I are rather unexpected. Since the maximum release, AN, is a monthly value, it does not give information about actual flood conditions. Therefore, it is kept constant ($AN = 300 \cdot 10^6$ m³) and is not further considered in this discussion.

The influence of the parameters AM, S_{min}, and V on the required reservoir capacity is, however, of particular interest. Alternatives 4 and 7 or 5 and 9 show that the flood storage V is merely an addition to the capacity required without flood storage and will thus not be considered further.

Alternative 1 shows that a reservoir, which can do virtually nothing ("useless reservoir"), i.e., it guarantees no minimum release, no minimum reservoir content and provides no flood storage, requires a capacity of $291.2 \cdot 10^6$m³ ! The only quality this reservoir can produce, is operation according to the linear decision rule, i.e., at the beginning of a month it can be said,

TABLE I

Required reservoir capacity k for various design and operational alternatives of the Kinzig reservoir (Deterministic constraints).

Alternative No.	Max. release AN (10^6 m³/month)	Min. release AM (10^6 m³/month)	Min. reservoir content S_{min} (10^6 m³)	Flood storage V (10^6 m³)	Required reservoir capacity k (10^6 m³)
1.	300	0	0	0	291.20
2.	300	5	0	0	291.20
3.	300	0	100	0	381.60
4.	300	5	100	0	381.60
5.	300	10	100	0	382.90
6.	300	1	100	50	431.60
7.	300	5	100	50	431.60
8.	300	9	100	50	431.60
9.	300	10	100	50	432.90

how much the release during this month will be :

$$A_t = S_{t-1} - E_t \qquad \ldots(6)$$

or

$$A_t = I_{t-1} + E_{t-1} - E_t \qquad \ldots(6a)$$

A_t may, however, be zero, if $I_{t-1} \leqslant E_t - E_{t-1}$, which is the reason, why we call this reservoir "useless".

The minimum release AM is often the most important parameter since it guarantees always a minimum quantity of water to the consumer. Alternatives 6 to 9 in Table I show that the required capacity hardly changes at all for minimum releases between 1 and $10 \cdot 10^6$m³ per month. Values greater than $10 \cdot 10^6$m³ for AM are not possible, because this leads to certain constraints to be in conflict. For comparison purposes it may be interesting to know that the average flow of the Kinzig River amounts to $AQ = 58 \cdot 10^6$m³ per month.

Solutions with the Aid of Chance Constraints

Equations $(2b) \div (5b)$, (I.1) and (I.2) in Appendix-I represent 50 constraints on the reservoir design problem. The main feature of these deterministic constraints is, that the inequality must be fulfilled 100 percent, e.g.,

$$k - E_t \geqslant V_t + I_t \qquad \ldots(4a)$$

or

$$k - V_t - E_t \geqslant I_t \qquad \ldots(4c)$$

In case the designer is satisfied, if the flood storage V_t is provided only in a certain percentage α of the time, say $\alpha = 95$ percent, the constraint Equation (4c) may be expressed in the following manner :

$$P(R_i \leqslant k - V_i - E_i) \geqslant \alpha \qquad \ldots(10)$$

A comparison of Equation (10) and Equation (4c) shows, that the deterministic inflow of month t, i.e., I_t is replaced by the random inflow variable R_i for the i^{th} month of year. Thus, Equation (10) reads as follows : the probability P for the random inflow variable R_i being less than $k - V_i - E_i$ in month i has to be at least $= \alpha$. In our case the 45 years of observed inflow data allow to establish a probability distribution for the inflows R_i of each month i. If the level α is given by the designer, the corresponding value of R_i will be found from this cumulative probability distribution.

Analogous to Equation (10) it is possible to formulate all constraints of Equations (2b) ÷ (5b), (I.1) & (I.2) as chance constraints. The transformation of the deterministic constraints into chance constraints is given in Ref. (1) and is briefly summarized in Appendix-II.

Trial designs were carried out again for the Kinzig reservoir. The probability level at which the constraints must be met was chosen to be 90 percent for all constraints (see Appendix-II) :

$$\alpha = \alpha_1 = \alpha_2 = \alpha_3 = \alpha_4 = 0.90$$

The results are given in Table II.

TABLE II

Required reservoir capacity k for various design and operational alternatives of the Kinzig reservoir (Chance constraints, α 0.90).

Alternative No.	Max. release AN ($10^6 m^3$/month)	Min. release AM ($10^6 m^3$/month)	Min. reservoir content S_{min} ($10^6 m^3$)	Flood storage V ($10^6 m^3$)	Required reservoir capacity k ($10^6 m^3$)
1.	150	0	0	0	141.8
2.	150	5	0	0	141.8
3.	150	5	0	50	191.8
4.	150	0	100	0	225.3
5.	150	5	100	0	225.3
6.	150	10	100	0	225.3
7.	150	19.5	100	0	233.2
8.	150	1	100	50	275.3
9.	150	5	100	50	275.3
10.	150	9	100	50	275.3
11.	150	10	100	50	275.3
12.	150	19.5	100	50	283.2

The results are similar to the ones of Table I for deterministic constraints as far as the flood storage is concerned, since it simply adds its value to the required reservoir capacity. The capacity k, however, is always lower than for deterministic constraints. This is shown for representative alternatives in Table III (flood storage $V = 50$ and $AN = 300$ for deterministic and $AN = 150$ for stochastic cases).

TABLE III

Comparison between deterministic and stochastic design alternatives.

Min. release ($10^6 m^3$/month)	Min. reservoir content ($10^6 m^3$)	Required reservoir capacity k		Difference Percent
		Deterministic ($10^6 m^3$)	Stochastic ($10^6 m^3$) $\alpha = 0.90$	
0	0	341.2	191.8	43.8
1	100	431.6	275.3	36.2
5	100	431.6	275.3	36.2
9	100	431.6	275.3	36.2
10	100	432.9	275.3	36.4
19.5	100	not feasible	283.2	—

The main result is shown by the fact, that reservoir capacities gained by application of chance constraints ($\alpha = 90$ percent) are at an average about 1/3 lower than those gained by the use of deterministic constraints.

This positive feature is, however, not very useful for practical purposes. Simulation runs on the computer with reservoirs designed according to the above-mentioned chance constraints and based on 45 years of observed data show, that not only the constraints are violated (which is allowed up to 10 percent of the time) but that negative release values occur, which is not allowed and physically not possible. Figure 1 shows such an example, where the minimum storage is sometimes less than S_{min}, but always positive. The release is sometimes less than AM, but sometimes even negative.

In order to avoid this impractical operation mode the constraints were made stronger, i.e., α was raised to 95 percent. For the alternative $AM = 9.0$; $S_{min} = 100$; $AN = 300$ and $V = 50$ the required storage capacity became $k = 326.7 \cdot 10^6 m^3$ which is by 18.6 percent larger than the corresponding value of $k = 275.3 \cdot 10^6 m^3$ for $\alpha = 90$ percent. For this case no negative releases occurred anymore.

One point of particular interest is the dependence between required reservoir capacity k and the probabi-

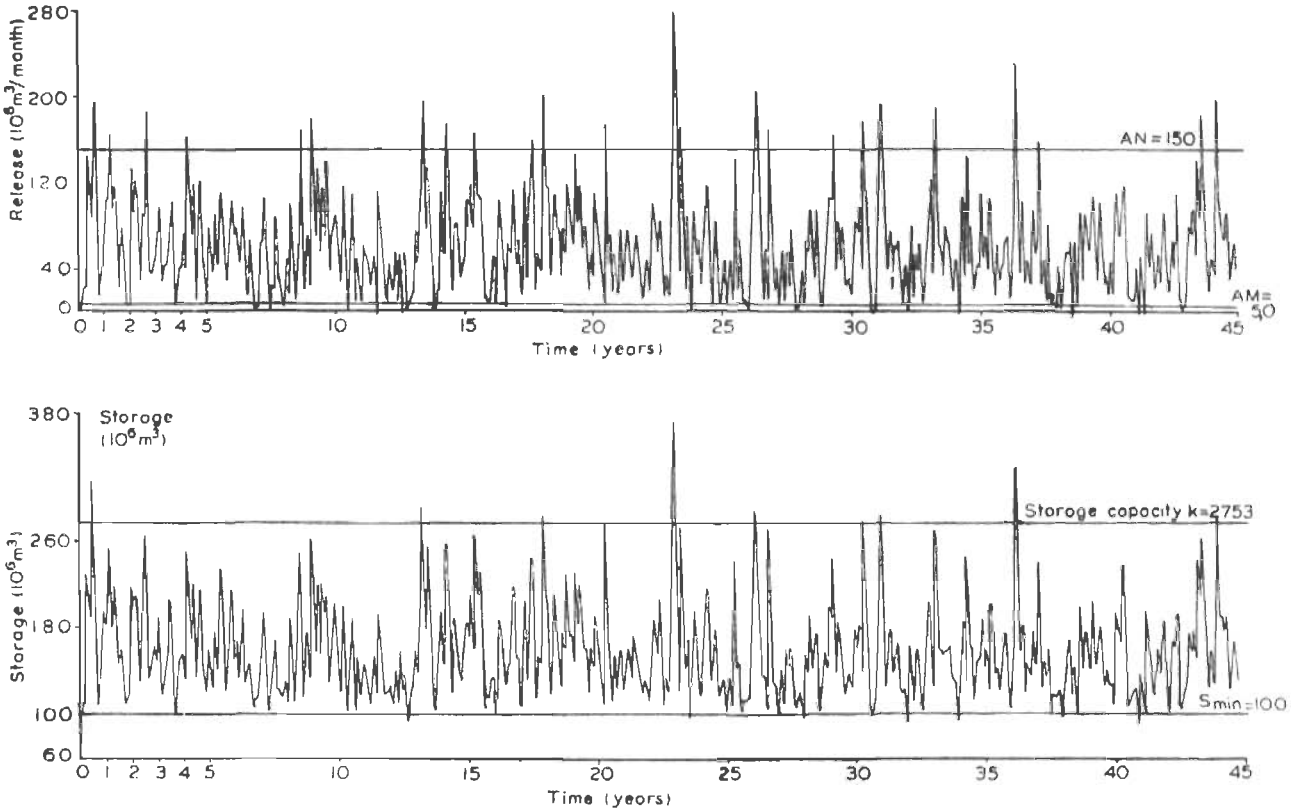

FIGURE 1: Simulation run for 45 years observed data. Chance constraints with α = 0.90, AM = 5.0·10^6m^3/month, S_{min} = 100 · 10^6m^3, V_i = 50 · 10^6m^3.

lity level α, by which the chance constraints must be met. Qualitatively it is obvious, that k must grow with α. Figure 2 shows the results of computations for the Kinzig River. For the linear decision rule

$$A_t = S_{t-1} - E_t \qquad \ldots(6)$$

as discussed so far, it can be seen from Figure 2 that the relationship between α and k follows a log-normal probability distribution function. The deterministic case of k=431.6 . 10^6m^3 corresponds to a level α=98.8 percent. For α = 0.90 the reservoir capacity k has to be 275.3 · 10^6m^3 and for α = 0.99 the k value is 451.7 . 10^6m^3, which amounts to an increase of 64 percent.

A Modification of the Conventional Linear Decision Rule (LDR)

In the discussion of the results of the deterministic case shown in Table I it was stated that the "useless" reservoir requires a capacity of 291.2 · 10^6m^3 for nothing else but verification of the linear decision rule as given in Equation (6):

$$A_t = S_{t-1} - E_t \qquad \ldots(6)$$

or Equation (6*a*):

$$A_t = I_{t-1} + E_{t-1} - E_t \qquad \ldots(6a)$$

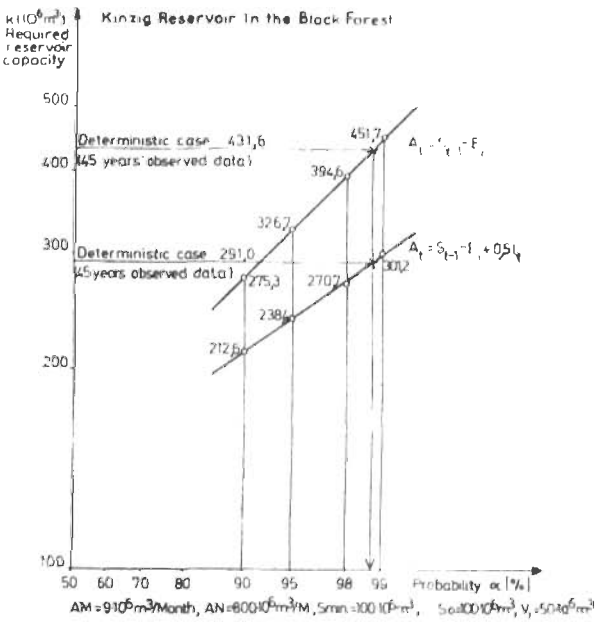

FIGURE 2: Required reservoir capacity versus probability level α, by which the chance constraints must be met.

In the many computations carried out during this study it was found that the E_t values are all of the same order of magnitude. This means for Equation (6*a*) that in a time interval t the release A_t has about the same value as the inflow I_{t-1} of the previous interval. In consequence the LDR boils down more less to a reservoir operation in which inflow is merely delayed by one month before release. Usually the objective of a reservoir is, however, to store water in wet months for use during dry periods. In order to come close to this aim the LDR may be altered. A simple way of doing this is to replace Equation (6*a*) by the following :

$$A_t = S_{t-1} - E_t + \gamma \cdot I_t \qquad \ldots(11)$$

with $0 \leqslant \gamma \leqslant 1$.

This way the release is partly dependent on the inflow during the same time increment which is advisable for flood control. Furthermore, the fraction $(1-\gamma)$ of the inflow will be released during the following months. The advantage of such a LDR is that the required reservoir capacity is no longer an almost direct function of the maximum inflow.

Results obtained by the LDR of Equation (11) are shown in Figure 2 for $\gamma = 0.5$ (lower curve). It can be seen in this case the same minimum release can be guaranteed by a much smaller reservoir.

For $\alpha = 0.99$ the required reservoir capacity will be $k = 301.2 \cdot 10^6 m^3$ when using the LDR of Equation (11), instead of $k = 451.70 \cdot 10^6 m^3$ according to the LDR of Equation (6*a*). Thus, the modification of the LDR yields a reduction of reservoir capacity by 1/3.

Conclusion

The paper shows the influence of chance constraints on required reservoir capacity for a design problem of a water supply reservoir in the "Black Forest" mountains in Southern Germany.

The reservoir, which is operated according to a linear decision rule (LDR), is subject to constraints concerning minimum release, maximum release, minimum reservoir content and provision of flood storage in each month. The objective is to find the minimum required reservoir capacity. Solutions were found by the application of linear programming. The following results were obtained :

(1) If the constraints are formulated in a deterministic mode, the required storage capacity was rather large, e.g., $k = 431.6 \cdot 10^6 m^3$ for alternative 8 in Table I.

(2) If the constraints are formulated as chance constraints, ($\alpha = 0.9$) the required reservoir capacity may be reduced considerably, e.g., $k = 275.3 \cdot 10^6 m^3$ for the case corresponding to the one mentioned above.

(3) A comparison of corresponding deterministic and stochastic design alternatives is given in Table III.

(4) The choice of the probability level $(1-\alpha)$, by which constraints may be violated can be crucial. In the case of $\alpha = 0.90$ negative reservoir releases were required. Only for $\alpha \geqslant 0.95$ this impossibility was avoided.

(5) Modification of the conventional LDR of Equation (6) into the formulation of Equation (11) for $\gamma = 0.5$ leads again to a reduction of required reservoir capacity. For example for $\alpha = 0.95$ the capacity was $326.7 \cdot 10^6 m^3$ according to Equation (6) and became $238.4 \cdot 10^6 m^3$ according to Equation (11) which means a reduction by 27 percent. Compared to the deterministic case it amounts to a reduction of 45 percent.

(6) Design alternatives found by application of deterministic constraints correspond to stochastic alternatives which have a probability level α corresponding, more or less, to the length of the observation period. Figure 2 shows, e.g., that the deterministic case for 45 years of observation corresponds to the stochastic case of $\alpha = 98.8$ percent.

As a conclusion one would suggest, that in a design problem where the minimum required reservoir capacity is to be determined, it is reasonable to apply chance constraints (as compared to conventional deterministic constraints), if a probability level is acceptable, which allows violation of constraints such that no negative releases occur (in the "Black Forest" example this probability level had to be less than 5 percent). Furthermore, one should investigate which type of LDR may be used (if any at all), because it considerably influences the required reservoir capacity.

Acknowledgements

The authors are grateful to Mr. J.W. Figlus, who did most of the computational work. The computations were carried out free of charge on the UNIVAC 1108 computer of the University of Karlsruhe.

References

(1) REVELLE, Ch. ; JOERES, E. and KIRBY, W. : "The Linear Decision Rule in Reservoir Management and Design. 1, Development of the Stochastic Model." Water Resources Research, Vol. 5, No. 4, 1969.

(2) REVELLE, Ch. and KIRBY, W. : "Linear Decision Rule in Reservoir Management and Design. 2, Performance Optimization." Water Resources Research, Vol. 6, No. 4, 1970.

(3) EISEL, L.M. : "Comments on the Linear Decision Rule in Reservoir Management and Design by Revelle, Kirby and Joeres." Water Resources Research, Vol. 6, No. 4, 1970.

(4) EISEL, L.M. : "Chance Constrained Reservoir Model." Water Resources Research, Vol. 8, No. 2, 1972.

(5) LOUCKS, D.P. : "Some Comments on Linear Decision Rules and Chance Constraints." Water Resources Research, Vol. 6, No. 2, 1970.

(6) NAYAK, S.C. and ARORA, S.R. : "Optimal Capacities for a Multi-reservoir System using the Linear Decision Rule." Water Resources Research, Vol. 7, No. 3, 1971.

APPENDIX—I

Reduction of 2,160 Constraints, given in Equations (2*a*)÷(5*a*), to (48+2=50) Constraints

$$k-E_i \geqslant V_i+I_i \qquad \ldots(4a)$$

$$E_i \geqslant S_{min}-I_i \qquad \ldots(3a)$$

$$E_{i-1}-E_i \geqslant AM_i-I_{i-1} \qquad \ldots(2a)$$

$$E_{i-1}-E_i \leqslant AN_i-I_{i-1} \qquad \ldots(5a)$$

The unknowns are the required reservoir capacity k and 12 values of E_i (one for each month). The initial conditions give another two constraints with a further unknown, the initial reservoir content S_o :

$$S_0 \geqslant S_{min} \qquad \ldots(I.1)$$

$$k-S_0 \geqslant V_1 \qquad \ldots(I.2)$$

Equations (2*a*) ÷ (5*a*) represent 540 (=12×45) constraints each. However, each constraint appears in the same form 45 times, except for a different value of I_i. If so, one constraint must be more restrictive than the others, and only this most restrictive one has always to be considered :

$$k-E_i \geqslant V_i+\max_j (I_{i+12j}) \qquad i=1\ldots12,\ j=0\ldots44 \qquad \ldots(4b)$$

$$E_i \geqslant S_{min}-\min_j (I_{i+12j}) \qquad \ldots(3b)$$

$$E_{i-1}-E_i \geqslant AM_i-\min_j (I_{i-1+12j}) \qquad i=2\ldots12,\ j=0\ldots44 \qquad \ldots(2b)$$

$$E_{12}-E_1 \geqslant AM_1-\min_j (I_{12+12j}) \qquad i=1,\ j=1\ldots44$$

$$S_o-E_1 \geqslant AM_1 \qquad i=1,\ j=0$$

$$E_{i-1}-E_i \leqslant AN_i-\max_j (I_{i-1+12j}) \qquad i=2\ldots12,\ j=0\ldots44 \qquad \ldots(5b)$$

$$E_{12}-E_1 \leqslant AN_1-\max_j (I_{12+12j}) \qquad i=1,\ j=1\ldots44$$

$$S_0-E_1 \leqslant AN_1 \qquad i=1,\ j=0$$

$$S_0 \geqslant S_{min} \qquad \ldots(I.1)$$

$$k-S_0 \geqslant V_1 \qquad \ldots(I.2)$$

Equations (2*b*) ÷ (5*b*) represent one constraint for each month, i.e., $4\times12=48$ equations. Including Equations (I.1) & (I.2) we have a set of 50 equations with 14 unknowns. The solution for minimization of the objective function

$$O.F. = k = min\,!$$

can easily be found by linear programming, e.g., by application of the simplex algorithm. Equations (2*b*)÷(5*b*), (I.1) & (I.2) represent the set of deterministic constraints of the problem investigated in this paper.

It should be noted, that some of the constraints are not independent. For example, Equations (2*b*) & (5*b*) read for extreme conditions :

$$E_{i-1}-E_i = AM_i-min\ I \qquad \ldots(2b)$$

$$E_{i-1}-E_i = AN_i-max\ I \qquad \ldots(5b)$$

$$AM_i-min\ I = AN_i-max\ I$$

$$AM_i = AN_i-max\ I+min\ I \qquad \ldots(I.3)$$

Since *min I* and *max I* are known observed discharges Equation (I.3) may be written

$$AM_i = AN_i+C \qquad \ldots(I.3a)$$

which shows, that the choice of AM_i and AN_i must be such that no constraint will be violated !

APPENDIX—II

Transformation of Deterministic Constraints into Chance Constraints

Following closely (1) a brief derivation of the chance constraints shall be given.

The inflow values I_i for each month i will be treated as random variable R_i having a cumulative empirical probability distribution F_{R_i} obtained from observed data (in our case 45 years) :

$$F_{R_i}(I) = P(R_i \leqslant I) \qquad \ldots(II.1)$$

The constraint (4*a*)

$$k-E_i \geqslant V_i+I_i \qquad \ldots(4)$$

shall now be changed into a chance constraint by replacing the observed value of I_i by the random variable R_i :

$$k-E_i \geqslant V_i+R_i \qquad \ldots(4d)$$

or

$$E_i+R_i \leqslant k-V_i \qquad \ldots(4e)$$

Constraint (4*e*) will be violated with a probability α, if

$$R_i \geqslant k-V_i-E_i$$

On the other hand α may be chosen such that

$$P(R_i \leqslant k-V_i-E_i) = F_{R_i}(k-V_i-E_i) \geqslant \alpha_1 \qquad \ldots(II.2)$$

The R_i-value corresponding to a given level of α will be called $r_i(\alpha_1)$, which changes Equation (II.2) into

$$k - V_i - E_i \geqslant r_i(\alpha_1) \qquad \ldots(\text{II}.3)$$

since $r_i(\alpha_1)$ is the solution of the equation

$$F_{R_i}(x) = \alpha_1 \qquad \text{for } x.$$

Analogous to constraint (4) the other constraints may be formulated as chance constraints :

deterministic : $E_i \geqslant S_{min} - I_i$ ...(3*a*)

stochastic : $P(E_i \geqslant S_{min} - R_i) \geqslant \alpha_2$ ...(II.4)

constraint (2*a*) :

deterministic : $E_{i-1} - E_i \geqslant AM_i - I_{i-1}$ ...(2*a*)

stochastic : $P(E_{i-1} - E_i \geqslant AM_i - R_{i-1}) \geqslant \alpha_3$ ...(II.5)

and constraint (5*a*) :

deterministic : $E_{i-1} - E_i \leqslant AN_i - I_{i-1}$ ...(5*a*)

stochastic : $P(E_{i-1} - E_i \leqslant AN_i - R_{i-1}) \geqslant \alpha_4$ ...(II.6)

The additional constraints for initial conditions now become irrelevant since S_o will become a fixed value, which was found by the deterministic computations. Analogous to the development of Equation (II.3) also the other constraints may be transformed as follows :

$$k - E_i \geqslant V_i + r_i(\alpha_1) \qquad \ldots(\text{II}.7)$$

Equation (II.4) then becomes :

$$S_{min} - E_i \leqslant r_i(1 - \alpha_2) \qquad \ldots(\text{II}.8)$$

Equation (II.5) becomes :

$$AM_i - E_{i-1} + E_i \leqslant r_{i-1}(1 - \alpha_3) \qquad \ldots(\text{II}.9)$$

and Equation (II.6)

$$E_{i-1} - E_i \leqslant AN_i - r_{i-1}(\alpha_4) \qquad \ldots(\text{II}.10)$$

For Equations (II.9) & (II.10) the initial conditions for first and second year have to be established analogous to Equations (2*b*) & (5*b*) in Appendix-I. Equations (II.7) ÷ (II.10) represent 48 chance constraints altogether.

The Approximate Probability Density Function of Range and Adjusted Range

PRATHET SUTABUTR
Senior Engineer
National Energy Administration, Pibultham Villa, Yodsae, Bangkok 5, Thailand.

SYNOPSIS

The objectives of this study are to develop the general expression approximately for probability density function and probability distribution function for the random variable range of both the independent random normal variable and dependent random normal variable of the first and second order Markov linear model.

Since the four basic parameters, the mean, the variance, the skewness coefficient and the excess coefficient of the maximum range for independent standard normal variable or dependent normal variable of the first and second order Markov linear model can be obtained by the data generation method.

Using these four basic parameters approximately obtained by the above method and applying the basic criteria set by Karl Pearson, the approximate probability density function of range is obtained as one of the best fitted from his family of curves. The parameters of this probability density function can then be computed by using the exact and approximate expression for the expected value and variance of the maximum range of the independent normal variable or dependent normal variable of the first and second order Markov linear model previously derived by many authors.

Introduction

If we let Z_i be sequence of random variables with $E(Z_i) = 0$, then

$S_n = Z_1+Z_2+Z_3+ \ldots\ldots + Z_n$ are its accumulate sum. If we take

$$M_n = \text{Max. } (0, S_1, S_2, S_3, \ldots\ldots, S_n)$$

$$m_n = \text{Min. } (0, S_1, S_2, S_3, \ldots\ldots, S_n)$$

as maximum and minimum of accumulated sums, with i taking all non-negative integer values from 0 to n, then the variable

$R_n = M_n - m_n$ is called the range of the cumulative sum S_n.

It is clear in this case that $E(S_n) = 0$, however, in some applications, especially for small value of n, if each component Z of the partial sum is subtracted by the sample mean $\bar{Z}_n$. Therefore, the above random variables will take the form

$$S_i^* = S_i - \frac{i}{n} S_n$$

$$M_n^* = \max.\left(0, S_1^*, S_2^*, \ldots\ldots, S_n^*\right)$$

$$m_n^* = \min.\left(0, S_1^*, S_2^*, \ldots\ldots, S_n^*\right)$$

where, S_i^* is called the adjusted partial sum, M_n^* the

This research paper is supported by the Alexander Von Humboldt Stiftung and performed at Technische Universität Braunschweig, West Germany.

adjusted maximum partial sum or adjusted surplus, m_n^* the adjusted minimum partial sum or adjusted deficit and R_n^* the adjusted range. Figure 1 represents graphically R_n, M_n, m_n, R_n^*, M_n^* and m_n^* respectively. Obviously, these six new variables are also random variables and they are very important in the application of reservoir storage capacity design. Several attempts have been made to find the exact expression for their density and distribution function but in general, finding these exact density functions is a very difficult mathematical problem even for cases of independent normal random variables. However, in the last past two decades several authors had derived and obtained their exact expected values for finite values of n or their asymptotic expected value and variance. Recently some approximate expression of variance for finite values of n of independent and dependent normal variable were also obtained.

Rippl (1883) was the first who injected the concept of mass curve for analyzing the relationship between the inputs, outputs and storage capacity. From then on several research works have been started following his concepts and they are mentioned here briefly only the ones which will be used in the further text.

Range of Cumulative Sums S_n

W. Feller (1951) derived the asymptotic distribution of the range of the cumulative sums of independent normal random variables. Feller obtained in particular the equation

$$E(R_n) = 2\sqrt{\frac{2}{\pi}}\,n = 1.60\ n \qquad \ldots(1)$$

$$\text{Var } R_n = 4n\left(\log 2 - \frac{2}{\pi}\right) = 0.2181\ n \qquad \ldots(2)$$

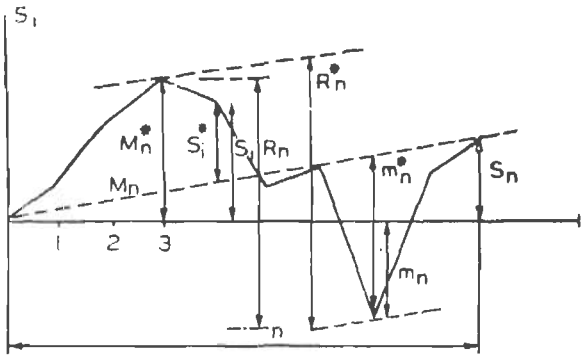

Definition of unadjusted and adjusted partial sum, S_i, S_i^* The unadjusted and adjusted maximum partial sum, M_n, M_n^* (unadjusted and adjusted surplus), the unadjusted and adjusted minimum partial sum, m_n, m_n^* (unadjusted and adjusted deficit), and the unadjusted and adjusted range R_n, R_n^*.

FIGURE 1.

A.A. Anis and E.H. Lloyd (1953) solved the problem of the storage capacity of a reservoir for which one would like to know the distribution of the water-level over a given number of "n" years. They concluded that the level after "i" years may be regarded as the sum of "i" annual increments, and that one may approximate this real problem by the ideal one in which the annual increments are independent variates with a common normal distribution. The application of these results to other storage problem is obvious. Anis and Lloyd derived the expected value of range, over "n" years as

$$E(R_n) = \sqrt{\frac{2}{\pi}} \sum_{i=1}^{n} i^{-1/2} \qquad \ldots(3)$$

P. Sutabutr (1967) investigated the reservoir design problem for within the year regulation assuming a constant standard deviation for variable at various positions during the year and the first order Markov linear model for the stochastic part of the monthly streamflow data. Based on his simulation, he suggested that the expected value of range for the standard normal variable can be expressed by

$$E(R_n) = \sqrt{\frac{2}{\pi}} \sum_{i=1}^{n} i^{-1}\,[\text{Var } S_i]^{1/2} \qquad \ldots(4)$$

and for the standard normal first order linear model, the expected value of range can be expressed as :

$$\text{for } \rho \geqslant 0 : E(R_n) = \sqrt{\frac{2}{\pi}} \sum_{i=1}^{n} i^{-1/2} \left[\frac{1+\rho}{1-\rho} - \frac{2\rho(1-\rho)^i}{i(1-\rho)^2}\right]^{1/2} \qquad \ldots(5)$$

V. Yevjevich (1967) using the data generation approach, also suggested that the expected value of range of all linearly dependent normal variables may be expressed by Equation (5). He specially obtained the general expression for the case linearly dependent normal variable as

$$E(R_n) = c\sigma \sum_{i=1}^{n} i^{-1/2}\left[1 + \frac{2}{i}\sum_{k=1}^{i-1}(i-k)\,\rho_k\right]^{1/2} \qquad \ldots(6)$$

According to Yevjevich, the factor

$$\left[1 + \frac{2}{i}\sum_{k=1}^{i-1}(i-k)\,\rho_k\right]^{1/2}$$

represents the effect of the auto-correlation of the time series on the expected value of range, whereas $\sigma \neq 1$ represents its effect on the change of standard deviation made by a linear dependence model. The constant "c"

for either independent or dependent normal variable will always be equal to $\sqrt{\frac{2}{\pi}}$.

Salas-La Cruz (1972), in his dissertation "Range Analysis for Storage Problems of Periodic-Stochastic Processes" obtained many interesting results concerning with non-stationary time series. One of his interesting results is his empirical equations for the variance of range of the first and second order Markov models with constant auto-correlation coefficients which will be used in the further text. These equations can be expressed as follows :

$$\text{for} \quad n \geqslant 6 \quad \text{Var } R_n = \sigma^2 (A + Bn) \qquad \ldots(7)$$

where, σ is the constant standard deviation of the input and the linear regression coefficients A and B are functional of the auto-correlation coefficients of the Markov models considered. The linear regression parameters A and B of Markov first order and second order linear model given in Equation (7) are given in Tables I & II.

Adjusted Range of Cumulative Sums S_n

H.E. Hurst (1951) was the first developing an expression for storage capacity for over year water regulation related to the concept of adjusted range. He collected an impressively large amount of statistical material relating to annual values of natural phenomena, including river discharges. According to Hurst, a quantity R_n^* enters into these which can be obtained by taking departures of the annual values from their mean for a period of n years. For the case of time series of various natural phenomena, of which a large quantity have been examined, the mean result is presented by the equation

$$\frac{R_n^*}{\sigma_n} = Kn^H \qquad \ldots(8)$$

where, σ_n is the standard deviation of the time series and H is a quantity which has a normal distribution and a mean of 0.73.

TABLE I*

Regression coefficients of linear function fit to variance of the range of the first order Markov Model.

	Value of ρ						
	0.0	0.1	0.2	0.3	0.4	0.6	0.8
A	0.1967	0.2069	0.2124	0.2293	0.1164	−0.5261	5.6682
B	0.2338	0.2753	0.3397	0.4422	0.5363	0.9403	2.1919
Standard error of regression coefficients	0.00285	0.00305	0.00402	0.00606	0.00696	0.01323	0.0219
Correlation coefficients	0.99956	0.99963	0.99958	0.99944	0.99950	0.99941	0.9997

TABLE II*

Regression coefficients of linear function fit to variance of the range of the second order Markov Model.

	$\rho_1 = 0.40$			ρ_1 0.60		
	$\rho_2 = 0.10$	$\rho_2 = 0.20$	$\rho_2 = 0.30$	$\rho_2 = 0.25$	$\rho_2 = 0.30$	ρ_2 0.40
A	−0.33983	−0.66148	−1.21142	−0.12678	−0.51548	−1.86086
B	0.47315	0.60505	0.77663	0.65861	0.77870	1.08101
Standard error of regression coefficient	0.00426	0.00519	0.00617	0.00609	0.00670	0.00860
Correlation coefficient	0.99931	0.99938	0.99946	0.99927	0.99937	0.99946

*These tables obtained from Jose D. Salas-La Cruz (1972).

W. Feller (1951) derived the asymptotic distribution of the adjusted range of the sum of n independent normal random variable Z_i, with $E(Z_i) = 0$, and Var $Z_i = 1$. In particular

$$E\left(R_n^*\right) = 1.25\, n^{0.5} \qquad ...(9)$$

and

$$\text{Var } R_n^* = 0.074\, n \qquad ...(10)$$

V. Yevjevich (1965) showed that the asymptotic expression for variance of adjusted range obtained by W. Feller does not depart significantly from the variance obtained by the data generation method, (100,000 random numbers). He concluded that the asymptotic variance in Equation (10) can be used in practical cases, except for very small values of n, such as $n = 2$–6.

Significance of the Study

Due to the statistical nature of inputs and outputs of a water resource system, most of the research in the last two decades regarding the method for planning, design and operation of the reservoir of the water resource system has been statistically approached. They can be classified into three :

(1) empirical

(2) simulation or data generation, and

(3) analytical (mathematical).

The method used generally known as the Rippl's diagram or mass curve is still the most oftenly used in designing the reservoir storage capacity. The basic assumption is that both reservoir input and output are known function of time and produce the storage capacity required for no water shortage during the period considered. This analysis which based on a single sequence of hydrologic events of a historical record may produce one important uncertainty. It is unlikely that the same historical sequence of flow will occur again during the life of the project. In another way of saying, the variable considered in the Rippl's diagram is also a random variable which must be analyzed statistically. Another disadvantage is the difference between the length of a historical record and the economic life time of a project.

The new expression "Probability density function of the random variable range" of both the independent random normal variable and dependent random normal variable of the first and second order Markov linear model which is the objective of this study can be very helpful with much less considerable risk is judging the storage capacity required by the water resource project.

Method of Determination of the Four Basic Moments of Range of Independent and Dependent Normal Variables

In most of the digital computer, the independent random numbers of a uniform density function in the interval (0, 1) are generally available. Several methods are also available in obtaining normal random variables from the uniform random variables, however, the least time consuming method was developed by Box and Muller (1958).

If U_1 and U_2 are two independent random numbers from the same uniform density function in the interval (0, 1), then the random variables

$$\epsilon_1 = (-2\, lnU_1)^{1/2} \cos 2\pi\, U_2 \qquad ...(11)$$

and

$$\epsilon_2 = (-2\, lnU_1)^{1/2} \sin 2\pi\, U_2 \qquad ...(12)$$

will be a pair of independent random numbers from the same normal distribution with mean zero and variance unity.

In case of dependent standard normal variable of the first and second order Markov linear model, Equations (13) & (14) below can be applied respectively for various values of ordered serial correlation :

$$Z_i = Z_{i-1} + \sqrt{1-\rho^2}\ \epsilon_i \qquad ...(13)$$

and

$$Z_i = \alpha_1 Z_{i-1} + \alpha_2 Z_{i-2} + \epsilon_i \qquad ...(14)$$

in which

$$\alpha_1 = \frac{\rho_1 - \rho_1 \rho_2}{1-\rho_1^2}$$

$$\alpha_2 = \frac{\rho_2 - \rho_1^2}{1-\rho_1^2}$$

Using the digital computer, any numbers of independent and dependent standard normal variable can now be generated. The random variable range, adjusted range and their first four moments are able to be obtained using the Fortran Program.

Method of Determination of Approximate Probability Density Function of Range and Adjusted Range

According to Karl Pearson (1965), the two general criteria for the best selection of one of his general probability density function are

$$K_1 = 2\beta_2 - 3\beta_1 - 6 \qquad ...(15)$$

and

$$K_2 = \frac{\beta_1 (\beta_2+3)^2}{2\,(4\beta_2 - 3\beta_1)\,(2\beta_2 - 3\beta_1 - 6)} \qquad ...(16)$$

where, β_1 = the skewness coefficient on square and β_2 = the Kurtosis coefficient. In term of these two coefficients, K_2 in Equation (16) which is the most important criteria can be expressed as

$$K_2 = \frac{C_s^2\,(E+6)^2}{4\,(2E - 3C_s^2)\,(4E - 3C_s^2 + 12)}$$

in which C_s and E are the skewness and Kurtosis coefficient respectively and preferable in the unbiased form. From the criteria K_2, one can select the best

fitted probability density function from the family of Pearson functions.

Generally speaking, if K_2 is negative, the best function is the Pearson-Type-I unbounded function (Beta-distribution). If the distribution is bounded by zero on the lower end or the considered random variable is positive-valued variable, the subcase of type I as the Pearson-Type-III distribution should be applied.

The Pearson-Type-II probability density function in general can be given in the form

$$y = y_0 \left(1+\frac{X}{m}\right)^{\gamma m} \quad e^{-\gamma m} \qquad \ldots(18)$$

where, γ and m are the parameters and the probability density function in Equation (18) has a range limited at $-m$ in a lower end direction.

Using the random variable range R_n as a variable and transforming Equation (18) by the expression $R_n = m+X$. Equation (18) can then be written as

$$f(R_n) = f(m)\left(\frac{R_n}{m}\right)^{\gamma m} \quad e^{-\gamma(R_n-m)} \quad 0 \leqslant R_n < \infty \qquad \ldots(19)$$

where, $f(m)$ is the probability density of the mode m.

If the alternative parameter $p = \gamma m$ is introduced, by direct integration of Equation (18) and Equation (19) it can be shown that the first and second moment about the origin

$$\mu'_1 = \frac{p+1}{\gamma} \qquad \ldots(20)$$

and

$$\mu_2' = \frac{(p+1)(p+2)}{\gamma^2} \qquad \ldots(21)$$

Subtraction Equation (21) by the square of Equation (20) the second moment about the mean or variance of range can be obtained as

$$\mu_2 = \frac{p+1}{\gamma^2} \qquad \ldots(22)$$

Dividing Equation (22) by Equation (20), then the parameter γ can be expressed in term of the first and the second moment as

$$\gamma = \frac{\mu'_1}{\mu_2}$$

and in term of expected value and variance of range as

$$\gamma = \frac{E(R_n)}{\text{Var } R_n} \qquad \ldots(23)$$

Therefore, the parameter m and $f(m)$ can be found as

$$m = \frac{\{E(R_n)\}^2 - \text{Var } R_n}{E(R_n)} \qquad \ldots(24)$$

$$f(m) = \frac{(\gamma m)^{\gamma m+1}}{m\, e^{\gamma m}\, \Gamma(\gamma m+1)} \qquad \ldots(25)$$

In conclusion, the necessary steps in finding the best function from the family of Pearson's probability density function for the random variable range or adjusted range require first calculating the first four moments from the generated data, then the skewness coefficient, excess coefficient and K_2 are computed. After selecting the best probability density function, the parameters of this density function can be found using the expression previously derived by many authors.

In this study, the data used consisted of 100,000 random numbers of an independent normal variable with mean zero and variance unity. In case of dependent normal variable of the first and second-order Markov linear model, the independent standard normal variable was replaced by the expression given in Equations (13) & (14) respectively. The Fortran Program used was such as to use random numbers in block of 1,000, with a total of 100 groups. The accumulative sums of this variable were calculated then the maximum, minimum of the accumulative sum (surplus and deficit) and the variable range or adjusted range at lag time $n = 10, 20, 30, 40$ and 50 were computed. The frequency density function, the first four moments both about the origin and about the mean, the skewness coefficient and the excess coefficient of the above random variable were also determined.

It has been found in this study that almost all of K_2 in Equation (17) are either negative or substantial large positive valued number, therefore, the best fitted probability density function from the family of Pearson functions is the Pearson-Type-I or Pearson-Type-III (which is the subcase of Type I). However, due to the random variable range or adjusted range is a positive valued variable and bounded at the lower end, the subcase of Type I as the Pearson-Type-III distribution should be applied.

Equation (19) represents the approximate probability density function of range of independent standard normal variable of the first and second order Markov linear model. This equation can also be applied for adjusted range but only when the expression for the expected value and variance is available which is the case of independent standard normal variable.

For comparison purposes, the frequency density function of range and adjusted range as obtained by the data generation method and by the approximate Equation (19) are shown together in Figures 2 & 3. It can obviously be concluded that Equation (19) fits relatively well both in range and shape with the frequency density function obtained by the data generation method. Equation (19) should be applicable as long as there are the expressions given both for the $E(R_n)$ and Var R_n.

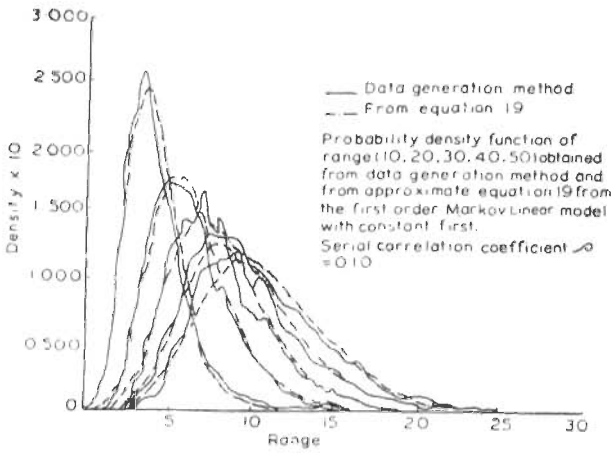

FIGURE 2.

Application of the Probability Density Function of Range*

Assumed a reservoir has been built for over year (long range) river flow regulation, with the ratio of the reservoir storage capacity, S_f, to the standard deviation of annual inflow, $s(z)$, given by $R_f = S_f/s(z) = 6$. Suppose also that the designer is interested in the probability that this storage capacity may regulate the flow for every 10-year period on the long-term average discharge, provided the annual inflows are normally distributed and follow the first order Markov model with $\rho = 0.20$.

In order to apply Equation (19), first the parameters γ, m and $f(m)$ can be calculated using Equations (23), (24) & (25) respectively. For this particular case $\gamma = 1.25$, $m = 3.72$ and $f(m) = 0.23$.

$$f(R_{10}) = 0.23 \left(\frac{R_{10}}{3.72}\right)^{4.66} e^{-1.25\,(R_{10}-3.72)}$$

Using Newton's difference method of integration, the integration of the above equation from $R_{10} = 0$ to $R_{10} = 6$ yields

$$P\,(R_{10} \leqslant 6) = \int_0^6 f(R_{10})\,dR_{10} = 0.8009$$

By the same integration but from $R_{10} = 0$ to $E\,(R_{10}) = 4.519$ yields

$$P\,\{R_{10} \leqslant E\,(R_{10})\} = 0.572$$

In conclusion, in four out of every five 10-year periods, the storage capacity is sufficient to regulate all inflows and produce approximately the long-term mean discharge as the constant outflow from the reservoir. In other words, to be certain in four out of every five 10-year periods, the designer should provide the storage capacity $R_{10} = 6\,s(z)$ to regulate all inflows and produce approximately the long-term mean discharge as the constant outflow from the reservoir. The storage capacity $E(R_{10})\,s(z)$ is sufficient to serve the same purpose approximately in six out of every 10-year periods.

* From "Stochastic Processes in Hydrology" by V. Yevjevich.

Conclusion

In the long range (over year) storage design with the application of concept of range, if the present practice of determining storage capacities by the so-called mass-curve (Rippl diagram) method is examined, it can be easily seen that we actually depend on only one random variable range instead of its probability distribution function. However, in the last past two decades, the concept of range with its mean, variance and other parameters has been intensively investigated to give a more reliable information for various planning and operational objectives.

In this study, the approximate probability density function and the approximate probability distribution function of maximum range, R_n, for the independent and dependent normal variable of the first and second order Markov model were investigated. Using the data generation method and the criteria set by Karl Pearson[5] (1965), one of the most suitable of the Pearson curve was selected. From the analysis made for this study, the following conclusions were reached :

(1) Using the criteria set by Karl Pearson with the practical reality, the most suitable function from the Pearson family of curve was the Pearson-Type-III a subcase of Type I.

(2) The probability density function of range of the normal variable given in Equation (19) (which in fact gamma function with 2 parameters) fitted relatively well both in range and shape with the frequency density fuuctions obtained by the data generation method.

(3) The two parameters γ and m in the probability density function Equation (19) could be obtained using the expression of $E(R_n)$ and Var R_n obtained previously from a number of authors for various values of ρ and n of the first order Markov and for various values of ρ_1, ρ_2 and n for the second order Markov.

Acknowledgements

The author wishes to express his sincere appreciation to his host professor, Dr. Ing. V. Maniak, Associate Professor of Leichtweiß—Institut für Wasserbau, Technische Universität, Braunschweig, to Mr. Nitipat Jalichan, the Secretary General of the National Energy Administration, Government of Thailand, to his former major professor, Dr. V. Yevjevich, Professor of Civil Engineering, Colorado State University, Fort Collins, Colorado, U.S.A., for providing the opportunity of doing this research investigation.

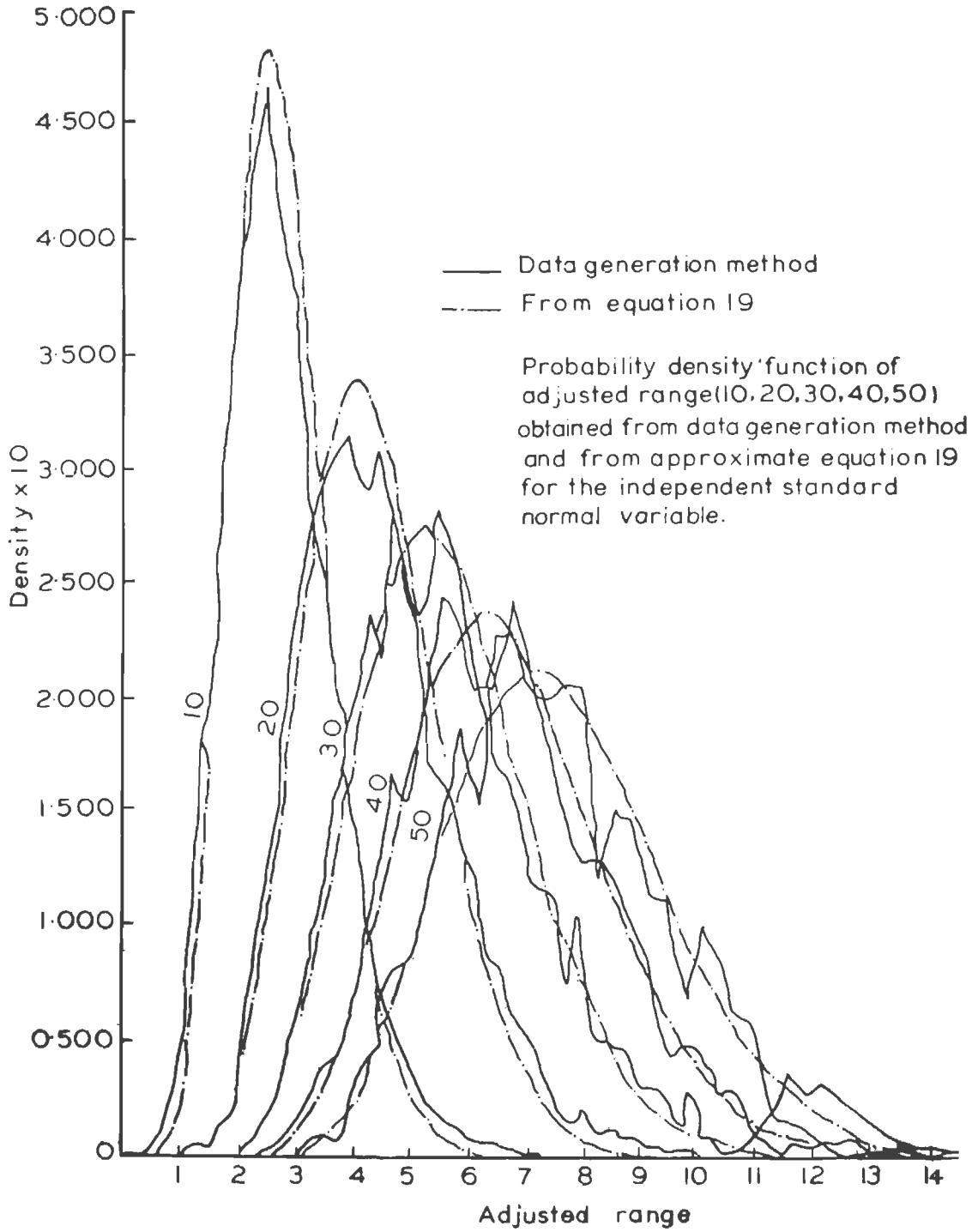
5·000
4·500
4·000
3·500
3·000
2·500
2·000
1·500
1·000
0·500
0
Density x 10
1 2 3 4 5 6 7 8 9 10 11 12 13 14
Adjusted range
10
20
30
40
50
Data generation method
From equation 19
Probability density function of adjusted range(10,20,30,40,50) obtained from data generation method and from approximate equation 19 for the independent standard normal variable.

FIGURE 3.

Gratitude is extended to the Alexander Von Humboldt Stiftung who funds this research project and to the Technische Universität Computer Center for the free computer time.

Gratefulness is also extended to Mrs. E. Dumpert and Mr. C. Ratanarak for their assistance in this investigation. Finally, to his wife M.L. Poonsang and his two sons Prathomrat and Tavarat for their patience throughout all his long absence from the country, goes the author's deepest sympathy.

List of Symbols

A = Regression coefficient of variance of range

B = Regression coefficient of variance of range

C_s = Coefficient of skewness

E = Excess coefficient

K_2 = Pearson's criteria in selecting the type of probability density function

m = Location parameter in the Pearson-Type-III probability density function

M_n = Maximum of the partial sum at time n

M_n^* = Maximum of the adjusted partial sum at time n

m_n = Minimum of the partial sum at time n

m_n^* = Minimum of one adjusted partial sum at time n

R_n = Range of the partial sum at time n

R_n^* = Adjusted range of the partial sum at time n

S_i = Partial sum of the random variable at time i

S_i^* = Adjusted partial sum of the random variable at time i

S_n = Partial sum of the random variable at time n

X = Random variable in the Pearson-Type-III

U_1 = Uniform random variable

U_2 = Uniform random variable

y = Random variable in the Pearson probability density function

ρ_1 = Population first order serial correlation coefficient

ρ_2 = Population second order serial correlation coefficient

ϵ_i = Independent standard normal variable with mean zero and variance unity

σ = Standard deviation of any random variable

μ'_i = The i^{th} moment about the origin

μ_i = The i^{th} central moment

β_1 = Skewness coefficient on square

β_2 = Kurtosis coefficient

γ = Shape parameter in the Pearson-Type-III probability density function.

Bibliography

(1) ANIS, A.A. and LLOYD, E. H. (1953) : "On the Range of Partial Sums of a Finite Number of Independent Normal Variates." Biometrika, Vol. 40, pp. 35-42.

(2) BOX, G.E.P. and MULLER, M.E. (1958) : "A Note on the Generation of Normal Deviates." Annual Mathematics, Statistics, Vol. 28, pp. 610-611.

(3) FELLER, W. (1951) : "The Asymptotic Distributions of the Range of Sums of Independent Random Variables." Annual Mathematics, Statistics, Vol. 22, pp. 427-432.

(4) HURST, H. E. (1951) : "Long-term Storage Capacity of Reservoirs." Transactions of the American Society of Civil Engineers, Vol. 116, pp. 770-808.

(5) PEARSON, K. (1965): "Table of Incomplete Gamma Function." Cambridge University Press, Cambridge.

(6) RIPPL, W. (1883) : "The Capacity of Storage Reservoir for Water Supply." Institution of Civil Engineers, Processes, Vol. 71, pp. 270-278.

(7) SALAS-LA CRUZ, J.D. (1972): "Range Analysis for Storage Problems of Periodic-Stochastic Processes." Ph.D. Dissertation, Colorado State University, Fort Collins, Colorado.

(8) SUTABUTR, P. (1967) : "Reservoir Storage Capacity Required when Water Inflow has a Periodic and a Stochastic Component." Ph.D. Dissertation, Fort Collins, Colorado, Colorado State University.

(9) YEVJEVICH, V. (1965) : "The Application of Surplus, Deficit and Range in Hydrology." Hydrology Paper No. 10, Fort Collins, Colorado, Colorado State University.

(10) YEVJEVICH, V. (1967) : "Mean Range of Linearly Dependent Normal Variables with Application to Storage Problems." Water Resources Research, Vol. 3, pp. 663-671.

A Method for Computing Storage Capacity of a Reservoir Serving Irrigation, Considering the Demand as a Probability Process

L. KOTOV
Doctor of Technical Sciences
Professor of Hydraulic Engineering, University of Civil Engineering
Sofia, Bulgaria.

G. KRAFTI
Associate Professor of Hydraulic Engineering
Academy of Agricultural Sciences
Sofia, Bulgaria.

A. POPOV
Doctor of Technical Sciences
Asstt. Professor of Hydraulic Engineering, University of Civil Engineering, Sofia, Bulgaria.

Regarding runoff event as a simple Markovian process requires to take into account the auto-correlation, i.e., the correlation between the runoffs of two consecutive years. There is a wealth of literature on streamflow regulation that takes into consideration this relation, typical of the random processes, treating, however, mostly the case of a constant reservoir release, or a release pattern that depends on the initial reservoir storage.

Unquestionably, a decisive step forward must be done in reservoir planning studies for the purposes of irrigation too. Moreover, it is to be noted that the problems which must be solved in runoff regulation analyses for the case considered are much more difficult in our opinion, and that not from the standpoint of the decision itself, but because of the difficulties involved in studying the specific nature of the processes. The complication is due to the fact that in runoff regulation analyses for irrigation we come across to the manifestation of two random events which are more or less pronounced. These are the runoff, which is a subject of constantly increasing consideration on the part of the investigators, and the irrigation demand. The formation of both the events is a result of some causes which are of the same character, though not always occurring in the same conditions. Because of the fact, as it can be expected, that there exists an internal relation in the course of runoff event or rather in the course of its formation, it can be assumed that there exists such a relation also in the course of the event "water requirements of crops". In the same time it must be considered the functional relation between the two events, which can be revealed in the course of their simultaneous occurrence; it is possible also that this relation should have some historical roots.

In the analyses made herein (in conformity with the recent investigation for the case of a constant reservoir release) it is assumed that the character of these relations is known and that it is possible to determine the transition functions (functions governing the process).

Subject of research is the case where there exists a relation between runoff and demand during a given period of time and in the same time, both the processes considered jointly as an united process depend on the recent history of the joint process, i.e., on the behaviour of the process during the preceding time period.

Presented herein are the possible solutions of the problem considered with full understanding that extensive studies in this direction are still to be undertaken by a large number of researchers.

1. Distribution of Irrigation Water Demands in case of Correlation between Rainfall and Consumptive use

Two major time periods are essential for the variation in the consumptive use. The one embraces the months of the growing season and the other—the winter months, when consumptive use consists only of water evaporating from soil surface (Figure 1).

The change in soil moisture content during one of these periods can be described by the water balance equation :

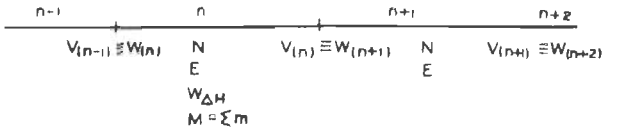

FIGURE 1.

$$V = W+N-E+W_{\triangle H}+M \qquad \ldots(1)$$

where,

W = soil water storage at the beginning of the time period considered;

V = soil water storage at the end of the same time period;

N = inflow due to precipitation;

E = total consumptive use for the time period considered;

$W_{\triangle H}$ = change in soil water storage resulting from the increasing depth of root zone;

M = depth of water to be applied, such that the storage should be $V_{min}^{(1)} < V \leqslant V_{max}^{(0)}$.

The existence of correlation between rainfall and consumptive use within a given time period permits to establish the distribution of their joint occurrence, using their unconditional and conditional distributions, i.e., the occurrence of N_E for an occurred event E, corresponding to a coefficient of correlation $\tau_{N_E} \neq 0$.

To find the distribution of their joint occurrence it is necessary to determine the distribution of the series

$$D = N_E-E+W_{\triangle H}.$$

Let $\bar{F}(D/E)$ denote the conditional occurrence probability of the deficit D for an occurred consumptive use E. Then the unconditional probability of the event D is :

$$F(D) = \int_E F(D/E)\, dP(E) \qquad \ldots(2)$$

The conditional probability of the event $\bar{F}(D/E)$ is identical with the occurrence probability of the event $N_E \geqslant D+E-W_{\triangle H}$. Hence,

$$F(D) = \int_E \bar{F}(D/E)\, dP(E) = \int_E F(N_E \geqslant D+E-W_{\triangle H})\, dP(E) \qquad \ldots(3)$$

As a result of this analysis, the distribution $F(D)$ of the deficits $D = N_E-E+W_{\triangle H}$ can be established. Thus, the water balance Equation (1), if $M = 0$, i.e., no irrigation has been applied, reduces to :

$$V = W \qquad \ldots(4)$$

If $\bar{\phi}(V/W)$ denotes the conditional occurrence probability of the water storage at the end of the time period for an occurred content W at the beginning of the same period, then using the relationship of the total probability we have :

$$\phi(V) = \int_W \bar{\phi}(V/W)\, d\phi(W) \qquad \ldots(5)$$

where, $\bar{\phi}(V/W)$ is the conditional probability of the event for the occurred event W. It is equal to the occurrence probability of the event $D \geqslant V-W$.

Thus, Equation (5) can be written as :

$$\phi(V) = \int_W \phi(D \geqslant V-W)\, d\phi(W) \qquad \ldots(6)$$

Equations (3) & (6) can be solved by numeral integration of the integral, or by its finite difference approximation :

$$\phi(V) = \sum_W \bar{\phi}(V/W) \cdot \triangle\phi(W) = \sum_W \phi(D \geqslant V-W) \cdot \triangle\phi(W) \qquad \ldots(7)$$

To find the steady state distribution of the soil water storage, Equation (7) is to be solved for each one of the consecutive periods, starting from a randomly selected initial state.

The solution of the problem, using Equation (7) can be found according to the following procedure :

The first step is to discretize the series of soil water storages V at the end of the time period considered, which is still unknown. For this purpose, taking into account $V_{max}^{(0)}$ and $V_{min}^{(1)}$, the basic intervals (Figure 2) can be established by the following recurrence relationship :

$$V_{min}^{(j)} = V_{max}^{0} - j\left(V_{max}^{0} - V_{min}^{(1)}\right) = V_{max}-jm \qquad \ldots(8)$$

where, $j = 0\,;\,1\,;\,2\,;\,3\ldots$

Then the basic intervals are to be divided into sub-intervals with a step of $\triangle m = \dfrac{V_{max}^{(0)} - V_{min}^{(1)}}{R}$ (R is an arbitrary whole number) according to the following recurrence relationship :

$$V_i^{(j)} = V_{min}^{(j)} - i\triangle m \qquad \ldots(9)$$

where, $i = 0\,;\,1\,;\,2\,;\,3\ldots k$

For all values of $V_i^{(j)}$ obtained in this way, represen-

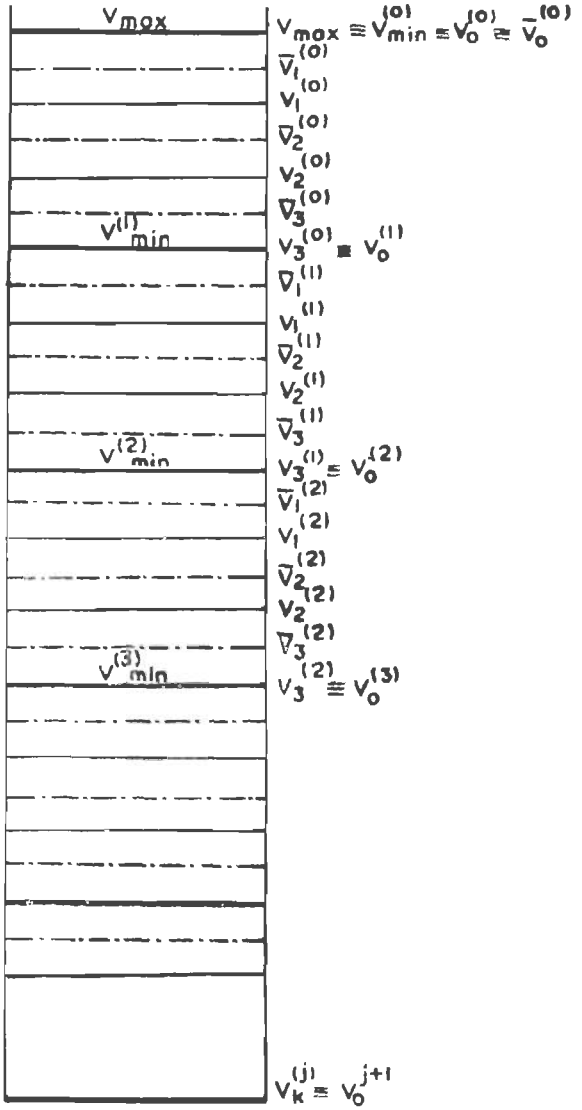

FIGURE 2.

ting soil water storages at the end of the time period considered using Equation (7) makes it possible to determine their probability of occurrence $\phi\left(V_i^{(j)}\right)$.

Considering that soil water content can be kept within the range $V_{min}^{(1)} < V \leqslant V_{max}^{(0)}$ by the application depths m, it follows that the occurrence probabilities of water storages $\bar{V}_i^{(0)}$ can be obtained by the following recurrence relationship :

$$\text{for } i = 0\ \bar{\phi}\left(\bar{V}_o^{(0)}\right) = \phi\left(V_o^{(0)}\right) = \phi\left(V_{min}^{(0)}\right) = \phi\left(V_{max}^{0}\right) \text{ where, } \bar{V}_o^{(0)} = V_{max}$$

$$\text{for } i = 1\ ;\ 2 \ldots . k\ \bar{\phi}\left(\bar{V}_i^{(0)}\right) = \sum_{0}^{j}\left[\phi\left(V_i^{(j)}\right) - \phi\left(V_{i-1}^{(j)}\right)\right] \quad \ldots 10)$$

where, $\bar{V}_i^{(0)}$ is the average value of the water storage, computed from $V_i^{(0)}$ and $V_{i-1}^{(0)}$, i.e.,

$$\bar{V}_i^{(0)} = \frac{V_{i-1}^{(0)} - V_i^{(0)}}{2}$$

Using the values of the water storages determined in this way and their probabilities of occurrence at the end of the period, Equation (7) can be solved in the next interval until the steady state is reached.

On the basis of the steady state, the application depths and their probabilities of occurrence for the time period considered can be obtained (Figure 3) using the following recurrence relationships :

$$M_j = j\left(V_{max} - V_{min}^{(1)}\right) = jm \quad \ldots(11)$$

$$\text{for } j = 0\ \bar{\phi}(M_j) = \bar{\phi}(M_o) = \phi\left(V_{min}^{j+1}\right) = \phi\left(V_{min}^{(1)}\right)$$

$$\text{for } j \neq 0\ \bar{\phi}(M_j) = \phi\left(V_{min}^{(j+1)}\right) - \phi\left(V_{min}^{(j)}\right)$$

(where, $j = 0; 1; 2; 3 \ldots$

2. Streamflow Regulation in Case of Correlation between Water Supply and Demand and Auto-correlation of the Series "Supply-Demand"

The solution of streamflow regulation problem can

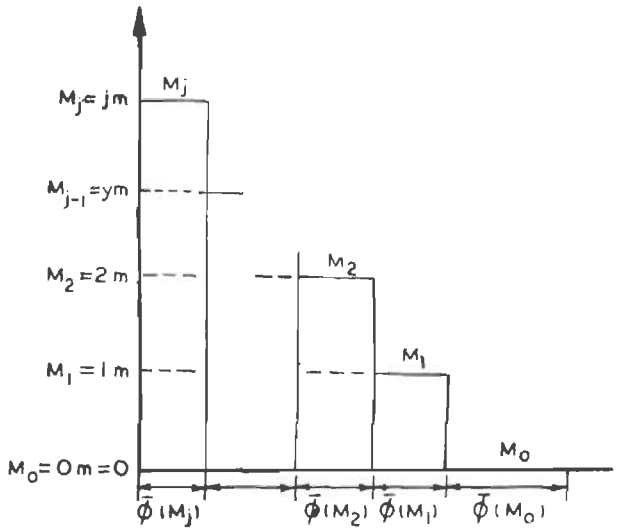

FIGURE 3.

be achieved by means of the reservoir balance equation describing its state during two consecutive years(1)(2)(3).

For the n-th and $(n-1)$th years the balance equation becomes (Figure 4) :

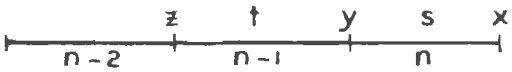

FIGURE 4.

$$x = y+S-\alpha_t$$

$$y = Z+t-\alpha_t \qquad \ldots(12)$$

where, x = reservoir storage at the end of the n-th year;

y = reservoir storage at the beginning of the n-th year, or at the end of the $(n-1)$th year, respectively;

Z = reservoir storage at the end of the $(n-2)$th year, or at the beginning of the $(n-1)$th year, respectively;

S = inflow to the reservoir during the n-th year;

t = the same during the $(n-1)$th year;

α_s = water delivered from the reservoir for irrigation during the n-th year;

F_δ^c = maximum area to be irrigated;

m_s = annual application depth during the n-th year, which determines in fact the random property of the reservoir release. The subscripts s denote the presence of relation between inflow to the reservoir and demand for water or release from the reservoir respectively;

α_t = release from the reservoir during the $(n-1)$th year, which depends also on the annual inflow t.

The presence of dependence connecting water inflow and use within a given year makes it possible to determine the distribution of their joint occurrence by means of their unconditional distributions and the conditional distribution, i.e., the occurrence distribution of α_s, for an occurred s [event α_s/s—$P(\alpha_s/s)$].

The distribution of their joint occurrence can be determined by means of Equations (3) & (7).

Because the series α_s is limited ($\alpha_{max} = F_\delta^c\, m_{max}$) it is more convenient to use another form of representation.

For the case considered Equation (3) can be written as :

$$\overline{F}(D) = \int_s F\left(\frac{D}{\alpha_s}\right) dP(\alpha_s) = \int_s F(S \geqslant D+\alpha_s)\, dP(\alpha_s) \qquad \ldots(13)$$

where, the conditional probability $F(S)$ is the probability of the inflow S (S must be equal or greater than $D+\alpha_s$), determined from the conditional distribution of S/α_s.

On the basis of this analysis the distribution $\overline{F}(D)$ of the deficits $D = S-\alpha_s$ can be found.

Thus, the balance Equation (12) can be rewritten as:

$$x = y+D_n\,; \qquad y = Z+D_{n-1} \qquad \ldots(14)$$

The joint solution of these equations yields :

$$x = Z+D_{n-1}+D_n \qquad \ldots(15)$$

Equation (15) shows that reservoir storage x at the end of the n-th year depends on the storage Z at the end of the $(n-2)$th year and on the deficits D during the n-th and $(n-1)$th years, which have the same unconditional distribution $\overline{F}(D)$, but according to the statement of the problem they have an auto-correlation and hence, D_n depends on the values that D_{n-1} had occupied.

If we denote by $\phi(x/Z)$ the conditional occurrence probability of the storage x for an occurred storage Z [during the $(n-2)$th year] then using the formula of the total probability (2) we have :

$$\phi(x) = \int_Z \phi\left(\frac{x}{Z}\right) d\,\phi(Z) \qquad \ldots(16)$$

Besides,

$$\phi\left(\frac{x}{Z}\right) = \int \phi\left(\frac{x}{Z},\, D_{n-1}\right) d\,\overline{F}(D_{n-1})$$

and the conditional probability $\phi\left(\frac{x}{Z}, D_{n-1}\right)$ of the event x for the occurred events Z and D_{n-1} equals the occurrence probability of the event

$$D_n \geqslant x-Z-D_{n-1}, \text{ i.e., } \overline{F}\left(D_n \geqslant x-Z-\frac{D_{n-1}}{D_{n-1}}\right)$$

Therefore, Equation (7) can be rewritten as follows :

$$\phi(x) = \int_Z \int_{D_{n-1}} \overline{F}\left(\frac{D_n}{D_{n-1}}\right) d\,\overline{F}(D_{n-1})\, d\phi(Z) \qquad \ldots(17)$$

Reaching the steady state (after N-transitions, where, N is a sufficiently great number) the two distributions $\phi(x)$ and $\phi(Z)$ coincide (in fact these are the same series) and Equation (8) can be written as follows :

$$\phi(x) = \int_x \int_D \overline{F}\left(\frac{D_n}{D_{n-1}}\right) d\,\overline{F}(D_{n-1})\, d\,\phi(x) \qquad \ldots(18)$$

In a finite difference form Equation (18) becomes :

$$\phi(x) = \sum_{y} \triangle\phi(y) \sum_{D} \overline{F}\left(\frac{D_n}{D_{n-1}}\right) \triangle \overline{F}(D_{n-1}) \qquad \ldots(19)$$

or

$$M_j = \sum_{j} M_{\triangle}^{i} \sum_{D_{n-1}} \overline{F}\left(\frac{D_n}{D_{n-1}}\right) . f_D \qquad \ldots(20)$$

where, M_j is the occurrence probability of the storage x_j that determines the unconditional distribution of the reservoir storages. The use of the new symbol means that it is considered not the theoretical distribution $\phi(x)$, but the distribution obtained by numeral calculations.

$M_{\triangle}^{i}$ represents the probability of the initial storages y_i determined according to the discretized series M_j. That is,

$$M_{\triangle}^{i=j} = M_{j-1} - M_j$$

where, f_D is the occurrence probability of the event D_{n-1} $(D = D_{n-1})$.

The solution of the problem by means of Equation (20) can be obtained according to the following procedure :

The series of the reservoir storages x_j, which is still unknown is discretized using the basic quantities $x_0 = 0$ and $x_\beta = \beta$ (β = storage capacity of the reservoir) as well as n_x values of x (in the interval 0.0– β).

It is convenient to divide the interval 0—β into $n_x - 1$ equal increments. The more the sturdied values of x the greater the accuracy, but longer the solution of the problem.

The discretized values of the water storages, denoted by y_j are determined as a mean value of x_j between two adjacent values of x, that is

$$y_{i=j} = \frac{x_{j-1} + x_j}{2}$$

The probabilities $M_{\triangle}^{i}$ which are in the sum represent the differences between the values of M_j that are to be determined :

$M_{\triangle}^{i=j} = M_{j-1} - M_j$. For $y_0 = 0$, $M_{\triangle}^{0} = 100 - M_0$;

for $y_{n_x+2} = \beta$ $M_{\triangle}^{\beta} = M_\beta$.

The unconditional distribution of the deficits D is

TABLE 1

Annual Runoff (W), Application Depth (M), Rainfall (N) and Consumptive use (E) for the period 1936-1971.

1936	441.0	120	230	397	1954	305.6	318	183	524
1937	554.4	38	358	360	1955	463.0	136	303	397
1938	453.6	242	193	508	1956	485.1	217	347	441
1939	296.1	177	242	451	1957	415.8	165	384	402
1940	516.6	63	434	322	1958	412.8	370	154	604
1941	500.8	112	372	342	1959	296.1	129	305	367
1942	425.2	203	228	448	1960	459.9	133	268	415
1943	333.9	184	263	442	1961	293.0	192	222	442
1944	752.8	115	250	417	1962	368.6	344	123	535
1945	378.0	345	128	654	1963	557.6	149	237	465
1946	346.5	320	135	663	1964	277.2	181	266	381
1947	302.4	166	322	470	1965	400.0	257	174	462
1948	633.2	186	222	477	1966	337.0	139	259	369
1949	201.6	151	272	461	1967	419.0	88	288	322
1950	293.0	442	84	650	1968	211.0	226	305	459
1951	396.9	126	242	434	1969	378.0	159	332	422
1952	201.6	354	130	599	1970	381.2	143	304	375
1953	419.0	274	176	469	1971	327.6	155	296	413

NOTE—The runoff is calculated for the hydrological year and the other values—for the maize growing season (May to August).

discretized and as a result of this the occurrence probabilities of a given discretized value of D is obtained.

It is assumed that x takes consequently the adopted values of x_j.

One equation of the type (20) corresponds to any particular value of x. For any particular value x_j the sum $\sum_{D_{n-1}}$ is evaluated. For a given value of (for an adopted already value of j) and for any discretized value of $D = D_{n-1}$ (computed from the unconditional distribution of D) the value of $D_n = x_j - y_i - D_{n-1}$ is determined. For this value, using the conditional distribution of D_n/D_{n-1}, $\bar{F}\ (D_n/D_{n-1})$, the conditional probability $\overline{F}_{dij} = \overline{F}(D \geqslant x_j - y_i - D_{n-1}/D_{n-1})$ can be obtained. The same procedure is to be repeated for all the combinations between y_i and D_{n-1}. The solution of this first part of the problem in matrix form, after determining the matrix of the transitions is :

$$[A_{0j},\ A_{1j},\ A_{2j} \ldots A_{n+2,j}] = [f_1 f_2 \ldots f_n] \parallel \bar{F}_{dij} \parallel \qquad \ldots(21)$$

where, $j = \text{const.}$

For the other values of x_j the new matrix of the transitions $\parallel A_{ij} \parallel$ is computed in a similar manner.

The second part of the solution is to work out a system of equations, through which the values of M_j can be determined. To obtain these equations the following recurrence relationship is used :

$$M_j\,(1 + A_{jj} - A_{j+1,\,j}) = 100\,A_{0j} + \sum_{i=0}^{n_{x+1}} (A_{i+1,\,j} - A_{ij})\,M_i \qquad \ldots(22)$$

(for $i = j$).

The solution of the system obtained gives the probabilities M_j of x_j as well as the unconditional distribution of the reservoir storages.

On the basis of the foregoing analyses, some relations between the runoff and demand for irrigation water have been developed for the natural conditions in Bulgaria. As an example, the annual runoffs of Iskar River, immediately upstream from Iskar Dam, and the average annual water application for the crops grown in Sifia Irrigation Project are listed in Table 1. Iskar Dam is the main supply source for this irrigation project.

It was found that the relation between the runoff and the demand for irrigation can be characterized by a coefficient of correlation $r = -0.389$. It was found also that a very poor auto-correlation ($r = -0.187$) exists between the annual demands but there is not any auto-correlation either between the application depths of the different years ($r = -0.078$) or between the differences "$W - M$" during the same years ($r = -0.098$).

A very good coefficient of correlation is obtained for the relation between rainfall and consumptive use during the growing season ($r = 0.80$).

It can be expected that for the other regions in Bulgaria the foregoing relations are characterized by similar values of the correlation and auto-correlation coefficients.

References

(1) KARTVELISHVILY, N.A. : "Theory of Probability Processes in Hydrology and Streamflow Regulation." Leningrad, gidrometeorogicheskoe Izd., 1967.

(2) KARTVELISHVILY, N.A. : "Formula for the Total Probability in the Theory of Streamflow Regulation." Problemi gidroenergetiki i vodnogo hosaistva, Alma-Ata, 1966, 4.

(3) KIKTENKO, V.A. et al : "Streamflow Regulation, Considering the Auto-correlation of Runoffs in the Consecutive Years." Problemi gidroenergetiki i vodnogo hosaistva, Alma-Ata, 1968, 6.

(4) POTAPOV, M.V. : "Streamflow Regulation." Selected Works, Volume 3, Moscow, Selhozgis, 1951.

The Rapid Emptying of Water Reservoir Systems

D. L. VISCHER
Professor of Civil Engineering

M. SPREAFICO
Civil Engineer

Laboratory of Hydraulics, Hydrology and Glaciology annexed to the Federal Institute of Technology Zurich, Zurich, Switzerland.

SYNOPSIS

In Switzerland there are principally three schemes for the protection of the areas lying below reservoirs in flood catastrophes caused by the failure of the dams. On the one hand, there are specifications laid down for the proper dimensioning of the dam to be carried out by experts and on the other hand, by constant supervision of the dam the danger of a possible failure of the dam is greatly reduced. The third scheme is concerned with the measures to be taken in an emergency. Included in these emergency measures is the lowering of the water in the reservoir. Of the many different questions which are of practical relevance with regard to the emptying of a system of reservoirs this paper concerns itself with two, namely, the minimum time span "beginning of water lowering" to "end of water lowering" of a reservoir system, and with the question of the least sum of lowering times for all the reservoirs. Here it is assumed that all the reservoirs are in equal danger, i.e., no one reservoir has priority with regard to emptying. Using a simple model the optimum emptying programme is determined within the given constraints, first for a single reservoir and then for various reservoir systems.

Introduction

Switzerland has about 50 reservoirs at its disposal for hydro-electric power production containing from 10 to 400 million m^3 of water. This means that in Switzerland having a surface area of only about 40,000 km^2, there is more than one reservoir to every 1,000 km^2. In the mountainous regions which are more suitable for the construction of reservoirs the relationship becomes as much as 2 or 3 reservoirs every 1,000 km^2.

It is, therefore, understandable that Switzerland, which is proportionately densely populated, pays great attention to the safety of its reservoirs and to the dams associated with them. In connection with this it is valid to consider various hazards which may arise, which can only be briefly outlined here :

(*a*) Failure under normal conditions

(*b*) Failure resulting from unforeseen earthquake effects

(*c*) Destruction by sabotage or in war.

In all 3 cases it is not only the dam itself which is affected but also, when the reservoir is completely or partly full, a low lying area which is usually extensive. For with a large breach in the dam the mass of water which is released rushes down the valley as a flood wave bringing devastation with it. The results are similar to those of a sudden flood catastrophe with the additional tragic element, that this catastrophe cannot simply be regarded as an 'act of God' over which we have no control, but can be traced back to a construction failure occurring under natural conditions or caused by human interference.

Three methods are employed to ensure the avoidance of such a catastrophe, which can be described under the following headings :

(1) Expert dimensioning of the dam.

(2) Constant supervision of the dam.

(3) Emergency measures for the dam and in the low lying areas.

Owing to lack of space the first two methods are only to be gone into here in as far as they influence the third, for it is the third method which we particularly wish to deal with.

The third preventive method, that is, measures to be taken in an emergency will be brought into action as soon as a failure of the dam, or its destruction, is to be feared. At the same time related information can be obtained from the constant supervision of the dam and from the intelligence service over possible sabotage or war designs. Depending on whether or not the danger is imminent two different plans may be followed, either the setting off of a water alarm together with the evacuation of the threatened area, or the rapid lowering of water in the reservoir.

1. Water Alarm and Evacuation

The so-called water alarm is set off when in a full or partly filled reservoir, a dam suddenly breaks or threatens to break. This is done by civil or military bodies which essentially have at their disposal the following means of action :

With the aid of a local alarm system, an alarm is sounded in the areas, which will be reached by the flood wave within a period of less than two hours. The alarm is given by deep toned sirens, which are set up in the areas and which can be set off by means of a very reliable transmission system. Figure 1 gives an idea of this scheme(1).

After the alarm has been sounded the population of the area concerned must take action itself in carrying out the evacuation of the zones mapped out before hand. This demands, of course, that the population has previously been made well aware of the possible scale of the flood wave and of the escape routes.

For this purpose leaflets are especially useful which give details of :

—the scale of flooding

—the means of giving the alarm

—purposeful behavior in the emergency.

Figure 2 shows a section from such a leaflet exemplifying this(2). It deals with information concerning the city of Zurich if the dammed upstream water mass of the Sihlsee (total water volume 96 million m^3) is suddenly set free. As calculations have shown(3) this water would reach the city of Zurich in $1\frac{1}{2}$ hours and certain quarters there would be flooded by up to 8 m of water. The area which is reached by the flood wave after 2 hours at the earliest will be informed by the so-called long distance alarm. This is broadcast primarily by radio and results in an evacuation organized by the specially trained civil service.

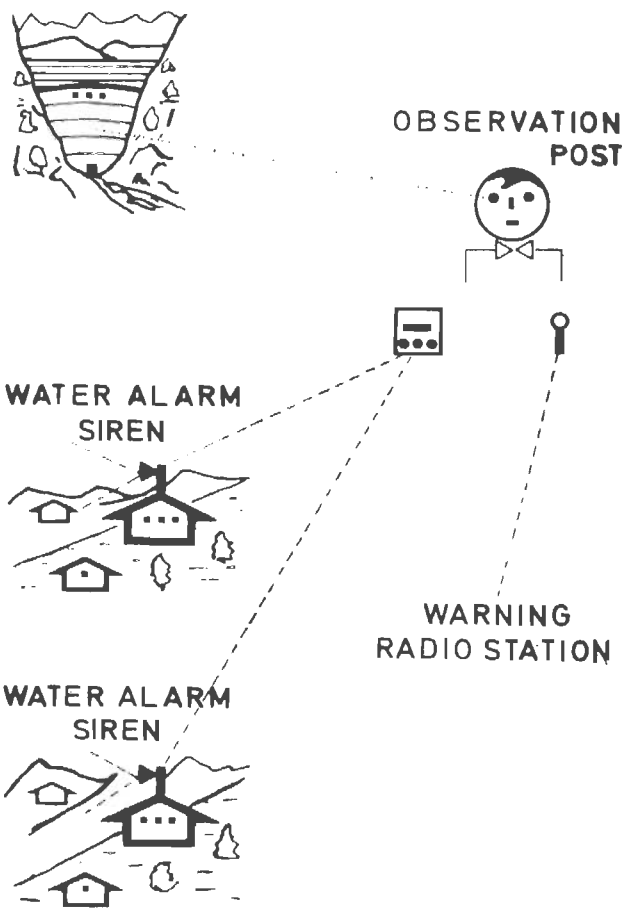

FIGURE 1 : Structure of a water alarm system.

2. The Rapid Emptying of Reservoirs

Prevention is, of course, to be preferred to a warning system.

A reservoir can be lowered if there is sufficient time between the awareness of the danger threatening and its actual occurrence. The method consists in a complete or partial emptying of the reservoir through outlets in the base (bottom outlets), and if possible by turbines. By this means attempts are made on the one hand to empty the reservoir as quickly as possible to a safe level, while on the other hand ensuring that the water which is released causes no damage further downstream.

For such a case the bottom outlets should be properly dimensioned. In addition the responsible organizations should be well trained. No difficulty arises when small or middle sized streams flow into the reservoir, but the case is different with large inflows. For it is not usually possible to conduct a lot of stored water away in addition to the big inflows without danger to the low lying regions. Fortunately, however, in the Swiss reservoirs—which act as seasonal reservoirs to store the surplus water from the summer for the winter—

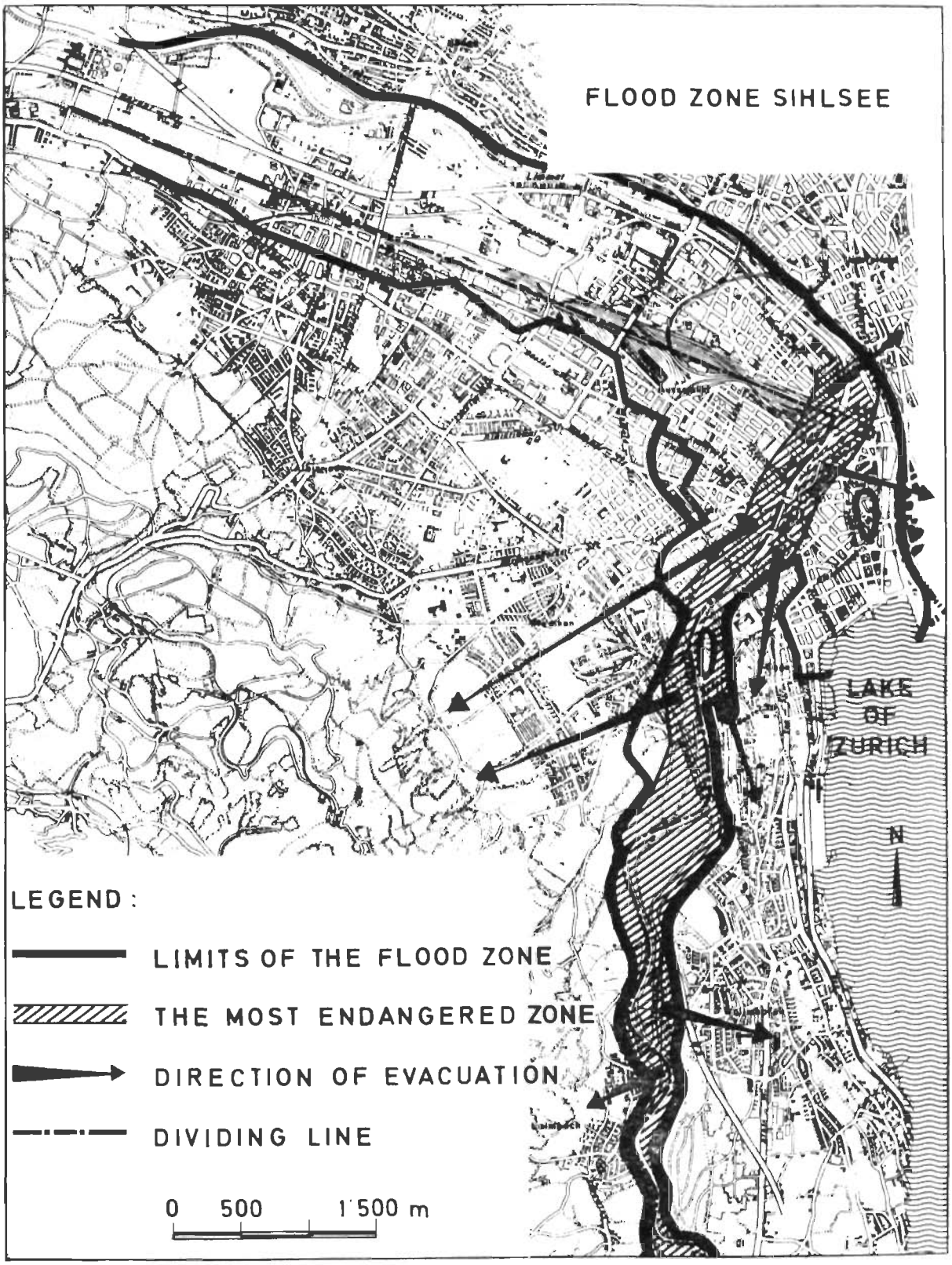

FIGURE 2 : Memorandum for the evacuation of the city of Zurich in the case of a flood alarm after ([2]).

it is seldom that large inflows and a full reservoir occur at the same time.

2.1 *Lowering the Water in a Single Reservoir*

The emptying of a single reservoir is an operation which can be easily summarized. The bottom outlets which are present as a means of discharging water, and the outlets for normal working must be opened as wide as possible if the reservoir is to be lowered in the shortest possible time to a safe reservoir level.

This means of draining away the water is limited on the one hand by the capacity of the bottom outlets and on the other hand by the ability of the downstream channels to discharge more water.

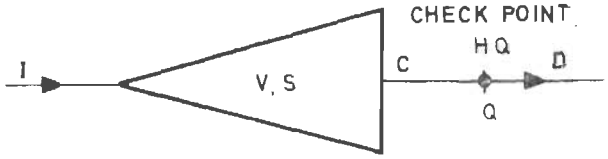

FIGURE 3 : Diagram of a single reservoir.

Using the symbols of Figure 3, namely

S = Volume of water to be emptied

V = Volume of water in reservoir

I = Reservoir inflow

D = Discharge from reservoir through bottom outlets

C = Capacity of bottom outlets

Q = 'Natural' flow at a check-point in the river course

HQ = Maximum possible flow at the check-point

t = Time

the hydraulic relationship can be simply formulated by means of the continuity equation,

$$I-D = \frac{dV}{dt}$$

whereby,

$$D \leqslant C$$

$$D \leqslant HQ-Q$$

$$C = C(V)$$

Of course, a lowering is only possible if the flow into the reservoir does not exceed its discharge capacity, i.e., if

$$I < C$$

or $$I < HQ-Q$$

The larger the difference

$$D-I$$

the quicker the lowering of the reservoir.

If one supposes that the inflow I and the 'natural' flow Q do not vary with time during the lowering period and that the outflow capacity is limited not by C but by HQ, the shortest lowering time results from

$$I-(HQ-Q) = \frac{dV}{dt}$$

or $$[I-(HQ-Q)] \int_T dt = \int_S dV$$

$$T = \frac{S}{HQ-Q-I}$$

If the outflow capacity is limited by C and not by HQ then the continuity equation cannot be solved so easily. For the capacity of the bottom outlets is dependent on the reservoir level and therefore, on the water content of the reservoir.

If this capacity depends only on the size of the bottom outlets—in an emergency the turbines are not used if possible—the relationship is mostly of this kind :

$$C \sim \sqrt[3]{V}$$

and so in the upper two-thirds of the reservoir it does not play an important part. As long as the reservoir does not have to be emptied of more than about these two-thirds, the approximate capacity of the bottom outlets can be taken to be an invariable.

Under these conditions the shortest lowering time becomes :

$$T = \frac{S}{C-I}$$

Of course, it would not be difficult to introduce the relationship $C = C(h)$ exactly into the continuity equation and to solve this numerically, to ascertain the shortest lowering time. The simplifications introduced here, however, are made in connection with the next section.

2.2 *The Lowering of a System of Reservoirs*

The lowering of several reservoirs within the same catchment area, i.e., of a system of reservoirs, is a complex operation because the outflows from the various reservoirs are superimposed at the check-points. In addition to this the outflows from higher-lying reservoirs add to the inflows into the low lying reservoirs. Because of this the lowering programme is all the more complicated; the optimum lowering programme—i.e., that which leads to the shortest lowering time for the whole reservoir system—cannot, therefore, be given directly. It must be ascertained much more on the basis of an optimum calculation, which is the usual procedure in Operations Research.

If one accepts the conditions introduced in the previous section :

(1) The inflows I are independent of time

(2) The capacity of the bottom outlets C is independent of volume

(3) The 'natural' flows Q are independent of time then linear programming is especially suitable for the treatment of the various questions arising.

Several questions and cases can be dealt with, for example :

Question A : which programme of lowering results in the shortest time span between the beginning and ending of water lowering in the reservoir system ?

Question B : which lowering programme results in the smallest total of lowering times of the individual reservoirs ?

Case (*a*) : all the reservoirs are equally in danger, i.e., no single reservoir has priority with respect to lowering of the water

Case (*b*) : the reservoirs are not in equal danger : one or several of them has claim to priority

Question A can be understood as it stands, but question B exhibits a certain heuristical character, and it is especially interesting in connection with case (*b*).

In what follows some relevant solutions will be put forward with regard to questions A and B and case (*a*). Case (*b*) is not treated on account of lack of space.

2.2.1 *Two Parallel Reservoirs*

Assuming case (*a*), where no reservoir has priority the optimum lowering programme for the reservoir system shown in Figure 4 should be sought. The definition of the problem in terms of linear programming runs like this :

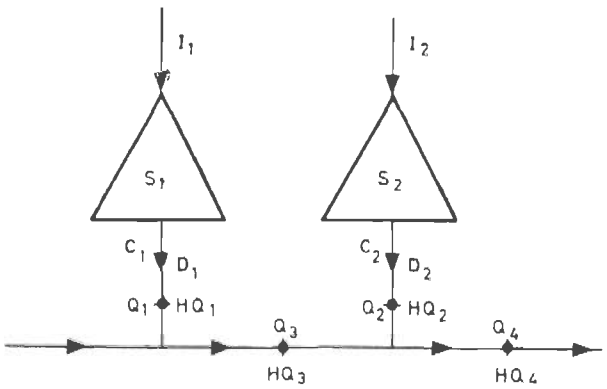

FIGURE 4 : Diagram of two parallel reservoirs.

Parameters of the System

S_1, S_2 = Volume of water to be emptied

I_1, I_2 = Reservoir inflows

C_1, C_2 = Capacity of bottom outlets

Q_1, Q_2, Q_3, Q_4 = 'Natural' flows at the check-points in the river course

HQ_1, HQ_2, HQ_3, HQ_4 = Maximum possible flows at the check-points

Decision Variables

D_1, D_2 = Discharges from the reservoirs

Constraints

$$D_1 \geqslant 0 \qquad D_2 \geqslant 0$$
$$D_1 \geqslant I_1 \qquad D_2 \geqslant I_2$$
$$D_1 \leqslant C_1 \qquad D_2 \leqslant C_2$$
$$D_1 \leqslant HQ_1 - Q_1 \qquad D_2 \leqslant HQ_2 - Q_2$$
$$D_1 \leqslant HQ_3 - Q_3 \qquad D_1 + D_2 \leqslant HQ_4 - Q_4$$

Assumptions

Continuous discharge.

The lowering times T_1 and T_2 of the individual reservoirs are equal (see below).

Objective Function

The discharges from the reservoirs should be maximum, which with respect to question A and case (*a*), means the same as the shortest time of lowering the water.

$$D_1 + D_2 \rightarrow \text{Max.}$$

This objective function leads in many practical cases to a parametric solution, i.e., the objective function coincides with a boundary of the feasible policy space. It can be proved, however, that the time span "beginning of lowering" to "end of lowering" of the whole reservoir system is smallest when the water lowering times T_1 and T_2 of the individual reservoirs are equal to each other. This is independent of whether the lowering of the reservoir is carried out continuously or discontinuously (Figure 5).

With two parallel reservoirs this conclusion leads to

$$T_1 = T_2$$

and

$$\frac{S_1}{D_1 - I_1} = \frac{S_2}{D_2 - I_2}$$

or

$$D_1 - D_2 \cdot \frac{S_1}{S_2} - I_1 + I_2 \cdot \frac{S_1}{S_2} = 0$$

So an additional constraint is obtained, viz., that the optimum solution must lie on the line $T_1 = T_2$. In this way a definite solution is obtained.

Now the objective function is to be maximized while observing the constraints. This can be carried out either analytically with the aid of the Simplex Algorithm, or in the two-dimensional case also graphically.

In Figure 6 the solution of the problem for the following values of the parameters of the system is

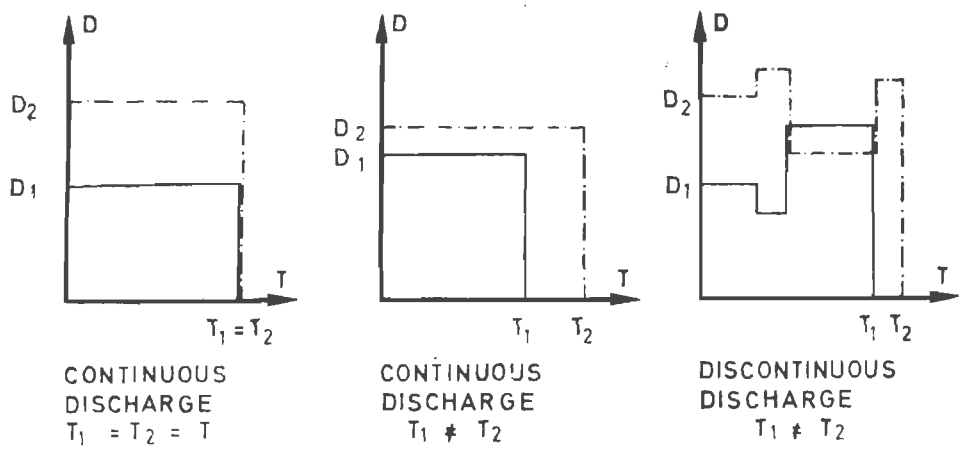

FIGURE 5 : Methods of lowering.

presented in graphical form :

$S_1 = 50 \cdot 10^6$ m³ $\quad S_2 = 40 \cdot 10^6$ m³

$I_1 = 5$ m³/sec $\quad I_2 = 3$ m³/sec

$C_1 = 50$ m³/sec $\quad C_2 = 40$ m³/sec

$Q_1 = 500$ m³/sec $\quad HQ_1 = 570$ m³/sec

$Q_2 = 400$ m³/sec $\quad HQ_2 = 460$ m³/sec

$Q_3 = 600$ m³/sec $\quad HQ_3 = 660$ m³/sec

$Q_4 = 800$ m³/sec $\quad HQ_4 = 880$ m³/sec

The optimum discharges obtained are :

$D_1 = 45$ m³/sec, $\quad D_2 = 35$ m³/sec

This gives a minimal time span from "beginning of lowering" to "end of lowering" for both reservoirs of :

$$T_1 = T_2 = T = 1{:}25 \cdot 10^6 \text{ sec} = 347.2\ h$$

If question *B*, case (*a*) is posed, regarding the optimum emptying programme by which the least sum is arrived at for the lowering times of all the reservoirs, then the answer cannot be found in this way. In this instance the condition $T_1 = T_2$ is no longer valid.

Figure 7 shows several emptying programmes.

Here it is shown that the time span "beginning of water lowering" to "end of water lowering" in the case $T_1 = T_2$ is smaller than or at most equal to the values obtained in the cases $T_1 \neq T_2$. On the other hand the total $T_1 + T_2$ of the times of water lowering in the case $T_1 = T_2$ can be greater than in cases $T_1 \neq T_2$.

If the lowering of water is continuous, the optimum lowering programme is obtained by minimizing the total of the times of water lowering of the individual reservoirs.

$$\frac{S_1}{D_1 - I_1} + \frac{S_2}{D_2 - I_2} \rightarrow \text{Min.}$$

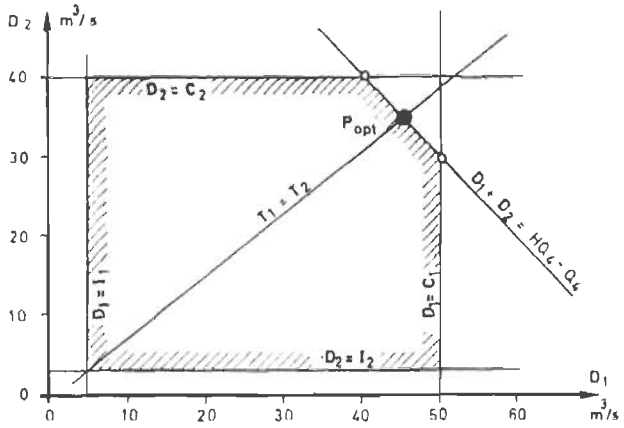

FIGURE 6 : Graphical solution for two parallel reservoirs [Question A, Case (a)].

By introduction of the additional parameters

$$B_1 = \frac{1}{D_1 - I_1} \qquad B_2 = \frac{1}{D_2 - I_2}$$

the objective function takes the form

$$B_1 S_1 + B_2 S_2 \rightarrow \text{Min.}$$

The constraints (with the same input values as before) are then formulated as follows :

$$B_1 \geqslant \frac{1}{45} = 0.022 \qquad B_2 \geqslant \frac{1}{37} = 0.027$$

$$B_1 \geqslant \frac{1}{65} = 0.015 \qquad B_2 \geqslant \frac{1}{57} = 0.017$$

$$B_1 \geqslant \frac{1}{55} = 0.018$$

and

$$\frac{1}{B_1} + \frac{1}{B_2} \leqslant 72$$

The objective function and all constraints are linear up to the last which is not linear, so that the problem

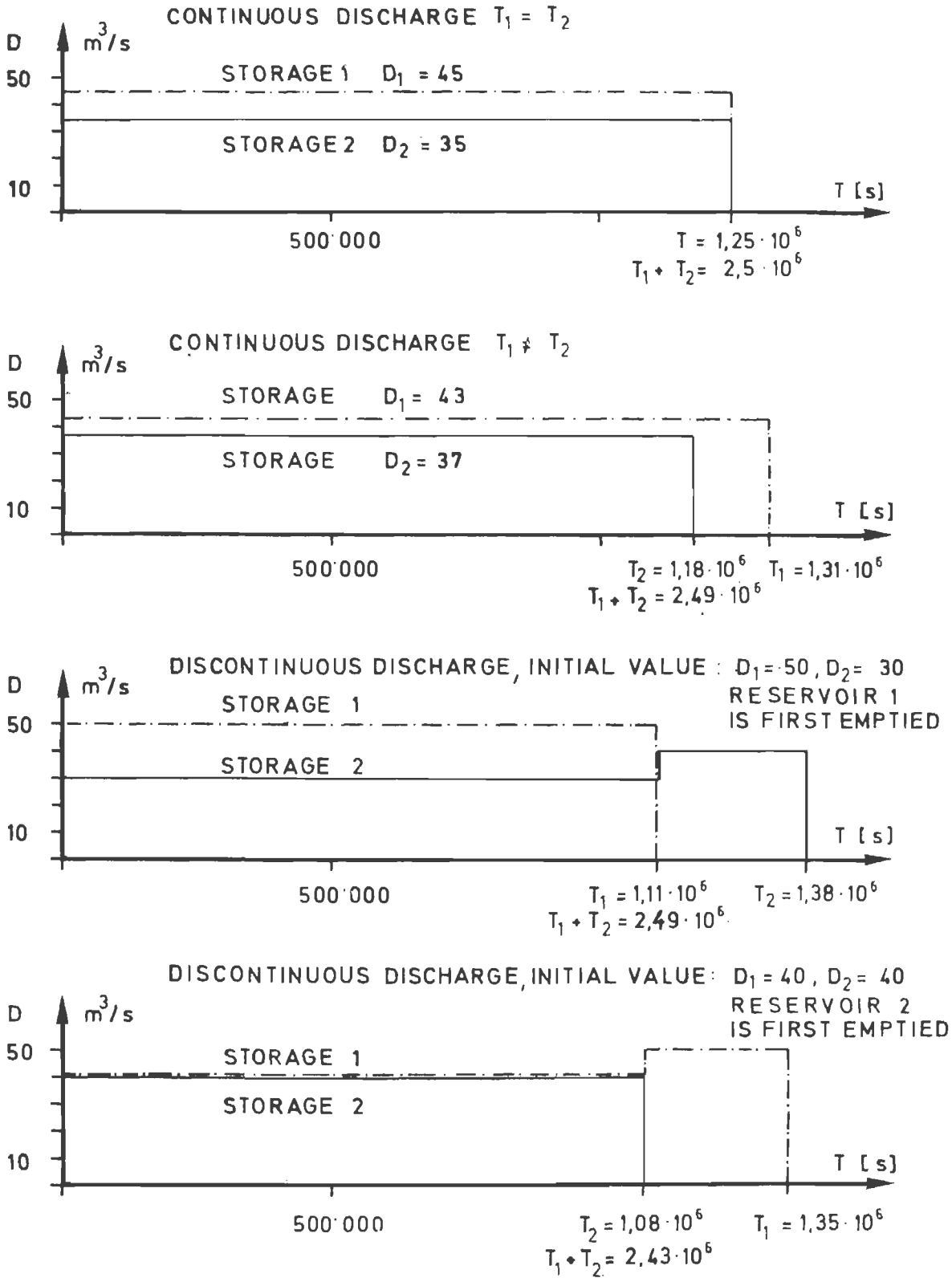

FIGURE 7 : Programmes of lowering for two parallel reservoirs.

can be solved in spite of this with linear programming. For the numerical solution the last condition has to be linearized. The problem is graphically portrayed in Figure 8.

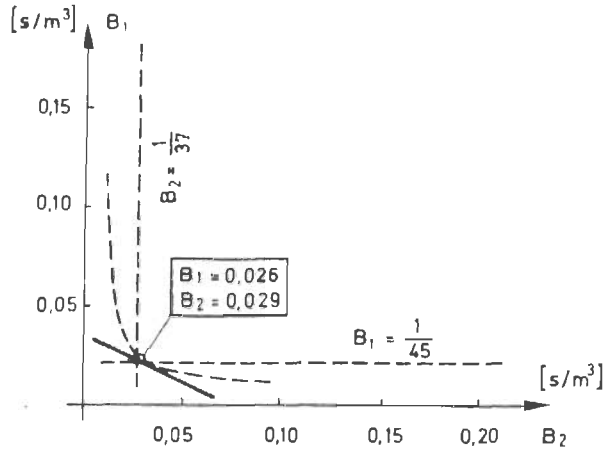

FIGURE 8 : Graphical solution for two parallel reservoirs [Question B, Case (a)].

The optimum rates of discharge resulting are

$$D_1 = 43 \text{ m}^3/\text{sec}, \qquad D_2 = 37 \text{ m}^3/\text{sec}$$

And the total of the water lowering times is

$$T_1 + T_2 = 1.31 \cdot 10^6 + 1.18 \cdot 10^6 = 2.49 \cdot 10^6 \text{ sec}$$

So this total is smaller than in the case $T_1 = T_2$ ($2.5 \cdot 10^6$ sec). On the other hand the time span "beginning of water lowering" to "end of water lowering" of both reservoirs togcther is greater ($1.31 \cdot 10^6$ compared to $1.25 \cdot 10^6$, see Figure 7).

If the lowering of water is discontinuous, taking the initial values as $D_1 = 40$ m³/sec, $D_2 = 40$ m³/sec, the smallest total of the lowering times obtained is

$$T_1 + T_2 = 1.08 \cdot 10^6 + 1.35 \cdot 10^6 = 2.43 \cdot 10^6 \text{ sec}$$

The shortest time span, from "beginning of water lowering" to "end of water lowering" of both reservoirs is greater too ($1.35 \cdot 10^6$ compared with $1.25 \cdot 10^6$ sec, see Figure 7 and Table I).

TABLE I

Summary of results.

Question/case	Lowering time in [10^6·sec]			Total of lowering times 1+2 [10^6·sec]
	Reservoir system	Reservoir 1	Reservoir 2	
A/a	1.25	1.25	1.25	2.50
B/a	1.31	1.31	1.18	2.49

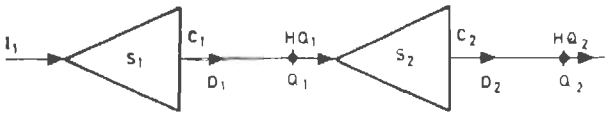

FIGURE 9 : Diagram of two reservoirs in series.

2.2.2 *Two Reservoirs in Series (Figure 9)*

For the same problem question A, case (*a*) as in 2.2.1, the shortest time span from "beginning of water lowering" to "end of water lowering" is determined by maximizing the objective function

$$D_1 + D_2 \rightarrow \text{Max.}$$

while observing the constraints

$$D_1 \geqslant I_1 \qquad D_2 \geqslant D_1 + Q_1$$
$$D_1 \leqslant C_1 \qquad D_2 \leqslant C_2$$
$$D_1 \leqslant HQ_1 - Q_1 \qquad D_2 \leqslant HQ_2 - Q_2$$

and the additional condition

$$T_1 = T_2 = T = \frac{S_1}{D_1 - I_1} = \frac{S_2}{D_2 - D_1 - Q_1}$$

$$D_1 - D_2 \cdot \frac{S_1}{S_1 + S_2} + Q_1 \cdot \frac{S_1}{S_1 + S_2} - I_1 \cdot \frac{S_2}{S_1 + S_2} = 0$$

2.2.3 *General Reservoir System*

According to question A, case (*a*), the smallest time span between "beginning of water lowering" to "end of water lowering" of the system shown in Figure 10 is to be found, when no reserovir has priority.

Parameters of the System

$S_1, S_2 \ldots\ldots S_8$: Volume of water to be emptied

$I_1, I_2, I_3, I_4, I_6, I_7, I_8$: Reservoir inflows

$C_1, C_2 \ldots\ldots C_8$: Capacities of bottom outlets

$Q_1, Q_2 \ldots\ldots Q_{15}$: 'Natural' flows at the check-points in the river course

$HQ_1, HQ_2 \ldots\ldots HQ_{15}$: Maximum possible flows at the check-points

Decision Variables

$D_1, D_2 \ldots\ldots D_8$: Discharges

Constraints

$$D_i \leqslant C_i \qquad i = 1, \ldots\ldots, 8$$
$$D_i \geqslant I_i \qquad i = 1, 2, 3, 4, 6, 7, 8$$
$$D_i \geqslant D_{i-1} + Q_{i-1} \qquad i = 5$$
$$D_i \leqslant HQ_i - Q_i \qquad i = 1, \ldots\ldots, 8$$
$$D_1 \leqslant HQ_{11} - Q_{11}$$
$$\sum_{i=2}^{3} D_i \leqslant HQ_9 - Q_9$$

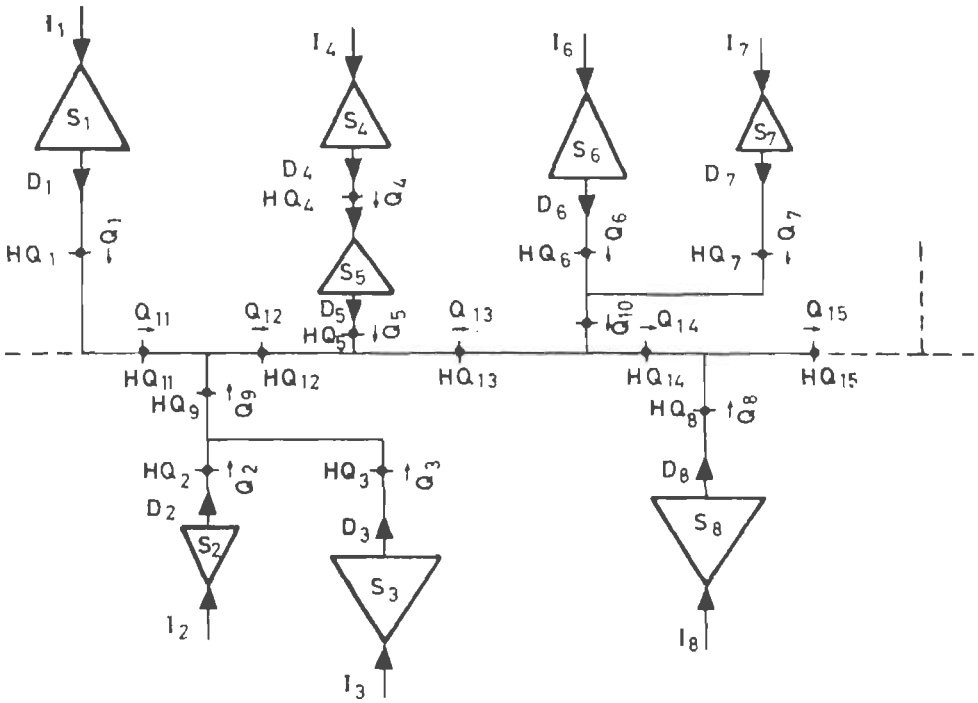

FIGURE 10 : Diagram of a system of 8 reservoirs.

$$\sum_{i=6}^{7} D_i \leqslant HQ_{10} - Q_{10}$$

$$\sum_{i=1}^{3} D_i \leqslant HQ_{12} - Q_{12}$$

$$\sum_{i=1}^{5} D_i \leqslant HQ_{13} - Q_{13}$$

$$\sum_{i=1}^{7} D_i \leqslant HQ_{14} - Q_{14}$$

$$\sum_{i=1}^{8} D_i \leqslant HQ_{15} - Q_{15}$$

Additional conditions for the lowering times :

$$T_1 = T_2 = T_3 = T_4 = T_5 = T_6 = T_7 = T_8 = T$$

Objective Function

$$\sum_{i=1}^{8} D_i \rightarrow \text{Max.}$$

i.e., the problem can be formulated through a system of a linear objective function and linear constraints and as a result it can be solved with the Simplex-Algorithm;

3. Final Remarks

In order to simplify the model it was assumed that the outflow D and the capacity of the bottom outlets C are independent of the volume of water in the reservoir. In reality, however, these are independent. As previously mentioned, for most of our reservoirs it is valid to neglect the changes of outflow for a lowering of the water in the upper half of the reservoir (or of the upper two-thirds of the reservoir storage capacity). If this assumption does not apply to a reservoir system, the reservoirs can be subdivided into sub-reservoirs according to their volumes. Within these sub-reservoirs the outflow D must in addition fulfil the condition

$$D_i \leqslant D_{i\,max}$$

$$D_{i\,max} = \sqrt{\frac{2 \cdot g \cdot h_{i\,max}}{1 + \Sigma \xi_i}} \cdot F$$

$h_{i\,max}$: Height of water of the upper limit of the i-th sub-reservoir above the bottom outlet

ξ_i : Losses

F : Cross-section of bottom outlet.

The inflows I and the 'natural' flows Q at the check-points are in reality not constant as assumed. Since, however, at the beginning and during the lowering process the future inflows are unknown and their prediction for the period of lowering is very uncertain, it is not possible to give the optimum lowering programme beforehand with any degree of certainty. Taking account of this fact the optimum emptying programme is only found by chance : in most cases a solution is obtained near to the maximum. As a consequence of these considerations, the values of I and Q in the resulting computation are time invariant, i.e., anticipated

values of I and Q were used. The inflows and the outflows are uniform during the complete lowering process.

With the aid of sensitivity analyses the sensitivity of the solution to parameter changes can also be investigated, and so valuable indications to critical factors can be obtained.

The solution of the problem is achieved by means of linear programming. The advantage of this analytical method of optimisation lies in its simple applicability and in the fact that a direct solution algorithm exists, which enables an optimum solution to be found. The disadvantages are the requirement of a linear objective function and of linear constraints.

For some possible questions linear programming is not suitable, or of only limited suitability. It is possible in these cases to use other solution techniques, like dynamic programming (for sequential decision processes), simulation (for mathematical or analogue models, coupling effects) and heuristical methods.

4. Bibliography

(1) FREHNER, P.: Wasseralarm Emosson. Bulletin des Schweizerischen Elektrotechnischen Vereins 24. November 1973.

(2) STADTRAT VON ZÜRICH: Wasseralarm Sihlsee. Weisungen über das Verhalten der Bevölkerung bei einer Ueberflutung der Stadt Zürich durch den Sihlsee, 1972.

(3) CHERVET, A.: Calcul de la propagation des crues dans un cours d'eau avec submersion de champs d'inondation. Schweiz. Bauzeitung, 17. Juni 1971.

Reservoir Models

S. P. CHEE
Professor of Civil Engineering
University of Windsor, Windsor, Ontario, Canada.

SYNOPSIS

A series of hydraulic models were used to study the sedimentation characteristics of reservoirs. Configurations of water bodies were moulded within a large basin which has its own water circulating, flow metering, and sediment feeding equipment. The physical aspects of siltation observed in the models included the formation of topset and bottomset beds, sediment bed slopes, disposition of the silt, and the effect of reservoir shape on sediment distribution. Bed load equations proposed by Kalinske and Einstein as well as other researchers were investigated. Flow resistance formulae determined by Richardson and Simons, Liu-Hwang, and others, were evaluated. The reservoir models were found to be very useful as a laboratory aid to resolve some of the problems associated with reservoir sedimentation.

Introduction

The feasibility whether a river basin development project could be undertaken successfully in economic terms sometimes depends on the useful life of the impounding reservoir. Most reservoirs eventually die of sedimentation. In the planning and development of water resources projects, it is essential to be able to estimate the useful life of the reservoir and in order to be able to determine this factor, a knowledge of the siltation characteristics of reservoirs is necessary.

The volume of a reservoir could often be expressed in terms of the depth by a relation of the form,

$$G = KH^m \qquad \ldots(1)$$

in which, G = reservoir capacity ; K = coefficient, H = reservoir depth ; m = a constant. The mode of silt deposition, besides other factors, would be influenced by the configuration of the water body. One method of classifying reservoirs would be by its shape and Equation (1) suggested a procedure which was adopted by the U.S.B.R.([1]). Sutherland([2]) defined mathematical shapes by assigning values to the exponent m consistent with the physical aspect in a similar manner to the U.S.B.R. as given in Table I.

TABLE I

Value of m	Reservoir shape
1.0 to 1.5	Gorge
1.5 to 2.5	Hill
2.5 to 3.5	Flood plain-foothill
4	Lake

For any given reservoir depth, H, the capacity increases as the value of m gets larger.

The rate of loss of life storage in a reservoir is always an important consideration to determine, besides the economic practicability of the project, also the planning of replacement storage. In this respect, the slopes assumed by the topset, foreset, and bottomset beds play an important role. It would, therefore, be very useful to be able to calculate the magnitude of the sediment gradients with good accuracy. The various bed load equations available, such as by Kalinske, Einstein, and others, were tested in the hydraulic models where non-uniform flow prevailed. Besides the sediment slopes, the manner in which the silt is distributed within the reservoir is also of great significance.

To resolve the many problems related to the deposition of silt in water bodies, some of which are not readily amenable to mathematical solutions, hydraulic models were used. This paper deals with the observations made on these reservoir models, analysis and discussion of the results.

Experimental Program

Sedimentation models of a wide range of simple and compound shapes were used to investigate reservoir siltation in the laboratory. The bed slopes of the model reservoirs were also varied over an appreciable range. Various inlet channel conditions were also tested. Overflow weir type and undersluice outlets were incorporated in the models. A calibrated hopper at the intake fed the sediment into the flow. The rate of sediment discharged into the inlet could be varied during the duration of the tests if desired. Reservoir models were built inside a large 1.52 m wide × 1.22 m high basin using cement-sand mortar, plexiglass and wood. The models have widths of from 0.15 m to 1.2 m. The cross-sectional shapes ranged from rectangular, trapezoidal, to sections with compound curved sides.

Water was circulated by a centrifugal pump motor unit capable of handling flows of up to 0.04 m^3/s. Triangular notch weirs were used to measure the flows. Water levels were measured by point gages. Miniature current meters were available to probe velocity profiles. Silica sand with a specific gravity of 2.65 was used as sediment. The grain size of the sediment varied from 0.05 mm to 2.0 mm.

Analysis and Results

Investigation of mobile boundary flow normally starts with an analysis of bedforms which controls the skin friction of the channel. An equation governing water flow and another expressing sediment discharge are also essential. Topset, foreset, and bottomset sediment beds are important features of the siltation process. The mode of disposition of the silt accounts for the filling of the peripheral reservoir space.

Bedforms

The division of channel roughness into two parts, namely, skin friction and form roughness due to bedforms, is a popular procedure adopted to determine the total resistance of the stream. Bedform diagrams delineating the state of the active bed, such as ripples, dunes, and others, were presented to describe the phenomenon. These figures are sometimes accompanied by visual sketches of the shapes of the bedforms but lack the exact detail dimensioning to define their geometric configuration.

One of the earliest bedform diagrams is that due to Shields as reported by Brown[3] in which the entrainment function $\tau/\gamma(S_s-1)d$ is related to the particle Reynolds' number $d\sqrt{\tau/\rho}/\nu$ to describe the incipient movement of the sediment in which τ = critical boundary shear ; γ = unit weight of water ; S_s = specific gravity of the sediment ; d = grain size ; ν = kinematic viscosity of the water ; ρ = water density.

Two other researchers who described bed activity in a manner not unlike that of Shields, is Liu and Hwang[4]. The Liu-Hwang bedform mechanics diagram utilizes the dimensionless products V_*/w and wd/ν in which $V_* = (gDS)^{1/2}$ = shear velocity ; g = acceleration due to gravity ; D = flow depth ; S = energy gradient ; w = fall velocity of spherical particles.

Departure from the use of dimensionless parameters was made in Simon's diagram given by Graf[5] which made use of the dimensional product τV termed stream power plotted as the ordinate and the mean grain size, d, as the abscisse where, V = mean velocity.

There is a close resemblance between the Shields and Liu-Hwang methods in relation to the choice of dimensionless products. In the procedure proposed by Simons, the specific gravity of the grain and fall velocity are not represented in the variables. There are advantages in the utilization of dimensionless products in describing transport phenomenon and appeals to other researchers such as Allen[6] and Yalin[7].

Both the bedform diagrams of Simons and Liu-Hwang were used to predict sediment activity in the models. Within the range of visual accuracy in relation to the two diagrams, there did not appear to be a strong preference for either. The two procedures predicted a proportionately greater percentage of dunes than ripples as compared to the visual results.

Water Flow

An equation relating the discharge or mean velocity to the energy gradient and channel parameters such as flow area, hydraulic radius and a roughness coefficient is necessary to calculate the conveyance of the stream. Depending on the nature of the problem as to which quantity is taken as the independent variable, the alternative description of flow resistance equation is also commonly used. The Chezy and the Manning equations have weathered the passage of time and are widely used in rigid boundary flow in which the skin friction roughness need only be considered.

It is, therefore, not surprising that the water discharge relations in erodible channels with sediment transport falls back on the rigid boundary equations. Richardson and Simons[8] made use of the Chezy equation for mobile channel hydraulics. In order to take into account roughness effects due both to surface grains and bedforms, they proposed different values of Chezy's coefficient, C, for various bedforms, viz.,

$$V = C\,(RS)^{1/2} \qquad \ldots(1)$$

where, V = mean velocity ; R = hydraulic radius

(*i*) Plane bed with negligible sediment transport

$$\frac{C}{g^{1/2}} = 5.9 \log D/d_{85} + 5.44 \quad \ldots(2)$$

(*ii*) Plane bed with considerable sediment motion

$$\frac{C}{g^{1/2}} = 7.4 \log D/d_{85} \quad \ldots(3)$$

(*iii*) Ripples

$$\frac{C}{g^{1/2}} = \left(7.66 - \frac{0.30}{V_*}\right) \log D + \frac{0.13}{V_*} + 11 \quad \ldots(4)$$

(*iv*) Dunes or anti-dunes

$$\frac{C}{g^{1/2}} = 7.4 \log D/d_{85} \left(1 - \frac{\triangle RS}{RS}\right) \quad \ldots(5)$$

in which $C/g^{1/2}$ = non-dimensional Chezy's coefficient ; d_{85} = fall diameter of the bed material in which 85 percent by weight of the grain sizes are finer ; $\triangle RS$= increase of RS due to form roughness. A graph was available to obtain values of $\triangle RS$ from known RS values. Except otherwise stated, the units of measurement are in the *FPS* system.

Based on the same principle as Richardson and Simons that curvilinear bedforms has a larger wetted perimeter, Einstein and Barbarossa[9] theorized that the hydraulic radius consisted of two portions, R' and $(R-R')$ where, R' = hydraulic radius due to surface grain roughness, $(R-R')$ = hydraulic radius due to moving sediment beds. Chow[10] using Manning's equation,

$$V = \frac{1.49}{n} R^{2/3} S^{1/2} \quad \ldots(6)$$

proposed that the Strickler relation for Manning's n could be expressed in the form,

$$n = \phi \left(\frac{R}{k}\right) k^{1/6} \quad \ldots(7)$$

in which k = roughness height. The function $\phi\,(R/k)$ was extended by Donald and Chow[11] to encompass surface grain and bedform roughness and suggested a formula,

$$\phi\,(R/k) = 0.0342/(R'/R)^{2/3} \quad \ldots(8)$$

A mobile boundary flow resistance equation would ensue by combining Equations (7), (8) & (9) to give,

$$V = \frac{43.6}{k^{1/6}} (R^{2/3}) (R'/R)^{2/3} S^{1/2} \quad \ldots(9)$$

A family of curves of (R'/R) were presented in graphical form as functions of $(R/k_{65})^{1/3}$ and (k_{35}/RS) in which k_{35} and k_{65} refer to sediment size just larger than 35 percent and 65 percent respectively of the material obtained from a mechanical analysis curve.

Liu and Hwang[4], after an intensive laboratory investigation of mobile bed flow ended with an exponential type of flow resistance formula not unlike that of Manning,

$$V = C_a R^x S^y \quad \ldots(10)$$

The coefficient C_a and the exponents x and y have changing values consistent with the sediment size and bedform. Graphs were given in their paper in which the values of C_a, x and y could be found depending on the grain size and bedform.

The methods developed by Richardson-Simons, Donald-Chow and Liu-Hwang were evaluated by testing them with the observations made in the reservoir models. The relationships were used in the form of resistance equations in which the computed slopes were compared with those observed in the reservoir models. The equations of Richardson-Simons and Liu-Hwang demonstrated appreciably better agreement than the relations of Donald-Chow. The Richardson-Simons and Liu-Hwang equations both showed good agreement with the experimental observations although the Richardson-Simons method gave greater accuracy and some of the results are shown in Figure 1.

Sediment Bed Transport

The slope of sediment beds is predominantly determined by the rate of solid discharge along the bottom as suspended sediments do not have such a marked influence. A sediment bed load discharge equation is, therefore, essential to ascertain both the quantity of material moving near the bottom as well as the energy slope of the flow system.

A few bed load equations are available but those by Kalinske and Einstein were used in the reservoir models.

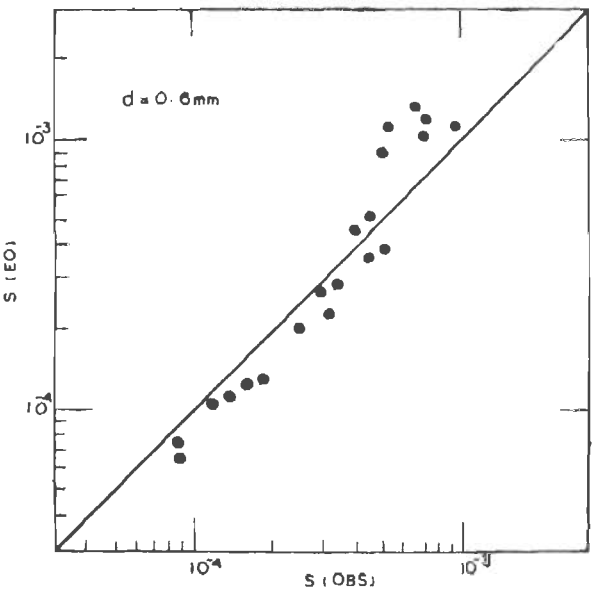

FIGURE 1 : Richardson-Simons' EQ.

These equations which were presented in Henderson[12] are,

Kalinske :

$$\frac{q_s}{d\,(\tau/\rho)^{1/2}} = 10\left(\frac{\tau}{\gamma\,(S_s-1)\,d}\right)^2 \qquad ...(11)$$

Einstein :

$$\frac{q_s}{d^{3/2}\,G[g\,(S_s-1)]^{1/2}} = 40\left(\frac{\tau}{\gamma\,(S_s-1)\,d}\right)^2 \qquad ...(12)$$

in which q_s = sediment discharge per unit width ;

G = sediment parameter.

Equations (11) & (12) were used in the form in which the sediment flow was computed and compared with the experimental bed load. Besides being easier to manipulate, the Kalinske bed load equation showed better agreement. Figure 2 illustrates typical results.

Bottom Sediment Beds

The main sediment transport in the reservoir consists of the bed movement and the suspended load. The bottom sediment beds comprise the topset, foreset and bottomset beds which are in active motion together with the passive clay accumulation deposited from the wash load adjacent to the dam and spillway structure. The sediment composition, reservoir configuration, and inlet velocity, are deterministic parameters which control the formation of the active bottom sediment beds. These variables determine the formation of topset, foreset, and bottomset beds besides their relative proportions and surface gradients. Depending on the range of the grain sizes of the sediment, more than one set of active bed sediments may be formed. Except during the initial phase of sedimentation, the original river bed slopes of the impounded reservoir did not have any effect on the final sediment slopes. The fluvial process of hydraulic sorting of the different size grains to form distinct sediment profiles proceeded continuously during siltation.

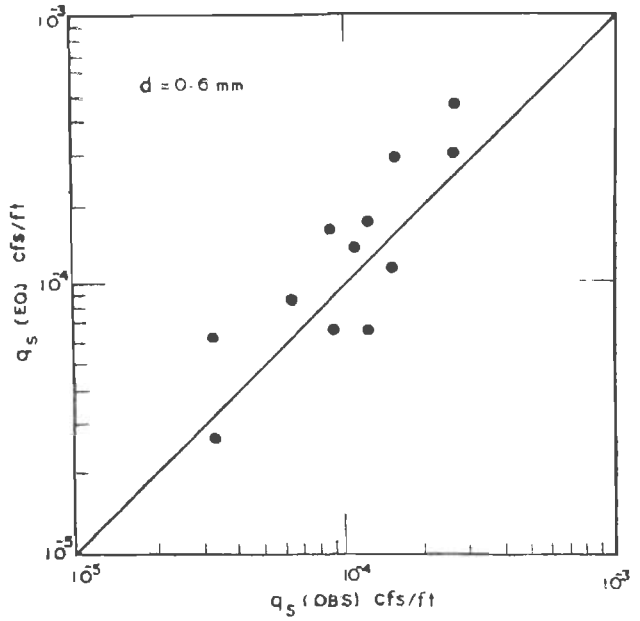

FIGURE 2 : Kalinske's EQ.

The almost quiescent settling of the clay size particles of suspended sediment at the downstream pool close to the main embankment and hydraulic outlet structures form a mud stratum. If favourable outlet bottom sluices are present, part of this silt-clay accumulation could be drawn off but the efficiency does not appear to be as high as reported by Duquennois[13]. Figure 3 shows the longitudinal distribution of sediments in a reservoir schematically.

Peripheral Sediments

The disposition of the peripheral sediments, which were brought about by the settling of the suspended silt in sluggish water, was influenced strongly by the shape of the water body. It represented a smaller proportion of the total sediments. A physical reservoir model would be very useful to observe this phenomenon as it would not lend itself easily to analytical predictions.

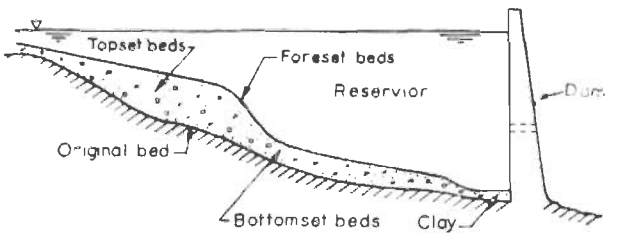

FIGURE 3 : Reservoir sediments.

Conclusions

(1) The Chezy equation using the Richardson-Simons coefficients was found to describe the resistance of mobile beds with good accuracy.

(2) Bed load transport could be determined adequately using Kalinske's equation.

(3) Topset, foreset and bottomset sediment beds could be readily reproduced in the reservoir models which would enable the study of their formation and movement with better understanding.

(4) The hydraulic models were found to be very useful in observing the siltation process in the periphery of the water bodies.

Acknowledgement

The research funds provided by the federal agencies now Environment Canada are gratefully acknowledged.

References

(1) U. S. B. R. : "Distribution of Sediment in Reservoirs." Interim Report, 1954, p. 15.

(2) SUTHERLAND, R. A. : "Some Aspects of Water Conservation." Trans. A. S. C. E., Vol. 96, 1932, p. 157.

(3) BROWN, C. B. : "Sediment Transportation." Rouse, H. (Ed.), "Engineering Hydraulics," Chapter 12, John Wiley and Sons, 1950.

(4) LIU, H. K. and HWANG, S. Y. : "Discharge Formula for Straight Alluvial Channels." Journal, Hyd. Div., A. S. C. E., 85 (Hy 11), 1959, pp. 65-97.

(5) GRAF, W. H. : "Hydraulics of Sediment Transport." McGraw-Hill Book Co., 1971, p. 282.

(6) ALLEN, J. : "Scale Models in Hydraulic Engineering." Longmans, Green and Co., 1952

(7) YALIN, M. S. : "Theory of Hydraulic Modes." The MacMillan Press Ltd., 1971.

(8) RICHARDSON, E.V. and SIMONS, D. B. : "Resistance to Flow in Sand Channels." Twelfth Congress, I.A.H.R., Vol. 1, 1967, pp. 141-150.

(9) EINSTEIN, H. A. and BARBAROSSA, H. L. : "River Channel Roughness." Trans. A. S. C. E., Vol. 117, 1952, pp. 1121, 1132.

(10) CHOW, V. T. : "Open Channel Hydraulics." McGraw-Hill Book Co., 1959, pp. 208–210.

(11) DONALD, J. J. and CHOW, V. T. : "Discussion of River Channel Roughness." Trans. A. S. C. E., Vol. 117, 1952, pp. 1121-1132.

(12) HENDERSON, F. M. : "Open Channel Flow." Chapter 10, The MacMillan Co., 1966.

(13) DUQUENNOIS, H. : "New Methods of Sediment Control in Reservoirs." Water Power, May 1956, p. 174.

Dynamic Programming as Applied to Substantiation of a Reliable Water Supply in Integrated Water Management Systems

A. L. VELIKANOV D. N. KOROBOVA
Institute of Water Problems
U.S.S.R. Academy of Sciences, Moscow (U.S.S.R.).

SYNOPSIS

Aspects of a reliable water supply substantiation in integrated water management systems are discussed. The necessity of reactivating the issue has been recently underlined by the formation of large-scale systems and redistribution of river flow over vast areas. The task of water resources distribution that constitutes the backbone of numerous water economy problems, including that of a reliable water supply substantiation, can be investigated with the aid of a dynamic programming method.

According to experts, dealing with problems of rational use of water resources, the second half of the 20th century has been the time of intensive formation of water management systems and their chains, stretching way beyond geographic and state boundaries.

The necessity of having large-scale water resource systems and the consequential redistribution of river flow over vast areas give rise to a number of new technological and scientific problems.

As regards the technical means employed in the realization of such systems (construction machinery) or the designing of structures (canals, dams, hydropower complexes), the achievements to-date are obvious enough to call for any doubt. However, there has been no significant progress lately in the field of controlling the river flow, a resource of nature, ever-replenished and constantly changing as time goes on. Reference is made, specifically, to two aspects of water resources control, i.e., (*a*) practical measures to control the formation of river flow as an element of the hydrologic cycle, and (*b*) a reliable long-term forecasting of river flow.

It can be asserted, that in the foreseeable future river flow regulation by reservoirs will continue to be the only means of eliminating the inconsistency between the nature of river flow variations and water requirements of the different water management system components. As far the dependable long-term forecasting of river flow in the future systems, this prediction must be treated in terms of a possible transition from unconditional to conditional distribution of the river flow probability values. In other words, one would take into account the dependence of the new flow on factors, already manifest by the time of forecasting, including geophysical processes, which can be predicted with a comparatively high degree of probability.

Taking further our analysis of the systems reliability, we proceed, then, from two assumptions : (*a*) river flow as the basic source of water essential for the development of society, is subject to natural fluctuations, forecast in terms of probabilities; (*b*) water resources control, i.e., gearing the resources both to economic/social needs of society to meet the requirements imposed by the environmental protection measures, is exercised through reservoirs, which are practically incapable of suppressing thoroughly the variations in the present pattern of water supply.

Water management system reliability aspects, one of which constitutes the subject of this paper, are by no means new either in practice or in the theory of river resource utilization. Reliability aspects have received

much attention in the works of S.N. Kritsly and M.F. Menkel(1)(2)(5), the Soviet authors of the River Flow Regulation Theory, and their school of thought. While tackling the reliability aspect, two tasks are generally distinguished : reliability of structures from the standpoint of safety of operation ; reliability of meeting water requirements. The former deals with the function of water facilities, operating under conditions of maximum water discharges ; the latter analyses the conditions of water users, when the flow is insufficient.

The reliable supply of water user demands is an important factor of any water management system ; in fact, it determines the system's efficiency. As far as the practical utilization of river flow in the U.S.S.R. is concerned, the problem of a reliable water supply was largely solved following the introduction of a "design probability" index in water economy calculations. This index, normally expressed as a percentage, provides a quantitative estimate of the needed probability of a continuous water supply. Although there are no unified standards for the design probability in the U.S.S.R., the index has acquired the significance of a standard, and is used at present as the basis to determine both the parameters of hydraulic structures, regulating and supplying the water, and the parameters of water users, abstracting the water from a given source. In addition to this, the design probability is used in the preparation of water balances and is a good indicator in setting the scale of inter-regional flow transfer schemes.

Because the economic and physical meanings of the design probability employed in water facility design and especially in determining the capacity of hydro-electric plants have been sufficiently discussed in a number of papers(1)(3)(4), we shall only confine ourselves to the fundamentals on which the solution of the problem is based.

It is generally assumed that there exists a direct relationship (although within certain limits) between a quantity of water diverted from a given source and economic efficiency of the water user, i.e., the greater the design quantity of the tapped resource, the higher the efficiency. However, flow variations, typical of the rivers, result in a situation, when an increase in water requirements limits water user consumption during low-water periods, with damage inflicted on the water user and his efficiency going down. In order to make water supply steadier and curtail the damage, it seems necessary either to increase the storage regulating capacity or resort to an extra source of water, or else to cut the design amount of the water being used. Thus, we get three inter-related parameters :

—water requirements ;

—irregularities in water supply, liable to occur with given requirements ;

—regulating capacity or measures aimed at stabilizing water supply.

In principle, economic assessment of reconsidering the water requirements and estimating the cost of measures providing for a more consistent water supply is not a problem, whereas it may be rather difficult, if not impossible, to evaluate the economics of a disrupted water user behaviour pattern. This unpredictable group of water users includes community water supply and environmental control programmes. It is equally difficult to assess the damage resulting from disruptions in agricultural water user pattern, since the efficiency of farming is not related to water consumption alone. All things considered, the design probability, on a practical level, is established on the basis of standards. The required degree of continuous water usage naturally depends on the type of water user. According to (Ref. 8) water supply for industrial and community needs is calculated on the basis of 95 to 99 percent probability. For those industries that can afford underutilization of river flow without breaking a steady production cycle, the probability standard goes down to 75-90 percent. For some water users, there exists another standard, applied to regulate the permissible degree of reducing water supply during low-water periods, when the amount of water available for use is far below the design probability. The above standards are established by synthesizing the design, operation and maintenance practices applied in the management of water projects as well as on the basis of economic analysis, which makes it possible to evaluate the relative significance of certain factors in decision-making.

Worthy of note are two points, at least, that necessitate further investigation of the design probability substantiation. First, the above standards, while providing for a choice to be optional, may at times lead to entirely different technological approaches.

For example, should the probability of water consumption from the seasonal water storage on the Dnieper River (relative storage capacity = 0.15) be reduced from 99 to 95 percent, the increment of water consumption will be about 20 percent, while the failure rate may increase five times. Definitely, in such a case it will not be that simple to make a decision.

Second, the design probability as a standard applies to a rather wide range of water users for whom, cost-wise, the extent of damage suffered during low-water periods is almost equivalent to the cost of a more reliable water consumption.

These two factors constitute a bottleneck in applying the design probability to the analysis of water economy systems.

A water economy system is a combination of water sources and water users, utilizing the resources for the benefit of various industries of a national economy, both to satisfy social demands and to protect environmental values. A river with tributaries is considered to be a typical water source.

Analysis of the entire set of water sources in combination with water users reveals some peculiarities of such systems. To begin with, a direct relationship is no longer there between water needs of an individual system component and anticipated shortage of water, because the latter is determined not by the variability characteristic of the river flow alone, but also by the standing procedure of water resources distribution. Besides, with a system scattered over an area, and the pattern of water utilization varied (non-returnable/returnable abstraction, the use of the river natural flow, backwater arrangements, etc.), the relationship between aggregate water requirements, water shortage and storage capacity proves to be functionally uncertain. The reliability of steady supplying the demands of individual water users turns out to be the function not only of the regulating capacity, but also of some other factors, which could not be taken into account in establishing the design probability as an operational standard for water supply reliability.

In this connection, it became necessary to try and see, and examine the problem of water use reliability in water economy systems. Originally, it was thought that some common index could be devised to measure the reliability of a system as a whole, similar to the design probability index. However, when dealing with scattered water resources and different modes of their use, such an index ceases to be meaningful. Our analysis clearly indicated that reliability of a steady supply of water users cannot be determined unless all operating conditions of the system are closely examined.

The reliability of water supply used to be an argument in economic substantiation of the design probability of individual water facilities ; when applied to water economy systems, the reliability is no longer an independent variable. In this case, an argument will be the design quantity of water needed for each water user X_i (i is the user number) ; this quantity determines the capacity, yield or design conditions of a resource utilization. Thus, the design value of water resources required is an argument of a given water user efficiency function $E_i(X_i)$. It is assumed that within certain limits this function increases. At the same time, as the design quantity of the resources used goes up, so does the probability of a failure occurring in the normal water supply pattern. This results in damages, that lower the efficiency of water user development, as system components. Each water user has his own damage curve (D_i), determined by the resources used (X) and the value of the design water consumption by water user (X_i)—$D_i(X/X_i)$.

The amount of water actually available to any one component under different conditions of water supply depends on the pattern of water distribution between individual water users. For the benefit of national economy as a whole, there should be a general trend toward deriving maximum effect from water resources of a given system, the effect being regarded as an integral evaluation of water utilization.

In such a case, on the basis of the principle of optimality, it can be assumed that for each variant of the design water consumption (X_1, X_2, ... X_m) any amount of water should be distributed between the system components in such a way that the total damage in the system could be minimal, i.e., $\sum_{i=1}^{m} D_i(X/X_i) \rightarrow min$.

Assuming further that water resources of a river adhere to the law of probability distribution, in estimating the efficiency of a system as a whole, one should deal with mathematical expectancy of the minimum total damage $M\left[min \sum_{i=1}^{m} D_i(X/X_i)\right]$.

It follows from the above that a substantiation of water consumption reliability in fact amounts to determining the design water consumption of all the components $X_1, X_2, \ldots, X_m$ which would minimize the cumulative effect $\sum_{i=1}^{m} E_i(X_i) + M\left[min \sum_{i=1}^{m} D_i(X/X_i)\right] \rightarrow min$.

Thus, our task has been reduced to a multiple distribution of the changing water resources with different variants of the design water consumption by the system components.

To investigate the so-called monomer processes of distribution, a dynamic programming method is widely used.

This method is based on the principle of optimality, formulated by R. Bellman (Ref. 5), who regards this as a feature of a multi-stage process.

The basic merits of this method consist in the possibility of obtaining the absolute rather than relative maximum, the absence of requirements to the analytical structure of the functions, as well as in the likelihood of introducing any number of limitations in the calculations. Ref. 5 provides a detailed description of the algorithm along with the computation scheme to be used for the solution of a number of distribution tasks. However, as R. Bellman points out, he failed to come up with a standard solution, that might be applied to all distribution processes, which caused the appearance of numerous papers devoted to practical uses of the dynamic programming method, employed in the solving of specific distribution problems in various industries, including water management.

The problem of water resources distribution between the components of an intricate water management complex is characterised by the non-linear, and analytically indeterminate functions of the components' effect from the used water resources as well as by a great number of limitations. The problem, then, belongs to monomer processes of distribution that easily yield themselves to investigation by the dynamic programming method.

Efforts of many authors toward the use of this method for investigations in the field of water management showed, on the one hand, the impossibility of a

direct application of Bellman's recurrent expression or of the algorithm that he devised for purposes of solving the distribution problems existing in the majority of water economy system patterns; on the other hand, it showed a good deal of contrivancy on the part of the authors in trying to solve some specific problems of water economy through the use of the guiding principle of dynamic programming, i.e., the principle of optimality.

The great popularity of this method with scholars engaged in solving water economy problems is due to the fact that the process of solution is illustrative, and each stage of the process yields results that can be analysed, which means that in case of point the method can be ideally interpreted in physical terms.

There are two groups of reasons to account for the complexity of a direct application of the dynamic programming method to solving the water resources distribution problems : (*a*) the dispersion and a definite direction of a resource preconditioned by the complexity of a river basin pattern, on which a water management complex is located (the main course, tributaries); (*b*) a variety of water resources utilization forms (water use conditions) and of economic estimates of the actual effect derived from the water used.

Hence, the two basic approaches to the application of the method. The first approach is characterized by a tendency toward devising a universal recurrent expression on the basis of the guiding principle of dynamic programming and a common solution algorithm at any one stage of the distribution process, that might be applicable to all kinds of water management complexes.

The second approach consists in reducing the overall complex problem of distribution to a number of simple problems, easily solvable by R. Bellman's method alone. The results of simple problems; solution can well be used as background data for further solving of the distribution problem as a whole involving other means and methods of solution.

In view of the unique nature of water management complexes, it is apparently difficult to predict the possibility of devising, on the basis of the guiding principle of dynamic programming, of a common recurrent expression and a solution algorithm applicable to any complex. Such a versatility, no doubt, would considerably complicate further the initial computation procedure of dynamic programming and thus rule out any possibility of a simpler solution in each particular case. Nevertheless, there is some benefit resulting from a certain complicating R. Bellman's recurrent expression and the solution algorithm thereof, quite obviously.

A combination of the two approaches seems, therefore, to be most effective, i.e., a reasonable complicating of the basic recurrent equation and of the solution algorithm, both devised by R. Bellman, and, at the same time, deduction of individual case problems, where it is more practical to employ other methods and means of solution.

Such an approach may prove sufficiently captivating and lead to good results, if applied to some water management problems.

However, it is more complicated compared with R. Bellman's method of solution.

As was pointed out earlier, the main difficulties of applying a dynamic programming method to water management problems are primarily determined by peculiar features of a given water resource and the variety of water consumption modes and the characteristics of the effect for the components.

Dispersion of a resource, expressed by a variable of the cumulative resource in different points of a river basin, and a definite direction of the source condition unequal opportunities for the components as regards the resource utilization. Thus, it is obvious that the possible extent of resource utilization by components located on the tributaries, in the upper reaches or in its mouth will be different. This necessitates an introduction of limitations to confine the extent of water consumption variation for each component and a group of components, and the use of a balance equation. The said limitations will not be the same on different sections of the river, which, in its turn, complicates the logic of computation. It is noteworthy, that R. Bellman's algorithm, if taken alone, is only good for the case of a water storage, as a common resource, and of components with a non-return flow consumption, located along the sides of the storage.

A suggestion was made in some papers (Ref. 6, 7) to build the summable R. Bellman's function in two stages : first, for components, located on the tributaries; then, for components spread along the river banks and for the earlier built cumulative functions of the effect for tributaries. The same procedure, although in a reverse order, can be used to advantage in a water resource distribution proper : first, between the components in the river bed and groups of components on the tributaries ; then between the components on the tributaries. This pattern is particularly suitable when all the components operate under the same water consumption conditions, the so-called non-return flow consumption. In some cases, such an approach may considerably reduce the amount of computation involved. The different ways of plotting the combined characteristics, known from literature, depending on the direction of a watercourse, i.e., from the upper reaches toward the mouth or vice versa, is of no consequence. The direction of adding up, adopted in our work—from the source to the mouth—does not seem to destroy the physical meaning of the problem and preserves the illustrative nature of the solution process at every stage of optimization, thus keeping us from being too formalistic.

Far more complicated is the removal of difficulties related to different form of a water resource utilization,

starting with the use of a water way in its natural state, e.g., fishing, and ending with a complete abstraction of part of the flow for the purpose of transfer to another river basin.

There are two widely used and yet sufficiently loose terms used to describe the modes of water utilization : a water consumer and a water user as well as their various modifications, such as a pure water user, a water consumer with a partial return flow, etc.

In line with the requirements of dynamic programming, it seems practical to express all the forms of water utilization through a single component having the characteristic of effect from the water that he uses $D_i(X)$ and the characteristic of water utilization conditions—the function of return flow $Y_i(X)$. An introduction of this function for all the components of a complex makes it possible to formalize the overall problem into a single-type (homogeneous) multi-stage process.

It must be stressed that a return flow in question is the water, coming back to the watercourse immediately downstream of the given component. Our investigations undertaken with a view to record the return flow several stages downstream, i.e., after several steps of the distribution process, showed that it is worthwhile to single out this sector of solution from the problem as a whole, and analyse it by other methods.

With this approach, the basic recurrent equation of R. Bellman can be presented as follows :

$$F_i(W) = \min_{a_i \, X \, b_i} D_i(X) + F_{i-1}[W - X + Y_i(X)],$$

where,

$F_i(W)$ = summable function of Bellman's effect at i's stage of the solution ;

$Y_i(X)$ = the value of the return flow function of i's component ;

$F_{i-1}[W - X + Y_i(X)]$ = summable function of Bellman's effect at the preceding stage.

The problem formalization, that we adopted both with respect to the resource and to water utilization modes, necessitates the devising and subsequent observance of a number of complicated water balance limitations and equations, which in turn, calls for a special logic of control, taking care of water balance peculiarities typical of different sections of a river basin.

Let us consider some of the points presented above, taking as an example a water management complex, that tentatively can be reduced to a scheme, including the main channel with primary tributaries and the components of the complex, having the characteristics of the effect $D_i(X)$ and of the return flow function $Y_i(X)$.

The adopted in our case algorithm of problem solution presupposes the availability of data about the results of the preceding solution stage, about the component at the given stage, and about the extent of variation of Bellman's summable function argument; the latter is to be obtained as a result of solution at the given stage. Let us turn to the algorithm of solution for k's stage of optimization.

The required information about the results of solution at the preceding $(k-1)$ stage boils down to the limits of Bellman's function argument variation, i.e., W_{k-1}^{min} and W_{k-1}^{max}, and to the data about the cumulative water resource, accumulated toward the $(k-1)$ stage.

Information about the component at the k's stage includes more accurate limits of the effect's function argument variation and of return flow fluctuations of this component a_k and b'_k, the effect's functions proper $D_k(X)$, return flow functions $Y_k(X)$, and the water resource W'_k, feeding the component. When a component is stationed on a tributary, W'_k corresponds to the magnitude of the tributary water resources. If the component abstracts water from the channel, $W'_k = 0$.

As for the summable function of the effect $F(W)$, it is sufficient to have the data on the limits of its argument variation W_k^{min} and W_k^{max}.

The background information about a water resource and the components of a complex can only provide partial data concerning the component at the k's stage. The remainder of the information is obtained in the course of computation, subject to verification prescribed by water balance limitation.

On the basis of R. Bellman algorithm, the data are produced on the zero stage of solution—zero component—regarded as a preceding solution relative to the first stage in the form of

$$F_o(W) = 0, \; W_o^{min} = 0, \; W_o^{max} = 0, \; \sum_{i=0}^{o} W_i = 0.$$

There are different ways of determining the limitations by the k's component b'_k, as well as of the limits set on the $F_k(W)$ summable function variation, produced as a result of solution on the k's stage. The difference is accounted for by the location of the component on the channel or on the tributary. For a channel :

$$b'_k = \min\left(b_k, \sum_{i=1}^{k-1} W_i - \sum_{i=1}^{k-1} a_i\right)$$

$$W_k^{min} = W_{k-1}^{min} + a_k - Y_k(a_k)$$

$$W_{k-1}^{max} + b'_k - Y_k(b'_k)$$

$$W_k^{max} = \min \sum_{i=1}^{k-1} W_i - Y_k(a_k)$$

For a tributary :

$$b'_k = min\ (b_k,\ W_k)$$

$$W_k^{min} = W_{k-1}^{min} + a_k - Y_k(a_k)$$

$$W_k^{max} = W_{k-1}^{max} + b'_k - Y_k(b'_k)$$

In the course of computation the W_k^{max} value can be reduced due to the horizontal areas on the functions of k's component return.

While making computations for components diverting water from a river channel, it is necessary to check up the following balance equation :

$$X_{k,1}\left(\sum_{i=1}^{k-1} W_i - \sum_{i=1}^{k-1} a_i\right) - W_{k-1,\,m}$$

When observing these limitations, the computation is carried out using an algorithm similar to the one proposed by R. Bellman.

The solution of the problem of distributing a water resource between the components of a water management complex yields results that can be used to investigate the problem of the reliability of water supply in integrated water management systems as well as other matters of water economy.

Conclusions

(1) The creation of large-scale water management systems and redistribution of flow over vast areas brings back the problem of substantiating the reliability of water supply.

(2) The present system of different standards of the design probability currently applied in project planning cannot fully account for a dispersed nature of water resources within complex systems.

(3) The problem of substantiating a reliable water supply in integrated water management systems for the benefit of the national economy, in fact, amounts to determining the design water consumption for all the components of a system.

(4) The problem of water distribution between the components of a complex water management system, constituting the substance of the problem of water supply substantiation, can be treated as a monomer distribution process, and hence, easily yields itself to an investigation by a dynamic programming method.

(5) Efficiency and practicability of applying a dynamic programming method to solving water management problems are underlined by the absence of requirements to the exact analytical structure of the functions and by a good many limitations that can be introduced in the computations, the process of solution being illustrative and allowing for an analysis of the results at each stage.

(6) The prospects of a dynamic programming method application in the field of water management, coupled with other optimization methods.

References

(1) KRITSKI, S.N. and MENKEL, M.F. : Vodohozaistvennyje raschety. Gidrometeoizdat, L., 1952.

(2) KORENISTOV, D.V.; KRITSKI, S.N. and MENKEL, M.F. : Problemy teorii regulirovanija stoka. Sb. "Problemy izuchenija i ispolzovania vodnyh resursov," Izd-vo "Nauka", M., 1972.

(3) KORENISTOV, D.V. : Issledovanije k byboru obespechennoi i ustanovlennoi moshnosti gidroelectricheskoi stancii, rabotayushei s sutochnym regulirovaniem v energeticheskoi systeme. Sb. "Problemy regulirovanija rechnogo stoka", M.-L., Izd-vo AN SSR, vyp. 4, 1950.

(4) VELIKANOV, A.L.; DRUZHININ, I.P.; KRITSKI, S.N. and MENKEL, M.F. : Metodika economicheskogo vybora obespechennoi moshnosti gidroelectrostancii. Sb. "Problemy energetiki i regulirovanija rechnogo stoka", M.-L., Izd-vo AN SSSR, 1960.

(5) BELLMAN, R. and DREIFUS, S. : Prikladny zadachi dynamicheskogo programmirovanija. Izd-vo "Nauka", M., 1965.

(6) VELIKANOV, A.L. and KOROBOGA, D.N. : Primenenije metoda dynamicheskogo programmirovanija k raspredeleniyu vodnyh resursov. Sb. "Problemy izuchenija i ispolzovanija vodnyh resursov, Izd-vo "Nauka", M., 1972.

(7) VELIKANOV, A. L. ; KOROBOVA, D. N. and SINITSYN, N.I. : Algoritm optimalnogo raspredelehija vodnyh resursov na EVM dlya slozhnyh vodohozaistvennyh system. Sb. "Problemy regulirovanija i ispolzovanija vodnyh resursov", Izd-vo "Nauka", M., 1973.

(8) KRITSKI, S.N. and MENKEL, M.F. : "Regularities in Flow Fluctuations and Requirements toward their Control" River Flow Control International Symposium of Flow Control. Sofia, October, 1967.

Response of Alluvial Channels to River Regulation

R. D. HEY
Lecturer in Hydrology
School of Environmental Sciences, University of East Anglia
Norwich, U.K.

SYNOPSIS

In the long-term all alluvial channels adjust their average bankfull capacity and dimensions to the flow which transports most sediments. Studies in America have shown that the frequency of occurrence of the flow doing most work and bankfull discharge are identical and this explains why bankfull flow appears to be the dominant discharge.

This model can be utilised to show that river regulation for water resource development purposes may be responsible for channels adjusting their overall dimensions to a new climate of flows. Analysis of the factors controlling erosional and depositional processes indicate that stability can be maintained provided that releases from reservoirs, and releases and abstractions from river outfalls/intakes, are below the threshold of bed material transport.

In the U.K. a major new reservoir has been proposed at Craig Goch to regulate the flows in the Rivers Wye and Severn. As river intakes/outfalls are to be used it is essential that abstractions as well as releases are below the threshold of bed material transport. The techniques available to determine these values are illustrated in a study of the River Severn.

Introduction

Regulating reservoirs and the associated use of river systems as natural aqueducts are increasingly being utilised for major water resource development schemes. In the United Kingdom the River Dee is already operating in this manner and further schemes are planned before the end of this century. It is predicted that some river regulation schemes may not be able to meet projected demands in certain areas, especially in Eastern England, and inter basin transfers are being planned to meet this eventuality (1).

As a result of these changes the flow regime of many rivers will be modified which, in turn, may be responsible for them adjusting their capacity and dimensions to the new flow conditions.

Ideally regulation should not cause unnatural amounts of erosion or deposition in the vicinity of the dam site or river intake/outfall. Indeed failure to maintain channel stability could result in a loss of agricultural land, a reduction in the flood capacity of the river, and a loss of river amenity.

The economic cost of channel maintenance could, in such circumstances, be quite considerable and it needs to be identified during the planning stage of a water resource development scheme. If it proves to be excessive composite or alternative schemes may have to be considered.

As sufficient is now known about natural channel adjustment processes regulation strategies can be identified at the planning stage which will maintain the channel in its natural state. Before this can be achieved it is necessary to review the factors controlling the bankfull geometry of stable natural channels.

Dominant Discharge

Although rivers adjust their bankfull shape and

dimensions to a range of flows it has been argued that the steady discharge which produces the same gross shapes and dimensions as the natural sequence of events is the dominant discharge ([2])([3])([4]). Flume experiments and observations of natural channels indicate that the flows at, or about, the bankfull stage are the effective ones for channel forming processes ([5])([6]). Indeed the channel is operating most efficiently at this particular stage because flow resistance is at a minimum ([6]). In spite of this evidence it does not explain why the channel adjusts to this particular flow.

Wolman & Miller ([7]) in their study of the magnitude and frequency of transport processes rationalises this problem. Although extreme discharges are individually responsible for transporting large volumes of sediment it is the smaller more frequent flows which are responsible for the transport of the largest volume of material in the long-term. The value and frequency of the flow doing most work is dependent on the flow regime and the sediment transport characteristics of the river ([8]). If coarse suspended and bed load is the predominant mode of transport then the intermediate flood flows collectively do most work [Figure 1 (*a*)]. As the calibre of the load is reduced and fine suspended and wash loads become dominant the smaller flows become responsible for the transport of the greatest amount of sediment because the shape of the sediment rating curve changes [Figure 1 (*b*)]. Variations in the flow regime also influence the magnitude and frequency of the flow doing most work. Changes in flow variability have the most significant effect; the larger its value the greater the influence of the high flows and vice versa [Figure 1 (*c*)]. In contrast variations in mean flow can only affect its magnitude and not its frequency of occurrence.

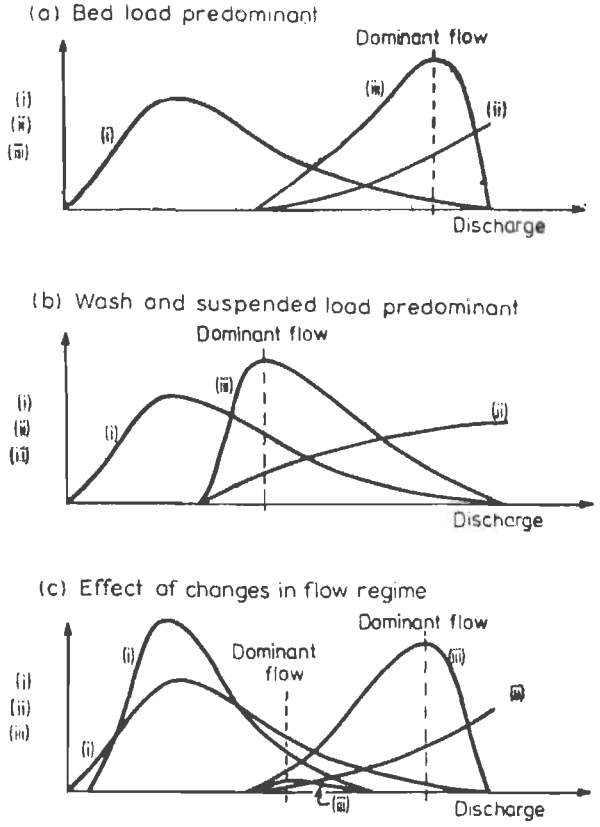

FIGURE 1 : Influence of sediment transport characteristics and flow regime on flow doing most work.
Key : (i) Frequency, (ii) Instantaneous sediment discharge, (iii) Collective sediment discharge.

Wolman & Miller's calculations have shown that the frequency of occurrence of the flow which collectively transports most sediment equates with the frequency of bankfull flow. Thus the bankfull capacity of natural channels adjusts to the flow doing most work, and this explains why bankfull flow appears to be the dominant discharge.

For stable gravel bed rivers in the United Kingdom the return period of bankfull flow is the 1.5 year flood on the annual series ([8]) and this compares favourably with the results obtained for similar rivers in the United States ([9]).

Effects of River Regulation on Dominant Discharge

River regulation and interbasin transfers, through their influence on flow variability and mean flows, can have considerable effect on the magnitude and frequency of the flow doing most work. Consequently the channel downstream from the regulation point could be susceptible to either erosion or deposition as it adjusts its capacity and hydraulic geometry to the new flow regime.

Regulation can be achieved either through the operation of surface water reservoirs, allowing control downstream from the dam site, or through the use of river intake/outfalls linked to surface or subsurface reservoirs. In both cases flow variability will be reduced downstream from the regulation point because the magnitude and frequency of the flood flows are reduced in order to decrease the number of exceedingly low flows. Mean flows will also be modified if interbasin transfers are involved.

Reservoirs

There are many examples of scour effects downstream from reservoir sites. Primarily it results from the reduction in sediment load consequent upon dam construction([10])([11]) although modification to the flow regime can be a significant influence ([12]).

Consider the situation immediately downstream from a dam site. Initially this section will retain its ability to transport sediment at certain flow stages. As input load is zero erosion will commence which, in turn, will reduce the slope of the channel, reduce the bed shear stress, and increase the average size of the bed sediment. Consequently, the sediment transport rate for a given discharge will decline to zero (Figure 2). This progressive reduction in sediment output will cause erosion at downstream

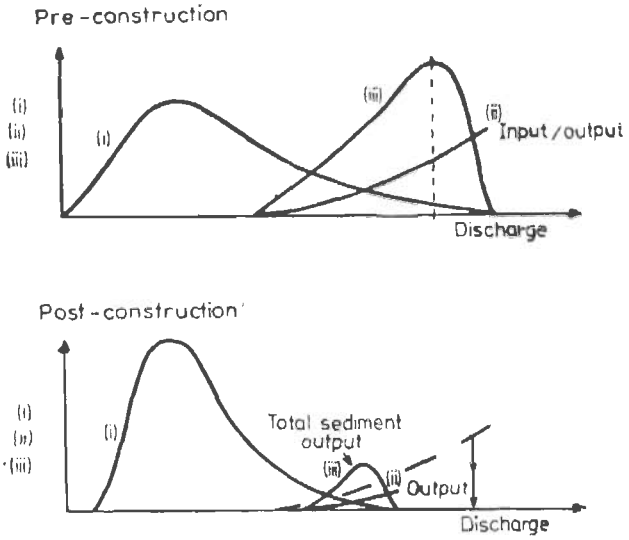

FIGURE 2 : Effect of dam construction on total sediment flow.

Key : (i) Frequency, (ii) Instantaneous sediment discharge, (iii) Collective sediment discharge.

sections and the process is repeated. The rate and extent of downstream erosion will depend on the nature of the alluvial material, the slope of the channel, the imposed flow regime, and the activity of tributary channels. If the tributary channels are unregulated sediment entering the main channel may not be transmitted by the reduced flow levels and this will tend to nullify its erosional ability. Even if the channel below the dam site is cut in bed rock erosion will probably be experienced in the alluvial stretches of the channel further downstream.

Stability can, in general, be maintained below reservoir sites by ensuring that the releases are kept below the sediment transport threshold. If localised deposition takes place at tributary junctions this can be flushed out by several large regulated releases.

River Intakes/Outfalls

Increasing use is being made of river sections for direct supply to, and releases from, regulating reservoirs. Often interbasin transfers are associated with such schemes. In this situation both the flow regime and the sediment transport characteristics of the channel are changed dramatically over a short stretch of channel and unlike the simple reservoir case, sediment input is not necessarily zero. The net long-term effect on the channel is governed by the pattern of abstractions and releases.

Channel instability would result if abstractions took place when sediment was being transported by the river and if the majority of the releases were above the threshold of sediment transport. Deposition would occur during abstraction because the input load would no longer be transmitted by the reduced flow levels. Conversely during releases erosion would occur because there would be negligible input load to be transmitted. Net erosion would result [Figure 3 (*a*)] and this would trigger complex upstream and downstream reactions as the river responds to the changed conditions.

If the majority of the releases are made below the threshold of sediment transport net deposition would occur because material deposited during periods of abstraction would not be removed [Figure 3 (*b*)].

Although regulation could, theoretically, produce a situation in which erosional and depositional activity are in balance, in practice this would be undesirable because it would promote similar fluctuations upstream and downstream due to the operation of feedback mechanism[8]. In addition there is no guarantee that the long-term stability of the channel could be maintained in this manner because experience with natural systems[6] indicates that erosional and depositional activity are rarely equal and opposite due to systematic changes in the hydraulic geometry of natural channels.

Thus if regulation precipitates any erosion or deposition at the intake/outfall point the feedback mechanisms will immediately operate to affect the stability of upstream and downstream sections. Equilibrium will only be achieved when the channel adjusts its hydraulic geometry and reduces its sediment transport capacity so that all abstractions and releases are below the threshold of sediment transport.

Clearly this defines the operational conditions for a river intake/outfall scheme : abstractions and releases

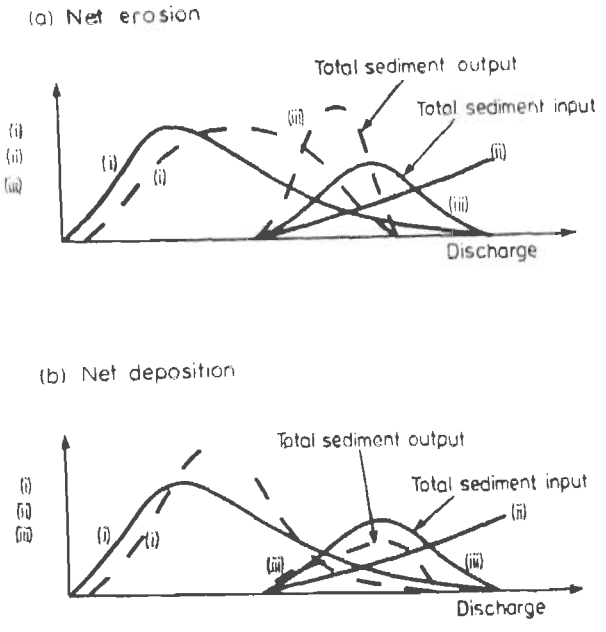

FIGURE 3 : Effects of regulation at river intakes/outfalls on total sediment flow.

Key : (i) Frequency, (ii) Instantaneous sediment discharge, (iii) Collective sediment discharge.

should be below the threshold and sediment transport if the stability of the channel is to be maintained and this applies to bed rock as well as alluvial channels.

Craig Goch Reservoir Investigation

Proposals for the largest single water resource development scheme ever planned in the United Kingdom were presented to Parliament for approval on 1 March 1975. The scheme, sponsored by the Severn-Trent, Welsh National, & Wessex Water Authorities is designed to meet the demands of the Midland region to the year 2001. To achieve this the capacity of Craig Goch reservoir in Mid Wales is to be increased from 9.09×10^6 cu m to 545.4×10^6 cu m by replacing the present dam with one 121.9 m high, making it the largest to be built in Europe. Unlike its neighbouring reservoirs in the Elan valley, which are direct supply reservoirs, Craig Goch will operate as a regulating reservoir drawing water in winter from the Rivers Wye and Severn and releasing it during summer drought periods (Figure 4). As demands are greater on the Lower Severn there will be a net transfer of water from the Wye to the Severn.

In order to ensure that regulation has minimal effect on the hydraulic geometry of the Rivers Wye and Severn it is essential that abstractions from and releases to these rivers are kept below the threshold of sediment transport. Both rivers have coarse gravel beds so the critical condition is the initiation of bed load movement. Transport of fine material in suspension is not particularly significant because the coarse material has to be moved before systematic erosion or deposition can proceed.

As interbasin transfers are an integral part of this scheme regulation is likely to have most impact on the River Severn. The results of a preliminary study on this river are illustrative of the techniques that are available to establish critical transport thresholds for gravel bed channels.

River Severn Intake/Outfall : Bed Load Transport Threshold

A lagoon excavated in the flood plain approximately 1 km downstream from Llanidloes is the proposed intake/outfall point on the River Severn. As no major tributaries enter the river for 13 km below this site

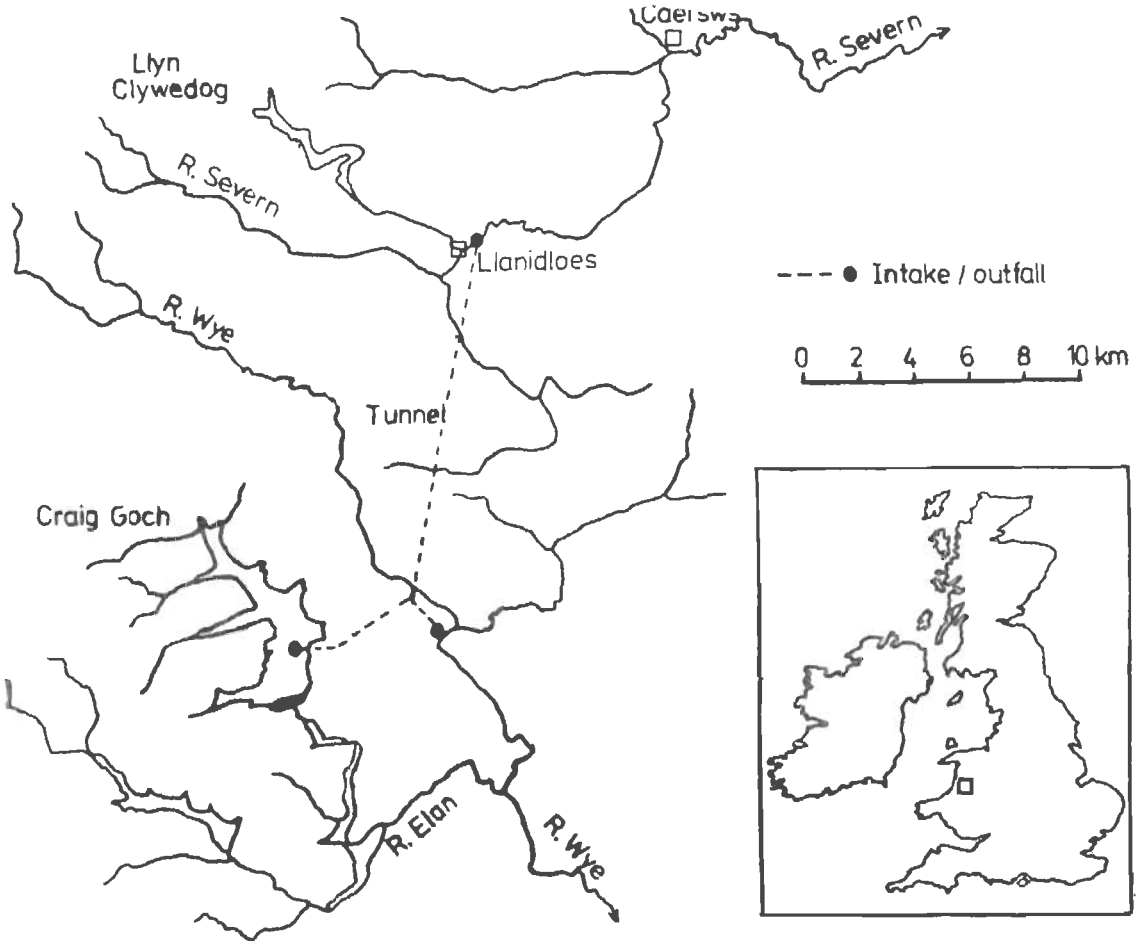

FIGURE 4 : Craig Goch Reservoir Scheme (from Sir William Halcrow & Partners, London).

regulation could have immediate effects as far downstream as Caersws.

Prior to the operation of Llyn Clywedog in 1967 river data collected from several surveyed sections on the Upper Severn indicated that the bankfull dimensions and capacity of the channel varied considerably between Llanidloes and Caersws (Table I). These variations were primarily due to downstream changes in channel stability because the river between the intake/outfall and a site 4 km downstream was basically stable, between 4 and 8 km it was eroding, and further downstream there was evidence of depositional activity ([6]). Thus though the proposed residual flow of 37 m^3/sec (releases and natural flow) may be below the transport threshold in the vicinity of the intake/outfall it may cause unnatural amounts of erosion of deposition further downstream. In these circumstances the maximum safe residual flow is defined by the maximum flow which will not transmit bed material in this stretch of channel. Although no upper discharge limit has yet been fixed for abstractions it is important that they should also be below the threshold of bed material transport if channel stability is to be maintained.

TABLE I

Bankfull capacity and hydraulic geometry of channel downstream from intake/outfall River Severn, U.K.

Distance Downstream from Intake/Outfall (km)	Estimated Bankfull Discharge (m^3/sec)	Estimated Bankfull Velocity (m/sec)	Median Grain Size Bed Sediment (mm)	Wetted Perimeter (m)	Hydraulic Radius (m)
1.6	114.3	1.78	35.5	33.53	1.91
2.8	165.5	1.98	40.2	39.01	2.38
4.0	137.8	1.73	60.0	35.84	2.23
6.8	52.1	0.87	48.0	78.27	0.76
11.4	54.8	1.27	57.5	56.08	0.77

Basically there are three techniques which can be employed to establish transport thresholds. They can be obtained either from reference to available sediment rating curves, from calculations based on sediment transport equations, or from observation of bed load transport events of various magnitudes.

Sediment Rating Curves

Although this would be the easiest way to establish critical transport thresholds such information is not available for this stretch of channel.

Sediment Transport Equations

Hydraulic data could be utilised to predict the critical discharge for the initiation of movement at each section. However, recent work by White et al ([13]) at the Hydraulics Research Station, Wallingford, U.K. has identified the inherent inaccuracy of many sediment transport equations. Three equations, namely those developed by Ackers & White([14]), Engelund and Hansen([15]), and Rottner ([16]), consistently showed the best conformance with the available flume and field data and any of these could be utilised to establish threshold discharges for sediment motion in sand bed channels with sufficient accuracy for a preliminary investigation. Their accuracy when applied to gravel bed channels is unknown and until further data is available from this type of channel their value, even for preliminary investigation, is doubtful.

Bed Load Transport Thresholds

In the absence of sediment rating curve information field experiments offer the most accurate solution to the problem. On the Severn releases from Llyn Clywedog can be used to simulate residual flows at the outfall and this allows the use of experimental procedures to establish critical threshold discharge for sediment transport.

A programme of research using these releases was planned for August 1974 but inclement weather caused postponement until 1975. However, experimental methods have been devised for use at a later date.

Six cross-sections will be utilised on the Severn, two in each of the major zones, stable, eroding and depositing, between Llanidloes and Caersws. A hundred cobbles and pebbles will be sampled ([17]) at each site painted and replaced. After the releases the sites can be inspected for bed load movement. If this indicates that the proposed releases are below the threshold of sediment transport at all sites they should not cause unnatural amounts of erosion or deposition. In order to establish the maximum discharge for abstractions the same techniques will have to be employed with natural flows.

However, if there is evidence of movement at one or more sites during the releases from Llyn Clywedog it will be necessary to establish the lowest critical threshold discharge, as this would constitute the upper discharge level for abstractions as well as releases. Unfortunately the releases have to be systematically increased in three stages over a three-day period so thus precludes inspection of the bed after each increase in discharge. To overcome this problem brightly painted spherical cork floats up to 1.5 cm in diameter will be attached by nylon line and pegs to the bed of the channel and placed under pebbles of known weight and dimensions. As soon as bed material movement occurs the corks will float to the surface. Ten floats will be installed at each section and, by using different coloured floats under particular sizes of pebble, the

threshold discharge can be established and also the percentage of the bed that is mobile at a given discharge. This information will identify the upper discharge limit for abstractions and releases if the channel is not to experience unnatural amounts of erosion or deposition.

Conclusions

Problems of channel instability associated with flow regulation are likely to be most acute in rivers where the critical threshold discharge for bed sediment transport is low. Even quite modest regulation schemes could have considerable effect on these channels.

In areas where this threshold is relatively high, as in the gravel bed rivers in the U.K., regulation has, until now, not constituted a major problem. Most storage reservoirs were constructed in upland areas and the compensation flows were normally insufficient to cause erosion. Even regulation reservoirs are unlikely to cause serious problems because the releases are usually below the threshold of sediment transport. The operation of river intakes/outfalls in conjunction with interbasin transfers constitute a more serious problem especially if one small headwater stream is used to regulate the flows of the main river. To achieve this aim releases to the headwater channel will have to be relatively large and, if this is above the bed sediment transport threshold, channel instability will result.

If this type of problem can be identified at the planning stage the various alternative strategies can be evaluated. These include the acceptable of channel maintenance costs, the relocation of the intake/outfalls lower downstream at section which can be regulated without causing instability, the construction of a number of intake/outfalls on other headwater channels, and the development of a number of smaller systems to replace the single large unit. At the moment it is impossible to assess the cost of channel maintenance because insufficient quantitative information is known about the operation of upstream and downstream feedback mechanisms as they respond to and control rates of erosion and deposition. With the others the optimum economic solution will depend on the relative costs of reservoir and pipeline construction.

Clearly it is important to recognise the possible effects of river regulation on alluvial channels so that appropriate measures can be taken to sustain their stability and prevent the destruction of valuable agricultural land, maintain their capacity to transmit flood flows, and retain their recreational appeal.

Acknowledgements

The section of this report concerned with the Craig Goch Reservoir Investigation describes research which is being carried out for the Severn-Trent Water Authority. The author gratefully acknowledges the assistance of Sir William Halcrow and Partners, London for the provision of flow data and the Severn-Trent Water Authority for permission to publish this information.

References

(1) WATER RESOURCES BOARD : "Water Resources in England and Wales." Vol. 1 : Report, Vol. 2: Appendices H. M. S. O., London, 1973.

(2) INGLIS, C. C. : "Meanders and their Bearing on River Training." Inst. Civ. Eng. Maritime and Waterways Paper No. 7, 1947.

(3) INGLIS, C. C. : "The Behaviour and Control of Rivers and Canals." Res. Pub. Cent. Board Irrig. India, No. 13 (Simla), 1949.

(4) NIXON, M. : "A Study of the Bankfull Discharge of Rivers in England and Wales." Proc. Inst. Civ. Eng., Vol. 12, 1959, pp. 157-174.

(5) ACKERS, P. and CHARLTON, F. G. : "Dimensional Analysis of Alluvial Channels with Special Reference to Meander Length." Jour. Hyd. Res., Vol. 8, 1970, pp. 287-315.

(6) HEY, R. D. : "Analysis of Some of the Factors Influencing the Hydraulic Geometry of River Channels." Unpublished Ph.D. Thesis, Cambridge, 1972, pp. 1-217.

(7) WOLMAN, M.G. and MILLER, J. P. : "Magnitude and Frequency of Forces in Geologic Processes." Jour. of Geol., Vol. 68, 1960, pp. 54-74.

(8) HEY, R. D. : "Design Discharge for Natural Channels." In R. D. Hey and T. D. Davies (Eds.), Science & Technology in Environmental Management, Saxon House, D. C. Heath Ltd., U.K., 1975, (in press).

(9) WOLMAN, M. G. and LEOPOLD, L. B. : "River Flood Plains : Some Observations on their Formation." U.S. Geol. Survey Prof. Paper 282-C, 1957, pp. 87-109.

(10) SONDEREGGER, A. L. : "Modifying the Physiographic Balance by Conservation Measures." Trans. Amer. Soc. Civ. Eng., Vol. 100, 1936, pp. 284-304.

(11) KOMURA, S. and SIMONS, D. B. : River Bed Degradation below Dams." J. Hyd. Div. Amer. Soc. Civ. Eng., Vol. 93, No. HY 4, 1967, pp. 1-14.

(12) GREGORY, K.J. and PARK, C. : "Adjustment of River Channel Capacity Downstream from a Reservoir." Water Resources Res., Vol. 10, No. 4, 1974, pp. 870-873.

(13) WHITE, W.R. ; MILLI, H. and CRABBE, A.D. : "Sediment Transport : An Appraisal of Available Methods." Hydraulics Research Station, Wallingford, U.K., INT 119, November 1973, pp. 1-54.

(14) ACKERS, P. and WHITE, W.R. : "Sediment Transport : New Approach and Analysis." J. Hyd. Div. Amer. Soc. Civ. Eng., Vol. 99, No. 11, 1973, pp. 2041-2060.

(15) ENGELUND, F. and HANSEN, E. : "A Monograph on Sediment Transport in Alluvial Streams." Danish Technical Press, Copenhagen, 1967.

(16) ROTTNER, J. : "A Formula for Bed Load Transportation." La Houille Blanche, Vol. 4, No. 3, 1959, pp. 301-307.

(17) WOLMAN, M. G. : "A Method of Sampling Coarse River Bed Material." Trans. Amer. Geophys. Union, Vol. 35, No. 6, 1954, pp. 951-956.

Economy through Hydraulic Designs in Water Utilisation Projects

C. V. GOLE
Member (Water Resources)
Central Water Commission, New Delhi (India).

P. C. SAXENA
Director

C. P. VENKATRAMAN
Chief Research Officer

V. N. DIWANJI
Assistant Research Officer

V. RAMANATHAN
Assistant Research Officer

Central Water and Power Research Station, Poona (India).

SYNOPSIS

Water is the most precious and an essential element for the existence of life. Harnessing the available water resources and wisely utilising them will bring increasing prosperity to the country. Many gigantic multipurpose river valley projects like Beas, Koyna, Ukai, etc., were undertaken mostly with indigenous technical know-how. Each project provided inherent incentive for ingenuity in planning, design, research and execution. Engineers had to accept the challenge to solve the peculiar problems posed by unfavourable topography, geology and economic considerations. Some unique hydraulic designs which were developed and successfully used have been highlighted. They also have potential economic utilisation in projects of similar situations.

1. Introduction

1.1 One of the most exhilerating aspects of development of water resources is the seemingly incessant challenge to solve unique problems. Even in the simplest of the Hydro Projects, there is a reasonable scope for ingenuity in design, construction and operation. More than often, new and daring approaches are demanded. No single answer can be applied indiscriminately to every project, because each has its own set of singularities.

1.2 The challenge may present itself in different forms. It may concern undesirable site conditions such as topography precluding the possibilities of economical layout, poor quality of rock for foundation, type of construction consuming considerable time and unusual hydrological considerations. Likewise, answers may be required to difficulties of operating the control gates under emergencies created by natural calamities which cannot always be predicted. Many times, special efforts are needed to give proper balance between benefits and costs to assure the economic justification of Water Resources Projects. Fundamentally, hydraulic problems posed by dynamic flow of water during diversion and ultimate stages of the project operation have to be solved by proper means to maintain the economic interests of the project at every stage as explained in the article.

2. Flow Deflector for Minimising Cost of Protective Works of adjacent Structures during Diversion Stage

2.1 The Ukai Hydro-electric Project which has been completed in the year 1972 consists of a composite masonry-cum-earthen dam near the village Ukai about 116 km upstream of Surat city of Gujarat State, India. The project provides irrigation to 1.5 lakh ha of land and would ultimately generate 300 MW of power. Protection

of downstream region which was being flooded frequently has also been achieved by this project.

2.2 Sub-surface investigations showed that the left terrace provided an ideal site for spillway as the rock profile was predominantly higher on the left flank and dipped rapidly towards the right bank of the river. The main river was closed by an earthen dam rising about 69 m above the river bed and involved laying of as much as 7.36 million m^3 of earth work which could not be tackled in one season but had to be spread over a minimum period of three working seasons. Passing the monsoon floods over the partly completed earthen dam, though achieved successfully on many projects in the country and elsewhere, was ruled out at Ukai because of the staggering flood peaks that had to be faced. The flood peak to be passed was as high as 45,000 m^3/sec. Suitable diversion of the river, therefore, presented a major problem.

2.3 The geological and topographical situations at the site and the immensity of the discharge to be faced made the choice of tunnels for diversion economically infeasible. Hence, the diversion of the river was effected through an open cut channel of suitable dimensions. The diversion channel at Ukai catered to a discharge of the order of 45,000 m^3/sec which was nearly four times the discharge of the River Nile at High Aswan Dam, Egypt. The layout of the diversion channel had to be curvilinear in order to be economical and this was expected to result in spiralling currents and cross waves (see Figure 1).

Literature available on open channel flow does not throw enough light on the design practices for curved reaches. The normal practice is to provide a radius of curvature equal to certain multiple say 7 to 15 of the bed or water surface width([1]). However, the effects of spiral or helicoidal flow are minimised when the radius of curvature is about 3 times the width of the channel. From economic considerations, the shortest curvature possible for the Ukai diversion channel was a radius of 541.5 m which gave a ratio of 2.3 for the radius to the width of the channel.

2.4 The layout of the diversion channel was studied in a 1/100 scale hydraulic model, initially for a discharge of 28,000 m^3/sec. As expected, the flow velocities at

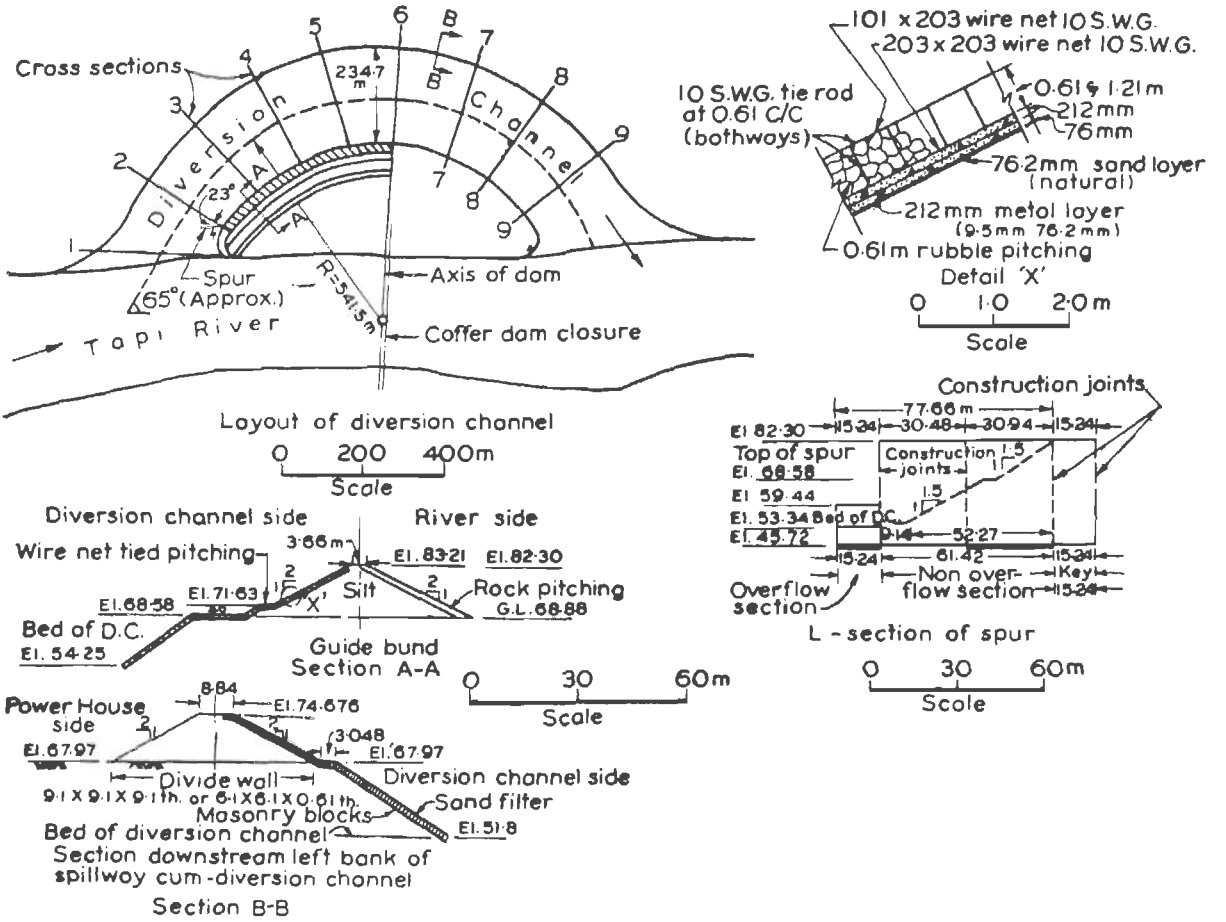

FIGURE 1 : Layout and details of the diversion channel, Ukai Dam Project, Gujarat.

the beginning of the bend were more at the inner bank when compared to the outer curve of the channel. High velocity filaments crossed gradually to the outer bank and the low velocity filaments moved nearer the inner bank in the initial reaches of the channel, until a section was reached from where the outer bank velocities were consistently higher in consonance with the theoretical expectations. The velocities on the right bank were as high as 14 m/sec in the beginning and sharply dropped to about 3 to 4 m/sec thereafter (see Figure 2). A most economical banking involving least rock cutting on the bed of the diversion channel gave only a marginal relief (see Figure 2) and the safety of the diversion dam was still jeopardised. Protective pitching against the bank velocities of the order of 14 m/sec would require blocks weighing about 680 tonnes(2). This would not only involve large investment but also considerable time and it was not possible for the project engineers to raise the diversion dam within a working season as scheduled.

2.5 Considerable discussions ensued to evolve a suitable hydraulic means to minimise the cost and time of construction of the protective works. It appeared necessary to supplement the action of the superelevation by a proper means to deflect the high velocity currents from the right bank. Studies on the hydraulic model proved the idea of a deflecting spur was the best under the circumstances. Various combinations of location, lengths and angle of the spur were studied on the model and the most economical choice for a diversion discharge of 28,000 m^3/sec appeared to be a deflector spur oriented at an angle of 23 degrees with respect to the radial line(3) (see Figure 1). With this means the local velocity at the entrance of the diversion channel dropped from 14 m/sec to about 3 m/sec and even 1 m/sec (see Figure 3). The ultimate economy on this account which depended upon the sixth power of velocity (stone size) is shown in Figure 5. As the studies were in progress, the River Tapi experienced a flood of 42,000 m^3/sec in the year 1968 against the original design flood of 28,000 m^3/sec. The hydrology of the river was reviewed and it was decided to check the design of the deflector spur for a revised discharge of 45,000 m^3/sec (Figure 4). It was not possible to alter the design of the diversion channel but the possibilities of increasing the height of the diversion dam and redesigning the protective measures were kept in view. The efficacy of the spur structure

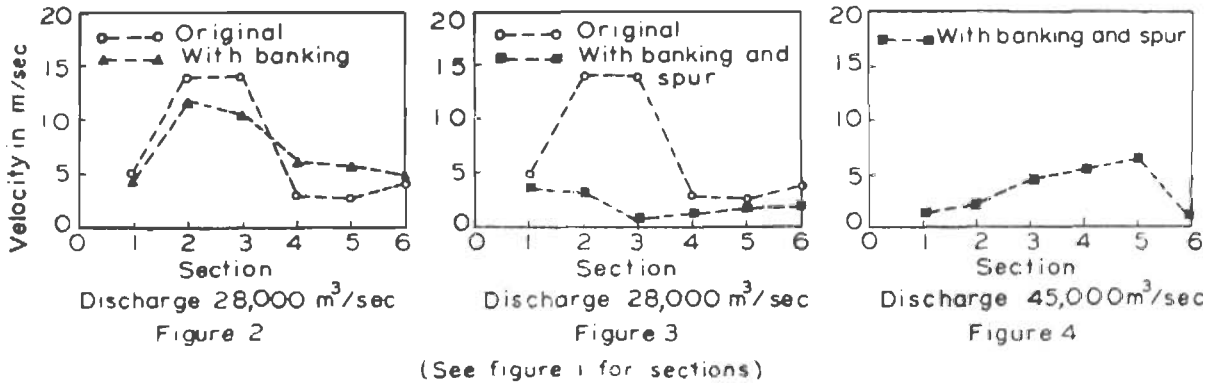

FIGURES 2, 3 & 4 : Velocity along upstream right bank of diversion channel.

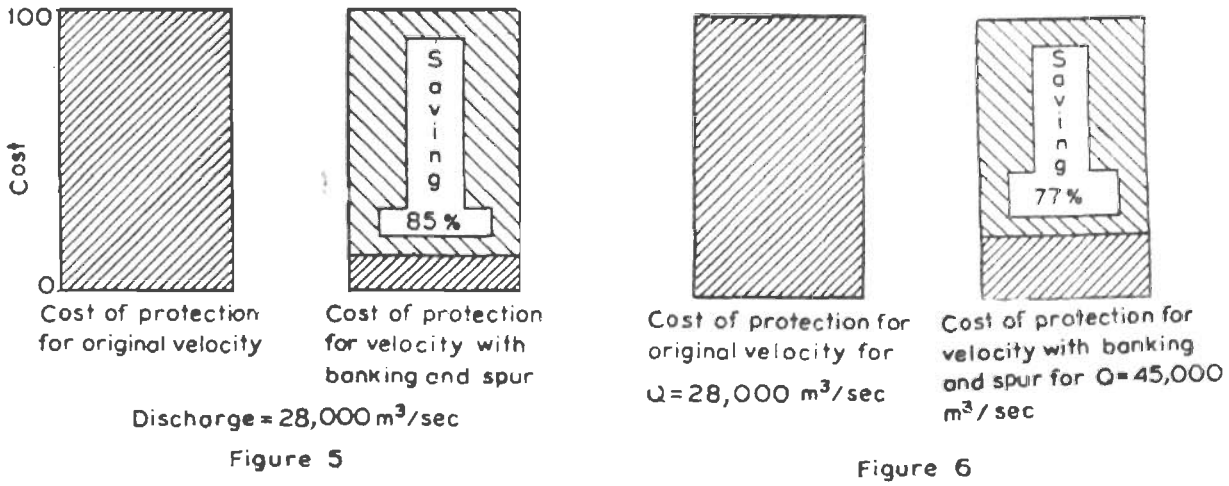

FIGURES 5 & 6 : Ultimate saving in protection of upstream right bank—Results of Studies on Diversion Channel, Ukai Project.

for the revised design discharge of 45,000 m³/sec is shown in Figure 6. The study indicated that masonry blocks of sizes ranging from 6.1m×6.1m×0.61m to 9.1m×9.1 m×0.91m were sufficient to withstand the local velocities of 9 to 12 m/sec respectively (see Section B-B of Figure 1). A special type of caged pitching using wire nets on the right bank was used for protection of the field structure (see detail 'X' of Figure 1). In the year 1969 a flood of 28,000 m³/sec passed in the diversion channel and in the year 1970 an increased flood of 37,000 m³/sec which was nearly equal to 80 percent of the revised design discharge passed through the diversion channel safely and thus proving the deflector spur as a hydraulic means to effect economy for the open channel diversion of the entire river during the construction of the Ukai Dam Project. The approximate saving on account of this hydraulic design was about 40 percent of the cost of the flood diversion works of the project.

3. Segmental Overflow Crests for augmenting Discharging Capacity over Spillways in a Narrow Width

3.1 The Badua Dam aims at harnessing the River Badua for irrigating 32,500 ha of land in Bhagalpur and Monghyr districts of Bihar State, India. The main river was blocked by a 457 m long and 40 m high earthen dam to create the reservoir. The spillway consisted of a concrete overfall and chute. A secondary weir with an Ogee crest was situated just at the lower end of the chute (Figure 7). Thus the energy of fall of 27.59 m of water head from the reservoir to the downstream channel was divided into three steps of 3.21 m, 22.75 m and 1.63 m respectively. The effluent energy from the lowest weir was passed into an artificial open channel before it ultimately cascaded into the river.

3.2 The maximum spillway outflow was of the order of 2,831 m³/sec. The spillway site was located in a saddle between two hillocks rising steeply in certain portions. The valley between the hillocks had gradual convergence followed by a diversion in plan. The minimum clear width between the hillocks was 75 m.

3.3 Considerable attention was paid to the optimisation of the spillway layout and basic design because of the relatively high cost of flood provision. The main problem lay in the proper choice of the spillway with the restrictions imposed on the width of the chute by the hillocks. The maximum width of the chute compatible with minimum side hill cutting was fixed at 91.4 m. Several alternative spillway arrangements were investigated and extensive hydraulic model studies carried out on the main spillway(4)(5). The development of the layout started with a straight alignment

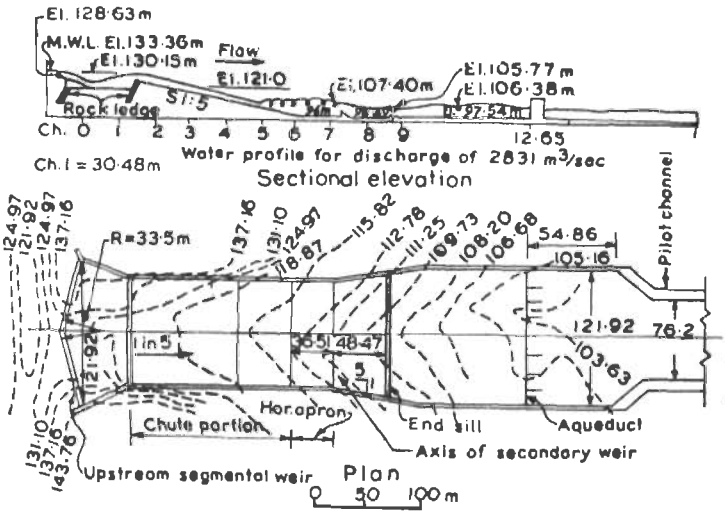

Figure 7

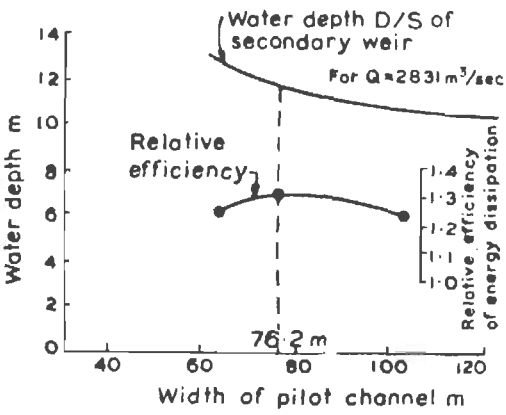

Figure 9: Design of pilot channel

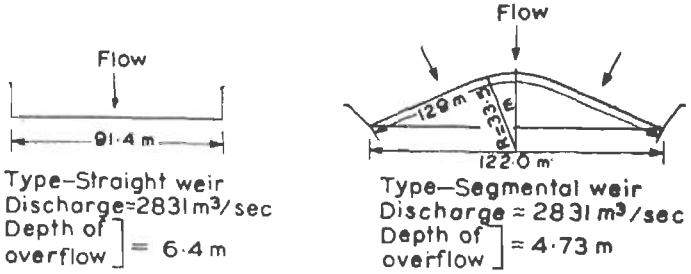

Figure 8. Comparative study

FIGURES 7, 8 & 9 : Chute Spillway, Badua Dam, Bihar.

which carried the maximum outflow of 2,831 m³/sec at a depth of 6.4 m (see Figure 8). Various crest alignments including semicircular, triangular and other curved and pologonal shapes were studied in order to achieve economy in the height of the dam. Some arrangements which were effective at lower discharges experienced hurdling action in the stilling basin at higher discharges due to the interference of the lateral flows. These designs were also found to involve larger costs for foundation.

3.4 Further study brought to light that it would be most economical if the spillway layout followed the shape of rock ledges in plan as revealed by the subsurface exploration carried out in the field when the hydraulic model studies were in progress. Accordingly, the layout of the spillway was modified keeping in view maximum hydraulic efficiency compatible with the economy of cost of foundation and also the hill cutting on the sides to create a good approach to the spillway. The finally adopted design was a segmental weir, consisting of two straight lines connected tangentially by a central arc of 33.5 m radius (see Figure 8). The relatively high capacity of this type of spillway was associated with fairly smooth flow conditions in the approach to the spillway, provision of suitable controlling chute slope to prevent throttling of the flow at higher discharges and also the necessary minimum chute width for the discharge in keeping with minimum side hill cutting. The increased capacity of the spillway resulted in a saving of about 2 m in the height of the earthen dam.

3.5 The discharge from the lower weir was passed into an artificial channel. In evolving the dimensions of this channel it was to be ensured that the excavation and the hill cutting remained minimum. At the same time, it was to be ascertained that the hydraulic jump did not get drowned to an extent to impair energy dissipation. Care was also taken to provide necessary sequent depth for the hydraulic jump after the pilot cut channel developed and attained the regime depth in due course of time. Thus the economical setting of the stilling basin level was also to be kept in view. All these factors were studied and an initial cutting of 76.2 m width was adopted for the pilot channel. Figure 9 shows the results of the studies made for the design of the optimum dimensions of the tail channel. It can be seen that the proper hydraulic design of the spillway crest and the tail channel resulted in saving in the height of the dam and also helped to avoid unnecessary hill cutting and earth excavation for the tail channel.

4. *Twisting and Laterally Spreading Ski-jump to Minimise Bank Cutting and Erosion in the River Bed*

4.1 The 70 m high concrete dam across the River Umium in Assam, India, is an integral part of the Umium Barapani Hydro-electric Project which generates 36,000 kW of hydropower. The dam site is situated slightly downstream of a sharp right angled bend in the river. Disposal of floods of the order of 2,100 m³/sec is effected through two spillway spans 12.19 m × 11.93 m provided with radial gates (see Figure 10).

4.2 Design of the energy dissipator for the spillway

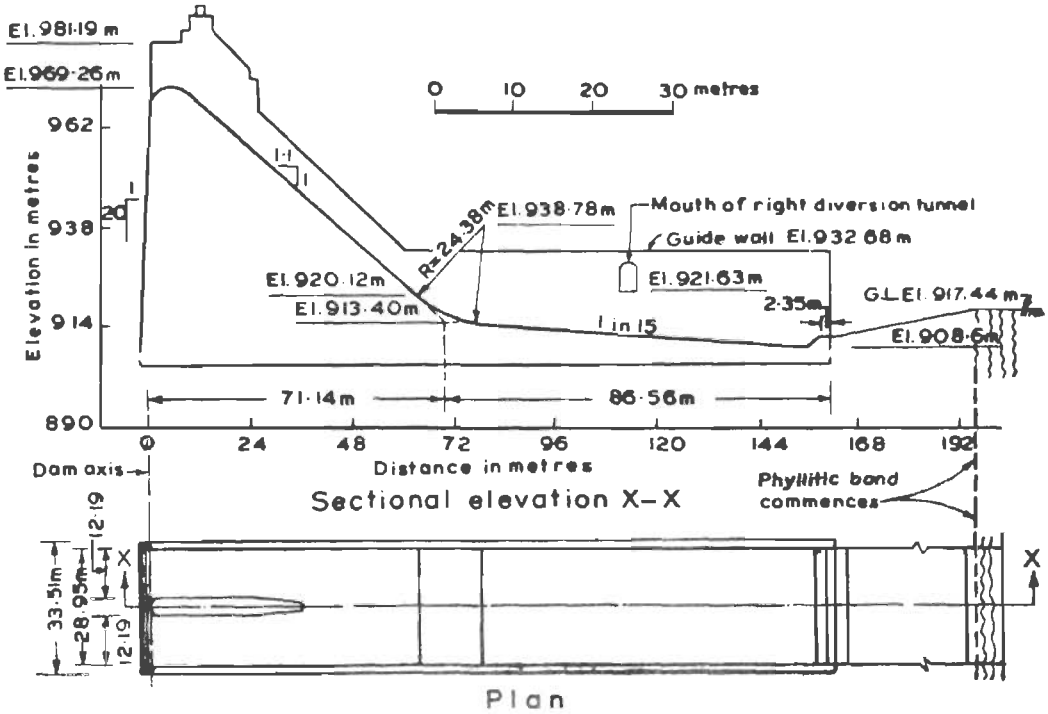

FIGURE 10 : Details of sloping apron—Studies on energy dissipators, Umium Barapani Hydro-electric Project, Assam.

posed numerous problems. There was a soft phyllitic band at a distance of 195 m from the axis of the dam. Design of the energy dissipating device was required to meet the needs of satisfactory hydraulic performance against inflow velocities as high as 35 m/sec and minimum impact on the phyllitic band.

4.3 A hydraulic jump type energy dissipator was considered the best in view of its efficiency of energy dissipation. The maximum conjugate depth for the stilling basin was of the order of 22 m. The floor level and dimensions of the sloping apron designed on this basis of the tail water rating curve at the site are depicted in Figure 11. Studies on this design revealed satisfactory hydraulic performance and there was a good degree of energy dissipation within the apron.

4.4 The sloping apron design was found to interfere with the outfall of the diversion tunnel at a distance of 112 m from the axis of the dam. Also, the design involved deep excavations and concreting over a long length. The excavation for the apron involved a depth of about 12 m below average ground level and a width of 36 m over a length of about 87 m. The huge quantity of rock excavation and concreting in the difficult terrain was very costly and hence called for an economic design with reasonable hydraulic efficiency.

4.5 Feasibility studies on a roller bucket did not yield satisfactory results from the point of view of economic energy dissipation. Hence, recourse was taken to ski-jump bucket type dissipator and investigations were carried out on the model to evolve a suitable design.

4.6 Three designs of ski-jump bucket with inverts at El. 917.45 m, 918.97 m and 920.49 m by maintaining the bucket radius at 24.38 m and lip angle at 40° were studied. In all the three cases, ski-jump action was perfect with good aeration for all depths of overflow. For the lowest bucket level, the jet impinged on the soft phyllitic band where supercritical flow occurred downstream. With the invert at 920.49 m the jet impinged on the ground at about 12.2 m upstream of the soft phyllitic band. At this stage, it was decided to device a suitable modification in the design to introduce more air-entrainment for the dimunition of the energy of the falling jet. The lip of the ski-jump bucket with invert at El. 920.49 m was modified into the form of a jet spreader with the lip angle of 40° in the middle, decreasing to 30° at the flanks. In plan, the lip conformed to the parabola $Y = 0.0167\ X^2$. The design was studied on the model(5). It was observed that the ski-jump jet spread over a large area due to differential throw off. Wider spreading of the divergent jet resulted in larger air-entrainment and consequently reduced impact pressures on the ground. The area of impact was more than in the case of a conventional ski-jump bucket with uniform lip angle throughout. The ski-jump jet was more divergent towards the right for discharges larger than 1,652 m³/sec and attacked the right bank of the river (see Photo 1). This divergence could be attributed to the asymmetrical approach of the river upstream of the spillway. The attack on the right bank was undesirable as it would lead to sliding of the hillock into the river. A cross superelevation was imposed in the bucket so as to twist the ski-jump jet in space and divert it towards the left. Radii of different magnitudes were considered for the curvatures between the invert and the lip. Starting with a radius of 24.38 m at the right, the radius progressively increased to 27.43 m at the centre and eventually to 30.48 m at the left extreme of the bucket. The spreading of the ski-jump was effected by altering the lip angles from 40° on the right

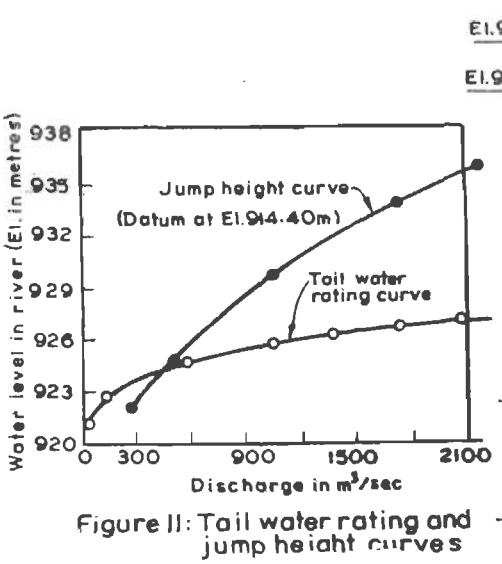

Figure 11: Tail water rating and jump height curves

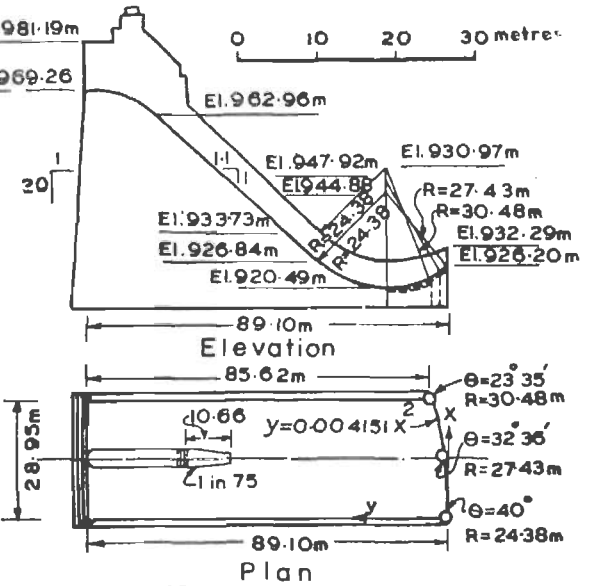

Figure 12: Superelevated skijump bucket

FIGURES 11 & 12: Studies on energy dissipators, Umium Barapani Hydro-electric Project, Assam.

flank to 23° 35′ on the left by imposing a parabolic shape to the lip in plan (see Figure 12). Studies on the design showed that the attack on the right flank was avoided except for the grazing of stray jets for the maximum discharge (see Photo 2). Thus, by providing a cross superelevation to the bucket, impingement of the jet on the right bank was avoided thereby eliminating protection works which would have entailed exhorbitant costs. In addition, by providing a ski-jump, the quantity of excavation required for the energy dissipating device was reduced by about 90 percent as compared to the sloping apron.

5. Use of Improvised Stilling Basin for Diversion-cum-Power Tunnels to Accommodate Power House

5.1 The Beas Dam Project has a 116 m high sand-gravel-boulder fill major dam on the River Beas, a tributary of River Indus near village Pong, Punjab, India. It is one of the units in the comprehensive plan for the development of irrigation and power potential for the Punjab and Rajasthan States. The outlet works for diversion of discharge during construction consisted of five tunnels of 9.14 m diameter each. Three of these tunnels (designated as P_1, P_2 and P_3) will house 7.5 m steel penstocks for the generation of power in the ultimate stage. Part of the first diversion stage discharge was passed through the power tunnels. In the design, two power tunnels (P_1 and P_2) have been separated from the third one (P_3) by a long divide wall. The tunnels P_1 and P_2 had a common stilling pool (see Figure 13). The tunnel P_3 had an elaborate design of stilling basin as this had to serve a longer period of diversion. However, the stilling basin requirements for the diversion stage power tunnels P_1 and P_2 were less demanding for the following reasons :

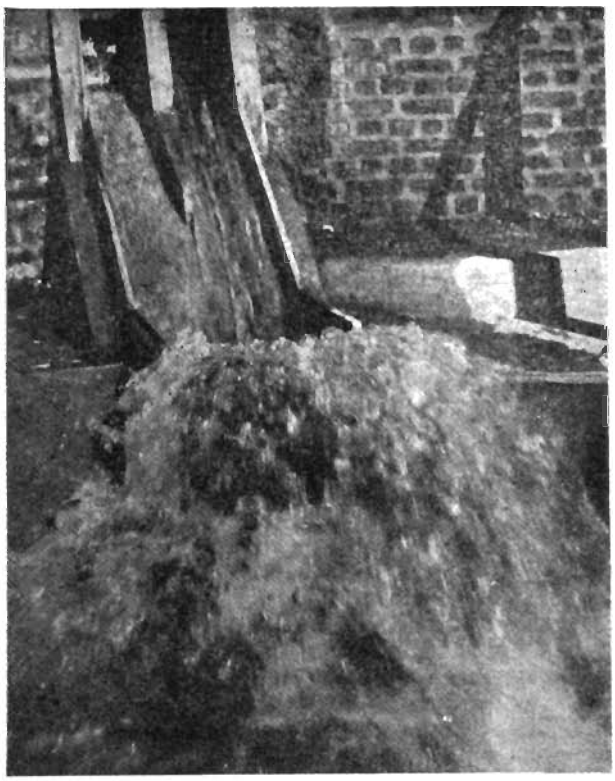

PHOTO 1 : Performance of ski-jump bucket—Energy dissipator, Umium Barapani Hydro-electric Project, India. ($R = 24.38$ m; $\theta = 40°$ at the centre and $\theta = 30°$ at the flanks).

PHOTO 2 : Performance of the ski-jump with cross superelevation downstream of the invert Energy dissipator, Umium Barapani Hydro-electric Project, India.

(*i*) the stilling basin would function for only two years or so during construction,

(*ii*) the channel downstream was proposed to be concrete lined completely up to the outfall into the river, and

(*iii*) after installation of power penstocks and the turbines in the valve house floor, the turbine efflux would have considerable lesser velocities.

5.2 The maximum head during diversion was of the order of 60 m with a maximum discharge of 1,286 m³/sec through each tunnel. Hydraulic studies on a 1/40 scale model indicated that the performance of the valve house floor as a stilling basin was very poor. The flow from the tunnel did not follow the rapid expansion resulting in high velocities along the centre line of the tunnel accompanied by the eddies on sides to a considerable distance (see Figure 13 and Photo 3).

5.3 It became evident from the studies that unless the momentum change from the tunnel exit took place in a more regular pattern, the energy dissipation would not be sufficient. Introduction of fine grain turbulence by formation of at least a partial hydraulic jump with

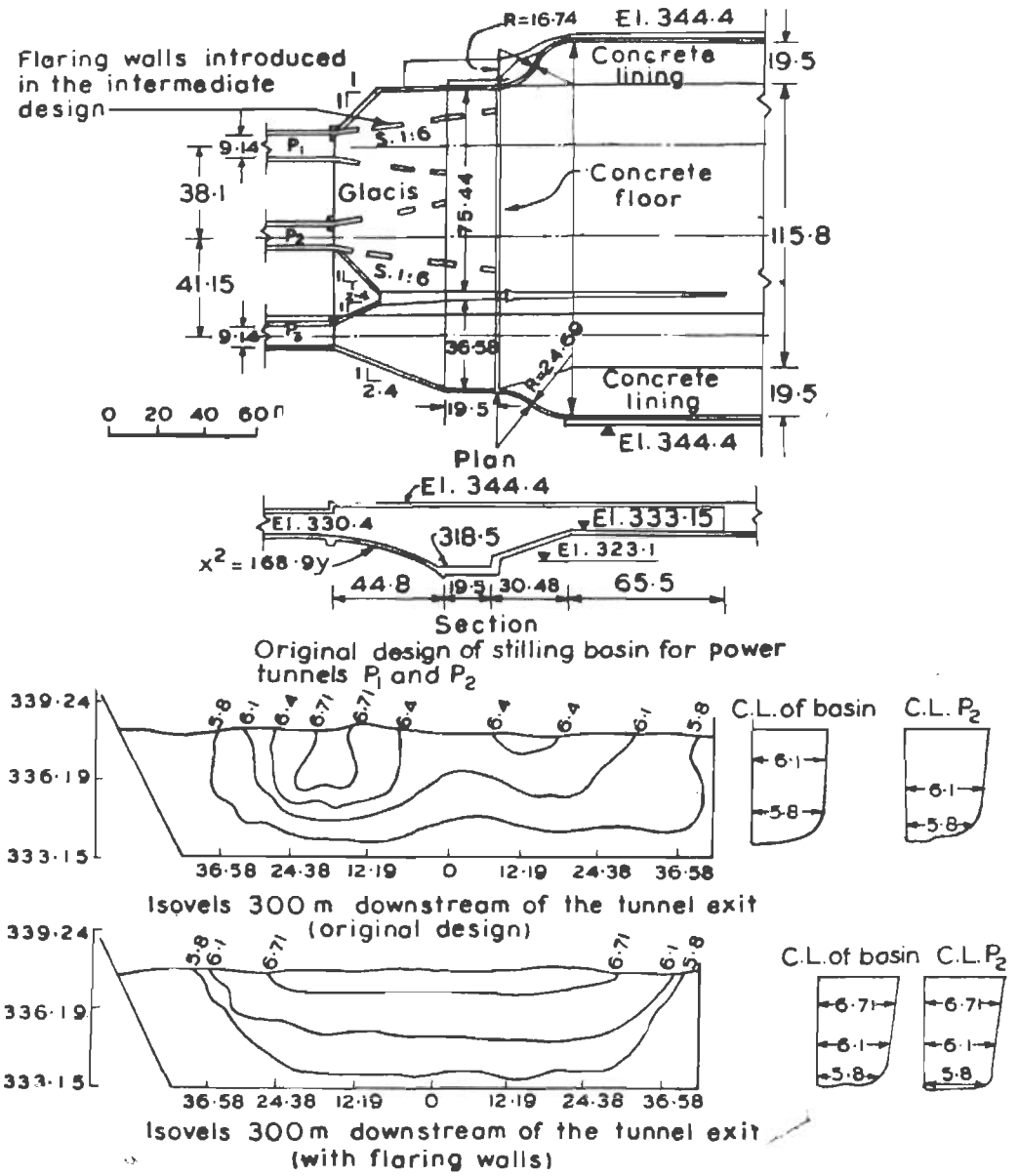

FIGURE 13 : Design of stilling basin power tunnel (diversion stage) Beas Project.

minimum horizontal reverse flow would achieve reasonable energy dissipation(6). On this background an improvised design of 1 : 6 flaring side walls was evolved to achieve gradual expansion of the jet (see Figure 13). Intermediate openings on the side walls at regular intervals were intended to equalise the lateral hydrostatic pressures and to effect economy in the design of walls. This design was an eventual step to increase energy dissipation. While the studies were in progress certain modifications were introduced in the design to suit the revised layout of the wye branches of the turbine penstock. The parabolic glacis was lengthened from 44.8 m to 52.0 m. The length of the valve house floor was also increased from 19.5 m to 47.0 m. Another major modification was lowering the bed level of the tail-race channel by 3.66 m to gain head on the turbine (see Figure 14). The experience on the previous model studies were kept in view while determining the radius of curvature of side wall to satisfy the hydraulic condition as well as the requirements of space necessary to accommodate the wye branches and the turbines in the ultimate stage. This resulted in reduced excavation (see Figure 14). The flow within the curved walls on the parabolic glacis resembled the phenomenon of a

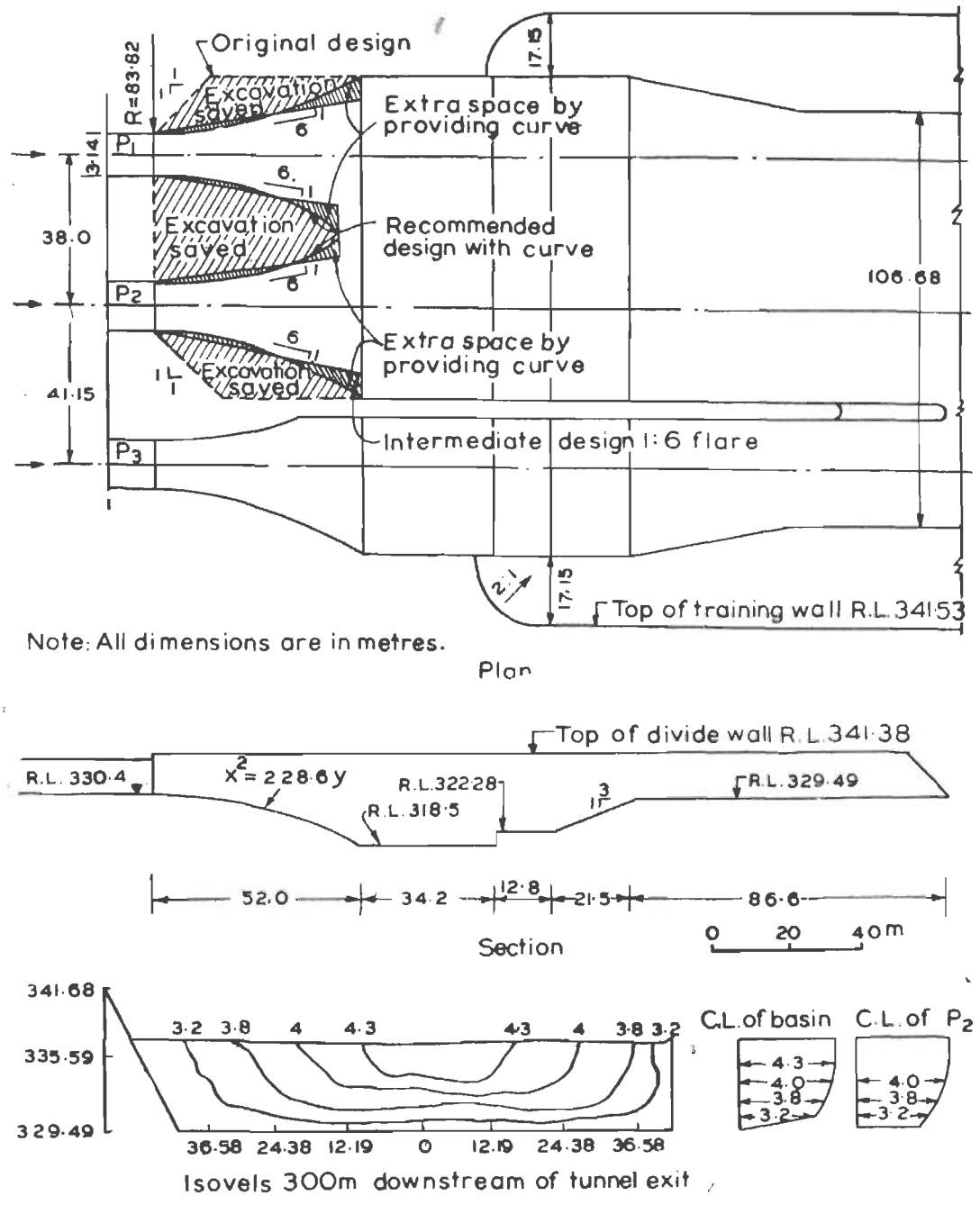

FIGURE 14 : Recommended design of stilling basin power tunnel (diversion stage) Beas Project.

PHOTO 3 : Performance of the stilling basin for power tunnels P_1 and P_2 (diversion stage), Beas Project, India (original design). Discharge through each tunnel = 1286 m^3/sec, tail-water elevation = 337.41 m.

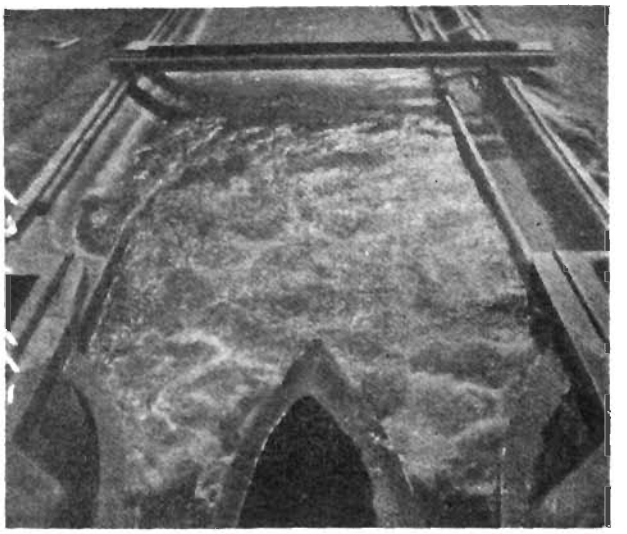

PHOTO 4 : Performance of the stilling basin for power tunnels P_1 and P_2 (diversion stage), Beas Project, India (modified design). Discharge through each tunnel = 1286m^3/sec, tail-water elevation = 337.41 m.

hydraulic jump forming partly on the parabolic floor and partly on the horizontal floor of the valve house. Basic studies conducted at CWPRS, Poona, indicated that the sequent depth requirement for hydraulic jumps on the parabolic floor would be lesser than that on the uniformly sloping floor. Thus it would seem that the utilisation of the parabolic glacis with a proper lateral divergence for the formation of hydraulic jump would give reasonable energy dissipation for the diversion stage design. However, in the present case the actual depth of flow above the valve house floor was about 8 to 10 percent more than that required for the hydraulic jump on the horizontal floor of the valve house. Studies showed spectacular improvement in energy dissipation (see Photo 4 and Figures 13 & 14). The velocities near the bank were reduced from about 5.8 m/sec to 3.2 m/sec. This resulted in a large saving of the cost of bank protection. In addition, proper choice of improvised stilling basin utilising the structures intended for the ultimate Power House Structure provided economical design of the energy dissipator for flow diversion through the power tunnel of Beas Project.

6. "Slot Flow Arresters" for Minimising Downpull of Emergency Gates in High Head Conduits

6.1 The epoch making earthquake in December 1967 necessitated immediate depletion of the Shivaji Sagar Reservoir for the inspection of possible damage to the Koyna Dam, India. Additional outlet facilities were, therefore, planned by converting the penstock pipes into outlets sluices with suitable terminal constrictions to bring the average velocities in the improvised sluice to a limit of 13 m/sec. The penstocks had individual bulk head gates at the bellmouthed entrances followed by intake gates operated by hydraulic hoists. The intake gate of size 1.98 m × 2.59 m designed for operation under a head of 71 m had upstream skin plate and upstream seals with supporting girders on the downstream side (see Figures 15 & 16). The design hoisting capacity of the gate was 28 tonnes which accounted for the weight of the gate (5.5 tonnes) frictional forces (19.3 tonnes) and water load (2.3 tonnes).

6.2 When the gate was operated under a head of 38 m in April 1968 it opened only up to a height of 0.6 m, from its closed position, when the oil pressure in the hoist cylinder indicated an intensity of 110 kg/cm^2 (100 kg/cm^2 was equivalent to 28 tonnes) which was 10 percent in excess of the design capacity of 28 tonnes[7]. Pressure on the bonnet cover was 0.7 kg/cm^2 which amounted a downpull force of 14 tonnes on the gate as against the design value of 2.3 tonnes under 71 m head.

6.3 Unless measures were taken to reduce the water load on the top of the gate it could not be opened further. In the hydraulic design of the fixed wheel gate with upstream skin plate and seals the inflow into the gate housing due to the leakage flow past deshaped seal and also the vertical flow within the gate slots caused by steep pressure gradients in the converging stream lines below the lip of the gate are to be considered[8]. Water entering the gate housing flushes out through the outflow gap on the downstream side between the body of the gate and the downstream face of the gate housing and also through the drain holes on the web plate of the girders. The outflow is a function of the residual head which stagnates on the top of the gate as a result of the unsteady inflow-outflow-storage balance in the gate housing. The residual head on the top of the gate augments the downpull forces on the gate.

6.4 In the present case, increasing the capacity of the

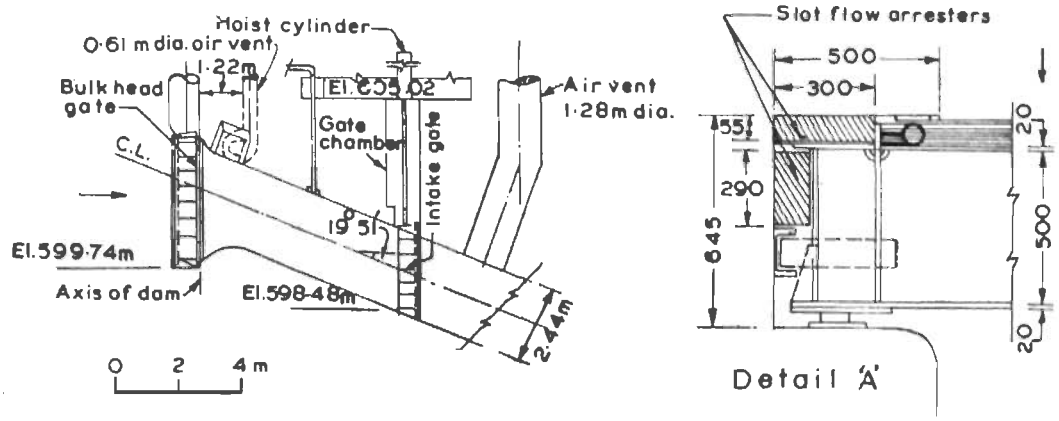

FIGURE 15 : Disposition of the gates in the penstock, Koyna Hydro-electric Project.

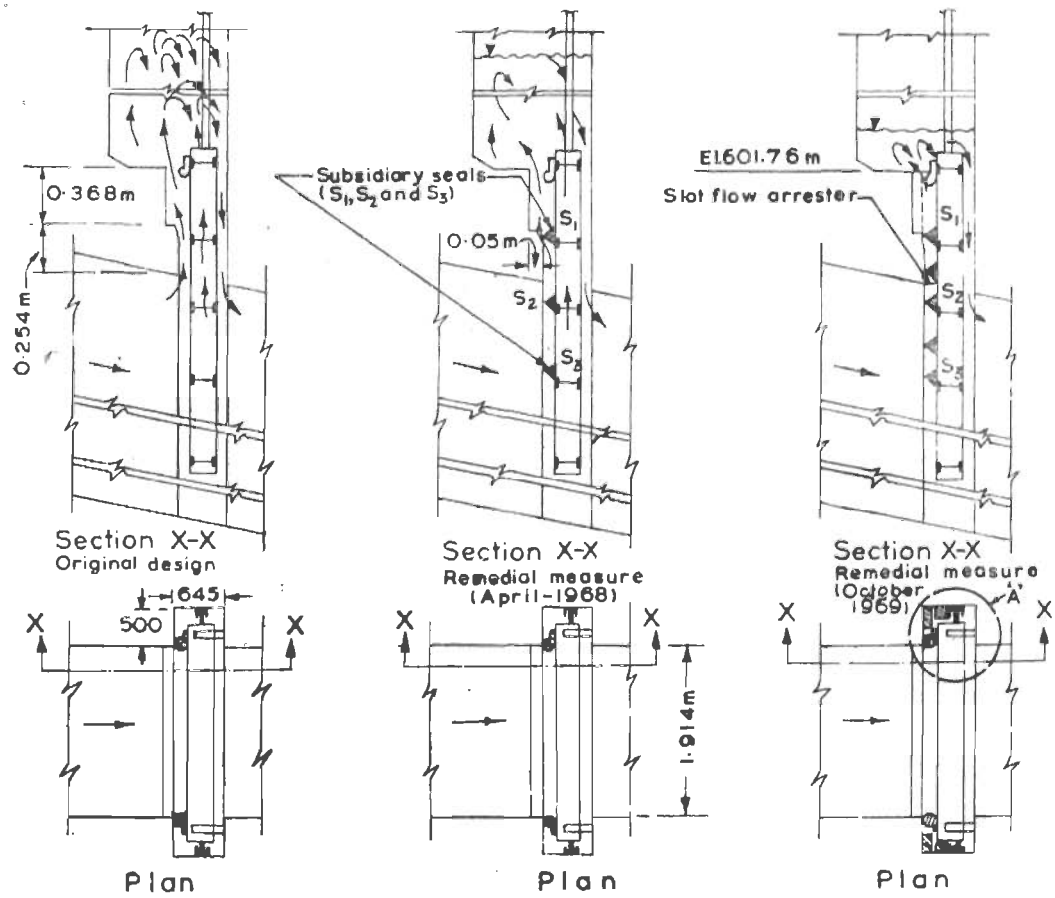

FIGURE 16 : Scheme of remedial measures, Koyna Hydro-electric Project.

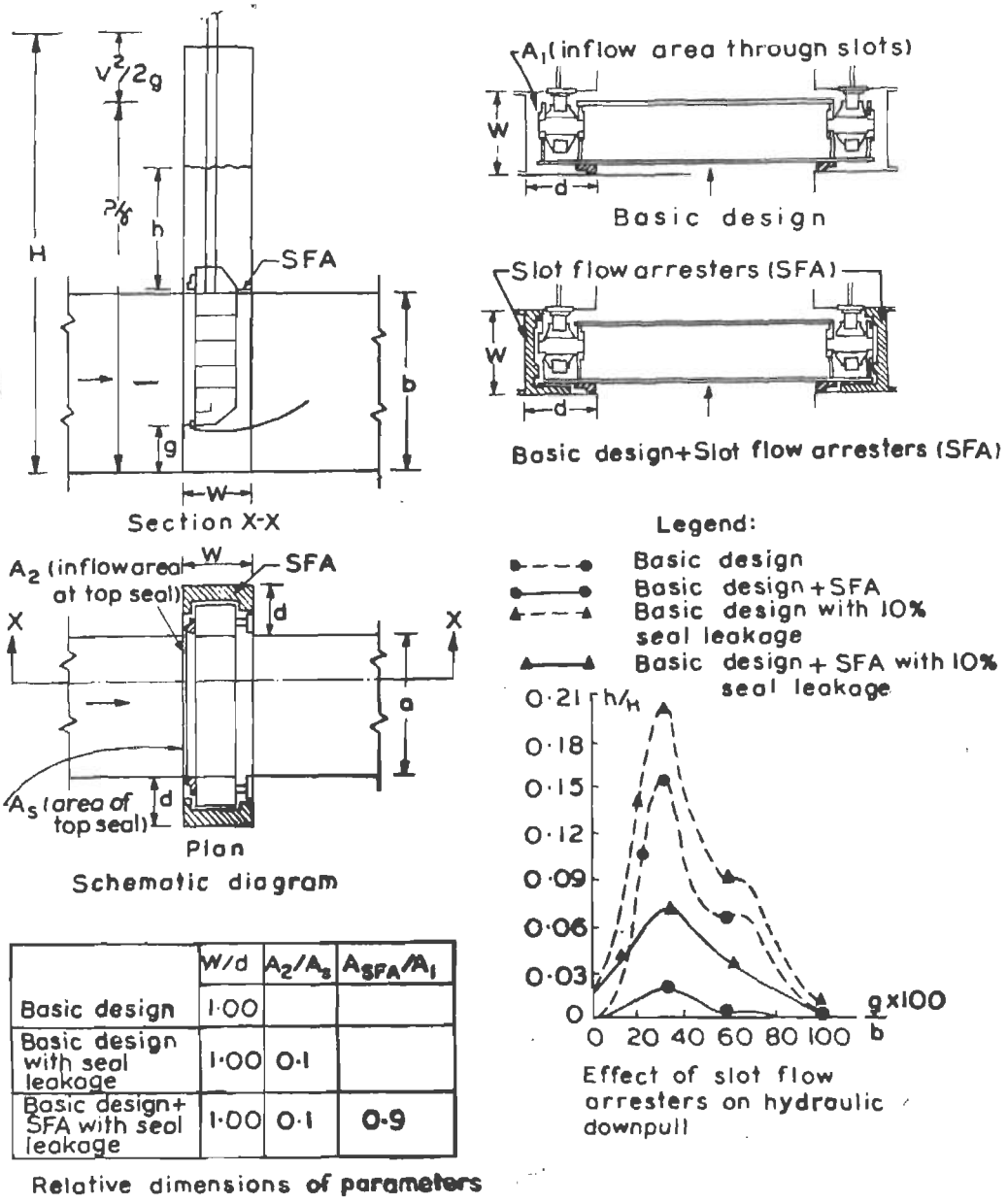

	W/d	A_2/A_s	A_{SFA}/A_1
Basic design	1·00		
Basic design with seal leakage	1·00	0·1	
Basic design+ SFA with seal leakage	1·00	0·1	0·9

Relative dimensions of parameters

FIGURE 17 : Studies on slot flow arresters.

hoisting equipment involved redesign and replacement of the hydraulic pumping machinery and the hydraulic circuits, in addition to loss of time and cost. Minimising downpull by increasing the outflow areas through the drain holes on the gate girders and through the clearance between the body of the gate and the downstream face of the gate housing was not possible as they involved structural problems. Hence, inflow control was thought of as the best remedial measure.

6.5 Filling up the working space above the step on the upstream side of the gate housing would help to close the seal gap. This would, however, necessitate the complete withdrawal of the gate from the gate housing for inspection and minor repairs to the seals and gate. This involved periodic expenditure for dismantling and refixing of the hoisting equipment.

6.6 Considering the economy and time involved for construction, it was proposed to weld mild steel angle subsidiary seals of size 65 mm × 65 mm on the skin plate with a small clearance of ± 4 mm which reduced the

seal gap by about 90 percent at 0.6 m gate opening (see Figure 16). The spacing of the subsidiary seals was based on the consideration of effecting sealing action with the existing seal plate in succession with the top rubber seal. With the incorporation of the subsidiary seals the gate opened successfully to the full height in April 1968 under the head of 38 m.

6.7 The intake gate which opened in April 1968 with the provisional arrangement of subsidiary seals at a head of 38 m could not be opened beyond 0.61 m under an increased head of 51 m in August 1969. Extending the vertical seal plate for a part height up to the level of the inspection platform and fixing two more subsidiary seals did not help to open the gate. Water pressure on the bonnet cover of the gate housing was observed to be of the order of 6 m indicating a water load of 14 tonnes on the gate. The total force required to raise the gate worked out to 35 tonnes, (25 percent in excess of the design hoist capacity).

6.8 Analysis of the flow circulation indicated that the inflow through the upstream seal gap after providing subsidiary seals would be only about 15 percent of the total inflow required to cause a pressure of 6 m on the bonnet cover of gate housing. This lead to the conclusion that additional inflow through the gate slots was responsible for the heading up of water on the gate. This was confirmed by a flow visualisation after removing a part of the bonnet cover at the site.

6.9 With a view to reduce the inflow through the gate slots, flat plates designated as "Slot Flow Arresters" were juxtaposed within the gate slots with a clearance of 3 mm so as to cover an area of about 71 percent slot flow (see Figure 16). The plates were located a little above the roof of the conduit so that the lowest edge of the gate will always be below the plate. After incorporation of the "Slot Flow Arresters", the gate was opened successfully under a head of 50 m. Thus incorporation of this device enabled the gate operation with the existing hoisting equipment which otherwise was to be redesigned for about 125 percent of the design capacity for operation under 70 percent of the design head.

6.10 Subsequent to the prototype experience at Koyna, the efficacy of "Slot Flow Arresters" was investigated on a specific model. Studies indicated that with a blockage of 90 percent of the slot flow area by means of "Slot Flow Arresters", the downpull force could be reduced by 85 percent of the value obtained in the basic design without them. Even with a deshaped bulb of the top seal, the "Slot Flow Arresters" reduced the downpull to the extent of 55 percent compared to the basic design without seal leakage (see Figure 17).

7. Conclusion

Efficient hydraulic designs such as the flow deflector for Ukai diversion channel, the double entry crest spillway of Badua Dam and the superelevated ski-jump bucket for the Umium Barapani spillway resulted in large savings in these water resources projects. In many cases, proper planning of the various structural elements of the project to serve different functions at different stages resulted in considerable economy as has been realised in the design of the stilling basin for the Power Tunnel of Beas Project. "Slot Flow Arresters" incorporated in the design of Koyna penstock intake gate was an example of a simple hydraulic expedient which saved time and money in post-construction stage.

8. Acknowledgement

The authors are highly indebted to Shri Y.K. Murthy, Chairman, Central Water Commission, New Delhi and Dr. K.C. Thomas, Member (D&R), Central Water Commission, New Delhi for the valuable discussions and guidance during the course of evolution of the hydraulic designs mentioned in the article. The authors are also very much thankful to all concerned Chief Engineers, Design and Field Engineers of the various projects with whose co-operation the economic interests of the projects were best served.

9. References

(1) GOLE, C.V. and CHITALE, S.V. (edited by FRAMJI K.K.) : "Design Practices of Irrigation Canals in the World." International Commission of Irrigation and Drainage—1972.

(2) HYDRAULIC DESIGN CHART 712—1. U.S. Army Engineer Waterways Experiment Station, Vicksburg, Mississippi.

(3) ANNUAL RESEARCH MEMOIRS—1967, Central Water & Power Research Station, Poona, India.

(4) ANNUAL RESEARCH MEMOIRS—1961, Central Water & Power Research Station, Poona, India.

(5) ANNUAL RESEARCH MEMOIRS—1962, Central Water & Power Research Station, Poona, India.

(6) ROUSE SIAS and NAGARATNAM : "Turbulence Characteristics of the Hydraulic Jump." Trans. of A.S.C.E., Vol. 124, 1959.

(7) GOLE, C.V. et al : "Prototype Observations of the Penstock Intake Gate of the Koyna Dam, Maharashtra State." Proceedings of the 40th Annual Research Session, Central Board of Irrigation and Power, India.

(8) VENKATRAMAN, C.P. et al : "Hydrodynamic Forces Caused by Unsteady Slot Flow on Vertical Leaf Gates." XIVth Congress of the International Association for Hydraulic Research, 1971, Paris.

Potential of Conventional and Nuclear Techniques in Water Resources Evaluation in India

UMESH CHANDRA K. BALU M. P. S. RAMANI

Desalination and Effluent Engineering Division
Bhabha Atomic Research Centre, Bombay (India).

SYNOPSIS

Various investigations involving the use of conventional and isotope methods for determination of filtration rate, stage speed, direction and vertical flow of ground water, streamflow measurements have been reviewed to highlight the merits and limitation of the methods involved. Study of infiltration of precipitation and supplemental irrigation in seventeen districts of western Uttar Pradesh, as initiated by Department of Atomic Energy is reported. The data of recharge for a year of normal monsoon is reported. In order to study aquifer response and predict water-level changes consequent to withdrawals from the aquifer, the technique of resistance-capacitance analog simulation is being studied for a basin between Hindon and Krishni Rivers in western Uttar Pradesh. Geohydrological data which serve as input to the analog and the complexity introduced by the presence of extensive clay bands in the aquifer are discussed. Various hydrological investigations employing stable isotopes have been reviewed and case studies for some investigations are being initiated. Application of nucleonic soil moisture and density gauges in various hydrological studies is reviewed. An increasing use of isotopic methods by various water resources agencies in the country is stressed.

Introduction

Many hydrologists in India are not using nuclear techniques [1][2][3][4] because there is lack of understanding among them of ; the principles, various applications and potential benefits of, these methods. These techniques find their applications in determination of velocity, direction, vertical flow of ground waters ; determination of seepage from hydraulic structures ; measurement of canal and river discharges; identifying the mode and extent of recharge to ground water ; determination of origin of ground waters and aquifer interconnections, etc. The potential of the nuclear techniques as supplement and as alternative to conventional hydrological methods has been reviewed and discussed in this paper.

Bore-hole Dilution Techniques

Determination of Aquifer Parameters : Filtration Rate, Stage Speed, Porosity, Transmissibility

Various radio-active isotopes in ground water investigations have been used in single-well and multi-well methods. Filtration velocity, Vf, obtained by single-well technique [5] when used with stage speed, V, which is deduced from multi-well method [6], helps a hydrologist in computing yet another important aquifer parameter, i.e., effective porosity, θ by the following relation,

$$Vf = \theta . V$$

By determining filtration velocity and if the gradient, i, is known the permeability of the ground water field, Kf,

can be obtained by Darcy's law, i.e.,

$$Vf = i.Kf$$

In addition to this, single-well pulse techniques [7] [8][9] have been developed to determine transmissibilities and porosities of a layered aquifer by injecting radio-active tracer into the aquifer and then pumping it out.

The traditional methods of determining permeability in situ are the pumping and packer tests. Many investigations in the recent past have been carried out to compare [10][11][12][13] the results obtained from these traditional methods with bore-hole dilution techniques [14][15] which use radio-active traces, while knowing that the methods cover a larger or smaller region of the aquifer. In the light of these comparisons it can be showed that dilution methods produce substantially the same results as the usually very onerous pumping tests. Dilution methods prove to be more economical in terms of operational time, cost and repeatability of the studies than pumping tests. Used to supplement the pumping tests, the dilution method yields the stratification of the permeability values in the vertical profile penetrated by a bore-hole.

By the use of the dilution techniques various interesting and new findings have been reported in various investigations of ground water exploitation [16], well installation [13], seepage from rivers [17] and canal [18][19] and soil consolidation[20].

Determination of direction of ground water flow while employing radio-active tracers [21][22][23] in the dilution techniques has proved an elegant aid for determination of, area of a ground water field ; protection zones of drinking water catchments [24] ; load on ground water as a result of foundations [10] and hydraulic engineering works, drainage, etc.

In addition, the dilution techniques have the advantages ; one needs only one bore-hole of a small diameter (about 5 cm) for measurement ; measuring time is very short about 1 hour for 1 m/day ; the range of measurable velocities lies between some mm/day to some hundred m/day.

Determination of Vertical Flow of Ground Water

Of vital information is the detection and estimation of vertical flow in bore-holes. For flows of medium and high velocity, mechanical current meters used in various investigations [25][26] have been found efficient and simple to use, but the precision of mechanical meters deteriorates as a result of friction and hence radio-active tracer logging methods [27] have been found reproducible and more efficient. Measurement of vertical flow in bore-holes yields valuable information in investigation of water production [10], seepage from dams [10][14][28][29], location of permeable zones [10][14] [15][28], and hydrological communication[30].

Stream Gauging

The measurement of the discharge of rivers and canals is of considerable importance to hydrologists and engineers and to economic development of water resources. Radio-active methods[31][33] of river measurement although are not universally applicable but are often complimentary to the other conventional methods and in time should take their place as a system which can provide highly accurate measurement of stream discharge.

Continuous measurement of streamflow is expensive and where the expense can be justified is conventionally carried out by the construction of a weir or flume. Such construction has to be carried out with great accuracy to enable the flow to be calculated from a rating formula which might have evolved from scale model calibration. Radio-active tracer methods can be of value for accurately checking the actual performance of such a structure after its construction or when there is some doubt about its performance due for instance to siltation.

Discontinuous or spot measurements of a streamflow are often carried out using current meters. The method is not easy or accurate under some conditions such as (*i*) high velocities (5-10 m/sec) which may occur during floods ; (*ii*) small and very variable depth streams ; (*iii*) in rivers where much debris is transported.

Tracer techniques provide another advantage over conventional method and are essentially for discontinuous measurement. The method is highly accurate when used under suitable conditions. The principal requirement is the complete mixing of the tracer across the width of the river. This can be difficult to establish in wide slow flowing rivers or where tributaries or bank discharge occur over the stretch of river where measurements are required.

The tracers which have been used and generally found to be satisfactory include ^{24}Na as bicarbonate, ^{82}Br as ammonium or potassium bromide, ^{51}Cr EDTA, ^{131}I in the presence of sodium thiosulphate, ^{3}H as tritiated water.

The measurement of rivers in flood [34][35] is difficult and can only be attempted at present when the river is fairly well restricted by its banks. If there is extensive flooding out of the channel, complete lateral mixing is not usually achieved and the measurement is not valid. With large flows, often occurring at short notice, tritium is the only convenient tracer.

Ground Water Recharge

The ground water reservoir beneath the Gangetic Plain in western Uttar Pradesh is very vast and potentially very productive. Tubewells with significant increase in their number every year are being installed in this region in order to tap water from shallow as well as deep aquifers. Any long-term plan for exploiting this

ground water for agriculture and industry should be preceded by a thorough investigation of water budget. The first step for this study is to know the rate of recharge in the region.

Department of Atomic Energy had initiated study of recharge in seventeen districts of western Uttar Pradesh by a more reliable technique using artificial tritium as water tracer, a technique first developed by Munnich [36]. Tritiated water was injected at 70 cm depth at about 4 or 5 sites in each district (Figure 1). The site selection was done random. The injection work was carried out just before the onset of monsoon of 1971. Periodical sampling of soil at the sites was carried out for determination of soil moisture and tritium contents of various layers through which the tracer had infiltrated.

The infiltration of precipitation and supplemental irrigation into the soil was studied at about 50 sites in 1971. The results [37] indicated an average recharge in western Uttar Pradesh of 21.5 cm of water per year. The year 1971 was a year of normal monsoon and the above value may be taken as typical for a normal year.

Further investigations to examine the influence of different crop on recharge are in progress, thus enabling the estimation of evapotranspiration losses from various crops. Tritiated water has also been injected at 10 sites (Figure 1), in the doab between Hindon and Krishni Rivers in Muzaffarnagar and Meerut districts so as to study more intensively the spatial variation of recharge.

Aquifer Response by Resistance-Capacitance Analog Simulation

In order to study aquifer response and predict water-level changes consequent to different withdrawals from the aquifer, resistance-capacitance analogs have been widely used elsewhere [38][39][40][41][42][43]. This useful and versatile technique is being adopted to simulate the ground water basins in western Uttar Pradesh. Out of the proposed project area for this study, a pilot area between Hindon and Krishni Rivers (Figure 1), has been chosen for initial investigations.

Pertinent geohydrological field data, viz., rainfall, water levels, withdrawals, transmissibility and storage coefficient, borelogs, evaporation for the pilot area have been obtained and processed. The typical geological profiles in the pilot area are shown in Figures 2 to 5. The presence of extensive and sometime indeterminate clay bands in the pilot area does not present a simplified case for simulation by resistance-capacitance analog. The aquifer can be said to be leaky-confined which is indicated by the data of pumping tests also. The typical values of storage coefficient and transmissibility in the pilot area vary from 4.5×10^{-4} to 1×10^{-1} and 28,277 to 153,000 U.S.G.P.D./ft respectively. For simulation in the analog, first the aquifer is being considered to be fairly homogeneous, neglecting the presence of clay bands and then the presence of clay bands will be simulated by designing a layered analog circuit connected by a suitable resister. Besides the small rivers which act as hydrological boundaries of the pilot area the water-level divide boundary based on the water levels of October 1971 is shown in vertical discontinuous lines in Figure 1.

Stable Isotopes for Hydrological Investigations

The heavier isotopes of water molecule are deuterium D and ^{18}oxygen, ^{18}O. They occur in natural waters in concentrations of about 320 ppm and 2000 ppm respectively. The varying proportions of these isotopes in terrestial waters can be measured with precisions of better than ± 2 percent for D and $\pm$ 0.2 percent for ^{18}O by commercial mass spectrometer.

Analysis of precipitation and water which have not got evaporated show a good linear relationship between D and ^{18}O contents [44]. Using this relationship, D and ^{18}O measurements on surface waters can furnish indications on the location of the catchment areas of these waters. Thus, it has been possible to detect for rivers of various countries of the earth a clear dependence of D contents on geographical latitude and orographic altitude [45][46].

Hydrologists are often facing the problem of determining the contribution of a river flowing into another one. In many cases this problem can be solved by deuterium, since the deuterium content of different rivers is unlikely to be the same. By measuring the D content of each river before the confluence and after the contributions of each river can be figured out.

Correlation of the isotopic contents of precipitation, ground and surface waters can be used in hydrographic investigations and for a determination of the variation pattern with respect to ground water[47]. Isotope measurements on lakes can contribute towards the balance of surface and sub-surface affluents and influents [47][48].

Studies of various problems of aquifer interconnections and determination of origin of recharge in western Uttar Pradesh are being initiated in collaboration with State Ground Water Investigation Organisation. Observation wells for sampling based on the network of spring wells maintained by various agencies are being selected depending upon the local hydrological problem.

Nuclear Logging

The neutron moisture gauge and gamma ray density gauge permit long-term studies on soil moisture movement, soil moisture deficiency[49], determination of rates of infiltration of precipitation and irrigation water[50][51], design of drainage paths, determination of aquifer porosity and amount of water in storage[52][53] and performance of an aquifer in response to recharge and discharge [54].

Neutron moisture and gamma ray density gauges and associated battery operated portable instruments developed [55] in Bhabha Atomic Research Centre in the

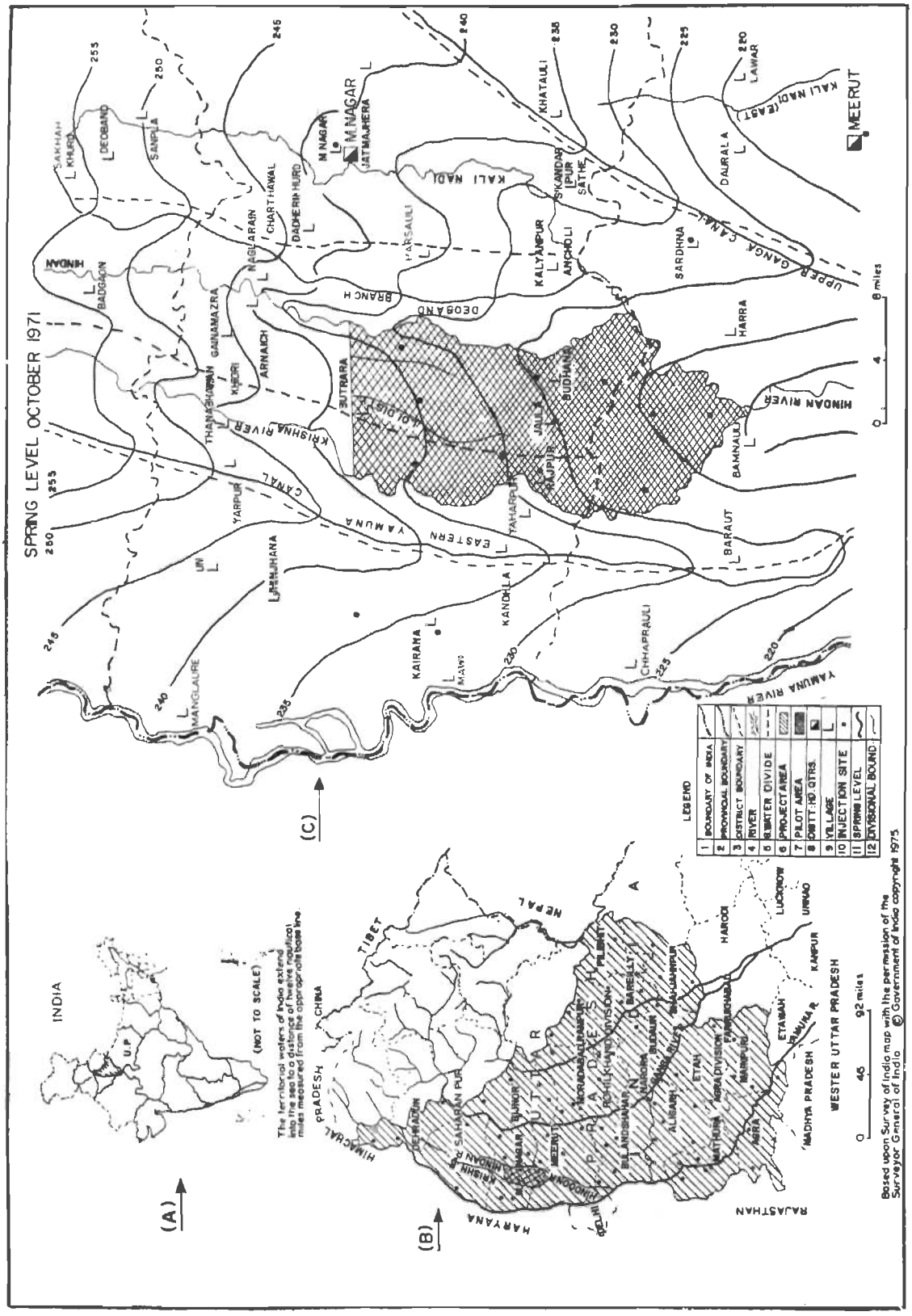

FIGURE 1 : (A) Location map of project. (B) Project area U.P. and tritium injection sites. (C) R.C. analog studies pilot area western U.P.

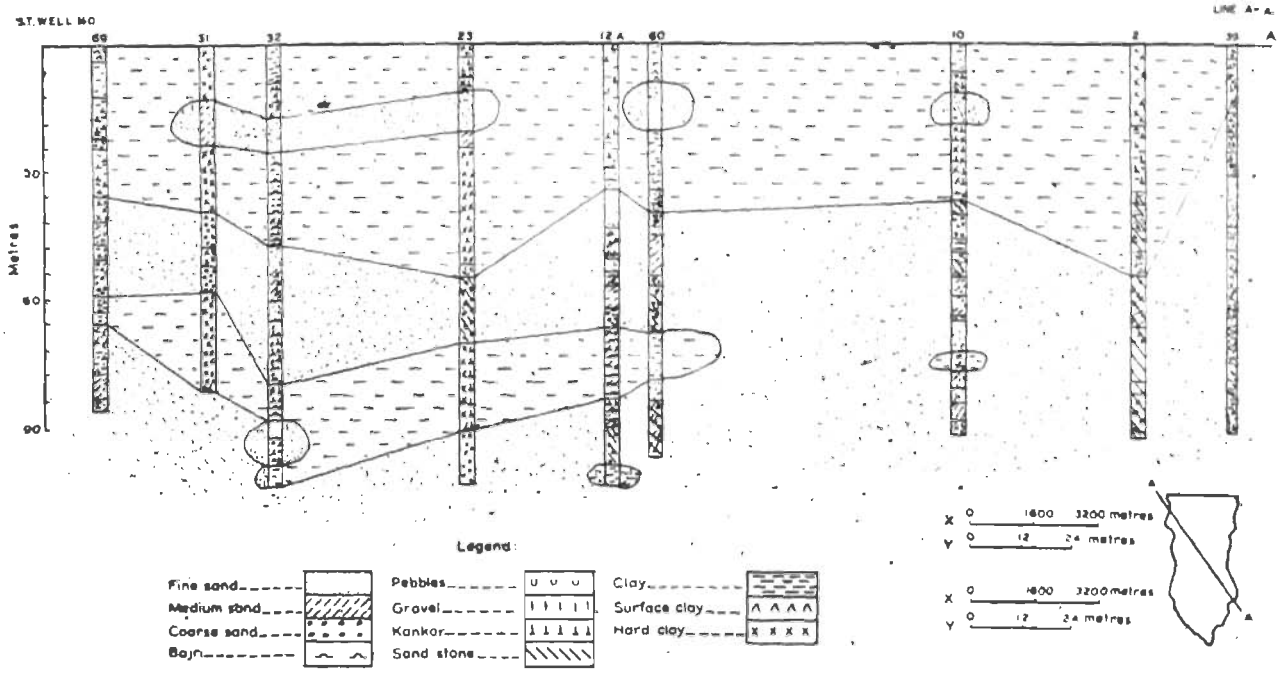

FIGURE 2 : R.C. analog pilot area geological cross-section line A-A.

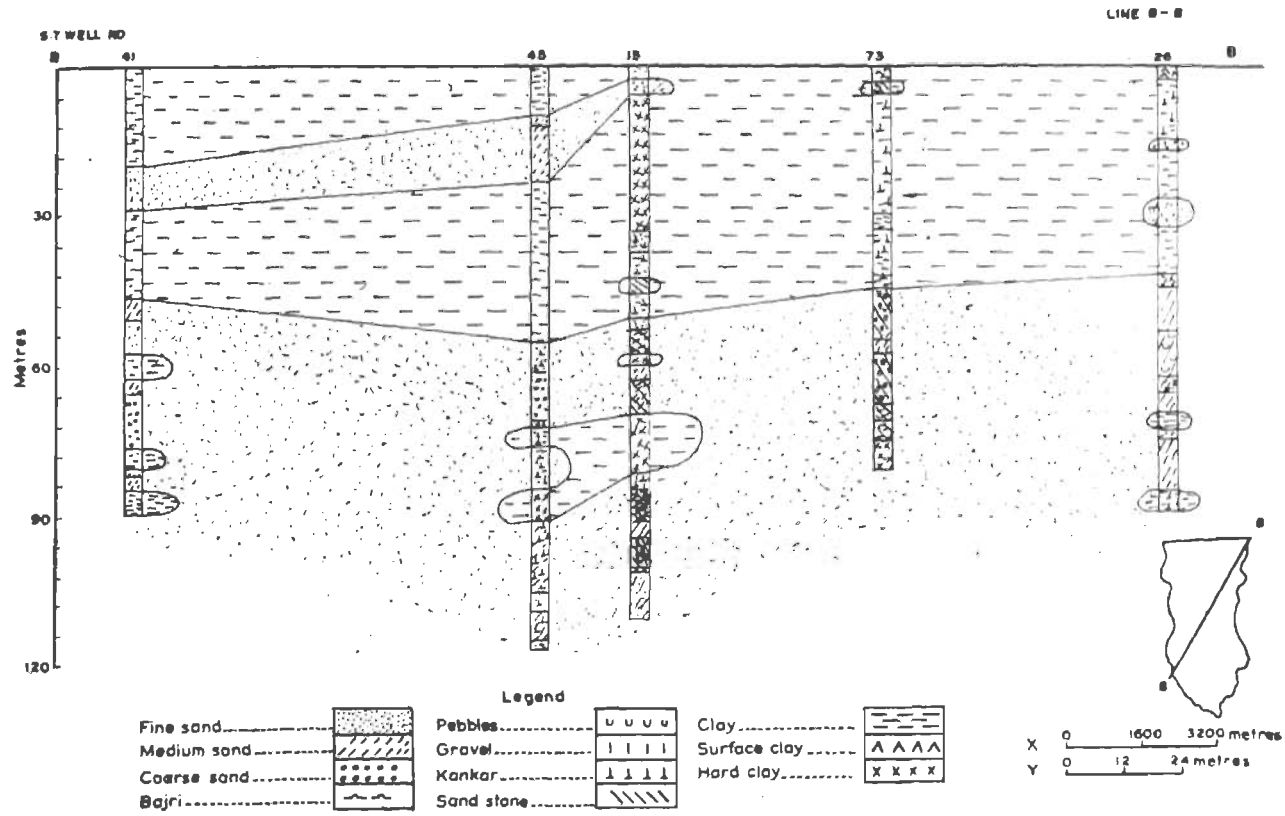

FIGURE 3 : R.C. analog pilot area geological cross-section line B-B.

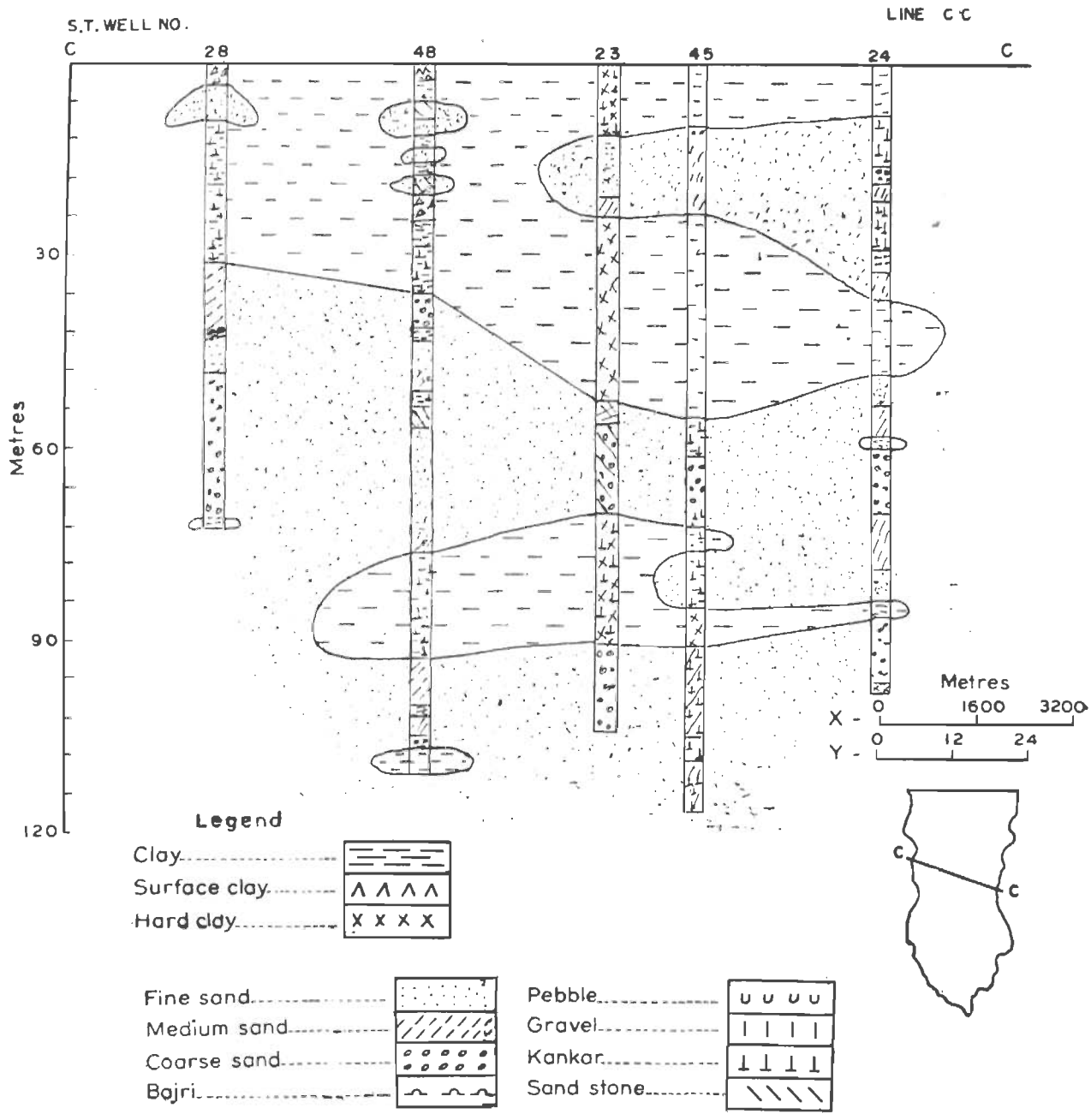

FIGURE 4 : R.C. analog pilot area geological cross-section line C-C.

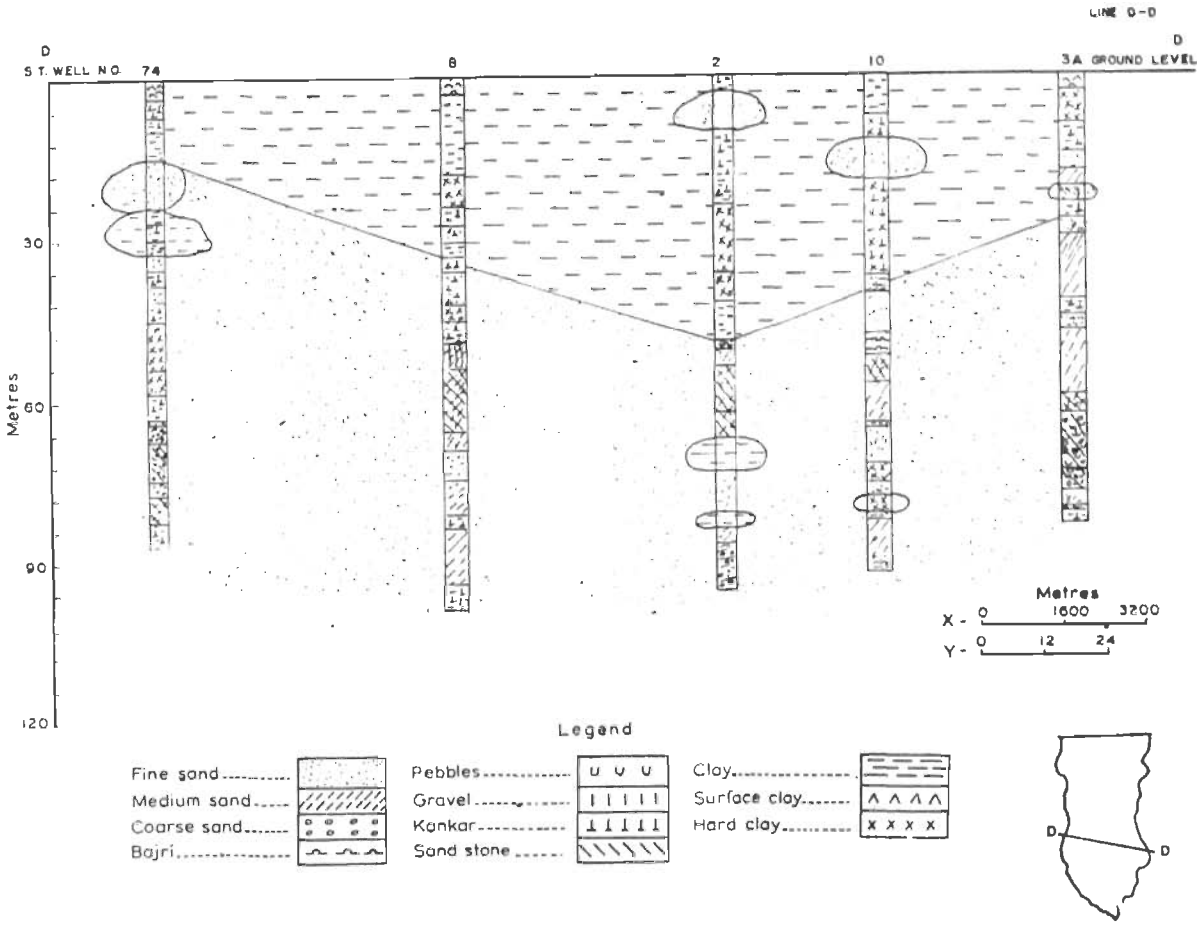

FIGURE 5 : R.C. analog pilot area geological cross-section line D-D.

past have been used at Trombay ([56]) and elsewhere to study the geological stratification, relative rates of infiltration and direction of soil moisture movement in unsaturated zone. Improved instrumentation often used ([14])([17]) in isotope methods renders the field investigations less laborious, more informative, quick and readily reproducible thus requiring minimum number of field personnel.

Conclusion

The potential of isotope techniques as supplement and alternative to conventional hydrological methods has been discussed. The application of nuclear techniques and instrumentation for various hydrological investigations by major water resources agencies in India is stressed. A combined approach, i.e., use of conventional methods in conjunction with bore-hole dilution technique or stable isotope method wherever possible yields best possible hydrological information of any region. By the use of artificial tritium as water tracer, average recharge to ground water in western Uttar Pradesh has been found to be 21.5 cm of water for a year of normal monsoon. Resistance-capacitance analog simulation of aquifer in a pilot area in western Uttar Pradesh is being attempted to predict water-level changes. Case studies for application of stable isotope methods for determination of origin and interconnection of ground water are being initiated.

Acknowledgements

The authors are thankful to Ground Water Investigation Organisation of Uttar Pradesh State Government for making the geohydrological data available for analog simulation study and for assistance in carrying out recharge studies in western Uttar Pradesh.

References

(1) I.A.E.A. : "Radio-isotopes in Hydrology." Vienna, 1963.

(2) I.A.E.A. : "Isotopes in Hydrology." Vienna, 1967.

(3) I.A.E.A. : "Isotope Hydrology." Vienna, 1970.

(4) I.A.E.A. : "Symp. Isotope Techniques in Ground Water Hydrology—1974." Vienna, (In Press).

(5) HALEVY, E. et al : "Bore-hole Dilution Techniques : A Critical Review". Isotopes in Hydrology, IAEA, Vienna, 1967, p. 531.

(6) BATSCHE, H. et al : "Kombinierte Karstwasser Untersucheungen im Gebiet der Donauversick erung (Baden-Württemberg) in den Jahren 1967-69." Steirische Beitrage zur Hydrogeologie, Vol. 22, 1970, pp. 5-165.

(7) MANDEL, S. : "Hydrogeological Field Work with Radioactive Tracers in Israel up to May 1960." Extract of Publication No. 52 of Commission of Subterranean Waters, Israel.

(8) HALEY, E. and NIR, A. : "The Determination of Aquifer Parameters with the Aid of Radio-active Tracers." J. Geophys. Res., Vol. 67, 1962, pp. 2403-9.

(9) BOROWCZYK, M. et al : "Single-Well Pulse Technique." Isotopes in Hydrology, IAEE, Vienna, 1967, p. 507.

(10) DROST, W. : "Grundwasser messungen mit Radioactiven Isotopen." Geologica Bavarica, Vol. 64, 1971, pp. 167-96.

(11) GASPAR, E. et al : "Field Determination of Soil Permeability by the Nuclear Methods". IFA Report MR-29, Bukarest, 1967.

(12) KRATZSCHMAR, H. : "Vergleichende Unter-schungen Bekannter und Neuerer Geohydrologischer Verfahren." Wiss. Zeitschr. T.U. Dresden, Vol. 13, 1964, pp. 1057-9.

(13) DROST, W. et al : "The Bore-hole Dilution Method of Measuring Ground Water Filtration Velocity." GSF Bericht R 16, Munchen, 1968.

(14) "Annual Reports" : Intitut fiir Radiohydrometrie, GSF, München, 1964, 1965, 1967, 1968.

(15) BOROWCZYK, M. et al : "A Single Well Pulse Technique : Outline of the Method, an Example of Application and Comparison with other Methods." IAEA Report, Contract No. 177 R2/RB, 1966.

(16) MAIRHOFER, J. : "Grundwassaruntersuchungen in Ungarn." Report of BVFA, Vienna for Institute of Water Resources, Budapest, 1965.

(17) "Annual Report" : Institut fiir Radiobydrometrie, GSF, München, 1969.

(18) KAUFMANN, W. J. and TODD, D. K. : "Application of Tritium Tracer to Canal Seepage Measurement," Tritium in the Physical and Biological Sciences, Vol. I, IAEA, Vienna, 1962, pp. 83-94.

(19) IYA, V. K. : "Application of Radio-isotopes and Radiation Sources in Industry, Radiation Processing and Hydrology—Current Status in India." A Conf. 49/P/539, Geneva, 1971.

(20) "Grundwasser-ges-churindigkeit und der Stromungsrichtung beim Wehr Gross Reifling." Report of BVFA to Stewcag, Graz, 1954.

(21) BOROWCZYK, M. et al : "Radio-isotope Measurements of Ground Water Flow Direction by Single Well Method." Nukleonika, Vol. 10, 1965, p. 19.

(22) MAIRHOFER, J : "Die Bestimmung der Grundwasserströmung am Ostufer des Neusiedlersees." Report of BVFA Vienna to Neusiedlersees Planungs-gesellachaft, Vienna, 1966.

(23) WURZEL, P. and WARD, P. R. B. : "A Simplified Method of Ground Water Direction Measurements in a Single Bore-hole." J. Hydrol., Vol. 3, 1965, p. 97.

(24) DROST, W. : "Die Anwendung Radioaktriver Isotope bei Grundwasser-messungen." Isotopenmethoden in Hydrologie, München, 1971.

(25) FIELDER, A. G : "The Au Deepwell Current Meter and its use in the Roswell Artesian Basin, New Mexico." U.S. Geol. Survey Water Supply, Paper 596, 1928, p. 24.

(26) MEINZER, D. E. : "Methods of Exploring and Repairing Leaky Artesian Wells." U. S. Geol. Survey Water Supply, Paper 596, 1928, p. 1.

(27) DROST, W. : "Der Tracerlog, ein neus Bohrlochverfahren Zur Grundwassermessung mit Radioaktiven Isotopen." Strah-lungs und Isotopenanwendung im Bauwesen, Brüssel, Report No. 23, 1970.

(28) "Annual Reports" : Forschungstalle für Radiohydrometrie, Universität München, München, 1963.

(29) MOSER, H. et al : "New Experiences with the Use of Radio-active Isotopes in Hydrology." Radio-isotopes in Hydrology, IAEA, Vienna, 1967, p. 93.

(30) MAIRHOFER, J. : "Ground Water Flow and Direction Measurement by Means of Radio-isotopes in a Single Well." Isotope Techniques in Hydrological Cycle, Geophysical Monograph Series 11, 1967, pp. 119-29.

(31) HULL, D. E. : "The Total Count Technique : A New Principle in Flow Measurement." Int. J. Appl. Radiet. Isotopes, Vol. 4, 1958, p. 1.

(32) FLORKOWSKI, T. : "Use of Tritium Tracer for River Flow Rate Measurements." Report to Government of Kenya, IAEA, Vienna, Technical Assistance Report, 1968.

(33) DINCER, T. : "Application of Radio-tracer Methods in Streamflow Measurements." Isotopes in Hydrology, IAEA, Vienna, 1967, pp. 93-110.

(34) PILGRIM, D. H. : "Radio-active Tracing of Storm Runoff on a Small Catchment, I. Experimental Technique." J. Hydrol., Vol. 4, 1966, p. 289.

(35) PILGRIM, D. H. : "Radio-active Tracing of Storm Runoff on a Small Catchment, II. Discussion of Results." J. Hydrol., Vol. 4, 1966, p. 306.

(36) ZIMMERMANN, U. et al : "Downward Movement of Soil Moisture Traced by means of Hydrogen Isotopes." Geophysical Monograph No. 11, Isotope Techniques in the Hydrologic Cycle, Washington, 1967, p. 28.

(37) DATTA, P. S. et al : "Ground Water Recharge in Western Uttar Pradesh." Proc. Ind. Aca. Sciences, Vol. LXXVIII, Sec. 'A', No. 1, 1973.

(38) BUNDESANSTALT FÜR BODENFORSCHUNG : "Electric Analog Studies of the Amman-Wadi Sir—Aquifer in the Shaubak-Ras en Naqb Area, South-Jorden." Federal Republic Germany, 1972.

(39) ANDERSON, T. W. : "Electrical-Analog Analysis of the Hydrologic System in Tuscon Basin, Arizona, U. S. A." Publication de AIHS No. 80, 1968, p. 15.

(40) PHILLIPS, H. B. and Mc DONALD, H. R. : "Analog of Ground Water in East-Central New Mexico." Proc. ASCE, Jr. Irrigation and Drainage Div., Vol. 95-IR 1, 1969, p. 27.

(41) SKISITZKE, H. E. : "The Use of Analogue Computers for Studies in Ground Water Hydrology." Jr. Instn. Water Engrs., London, Vol. 17, 1963, p. 216.

(42) HERBERT, R. and RUSHTON, K. R. : "Ground Water Flow Studies by Resistance Networks." Geotechnique, Vol. 16, 1966, pp. 53-75.

(43) BATTERMANN, G. and MULL, R. : "Analoge und Hybride Simulation-nichtlinearer. Ausbreitungsvorgänge." Jahresbericht 1971 des SFB 79 der TU Hannover, 1972.

(44) DANSGAARD, W. : "Stable Isotopes in Precipitation." Tellus, Vol. 16, 1965, p. 436.

(45) FRIEDMAN, I. et al : "The Variation of the Deuterium Content of Natural Waters in the Hydrologic Cycle." Rev. Geophys., Vol. 2, 1964, pp. 177-224.

(46) EICHLER, R. : "Über den Isotopengehalt des Wassers in Niederschlags, Boden-und Grundwasser." Dissertation Universitat Bonn, 1964.

(47) I.A.E.A. : "Guidebook on Nuclear Techniques in Hydrology." Vienna, 1968.

(48) ZIMMERMANN, U. : "Bilanzierung von Seen mit Hiffe von Stabilen Isotopen." Dissertation Universitat Heidelberg, 1969.

(49) GIESEL, W. et al : "Water-flow Calculations by Means of Gamma Absorption and Tensiometer Field Measurements in the Unsaturated Soil Profile." Isotopes in Hydrology, IAEA, Vienna, 1967, p. 663.

(50) COLE, J. A. and GREEN, M. J. : "Measuring Soil Moisture in the Brenig Catchment Area : Problems of using Neutron Scatter Equipment in Peaty Areas." Water in the Unsaturated Zone, Proc. Sump. Wagningan, UNESCO, Paris, 1969, p. 74.

(51) DANFORS, E. : "Changes in Moisture Content of Top Soil Measured with a Neutron Moisture Gauge." Water in the Unsaturated Zone, Proc. Symp., UNESCO, 1969, p. 96.

(52) I. A. E. A. : "Nuclear Well Logging in Hydrology." Vienna, 1971.

(53) KEYS, U. S. : "The Application of Radiation Logs to Ground Water Hydrology." Isotope in Hydrology, IAEA, Vienna, 1967, p. 477.

(54) MEYER, W. R. : "Use of Neutron Moisture Probe to Determine the Storage Coefficient of an Unconfined Aquifer." U. S. Geol. Survey Prof. Paper 450-E, 1963, p. 174.

(55) "Division of Radiation Protection." Bhabha Atomic Research Centre, Bombay.

(56) CHANDRA, U. : "Hydrological Investigations carried out with Nucleonic Soil Moisture and Density Gauges Developed at Trombay." HYD/19, Application of Isotope Techniques in Hydrology and Hydraulics, Symp., Poona, 1974.

Nuclear Techniques for Water Resources Technology

JAGDISH BAHADUR
Radiation Physicist
Nuclear Research Laboratory
Indian Agricultural Research Institute
New Delhi (India).

SYNOPSIS

Nuclear techniques available for studies on water resources problems involve the use of one or the combination of methods, e.g., environmental isotope approach, injection and monitoring of radiotracers, or the logging with the help of sealed radiation sources. The environmental isotope approach could give information on the basic facts about a hydrological system, e. g., its origin, mixing process, age or residence time and rates of water movement. Radioactive tracers could be used for stream discharge measurements, sediment transport, direction and velocity of ground water movement, leakages from water carriers and reservoirs. Sealed radioactive sources are normally used for making non-destructive and repeated measurements of water equivalent of snow mass, soil density and its moisture, permeable characteristics of man-made structures or fractured rocks, water-level fluctuations and suspended sediment load.

Indian contribution to the development of water resources adopting nuclear techniques is reviewed and a mention is made about the global status of these versatile methods.

A few observations are made for the economic solutions of some of our hydrological problems where the nuclear tools have greater advantages over the conventional approaches.

1. Introduction

The use of nuclear techniques in water resources research forms probably one of the most significant peaceful use of atomic energy after nuclear power production.

By the end of twentieth century, it is expected that the water consumption throughout the world will touch a figure of 5,000 km^3/yr. This amount represents about 5 percent of the average precipitation or 15 percent of the average runoff [1] and may not appear large at the first instance. Considering the spatial and temporal variability of water distribution and the poor water use efficiency, one can realise the enormous quantities of water to be stored and redistributed for satisfying the need based requirements of local agriculture, industry and the community as a whole. Another paradox is that the progress of civilisation is linked up with the increase in pollution of the fresh water resources having serious implications of the very existence of man in his environment. The above consideration calls for an organised research effort to work out the local and regional water balance with adequate knowledge of all the hydrologic processes.

The concept of hydrology can be summarised as the hydrological cycle, describing the various channels and patterns of water circulation, mainly within the earth's hydrosphere, in glaciers and ice-caps, as underground

water, in rivers and lakes, and over and above in oceans. The subject of hydrology is considered as a 'Dynamic Sequential System' consisting of an input and output of water. Backed by strong and powerful analytical tools like Laplace's transforms, probability theory, computers, remote sensing, etc. Hydrologists have been able to accumulate, analyse and interpret colossal amount of field and laboratory data. More recently, nuclear techniques have become available to the hydrologist.

The use of radiation sources for determination of water equivalent of snow were reported as early as 1950([2]). The first researches on knowing the isotopic variations of water molecule were reported in 1953([3]). Followed by these, Bengemann and Libby([4]) reported on the potential use of environmental tritium in hydrology. These discoveries were followed by many other investigations but the actual impetus for the development of nuclear techniques in hydrology was given by a panel of experts who met in 1961 at the instance of International Atomic Energy Agency, Vienna. Thereafter, the Agency has sponsored four international symposia : first in 1963 at Tokyo ; second, third and fourth at Vienna in 1966, 1970 and 1974 on the subject and also brought out several special reports for the benefit of users. A number of reviews on the potential applications of these techniques ([5-11]) have been published which are of great importance to the persons who are looking for introducing these methods of investigations.

It is now widely realised and accepted that the nuclear techniques for water resources technology are one of the powerful tools available to practically all aspects of the hydrological cycle.

The present article introduces various nuclear techniques, their applications in water resources technology, Indian contribution to the isotopic hydrology, global status of advancement in the field with some comments on the economic solution of some of the hydrological problems in India.

2. Nuclear Techniques

The nuclear techniques make use of changes occurring in both physical and chemical properties of isotopes.

In stable isotopes, one makes use of the fact that a mass difference between isotopes of the same element produces small differences in their physical and chemical behaviour which in turn establish slightly different isotopic compositions (isotopic fractionation) among co-existing chemical compounds or phases.

In radioactive isotopes, use is made of the basic property of radioactivity with high sensitivity of detection made possible due to developments in electronic instrumentation.

For convenience of description, these techniques can be divided in three sub-heads, viz., environmental isotope approach, use of artificial radioactive tracers and use of sealed radiation sources.

2.1 *Environmental Isotope Approach*

In environmental isotope approach, one makes use of isotopic variations caused by natural processes. These isotopic variations can not be controlled by man and have been useful in studying several problems in hydrology. Problems like origin, turnover and transit time of water in a system which can not be tackled by conventional techniques are amenable to isotopic techniques.

Commonly used isotopes for such studies are $^{18}O/^{16}O$, $^{2}H/^{1}H$, $^{13}C/^{12}C$ (stable) and ^{3}H, ^{14}C (radioactive) and sparsely used ones are $^{34}S/^{32}S$ (stable) and ^{32}Si, ^{234}U, ^{238}U, ^{228}Th, ^{230}Th, ^{228}Th, ^{226}Ra, ^{222}Rn, ^{210}Pb, ^{81}Kr, ^{39}A (radioactive). The characteristics of main environmental isotopes used in hydrology([12]) are given in Table I.

TABLE I

Some characteristics of main environmental isotopes used in hydrology.

Isotope	Relative abundance in nature (percent)	Decay	Half life	Maximum energy (KeV)
^{1}H	99.985	Stable		
$^{2}H=D$	0.015	Stable		
$^{3}H=T$	10^{-16}—10^{-12}*	β^-	12.26*y*	18.1
^{12}C	99.89	Stable		
^{13}C	1.11	Stable		
^{14}C	1.2×10^{-10}**	β^-	5.370*y*	156
^{16}O	99.76	Stable		
^{17}O	0.04	Stable		
^{18}O	0.20	Stable		

* The lower figure refers to the tritium content of precipitation before 1952 and higher to that reached in 1963 in the northern hemisphere.

** In modern carbon before 1950.

Among all the environmental isotopic species of water HTO, $H_2{}^{16}O$, $HD^{16}O$, $H_2{}^{18}O$ are of practical interest in hydrology. The tritium concentration is expressed in T. U. (1 atom of tritium in 10^{18} atoms of protium) while the stable isotopic ratios D/H or $^{18}O/^{16}O$ are expressed in terms of per mille difference ($\delta\,{}^{\circ}/_{\circ\circ}$) expressed as :

$$\delta = \left(\frac{R_s}{R_{SMOW}} - 1\right) \times 1000$$

where, R_s and R_{SMOW} are the isotopic ratios for the sample and standard mean ocean waters.

2.2 *Use of Artificial Radioactive Tracers*

The artificially produced radioisotopes are introduced as tracers in larger concentration and evolution of concentration with time is followed at one or more locations. This kind of study can yield detailed information about the system but the results are always of limited applications in time and space.

In general, the following criteria must be satisfied by an ideal water tracer :

(*i*) The tracer should travel with the natural speed of water, i.e., the presence of tracer should not affect the physical properties, e.g., density, viscosity and temperature of water.

(*ii*) It should not be lost by absorption or adsorption.

(*iii*) It should have a suitable half life.

(*iv*) It should be least toxic and hazardous.

(*v*) It should be easily detectable in situ.

(*vi*) It should not be expensive.

All the above criteria are not satisfied by any single tracer but several tracers[10] have been found useful for hydrological studies (Table II).

2.3 *Use of Sealed Radiation Sources*

The fundamental properties of radiations, e.g., attenuation, elastic or inelastic scattering while traversing a medium are utilised when use is made of sealed radiation sources. Sealed beta, gamma and neutron sources are used for hydrological studies.

Most commonly used methods employing radiation sources are gamma-gamma for soil density, neutron-neutron for soil moisture.

In gamma-gamma method, photons emitted from a gamma source interact with the electrons of the media to produce scattered photons due to elastic scattering. The measured intensity of scattered photons is proportional to the electron density of media. Some of the characteristics of commonly used gamma sources[9] are given in Table III.

In neutron-neutron method, the fast neutrons are thermalised due to elastic scattering with hydrogen nuclei predominantly present in the form of soil moisture and the thermalised neutrons are captured by a detector whose response is proportional to the moisture present in the soil. The fast neutron sources used for moisture studies[18] are given in Table IV.

Sealed gamma sources are used with collimated detector in twin probes for determining the water equivalent of snow cover and also small changes in the values of soil moisture and density. Small pellets of radiation sources are used with floats for monitoring the fluctuations of water levels.

TABLE II

Some characteristics of commonly-used artificial radioactive tracers in hydrology.

Isotope	Chemical form	Half life	Decay models	γ-energies in MeV	Min. permissible concentration in drinking water μ Ci/ml	Min. amount detectable in water μ Ci/ml
^{3}H	H_2O	12.26 *y*	β^-	No γ	3×10^{-3} (10^6 TU)	10^{-6}* (300 TU)
^{24}Na	Na_2CO_3	15.0 *h*	β^-	1.37, 2.75	2×10^{-4}	10^{-8}
^{51}Cr	*Cr-EDTA*, $CrCl_3$	27.8 *d*	*EC*	0.324	2×10^{-3}	8×10^{-7}
^{58}Co	*Co-EDTA* $K_3[Co(CN)_6]$	71 *d*	*EC* (85%) β^+ (15%)	0.81, 0.511 from positron annihilation	10^{-4}	6×10^{-8}
^{82}Br	NH_4Br	35.7 *h*	β^-	0.55 to 1.46	3×10^{-4}	2×10^{-8}
^{110m}Ag	$K[Ag(CN)_2]$	249 *d*	β^- (98%) *IT* (2 %)	0.66, 0.88	3×10^{-5}	3×10^{-8}
^{131}I	*KI*	8.05 *d*	β^-	0.08 to 0.64	2×10^{-6}	8×10^{-8}
^{198}Au	$AuCl_3$	64.8 *h*	β^-	0.41, 0.68	5×10^{-5}	10^{-7}

*Detection level without isotopic enrichment.

TABLE III

Radiation characteristics of some gamma sources.

Isotope	Half life (years)	Gamma energies emitted (MeV)	γ-dose mr/hr at 1 m from 1 m Ci
^{60}Co	5.26	1.17, 1.33	1.30
^{137}Cs	30	0.66	0.33
^{226}Ra	1620	0.19 to 2.43	8.25

TABLE IV

Radiation characteristics of some neutron sources.

Neutron source	Half life	Neutron emmission	γ-energy of the radio-nuclide	γ-dose rate mr/h per m Ci at 1 m
^{210}Po-Be	138 d	2.5×10^{3}	0.8	0.0001
^{226}Ra-Be	1608 y	1.3×10^{4}	0.61 to 1.76	0.83
^{239}Po-Be	24400 y	2.2×10^{3}	0.04, 0.05, etc.	0.01
^{241}Am-Be	458 y	2.5×10^{3}	0.03, 0.06, etc.	0.0025

3. Applications in Water Resources Technology

3.1 *Problems in Hydrometeorology*

For quite sometime now, primary, cosmogenic and artificial radiomiclides have been used for atmospheric studies[13] in addition to stable isotopes of hydrogen and oxygen ([14])([15]). These have been used to trace the origin of atmospheric moisture and study of other atmospheric phenomena, e.g., mixing, orographic effects, evaporation, evapotranspiration, condensation, freezing, hurricanes and also exchanges between atmospheric water vapour and surface waters of land and sea.

Commonly used tracers are ^{3}H, $^{2}H/^{1}H$, $^{18}O/^{16}O$, ^{90}Sr, ^{222}Rn and other fall-out radionuclides.

3.2 *Problems in Surface Hydrology*

3.2.1 *Snow and Glacier Hydrology* : The water content of the snow profile is of prime importance for forecasting snow melt runoff from inaccessible areas in mountains. With the help of radioisotope gauges, it has been possible to detect ice-lenses and sudden changes in the density of snow pack for avalanche forecasting. Several variations of automatic and remotely controlled gauges have been developed. Areal measurement of water equivalent up to 60 cm of water has been possible by measuring the natural radioactivity of the earth. Some investigators have also used sealed gamma-sources for the purpose.

Studies on dating the snow by radioactive fall-out have been employed to determine the rate of snow accumulation on glaciers. Gross beta-activity and the concentration of radioisotopes, e.g., ^{210}Pb, ^{32}Si, ^{14}C and ^{3}H have been used to date the glacier ice. Variations in the deuterium and oxygen-18 concentrations have been helpful in resurrecting past climatic oscillations. Inter-glacial drainage is also studied by means of radiotracers and the use of stable and radioactive isotopes for ice flow studies has also been reported.

3.2.2 *Stream Discharge Measurements* : The stream discharge measurements were one of the early applications of radiotracers (e.g., ^{82}Br, ^{131}I, ^{198}Au, ^{3}H) in hydrology. Lately environmental tracers, e.g., ^{3}H, $^{2}H/^{1}H$ and $^{18}O/^{16}O$ are used for studies connected with river discharges.

There are two main radioisotope technique for discharge measurements, viz., a constant injection of a tracer or an instantaneous injection of a known quantity of a radioisotope([10]).

3.2.3 *Leakage from Man-made Structures* : When water leaks from a storage or conveyance system, it normally endangers its structural stability and also impairs economic operation of the hydraulic structure. The case of leakage, it can be usually ascertained that the water loss is occurring but difficulties arise in knowing the exact leakage paths. For this both the stable isotopes and radioactive tracers can be used.

The stable isotopes of hydrogen and oxygen usually have higher concentration in lake waters due to preferential enrichment by evaporation. This property can be utilised in studying the hydraulic connections between lakes and reservoirs.

Methods of radiotracer absorption and tracer labelling are used for seepage studies. In the first approach a strongly and readily adsorbable radiotracer is injected at the bottom of the water carrier system or a reservoir and then the radiotracer concentration is monitored by submersible radiation detectors. The region of maximum activity gives the location of seepage entry points. In the technique employing tracer labelling, the whole reservoir is labelled and the appearance of the tracer at seepage points gives information about the seepage path.

3.2.4 *Study of Dynamics of Lakes and Reservoirs* : The mixing pattern and water balance are the dynamic properties of lakes and reservoirs and these properties can be studied by both environmental and artificial isotopes.

In general, the vertical stratification is a common feature with all the lakes. When the layers are well separated, the reservoir can be treated as a system of one or more boxes each being an ideal reservoir, i.e., the rate of loss or gain of water can be found out applying simple water balance considerations. In case of radiotracers, the degree of mixing can be studied by monitoring the changes in the tracer concentration with time.

Mathematical equations have been used to describe the vertical distribution of ^{3}H, ^{14}C and ^{222}Rn. For study of mixing characteristics of lakes, artificial tracers like ^{131}I, ^{82}Br and ^{60}Co have also been employed and the radioactivity has been monitored by fixed detectors or detectors mounted on a mobile platform.

3.2.5 *Sedimentation and Erosion* : Both transmission and scattering type of gauges have been used for evaluation of suspended load. In the transmission type of gauge, ^{109}Cd or ^{241}Am or ^{170}Tm is used as a radiation source. Continuous and un-attended evaluation of suspended sediments at fixed location has been made possible by the use of transmission gauges. For both gauges, the response is dependent on the chemical nature of the suspended material and hence the need for calibration curves for different material parameters.

For bed load transport studies, injection of activated sediments (^{46}Sc or ^{198}Au) is followed by immersed detectors or spot sampling or both. Normally crushed glass, having grain-size distribution similar to natural sediments, activated in reactor, forms the tracer. Such tracer studies have given qualitative and quantitative information on sand and silt movement under the influence of natural forces. Several radionuclides belonging to *U-Th* series have been used for sedimentation in river and ocean studies.

Investigations regarding soil erosion have been performed by autoradiography making use of beta emitters, e.g., ^{32}P.

3.3 *Problems in Sub-surface Hydrology*

3.3.1 *Study of Soil Density and Moisture* : The study of density and moisture is important for compaction of soil mass and the movement of water in sub-soils. The back scatter radiation gauges are being utilised for this purpose for the last two decades or more.

The nucleonic method for soil and moisture determination gives reliable results in less time and eliminates human error. The test employs a non-destructive process and samples a large volume of soil, giving a more representative picture of the sub-soil. These instruments can be used for both absolute and relative determination of in situ sub-soil conditions. The other important advantage is that an access tube can be left in place over a long period without disturbing the drainage or other characteristics of the surrounding terrain thereby facilitating studies on the dynamic behaviour of soil-water systems. The preparation of a suitable calibration curve is the main bottleneck for the quantitative evaluations.

Gamma-attenuation is used for studying water movement in the unsaturated zone. Various gamma sources, e.g., ^{60}Co, ^{137}Cs, ^{55}Fe, ^{65}Zn, ^{75}Se, ^{109}Cd, ^{170}Tm and ^{241}Am have been used for the purpose. The most commonly used source for measurement of soil moisture content has been ^{137}Cs. A number of other nuclear well logging techniques[16] are available for non-destructive evaluation of sub-soil characteristics.

3.3.2 *Dating of Ground Waters* : In dating, the use of radioactive decay as a basis of time determination rests on the premise that a parent element decays at a known constant rate into a daughter element either directly or in a radioactive chain and that nothing is added or removed during the process.

The four methods which offer possible approaches for the purpose are dating from ratios of the member of natural radioactive series, carbon-14, tritium and silicone-32. Several physical and mathematical models have been used to explain the experimental data.

3.3.3 *Infiltration and Recharge* : The water movement in unsaturated soil is a very complex phenomenon having great spatial and temporal variability. Blume et al[17] used artificial tritium tagging technique which is based on the observed fact that the soil water in unsaturated zone moves layer by layer. The phenomenon takes place because of lateral molecular diffusion which mixes the percolating water with the stationary water present in the soil column. In this technique, a small quantity of tracer is injected at a marked point, along a line or in a plane below the soil surface. The tagged layer is then sampled at different times to study the dispersion of activity and movement of peak concentration. Knowing the shift, initial and final moisture content of soil, one can easily estimate the amount of vertical recharge in alluvial soils. Environmental tritium has also been used for this purpose[18].

In general, one has to make several measurements to derive an average value of recharge rate to account for the variability in the physical properties of the soil. Accuracy of the method is estimated to be better than ± 10 percent under favourable conditions.

3.3.4 *Ground Water Flow Velocity and Direction* : For ground water tracing, single well tracer logging, dilution, pulse technique or multiwell tracer technique are adopted. In single well tracer logging technique, a radiotracer is thoroughly mixed in the open or perforated bore-hole and the tracer activity is logged at different intervals of time. In single well pulse technique, radiotracer is injected in the aquifer through a well and the well is recharged so as to push the tracer pulse. After sometime the tracer pulse is pumped out. Working with different delay times, the velocity of ground water flow is determined. In multiwell technique, tracer is injected in one well presumably located on the upgradient and the downgradient wells are monitored.

For ground water flow velocity determination special instruments have been developed for horizontal and vertical flows[19].

For finding out the direction of ground water flow, the water column in the well is labelled with a radioactive tracer solution and allowed to flow into the aquifer. The distribution of the tracer in the ground is measured with reference to filter tube of the well by means of a

direction-sensitive detector employing an array of detectors or a directionally oriented collimated detector. Usually a collimated scintillation probe is used. Either the probe as a whole is rotated from above or by a motor placed within[20]. More recently, a ring shaped film mounted on a cylindrical lead shield is used as a detector. The probe with the film is left in the bore-hole for a suitable exposure and the developed image gives the predominant direction of flow.

3.3.5 *Aquifer Characteristics* : Several aquifer characteristics, e.g., effective porosity, transmissivity and dispersivity can be determined by the use of radiotracers and logging devices.

The effective porosity, i.e., the effective pore space to total volume can be determined by injection and monitoring of the radio tracer. The volume V of water pumped between the wells at distance r apart of an aquifer of thickness b, is given by

$$V = \pi r^2 bs$$

where, s is the effective porosity. Prime requirements are that the distance between wells be large compared to the aquifer thickness, i.e., $r > b$; radial pumping velocities are larger than the natural flow velocities and the cone of depression at the pumping well be small compared with the volume of the water pumped. Details of field experiment have been described by Halevy and Nir[21].

The transmissivity is a measure of the ability of an aquifer to transmit water and is given by

$$T = b\,k$$

where, T is the coefficient of transmissivity, b, the thickness of the aquifer and k the coefficient of permeability. The use of tracers in two injection and one observation well have been made. Alternately, k can be determined by knowing the average value of filtration velocity and hydraulic gradient by application of Darcy's law.

The dispersivity characterises the mixing property of an aquifer and is of importance for large scale artificial recharge of aquifers by water of a lower quality, waste disposal in the ground or the intrusion of salt water into fresh water. The coefficient of dispersion D is involved in the transport equation :

$$\frac{\delta c}{\delta t} = D\frac{\delta^2 c}{\delta x^2} - v\frac{\delta c}{\delta x}$$

where, c is the concentration of the tracer and x, t are the space and time variables.

3.3.6 *Regional Studies of Origin and Dynamics of Ground Water* : For regional ground water investigations, environmental isotopes, e.g., ^3H, $^{18}O/^{16}O$, $^2H/^1H$ have been extensively used. Their distribution gives information which is sometimes unique in making decisions on the origin of waters, ground water flow regimes, interconnections between different aquifers.

In mountainous regions, altitude effects are observed in stable isotopic species of hydrogen and oxygen. These effects can be used to study the source of ground water recharge and the extent of intermixing of recent recharge with old ground waters. The changes in tritium concentration with time can be helpful in evaluating the transit and turnover times of a ground water basin.

Usually, it is possible to determine the interconnections between surface and sub-surface waters as it is known that the surface water of lakes or reservoirs have an enriched stable isotopic composition such that they do not fall on the meteoric line and thus are provided with a natural isotope labelling. Further, isotopic composition is not altered for the water in the ground where it escapes evaporation except at very high temperatures.

In semi-arid and arid regions, environmental tritium content can give qualitative information about the recharge processes while the stable isotopic contents in surface and sub-surface waters have been useful to demarcate the recent water from paleowaters. To supplement information, ^{14}C-dating has been helpful for studies with old ground waters.

3.3.7 *Quality of Ground Water* : In general, some quantitative limits are placed for physical, chemical and bacterial quality of drinking water. The physical characteristics are mainly fixed on the basis of turbidity, colour and taste. The chemical control depends on the concentration of various elements and compounds in water while the bacterial control is based on the number of colonies obtained from a known volume of water. These limits change from place to place depending on climate, geography and geology of the area. Eutrophication, i.e., the process where the bacterial productivity of water is progressively increased by the addition of nutrient salts specially nitrates and phosphates. It occurs in undisturbed nature, but may be greatly accelerated in waters which receive nutrients from discharges of sewage and industrial waste or from agricultural fertilisers. Usually the process leads to deterioration of the environment but there are cases, e.g., in fish ponds where it encouraged to increase the crop of fish. These are subjects requiring careful studies[22].

For finding out the traces of elements, atomic absorption spectrophotometric, mass-spectrometric and radioactivation analyses are routinely used. In radioactivation nuclear particles (e.g., thermal neutrons or protons) are used to produce radioactive isotopes. This method requires a few milligrams or less of sample in solid or liquid form. The sensitivity of the method range from 10^{-8} to 10^{-12} gram per gram of sample depending on the element to be detected and the flux of the incident radiation. Radiation sterilisation for the control of bacterial activity in waste waters is now in routine use in developed countries.

4. Indian Contribution to Isotopic Hydrology

The Indian status of applications of radioisotopes and radiation sources in hydrology is discussed by Iya,

et al[23]. This review has dealt with investigations conducted to obtain specific information regarding the study of ocean sediment transport, seepage in dams and canals, flow measurement in turbulent streams, and application of environmental isotope. The first radiotracer application in India was carried out in 1959 to select suitable dumping site for the dredged material at Bombay port. Since then as many as 34 investigations have been conducted for studies connected with the bed load transport[24] and 45 trials are made for streamflow measurements. Another review has been prepared by Bahadur[25]. Most of the major investigations performed with the help of environmental and artificial isotopes were described in the proceedings of first national symposium on the application of isotope techniques in hydrology and hydraulics held at Poona during 26-27 November 1974.

4.1 *Hydrometeorological Studies*

Cosmically produced silicone-32 in nature has been reported by Lal et al[26]. Bhandari[27] reported on some physical processes occurring in the atmosphere based on radionuclides of natural and artificial origin. The concentration of radon daughters as well as the activity ratios of ^{214}Bi to ^{210}Pb in rains can be used for estimating the ratios of continental to maritime air in an air mass. Rama[28] used ^{222}Rn to delineate the pathway of southwest monsoon over Arabian Sea. Athavale et al [29] reported on the bomb-produced tritium in the Indian precipitation distributed over 17 stations all over India during 1961-64 with the principal aim of studying the prevalent meteorological processes. One of the main conclusion of their work is that the spatial variation of tritium suggests the existence of two well defined cells which are internally well mixed. Estimates of 2 to 3 years were obtained for the stratospheric residence time for tritium.

4.2 *Surface Hydrological Studies*

Lal et al[30] measured the concentration of silicone-32 and found it to be 0.33 ± 0.07 dmp/10^3 litres in snowmelt waters feeding Jhelum and this concentration was reported to be the same as observed from the mean precipitation over the region. During interdepartmental glaciohydrological expedition 1971, a few snowmelt water samples were collected from central Himalayan Region. The deuterium content varied from -175 percent to -103 percent for these samples. With the help of global data, it was possible to estimate the altitudes where the precipitation might have taken place. The results demonstrate that the origin of these waters is due to summer precipitations over the glaciated region[31] with an altitude variation of 3.45 percent per 100 m.

The first trials for measurement of stream discharge were made in early sixties by Bhabha Atomic Research Centre, Bombay in collaboration with Central Water and Power Research Station, Poona in a canal followed by river discharge measurements in other rivers making use of total count technique. The method suffers from inherent defects for high discharges but is very useful for finding the discharge of turbulent streams.

Leakages from several man-made structures have been investigated. Iya et al[32] utilised ^{82}Br as a tracer to study the flow paths of seepage in the coffer dams at Srisailam. The major points of seepage entry and the flow paths of seepage across the dam were established. Krishnamurthy et al[33] located the fissures at Aliyar Dam. Rao et al[34] confirmed the suspected seepage entry from Bhadra Reservoir. Krishnamurthy et al[35] reviewed conventional techniques for canal seepage estimation and gave a new theoretical and experimental approach based on single well tracer dilution technique for Ganga Canal. Mixing and residence time of primary sewage were determined by radiotracer method[36].

The stable isotopes D and ^{18}O were successfully used to study the influence area of a percolation tank in basaltic formation. The method was also applied to study leakage from Jowai Reservoir.

Several laboratory studies have been conducted for measurement of suspended sediment load in water but no continuous field measurements have so far been carried out. Bed load studies are taken as a routine as outlined earlier.

4.3 *Sub-surface Hydrological Studies*

For the first time, back scatter nucleonic gauges for soil density and moisture determination were used by Central Water and Power Research Station, Poona. These gauges were calibrated in different soil materials under different geometrical conditions[37] in the laboratory. Field investigations, e.g., borrow evaluation, in situ density and porosity of loose river deposits, nondestructive testing of concrete dam were also described with a review of various factors affecting the performance of gauges. Since then, these instruments have been routinely used for sub-surface investigations at river valley projects. At Central Arid Zone Research Institute, the neutron moisture meter was used to study the soil moisture dynamics for stabilisation of sand dunes. Bardhan[38] utilised these gauges for determination of aquifer parameters using a neutron absorber. More recently, combination of soil density and moisture gauges with tritium tagging were used by Arora et al[39] for monitoring the deep drainage in an irrigated field where an irrigation experiment was laid on water-use efficiency studies.

On chronology, Rama[9] contributed a chapter to IAEA guidebook on nuclear techniques in hydrology. Lal et al[30] concluded that the apparent silicone-32 ages for ground water (500-2000 year old) in arid to semiarid to wet regions of India are found to be in good agreement with C-14 ages.

Environmental ^{3}H has been used by Sukhija[40] for evaluation of ground water recharge in semi-arid regions of India. Results of two different samplings performed during 1967 and 1969 were in fair agreement and it was

concluded that about 5 percent of the precipitation recharges the ground water. Environmental ^{3}H has also been used to evaluate the recharge in hard rock areas of Andhra Pradesh. The artificial tritium technique was used by Datta et al[41] to evaluate the ground water recharge in Western U.P. These studies have also been extended to regions in Punjab and Haryana. Bahadur et al[42] used this technique to work out the water balance in microplots where surface runoff was measured. Fraczek and Bahadur[43] made use of two tracers, viz., ^{51}Cr-*EDTA* and *HTO* for determination of effective porosity of a unconfined sandy aquifer in Rajasthan employing two well technique. The tritium activity distribution curve showed three distinct peaks corresponding to three values of effective porosity, demonstrating the stratified nature of the aquifer. In another study[44] filtration velocities in sandy loam were used to compute the transmissivities and values compared with those obtained by other investigators.

The first radiotracer study for ground water flow was undertaken at Mula Dam site for location of pervious pockets[45]. During 1966 artificial tritium was used to locate the subterranean interconnections in Assam[37] for distances up to 6 km. Mahajan et al[46] reported the use of nucleonic gauges and radiotracers for locating the pervious zones in quartzitic formations and also below the foundation of an earth dam.

The environmental tritium concentration of ground waters in karst terrain of Kopili Project, Assam showed evidence of quick recharge even under a thick cover of shale[36]. In another ground water study, ^{3}H, ^{2}H, ^{18}O were used to study the regional ground water situation in semi-arids of Gujarat and Rajasthan[47]. The high tritium values in shallow aquifers of Gujarat indicated that the aquifer is fast replenished by rainfall. The absence of ^{3}H in confined aquifers of Gujarat and water samples taken 14 m below the water-table in Rajasthan show that these waters are older than twenty years. Deuterium and ^{18}O data of Rajasthan indicate that the aridity enriches the stable isotopes and this is related to salinity development. Depth profiles show the presence of old waters having less negative δ-values which could be due to higher precipitation in the past (a few thousand years back). The stable isotopic contents do not follow the Craig line and this could be due to enrichment by evaporation before recharge.

5. Global Status of Isotopic Hydrology

The evaluation of production rate of cosmically produced isotopes and their applications in atmospheric sciences have been developed at Tata Institute of Fundamental Research, Bombay in collaboration with several leading institutions of the world. For snow and glacier hydrology, isotope gauges were developed at Sierra Nevada Laboratory, U. S. A., stable isotopic applications were developed at University of Copenhagen, Denmark and support from Cold Regions Research Laboratory, New Hamphire. Its use has been extended by Friedman in U. S. A., Amback at Innsbruk, Austria, Krouse in Canada and Moser at Munnich, F. R. G., Russians developed the method for utilisation of gamma activity of ground for areal snow surveys. These were subsequently used in European countries. The developments for stream discharge evaluation has taken place in France, U. K., etc. Environmental tritium was first used in U. S. A. for river basin studies followed by Canada, F. R. G. and others. Extensive use of nuclear techniques in civil engineering were made in U. S. A., U. S. S. R., Japan, etc. Ground water tracer studies were first reported in U. S. A. followed by other countries.

Several distinguished scientists, e. g., W. F. Libby (California, U. S. A.), Don Kirkam, (Illinois, U. S. A.), E. Eriksson (Uppsala, Sweden). W. Dansgaard (Copenhagen, Denmark), H. Moser (Munnich, F. R. G.), D. B. Smith (U. K), A. Nir (Israel), Lal (India) have contributed significantly to the subject of isotopic hydrology. No doubt, that the developmental work in the field was undertaken by a few painstaking chemists and physicists but the main credit goes to the efforts made by Hydrology Section of International Atomic Energy Agency, Vienna for taking these techniques to field hydrologists and hydrogeologists.

The isotope hydrology has now developed to a stage that the techniques are now accepted as tools of investigations in the hands of a hydrologist to solve problems in agriculture, engineering and industry.

6. Concluding Remarks

At Bhabha Atomic Research Centre, Bombay, Isotope Division has developed facilities for sediment transport studies and instruments for radiotracer work. The group plans to have a mass spectrometer for application of stable isotopes in hydrological studies. Group working at Desalinisation and Effluent Engineering Division of this centre is engaged in the development of ground water velocity and direction probes while nucleonic gauges have been developed at the Division of Radiological Protection for routine use. The Central Water and Power Research Station, Poona has a set of nucleonic gauges, natural gamma logging equipment with other facilities for radiotracer work. Facilities for environmental radiotracers, e.g., ^{3}H, ^{14}C and ^{32}Si exist at Physical Research Laboratory, Ahemdabad. The National Geophysical Research Institute at Hyderabad has a ^{3}H laboratory for environmental isotopic work and plans to procure a mass spectrometer and other facilities for ground water research are underway. The Nuclear Research Laboratory at Indian Agricultural Research Institute, New Delhi has Troxler's nucleonic gauges and indigenous tracer logging probes. Facilities for tritium tagging work have been developed and it is proposed to procure a mass spectrometer, a tritium enrichment facility and a low background liquid scintillation counter for environmental isotopic work. The Geological Survey of India and Central Ground Water Board have radiation logging equipments and the later organisation is proposing to

set up a laboratory for isotopic work at Faridabad. Many other research institutes and universities are interested in the application of the nuclear techniques to hydrological problems.

With the available know-how and the resources, it is possible to develop remotely controlled snow gauges for studies connected with the evaluation of water resources of Himalayan Region. It would also be desirable to go into the feasibility of snow-survey studies for determination of water content by natural gamma activity of the earth. These will help evaluate and predict the inflows to reservoirs like Gobindsagar Lake. The stable isotopes can be used for snowmelt-runoff and glacial drainage studies to understand the flood problems in north India rivers as the time of maximum insolation and monsoon activity coincides. Radiotracer method for turbulent streams in mountainous regions offers a unique opportunity. Continuous data collection for suspended sediments would be extremely useful in taking measures for increasing the life of reservoirs and soil conservation from erosion of valuable agricultural lands. Seepage studies from canals and reservoirs are being conducted as a routine but a more systematic work on ground water investigations, e.g., their origin, recharge and flow characteristics need to be developed with emphasis on interdisciplinary approach. The stable isotope approach offers an attractive possibility to understand arid zone hydrology of Rajasthan, Gujarat and Himachal Pradesh and also the influence of geothermal fields in the neighbouring aquifers. The mixing of sea water with fresh water in coastal aquifers needs to be investigated.

The interrelationship of surface with sub-surface water can be studied by making use of environmental isotopes in order to study the influent and effluent characteristics of rivers for optimal utilisation of water resources. The above only outlines some of the complex hydrological problems which could be undertaken for economic solution with the help of nuclear techniques.

7. Acknowledgements

The author is grateful to Project Director, Nuclear Research Laboratory and Director, Indian Agricultural Research Institute for their permission to present the paper.

8. References

(1) BOCHIN, N. et al : "Status of and Reasons for using Isotope Techniques in Hydrology." Proc. 'Peaceful uses of Atomic Energy.' Vol. 14, 1972, pp. 411-423.

(2) GERDEL, R.W. et al : "The use of Radioisotopes for the Measurement of the Water Equivalent of a Snowpack." Trans Am. Geophys. Union, Vol. 31, 1950, pp. 449-453.

(3) FRIEDMAN, I. : "Deuterium Content of Natural Waters and other Substances." Geochim, Cosmochin Acta, Vol. 4, 1953, pp. 89-103.

(4) BENGEMANN, F. and LIBBY, W.F. : "Continental Water Balance Ground Water Inventory and Storage Times, Surface Ocean Mixing Rates and Worldwide Circulation Patterns from Cosmic Ray and Bomb Tritium." Geochin Cosmochin Acta, Vol. 12, 1957, pp. 277-296.

(5) FEELY, H.W. et al : "The Potential Applications of Radioisotope Techniques to Water Resources Investigations and Utilisation." Westwood, N.J., Isotope Inc. USA. NYO-9040, 1961, pp. 1-352.

(6) BELIKOV, M.P. et al : "Applications of Radioisotopes in Hydrotechnology." Publishing House of Literature on Construction, Agriculture and Construction Materials, Moscow, 1961, pp. 1-164. (Russian)—English Translation by Israel Programme of Scientific Translations Ltd., Catalog No. 1176 (1964).

(7) BAHADUR, J. : "Utilisation of Isotopes for Sub-soil Investigations and Soil Compaction Control." Central Board of Irrigation and Power, New Delhi, 1968, pp. 1-477.

(8) FERRONSKIY, V.I. et al : "Radioisotope Investigation Methods in Engineering, Geology and Hydrogeology." USAEC Report, No. AEC-tr-7230, 1969, pp. 1-254.

(9) IAEA : "Guide Book on Nuclear Techniques in Hydrology." Tech. Rep. Ser. Int. At. Energy Ag., No. 91, 1970, pp. 1-214.

(10) PAYNE, B.R. : "Isotope Hydrology." Advances in Hydroscience, Vol. 8, 1972, pp. 95-138.

(11) GASPER, E. and ONCESCU, M. : "Radioactive Tracers in Hydrology." Elsevier Publishing Co., Amsterdam, 4, 1972.

(12) BROWN, R.H. et al : "Ground Water Studies—An International Guide for Research and Practice." UNESCO, 1972 pp. 1-40.

(13) LAL, D. and SUESS, H.E. : "The Radioactivity of the Atmosphere and Hydrosphere." Ann. Rev. of Nucl. Sc., Vol. 18, 1968, pp. 407-434.

(14) DANSGAARD, W. : "Stable Isotopes in Precipitation." Tellus, Vol. 16, 1964, pp. 436-468.

(15) ERIKSSON, E. : "Isotopes in Hydrometeorology." Proc. Symp. Isotopes in Hydrology, Vienna, 1967, pp. 21-23.

(16) IAEA : "Nuclear Well Logging in Hydrology." Tech. Rep. Ser. Int. At. Energy Ag., No. 126, 1971, pp. 1-90.

(17) BLUME, H.P. et al : "Tritium Tagging of Soil Moisture. The Water Balance of Forest Soils." Proc. Symp. 'Isotope and Radiation Techniques in Soil Physics and Irrigation Studies', Istanbul, 1967, p. 315.

(18) SMITH, D. B. et al : "Water Movement in the Unsaturated Zone of High and Low Permeability Strata using Natural Tritium." Proc. Symp. 'Isotope Hydrology', Vienna, 1970, p. 73.

(19) DROST, W. et al : "Isotope Methods in Ground Water Hydrology." Commission of the European Communities—EURISOTOP, 61-Series, Monograph-16, 1974, pp. 1-176.

(20) DINESCU, L. et al : "The Determination of Underground Water Flowing Direction by the Single Well Method." Report No. MR-27, 1967, pp. 1-14.

(21) HALEVY and NIR, A. : "The Determination of Aquifer Parameters with the Aid of Radioactive Tracers." J. Geophy. Res., Vol. 67, 1962, pp. 2403-9.

(22) ERIKSSON, E. : "World Water Problems." Report on the Nobel Workshop, May 7-11, 1973 IHD, Sweden Report 34, 1973, pp. 1-35.

(23) IYA, V. K. et al : "Applications of Radioisotopes and Radiation Sources in Industry, Radiation Processing and Hydrology." Proc. Symp. 'Peaceful Uses of Atomic Energy', New York, IAEA, Vol. 14, 1972, pp. 3-18.

(24) BANERJEE, S. : "Radioisotope Techniques in Water Resources Research and Management with Special Reference to India." Proc. Symp. Application of Isotope Techniques in Hydrology and Hydraulics, Poona, 1974.

(25) BAHADUR, J. : "Status Report on Nuclear Techniques in Hydrology for the End of International Hydrological Decade." Report prepared for Indian National Committee on IHD, Jan.' 74, p. 1.

(26) LAL, D. et al : "Cosmic Ray Produced Silicone-32 in Nature." Science, Vol. 131, 1960, pp. 332-337.

(27) BHANDARI, N. : "Studies of Some Physical Processes Occurring in the Atmosphere based on Radionulides of Natural and Artificial Origin." Ph. D. Thesis, University of Bombay, India, 1965.

(28) RAMA, S. N. I. : "An Attempt to Trace the Monsoon Flow Using Natural Radon." Indian J. Met. Geophys., Vol. 18, 1967, p. 403.

(29) ATHAVLE, R. N. and LAL, D. : "The Measurement of Tritium Activity in Natural Water". Proc. Indian Acad. Sci., Vol. 15, 1967, pp. 73-101.

(30) LAL, D. et al : "Silicone-32 Hydrology", Proc. Symp. Isotope Hydrology, Vienna, 1970, pp. 847-863.

(31) BAHADUR, J. : "Altitudinal Variation in Deuterium Concentration of Water Samples of Central Himalayas." Accepted for Indian J. Met. and Geophys., 1975.

(32) IYA, V. K. et al: "A Radiotracer Study on Flow Path of Seepage in Coffer Dams at Srisailam." Intern. Jour. of Appl. Rad & ISO, Vol. 18, 1967, pp. 349-57.

(33) KRISHNAMURTHY, K. et al : "A Radiotracer Study on Seepage Lines in Aliyar Dam." Report BARC/Isotope/13, 1967, pp. 1-15.

(34) RAO, S. M. et al : "Seepage Studies at Bhadra Dam using Radioactive Tracer." Report BARC/Isotope/15, 1968, pp. 1-15.

(35) KRISHNAMURTHY, K. et al : "Theory and Experiment in Canal Seepage Estimation using Radioisotopes." J. Hydrology, Vol. 9, 1969, pp. 277-293.

(36) EAPEN, A. C. et al : "Determination of the Retention Period of Sewage in a Primary Sedimentation Tank using a Radioactive Tracer." Report AEET/Radiochem/28, 1962.

(37) BAHADUR, J. : "Application of Radioisotope Techniques to Civil Engineering Problems." Univ. of Poona, Ph. D. Thesis, 1968, pp. 1-223.

(38) BARDHAN, M. : "A Geophysical Method for Determination of Aquifer Parameters of Hard Rocks." Proc. Intern. Symp. 'Development of Ground Water Resources', Madras, Nov.' 73, Vol. 1, see 1-b, pp. 11-21.

(39) ARORA, R. P. et al : "Radiation Techniques for Monitoring Deep Drainage in an Irrigated Wheat Field." Proc. Symp. 'Application of Isotope Techniques in Hydrology and Hydraulics' Poona, 1974.

(40) SUKHIJA, B. S. and RAMA : "Evaluation of Ground Water Recharge in Semi-arid Region of India using Environmental Tritium." Proc. Ind. Acad. Sci., Vol. 73, see A, No. 6, 1973, pp. 270-292.

(41) DATTA, P.S. et al: "Ground Water Recharge in Western Uttar Pradesh". Proc. Ind. Acad. Sci., Vol. 73, see A, No. 1, 1973.

(42) BAHADUR, J. et al : "Tritium Tracer Technique for Study of Water Movement in Alluvial Soils." Proc. Symp. 'Use of Radiations and Radioisotopes in Studies of Plant Productivity', Pantnagar, Feb. 1974.

(43) FRACZEK, E. and BAHADUR, J. : "A Radiotracer Experiment for Effective Porosity Determination of Quarternary Aquifer at Setala, Rajasthan." Proc. Symp. 'Application of Isotope Techniques in Hydrology and Hydraulics', Poona, Nov. 1974.

(44) BAHADUR, J., et al : "^{51}CR-EDTA as a Radiotracer for Natural Ground Water Flow Measurement in a Tube-well at IARI." Sent for Publication in Indian J. of Agri. Engg., 1974.

(45) BAHADUR, J. :"Study of Ground Water Flow by Radioactive Tracers at Mula Dam site, Ahmednagar, Maharashtra." Proc. Symp. 'Ground and Lake Water Resources in India', Hyderabad, Dec. 1967, pp. 91-101.

(46) MAHAJAN, N. M. et al : "Use of Radioisotopes in Seepage Studies below the Foundation of an Earthen Bund and its Embankments." Journal Irrigation and Power, Vol. 30, No. 3, 1973, pp. 209-15.

(47) BAHADUR, J. et al : "Environmental Isotope Approach for Study of Ground Water in Semi-arid Regions of Rajasthan and Gujarat." Proc. Symp. 'Application of Isotope Techniques in Hydrology and Hydraulics', Poona, Nov. 1974.

Time Series Analysis and its Application to Water Resources

SUN-FU SHIH
Systems Engineer
Department of Resource Planning
Central and Southern Florida Flood Control District
West Palm Beach, Florida, U.S.A.

SYNOPSIS

Time series analysis has been used widely in several fields of stochastic approaches to analyze the water resources data. A systematic model of time series analysis which uses the F-test as a statistical criterion to determine the possibility of any component existing in series is developed. The data obtained from the Kissimmee River Basin and Lake Okeechobee, Florida, such as annual water demand, crop rooting depth, evaporation, lake stage, water quality, streamflow, precipitation, and accumulated irrigation requirements are used to demonstrate the seven categories of time series. Both correlogram and spectral analyses which include the end of month stages of Lake Okeechobee is taken as sample data used to analyze the deterministic portion of the series. The results show that the correlogram reveals more about the relationships between values of series, while the spectrum provides the extent to which the series exists in some fundamental periodicities. Based on the Chi-square test for goodness-of-fit between synthetic sequences and record data, the synthetic streamflow with joint distribution is more applicable in the Kissimmee River. The results of time series analysis can furnish means for forecasting and prediction which are increasing in use in the fields of resources planning, design, management, and synthetic data.

Introduction

Present water resources problems have been approached by three methods, i. e., stochastic, deterministic and parametric approaches. The time series analyses have been used extensively in several fields of stochastic approaches. Time series of interest to the water resources workers include water demand, evapotranspiration, streamflow, rainfall, lake stage variation, and stream water quality, etc. The results of analyses not only can look into the cause, interaction, and effect of water resources systems, but also can provide means for forecasting and prediction which are increasing in use in the fields of resources planning, design, management, and synthetic data.

Pioneering studies of time series analyses, serial correlation, spectral analyses and mathematical statistics are those of Blackman and Tukey[1], Wilks[2], Brown[3] Cramer[4], Kendall and Stuart[5], Box and Jenkins[6] and Anderson[7].

Applied time series analyses to hydrologic data and water quality parameters are those of Chow[8], Roesner and Yevdjevich[9], Kisiel[10], Chow and Kareliotis[11], Yevdjevich[12], Rich[13] and Bourodimos et al[14]. The time series techniques have also been used to analyze the plant growth dynamics and water use model by Shih et al[15][16][17]. Chow and Kareliotis[11] indicated that the stochastic method, employing the concept of probability as well as its sequential relationship, has not been well introduced in the practical design and planning of hydrologic projects because such methods have not been fully developed. Hence, there is a great need for more practical applications in order to better describe the processes involved.

The objectives of this study are :

(1) A general concept of time series is introduced. This time series is considered as a sum of three components; a trend, a cyclical movement, and a randomness.

(2) A systematic model of time series analyses is developed. This model comprises several techniques such as multiple regression analysis, asymptotic expansion, harmonic analysis, serial correlation, spectral analysis, and Monte Carlo simulation, etc.

(3) The systematic model has been converted into a computer program with Fortran IV Language. The computer results are compared with the field data obtained from the Kissimmee River basin and Lake Okeechobee area, Florida.

(4) After applying this analyses based on the F-test, the water resources data in South Florida is divided into seven categories :

(*a*) a simple time trend ;

(*b*) some periodicity ;

(*c*) entirely random variation ;

(*d*) a time trend with some periodicity ;

(*e*) a time trend with some degree of randomness ;

(*f*) several periodicities with some degree of randomness; and

(*g*) a time trend with some periodicity and randomness.

(5) The techniques of correlograms and spectral analyses are demonstrated and the differences between those two analyses are also discussed.

(6) The time series analysis of existing records is used in synthesizing time series. Synthetic streamflow is used as an example.

Mathematical Analysis

Four classes of analyses are introduced in this study :

Time Series Analysis and Forecasting

When the behavior of a water resources system is not immediately evident, a stochastic approach may be used to discover underlying patterns. For example, time series analysis which includes three kinds of movements can be utilized to observe the trend, cyclical movement and residual pattern of a water resources system.

Trend Movements : The trend movement expresses a smooth, continuous, relatively irreversible long-run trend. The typical time trend lines, $X_T(t)$, are :

(1) *Polynomial Model* :

$$X_T(t) = a_0 + a_1 t + \ldots + a_n t^n \qquad \ldots(1)$$

where, $a_0, a_1, \ldots, a_n$ = constants; and

t = time expressed as an integer in a series of consecutive integers ranging from 1 through n.

The values of constants can be obtainedjby the least squares method [Steel and Torrie([18])].

(2) *Asymptotic Expansions Model* :

$$X_T(t) = \alpha + \beta \cdot \gamma^t \qquad \ldots(2)$$

where, α, β, γ are all constants, t is the same as expressed in Equation (1). If a series plotted on semi-logarithmic paper yields an approximately straight line, this type of model can be used to discover the time trend. The least squares method also can be used to obtain the constants of α, β and γ.

(3) *Moving Averages Model* :

$$X_T(t) = \theta_0 Z_t + \theta_1 Z_{t-1} + \theta_2 Z_{t-2} + \ldots + \theta_q Z_{t-q} \qquad \ldots(3)$$

is called a moving average process of order q.

where, Z is a random variable ; $\theta_0, \theta_1, \ldots, \theta_q$ are the weights.

The moving average is in common use for the value which can change gradually with time, because the average computed at any time should place more weight on current observations than on those obtained a long time ago.

Extrapolation on the basis of the trend line shows the influence of the trend movement in the future state of the environmental phenomenon under study, but it does not give its expected probable value unless the cyclical influences are introduced.

Cyclical Movements : Cyclical movements represent the periodic variation of the series. Sum of the harmonic model is utilized to express the cyclical movement, $X_c(t)$, and can be described as:

$$X_c(t) = \frac{A_0}{2} + \sum_{K=1}^{M} (A_K \cos KWt + B_K \sin KWt) \qquad \ldots(4)$$

where, M = total number of harmonics considered non-negligible ;

K = harmonic number ;

$W = 360/P$;

P = the period of fundamental cycle ; and

A_K, B_K = Fourier coefficients of K^{th} harmonic.

Let $2N$ equal the total number of tabulated data points. In practical application, the upper limit M in Equation (4) is much less than N. The estimate of the Fourier coefficients is given by Anderson and

Anderson[19] as

$$A_0 = \frac{1}{2N}\sum_{i=1}^{2N} X_i \qquad \ldots(5)$$

$$A_K = \frac{1}{N}\sum_{i=1}^{2N} X_i \cos KWt \qquad \ldots(6)$$

$$B_K = \frac{1}{N}\sum_{i=1}^{2N} X_i \sin KWt \qquad \ldots(7)$$

where, X_i is the discrete data at time i, N is the half number of data points.

Ralston and Wilf[20] introduced a numerical procedure to calculate the Fourier coefficients. The procedure was described briefly as follows :

Let $K\pi/N$, $K = 0, 1, \ldots, 2N-1$

$$c_1 = \cos(\pi/N),\ d_1 = \sin(\pi/N) \qquad \ldots(8)$$

$$U_2 = 0,\ U_1 = 0,\ c = 1,\ d = 0,\ i = 1 \qquad \ldots(9)$$

The following recursive sequence is used to compute U_0, U_1 and U_2

$$U_0 = F\left(\frac{m\pi}{N}\right) + 2\,c\,U_1 - U_2 \qquad \ldots(10)$$

in which $F(m\pi/N)$ is a vector matrix of tabulated function values of length $2N$.

$$U_2 = U_1,\ U_1 = U_0 \qquad \ldots(11)$$

for values of $m = 2N-1,\ 2N-2, \ldots, 1$. The Fourier coefficients are then

$$A_i = \frac{1}{N}\left[F(0) + c\,U_1 - U_2\right] \qquad \ldots(12)$$

$$B_i = \frac{1}{N}\,d\,U_1 \qquad \ldots(13)$$

the values of c and d are updated to :

$$q = c_1 c - d_1 d,\ d = c_1 d + d_1 c,\ c = q \qquad \ldots(14)$$

where, i is increased by 1 and the sequence starting at Equation (10) is repeated until the desired order of Fourier coefficients have been computed.

Since each of the amplitude coefficients of a series makes up a variance and the sum of the squares of the amplitude coefficients is related to the total variance of the mean by the equation [Brooks and Carruthers[21]].

$$\sum_{i=1}^{N} Q_i^2 = 2\sigma_{\bar{X}}^2 \qquad \ldots(15)$$

in which $\sigma_{\bar{X}}^2$ is the total variance of mean; $Q_i = \left(A_i^2 + B_i^2\right)^{1/2}$, is the magnitude of amplitude. Percent of the total variation in series of each harmonic, H_i, can be expressed by

$$\text{Percent of the } H_i \text{ harmonic} = \frac{Q_i^2 \times 100}{2\sigma_{\bar{X}}^2} \text{ for } i<N \qquad \ldots(16)$$

and

$$\text{percent of the } H_i \text{ harmonic} = \frac{Q_i^2 \times 100}{\sigma_{\bar{X}}^2} \text{ for } i=N.$$

The objective of this harmonic analysis is to seek out deterministic regularities.

Residual Movements : Removal of the trend and the cyclical components from the series leaves the random component, or the residuals. The random component has no deterministic pattern of behavior. This component, $X_R(t)$, can be expressed as

$$X_R(t) = Z_n\,\sigma_R + \mu_R \qquad \ldots(17)$$

where, μ_R is the mean value of residuals, σ_R is the standard deviation of the residuals. Z_n is the standardized random, normal, and independently distributed variate. Values can be obtained from prepared tables or generated by computer.

The procedure for simulating normal variates on a computer involves taking the sum, S, of the uniformly distributed random variates $x_1, x_2, \ldots, x_S$, where, x_i is defined over the interval $0 \leqslant x_i \leqslant 1$. Then applying the central limit theorem and the uniform distribution, we find that the expected value and variance of a uniformly distributed random variable over the interval (a, b) is given by

$$\mu_R = \int_a^b \frac{1}{b-a}\,R\,dR = \frac{b+a}{2} \qquad \ldots(18)$$

$$\sigma_R^2 = \int_b^a \frac{(R-\mu_R)^2}{b-a}\,dR = \frac{(b-a)^2}{12} \qquad \ldots(19)$$

If $a = 0$, and $b = 1$ then Equations (18) & (19) can be rewritten as

$$\mu_R = \frac{1}{2} \qquad \ldots(20)$$

$$\sigma_R = \frac{b-a}{\sqrt{12}} = \frac{1}{\sqrt{12}} \qquad \ldots(21)$$

and the standardized normal variate, Z_n, is

$$Z_n = \frac{\sum_{i=1}^{S} x_i - \frac{S}{2}}{\sqrt{S/12}} \qquad ...(22)$$

Equating Equations (17) & (22) together, we obtain

$$X_R(t) = \sigma_R \left(\frac{12}{S}\right)^{1/2} \left(\sum_{i=1}^{S} x_i - \frac{S}{2}\right) + \mu_R \qquad ...(23)$$

The value of S is usually determined by balancing computation efficiency against accuracy. Based on the asymptotic convergence implied in the Central Limit approach, a large number for S would be desirable. However, the time involved in generating S uniform variates for each normal variate would result in a small value of S. There is some computational advantage in using a value of $S=12$ in this simulation [Hamming(22)]. Then, Equation (23) can be rewritten as

$$X_R(t) = \sigma_R \left(\sum_{i=1}^{12} x_i - 6\right) + \mu_R \qquad ...(24)$$

Now, Equation (24) furnishes a simple formula to generate the normally distributed variates with the mean equal to μ_R and the variance equal to σ_R^2.

Combining the above three components together, a time series, $X(t)$, can be represented as

$$X(t) = X_T(t) + X_C(t) + X_R(t). \qquad ...(25)$$

Any one or a combination of these components may exist in practical water resources problem. A discussion of more refined methods of approach must await the account of correlogram and spectral analyses. A systematic flow chart shown in Figure 1 illustrates a procedure for time series analysis. This procedure has been programmed in Fortran IV Language for use on a CDC 3100 computer.

Serial Correlation

A series which is not random can be correlated with neighboring observations. One very useful measure of this effort is the product-moment correlation between successive observations. Given n values $X_1, \ldots, X_n$, the so-called serial correlation of lag k is the correlation between pairs of terms k units apart :

$$r_k = \frac{cov(X_i, X_{i+k})}{[var(X_i).\ var(X_{i+k})]^{1/2}} \qquad ...(26)$$

where, $cov(X_i, X_{i+k})$ is auto-covariance of the sample, or

$$cov(X_i, X_{i+k}) = \frac{1}{n-k} \sum_{i=1}^{n-k} (X_i - \mu_i)(X_{i+k} - \mu_{i+k}) \qquad ...(27)$$

and $var(X_i)$ and $var(X_{i+k})$ are sample variance, or

$$var(X_i) = \frac{1}{n-k} \sum_{i=1}^{n-k} (X_i - \mu_i)^2 \qquad ...(28)$$

$$var(X_{i+k}) = \frac{1}{n-k} \sum_{i=1}^{n-k} (X_{i+k} - \mu_{i+k})^2 \qquad ...(29)$$

where,
$$\mu_i = \frac{1}{n-k} \sum_{i=1}^{n-k} X_i \quad \text{and} \qquad ...(30)$$

$$\mu_{i+k} = \frac{1}{n-k} \sum_{i=1}^{n-k} X_{i+k}$$

For $k = 0$, it follows that $r_0 = 1$; and $k \geqslant 1$,
$-1 \leqslant r_k \leqslant 1$.

Spectral Analyses

The sample spectrum is an appropriate tool for analyzing time series made up of mixtures of sine and cosine waves. The sample spectrum is of great help in detecting the frequencies that should be included in a periodic model. Three main steps are involved in this spectral analyses :

Step 1 : The auto-covariance function of the data is formed based on Equation (27).

Step 2 : The Fourier cosine transformation of the auto-covariance function from the time domain to the frequency domain is computed. This computation can be expressed mathematically as

$$V_k = \frac{E}{m}\left[R_0 + R_m \cos k\pi + 2\sum_{j=1}^{m-1} R_j \cos \frac{jk\pi}{m}\right] \qquad ...(31)$$

where, V_k = Fourier cosine transform of auto-covariance at lag k ;

R_0, R_m, R_j = auto-covariance at lags $k = 0$, m and j, respectively ;

j = lag index, having all integer values between 1 and $m-1$;

m = total number of lags ;

E = constant ;

$E = 1$ for $k = 1, 2, \ldots, m-1$;

$E = \frac{1}{2}$ for $k = 0$, $k = m$; and

k = lag number $= 0, 1, \ldots, m$.

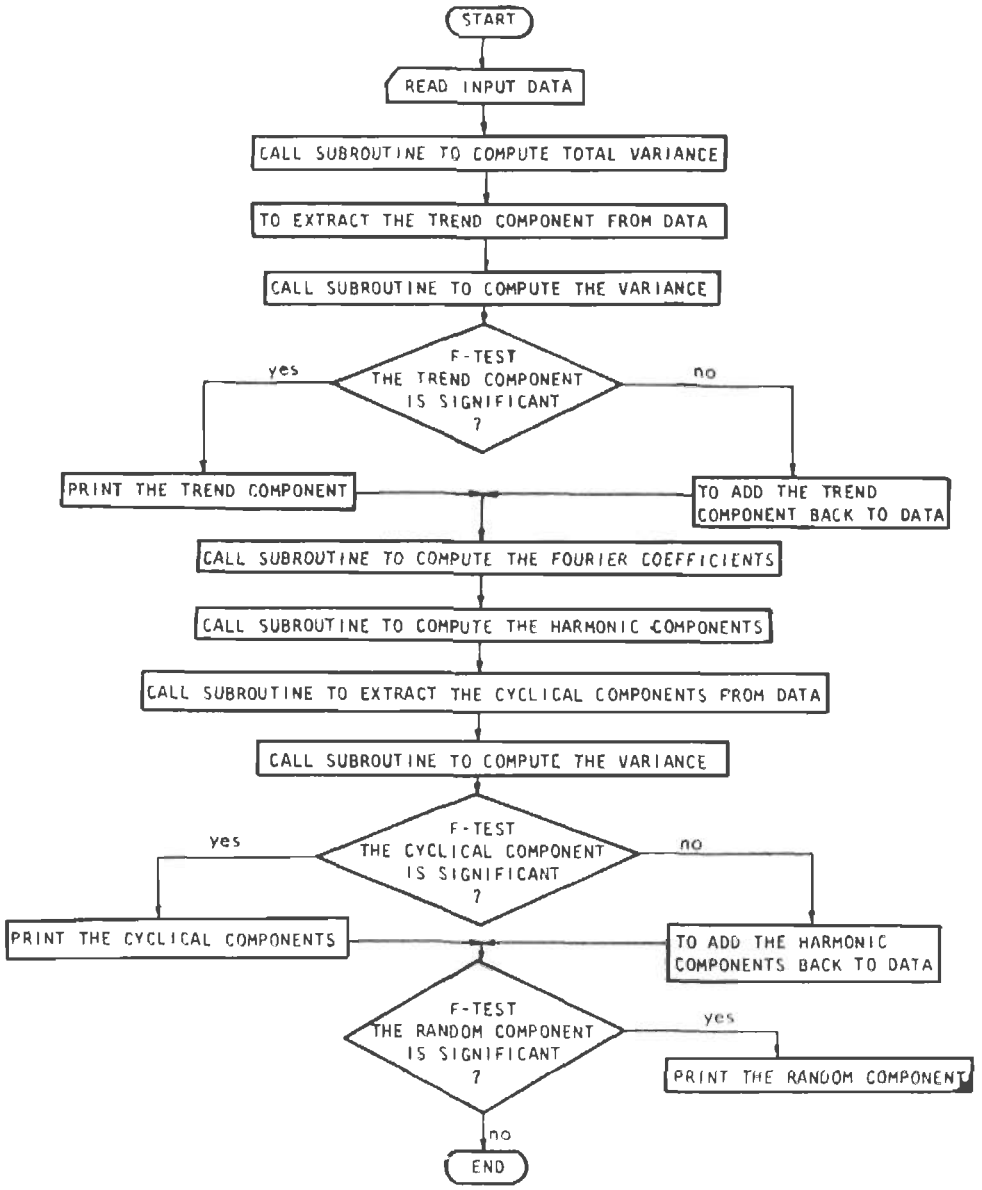

FIGURE 1 : Systematic flow chart for time series analysis.

Step 3 : A weighting computation that counteracts some of the distribution of the spectrum resulting from the analysis of a single record is smoothed. One such computation can be expressed mathematically as

$$U_0 = 0.5\ (V_0+V_1)$$

$$U_k = 0.25\ (V_{k-1}+V_{k+1})+0.5\ V_k \quad \text{for } 1 \leqslant k \leqslant m-1 \qquad \ldots(32)$$

$$U_m = 0.5\ (Vm^{-1}+V_m)$$

where, U = smoothed estimate of variance spectrum.

Sometimes, it is more helpful that the period corresponding to each lag is determined from the lag number and the sampling time interval by this relation :

$$T_k = \frac{2m\triangle t}{k} \qquad \ldots(33)$$

where, T_k = period corresponding to lag k; and

$\triangle t$ = sampling time interval.

Each of these variance spectrums represents a part of the total record. Any generating process contains periodic terms and the frequencies of these terms will appear as peak in the spectrum.

Auto-Regressive Model

As mentioned in previous sections, time series analysis

of existing records can be used in generating the forecasting time series. The auto-covariance function is usually used as a measure of the correlation between the observations X_{t-1}, X_{t-2},.... The general KI^{th} order auto-regressive model can be written as

$$X_{i+1,\,j+1} = \mu_{j+1} + \sum_{l=1}^{KI} b_{j+1-l}\,(X_{i+1-l,\,j+1-l} - \mu_{j+1-l}) + Z_{i+1}\,\sigma_{j+1}\,(1-\rho_j^2)^{0.5} \quad \ldots(34)$$

if $KI = 1$, the Equation (34) is reduced to

$$X_{i+1,\,j+1} = \mu_{j+1} + b_j\,(X_{i,\,j} - \mu_j) + Z_{i+1}\,\sigma_{j+1}\,(1-\rho_j^2)^{0.5} \quad \ldots(35)$$

Equation (35) has been introduced by Thomas and Fiering[23] to synthesize the streamflow sequence at a single site. In which $X_{i,\,j}$, $X_{i+1,\,j+1}$ = synthetic flow during j^{th} and $(j+1)st$ seasons reckoned from the start of the sequence;

μ_j, μ_{j+1} = average flow for the j^{th} and $(j+1)st$ season, within a repetitive annual cycle ;

σ_{j+1} = standard deviation of streamflows for $(j+1)st$ season;

ρ_j = lag one correlation between flows in j^{th} and $(j+1)st$ seasons, i.e., Equation (26) can be reduced as follows :

$$\rho_j = \frac{\sum_{i=1}^{n-1} (X_{i,\,j} - \mu_j)\,(X_{i+1,\,j+1} - \mu_{j+1})}{(n-1)\,\sigma_j\,\sigma_{j+1}} \quad \ldots(36)$$

b_j = regression coefficient for estimating flow in $(j+1)st$ season from that of j^{th} season, i.e.,

$$b_j = \frac{\sum_{i=1}^{n} X_{i,\,j}\,X_{i+1,\,j+1} - n\mu_j\,\mu_{j+1}}{\sum_{i=1}^{n} X^2_{i,\,j} - n\mu^2_j} \quad \ldots(37)$$

j = serial index identifying season;

n = number of years of record; and

Z_{i+1} = standardized random variate.

The term "season" implies the time interval varying from 1 to 6 months. There are three steps involved in this model application :

Step 1 : The parameters of μ_j, μ_{j+1}, b_j, σ_j and ρ_j for each season are computed based on the historical record.

Step 2 : The distribution of the data is determined either by prior knowledge or by specific testing.

Step 3 : A streamflow sequence is generated based on the model indicated in Equation (34).

Applications of the Models

In order to observe the applicability of the mathematical models to practical problems, the field data obtained from the Kissimmee River basin and Lake Okeechobee area, Florida, are used in this study. The time series analyses applied to water resources systems are divided into seven categories.

Category 1. A Simple Time Trend

The Corps of Engineers' study[24] of the annual water demand from Lake Okeechobee is plotted on Figure 2. The polynomial model with 3rd order is used to simulate the trend, i.e.,

$$DM = 0.71481355 + 0.02746433t - 0.00048254t^2 + 0.00000387t^3 \quad \ldots(38)$$

where, DM = the annual water demand, 10^6 acre-ft; and
t = year, 1971 treated as a first year.

Each coefficient of this model has been tested by the F-test at the 5 percent significant level. The cyclical component and random component are insignificant in this set of data. The result of this model is also plotted on Figure 2. As can be seen from Figure 2, the simulated results are very close to the data as reported by the Corps of Engineers[24].

Rooting depth data obtained from Weaver[25] has been used by Shih et al[17] to obtain coefficients for rooting depth models as introduced in Equation (2). The rooting depth models of two crops are shown as :

for sweet potatoes,

$$RD = 118.81 - 115.14 \times 0.9933^t \quad \ldots(39)$$

for soybeans,

$$RD = -21.42 + 284.98 \times 1.0142^t \quad \ldots(40)$$

where, RD = rooting depth, inches; and
t = days after planting.

In these rooting depth models, only trend components are tested at the 5 percent significant level by using the

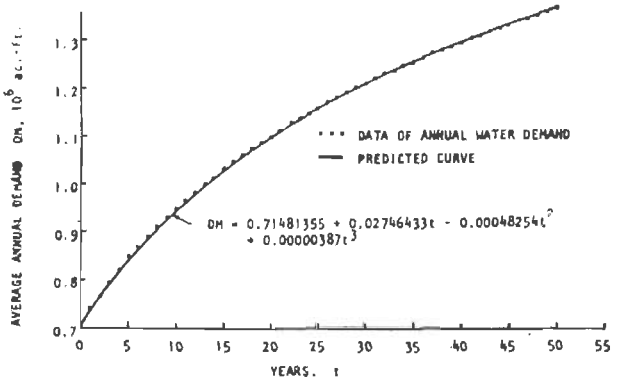

FIGURE 2 : Annual water demand from Lake Okeechobee, Florida.

F-test. The simulated results are given in Figure 3 are compared to the experimental data [Weaver ([25])]. The results also indicated that the asymptotic expansion model is a very applicable tool to simulate the trend of rooting depth.

Category 2. Some Periodicities

Corps of Engineers' data([24]) of monthly evaporation in Lake Okeechobee are plotted on Figure 4. After applying the time series analysis program to the data, the variances of trend, cycle, and randomness are found equal to 0.0002, 1.2033 and 0.0210, respectively. About 98 percent of variance belongs to the cyclical component. The *F*-test also indicates that the cyclical component is very highly significant at the 0.001 level, i.e., the cyclical movement is a most important factor in this monthly evaporation data. The three harmonic coefficients are shown in Table 1. The results of simulation are also shown in Figure 4.

Category 3. Entirely Random Variation

A set of short period records of alkalinity data from the S65E structure at Kissimmee River [Shih, et al ([26])] is plotted on Figure 5. This type of data belongs entirely to the random variation. The time series analysis indicates that the variances of trend, cycle, and randomness are equal to 0.0010, 0.0065, and 0.0135, respectively. The *F*-test shows that only the random component is significant at the 0.05 level.

Category 4. A Time Trend with Some Periodicities

Experimental data on plant's water requirement

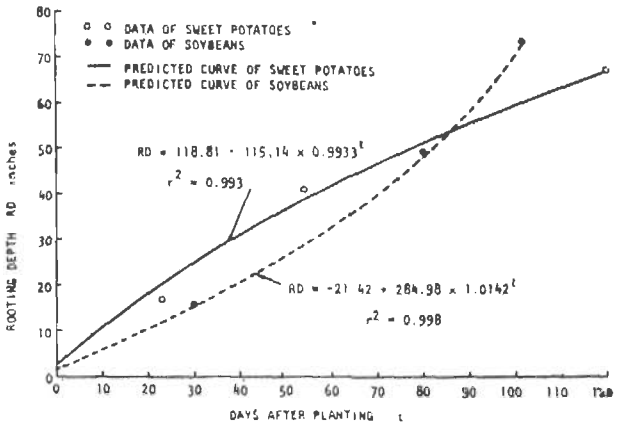

FIGURE 3 : Rooting depth related to the days after planting.

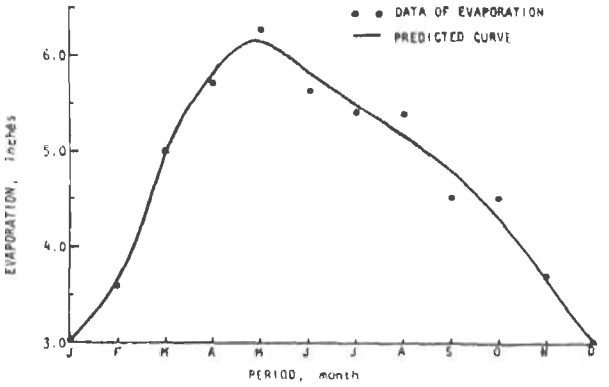

FIGURE 4 : Harmonic analysis of evaporation in Lake Okeechobee, Florida.

TABLE 1

Fourier coefficients and percent of variance in each harmonic.

Examples		1st Harmonic			2nd Harmonic			3rd Harmonic		
		A	B	Var. %	A	B	Var. %	A	B	Var. %
Evap. of Lake Okee.		−1.210	0.714	81	−0.458	−0.014	9	−0.050	−0.067	0
Wat. Use	Field Corn	−0.108	−0.012	87	0.027	0.003	6	−0.006	0.009	1
	Sweet Potato	−0.061	0.004	83	0.002	0.017	0	0.001	0.006	1
Lake Okee. Stage	12-month period	0.514	−0.344	62	−0.057	0.246	10	0.248	0.016	6
	72-month period	−0.184	0.314	40	−0.087	0.055	3	−0.028	0.063	1
Accu. Irreg. Requirement		−0.329	0.780	22	−0.244	−0.735	18	−0.310	−0.421	8

[Shih et al[17]] can be used to demonstrate this category 4 series. The time series analyses for the water use of field corn and sweet potato indicate that the plant's water requirement involves two components—trend and cycle.

The results are shown as

$$\textit{field corn}: WR = 0.08787 + 0.00362t + X_c(t) \quad \ldots(41)$$

$$\text{and } \textit{sweet potato}: WR = 0.0331B + 0.01886t + X_c(t) \quad \ldots(42)$$

where, WR = water requirement, inches per day; and
t = days after planting.

The harmonic coefficients of $X_c(t)$ are given in Table 1. Table I also shows the percentages variation accounted for by the first, second and third harmonic component. In many cases the first three harmonics accounted for a high percent of the variation. Therefore, only three harmonics were used in this study. Comparison of simulated water use, using the models of Equations (41) & (42), with observed water use are shown in Figure 6. The simulated water use is in close agreement with the observed data for each crop considered.

Category 5. A Time Trend with Some Degree of Randomness

The sequential generation of streamflow in the Kissimmee River is a type of time trend with some degree of randomness. The detailed description will be presented in a later section of synthetic streamflows succession.

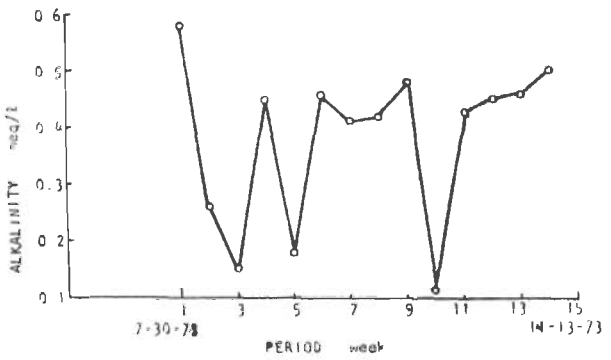

FIGURE 5: Alkalinity data of Kissimmee River at S65E, Florida.

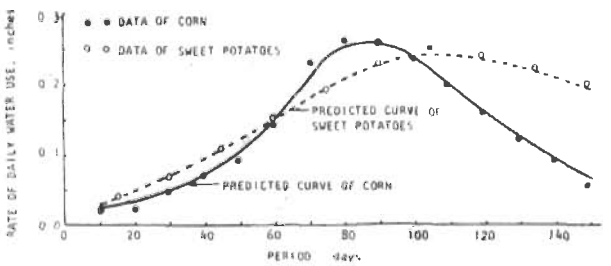

FIGURE 6 : Moisture use for corn and sweet potatoes.

Category 6. Several Periodicities with Some Degree of Randomness

The end of the monthly stage of Lake Okeechobee can be used to describe the phenomena of several periodicities with some degree of randomness. The time series analysis indicates that the variance of trend, periodicity, and randomness recorded in these stages are equal to 0.0035, 0.5577, and 1.1560, respectively. The F-test shows that the trend component is insignificant and the components of periodicity and randomness are all highly significant at the 0.01 level. The harmonic coefficients with 12 monthly periods and 72 monthly periods are also shown in Table I. The reason for using different periods will be discussed later under sections of correlogram and spectral analyses.

Category 7. A Time Trend with Some Periodicities and Randomness

Accumulated irrigation requirements for composite vegetables in the Lake Okeechobee area can be used to demonstrate the concept of a time trend with some periodicity and randomness. Data used to determine the coefficients for the model were obtained from the Corps of Engineers[24]. Time series analyses show that the variance of trend, periodicity and randomness are equal to 2.0253, 2.0383, and 3.3929, respectively. The F-test indicates that three components are all significant at the 0.1 level. This implies that the time series, $X(t)$, involves three components, i.e.,

$$X(t) = -1.9741 + 1.3048t + X_C(t) + X_R(t) \quad \ldots(43)$$

where, t is the month and the basic period of harmonic component is 12 months. The coefficients of harmonic components, $X_C(t)$, are shown in Table I. The data and simulated results are shown in Figure 7.

The time series analysis involved two portions, first portion is a deterministic part and the other is random

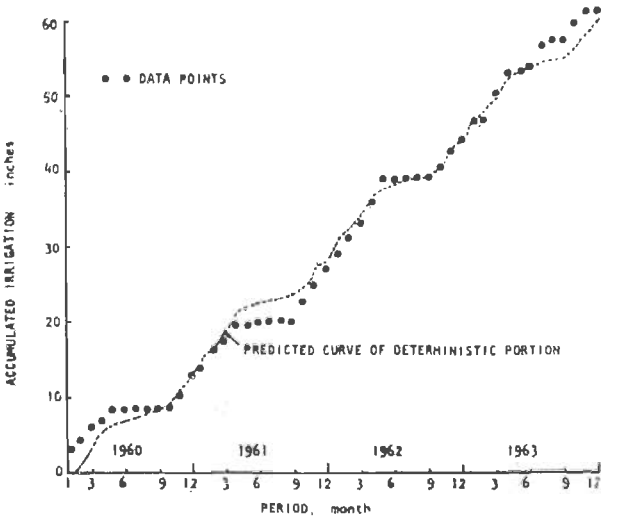

FIGURE 7 : Accumulated irrigation requirement for composite vegetables.

and uncorrelated to the deterministic part. The deterministic portion turns out to be a cyclical function rather than a polynomial of time. Hence, the correlogram and spectral analyses can provide insight into the existence of harmonic components in the process.

Correlogram

The Equations (26), (27), (29) & (30) are used to calculate the serial correlation r_k of lag k for the monthly discharges of the St. John River, Florida, and the end of month stage of Lake Okeechobee. In these examples, L is the length of record equal to 432 months in discharge data, and 504 months in stage record. The value k is between 0 and k/L which is recommended by Blackman and Tukey([1]) and should not exceed 0.1, for instance, 43 in discharge and 50 in stage. The array of coefficients r_0, r_1,...shows a good deal about the nature of the internal dependence of the series. Their sum is called the correlogram which is used to express the graph of k as abscissa versus r_k as ordinate. The correlogram for discharge and stages are shown in Figures 8 & 9, respectively. As can be seen from Figure 8, the correlogram is oscillating along the abscissa $r_k = 0$, with a 12 months period same harmonic components of the model. However, as Figure 9 shows, the correlogram is oscillating with a 12 months period and dumping curve. This implies that the data of time series used to compute the correlogram is too short and thus may conceal its actual form. Hence, the spectral analysis is needed because the significance between spectrum and the corresponding correlogram is that the spectrum exhibits a fewer sampling variation.

Spectral Analyses of the Stage of Lake Okeechobee

The power spectrum for the end of month stage of Lake Okeechobee can be analyzed by using Equations (27), (31), (32) & (33). The techniques used to decide the sampling time interval, $\triangle t$, and maximum lag number, k, should be discussed further based on the following two cases :

Case 1. Constant k with Varying $\triangle t$

A general decision is that a smaller time interval is used to observe the shorter period of environmental phenomena and a larger time interval is used to seek the longer period of process. However, no matter what size of sampling time interval is chosen, the population mean of the original series should not be distorted significantly. The reason is because the larger time interval may affect the sampling accuracy. For example, different time intervals used in the lower east coast of Florida's rainfall and Lake Okeechobee's stage are used to exemplify this effect. The results are shown in Table II. As can be seen from Table II, the sampling time interval equal to a 6-month in rainfall data indicates that the

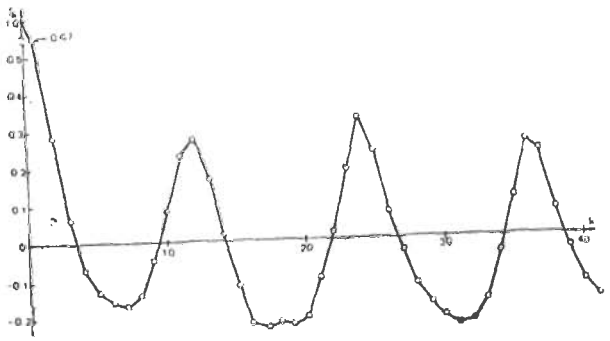

FIGURE 8 : Correlogram of the monthly discharge of St. John River, Florida.

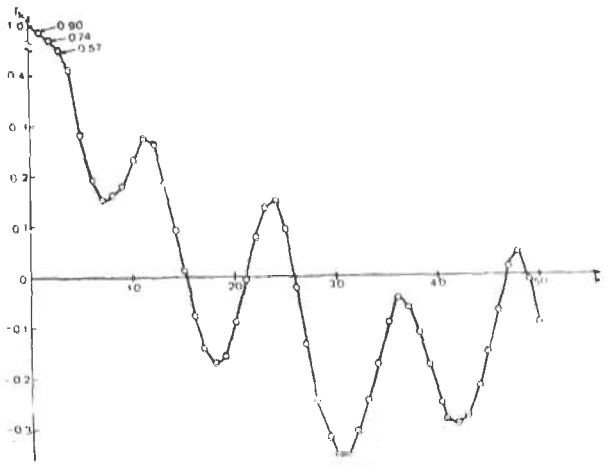

FIGURE 9 : Correlogram of the stage of Lake Okeechobee, Florida.

TABLE II

Testing difference among the variances of time interval, $\triangle t$.

Source of variance	*F*-value					
	Time Interval, Month					
	1	2	3	4	5	6
Time Interval, Month	Precipitation of Lower East Coast of Florida					
	2	1.07				
	3	1.03	1.03			
	4	1.26	1.34	1.30		
	5	1 29	1.38	1.33	1.03	
	6	1.62*	1.52*	1.57*	2.04**	2.10**
	Stage of Lake Okeechobee					
	2	1.02				
	3	1.07	1.05			
	4	1.04	1.02	1.03		
	5	1.05	1.04	1.02	1.02	
	6	1.16	1.18	1.25	1.21	1.23
	12	1.15	1.17	1.23	1.19	1.21 1.01

* = The *F*-test is significant at the 0.05 level.
** = The *F*-test is highly significant at the 0.01 level.

series sampled by a 6-month interval is not same as the original monthly series because the F-test is significant at least at the 0.05 level.

The results of the stage of spectral estimates from which the Figures 10.1A & 10.1B are plotted are based on $k = 12$ with $\triangle t = 1$ and 3, respectively. As can be seen from those figures, the resolution of components with a period as short as 2 months in 10.1A, instead of the 6 months possible in the 10.1B. This indicates that the 10.1B is unable to show the components which are shorter than 6 months. However, the 10.1B can show a longer period of component such as 72 months which are not visible clearly in 10.1A.

Case 2. Constant $\triangle t$ with Varying k

The L is the length of record equal to 504 months of stage data. According to Blackman and Tukey([1]) who suggested that the k/L should not be greater than 0.1. For this example, k is equal to 50 and 25, for a Sampling time interval equal to 1 month and 2 months, respectively. The effect of increasing the number of lags from 10 to 25 with constant $\triangle t = 2$ are shown in Figures 10.2A & 10.2B. As can be seen from these two figures, the resolving power in 10.2B is greater than 10.2A because the spectrum estimates computed by larger lag number are made for a greater number of spectral bands.

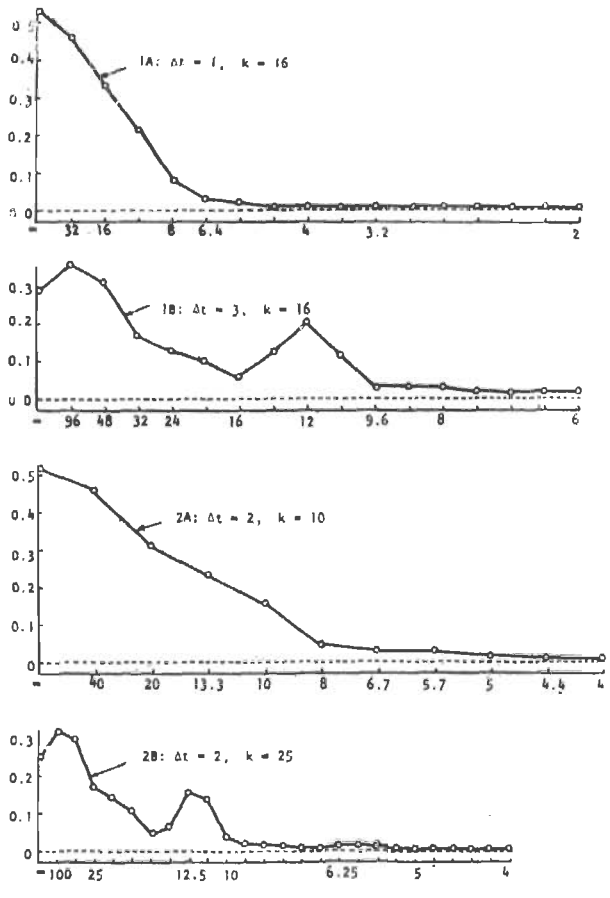

FIGURE 10 : Spectrum of the stage of Lake Okeechobee, Florida.

Both the correlogram and spectrum can be used to explore the internal structure of a time series. The correlogram reveals more about the relationship between values of the series which are separated in time. The spectrum provides the extent to which the series exists in some fundamental periodicities and the peak of the spectrum is identified with the harmonic terms in the system.

Synthetic Streamflow Succession

The time series analysis of existing data as described in previous sections can be used in generating a predicted sequence. The mean monthly discharges of the Kissimmee River, Florida, are used in this synthetic study. The length of record is 540 months. Equations (28) & (29) are used to calculate the standard deviation for the j^{th} and $(j + 1)st$ month of the streamflow. The results are listed in Table III. Equations (5), (36) & (37) are used to calculate the means, correlation coefficients, and regression coefficients, respectively. The results are also listed in Table III. The first order of the Markov model as mentioned in Equation (35) is used to generate the monthly streamflow. A normal distribution of the data which is used in this study is also suggested by Thomas and Fiering([23]). Equation (24) is used to generate the normally distributed variates with mean equal to 0 and variance equal to 1. In order to observe the possibility of other types of distribution, a log-normal distribution is also used. Comparison of the synthetic mean monthly flow standard deviation with those of 45 years of observed data are shown in Tables IV & V, respectively. As can be seen from Table IV, a significant difference between normal and log-normal distribution is that the negative values occurred in the synthesized sequence found by using normal distribution. The moments included in these negative results are subsequently set to zero. The significance of negative values are listed in Table IV. The percentage of the total synthetic flows affected by setting negative values to zero is less than 3 percent, which is still within the 95 percent statistical conference limits. Hence, setting negative values to zero do not distort the population significantly. As can be seen from Tables III & V, the standard deviation with minimum values such as May, and with maximum values such as October, are used to observe the cumulative frequency function. The results of the frequency distribution are plotted on Figure 11. As Figure 11 shows, the synthetic flow with normal distribution is slightly better in May but not in October. The distribution of synthetic results for annual and mid-year such as July are plotted on Figure 12. As Figure 12 shows, the cumulative frequency function for annual synthesized by both distributions are fitted closely to the record results. However, the synthetic July's flow with log-normal distribution is better fitted than the normal distribution. Therefore, a Chi-square test is used to examine the goodness-of-fit between synthetic results

TABLE III

Serial correlation parameters of mean monthly flows at Kissimmee River obtained from 45 years of observed record.

Month	Regression coefficient b_j	Correlation coefficient ρ_j	Standard deviation σ_j	Mean flow q_j
January	0.6794	0 8507	2267	3129
February	0.8598	0.7185	1829	2999
March	0.8913	0.8316	2180	3149
April	0.6706	0.8397	2302	2968
May	1.2007	0.6442	1747	2334
June	0.9495	0 8540	3328	3007
July	0.7136	0.7685	3683	3779
August	1.1508	0.8075	3429	4265
September	0.9934	0.7919	4866	5963
October	0.5639	0.8945	6970	7022
November	0.7361	0.9215	3810	4512
December	0.1405	0.1609	2953	3443

TABLE IV

Comparison of the mean monthly flows and magnitude of negative values generated in different period of years with those of 45 years of observed data, acre-ft.

Month	Observed mean monthly flow 45 years	Synthetic mean monthly flow					
		45 years		100 years		500 years	
		*ND**	*LD**	*ND*	*LD*	*ND*	*LD*
January	3129	3376	3101	3291	3407	3157	3268
February	2999	3042	2890	2966	2880	3008	2960
March	3149	3129	3099	3338	3408	3104	3090
April	2960	2988	3508	3028	3346	2953	3133
May	2334	2458	3209	2503	2988	2339	2628
June	3007	2874	2515	3005	2614	3224	2623
July	3779	4476	3801	4072	3400	4056	3373
August	4265	4362	4065	4364	3922	4434	3946
September	5963	6359	5668	6001	5172	6089	5391
October	7022	6678	6361	7128	6747	7334	6671
November	4512	4396	3898	4695	4181	4660	4272
December	3443	3419	3005	3542	3310	3592	3644
Sum	46562	47557	45140	47933	45375	47950	44999
Average	3880	3963	3762	3994	3781	3996	3750
Negative value, 10^2		575		1033		5544	
Percent, %		2.69		2.16		2.31	

* *ND* = Synthetic flow with normal distribution.

* *LD* = Synthetic flow with log-normal distribution.

TABLE V

Comparison of the standard deviation of synthetic flow with those of 45 years of observed data.

Month	Standard deviation of observed data	Standard deviation of synthetic flow					
		45 years		100 years		500 years	
		*ND**	*LD*	*ND*	*LD*	*ND*	*LD*
January	2267	1811	2382	1990	2926	2069	3322
February	1829	1609	2019	1664	2310	1702	2351
March	2180	2064	2840	2058	3446	1976	3096
April	2302	2298	4431	2161	3933	2051	4061
May	1747	1840	4444	1698	3756	1593	3593
June	3326	2870	2482	2858	2542	2698	2338
July	3683	3104	3168	3045	2792	3018	2893
August	3429	2927	3258	2904	2993	2906	3120
September	4866	4112	4380	3958	3942	4075	4454
October	6970	4937	8857	5215	7738	5138	7126
November	3810	3001	3997	3064	4322	3172	4790
December	2953	2217	2830	2394	3680	2453	4861
Sum	39362	32790	45088	33009	44380	29945	46005
Average	3280	2733	3757	2751	3698	2495	3833

* *ND* = Normal distribution, *LD* = Log-normal distribution.

TABLE VI

Comparing the Chi-square test for goodness-of-fit of log-normal and normal distributions in different periods of years with those of 45 years of record.

Month	Chi-square values of synthetic flow					
	45 years		100 years		400 years	
	ND†	*LD*	*ND*	*LD*	*ND*	*LD*
January	31.74*	22.49	48.68**	25.54	27.81	23.09
February	34.60*	47.20**	11.67	39.04**	40.22**	32.94*
March	25.83	32.11*	23.02	46.04**	24.01	40.71**
April	16.99	53.04**	17.00	76.74**	16.62	62.89**
May	27.82	32.20*	26.05	47.46**	20.01	41.58**
June	23.08	17.13	16.07	19.78	17.30	9.76
July	58.35*	11.27	60.60**	12.15	47.62**	19.71
August	32.50*	23.46	41.11**	32.71*	20.95	19.84
September	66.90**	21.41	42.59**	14.32	34.39*	16.74
October	21.02	37.53**	26.10	17.29	22.10	10.23
November	25.82	22.09	12.39	22.86	18.58	17.94
December	17.70	31.86*	21.12	45.65**	13.07	30.73*
Annual	14.85	28.37	26.97	17.92	25.23	14.80

† *ND* = Normal distribution, *LD* = Log-normal distribution.
*, ** = The Chi-square tests are significant at the levels of 0.05, 0.01, respectively.

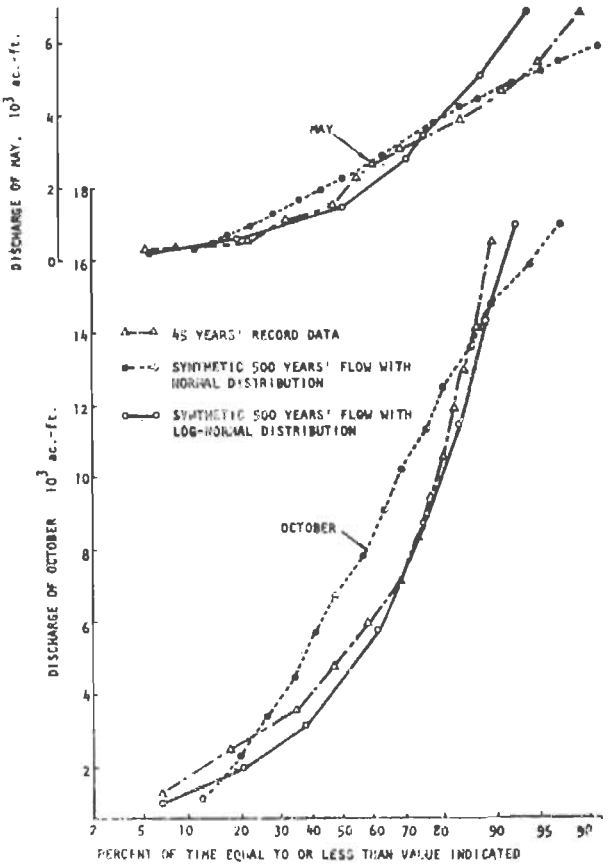

FIGURE 11 : Distribution of streamflow for May and October.

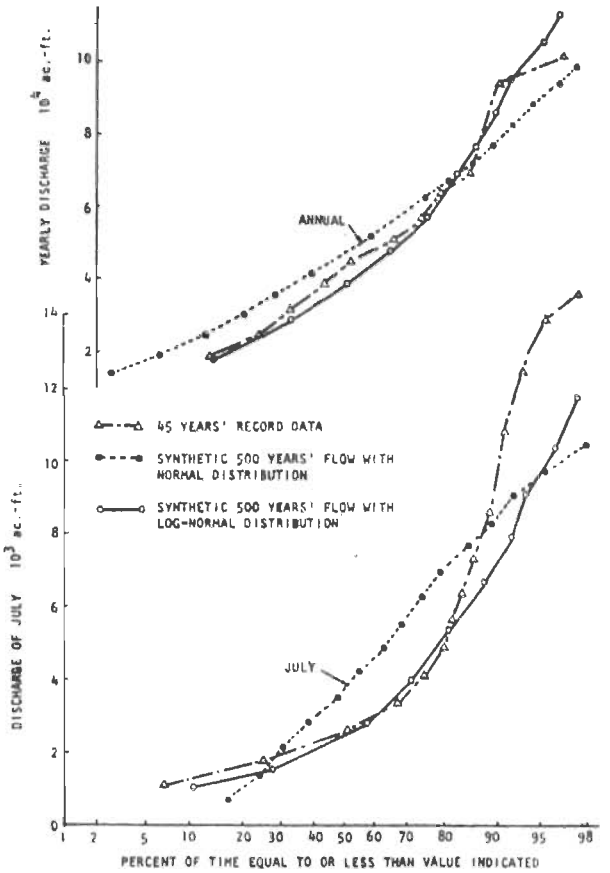

FIGURE 12 : Distribution of streamflow for July and annual.

and record data. Twenty frequency intervals are used in this example, the results of Chi-square values are listed on Table VI. For instance, comparing the Chi-square test for normal and log-normal distributions in a synthesized 400 years' sequence with those of 45 years of record indicates the following results:

(1) The synthetic flows with both types of distributions in January, June, August, October, November, and annual render the cumulative frequencies which agree closely with the cumulative frequency performed by historical record.

(2) The synthetic flows with log-normal distribution are better in February, July, and September. However, the results for months such as March, April, May, and December are not as good as the synthesized sequence with normal distribution.

These results imply that the synthetic streamflow sequence with joint distributions are more applicable in the Kissimmee River flow.

Conclusions

A general concept of time series which includes three components such as trend, periodicity, and randomness is introduced. A systematic model of time series analysis is also developed. The *F*-test is used as a statistical criterion to determine the number of components which may include in each series. Based on this criterion, the water resources systems can be classed into seven categories. The data obtained from the Kissimmee River Basin and Lake Okeechobee area, Florida, are taken as examples to demonstrate these applications. Examples are included such as a water demand, crop rooting depth, evaporation of lake, lake stage, water quality, streamflow, rainfall, and accumulated irrigation requirements.

Both the correlogram and spectral analyses are used to analyze the deterministic portion of the data. The techniques used to decide the sampling time interval and lag number of the serial correlation are separated into two cases to explore how the spectrum is affected by the sampling intervals and the lag number. No matter what size of sampling time interval and number of lags are chosen, the population mean of original series should not be distorted significantly. The correlogram reveals the relationships between values of the series, while the spectrum shows the extent to which the series exists under certain fundamental periodicities.

Synthetic streamflow succession is used as an example to demonstrate the application of the auto-regressive model. Based on the Chi-square test for goodness-of-fit between synthetic sequence and record data, the synthetic streamflow with joint distributions are more applicable in the Kissimmee River.

Acknowledgements

The author wishes to express sincere thanks to Mr. W.V. Storch, Director of the Resource Planning Department, and to Mr. R.L. Hamrick, Chief of the Water Planning Division for their supervision and guidance in this study.

References

(1) BLACKMAN, R.B. and J. W. TUKEY : "The Measurements of Power Spectra." Dover, New York, 1958, pp. 1-30.

(2) WILKS, S.S. : "Mathematical Statistics." John Wiley & Sons, Inc., New York, 1962, pp. 514-540.

(3) BROWN, R.G. : "Smoothing, Forecasting and Prediction of Discrete Time Series." Prentice-Hall, Inc. Englewood Cliffs, N.J., 1963, pp. 49-84.

(4) CRAMER, M. : "Model Building with the Aid of Stochastic Processes." Technometrics 6, 1964, pp. 133-160.

(5) KENDALL, M.G. and A. STUART : "The Advanced Theory of Statistics." Vol. 3, Hafner Publishing Company, New York, 1968, pp. 342-471.

(6) BOX, G.E.P. and G.M. JENKINS : "Time Series Analysis Forecasting and Control." Holden-Day, San Francisco, California, 1970, pp. 53-72.

(7) ANDERSON, T.W. : "The Statistical Analysis of Time Series." John Wiley & Sons, Inc., New York, 1971, pp. 30-159.

(8) CHOW, V.T. : "Handbook of Applied Hydrology." McGraw-Hill Book Company, New York, 1964, pp. (8) 78-(8) 89.

(9) ROESNER, L. A. and V.M. YEVDJEVICH : "Mathematical Models for Time Series of Monthly Precipitation and Runoff." Hydrology Paper No. 15, Colorado State University, Fort Collins, Colorado, 1967.

(10) KISIEL, C. C. : "Time Series Analysis of Hydrologic Data." in Advances in Hydroscience, edited by V.T. Chow, Academic Press, New York, Vol. 5, 1969, pp. 1-30.

(11) CHOW, V.T. and S.J. KARELIOTIS : "Analysis of Stochastic Hydrologic Systems." Water Resources Research, Vol. 6, No. 6, 1970, pp. 1569-1582.

(12) YEVDJEVICH, V.M. : "Stochastic Processes in Hydrology." Water Resources Publication, Fort Collins, Colorado, 1972, pp. 1-67.

(13) RICH, L. G. : "Environmental Systems Engineering." McGraw-Hill Book Company, New York, 1973, pp. 214-251.

(14) BOURODIMOS, E.L.; S L. YU and R.A. HAHN : "Statistical Analysis of Daily Water Quality Data." Amer. Water Resources Assoc., Water Resources Bulletin, Vol. 10, No. 5, 1974, pp. 925-941.

(15) SHIH, S.-F.; B.K. HUANG and G.J. KRIZ : "A Simulation Analysis of Plant Growth Dynamics as Affected by Water Tables, Depth to Drain and Soil Types." Proc. of 1970 Summer Computer Simulation Conference, Denver, Colorado, June 1970, Vol. 11, pp. 980-989.

(16) SHIH, S.-F. and B.K. HUANG : "Digital Simulation Techniques in Analyzing the Effect of Soil Temperature on Plant Growth Dynamics." Proc. of 1971 Summer Computer Simulation Conference, Boston, Mass , June 1971, Vol. 11, pp. 801-811.

(17) SHIH, S.-F.; R.E. SNEED and R.S. SOWELL : "Water Requirements for Optimum Crop Yield." 1972 Annual Meeting of Amer. Society of Agri. Engineers, St. Joseph, Michigan, December 1972, Paper No. 72-773.

(18) STEEL, R.G.D. and J.H. TORRIE : "Principles and Procedures of Statistics." McGraw-Hill Book Company, Inc., New York, 1960, pp. 332-341.

(19) ANDERSON, R.L. and T.W. ANDERSON : "Distribution of the Circular Serial Correlation Coefficient for Residuals from a Fitted Fourier Series." Ann. Math. Statist., Vol. 21, 1950, pp. 59-89.

(20) RALSTON, A. and H.S WILF : "Mathematical Methods for Digital Computers." John Wiley & Sons Company, Inc., New York, 1960, pp. 2582-279.

(21) BROOKS, C.E.P. and N. CARRUTHERS : "Handbook of Statistical Method in Meteorology." Her Majesty's Stationary Office, London, England, 1953, pp. 1-150.

(22) HAMMING, R.W. : "Numerical Methods for Scientists and Engineers." McGraw-Hill Book Company, Inc., New York, 1962, pp. 34, 389.

(23) THOMAS, H.A. Jr. and M.B. FIERING : "Mathematical Synthesis of Streamflow Sequence for the Analysis of River Basins by Simulation." Chapter 12 of Design of Water Resources Systems by Mass et al. Harvard University Press, Cambridge, Massachusetts, 1962, pp. 459-493.

(24) CORPS OF ENGINEERS : "Water Resources for Central and Southern Florida." Appendix I, Serial No. 54, Department of the Army, Jacksonville District, Corps of Engineers, Jacksonville, Florida, February 1968, pp. (C) 10-(C) 30.

(25) WEAVER, J.E. : "Root Development of Field Crops." McGraw-Hill Book Company, Inc., New York, 1926, pp. 95-180.

(26) SHIH, S.-F.; D.W. HALLETT and R.L. HAMRICK : "Analysis of Kissimmee River Flows for Water Quality Effects." Proceedings of International Seminar and Exposition on Water Resources Instrumentation, International Water Resources Association, June 4-6, 1974, Chicago, Illinois.

Non-Linear Modelling of the Water Resources Systems

JAGAT N. SHARMA
Graduate Assistant
Coastal Engineering Laboratory
University of Florida
Gainesville, Florida 32611, U.S.A.

SYNOPSIS

Non-linearities in the water resources systems were recognized early[3], but due to lack of sound theory for non-linear systems the water resources system planning has heavily depended on the linear system theory thus far. In recent years the non linear systems have received considerable attention due to their extreme importance in several disciplines. The present paper will develop a new method of analysis and identification of a non-linear system such as drainage basin or reservoir. The proposed method consists in estimating the parameters of the non-linear system through the known relation between the correlation functions of the input and output records. The unknown function representing the non-linear system is expanded into series of Hermite polynomials. Also the probability density of the input is expanded into the equivalent series of Hermite polynomials. The output autocorrelation function is expressed in terms of the input autocorrelation and unknown system function. This provides as many equations as there are correlation function estimates. From these equations the same number of parameters of the function representing the non-linear system can be estimated.

The above method will be applied to numerically simulated system and some of the actual water resource systems such as drainage basin or reservoir.

Introduction

Linear models of water resources systems are extensively used not because the systems in question are linear but mainly because a suitable theory and computational methods for non-linear systems are not available. Linearization, piecewise linearization and Weiner's method for non-linear systems constitute the presently available tools for building a model for non-linear systems. A new method for analysis and identification of non-linear systems will be presented in this paper.

The proposed method utilizes the relation between input autocorrelation and output covariances obtained by the characteristic function method first used by Rice[7]. The above well-known result has been modified and simplified by expressing the non-linear functional relation in a series of Hermite polynomials and reducing the resulting expression using the orthogonality properties. Thus the output covariances are expressed as an infinite series in terms of input correlation and the coefficients of the Hermite polynomial describing the non-linear system.

Now the identification problem is posed. Can we estimate the coefficients of the Hermite polynomial describing the non-linear system given the input correlations and the output covariances? The answer is a conditional yes. In certain conditions, such as Gaussian input, the zero memory non-linearity can be easily evaluated by the new method developed in this exposition. The new method has been applied successfully to the simulated

random sequences. The method has been further modified so that it can be applied to systems such as catchment basins which have non-Gaussian input such as rainfall. This modified identification method has been applied to monthly rainfall runoff data from an experimental catchment basin in Florida. The predicted and the actual runoff has been presented for comparison. It can be seen that even the simplest type of non-linear model can be an effective prediction tool. The ways to improve the model further have been indicated.

In summary a new method for building a non-linear model for water resources systems has been developed and successfully applied to a simulated non-linear system and an actual catchment basin.

Mathematical Derivation

Given a stationary Gaussian random sequence x_n, $n = 1, 2,...$ as input to a zero memory non-linear device represented by function $f(x)$. We wish to estimate the correlation function and spectrum of the output random sequence $y_n = f(x_n)$, $n = 1, 2$. The characteristic function method of non-linear systems analysis has been well described in literature beginning from Rice's paper([7]) and several textbooks([5])([8]). Following Brown([2]) let us consider the more general result for the cross-correlation function $\psi = E\{f(x_1) \cdot g(x_2)\}$, where, f and g are given arbitrary functions represented by their respective Fouriers integrals

$$f(x) = \frac{1}{2\pi} \int_{-\infty}^{\infty} F(w_1)\, e^{iw_1 x}\, dw_1 \qquad ...(1)$$

$$g(x) = \frac{1}{2\pi} \int_{-\infty}^{\infty} F(w_2)\, e^{iw_2 x}\, dw_2 \qquad ...(2)$$

and the random variables x_1 and x_2 have bivariate Gaussian distribution with zero means and variances σ_1 and σ_2 and correlation ρ. The cross-correlation function is then expressed by

$$\psi = \sum_{n=0}^{\infty} \left[\int_{-\infty}^{\infty} f(x)\, H_n\left(\frac{x}{\sigma_1\sqrt{2}}\right) P_1(x)\, dx \right] \left[\int_{-\infty}^{\infty} g(x)\, H_n\left(\frac{x}{\sigma_2\sqrt{2}}\right) P_2(x)\, dx \right] \frac{\rho^n}{2^n n!} \qquad ...(3)$$

where, H_n is Hermite polynomial defined by

$$H_0(x) \equiv 1$$

$$H_{n+1}(x) = -e^{x^2} \frac{d}{dx}\left[e^{-x^2} H_n(x) \right] \text{ for } n \geqslant 0 \qquad ...(4)$$

$P_1(x)$ and $P_2(x)$ are the marginal probability densities of x_1 and x_2.

In case $\sigma_1 = \sigma_2 = \sigma$, we have $P_1(x_1) \equiv P_2(x_2)$ and if also $f(x) = g(x)$ we get the auto-covariance ϕ for the output $y_n = f(x_n)$ $n = 1, 2, \ldots n$ in terms of the auto-correlation of the input.

$$\phi = \sum_{n=0}^{\infty} \left[\int_{-\infty}^{\infty} f(x)\, H_n\left(\frac{x}{\sigma\sqrt{2}}\right) p(x)\, dx \right]^2 \frac{\rho^n}{2^n n!} \qquad ...(5)$$

where,

$$P(x) = \frac{1}{\sigma\sqrt{2\pi}}\, e^{\frac{-x^2}{2\sigma^2}}$$

In order to get the answer to the question posed in the beginning of this section the above formula is used in the following manner.

The stationary input Gaussian random sequences x_n, $n = 1, 2...$ has correlations $\rho_n = E(x_m \cdot x_{m+n})$, $n=0, 1, 2....$ The output auto-covariance $R_{xy}(n) = E[f(x_m) \cdot f(x_{m+n})]$ is obtained by the Equation (5) substituting $\rho = \rho_n$. Thus the output auto-covariance function is obtained as a function of the input autocorrelation function given by ρ_n, $n = 0, 1, 2, 3...$. The spectrum of the output from the non-linear device can easily be obtained by applying cosine transform to the auto-covariance function. The spectrum provides information on generation of harmonics due to non-linearity of the system.

New Formula for Output Auto-Covariances

For computation of the auto-covariance of the output and also for the identification of the non-linearity the Equation (5) has been modified in the following way.

The function $f(x)$ describing the non-linearity can be expressed as the sum of Hermite polynomials, i.e.,

$$f(x) = \sum_{m=0}^{\infty} C_m\, H_m\left(\frac{x}{\sigma\sqrt{2}}\right) \qquad ...(6)$$

For types of non-linearity for which the Hermite polynomial approximation is convergent the Equation (5) can be expressed as

$$\phi = \sum_{n=0}^{\infty} \left[\int_{-\infty}^{\infty} \sum_{m=0}^{\infty} C_m \cdot H_m\left(\frac{x}{\sigma\sqrt{2}}\right) \cdot H_n\left(\frac{x}{\sigma\sqrt{2}}\right) \frac{1}{\sigma\sqrt{2}\cdot\sqrt{\pi}}\, e^{\frac{-x^2}{2\sigma^2}}\, dx \right]^2 \frac{f^n}{2^n . n!} \qquad ...(7)$$

Substituting $z = \frac{x}{\sigma\sqrt{2}}$ and interchanging

summation and integration we get

$$\phi = \sum_{n=0}^{\infty} \left[\sum_{m=0}^{\infty} \frac{C_m}{\sqrt{\pi}} \int_{-\infty}^{\infty} H_m(z) \cdot H_n(z) \cdot e^{-z^2} \cdot dz \right]^2 \frac{\rho^n}{2^n \cdot n!} \quad \ldots(8)$$

Using the orthogonality relation

$$\int_{-\infty}^{\infty} H_m(z)\, H_n(z) \cdot e^{-z^2} \cdot dz = \begin{cases} \sqrt{\pi} \cdot 2^n \cdot n! \text{ for } m=n \\ 0 \text{ for } m \neq n \end{cases} \quad \ldots(9)$$

we get

$$\phi = \sum_{n=0}^{\infty} C_n^2 \cdot 2^n \cdot n!\, \rho^n \quad \ldots(10)$$

Thus if $\rho(m)$ is the autocorrelation of the input for lags $m = 0, 1, 2, \ldots$ and $\phi(m)$ auto-covariance of the output for lags $m = 0, 1, 2, \ldots$ where input x and output y are related by

$$y = f(x) = \sum_{n=0}^{\infty} C_n H_n \left(\frac{x}{\sigma \sqrt{2}} \right)$$

then

$$\phi(m) = \sum_{n=0}^{\infty} C_n^2 \cdot 2^n \cdot n!\, \rho^n(m) \text{ for } m = 0, 1, 2, \ldots \quad \ldots(11)$$

The above can be interpreted as if the covariance of the output has been broken into its orthogonal components corresponding to each of the terms in the Hermite polynomial representation of the non-linearity. This interesting property of the Equation (11) allows one to compute $\phi(m)$ as accurately as a particular application demands. Many types of simple non-linearity can be well approximated by the sum of a few terms of Hermite polynomials. Thus the output correlations can be calculated very quickly.

New Identification Method

Now we have all the necessary tools to discuss the question posed in the introduction. Given autocorrelation $\rho(m)$, $m = 0, 1, 2, \ldots$ of the input zero-mean Gaussian sequence and the auto-covariance $\phi(m)$, $m = 0, 1, 2, \ldots$ of the output from a non-linear device, we would like to identify the non-linear device $y = f(x)$. Let the non-linear device be represented by the sum of Hermite polynomials, i.e., Equation (6). If there are m significant estimates of autocorrelation and auto-covariances, then from Equation (11) we can get m equations in terms of the coefficients of the Hermite series. Up to m coefficients C_n^2 can be solved in such a way that $C_n^2 > 0$. In many of the practical cases we will have more equations than the number of unknown then the equation should be solved in the least square sense. Since the coefficients C_n are present in the equations as C_n^2, their actual sign will depend on the mean value of the output signal.

Adaptation of the Method for Non-Gaussian Input

If the inputs are non-Gaussian the above method cannot be applied. But we can look at the problem in this way. The input itself can be pictured as an output from a non-linear device $x = f(z)$ where, z is zero-mean Gaussian random variable. Similarly system output can be considered as an output from a non-linear device $y = g(z)$. Using Equation (11) we solve for the functions f and g. Now $z = f^{-1}(x)$. Therefore, $y = g\{f^{-1}(x)\}$ is the required system non-linearity. We need to consider only the real value of $z = f^{-1}(x)$. In case of the multi-valued real solutions, the sequence $z_n = f^{-1}(x_n)$, $n = 1, 2, \ldots$ which has zero mean should be kept for y_n computation.

Numerical Simulation and Application

Uncorrelated Gaussian random variables were generated by the direct method as follows([1]). Generate a pair of independent random variables U_1 and U_2 uniformly distributed over the interval (0, 1). Then

$$x_1 = (-2 \ln U_1)^{1/2} \cos 2\pi U_2$$

$$x_2 = (-2 \ln U_1)^{1/2} \sin 2\pi U_2$$

are a pair of Gaussian random variables with zero mean and unit variance. Correlated Gaussian random variables were generated by the relation $x_t = 0.5\, x_{t-1} + a_t$ where, a_t is independent uncorrelated Gaussian random variable $y_t = f(x_t)$ was computed for several functions. Covariance of y_t has been computed and compared in Table I.

TABLE I

Function	Covariance	Covariance from Equation (10)
$(x-1)^2$	7.548	7.551
x^2+x-1	3.808	3.770
x^2-1	2.759	2.636
$0.25\,(x^2-1)+0.1x^3$	0.346	0.393

Results are very good for simple functions. For functions involving high powers error comes from the deviation of higher moments of the random variable x_t from the ideal moments of a Gaussian random variable. In order to test the efficiency of the identification

method, the autocorrelation of x_t and auto-covariance of $y_t = x_t^2 - 1$ for 0, 1 and 2 lags was used in Equation (11). Solving the equation for non-negative solutions for coefficients C_n^2 and then reducing we recover the function $f(x) = 1.0106x^2 - 1.1433$ which is very close to the simulated non-linearity.

The monthly rainfall and runoff data collected from the experimental watershed No. W-2 near Vero Beach, Florida([6]) has been used to build a non-linear model for the catchment basin. Monthly precipitation and discharge are $P = f(z)$ and $Q = g(z)$. By the method used in the previous paragraph the functions of f and g are determined. In the next step $z = f^{-1}(P)$ is calculated. Finally $Q = g\{f^{-1}(P)\}$ is obtained. The results of the calculation are presented in Figure 1. Despite the facts that auto-covariances up to only 3 lags were used even though the data showed strong periodicity for 12 months and weak periodicity for 3, 4, and 6 months([4]), and that the memory effect, i.e., in this case storage has not been considered, the predictions come quite close to the actual value of the discharge.

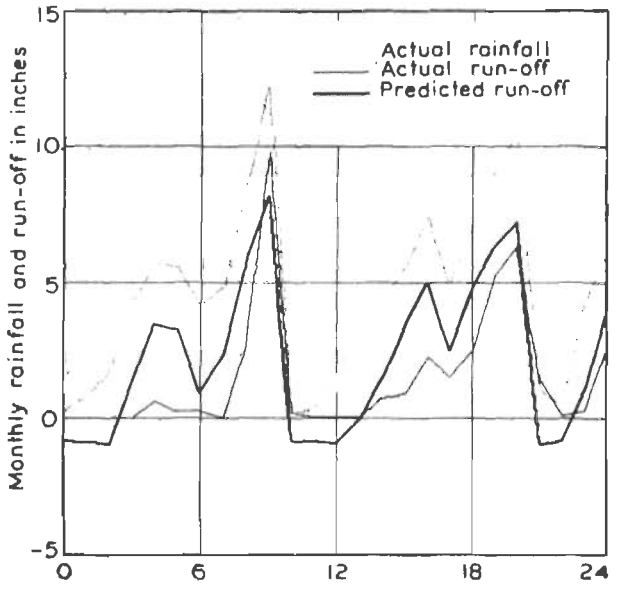

FIGURE 1 : Comparison of the actual and predicted monthly runoff.

Conclusions

(1) Characteristic function method for analyzing non-linear systems has been modified for Gaussian input and non-linearity expressible in a convergent series of Hermite polynomials.

(2) Formula for output autocovariance has been derived as a series in terms of the coefficients of Hermite polynomials and the powers of the input autocorrelations.

(3) A new method for identifying the non-linearity of a system with Gaussian input has been developed and applied successfully to the simulated data.

(4) The new identification method has been further modified to a general case of non-Gaussian input.

(5) The modified identification method has been successfully applied to build a model for an experimental watershed in Florida.

(6) It has been effectively demonstrated that the inherently non-linear hydrologic systems can be tackled easily by the new methods developed.

Acknowledgement

The author sincerely thanks Dr. Omar H. Shemdin, Director, Coastal Engineering Laboratory, University of Florida, Gainesville for his encouragement and financial support for developing non-linear prediction model particularly for wave run-up on beach.

References

(1) ABRAMOWITZ, M. and SEGUN, I.A. : "Handbook of Mathematical Function." Dover Publication, Inc., New York, 1965, pp. 953.

(2) BROWN, J.L. : "On the Expansion of the Bivariate Gaussian Probability Density using Results of Non-linear Theory." IEEE Transaction on Information Theory, Vol. IT-14, No. 1, January 1968, pp. 158-59.

(3) CHOW, VEN TE (Ed.). : "Handbook of Applied Hydrology, a Compendium of Water Resources Technology." New York, McGraw Hill, 1964.

(4) CHOW, VEN TE : "Analysis of Multiple Input Stochastic Hydrologic System." Research Report No. 67, Water Resources Center, University of Illinois at Urbana-Champaign, July 1973, pp. 65.

(5) DAVENPORT, W.B. and ROOT, W.L. : "An Introduction to the Theory of Random Signal and Noise." New York, McGraw Hill, 1958, pp. 393.

(6) HAROLD, W.H. and CRAMMATE, F.B. : "Hydrologic Data for Experimental Agricultural Watersheds in the United States." Misc Publication No. 994, Agricultural Research Services, U.S. Department of Agriculture, Washington, D.C., 1965.

(7) RICE, S.O. : "Mathematical Analysis of Random Noise." Bell System Technical Journal, July 1944 and January 1945. Also in "Selected Papers on Noise and Stochastic Processes", edited by Nelson Wax.

(8) STRATONOVICH, R.L. : "Topics in the Theory of Random Noise." Volume 1, Gordon and Breach, New York, 1963, pp. 292.

Integration of Filtration Equations and Parameter Optimization Techniques

A. C. PAYATAKES* R. M. TURIAN C. TIEN
Department of Chemical Engineering and Materials Science
Syracuse University
Syracuse, New York 13210.

SYNOPSIS

The system of differential equations describing filtration through filter bed of granular material and its integration are discussed A new method for the determination of the optimum set of the values of the filtration parameters, namely those parameter values which give the best fit to a given set of filtration data, is developed. This method is a combination of a non-linear least square algorithm and a pattern search technique and is found to be effective in determining pertinent filtration parameters from raw filtration data. Furthermore, unlike previous methods, it does not require generation of indirect data by cross-plotting. Illustration of this method is provided through an example which treats data obtained from filtration of aqueous clay suspension through deep bed filter composed of granular activated carbon.

1. Introduction

The mathematical description of filtration through granular bed is governed by a system of two equations : the macroscopic conservation equation and the so-called filtration equation. The latter is a phenomelogical description of the rate of retention of particulate matters, even though significance in terms of the mechanism of particle deposition is often attached to it. Strictly speaking, none of the models proposed for this rate expression can claim a broad theoretical basis, although some of them have been proved to be useful as frameworks for interpretation of the phenomena underlying filtration. For example, assuming that the parameters of the rate expression are known, the solution of these equations enables the prediction of the dynamic behavior of the filtration process, which can be used as a basis of rational design. Equally important, the solution of these equations, together with experimental data, can be used for the evaluation of the filtration parameters. The problem in essence, is to establish these model parameter values which are consistent with experimental observations and it is, therefore, intimately related to the solution of the problem.

The work reported here is concerned with the latter problem ; namely, the evaluation of the filtration parameter from the solution of the phenomelogical equation and experimental data. The main emphasis is on the development and formulation of an optimization search method which can be used in evaluating filtration parameters on a consistent and unambiguous basis. The development and application of optimization techniques has been one of the major technological innovations. However, it is surprising to note that this particular application has not yet been explored.

2. Filtration through Beds of Granular Porous Media

2.1 *Phenomelogical Equations*

We consider a deep bed filter consisting of a packed bed of solid grains. Initially, the filter bed is filled with clear liquid and free of any particulate matters. At a given time, a suspension of solid particles flows into and through the bed at a constant flow rate.

* *Present Address* : Department of Chemical Engineering, University of Houston, Houston, Texas 77004.

Filtration takes place throughout the entire depth of the filter. The problem is to predict the quality of filtrate (i.e., concentration of solid particles in the fluid stream, y) and the extent of particle retention (i.e., specific deposit of filter bed, volume of deposited matters per unit volume of filter bed) as functions of the depth of filter and time.

The mass balance of the solid particle as the suspension flows through the filter yields the conservation equation, i.e.,

$$\frac{\partial}{\partial t}(\sigma + \varepsilon y) + u_m \frac{\partial y}{\sigma z} - D\frac{\partial^2 y}{\partial z} = 0 \qquad \ldots(1)$$

Equation (1) is written on the basis that there is no radial dependence and the flow is uniform. The meanings of the symbols are given in the nomenclature.

The porosity of the filter bed, ε, will change depending upon the extent of particle retention, or

$$\varepsilon = \varepsilon_o - \beta\sigma \qquad \ldots(2)$$

where, ε_o is the initial porosity and β is the ratio of that apparent volume of deposited matter to the actual volume of the deposits. The term $D\frac{\partial^2 y}{\partial yz}$ in Equation (1) represents the Brownian diffusional flux along the axial direction which in most cases can be ignored. Moreover, for dilute suspensions, $\varepsilon \simeq \varepsilon_o$. Under these considerations Equation (1) becomes

$$\frac{\partial \sigma}{\partial t} + \varepsilon_o \frac{\partial y}{\partial t} + u_m \frac{\partial y}{\partial z} = 0 \qquad \ldots(3)$$

Equation (3) can be further simplified by introducing the so-called retention time, τ, or

$$\tau = t - \int_0^t \frac{dz}{u_m/\varepsilon_o} \qquad \ldots(4)$$

Namely, at any depth of the filter, time is counted from the moment when the suspension reaches the particle position. Equation (1) is reduced to

$$\frac{\partial \sigma}{\partial \tau} + u_m \frac{\partial y}{\partial z} = 0 \qquad \ldots(5)$$

Equation (5) has two dependent variables (σ and y) and two independent variables (τ and z). To express σ (or y) as function of τ and z, one more equation relating these quantities is required. Iwasaki (1937) observed almost forty years ago the linear relationship between y and z on a semi-log scale during the initial period of filtration and suggested that

$$\left(\frac{\partial y}{\partial z}\right) = -\lambda y \qquad \ldots(6)$$

where, λ is the filter coefficient and is related to its initial value, λ_o, by the following expression

$$\lambda = \lambda_o F(\sigma) \qquad \ldots(7)$$

namely, the effect of particle retention on λ can be expressed in terms of the specific deposit entirely. More recently, Deb (1970) proposed that

$$\frac{\partial \sigma}{\partial t} = \lambda' \left[\varepsilon_o - \frac{\sigma}{1-\varepsilon_s}\right] y \qquad \ldots(8)$$

when, ε_s designates the porosity of the deposited matter. Similarly, Herzig et al (1970) suggested that

$$\frac{\partial \sigma}{\partial t} = Ky = K_o F(\sigma)\, y \qquad \ldots(9)$$

In fact, all these expressions can be shown to be equivalent. For example, it is simple to show that

$$K = \lambda u_m \qquad \ldots(10)$$

or

$$K_o = \lambda u_m \qquad \ldots(11)$$

and

$$\lambda' = \frac{K}{\varepsilon_o - \beta\sigma} = \frac{K_o}{\varepsilon_o} \frac{F(\sigma)}{1 - \frac{\beta}{\varepsilon_o}\sigma} = \lambda'_o Fn(\sigma) \qquad \ldots(12)$$

where,

$$\lambda_o' = \frac{K_o}{\varepsilon_o} \qquad \ldots(13)$$

$$Fn(\sigma) = \frac{F(\sigma)}{1 - \frac{\beta}{\varepsilon_o}\sigma} \qquad \ldots(14)$$

2.2 *Method of Integration*

From the above discussion, the phenomelogical description of deep bed filtration is given by the following system of equations

$$\frac{\partial \sigma}{\partial \tau} + u_m \frac{\partial y}{\partial z} = 0 \qquad \ldots(5)$$

$$\frac{\partial \sigma}{\partial \tau} = K_o F(\sigma)\, y \qquad \ldots(9)$$

with the following initial and boundary conditions

$$y = y_i \qquad z = 0 \qquad \tau > 0 \qquad \ldots(15)$$

$$\sigma = 0 \qquad \tau \leqslant 0 \qquad z > 0 \qquad \ldots(16)$$

Equations (5) & (9) are known as semi-linear hyperbolic equations which can be solved conveniently with method of characteristics. However, because of the particular form of expression used for the rate equation, Equations (5) & (9) can be reduced to two ordinary differential equation which can be solved sequentially. This possibility was first pointed out by Herzig et al (1970) and will be used in this work.

Herzig et al (1970) showed that Equations (5) & (9) can be reduced to two ordinary differential equations. In terms of dimensionless variables they are

$$\frac{d\sigma_i}{d\tau^*} = F(\sigma_i) \qquad \ldots(17)$$

$$\sigma_i = 0 \qquad \tau^* = 0 \qquad \ldots(18)$$

$$\frac{d\sigma}{dz^*} = -\sigma F(\sigma) \qquad \ldots(19)$$

$$\sigma = \sigma_i(\tau^*) \quad \text{at} \quad z = z^* \qquad \ldots(20)$$

where,

$$\tau^* = \tau K_o y_i \qquad \ldots(21)$$

$$z^* = z\frac{K_o}{u_m} \qquad \ldots(22)$$

Thus, one can determine σ_i as a function of τ^* from direct integration of Equation (19) with the initial conditions of Equation (18). Once σ_i is known, it can be used as initial condition for Equation (19), the integration of which gives the distribution of σ throughout the column for a specified time. The relationship between the liquid phase concentration, y, can be found from the relationship

$$\frac{y}{y_i} = \sigma \qquad \ldots(23)$$

The actual integration can be carried with a number of methods such as the fourth order Runge-Kutta algorithm or the Adams-Moulton predictor-corrector algorithm. Furthermore, with certain particular forms of $F(\sigma)$, integration may even be made analytically.

2.3 *Determination of Functional Form of* $F(\sigma)$

In order to integrate the phenomelogical equations [i.e., Equations (17) through (23)] and to predict the dynamic behavior of filtration processes, a form of the function $F(\sigma)$ has to be specified. The functional form and values of the model parameters, generally speaking, cannot be determined a priori, but have to be based on experimental data. A brief discussion of the various available methods is given below to provide a perspective and basis of comparison for the work presented here.

(*a*) *Differential Methods* : Various methods can be classified under this class which are based on experimental data taken from shallow as well as deep beds. In the former case, a thin bed element is used for measurement and the dependence of axial distance is assumed to be negligible. A form of $F(\sigma)$ and the values of parameters are obtained directly from the data of the form of rate of filtration versus σ. Various problems arise. Perhaps the most serious one is that of bed packing as pointed out by Ives & Pienvichitr (1965).

The determination of $F(\sigma)$ can also be made from measurements of deep bed. Both Ives (1960) & Deb (1969) employed this approach in their respective works. The data obtained are in the form of y and σ as functions of z and t. By cross-plotting and interpolation, the various derivatives in the phenomelogical equations can be estimated from numerical differentiation, which then can be used for determining $F(\sigma)$. The main disadvantage is the lack of accuracy which inevitably arises from numerical differentiation.

(*b*) *Integral Method* : The name "integral method" derives from the fact that the integrated forms of the filtration equations are used instead of their differential forms and the formulation of this method is the purpose of this work. In principle, the selection of $F(\sigma)$ and its parameters are to be made so that the predicted behavior gives "best fit" to experimental measurements. The problem, therefore, is one of optimization and integration of the phenomelogical equations.

The major advantage of the integral method is that the data fitting used in determining $F(\sigma)$ is performed directly on experimental data. Futhermore, the computation is made with a framework suitable for computer calculation. On the other hand, it has a major disadvantage : namely, it requires an assumption of $F(\sigma)$. However, reasonable guidelines can be developed for its selection. By inspecting the data, one can deduce the general form of $F(\sigma)$ from the behavior of curves such as y^* versus z for fixed τ. In this connection, the following remarks may be of some use :

(1) $F(\sigma) = 1$ should be used if the concentration profile (y^* versus z) is invariant with time.

(2) For $F(\sigma) = 1-b\sigma$ or $F(\sigma) = 1 = b\sigma^2$, one has

$$\text{Sign}\left[\frac{\partial y^*}{\partial q^*}\right] = \text{Sign } b$$

When either form is valid, the (y^* versus z, fixed τ) curves are progressively displaced as τ increases for $b > 0$. For $b < 0$, the reverse behavior is obtained.

(*c*) *Mixed Behavior* : This is the most usual case and can be detected from the behavior of the (y^* versus z, fixed τ) curves which exhibit a weakening or even inversion of the initial trend of displacement of curves. For such cases, at least one more parameter has to be added. The following expression can be used to describe behavior of this type.

$$F(\sigma) = 1 + b\sigma - \frac{a\sigma^2}{\varepsilon_o - \sigma} \qquad a, b > 0 \qquad \ldots(24)$$

$$F(\sigma) = 1-b\sigma+\frac{a\sigma^3}{\varepsilon_o-\sigma} \qquad a, b>0 \qquad ...(25)$$

$$F(\sigma) = (1\pm\gamma\sigma)^n \qquad \lambda>0 \qquad ...(26)$$

$$F(\sigma) = \left(1+b\frac{\sigma}{\varepsilon_o}\right)^{n_1}\left(1-\frac{\sigma}{\varepsilon_o}\right)^{n_2}\left(1-\frac{\sigma}{\sigma_u}\right) \qquad ...(27)$$

3. Procedures of Optimization and Parameter Search

The purpose of this work is to develop a systematic procedure which determines the filtration model parameters from experimental data so that the predicted behavior from the filtration equations gives a best fit to experimental data. The procedure consists of two parts : integration of the filtration equations and minimization procedure for the determination of the model parameters. For the latter purpose, a combination of a pattern search scheme together with a least square curve fitting method (Levenberg's modification of the Gauss-Legendre method) is used. A detailed description of the procedure developed is given in this section.

For the discussion of the minimization technique developed here, the filtration rate is assumed to be described by either of the following two expressions :

$$\frac{\partial\sigma}{\partial\tau} = K_o(1-b\sigma)(y-\alpha y_l) \qquad y\geqslant\alpha y_l \qquad ...(28)$$

$$\frac{\partial\sigma}{\partial\tau} = K_o\frac{y}{(1+\gamma\sigma)^n} \qquad n>1 \qquad ...(29)$$

The use of Equation (29) is consistent with the rate expression of Equation (9) with $F(\sigma)$ of the form of Equation (26). Equation (28) can be considered as a generalization of the rate expression of Equation (9) which is commonly used in deep bed filtration. It assumes that a given fraction of particles of the inlet stream is non-filtrable. Thus, the effective concentration is $y-\alpha y_l$. This kind of behavior was observed for the filtration of clay suspension through activated carbon bed (Mehter 1970; Mehter et al 1970). It is also interesting to note that both expressions can be considered as special cases of the following expression

$$\frac{\partial\sigma}{\partial\tau} = K_o\frac{(y-\alpha y_l)}{(1+\gamma\sigma)^n} \qquad ...(30)$$

which reduces to Equation (25) for $\alpha = 0$ and to Equation (28) for $b = n\gamma << 1$.

3.1 *Integration of Filtration Equations*

The integration method was discussed in detail under para 2.2. A few remarks will be made in connection with the particular models chosen in this work [i.e., Equations (28) & (29)]. When Equation (28) is used, the integration can be performed analytically to give :

$$\sigma(z^*, \tau^*) = \frac{e^{b\tau^*}-1}{b(e^{z^*}+e^{b\tau^*}-1)} \qquad ...(31)$$

and

$$y^*(z^*, \tau^*) = \alpha+(1-\alpha)\frac{e^{b\tau^*}}{(e^{z^*}-e^{b\tau^*}-1)} \qquad ...(32)$$

For Equation (29), σ and y^* cannot be obtained analytically in explicit form (although they can be obtained implicitly in series expansion). However, $\sigma_i(\tau^*)$ can be obtained analytically and is given by

$$\sigma_i(\tau^*) = \frac{1}{\gamma}\left\{\left[1+(n+1)\gamma\tau^*\right]^{\frac{1}{(n+1)}}-1\right\} \qquad ...(33)$$

Numerical integration is necessary only in terms of z^* [integration of Equation (19) with initial values $\sigma(0, \tau^*)$ given by Equations (20) & (23)]. The Adams-Moulton predictor-corrector algorithm, initiated by a fourth order Runge-Kutta scheme was used.

3.2 *Minimization Technique for Parameter Search*

The basis for the minimization technique is Levenberg's modification of the Gauss-Legendre algorithm for least-squares (Wilde and Beightler 1967). The method, adapted to the problem at hand, is discussed briefly here.

Consider a filtration experiment in which the concentration in the liquid is determined through periodic sampling at various depths of the filter bed. Let τ_k be the time of sampling with $k = 1,..., K$, where, K is the number of $\{y^*$ versus $z^*\}$ data sets available. Let

$$y^*_{km} = \frac{y_{km}}{y_l} \quad m = 1,..., M \qquad ...(34)$$

be the data values (reduced concentration) at time τ_k from the M sampling sites at depths z_m ($m = 1, ..., M$), and $y^*\left(z^*_m, \tau^*_k ; \underline{x}\right)$ be the corresponding calculated values for a given form of $F(\sigma)$, where $\underline{x}$ is the vector of N parameters [for example, if Equation (29) is used, $\underline{x}$ contains K_o, γ and n]. The objective functions to be minimized are :

$$\psi_k(\underline{x}) = \sum_{m=1}^{M}\left[y^*_{km}-y^*\left(z^*_m, \tau^*_k ; \underline{x}\right)\right]^2 \qquad k = 1,..., K \qquad ...(35)$$

It should be noted that it is more proper to minimize $\sum_{k=1}^{K}\psi_k$. However, the minimization of each ψ_k separately has the advantage that possible inadequacies of a model under consideration will be revealed through a trend in the discrepancies between the various $\underline{x}_{k,opt}$, resulted from the K independent minimizations. Accordingly, one should use the separate minimization of each ψ_k to test the different forms of $F(\sigma)$ and the one step

minimization of $\sum_{k=1}^{K} \psi_k$ should be used for the computation of $\underline{x}_{opt}$ for an accepted $F(\sigma)$. We will return to the latter method later on.

For simplification, the index k is dropped for the time being but will be restored when needed. If we define

$$\phi_m(\underline{x}) = y_m^* - y^*\left(z_m^*, \tau^*; \underline{x}\right) \quad m=1,\ldots, M \qquad \ldots(36)$$

Equation (35) can be written as :

$$\psi(\underline{x}) = \sum_{m=1}^{M} \phi_m^2 \qquad \ldots(37)$$

We use the notation $\underline{\phi}$ for the column vector of the M functions $\phi_m(\underline{x})$ defined by Equation (36), and $\underline{\phi}^T$ for its transpose. Equation (37) can be written (in vector notation) as

$$\psi(\underline{x}) = \underline{\phi}^T \underline{\phi} \qquad \ldots(38)$$

By differentiation with respect to $\underline{x}$, one obtains

$$\nabla\psi = \frac{\partial\psi}{\partial \underline{x}} = 2\underline{\underline{J}}\,\underline{\phi} \qquad \ldots(39)$$

where, $\underline{\underline{J}}$ is the Jacobian

$$\underline{\underline{J}} = \begin{bmatrix} \frac{\partial\phi_1}{\partial x_1} & \cdots\cdots & \frac{\partial\phi_M}{\partial x_1} \\ \frac{\partial\phi_1}{\partial x_N} & \cdots\cdots & \frac{\partial\phi_M}{\partial x_N} \end{bmatrix} \qquad \ldots(40)$$

Let $\underline{\underline{J}}^T$ denote the transpose of $\underline{\underline{J}}$. It can be proven that

$$\nabla\psi(\underline{x} + \Delta\underline{x}) \approx 2\underline{\underline{J}}\,[\underline{\phi} + \underline{\underline{J}}^T\,\Delta\underline{x}] = 2(\underline{\underline{J}}\,\underline{\phi} + \underline{\underline{J}}\,\underline{\underline{J}}^T\,\Delta\underline{x}) \qquad \ldots(41)$$

For a given $\underline{x}$, a better approximation to $\underline{x}_{opt}$, for which $\psi(\underline{x}_{opt}) = \min_{\underline{x}} \psi$, can be obtained from $\underline{x} + \Delta\underline{x}$, where,

$$\Delta\underline{x} = -(\underline{\underline{J}}\,\underline{\underline{J}}^T)^{-1}\,\underline{\underline{J}}\,\underline{\phi} \qquad \ldots(42)$$

If ϕ_m are linear functions of $\underline{x}$, Equation (41) is exact, and only one step is required for convergence to the minimum. The method often converges for systems which are non-linear, but the convergence is not guaranteed. For strongly non-linear systems (as the case is with the filtration system) a modification introduced by Levenberg (1944) should be used

$$\Delta\underline{x} = -(\underline{\underline{J}}\,\underline{\underline{J}}^T - \chi\underline{\underline{I}})^{-1}\,\underline{\underline{J}}\,\underline{\phi} \qquad \ldots(43)$$

where, $\underline{\underline{I}}$ is unit $N \times N$ matrix, and χ a Lagrange multiplier, also known as the Levenberg parameter.

The physical interpretation of Equation (43) is the following. Consider the point $\underline{x}$ in N-dimensional space, and a hypersphere of radius r centered on $\underline{x}$. A step $\Delta\underline{x}$ starting from $\underline{x}$ and ending on the hypersphere is taken toward $\underline{x}_{opt}$. The function of the hypersphere is to confine the step $\Delta\underline{x}$, so that it will not lead away from $\underline{x}_{opt}$. Within the hypersphere the method treats the objective function as if ϕ_m were linear in $\underline{x}$. The parameter χ is introduced through the equality constraint

$$|\,\Delta\underline{x}\,| = r \qquad \ldots(44)$$

by forming the Lagrangian. χ is related to r through the following equation

$$r^2 = |\,\Delta\underline{x}\,|^2 = \underline{\phi}^T\,\underline{\underline{J}}^T\,(\underline{\underline{J}}\,\underline{\underline{J}}^T - \chi\underline{\underline{I}})^{-2}\,\underline{\underline{J}}\,\underline{\phi} \qquad \ldots(45)$$

Solving Equation (45) for χ in terms of r, and substituting into Equation (43) in order to obtain $\underline{x}$, is not justified in view of the fact that the computations are lengthy, and r is an estimate at any rate. Levenberg's original suggestion was to assign a value to χ directly. Wilde and Beightler (1967), however, point out that the value of r is easier to guess than that of χ and suggest the maximum permissible value of r to be

$$r_{max} = |\,(\underline{\underline{J}}\,\underline{\underline{J}}^T)^{-1}\,\underline{\underline{J}}\,\underline{\phi}\,| \qquad \ldots(46)$$

and r is estimated as some fraction of r_{max}. For the present work it is suggested that

$$r = \frac{r_{max}}{20} \text{ for the model given by Equation (28)} \qquad \ldots(47)$$

$$r = \frac{r_{max}}{10} \text{ for the model given by Equation (29)} \qquad \ldots(48)$$

In the case of the model given by Equation (28), for $r = r_{max}$ the search diverges. It is this fact that necessitates the use of the Levenberg modification of the Gauss-Legendre method. This problem does not arise very often for the model of Equation (29). However, the Levenberg modification is used since it guarantees convergence for the proper χ which is given as

$$\chi = -\frac{|\,\underline{\underline{J}}\,\underline{\phi}\,|}{r} \qquad \ldots(49)$$

This approximation usually leads to some $|\,\Delta\underline{x}\,|$, which is less than r. A better approximation can be obtained through iteration. Let $\chi^{(0)}$ and $\Delta\underline{x}^{(0)}$ be the values of χ and $\Delta\underline{x}$ obtained as described. Form

$$\chi^{(n+1)} = \chi^{(n)}\frac{|\,\Delta\underline{x}^{(n)}\,|}{r} \qquad n = 0, 1, 2, \ldots \qquad \ldots(50)$$

until

$$cr \leqslant |\,\Delta\underline{x}^{(n)}\,| \qquad \ldots(51)$$

where, cr is a specified fraction of r (e.g., 0.95 r). This iteration, proposed by Wilde & Beightler (1967), amounts to an iterative solution of Equation (50) in terms of χ.

At the minimum (hopefully the global minimum)

$$| \underline{J}\underline{\phi} | = 0 \qquad \ldots(52)$$

This is the criterion for convergence to the minimum. In practice, the condition in Equation (52) is replaced by

$$| \underline{J}\underline{\phi} | \leqslant \varepsilon \qquad \ldots(53)$$

where, ε is a specified small positive number (e.g., 10^{-5}). It is not necessary to repeat the computation of χ at each step. One may use the value of χ obtained from the first step.

In this work the value of r_1 at the first step is stored. Subsequent steps are taken with this initial r_1. However, r_{max} is computed at each Gauss-Legendre-Levenberg step, and is compared to r_1. If, at some step, r_{max} is less than or equal to r_1, the step is taken without constraint (by letting $\chi = 0$). In this way, when the search comes with "sight" of the minimum, the constraint introduced by Levenberg is relaxed. The step is taken according to Equation (42).

The Gauss-Legendre-Levenberg algorithm (GLL), powerful though it is, requires a certain amount of computation, especially when numerical integration and differentiation are necessary. This, together with the fact that the form of $F(\sigma)$ may require r_1 to be a small fraction of r_{max}, may make it profitable to use a pattern search technique (PST) in combination with the GLL method. The PST is usually effective in direct search optimization problems. It requires a minimum amount of computation, while it reduces the value of the objective function considerably, each time it is successfully used. The first step is taken by GLL. Then the PST takes a tentative step in the same direction, from the new position. At the new tentative position the objective function is calculated. If the tentative step proves to be an improvement, it is adopted, and another tentative step is taken in the same direction. The length of the PST step is increased after each success by a certain empirical factor q, since successive successes in the same direction make the latter increasingly more promising. The value of this empirical factor has to be determined for each particular problem. In this work it was found that a satisfactory range is $1 < q < 2$. The PST proceeds in the same direction with ever-increasing steps, until it runs into a tentative position at which the objective function has a value higher than that one at the exactly previous position. This last step is not taken. The GLL algorithm is used, instead, to provide a new step. The PST takes over in the direction of the GLL step. The GLL algorithm will be used more than once at a time, only if the first PST step fails to produce an improvement. Successive failures mean that either the contour lines are very twisted in this region, or that the region of a minimum has been reached. For this reason, if the GLL is called more than one time in a row, the search becomes more "cautious" by automatically reducing r by a certain factor (in this work by 2). The value of r is restored to the initial estimate r_1 after the PST takes one successful step. Each time the GLL is used the value of $| \underline{J}\underline{\phi} |$ is checked. When the criterion expressed by inequality (53) is satisfied, the computation is discontinued. The computation is also discontinued if the GLL is called more than seven times in a tow, since then even steps of the order of $\frac{r_1}{100}$ in the GLL step direction lead away from the minimum.

As mentioned earlier, the minimization for a given form for $F(\sigma)$ should be performed with $\sum_k \psi_k$ as the objective function. Let us define

$$\psi(\underline{x}) = \sum_{k=1}^{K} \psi_k = \sum_{k=1}^{K} \sum_{m=1}^{M} \left[y^*_{km} - y^* \left(z^*_m , \tau^*_k ; \underline{x} \right) \right]^2 \qquad \ldots(54)$$

The vector of differences is

$$\underline{\phi} = \begin{bmatrix} y^*_{11} - y^* \left(z^*_1 , \tau^*_1 ; \underline{x} \right) \\ \vdots \\ y^*_{1M} - y^* \left(z^*_M , \tau^*_1 ; \underline{x} \right) \\ \vdots \\ y^*_{K1} - y^* \left(z^*_1 , \tau^*_K ; \underline{x} \right) \\ \vdots \\ y^*_{KM} - y^* \left(z^*_M , \tau^*_K ; \underline{x} \right) \end{bmatrix} = \begin{bmatrix} \phi_1 \\ \vdots \\ \phi_R \end{bmatrix} \qquad \ldots(55)$$

where, $R = KM$. The minimization of ψ can be performed in exactly the same way as for the case of each ψ_k. The Jacobian in this case will be

$$J = \begin{bmatrix} \frac{\partial \phi_1}{\partial x_1} & \cdots\cdots & \frac{\partial \phi_R}{\partial x_1} \\ \vdots & & \vdots \\ \frac{\partial \phi_1}{\partial x_N} & & \frac{\partial \phi_R}{\partial x_N} \end{bmatrix} \qquad \ldots(56)$$

The minimization technique described proved to be very effective for the problem considered. The CPU time for $K = 6$, $M = 5$ and for the two-parameter model given by Equation (28) is about 50 seconds in an IBM/360 digital computer (execution time $\sim$ 30 sec), when each ψ_k is minimised separately. The number of steps required for the minimization is usually in the neighborhood of 20. The ratio of the number of steps taken by the PST to that taken by the GLL algorithm is usually about 1:1.

Longer CPU times are required for three-parameter models, mainly because of the required numerical integration and differentiation. Fortunately, the integration of Equation (17), in many cases, can be performed analytically. The CPU time for $R = 30$

($K = 6$, $M = 5$) for the three-parameter model given by Equation (32) is of the order of 240 sec (execution time $\sim$ 220 sec), when the objective function is ψ. The number of steps required for the minimization is in the neighborhood of 20. The ratio of the number of steps taken by the PST to that taken by the GLL algorithm is usually about 1:1.

Two separate programs based on models of Equations (28) & (29) were developed*. They can very easily be modified for any model containing 2 and 3 parameters and by a straightforward extension can be adapted for models containing more than three parameters.

3.3 *Initiation of the Parameter Search*

To initiate the optimization and parameter search procedure, the model parameters have to be assigned with proper values. The selection of these values is discussed in terms of the two model expressions [i.e., Equations (28) & (29)], although the same reasoning can be adapted to other models as well.

For the model given by Equation (28), the value of α, and initial guesses for K_o and b are needed.

(*a*) *Value of* α : Since most of the filtration occurs in the beginning section of the column, a crude estimate of α can be taken to be the value of y^* for large bed depth. Letting z_M be the depth beyond which the filtrate quality (i.e., value of y') remains essentially constant, one has

$$\alpha = y^*_{1M} \qquad \ldots(57)$$

An alternate approach is to assume that

$$\alpha = \frac{1}{K}\sum_{k=1}^{K} y^*_{kM} \qquad \ldots(58)$$

where, as before, y^*_{kM} is the measured value of y^* at z_M and τ_k.

As to be expected, different values for K_o and b are obtained for the two different values of α. From the physical point of view, Equation (57) is more attractive, although Equation (58) leads to a slightly better fit.

(*b*) *Initial Guess for* K_o : In order to obtain an estimate for K_o, the filtration data for the initial period of measurement (i.e., y^* versus z for smallest value of τ) should be utilized. The estimation that follows does not depend on the particular form of $F(\sigma)$, since $F(\sigma) \simeq 1$ for small times or

$$K \approx K_o \qquad \ldots(59)$$

Also, for $K \simeq K_o$, the integration of the filter equation yields

$$y^*(z^*, \tau_1^*) \approx y^*(z^*, 0) = \alpha + (1-\alpha)\, e^{-z^*} \qquad \ldots(60)$$

from which, one has

$$K_o \approx \frac{u_m}{z} \ln \frac{(1-\alpha)}{[y^*(z^*, 0) - \alpha]} \qquad \ldots(61)$$

It is reasonable to assume that $y^*(z^*_m, 0) \approx y^*_{1m}$ for $m = 1, \ldots, M$, or

$$K_o \approx \frac{u_m}{z_m} \ln \frac{(1-\alpha)}{(y^*_{1m} - \alpha)} \quad m = 1, \ldots, M' \qquad \ldots(62)$$

where, M' is the number of data points for which $(y^*_{1m} - \alpha) > 0$.

For practical purposes the average value should be taken

$$K_o^{(0)} = \frac{u_m}{M'}\sum_{j=1}^{M'} \frac{1}{z_j} \ln \frac{(1-\alpha)}{(y^*_{1j} - \alpha)} \qquad \ldots(63)$$

The value $K_o^{(0)}$ obtained from Equation (63) is, in most cases, within 20-40 percent of $K_{o,\,opt}$.

(*c*) *Initial Guess for* b : No fast simple method is available for an initial guess for b. However, the optimization technique is powerful enough that this is not a major obstacle. In most cases, b is expected to be quite small. On the other hand, trial calculations with the program indicate rapid convergence to small values of b even if the initial guess is as large as 100. As a rule, one may use

$$b^{(0)} = 10 \qquad \ldots(64)$$

For the model given by Equation (29), the value of α and initial guesses for K_o, γ, and n are needed.

(*a*) *Value of* α : Equations (57) or (58) should be used if particulate matters in the suspension contain fractions of non-filtrables.

(*b*) *Initial Guess for* K_o : As before, $K_o^{(0)}$ can be obtained from Equation (63).

(*c*) *Initial Guesses for* γ *and* n : For σ small enough, one can write the approximate relation

$$(1 + \gamma\sigma)^{-n} \approx 1 - b\sigma \qquad \ldots(65)$$

Assuming that this relation holds for the first and second sets of data, one can minimize ψ_1 and ψ_2 separately. For initial guess of b, let

$$b^{(0)} = 100 \qquad \ldots(66)$$

* These programs are available upon direct request from the authors.

This minimization usually is very fast (CPU time $\sim$ 25 sec). Let b_{opt} be the average of the two values of b to which the search converged. In order to obtain γ and n, one can use a one-dimensional Fibonacci search for n, with ψ as the objective function. In the Fibonacci search for each n, the corresponding value of γ can be obtained from

$$\gamma = \frac{b_{opt}}{n} \qquad ...(67)$$

or more accurately

$$\gamma = \frac{3n - \sqrt{9n^2 - 12 b_{opt}\, n(n-1)\sigma_c}}{2n(n-1)\sigma_c} \qquad ...(68)$$

where,

$$\sigma_c = \frac{1 - e^{-b_{opt}\,\tau_1^*}}{b_{opt}}, \text{ if } \tau_1 < 2 \text{ hr} \qquad ...(69)$$

The Fibonacci search converges consistently within a certain region. For this work it is suggested that the search be performed in the region $1 < n < 6$. The objective function is not always convex within the above region. For this reason, if the Fibonacci search happens to diverge in a certain region in which the optimum value of n is expected to be, the search should be performed piece-wise in sub-regions. This provision is provided in the computer program developed in this work.

When the method converges in the initial region, the CPU time for $K = 6$, $M = 5$ is $\sim$ 50 sec (execution time $\sim$ 40 sec). The main weakness of the two-stage procedure described here for K_o, γ and n is that it relies heavily on the first one or two sets of data. This is the reason why the results should be regarded only as good approximations to the optimum set of values of the parameters, and not as the optimum values themselves.

Once the range of values of K_o, γ and n is known, the two-stage procedure is not necessary any more The one-stage optimization of all parameters simultaneously can be used directly. This is shown in the illustrative example given below.

4. Illustrative Example

Consider the following filtration data from which the model parameters are to be evaluated (Mehter 1967).

Filter Bed : Granular Activated Carbon Darco 20×40
Particle Geometric Mean Diameter $= 0.594$ mm
Filter Bed I.D. $= 7.6$ cm
Filter Bed Depth $= 130$ cm
Macroscopic Porosity, $\varepsilon_0 = 0.49$

Suspension : Clay (EPK) Suspension in Tap Water
Suspended Particle Size : Non-Uniform
$4\mu < d < 40\mu$

Operating Conditions : Approach Velocity,

$$u_m = 496 \text{ cm/hr} \left(2.034 \frac{\text{gpm}}{\text{sq ft}}\right)$$

Feed Concentration,

$$y_l = 88 \times 10^{-6} \frac{\text{cm}^3}{\text{cm}^3} \left(218 \times 10^{-6} \frac{\text{gm}}{\text{gm}}\right)$$

Experimental filtration data using darco 20×40

z (cm) \ τ (hr)	Concentration ratio y^*					
	1.0	2.0	6.0	9.5	13.0	16.0
0.0	1.000	1.000	1.000	1.000	1.000	1.000
13.0	0.317	0.615	0.762	0.791	0.837	0.837
33.0	0.098	0.128	0.214	0.372	0.535	0.581
65.2	0.024	0.026	0.024	0.047	0.070	0.070
102.8	0.000	0.026	0.024	0.023	0.023	0.023
126.0	0.000	0.000	0.024	0.023	0.023	0.023

The kinetic expression of Equation (29) will be used to describe the filtration behavior. Initial guesses of the filtration parameters were assumed as follows :

(*a*) $K_o^{(0)}$ can be obtained using Equation (63) and the first data column in the Filtration Data Table :

$$K_o^{(0)} = 35.6 \text{ hr}^{-1}$$

(*b*) An initial guess for $\gamma^{(0)} n^{(0)} = b_{opt}$ can be obtained by using the computer program based on Equation (28) and the first two or three data columns in the Filtration Data Table. In this minimization we take the value of $K_o^{(0)}$ to be 35.6 hr^{-1} and $b^{(0)} = 100$ [see Equation (66)]. The optimal parameter values from the minimization of ψ_1, ψ_2 and ψ_3 are as follows :

τ	$K_{o,\,opt}$	b_{opt}
1.0 hr	41.66 1/hr	0.73
2.0	51.96	167.37
6.0	54.48	80.30

These results may appear confusing and to have a lack of consistency. However, if one continues the search by using the next three sets of data of the Filtration Data Table, the trend of decrease of b for $\tau > 2$ hr, (as well as the trend of increase of K_o) continues for $\tau > 6$ hr. This suggests the inadequacy of the model $F(\sigma) = 1 - b$.

The exceeding low value of b_{opt} for $\tau = 1.0$ hr can be attributed to the fact that for the small flow rate, and the dilute suspension used in this run, the effect of σ (which is very small) on the value of $K = K_o F(\sigma)$ is negligible. Indeed, parameter search based on data obtained under exactly the same conditions, except for a higher flow rate $\left(3.141 \frac{\text{gpm}}{\text{sq ft}}\right)$, and higher feed concentration (190×10^{-6} cm^3/cm^3, or 470×10^{-6} gm/gm), did not exhibit this deviation from the trend of decreasing b_{opt}. This particular example was used in order to emphasize that judicious interpretation of the computer output is necessary. Under these circumstances, a better initial guess will be

$$K_o^{(0)} = \tfrac{1}{2}(41.66 + 51.96) = 46.8 \text{ hr}^{-1},$$

$$\gamma^{(0)} n^{(0)} = b_{opt} = 167$$

and *not*

$$\gamma^{(0)} n^{(0)} = \tfrac{1}{2}(0.73 + 167.37) = 84.05$$

(*c*) With this information, $\left(K_o^{(0)} = 46.8 \text{ hr}^{-1} \text{ and } b_{opt} = 167\right)$, the Fibonacci search described before can now be used in order to obtain $\gamma^{(0)}$ and $n^{(0)}$. The search is performed in the region (1,6). The following values are obtained :

$$\gamma^{(0)} = 59.25, \; n^{(0)} = 2.82$$

The sum of the least squares (designated by ESQMIN) is

$$\text{ESQMIN} = 0.04747325$$

The standard deviation for this value of ψ_{min} is

$$s = \sqrt{\frac{\text{ESQMIN}}{(30-3)}} = 0.0419$$

(*d*) The values of $K_o = 46.8$ hr^{-1}, $\gamma = 59.25$ and $n = 2.82$ can be used as initial guesses for the one-stage minimization. The values of the parameters to which this search converges are

$$K_{o,\,opt} = 50.47 \text{ hr}^{-1}, \; \gamma = 30.46, \; n = 5.095$$

The predicted concentration profiles, y^* versus z, for various times based on these parameters are given in Figure 1. For comparison purposes, the experimental

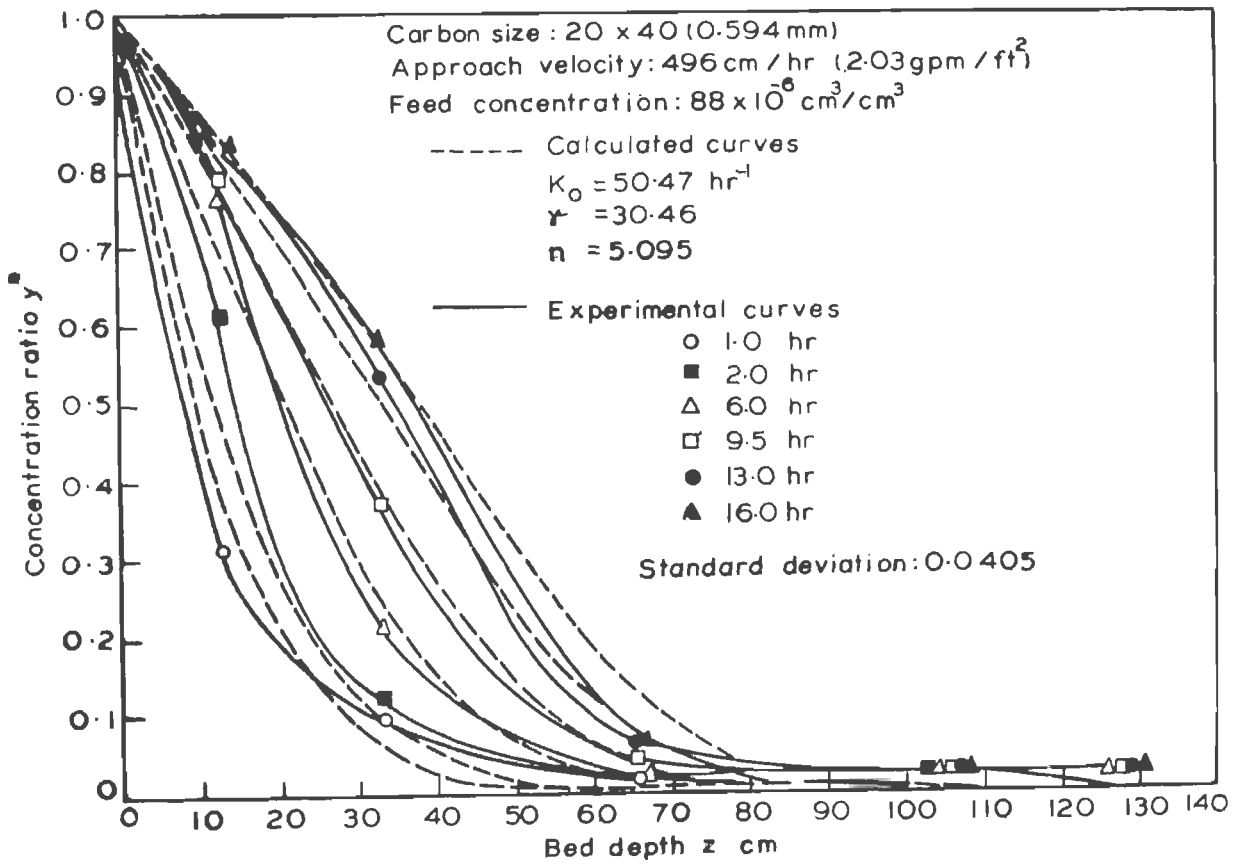

FIGURE 1 : Suspension concentration distribution for filtration through 20 x 40 carbon bed.

data are also included in the figures with

$$\psi_{min} = \text{ESQMIN} = 0.04425633,$$

$$s = \sqrt{\frac{\text{ESQMIN}}{(30-3)}} = 0.0405$$

(*e*) *One-Stage Minimization Directly* : The previous procedure would be necessary only if the order of magnitude of the parameters were unknown ; it was presented here only for purposes of illustration. In practice, one can use directly as initial guesses

$$K_o^{(0)} = 35.6 \text{ hr}^{-1}, \gamma^{(0)} = 50, \quad n^{(0)} = 3$$

for the one-stage minimization (i.e., with the use of the three-parameter computer program). The search converges to the following values :

$$K_{o,opt} = 50.08 \text{ hr}^{-1}, \gamma_{opt} = 26.06, n_{opt} = 5.812$$

with

$$\psi_{min} = \text{ESQMIN} = 0.04425775$$

and

$$s = \sqrt{\frac{\text{ESQMIN}}{(30-3)}} = 0.0405$$

(*f*) *Discussion* : The discrepancies in the values of the parameters and the values of ESQMIN, which the one-stage minimization, starting from slightly different initial values, produced, i.e., those used in (*d*) and those in (*e*), are accounted for by the fact that the search is, in practice, discontinued when the criterion expressed by Equation (53) is satisfied*. The exact criterion expressed by Equation (52) is not satisfied at these points, and it is questionable whether it can be satisfied at all, considering the fact that the computation of the profiles is performed, at least in part, numerically. From continuity considerations it is expected that there exists a locus of points in the *N*-dimensional space, at which the criterion expressed by Equation (53) is satisfied. It is then obvious that starting from different points the search will be discontinued at different, in general, points of the aforementioned locus. One hardly needs to mention that the exact optimum belongs to this locus, too.

Another observation of importance is the following. Despite the considerable difference between the values of the parameters obtained with the two-stage minimization ($K_o^{(0)} = 46.8$ hr^{-1}, $\gamma^{(0)} = 59.25$ and $n^{(0)} = 2.82$), and the ones obtained with the one-stage minimization ($K_{o,opt} = 50.47$ hr^{-1}, $\gamma = 30.46$ and $n = 5.095$), the difference between the values of the objective function (0.04747325 versus 0.04425633) is not very large. It seems that the minimum lies in a four-dimensional, rather flat, valley in which relatively large changes in the parameters (especially γ and n) produce small changes in the objective function. The sensitivities with regard to these parameters are rather weak.

* In this case $\varepsilon = 0.00005$.

5. Acknowledgment

This work was performed under Grant 17020 DZO, Federal Water Quality Administration.

6. Literature Cited

(1) DEB, A.K. : "Theory of Sand Filtration." J. San. Eng. Div., Proc. ASCE, 95, SA3 399 (1969).

(2) HERZIG, J.P. ; LECLERC, D. and LeGOFF, P. : "Flow of Suspensions through Porous Media-Application to Deep Bed Filtration." Ind. Eng. Chem., 62, 8 (1970).

(3) IVES, K.J. : "Rational Design of Filters." Proc. the Int. of Civ. Engrs. (London), 16, 189 (1960).

(4) IVES, K.J. and PIENVICHITR, V. : "Kinetics of the Filtration of Dilute Suspensions." Chem. Eng. Sci., 20, 965 (1965).

(5) IWASAKI, T. : "Some Notes on Sand Filtration." J. AWWA, 29, 1591 (1937).

(6) LEVENBERG, K. : "A Method for the Solution of Certain Non-linear Problems in Least Squares." Quart. App. Math., 2, 164 (1944).

(7) MEHTER, A.A. : "Filtration in Deep Beds of Granular Activated Carbon." M.S. Thesis, Syracuse University (1970).

(8) MEHTER, A.A. ; TURIAN, R.M and TIEN, C. : "Filtration in Deep Beds of Granular Carbon." Report No. 70-3, Submitted to FWQA, Deptt. of Chem. Eng. and Mat. Sci., Syracuse University (1970).

(9) WILDE, D.J. and BEIGHTLER, C.S. : "Foundations of Optimization." (Prentice-Hall, Englewood Cliffs, N.J., 1967), pp. 298-304.

Nomenclature

a	= filtration parameter
b	= filtration parameter
D	= effective dispersion coefficient of suspended particles
$ESQMIN$	= the minimum value of the particular objective function
$F(\sigma)$	= arbitrary function of σ, such that $F(0) = 1$; [Equations (7) or (9)]
g	= acceleration of gravity
i	= index
I	= $N \times N$ identity matrix
j	= index
$\underline{J}$	= Jacobian matrix [Equation (40) ; also Equation (56)]
k	= index
K	= filter coefficient [Equation (9)] ; also : number of $\{y^*$ versus $z\}$ data sets available
m	= index
M	= number of sampling sites

n = empirical exponent [Equation (26), and Equation (29)]

n_1, n_2 = empirical exponents [Equation (27)]

N = number of the parameters (including K_o) of the filtration model under consideration

r = radius of hypersphere [Equation (44)]

r_{max} = maximum value of r at a particular position [Equation (46)]

r_1 = length of the first step taken by the GLL algorithm

s = standard deviation

t = time since start-up of filtration, that is, since the moment of first contact between suspension and filter bed

u_m = approach on superficial velocity of suspension

$\underline{x}$ = vector of the N parameters (including K_o) of the filtration model under consideration

y = volume fraction of solids in suspension

y_i = feed value of y

y^* = y/y_i, reduced concentration of solids in suspension

y^*_{km} = experimental value of the reduced concentration at time τ_k, and depth z_m

z = depth in bed

z^* = zK_o/u_m, dimensionless depth in bed

Greek Letters

α = the non-filtrable fraction of the feed concentration, y_i

β = ratio of the apparent volume of deposited matter to the actual volume of the deposit

γ = filtration parameter [Equation (26)]

ϵ = macroscopic porosity of the bed; also: a small positive number [Equation (53)]

λ = filter coefficient [Equation (6)]

λ' = filter coefficient [Equation (12)]

ρ = density

σ = specific deposit, or retention; actual volume of deposited particles per unit volume of filter

σ_i = specific deposit at zero depth, that is, at the top differential layer of the bed

σ_u = critical value of [Equation (27)]

τ = $t - \epsilon_o\, z/u_m$, corrected time

τ^* = $\tau K_o\, y_i\, (1-\alpha)$, dimensionless corrected time

$\underline{\phi}$ = vector of differences between the experimental values of y^*, and the corresponding calculated values for a given time [Equation (36)]

$\underline{\phi}$ = vector of differences between all the experimental values of y^*, and the corresponding calculated values [Equation (55)]

χ = Levenberg's parameter [Equation (35)]

ψ_k = sum of the squares of the differences between the experimental values of y^*, and the corresponding calculated values for a given time τ_k [Equation (35)]

$\psi = \sum_{k=1}^{K} k$, sum of the squares of the differences between all the experimental values of y^*, and the corresponding calculated values

Subscripts

i = refers to conditions at zero depth

o = refers to clean bed conditions

$\underline{\ }$ = designates a vector

$\underline{\underline{\ }}$ = designates a matrix

Super T = designates the transpose of a vector, or a matrix

Combined Water Quality and Flow Monitoring Stations Employing New Techniques

S. J. GILLAM-SMITH
Sales Manager
Hydrological Systems, Plessey Radar, Addlestone, England.

SYNOPSIS

For both water resource studies and river management, knowledge of quality and quantity are important. Even in remote areas the quality of rivers can be as variable as the flow. Continuous measurement of quality and flow must, therefore, be undertaken if effective decisions are to be made regarding the storage and use of water.

New techniques recently perfected in the United Kingdom enable flow to be measured continuously at sites which have previously been unsuitable for classical methods such as structures and discharge/level calibrations. The new techniques, which do not interfere with navigation, fish movement or water-level, use electronic methods to provide an output indication directly in conventional units. Water quality parameters are measured automatically to provide outputs which are displayed and recorded in the same way as flow. Unattended operation is feasible with date either being telemetered to a control centre or recorded locally.

The application, operation and principles are presented and future developments discussed.

Introduction

The object of any study of water resources is to obtain reliable, statistically meaningful information about the quantity of usable water in a geographical area. The measurement of usable water cannot be made without reference to the way in which the water is to be used. For example, the quality of water required for irrigation is different from that required for drinking supply. This frequently requires the continuous acquisition of information about both quantity and quality with the data presented in a form easily handled by the ubiquitas computer which can be used to undertake detailed analysis. This paper presents some of the new techniques which have been developed by the electronics industry specifically to help those concerned with the management of water. Two techniques are for the measurement of quantity, whilst a third is for the measurement of quality.

Rivers have, of course, been gauged using conventional techniques for many years. The frequency of measurement and accuracy of the gauging method used has depended on two factors. Firstly, the application or use of the data and, secondly, the limitations of the river or canal itself. The electronic flow gauges were designed because, in the United Kingdom as in many other parts of the world, demand for good quality water, especially for industrial and domestic use has been growing rapidly. Despite the famous English weather, it has been calculated that, apart from the island of Malta, England has less rainfall per head of population than any other European country. The gauges allow reliable measurements to be made on stretches of river which previously defied traditional methods ; such conditions are very low flow rates, bi-directional flow, the need for navigation and fish movement to be unimpeded, the presence of weeds, the control of the level by sluices and unstable cross-sections. The traditional

methods referred to for obtaining continuous measurements are those relying on a relationship between water-level and volumetric flow whether in the natural channel or past a man-made structure such as a weir or flue.

The water quality monitor was likewise designed to provide information which could not be obtained economically manually. The ninety-six samples taken each day provide a comprehensive picture of the river showing up both the natural diurnal variation and the pollution surges which frequently occur whilst noone, except automated equipment, is likely to be sampling.

Combined Monitoring Stations

Because of the importance of knowing the flow at the same point as quality, it is normal practice to combine the measurement points wherever this is possible. The specific advantages of combining automated measuring equipment are obvious; savings can be made by the use of a single building with a single power supply and a common data recording unit. Operational benefits include the reduced cost of maintenance and of data processing.

The first part of the system is the measurement of quantity or discharge defined as the product of the average velocity and the cross-sectional area. Both of these are variables which may or may not be related. The cross-sectional area of many rivers is simply related to water-level whilst in others the bed shape is constantly changing. In such rivers the velocity profile is likely to be irregular. However, at sites where the bed is stable it is usually possible to obtain repeatable velocity profiles and so to define, for a particular river level, a single depth at which the measured velocity is equal to the mean velocity of the river. This is the principle exploited by the ultrasonic flow gauge which has been developed in the United Kingdom.

The Measurement of Flow by Ultrasound

(1) The human ear responds to vibrations of up to 20,000 Hertz; frequencies higher than this are said to be ultrasonic. The frequency used in the gauge described is 500,000 Hertz.

(2) The operation of the gauge, which is designed to give an immediate output in cubic metres per second, is based on the fact that discharge can be calculated from knowledge of the average velocity and the cross-sectional area, and that this average velocity may be represented by the measured velocity in a single horizontal plane. The cross-sectional area of the water is defined by the form of the channel and the depth, and the depth of the horizontal plane is chosen empirically so that the measured velocity in this plane is equal to the average velocity of the whole channel when the river is at its normal level.

(3) The measurement of the velocity in the horizontal plane is made using ultrasonic techniques. The time for a pulse of sound to travel diagonally across the channel is influenced by the average component of the velocity of flow along the path of the sound as well as by the instantaneous velocity of sound in the water. The gauge is made independent of the velocity of sound by transmitting short regular pulses in both directions across the channel so that the velocity of sound can be cancelled out during the calculation of discharge.

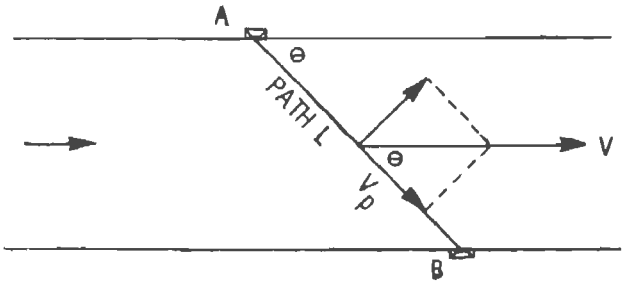

FIGURE 1 : Determination of streamflow.

If V is the velocity of flow parallel to the bank at a depth Y,
Vp is the component of velocity along the sound path,
L is the length of the sound path
and C is the velocity of sound,
the time taken for a pulse to travel from A to B is:

$$t_1 = \frac{L}{C+V_p} \qquad \ldots(1)$$

Similarly the time taken for a pulse to travel from B to A is:

$$t_2 = \frac{L}{C-V_p} \qquad \ldots(2)$$

thus, $$\frac{1}{t_1} - \frac{1}{t_2} = \frac{2V_p}{L} \qquad \ldots(3)$$

or $$V_p = \frac{L}{2}\left(\frac{1}{t_1} - \frac{1}{t_2}\right) \qquad \ldots(4)$$

Expression (4) does not contain the velocity of sound term C.

also $$V_p = V \cos\theta \qquad \ldots(5)$$

and combining (4) and (5)

$$V = \frac{L}{2\cos\theta}\left(\frac{1}{t_1} - \frac{1}{t_2}\right) \qquad \ldots(6)$$

(4) The layout of a typical ultrasonic flow gauge, such as those now in operation on the River Thames, is shown in Figure 2. It comprises two ultrasonic transducers, two transmitter/receiver interface units, a level sensor and two cabinets of electronics housed in an instrument building. The transducers are mounted one at each bank on a slide assembly which allows its vertical position to be adjusted. The mountings are fixed to a suitable vertical surface such as a steel pile or a concrete pier so that the line between the transducers

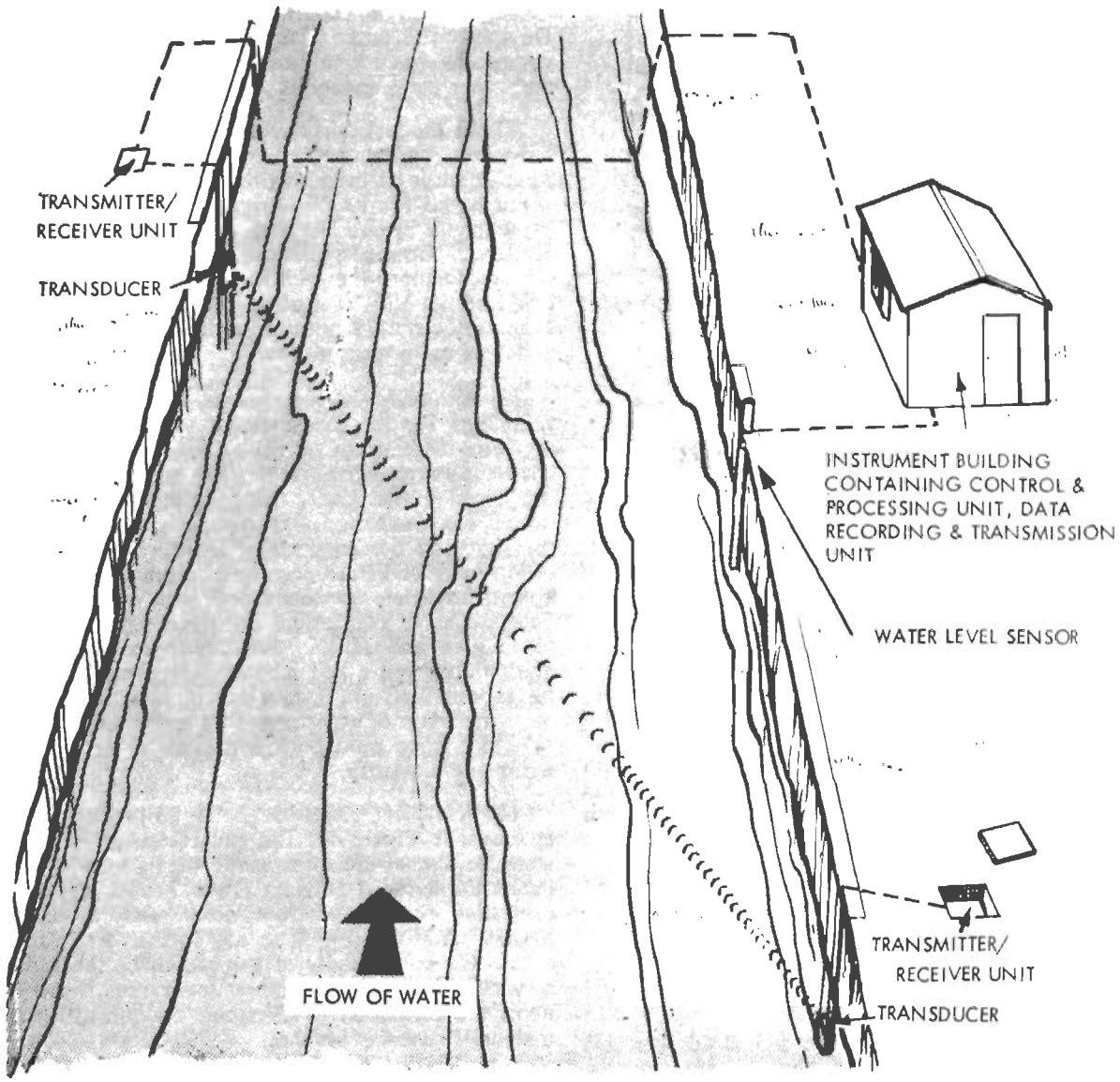

FIGURE 2 : Typical installation ultrasonic flow gauge.

makes an angle of between 30° and 60° with the direction of flow. The slide assemblies enable the vertical velocity profile to be determined and thus the system to be self-calibrating.

(5) The operation of the ultrasonic flow gauge is illustrated in Figure 3. A series of short ultrasonic pulses is transmitted by each transducer in turn. The transducers at both banks act as receivers detecting the pulses emitted by the opposite transducer. Each receiving transducer controls the frequency of an oscillator which determines the transmitted pulse repetition frequency for the opposite transducer. The period of the frequencies F_1 and F_2 in Figure 3 is adjusted to be a function of the transit time of the pulse across the channel. Thus the frequency of the oscillator controlled by the pulses travelling with the flow will be higher than that of the oscillator controlled by the pulses travelling against the flow. The two frequencies are then compared by the signal processing equipment and a difference frequency derived. This frequency is low enough to be treated as a series of individual pulses which may be counted. The time for which they are counted is determined by the cross-sectional area of the channel. As the channel shape is assumed to be constant for any one site, the time window needs only to be adjusted to accommodate changes in the water-level.

At the time of writing three such stations were in operation with ten more stations planned in detail for installation in following months. The results of the first few indicate that for approaching 95 percent of the

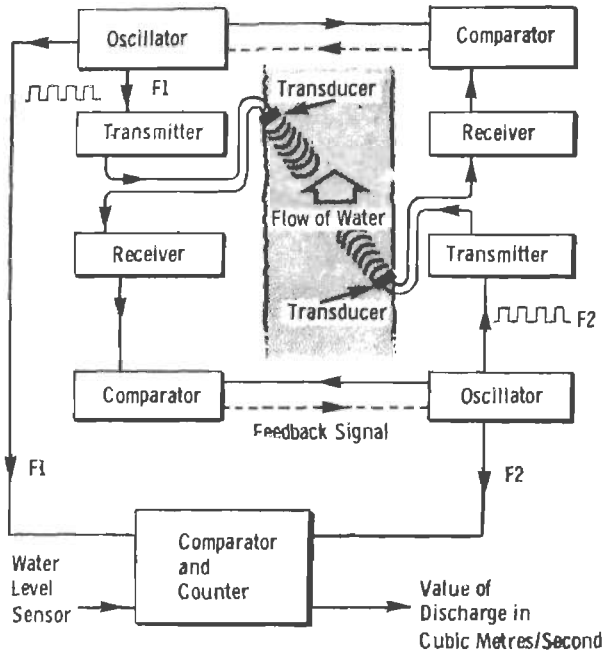

FIGURE 3 : System operation ultrasonic flow gauge.

time, the accuracy of the displayed (and recorded) data, in cubic metres per second, was better than 3.5 percent and that with an increase in the water-level of up to half the normal depth the accuracy of these data was still better than—11 percent without any correction for the fact that the ultrasonic path was no longer at the depth representing the mean velocity.

The optimum conditions for a gauge may be summarised as being

(*i*) A stable channel cross-section

(*ii*) Freedom from weed growth and turbulence

(*iii*) A limited range of water-level

(*iv*) The ability to mount the transducer carriage assemblies vertically.

Naturally not all rivers conform to the above specification. Currently work is in progress to develop a more complex ultrasonic gauge with more than one measurement path. This, it is hoped, will overcome the problem of the limited range of water-level and the need for a rectangular cross-section. However, as the ultrasonic technique itself is limited by the first two constraints listed above, it is apparent that a second approach to the problem of flow gauging is required.

The Measurement of Flow by Electromagnetic Methods

(1) In 1832 Michael Faraday demonstrated that when water flowed through a magnetic field, a potential difference could be detected across electrodes placed at each side of the channel. This electrical potential is proportional to the strength of the magnetic field and the average velocity of the entire cross-section of the channel. Obviously this latter relationship makes the electromagnetic technique a highly desirable one for gauging rivers and other large channels.

(2) In the last thirty years, a number of experiments have been undertaken using the earth's magnetic field: notable amongst these was the measurement of the flow through the Straits of Dover in 1953 and a series of experiments in the last few years along the coast of Holland. However, all these experiments were hindered by two factors—the weakness of the earth's magnetic field and the high level of electrical noise which exists as a result of electrical power transmission, electric railways and even radio transmitters.

(3) Although these problems were overcome some years ago for the measurement of flow in pipes by applying large magnetic fields, they have only recently been surmounted for rivers. The solution has been to use a coil buried under the river together with sophisticated electronic signal processing techniques to detect the signal in the presence of noise. Since the advent of low cost solid state electronics, a practical and reliable system has been developed and is now undergoing the final stages of evaluation on rivers where traditional techniques had failed. The development which was started four years ago incorporates some ideas which have been used in previous experiments, some of which were the result of experience on a test channel, and some of which have been borrowed from other parts of the electronics industry.

(4) A typical electromagnetic flow gauging station is shown in Figure 4. The gauge consists of a coil to generate the artificial magnetic field, two probes to detect the induced potential, four probes to assist in cancelling out the ambient noise and a water-level sensor. Additionally, there are further two probes to enable the conductivity of the bed to be measured and a water conductivity measurement cell. All these items are connected to electronic equipment housed in a suitable riverside building.

(5) Installation of the coil involves digging two trenches across the river and laying a plastic duct so that the cable may be drawn through to form a coil, rectangular in plan and trapezoidal in section. This operation can be undertaken, without the need for temporary dams, using a drag line excavator and divers.

The two signal probes are placed just in the bank in line with the middle of the coil so that their ends are below the lowest point of the river bed. The four noise cancellation probes are placed two on each side of the coil to match the signal probes. The river bed conductivity probes are driven in, one on each bank, some distance back but in line with the signal probes.

(6) The sequence of operation is as follows:

A direct current is switched twice per second through the coil so that the magnetic field is

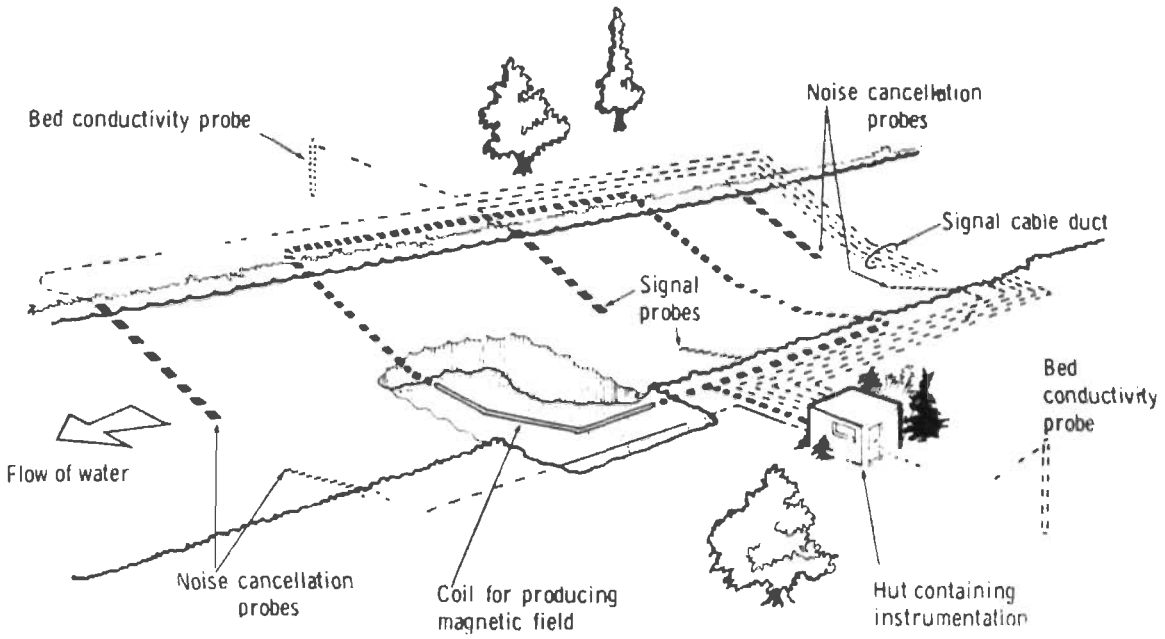

FIGURE 4 : Typical installation electromagnetic flow gauge.

reversed. Each reversal causes the polarity of the induced electrical potential in the signal probes to change in synchronism. The associated electrical signals can be as small as one microvolt in the presence of one hundred millivolts of noise, and to recover the signal several special techniques must be used. Firstly, the random noise picked up by the signal probes can be partially cancelled by subtracting from the signal voltage the voltage picked up by the noise cancellation probes. Secondly, the fact that the polarity of the wanted signal changes synchronously with the current in the coil, enables further random noise to be rejected by use of a phase sensitive detector and, thirdly, the resultant signal is filtered using digital filters before being averaged and combined with information from the water-level and conductivity sensors to give an on site output of discharge averaged over 15 minutes.

(7) The advantage of the electromagnetic gauge is that it is insensitive to changes in the cross-sectional area of the river. This is because the cross-sectional area of the measurement is defined by the signal probes and not by the bed. Both theory and practice show that the signal detected at the probes is proportional to the average velocity for this area, and that if there is a build up of silt, it appears to the gauge much the same as stationary water.

At the time of writing, one station was in operation whilst two others were being installed and surveys for further stations were being made. The results from the first station have been encouraging especially during the comprehensive series of tests with various obstacles placed in the channel.

Automatic Monitoring of Water Quality

(1) Whilst quantity is a totally objective variable, quality is a largely subjective one. There are at least one hundred chemical, biological and physical tests which can be undertaken to determine the quality of water. Of these some are analytical, such as the determination of the concentration of a particular chemical, whilst others are simply indications of the effect of pollutants. Obviously, it would be highly desirable to be able to monitor every substance that is likely to be present in water, but economic and technical considerations limit the field to about ten variables.

(2) The basic requirements of sensing systems for use at remote sites are that they should provide an electrical output proportional to the variable being monitored and that they should work reliably without loss of accuracy for periods of up to at least one month. An added advantage is that a particular sensor should respond to only one variable.

(3) Automatic monitoring of rivers began about ten years ago, motivated by the desire to reduce man-made pollution and to obtain more information on how natural rivers behave. One of the first parameters to be monitored was that of the dissolved oxygen concentration, for this not only indicates the possibilities for the river to support fish, but also the ability of the river to be self-purifying and so cope with additional pollution loads. The next parameter to be monitored continuously was that of turbidity. Turbidity, which is the measurement

of the transmission of light through the water, is a practical if not particularly accurate way of assessing the suspended solids load being carried by a river. Suspended solids are undesirable where water is to be pumped through a pipeline or allowed to flow slowly along canals, for apart from the scouring effect of the particles, the solids will settle and silt up the system.

Having tried various simple configurations of sensors for these two variables, it was decided that multi sensor systems were required to extend the interval between service visits and to collect all the data on one data logger. The variables chosen to be monitored in a standard monitoring station are:

Dissolved oxygen

Turbidity

pH

Conductivity, and

Temperature

The sensors, which have to withstand the environment and satisfy the criteria of low drift and minimum maintenance, have been chosen from among those in current use in the process control industry.

(4) Dissolved oxygen is measured using a Mackereth probe. This consists of a perforated cylindrical silver cathode enclosing a porous anode. The cell, which is filled with saturated potassium hydrogen carbonate solution, is isolated from the external medium by a tubular polythene membrane, sealed at each end by 'O' rings. A thermistor is incorporated in the cell to compensate for the temperature coefficient of the probe. The oxygen partial pressure in the water sample causes the dissolved gas to permeate through the polythene membrane into the solution. Inside the cell the oxygen is reduced at the silver cathode surface, generating a galvanic current which is proportional to the concentration of dissolved oxygen. The operational range of the sensor is 0 to 200 percent saturation with an accuracy of $\pm$ 5 percent.

(5) The turbidity sensor uses two light paths, one short and one long to minimise the effect of fouling of the optical surfaces. Turbidity is measured as the ratio of the light received by the two photocells. The measurement ranges are 0 to 100, 250, 500 or 1000 mg per litre (against a formazin standard) with an accuracy of 10 percent of the calibrated maximum value.

(6) The *pH* sensor which indicates the degree of acidity or alkalinity of the water contains two concentric electrodes, a glass membrane electrode sensitive to hydrogen ions, and a silver/silver chloride reference electrode connected by means of a porous ceramic plug. The potential difference between the glass and reference electrodes is proportional to the *pH* of the sample. The sensor has an operating range of 2 to 10 with an accuracy of $\pm$ 0.2 *pH*.

(7) The conductivity sensor is a cylindrical epoxy resin casting containing three concentric carbon rings.

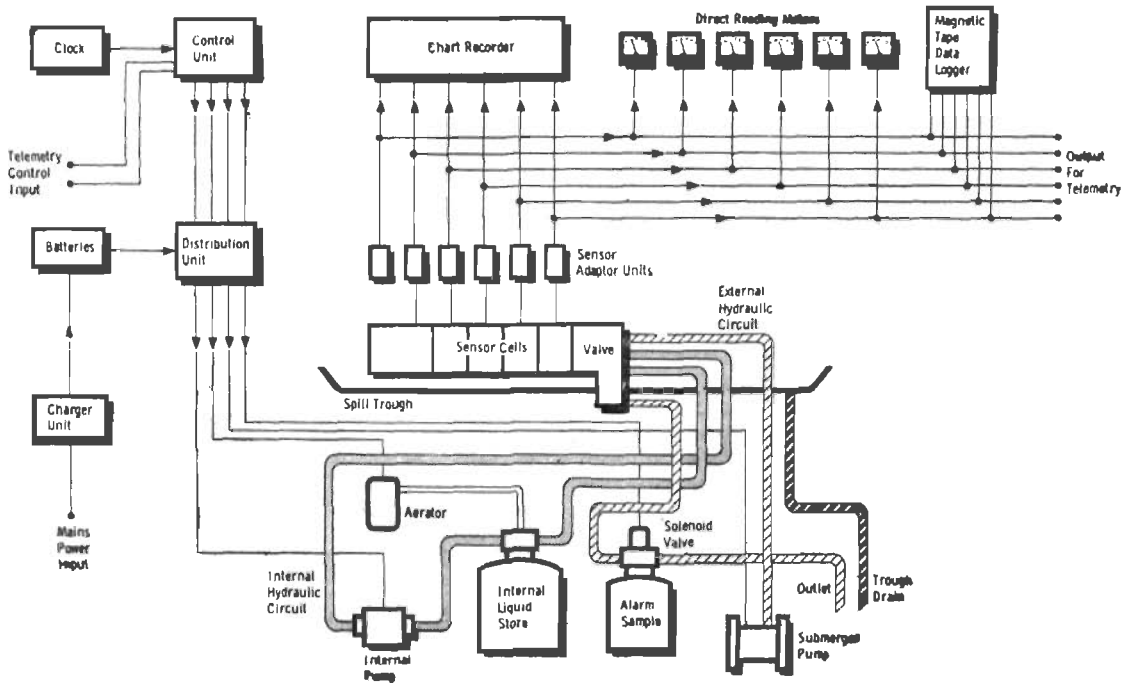

FIGURE 5 : System diagram water quality station.

To obtain a measurement, an alternating voltage is applied between the outer (pair) and the inner electrodes. The resistance of the water sample, which is inversely proportional to the conductivity is detected by a high input impedance amplifier circuit.

The conductivity range depends upon the sensor used, the lowest range being 0.1 to 10μ Siemens/cm and the highest 50 to 55 000μ Siemens/cm with an accuracy of $\pm$ 2 percent of the calibrated maximum value.

(8) The temperature is sensed by a precision platinum resistance thermometer with a working range of -5°C to $+35$°C and an accuracy of $\pm$ 0.2°C.

(9) The sensors are placed in a specially designed clear plastic flow block which optimises the performance of the sensors and prevents the build up of silt or slime. The flow block can be fed from two sources via a fluidic valve. This valve which is operated by the pressure of the water at the inlets connects the flow block into one of two flow systems. (See Figure 5).

The first of these systems allows water to flow from a pump in the river past the sensors and then back into the river. The second connects the flow cell to a pump inside the unit which circulates a cleaning liquid which is stored in a 10 litre container.

(10) The sequence of operation of the station is as follows : the pump in the river is started every fifteen minutes by a clock mechanism. After allowing sufficient time for the sensors to stabilise with a representative sample the interface electronics are switched on and the information recorded. On completion of the recording cycle, the pump is switched off and the hydraulic systems drains. This results in the sensors only being subjected to contamination for about three minutes in every fifteen. Any contamination that does build up, whilst the sample is being pumped, is removed once a day by pumping from the internal store a mixture of a detergent and sodium hypochlorite. This cleans the surfaces and kills any algal growth.

(11) As indicated previously, the practical sensors for automatic monitoring do not necessarily identify the cause of a problem. Two approaches are, therefore, possible. Firstly, to collect a sample for laboratory analysis whenever the automatic station detects a value beyond some preset alarm limit and, secondly, to interface more complex sensing units, accepting that they will require more attention than the basic station. Although it is not the purpose of this paper to describe the operation, or use of these more complex systems, it is worth mentioning that the basic station has already been used to control and record the data from units monitoring the values of:

Ammonium Ion Concentration

Nitrate Ion Concentration

Chemical Oxygen Demand, and

Organic Pollution Concentration.

(12) Automatic water quality monitoring stations, similar to that described in this paper, are known to be in operation in twenty countries protecting water intakes, preventing discharges of untreated effluent from factories and assisting water resource and environmental improvement planners.

Conclusion

Electronic systems for the study and management of water are now an established part of hydrology. Without electronics, everyday items such as communications systems and computing facilities would not exist and hydrology would not have reached the advanced state that it has today. It is only natural, therefore, that electronic methods should have been developed which challenge and improve upon the traditional techniques of measurement and surveillance.

The combined station and its component parts have already solved many of the operational problems of hydrology. In particular, the flow gauges offer a new degree of freedom to obtain information at the point that it is required, regardless of the fact that the velocities may be too low to turn current meters or that weeds would foul their propellers, thus preventing the establishment of a stage/discharge rating.

Likewise, automatic water quality monitors have demonstrated unexpected variations in rivers and have provided a very firm data base on which to build pollution models and future constructional plans.

Having experienced for several years the benefits gained by close liaison between the water and electronics industries, it is only to be hoped that this can be continued and progress maintained.

Acknowledgements

Acknowledgement is made to the Director of the Department of the Environment, Water Data Unit, and to the Director of the Water Research Centre for the financial support during the development of the flow gauges. Thanks are also due to Mr. W. R. Loosemore of the Atomic Energy Research Establishment, Harwell, who designed the ultrasonic gauge, to Mr. J.D. Newman of Plessey Radar Limited, who designed the Electromagnetic Gauge, and to Mr. R.W. Herschy of the Water Data Unit for his enthusiastic support and guidance. Acknowledgement is also made to the Directors of the Plessey Company Limited for their permission to publish this paper.

Bibliography

(1) HERSCHY, R.W. and NEWMAN, J.D.: "Electromagnetic River Gauging." Proceedings of the Symposium on River Gauging by Ultrasonic and Electromagnetic Methods, Water Research Centre and Department of the Environment Water Data Unit, December 1974.

(2) HERSCHY, R.W. and LOOSEMORE, W.R.: "The Ultrasonic Method of River Flow Measurement." Proceedings of the Symposium on River Gauging by Ultrasonic and Electromagnetic Methods, Water Research Centre and Department of the Environment Water Data Unit, December 1974.

(3) NEWMAN, J.D.; GREEN, M.J. and ELLIS, J.C.: "Analysis of Gauging Result." Proceedings of the Symposium on River Gauging by Ultrasonic and Electromagnetic Methods, Water Research Centre and Department of the Environment Water Data Unit, December 1974.

(4) Plessey Radar Limited :
The Ultrasonic Flow Gauge RSL 1603

(5) Plessey Radar Limited :
The Electromagnetic Flow Gauge RSL 1522

(6) Plessey Radar Limited :
The Land Based Water Quality Station RSL 1451

The Potential Impact of Satellite Data-Relay Systems on the Operation of Hydrologic Data Programs

D. W. MOODY
Hydrologist
U.S. Geological Survey
National Center, Reston, Virginia 22092.

D. M. PREBLE
Electronic Engineer
U.S. Geological Survey
Bay St. Louis, Mississippi 39520.

SYNOPSIS

The development of satellite communication systems presents new opportunities to improve the performance characteristics of hydrologic data collection programs. Data telemetry, via a communications link from remote field sites to a central station, alerts the manager of a data collection program to possible malfunctions of remote station equipment. By dispatching fields crews to repair stations as soon as malfunctions have been detected, the manager can substantially reduce data losses that would be incurred under non-telemetered modes of operation and, thus, improve the quality and continuity of the station's historical record. Telemetry, moreover, has the potential for reducing the labor, travel, and costs of operating a hydrologic network.

This paper reviews the operation of a non-telemetered hydrologic data collection system and identifies work elements which will be affected by telemetry. Estimated costs and the performance of non-telemetered stations are compared with those of stations telemetered via land-line, line-of-sight radio, meteor burst, and satellite communication links. It is concluded that the total costs of a large network of automatic hydrologic data collection stations whose data are transmitted via satellite to a central station are comparable to the total costs of a non-telemetered network. Because of their extensive geographic coverage, satellite systems will play an important part on the design and operation of future water resource management systems and global environmental monitoring programs.

Introduction

In July 1972, the launching of the Earth Resources Technology Satellite (ERTS-1) placed in orbit a Data Collection System (DCS) that could relay data from field site instruments to ground stations. Over the past 3 years, numerous experiments have demonstrated the technical feasibility of using satellite-based data relay to provide real-time hydrologic data services. Moreover, these experiments have suggested that under certain conditions, the use of satellite data-relay systems may not only reduce the funds and manpower needed to operate a hydrologic data program but also may improve the quality of the data.

This paper briefly outlines the recent history of hydrologic data collection technology in the United States, describes several satellite and non-satellite real-time data systems and programs, and describes the potential applications and impacts of satellite data-relay systems on water resources data programs.

Existing Hydrologic Data Collection Programs

Systematic stream gaging in the United States was begun by the U.S. Irrigation Survey in 1888 under the direction of Major John Wesley Powell[1]. Major Powell, who at the time was also Director of the U.S. Geological Survey, had a camp established on the Rio Grande at Embudo, New Mexico, to develop streamflow

measuring techniques and to train engineers in the art of stream gaging. From these early efforts to provide hydrologic data for planning and designing irrigation projects in the Western United States, the Geological Survey's National Water Data Program has grown to encompass data from more than 10,000 stream gaging stations, 4,300 water quality stations, 880 sediment stations, and 2,500 key wells. This program supports a wide range of Federal, State, and local land and water-resource related activities including :

—Management and operation of water resources projects

—Planning and design of land and water resources development programs

—Monitoring and assessing man's impact on the environment

—Water resources investigations and research.

The techniques and methods used by the Geological Survey and other Federal agencies in the United States to collect water data are summarized and documented in a recent report by the Federal Interagency Work Group on Designation of Standards for Water Data Acquisition([2]).

Some of the significant milestones in the development of the Geological Survey's National Water Data Program include :

1954—Development of the servo-manometer or bubble gage which greatly reduced the installation costs of water stage stations by eliminating the requirement for a stilling well. In addition, it substantially improved the ability to gage streams with unstable beds([3]).

1958—Development of an analog-to-digital recorder (ADR) which records data in computer-compatible format to facilitate direct entry of data into computers([4]).

1961—Introduction of water-quality monitoring equipment which provides continuous field measurements of certain water-quality parameters such as water temperature, dissolved oxygen, conductivity, and *pH*([5]).

1964—Establishment of remote computer terminals in selected field offices of the Geological Survey.

1971—Introduction of digital tape transmitters to transfer ADR punched paper tape data from field offices via telephone lines to the Survey's central computer facility([6]).

These milestones reflect a trend of increasing capability and automation of field instrumentation and increasing use of computers.

Originally, all historical basic records were manually processed in field offices. Later, much of the data-processing work was centralized to take advantage of labor-saving automatic data-processing techniques. The most recent trend has been to place data-processing activities again under the control of the field offices by using computer terminals and digital tape transmitters to communicate with the central computer facility. While these innovations have greatly reduced the time required to process records (a reduction from 6 weeks to less than 24 hours), the records are historical and do not reflect current hydrologic conditions.

Real-Time Data Systems

The availability of general purpose computers in the 1960's accelerated the development of mathematical models for use in operating water resources projects. Commonly, flood warnings and the operation of flood control structures are based on forecasts of streamflow. In addition, hydrologic forecasts may be used to operate multipurpose reservoirs, to schedule hydro-electric power generation, and to operate water-supply and waste-treatment plants. While computer technology provides the computational ability needed to process large amounts of data to make and update flood forecasts or schedule reservoir releases in response to current hydrologic conditions in a river basin, the problem remains of how to acquire current observations of hydrologic conditions from many geographically scattered points within a short enough time period to make forecasts and operational decisions.

Within the past decade, several real-time data systems have been established in the United States which reflect the growing demand for this type of data service :

—The National Weather Service (NWS) has established 12 regional River Forecast Centers (RFC) which use reports from approximately 2,000 stage stations. Stage reports and precipitation measurements obtained by local observers or by automated land-line systems are used to make flood forecasts([7]).

—The U.S. Corps of Engineers, Northeast Division, uses VHF, UHF, and microwave radio equipment to transmit hydrologic data from 41 points in New England to their Flood Control Center near Boston, Massachusetts. The data are used to operate about 70 dams and other structures in New England for flood control, hurricane protection and associated purposes([8]).

—The Columbia River Operational Hydromet Management System (CROHMS), a cooperative hydrometeorological data network supported by Federal agencies and power companies in the Pacific Northwest, utilizes data from over 750 stations to make river forecasts and schedule hydro-electric power generation.

In addition, numerous smaller networks of gaging stations and water quality monitors are supported by

State and municipal agencies and river basin commissions to control water-supply systems and monitor water pollution.

Land-line telephone systems are probably the most familiar form of data communications. The simplest form of a real-time data system uses a local observer who reads a river or reservoir stage and telephones the value to a central location where the forecasts and operational decisions are made. Where local observers are not available, encoders, which can be attached to water-level recorders, respond to a telephone call to the station with a series of audible tones (beeps) that represent the coded stage value([8]). Another approach is to transmit data over telephone or telegraph lines dedicated to the exclusive use of the data collection agency. An automated central station periodically polls the remote sites for data.

Line-of-sight communications using very-high frequency (VHF) or ultra-high frequency (UHF) radio links are often used in remote areas where land lines are not available. Tall radio antennas and repeater stations are usually necessary to relay data from remote sites to a central station, because local topography or the curvature of the earth limits the length of the line-of-sight communications link.

A potentially attractive alternative to land-based data acquisition systems is the Meteor Burst Communications System([9]). This system utilizes the ionized trails of meteors which form at altitudes of 80 to 120 km to passively reflect or re-radiate VHF radio signals and, thus, establishes a temporary communications link between a central station and remote sites. Because the frequency of meteors entering the atmosphere varies both annually and diurnally, it is estimated that a central station can expect to receive 12 (worst case at 1800 hours in February) to 400 (best case at 0600 hours in August) error-free, 100-bit messages per hour from remote stations assuming data transmission rates of 2,000 bits per second in 50 millisecond bursts. The average annual waiting time for the reception of an error-free message is approximately 5 minutes. The system operates best for remote sites located between 640 km and 1,280 km from the central station and has a maximum range of 1,900 km. The U.S. Soil Conservation Service is currently examining a meteor burst system for the collection of snow data in the Western United States.

In summary, advances in hydrologic modelling and the development of water resources management tools, made possible by modern computer technology, have created a demand for real-time data services. Field instrumentation exists for a wide range of hydrometeorological variables to meet these demands, although improvement in equipment standards, operational simplicity, and reliability is needed([10]). Land-line networks, while based on relatively simple, time-tested technology, are subject to disruption during periods when the data will be needed most, e.g., during hurricanes and storms, and tend to be prohibitively expensive in remote areas where the user may have to bear all installation costs. Line-of-sight radio systems are costly to install, difficult to maintain, require tall, unaesthetic antenna towers, which are vulnerable to wind and lightening damage, and are subject to poor quality radio transmissions owing to stormy weather or other forms of interference([11]). Despite these difficulties, line-of-sight radio systems have been extensively used in remote and mountainous areas where land-line systems are not economically feasible. The meteor burst communication system, although untried as a means of telemetering hydrologic data, appears to be a feasible technique for handling small amounts of data from networks of approximately 500 stations. For best reception the receive site must be placed from 640 to 1,280 km away from the stations being interrogated and land lines must be used to transmit the data back to regional users. It does not appear to be feasible for individual agencies to maintain their own receive sites. The relatively high costs of these systems and the growing demand for real-time data services have led network planners to examine the feasibility of satellite data-relay systems.

Satellite Data-Relay Systems

A satellite data-relay system is basically a line-of-sight repeater communication system in which the satellite transceiver relays data transmissions from a large number of remote stations to one or more central stations. There are two types of satellite data-relay systems currently being used to transmit hydrologic data: the low-altitude or biting satellite systems such as the Earth Resources Technology Satellite (ERTS)—now referred to as LANDSAT—operated by the National Aeronautics and Space Administration (NASA), and geostationary satellite systems such as the Geostationary Operational Environmental Satellite (GOES), operated by the National Oceanic and Atmospheric Administration (NOAA).

ERTS-1, launched in July 1972, orbits the earth about once every 103 minutes at an altitude of 900 km*. The orbit is nearly polar (87 degrees inclination) as well as sun synchronous to facilitate the collection of earth resources imagery—the primary mission of the satellite. The Data Collection System (DCS) on board ERTS-1 begins to relay data when both the specialized transmitter, known as a Data Collection Platform (DCP) at the remote site, and the receive site are simultaneously visible to the satellite. The number of periods of simultaneous visibility per day and the duration of reach period are functions of the latitudes and longitudes of the DCP and of the receive sites, and the elevation above the horizon that the satellite must reach before it is

* LANDSAT, 2, the second satellite of the LANDSAT series, was launched in January 1975, into a polar orbit 13 degrees out-of-phase with ERTS-1. ERTS-1 is now used as a backup to LANDSAT 2, but may be used to double the length of mutual visibility time.

visible to the antenna of either site. For example, assuming the receive site antenna can operate within 5 degrees of the horizon, the satellite will be visible at a range of 2,680 km. Similarly, if the DCP antenna can operate within 15 degrees of the horizon, then the satellite will be visible at a range of 1,900 km. Given the relative positions of the DCP and the receive site, the area of mutual visibility may be mapped, and the number of mutually visible periods and their durations may be calculated (Figure 1).

For DCPs located in the conterminous United States communicating with receive sites located in California and Maryland, the average duration of mutually visible periods is 9 minutes at least once every 12 hours, although two to three *successive* orbits during a 12-hour period are capable of relaying data for most DCPs. The number of orbits visible to the receive site in a given 12-hour period increases with latitude (Figure 2).

ERTS-DCS is designed to relay at least one message from as many as 1,000 DCPs simultaneously in view of the satellite to accomplish this, a random access mode of operation was chosen for the DCPs. Each DCP transmits a message of 38 milliseconds duration about once every 3 minutes. During transmission the DCP sends its identifier code and 64 bits of hydrologic information.

The ERTS-DCP is designed to be installed and

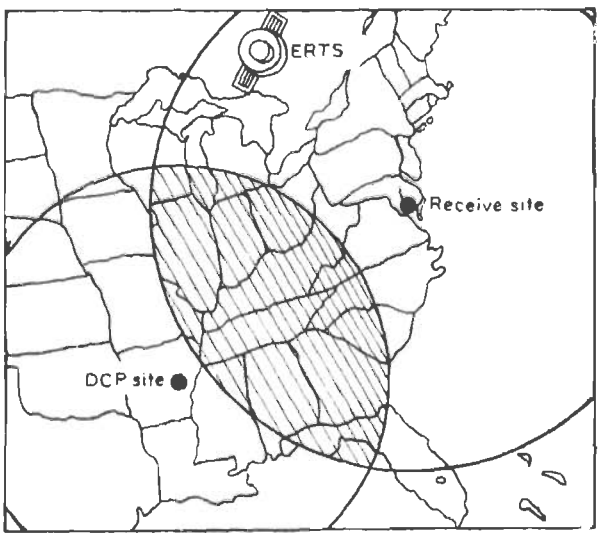

Area simultaneous visibility for ERTS-DCS (shaded area). Solid circles drawn about the DCP and receive site represent the maximum range at which ERTS is visible to the site. During the period of time that the orbit of the satellite takes it over the shaded area, data transmission is realized.

FIGURE 1 : Definition of periods of mutual visibility.

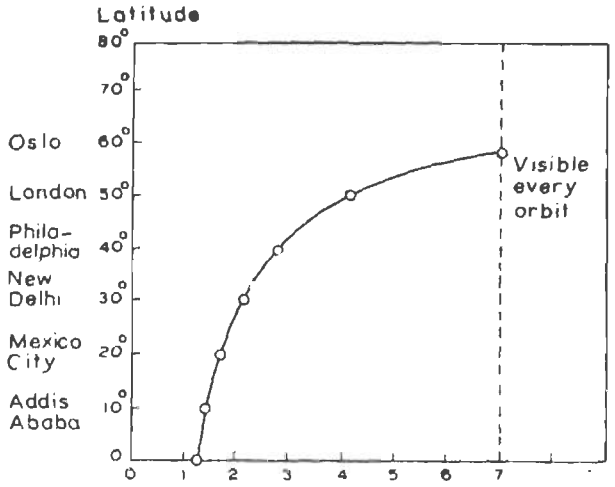

Average number of orbits in 12-hour period visible to a receive site for various latitudes N and S of the equator assuming antenna elevation of 5 degrees looking at a 900 km altitude polar orbitor-ERTS. Average visibility time 9 minutes.

FIGURE 2 : Frequency of periods of LANDSAT visibility to a receive site located at different latitudes.

operated by technicians with very little training in electronics. Since each DCP transmits its message on a common channel at random relative to the other DCPs, interference between remote site transmissions is designed to be less than 5 percent. Furthermore, the user need not know the satellite's position, nor need he synchronize the station's reporting interval with other DCPs. The technician just connects the antenna, sensors, batteries, and switches on the DCP (Figure 3). A simple radio frequency meter may be used to assure that the DCP is transmitting a signal.

GOES Data Collection System

In May 1974, the first GOES satellite was launched*. GOES is a geostationary satellite which maintains a constant position relative to a point on the earth's equator at an altitude of 36,000 km. Present plans for the GOES system call for three satellites in orbit: one satellite will be positioned at 70° W. Longitude; one satellite will be at 135° Longitude; and the third satellite will be located in between as an in orbit spare. In addition, a fourth satellite will be available on the ground for launch within 30 days of a failure of one of the satellites in orbit.

Although the primary mission of GOES is the collection of meteorological imagery, each satellite will contain a Data Collection System. Management of the GOES system is the responsibility of NOAA's National Environmental Satellite Service (NESS). NOAA's policy is to make GOES-DCS available to meet national

* A second geostationary satellite in the GOES series was launched in January 1975.

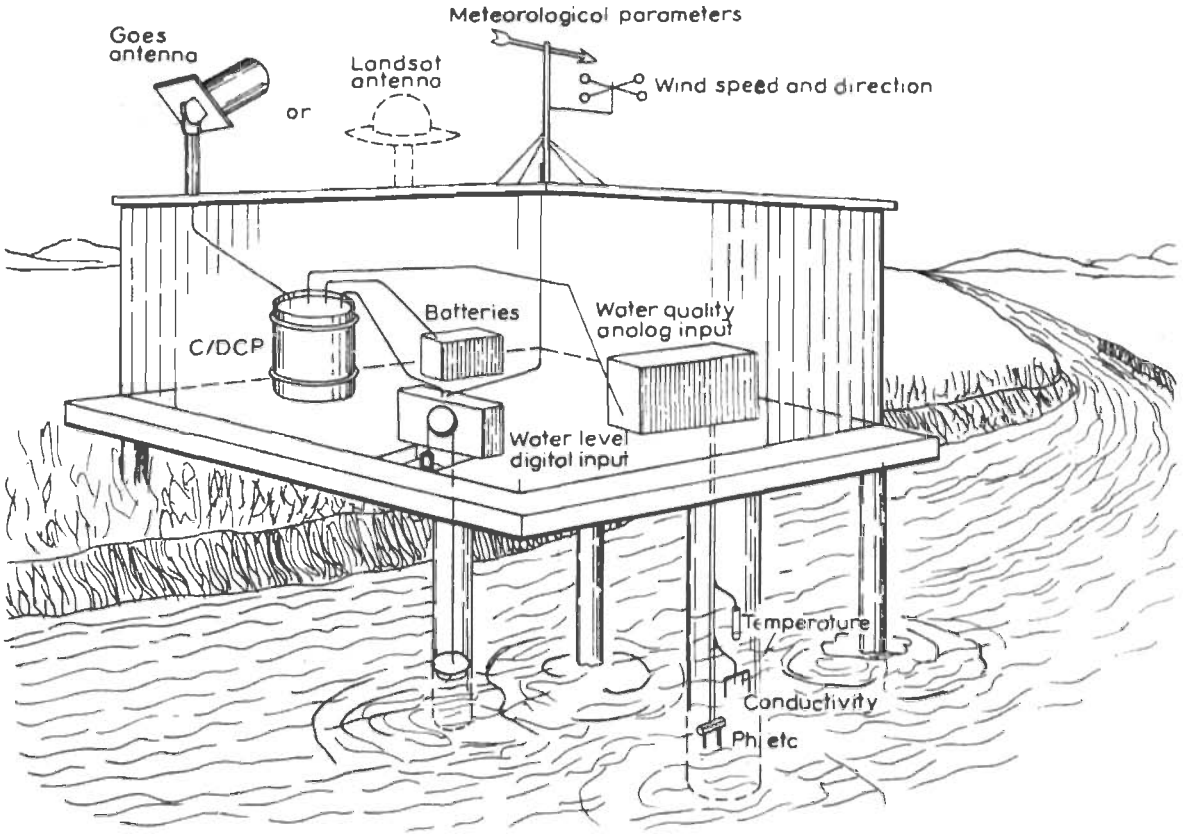

FIGURE 3 : Artist conception of major components of ERTS-GOES Data Collection Platform (C/DCP) stage monitor station. Users supply sensors, antenna mount, and shelter to protect equipment.

requirements for environmental data collection([12]). System use must conform to NESS regulations and those of the International Telecommunications Union.

Each GOES will provide a communications link, available 24 hours a day, for all DCPs within a 60 degree earth disc about the satellite's subpoint on the earth's equator. In contrast to ERTS-DCS, GOES-DCS operates in either an interrogate or self-timed mode. Present bandwidth management assigns 100 1.5-KHz channels for interrogatable DCPs and 50 3.0-KHz channels for self-timed DCPs. One hundred KHz capacity is reserved for spare channels. Because of its large UHF bandwidth allocation (400 KHz), GOES has a large data capacity.

When operating in the interrogate mode, a signal can be sent from the NESS Command and Data Acquisition Site at Wallops Island, Virginia, to GOES which retransmits it on a single interrogation channel to all DCPs. The particular DCP addressed then transmits its message. Since the interrogate message requires about 0.6 seconds to transmit, a maximum of 6,000 individual DCPs or groups of DCPs may be addressed per hour. If each DCP message requires about 15 seconds, then 240 DCPs can respond on each of the 100 channels allocated to interrogatable DCPs each hour for a total of 24,000 bits per hour.

In the self-timed mode of operation, each DCP is equipped with an accurate clock which periodically commands the DCP to transmit a message. The number of DCPs per channel is dependent upon the accuracy of the timer. Assuming a clock which is accurate within ± 30 seconds per year and a 15-second message, DCPs should be scheduled to report at minimum intervals of 45 seconds in order to avoid interference with one another's transmission. Therefore, each of the 50 GOES channels allocated to self-timed operation can handle a maximum of 80 DCP reports each hour for a total of 4,000 sites per hour.

An additional characteristic of GOES-DCS is its requirement for a moderate gain antenna which must be pointed at the satellite. Figure 4 shows the approximate azimuth and elevation of the DCP's antenna pointing at a geostationary satellite located at an arbitrary longitude at the earth's equator from various DCP locations. Note that at higher latitudes, the elevation angle approaches the horizon increasing the probability that the line-of-sight path might be blocked by local

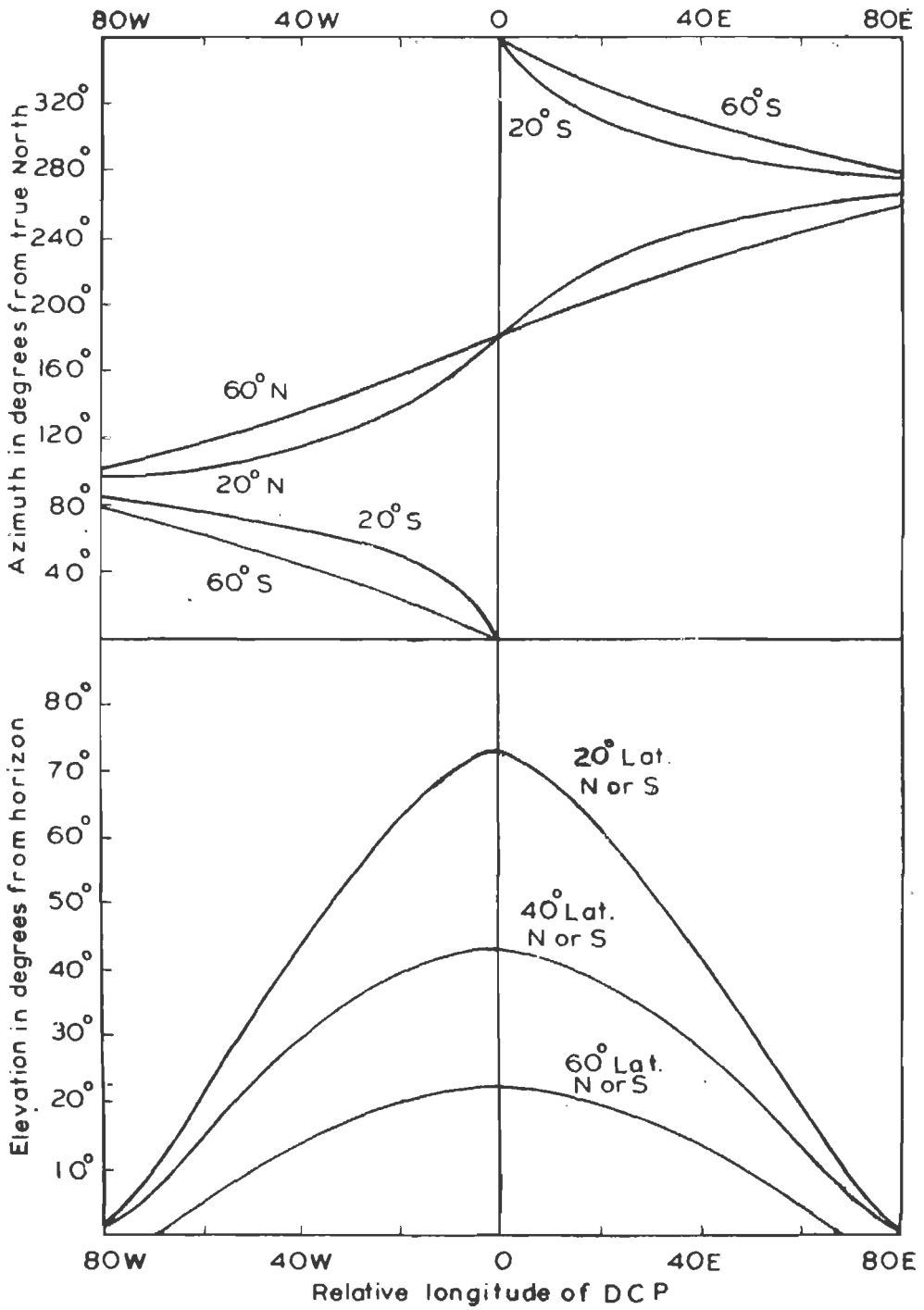

FIGURE 4 : Geostationary Satellite DCS coverage relative to satellite position. Azimuth and elevation are antenna pointing angles from given latitude and longitude of the DCP position relative to Geostationary Satellite subpoint.

topographic features. Minimum antenna elevation angle defines the maximum communication coverage of a geostationary satellite.

Data Collection System Experiments

Between 1967 and 1969, river stage and rainfall data from three stations in Arkansas, California, and Oregon were transmitted via NASA's Applications Technology Satellite (ATS-1) to NWS offices in Maryland([13]). These small-scale experiments first demonstrated the technical feasibility of using a satellite-base data collection system to transmit real-time hydrologic data as part of NWS's river and flood forecast and warning services. NWS proposed that such a system could form the basis for a national data collection system to serve the needs of water resources managers([14]).

After the launch of ERTS-1, ten moderate-scale experiments were conducted during the 1972-74 period([15]). These experiments included :

—U.S. Geological Survey, Pennsylvania—water stage, water quality data, and ground water levels from 24 sites in Pennsylvania and New Jersey reported daily to local officials.

—U.S. Geological Survey, Florida—water stage, water quality data, and meteorological data from 20 sites used by local water management agency and as an aid to interpret concurrent earth resources imagery.

—Canadian Water Survey—installed nine DCPs at widely scattered points in Canada to assist in managing water data network.

—U.S. Corps of Engineers—river flows, reservoir levels, and meteorological data collected at 25 sites in New England to provide information for operating flood control structures. Stations were integrated into the existing 41-station Automatic Hydrologic Radio Reporting Network referred to earlier in this paper.

—U.S. Geological Survey—seismic event counters and tiltmeters used to monitor volcanoes at 16 widely scattered sites including Alaska, Washington, California, Hawaii, Guatemala, Nicaragua, San, Salvador, and Iceland, which effectively demonstrated the world-wide monitoring potential of satellite data collection systems.

The experiments with ERTS-1 have generated considerable enthusiasm among the users of the DCS, particularly in those agencies which were planning extensive investments in real-time data systems. The launch of GOES in May 1974, however, presented a quandary for the potential users as to which system to use.

The solution lay in the fact that both the ERTS—and the GOES-DCP have a large number of common subsystems. The most significant differences are the antenna design and the accurate clock needed to synchronize the GOES-DCP data transmissions. Therefore, the Geological Survey sponsored the development of the ERTS-GOES Convertible Data Collection Platform (C/DCP). The GOES interrogate mode of operation was not included in C/DCPs because the GOES-DCP developed by NWS already had this feature; an interrogatable DCP costs 1.5 to 2 times as much as self-timed DCPs ; power consumption is about four times greater than the self-timed mode ; and increased complexity of the DCP increases maintenance difficulties and decreases reliability. In the process of development, many improvements were made to the original ERTS-DCP including interfacing the DCP with a 384-bit memory which permits up to six 64-bit sets of previously observed data to be stored for later transmission. The Survey, in cooperation with the U.S. Corps of Engineers, has recently purchased 180 C/DCPs to evaluate the impact of telemetry on hydrologic data program operations.

Impact of Telemetry on Hydrologic Data Program Operations

The most obvious impact of data telemetry is to make data available on a real-time or near real-time basis to users. Demand for such data services is increasing in the United States, although the magnitude of the demand and its relationship to cost is difficult to estimate. Of considerable concern to a data collection agency is the impact data telemetry might have on its own internal operations. How will a shift from providing predominantly historical data on an annual basis to providing current records on a daily or more frequent basis affect the utilization of available resources and the quality of the basic records? The analysis of impacts will proceed in four parts :

—Overview of data program operations

—Discussion of record quality and station failure rates

—Comparison work elements

—Comparison of the performance of alternative systems and costs

Overview of Operating Procedures

As part of the work associated with operating a network of gaging stations and water-quality monitors, technicians periodically visit the field sites to make sure that the station is operating satisfactorily, to perform minor maintenance on equipment, to make discharge measurements and calibrate water quality sensors, and to collect field recorded data. The frequency of gaging station visits depends primarily upon the stability of the stage-discharge relation. The more frequently the relation shifts, the more frequently discharge measurements must be made in order to maintain the accuracy of the discharge calculations which are made on the stage record. Most streams in the U.S. are gaged at

6-week intervals or about nine times per year. The frequency of visits to stage/monitor stations is controlled by the reliability of the water-quality monitor equipment. Existing equipment generally requires servicing at 10-day intervals to avoid excessive loss of record.

Usually, the technician is away from his office up to 1 week at a time, travelling from one station to another in a predetermined sequence. The travel time between stations will vary depending upon the distance and condition of the roads. In addition to periodic trips, several major maintenance trips are scheduled during the year, as well as unscheduled trips to measure flood flow. This kind of maintenance routine is called periodic maintenance.

The operation of a telemetered network is considerably more flexible because the program manager knows at any given time which stations are not operating properly and which stations are experiencing extreme events. Thus, he can schedule repair trips as the need arises and schedule discharge measurement trips to coincide more closely with the occurrence of extreme events or with periods when the stage-discharge relation is most likely to shift. This kind of maintenance routine is called service-when-failed maintenance.

Record Quality and Station Failure Rates

Errors in computed daily discharge records are attributed to three major sources:

—Loss of record or erroneous measurement owing to malfunctions of sensing of recording equipment.

—Backwater conditions caused by ice or other obstructions, either in the channel or on the station's control.

—Alterations of a stream channel's geometry caused by erosion and sedimentation.

Water-quality record errors are primarily due to sensing and recording equipment malfunctions.

The observed frequency of station failures depends upon the type of station equipment, the frequency of station visits, and the operating environment. Data based on the performance of 600 surface-water gaging stations located in several parts of the United States suggest that float-stage gages tend to fail an average of 0.6 times per year and bubble gages tend to fail about 1.2 times per year given station visits at 6-week intervals. About 70 percent of the float gage and 30 percent of the bubble gage failures are caused by malfunctions of the digital recorder or the electromechanical clock which controls the recorder. Once a station fails, the amount of record lost depends upon the length of time which passes before the next station visit. Assuming that the time to failure of the data collection system follows a negative exponential distribution function, the expected downtime of the system can be expressed as a function of the system's failure rate (number of failures per unit time) and the length of time between station visits. For example, given failure rates of 0.6 and 1.2 and a periodic inspection interval of 6 weeks, the expected loss of record would be 3.4 percent and 6.6 percent respectively [Figure 5(*a*)]. The observed loss of record for surface-water gaging stations in the United States averages about 4 percent.

Water-quality monitors, serviced at intervals of 10 days, experience failures at the rate of 15 to 30 events per year. Failure of the monitor's submersible pump accounts for about 50 percent of the malfunctions; sensor fouling or failure 25 percent; and electronics failure, 25 percent. Observed loss of record runs about 20 to 30 percent.

Under a service-when-failed maintenance policy for a telemetered data network, the loss of data at a station depends upon the number of stations in the network, the number of technicians available to service stations when they fail, the station failure rate and the technician's station service rate (the average number of stations which one technician can repair in an 8-hour day). As stations fail, the program manager dispatches technicians to the field to repair the stations. At times queues of stations develop because the technicians are unable to keep up with the workload, and data will be lost. A mathematical model, which describes this queuing problem, has been described by Panico[10]*.

The results of the queuing model suggest that one technician can operate 100 surface-water gaging stations with average record losses of less than 2 percent if he can service stations at the rate of 0.5 stations per 8-hour day [Figure 5(*b*)]. Similarly, five technicians can keep 100 water-quality monitors operating with less than 10 percent record losses if they can each service 1.0 to 1.5 stations per 8-hour day [Figure 5(*b*)]. While the technicians would need to be available for field work, they would not necessarily be in the field all the time. For example, if three technicians were assigned to operate a 100-station stream-gaging network having an average failure rate of 1.0 events per year and a service rate of 0.5 stations per day, the probability of each technician being in the field on a given day would be 0.18. Record losses under these conditions would average about 0.5 percent.

Even though telemetry will reduce record losses and the manpower required to maintain a station, field visits still have to be made to calibrate the stage-discharge relation and water-quality sensors. Unfortunately, few studies have been made of the relation between the frequency of discharge measurements used to define the stage-discharge relation and the errors of computed

* Mathematical development of the periodic maintenance model and the service-when-failed maintenance model is available from the authors upon request.

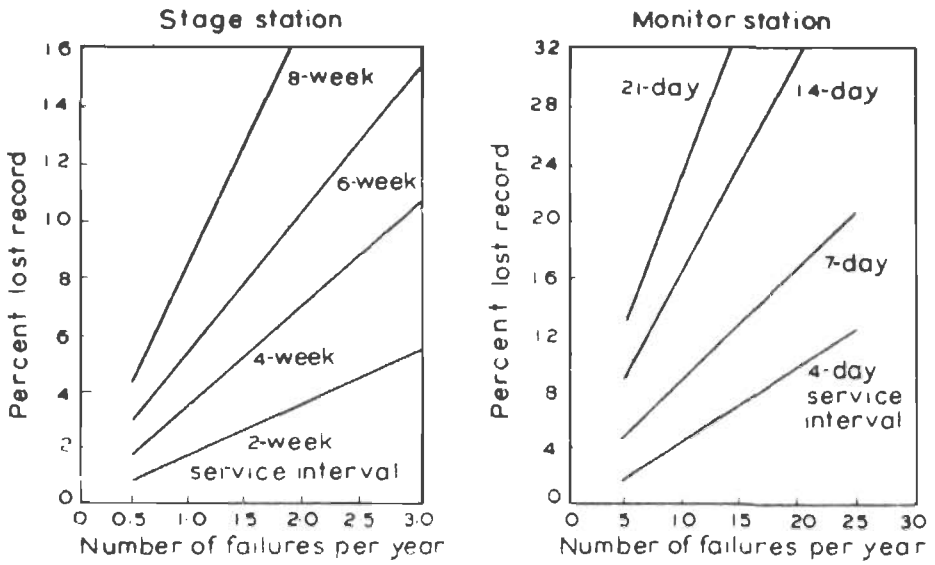

A. Record losses given for different service intervals under periodic maintenance policy

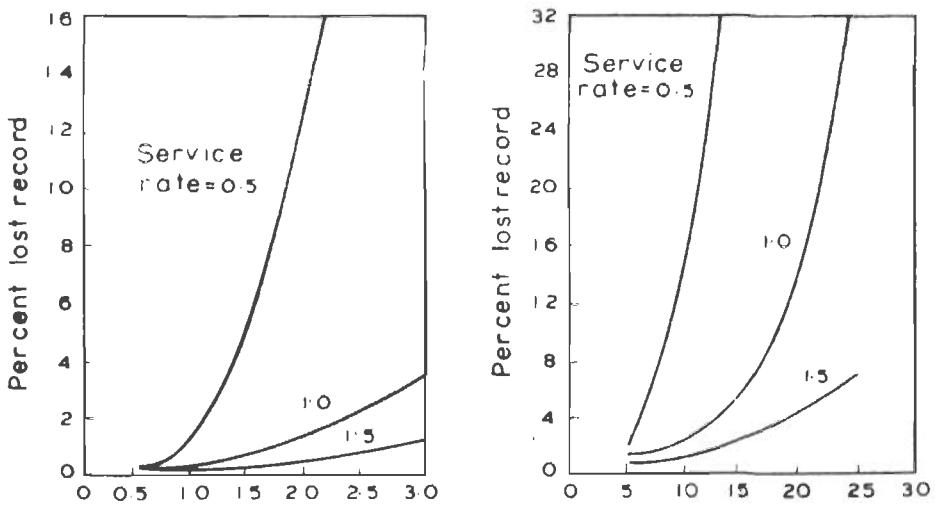

B. Record losses given for different service rates (the average number of stations which one technician can repair in an 8-hour day) assuming one technician per 100 stage stations and five technicians per 100 monitor stations are available under service-when-failed maintenance policy.

FIGURE 5 : Comparison of stage station and water-quality monitor station record losses under different maintenance policies.

discharge records. Some streams are very stable and require very few discharge measurements to maintain record accuracy. On the other hand, alluvial streams may need to be measured quite frequently to maintain a given level of accuracy[17]. Telemetry, however, permits the manager of a data collection program considerable flexibility in allocating and scheduling his manpower resources to meet network accuracy objectives. For the purpose of this analysis, it is assumed that the increased flexibility in scheduling field trips will permit the annual number of discharge measurements per station to be reduced from nine to five per year.

Work Elements

Figure 6 compares the estimated manhours spent on major work elements to operate non-telemetered and telemetered gages and stage/monitor stations. Non-telemetered time estimates are based on a survey of 40 Geological Survey districts and reflect nationwide *averages*. The telemetered time estimates are computed on the basis of assumptions about the impacts of a service-when-failed maintenance policy and the feasibility of utilizing computers to automatically screen and check data—operations previously done manually.

The stage station is assumed to fail once per year and the stage/monitor, 20 times per year. Periodic maintenance (non-telemetered operation) calls for servicing the stage station at 6-week intervals and the stage/monitor station at 10-day intervals. Nine discharge measurements are made per year. Service-when-failed maintenance (telemetered operation) assumes a reduction of discharge measurements from nine to five per year and

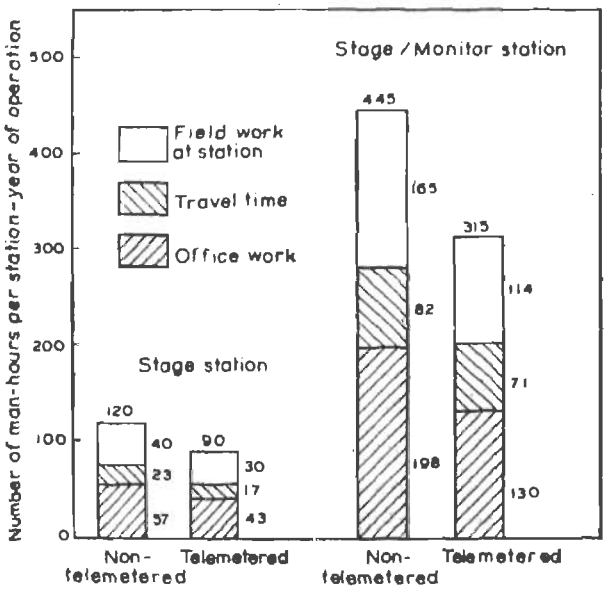

FIGURE 6 : Comparison of manhours spent on major work elements to operate non-telemetered and telemetered stage and stage/monitor stations. (See text for assumptions).

a technician service rate of one station per day. In addition, it is assumed that the use of computers will substantially reduce the office time spent checking discharge records against those of other stations.

The time required to make a scheduled field trip to and from a station averages about 2 hours per trip since a number of stations are visited over several days. The travel times in Figure 6 assume that unscheduled trips require 3 hours per trip. Telemetry reduces the total number of field trips but increases the number of unscheduled trips because of the service-when-failed maintenance policy. If the unscheduled trips take more than 3.5 hours per trip, then the travel time for the telemetered stage/monitor station would be greater than that for the non-telemetered station, and the net reduction in manhours would be less. Similarly, an improvement in the reliability of the monitor, which reduced the failure rate from 20 to 10 events per year, would reduce the total number of manhours needed to operate the non-telemetered stage/monitor from 445 to 348 hours and the telemetered station, from 315 to 267 hours. The net savings attributable to telemetry would be reduced from 130 to 81 hours.

In summary, telemetry is estimated to save on the average about 30 ± 4 manhours per year in the operation of a stage station, and about 130 ± 23 manhours per year in the operation of a stage/monitor station.

Comparison of Performance and Costs

The average annual total system costs (1975 U.S. Dollars), computed as the sum of equipment costs and the present value of 10-year operating costs (assuming an 8 percent discount rate) averaged over the 10-year period, of non-telemetered and telemetered stage and stage/monitor stations are compared for alternative systems in Table I and in Figure 7. Labor costs are assumed to range from $7.50 per hour for technicians to $12.80 per hour for engineers. Travel costs are based on $0.10 per km for vehicle operation and $25 per day for per diem. Central receive site equipment and operating costs are averaged over 100 stations for land line and line-of-sight radio systems, 500 stations for the meteor burst system, and 3,000 stations for satellite systems. The costs do not include installation of a cableway from which to make discharge measurements nor do they include administrative costs.

The costs of the leased-line system and the line-of-sight radio system are very sensitive to the geographic distribution of stations and local terrain. These systems are most suitable for small networks (less than 100 stations) with limited geographic coverage. Because of their relatively high cost, compared with the meteor burst or satellite alternatives, and their vulnerability to storm damage, both are eliminated from further consideration.

The LANDSAT/GOES appears to be the least costly of the telemetry options considered if no communication

TABLE I

Comparison of performance and costs of alternative telemetry systems.

Alternative	Annual average system cost (1974 U.S. Dollars)		Remote Station Capacity	Frequency of Reporting	Timely Accessability of other users to data	Remarks
	Stage	Stage/Monitor				
Non-telemetered	$1,620	$5,100	NA	~6 weeks	Poor	Only historical record available.
Leased-line	$2,920	$6,010	~100	Hourly or on demand	Fair	Land-lines vulnerable to storm damage.
Line-of-sight radio	$3,100	$5,720	~100	Hourly or on demand	Fair	Radio antenna towers and repeater stations vulnerable to storm and wind damage; signals subject to atmospheric interference.
Meteor burst	$2,300	$4,920	400-1,000	Hourly or on demand with up to 20-minute delay	Fair	Communication link based on natural phenomenon.
LANDSAT/ GOES	$1,860	$4,480	3,000-10,000 plus	12 hrs (LANDSAT). Hourly or on demand (GOES) at additional cost	Excellent	Possible catastrophic failure if only one satellite is used in system.
Commercial satellite (2 satellite system)	$2,530	$5,150	10,000	1.6 to 3 hrs.	Excellent	Very low risk of catastrophic failure. Performance may degrade from reporting every 3 hrs to reporting every 6 hrs should one satellite fail.

changes are levied against the users. Using this method of data-relay, a stage station would cost an average of 240 ± 30 per year *more* to operate than a non-telemetered station*. On the other hand, the stage/monitor is estimated to cost 620 ± 170 per year *less* to operate than the non-telemetered station. The meteor burst system also appears to be a viable choice for telemetry systems which will carry small amounts of data gathered from medium-sized networks (400 to 1,000 stations). It appears doubtful, however, that the system could handle the daily volume of hourly (or more frequent) observations from a network of 3,000 or more stream gages and water-quality monitors projected for the United States.

As noted above, the LANDSAT/GOES cost data do not include the cost of the satellite. This is because both the LANDSAT and GOES satellites have imagery acquisition as their primary mission with DCS as a secondary function. Thus, it is very difficult to estimate the "fair share" of DCS. Furthermore, the satellite-DCS capability already exists, and it is being under utilized.

A commercial satellite DCS consisting of two low-orbiting satellites could provide world-wide coverage at intervals of about 1.6 hours with occasional skips of 3 hours several times a day. A proposed commercial system, modelled after the LANDSAT-DCS, could have

* Uncertainty in costs reflects only that associated with labor costs.

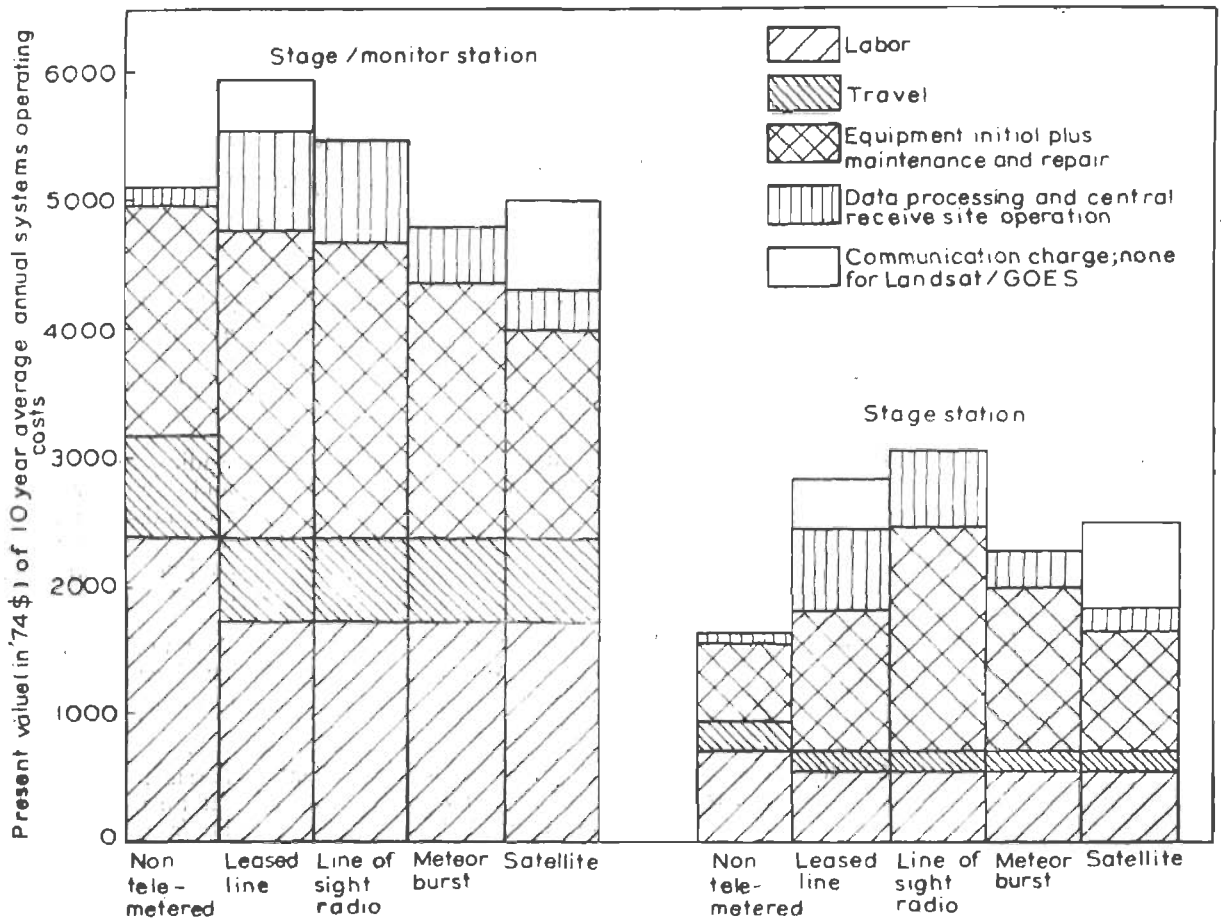

FIGURE 7 : Comparison of 10-year average annual system operating costs for stage/monitor and stage station.

TABLE II

Item	Stage station		Stage/Monitor	
	Non-telemetered	LANDSAT/GOES	Non-telemetered	LANDSAT/GOES
Average annual total cost	$1,620	$1,860	$5,100	$4,480
Average annual operating costs	$1,160	$1,150	$3,760	$3,250
Equipment costs	$4,600	$7,030	$13,400	$12,300
Annual labor (manhours)	120 hrs	90 hrs	445 hrs	315 hrs
Annual travel (kilometres)	1,100 km	820 km	3,940 km	3,500 km
Expected record loss (percent)	4%	<1%	20%	<10%
Historical record accuracy	—	Improved	—	Improved

a capacity of relaying data from up to 10,000 stations simultaneously visible to the satellite and the receive site. The same channel space may be used in many different visibility areas. Ten communications channels, each with a capacity of 1,000 stations, may lease for approximately $ 1 million per year. At full capacity, this amounts to $1,000 per station-year and would increase the 10-year present value of LANDSAT/GOES system costs by $6,700 or an average of $670 per year. If these costs are shared by users in more than one geographic area, they may be substantially reduced.

Low-cost receive sites (about $50,000 per station) are also under design as opposed to the $210,000 cost used to calculate equipment costs in Figure 7. Development of low-cost receive sites will greatly increase the utility of the data-relay system by making it economically feasible for users to directly receive data rather than waiting for it to be distributed over land lines from the data collection agency's computer facilities. In all the non-satellite telemetry options, the user would have to rely on the data collection agency to periodically distribute the data by conventional means. The average costs and impacts of using LANDSAT or GOES to relay data from a U.S. Geological Survey water stage station and from a combined stage and four-parameter water-quality monitor station network are summarized in Table II.

Conclusions

We have attempted to demonstrate the potential benefits of telemetered data to the *manager* of a hydrologic data network in terms of decreased operating costs, reduced manpower, less travel, less record loss, and improved record accuracy. Of course, the data user also benefits from having access to the water information within a few hours of its collection.

At current (1975) prices, the use of the LANDSAT/GOES system option to acquire near real-time stage data will cost about $240 more per station-year than non-telemetered station operation. However, cost of electronics equipment is rapidly decreasing. For example, the development of microwave integrated circuits and the introduction of large-scale integration of electronics components is expected to reduce the cost of LANDSAT/GOES-DCPs from $2,700 to $1,500 in quantities of 1,000 within a few years. On the other hand, the cost of labor and travel is rapidly increasing network operating costs. These trends should increase the attractiveness of investment in satellite data-relay systems in the years to come as a fundamental tool in the development of national, multinational, and global environmental monitoring and resource management systems.

References

(1) FRAZIER, A.H. and HECKLER, WILBUR: "Embudo, New Mexico, Birthplace of Systematic Stream Gaging." U.S. Geological Survey Prof. Paper 778, p. 23, 1972.

(2) FEDERAL INTERAGENCY WORK GROUP ON DESIGNATION OF STANDARDS FOR WATER DATA ACQUISITION : "Recommended Methods for Water Data Acquisition." U.S. Geological Survey, Office of Water Data Coordination, D.C., 1972.

(3) BUCHANNAN, T.J. and SOMERS, W.P. : "Stage Measurement at Gaging Stations." U.S. Geological Survey Techniques Water-Resources Inv., Book 3, Chapter A7, p. 28, 1968.

(4) ISHERWOOD, W.L.: "Digital Water-Stage Recorder" *in* MESNIER, G.N. and ISERI, K.T. : "Selected Techniques in Water Resources Investigations." U.S. Geological Survey Water-Supply Paper 1669-Z, p. 64, 1963.

(5) SMOOT, G.F. and BLAKEY, J.F. : "Systems for Monitoring and Digitally Recording Water Quality Parameters." U.S. Geological Survey Open-File Report, p. 14, 1966.

(6) SHOWEN, C.R. : "Transmission of Digital Data." U.S. Geological Survey Open-File Report, p. 13, 1971.

(7) FLANDERS, A.F. and BAKER, D.R. : "Future Developments in Network Design and Operation for River Forecasting" *in* WORLD METEOROLOGICAL ORGANIZATION : "Casebook on Hydrological Network Design Practice." WMO Publication No. 324, p. VI-1. 1-1 to VI-1. 1-4, 1972.

(8) GRAY, C.H. : "The Automatic Hydrological Radio Reporting Network." 38th Annual Western Snow Conf., Victoria, British Columbia, Proc., pp. 102-107, 1970.

(9) LEADER, R.E. : "Meteor Burst Communications." 42nd Ann. Western Snow Conf., Anchorage, Alaska, Proc., pp. 29-36, 1974.

(10) WORLD METEOROLOGICAL ORGANIZATION : "Automatic Collection and Transmission of Hydrological Observations." WMO Publication No. 337, p. 69, 1973.

(11) SWIFT, C.H. : "Radio-telemetry Network Used by the U.S. Geological Survey for Reporting Hydrologic Data in Western Washington." 39th Ann. Western Snow Conf., Billings, Montana, Proc., pp. 20-22, 1971.

(12) NATIONAL OCEANIC AND ATMOSPHERIC ADMINISTRATION : "The United States Geostationary Operational Environmental Satellite Data Collection System." Federal Register, October 14, 1972.

(13) FLANDERS, A.F. ; KOHL, F.V. and DAVIS, T.W. : "Hydrologic Communications Experiment on the Applications Technology Satellite (ATS-1)." Internat. Symp. on Remote Sensing of Environment, Ann Arbor, Michigan, Proc., V. 1, pp. 197-204, 1969.

(14) FLANDERS, A.F. and SCHIESL, J.W.: "Hydrologic Data Collection via Geostationary Satellite." IEEE Trans. Geoscience Electronics, V. GE-10, No. 1, pp. 47-51, 1972.

(15) NATIONAL AERONAUTICS AND SPACE ADMINISTRATION : "Earth Resources Technology Satellite-1 Data Collection System Workshop." NASA, Wallops Island, Va., Proc., 1973.

(16) PANICO, J.A. : "Queuing Theory." Englewoods Cliffs, N.J., Prentice Hall, p. 200, 1969.

(17) BURKHAM, D.E. and DAWDY, D.R. : "Error Analysis of Streamflow Data for an Alluvial Stream." U.S. Geological Survey Prof. Paper 655-C, p. 13, 1970.

Remote Sensing in Hydrogeological Mapping

(WITH SPECIAL RESPECT TO INDIA AND CANADA)*

G. OZORAY
Research Officer
Alberta Research, Edmonton, Alberta, Canada.

SYNOPSIS

The remote sensing techniques most suitable for hydrogeological mapping are reflected light (both visible and infrared) and thermal imaging from aircraft and spacecraft. (Conventional air photography is excluded from the present paper). Examples of application are mostly drawn from Southern India and Alberta, Canada.

Large, scale imagery may be used for solving local problems and carrying out detailed investigation. Thermal images show ground water discharge forms, such as diffuse discharge (linear or areal seepages) or submerged springs, which are not often visible on conventional air photographs ; differences in moisture content of soil or rock outcrops are also discernible. Obtaining large-scale imagery is costly, mainly special projects may afford its use.

Regional hydrogeological mapping can use small-scale images, representing extensive areas, taken from spacecraft (being either conventional photographs or scanner images), available at nominal cost.

The best source of space imagery for hydrogeological mapping purposes is the first Earth Resources Technology Satellite (ERTS-1) which has a polar orbit and repeats its observations every 18 days. ERTS-1 has a Multispectral Scanner System which images in the green, red, near-and far-reflected infrared spectral bands.

Phenomena useful for hydrogeological mapping and discernible from space imagery are: general topography and hydrography; surface geology, including the extent of surficial aquifers ; surface expressions of tectonic and atectonic structure ; morphology which often controls special ground water phenomena ; fine texture of local orography usually not shown on topographic maps; vegetation and soil types; distribution of marshlands.

Use of images of the same area taken in different seasons and application of color-enhancement can facilitate better interpretation.

Remote sensing interpretation must be checked on the ground (ground truth).

Introduction

The purpose of this paper is to investigate the use and applicability of remote sensing in hydrogeologic mapping through theoretical considerations and case histories. Examples of application are drawn preferably from India and Canada because during recent years the author has worked in these countries.

Remote sensing is defined by Gregory[1] (p. 33) as "the aerospace practices of surveying the ultraviolet, visible, infrared and microwave radiations emitted and

* Alberta Research Contribution No. 706.

reflected from the surface of the Earth."

A hydrogeological map by my definition "represents ground water conditions in their geological context"([2]), (p. I-*a* 2); see also discussion by and reply to M. Bardhan:([2]), (p. 2-12-13). The expression "hydrogeological mapping" is used in the present paper in its broadest meaning and includes the process of observation and testing of relevant phenomena, collection, evaluation, interpretation of data, and actual construction of maps.

The application of remote sensing is manifold and quite inter-disciplinary. For example, far removed sensors can delineate the light reflection and heat emission properties of the vegetation which are related to soil moisture([3]). Such applications are not only useful in many ways, but also eyecatching([4]). Connections with such fast developing technologies are telecommunication or spacetravel gave remote sensing a "modern" and "miraculous" appearance in the eyes of the general and professional public. Moreover, because of its inter and multi-disciplinary character, remote sensing is an ideal tool for environmental observations—whatever that broad but shapeless concept may cover. There was, for instance, a whole series of symposiums on the "Remote Sensing of Environment" (see Ref. 3). The word "environment" and its derivates are quite in fashion now-a-days—they used to be a fad in the near past. The popularity of remote sensing was enhanced (for better or worse) by its name being connected with that of the environment, because our thoughts are shaped to a great extent by the words we express them as it is so lucidly elaborated by Orwell in the "Nineteen Eighty-four"([5]).

Although there is an exaggerated anticipation towards remote sensing and it is over-valued, it has already proved to be very useful in the earth, water and atmospheric sciences and its further application for those fields (including hydrogeology) is promising. Usually qualitive areal differences or the areal distribution of some phenomena are remotely sensed. For that reason, hydrogeological mapping can most obviously gain from the use of remote sensing, because it is an operation directed towards an areal perception of phenomena.

The remote sensing techniques suitable for hydrogeological mapping are visible and infrared reflected light and thermal imaging from aircraft and spacecraft. For practicality's sake, conventional visible light air photography is excluded from the present paper except when it is complimentary to remote sensing operations.

The Author's interest was first drawn to the topic in 1967 when a space photograph proved to be useful in solving a hydrogeological mapping problem([6])([7]) in the Cauvery Delta (Tamil Nadu, India).

Since 1968 the author has worked on the reconnaissance hydrogeological mapping of the Province of Alberta, Canada. The area of the province([8]) (p. 41) is 255,285 sq miles (660,902 km^2). It includes extensive unpopulated and roadless areas and some parts of it are as yet not covered by high quality topographic maps. The available ground water and geological data are unequal in quality and unevenly distributed. Remote sensing offers ways to supplement areal reconnaissance.

Airborne reflected infrared and thermal sensing methods were successfully used in several cases in Alberta and in other parts of Canada to solve local hydrogeological problems, partly by directly observing elements of the ground water regime, i.e., discharge features.

For reconnaissance hydrogeological mapping of extensive areas the small scale remote sensing of relevant elements of the hydrogeological environment especially the use of ERTS-1 Satellite Scanner images seems to be most helpful. Although geologic structure as reflected on the surface by lineaments is one of such observable elements of the hydrogeologic environment([9]), in this paper the non-structural applications of the ERTS-images are emphasized because the author's observations regarding the morphotectonic analysis of ERTS-1 images in Alberta are included in another IWRA publication([10]).

Application of Large-Scale (Airborne) Imagery

To solve local problems and carry out detailed investigations large-scale imagery with sufficient ground resolution is required. The actual scale is project-dependent: it can be as small as 1:50,000 for an extensive mapping operation or as big as 1:1,000 for an engineering survey. Large-scale imagery is obtained by airborne sensing.

Aerial photography is extended from the visible to the infrared spectrum, the latter being applied either in black and white or in false colour. The different light bands can be applied separately (by use of special filters) and can be recombined into desired combinations. Infrared light penetrates foggy, unclear and dusty air better than visible light: the longer wave length minimizes the obstacle caused by small suspended particles.

In addition to visible and reflected infrared photography (and preferably applied together with them) thermal sensing is a promising tool in hydrogeological investigations. Thermal sensing measures the infrared radiation of wave lengths longer than 3.5 microns, especially in the ranges of the 3.5-5.5 and 8-14 microns so called "atmospheric windows" for which atmosphere is transparent([11]) (p. 251). Thermal imagery, therefore, shows the temperature of the surface. For interpretation many factors must be taken into account, such as time of the day, season of the year, weather, vegetation, uneven surface, human activity and so on. Images of the same area, taken at different times of the day, for instance after sunrise and after sunset, can be helpful.

Distribution of water is one factor responsible for differences in surface temperature. Therefore, careful interpretation of thermal images can delineate areas of dry and wet soil (rocks) and open water bodies, locate

discharge features such as springs or seepages, including areas (lines, zones, patches) of diffuse or hidden discharge. Salts also have peculiar thermal properties. therefore, areas of salt precipitation may also be located on thermal images. Among recharge features swallow-holes may be spotted by thermal methods. Micro- or meso-tectonic lines show up on thermal images as lines of soil moisture difference.

The hydrogeological interpretation of large-scale (airborne) remote sensing images consequently may be based on observation of :

(*a*) elements of the ground water regime (such as springs, seepages, swallowholes) ;

(*b*) alterations caused by ground water (such as salt precipitates, alkaline patches, spring cones, sinkholes) ;

(*c*) surface waters ;

(*d*) elements of hydrogeologic environment (such as geology, structure, morphology, topography).

Infrared remote sensing (both reflected infrared light and thermal images) offers solution to a great variety of scientific and practical water-related problems: hydrogeological, surface-geological or geomorphological mapping, surface analysis ; engineering geological analysis ; land use planning ; ground water prospecting ; check on infiltration losses and efficiency of water-transport systems (canals, pipelines); detection of thermal water or hidden (submerged, ice-covered) springs, and so on. Some Canadian examples are :

In the Maligne karst system of the Rocky Mountains, Alberta, investigated by Brown[12], the discharge point of a karst polje was unknown. Thermal scanner images (8-14 microns wave length) indicated, that the water disappearing in the polje was reappearing as a submerged spring under the surface of the Medicine Lake.

There was a catastrophic landslide at St-Jean-Vianney, Quebec, in 1971. It was urgently needed to determine whether the slide could extend further. A combined thermal, reflected infrared, visible light remote sensing and air-photo survey was carried out to locate seepage zones, wet soils and other unstable places and also to direct drilling operations and detailed engineering geological (soil-mechanics) studies. As evaluated by Tanguay and Chagnon[13] the remote sensing operation was successful. It was possible to determine the weak spots very quickly and take immediate practical measures.

An operation was carried out in 1969 by Holmes and Thompson [11] to assess the value of infrared sensing in Quaternary research. Among other features, lines of diffuse ground water discharge were located along some of the coulee-s (deep ravines) on thermal images of the Lake Pakowki Area, Alberta.

In 1967 a combined thermal, reflected infrared and visible light study was carried out at Granum, Alberta to evaluate the usefulness of remote sensing in ground water exploration in the prairie (grassland) environment. One of the aims was to determine seepage along irrigation canals. It was concluded by E. Chase[14] that the technique was promising but a better ground check would have been needed.

These examples show that large-scale remote sensing has been used recently in hydrogeology, mainly to solve special problems. In hydrogeological mapping its use is presently either experimental or is aimed at problem-oriented "project-maps" (such as a map of water-saturated, landslide-prone weak spots of a limited study area).

Detailed regional hydrogeological mapping could profit from the use of airborne remote sensing methods. Unfortunately, it cannot afford it. Remote sensing is costly (and the present tendency of prices does not promise much for the near future), as it has to be specially ordered. It, therefore, depends on the financial standing of the mapping operation, whether and to what extent remote sensing can be applied.

Application of Small-Scale (Space) Imagery

Pros and Contras of Space Imagery Application

Regional hydrogeological mapping, especially on the reconnaissance level, however, can make excellent use of small-scale images representing extensive areas. Pictures taken from spacecrafts, being either conventional photographs[15] or scanner images, can be suitable for such mapping. These pictures are available at nominal cost as they are byproducts of other programs such as space research, instrumentation experiment, meteorological or earth resource observation, etc. In 1974 a black and white (single band) negative ERTS-1 scanner image cost only $3.00 and a combined false colour transparency $5.00. Another advantage is that space images cover extensive areas and the use of photo-mosaics can be avoided. Even the best photo-mosaic displays confusing variations of contrast between individual shots due to the time lapse between exposures.

On the other hand, space images are not tailor made for our purposes, the sensing methodology is not directed towards observation of ground water connected phenomena. We have to make the best use of what there is by assessing secondary phenomena, deducing from slight indications and analogues, applying enhancement techniques and a good deal of imagination. An overdose of imagination should be counter-balanced by obtaining every possible bit of "ground truth", verification from conventional airphotos, existing maps, helicopter, ground vehicle and foot field trips, drilling and sampling operations, etc.

Space observations by their very nature are of a small-scale and even the best enhancement technique cannot overcome this basic fact. To make the best of it we have to concentrate on the extensive, the linear, the naturally enhanced, the sharply contrasting, and the

repeating phenomena. A narrow, linear feature such as a river or a highway may show up well on a small-scale image even if its narrowest diameter is just a fraction of a scanning point. Shadow, wetness and vegetation are the best natural enhancers. Shadows emphasize the slopes and especially the escarpments. An oblique view and a low sun angle may stress shadow enhancement even more. The presence of snow is usually a disadvantage; however, it can be an enhancing factor, too, when it is swept into the shallow gullies or when it covers only the higher ground. For example the structural analysis of Western Canada and Alaska by Lathram[16] is based on a Nimbus IV meteorological satellite scanner image taken at a low sun angle when snow enhanced differences in elevation. Vegetation change or human operations (agriculture) may result in sharp contrast on the space imagery. Repeating patterns are easier to notice, recognize and evaluate than a single small object. In addition to this, repeating patterns (for example drumlins, sinkholes, dunes) may result in a characteristic image texture even if the individual features are too small to be discernible themselves. Examples of these type will be given later.

A True Colour Photo Application in India

The first spacecrafts had more or less equatorial trajectories or orbits. It is understandable that the first hydrogeological use of a space photo (was in 1967, by the author of this paper) concerned a tropical area : Tamil Nadu, India[6][7]. The problem was one of mapping type : namely the distinction of alluvial plains from the hydrogeologically different laterite plateau in and around the Cauvery Delta area. Suitable air photos were not available, the topographical maps did not show minute morphological differences clearly, and deluvial phenomena obscured the elevation differences. The mentioned formations were successfully recognized and delineated on a true colour space photo[17][18], (p. 130) on the basis of colour difference.

ERTS-1 Imagery

Presently the best source of space imagery for hydrogeological mapping purposes is the first Earth Resources Technology Satellite (ERTS-1)[19]. It has a polar orbit (therefore, covers the entire planet systematically) and repeats its observations every 18 days[20]. The altitude of the orbit varies between 490-510 nautical miles (about 907-945 km). The presently operational Multispectral Scanner System (MSS) images in the following four spectral bands (wave lengths in microns given in brackets):

band 4	: green	(0.5-0.6)
band 5	: red	(0.6-0.7)
band 6	: reflected infrared	(0.7-0.8)
band 7	: reflected infrared	(0.8-1.1)

The field view of the scanner is 230 ft (70.1 m) in diameter.

The Canadian data are received by the Prince Albert Satellite Station (Saskatchewan), recorded on magnetic tape and later, in Ottawa, made into film negatives. One image represents an area of a 100 nautical miles (185.2 km) square (10,000 sq nautical miles=34,299 km^2), about two and one half to three times larger than the two-square geographical degree area represented by a 1: 250,000 topographical or hydrogeological map in Alberta.

During reconnaissance hydrogeological mapping of Alberta, 1:1,000,000 scale ERTS images were used as a base for the interpretative work. They are available both in negatives and positives, either as separate spectral band images (black and white paper prints or transparencies) or as MSS False Colour Composites (colour paper prints or colour transparencies).

Among black and white paper prints the infrared bands 6 and 7 images were the most suitable for interpretation. Bands 4 (green) and 5 (red) tend to be hazy.

Colour composite positive transparencies show finer details because shades of colour enhance small differences in type and water content of soil, and also in vegetation and elevation. It is unfortunate that ERTS image coverage is available in colour composite transparency only for some parts of Alberta.

Corroboration and Enhancement

Nearly always part of the image is cloud covered or unclear for other reasons. In these cases different images covering the same area may be used to corroborate the incomplete image. Images taken at a different sun angle emphasize different details. Also, use of images of the same area taken in different seasons of the year can facilitate better interpretation.

In the above mentioned Alberta program, where ERTS-1 colour transparencies were not available, additive colour enhancement was applied based on black and white transparencies of different spectral band images of the area. The method was similar to those described by Lent[21]. From the original positive transparencies half tone filtered negative, black and white transparencies were produced photographically. The half tone filtering made the details more plastic and brought out fine shades.

From the photo negatives, single colour transparencies were produced (either positive or negative) by the inexpensive Diazo technique. The different colour transparencies representing (by arbitrary false colours) different original spectral bands were laid over each other and taped together. The resulting colour composites effectively enhanced small details.

Using different kinds of colour combinations, different details can be enhanced or suppressed. For instance, a red negative overlay of band 7 and a negative blue of band 6, when combined, result in a good enhancement (in shades of violet colour) of ground details. The shortcoming is that small puffs of clouds can be mistaken for small lakes. A combination of red positive with

blue and yellow negatives of different bands effectively separates water surfaces (lakes, rivers), seen as red, from clouds, seen as green. This combination also separates vegetation types.

Discernible Phenomena

The essential phenomena useful for hydrogeological mapping and discernible on satellite images are treated below. (It must be kept in mind that direct ground water features usually cannot be recognized on small-scale images).

(*a*) General topography and hydrography (where suitable topographic maps are not available);

(*b*) surface geology, including the presence and extent of surface aquifers (as in the case of the above mentioned Indian application) ;

(*c*) surface expression of tectonic and atectonic structures;

(*d*) morphology which often controls special ground water phenomena (such as inactive drainage channels, pitted ground moraines, badlands, karst plateaus);

(*e*) fine texture of local orography usually not shown on topographic maps (such as in areas of glacial fluting or dune fields);

(*f*) distribution of muskegs and other types of marshland.

Examples from Alberta

The two attached space image details (Figures 1 and 3) are used as examples for the above discussed phenomena, each of them representing 5,790 sq miles (15,000 km²). Figure 2 is an interpretative sketch to Figure 1; Figure 4 is to Figure 3. Description is given in the text. The reference points are marked on the interpretative sketches by capital letters, from *A* to *K* on Figure 2, from *L* to *R* on Figure 4 ; but, of course, the relevant point of the space image (Figure 1 or 3, respectively) must be consulted.

Figure 1 is part of a black and white band 7 (infrared) ERTS-1 image (E-1414-17543-7) taken on September 10, 1973. Orientation and geographic location is given by the latitude and longitude network. The area lies in east-central Alberta (its eastern margin, east from the 110° western longitude falls within the Province of Saskatchewan). Most of the area is covered by the NTS (Canadian National Topographic System) 73L (Sand River) topographic map. The NTS 73L map area has recently been hydrogeologically mapped[22]. Only a part of the area is settled and cultivated : the farm lands show up on the image as a quilt of rectangular light and dark patches. The remaining part is mainly tayga or park type forest ; muskeg (marshland) and lake. Topography is hilly or rolling plains with small difference in elevation, between 1,700 and 2,100 ft (about 520-640 m).

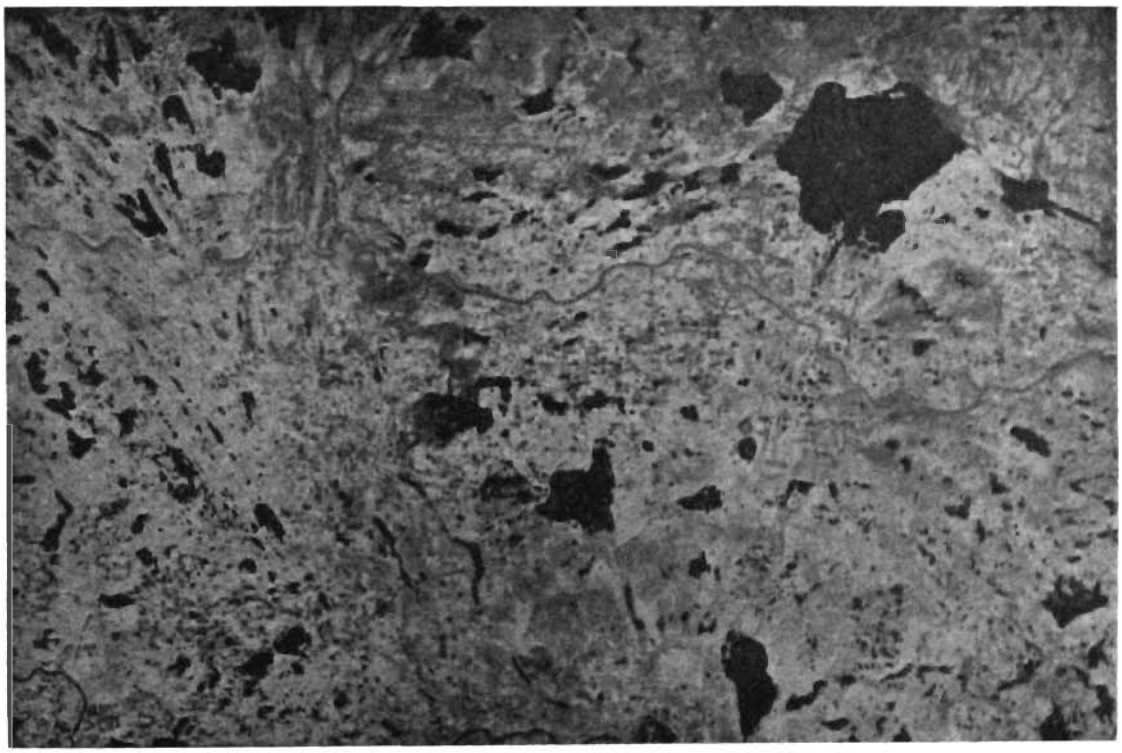

FIGURE 1 : ERTS-1 Image of the Beaver River—Sand River area; Band 7 reflected infrared (0.8—1.1 microns).

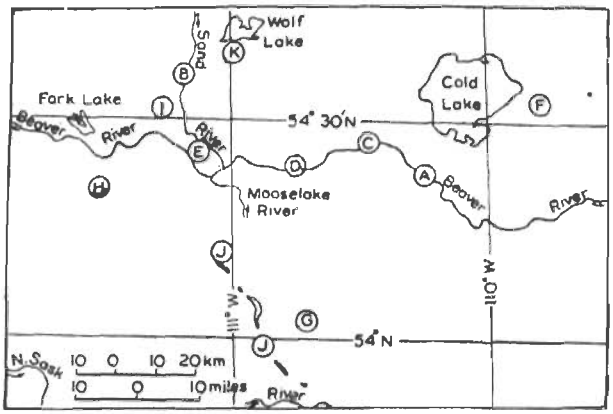

FIGURE 2 : Interpretative sketch to Figure 1.

The general topography and hydrography is well discernible on the image. It gives a good overview of the area which is useful, though the relevant topographic maps (both in 1 : 250,000 and 1 : 50,000 scale) are quite good. Note, that even such details as actual channel meanders on the bottom of rather narrow, non-meandering valleys are clearly visible (*A* : Beaver River; *B* : Sand River). Shadows enhance slopes and escarpments such that there is a conception of the third dimension (e.g., at the cut of the valley at *A*).

One of the important surface aquifers in the area is the sand and gravel accumulation along the Beaver River. At *C* and *D* locations, on the right (southern) bank of the river the terraces are extraordinarily wide and massive. After checking on conventional air photos and field visits (by helicopter and car) at *D* a test hole was drilled and a thick sand and gravel sequence was found with positive artesian ground water conditions. [The topic of ground water prospecting in Canada, via, ERTS image applications is elaborated by Mollard and Carr([19])].

Morphotectonic features are visible at the confluence area of the Beaver, Sand and Mooselake (the right tributary) Rivers (*E*). That area has a fluted (groove and ridge morphology) surface. However, the rivers do not follow the roughly N-S direction of the glacial grooves. The rivers from NW-SE and SW-NE reaches. NW-SE and NE-SW are main morphotectonic direction in Alberta([23])([24]). A NW-SE morphotectonic line is also discernible at *F* by several lakes and a river. The roughly E-W ravines, on the left side of the Sand River upstream from *B* are also supposed to be structurally controlled.

Morphology often controls special ground water phenomena. "Hummocky moraine", an icy disintegration phenomenon([2,3]), is characterized by small round mounds and small depressions often containing lakes, ponds or "sloughs" (marshes). Local ground water

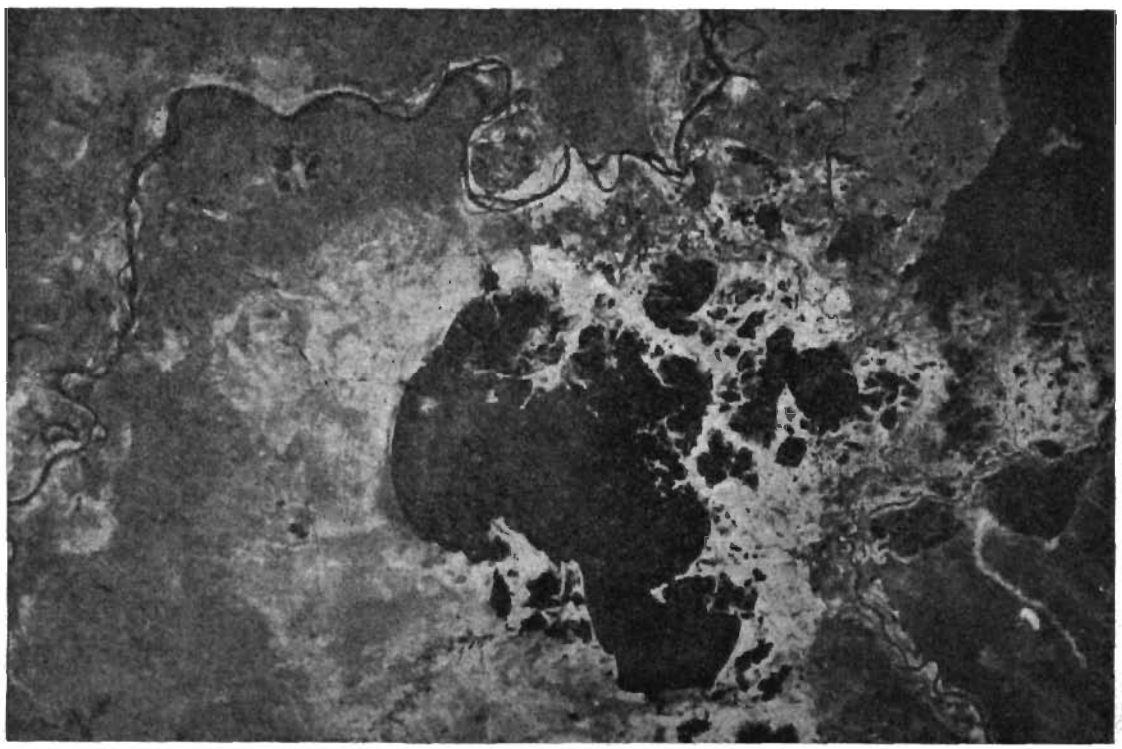

FIGURE 3 : ERTS-1 Image of the Athabasca Delta area; Band 6 reflected infrared (0.7—0.8 microns).

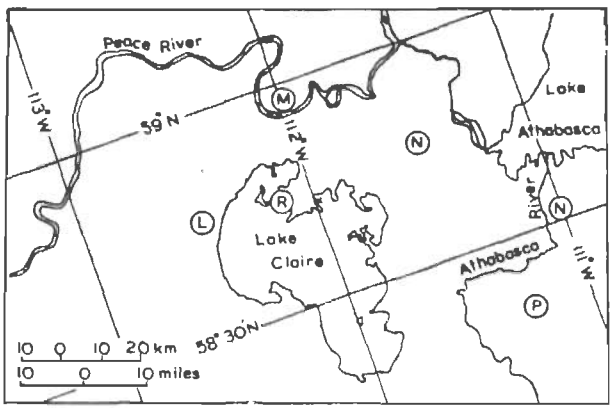

FIGURE 4 : Interpretative sketch to Figure 3.

flow systems tend to be short, the hydrogeological picture seems to fall into fragments like a mosaic. The hydrogeology of hummocky moraines was studied by Meyboom[20]. On the satellite-image an extensive hummocky moraine field (verified by ground check) is represented at *G* by a "pepper and salt" appearance caused by alterating very fine lighter and darker dots. This is a good example of the detection of an area of repeating features, although the individual features are too small to be discernible. Glacial flutings, long narrow grooves or furrows separated by elongated ridges are also widespread in Alberta[27]. They are elongate in the direction of ice-movement during the last (Wisconsin, about equivalent to the European Würm) glaciation, tends to fragment local ground water flow systems. Flutings may be individually too small (though numerous) to be represented on topographic maps. Two big fluting systems can be recognized on the ERTS-image, at *H* and *I*. The two arched systems are fused together at the Fork Lake.

Inactive valleys and more or less buried channels are important ground water flow controlling elements. A clearly discernible inactive valley is marked by *J* at two points ; the Mooselake River flows along its northern extension.

The Wolf Lake on the north-central margin of the area is shaped by NE-SW directed esker-type glacial accumulation ridges (*K*). Eskers are ridges of porous material (sand and gravel), consequently they are important recharge areas.

Figure 3 is part of a black and white band 6 (infrared) ERTS-1 image (E-1345-18113-6) taken on July 3, 1973. The figure is not orientated towards north but the cardinal directions are clear from the latitude and longitude network (Figure 4). The area lies in north-east Alberta and includes the gigantic inland delta usually referred to as the Athabasca Delta. The area is uncultivated, practically unpopulated and is covered by tayga-forest, lakes, and muskeg (peat-bog, boreal marshland). It abounds in interesting natural features.

L denotes the center of a 60 miles (100 km) long arched zone of repeated fossil beach-ridges[10] mapped by Bayrock[28]. Beach ridges are good recharge areas.

M denotes another repeating morphological feature: a series of oxbows and levees of a giant meander migrating towards a structurally fixed position. *N* marks two points within the inland delta system.

Delicately branching rivers build finely structured delta-complexes into the quiet Lake Claire (*R*). The shade-difference between the more sandy and tree-covered levees and the more silty, bush, sedge and reed covered lower wetlands is noteworthy.

By colour enhancement the main types of vegetation can be differentiated. The muskeg-covered broad valley at *P* is discernible even on the black and white image.

Conclusions

Remote sensing is a useful tool in hydrogeological mapping. Detailed hydrogeological mapping could make excellent use of large-scale (airborne) remote sensing, preferably a combination of photographic (including infrared) and thermal methods. At the present time airborne remote sensing is applied mainly in connection with special hydrogeological problems and "project" maps because of the high costs involved, however, extension of the method to routine mapping would be desirable.

Small-scale (space) images are inexpensive and they are applicable in many ways to small-scale (reconnaissance) hydrogeological mapping. Colour true photographs (in India) and scanner images (in Alberta, Canada) were successfully applied in determination of the extent of surface aquifers and in structural analysis. There are further possibilities of extension of the field of application to analyse: general topography and hydrography in absence of suitable topographic maps; morphology which often controls special ground water phenomena; fine texture of orography not shown on topographic maps ; vegetation and soil types ; distribution of marshlands.

Use of images of the same area taken in different seasons and application of colour enhancement can facilitate better interpretation.

Verification and checking of remote sensing interpretation on the ground (obtaining ground truth) is very important. Without ground check (in a broad sense, including helicopter survey) more harm can be done than profit gained.

Acknowledgments

For the space imagery used, credit is due to NASA, for operating the ERTS-1 and thus making the original observations; and to the Canadian Centre of Remote Sensing and the National Air Photo Library, Ottawa, for recording, reproducing and distributing the imagery in Canada.

During the entire project assistance was given by A.T. Lytviak. The manuscript was critically read by R. Barnes, Dr. D. Borneuf and R. Stein. Drafting work was done by D. Keeling. The manuscript was typed by Mrs. B.M. Stemp. The author gratefully acknowledges their help.

References

(1) GREGORY, A.F. : "What Do We Mean by Remote Sensing?" First Canadian Remote Sensing Symposium, Ottawa, February 1972, Vol. 1, pp. 33-37.

(2) OZORAY, G.: "Ground Water Mapping: a Prerequisite of Successful Ground Water Resource Estimation and Management." International Symposium on Develpoment of Ground Water Resources, Madras, November 1973, Vol. 1, pp. I-a. 1-8; Discussions : Vol. 4, pp. 2-6—15.

(3) MYERS, V.I. ; WIEGAND, C.L. ; HEILMAN, M.D. and THOMAS, J.R. : "Remote Sensing in Soil and Water Conservation Research." Fourth Symposium on Remote Sensing of Environment, Ann Arbor, Michigan, April 1966, Revised Edition, pp. 801-813.

(4) WEAVER, K.F. : "Remote Sensing : New Eyes to See the World." National Geographic, Vol. 135, No. 1, January 1969, pp. 46-73.

(5) ORWELL, G. : "Nineteen Eighty-four." Republished by Penguin, 1969, 251 pages.

(6) OZORAY, G. : "Final Report, 1966-67 (on the Hydrogeology of the Cauvery Delta Area, India)." Manuscript, United Nations, June 8, 1967, 44 pages.

(7) OZORAY, G. : "The First Hydrogeological Application of a Space Photograph, Tamil Nadu, India, 1967." International Symposium on Development of Ground Water Resources, Madras, November 1973, Vol. 1, pp. I-a. 9-11; Discussions : Vol. 4, pp. 2-15—16.

(8) RALSTON, E., ed. : "Canada Year Book 1973." Information Canada, Ottawa, 1973, 951 pages.

(9) OZORAY, G.: "Tectonic Structure as a Hydrogeologic Factor." Seminar on Problems in Ground Water Development, Madras, October 1972, pp. 155-158.

(10) OZORAY, G. : "Lineament Analysis Using ERTS-1 Images of Alberta." International Water Resources Association, International Seminar and Exposition on Water Resources Instrumentation, Chicago, June 1974, in press.

(11) HOLMES, R.M. and THOMPSON, D. : "Infrared Remote Sensing in Quarternary Research." Geoexploration, Amsterdam, Vol. 11, 1973, pp. 249-267.

(12) BROWN, M.C. : "Karst Hydrogeology and Infrared Imagery: an Example." Geological Society of America Bulletin, Vol. 83, October 1972, pp. 3151-3154.

(13) TANGUAY, M.G. and CHAGNON, J.Y. : "Thermal Infrared Imagery at the St-Jean-Vianney Landslide." First Canadian Symposium on Remote Sensing, Ottawa, February 1972, Vol. 2, pp. 387-402.

(14) CHASE, E.M. : "Ground Water Exploration and Evaluation by Infrared Remote Sensing, Granum East." Alberta Department of Agriculture, Edmonton, 1968, 73 pages.

(15) LOWMAN, P.D., J.R. and TIEDEMANN, H.A. : "Terrain Photography from Gemini Spacecraft : Final Geologic Report." Goddard Space Flight Center, Greenbelt, Maryland, X-644-71-15, January 1971, 75 pages.

(16) LATHRAM, E.H. : "Nimbus IV View of the Major Structural Features of Alaska." Science, Vol. 175, No. 4029, 31 March 1972, pp. 1423-1427.

(17) GORDON, R. : "Astronaut's View of India." Span, New Delhi, December 1966.

(18) NASA: "Earth Photographs from Gemini VI through XII." National Aeronautics and Space Administration, Washington, D.C., 327 pages.

(19) MOLLARD, J.D. and CARR, P.A. : "Applications of the ERTS-1 Satellite in Remote Sensing of Water Resources Data in Canada." Cospar XVIth Plenary Meeting, Symposium on Approaches to Earth Survey Problems through the Use of Space Techniques, Session 4, May-June 1973, Konstanz, Germany.

(20) CANADIAN CENTRE FOR REMOTE SENSING : "The ERTS System." CCRS Newsletter, CCRS Remote Sensing Office, Calgary, No. 1, February 1973, pp. 1-4.

(21) LENT, J.D. : "Additive-Color Image Enhancement-Techniques and Equipment." In COLWELL, R.N., Monitoring Earth Resources from Aircraft and Spacecraft, National Aeronautics and Space Administration, Washington, D.C., NASA SP-275, 1971, pp. 9-14.

(22) OZORAY, G. and LYTVIAK, A.T. : "Hydrogeology of the Sand River Area, Alberta." Alberta Research Report and 1 : 250,000 Hydrogeological Map, Edmonton, to be published.

(23) OZORAY, G. : "Structural Control of Morphology in Alberta." The Albertan Geographer, Edmonton, No. 8, 1972, pp. 35-42.

(24) OZORAY, G.: "Tectonic Control of Morphology on the Canadian Interior Plains." Twentysecond International Geographical Congress, Montreal 1972, International Geography, Vol. 1, pp. 51-54.

(25) GRAVENOR, C.P. and KUPSCH, W.O. : "Ice-disintegration Features in Western Canada." The Journal of Geology, Vol. 67, No. 1, January 1959, pp. 48-64.

(26) MEYBOOM, P. : "Mass-transfer Studies to Determine the Ground Water Regime of Permanent Lakes in Western Canada." Journal of Hydrology, Vol. 5, 1967, pp. 117-142.

(27) GRAVENOR, C.P. and MENELEY, W.A. : "Glacial Flutings in Central and Northern Alberta." American Journal of Science, Vol. 256, December 1958, pp. 715-728.

(28) BAYROCK, L. : "Surficial Geology, Lake Claire, NTS 841, 1:250,000." Research Council of Alberta Map, Edmonton, 1972.

The Role of Direct Analogue Computers in the Solution of Water Resources Problems

K. V. RAMANA MURTHY
Chief Research Officer (Physics)
Central Water and Power Research Station
Poona (India).

SYNOPSIS

In the judicious utilisation of water resources for human needs, a number of problems arise right from planning to execution. For example, it is required to estimate the ground water potential and plan its prudent utilisation. In a similar way, it is also required to estimate the water resource available from either rainfall or snowmelt and plan and execute its conservation for lean periods. The processes by which water resource becomes available and lost for human utilisation are highly non-linear in nature. These problems by virtue of their complexity, can best be solved by a computer approach. The direct analogue computer comes as a handy tool for this purpose. It is inexpensive, accurate and quick. These computers can be used for the solution of piece meal problems like assessment and utilisation of ground water resource, estimation, planning, storage and budgeting of open channel flow either for short-term or long-term duration, municipal water distribution, flood routing and forecasting. However, they find their potential use for basinwise simulation and analysis of water resources systems.

1. Introduction

1.1 Fresh water is available for human needs either as ground water or as surface water. In the optimum utilisation of ground water, one comes across a number of problems like the rate of pumping, spacing of wells, recharge, etc., for aquifers. In the utilisation of surface waters, problems arise regarding storage, its losses, usage variation with time, water budgeting, etc. The rational distribution of drinking water in urban localities also poses problems. The surface water on account of its uneven time distribution causes human misery by floods and droughts. To alleviate this, one has to store water during the period of abundance, to distribute it to needy in lean periods. This entails losses in the distribution networks. All these aspects can be studied on Direct Analogue Computers so that the available water resource can be put to optimum use.

1.2 Computers can be classified as digital and analogue. The analogue computers can be further subdivided as Direct and Indirect. The Direct Analogue Computer works on the principle of identity of mathematical equations representing the original phenomenon and the computer. After establishing the identity of parameters, the problem has to be scaled, for obtaining solution on these computers. These are economical, accurate and quick. As such they offer potential use for the solution of problems. The various facets of water resource problems can be conveniently solved by Direct Analogue Computers. The following enumerates this.

2. General Method of Solution by Direct Analogue Computers

2.1 When the mathematical equations representing two physical phenomena are similar then the two phenomena

are said to be analogous. For obtaining solutions by Direct Analogue Computers, the mathematical equation governing the physical problem for which a solution is required has to be first written. Writing the equation governing the electrical circuit under consideration, then the two equations have to be shown to be similar, to establish that the electrical circuit functions in an analogous way to the problem under consideration. Then identifying, which electrical parameter represents which one of the problem, the scale factors have to be chosen. Developing the hardware for the computer, the solution of the problem is then obtained.

3. Direct Analogue Computers for Ground Water Problems

3.1 For the proper utilisation of ground water resource, pumping has to be related to water-level change with respect to time and space. For this, the quantitative description of this resource and its physical parameters like, transmissibility, storage, area, boundaries, etc., are to be known. To evaluate the response of the aquifers to development, various alternative schemes have to be examined and the consequences forecast. Direct Analogue Computers come handy for this purpose[1][2][3][4].

3.2 The partial differential equation governing the non-steady state, two-dimensional flow of ground water in a homogeneous, isotropic and infinite aquifer is

$$\frac{\partial^2 h}{\partial x^2} + \frac{\partial^2 h}{\partial y^2} = \frac{S}{T} \cdot \frac{\partial h}{\partial t} \qquad \ldots(1)$$

where, h is hydraulic head, S is coefficient of storage of the aquifer, T is coefficient of transmissibility of the aquifer, t is time and x and y are rectangular co-ordinates.

3.3 The finite difference form of Equation (1) is

$$\frac{(h_2 + h_3 + h_4 + h_5 - 4h_1)}{a^2} = \frac{S}{T} \cdot \frac{\partial h}{\partial t} \qquad \ldots(2)$$

where, h_1, h_2, h_3, h_4, h_5 are the hydraulic heads at the nodal points 1, 2, 3, 4 and 5 and $a^2 \simeq \Delta x \,.\, \Delta y$.

3.4 Considering the resistor capacitor network shown in Figure 1 the relation of voltages around the junction can be expressed as

$$(V_2 - V_1)\frac{1}{RA} + (V_3 - V_1)\frac{1}{RB} + (V_4 - V_1)\frac{1}{RC} + (V_5 - V_1)\frac{1}{RD} = C \,.\, \frac{\partial V_1}{\partial t} \qquad \ldots(3)$$

where, V_{1-5} are the voltages at the ends of resistors, $RA - D$ are the values of resistances and C is the capacitance. If the values of the resistors are equal, Equation (3) can be written as

$$(V_2 + V_3 + V_4 + V_5 - 4V_1)\frac{1}{R} = C \,.\, \frac{\partial V_1}{\partial t} \qquad \ldots(4)$$

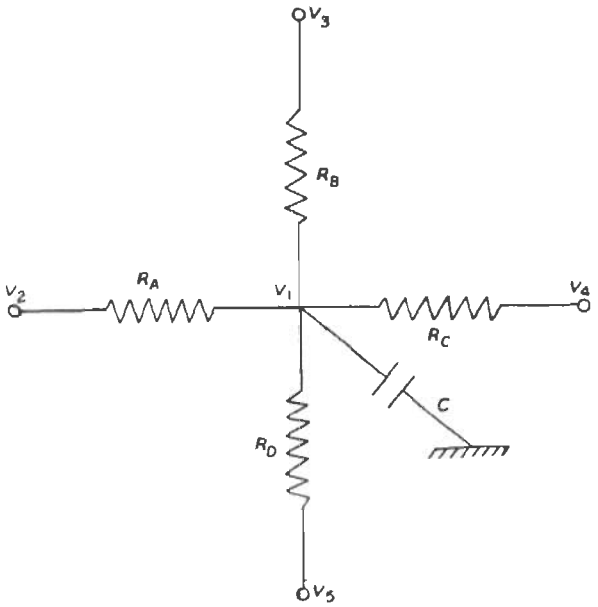

FIGURE 1 : Resistor Capacitor Network.

It can be seen that the Equation (4) governing the electrical circuit given in Figure 1 is similar to the Equation (2) governing the flow of ground water in an aquifer. Thus the electrical circuit is analogous to the aquifer and the water resource problems related to the aquifer can be solved with the help of this circuit. In this, the voltages are analogous to hydraulic heads, conductivity is analogous to transmissibility and the capacitance is analogous to the product of coefficient of storage and the area of the grid. The following scale factors relate the hydraulic and electrical quantities :

$$q = K_1 Q' \qquad \ldots(5)$$

$$h = K_2 V \qquad \ldots(6)$$

$$Q = K_3 I \qquad \ldots(7)$$

$$t_d = K_4 t_s \qquad \ldots(8)$$

where, q is cubic metres, Q' is Coulombs, Q is cubic metres per day, I is amperes, h is metres, V is volts, t_d is days and t_s seconds.

3.5 Knowing the aquifer parameters and the conversion scale factors the electrical quantities are to be calculated.

3.6 *Computer Hardware*

3.6.1 The computer hardware, for the solution of aquifer problems consists of a R-C network, a waveform generator, pulse generator and an oscilloscope. The schematic diagram of the computer is shown in Figure 2. The computer set-up is shown in Figure 3. The waveform generator is coupled to the pulse generator and the oscilloscope. The sawtooth pulses emerging from the waveform generator trigger the pulse generator

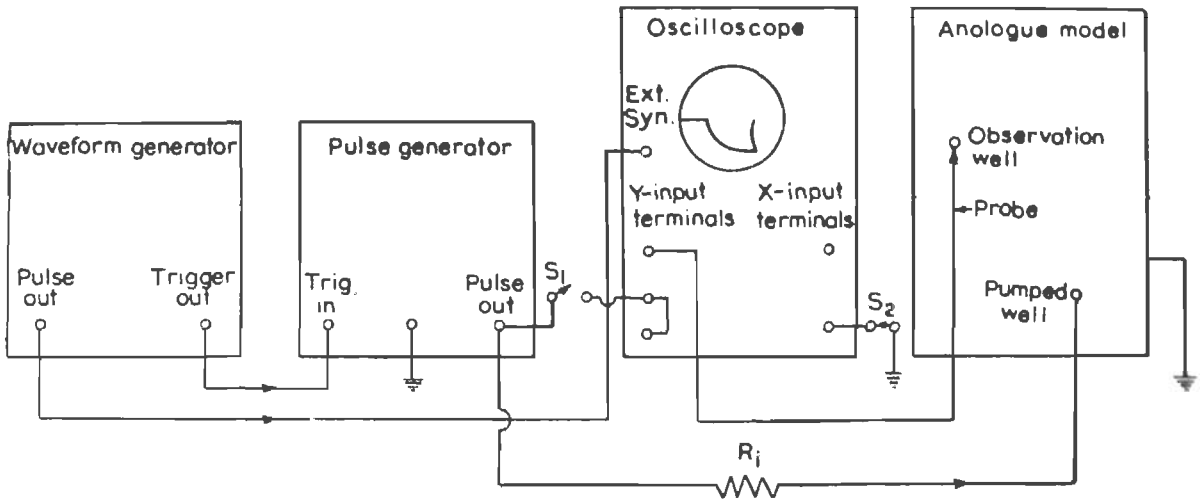

FIGURE 2 : Schematic diagram of the computer for aquifers.

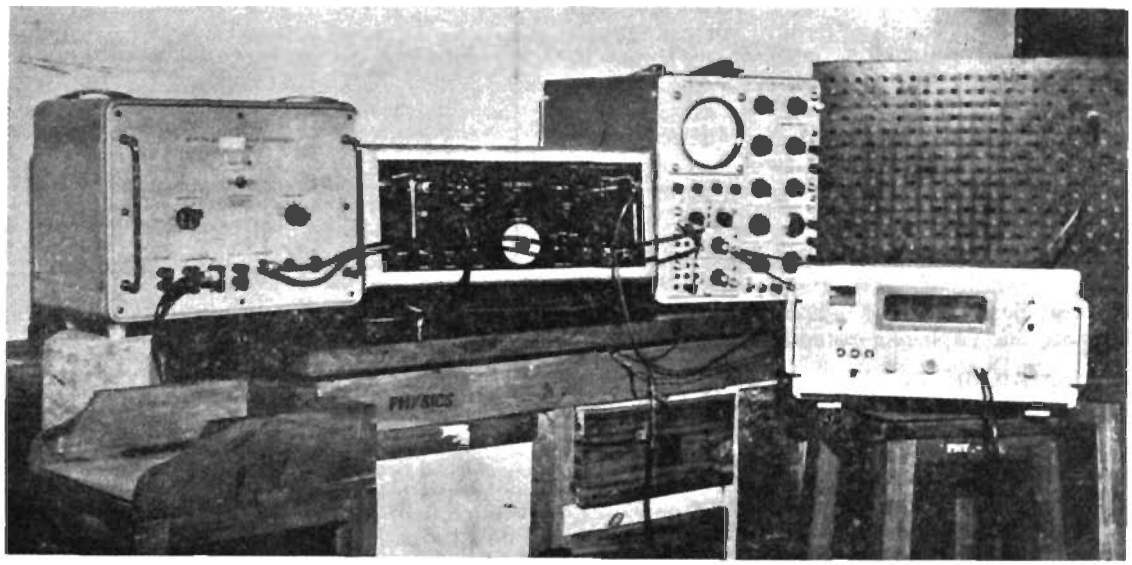

FIGURE 3 : Direct analogue computer for aquifers.

and the horizontal sweep of the oscilloscope. The output of the pulse generator, comprising rectangular shaped pulses of various durations and magnitudes, representing various draws is coupled to the *R-C* network node representing pumped well. The oscilloscope is connected to the node of the *R-C* network where the response of the aquifer to pumping is to be observed. On the screen of the oscilloscope a time voltage graph is produced which is analogous to the time drawdown graph of an observation well.

3.7 This computer is useful to determine the effect of various pumpings on the water-level change with reference to time and space of aquifers with various boundary conditions so that the available ground water resource is put to optimum use.

4. Direct Analogue Computers for Sub-soil Flow Problems

4.1 The surface water resource is unevenly distributed with respect to time and space. On account of this, it is required to store and conserve it, for use in lean periods. It is also required to convey the stored water to required locations. To store the water in open channels, structures are constructed. These may be earthen, masonry, etc. The stored water percolates through and underneath the structures, the quantity per unit time per unit width depending on the differential head and the permeability coefficient of the material through which it seeps. Water is lost in the process of conveyance to the required areas also. Thus the water resource available in the open channel flow is lost to

human needs on account of this seepage. The Direct Analogue Computer, traditionally called as electrical analogy method ([5])([6]) comes handy for estimation and assessment of the efficacy of various measures to reduce seepage.

4.2 The slow flow of water through earth masses is given by Darcy's law, which can be written as

$$Q = \frac{KAH}{L} \qquad ...(9)$$

where, Q is the rate of flow of water, K is coefficient of permeability of the soil, A is cross-sectional area, H is head producing flow and L is length of path of percolation.

4.3 The Ohm's law governing the flow of electric current in a conductive medium can be written as

$$I = \frac{K'A'V}{L'} \qquad ...(10)$$

where, I is current, K' is conductivity, A' is cross-sectional area, V is voltage, L' is length of path of current. It can be seen that the Equation (10) is similar to the Equation (9), thus the electrical circuit represented by Equation (9) is analogous to the slow flow of water in a permeable medium represented by Equation (10). The current in the electrical circuit represents the rate of flow of water, the conductivity represents the coefficient of permeability and the voltage represents the head producing flow.

4.4 The analogy can also be seen from the angle that both the steady flow of water in a permeable medium and the flow of electric current in a conductive medium are governed by the Laplacian potential

$$\triangle^2\phi = 0 \qquad ...(11)$$

4.5 The electrical analogy tray set-up utilised for the solution of seepage problems is given in Figure 4. In this, in the tray of the size 1.5 m × 1.5 m × 15 cm the structure to the reduced scale represented by conducting or non-conducting surfaces is put. The permeable medium is represented by an electrolyte. The stratification in the soil is represented by either changing the depth of the electrolyte or by placing electrolytes of conductivities in the same ratio as permeabilities, in watertight compartments. Copper strips mounted on non-conducting partitions are used for transferring electrical potentials from one electrolyte compartment to the other. Voltage representing the differential head is given with the help of an oscillator to the upstream and downstream side of the structure. The same voltage is given to the potential divider which resolves it into a thousandth part. The difference of the voltage between the potential divider and the variable probe point in the tray is fed to the null indicator. This is of magic eye type. It opens wide when the two potentials are equal. Thus the potential at any point in the tray is determined. Normally after simulating appropriate boundary conditions in the tray the equipotential lines at 5 percent intervals are plotted. The streamlines are drawn

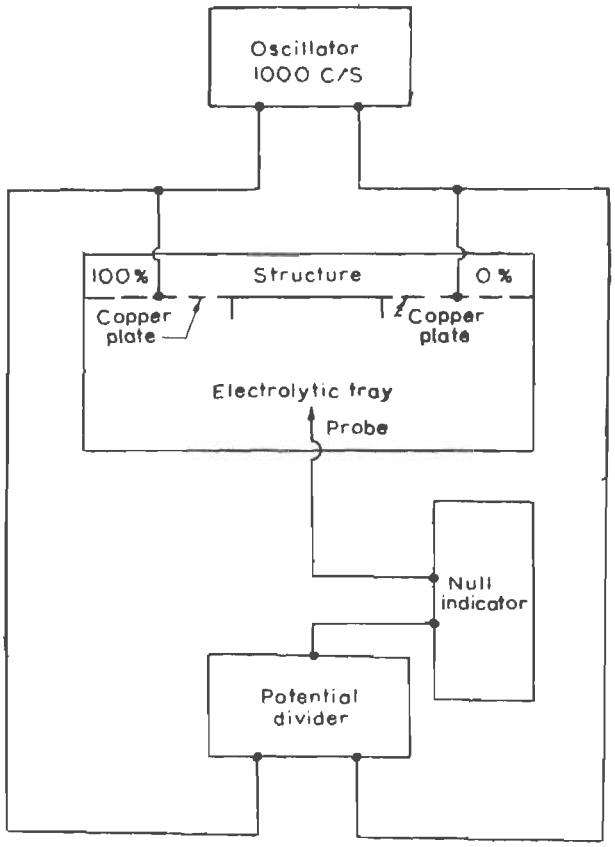

FIGURE 4 : Electrical analogy tray set-up.

orthogonal to the equipotential lines, so that curvilinear squares are formed. The quantity of seepage Q is calculated from the formula

$$Q = K.\left(\frac{n_f}{n_e}\right).H \qquad ...(12)$$

where, K is the permeability coefficient, n_f is the number of flow tubes, n_e the number of increments into which the differential head is divided while plotting the equipotential lines and H is the differential head. While obtaining solutions by the electrical analogy method the boundary conditions have to be properly represented, otherwise the results will be erroneous. The Teledeltos paper can also be used as a conductive medium. However, the order of accuracy of the results will be low as the commercially available Teledeltos paper is non-homogeneous in its resistance. Its vertical and horizontal resistances also differ. But quick solutions can be obtained by Teledeltos paper as compared to the tray. A practical approach would be, to use the Teledeltos paper for rough solutions of various, alternate combinations and to obtain accurate solution for the final choice by tray. This method is also useful to find the exit gradients and uplift pressures to assess the safety of the structure apart from determining the quantity of seepage. The set-up of a three-dimensional tray is shown in Figure 5.

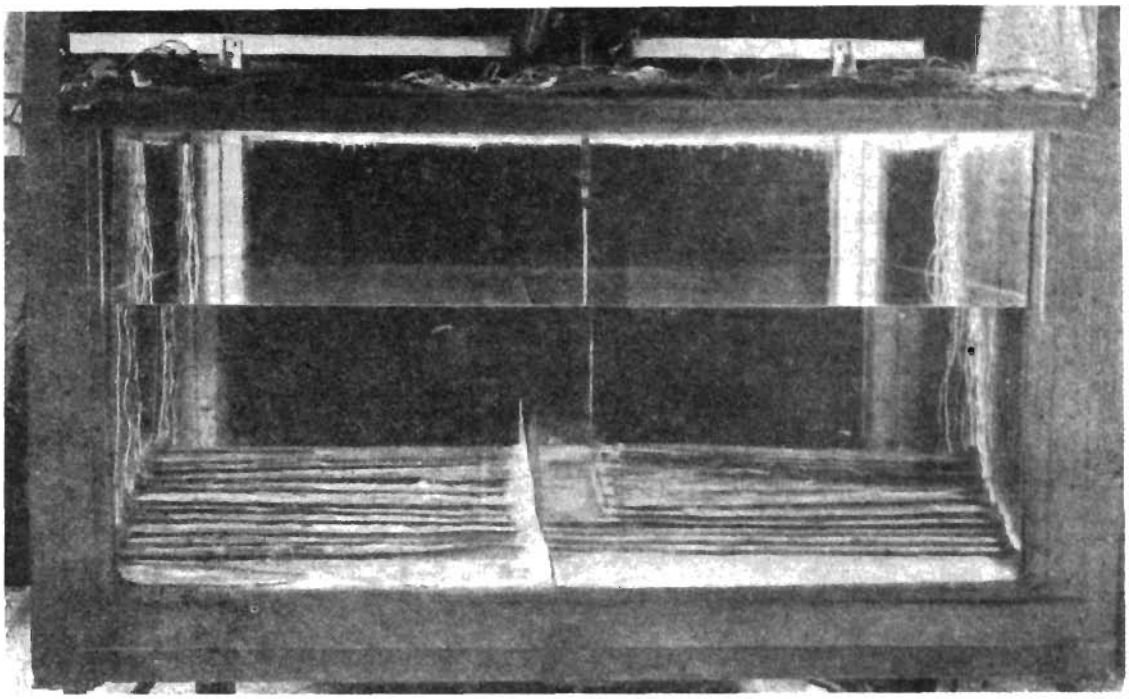

FIGURE 5 : Three-dimensional electrical analogy tray.

5. Direct Analogue Computers for Water Budgeting Problems

5.1 Water is stored in reservoirs to cater to human needs. The water thus stored is required to be budgeted for various requirements like irrigation, power generation, drinking, recreation, etc. These requirements can also be sometimes, conflicting. The budgeting has to be done on a short-time basis, where the inflow is high during peak monsoon and on a long-term basis when the inflow varies from very low to very high flows the period comprising a year or many years.

5.2 *Computer for Short-term Water Budgeting*

5.2.1 The inflow, outflow and storage in a water impounding structure are related by the equation

$$I - O = \frac{dS}{dt} \qquad \ldots(13)$$

where, I is inflow, O is outflow and $\frac{dS}{dt}$ is rate of change of storage. Considering the basic circuit of Figure 6 the relation between the current i flowing into the circuit, the current o flowing through the resistor R and the rate of change of charge across the condenser can be written as

$$i - o = \frac{dQ}{dt} \qquad \ldots(14)$$

5.2.2 It can be seen that the Equation (14) is similar to the Equation (13) and as such the electrical circuit given in Figure 6 acts analogous to the storage in a reservoir. The currents in the circuit represent the flows and the charge represents the storage. The practical circuit utilised for the solution of short-term water budgeting problems is given in Figure 7. In this, the surcharge storage is divided by the outflow discharge to obtain the time of emptying. Selecting a suitable analogue time scale, a rectifier, resistor condenser combination is arrived at, the current versus time curve of which has the same shape as that of the time of emptying curve. The inflow hydrograph is plotted on the "Inflow recorder" and a current proportional to the inflow hydrograph is pumped into the circuit by varying the 180 Meg ohm potentiometer. The outflow is automatically plotted on the "Outflow recorder". The levels of the reservoir also can be directly read from the digital voltmeter. The computer set-up is shown in Figure 8.

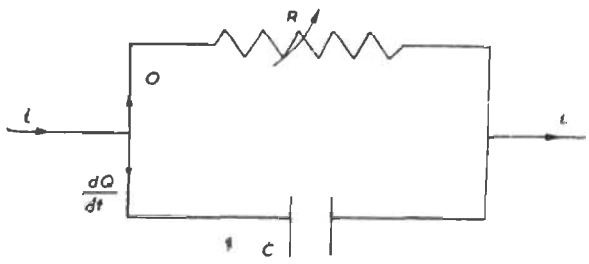

FIGURE 6 : Basic circuit.

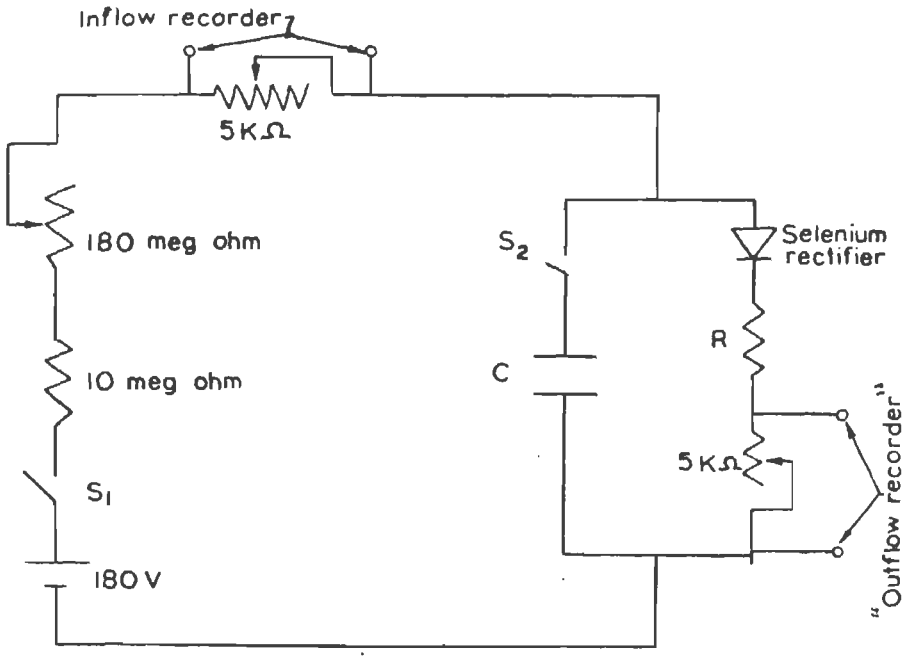

FIGURE 7 : Practical circuit.

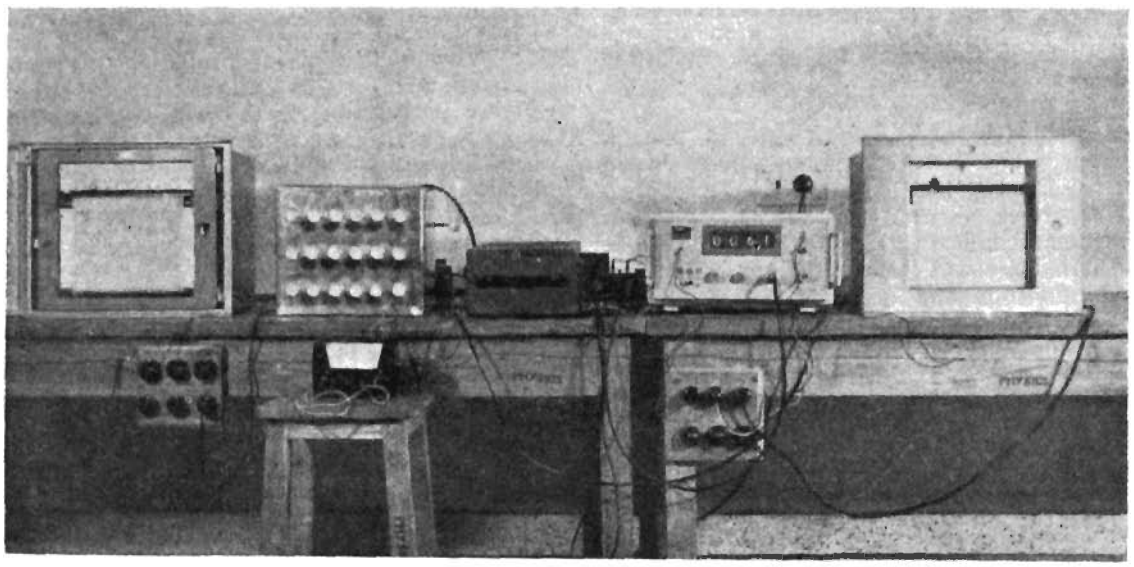

FIGURE 8 : Short-term water budgeting computer.

This computer is helpful to plan the storage and its budgeting on a short-term basis.

5.3 *Computer for Long-term Water Budgeting*

5.3.1 On a long-term basis the variation in inflows will be extreme and the minor outflows also have to be accounted as they will be cumulative. The losses like evaporation also have to be accounted. Moreover, the flows vary with respect to the level of the reservoir which has to be programmed.

5.3.2 Taking all these into account a computer has been developed[7]. The set-up of this is shown in Figure 9. This works on a fast time scale of a month in the prototype equal to 7.5 sec in the computer. Thus a hundred-year budgeting can be carried out in 2½ hours time.

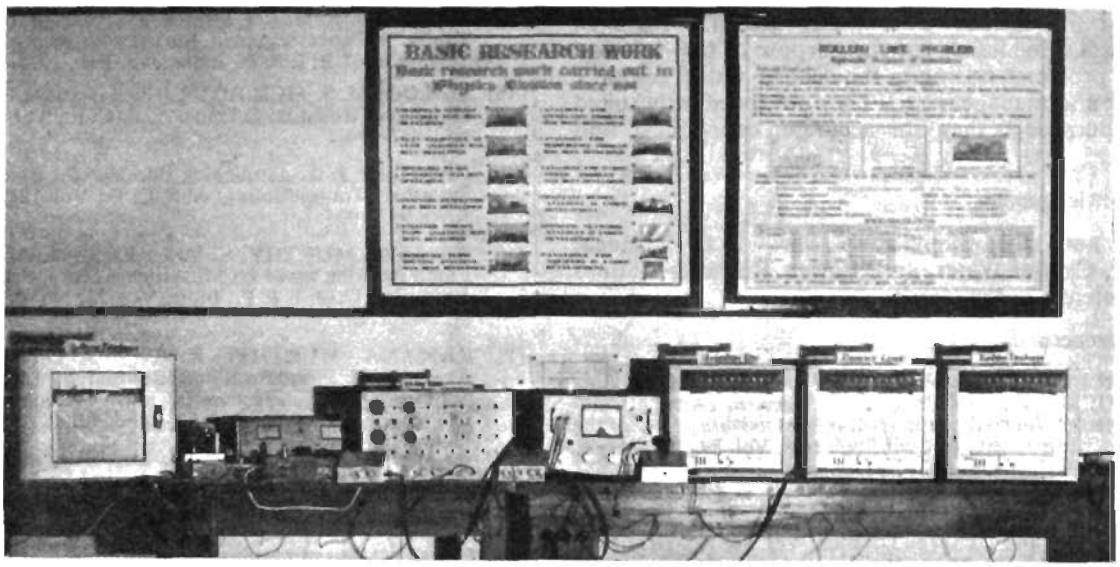

FIGURE 9 : Long-term water budgeting computer.

6. Direct Analogue Computer for the Solution of Municipal Water Distribution Problems

6.1 With increasing urbanisation the distribution of municipal waters for domestic needs poses a problem. It is difficult to solve the complex network problem with traditional methods. As such a computer is developed[8] for this purpose. This is called Macilroy network analyser. It works on the following principle. The law governing the flow of water through a pipe can be stated as

$$H = C \cdot Q^x \qquad \ldots(15)$$

where, H is loss in head, C is a coefficient depending upon the length, diameter and roughness of the pipe, Q is the discharge and x an exponent having a value between 1.7 to 2.0. In Hazen-Williams formula x is taken as 1.85.

6.2 If we take a tungsten filament wire having a cold resistance Ro, its resistance R with respect to temperature, changes according to the equation

$$R = Ro(1 + \alpha t) \qquad \ldots(16)$$

where, α is the temperature coefficient of resistance for tungsten. The voltage versus current relationship of a tungsten filament wire mounted in a vacuum bulb with suitable leads will be of the type

$$V = K \cdot I^x \qquad \ldots(17)$$

This type of bulbs are called fluistors. It can be seen that the Equation (17) is similar to Equation (15). Thus the fluistors behave analogous to pipes. The voltage across a fluistor respresents the loss in head across the pipe, the current represents the flow through the pipe. By a suitable design of the fluistor, the coefficient of current is made equal to the coefficient of flow through a pipe and a number of fluistors with varying K values developed. For solving a municipal distribution problem with the help of this network analyser, one has to first reduce the pipe line network to its essentials and connect the fluistors with appropriate K values in a similar fashion. Giving the voltages to the network of fluistors corresponding to the heads at the feeding points, one can observe the current through various fluistors to know the flows. Knowing the voltage at any point in the analyser one can know the head available. The analyser can be used for designing a completely new pipe line network or modifications for an existing one.

7. Direct Analogue Computers for Flood Routing and Forecasting Problems

7.1 A number of computers have been developed for flood routing [9][10][11][12][13][14] and forecasting purposes. These are based on Muskingum storage equation, mean velocities of flow. Computers are also developed for obtaining the stages directly from them. Computers for reservoir flood routing have also been developed[15]. These can be interconnected for basin-wise simulation and for flood forecasting purposes.

8. Conclusion

8.1 In the utilisation of available fresh water resources one comes across a number of problems. For example, the spacing of wells, amount of draw have to be determined for judicious utilisation of ground water potential. A number of schemes of utilisation have to be tried, to forecast the effect of these on the levels of ground water. In the conservation of surface water during the time of abundance, for use in lean periods, one comes across a number of problems like seepage which cause

water losses. In addition, the stored water has to be budgeted for various uses. The Direct Analogue Computers come handy for the purpose of the solution of these problems arising in the field of water resource planning and management. They are specifically suited for this purpose as they are accurate, economical and quick.

9. Acknowledgement

9.1 The author is thankful to Shri P. C. Saxena, Director, Central Water and Power Research Station for his interest in this work.

10. References

(1) WILLIAM, C. WALTON and THOMAS, A. PRICKETT : "Hydrogeologic Electric Analog Computers." Journal of the Hydraulics Division, Proc. of the American Society of Civil Engineers, Vol. 89, No. Hy 6, Nov. 1963, Part 1, pp. 67-91.

(2) HERMAN BOUWER : "Analyzing Ground Water Mounds by Resistance Network." Proc. A. S. C. E., Irrigation and Drainage Division, Vol. 88, No. IR3, Sep. 1962, Part I.

(3) ROBIN HERBERT : "Time Variant Ground Water Flow by Resistance Network Analogues." Journal of Hydrology, Vol. VI, No. 3, June 1968, pp. 237-264.

(4) KARPLUS, W. J. : "Analog Simulation." McGraw-Hill Book Co., 1958.

(5) CARL, N. ZANGAR : "Theory and Problems of Water Percolation." Engineering Monographs, U. S. B. R., Denver, Colorado, April 1953, p. 19.

(6) VAIDHIANATHAN, V. I. : "The Application of Electrical Analogy to the Design of Hydraulic Structures." C. B. I. P. Publication No. 55, New Delhi, July 1954.

(7) RAMANA MURTHY, K. V. and BELGAL, P. R. : "Electronic Analogue for the Preparation of Working Tables." Paper accepted for the 44th Annual Research Session of C. B. I. & P., India, Jan.-Feb. 1975.

(8) MALCOLM, S. MCILROY : "Pipe Networks studied by Non-linear Resistors". Trans. A. S. C. E., Vol. 118, 1953, pp. 1055-1067.

(9) HARDER, J. A. : "Analog Models for Flood Control Systems." Transactions of A. S. C. E., Vol. 128, 1963, Pt. I, pp. 993-1004.

(10) RAMANA MURTHY, K. V. : "Electronic Analogue for Flood Routing based on Muskingum Storage Equation." Journal of C. B. I. & P., India, Vol. 22, No. 4, Oct. 1965, pp. 443-452.

(11) RAMANA MURTHY, K. V. : "A Direct Discrete Analogue for Flood Routing." Journal of Institution of Engineers, India, Electronics and Telecommunication Division, No. 5, January 1967, pp. 66-80.

(12) RAMANA MURTHY, K. V. and BELGAL, P. R. : "Flow Routing Analogue based on Mean Velocities." Journal of the Institution of Engineers, India, E&T Division, May 1968, pp. 777-783.

(13) RAMANA MURTHY, K. V. : "Electronic Analogues representing Non-linear Flow through Open Channels and Flood Control Structures." Proc. of XIIIth Congress of I. A. H. R., Kyoto, Japan, August-September 1969, Vol. I, pp. 247-258.

(14) RAMANA MURTHY, K. V. : "Flood Routing Analogue." Journal of the Institution of Engineers, India, Electronics and Telecommunication Division, September 1970.

(15) RAMANA MURTHY, K. V. and BELGAL, P. R. : "Reservoir Flood Routing Analogue." Journal of Institution of Engineers, India, E & T Division, Vol. 52, No. 3, Pt ET2, November 1971, pp. 108-112.

Flow in a Leaky Aquifer with Time-Dependent Drawdown in the Well

ROBERT Y. S. LAI
Assistant Professor of Hydraulic Engineering, College of Engineering and Applied Science
University of Wisconsin—Milwaukee, Milwaukee, Wisconsin 53201 U.S.A.

SYNOPSIS

This study deals with the non-steady flow to a well of finite size fully penetrating an extensive homogeneous, isotropic leaky artesian aquifer of uniform thickness. The drawdown inside the well is a time-dependent function. The leakage is assumed to be at a rate proportional to the drawdown at any point in the aquifer. The exact analytical solution for the drawdown distribution around the well is presented. The solution is given in the most general form, i.e., it is valid for any specified time-dependent drawdown in the well. Two special time-dependent drawdown functions in the well, exponential and linear functions of time, are chosen as examples for numerical evaluation of the solution and discussion of the results. The solution for the corresponding well discharge is also presented. Typical drawdown curves and well discharge are presented in graphs by numerical evaluation of the analytical solution.

Introduction

The existing theoretical solutions for non-steady flow toward a well which is fully penetrating in an extensive, homogeneous leaky aquifer of uniform thickness consider either constant flow rate or constant drawdown in the well. Hantush and Jacob[1] obtained the solution for the drawdown distribution near a well discharging steadily from an infinite leaky aquifer of uniform thickness and permeability. In their study, the well is idealized as a mathematical line sink. A similar problem but for the case of constant drawdown in the well of finite diameter was considered by Hantush[2]. In both studies, the leakage into the aquifer is assumed to be vertical and proportional to the drawdown, i.e., linear leakage. The aquifer is treated as perfectly elastic.

Practical problems are, as a rule, much more complex. The boundary condition of either constant flow rate or constant drawdown in the well only approximates the actual situations. For instance, the assumption of constant discharge is associated with a time-dependent drawdown in the well which in turn results in the increase of the suction head and a corresponding decrease in discharge. This effect may be insignificant in certain cases, while it may become important in others. Lai and Su[3] studied the non-steady flow to a large well in a leaky aquifer induced by a time-dependent pumping rate. The effect due to the storage capacity of the well is also considered. They concluded that at large time the drawdown in the well is significantly larger and the time required for the drawdown to approach its steady state volume is longer for smaller values of the leakage factor. The effect of the storage capacity of the well on the drawdown is found to be significant when the time is not large or the ratio of the transmissibility of the aquifer to its storage coefficient is small

The study deals with the non-steady flow to a well of finite size fully penetrating an extensive, isotropic leaky artesian aquifer of uniform thickness when the drawdown in the well is a prescribed time-dependent function. Linear leakage will be assumed but the storage capacity of the well will not be taken into consideration. The theoretical development of the solution for the drawdown distribution around the well is presented in the next section. The solution is expressed in the most general form, i.e., it is valid for

any specified time-dependent drawdown in the well. Two special time-dependent drawdown functions in the well, exponential and linear functions of time, are chosen as examples for numerical evaluation of the solution and discussion of the results. The solution for the corresponding well discharge is also presented. Typical drawdown curves and well discharge are presented in graphs.

Analysis

Consider a non-flowing well of finite size cased to the top of an extensive homogeneous, isotropic, leaky aquifer of uniform thickness and screened throughout the thickness of the artesian sand (Figure 1). Assuming that the leakage into the aquifer is perfectly elastic, then the differential equation derived by Jacob[4] describing the non-steady radial flow in the leaky aquifer may be given as :

$$\frac{\partial^2 s}{\partial r^2} + \frac{1}{r}\frac{\partial s}{\partial r} - \frac{s}{B^2} = \frac{1}{\alpha}\frac{\partial s}{\partial t}\,;\ r \geqslant r_w, \qquad \ldots(1)$$

in which $s(r, t)$ is the drawdown in the aquifer ; r is the radial distance from the center of the well; t is the time ; B^2 is the ratio of the transmissibility of the artesian sand, $\tau = Kb$, to the specific leakage, K'/b', (K, K' and b, b' are, respectively, the permeabilities and the thickness of the artesian sand and semi-confined bed); α is the ratio of τ to the storage coefficient of the artesian sand, M ; r_w is the radial of the well.

If the initial piezometric head is horizontal throughout the aquifer and the storage capacity of the well is not considered, then the initial and boundary conditions that are to be satisfied by the drawdown, $s(r, t)$ are :

$$s(r, o) = 0\,, \qquad \ldots(2)$$

$$s(\infty, t) = 0\,, \qquad \ldots(3)$$

$$s(r_w, t) = f(t)\,, \qquad \ldots(4)$$

in which $f(t)$ is a prescribed time-dependent drawdown in the well. The flow rate $q(t)$ is given by

$$q(t) = -2\pi r_w \tau \left.\frac{\partial s}{\partial r}\right|_{r=r_w} \qquad \ldots(5)$$

For convenience, Equations (1) through (5) are transformed into dimensionless form :

$$\frac{\partial^2 S}{\partial R^2} + \frac{1}{R}\frac{\partial S}{\partial R} - A^2 S = \frac{\partial S}{\partial T}, \qquad \ldots(6)$$

$$S(R, o) = 0\,, \qquad \ldots(7)$$

$$S(\infty, T) = 0\,, \qquad \ldots(8)$$

$$S(1, T) = F(T)\,, \qquad \ldots(9)$$

$$Q(T) = -2\pi \left.\frac{\partial S}{\partial R}\right|_{R=1} \qquad \ldots(10)$$

In the above set of equations, the dimensionless parameters,

$$R = r/r_w,\ T = t\alpha/r_w^2,\ S = s/H_0,\ A = r_w/B,$$

and $Q(T) = q(t)/KH_0$.

Equations (6) to (9) form a boundary value problem for the dimensionless drawdown $S(R, T)$ and will be solved by Laplace transform technique.

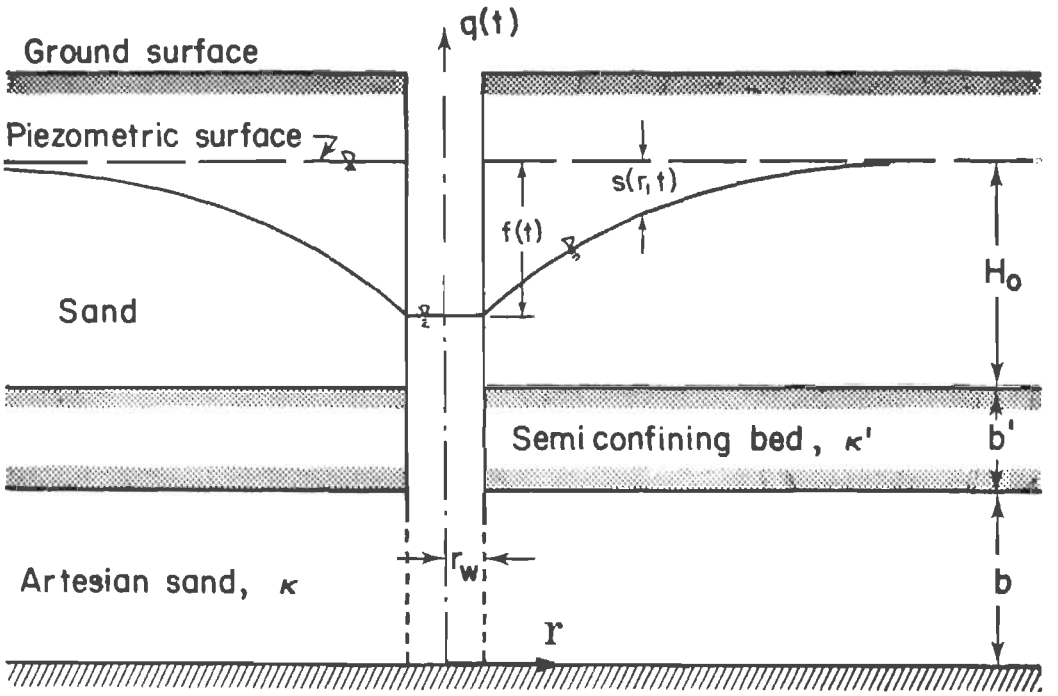

FIGURE 1 : Definition of sketch for non-steady flow to a finite size well in a leaky artesian aquifer.

The Laplace transform of Equations (6) to (9) are

$$\frac{\partial^2 \bar{S}}{\partial R^2}+\frac{1}{R}\frac{\partial \bar{S}}{\partial R}-A^2\bar{S}=p\bar{S}, \qquad ...(11)$$

$$\bar{S}(\infty, T)=0, \qquad ...(12)$$

$$\bar{S}(1, T)=\bar{F}(p), \qquad ...(13)$$

in which $\bar{S}(R, p)$ and $\bar{F}(p)$ are, respectively, the Laplace transform of $S(R, T)$ and $F(T)$. p is the Laplace transform parameter. Note that the initial condition Equation (7) has been used in obtaining Equation (11). The solution that satisfies Equations (11) & (12) is found as

$$\bar{S}(R, p)=C K_0(\sqrt{p+A^2}\,R) \qquad ...(14)$$

where, K_0 is the modified Bessel function of the second kind of order zero. The integral constant C can be easily determined by the boundary condition Equation (13). Thus the solution for $\bar{S}(R, p)$ is

$$\bar{S}(R, p)=\frac{\bar{F}(p)\,K_0(\sqrt{p+A^2}\,R)}{K_0(\sqrt{p+A^2})}, \qquad ...(15)$$

The solution for the drawdown distribution, $S(R, T)$, which is the Laplace inversion of Equation (15), can be, for convenience, written as follows :

$$S(R, T)=L^{-1}[\bar{S}(R, p)]$$
$$=L^{-1}\left\{[p\,\bar{F}(p)]\left[\frac{K_0(\sqrt{p+A^2}\,R)}{p\,K_0(\sqrt{p+A^2})}\right]\right\} \qquad ...(16)$$

By using convolution theorem, the solution may be given by

$$S(R, T)=\int_0^T \phi(T-\lambda)\,\psi(R, \lambda)\,d\lambda, \qquad ...(17)$$

in which

$$\phi(T)=L^{-1}[p\bar{F}(p)] \qquad ...(18)$$

$$\psi(R, T)=L^{-1}\left[\frac{K_0(\sqrt{p+A^2}\,R)}{p\,K_0(\sqrt{p+A^2})}\right] \qquad ...(19)$$

The function $\psi(R,T)$ has been found by Hantush(2) and is given by

$$\psi(R, T)=\frac{K_0(AR)}{K_0(A)}+\frac{2}{\pi}\int_0^\infty e^{-(\mu^2+A^2)T}\eta(R, \mu)d\mu \qquad ...(20)$$

where,

$$\eta(R, \mu)=\frac{\mu}{(\mu^2+A^2)}\left[\frac{J_0(\mu R)\,Y_0(\mu)-Y_0(\mu R)\,J_0(\mu)}{J_0^2(\mu)+Y_0^2(\mu)}\right] \qquad ...(21)$$

In the above equation, J_0 and Y_0 are Bessel functions of the first and second kind of order zero, respectively.

Equation (17) is the exact solution for the drawdown distribution, $S(R, T)$, due to an arbitrary time-dependent drawdown in the well. For a given drawdown function in the well, $F(T)$, $\phi(T)$ may be found by Equation (18). The infinite integral given in Equation (20) can not be integrated analytically. Therefore, numerical technique has to be used to evaluate the drawdown distribution. In order to gain more insight to the problem, two particular time-dependent drawdown functions in the well are chosen as examples for further study.

A. Solution for Exponential Time-Dependent Drawdown in the Well

The first example concerns the case where the drawdown in the well is an exponential function of time. Without loss of generality, the dimensionless form of the drawdown in the well may be expressed by :

$$F(T)=S_f+(S_0-S_f)\,e^{-\beta^2 T} \qquad ...(22)$$

in which S_0 is the initial drawdown, S_f is the final drawdown corresponding to $T\to\infty$, β is an arbitrary constant. Equation (22) represents an exponentially decaying function of time. The function $\phi(T)$ given in Equation (18) can be easily found as

$$\phi(T)=S_f\,\delta(T)+(S_0-S_f)\,\delta(T)-\beta^2(S_0-S_f)\,e^{-\beta^2 T} \qquad ...(23)$$

where, $\delta(T)$ is the dirac delta function. Substituting Equation (23) into Equation (17) and carrying out the integration with respect to λ, yields

$$\frac{S(R, T)}{S_f}=\frac{K_0(AR)}{K_0(A)}\left[1+\left(\frac{S_0}{S_f}-1\right)e^{-\beta^2 T}\right]$$
$$+\frac{2}{\pi}\int_0^\infty \left\{\frac{\beta^2[e^{-(\mu^2+A^2)T}-e^{-\beta^2 T}]}{(\beta^2-\mu^2-A^2)}\right.$$
$$\left.+\frac{S_0}{S_f}\left[\frac{\beta^2 e^{-\beta^2 T}-(\mu^2+A^2)e^{-(\mu^2+A^2)T}}{(\beta^2-\mu^2-A^2)}\right]\right\}\eta(R, \mu)\,d\mu \qquad ...(24)$$

Equation (24) is the exact solution for the drawdown distribution when the time-dependent drawdown in the well is given in Equation (22).

The solution given in Equation (24) involves an infinite integral which can not be integrated analytically. Numerical technique developed by Gemant(5) is adopted in this study. For demonstration purpose, Equation (24) is evaluated and plotted in Figure 2 for $A=0.01$, $S_0/S_f=2$ and $\beta=0.01$. Figure 3 is for $A=0.001$, $S_0/S_f=2$, and $\beta=0.01$. By comparing Figure 2 with Figure 3, the time required for the drawdown to reach its steady state is longer for small values of the leakage factor A ($=10^{-3}$) than for larger

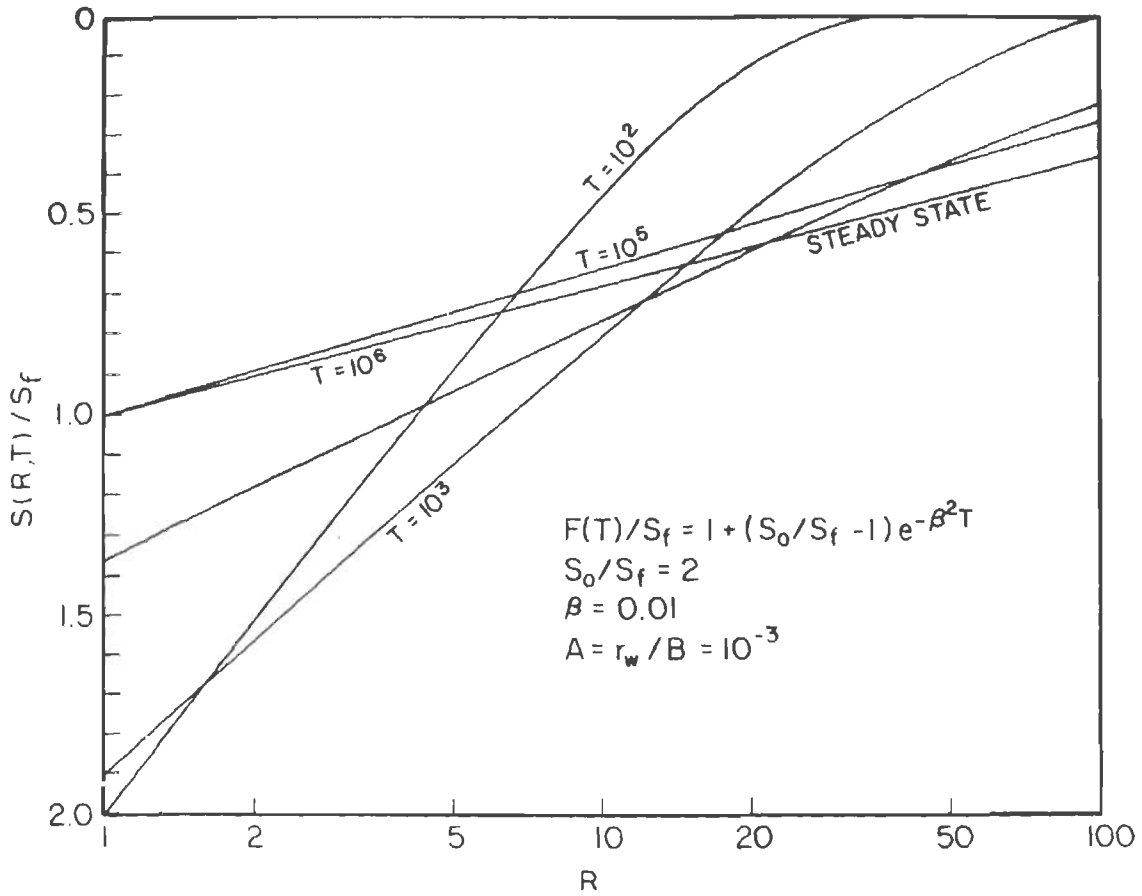

FIGURE 2 : Drawdown curves with exponential drawdown in the well ($A=10^{-3}$).

$A(=10^{-2})$. The slopes of the drawdown curves are smaller for $A = 10^{-3}$ and larger for $A = 10^{-2}$. This implies that the radius of influence by the pumping well is larger for smaller values of the leakage factor.

The corresponding flow rate can be found by Equation (10) and the result may be given by

$$\frac{Q(T)}{2\pi S_f} = \frac{AK_1(A)}{K_0(A)}\left[1+\left(\frac{S_0}{S_f}-1\right)e^{-\beta^2 T}\right] + \frac{4}{\pi^2}\int_0^\infty \left\{ \frac{\beta^2\left[e^{-(\mu^2+A^2)T} - e^{-\beta^2 T}\right] + \frac{S_0}{S_f}\left[\beta^2 e^{-\beta^2 T} - (\mu^2+A^2)e^{-(\mu^2+A^2)T}\right]}{(\beta^2-\mu^2-A^2)} \right\} \zeta(\mu)\,d\mu \quad \ldots(25)$$

in which K_1 is the modified Bessel function of the second kind of order one, and

$$\zeta(\mu) = \frac{\mu}{(\mu^2+A^2)} \frac{1}{[J_0^2(\mu) + Y_0^2(\mu)]} \quad \ldots(26)$$

Figure 4 shows the variation of discharge with time for $A = 0.02$, 0.01, and 0.001. For large time, the discharge increases with the value of the leakage factor. But as shown in Figure 4, for $T<10^2$, the effect of leakage on the discharge is insignificant. The dashed curves shown in Figure 4 are the corresponding discharge curves for constant drawdown in the well as obtained by Hantush(2).

B. Solution for Linear Time-Dependent Drawdown in the Well

In this section, we consider a particular time-dependent function of the drawdown in the well, i.e., it increases linearly with time until $t = t_i$ and then remains constant. Mathematically, its dimensionless form can be expressed by

$$F(T) = S_0 + \frac{S_0}{T_i}(T-T_i)[1-H(T-T_i)], \quad \ldots(27)$$

in which S_0 is the constant drawdown, $T_i = t_i\alpha/r_w^2$, and $H(T)$ is the heavyside function. The corresponding function $\phi(T)$ given in Equation (18) is found as

$$\phi(T) = \frac{S_0}{T_i}[1-H(T-T_i)] \quad \ldots(28)$$

Substituting Equation (28) into Equation (17) and

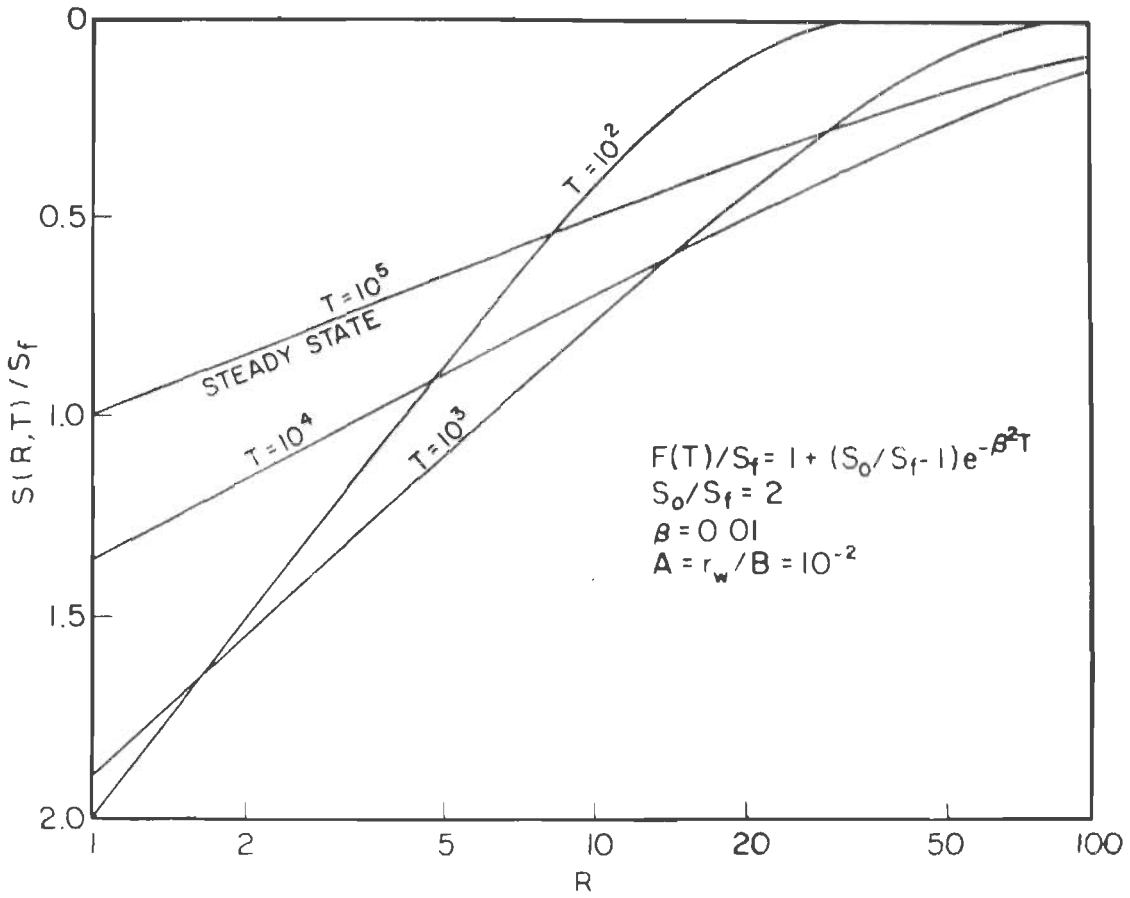

FIGURE 3 : Drawdown curves with exponential drawdown in the well ($A = 10^{-2}$).

carrying out the integration with respect to λ, the solution for the drawdown distribution is

$$\frac{S(R,T)}{S_0} = \frac{K_0(A,R)}{T_i K_0(A)}[T-(T-T_i)H(T-T_i)] + \frac{2}{\pi}\int_0^\infty \left\{\frac{1-e^{-(\mu^2+A^2)T}+H(T-T_i)[e^{-(\mu^2+A^2)(T-T_i)}-1)}{T_i(\mu^2+A^2)}\right\} \eta(R,\mu)d\mu \quad \ldots(29)$$

The solution given in the above equation is evaluated numerically for some particular values of the parameters involved. Figure 5 shows the drawdown curves at various time instants. T_i is set equal to 10^{-3} and the dashed curves are for $A = 10^{-2}$. For small time, the effect due to the leakage is insignificant. It takes longer time for smaller leakage factor to reach its steady state. As shown in the previous example, the slopes of the drawdown curves for $A = 10^{-2}$ are consistently larger than those for $A = 10^{-3}$.

The corresponding flow rate is found by substituting Equation (29) into Equation (10), and the result is

$$\frac{Q(T)}{2\pi S_0} = \frac{AK_1(A)}{T_i K_0(A)}[T-(T-T_i)H(T-T_i)] + \frac{4}{\pi^2}\int_0^\infty \left\{\frac{1-e^{-(\mu^2+A^2)T}+H(T-T_i)[e^{-(\mu^2+A^2)(T-T_i)}-1]}{T_i(\mu^2+A^2)}\right\} \zeta(\mu)\,d\mu \quad \ldots(30)$$

where, $\zeta(\mu)$ is given in Equation (26). Figure 6 shows the variation of flow rate with time for various values of A. The flow rate increases with the value of A. The results for constant drawdown in the well by Hantush[2] are also presented in Figure 6 for $A = 10^{-2}$ and 10^{-3}.

Conclusion

The exact analytic solution for the drawdown distribution around a well of finite size fully penetrating an

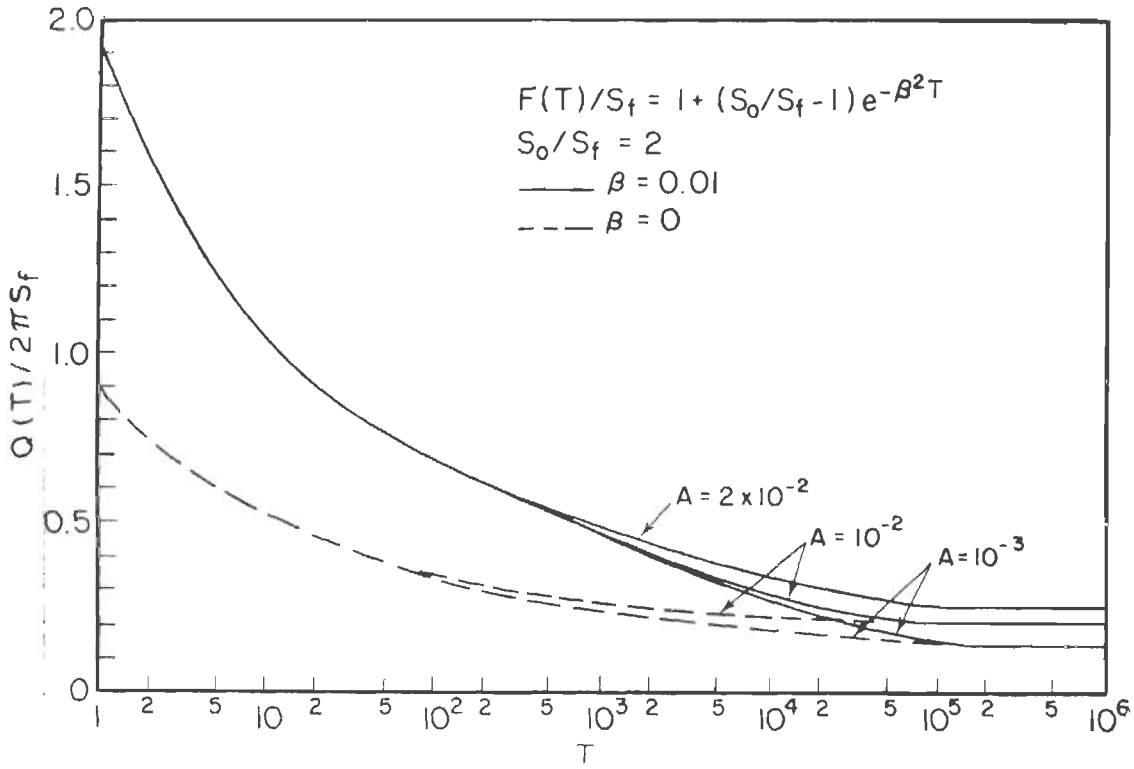

FIGURE 4 : Discharge-time relationship (Exponential time-dependent drawdown in the well).

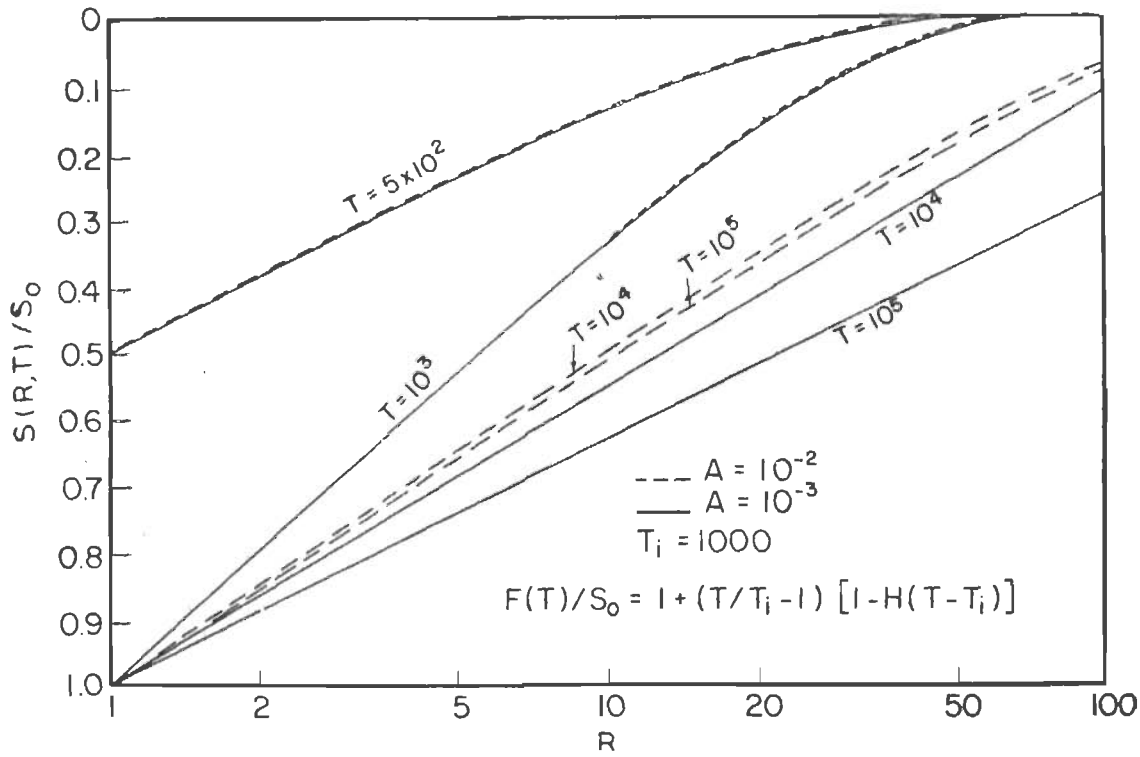

FIGURE 5 : Drawdown curves with linear drawdown function in the well.

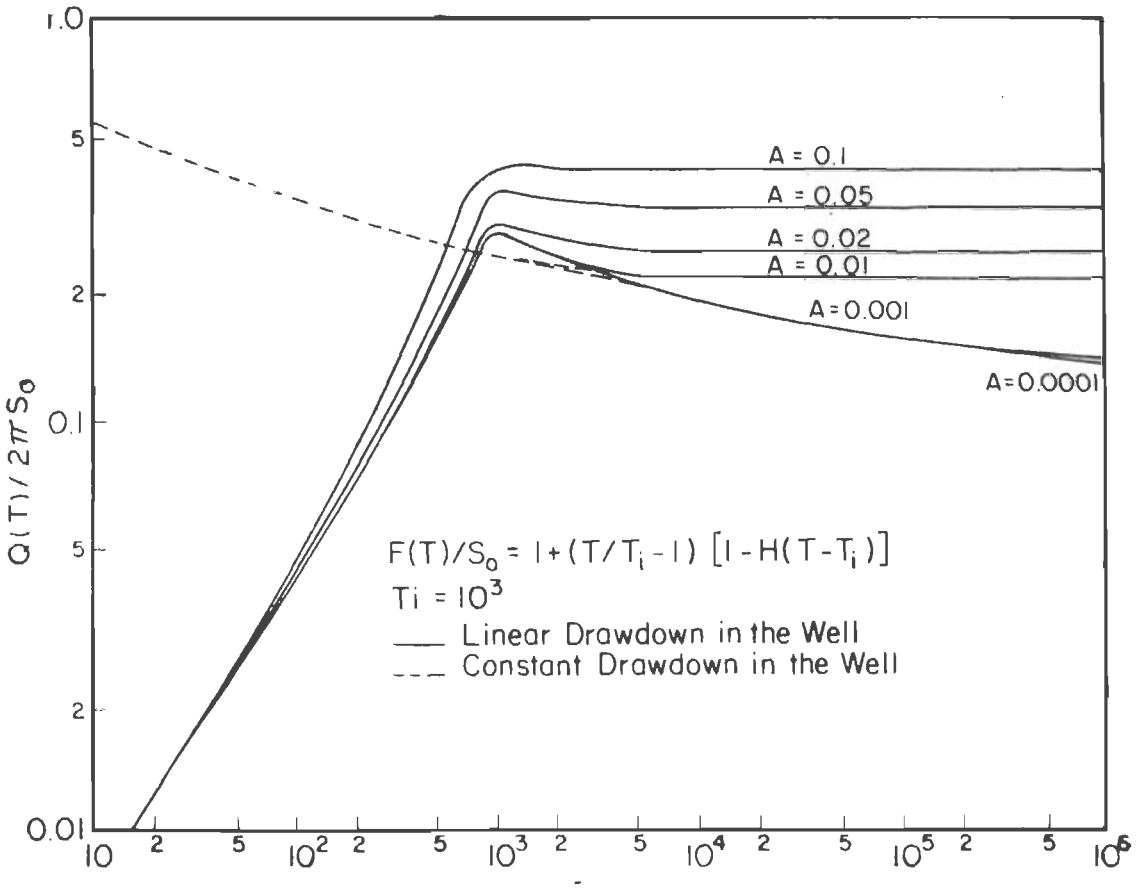

FIGURE 6 : Discharge-time relation (Linear time-dependent drawdown in the well).

extensive homogeneous, isotropic leaky aquifer due to a time-dependent drawdown in the well is presented. The solution is valid for any given time-dependent drawdown in the well. Two special time-dependent drawdown functions in the well, i.e., exponential and linear functions of time, are chosen as examples for further study. The solutions, which are expressed in terms of infinite integrals, have been evaluated numerically by a technique by Gemant([5]). It is found that the time required for the drawdown curves to reach its steady state is longer for smaller values of the leakage factor. The radius of influence is greater for smaller values of the leakage factor. The solutions for the corresponding flow rate are also presented. The variations of flow rate with time for various values of the leakage factor are presented in graphs. It is shown that the flow rate increases with the value of the leakage factor. The corresponding results for the case of constant drawdown in the well obtained by Hantush([2]) are also presented in graphs for comparison purpose.

References

(1) HANTUSH, M. S. and JACOB, C. E. : "Non-steady Radial Flow in an Infinite Leakage Aquifer." Trans. Amer. Geophys. Union, Vol. 36, 1955, pp. 95-100.

(2) HANTUSH, M. S. : "Non-steady Flow to Flowing Well in Leaky Aquifer." J. Geophys. Res., Vol. 64, 1959, pp. 1043-1052.

(3) LAI, R. Y. S. and SU, C. W. : "Non-steady Flow to a Large Well in a Leaky Aquifer." J. Hydrology, Vol. 22, 1974, pp. 333-345.

(4) JACOB, C. E. : "Flow in a Leaky Artesian Aquifer." Trans. Amer. Geophys. Union, Vol. 27, 1946, pp. 198-205.

(5) GEMANT, A. : "Transient Temperature Around Heating Pipes Maintained at Constant Temperature." J. Applied Physics, Vol. 17, 1946, pp. 1076-1081.

Least Cost Design of Water Distribution Networks

R. G. CEMBROWICZ
Research Associate
Institut für Siedlungswasserwirtschaft Universität Karlsruhe
75 Karlsruhe, Postfach 6380 (Germany).

SYNOPSIS

A Linear Programming model is developed to derive minimum cost solutions of water supply networks using a decomposition principle from graph theory. The costs are formulated as capital cost related to the diameter size. Additional pumping costs corresponding to the energy loss in the system may be included. There are no requirements concerning the convexity of the cost functions. The graph of the network is assumed to be known as well as the demand or inflow at any node, minimum pressure requirements and minimum admissible diameters and flows. The results of the model are optimal standard diameter sizes of the distribution system.

1. Introduction

The distribution network usually contributes the largest share of the total water supply systems costs. Therefore, optimal designs are desirable in particular for numerous expanding cities of the less industrialized nations. Traditionally, trial and error selection of diameters and subsequent verification of the hydraulic network balance have been used for cost optimization. This method proves insufficient except for a relatively small number of conduits.

Over the last decades research results in the area have improved with the help of mathematical programming techniques. Jacoby([1]) formulates the problem as unconstrained sequential optimization, Smith([2]) compares different solution algorithms: linear programming, steepest descent, random sampling.

Cembrowicz([3]) employs graph theory to decompose the nonconvex problem into convex subsets. Gupta([4]) derives the cost minimum of a branch network using Linear Programming.

However, the research results are not in general applicable in practice. Apart from preventive computational intricacy either of the following drawbacks occur:

(1) The optimal design is based on continuous diameters instead of available standard sizes.

(2) Local optima are derived instead of a global solution.

(3) Branch networks are used instead of existing loop grids.

The approach presented in this paper uses Linear Programming and derives a global cost solution for standard diameters based upon free configurations of the network graph. Costs may include capital and pumping costs. The model assumes given input flows and potentials, minimum flow requirements in any branch, minimum pressure potentials and the demand at the nodes. The method is supplemented by a random search that offers an abbreviation of the computational efforts.

2. Definitions

The configuration of branches and nodes of a network and the direction of flows in the branches are described in graph theory using an incidence matrix A. The

elements are $a_{ij} = +1$ if flow f_j in branch j enters node i, $a_{ij} = -1$ if the flow f_j leaves node i, $a_{ij} = 0$ if branch j is not incident to node i. The demand at any node i is called q_i, and the head loss in branch j is h_j.

Kirchhoff's node law states that the inflow equals the outflow at any node :

$$Af = q \qquad \ldots(1)$$

One node, e.g , the reference node, has been omitted in A since otherwise one node equation of (1) would be redundant with A being singular in this case. Kirchhoff's loop law balances the head losses of a network :

$$A^T p = h \qquad \ldots(2)$$

or

$$\sum_j h_j = 0, j \in J_s, \forall s, \qquad \ldots(3)$$

J_s designating the set of branches contained in a loop s.

Let the number of nodes in a network be NN, the number of branches be NP, and the number of loops be NL. Then, matrix A may be partitioned into an $(NN-1)\times(NN-1)$ square matrix E and into an $(NN-1)\times(NL)$ matrix G :

$$A = [EIG] \qquad \ldots(4)$$

According to Euler's theorem on connected graphs[5] the number of columns in A equals :

$$NP = (NN-1)+NL. \qquad \ldots(5)$$

If E represents a subset of the total branches in a network such that every node is connected without forming loops, this subset is called a tree, G being the associated cotree. From Equations (4) & (5) follows that the number of loops equals the number of cotree branches called chords. Any loop contains one chord. E represents a tree if

$$| E | = \pm 1, \qquad \ldots(6)$$

and E is not a tree if

$$| E | = 0 \qquad \ldots(7)$$

Subsequently E will be taken to designate a tree.

The number of possible tree configurations of a graph with an incidence matrix A follows from :

$$T = | AA^T | \qquad \ldots(8)$$

The tree configurations are derived using criterion (6) or others[6].

Combining Equations (1) & (4) and partitioning f in accordance with Equation (4) into f_1, the flows in the tree, and f_2, the flows in the chords :

$$[EIG]\begin{bmatrix} f_1 \\ \\ f_2 \end{bmatrix} = q \qquad \ldots(9)$$

$$f_1 = E^{-1} q - E^{-1} G f_2 \qquad \ldots(10)$$

Equation (10) states that the flows f_1 in a tree are uniquely determined by a set of linear equations given the flow in the chords. Hence, any loop has one degree of freedom to choose the flow. If the flows in the chords are assumed the entire flow in the network follows.

The simultaneous solution of Equations (1), (3) & (11) is called the hydraulic balance of a network. In this case the diameters and the demand or input at the nodes are known and the $2\times NP$ elements of the unknown vectors f and h are computed. The corresponding number of the Equations (1), (3) & (11) corresponds to the number of unknowns :

$$(NN-1)+NL+NP = 2\times NP$$

3. Optimization Concept

Consider a branch j, length L_j, between two nodes consisting of $k = 1, \ldots K$ sections of increasing standard diameter sizes d_{jk}, lengths l_{jk}. The number of available standard diameters is relatively small with large capacity differences between subsequent sizes. Accordingly, an appropriate choice of K will cover any feasible capacity range.

Since in practice the capital cost including installment, c^c_k, of a conduit is given per unit length, the total cost of a branch consisting of sections k amounts to :

$$C_c(l) = \sum_k c^c_k l_{jk} \qquad \ldots(15)$$

It is presumed that the cost c^c_k increases with increasing diameter.

In addition, a general hydraulic formula is introduced relating flow, head loss, diameter d_j and length l_j of a pressure conduit :

$$h_j = \gamma_j \lambda_j \frac{f_j^{\delta}}{d_j^{\epsilon}} l_j \qquad \ldots(11)$$

The parameter γ_j includes dimensional adjustments and the friction factor λ_j as a constant according to Hazen-Williams ($\delta = 1.85$, $\epsilon = 4.85$) or Darcy-Weisbach ($\delta = 2.0$, $\epsilon = 5.0$)[7]. In Germany hydraulic computations for water supply networks are required to use the Prandtl-Colebrook formulation[7]. Commonly, the hydraulically "critical zone" applies, and the friction factor λ is an implicit function of the Reynolds' number Re and of the roughness r :

$$1/\lambda^{1/2} = \log [2.51/(Re\ \lambda^{1/2}) + r\ (3.71\ d)]^{-2} \qquad \ldots(12)$$

Outside the critical zone λ is either independent of Re or of the relative roughness r/d. The sensitivity of the friction factor with respect to the Reynolds' number

is small. Adjustments of the exponents δ, ε and of the constant γ in Equation (2) yield sufficiently accurate approximations of expression (2) based on Equation (3) if λ is assumed constant. Accordingly, for simplification the general hydraulic formula, Equation (2), with λ being constant is used in the following mathematical considerations.

If the pipe material, i.e., the roughness r, diameter and flow are known, Equation (11) reduces to :

$$h_j = a_j \, l_j \qquad \ldots(13)$$

$$a_j = \gamma_j \, \lambda_j \, f_j^{\delta} \Big/ d_j^{\epsilon} \qquad \ldots(14)$$

with a_j being constant.

Also, if a total head loss h_j of the branch j is to be observed and Equation (15) to be minimized, the following Linear Program obtains :

$$\text{Min } C_c(l) = \sum_k c_k^c \, l_{jk} \qquad \ldots(16)$$

subject to

$$\sum_k l_{jk} = L_j \qquad \ldots(17)$$

$$\sum_k a_{jk} \, l_{jk} = h_j \qquad \ldots(18)$$

However, at most two adjacent diameters d_{jk} enter the optimal solution of the program (16) to (18). Consider, e.g., the sections with the three largest diameters out of a number of increasing standard diameter sizes in branch j. The section in the middle shall be expanded to either side and the adjacent sections shortened accordingly, such that the total length and overall head loss of the three sections are maintained. For hydraulic reasons, as stated by Equation (11), the length of the largest diameter is to be reduced more than the shortest one in order to balance the head loss differences generated on either side of the middle section. Hence, the greatest cost savings occur if the largest diameter is replaced entirely by the middle section. Repeating the procedure at most two sizes remain if minimum costs are desired.

The Lagrangian form of expressions (16) to (18) is :

$$\text{Min.} \sum_k c_k \, l_{jk} + \lambda_{j1} \left(L_j - \sum l_{jk}\right) + \lambda_{j2} \left(h_j - \sum a_{jk} \, l_{jk}\right) \qquad \ldots(19)$$

Using the previous result that at most two diameters, $k = 1, 2$, are contained in a minimum cost branch, and assuming, e.g., $c_1 > c_2$, $a_{j2} > a_{j1}$, the values of the Lagrangian multipliers obtain :

$$\lambda_{j1}^* = (c_1 a_{j2} - c_2 a_{j1})/(a_{j2} - a_{j1}) > 0 \qquad \ldots(20)$$

$$\lambda_{j2}^* = (c_2 - c_1)/(a_{j2} - a_{j1}) < 0 \qquad \ldots(21)$$

The sign of the multipliers follows from their interpretation as dual variables if the original *L.P.*, expressions (16) to (18), is transformed into the following equivalent :

$$\text{Min} \sum_k c_k \, l_{jk} \qquad \ldots(22)$$

subject to

$$\sum l_{jk} \geqslant L_j \qquad \ldots(23)$$

$$\sum a_{jk} \, l_{jk} \leqslant h_j \qquad \ldots(24)$$

At the optimum or minimum solution the equality sign of expressions (23) and (24) holds, and the programs (16) to (18) and (22) to (24) yield identical results.

However, the transformation allows interpretation of the dual variables, $\lambda_{j1} > 0$ indicating a cost increase for increasing length L_j, and $\lambda_{j2} < 0$ a cost decrease for increasing head loss h_j (cost increase for decreasing head loss h_j). The first dual variable, λ_{j1}, is independent of the flow in branch j [Equation (20)], whereas λ_{j2} decreases hyperbolically with increasing flow [Equation (21)]. This is tant amount to an overall decrease of the marginal cost for increasing flows implying a concave curvature of the cost function with respect to the flows. The concave cost function is defined by the value of the dual function of the program (22) to (24) which, by definition, equals the value of the original primal at the optimum :

$$C^*(l) = \lambda_{j1}^* \, L_j + \lambda_{j2}^* \, h_j \qquad \ldots(25)$$

The principle of concavity or economies of scale of the cost of a branch with respect to the flows holds for any head loss h_j that is assumed. Hence, given a hydraulically feasible head loss distribution according to Equation (2) or (3), it will be desirable to concentrate the flows in the network as much as possible in order to utilize the economies of scale. This can be visualized by assuming a network hydraulically balanced, i.e., Equations (1), (3) and (11) are observed. Then, without changing the head losses h_j and without violating Equation (1), the flows leaving a node are redistributed at the node by reducing as many flows as possible to zero and increasing the flows correspondingly in the remaining mains leaving the node. The resulting flow configuration equals that of a tree the chords being zero.

Because of different and/or identical economies of scale a flow unit decreased in one of the branches leaving a node will generate a cost decrease greater than and/or equal to a corresponding flow increase in another branch leaving the same node. However, the branches of which the flows are to be increased and decreased are unknown at this point since according to Equation (25) the associated cost curves depend on the diameters of the branch sections and of the flow itself that have been assumed so far. Hence, the problem arises to investigate any tree configuration.

In summary, the minimization of the capital cost requires the following input :

I —design demand q_i at any node i

II — minimum supply pressure p_i at any node i

III — input flow and potential at the input nodes

IV — length L_j of any branch j

V — roughness r_j of any pipe j

VI — price p_k^c per unit length of standard diameter sizes d_k

VII — range K_j of potential diameter sizes for any branch j

VIII — viscosity of the water

IX — configuration of all the trees of the network graph.

The formulation of the Linear Program for any tree follows to :

$$\text{Min} \sum_j \sum_k c_k^c \, l_{jk} \qquad \ldots(26)$$

subject to

$$\sum_k l_{jk} = L_j, \quad \forall\, j \qquad \ldots(27)$$

$$\sum_k a_{jk} \, l_{jk} = 0, \quad j \in J_s, \; \forall\, s \qquad \ldots(28)$$

$$\sum_k a_{jk} \, l_{jk} \leqslant H_e, \quad j \in J_e, \; \forall\, e \qquad \ldots(29)$$

J_e denotes the set of branches j leading from an input node to an end node e of a tree. The maximum admissible head loss H_e is the difference between the input node potential and the minimum potential requirement at the end nodes.

If pumping costs are to be included the conditions I through IX are supplemented by :

X — pumping efficiency factor η

XI — pumping cost c^p per kWh

XII — present value factor v based on a design period τ and a discount rate z.

XIII — peak factor p_f, ratio of the design demand to the daily mean.

The pumping costs $C_p(l)$ for any branch are based upon the energy loss which is proportional to the product of flow and head loss :

$$C_p(l) = \alpha \frac{v \, c^p \, p_f}{\eta} f_j \sum_k a_{jk} \, l_{jk} \qquad \ldots(30)$$

where, α includes the specific weight of the water, conversion from kW to [m · kg/sec], the yearly pumping duration time and dimensional adjustments. Equation (30) may be simplified by introducing a lump sum pumping cost c_j^p :

$$C_p(l) = c_j^p \sum_k a_{jk} \, l_{jk} \qquad \ldots(31)$$

Accordingly, the objective function of the summarized capital and pumping costs follows to :

$$\text{Min.} \sum_j \left\{ c_j^p \sum_k a_{jk} \, l_{jk} + \sum_k c_k^c \, l_{jk} \right\} \qquad \ldots(32)$$

The associated constraints set equals expression (27) to (29).

4. Example

4.1 *Input*

Figure 1 shows the water supply mains of an example network. Inside the main grid smaller supply lines may be assumed with diameter sizes corresponding to minimum regulations that are not subject to optimization. Discounting the carrying capacity of this subgrid is an assumption similar to the convention that the demand is exerted at the nodes only. In accordance with the concave behavior of the cost and economies of scale with respect to the flows the main grid provides an arterial skeleton to facilitate a concentration of the flows based on the previous tree concept. The diameters of the chords will fall into the range of those of the subgrid. For the layout of the main grid, engineering judgement must be employed supplemented by feedback from this analysis. For example, if the main grid is extended to include smaller supply lines, substantial computational efforts may be wasted since the model tends to concentrate flows at the expense of smaller lines whose size cannot be further reduced because of minimum flow and diameter requirements.

On the other hand, if the main grid is designed too spacious, the assumption of neglecting the carrying capacity of the subgrid may have to be verified. Dividing any branch into sub-branches between additional nodes to refine the demand distribution may offer an improvement.

As it is common practice the network of Figure 1 will be optimized for a steady state design demand. It is recognized that this criterion may not prove adequate. Though research has been developed to include more realistically fluctuation patterns[8][9], this model uses a conventional steady state "peak load".

The following input data refer to a city in a developing nation. Design demand at any node i is $q_i = 80$ l/sec. This corresponds to a daily mean of 70 l/inhabitant, a peak factor $p_f = 5.0$, and a population density of ~200 inhab./ha (1 ha = 10^4 m^2). Flow input is at node 1 with 510 l/sec at 300 m and at node 4 with 450 l/sec at 310 m, respectively. The approximation based on a constant friction factor λ employed in the

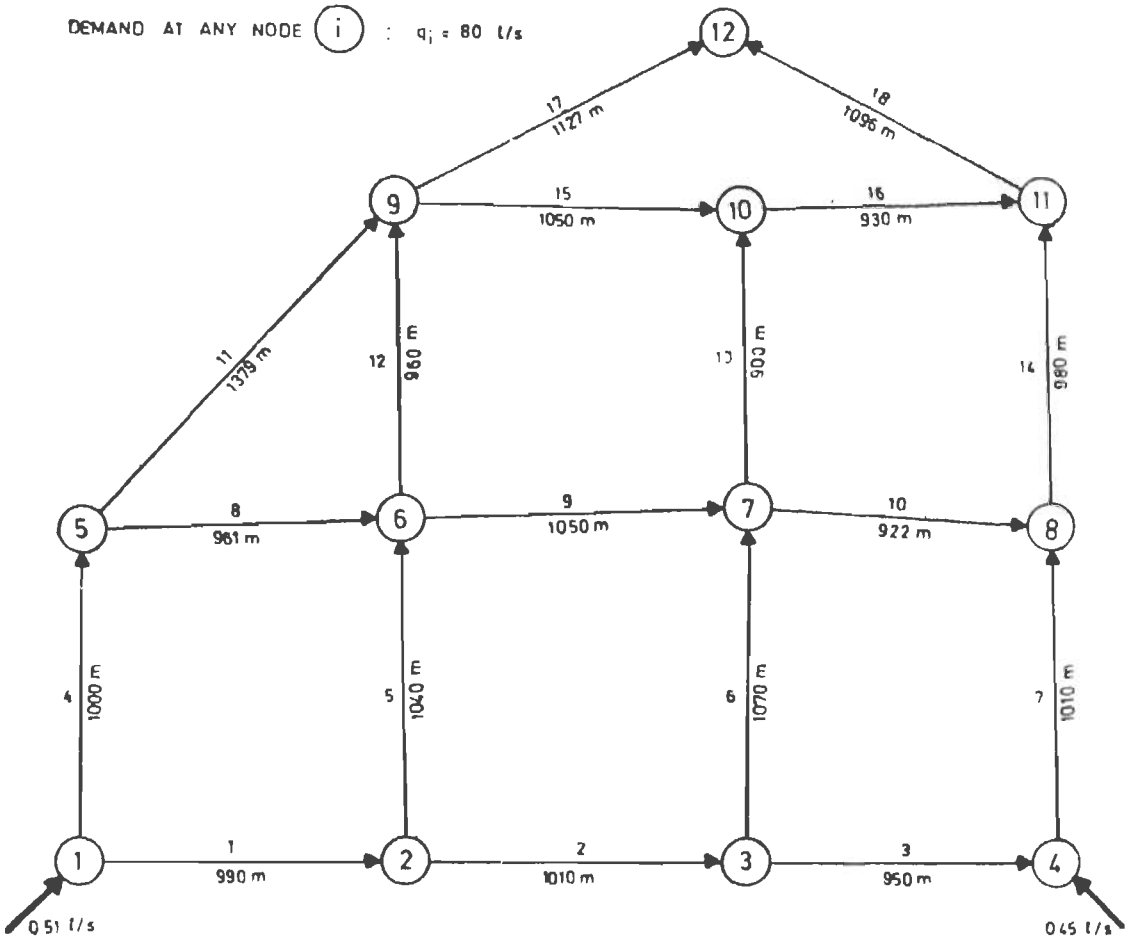

FIGURE 1 : Network designations.

TABLE I

node i	(input) 1	2	3	(input) 4	5	6	7	8	9	10	11	12
p_i m	(300)	202	203	(310)	205	206	207	208	209	210	211	212

derivation of the mathematical concept was dropped and replaced by Prandtl-Colebrook, Equation (12), using an iteration routine. Viscosity of the water is $\nu = 1.31 \times 10^{-6}$ m²/sec and the roughness $r = 0.0004$ m (cement lining) for any diameter. The minimum pressure requirements at the nodes are given in Tables I & II.

Pumping costs are computed using an energy price of $c^P = 0.1$ DM/kWh and an overall efficiency factor of $\eta = 0.7$ to pump the daily mean q_i/p_j during a design period of $\tau = 20$ years. Considering a discount rate of $z = 8$ percent, the present value factor obtains to $v = 9.818$. The lump sum pumping cost, expression (31),

TABLE II

Capital cost including instalment of the pipes according to[10].

Diameter m	Cap. cost DM/m	Diameter m	Cap. cost DM/m	Diameter m	Cap. cost DM/m
0.080	48.0	0.250	110.8	0.500	249.0
0.100	52.0	0.300	134.0	0.600	307.0
0.125	58.3	0.350	160.0	0.700	355.0
0.150	64.5	0.400	185.0	0.800	400.0
0.200	87.5	0.450	217.0	0.900	564.0

follows to :

$$c_j^p = \alpha \frac{\gamma c^p p_f}{\eta} = (10^3 \times 9.818 \times 365 \times 24 \times 0.1 \times 0.2)/$$
$$(102 \times 0.7 \times 5.0) = 2.407 \times 10^4$$

The minimum flow requirement for the chords was chosen to be greater than 5 l/sec with a corresponding diameter of either 0.080 m or 0.100 m depending upon the optimal head losses generated in the tree.

Based on engineering judgement the branches 1, 3, 4, 7 were assigned the property to be main trunks and members of any tree in order to reduce the number of possible trees, expression (8), in the graph of Figure 1.

The optimization concept requires that any branch consists of $k = 1, \ldots, K$ sections of increasing diameter size. The minimum diameter size was chosen to be 0.1 m. The ten sections ($K = 10$) (Table III) correspond to a capacity range such that the smallest flow and the smallest diameter yield a head loss in the order of 80—100 m, and that the head loss generated by the largest flow and largest diameter is < 1 m for any branch.

4.2 *The Algorithm*

The algorithm encompasses the following steps :

(1) Determination of the tree configurations by evaluating the possible combinations of $(NN-1)$ columns representing E out of NP columns of A according to Equation (4) considering the preassig ed tree branches.

(2) Computing the flows in the tree branches using Equation (10) and assuming zero flows in the chords.

(3) Selecting ten standard diameter sizes for any branch of the tree according to the range of the flows in Table III.

(4) Solving the *LP*, i.e., either expression (26)—(29) for minimum capital cost only or expression (32) and (27)—(29) if pumping costs are to be added.

(5) The results are the optimal diameters for any branch and the associated head loss distribution in the network and/or pressure potentials for any mode.

(6) The pressure potential differences between nodes that are connected by chords constitute an input as head loss constraints for a second *LP* run.

(7) The flows for the second *LP* run are computed by introducing the chord flows into Equation (10) that are based upon the head loss constraint of point 6 using either a 0.08 m or 0.10 m chord diameter to generate a flow close to 5 l/sec.

(8) If the pressure potential difference of point 6 is not sufficient to generate a chord flow $\geqslant$ 5 l/sec a head loss constraint is introduced into the second *LP* run corresponding to a 5 l/sec flow and 0.10 diameter size.

(9) The *LP* is solved a second time.

4.3 *Results*

The total number of trees of the example graph equals 5407. Preassigning the tree branches Nos 1, 3, 4, 7 reduces the number of trees to 801 that are produced in a systematic sequence according to the combinations of $(NN-1)$ elements out of a set of NP branches corresponding to Equation (4). The optimization routine was applied to any tree encountered. The results are shown in Figures 2 & 3 covering a reach of 200 subsequent trees. Figure 2 displays capital cost only (Case I), and Figure 3 includes pumping cost (Case II). Each figure indicates the total cost of the entire network and the cost of the tree only, without the chords. The cost curves are interrupted if the *LP* solutions are infeasible because of the artificial head loss constraint introduced to guarantee minimum flows in the chords. Since the total cost and the cost of the

TABLE III

Flow range m³/sec	Diameter m									
	$k = 1$	2	3	4	5	6	7	8	9	10
0=0.041	0.1	0.125	0.15	0.20	0.25	0.30	0.35	0.40	0.45	0.50
0.041-0.067	0.125	0.15	0.20	0.25	0.30	0.35	0.40	0.45	0.50	0.60
0.067-0.128	0.15	0.20	0.25	0.30	0.35	0.40	0.45	0.50	0.60	0.70
0.128-0.230	0.20	0.25	0.30	0.35	0.40	0.45	0.50	0.60	0.70	0.80
0.230-1.00	0.25	0.30	0.35	0.40	0.45	0.50	0.60	0.70	0.80	0.90

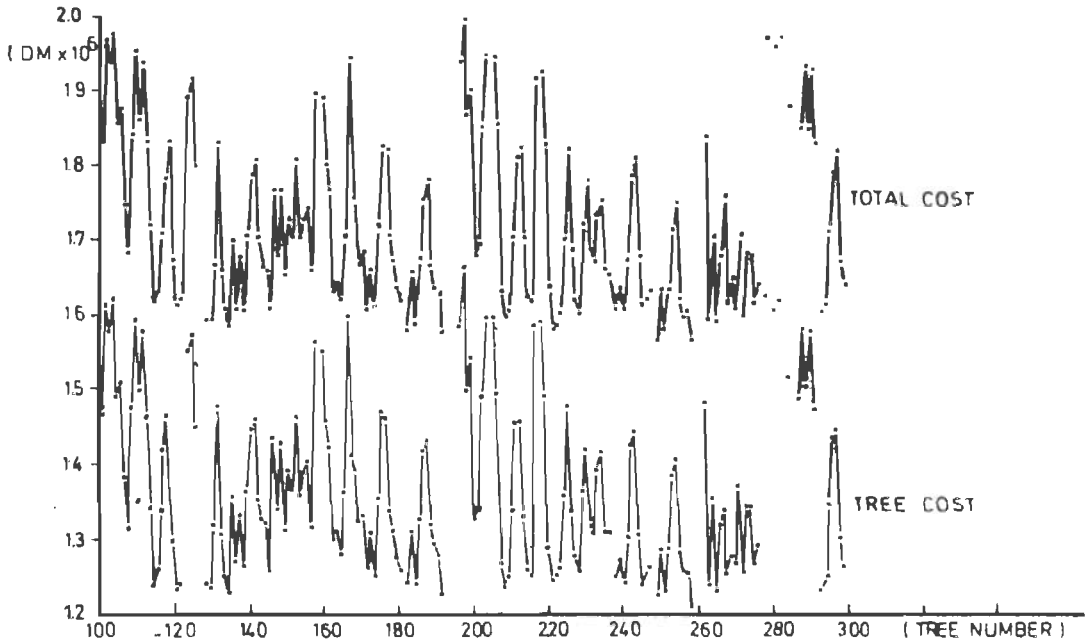

FIGURE 2 : Capital cost.

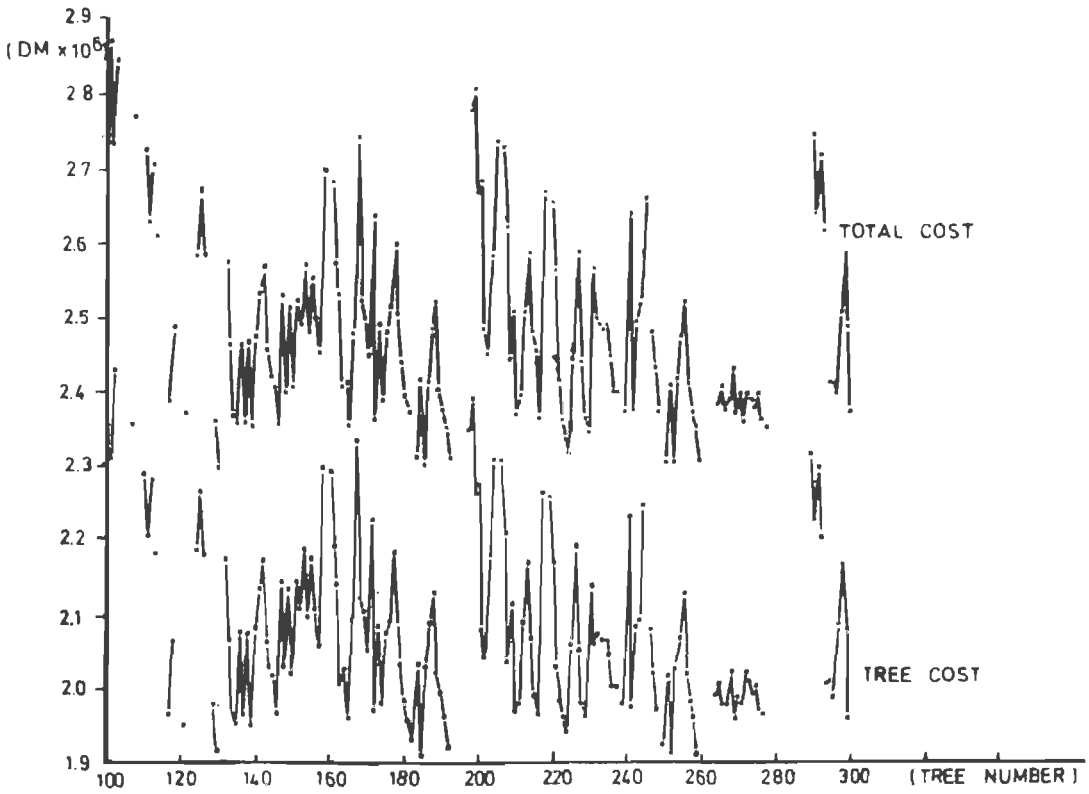

FIGURE 3 : Capital and pumping cost.

tree only run almost parallel it may be an expedient and computation saving alternative to omit the chords in order to find optimal tree configurations.

The cost curves of Figures 2 & 3 give the impression of random fluctuations inspite of the systematic derivation of the tree configurations. However, the fluctuations are clearly limited within a reach displaying cost deviations of < 25 percent in Case I and of < 20 percent in Case II.

Figures 2 & 3 also indicate that local optimal solutions at about the same cost level occur based on rather different flow configurations. In practice, the final choice of different designs will depend on other social, environmental, political criteria given an equal level of engineering costs. For example, Figures 4 & 5 show the three best solutions for Case I and II.

The total costs of the ten best solutions for Case I and II are summarized in Table IV. Again, through the response surface appears smooth, the flow configurations and distribution of optimal diameter sizes vary substantially in these solutions. The total computation time for Case I was ~ 45 min. and for Case II ~ 55 min., respectively, using the UNIVAC 1108 of the University of Karlsruhe.

4.4 *Random Search*

For large networks the computational volume may increase significantly. As an abbreviation of the previous algorithm, a random search has been successfully employed based on a principle by Rechenberg[11] which comprises the following steps :

(1) Random sample of the combinations of $(NN-1)$ columns, representing E, out of NP columns of A according to Equation (4) and selecting the included trees.

(2) Applying the previous algorithm to obtain a number (e.g., 10) of the best local minima.

(3) Checking for common tree branches contained

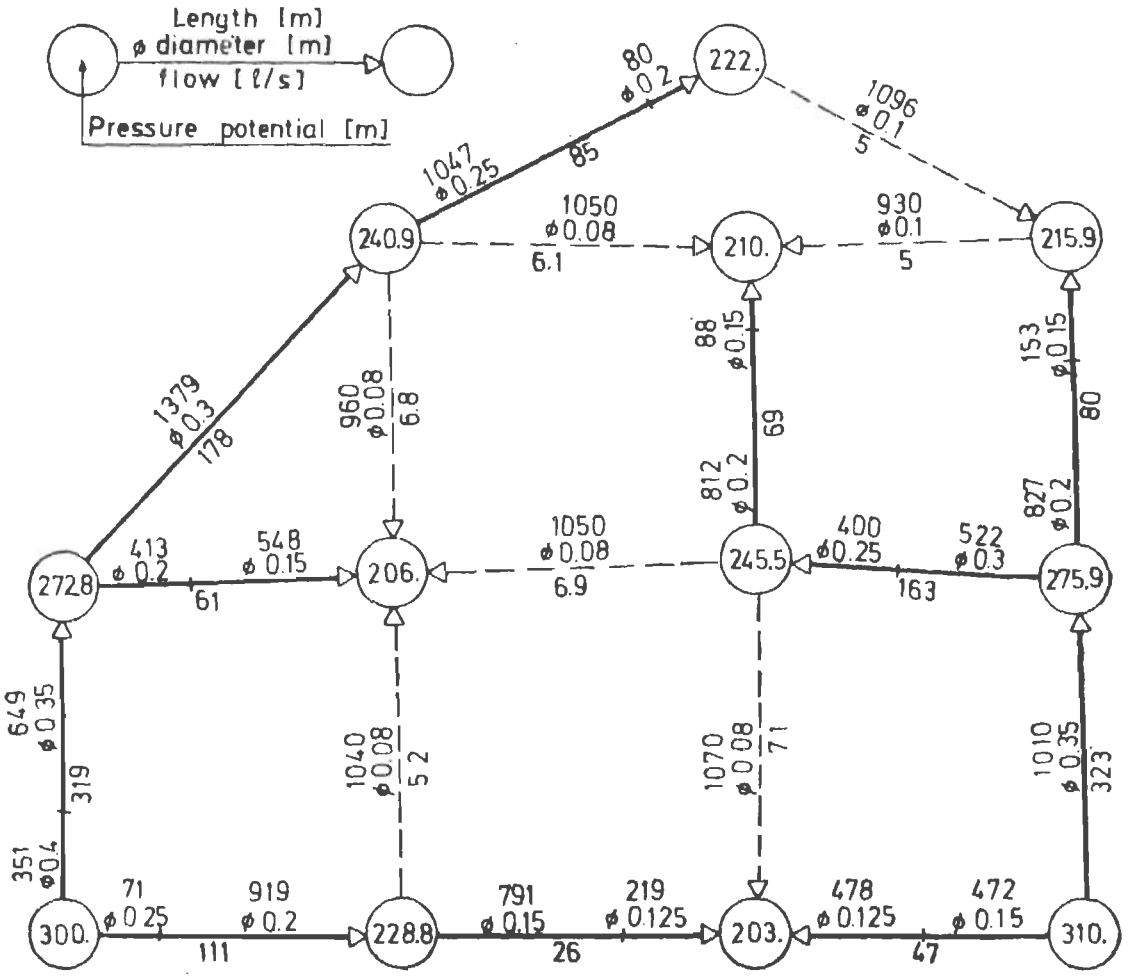

FIGURE 4 : Case I—Capital cost—Best solution.

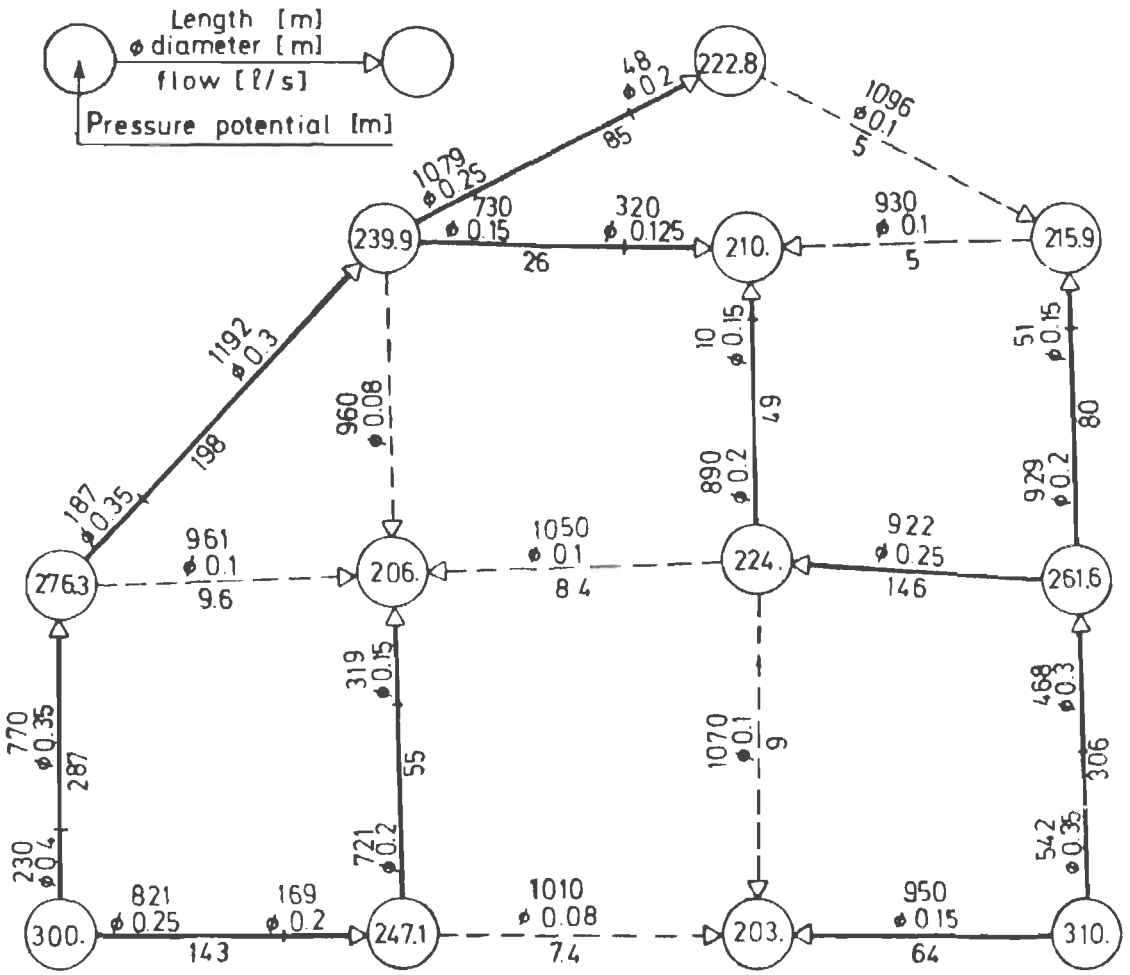

FIGURE 4 (Contd.) : Case I—Capital cost—Second best solution.

TABLE IV

Total cost 10^6 DM		
No.	Case I	Case II
1	1.547	2.298
2	1.567	2.302
3	1.569	2.304
4	1.573	2.306
5	1.578	2.308
6	1.580	2.309
7	1.581	2.311
8	1.582	2.313
9	1.582	2.314
10	1.584	2.317

in the best solutions.

(4) The common branches are preassigned as tree branches in a subsequent random sample (and/or total evaluation if the number of possible combinations is sufficiently reduced by the preassignment).

In the example the global optimum was obtained saving about half of the computation time. The efficiency of the random method suggested that even for large networks a global or near-to global solution can be derived with reasonable computation time.

5. Conclusions

A tractable method to design cost-optimal water supply networks is not available in practice. Research results show either preventive numerical intricacy, produce non-standard diameter sizes, are restricted to

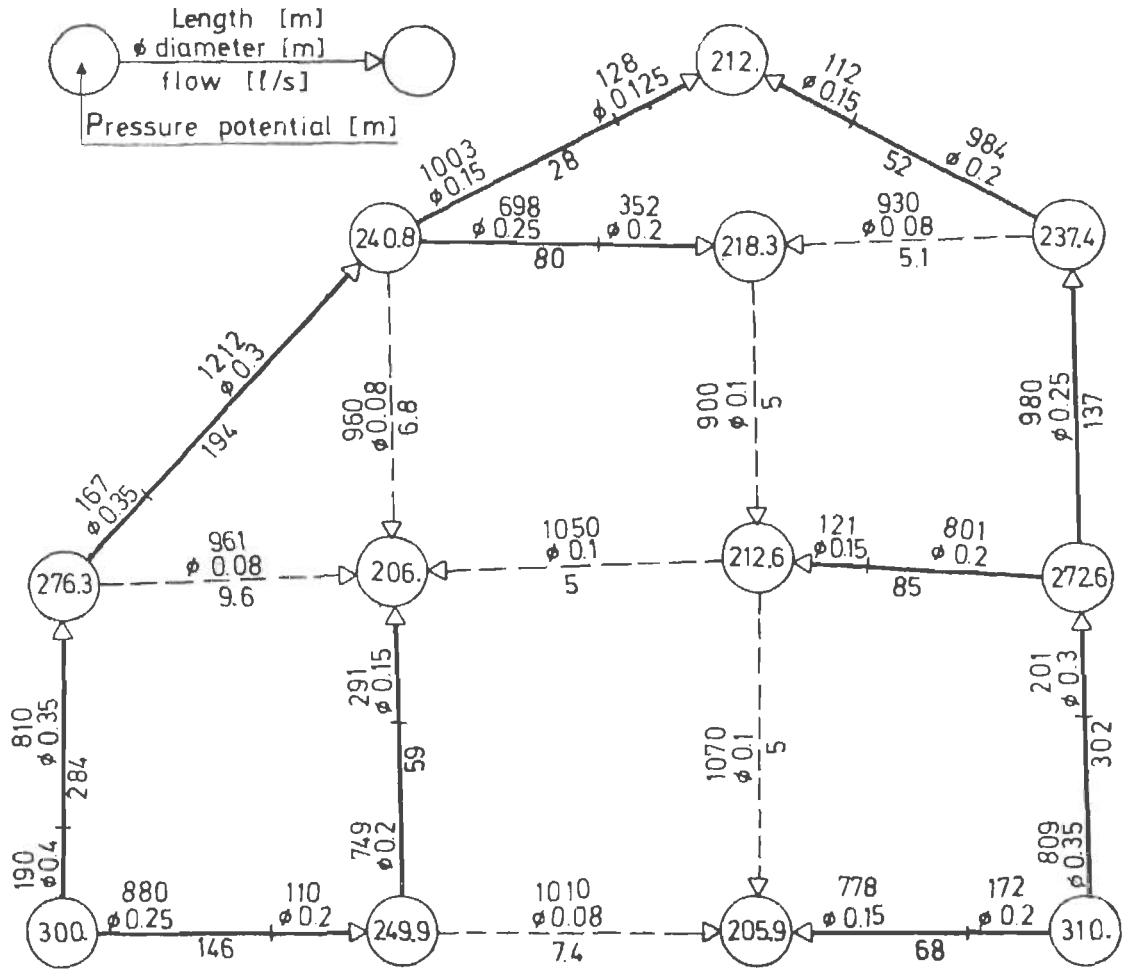

FIGURE 4 (Contd.) : Case I—Capital cost—Third best solution.

branch networks, or yield local suboptima. The general formulation of the problem is to find optimal standard diameter sizes that minimize capital and pumping cost. Given is the graph of the network, a steady state demand at the nodes, input flow and pressure potentials, minimum flow and/or diameter requirements for any branch, and minimum pressure requirements for any node. The algorithms of the proposed model use Linear Algebra and Linear Programming only.

It can be shown that a branch consisting of two subsequent standard diameter sizes is adequate to fulfil any consistent hydraulic condition imposed upon the branch. The associated costs are a concave function of the flow in the branch. The resulting economies of scale with respect to the flows lead to a concentration of the flows in main trunk lines of the network. Consequently, tree configurations from graph theory develop as the basis of local minima assuming minimum flows in the chords.

The flows in any tree are determined by a set of linear equations. Dividing any branch into a sequence of standard diameter sizes according to the size of the flow the lengths of the sections are introduced as variables in the following Linear Program. The optimal solution of the *LP* for any tree consists of at most two diameter sections.

The capital cost of a standard diameter section is a linear function of the length of the sections. The same holds for pumping costs being proportional to the

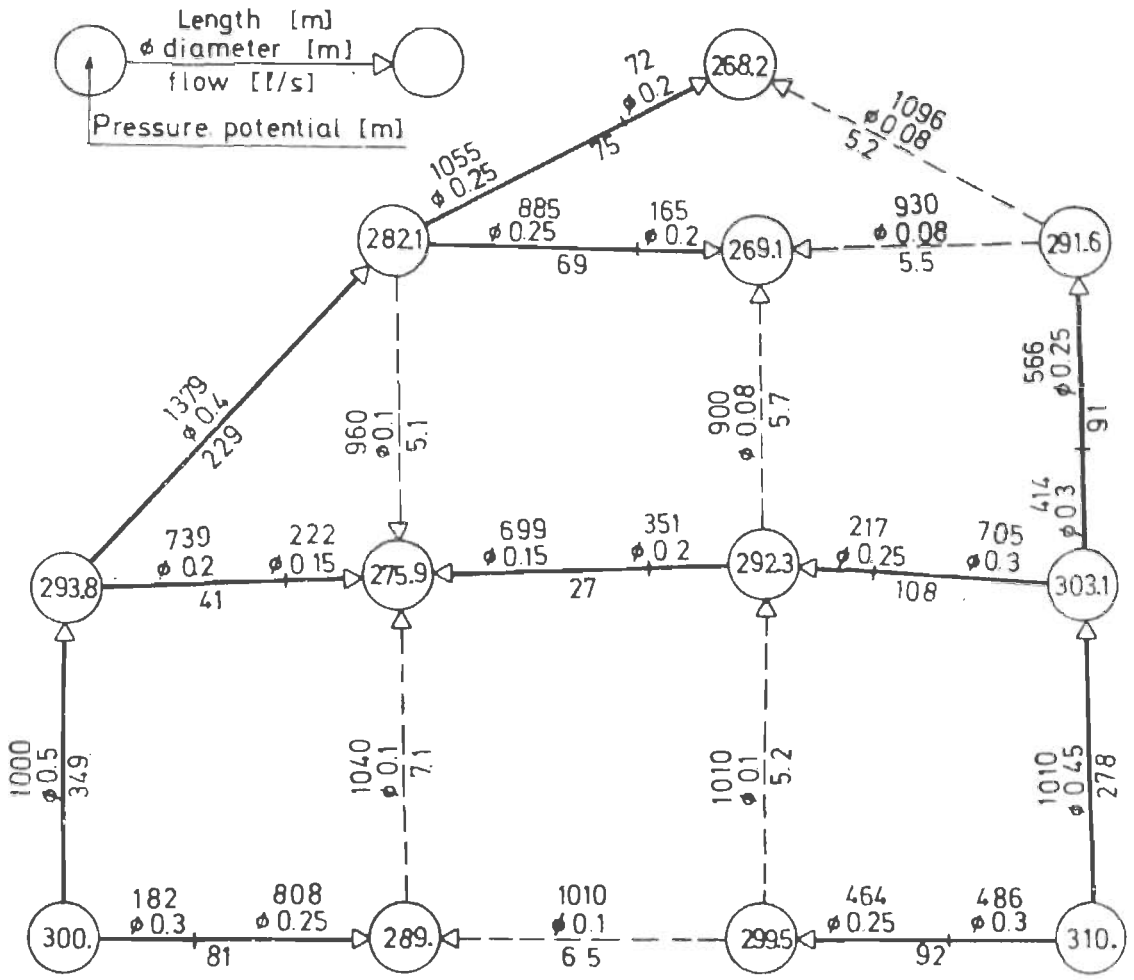

FIGURE 5 : Case II—Capital and pumping cost—Best solution.

energy loss which corresponds to the product of flow and head loss in any branch. The flows are known and the head losses are likewise linear functions of the lengths of the assumed sequence of diameter sections. Constraints of the *LP* observe minimum pressure requirements formulated as maximum admissible head losses, the head loss balance for any loop of the network, the total length for any branch. The result of the *LP* are (at most two) optimal standard diameter sizes for any tree configuration. Comparing the solution of all possible trees of the network graph yields the global optimum.

The number of trees in a graph may be substantial, but is reduced by preassigning a number of branches of the network as permanent tree members. The preassignment can be based on engineering judgement.

As an alternative the abbreviation of a random sampling approach of tree configurations was introduced. Recurring tree branches in the optima of the random sample are subsequently employed as preassigned tree branches. For the reduced sample size, the random procedure is repeated or a complete evaluation performed if the sample size was sufficiently small. The results indicated the same global solution of the original approach with less computation time. For large problems the random approach is considered an expedient alternative.

6. Acknowledgement

The programming assistance and constructive suggestions of Gerhard Krauter were appreciated. The work was indirectly supported during research on Water Quality Models sponsored by the German Ministry of the Interior.

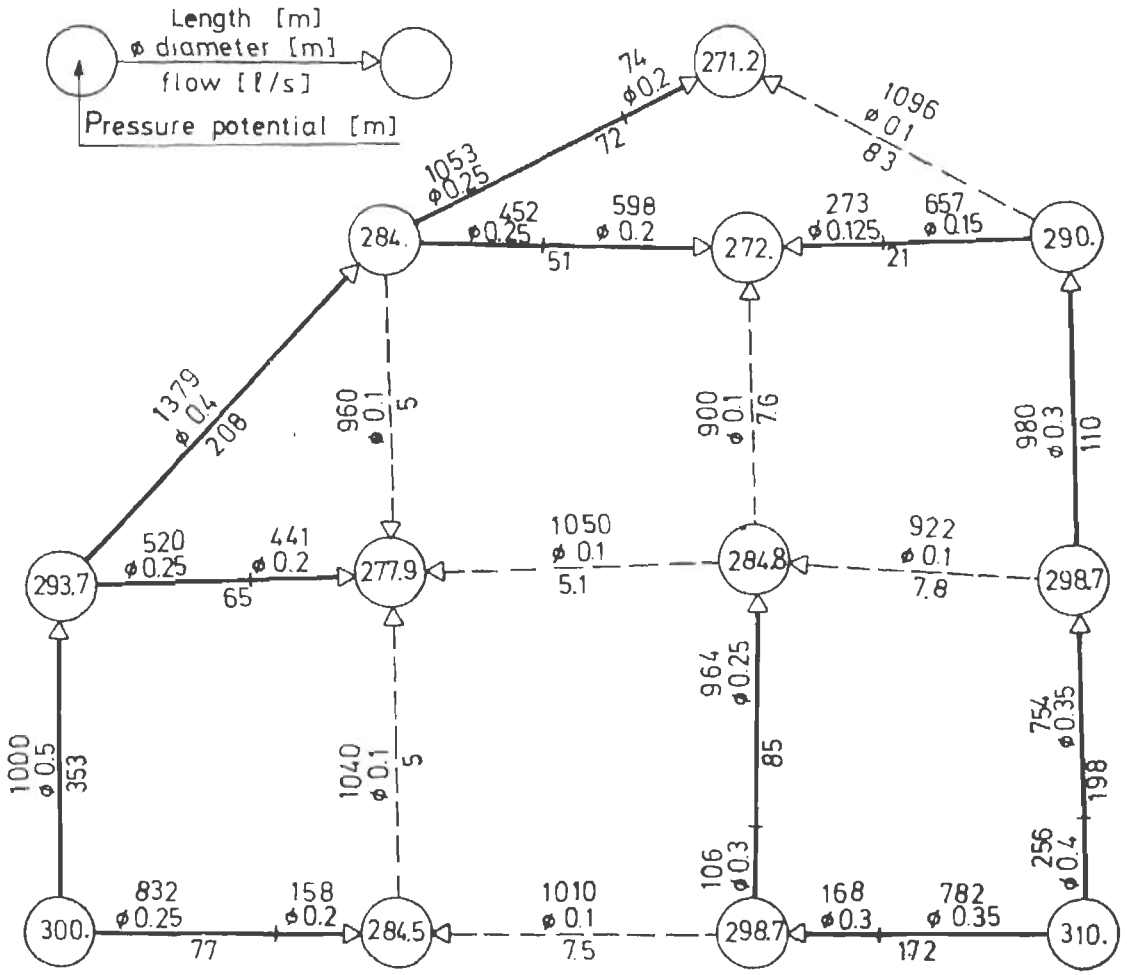

FIGURE 5 (Contd.) : Case II—Capital and pumping cost—Second best solution.

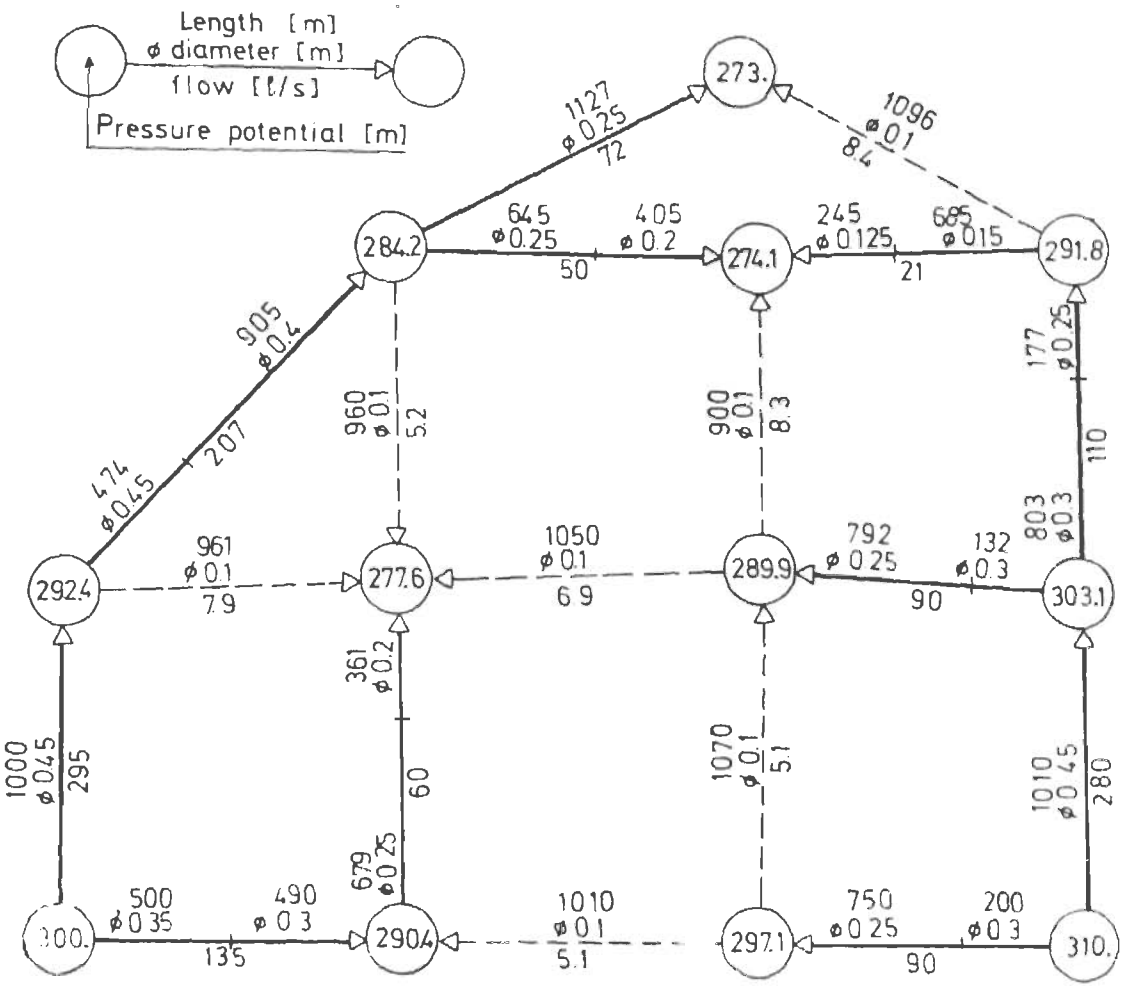

FIGURE 5 (Contd.) : Case II—Capital and pumping cost—Third best solution.

7. References

(1) JACOBY, L.S. : "Design of Optimal Hydraulic Networks." Jour. Hydr. Div. Proc. ASCE, Vol. 94, HY 3, 1967.

(2) SMITH, D.V. : "Minimum Cost Design of Linearly Restrained Water Distribution Networks." M.I.T., Cambridge, Mass., 1966.

(3) CEMBROWICZ, R.G. : "Capital-Cost Minimization of Hydraulic Networks." Jour. Hydr. Div. Proc. ASCE, Vol. 99, HY 3, 1973.

(4) GUPTA, F. ; HASSAN, M.F. and COOK, J. : "Linear Programming Analysis of a Water Supply System with Multiple Supply Points." Trans. Amer. Inst. Ind. Eng., 4 (3), 1972.

(5) BERGE, C. and CHOUILA-HOURI, A. : "Programming Games and Transportation Networks." Methuen and Co. Ltd., London, U K., 1956.

(6) TRENT, H.M. : "A Note on the Enumeration and Listing of all Possible Trees in a Connected Linear Graph." Proceedings of National Academy of Science, Vol. 40, No. 10, 1954.

(7) FAIR, G.M. ; GEYER, J.C. and OKUN, D.A. : "Water and Wastewater Engineering." Vol. 1, John Wiley and Sons, New York—Sidney—London, 1966.

(8) McPHERSON, M.B. : "Distribution System Equalizing Storage Hydraulics." Jour. Hydr. Div. Proc. ASCE, Vol. 99, HY 3, 1973.

(9) CEMBROWICZ, R.G. : "Mathematical Model of a Water Supply System Under Fluctuating Demand." Harvard University, Environmental Systems Program, 1971.

(10) SCHNAPAUFF, J. : "Aachener Kurve in der Praxis." gwf., Wasser-Abwasser, Heft 18, 1968.

(11) RECHENBURG, I. : "Evolutionsstrategie—Optimierung technischer Systeme nach Prinzipien biologischer Evolution." Fromann Verlag, Cannstadt—Stuttgart, 1973.

Water Conveyance Capacity of Channels with an Ice Cover

S. P. CHEE
Professor of Civil Engineering
University of Windsor
Windsor, Ontario, Canada.

SYNOPSIS

The discharge capacity of an ice covered channel is studied analytically and with the aid of experiments. The flow of water in an open channel with an ice cover simulates pressure flow in a closed conduit with respect to the velocity profile and the presence of retarding boundaries around the entire wetted perimeter. The mechanics of the flow also resemble open channel hydraulics in that it possesses the freedom to adjust its top surface. Owing to the dual nature of the phenomenon, a two horizontal cell flow concept is invoked to derive the resistance equation relating the discharge to the roughnesses of the ice cover and channel bed, hydraulic radius, conveyance section and energy gradient. A formula giving the overall roughness coefficient of the ice covered channel in terms of the ice and channel rugosities has also been obtained. The theoretical findings are verified in laboratory channels using polyethylene plastic, which has a specific gravity very close to natural ice, to simulate an ice cover.

Introduction

The conveyance of water in an open channel in countries which have a long winter presents problems when an ice cover forms and remains in the channel for an extended period of the year. If the stream depth is shallow, a considerable portion or even the entire cross-section could be frozen. Under these conditions it is no longer valid to ignore the presence of the ice cover in the computation of the flow rate. For the proper planning of water resources projects which require predetermined flow quantities throughout the year it is essential to know the capacity of channels with a top constraint imposed on the upper boundary of the flow.

The formation of an ice cover begins with the thickening of ice sheets and also the gradual massing together of ice floes into a large cover with its thickness increasing in the downstream direction. The cover increases in size with the accumulation of ice blocks on the upstream leading edge; this phenomenon will take place only if the ice cover has attained a certain thickness otherwise the ice blocks will dive under the ice canopy giving rise to undercover ice runs. The ice discharge, under certain conditions could form hanging ice dams. Kivisild[1] set forth the hydraulic conditions for the required thickness of the ice cover necessary for its progressive growth upstream. The present paper deals with the discharge capacity of open channels when a solid stable ice cover has been formed.

Experimental Program

A series of hydraulic models were used to determine the conveyance of channels with an ice cover. A 0.45 m wide × 0.61 m high channel was utilized initially for the basic observations and a 1.52 m wide × 1.22 m high flume was employed to extend the range of the observations. Within the latter 1.52 m wide basin, channels of various cross-sections were moulded including uniform and composite sections. Plexiglass, timber, and sand-cement mixes were employed in fabricating the channels.

Centrifugal pump-motor units with discharge capacities of up to 0.16 m^3/s were used to circulate the water. Measurements of water elevations were made by point gages and manometers. Pitot tubes were used to make velocity traverses. An electronic flow recorder and sharp edged *V*-notch and rectangular weirs were available to meter the flow.

To simulate natural ice, polyethylene plastic pellets and sheets with a specific gravity very close to ice, were used. A calibrated hopper located at the inlet end of the channel was also used to feed the polyethylene pellets into the streamflow. A stable ice cover was first formed before readings were taken.

Whenever desirable, photography was made use of to record flow conditions in the channel. This method was particularly useful to delineate the roughness profiles of ice covers.

Analysis

In an ice covered channel, the ice imposes an additional top constraint on the flow resulting in a change of velocity distribution from a free surface velocity profile with the maximum velocity filament close to the surface to one resembling closed conduit flow with its maximum located near mid-depth and no slip conditions at the bottom and top in addition to the other parts of the wetted perimeter (Figure 1). The ice cover bottom surface would have a different roughness to the channel. The ice roughness would also vary with the age of the cover and the presence of floating ice blocks. The increased wetted perimeter and roughness would result in a larger flow depth.

The dynamic flow resistance equation is first developed relating the shear stresses around the wetted perimeter to the flow parameters. Consider the longitudinal channel reach and flow cross-section illustrated in Figure 2. The assumptions of relatively small bed and water slopes are invoked. Using the notation given in Figure 2 and by Newton's second law of motion, the following dynamic equation can sensibly be written,

$$\gamma A\, d(z+y) - (\tau_c P_c\, dx + \tau_i P_i\, dx) = \rho A\, v \frac{dv}{dx} dx \qquad \ldots(1)$$

in which the terms have the following meanings :

$\gamma A\, d(z+y)$ = total gravity forces

$\tau_c P_c\, dx$ = shear resistance of the channel

$\tau_i P_i\, dx$ = shear resistance of the ice cover

$\rho A\, v \frac{dy}{dx} dx$ = mass accelerating force

γ = unit weight of water; A = flow area; z = elevation of bed from a fixed datum ; y = distance of the water surface referred to the channel bed ; τ_c = mean shear stress of the channel ; τ_i = mean tangential shear stress acting on the bottom surface of the ice cover; P_c = wetted perimeter of the channel; P_i = wetted perimeter of the ice cover ; dx = short section of channel ; ρ = density of water ; v = mean flow velocity ; dv = small change in velocity.

With the coordinate system used in Figure 2, $d(z+y)$ is negative and putting in the proper sign and solving

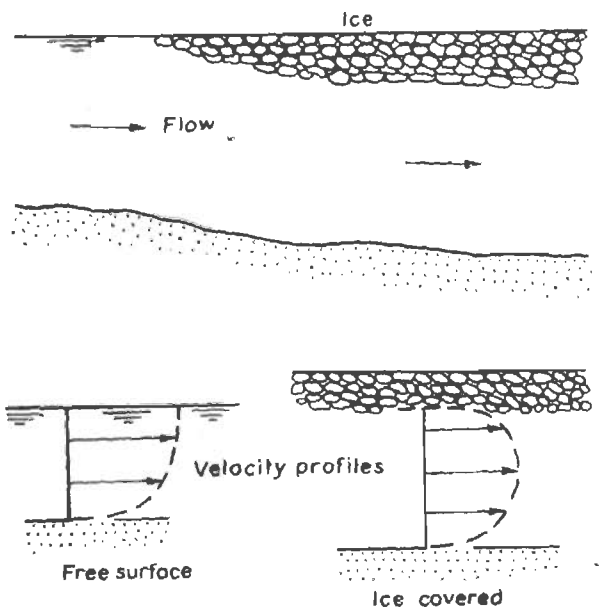

FIGURE 1 : Ice covered flow.

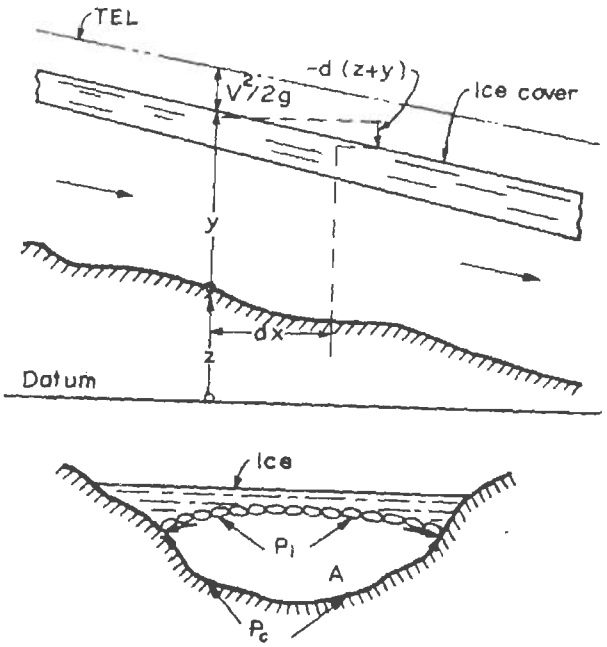

FIGURE 2 : Definition sketch.

for the resisting shear forces per unit channel length,

$$(\tau_c P_c + \tau_i P_i) = -\gamma A \left[\frac{d(z+y)}{dx} + \frac{v}{g} \frac{dv}{dx} \right] \quad \ldots (2)$$

Dividing Equation (2) by the total wetted perimeter $P=(P_c+P_i)$ and noting that $\frac{v}{g} \frac{dy}{dx} = \frac{d}{dx}\left(\frac{v^2}{2g}\right)$, and $R = A/P$ = hydraulic radius,

$$(\tau_c P_c + \tau_i P_i)/P = -\gamma R \frac{d}{dx}\left(z+y+\frac{v^2}{2g} \right) \quad \ldots(3)$$

or $$\tilde{\tau} = \gamma R S \quad \ldots(4)$$

in which $\tilde{\tau}=(\tau_c P_c + \tau_i P_i)/P$=average shear stress over the entire wetted perimeter; $S = -\frac{d}{dx}(z+y+v^2/2g)$ =energy gradient,

and $$\tilde{\tau} P = \tau_c P_c + \tau_i P_i \quad \ldots(5)$$

The shear resistance dynamic equation is embodied in Equation (4). The resisting shear force components are given in Equation (5).

Before the discharge of an ice covered channel could be computed, it would be necessary to develop an equation relating the total roughness coefficient, n, in terms of the roughness of the channel, n_c, and the rugosity of the base surface of the ice cover, n_i. Based on the velocity profile, the concept of two cell flow is postulated as shown in Figure 3 in which one cell lies above the other.

Employing this theory, the hydraulic radii could be expressed as $R = A/P$; $R_c = A_c/P_c$, and $R_i = A_i/P_i$; $A = A_c + A_i$. The rate of energy dissipation, S, could also be obtained from the Manning equation,

$$S = v^2 n^2/2.22\ R^{4/3} \quad \ldots(6)$$

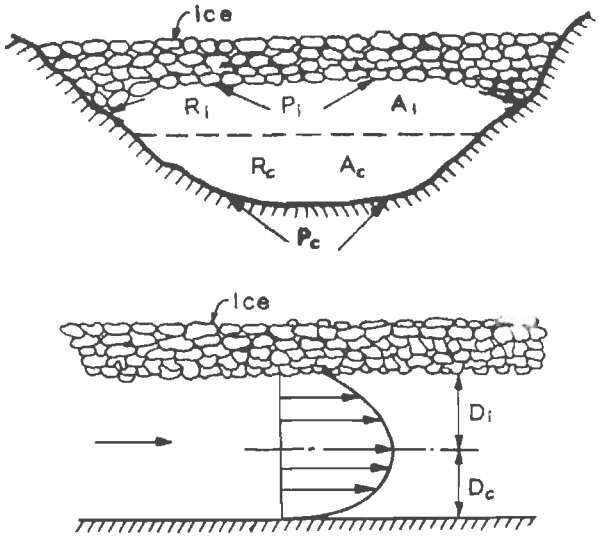

FIGURE 3 : Two cell flow.

Combining Equations (4), (5) & (6),

$$\frac{n^2}{R^{1/3}} P = \frac{n_c^2}{R_c^{1/3}} P_c + \frac{n_i^2}{R_i^{1/3}} P_i \quad \ldots(7)$$

Using the wide channel approximation in which, $P_c = P_i = P/2$; $R = (R_c + R_i)/2$ and $R_c = R_i = R$; Equation (7) on substituting these values gives,

$$n = \frac{n_i}{2^{1/2}} [1 + (n_c/n_i)^2]^{1/2} \quad \ldots(8)$$

The value of the total roughness coefficient as given by Equation (8) could be used in the Manning equation to determine the discharge, Q, of an ice covered channel, namely,

$$Q = \frac{1.49}{n} A R^{2/3} S^{1/2} \quad \ldots(9)$$

If the assumption that $R = R_c = R_i$, which was used to derive Equation (8), is not employed, an equation relating n with the ratio n_c/n_i could be found, for the condition of maximum discharge, by differentiating Equation (7) and setting $dn/d(n_c/n_i) = 0$. Performing this operation and solving explicitly for n, would give the equation,

$$n = \frac{n_i}{2^{2/3}} [1 + (n_c/n_i)^{3/2}]^{2/3} \quad \ldots(10)$$

Results and Discussion

The material employed in the laboratory to simulate natural ice was polyethylene plastics used in the form of sheets, blocks, and pellets. The coefficient of friction of the material was first determined for the case of smooth sheets, which would be different when used in the form of random blocks and pellets. The equation obtained by Alien and Chee(2) for smooth painted sheet metal followed very closely that for polyethylene sheets,

$$f = 0.124\ (VR/v)^{-0.17} \quad \ldots(11)$$

in which f = Darcy's friction factor; v = kinematic viscosity of the fluid. Except otherwise noted, equations and units are given in the FPS system.

In the series of experiments in which a prismatic channel was used, the flume was made of timber on one side and plexiglass on the other. The friction factor of the rectangular channel was found to fit the equation obtained by Allen(3) using a flume with glass on one side and smooth pine on the other wall,

$$f = 0.0936\ (VR/v)^{-0.16} \quad \ldots(12)$$

The Darcy friction factor, f, is related to the Manning equation by,

$$n = 0.093\ f^{1/2} R^{1/6} \quad \ldots(13)$$

The channels in which composite sections were used were moulded from sand-cement mortar utilising templates to obtain the desired configuration. The value

of Manning's n for the skin friction coefficient for these channels is 0.013.

Before the evaluation of the conveyance capacity of stream channels with an ice cover is considered, the roughness coefficient of these channels should first be calculated. The computation of the roughness of channels with compound rugosities such as an ice cover has been derived and given by Equations (8) & (10) based on different assumptions. Equation (10) was derived on a method postulated by Pavlovskii as reported by Chow[4] by setting $dn/d\,(n_c/n_i) = 0$ but with different assumptions with regard to the hydraulic radius of the ice covered channel. In Pavlovskii's derivation, he assumed that the hydraulic radius of the ice covered channel is the sum of the hydraulic radii due to the channel bed and that due to the ice cover. With this assumption that $R = (R_c + R_i)$ and putting

$$dn/d(n_c/n_i) = 0,$$

the equation obtained for wide channels is,

$$n = \frac{n_i}{2^{1/2}} \left[1 + (n_c/n_i)^{3/2}\right]^{2/3} \qquad \ldots(14)$$

Equation (14) is not in total agreement with Equation (10). However, if $n_c = n_i$, then, $n = n_c = n_i$ as it should be and this result would be given by Equations (8) & (10) but a different conclusion would be reached with Equation (14).

Equations (8) & (10) were tested by comparing the calculated values of Manning's n obtained from these equations with the experimental values. These formulae gave close agreement with the observed results to an accuracy of ± 5 percent. The results obtained from Equation (8) differed by approximately 2 percent from that of Equation (10). These results indicated that the assumption of two cell flow which was used in its derivation has been justified. Equation (14) would give results incompatible with their physical interpretation.

Computation of the discharge capacity of ice covered streams can be obtained relative to the channels when they are free of ice. Let suffix "i" when attached to flow parameters refer to the case of an ice covered channel, and its absence denote flow free from ice. Then, by Manning's equation and using the assumption that $R = 2R_i$ for the condition $D_i = D$, $S_i = S$,

$$Q_i/Q = 0.63\,(n/n_i) \qquad \ldots(15)$$

Equation (15) gave reasonable agreement with experimental observations to an accuracy of ±15 percent. The main discrepancy was due to the assumption that $S_i = S$ which was not fully valid.

Conclusions

(1) The treatment of the problem of ice covered channels by taking the total force retarding the flow as equal to the resisting forces due to the channel and ice cover has made possible the derivation of an equation relating the total channel roughness coefficient to the individual rugosity factors of the ice cover and that of the channel without the ice.

(2) Applying the concept of two cell flow to the ice covered stream with a top retarding surface has enabled an equation for the total roughness coefficient to be readily computed.

(3) The conveyance capacity of ice covered streams can be determined relative to the flow without the ice by making the assumption that the energy slope remained the same after formation of the cover with reasonable accuracy.

Acknowledgement

The research grant provided by the National Research Council of Canada is gratefully acknowledged.

References

(1) KIVISILD, H. R. : "Hanging Ice Dams." Proceedings, Vol. III, I.A H.R. Eighth Congress, Montreal, August 1959, pp. 1-S1-1—1-51-3.

(2) ALLEN, J. and CHEE, S. P. : "The Resistance to the Flow of Water Round a Smooth Circular Bend in an Open Channel." Proceedings, Instn. Civ. Engrs., Vol. 23, November 1962, pp. 423-434.

(3) ALLEN, J. : "Streamlining and Turbulent Flow in Open Channels." Phil. Mag., S7, Vol. 17, No. 116, June 1934, pp. 1081-1112.

(4) CHOW, V. T. : "Open-Channel Hydraulics." 1st Edition, McGraw-Hill Book Co., Inc., 1959, pp. 137-138.

Inflatable Dams for Irrigation Projects

H. O. ANWAR
Principal Scientific Officer
Hydraulics Research Station, Wallingford, England.

SYNOPSIS

An inflatable dam provides an inexpensive and simple device for raising and controlling the water-level in a river or canal. The dam is inflated with air or air and water and anchored to a concrete foundation slab, or inflated with water alone and either anchored to a concrete foundation or laid directly on the bed. This paper deals, both theoretically and experimentally, with the performance of a water-inflated dam when anchored and when laid directly on the bed.

The dam was operated under both non-overflow and overflow conditions and behaved satisfactorily, provided the overflow was not high. The calculated shapes were in good agreement with the measured profiles, provided that the depth of overflow was less than half the dam height. Observations showed that a dam with high internal pressure is prone to vibration, due to the large curvature of the crest; however, a trip wire reduced this vibration by inducing aeration of the nappe. Coefficients of discharge were determined experimentally for three different shapes of dam.

Introduction

An inflatable dam constructed of a flexible but inextensible material provides a simple yet relatively cheap means of raising or controlling the water-level in a river or canal. This type of dam has the advantage that it may be used at sites where conventional dams are too costly or take too long to construct. The dam may be inflated with air or air and water and anchored to a concrete foundation, or it may be inflated with water alone and either anchored to the foundation or laid directly on the bed. When laid directly on the bed an apron of the material is extended upstream from the dam so that, under the weight of water, it provides an effective seal against underflow. The dam can be deflated when not required and produces only a small effect on flow characteristics at existing installations. A typical material for the dam, when used with an anchorage, consists of a two-ply neoprene and nylon lamination coated with hypalon. The coating is silvery in appearance and protects material from the effect of the weather. A typical material for the dam without anchorage is polyester fabric coated with PVC.

Most inflatable dams have been used under non-overflow conditions and are known to operate satisfactorily ([1-3]); there is, however, little information about their behaviour when overflow occurs. A theoretical and experimental investigation has, therefore, been conducted at the Hydraulics Research Station to determine various features of a water-inflated dam. Experimentally, the shape of the air-face and of the water-face of the dam, operating under both non-overflow and overflow conditions, was measured when the dam was (*a*) anchored to the floor of a flume, and (*b*) laid without anchorage on the bed. Good agreement was obtained between theoretical and measured shapes. The coefficient of discharge for the dam for various values of the internal water pressure was determined experimentally. It was observed that the dam anchored to the floor of the flume vibrated when the overflow was high.

Shape of Water-inflated Dam

The Air-face of the Dam—The shape of the dam, operating under non-flow condition, was calculated for a two-dimensional model. In this calculation it was

assumed that the fabric material of the dam was perfectly flexible. This assumption is reasonable since the fabric materials have a low Young's modulus. It was also assumed that the weight of the fabric itself was negligible. The shape of the air-face of the dam can be described by the following equation (See Appendix I) :

$$\frac{X}{H}+C_1 = \frac{\alpha+2\beta}{\sqrt{1+4\frac{\beta}{\alpha}}}F(\theta, K)-\alpha\sqrt{1+4\frac{\beta}{\alpha}}E(\theta, K) \qquad ...(1)$$

in which H is the height of the dam (See Figure 1), F and E are the elliptic integrals of the first and of the second kind respectively, α is the proportional pressure factor which relates the excess of the internal water pressure, P_i, to the height of the dam ($\alpha = \frac{P_i}{\rho g H}$, ρ being the density of the fluid inside the dam and g the acceleration due to gravity) ; β is a constant ($\beta = \frac{1+2\alpha}{4\alpha}$, See Appendix I). The constant C_1 can be determined from the initial condition that the face of the crest of the dam is a tangent to the x-axis at the origin, 0, of the coordinate system shown in Figure 1.

The Water-face of the Dam—It is shown in Appendix I that the shape of the water-face of the dam is a part of a circle with the radius R defined by

$$R = \frac{1+2\alpha}{4\alpha}H \qquad ...(2)$$

and is a tangent to the x-axis at the origin 0 (See Figure 1).

The periphery, S, of the air-face of the dam can be calculated from the following equation (See also Appendix I).

$$\frac{S}{H}+C_2 = -\frac{2\alpha\beta}{\sqrt{4\alpha\beta+\alpha^2}}F(\theta, K) \qquad ...(3)$$

in which C_2 is a constant and can be determined from the initial condition, namely $S/H = 0$ at the origin 0. Equation (3) has been evaluated for various values of the proportional factor α and the results are shown in Figure 2.

Equations (1) & (2) have been evaluated for three different values of α. The results of evaluation, together with those obtained from measurements (to be described subsequently) are shown in Figure 3; agreement is seen to be good. The results shown for $\alpha = 0.16$ correspond to the case in which the dam, laid without anchorage, was operating under non-overflow and also overflow conditions. These results, together with those obtained for the dam with anchorage[4], indicate that when the dam operates under overflow conditions its shape does not differ greatly from that which operates under non-overflow conditions, provided the depth of overflow

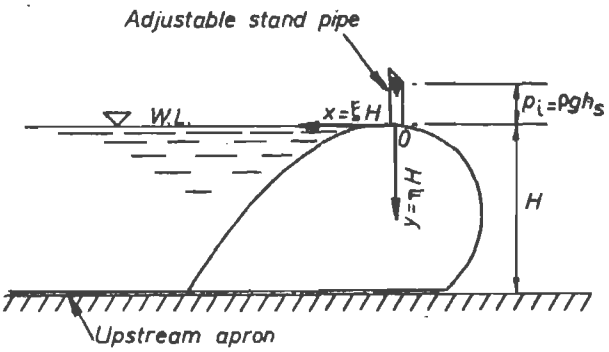

FIGURE 1 : Definition of terms for a water-inflated dam.

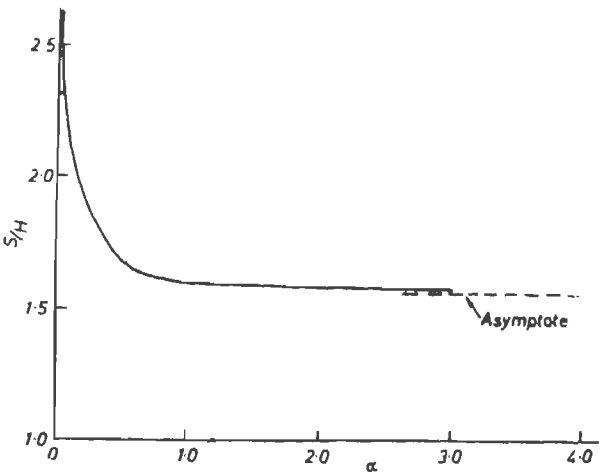

FIGURE 2 : Non-dimensional periphery S/H of the air-face of the dam.

does not exceed one-half the total height of the dam. Figure 3 further shows that the periphery of the dam and the length of its base depends on the factor α, hence on the pressure P_i and on the dam height H, for which the dam is designed. An increase in P_i or H will cause an increase in the tension of the fabric material and hence may cause failure of the dam.

Experiments

The first series of experiments was conducted two-dimensionally with the dam anchored to the floor of a glass-walled flume 0.6 m wide and 0.5 m high. The inflated dam, 0.30 m and 0.22 m high operating under non-overflow and overflow conditions respectively, was constructed of commercial polythene sheeting 0.25 m thick. The end panels were cut from the polythene sheeting to give the shape obtained from Equations (1) & (2). These end panels were welded to the polythene skin and the shape of the dam was measured using a point gauge.

When the dam was operating under overflow conditions its shape depended on the variation of pressure over the curved crest ; thus the shape of the dam varied

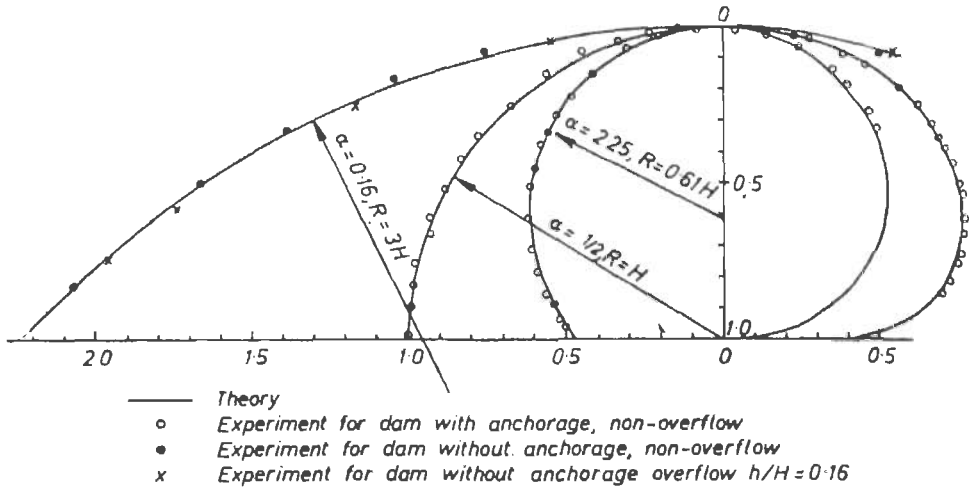

FIGURE 3 : Profiles of the water-inflated dam.

as upstream and downstream water levels varied over a wide range. It was observed that the pressure over the crest of the dam also varied periodically when the aeration of the nappe was not fully developed. This caused vibration of the dam resulting in oscillation of the upstream water-level. A trip wire of 5 mm diameter placed near the crest induced full aeration of the nappe and reduced vibration considerably.

The second series of experiments was carried out three-dimensionally in order to include end-effects which influence the dynamic behaviour of the dam. The water-inflated tube (see Figure 1) was laid with an upstream apron in a trapezoidal flume having 1:2 side slopes. The dam was 0.6 m high and about 4.50 m wide at its crest; the length of the apron was 3 m. The dam had three stand pipes along its crest, each of adjustable length, so that its height could be altered for a given overflow. The excess overflow would depress the crest of the dam causing the expulsion of water from within and thus self-deflation of the dam. The experimental results showed that self-deflation can occur when the overflow $Q > 0.4 \sqrt{2g}\, bh^{3/2}$, where b is the width of the dam, measured along the crest, and h is the depth of overflow which was equal to h_s the length of the stand pipe measured from the crest. These results were obtained when the downstream water depth was small and its effect was negligible.

The anchorage of the dam, as mentioned earlier, depends only on the pressure differences between upstream and downstream water levels. The model tests showed that the dam became unstable during self-deflation when the difference between upstream and tail-water levels was about 0.1 m. It was also observed that the dam oscillated when the tail-water-level was rising. The highest overflow depth, h, that could be obtained in the experimental set-up was about 0.15 m: Thus the overflow ratio h/H was much less than that defined before $\left[\frac{h}{H} \approx \frac{1}{2}\right]$ for the appearance of dam oscillation.

Coefficient of Discharge

The coefficient of discharge, C, was determined from the measured data. The coefficient C can be expressed by

$$C = f\left(\frac{h}{H}\right) \qquad \ldots(4)$$

The function $f(h/H)$ was determined experimentally, as shown in Figure 4. In this figure the coefficient C is plotted against overflow ratio h/H for three values of the pressure factor α. It can be seen that the value of C, as to be expected, increases with the increase of α due to the fact that dams with lower value of α have broader crests and the coefficient C is about that of a broad crest weir when $\alpha \simeq 0.16$ (See also Figure 3). The water discharge per unit width can be calculated from

$$g = Ch\sqrt{2gh} \qquad \ldots(5)$$

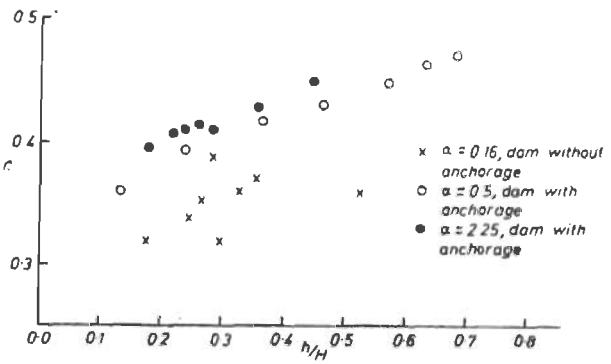

FIGURE 4 : Variation of coefficients of discharge with overflow ratio h/H.

Summary and Conclusion

An inflatable dam, constructed of a flexible but inextensible material, provides a simply, yet relatively cheap, means of raising or controlling the water-level in a river, canal, or reservoir. The dam is inflated with air or water or a mixture of the two and anchored to a rigid foundation or is inflated with water and either anchored to a rigid foundation or laid directly on the bed. When it is laid on the bed, an apron of the material is extended upstream from the dam which, under weight of water, provides an effective seal to prevent flow passing under it. The dam has stand pipes of adjustable length along its crest. The length of these pipes can be adjusted for a given overflow ; excess overflow will depress the crest of the dam causing the expulsion of water from within and thus deflation of the dam. Suitable materials for the dam are synthetic fabric coated with hypalon or PVC. Inflatable dams have been operating satisfactorily under non-overflow conditions, but there is little information about their behaviour when overflow occurs.

Equations for the profiles of a water-inflated dam have been derived when the dam is operating under non-overflow conditions. Calculated profiles are in good agreement with measured shapes. The profiles of the dam operating under overflow conditions did not differ greatly from that of the dam when operating without overflow, provided the depth of overflow was less than half the height of the dam. It was found experimentally that the dam became unstable during deflation when the difference between upstream and downstream water levels was about 0.1 m. Observation showed that the dam with anchorage vibrated under high overflow if aeration of the nappe was not fully achieved. A trip wire placed near the crest of the dam induced full aeration of the nappe and thus reduced vibration.

Coefficients of discharge were determined experimentally for the dam when anchored to the floor and when laid on the bed. These were found to depend largely on the shape of the dam ; they approached the coefficient for a broad crest weir when the internal water pressure was small.

Acknowledgement

The work described herein was carried out as part of a research programme undertaken for the Ministry of Overseas Development, and the paper is published by permission of the Director of the Hydraulics Research Station. The Author also wishes to express his thanks to J.A. Weller and R. Barnsley who carried out the experimental work.

References

(1) IMBERTSON, N.M. : "Collapsible Dam Aids Los Angeles Water Supply." Civil Engineering, Vol. 30, September 1960, pp. 42-44.

(2) SHEPHERD, M.E. ; McKEY, F.A. and HODGENS, V.T. : "The Fabridam Extension on Koombooloomba Dam of the Tully Falls Hydro-electric Power Project." The Journal of the Inst. of Eng., Australia, No. 1-2, Vol. 41, Jan.-Feb. 1969, pp. 1-7.

(3) CONNOR, L.J. and GRAD, B.E. : "Fabridams—Their Application on Flood Mitigation Projects in New South Wales." ANCOLD Bulletin No. 29, October 1969, pp. 56-65.

(4) ANWAR, H.O. : "Inflatable Dams." Proc. A.S.C.E., Vol. 93, No. HY 3, May 1967, pp. 99-119.

APPENDIX I

Air-face of the Water-inflated Dam—It will be assumed that the material of the dam is inextensible and perfectly flexible and that its own weight is negligible. It will be also assumed that the water surface reaches the crest of the dam. Hence the tension, T, in the fabric per unit length will be as follows :

$$T = PR \qquad \ldots(6)$$

in which P is the pressure difference across the fabric and R is the radius of curvature. The pressure difference P according to Figure 1 can be written as

$$P = \rho g(\alpha H + y) \qquad \ldots(7)$$

Similarly the tension T, which is proportional to P, can be written in the following form :

$$T = \alpha\beta\rho g H^2 \qquad \ldots(8)$$

in which β is the factor of proportionality and will be defined later. Substituting Equations (7), (8) and the expression for R into Equation (6) yields

$$\alpha\beta H^2 = (\alpha H + y)\,\frac{(1+y'^2)^{3/2}}{y''} \qquad \ldots(9)$$

The above equation can be made dimensionless by introducing the following non-dimensional coefficients : $\xi = xH$; $\eta = yH$. Thus,

$$\alpha\beta\,\frac{\eta''}{(1+\eta'^2)^{3/2}} = \alpha + \eta \qquad \ldots(10)$$

in which dashes denote differentiation with respect to ξ and the boundary conditions are :

$$\left.\begin{aligned}\eta'(0) &= 0\\ \eta(0) &= 0\end{aligned}\right\} \qquad \ldots(11)$$

Equation (10) can be integrated by putting $\eta' = P$, i.e.

$$-\frac{1}{\sqrt{1+P^2}} = \frac{1}{\beta}\eta + \frac{1}{\alpha\beta}\eta^2 + C_o \qquad \ldots(12)$$

where, C_o is a constant of integration equal to -1 ($C_o = -1$) according to the first boundary condition of Equation (11). The following equation can be obtained by integrating Equation (12) and making use of $C_o = -1$:

$$\xi + C_1 = \int_o^{\eta} \frac{\left(\frac{2}{\beta}\eta + \frac{1}{\alpha\beta}\eta^2 - 2\right) d\eta}{\sqrt{\left(\frac{2}{\beta}\eta + \frac{1}{\alpha\beta}\eta^2\right)\left(4 - \frac{2}{\beta}\eta - \frac{1}{\alpha\beta}\eta^2\right)}} \quad \ldots(13)$$

By substituting $\eta = x - \alpha$ in the above equation

$$\xi + C_1 = \int \frac{(x^2 - \alpha^2 - 2\alpha\beta)}{\sqrt{(x^2 - \alpha^2)(\alpha^2 + 4\alpha\beta - x^2)}}\, dx \quad \ldots(14)$$

Substituting $\mu^2 = \alpha^2 + 4\alpha\beta - x^2$ in Equation (14) yields

$$\xi + C_1 = \int \frac{(\mu^2 - 2\alpha\beta)d\mu}{\sqrt{(4\alpha\beta - \mu^2)(\alpha^2 + 4\alpha\beta - \mu^2)}} \quad \ldots(15)$$

Making the substitution

$$\mu^2 = 4\alpha\beta\, Sin^2\theta \quad \ldots(16)$$

Equation (15) becomes

$$\xi + C_1 = \frac{2\alpha\beta}{\sqrt{\alpha^2 + 4\alpha\beta}} \int \frac{(2Sin^2\theta - 1)d\theta}{\sqrt{1 - \frac{4\alpha\beta}{\alpha^2 + 4\alpha\beta} Sin^2\theta}} \quad \ldots(17)$$

The above equation can be integrated only in terms of elliptic integrals, in the form of Equation (1) given in the text.

The constant β can be determined as follows :

From relation (16)

$$\theta = arc\ Sin \frac{(\alpha^2 + 4\alpha\beta - x^2)^{1/2}}{2\sqrt{\alpha\beta}} \quad \ldots(18)$$

or

$$\theta = arc\ Sin \frac{(4\alpha\beta - \eta^2 - 2\alpha\eta)^{1/2}}{2\sqrt{\alpha\beta}} \quad \ldots(19)$$

This shows that $\theta = \frac{\pi}{2}$ when $\eta = 0$. The value of θ must be real when the non-dimension height η varies $0 \leqslant \eta \leqslant 1$. On the other hand, the shape of the dam will take up a position of minimum potential energy of the liquid contained in the downstream side of the dam, hence the tension in the fabric will have a minimum value and the curve described by Equation (17) will thus be an extremal. Since θ must have a real value at the anchorage, where, $\eta = 1$, the following expression can be written from Equation (19) when $\eta = 1$

$$4\alpha\beta - \eta^2 - 2\alpha\eta \geqslant 0 \quad \ldots(20)$$

This is minimum when

$$4\alpha\beta - 1 - 2\alpha = 0$$

or

$$\beta = \frac{1 + 2\alpha}{4\alpha} \quad \ldots(21)$$

Equation (21) shows that the constant β depends on the proportional pressure factor α.

Water-face of the Dam—For the water-face the pressure difference P across the fabric is constant, hence the following equation can be written from Equation (6) and by making use of Equation (8)

$$R = \beta H \quad \ldots(22)$$

or

$$R = \frac{1 + 2\alpha}{4\alpha} H \quad \ldots(23)$$

which indicates a circle of radius R. The centre of the circle is on the y-axis and is tangent to x-axis at the origin O (see Figure 1).

Periphery of the Downstream Face: The length of the periphery, S, can be written in the following form

$$S = \int_o^s \sqrt{1 + y'^2}\, dx \quad \ldots(24)$$

and in the non-dimensional form

$$\frac{S}{H} = \int \sqrt{1 + \eta'^2}\, d\xi \quad \ldots(25)$$

The above equation can be written in the following form by making use of the substitutions used in Equations (12), (14), (15) and making use also of Equation (16)

$$\frac{S}{H} = -\frac{2\alpha\beta}{(4\alpha\beta + \alpha^2)^{1/2}} \int \frac{d\theta}{\sqrt{1 - \frac{4\alpha\beta}{4\alpha\beta + \alpha^2} Sin^2\theta}} \quad \ldots(26)$$

The above equation can be integrated in terms of the elliptic integral of the first kind, in the form of Equation (3), given in the text.

Uniformly Discharging Outlets for Irrigation Systems

A. S. RAMAMURTHY
Associate Professor
Civil Engineering Department
Concordia University, Montreal, Canada.

K. SUBRAMANYA
Asstt. Professor
Civil Engineering Department
Indian Institute of Technology Kanpur (India).

L. CARBALLADA
Grad. Student
Civil Engineering Department
Concordia University Montreal, Canada.

SYNOPSIS

In certain applications such as automated irrigation systems, lateral weirs are housed in open channels in which spatially decreasing flow occurs. When the channel bed slope and the friction slope are very small, spatially decreasing subcritical channel flow results in a rising profile in the reach containing the lateral weirs. This causes non-uniform distribution of weir outflows. For purposes of analysis, a single equivalent weir is considered and it is shown that uniform water surface profile ensuring uniform outflow can be obtained by modifying the weir system geometry. The proposed method is simple and easy to construct, even in existing channels.

Introduction

Water is becoming universally accepted as a national resource. The increasing use of this resource suggests the need to adopt methods for its wise and efficient use. Intensification of agriculture in existing farmlands also points out the need to improve the existing methods of applying irrigation water. Conventional surface irrigation systems resulting in non-uniform application of water lead to increased runoff and deep percolation. Recently, methods such as automated furrow irrigation([1]), cutback systems([2]), etc., have come into vogue.

The Lateral Weir

The side weir, also known as a lateral weir is a free overflow type outlet set in the side of an open channel which allows part of the liquid to spill over to the side when the surface of the flow in the channel rises above the weir crest. Useful information about the side weir can be found in the earlier papers by Ackers([3]), Allen([4]) and Collinge([5]). Recently, Subramanya and Awasthy([6]) have determined the variation of the De Marchi Coefficient, C_M, with the Froude number of the flow.

Automated Surface Irrigation

Automated irrigation systems permit the use of less skilled labour besides allowing substantial reduction in the labour force required for farm work. Humphreys([1]) provides a useful summary of existing automatic surface irrigation systems. Sweeten et al([7]) studied the uniformity of discharge from a bank siphons set in the side of an open channel under conditions of spatially varied flow. Sweeten and Garton([8]) have conducted field experiments to find the non-uniformity of outflow from multiple lateral weir systems.

In the present paper, the methods of obtaining uniform discharge distribution along the length of the side weir by altering the geometric parameters of the weir system are discussed.

Theoretical Considerations

For purposes of analysis, it is convenient to examine

an equivalent single lateral weir in place of multiple weirs housed in the channel side. It is reasonable to assume that the outflow distribution will be uniform along the weir span when the water surface elevation in the channel is uniform along this reach. Uniformity of water surface elevation for spatially decreasing flow in the channel can be achieved by any one of the following methods :

(1) plain contouring of the channel bed [Figure 1 (*a*)]

(2) plain contouring of the channel side [Figure 1 (*b*)]

(3) plain contouring of the weir sill [Figure 1 (*c*)]

Channel Bed Contouring

Assume that the channel bed is originally horizontal and that friction losses are negligible in the section considered. For a rectangular channel whose bed is raised to a height Z_1 locally in the vicinity of the weir [Figure 1 (*a*)] of length L, the basic equations of motion are given below :

$$Y_1+\frac{V_1^2}{2g} = Y+\frac{V^2}{2g}+Z \qquad ...(1)$$

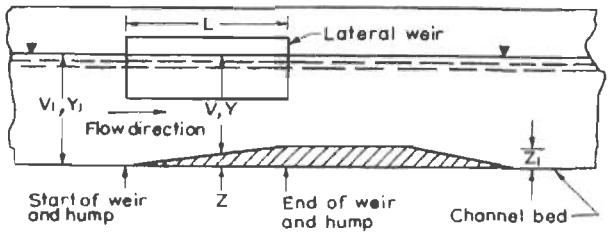

Figure 1 (a): Contouring of channel bed (elevation)

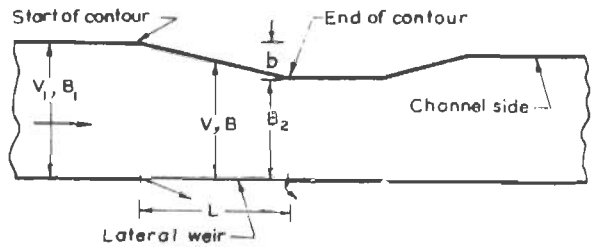

Figure 1 (b): Contouring of channel side (plan)

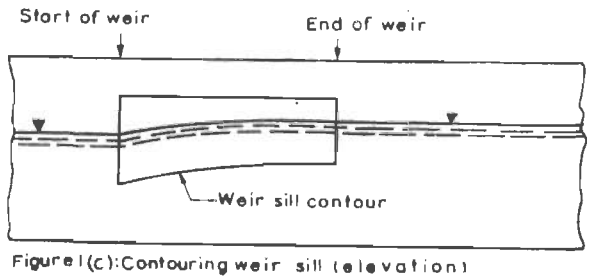

Figure 1 (c): Contouring weir sill (elevation)

FIGURE 1 (a), (b) & (c).

$$Q_1 = Y_1V_1B_1 = Q^*+[YVB_1]_{exit\ end} \qquad ...(2)$$

where, $Q^* = \frac{2}{3} C_M \sqrt{2g}\, Lh^{3/2}$ (weir outflow) ...(3)

and h = water surface elevation above the weir sill. Also $h = Y-s$ [Figure 1 (*a*)].

The inlet Froude number is given by :

$$F_1 = V_1/\sqrt{2gY_1} \qquad ...(4)$$

Further,

$$C_M = C_M[F_1] \qquad ...(5)$$

Since the water surface elevation has to be set uniform along the weir span, one can impose the following conditions :

$$Y_1 = Y+Z \qquad ...(6)$$

Consequently, from Equations (6) & (1), $V = V_1$, and

$$Q^* = B_1Z_1V_1, \text{ i.e., } \frac{Q^*}{Q_1} = \frac{Z_1}{Y_1} \qquad ...(7)$$

From Equation (7), one can compute the total rise in the channel bed hump Z_1 required to keep the water surface elevation horizontal for the given V_1 and the discharge ratio Q^*/Q.

Channel Side Contouring

For the case where the channel side is contoured to provide uniform water surface in the vicinity of the weir [Figure 1 (*b*)], the following equations hold good :

$$Y_1+\frac{V_1^2}{2g} = \left[Y+\frac{V^2}{2g}\right]_{exit\ end} \qquad ...(8)$$

$$B_1Y_1V_1 = Q^*+B_2YV = Q_1 \qquad ...(9)$$

For the water surface elevation to be uniform $Y_1 = Y$ and $V_1 = V$. Hence the side contraction b [Figure 1 (*b*)] is related to the discharge ratio as follows:

$$\frac{b}{B_1} = \frac{Q^*}{Q_1} \qquad ...(10)$$

with $b = B_2-B_1$

Weir Sill Contouring

For the case where the weir sill is contoured to provide uniform head causing lateral flow along the weir span [Figure 1 (*c*)], the differential equation governing the flow is given below :

$$\frac{dY}{dX} = \frac{S_o-S_f-Q_1/gA^2\,(dQ/dX)}{1-F^2} \qquad ...(11)$$

where,

$$F = V/\sqrt{gY} \quad \text{and} \quad Q_1 = B_1Y_1V_1$$

Let q^* be the constant outflow per unit length of the weir.

$$q^* = \tfrac{2}{3} C_M \sqrt{2g}\,[Y_1-s_1]^{3/2} = -dQ/dx$$

Since the channel floor is horizontal and friction is neglected, one can rewrite (11) after simplification, as :

$$\frac{dY}{dX} = \frac{Vq^*}{B_1(gY - V^2)}$$

The specific energy $E = Y + (V^2/2g)$ is constant and $V = \sqrt{2g(E-Y)}$.

Hence, $$\frac{dY}{dX} = \frac{\sqrt{2g}\, q^* \sqrt{E-Y}}{B_1[gY - 2g(E-Y)]}$$

or $$\frac{dY}{dX} = \frac{K\sqrt{E-Y}}{3Y-2E} \qquad \ldots(12)$$

where, $$K = \sqrt{2g}\, q^*/gB_1$$

Equation (12) is a simple differential equation which can be easily integrated to determine the variation of the water surface profile along the weir span. The boundary condition is $Y = Y_1$ at the start of the weir. Accordingly, upon integration, one gets

$$X = \frac{2E^{3/2}}{K}\left[\eta_1(1-\eta_1)^{1/2} - \eta(1-\eta)^{1/2}\right] \ldots(13)$$

where,

$$\eta = \frac{Y}{E} \quad \text{and} \quad \eta_1 = \frac{Y_1}{E} \qquad \ldots(14)$$

Having obtained the water surface profile, the weir sill can be contoured to provide a uniform driving head [Figure 1 (*c*)] along the weir span. At any location X, the sill level s of the weir can be obtained using the following relation :

$$(Y - s) = (Y_1 - s_1)$$

Experimental Verification

The Test Set-Up

A few preliminary tests were conducted in a rectangular steel plate flume which housed a lateral weir. The flume was 18 in. (45.7 cm) wide and 15 in. (38.1 cm) deep (Figure 2). The sharp edged lateral weir was 18 in. (45.7 cm) wide and the sill of the weir was 3.86 in. (9.7 cm) above the floor of the channel. Sufficient entry and exit and lengths were provided to reduce external interference effects in the vicinity of the weir. The depth measurements were made with a point gage and the inflow into the test flume was metered by an orifice meter. The weir flow was measured with the help of a 90° V notch.

The tests reported are limited to preliminary studies to determine the effectiveness of the channel floor hump in providing a uniform water surface profile, which in turn is assumed to provide uniform spanwise weir outflow distribution. The depth measurements were made along the center line of the channel. A plexiglass sheet hump of 1 in. (2.54 cm) height was set in the weir section as shown in Figure 2. Tests were made with and without the hump in place.

Discussion of Results

The test data related to the center line flow profile along the weir span is shown in Figures 3 & 4. The rising flow profile for the no-hump case is characteristic of sub-critical flows. The use of the 1 in. (2.54 cm) hump provides the nearly horizontal water surface profile

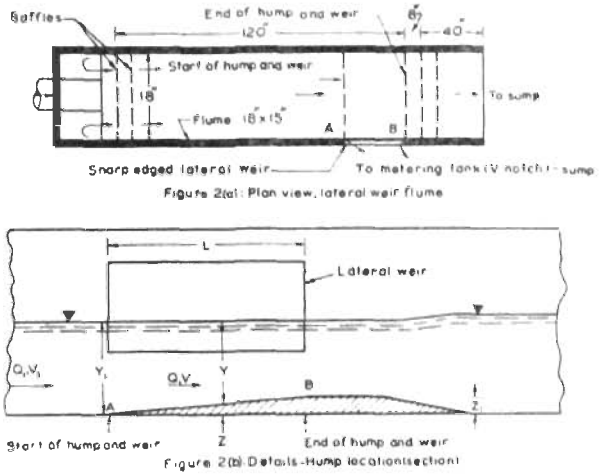

FIGURE 2 (a) & (b).

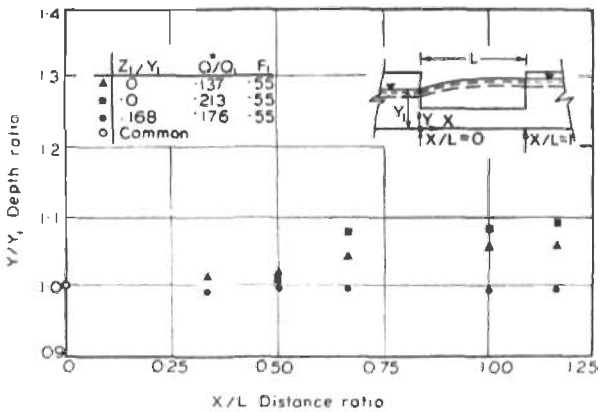

FIGURE 3 : Center line flow profiles ($Z_1 = 0$, $Z_1 = 2.54$ cm).

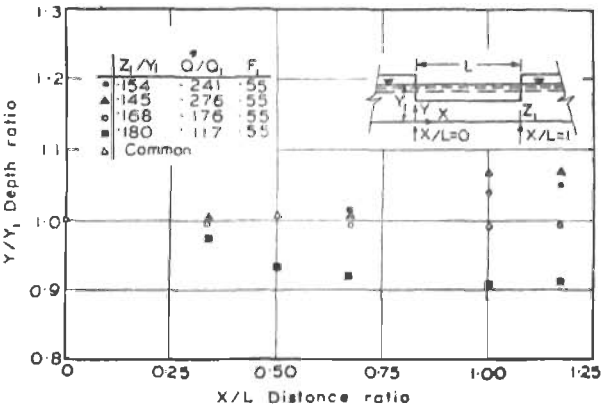

FIGURE 4 : Center line flow profiles ($Z = 2.54$ cm).

when the ratio Z_1/Y_1 is close to the discharge ratio Q^*/Q_1. Consider it as the design condition, the behaviour of the surface profile can be examined for off-design cases when the hump is present (Figure 4). When the ratio Z_1/Y_1 is not equal to Q^*/Q, the flow gets accelerated or decelerated in the channel as it negotiates the hump and this results in a falling ($Y_1 > Y+Z_1$) or a rising surface ($Y_1 < Y+Z_1$) profile which is indicative of non-uniform outflow distribution. This is also indicated by Equation (1).

Conclusions

(1) Simple geometric changes to the channel floor, channel sides or the weir sill are shown to provide uniform water surface profiles which in turn are expected to provide uniform flows lateral outlet systems.

(2) The preliminary results related to the use of a hump on the channel floor appears to be effective in ensuring a uniform surface profile for design conditions ($Q^*/Q_1 = Z_1/Y_1$).

Notations

b = side contraction
B = channel width
B_1 = channel width (at entry)
B_2 = channel width (at exit)
C_M = weir coefficient
E = specific energy
F = Froude number
F_1 = Froude number (at entry)
K = a constant
L = weir span
q^* = outflow/unit length
Q^* = weir outflow
Q = channel discharge
Q_1 = channel discharge (entry)
s = weir sill height
s_1 = weir sill height (at entry)
S_o = channel bed slope (o)
S_f = friction slope (o)
V = channel flow velocity
V_1 = channel flow velocity (at entry)
X = distance from entry end of weir
Y = channel flow depth
Y_1 = channel flow depth (at entry)
Z = hump height
Z_1 = hump height at exit
η = ratio of Y to E
η_1 = ratio of Y_1 to E.

References

(1) HUMPHREYS, A.S. : "Mechanical Structures for Farm Irrigation." J. Irrigation and Drainage Div., ASCE, Vol. 98, IR 4, 1969, pp. 463-479.

(2) GARTON, J.E. : "Designing an Automatic Cutback Furrow Irrigation System." Oklahoma State University, Exptl. Station, Bulletin B-651, Oct. 1966.

(3) ACKERS : "A Theoretical Consideration of Side Weirs as Storm Water Overflows." Proc. Inst. Civil Engineers, Vol. 6, 1957, pp. 250-269.

(4) ALLEN, JOHN WILLIAM : "The Discharge of Water Over Side Weirs in Circular Pipes." Proc. Inst. Civil Engineers, Vol. 6, 1957, pp. 270-287.

(5) COLLINGE, VINCENT KNIGHT : "The Discharge Capacity of Side Weirs." Proc. Inst. of Civil Engineers, Vol. 6, 1957, pp. 288-304.

(6) SUBRAMANYA, K. and AWASTHY, S.C. : "Spatially Varied Flow Over Side Weirs." J. Hydraulics Div., ASCE, Vol. 98, HY 1, 1972, pp. 1-10.

(7) SWEETEN, J.M. ; GARTON, J.E. and MINK, A.L. : "Hydraulic Roughness of an Irrigation Channel with Decreasing Spatially Varied Flow." T. ASAE, Vol. 12, No. 4, 1969, pp. 466-470.

(8) SWEETEN, J.M. and GARTON, J.E. : "The Hydraulics of an Automated Furrow Irrigation System with Rectangular Side Weir Outlets." T. ASAE, Vol. 13, No. 6, 1970, pp. 746-751.

Air Photo-Interpretation of Hydromorphology of Asan Basin, Doon Valley, India

S. K. SHARMA
Hydrogeologist (Jr.)

S. C. SHARMA
Hydrogeologist (Sr.)

Central Ground Water Board
Ministry of Agriculture and Irrigation, Government of India, New Delhi (India).

SYNOPSIS

The paper describes a geomorphological approach in deciphering ground water from aerial photographs of a part of Asan Basin in western half of Doon Valley. The technique involves deductions of properties of deciphered surface formations. A large part of the photo interpretations is based on landscape indicatory studies. Aerial landscape methods have been fruitfully used wherein such methods allow to readily observe, certain indicators over large areas. The method of hydrological deciphering incorporates observations and inferences from air photos. The validity of interpretation has been checked in the field.

The diverse geologic-geomorphic system in Western Doon Valley called for the need to construct a water resource characteristic map. A hydromorphological map prepared in this regard is considered useful in deciphering features of ground water of the "Intermontane hallow" in which Asan assumes a more or less Central position. Geomorphic, vegetation and structural indicators of ground water have considerable bearing on the ground water situation of the area. The lower realm of "Principal Doon Fan" and alluvial terraces are rated as productive aquifers to support good deal of irrigation-agriculture.

Application of the technique of air photo-interpretation in hydrologic data acquisition would achieve the purpose accurately and readily.

Introduction

A prolific growth in population and ever expanding technology place demands on our natural resources. Humanity, however, can no longer treat his resources strictly according to immediate economic dictates; a balance must be struck between short-term demands of technological and industrial development and the long-term effects on the environment.

The authors wish to examine here basic and quick method of hydrologic data acquisition. The technique for such an appraisal is one of air photo-interpretation. The black and white aerial photography has been used stereoscopically to obtain accurate measurements of shape, size, and location of objects. Panchromatic photography has, thus, been found most useful in mapping geologic, geomorphic, structural and vegetation indicators of ground water. This technique utilizes, largely a geomorphic approach in describing environmental characteristics accurately and readily in forms suitable for analysis and prediction of cause and effect relationship in hydrology. Basic data acquired by interpretive technology have been utilised in preparing resource characteristic map.

Hydromorphological map of part of Asan Basin has been constructed to describe static and dynamic elements of geohydrologic system in western part of Doon Valley. We have chosen to present our resources information

at a photo scale, 1:60,000. This scale provides reasonably detailed information in the mapping and description of ground water features.

The methodology is, however, thought to prove stimulus in the exposition and extension of technique of air photo-interpretation to hydrogeological surveys and making quick appraisal of events.

Area of Study

Location and Extent

The area chosen for hydrogeomorphological descriptions is that part of Western Doon Valley lying between this Sub-Himalayan belt in the north and Siwalik belt in the south, within which flows the Asan River in a westerly direction. The area of our study also includes, partly, Trans-Yamuna area. The entire area lies approximately between 30° 19′ north latitude and 77° 37′ east longitude and forms part of Survey of India topographical sheet No. 53F. It is 25 km from east to west and 12 km from north to south.

Geographical Features

Asan Valley and Trans-Yamuna area is divisible into three physiographic units, namely :

(*a*) The Sub-Himalayan belt in the north,

(*b*) The Siwalik belt in the south, and

(*c*) The synclinal depression in the middle.

Mean annual rainfall for the area is 2,199 mm. Ambari hill forest records 1,865 mm of rainfall. The whole climatic year is divisible into three seasons, each constituting four months :

Winter Season	1904 mm
Summer Season	2007 mm
Rainy Season	94 mm

The rainfall intensities are high and they are responsible for high peak flows. The area has been endowed with thick forest vegetation which is considered good in hydrologic sense.

Asan Basin

Asan Basin has an area of about 681 sq km with Asan being the trunk stream, flowing in a west-northwesterly direction. It bisects the basin into two unequal halves, the northern half having larger areal extent. Asan River gives the basin an asymmetric look and the valley thus bears dextral asymmetry.

Asan forms confluence with Yamuna near Paonta, where another stream, the Giri River meets River Yamuna little upstream of Asan-Yamuna confluence. The northern tributaries of Asan have larger catchment area than those issuing from Siwalik hill range in the south.

The left and right-hand hill torrents of the basin have seasonal flow. The upstream course of right-hand slope tributaries is perennial but they readily lose track in their lower reaches on crossing permeable gravel-fan deposit of Himalayan piedmont plain. The upstream course of such tributaries is fed partly by spring seepage and partly by base flow at the foot of Sub-Himalayan range. Similarly, the tributaries which originate in sandstone strata of Siwalik range and drain the left-hand slope of Asan Basin do also behave as perennial channels. They too, become suddenly absorbing streams when cross the piedmont-fan realm of Siwalik clothed with dense 'bhabar' sal forest. Asan, thus, has perennial flow character governed by base flow component of runoff water.

Antecedent moisture condition for the basin works out to be AMC-III, since 5-day rainfall total for growing season exceeds 53.3 mm. AMC-III condition means the highest runoff potential. Antecedent moisture condition is an index of watershed wetness and the watershed is practically saturated from antecedent rains.

Table I shows certain characteristic features of Asan Valley having bearing on hydrogeological system.

TABLE I

Characteristic	Left-hand slope	Right-hand slope
1. Declivity	Steep slope 5° to 10°	Gentle slope 1½° to 5°
2. Moistness	Wet due to thick 'Bhabar' sal forest	Variably dry and wet due to sporadic forest cover
3. Surface mantle of stones	Coarse, well rounded	Fine, sub-angular to sub-rounded and platy fragments
4. Piedmont vegetation	Mixed sal forest	Oak sal forest
5. Density of cover	Dense cover over 80 percent density	Open to dense cover
6. Drainage density	Medium; absorbing streams	Medium high; absorbing streams
7. Postulated most important process	Slope wash due to creep	Debris flow

Photo-Geomorphology

The mapable features of the valley, in terms of flood plains, alluvial terraces, piedmont-fan deposit, etc., have been identified from aerial photographs. One of the first step in the study of hydrogeology is, therefore, a comprehensive effort in photogeology. For the preparation of comprehensive geomorphic map(s) large part of geomorphologist deals with distribution and boundaries of landsurface. Photographs enable one to survey the

area readily through perspective view of large terrain and yield adequate data, simultaneously.

Geomorphology discussed, herein, is related to the study and distribution of landforms and various salient but obvious processes that promote formation of specific geomorphic forms. A descriptive geomorphology has been attempted from mere photo-interpretation and the validity of conclusions is field checked. The area has been divided into different geomorphic regimes depending upon the allowance of scale. A reference in this connection is made to Figure 1 with explanatory notes.

Landforms show the imprint of internal crustal movements, erosion and deposition. Tone and colour patterns, tonal alignments, irregularities in topography and drainage patterns indicate variation in conductivity of soil and vegetation. Both soil and vegetation are related to geomorphic features.

Morphological description of some important geomorphic units is given below. The distribution of these is shown in Figure 1.

Fluvial Morphology

In an analysis of geomorphic surfaces, the first step is the consideration of photo scale. Different landforms have different image and spatial look on air photos. A second consideration which receives an immediate attention of eye is the presence of major/minor relief features.

Landforms of the area are of fluvial nature. Fluvial forms call for the study of : (*i*) valley distribution, (*ii*) congurent and incongurent drainage patterns and (*iii*) the accumulation and erosional forms. Accumulation forms include :

(*a*) valley floor,

(*b*) flood plain, and

(*c*) uplands.

Alluvial deposits are thus developed into three types. They are :

(*a*) channel sediment,

(*b*) flood plain deposit,

(*c*) fluvial terrace, and

(*d*) alluvial fan.

Stream Morphology

Streams originating from Himalayan and Siwalik ranges have variably incised their courses. Their gradients are steep and they carry heavy sediment load. The headwater portions of tributaries have perennial drainage. The vertical incision is common with such tributaries when they deeply carve in their headwaters through the Siwalik strata. The erosive power and perennial character of such tributaries is exhausted as they cross the piedmont-fan realms in their lower reaches. By and large, the streams of Asan Valley have graded long profiles and have developed large flood plains along their courses. They are, therefore, classed as matured streams. The lateral erosion is a common feature with streams of Western Doon Valley. They are generally of aggradational nature. The main effect of such an erosion is the loss of agricultural land adjacent to stream beds. The stream widening is ascribed to excessive channel bed infiltration.

Braided Channels

Trunk streams as well as their tributaries in Western Doon Valley are braided. High intensity of rainfall, moderately steep gradients and large supply of coarse detritus from uplands are some of the factors responsible for formation of braided channels and braided deposits. Sand bars having downstream elongation are a common feature of braided streams. Riverine vegetation have occasional association with sand bars. Braided nature of streams accounts for the occurrence of coarse permeable materials in their channels.

Flood Plain

The lateral and longitudinal migration of alluvial rivers have generated new flood plain lands in about two types of accretion :

(*i*) Sand bar or island, and

(*ii*) Sheet.

Flood plain deposit distribution is shown by area symbol in Figure 1. A more or less smooth outline of landsurface, mottled texture due to variation in soil moisture and vegetation, topographically low-land strewn between the present-day channels and higher fluvial system, are some of the diagnostic photo elements of flood plain region of streams. They mostly comprise pebble-gravel assemblage and perhaps been formed as a single sheet by accretion. Dark colour plumes on the flood plains in air photos is index of moisture content and shallow ground water.

Himalayan Piedmont-Plain

The plain is the product of coalescence of older alluvial fans. It is built up by debris swept out by Sub-Himalayan drainage. Piedmont-plain has a concave upward profile with the mountain front. The main boundary fault forms a topographic break between hills and the piedmont-plain. The upper segment of the plain bears steeper slope and entrenched drainage having flat bottoms. It is variably dissected. The lower segment of the piedmont is a colluvial plain. Piedmont-plain constitutes comparatively fine clastics. They are angular to sub-rounded and platy fragments of quartzite limestone, phyllite and shale. This is the principal alluvial-fan deposit of the valley.

Siwalik Piedmont-Plain

This plain developed along the left flank of Asan on the dip controlled topography of Upper Siwalik strata.

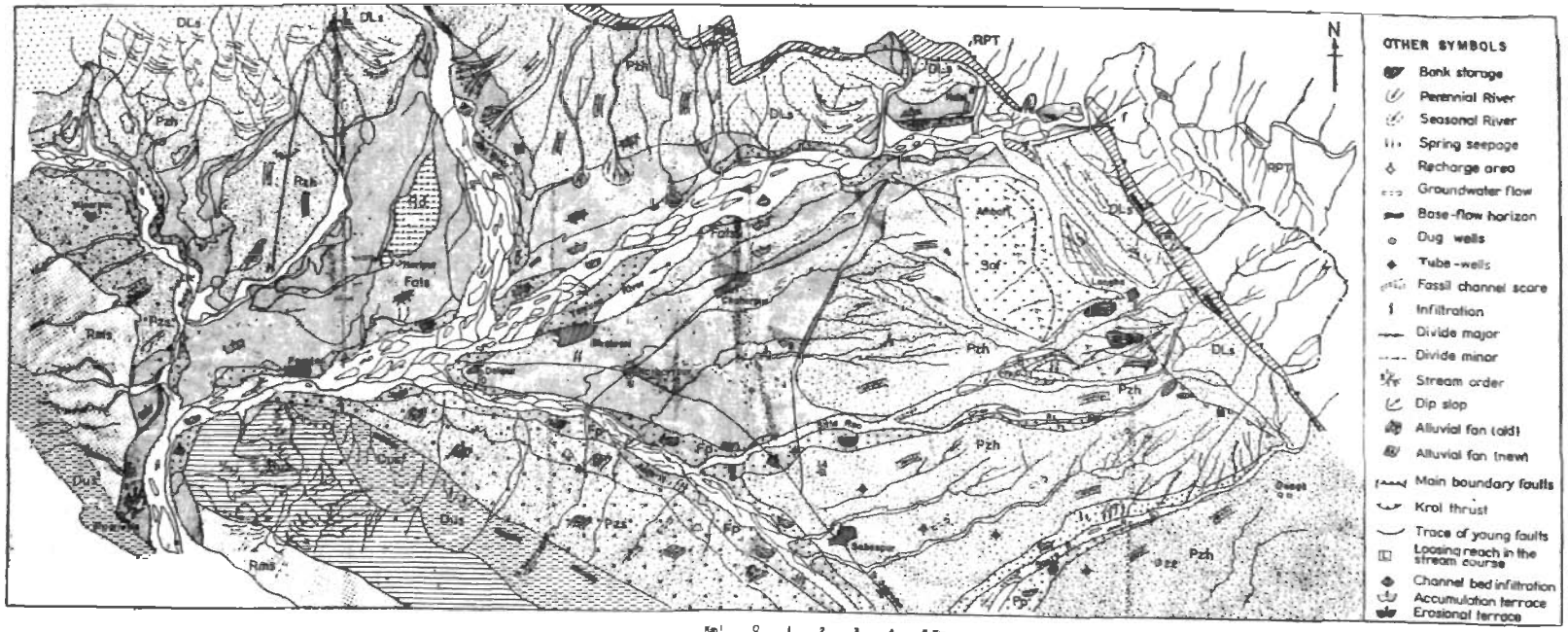

HYDROMORPHOLOGICAL UNITS

Fp	Flood-plain	Higher permeability, bank storage	Rms	Relief type Middle Siwalik	Zone of contact type springs with perennial drainage
Fats	Fluvial accumulation terrace system of River Yamuna	High permeability : yield water to dug wells	DLs	Denudational Lower Siwalik	Ill permeability ; catchment area for confluent plain between Bata and Giri Rivers
Tf	Terrace system of tributaries	Moderate permeability	Intra	Intra-thrust zone	Base-flow horizon
Pzs	Piedmont zone of Siwalik	Medium to low permeability	RPT	Relief type pre-tertiaries	Rain catchment horizon, source of base-flow at the foot of mountain-NE margin, Doon Valley
Pzh	Himalayan piedmont zone	Large permeability ; source of irrigation and domestic water supply	Rd	Anomalus residual hill	Medium permeability; upland providing run-off water to the surrounding permeable Yamuna-Giri River terraces
Saf	Solifluctional fan ridge	Permeable, catchment area for piedmont (Pzh) fans		High level fan surfaces	Medium to low permeability ; local catchments
Dus	Dissected zone of Upper Siwalik	Zone of low transmission; base-flow bed			
Rus	Ravinous tract of Upper Siwalik	Zone of seeps and spring with perennial streams			

FIGURE 1 : Hydromorphological map, area Western Doon Valley.

The plain has distinct break in slope with Upper Siwalik boulder bed. It is, ascribed possibly to the longitudinal down-shift of solid debris by hill torrents accentuated by the action of creep on permeable fan-deposit. The deposit constitutes well rounded boulders and gravels of quartzite. It is clothed by thick sal forest vegetation. The drainage on the fan-deposit is ephemeral.

Alluvial Terraces

Water borne deposits have been differentiated into various terrace levels along the stream courses. The oldest or the highest are characterized by erosional development along their scarps. The low level terraces are accumulation terraces.

Photo-elemental studies in conjunction with field checks have revealed that accumulation terraces bear relatively high permeable material assemblage than erosional terraces.

Soliflucional Fan-ridge

Upper Siwalik fan-ridge making the Ambari hill watershed has rounded topography. The rounded crestline and convexity of slopes on the ridge are produced by the action of creep on permeable soliflucional fan. The ridge comprises permeable boulders and gravel held loosely in silty and clay matrix. It is densely vegetated. This upland serves recharge area for fluvial terrace plain fringing it.

Hydromorphology

This chapter deals with method of extraction of hydrogeologic information from aerial photography and hydrological evaluation of morphological features. Hydromorphological map (Figure 1) divides the area into various geomorphic units which are geologically homogeneous. The preparation of such special purpose resources map by conventional method of mapping would be time consuming and much less informative as compared to the method of air photo-interpretation. It may be of importance to note that the interpretation of this area from air photos has taken only 12-man hours besides cartographic work. Such work is, however, directly related to the experience and capacity of an interpreter trained in the discipline.

Photo Hydrological Mapping

Hydrogeologic mapping from air photos is based on landscape-indicatory studies and the approach used is one of geomorphic. The notes record methods of hydrologic deciphering wherein the results of observations and inferences from air photos in conjunction with field data, have been incorporated. A careful interpretation based on terrain analyses method, which utilises 9-steps provides valuable information on the surface drainage condition, morpho-conservation patterns, spring seeps and marshy lands, soil and channel bed infiltration and losing and gaining reaches in the streams. Sub-surface condition can be analysed from study of well records in conjunction with alluvial morphology inferred from aerial photographs.

Various terrain analyses methods in this respect are:

(1) Stream course delineation,
(2) Drainage pattern and form analyses,
(3) Drainage and sub-basin delineation,
(4) Landform analyses,
(5) Drainage texture analyses,
(6) Tone-texture analyses,
(7) Fracture pattern analyses,
(8) Outcrop pattern analyses, and
(9) Geobotanical analyses.

Some of the observations and inferences of geologic and ground water conditions from the study of aerial photographs are brought out here.

A qualitative description is given below.

(A) Water Features at the Landsurface

(1) *Drainage Density*: It has direct bearing on the permeability of materials. Drainage density is inversely proportional to base flow in the area.

Streams draining the piedmont-fan deposits have low drainage density. They are braided and ephemeral. The channels have width greater than depth. The wider cross-section and braided nature of streams is a function of permeability of the materials. Such channels are expected to register excessive channel-bed infiltration.

Landforms on lower and middle Siwalik have relatively high drainage density. They are the tracts of rather low permeability.

Ambari hill watershed forms upland. It has a 2.24 km/km^2 drainage density and infiltration number valued at 11.4. Infiltration number directly reflects the permeability of a deposit. The higher the infiltration number greater is the permeability. Hence, this watershed has greater infiltration possibilities. The infiltrated water and overland flow is thought to recharge the alluvial piedmont-plain fringing the Ambari ridge.

Fluvial terrace regime form table-lands. They are devoid of drainage lines. These are the areas of rather high permeability. They are considered to obtain recharge by subtraction of overland flow.

(2) *Localized Gain or Loss of Stream Flow* : Perennial streams of Siwalik become losing streams when they enter the subrecent-fan deposits. The losing nature of streams is also a function of recharge in the piedmont materials. The Asan and Yamuna are gaining streams. The ground water in piedmont-plains is a sequel to topography being deeper in upper reaches and shallow in their lower segments.

(B) Character and Aerial Distribution of Rocks

(1) *Specific Type(s) of Rock(s) and Geomorphic Regimes* : Flood plain deposit is tract of rather very high permeability having greater possibility of bank storage. Black colour plumes on the flood plain in air photos are related to the hydromorphic nature of the soil. Such evidence permits inference on the occurrence of shallow ground water in such a deposit. Recharge to this unit is partly effected through infiltrated water from contiguous piedmont-plains. Shallower ground water is expected to occur more or less along the interface of Himalayan piedmont-fan and flood-plain deposit of Asan River.

(2) *Spatial Form and Interrelations of Rock Units* : The dissected zone of Upper Siwalik comprises clay and gravel beds. It is a zone of low transmission. It is probably an aquiclude with Siwalik piedmont-fan deposit representing aquifer above it. The Upper Siwalik beds in their up-dip exposures are expected to conduct water down-dip towards Asan Valley. The thickness of Siwalik fan deposit is expected to be small because of the shallow dip of the underlying bed-rock. The width of Siwalik fan deposit is also lesser as compared to Himalayan fan deposit.

(C) Geomorphic Indicators of Ground Water

Some geomorphic features have been taken to indicate the location of ground water. The principal piedmont-plain or "bajada" formed by the coalescence of alluvial fans which occur on the Himalayan slope may serve as excellent source of ground water. The lower realm of this plain is expected to form principal aquifer in Western Doon Valley.

The recharge to the principal aquifer possibly taken place by infiltration through the soil and subsequent percolation through the coarse boulder-gravel assemblage, during and after periods of heavy rainfall.

The second mode of recharge may be by channel bed infiltration. The base flow, at the foot of mountain in the north, is yet another source of recharge.

Fluvial terrace regime of Yamuna and confluence terrace plain of Yamuna-Giri River would likely hold appreciable quantities of ground water in their permeable materials. Fluvial accumulation terraces would expectedly bear higher permeability and ground water than fluvial erosional terraces. They are inferred to bear shallow ground water than their higher piedmont realms.

(D) Vegetation Indicators of Ground Water

Certain type of plants are fairly reliable indicators of ground water. Thick sal forest vegetation on Siwalik piedmont-fan deposit has been considered good in hydrologic sense. The thick canopy density of the vegetation stand is likely to intercept large amount of rainfall. But it would on the other hand reduce surface runoff during monsoon and conduct sub-surface flow to the Asan River.

Riverine forest vegetation on islands of streams and flood plain deposits has been taken to account for the occurrence of shallow ground water. Such areas have high infiltration opportunities.

(E) Structural Indicators of Ground Water

Intermontane hallow of Asan Valley having synclinal disposition together with its alluvial-fill establishes conditions favourable for formation of ground water basin and medium artesian basin. Thrust planes and their sheared zones offer greater opportunity for infiltrated waters to recharge the Asan Valley-fill. Intra-thrust zone comprises shaly material and is an area of low transmission. The rocks of Krol to the north of Krol thrust have more or less perched synclinal disposition. The obsequent drainage is expected to gather discharge by way of spring seepage and base flow.

Surface Runoff and Ground Water Runoff

Surface Runoff : Overland flow is distributed down the valley slopes as sheet and rills. This has distinction with channel flow in which broad and flat bottom drainage channels are confined by lateral banks. Overland flow on the Siwalik piedmont slope with thick vegetal litter mat on forest floor possibly carry concealed flow. Overland flow in the area is directly proportional to the rate of precipitation and length of slope but inversely proportional to both, the infiltration capacity of the soil and resistance of the land surface. The steeper upper realm of Himalayan piedmont generates faster overland flow and moderately intensive erosion.

Table II has been prepared to outline the runoff producing characteristics in the basin.

TABLE II

Designation of watershed characteristics	Left-hand basin slope	Right-hand basin slope
1. Relief	Rolling with average slope of 5 to 10 percent on Siwalik piedmont (50)	Relatively flat land with average slope of 0-5 percent (25) on Himalayan piedmont
2. Soil infiltration	Deep loam gravel, coarse textured soil that takes up water readily and rapidly (5)	Deep loam gravel, relatively medium coarse textured soil that takes up water rapidly (5)
3. Vegetal cover	Good to excellent; about 90 percent drainage area under sal forest (5)	Fair to good; about 50 percent of the area under forest vegetation; rest of the area is clear cultivated (10)
4. Surface storage	Negligible surface depression; rare marshy or hydromorphic soil (2)	Negligible surface depression rare ponds (20)

For the hilly tract north of the thrust, the runoff producing characteristics are given in Table III.

TABLE III

1. Relief	Hilly with average slopes of 10 percent to 30 percent (30)
2. Soil infiltration	No effective soil cover; rock with thin soil mantle (20)
3. Vegetal cover	No effective plant cover, sparse cover (20)
4. Surface storage	Negligible

Streamflow hydrograph has been prepared for Asan (Figure 2) based on the discharge data collected from the gauging station at Dalipur. The high flows during August through September are the result of high intensity rains over large parts of the drainage area. Generally, there are about two major peak flows during above period with recession to medium stages between storms. During winter months there is a gradual recession in the flow. The seasonal flow characteristic of northern tributaries of Asan Valley is higher than the southern tributaries.

Base Flow

Ground water runoff or base flow is that part of precipitation which infiltrates into soil or to the water-table and then expected to percolate in the Asan River channel. The possibility of the occurrence of base flow can be read from air photos but the volume of its flow can be measured from stream hydrographs. Such a data is useful in estimating recharge to the aquifer(s).

The hydrograph of Asan River shows the effect of base flow and surface water flow. The river receives prolonged base flow during August and September. It is seen to recede thereafter and before onset of monsoon as observed from base flow recession curve (Figure 1).

Sustained flow in Asan River indicates that highly permeable aquifer is contained within the drainage basin. Water infiltrating into the coarse materials of upper piedmont slopes and braided river beds may emerge in areas further downstream and increase the base flow.

Conclusions

Air photo-interpretation of hydromorphology of Asan Basin, Western Doon Valley, has been brought out with sole purpose of exposing this technique of deciphering ground water to the students of its interest. The technique utilises morphological approach. Hydro-morphological map is an illustrative example of

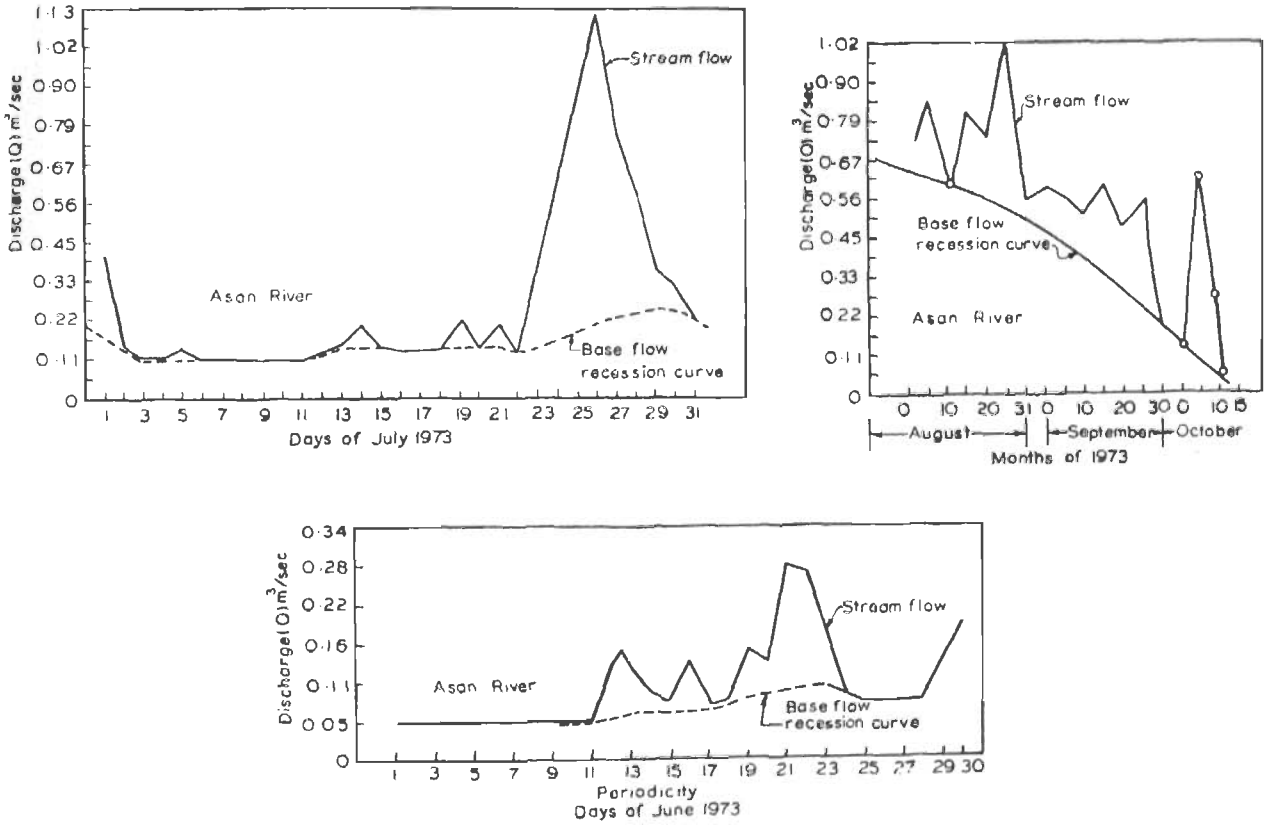

FIGURE 2 : Asan River hydrograph.

delineation of hydrologically homogeneous landscapes. Each morphological regime is hydrologically evaluated and the legend to the map is self-explanatory.

Alluvial valley in the area occupies shallow depression bounded by Siwalik hills in the south and Sub-Himalayan tract in the north. Piedmont-fan deposits or "bajada" and fluvial river terraces are among the common landforms having sound hydrologic properties. Essentially, the lower realm of Himalayan piedmont-fan is considered to bear large ground water potentials. Fluvial accumulation terraces afford greater possibility than fluvial erosional terraces in obtaining ground water supplies by way of wells and tubewells. Flood plain deposits have larger bank storage possibilities and ideal situation to irrigation-agriculture by dug wells.

Runoff producing characteristics operative on right and left-hand slopes of Asan Valley have been catalogued. Erosional processes accentuate larger runoff on the right-hand side slope. Sustained flow in Asan River as observed under stereomodels of winter air photography and checked by field observations indicate that a highly permeable aquifer is contained in the Western Doon Valley. This aquifer is the piedmont-fan aquifer.

Qualitative analysis from air photos is a first attempt of its kind in describing features of ground water of an Intermontane hallow. Geomorphic, vegetation and structural indicators of ground water have central role in such interpretations. Aerial landscape methods are considered useful in the acquisition of hydrogeologic data and compilation of water resource characteristic map(s).

Acknowledgements

The authors are thankful to Shri D.S. Deshmukh, Chief Hydrogeologist, Central Ground Water Board in critically examining the manuscript. They are thankful to Shri B.N. Raina, Head Geology Division, Indian Photo-Interpretation Institute, Survey of India, Dehra Dun for his valuable suggestions.

References

(1) HOWEL, R.H.L. : "Procedures of Applying Air Photo-Interpretation in the Location of Ground Water." Photogrammetric Engineering, Vol. 24, No. 1, pp. 35-49.

(2) KUDRITSKI, D.M.; I.V. POPOV and ROMANOVA, E.A. : 'Hydrographic Interpretation of Aerial Photographs." Israel Program for Scientific Translation, Jerusalem, 1966.

(3) MALLICK, S. and NIYOGI, D. : "Application of Geomorphology in Ground Water Prospecting in the Alluvial Plains Around Burdwan, West Bengal." Indian Geohydrology, Vol. VIII, No. 2, December 1972, pp. 86-98.

(4) SHARMA, S.K. and ROY, A.K. : "Hydrogeology of Motichur Rao Forest Watershed." Indo-Soviet Symposium on Recent Trends in Exploration of Mineral, Oil and Ground Water, New Delhi, October 15-20, 1973.

(5) SHARMA, S.K. and SHARMA, S.C. : "Hydrological Evaluation of Morphological Features of some parts of Hamirpur, Jhansi, Banda and Fatehpur Districts, U.P.—Using Air Photo Interpretation Techniques." 'Photonirvachak' Jour. Ind. Soc. Photo-Interpretation, Vols. I & 2, 1973.

Some Considerations Concerning the Sorption Capacity of Several Radionuclides of the Black Sea Water in Sediments on the Black Sea Bottom

VALENTINA VOLJIN
Lecturer
Department of Nuclear Physics, Faculty of Physics
University of Bucharest, Romania.

E. ZAMFIR
Physicist
Research Institute of Land Reclamation
Bucharest, Romania.

MIHAELA BLIDARU
Senior Research Engineer
Research Institute of Land Reclamation, Bucharest, Romania.

SYNOPSIS

A study has been made of the transfer of radionuclides ^{90}Sr, ^{137}Cs, ^{59}Fe, ^{65}Zn, ^{60}Co, ^{54}Mn, ^{144}Ce, of the Black Sea water in samples of sediments on the Black Sea ground taken over from different points of the Romanian Coastal region. For determining the diffusion coefficients of these radionuclides, the following methods were used: the method of sedimentation, method of the thin layers and the method of suspension. The sorption mechanism is affected by the physico-chemical properties and for biological conditions of sediments different analyses were made by using chemical and physical methods : the global chemical analysis of the sediments and chemical analysis of the Black Sea water, determination of soluble salts, cationic-exchange capacity and identification of mineralogical composition using the method of X-ray diffraction and infrared absorption spectrometry. The analyses effectuated indicate that from the point of view of composition, the analyzed samples are grouped themselves into two different categories, some with a high content of $CaCO_3$, others of SiO_2 and clays. It has been established that the content of clays increases appreciably sorption capacity of ^{137}Cs. It is observed that the samples with high content from $CaCO_3$ and with a close mineralogical composition have not the same sorption capacity for some radionuclides, thus indicating that the sorption phenomenon is very complex and that the factors upon which this phenomenon depends are not yet known. The diffusion coefficient values obtained indicate that the analyzed Black Sea sediments present a high exchange capacity and can serve as depollutant for some radionuclides.

Introduction

The sediment particles have the propriety to remove the radionuclides from the sea water and to concentrate them at the bottom of the sea, contributing thus to the process of depollution of the sea water. This migration process of the radionuclides in sediments can be considered at the first approach as being a diffusion process. The physical bases of this process, different mathematical limit cases as well as experimental

methods used, were fully described in papers (1)-(8). The presence of radionuclides in the Black Sea water and in sediments from the Black Sea bottom brought into evidence in Ref. (7), permitted the establishment of the transfer of different materials from water in sediments. The studies effected with radionuclides and the Black Sea sediments of the Black Sea bottom, indicated that these sediments present a high sorption capacity for some of the radionuclides(8). For the present paper, many problems of the radionuclides dynamics in the region of the Romanian Littoral of the Black Sea which due to the Danube influences, present certain particularities were studied. Sorption processes of the radionuclides in particles of sediments are affected by the physico-chemical properties and by the mineralogical structure of these sediments, by the conditions in which the sorption takes place : *pH* and salinity of the sea water, concentration of the stable isotope in sea water, by biological conditions, as well as by the chemical nature of the radionuclide used. With the aim of determining this dependence, different analyses have been effectuated, using physical and chemical methods of analysis.

Model of Uptake and Preparation of Samples

Samples of surface and deep water have been collected from the Musura gulf starting from the point Cardon to Mangalia—Vama Veche (Photo 1). The deep samples were taken from the same points from where also the sediment samples were collected. Sediment samples were collected starting from the Stambului Vechi inlet and Musura gulf to Vama Veche (228 km). The depth from which the samples were collected varied from between 10-12 m, the distance from the shore being 5-1 km. The samples were extracted mechanically, the thickness of the blocks being $\sim$ 10 cm. At the depth from which the samples were taken up, the bottom of the sea is pretty uniform as relief and flora all over the length of the Romanian Littoral, with the exception of Agigea zone, where the land is troubled, where there are huge blocks and sea-walls in a form of stairs towards the depth, deep cracks and pits. The remainder is covered by the alternations of the chelate stone, sand and clusters of plants composed of fungus Ulva and brown fungus (Photo 2) (9)(10). The silt is not to be found at these depths, except in deep pits, where the currents cannot operate.

The surface water salinity did vary from between 10-16 percent (*pH* 8-8.2) as a function of the place from where sample was taken. The salinity of the deep water varied up to 20 percent. The water was filtered through Millipore filter 0.45 μ. In some tests the following parameters were determinated which characterise sea water and sediments used in the analysis : electrical conductivity, viscosity, capillarity of interstitial water, porosity, dimensions of the sample grains, density of sediment suspension and electrokinetic potential. Some of the results were presented in Refs. (11)-(13).

Petrographic Analysis

The sediments have been analyzed by the optical and

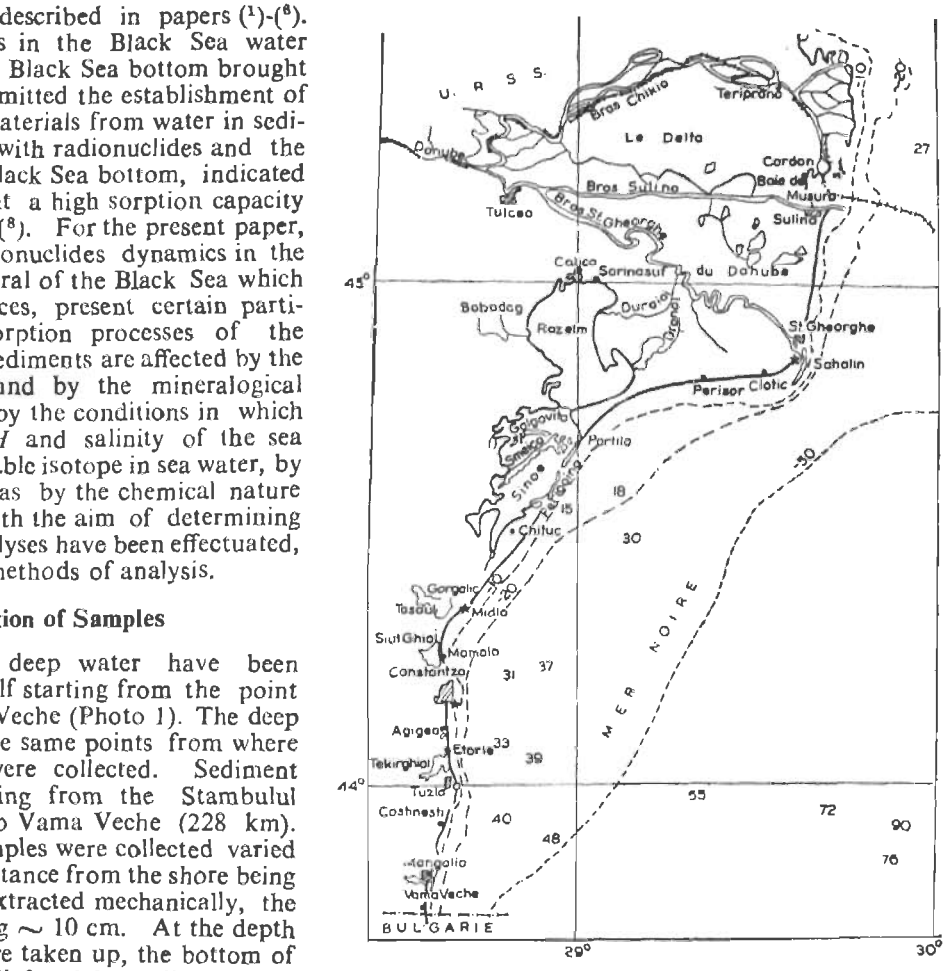

PHOTO 1 : Chart of the Black Sea Romanian Coast.

PHOTO 2.

polarization microscope. The calcareous mass mostly represented foraminifera schells, amongst which there were bivalvous ostrocode schells, calcareous fungus, and organic rests inside the calcareous mass.

Analysis by Neutron Diffraction Method

The crystalline properties as well as those magnetic ones of the crystals, undergo different phase-transformations under the influence of pressure and temperature. The structures of the minerals of the marine origin were relatively little studied from this point of view, so that these characteristics cannot yet be used as indicators for the dynamic and static characteristics of the sea bottom. By effecting the analysis by the neutron diffraction of some samples taken from the Black Sea bottom, it could be established that neither temperature and pressure conditions, at which the rocks had been formed at the bottom of the Black Sea—the Romanian Littoral—nor the biological conditions, specific to the Romanian Littoral in which organic combinations had been formed for ex. hematite, had not influenced their magnetic properties, hematite properties of marine origin being identic with those of hematite of the earth's crust[14][15].

Analysis by the X-Ray Diffraction

Analysis by the X-ray diffraction has been effectuated by using an automatic diffractometer URS-50, the tube of the X-ray having an anode of *Fe*. It was considered $\lambda_{Fe}\ K\alpha = 1.932076\ Kx$; a filter of *Mn* was used. In Figures 1 (*a*) & 1 (*b*) are represented the diffractograms thus obtained. For each sample there have been effectuated two diffractograms. A recording was made of the natural sample, and the second one from which carbonates were removed by leaching them with the weak acid.

Using the indicated method in Ref. (17) (18), the chemico-mineralogical composition of the analyzed samples was established[20]. The samples were taken from the following zones :

(1) Mamaia, (2) Agigea, (3) Vama Veche, (4) Mangalia (Table I).

Infrared Absorption Spectral Analysis

The infrared absorption spectrometer UR-10 K. Zeiss Jena with double fascicle, null optic and with three dispersion prisms was used. The same as in the case of the analysis by diffraction of the X-ray, two spectra were traced, one spectrum on the natural sample, and the other on the sample from which the carbonates were removed. In Figures 2(*a*) & 2(*b*) are represented the spectra thus obtained[18][19].

Spectrographic Analysis of the Sediment Samples

The spectrographic analysis has been effectuated by using a spectrograph with a diffraction grating the type PGS-2 GDR and the ultraviolet region of the spectrum comprised between 2,200 Å and 4,600 Å. The presence of the following elements in the sediment samples could be determinated *Ca, Mg, Fe, Mn, Al, Si*. There were also identified the trace elements contained in these sediments. In Table II are shown the results of the spectrographic analysis of the rock sample from the continental platform of the Black Sea (between Constantza and Mangalia) collected in 1968[21]. Analyzing the results, it was established that a higher

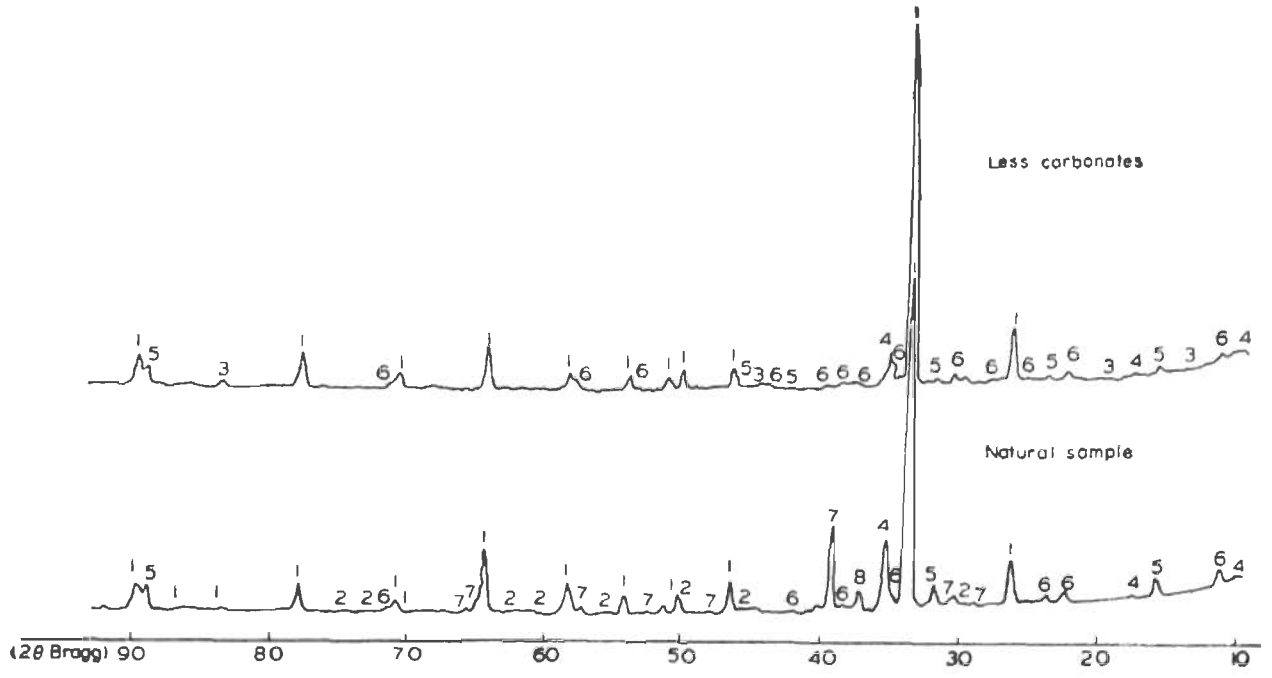

FIGURE 1 (a) : X-ray diffraction analysis of the sediment sample from Mamaia.

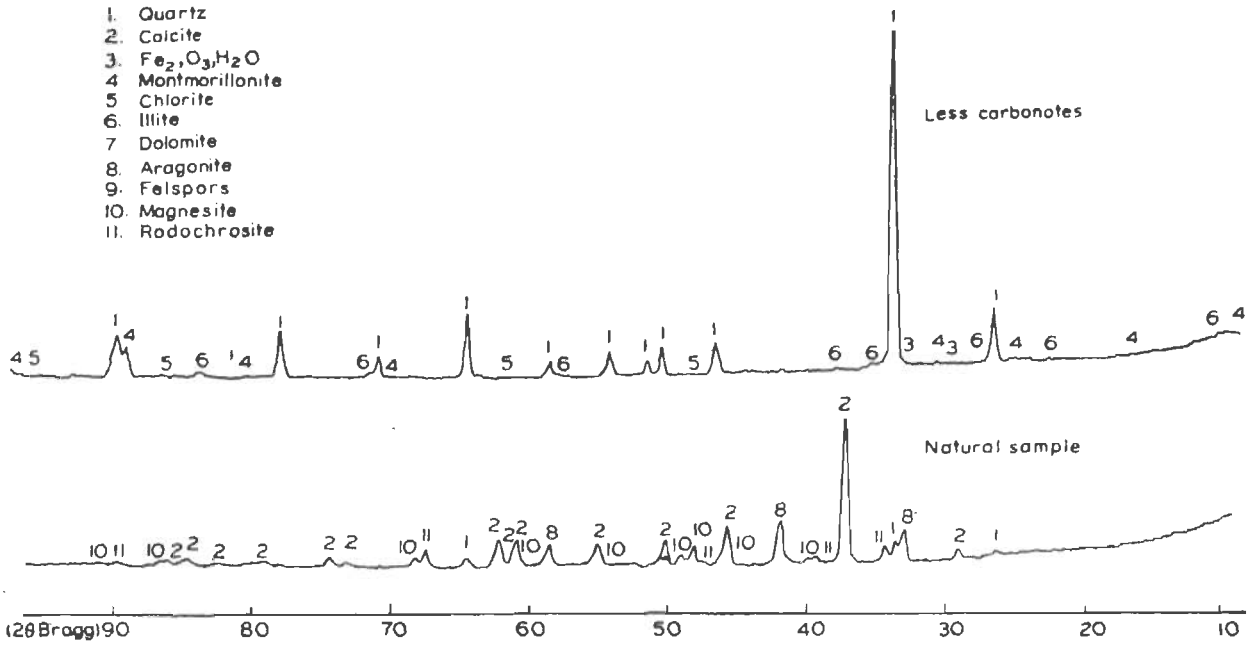

FIGURE 1 (b) : X-ray diffraction analysis of the sediment sample from Agigea.

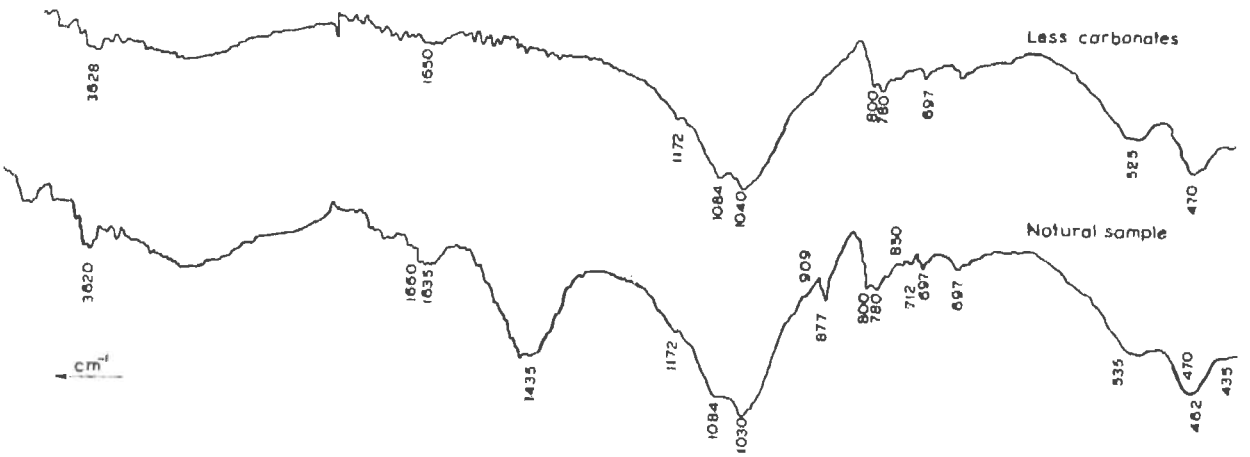

FIGURE 2 (a) : Infrared spectra of the sediment sample from Mamaia.

concentration of *Ti* and *Ba* occurred in the analyzed samples, which can be explained by the ionic exchange with calcium, especially from the calcite, which predominates the analyzed sample.

The quantity of iron oxide accumulated in rock is relatively large. The large quantity of titanium can be attributed to the fact that iron oxide collects titanium. Concentration of *Ni* and *Cu* depends on the quantity of *Mn* ([22]). In case of the samples studies, the contents of *Mn* are smaller than the iron, the rate $Mn/Fe = 6.810^{-2}$. Generally, it has been, however, established that in case of marine samples, the quantity of the trace elements is a little smaller than the average value of their content in terrestrial samples.

Chemical Analysis

(a) *Chemical Analysis of Black Sea Water*

Electrokinetical Potential

With the purpose of establishing of the electric charge of sediment particles as well as of the modifications of this charge in accordance with the sea water

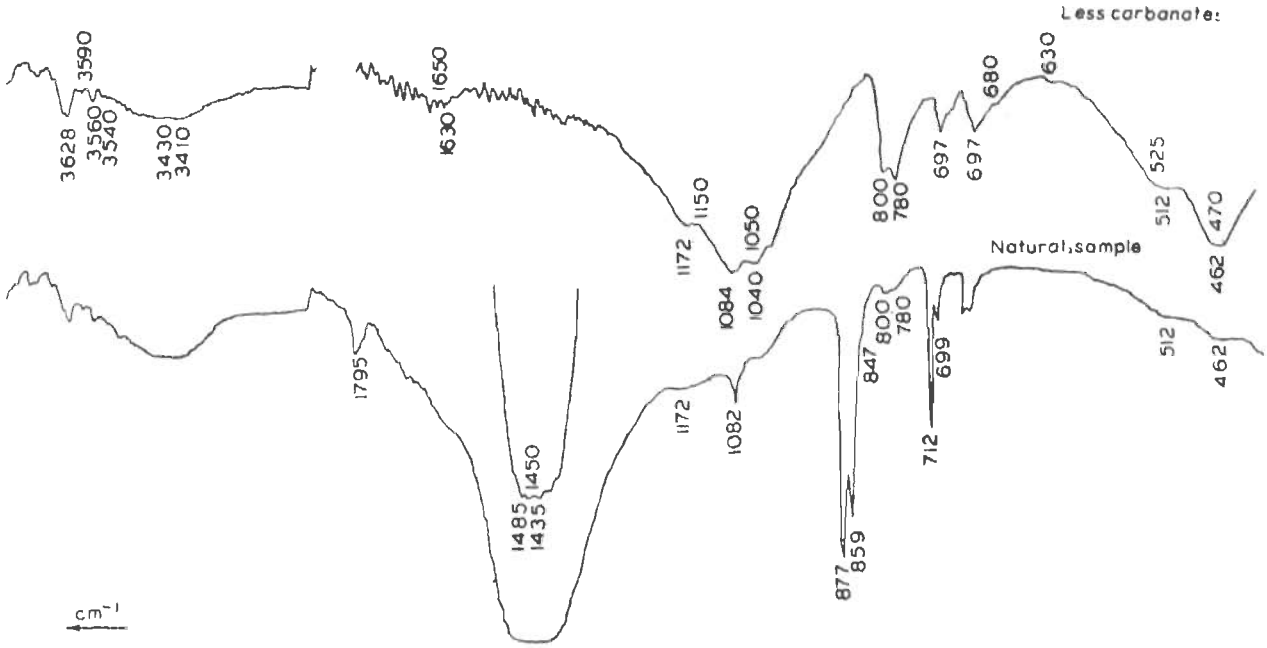

FIGURE 2 (b) : Infrared spectra of the sediment sample from Agigea.

TABLE I

Mineralogical composition of some sediments from the Black Sea bottom.

Components % \ Sample	1	2	3	4
Montmorillonite	3.1	0.43	6.53	—
Illite	7.85	0.76	1.87	0.31
Caolinite	—	—	—	1.47
Quartz	58.43	3.94	51.92	1.50
Fe_2O_3, H_2O	7.90	0.80	7.51	0.54
Felspars	—	—	11.58	0.75
Calcite	12.12	—	—	88.48
Calcite + aragonite	—	90.92	14.32	—
Dolomite	0.15	—	—	—
Magnesite	—	1.12	1.82	—
Siderite	—	—	2.08	—
Total	92.10	98.08	97.63	93.55
Unidentified substances	7.90	1.92	2.37	6.45

TABLE II

Trace elements contained in sediments from the Black Sea bottom.

Element	Mg/g sample	Compared with *Fe*		Compared with *Mn*
Ti	1000	$35.7 \cdot 10^{-3}$		0.52
Ba	300—1000	$(10.7—35.7)10^{-3}$		0.16—0.52
Sr	100	3.6	10^{-3}	0.052
Ni	30	1.07	10^{-3}	0.016
Cr	20	0.7	10^{-3}	0.0105
V	20	0.7	10^{-3}	0.0105
Co	10	0.36	10^{-3}	0.0052
Cu	10	0.36	10^{-3}	0.0052
Pb	10	0.36	10^{-3}	0.0052

saltness, the electrokinetic potential of sea sediments collected in the region of the Romanian Littoral of the Black Sea was determined.

Microelectrophoretic method for the determination of the speed of the *electrophoresis*[11][12] was used. In case of the studied sediments, a modification of the sign of the zeta potential which remains negative for very different salinities of the interstitial water was observed (Figure 5). The analyzed samples have been taken from the following Romanian Littoral :

(1) Mamaia, (2) Agigea, (3) Vama Veche (Table III).

TABLE III

The chemical composition of Sea Water—Romanian Littoral—uptaken in August 1973.

Ions mg/l / Sample	Na^+	K^+	Ca^{2+}	Mg^{2+}	Zn	Fe	Cr	Cl^-	SO_4^{2-}	HCO_3^-
1	9030	252	300	790	0.02	0.15	0.04	8875	815	213.5
2	10000	256	280	1064	0.024	0.19	0.06	9230	856	213.5
3	9030	254	280	711	0.018	0.15	0.04	8591	767	213.5

1. Mamaia, 2. Agigea, 3. Vama Veche.

The dosage of the ions, indicated in Table III, has been determined in the following way : *Ca* and *Mg* have been determined by complexometric titration with EDTA, *Na* and *K* were determinated using K. Zeiss plame—photometer type III, *Zn*, *Fe* and *Cr* were determined by the atomic absorption with help of the Perkin Elmer spectrometer 303, anions were determined volumetrically. Besides these elements identified in a chemical way, sea water contains also the artificial radionuclides resulted especially from the precipitations. Presence of ^{137}Cs was identified from γ spectrograms of the non-treated water samples, as well as after its separation under the form of $Cs_2\,Na\,[Co\,(NO_2)_6]$, the quantity varying between 0.3-0.4 pCi/l. A larger quantity was recorded in 1966-68[23]. ^{90}Sr (^{90}Y) was separated by precipitation in the form of oxalate. In the precipitate was entrained ^{90}Sr (^{90}Y). It has been established that concentration ^{90}Sr (^{90}Y) varies between 0.4-0.6 pCi/l. In Table IV are shown the values of concentrations of these radionuclides in water samples taken up between 1969-1973.

(b) Total Chemical Analysis of the Sediment Samples

Sediment samples have undergone an alcaline disaggregation and the metal constituents have been dozed in the respective melt. Free iron has been determinated by gravimetrical and photocolorimetrical methods. The results of these analyses are shown in Table V.

(c) Determination of Soluble Salts and of Cationic Exchange Capacity of the Sediment Samples

Soluble salts have been determinated in watery extract, the ratio water—sample being 5 : 1.

The cationic-exchange capacity, respectively exchangeable cations, has been determinated by percolating of the sample with ammonium acetate at $pH=7$ and analysis of the cations in a collected solution. In Table VI are shown the results of these analyses. In the case 2 and 4 samples, which contain high quantity of $CaCO_3$, the cationic content in the percolate give

TABLE IV

Concentration ^{137}Cs and ^{90}Sr in Black Sea Water—Romanian Littoral—uptaken in the period 1969-1973.

Collecting zone	year of collecting	pCi ^{137}Cs	pCi ^{90}Sr	$^{137}Cs/^{90}Sr$
Constantza	1969	0.70	0.60	1.116
Constantza	1970	0.55	0.50	1.100
Mangalia	1971	0.45	0.40	1.125
Mangalia	1972	0.40	0.35	1.142
Vama Veche	1973	0.40	0.35	1.142

TABLE V

Global chemical analysis of the sediment samples collected in different points of the Romanian Littoral in August 1973.

Constituents g/100 g / Sample	1	2	3	4
SiO_2	65.84	4.62	64.32	3.70
CaO	7.70	51.00	9.25	51.60
MgO	1.26	0.62	1.26	0.42
Fe_2O_3	9.25	0.72	9.50	0.85
Al_2O_3	2.85	0.28	3.10	0.45
Na_2O	1.95	0.73	1.69	0.32
K_2O	1.53	0.07	1.39	0.17
Lost at calcination 1000°C	9.54	41.00	9.45	42.23
Total	98.92	99.94	99.96	99.70
Fe_2O_3 free	7.10	0.72	6.75	0.48

1. Mamaia, 2. Agigea, 3. Vama Veche, 4. Mangalia.

TABLE VI

Soluble salts and cationic-exchange capacity of the sediment samples collected in different points of the Romanian Littoral in August 1973.

Sample	Soluble salts (me/100 g)							Exchange capacity				
	Na^+	K^+	Ca^{2+}	Mg^{2+}	SO_4^{2-}	Cl^-	HCO_3^-	Ca^{2+}	Mg^{2+}	Na^+	K^+	Total
1	36.6	0.95	2.4	1.6	12.8	22	2	30.2	0.17	2	1.65	34.02
2	17.7	0.53	2.8	0.2	—	18	2.5					
3	30.4	1.14	5.6	0.4	16.04	18	3.5	38.3	6.54	7.5	2.38	54.72
4	16.4	0.54	2.8	0.3	0.5	16	3.5					

1. Mamaia, 2. Agigea, 3. Vama Veche, 4. Mangalia.

erroneous results, and were not mentioned in the above table.

γ Analysis Spectrometry

The spectrometry analysis permits identification of some radionuclides present in the samples of marine medium. In this case has been used a γ spectrometer with a crystal of scintillation *NaI (Te)* of 75×75 mm and resolution 8 percent for the $E_\gamma = 661$ *KeV* of ^{137}Cs, as well as a detector *Ge (Li)* of 12 cm³, coupled to the impulse analyzer of 4096 channel. From γ spectrograms obtained it has been established that the radioactivity of samples of the marine medium (water and sediments) is due mostly to ^{40}K, natural radionuclide having $E_\gamma = 1456$ *KeV*.

In Figure 3 is represented the spectrogram of the sample obtained by a detector of *Ge (Li)*. Determining the *K* quantity from spectrograms obtained and comparing the results with those obtained by flame photometric method, a rather good agreement has been established.

The quantity of *K*, however, varies with the season, in which the samples have been taken, being larger in water samples collected in spring.

Generally, the *K* quantity in the Black Sea water, determinated by these methods varied between 250-300 mg/l in the samples of sea water in the Black Sea zone of the Romanian Littoral.

Besides that, from the spectrograms obtained, it has been established the presence of some artificial radionuclides in all the analyzed samples, the quantity of ^{137}Cs varying with the season, the accumulation of this radionuclide being connected with its quantity, in the atmospheric precipitations. Concentration ^{137}Cs has

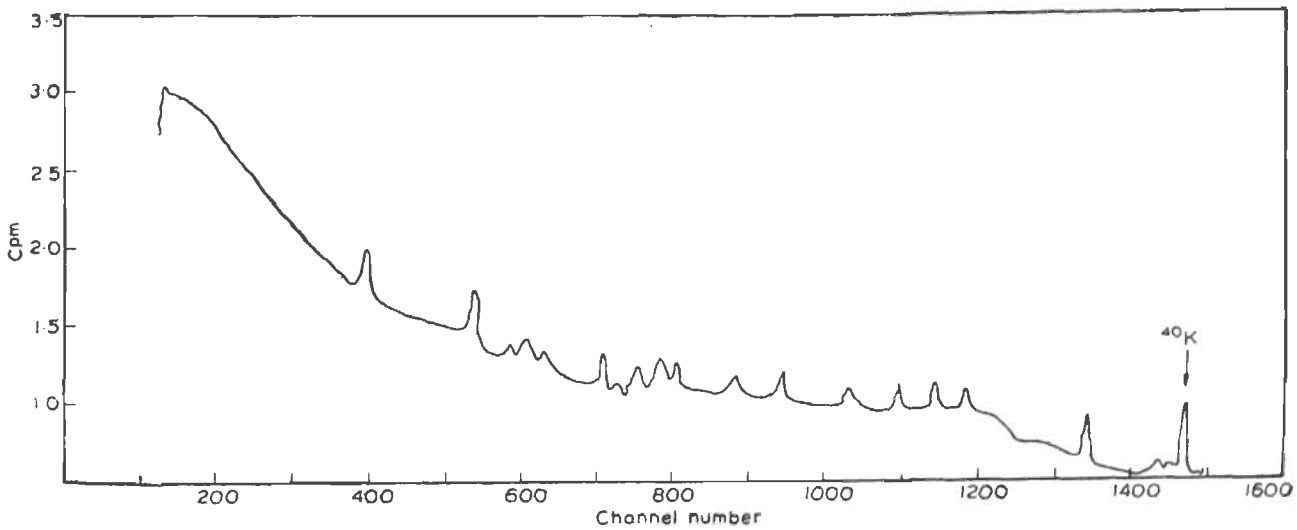

FIGURE 3 : Gama spectrogram of sediment of Black Sea ground from Mangalia.

varied between 0.1-0.3 pCi/g dry sample at 105°C and 0.3-0.7 pCi/l sample of used sea water. The quantity of ^{137}Cs from the sediment sample is pretty close from that of the sea water and a conclusion can be thus drawn that there exists an accumulation of this radionuclide in the sediments at the Black Sea bottom, and the establishment of an equilibrium between its concentration in water and sediment. For the establishment of this equilibrium there is need of long interval of time.

In natural conditions, in the marine medium are introduced simultaneously different radionuclides. In that case, their behaviour is not identical as in the case of one single radionuclide.

Determination of Sorption Capacity of Some Radionuclides in Sediments of the Black Sea Bottom

For the determination of distribution coefficients have been used the methods indicated by E.K. Duursma and C.J. Bosch[3] namely : the methods of sedimentation, of thin layers and that of suspension. The results obtained for samples uptaken in the region of Mangalia harbour, in August 1972, have been shown in Refs. (8) & (25). Distribution coefficient values obtained for the samples collected in August 1973 in different points of the Romanian Littoral [(1) Mamaia, (2) Agigea, (3) Vama Veche, (4) Mangalia] are shown in Table VII.

TABLE VII

Radionuclides sorption distribution coefficients as determinated by : 1. the suspension technique ; 2. the thin layer technique; 3. the sedimentation technique.

Sediment sample	Distribution coefficients K.10⁴						
	Sorption method	^{137}Cs	^{59}Fe	^{65}Zn	^{60}Co	^{54}Mn	^{144}Ce
Mamaia	1	1.5	5	2.2	1.5	5.8	7.8
	2	1.7	5.5	1.9	1.2	5.5	8
	3	1.3	4.5	2.1	1.1	6	8.2
Agigea	1	0.9	3.5	2.5	1.1	5.5	8.5
	2	1.1	3.5	2.8	1.3	5.8	8.1
	3	1.1	2.8	2.9	2.1	5.1	8.1
Vama Veche	1	1.0	3.5	2.8	1.5	5.4	7.9
	2	1.05	2.9	2.6	1.5	6.2	8.8
	3	1.2	3.8	2.6	2.1	5.8	8.7
Mangalia	1	1.9	2.8	2.9	1.6	5.1	8.8
	2	2.2	3.1	3.3	2.1	5.9	8.2
	3	2.2	4.5	3.4	1.8	6.2	8.4

Conclusion

From the analysis of the results presented in Table VII, the following conclusions can be drawn :

(1) The sediments from the Black Sea bottom—Romanian Littoral—present a high sorption capacity. This capacity was represented by distributing coefficients K, determinated in the case of those three methods used and namely: of suspension thin layers and sedimentation after the indications in Ref. (3), [Figures 4 (*a*), 4 (*b*), 4 (*c*)]. Coefficient values K have pretty high values, that which indicates that the radionuclides are retained on sediments.

(2) The distribution coefficients K are influenced by the physico-chemical properties of the analyzed sediments. Variation value of the distribution coefficients in

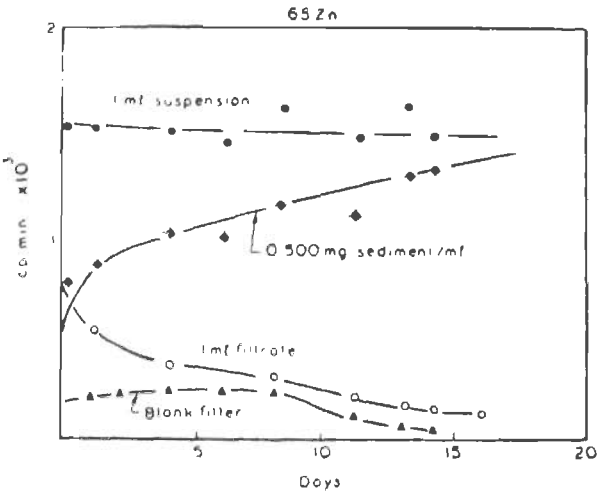

FIGURE 4 (a) : Suspension sorption technique.

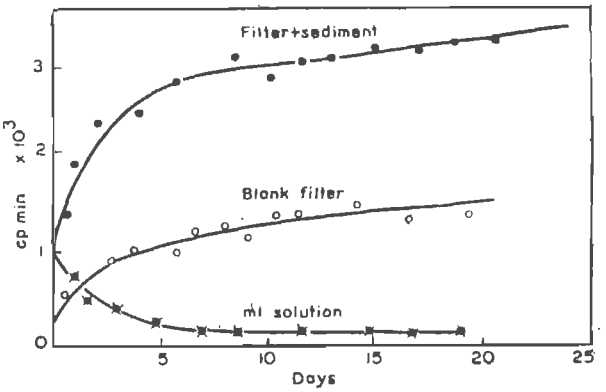

FIGURE 4 (b) : Thin layer technique.

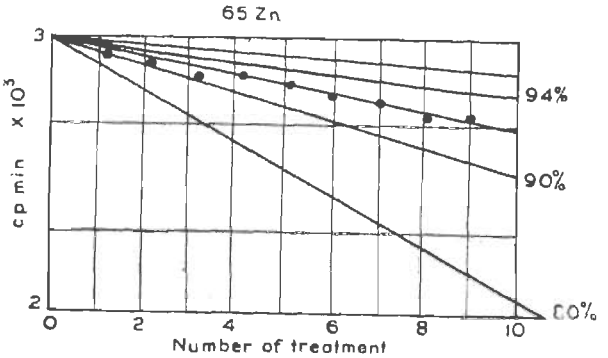

FIGURE 4 (c) : Sedimentation technique.

function of electrokinetic (zeta) potential and salinity of interstitial water, is represented in Figure 5.

(3) Sorption capacity is in function of the nature of used radionuclide. Cations are more powerfully retained due to the negative sign of the electrokinetic potential. Amongst cations, those which have greater charge and the smaller ionic radius, are more powerfully retained. Analyzing the behaviour of each radionuclide in part, it is observed that :

—in the case of radionuclide ^{144}Ce the distribution coefficient K is higher, but, however, there is not observed a variation of it in function of the chemico-mineralogical composition of the sample. Concerning the radionuclide ^{90}Sr (^{90}Y), the least retained by the sediments, the distribution coefficient K varies between the limits $(0.4 + 1)\ 10^2$ and does not represent a variation in function with the chemical composition of the sample. The values of this coefficient represent, however, high variations in function with the used method, that which makes that the results are not pretty conclusive. Using of other method for determination of this coefficient, indicated in Ref. (3), will permit more precise determination of K for the sorption ^{90}Sr (^{90}Y).

The distribution coefficient for the sorption of the radionuclide ^{137}Cs represents a higher value for the samples which contain more clays (illite, chlorite, montmorillonite) for example, the samples collected in Mamaia and Vama Veche zone variation of the coefficient K for sorption of the radionuclide ^{137}Cs in function with content of clays is shown in Figure 6.

It is also observed that as in the case of the radionuclide ^{137}Cs as well as of ^{65}Zn its distribution coefficient

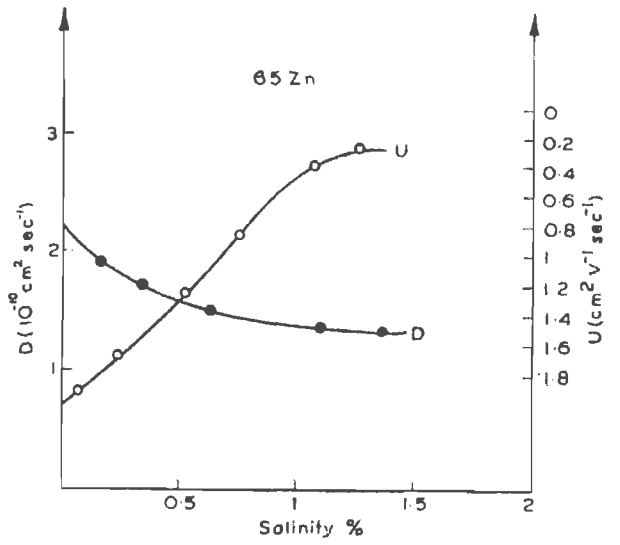

FIGURE 5 : Variation of diffusion coefficient D of ^{65}Zn in Black Sea bottom sediments (Mangalia) as function of salinity of interstitial water and the electrokinetic potential V.

for the sorption of these radionuclides represents a growth in function of cationic exchange capacity of the sample, Figure 7. However, this is only based on 2 observations.

Concerning the value of distribution coefficients for sorption of other radionuclides ^{59}Fe, ^{60}Co, ^{54}Mn a variation of this coefficient was observed which did not have a connection with chemico-mineralogical composition or other properties of the analyzed sediments in the present paper.

It is also remarked that samples with higher content of $CaCO_3$ and with close mineralogical structure, have not the same capacity of sorption for the same radionuclides in the same conditions of sorption that which indicates that sorption is very complex and all the factors on which depends this phenomenon are not yet

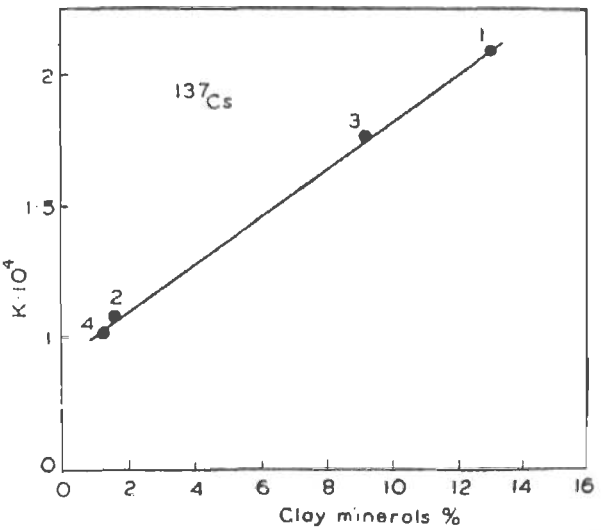

FIGURE 6 : Variation of distribution coefficient K for ^{137}Cs determinated using the thin layer method as function of clay minerals content in sediment.
(1) Mamaia ; (2) Agigea ; (3) Vama Veche ; (4) Mangalia.

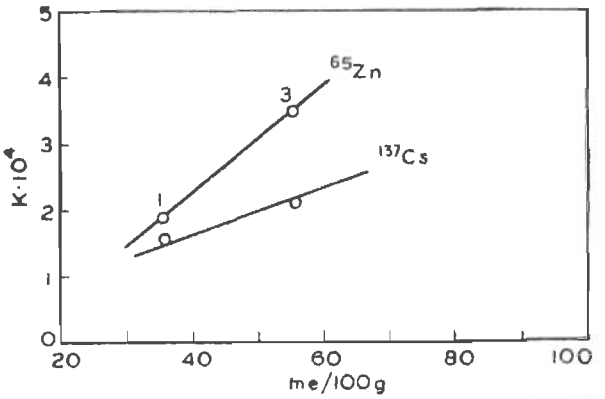

FIGURE 7 : Variation of distribution coefficient K for ^{137}Cs and ^{65}Zn as function of cationic-exchange capacity of sediments of Black Sea ground.
(1) Mamaia ; (2) Vama Veche.

known. In closing, it is specified that conditions under which were effectuated determinations, could not reproduce natural conditions in which intervene a series of processes which change conditions of sorption of the radionuclides.

It may be considered that the analyzed samples result generally in aerobic layers, but specific to the Romanian Littoral of the Black Sea, because the oxygenated conditions of sediments in the zone of the Romanian Littoral are influenced by the presence of the River Danube.

Acknowledgements

Present paper is the result of the studies carried out concerning the radioactivity of the Black Sea, initiated at the proposal of Dr. R. Fukai and suggestion of Dr. E. K. Duursma, of the International Laboratory of Marine Radioactivity, International Atomic Energy Agency, Musée Oceanographique Monaco, to whom the authors address here their most sincere thanks for the critical analysis of some results and for the materials put at their disposal.

The authors also address their most sincere thanks to Acad. Prof. I. Ursu, Chairman of the Romanian National Council for Science and Technology for the special efforts made for the creation of most adequate conditions for work at the National Physical Center, conditions that permitted elaboration of this paper.

The authors also ask Prof. V. Grecu and the colleagues at the Faculty of Physics of the University of Bucharest and the Institute of Atomic Physics (IFA) in Bucharest, who have helped them in the effectuation of some of the analyses, to receive their expression of most sincere thanks.

The authors further thank Eng. E. Alexandru from the Research Institute for Water Management for the analyses made of samples of sea water, as also to the Physicist I. Posircă from the Research Institute of Metallurgy for the analysis by diffraction of X-rays of the sediments samples.

The authors are also deeply grateful to Dr. Eng. R. J. Bally for his scientifical indications.

The efforts of the group divers from the Faculty of Physics of the Bucharest University organized and conducted by Eng. A. Ionescu have made possible the obtaining of subaquatic photographing in the zones where the samples were taken, as well as the taking of the used samples in our work.

The authors address to them all their most sincere thanks.

References

(1) DUURSMA, E. K. : "Molecular Diffusion of Radioisotopes in Interstitial Water of Sediments." Disposal of Radioactives Wastes into Seas, Oceans and Surface Waters, IAEA, Vienna, 1966, pp. 355-371.

(2) DUURSMA, E. K. and C. NOEDE : "Theoretical, Experimental and Field Studies concerning Molecular Diffusion of Radioisotopes in Sediments and Suspended Solid Particles of the Sea. Part A. Theories and Mathematical Calculations." Neth. J. Sea. Res., 1967, 3, pp. 423-457.

(3) DUURSMA, E. K. and C. J. BOSCH : "Theoretical, Experimental and Field Studies Concerning Diffusion of Radioisotopes in Sediments and Suspended Particles of the Sea. Part B. Methods and Experiments." Neth. J. Sea. Res., 1970, 4, pp. 395-469.

(4) DUURSMA, E. K. and M. G. GROSS : "Marine Sediments and Radioactivity." In Radioactivity in Marine Environment, U.S. Nat. Ac. Sc. NRC, Washington D.C., 1971, pp. 147-160.

(5) "Specific Activity of Radionuclides Sorbed by Marine Sediments in Relation to the Stable Element Composition." In Radioactive Contamination of the Marine Environment, AIEA, Vienna, 1973, SM-158/4, pp. 57-71.

(6) DUURSMA, E. K. and D. EIAMA : "Theoretical, Experimental and Field Studies Concerning Reactions of Radioisotopes with Sediments and Suspended Particles of the Sea. Part C. Applications to Field Studies." Neth. J. Sea. Res., 1973, 6, pp. 265-324.

(7) VOLJIN, V. and P. BULUMAC: "Sur la Radioactivité du Milieu marin de la Mer Noire." 1972, Rapp. Comm. Int. Mer. Medit. 20, 4, pp. 743-745.

(8) VOLJIN, V. and L. DINESCU : "Etude du transfer de quelques radionuclides de l'eau de la Mer Noire dans les sediments du fond de la Mer Noire." 1974, Rapp. Comm. Int. Mer Medit. 22, 8, pp. 39-41.

(9) VOLJIN, V. and A. IONESCU : "Prélévment des échantillon de sédiments du fond de la Mer Noire (documentation interne)." 1972.

(10) VOLJIN, V ; L. DINESCU and A. IONESCU : "Etude des processus de sorption de quelques radionuclides dans les sédiments du fond de la Mer Noire côte romaine." Analele Univ. Bucuresti (souss presse).

(11) VOLJIN, V. and A. MARINESCU : "Sur quelques paramétres de l'eau interstitielle et de la roche du fond de la Mer Noire, côte Roumaine." 1971, Rev.Roum. Phys. 16, 6, pp. 621-631.

(12) VOLJIN, V. and M. OLTEANU : "Determination du potentiel électrocinétique des sédiments du fond de la Mer Noire." 1974, Rapp. Comm. Int. Mer. Medit. 22, 8, pp. 71-73.

(13) VOLJIN, V. and M. OLTEANU : "Determination du potentiel électrocinétique des sediments du fond de la Mer Noire". Thallasia Yugoslavica.

(14) VOLJIN, V. and R. ALIKHANOV : "Diffraction Method used in Determination of Composition and Structure of Black Sea Bottom Rock." Preprint Univ. Bucharest, 1970, pp. 29 (in Russian).

(15) VOLJIN, V. and R. ALIKHANOV : "Etude de la roche de la platforme continentale de la Mer Noire par méthodes de diffraction." 1971, Rev. Roum. Phys. 16, pp. 633-642.

(16) STUBICAN, V. and RUSTUM ROY : "Isomorphous Substitution and Infrared Spectra of the Layer Lattice Silicates". 1961, The American Mineralogist, Vol. 46, pp. 32-51.

(17) BRINDLEY, G. W. : "X-Ray Identification and Crystal Structures of Clay Minerals." 1961.

(18) VAN DER MAREL, H. W. : "Quantitative Analysis of Clay Minerals and their Admixtures." 1966, Contr. Mineral and Petrol. 12, pp. 96-138.

(19) MOENKE, H. : "Mineralspektren." 1966.

(20) HEJER, K. S. : "Estimation of Chemical Composition of Rocks." 1961, The American Mineralogist, Vol. 46, 5 and 6, pp. 728-733.

(21) VOLJIN V. and BULUMAC, P. : "Spectrographic Analysis of Black Sea Bottom Rock—Romanian Coast." Preprint Univ. Bucharest, 1970.

(22) FUKAI, R. : "Chemical Composition of Shallow-water Sediments in the Bay of Roquebrune." Bull. Inst. Oceanogr. Monaco, 1965, 65 (1337), pp. 1-15.

(23) VOLJIN, V. and BULUMAC, P. : "Sur la radioactivité du milieu marin de la Mer Noire." Rapp. Comm. Int. Mer. Medit., 1972, 20, 4, pp. 743-745.

(24) VOLJIN, V. : "Analyse spectrométrique et dosage du ^{90}Sr dans les échantillons de l'eau de Mer Noire—côte Roumaine." Preprint Univ. Bucharest, 1970, pp. 10.

(25) VOLJIN, V. and DINESCU, L. : "Etude du transfer de quelques radionuclides de l'eau de la Mer Noire dans les sédiments du fond de la Mer Noire." Thallasia Yugoslavica, 1975 (souss presse).

WATER FOR HUMAN NEEDS : GENERAL

(ECOLOGY)

Environmental Aspects of River Development in Tropical Asia with Particular Reference to the Mekong Basin

V. R. PANTULU
Fishery Advisor
Mekong Secretariat, c/o ESCAP of the United Nations
Sala Santitham, Bangkok, Thailand.

SYNOPSIS

Environmental effects of dam construction are generally assumed to be harmful, largely as a result of experiences in the Pacific northwest of the American continent and in parts of arid Africa, and because of the undue emphasis given in popular press to the negative aspects of dam construction. This paper analyses environmental conditions in tropical Asia, with particular reference to the Mekong River system, identifies the observed and anticipated environmental effects of water resource development activities as functions of particular types of environmental situations, and points out that environmental effects of river development are not necessarily always harmful. This paper makes reference to the fact that no two river systems are alike, especially if they are located in different ecological zones. It concludes that extrapolations of experiences from one river system to another are not necessarily valid. The paper also concludes that through adequate preparatory studies and implementation of effective precautionary measures, it is possible to alleviate or offset the adverse effects and to enhance the benefits of river development, thereby rendering it a beneficial enterprise, on balance, in this region.

Introduction

River systems are complex environments, each with its own characteristic features. Tropical river environments in particular, with their infinite diversity of fauna and flora, and highly fluctuating physical and chemical features, are known to be more complex than those of rivers in other ecological zones of the earth. One of the important and widely applicable principles in ecology is that stability in an ecosystem is a function of the diversity (homeostatis). Thus, complex, normally saturated ecosystems, where all or the majority of the ecological habitats (and within habitats, the micro-habitats) are filled and exploited by many species, or life history stages, are least likely to be seriously disrupted by the alteration of a few habitats or by the elimination of a few kinds of organisms. Conversely, simple or undersaturated ecosystems, where fewer kinds of organisms and habitats are involved, are most likely to be catastrophically affected by environmental changes that remove or destroy a few habitats or eliminate a few species. It also follows that readjustment to rapid environmental change comes about most readily and with less basic disruption of biological production in complete systems. Even great population fluctuations tend to be more effectively damped out in complex or diverse systems.

Viewed in the light of these basic principles of ecology, the irrefutable fact that emerges is that environmental alterations resulting from water resource development are far less likely to be disruptive of useful biological production in tropical Asia than in arid Africa, in Europe, or in the Artic. However, even in complex environments, there are threshold levels of perturbations which, if exceeded, result in a delayed rather than rapid recovery. Sound as these principles are in theory, in practice, adequate techniques with which to gauge the health of an ecosystem, or to measure threshold levels of perturbations of differing magnitudes are only now

being developed. Therefore, the best way at present for assessing effects of human activities in river basins on aquatic production is to study case histories of environmental manipulations and to take note of disruptions that have resulted therefrom.

An accurate assessment of environmental effects of any river development programme is possible only if adequate basic information is available ; unfortunately, such information is scarce in respect to most of the river systems on earth. There is no gain saying the fact that most river development in different parts of the world historically has given scant regard to, and had only limited concern with the resultant environmental disruptions.

In "the environmental decade" now drawing to its close, alleged and potential disruptions have received disproportionately wide publicity. In such publicity, benefits accruing from river development in contrast, have often been ignored or given only "lip service." Many articles in public presses have thus been one-sided, unbalanced and even falsely alarmist. This publicity often attributes all the known previous environmental disruptions of river development activities to each new or projected river development scheme regardless of the unique environmental characteristics that prevail at each site. This has created an impression in the public mind that river development anywhere in the world would necessarily be uncompromisingly incompatible with environmental well-being. Such an impression is doing a great disservice by confusing the public and impairing its ability to recognize its own interest and thus impeding social and economic developments, particularly in countries where centuries of neglect have made the rapid development of resources imperative, if standards of living are to be elevated.

It is necessary to bring to a halt this undesirable trend, and to place the whole problem of environmental aspects of river development in a properly balanced perspective. It is necessary to emphasize that environmental effects of river development are not always harmful, but that they are multi-faceted and could at once be harmful, beneficial or innocuous depending on the facet observed. Also underlined should be the fact that no two river systems are alike, especially if they are located in different ecological zones, and that blind extrapolations of experience from one river system to another are not necessarily valid. Further, due cognizance should be taken of the fact that through adequate preparatory studies and implementation of effective precautionary measures, it is possible to alleviate or offset adverse effects and to enhance benefits, thereby rendering river development activity a beneficial enterprise on balance. It is, therefore, the objective of this paper to identify probable environmental effects of river development as functions of particular types of environmental situations and to examine actual experiences in the tropics, both harmful and beneficial, with special reference to the Mekong River development project in Southeast Asia.

The Aquatic Environment

It is obvious that effects of water resource development are most direct on the land that is actually inundated and on the aquatic environment. In the hydrologic system, major disruptions of dam construction usually arise through changes in water quality and water budget. The effects of these changes manifest themselves in several ways as elaborated in this section.

Sedimentation

Deposition of silt carried by river waters into reservoirs creates several environmental problems. Besides aggradation of the reservoir itself, sedimentation removes nutrient rich material from residual river flows and locks much of it into the lacustrine substrate. Abrupt changes in quality and quantity of sediments along with concomitant changes in the natural flooding pattern are believed to affect agriculture and fish production in many ways. Whereas, theoretically the principles involved in the foregoing surmises are sound, whether the apprehended effects do, in fact, occur in a given river is debatable and is dependent on various features of the river itself, such as the silt content of the waters, the nutrient status of the silt, the extent of flooding, and so on. It is often cited that in the case of the Aswan High Dam, due to deprivation of the annual nutrient silt deposits, Egyptian farmers have to spend millions of dollars every year for the purchase of large quantities of fertilizers, to recharge their soils with nutrients. Now this may be the case in Egypt, but directly to extrapolate the Nile experience to other rivers would be incorrect.

Water quality changes such as the foregoing, would depend on the volume, and nutrient content of silt carried by the river in question and also the silt contribution from the tributaries flooding the main river below the dam. For instance, in the Mekong, a careful study of the sediment problem has indicated that the silt content of Mekong waters ranges from a low of about 20-40 ppm between January and May to a peak of about 500 ppm in late August([23]). This shows that the Mekong is a relatively "clean" river, carrying a small quantity of alluvium in comparison to the Nile (1500 ppm), the Ganga (1950 ppm) and the Mississippi (1750 ppm). The Mekong study has further shown that the "sediment deposition does not measurably increase soil fertility in the Mekong delta"..."if the role of sediment on agriculture is considered without consideration of other side effects, water control in the delta is the single, most important change that can bring about dramatic increase in the delta's agriculture production. Elimination of silt deposition on delta soils should no longer be considered a negative factor against dam construction on the Mekong River."

Another reported disaster resulting from the trapping of silt in the Aswan Dam is the collapse of a fishery yielding annually 18,000 tons of sardines (value estimate US $ 13 million). Since the disappearance of the sardine

coincided with the completion of the Aswan Dam, it is surmised that "since the floods stopped, the aquatic food chain in the eastern Mediterranean has been broken along a stretch of continental shelf 12 miles wide and 600 miles long. The lack of Nile sediment has reduced plankton and organic carbons to a third of what they used to be, either killing the sardines, scombroids and crustaceans in the area or driving them away"([21]). There were no studies prior to the dam construction on the ecological features responsible for the appearance of sardine stocks in the eastern Mediterranean. Also, there are no precise studies establishing a cause and effect relationship between the Aswan and the disappearance of the sardines, notwithstanding the fact that the postulates in support of this surmise appear to be theoretically sound. Sardines have disappeared elsewhere in the world in situations completely unrelated to dam construction. They have equally mysteriously reappeared after a lapse of some years (for example, in the Indian Ocean). Cyclic fluctuations in numbers is a normal phenomenon in animal populations and is a well recorded scientific fact. Therefore, before it could be categorically asserted on the basis of the Nile experience that there is a cause and effect relationship between the disappearance of fish in inshore areas and dam construction, positive proof based on information derived from carefully planned and executed ecological studies would have to be provided.

Soil Erosion

Deposition of silt in reservoirs and resultant changes in the pattern of sedimentation in deltaic areas, combined with the increased impact of marine currents on the shoreline, due to reduced flooding from the river, are reported to cause erosion and crumbling of the delta shoreline. Increased aggressiveness of flow of silt-free waters in residual rivers, scours river beds and banks much faster than in a normal river. Erosional aberration of the substrate, of the shores and water sheds of reservoirs has been reported in many cases. The adverse effects of such erosion are obvious. Coastline erosion could cause the loss of valuable deltaic lands. Scouring of river beds and banks could result in collapse of barrages, bridges, and other structures. Reservoir erosion could reduce biological productivity by smoothening the configuration of the reservoir and smoothening fish food, fish nests and nesting grounds. Harbours could be silted up. Examples of one or more of such adverse effects are reported from the Aswan Dam in Egypt, the Kainji Lake in Niger, Lake Rybansk in USSR, among others.

Erosion is a result of interaction among several natural forces : water, climate and weather, and substrate. Environmental disruptions due to erosional extremes do occur, but they need not necessarily be aggravated by all river development activities. For example, in the Laotian Nam Ngum of the Mekong Basin, "there is no evidence of erosion problems prior to the project or after phase 1. No change is foreseen as a result of phase 2"([1]).

Removal of sediments by dams could be of some advantage to water-using industrial establishments, like paper mills. Furthermore, relatively sediment-free water from a reservoir is cheaper to treat for domestic consumption than silt-laden waters.

Fisheries

Fisheries are very important economically and nutritionally in Asia. Modification of riverine environment into a lacustrine environment by dam construction, affects the fisheries of the river system in many ways. The two major premises fundamental to the understanding of such effects in relation to modern concepts of protection and management of fisheries relative to river development are the following([13]) :

(*A*) Impoundment drastically alters the riverine environment by bringing about substantial changes in the morpho-ecological nature of rivers. Fast-flowing sections are converted into relatively static environments and long established inter-relations between organisms are transformed radically. Changes in temperature regimen, volumes and cycles of discharge, velocity of current, gradient, temperature, substrate, mineral content and other parameters take place. Alterations of spawning grounds resultant on flow and erosional depositional shifts inhibit propagation and development of both lythophilous and rheophilous species. If spawning grounds are eliminated, species may even disappear. Both qualitative and quantitative changes also take place in food chains and available foods. Fishes narrowly adapted to specific set of environmental conditions, cannot withstand sudden environmental alterations beyond rather narrow limits. Hence, many components of riverine fish faunas can be adversely affected by sudden and drastic changes that follow upon dam building.

(*B*) In many species of fishes, there are races or populations that are perpetuated from specific spawning areas or 'homes'. When dams deprive access to spawning areas for homing spawners, a specific race can be destroyed.

These basic premises which place rigid restrictions on the latitude available for modification of riverine environments have emerged largely as a result of the vast experience in the Pacific northwest of the American continent, with particular reference to the Pacific salmon populations. Unfortunately, assessment of fishery problems in relation to dams everywhere in the world has now been conditioned by these premises, irrespective of such considerations as levels of tolerance of different species to environmental change, their migratory habits, biology and ethology.

Tropical river environments exhibit violent seasonal fluctuations. As a measure of adaptation to widely fluctuating environmental factors, many of the fish species that inhabit these rivers have evolved a wide range of tolerances. Any realistic assessment of effects of river development on species populations should take this into account.

A tropical river has a seasonally conditioned regimen, and is thus a violently fluctuating environment. In the

Mekong system, the conditioning factor is the monsoons. In tropical rivers in general, flash-floods and large-scale inundations are common features. The annual amplitude of variation in discharge between the dry and flood periods is very high ; in the Mekong at Kratie, Khmer Republic, it ranges on the average between 1,764 m^3/sec for the dry period and 52,000 m^3/sec during floods. Due to differences in substrate and continued scouring action of floods over a long period of time, depressions or 'pools' are formed in the beds of rivers at several places. These pools often assume considerable proportions ; in the Mekong, some of them in Laos/Thailand region are a few kilometres long and more than 50 m deep. In the stretch of the river in the Khmer Republic, D'Aubenton(6) located several "troughs 40 to 60 m deep." These deep pools retain water all the year round and offer a sort of 'transient lacustrine' environment during the dry months. The months February to May usually constitute the low water period, when the wetted perimeter in the river is at the lowest. During this time of the year, fluvial sections of many of the tributaries are reduced to a mere trickle of water and the only relatively stable aquatic environment is provided by the often isolated pools in the stream beds. It is here that the residual fish population takes refuge.

In the lower Mekong, water temperatures generally are high and fluctuate within the wide range of 20°C to 37°C at different points during different months of the year. Hydrogen ion concentration values range between *pH* 6.0 and 8.2, and dissolved oxygen values run between 2.8 and 7.5 ppm (from oxygen deficient to saturated) in different sections of the river. Water-level in the river starts rising by about the end of May, reaches its peak in August or September, and finally subsides in November. With the onset of floods, water temperatures rise and dissolved oxygen and *pH* levels fall, mainly as a result of decomposition of the vast amount of organic debris brought in or inundated by flood waters. In the Mekong basin, it is estimated that in Viet-Nam delta alone, an area of about one million hectares is inundated and that water-level rises by 4 to 5 m with current velocities varying from 0.2 m/sec in February to about 1.4 m/sec or more in August. Flood induced changes in the environment return to normality and conditions of the dry period begin to set in during December or January.

Fluviatile sections of the river itself are not very productive, due to the relatively high turbidity, fast current and shifting sandy nature of the bottom. Plankton production in this fluviatile environment is low compared to that in the pools, the oxbows, and other inundated regions beside the rivers. These three regions are the true pockets of biological production in the river system.

More then 400 different species of fishes have been recorded from the lower Mekong basin. In contrast, the basin of St. Lawrence River with its Great Lakes, in the Temperate Zone at some 45°N latitude in North America, has only 150 species. In the Mekong, during the dry months of the year, carps (family : *Cyprinidae* ; 54 percent), catfishes (families : *Siluridae*, *Clariidae*, *Schilbeidae*, *Bagridae*, *Sisoridae* and *Akysidae* ; 19 percent) and murrels (family : *Ophicephalidae* ; 8 percent), together constitute about 81 percent of the fish fauna. The remaining 19 percent consists of feather-backs (*Notopteridae*), herrings (*Clupeidae*), climbing perches and gouramis (*Anabantidae*) and other miscellaneous groups. This composition varies slightly during different seasons, but averages substantially the same from year to year.

The life cycle of a vast majority of fishes depend prominently on the annual flooding and inundation cycle in many tropical rivers. With the onset of floods and concomitant submergence of fields, ditches, swamps, bayous, oxdows, and other low lying areas over considerable distances on either side of the river bank, a predominant section of the fish population "migrates" laterally from the rivers to the inundated areas, mainly for spawning. These migrations, barring a few exceptions, are more lateral (towards and into the inundated land bordering the rivers) rather than up or down the rivers (from estuaries to headwaters, or vice versa or from pools to rapids, etc.). The distances traversed in the 'lateral migrations' and the duration of sojourn in the inundated zone differ with different species, depending on their physiological requirements and environmental tolerances. Fishes with low oxygen requirements, or those with accessory respiratory mechanisms in addition to gills, like murrels, some catfishes, and climbing perches and related species remain for longer periods in the peripheral zones of inundation, where dissolved oxygen and *pH* are generally low, due to decomposing organic matter including submerged terrestrial vegetation. Many carp family members (*Cyprinidae*) which generally have higher oxygen requirements and lower tolerances to *pH* fluctuations than the foregoing occupy the proximal zone of inundation, spawn there and are among the earliest to move riverwards with receding floods. If the flood recedes quickly, as it happens during years of relatively sparse rainfall, large numbers of eggs and hatchlings become stranded and die due to desiccation. In contrast, when flood waters remain for a relatively long period, as in years of heavy rainfall, there may be large-scale mortalities of fry and fingerlings due to deoxygenation and drastic changes in *pH* resulting from decay of organic matter in flood waters. In some areas, then, flood regulation which eliminates either very high or very low flood, might actually be beneficial to fisheries.

The observed high fecundities in most of the tropical river fishes, except in those that exhibit parental care, are an adaptation for species survival in the face of natural periodic large-scale mortalities. Some of the young that result from the spawning activity in the inundated zone, enter the main river and repopulate it. Others are left behind in the water bodies inland, grow there and provide a rich crop of fish. Thus, a sort of natural restocking of the water bodies on either side of the river takes place annually when floods occur. The fact that fish fauna represented in residual stagnant water bodies is essentially the same as the riverine fauna

is an indication that many tropical river species can thrive in relatively still water environments. It is also obvious from the above, that annual inundation is of paramount importance to the propagation and survival of the vast majority of tropical river fishes. Any river development programme that completely eliminates annual flooding is bound to cause disruption in natural fish production and thus cause damage to fisheries.

While dams do change the inundation pattern in different degrees of magnitude depending on how discharges through them are regulated, in general they do not significantly alter other critical environmental features, such as temperature, dissolved oxygen and *pH* (except in deep stagnant waters of some reservoirs). Pantulu[14] citing the example of post-impoundment situation in the Nam Pong River (Mekong basin), concludes, with supporting data, that changes that occur in these critical environmental features in the top strata of reservoir waters and the residual river, are well within the normal range of fluctuations to be expected in natural rivers in the pre-impoundment phase. Thus they are within the adaptive tolerance ranges of most fishes concerned.

It is apparent from the above that the Temperate Zone—derived rigidity of restrictions on the latitude available for modification of the riverine environment, need not necessarily be applicable to tropical situations. This contention is further substantiated by the observed species composition of fish populations in the pre- and post-impoundment phases. Many tropical river species thrive in the relatively stable lacustrine environments that replace the widely fluctuating tropical river environment above the dam. It has been observed that consequent on the creation of different reservoirs, 2 to 30 percent of the original river species have disappeared, depending on the location of the dam. Fewer species have disappeared in mainstem reservoirs which have access to unaltered rivers and tributaries, than in tributary reservoirs. Notwithstanding the reduction in the number of species, there has invariably been an increase in fish production in a submerged river as a result of large quantities of fish food that develop in the reservoirs, in the expanded aquatic environment. The average production per hectare in an unaltered tropical river is estimated at about 12 kg/ha/year, whereas reservoirs have produced anywhere between 30-180 kg/ha/year and more, depending on their location, morpho-edaphic features, and efficiency of fishery management measures implemented. To cite two outstanding examples in the Mekong, the Nam Pong reservoir in Thailand has been producing on an average 1,600 tons of fish, valued at US $ 800,000 equivalent annually, while the Nam Ngum reservoir in Laos yields 1,800 tons annually, valued at $ 1.4 million equivalent at current market prices in that country. In both these instances, fishery benefits compare favourably, even exceed, electric power benefits. Similarly, representative conservative approximations that have emerged to date for stabilized annual metric tonnage of fish catch sustainable with good management for some African reservoirs are : Lake Nasser, 12,000; Lake Volta, 40,000; Lake Kainji, 4,500; and Lake Kariba, 6,000 (Lagler, personal communication). In view of the foregoing, it is ironic that despite the magnitude of benefits they generate, fisheries are often relegated to an ancillary role in planning water resource development projects.

It is sometimes argued that the fishery 'largesse' does not always last. Whereas it is true that in many reservoirs there is typically a decline in fish production after the first peak of increase, due to a phenomenon known as trophic decline, even the lesser ultimate levels of stable production are invariably much higher than those in unaltered rivers. Also, proper fishery management efforts can minimize the extent of decline in production, as exemplified in various reservoirs in the USSR. In the Nam Pong reservoir in the Mekong basin, even ten years after the creation of the lake, there is as yet no evidence of decline in catches. Dam construction, thus has seldom brought about changes in water quality in the freshwater stretches, which are outside the range of fluctuations occurring in natural rivers, but has only removed or dampened the amplitude of fluctuations. By virtue of the fact that many fish species of tropical rivers are adapted to life in the relatively static environments of pools in river beds or inundation zones beside the rivers, a vast majority of them actually thrive in the relatively newly stabilized environment of man-made lakes. Whereas undoubtedly, a few riverine species do locally disappear in the lakes made by damming rivers, this loss is more than compensated by the increase in actual fish production. Furthermore, although dam construction in the tropics has not appreciably affected fisheries in the freshwater stretches of the rivers due to water quality changes, water budget changes have either precipitated or could precipitate adverse effects on site in the residual river immediately downstream the dam, or off-site effects in estuaries and adjacent inshore marine areas.

A case in point is the observed sudden steep decline in the Indian shed (*Hilsa ilisha*) fishery in the inshore areas of the Bay of Bengal and the Hooghly estuary coinciding with the construction of the Maithon Dam in 1957[16] ; the third to be constructed in a series in the Damodar Valley in India. The Indian shad catches, which prior to 1957 used to comprise 60 percent of the total landings of fish in the area suddenly declined to 5 percent of the total landings. This decline was attributed to the drying up of a 90-mile stretch of spawning grounds of the fish in the residual Damodar and the Rupnarain Rivers. However, since 1972 there are indications that these populations are building up, perhaps as a result of increased survivals in adjacent spawning areas in the Hooghly.

Off-site effects of dam construction could be very significant in the dynamic tropical estuarine ecosystems, about which, admittedly, very little is known. Estuaries generally are among the most highly productive ecosystems on earth. This productivity is usually attributed to delicately balanced interactions amongst various biotic

and abiotic factors in an unusually shallow and fertile water area. Crucial among these factors are shifting salinity and temperature gradients ; allochthonous nutrients that regularly flow into the system and are quickly recycled there ; the nutrient-laden substratum that is constantly in photic zone ; a general freedom from predators ; and an optimization of the ecosystem by a delicately balanced, long-time evolved form of time sharing in which larvae, young, juveniles, and even adults of a host of different organisms utilize the food resources at different times and thus minimize competition. Estuaries are valuable nursery grounds for many marine and freshwater species. Many principal offshore fisheries are dependent on fish stocks the young of which must have access to the protection and nourishment afforded by estuarine tidal flats during the early stages of their life histories([16]). Despite the great advances of techniques in offshore fishing, most of the world's marine fish catches still comes from coastal waters and predominantly from those under estuarine influence.

Any water control in the estuaries could bring about far-reaching environmental changes. The magnitude of the environmental changes would naturally depend on the scale of water control that is practised. Only specific studies in a given situation can give the necessary insights into the actual effects that should be anticipated in a particular area. Changes in the configuration of the basin and reduction in net volume of flow into estuaries, by water resource development activities like upstream dam construction and poldering, bulkheading and filling, dredging, ditching of marshes, diversions, barriers, seawalls, tide control structures in the estuaries themselves, could result in alteration of drainage pattern and circulation which in turn could affect seasonal and special distribution of critical environmental factors such as salinity, temperature, magnitude of flows and velocity of currents. Changes in volume and seasonal distribution of freshwater inflow could also result in reduction of influx of terrigenous nutrient materials resulting in a general deterioration of the estuarine habitat and in a measurable loss of productivity. Changed hydrographic structure and behaviour in the estuary, could lead to upstream movement of deoxygenated bottom waters due to combined salinity and thermal stratification effects. Besides, siltation and intrusion of seawater could increase and the wetted perimeter (land-water interface) could decrease, leading to destruction of food and cover for fish. All these environmental changes could lead to alterations in vegetative cover, loss of nutrient material, reduction of spawning, nursery and feeding areas and an overall reduction of potential for fishery production.

Although changed river flows can have adverse effects on aquatic life, there are also instances on record where upstream movement of higher isohalines in an estuary could be beneficial under certain conditions to some estuarine populations. Steadied transport of nutrients could also potentially benefit the fisheries in that regulated flow could affect the estuarine penetration and abundance of both desirable and nuisance organisms and also enhance the spawning success of some species.

Instances of both positive and negative effects of water management on aquatic life in estuarine abound in scientific literature, a few of which are cited below as pertinent examples. According to Gunther([8]), alterations in the drainage pattern of marsh lands have led to significant ecological changes in the Mississippi delta. Rich oyster grounds and other shellfish spawning areas have become barren as a result of these changes, though finfish yields have not apparently been affected. Also, leveeing the main streams has resulted in an increase in the velocity of current, leading to an increased transportation of silt ; resultant alluviation, sedimentation and flooding of swamps has virtually eliminated marshes and estuarine conditions. Other important effects in the Mississippi estuary are, deposition of enormous quantities of silt directly in the Gulf of Mexico ; decrease in nutrient drainage from land ; increase in salinity and its stability ; and occurrence of island erosion and inland movement of bays. The estuary has changed, usually in ways detrimental to aquatic life. Sudden influxes of freshwater and resultant instability of the estuarine system around the river mouths have generally lead to a decrease in fertility([5]).

Korringa([9]) cites an instance in the Netherlands where closure of the Zuiderzee by diking, eliminated the traditional fisheries for herring and anchovies in that body of water, though it resulted in an increase in eel populations and the consequent development of new fishing industry. Segerstraale([19]) cites an instance in Finland, where average changes of 0.5 to 0.75 percent in salinity have produced beneficial alterations in the effective distribution of estuarine species.

Despite the alarming possibilities of adverse effects of water resource development, estuaries are remarkably resilient systems that resist change; they also have the capability of quickly healing many of their man-inflicted scars([5]). Well planned manipulations based on an adequate understanding of the estuarine environment could well result in overall benefits. The gross ecology of an estuary can be managed advantageously. There is room for a great deal of new thinking in the release systems of river water, diversion of large volumes and alterations of channels, currents and tides([9]). Aquaculture possibilities can be vastly developed. For instance with good upstream management, certain areas could be reclaimed more profitably, more quickly and at a lower cost for aquaculture than for agriculture. There are examples in Asia (India, Taiwan, Philippines, etc.) where brackish water areas reclaimed for aquaculture at an average one-time-cost of US $ 500 per hectare are yielding an annual finfish or shellfish crop valued at over US $ 1,200 per hectare. Net returns in such aquaculture operations are said to average between US $ 500 to 650 per annum. It is understood that average cost of reclaiming deltaic lands for agriculture are far higher and that the returns from agricultural operations are far lower

than for aquaculture. There is, therefore, an urgent need for understanding the ecology of any specific estuarine system, before attempts are made to forge any far reaching changes that would adversely affect its valuable resources. Otherwise the very object of water resource development, could be negated.

Migratory Fish

It has almost become axiomatic that dams interrupt life cycles of fish by inhibiting or obstructing their migrations and consequently lead to decline in the fisheries. Some calamitous consequences of dam construction have indeed taken place under certain environmental conditions, with specific fish species that perform long range migrations and have 'homing' requirements. In the rivers of the Pacific northwest of the American continent, for instance, the predominant commercially important fish are five species of the migratory Pacific salmon. These fish have a remarkable life story. Spawned in freshwater, they grow to adulthood in the high seas and perform spectacular migrations, sometimes of more than a thousand miles to reach upstream spawning grounds in river systems. The destination of each and every fish is the very same spawning ground where it had hatched and passed its early larval stages. There is so little straying from the parent stream that homing access to this stream determines the survival of the species stock in each spawning stream. This access can be denied by a dam.

Research indicates that the fish migrations such as those of the salmon are not consciously performed acts in the anthropomorphic sense, but a series of movements executed in response to imprints in the fish brain of environmental gradients. Specific features of environment, including water chemistry, current velocities and temperature, release specific behaviours comprising a series of directed movements that make up the entire pattern of migration and spawning. If a dam caused environmental changes beyond rather narrow limits, the environmental clues that trigger the pattern of homing migration are lost. Almost all salmons unable to reach the parent stream spawning ground, die without reproducing. In such cases, dams that obstruct migrations are rightly adjudged harmful to the fish.

What has happened to the Pacific salmon in dammed North American stream systems, has unfortunately formed the basis for present-day popular thinking that dams anywhere in the world are inevitably detrimental to fisheries. In tropical rivers like the Mekong, however, commercially important migratory fishes are generally few. Consequently, the detrimental impact of dams as barriers to migration may be very small. In contrast the Indian shad, which performs seasonal migrations in most of the rivers in the Indian sub-continent and in Burma, is of very considerable commercial value. Dams on the Indus, Cauvery, Krishna and the Godavari Rivers have, by virtue of their location, had different degrees of adverse effects, on migrations of this shad although they have not been of catastrophic proportions. The main effect had been a restriction in the range of its distribution to the stretches of the rivers below the dams. In this case, obviously the dams have not barred access to all the spawning grounds of the fish. However, in the Hooghly River in India, construction of a series of dams on its major tributary system have resulted in a catastrophic decline in the fishery as previously cited.

Another group of important migratory fishes in the tropics are the eels, *Anguilla* spp. These eels grow and become adults in freshwater rivers and, at maturity, migrate to unknown spawning grounds in the sea. Their young elvers return to freshwater rivers to complete the life cycle. Eels are hardy fish, which are known to even take short cuts around river bends by wriggling through moist grass, or to climb even steep wet walls, or waterfalls. They have considerable commercial value both locally and as an export commodity, but this potential has not yet been tapped in many of the countries in Southeast Asia. Considering the hardy nature of the eels, and their capacity to survive out of water for prolonged periods, only a large dam could limit their production.

Besides the two migratory groups of fishes mentioned above, in tropical Asian river systems, there are about a dozen important species of marine or euryhaline fishes which are known to perform relatively short seasonal migrations in the marine estuarine zone for feeding or breeding purposes. Very little information is available about the directive and causative factors for these migrations. It is conceivable that dams would affect these valuable fisheries adversely, but precise information on their stock movements and biology is essential before any specific statements regarding the effects of dams on these fisheries could be made.

The important potomodromous fishes species which are known to perform within river migrations in Asian Rivers, and which could be adversely affected by dam construction, either as a result of environmental changes brought about by dams or by obstruction to migrations include catfishes of the genera *Pangasius* and *Pangasianodon*, the major barbels, *Barbus* (*Tor*) spp., *Probarbus* spp. and the giant freshwater or river prawn (*Macrobrachium rosenbergii*). The giant freshwater prawn makes up high valued catches from freshwater rivers and estuaries and has a great aquaculture potential with a growing demand in both local and world markets. This species is known to spend its adult life in freshwater areas and migrates to estuaries and brackish waters for spawning where environmental salinity is the important factor for the reproduction and survival of the young. Salinity regimen changes in estuarine areas caused by impoundments upstream are known to affect the species. Decline in the fishery of the giant freshwater prawn due to dam construction was reported in the Krishna and the Godavari estuaries in India. In the Mekong, detailed studies are being conducted to elucidate the problem and also to develop large-scale culture of the species as a rehabilitative measure taken in advance of the onset of the apprehended adverse effects.

The other riverine migratory species also—the catfish and the major barbels—are of considerable commercial

value ; in a river like the Mekong and the Ganga their fishery may be worth a million dollars (equivalent) or more annually. In such waters a careful evaluation has to be made of the probable effects of dam construction on the fisheries, and rehabilitative measures to offset any anticipated losses have to be implemented as a part of the new water management scheme. In the Mekong development programme, artificial propagation of endangered species and their large scale cultivation in water bodies is the principal ameliorative measure that is being adopted to offset anticipated losses([14]).

Stratification

Stratification, which is a result of the tendency of lighter, warm water to float over denser cooler water, is a phenomenon observed seasonally in many deep reservoirs. When a reservoir is thus thermally stratified, oxygen from the previous vertical mixings may be depleted soon in deepest layers. In these layers, hydrogen sulphide is also produced, imparting obnoxious odour and creating a fishless void. However, even in deep tropical reservoirs where stratification generally occurs, the top ten metre (or so) layer always remains well oxygenated as a result of wind action and oxygen produced by the hordes of microscopic green plants (photoplankton). Stratification often breaks down with the onset of strong winds, generally during monsoons, and during heavy cool rains. The obnoxious presence of hydrogen sulphide in the deep reservoirs results from decay of submerged vegetation and the decomposition of organic matter that settles down. This along with concomitant depletion of oxygen may cause fish kills during the initial months or years of reservoir formation or when there is a sudden turnover of the water mass. This is, however, a transitory feature, and the magnitude of such fish losses is insignificant compared to the high levels of fish production that follow. Water low in suspended solids and acidic from flooded forests, marshes, and brooks corrodes hydraulic machinery and pipelines; bacterial slime develops in closed conduits and algae and moss grow in open concrete lined canals impeding water flow and resulting in power generation losses.

However, on the positive side, the fertilizing action of decaying vegetation generates the explosive proliferation of phytoplankton, which is the basis of production of all aquatic life including fish. It is to this fertilizing action of decaying vegetation, that the phenomenally high fish production in tropical reservoirs is generally attributed.

Ameliorative action often suggested for the problem of stratification is the selective withdrawal of water from the deep stagnant levels of man-made lake. Release of deoxygenated water could conceivably harm fish and other aquatic life downstream of the dam. To overcome this problem, outlets could be positioned in dams at different levels between the surface and bottom, facilitating simultaneously selective withdrawals from discrete levels of a density-stratified impoundment, to ensure release of innocuous water to downstream users. However, even when this cannot be done, the turbulence of the discharge soon drives oxygen back into the water and hydrogen sulphide out of it.

Water Weeds

One of the undesirable consequences of creation of man-made lakes is the proliferation of nuisance, aquatic macro-vegetation. Virtually every major hydro-electric project built in the tropics, has been plagued by one or more pest plants([11]). Principal offenders in this category are the water hyacinth (*Eichhornia crassipes*), water fern (*Salvinia auriculata*) and water lettuce (*Pistia stratiotes*). Water weeds can harbour vectors of several waterborne diseases. In Ghana, water lettuce infestation in Lake Volta caused the spread of disease, as this plant is the prime habitat for several mosquito larvae. One species of mosquito obtains its oxygen directly from the roots of the plant and thus never surfaces, rendering its control with insecticides virtually impossible, without clearing the weed. Similarly, water hyacinth is reported to harbour several snail vectors of human diseases.

Besides being instruments of spread of diseases, weeds impede water flow and navigation by clogging water ways with their thick growth. Fish populations are adversely affected due to shutting off of solar energy from the phytoplankton and due to pollutional effects of dead and decaying weeds. Furthermore, weeds utilize nutrients which would otherwise be available in the production of fish food organisms, and themselves also cause oxygen loss, during hours of darkness and very cloudy days. Perhaps the most insidious consequence of weed proliferation is transpirational loss of water generated by these plants. Compared to the loss of water by evaporation from a flat surface like that of the lake, a hyacinth-covered surface increases water loss through evapotranspiration by a factor of about 3.5 in semi-tropical areas and by as much as eight times in parts of India, where there are long periods of relatively low humidity([4]).

Proliferation of undesirable aquatic vegetation in reservoirs is a manifestation of unutilized productive potential of the waters. Fortunately, man is learning that this vegetable production potential can be diverted to channels advantageous to him([10]). Introduction of 'large numbers of phytohagous fishes is reported to withdraw 30 percent from the quantities (of water plants) being formed annually'([7]). It is, however, recognized that introduction of new species could cause several problems of a different nature in its wake, and that considerable care has to be exercised in deciding on any introduction. Gaziev([7]) further reports that 200,000 tons of protein concentrate, utilizable in cattle feeds, is extracted from blue-green algae harvested annually from a reservoir in Dnieper River. Useful aquatic plants like water cress and water chestnut which are valued ingredients of Asian cuisine could be grown extensively in reservoirs, thus inhibiting growth of obnoxious weed plants. Above all, weeds themselves can be utilized after

suitable processing, as animal feeds. Thus, given adequate research effort, it is possible that human intervention could greatly alleviate if not eliminate the nuisance value of aquatic vegetation. Also, while considering the disease-vector-harbouring potential of water weeds in relation to Southeast Asian situation, one has to bear in mind the fact that these weeds already occur in profusion in the innumerable water bodies spread over the landscape. Water borne diseases that could be spread through the intermediacy of vectors harboured by the weeds, are already rampant. Water resource development in such a situation might have a positive effect, be focusing the need to take adequate remedial measures.

The Terrestrial Environment

Forests and Wild Life

The most obvious adverse effect of impoundments on the terrestrial environment is the loss of productive farm lands through inundation. Loss of valuable forests, pasture lands for live stock and grazing, or browsing lands for big game animals could also contribute to considerable losses. For instance, it is estimated that scientifically managed and harvested biomass of wild animals in tropical savannahs could exceed that obtainable from cattle raising in the same locations([22]). The value of game yields in Africa is estimated at US $ 600 to 900 per km^2. It is, however, possible with adequate studies and investment to replace these losses, at least partially, through fishery development and management in the man-made lakes, and the development of pasture lands, utilizing irrigation water from the reservoirs. Further, given the economic and dietary importance of agricultural crops that could be grown on lands irrigated through dam construction, 'the loss of a few low land forests to flooding is probably not very significant in the total economy of the country'([4]).

Survival of rare plants or animal species with limited ranges or habitat requirements, could be endangered through submergence of special habitats. For instance, it has been suggested that the survival of the Kouprey (*Ovibos moschatus*) in northern Cambodia could be endangered by one of the proposed Mekong dams([2]). Apart from the scientific, ethical and conservational interests, some of the rare animal species could provide gene pools which could be of considerable value in the development process. Crossbred with domesticated varieties, these rare species could be instrumental in the production of superior strains leading to expanded animal or plant production.

Whereas such problems as the above are well recognized by environmentalists, it is often overlooked that man-made lakes could also create opportunities for environmental improvement, by stimulating the establishment or enlargement of adjoining game preserves (e.g., Kainji and Volta Lakes). Isolated islands and peninsulas in the lakes appear to afford excellent opportunities for development as game parks or wildlife preserves.

Ground Water

Ground water flow changes resultant on seepage from man-made lakes depend evidently on the permeability of the substrate. Negative effects of such changes are on record. In some instances, due to changes in the pressure of ground water and the direction of its flow, levels in some areas rise to the extent of producing bog effect adversely affecting the agricultural use of the soils([9]). Seepage losses in some cases are reported to be of such magnitude as to defeat the very purpose of dam construction for water storage. A case in point often cited is Lake Nasser in Egypt, where lateral seepage is estimated to reach 1,000 million cubic metres per year, representing 0.6 percent of the lake's content. On the positive side, there is the possibility of changes in volume and direction of ground water flow, facilitating reclamation of low-lying, arid lands considerable distances away from the dam. It appears that such a possibility has been foreseen in Egypt (Lagler, personal communication).

Earthquakes

Earthquakes are known to have accompanied the construction of about a score of dams in different parts of the world. Seismic activity following the filling of reservoirs, particularly those which are more than 100 metres deep, has been noticed in such divergent regions, from a geological point of view, as the Zambezi graben, Greece, or the Deccan Plateau([17]). While there is no complete agreement among geologists on the exact causative factors for this seismic activity, there is a general consensus that such activity occurs where the rock masses were already close to failure, and where water injection from the impoudment into faults may lubricate the slippage of rock blocks to produce termors. It follows that gathering the relevant seismic and geophysical data has become a prerequisite to dam citing and construction planning.

Climate

Climatic changes are known to have resulted from dam construction ; the magnitude of changes depending on the size of the lake created and the extent of alteration of, and interaction with, natural factors that determine the existing climate. These effects manifest themselves in the form of blinding fogs, where ambient air temperatures fall sufficiently beneath those of water surface. In some cases, as for example Lake Rybansk in USSR (Temperate Zone), normal precipitation might decrease in the spring and double in the Autumn. Climatic effects are known to extend as much as 2-15 km around the lake and may interfere with planned land uses around the lake. However, collection of adequate meteorological data and analyzing them prior to dam construction can made possible the prediction of climatic effects and enable modification of land use plans to conform to predicated changes in climate. However, man-made reservoirs that have an influence in macroscale and mesoscale on meteorological processes are rather few([12]).

Agriculture

Besides power development, improvement of agriculture is generally considered the 'raison de être' of water resource development. Intensive agricultural operations themselves, involving the use of pesticides, herbicides and fertilizers, have been very harmful to fisheries. Rapid increase in the use of artificial fertilizers, particularly phosphorus and nitrogen compounds, have led to serious pollution of the water bodies receiving the agricultural return flows either in surface runoff or in ground water. Increased fertilizer loads would lead to development of excessive algal blooms with associated massive oxygen depletion and fish kills. While on the one hand pesticidal and herbicidal pollution is a serious hazard to aquatic life (and to consumers of aquatic organisms) that intensive agriculture could introduce, on the other hand the absence of herbicides and pesticides could be a serious hazard for agricultural production.

The Human Environment

Resettlement

Resettlement of population displaced from reservoir basins, and spread of water borne diseases are two of the major environmental disruptions reported to result directly from water resource development. Reservoirs have shown themselves to be major factors in human migration not readily countered by the conveniences of previously constructed resettlement villages. In the history of man-made lakes to the present, hundreds of thousands of people have had to be resettled. It has been repeatedly alleged that results have been mostly unsatisfactory. Historically, improper location of resettlement villages have made the new homes uninhabitable or uninhabited, however attractive. Occupational changes necessitated by migration have usually found the resettlees unprepared and untrained to take advantage of the new opportunities. Resettlement syndrome caused by the 'wrench of departure' from familiar home locale and cultural incompatibility with co-settlees or host populations have resulted in an increase in mortality and morbidity rates of the resettled populations. Examples to substantiate these allegations are often cited from Africa and Asia.

Undoubtedly, there have been disruptions of the nature alleged above, arising out of faulty planning and inadequate attention to the problem. There are an equally large number, if not more, of instances where unprecedented prosperity followed forced resettlement. To give only one instance, the T.V.A. region of the United States illustrates well the nature of secondary long-term dividends of changing careless agricultural practices to profitable farming based on good soil conservation and on economic land use planning. Human betterment invariably accompanied effective resettlement planning based on ecological, social and economic aspects and water management schemes, as illustrated by many examples in Europe and USSR.

Water-borne Diseases

Explosive spread of water borne, human disease is known to accompany environmental changes in the aquatic environment consequent on dam construction. In several parts of Africa, the creation of vast areas of placid water environment by dam construction favoured the increase of populations of the intermediate snail host of a human disease known as Bilharziasis (schistosomiasis). This contributed to spread of the disease in epidemic preportions. Similarly, placid waters in shallow, twisting lakes shores could provide ideal breeding conditions for the mosquito vectors of malaria and yellow fever and the waterflea host of the guinea worm. Whereas placid waters of man-made lakes favour the spread of some diseases, the rapid water flow induced by flows through dam sluices have, in parts of Africa, encouraged the breeding of a black fly, *Simulium*, which carries a human disease known as river blindness (onchocerciasis). An imaginative writer, deluded by enthusiasm, even attributed the spread of dengue fever and elephantiasis to dams ! Of course, this particular allegation is ridiculous considering that *Aedis egypti*, the mosquito that carries hemorragic dengue fever always breeds indoors, in water stored in pans, pots and other containers, and never in the open. Also, the elephantiasis carrying mosquito, *Culex fatigans*, always breeds in polluted cess-pools in the neighbourhood of habitations and not in relatively clean, lake waters.

A particular environmental situation that has spurred the dramatic spread of many water borne diseases is that in arid Africa dam construction conveyed water to erstwhile dry areas. In the case of tropical Asia, however, where stagnant waters abound in the countless ponds, swamps, natural lakes and so on, still water conditions that favour the proliferation of the disease vectors exist even before the creation of man-made lakes. Therefore, dam construction in this region may not become instrumental in creating conditions favourable to the spread of the diseases in new areas, though increase in the extent of shoreline area created by dams could well serve as a multiplying factor in the spread of the diseases. Further, diseases like river blindness do not occur in this region and schistosomiasis is highly restricted in its endemicity. For instance, in India, despite the construction of a large number of dams, there has been no indication of explosive spread of bilharziasis. Similarly, in the Mekong basin, bilharziasis is restricted to a few small areas. Painstaking research in the Mekong basin has further indicated that the intermediate host of the blood fluke (apparently a new strain of *Schistosoma japonicum*) which causes bilharziasis, is the tiny snail, *Lithoglyphopsis aperta*, which is essentially a rapid-flowing-water species. Therefore, it would appear possible that water resource development in this region may not encourage the spread of the disease, unless the snail could adapt to the lacustrine environment of man-made lakes or to the slow-flowing-water environment of irrigation systems. Notwithstanding this probability, at the present time "it is not possible to predict if and to what extent the disease

may be spread by the construction of dams below this (its correct) focus"([20]) of infestations.

There are also indications to the effect that in northeast Thailand, the occurrence of another schistosome (*Schistosoma spindale*) which can cause a minor inconvenience known as "bathers' itch" or "swimmers' itch" in humans, might offer some protection against the bilharziasis causing schistosome. Such a possibility is now being studied by the World Health Organization. If such protection could be demonstrated, it could indicate that people of northeast Thailand may be able to resist *S. japonicum* (bilharziasis) infection, as a result of cross immunity from *S. spindale* (bathers' itch) infection([3]). This is yet another clear pointer to the fact that extrapolations or generalizations from experience from one region are not necessarily applicable to others.

Nevertheless, there are other diseases which are characteristic of the area that could spread extensively as a result of placid water environments created by dams, coupled with the eating habits of the populace. Some important endemic diseases of that nature are briefly described in the following paragraphs.

Opisthochiasis is a disease caused by the liver fluke, *Opisthorchis viverrini*, that parasitizes many carnivores such as man, dog, fox, cat and other fish eating mammals, which are the definitive hosts of the parasite. The disease causes cirrhosis of the liver, occasional obstruction of bile flow, and, after prolonged periods of infection, even perhaps carcinoma of the liver. Earliest indications of the disease in humans are abdominal pains, low fever, nausea and some diarrhoea. The fluke is transmitted to the definitive host through two intermediate hosts ; the first, a snail, *Bithynia goniomphalus*, and the second, fishes of the family cyprinidae, in particular *Cyclocheilichthys sp.* and *Hampala sp.* Man acquires the fluke parasite by ingesting raw or insufficiently cooked fish, carrying the metacercariae (second stage young) of the fluke. Leptosporiasis is from another liver fluke also, transmitted to man by the consumption of improperly cooked fish. This parasite completes its life cycle by passing through two intermediate hosts, snail and fish. Pulmonary paragonimiasis, a debilitating disease of the lungs, is also contracted by humans through the ingestion of improperly cooked or raw freshwater crabs and prawns or by drinking water contaminated by metacercariae, that have escaped from crabs and prawns. A nematode (round worm), *Angiostrongylus cantonensis*, contracted by humans through the ingestion of raw or improperly cooked snails, particularly of the genus *Pilidae*, causes eosinophilic meningo-encephalitis.

All these diseases are endemic to the Southeast Asian region and are wide-spread even before the construction of dams. For instance, rates of infection of liver flukes are up to 90 percent in some villages, and of *A. cantonensis* up to 93 percent, in certain locations. Pre-impoundment studies related to the Mekong development served to bring these problems into focus and to highlight the need to take up remedial measures ; otherwise they would have continued to remain in the penumbra of ignorance and neglect that characterize familiarity with disease. To that extent, water resource development in the Mekong has a beneficial effect in initiating measures that might ultimately lead to control of water borne diseases. In the mean time, however, the pattern of incidence of these diseases and the nature of their propagation render it extremely important to study carefully how the creation of man-made lakes and intensive irrigation systems would affect the distribution and intensity of the diseases.

Conclusion

A realistic assessment of environmental effects of water resource development, must necessarily take into consideration the effects of leaving the environment unchanged. In tropical Asia, people are only too familiar with environmental effects of 'non-development'. Towns and villages are repeatedly devastated and crops are frequently destroyed by floods. Absence of regular supply of irrigation water and consequent low-yield agricultural operations precipitate food shortages. Non-availability of adequate electrical power is reflected in lack of basic industries to exploit natural resources and to supply day to day needs of the population. The perpetuation of penurious state of human society, as a combined consequence of all the above factors, is all too common a situation in Asia to need any elaboration. In recent years, anthropologists have discovered human societies that live in complete harmony with nature ; societies that did not strive to modify their environment. We have examples of such societies in the forests of Andamans, in the mountainous regions of the Philippines, in the Amazon basin, and elsewhere in other isolated corners of the world. These societies have in them a life expectancy of a score or so of years ; they are constantly plagued by pestilence, disease and starvation and live in perennial fear of predatory animals. If the human race is to survive under better conditions, it has to modify its environment ; not carelessly but judiciously ; not in ignorance, but after a proper understanding of the consequences of such modifications. Therefore, water resource developments undertaken after adequate studies and with due caution and ameliorative action could be most valuable instruments of economic development, of improvement of environmental quality, and furtherance of human well being. Many water resource development projects around the world have scored very highly in the achievement of purposes for which they were constructed and have generated unprecedented benefits; some have failed in more ways than one and have created unanticipated costs and woes, not because of any evil intrinsic to water resource development itself, but because of human failures—short-sightedness and lack of perspective on the part of development agencies, imperfect co-ordination among and within the agencies involved, inadequate research on immediate and long-range effects, poor scheduling and implementing of relevant activities, and inadequate supply of technically trained manpower([18]). Fortunately, ways to minimize unwanted effects of water resource development are fast becoming more clear.

The author works for the Mekong development programme. The planning of this project represents the type of environmental concern that should be exhibited by water resource projects everywhere. It has already a fifteen year history of research and planning prior to the construction of the first mainstream dam. It is one of a few projects of its type in the world, which has adopted a truly broad and yet intensive multidisciplinary approach for its long-range planning in water resource development. Painstaking studies are conducted far in advance of the construction of dams and projects are executed in logical sequence in so far as available funding permits. The programme may not completely eliminate environmental hazards, but it will certainly minimize ecological costs. In the final analysis people will be better off and that, after all, is the ultimate purpose of our quest.

Acknowledgements

The Author is grateful to Mr. W.J. van der Oord, Executive Agent, Mekong Committee, for reading through the manuscript and giving helpful suggestions, and to Prof. Karl F. Lagler, Professor of Natural Resources, The University of Michigan, Ann Arbor, Michigan, U.S.A. for a critical review of the manuscript.

References

(1) ACRES INTERNATIONAL LIMITED : "Environmental Analysis of the Construction of the Nam Ngum, Laos, Hydro-Electric Project." Prepared for the International Bank for Reconstruction and Development by Acres International Limited, Canada, 1974.

(2) BARDACH, JOHN E. and B. DUSSART : "Effects of Man-Made Lakes on Ecosystems." (in) Man-Made Lakes: Their Problems and Environmental Effects : pp. 811-817. American Geophysical Union, Washington D.C., 1973.

(3) BIERDRAGER, J. and Z.J. BUZO : "Summary Report on a Health Survey of the Lower Mekong Basin." World Health Organization, Manila, 1967.

(4) CHALLINOR, D. : "The Effect of Development on Tropical Forests." (in) Some Environmental Considerations for the Mekong Basin Project. SEADAG group of the Asia Society U.S.A., 1973.

(5) CRONIN, L. EUGENE : "The Role of Man in Estuarine Process." (in) Estuaries American Advancement of Science, Publication No. 83 : pp. 667-689, U.S.A., 1967.

(6) D'AUBENTON, F. : "Report on the Operation of a Barrage on the Tonle Sap." Economic Commission for Asia and the Far East Committee for Co-ordination of Investigations of the Lower Mekong Basin, Bangkok, 1963. Mimeo.

(7) GRAZIEV, E. : "Discussion on Question 40." (in) The Transactions of the Eleventh International Congress on Large Dams. Vol. V. pp. 132-133. Madrid, 1973.

(8) GUNTER, GORDON : "Some Relationships of Estuaries to the Fisheries of the Gulf of Mexico." (in) Estuaries. American Association for the Advancement of Science, Publication No. 83 : pp. 637-638, U.S.A., 1967.

(9) LAGLER, KARL F. : "Fishery Development in the Estuarial and Adjacent Waters of the Mekong Delta, Southeast Asia." SEADAG Seminar on Fishery Development in the Mekong Basin, Santa Barbara, California, U.S.A., 1972.

(10) LITTLE, E.C.S. (Ed.) : "Handbook of Utilization of Aquatic Plants." Food and Agriculture Organization of the United Nations, Rome, 1963.

(11) NELSON, M.; E.O. GANGSTAD and D.E. SEAMAN : "Report on Potential Growth of Aquatic Plants of the Lower Mekong Basin, Laos-Thailand." Prepared for U.S. Agency for International Development, 1970.

(12) NEMEC, J. : "Summary : Interaction between Reservoirs and the Atmosphere and its Hydrometeorological Elements." (in) Man-Made Lakes : Their Problems and Environmental Effects : pp. 398-405. American Geophysical Union, Washington D.C., 1973.

(13) PANTULU, V.R. : "Fishery Problems and Opportunities in the Mekong." from : Geophysical Monograph Series, Vol. 17. Man-Made Lakes : Their Problems and Environmental Effects : Ef. by W.C. Ackermann, G.F. White, and E.B. Worthington, 1973.

(14) PANTULU, V.R. : "Mekong Fishery Progamme – Its Background and Rationale." Mekong Secretariat. United Nations ESCAP, Bangkok, 1973 (a).

(15) PANTULU, V.R.; K. ALAGARAJA and B.S. BHIMACHAR : "Fisheries of the Damodar Valley in Relation to Construction of Dams." Proceedings of the National Institute of Sciences of India 32 : 5 & 6. pp. 191-207, New Delhi, 1967.

(16) PEARSE, A.S. and G. GUNTER: "Salinity." (in) Treatise in Marine Ecology and Paleoecology, Vol. 1. Memoirs of Geological Society of America No. 67; 1957.

(17) ROTHE, J.P. : "Summary : Geophysics Report." (in) Man-Made Lakes : Their Problems and Environmental Effects : pp. 441-454. American Geophysical Union, Washington D.C., 1973.

(18) SCUDDER, T. : "Summary : Resettlement." (in) Man-Made Lakes : Their Problems and Environmental Effects: pp. 707-719. American Geophysical Union, Washington D.C., 1973.

(19) SEGERSTRAALE, S.G.: "The Recent Increase in Salinity off the Coast of Finland and its Influence on the Fauna." Journal du Conseil; Conseil International pour l'Exploration de la Mer, 17 : 103-110; Copenhagen, 1951.

(20) SMITHSONIAN INSTITUTION : "Snail Transmission in the Lower Mekong Basin, with Observations on other Waterborne Diseases." Summary of a Report submitted to the Mekong Committee by the Office of International and Environmental Programs, Smithsonian Institution, Washington D.C., 1973.

(21) STERLING, CLAIRE : "The Trouble with Super Dams." Britannica Yearbook of Science and the Future. Encyclopedia Britannica, Inc., Chicago, 1973, pp. 112-127.

(22) TALBOT, LEE M. : "Effects of Mekong Development on Wildlife, Parks and Reserves." (in) Some Environmental Considerations for the Mekong Basin Project. SEADAG Group of the Asia Society, U.S.A., 1973.

(23) UNIVERSITY OF HAWAII : "The Composition of Mekong River Silt and its Possible Role as a Source of Plant Nutrient in Delta Soils." Department of Agronomy and Soil Science, College of Tropical Agriculture, University of Hawaii, Honolulu, 1974, pp. 1-104.

Water Resources Ecology

S. H. C. de SILVA
Divisional Irrigation Engineer
Department of Irrigation, Colombo (Sri Lanka).

SYNOPSIS

Rapid growth of the world population has taxed the earths' resources to sustain it. Enormous demands for water by man and his polluting habits have threatened the ecology of the earths' water resources including marine life in the oceans. The limit of readily available fresh water is about 1.5×10^{10} M gal/year, being the sum of the runoff and safe ground water withdrawal.

In the exploitation of this limited water resources man has acted with increasing irresponsibility and brought about ecological disasters from which even man is not immune.

In developing countries caught in the web of feeding populations their economies cannot sustain, a desperate program of intensifying agricultural and industrial production is in motion. In this exercise the main resources of land, air and water are being increasingly polluted. Since the life giving water is in intimate contact with the land and the atmosphere via the hydrologic cycle the pollution of one resource is cycled to the next and living organisms on the land, water and air, including man himself becomes a victim.

Man has scant regard for an amenity once its usefulness has declined. Witness the wastes that empties into the rivers and oceans degrading the environment, disturbing the ecology and destroying the fish, the only source of inexpensive protein available to people in the lesser developed countries.

Introduction

1.1 Engineering is described as the art of directing the Great Sources of power in nature for the use and convenience of man. As man dominates all ecosystems on earth, he has manipulated natural systems to serve his immediate needs, regardless of consequences.

Water Resources has been the most exploited natural system since man strode the earth as a colossus from the dark ages.

Ego centred as an individual or patriotic in terms of his artificial national boundaries man has been selfish and extremely short-sighted in the exploitation of the natural resources, which he believed to be infinite.

Human Growth

1.2 With growth of civilisation, technological advancement, conquest of disease, the quality of life improved and man having no predator, multiplied by leaps and bounds to the present 4 billion (1975).

The phenomenal increase of his number and the need to fulfil their basic demands of food, clothing, shelter and energy have taxed the world's natural resources to such an extent that danger signals have appeared all round warning him of the ecological disasters ahead. It took man 200,000 years to grow in numbers to 1 billion. A century later, 2 billion comprised the earth's population. In 30 years (1930-1960), the third billion was added and this year (1975),

will pass the fourth billion to reach 6.2 billion in the year 2000. Realising that every day, when it is available, a human being consumes an average 2 lb of dry food, 6 lb of water and inhibits the amazing amount of 60 lb of air out of which he consumes 6 lb oxygen, supplying these 3 needs for 4×10^9 souls for a single day in 1975, is a staggering proposal by itself. But, he keeps increasing in numbers at an estimated 120 every minute and to crown it all, a man discharges 5 lb solid wastes each day in the form of food waste, paper, plastic and trash. The greatest danger to man's environment has arisen from the unbridled expansion of his numbers —the population explosion.

Water Resources and Ecosystems

1.3 Although the earths' surface is covered by over 70 percent water, most of this is either salty or frozen and what is available is less than 1 percent.

It is this 1 percent fresh water that man has harnessed in planning and execution of water resource projects. Since water quantity-wise is constant in the scale of time, the hydrologic cycle sets its motion through air, and land, plant, animal and man. Water resources ecology cannot, therefore, be singled out, due to interdependence and interplay of environmental pollution, ecosystems disturbance and degradation of soil.

Due to the interdependence and interaction of the principal resources of water, air, land and the biota sustained on this earth, housekeeping or the ecology of any one item cannot be pursued independently. Study of water resources from the ecological view point, thus form an indivisible part of the total picture, involving land, air and biota.

1.4 The increase in CO_2 content in the atmosphere at the rate of 6 billion tons/year from combustion of fossil fuels is expected to raise its concentration from 300 ppm by volume to 375 in the next quarter century. This 25 percent increase in CO_2 content could have far reaching global effects, melting of polar ice cap, rise of sea levels, alter climatological sequences, expand desert and will result in general environmental disruption. Such a chain of events, not unforeseeable today (1975) may immutably change not only the abiotic, but also, the biotic aspects of this planet earth, including man.

1.5 In the animal kingdom, a balance of population is reached by predation generally. The highest form of life is ordained to man. Imbued with a rational outlook, he has increasingly exploited the earths' resources with the aid of the technology he has perfected. His belief that nothing is impossible to achieve has been rewarded with his conquest of space and the ocean depths, two environments alien to his habitat on earth.

1.6 With the first space flight, man realised the value of the earths' resources. Into his space capsule, he packed not only his travel requirements but also, the "air" to breathe, water for his consumption and the food for his sustenance, signifying his utter helplessness in an environment alien to his home on earth. His exclamations from the darkness of space at the sight of the greenery on earth was nothing, but the yearning to be back amongst the vegetation inspired by the limited resources of land, air, water and biota on earth.

Water Resources

2.1 The past 200 years encompasses the technological revolution. In this period, starting from the steam engine to the nuclear power plants, man's energy requirements have expanded exponentially. In the search for more and more energy, vast changes took place in the earths' ecology and environment. The 1 percent available water resources on earth suffered most in this exercise.

The earths' water resources usable by man, could be grouped into the following :

(*i*) Rain and snow and the carrier clouds.

(*ii*) Ground water which is storage in earth of precipitation.

(*iii*) Rivers, lakes and man-made reservoirs.

(*iv*) Sea water converted by costly desalinisation.

(*v*) Small quantity of vapour in atmosphere obtained as dew.

2.2 Based on the almost clockwork regularity of the arrival of monsoons, man placed so much trust, that his cultivation patterns and dates rarely changed year to year.

Sri Lanka is one of the countries that depended on the monsoon rains to replenish her reservoirs in the dry zone and provide water for rain fed cultivations in the wet zone. The shifting patterns of slash and burn agriculture or "chena" cultivation depended primarily on these regular monsoon rains to broadcast seeds.

But, since 1973, the monsoon rains have failed in timing and intensity and Sri Lanka, like the other countries, in East Asia and Central Africa, have experienced prolonged droughts and poor rainfall. Dry zone reservoirs normally storing only a part of the year's precipitation runoff, went dry destroying the entire lacustrine habitat and driving man, cattle and wild animals to seek new pastures and water sources. According to climatologist Reid Bryson, Director of the Institute of Environmental Studies, University of Wisconsin, "important climatic changes are going on right now, if continued, will affect the whole human occupation of the earth".

Drought persists in India, countries of the Sahelian belt, Mauritania, Mali, Chad, Senegal, Upper Volta and Niger, have suffered the sixth consecutive year of drought, freak floods of 1973 in Pakistan and the advance of the Sahara southwards, are evidence of this conclusion.

2.3 Whatever form man's technology takes, his advances in water resource exploitation from surface, ground or river flow or high yielding grain and profitable breeds of livestock are all pivoted on the availability of water resource replenishment by rainfall. If rains fail, agriculture, fauna and flora and man must necessarily suffer.

With the present world food shortage, the spectre of increased famine and reduction of population in man accompanied by irreversible changes in the biotic and abiotic aspects of the affected regions is inevitable.

The much vaunted green revolution of the late 60s, is rapidly fading. The increased demands of fertilizer by the miracle rice and miracle wheat at a time of soaring fertilizer prices, following the fuel price hike, could never be met by the developing countries. Another cause for the decline of the miracle grain was the lack of resistance to climatic change.

Exploitation of Water Resources in Sri Lanka

2.4 In Sri Lanka, a developing country, freed from 4 centuries of western domination in 1948, the exploitation of her water resources has been comparatively systematic. Figure 1 shows the map of Sri Lanka. The presence of over 10,000 reservoirs in various stages of repair in a land area of 25,332 sq miles (6,580,000 ha), is eloquent testimony of the enlightened water resource exploitation for the past 2,500 years. History records the construction of the first reservoir in Fifth Century B.C. by King Ponduvasdeva in Sri Lanka.

Sri Lanka has essentially an agricultural based economy. Tea, Rubber and Coconut exports realised the foreign exchange earnings to purchase her consumer needs. The choice of these products was at the behest of past colonial governments, which gave low priority to food production.

The Island is blessed with rainfall from 2 monsoons per year, yielding annual runoff of 43×10^9 m^3 (35 million acre-ft) of water. Looking back to history, the ancient Sinhalese tank building kings had as their motto, the conservation of all waters that fell from the heavens and not a drop be wasted. The vast number of 10,000 reservoirs would doubtless have been the response from the loyal subjects executing regal orders.

The Malaria Vector

2.5 The causes for the collapse of this reservoir based irrigation, the decline of the Sinhalese monarchy, the shrinking of her population to 2,400,380 in 1871 can be traced to the ecological aspects, viz., the malaria vector. Could it be that the very idea of storing all water in reservoirs led to the profuse multiplication of the malaria vector at a time eradication methods were yet unknown ? Vector control or the anti-malaria campaign started in 1948, led Sri Lanka to reduce the death rate to 12 per thousand, the lowest in South-East Asia. This caused a complaisant atmosphere and D.D.T. campaign dwindled owing to the high cost of operation. In 1958, the vector control was renewed and relaxed in 1963, when the disease was brought under control again. But, since 1967, a resurgence has been observed as shown below :

Year	1966	1967	1968	1969	1970
Cases	207	3,465	425,937	552,234	468,202
Year	1971*	1972	1973	1974	
Cases	145,368	132,604	227,713	285,478	

The incidence of malaria continues unabated. For the P. Vivax or ordinary type, 12,000 to 13,000 cases have been recorded monthly in 1974, whilst the more virulent P. Falciparum which affects the brain has recorded an alarming increase as shown in table below for the first eight months of 1974 :

Month	Jan.	Feb.	Mar.	Apr.	May
New Cases	910	733	1,181	897	1,168
Month	June	July	Aug.		
New Cases	1,904	2,116	1,909		

The incidence of the disease from 1974, is linked with the curtailment of transport following the fuel price hike, sequel to the outbreak of the Middle East War in October 1973, and resultant relaxation of the D.D.T. spraying campaign.

2.6 In this, a developing country like Sri Lanka is caught in the horns of a dilemma. With 20 out of the 22 districts affected by this debilitating disease, a setback on the efforts for increased food production is likely. D.D.T. is a deadly chlorimated hydrocarbon insecticide, banned for use in the United States due to its harmful effects on the ecology and the environment. If this is intensively sprayed for vector control, the incidence of the disease may be curbed temporarily at an enormous cost in scarce foreign exchange, whilst introducing a pollutant to Sri Lanka's resources of water, land, and fauna and flora and man himself.

In the words of Rachel Carson "The chemical war is never won and all life is caught in its violent crossfire."

The Coral Habitat

3.1 The Western, South-Western and Eastern coastline of the Island is hemmed by surface or submarine coral—Ancropora. Corals are predacious, primarily carnivorous animals, but of late, the coral reef has fallen prey to man's greed. The ecology of the coral habitat, has been intruded into by man—(*i*) to provide limestone by burning of the live coral, (*ii*) by excessive exploitation of the tropical fish that form part of the submarine ecology.

* Data collection interrupted by Civil disturbance.

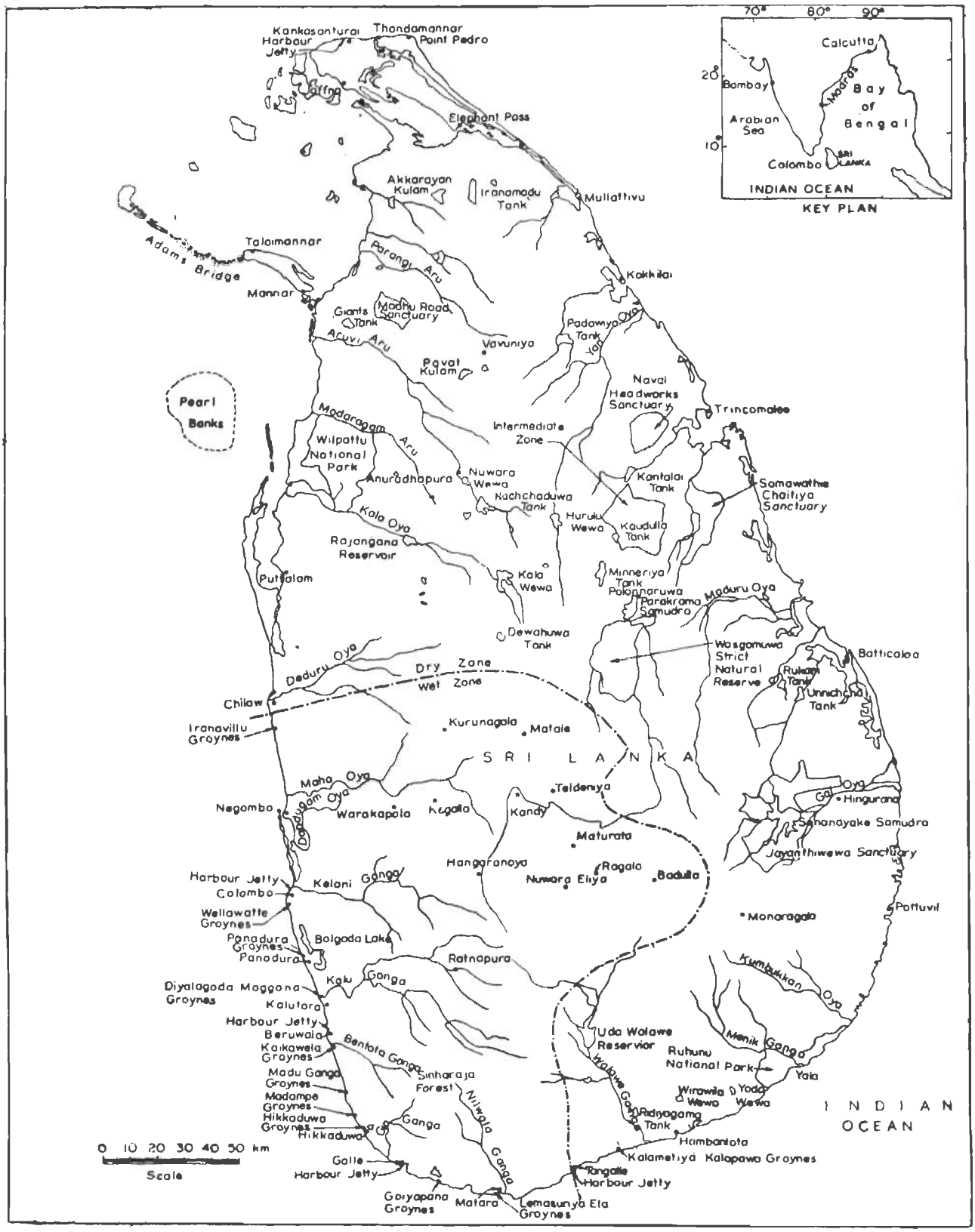

FIGURE 1 : Map of Sri Lanka.

FIGURE 2 : Coral reef hunters, Hikkaduwa. Live coral broken from submarine reef being transported by raft. Blackspots in background indicate divers mining coral.

3.2 The limestone industry has attracted a section of the unemployed, living in the affected maritime regions to gather coral from coral pits in the low-lying coastal dunes, foreshore or from the submarine reef (see Figure 2). In the case of inland pits, the coral is mined in some cases up to 30 ft depth in open pits. Pumps are used to evacuate the fast inflow of sea water into the pits through the open passages in coral formation. The limit of this operation is generally the depth at which pumping fails to lower the salt water-level in pit. The pumped outflow of saline water becomes overland run-off to low-lying lands and coastal lagoons. In this operation already brackish waters of the low-lying coastal strip are made increasingly saline and the chances of reclaiming this soil for productive paddy cultivation made very remote, if impossible. The abandoned pits fill up with sea water created by the steep hydraulic gradient during pumping and form the habitat for the larvae of the filaria bearing mosquito which multiplies rapidly in the salvinia infested pits unpestered by other aquatic life forms or fish. This ecological disturbance has bequeathed the island with a crop of filarial victims on the western coastal belt.

Intensive fishing of prawns, lobsters and exotic tropical fish that abound the coral reefs has caused a population explosion of the Acanthaster plancki (crown of thorns starfish). Unwittingly the "acropora" coral is now the victim of simultaneous predation by man and the starfish. Unemployment pressure and the readily available building material, limestone have decreed this ecological catastrophe, to continue (see Figure 3).

The reef coral in Sri Lanka's first defence against coastal erosion from the fierce South-West monsoon wind ripped waves and the lesser Southern swell. Though the reef can withstand, as it has withstood in the past, the might of crushing breakers, it readily succumbs to a pickaxe or picket. A change in the coastline may be the best epitaph for this monumental folly.

Gem Mining

3.3 Gem mining industry has emerged as the foremost

FIGURE 3 : Broken coral ready for transport to kilns, Hikkaduwa. Much of this is live coral with sea weeds still growing on it. While "Crown of thorns"—starfish strips polyps from coral leaving dead limestone, man removes it en bloc exposing the coast to serious erosion.

earner of valuable foreign exchange in the last three years in Sri Lanka. With stakes higher than for coral, this is an enterprise ably encouraged by the state and vigorously pursued by entrepreneurs. But, the methods used in the mining are generally inimical to the interests of environment and ecology. Mining along river banks pursuing seams, have disturbed the fragile environment between soil and water, promoting soil erosion and earth slips. Destruction of the timeless forest cover on land too steep for any cultivation will guarantee prolonged sediment transportation down the rivers.

3.4 The numerous lagoons dotting the coastal belt of the island are fast filling up with sediments. This has reduced the minimum depth required for the biannual circulation of water necessary for the lacustrine habitat. Construction of the Senanayake Samudra in the Gal Oya Valley and the opening up of 44,500 ha, has introduced a heavy drainage discharge into the Batticoloa lagoon resulting in the progressive decline of its salinity and endangering the lagoon ecology of penacid and prawn cultures.

Persistent demands by fishery industry to dredge the Batticaloa lagoon and bypass the drainage waters direct to sea have been made to restore that ecology. Similar condition occurs in Negombo lagoon by siltation from the Dandugam Oya and the famed prawn culture is endangered.

Pearl Fisheries

3.5 Lack of an ecological understanding has completely ruined Sri Lanka's pearl fisheries by over exploitation of the Pearl Banks. A survey conducted in 1965 yielded this forelorn conclusion.

Deforestation

4.1 The opening up of vast tracts of jungle land with the execution of large irrigation and hydropower schemes has spelled ruin to the ecology of the lush tropical evergreen forests of the island. The number of

species lost in these exercises will never be known as ecological, and environmental impact studies were totally ignored in attempting favourable benefit-cost ratios at project evaluation.

In dam construction for reservoir projects the clearing of forest, was on the primitive methods of slash and burn even though heavy machinery was utilised in the "slashing." Although wind belts and forest reserves were allowed in blocking out plans of irrigable tracts, on the land, what met the eye of the beholder after the bulldozer left, was a forelorn sweep of smouldering stumps and ashes. The situation was no different from the nomadic type of shifting cultivation or "chena" cultivation.

Eutrophication of Reservoirs

4.2 Potential Reservoir beds suffered most. Borrow areas were stripped of all vegetation and fauna and flora of the region suffered total destruction. Animals fleeing from man's terror were invariably destroyed, sometimes for their flesh. Since the entire water spread area was too vast, large sectors were left to be destroyed by the rising waters once the dam was complete.

The dying trees, plants and animals submerged in reservoir construction gave rise to eutrophication of the reservoir waters. Deoxygenation caused by decomposition of submerged land vegetation gave an insipid taste to the water and reduced fish population (see Figure 4).

4.3 No data whatsoever exists of pre-reservoir period on the chemical, microbiological, botanical, zoological and ecological aspects. It has been proved that dams reduced by tenfold invertebrates such as insect larvae and snails for several miles downstream. This plunder of life which takes place when the dam stops the flow and dries up part of the stream bed probably affected the river's capacity to cleanse itself.

The reservoirs with sprouting dead tree trunks and branches over the shimmering water spread stand as

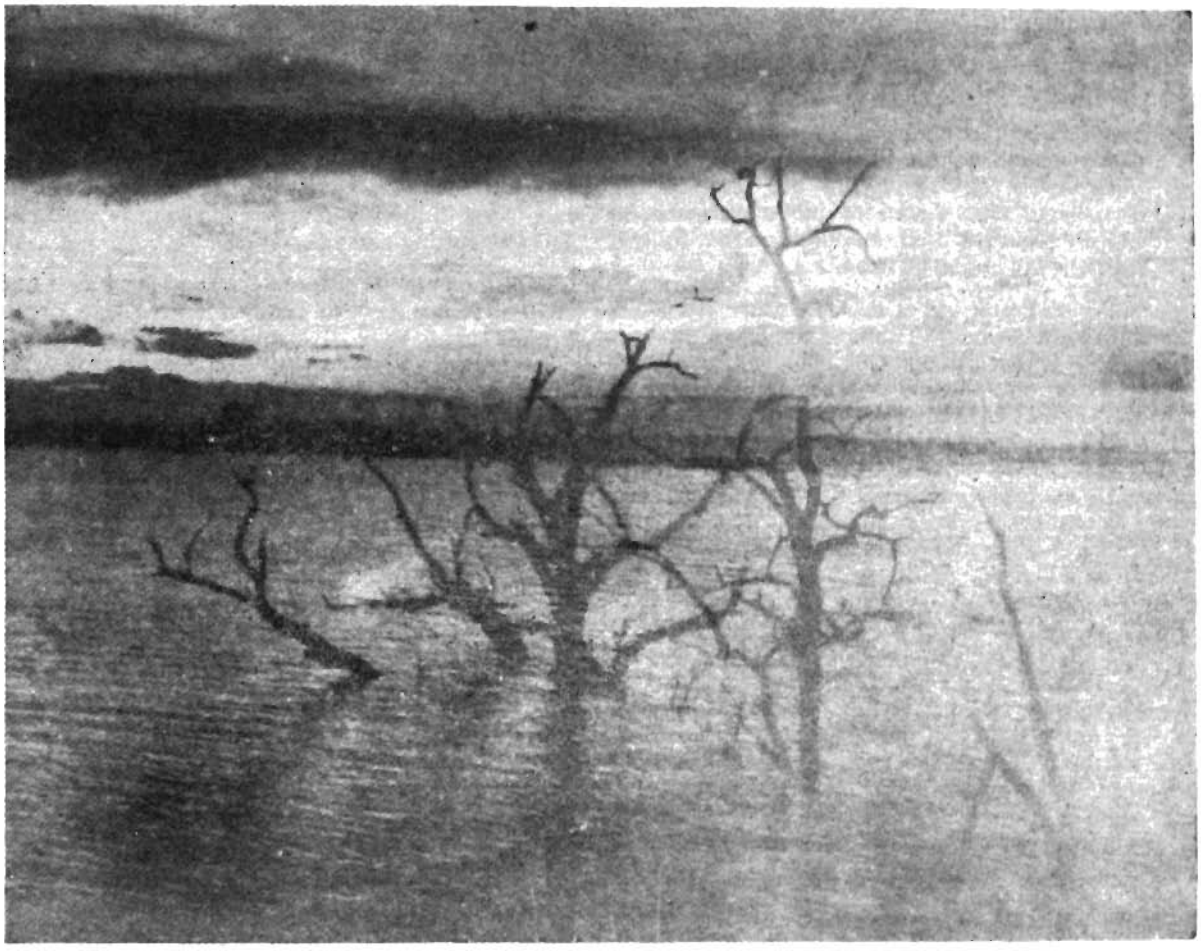

FIGURE 4 : Reservoir formed on uncleared lake bottom, Padaviya. Impoundment spells death to most biota, and causes deoxygenation affecting ecology. Dead trees obstruct boating and recreation. Calm waters help weed growth and disease vectors.

eloquent epitaphs of man's indifference to the wanton haste and ecological blindness.

The conversion of a perennial or non-perennial stream into a reservoir of fluctuating water levels responding to irrigation or power demands is potentially an environmental hazard. The knowledge necessary to quantify the benefits and hazards from such situation, is yet very meagre. As each location has its own native biota and no monitoring was done under pre-impoundment the ecological changes cannot be properly assessed. But in small reservoirs in the dry zone the dead storage (storage below irrigation sluices) is exploited in many ways as listed below :

(*i*) as a source of drinking water sometimes by sinking wells in reservoir bed.

(*ii*) focal point for all ablutious, washing of clothes using detergents.

(*iii*) water point for cattle who always pollute the reservoir bed with dung.

(*iv*) concentrated fishing in depleted waters.

(*v*) drying fish, caught after removing the entrails which are discarded indiscriminately in the dried reservoir bed.

(*vi*) tank bed or impoundment area cultivation for paddy or other short period crop, during falling water levels. Ploughing up the reservoir silt deposits, disrupts the entire biotic environment and if fertilizer is used the pollution that follows reservoir filling can be imagined.

Depending on the period of drought some reservoirs dry up completely. Under the above circumstances it is not difficult to see that fish cultures in inland reservoirs in Sri Lanka can only atrophy. The only species of note is the "Tilapia mossampica" introduced into reservoirs in 1951 but fighting a losing battle against human predation, as no conservation or preservation measures are enforced. Indeed dynamiting of fish in lagoons and reservoirs is an occasional occurrence, carried out by ignorant and lazy fishermen oblivious of the ecological holocaust they perpetrate on dumb nature.

Weed Control

4.4 Use of water as an agent for weed control is practised extensively in Sri Lanka. Ecologically this should be more beneficial than the introduction of chemical weed killers into the paddy to be ultimately washed into the streams and rivers and affect the fish and eutrophication of river waters. A further advantage is the saving in foreign exchange if the chemicals were imported.

Paradoxically in some parts of Sri Lanka, viz., Dewahuwa, experimentation has proved that the highest paddy yields were obtained by tracts having at least 5 cm (2 in.) of standing water covering the land during most of the growing season, including heading stage. The effect of this standing water in tillering stage was negligible on the yield.

This concept is in agreement with the notion of rustic farmers who from ancient times have handed down the traditional methods of paddy cultivation. But from a water resource point and consumptive use analysis such practice is detrimental and wasteful of limited water resource.

4.5 In the case of terraced paddy cultivation on hilly country, storage of water in paddy lands will cause an artificial high water-table and could promote earth slips. However, a beneficial aspect of this practice is the increased infiltration and thus greater ground water storage, an ecological aspect achieved in the natural forests the largest self-perpetuating ecosystem on earth. Basin furrowing or the excavation of thousands of shallow depressions practised in parts of the U.S.A. is a similar artificial measure to promote infiltration and arrest erosion.

Lumber Trade

4.6 Forests are felled not only for shifting agriculture which is wasteful but also for the timber for feeding the state timber complexes, viz., plywood, chipboard and building industry. The ecosystem that was the result of thousands or even millions of years of continuing evolution was being destroyed in the Sinharajah Mechanical Logging Project. Here the last bastion of the tropical rain forest in the island is yielding to heavy earth moving and tree cutting machinery.

On the impetus given to the food drive vast tracts of timeless forests have succumbed to the axe or tractor. Forests that took a foothold on steep slopes after centuries have crumbled to be replaced by tobacco as at Maturata and Teldeniya, on slopes over 45° (1 in 1). In other places once the timber was exploited the naked soil was left to brave the tropical heat and torrential rain as the soil was unsuitable for cultivation. This was soil conservation on the retrograde. Denied of the protective forest cover, the exposed hillsides promoted flash floods and intense soil erosion which ultimately collected as sediment deposits in water storage reservoirs. Unprecedented floods in the hill country towns of Nuwara Eliya, Halgran Oya, Ragala, Warakapola and Teldeniya in 1973/74 provide adequate proof of the dangers of tampering the fragile zone especially the lands over 1,525 m (5,000 ft) elevations. The increased turbidity of the silt laden waters affected the ecology of the rivers and reservoirs.

Forest and Climate

4.7 The effect of forests on the climate rainfall and water resources, have now been well defined. Forests contribute significantly to the global cycling of CO_2 a commodity nearly getting out of hand by the increased combustion of fossil fuels. Over half the photosynthesis on earth is attributed to forests cover. Thus excessive deforestation impairs the rate of natural removal of CO_2

from the atmosphere and may produce the "green house" effect with all its attendant evils of melting polar ice caps and inundating vast areas of the coastal belt of the entire world.

4.8 Molchanov has shown that for maximum water yield, forest should be distributed in the form of shelter belts on the contour. 6 percent of watershed area under contoured forest strips have been shown to halve the overland runoff of a completely agricultural watershed. 30 to 40 percent of the areas if afforested ensures transfer of the entire surface runoff to the sub-soil and prevent surface erosion.

Waterlogging

5.1 In overpopulated developing countries the form of land tenure system leads to fragmentation. Units uneconomic to handle are prolific. Even if the entire tract is under one crop, failure to synchronise cultivation leads to water issues, non-stop all round the year, resulting in waste of scarce water resources and maintaining high water tables even at harvesting time for some lots. Ecologically this promotes in the canals profuse growth of weeds, viz., water hyacinth, salvinia and the Bulinas Snail, a vector of the trematode worm which causes "Schistosomiasis", a disease endemic in Egypt and China. In Sri Lanka the filarial mosquito has been found to breed in waters infested with salvinia and water hyacinth especially in the coastal regions.

Water Hyacinth (Eichichornia Crassipes)

5.2 Water hyacinth is a plant with explosive growth rate, has become a nuisance in covering reservoirs, canals and lakes in Sri Lanka. Some of the eutrophied canals in the city of Colombo are completely covered by this growth causing impediment to water flow in times of flood. Abatement measures as manual or mechanical removal have met with little success as the "Water Hyacinth community doubles every two weeks, with one plant generating 65,000 offspring in a single growing season".

However, tests carried out at the National Aeronautics and Space Administration (NASA) laboratories in Bay St. Louis, Mississippi from 1971 to 1974 have discovered in water hyacinth "a remarkably efficient and inexpensive filtration and disposal system for toxic materials and sewage released into waters near urban and industrial areas".

This represents a major breakthrough in the fight for restoring sewage polluted estuaries, rivers and lakes, in tropical areas.

Monoculture Dangers

5.3 Monoculture propagation has followed the execution of large irrigation projects in Sri Lanka. This has been the rule as in the early days no land use study was undertaken before the project execution.

Under these circumstances vast acreages were earmarked for paddy cultivation, a monoculture, which all good ecologists abhor. Sri Lanka had a taste of this bitter result in November 1974 when the Brown Hopper pest devastated over 5,000 ha (13,000 acres) of paddy reaching its maturity and affected a further 14,000 ha (35,000 acres) in the Amparai District. As the country was in the throes of a food crisis aerial spraying was restored to using the insecticide "phosvel" and in 2 weeks 90 percent of the pest was destroyed and the crop partly saved. But the ecological disturbances following this have not been monitored as such exercises are deemed dispensable in developing countries.

5.4 In 1971 the coconut belt down the west coast was attacked by the Cummingi pest. Fortunately no insecticide was used to control this and resort made to biological control that had the least impact on the water, land and air resources.

Land Misuse

6.1 From the early 60s systematic land use surveys have generally preceded the opening up of new land for agriculture. Today the entire island is covered by reconnaissance soil surveys and selected zones covered by detailed soil study. The cultivation of paddy in tracts 2 to 7 of the Uda Walawe Right Bank channel on lands reserved for sugarcane resulted in the gross waste of expensive irrigation water. As the soils were too porous over 37,000 m^3 (30 acre-ft) of water had to be fed to cultivate paddy in that soil whereas 7,400 to 8,635 m^3 (6 to 7 acre-ft) sufficed in the lands earmarked for paddy per 0.4 ha (one acre).

Excessive infiltration caused further disruption to the low-lying paddy lands round Kachchigal Ara and the Kalametiya Kalapu (lagoon) by raising the water-table and causing waterlogging of once fertile paddy land. The Kachchigal Ara which ran dry in pre-impoundment days in drought, now flows brimful and has further endangered the lagoon fisheries by reduced salinity.

6.2 On the east coast the very same abuse has occurred in the sugarcane cultivation at Hingurana under the Senanayake Samudra.

Land earmarked for sugarcane was used for paddy cultivation on the left bank of Gal Oya and sugarcane cropped on the right bank, resulting in waterlogging of half the acreage. Costly measures to rehabilitate the land by improved drainage are now under execution in an attempt to salvage the situation. The keynote of such costly mistakes on countries with a shoe string economy indicate the necessity for thorough investigation at the planning stage of water resource projects including the ecological effects and the impact on the environment.

6.3 A kindred misuse of land is encroachments into areas reserved for wind belts, drainage lines, tank bunds and forest reserves. Unauthorised stick dams on drainage streams to divert water for cultivation have upset water distribution practices and leading to waterlogging of some areas and wasteful use of the scarce water resource. In general such encroachments increase

the areas under cultivation of a single variety of crop as crop diversification is rare. Stripped of the complex forest ecology that help to keep a balance and creating monoculture (paddy), the new cultivation is exposed to ravages of variety of pests that rapidly multiply. The Brown Hopper pest of Amparai District in late 1974 being a good example.

Drainage of the Wetlands

6.4 Another aspect of water resource utilisation are the coastal drainage and salt water exclusion projects in Sri Lanka. Low-lying lands below 1 m elevation above mean sea level are generally covered by mangrove swamp, pandans, or long leaf varieties, e.g., ketala, or water hyacinth =eichichornia crassipes, or salvinia auriculata. The lush vegetation is nature's device to provide enormous extent of evapotranspiration area to reduce the water in the low-lying lands. Along river banks these aquatic weeds introduce sufficient friction to reduce water velocities and hence act as sediment traps.

6.5 The only cultivation possible in these swampy areas which have brackish water is water loving paddy having a certain degree of saline resistance. In the quest for increased food production these marginal lands on the lower fragile zone have been exploited intensively in Sri Lanka. The streams have been cleared of all vegetation, straightened of meanders and dredged. The Sea outfalls have been deepened for rapid flood discharge by blasting of the protective coral formation or rock.

These operations drastically affect the ecology of these wetlands. Increased turbidity of the water reduces sunlight from reaching the photosynthetic organisms and disturbs the biological reactions, upsetting ecological stability of the larvae and crustacean population. The greater damage, is the increased flow of sediments into the sea, once the retarding apparatus of the marshland vegetation is disturbed. The river sea interface at the sea outlet introduces the environmental factors of the marine habitat, which are of greater complexity and international in character.

Coastal Structures

6.6 To counteract the deposition of silt at river estuaries coastal structures are required. These constructions have considerable influence on the hydraulic conditions of the shoreline, which is again a fragile zone being the interface of land air and water. The mobility of this interface due to littoral drift, is disturbed by artificial structures leading to fresh sedimentation and erosion elsewhere.

An ecological disturbance that will affect the very existence of the famous Hikkaduwa coral garden and the tropical fish of variegated hues, by sedimentation has been triggered by the series of groynes or jetty constructions done at Hikkaduwa to : (*i*) keep river outfall open, (*ii*) prevention of coastal erosion.

Although this submarine coral garden is one of the star attractions of tourists visiting the island its continuity is endangered. Yet little is done to prevent the catastrophe as conservation has never stood against man's hunt for food.

6.7 With the free movement of water assured at sea outfalls, the problem arises of increased saline intrusion landwards by tides and storm surge. Preventive measures for this are construction of salt water exclusion bunds and structures. Such structures opened at only low tide seriously interfere with the migration of anadromous fish seeking sheltered creeks and lagoons at high tide.

Fishermen interfere in operation of structure gates to achieve the entry of tide inland, even to the extent of causing wilful damage as occurred in Thondamannar, leading to the nullification of the salt water exclusion project there.

6.8 Another industry that has cross purpose with the salt water exclusion schemes is the coir fibre industry. Coconut husks are soaked in brackish water pits surrounded by wooden pens, erected on river or lagoon banks. The hydrogen sulphide gas emanating from the process kills fish larvae and endangers lagoon and estuarine life. The irregular promontories caused to the river bank by the enclosures reduces the waterway available for flood flows and act as submerged groynes interfering with the free flow of water.

Industrial Pollution

7.1 Several industries in the recent past have made a big contribution to the pollution of water resources of the island. The effluent from weaving mills, and sewage have grossly polluted the canals in the city of Colombo. The proliferation of shanty houses encroaching on canal banks and reservations have compounded the problem with domestic refuse and human waste. Toxic chemicals, acid and alkali waste find a ready receptacle in the numerous canals in the city that have consequently registered alarming Biochemical Oxygen Demand counts of 300 to 350 for 3 days at 28°C in the densely populated areas of Colombo North.

Realising the tolerable BOD is of the order of 30 the rapid eutrophication of these waters is apparent.

7.2 Although the major portion of city of Colombo is sewered the areas in the low-lying areas have only septic tanks and cess pits for disposal of human excreta, without sewers. Combined systems of storm water and sewerage also exist. With high water tables movement of bacterial contaminants is assured by ground water flow. The outbreak of frequent epidemics like cholera, typhoid has been the result.

Ground Water

7.3 Ground water resources are a nation's capital investment. Yet this capital has been "borrowed" into,

in many countries recently. The prolonged droughts of 1973 and 1974 and the increasing demands for agriculture by opening up of new lands have prompted the demand for more and more wells.

Systematic investigation commenced in 1965 for the exploitation of this water resource in the island. The most intensive application of this form of mining centred round the Jaffna Peninsula, where over 100,000 wells are in use, generally of the shallow well type. Due to karst limestone formation at a shallow depth, recharge from rainfall drains to the sea through the numerous network of subterranean canals. The optimum use has already been made of the lenses of available fresh water. Further mining introduces the danger of drawing in saline water, which will negative the efforts for irrigated agriculture.

In the other parts of the island metamorphic hard rock predominate except in coastal areas between Puttalam and Paranthan where deep well pumps are now located.

The danger of subsidence of the soil by over-extraction of ground water and subsequent reduction of aquifer is a possibility not yet encountered. In a developing country capital costs of ground water extraction alone mitigate the chances of widespread use of this water resource and attention will necessarily gravitate towards exploitation of surface water potential as is being done in the Mahaweli Diversion Scheme.

7.4 In this project area affecting 39 percent of the island's surface comprising 55 percent of the dry zone, lands will be opened up for irrigated agriculture mainly paddy and cash crops. Depriving the forest cover for such a substantial area of the island to be replaced by a monoculture can lead to a dangerous ecological disturbance, as witnessed in Amparai with the Brown Hopper pest in 1974.

One of the first victims of this experiment will be the destruction of the wildlife, already the elephant population in the island has dwindled to around 2,500. Will this quest for food to increasing numbers of the human population deprive these giant animals of the wild habitat ? The opening up of more and more forests will drive the native fauna to the only havens of the national sanctuaries, which are too confined and merely glorified zoos.

Conclusions

Could the opening up of such large extents of nature's preserves, affect the climate and the rainfall ? If the wind patterns are changing as forecast by some climatologists, then the danger will be multiplied several fold and the reservoir complexes constructed at great cost to fill once or twice a year will do so at every 5 or 10-year intervals, following cyclone patterns and not regular monsoons.

Denied the regular rains the lands will be parched up and desert conditions will result. The failure of the monsoon in 1973 and 1974 produced depleted reservoirs, electricity cuts and destruction of crops. The portents for the sowing season of April 1975 seem as gloomy. Yet designs and construction projects proceed on the old assumptions based on annual precipitations of 2,000 to 3,000 mm. None dare revise annual rainfall yields as population pressures build up clamouring for land in desperate drive to grow more or perish.

After belligerent methods failed—Men have congregated from time to time to settle irritating problems affecting them. By general agreements man has placed constraints on the use of the sea bed, territorial water, fishing, immigration and emigration, air-corridors, sharing of river waters, differential tariff, speed limits, building codes, effluent restrictions, carrying capacity of jumbo jets, trains, ships, bridges, elevators, and infinitum.

His humanitarian approach has thus far not ventured or dared at the optimum size of his own numbers. Religious and ultra nationalist beliefs which led people to multiply themselves to demonstrate strength in numbers are fast crumbling since he nuclear weapons race. Today with the dwindling earths' resources and concomitant plunge in the quality of life, man is at the threshold of a new era where, he has to limit his own growth if has to survive. "In a finite world growth cannot be infinite". The day is not far off when the size of a country's population is fixed by a world body on the basis of her own available resources to sustain it. "Stabilizing the world population is at some point a condition for survival". The population problem—is a social problem and at the same time an ecological problem. Man armed with his technology and intelligence is the greatest predator preying on all other forms of life and the resources of this planet earth.

One of the immutable laws of Biology is that unrestrained multiplication of any species within a given space leads to its ultimate disappearance. From this law man is not immune.

Once the optimum carrying capacity of the planet is known the danger levelled at the water resources can be contained.

Regrettably in global politics ecological issues are confined to platitudes. The only silver lining in this dismal picture is that man is now aware of the ecological misbehaviour he and his forbears have so far indulged. The 2 Earth Resources Technology Satellites (ERTS) set in the heavens to monitor global pollution is a consequence of this realisation.

Present abuses of the earths' resources pale into insignificance by nuclear explosions meticulously planned and deliberately carried out. The recommendations of the 1972 Stockholm Conference on Human Environment could very aptly be part of history as were Plato's observations, made 2,300 years ago, unless man learns to live in harmony not only with nature but also his kin.

Bibliography

(1) JOHN LAWRENCE HARGROVE : "Law Institutions and the Global Environment." Oceana Publishers, New York (1972).

(2) BUCKMINSTER, R. FULLER : Utopia or Oblivion – Overlook Press, New York (1972).

(3) S.H.C. de SILVA : "The Sediment Problem." Quarterly Bulletin, Institution of Engineers, Ceylon (March 1966).

(4) S. H. C. de SILVA and L. V. TALGODA : "Waterlogging Causes and Measures for Prevention." Symposium C.B.I. & P., India, Vol. II, Publication No. 118, New Delhi (1972).

(5) Report of Study of the Critical Environmental Problems : "Man's Impact on Global Environment." Massachussets Institute of Technology (1970).

(6) RACHEL CARSON : Silent Spring – Houghton Mufflin & Co., Boston (1970).

(7) BARBARA WOOD and RENE DUBOS : Only One Earth – W. Norton & Co., New York (1972).

(8) H. C. PEREIRA : "Land Use and Water Resources." Cambridge University Press (1973).

(9) PAUL, B. SEARS : "Biology of the Living Landscape." George Allen & Unwin Ltd., London (1962).

(10) PIERRE DANSEREAU : "Challenge for Survival." Columbia University Press (1970).

(11) EMIL, T. CHANLETT : "Environmental Protection." McGraw Hill (1973).

(12) NASA-NEWS : Release No. 74-332, National Aeronautics and Space Administration, Washington, D. C. (18 Dec. 1974).

(13) WILLIAM, C. ACKERMAN; GILVERT, F. WHITE and E. B. WORTHINGTON : "Man-Made Lakes – Their Problems and Environmental Effects." American Geophysical Union, Washington (1973).

(14) DARRELL HAUG DAVIS : "The Earth and Man." Macmillan Co., New York (1948).

(15) Report of the Special Committee : Wallawatte Canal Pollution (1972).

(16) GOLDBERG, G.F.A. : "Assessment of Ground Water Potential in Sri Lanka." Advisory Services Report HG/2 United Nations (1974).

Ecological Aspects of Water Resources Management—Study of a Case

ERNEST H. RAZVAN
Head, Environmental Hydraulics Research Group
Spl. Independentei 294, Bucharest 17, Romania.

SYNOPSIS

After some basic concepts (as environment, ecological motion, stability, etc.) were introduced, the complex role of the water in the ecosystems is commented. The water represents much more than a natural resource and its use must be limited by ecological considerations. This is particularly important for a river scheme, rivers being a main factor in many ecosystems. To avoid undesirable effects of a river scheme, its environmental impact must be evaluated at the planning stage. A general method for this purpose is lacking and even particular methods are giving a first approximation. Research is to be continued, the present paper representing a modest contribution in this direction.

This contribution concerns a particular river scheme, a massive diversion ; the environmental impact was evaluated using the results of six special studies. To integrate these results, a graph and an ecological matrix were conceived and some of the effects were determined in monetary expression. Such procedure made possible the choice between alternative schemes considering also ecological effects.

Introduction

In the last twenty years phenomena of local degradation of the environmental factors, including the hydrosphere, were constated in different countries. Such phenomena appeared and developed before a body of concepts, a coherent theory or some provisional method.

Even for existing phenomena of degradation, the far going consequences are often unevaluated. The ecological impact of the planned works (for instance a river scheme) was generally ignored, is often underevaluated and sometime overevaluated. This paper begins with definitions of some main concepts of the matter—environment, pollution, a.o.—broadly used (incl. by the mass media), but with different meanings. Then the general concepts are applied to the domain of water resources, considering the very special role of the water in the natural ecosystems. Finally, a particular method to evaluate the environmental impact of a determined river scheme, using the previous theoretical ideas, is presented. This method is similar but not identical with some others, elaborated independently by Batelle Organisation or U.S.A. Geological Survey(1).

1. Some Definitions and Theoretical Aspects

1.1 *Environment*

In a previous work the environment was defined as an ecological system (or rather a supersystem) attached to a determined human community(2). Such a definition can be represented graphically (Figure 1). There are two characteristics of the graph :

—the environment results from the activities of a certain *social group*, influencing different ecological subsystems ;

—the dynamic *connections* between the ecological subsystems and the social group represents the essential feature.

Both characteristics reflect the specificity of man like a specia : when all other living species are adapting themselves to the environmental conditions, man's activities are adapting the environment to his own needs. These activities started with the beginning of the mankind, but become extremely intensive during the contemporary scientific-technological revolution ; it is

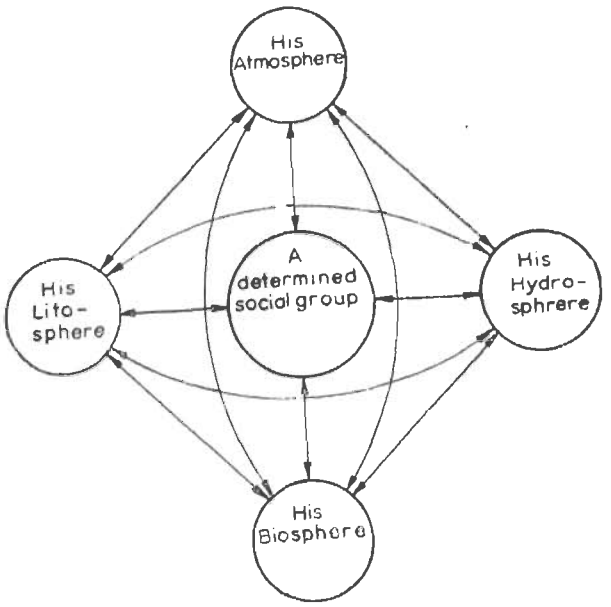

FIGURE 1 : Environment : definition graph.

precisely during this period that the concept of "environment" was broadly introduced.

1.2 *"Pollution" or "Degradation"? Resources*

From scientific point of view "pollution" is a rather vague term, including quite different physical, chemical and biological processes. More convenient and correct is the concept of *degradation* (of the environmental factors, etc.) instead of pollution. Another reason for using this term is that pollution reflects a manicheian philosophy: on one side we have a pure, "unpolluted" environment, on the other side, some malignant persons or "pollutant" activities. In fact, the actual so-called "pollution" represents the end of a process started long-time ago; practically at the same time with the human communities; this process is the use of the natural resources.

At a first sight, the concept of "resource" seems to be clear; in fact, this concept includes the source of the actual environmental degradation. Obviously, in the present vision, "resources" means substances that men can find in their environment, extract and processes to obtain determined useful items; at the end of the technological processes some useless, residual by-products are also yielded; these by-products are finally returned to the same environment. The degradation of the environment became obvious, when the intensity of this process is trespassing a certain critical level.

1.3 *Ecological Motion and Ecological Velocity— Stability and Impact*

The set of dynamic connections between the environmental factors reflects the existence of a new form of motion, the *ecological motion*. The previous, well-known forms of motion are the mechanical, thermal, electromagnetic, chemical, biological, social motions. Each of them is more complex than the precedent one; each includes some of the previous characteristics but adds some new, specific characteristics. Each form of motion is defined by a certain *velocity*, measuring the intensity of the changement; and each range of velocities include a certain critical value, limiting the *stability* domain of the motion. In the case of the ecological motion, the critical ecological velocity corresponds to the break of the main connections between the environmental factors; the loss of system stability follows, under the ecological impact (the disturbing effect of the some external or social action).

To quantify the environmental stability, it is necessary to find some parameter q (or rather a tensor q_{jk}) defining the qualities of the system. The fluctuations $\pm \Delta q$ are due to a determinated environmental impact. A simplest relation to define an environmental stability coefficient is :

$$C_{stab} = \frac{q - |\Delta q|}{q} \qquad \ldots(1)$$

It is not easy to measure the ecological impact and we have not a general method yet to express a coefficient of the environmental impact, C_{imp}. Different particular methods can be conceived for different particular conditions (see for instance Section 3.2). In any case a relation (or a curve) :

$$C_{stab} = f(C_{imp}) \qquad \ldots(2)$$

is a characteristic of the stability of every dynamic system. The stability coefficient will be equal to 1,0 only for a zero-impact and will be zero for $C_{imp} = 1{,}0$. Between these two theoretical points (0:1 and 1:0), the shape of a typical curve has three sections (Figure 2):

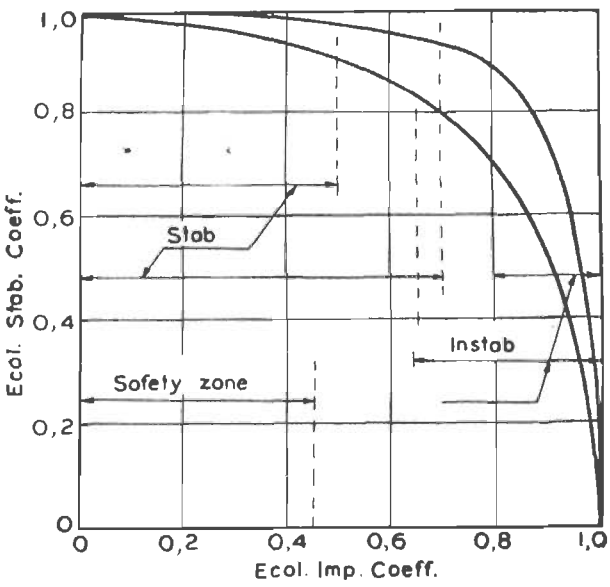

FIGURE 2 : Stability characteristic of a dynamic system.

—in the first, the stable one, for an increasing impact, the stability decreases very slowly ;

—in the second, a transition one, for a progressively increasing impact, the stability decreases rapidly;

—finally, in a last, unstable zone, for an insensible increase of the impact, the stability is fast dropping.

The different known stability curves, for different physical systems show that the first domain is limited by values of the impact $C_{imp} < 0{,}25...0{,}35$ and the last one, for $C_{imp} > 0{,}5...0.6$.

The shape of the curve suggests that, mathematically, this is a product of two other different curves, and, physically the coexistence of two set of factors, the first ones stimulatives, the others, inhibitors.

But the shape of the stability characteristic is important also for a practical point of view: in fact it is not necessary to plot the curve (2) for each system, it is enough to calculate the range of values of the environmental impact, and to have $C_{imp} < (C_{imp})$ critical.

1.4 *Two Sources of Environmental Degradation : Two Types of Solutions*

To avoid the instability it is important to have a very clear idea about the sources of environmental degradation. Considering the actual vision of the natural resources (see Section 1.2), there are two types of such sources :

—the first is connected with the rate of extraction of resources (as raw materials) from the nature;

—the second is connected with the rate of production and the nature of the residual substances, resulting in the processing of the raw materials.

Both sources are connected with the technologies, used by the respective social groups; in the present world the hottest points of environmental degradation occur in zones with highest GNP/cap and in connection with the top technologies.

To avoid the environmental degradation two types of solution can be conceived :

—the treatment of the residual substances resulting from socio-economic activities, using existing technologies ;

—the introduction of new technologies with integrated cycle of processing, without residuals (simulating natural processes).

Both types of solution are confronted with economical considerations : the social cost of the environmental degradation is still a crude approximation. The lack of some objective economical incentive to the environmental protection is probably a source of the continuity of degradation.

Unfortunately it is highly improbable that such incentives can be found using the actual economical theories. According to these theories, the economical value of an item is equal to the value of the incorporated social labour. It follows that such natural factors, which do not include human labour—as the air, the rivers and the sea water or the virgin land, have *no economical value*! Or these are precisely the environmental factors to be protected ; and it is very difficult to justify the considerable expenses required to protect some items without value (according to the respective theories). In fact, the traditional theories were formulated 200—300 years ago, long time before the actual scientific-technological revolution : obviously its validity domain is not unlimited. The contemporary conditions, essentially different from those of Adam Smith and Ricardo's time, require new economic theories and methods, including also the value of the environmental factors.

2. Ecological Aspects of Water Resources Management

The ecological aspects of water resources management follow from the previous theoretical aspects concerning the natural resources and from the very special part played by water in the environment.

2.1 *The Special Part played by Water in the Environment*

This part is very complex :

Long time before becoming a "resource", water had his part in the evolution of our planet, called also the "blue planet". The action of the water, under different forms (rains, streams, glaciers, etc.) was extremely important in landscape modelling. The hydrological cycle within the nature was, and continues to be, veryi mportant for the general climate, as well as for the local climate. The water bodies have a decisive role in the heat balance. The hydrological cycle must remind as that the quantity of water within nature is limited and fairly constant.

Long time before becoming a "resource", water had a special role in the biological processes. We actually do not know all about this role, but it is certainly decisive, because it is at least triple :

—water is a *component* of the living matter (up to 90 percent for certain species);

—water is the main *vector* for food, heat and residual substances;

—water is an important biological *habitat*.

In fact, each cell of a living body (including man) exists in a water flow. This is a reason why each man needs daily at least 2-3 l (and some times up to 8-10 l) of water for the alimentation.

But to fulfil its role in the biological processes, the quality of the water must be the same that makes life possible. The presence and concentration of strange substances in the water is a challenge for the life and the reactions of the living matter are incompletely known. The possible consequences, for life in general and

particularly for man could be very far going (diseases, deformations or destruction of some species, instability of biocenosis, etc.).

Water became a "resource" long time ago, when the first human communities appeared on earth. Historically, all the great civilisations developed along the river valleys. At present, the water resources are so important that any social-economical development is unconceivable without water. Compared to other natural resources, water resources have two specific characteristics :

—the use of water is *universal* (in all branches of economy, etc.) ;

—water is irreplaceable (by any synthetical products).

Water is an important esthetic element of the landscape, as well as of the urban and recreational areas (for swimming, fishing, etc.).

Water is not only a resource like others, but it is an important factor of the life quality. For this reason its use must be limited by ecological considerations.

2.2 *Rivers and Schemes*

Traditionally, rivers were considered sources for direct or indirect benefit and rivers schemes were designed without any consideration to the long-term consequence. But in last time important damages resulted from some schemes achieved 20-30 years ago. We realise now that a river has also some ecological functions, or is even the main factor in some ecological systems. The main ecological functions of a river are:

—the drainage of the watershed, including surface and ground waters (for the latter the river is a regulator, sometimes supplying the phreatic stratum);

—the transport of the debris collected from the watershed surface, including the vegetal detritus and different residual substances; some times all these became fertilizers for the valley soils during the flood periods (for example the River Nile);

—the habitat for water biocenosis.

Damming or diversions represent the starting points of a long perturbation chain of the ecosystems. The most direct one is the perturbation of the sediment transport: the downstream bed deformation and the reservoir sedimentation. These ones, cumulated with the levels changements became perturbation sources for the ground water flow; the natural vegetation and the agriculture; certain species can be stimulated, others inhibited by the ground waters modifications. Material damages can be so substantial so as to balance the positive effects of the scheme. Obviously, the prevision of the environmental impact is necessary at the planning of every important river scheme.

To make such previsions, there are many problems to solve :

—first, the main connections and characteristics of the natural ecosystems are to be determined ;

—second, the disturbing action of the structures, their propagation along different connections and the feed-back effects are to be estimated ;

—finally, different solutions to prevent or compensate the undesirable effects are to be designed.

Now-a-days we have not a general method to make environmental prevision ; but the above ideas were applied to some schemes planned on the Romanian rivers. A case study will be illustrative.

3. A Case Study

3.1 *The River Scheme*

The main purpose of the scheme is the river diversion for the irrigation of 540,000 ha in a first stage, and 1,000,000 ha in the final stage (Figure 3). For this purpose a large amount of water is necessary; the projected discharge of the main aqueduct is 270 m³/sec, representing the double of the average discharge in the intake section. The intake structure is located upstream from a diversion dam, overflowed during the floods. It follows that the hydrological cycle in the river valley will be strongly disturbed; the actual annual cycle will be broken in two quite different periods :

—the period of the flood (270 m³/sec $< Q <$ 6,000 m³/sec), about two months per year ;

—the period between two floods, when the river valley is practically dry ($Q <$ 5 m³/sec...25 m³/sec).

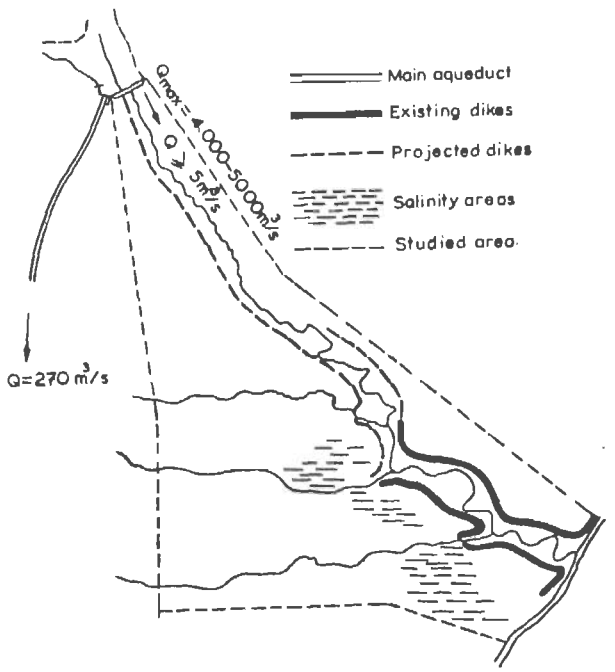

FIGURE 3 : A study case : diversion of a river.

Such an important change in flow is only an initial disturbance of the environment where more than 100,000 people, mainly farmers, are living and working. This initial disturbance propagates to the ground waters and then to the soils, vegetation, etc.

For the estimation of the impact in the system, i.e., the actual river valley, the following special studies were carried out :

—the study of the geography of the region (including the study of the soils) ;

—a hydrological study on the discharges in the actual river valley after diversion and on the water quality dynamics ;

—a hydraulic study on the sediment transport and bed deformation after diversion (increased roughness, general erosion, etc.) ;

—a study of the ground water levels before and after diversion ;

—a biological study on the present biocenosis and its predictable adaptation to the new conditions;

—a social study of the territory, including the populations' and economics problems relating to the existent river valley and to the foreseeable changes.

These studies were extended to the area likely to be influenced by the changes in river valley, i.e., about 250,000 ha on both sides.

3.2 *Integration of Partial Results*

Each study was provided with specific methods and ended with specific results. To estimate the environmental impact, it was necessary to integrate an important set of non-homogeneous informations.

The integration of these was provided in three steps :

—a graph of the ecological effects plotting together the informations ;

—an ecological matrix based on the previous and giving a measure of the environmental impact ;

—a listing of the evaluable effects (damages or supplementary works).

Using this procedure different alternative solutions were elaborated to minimise the environmental impact.

The graph of the ecological effects is constructed by plotting together logically the set of informations from all special studies (Figure 4). The graph is structured on several levels : the upper one is the sources or

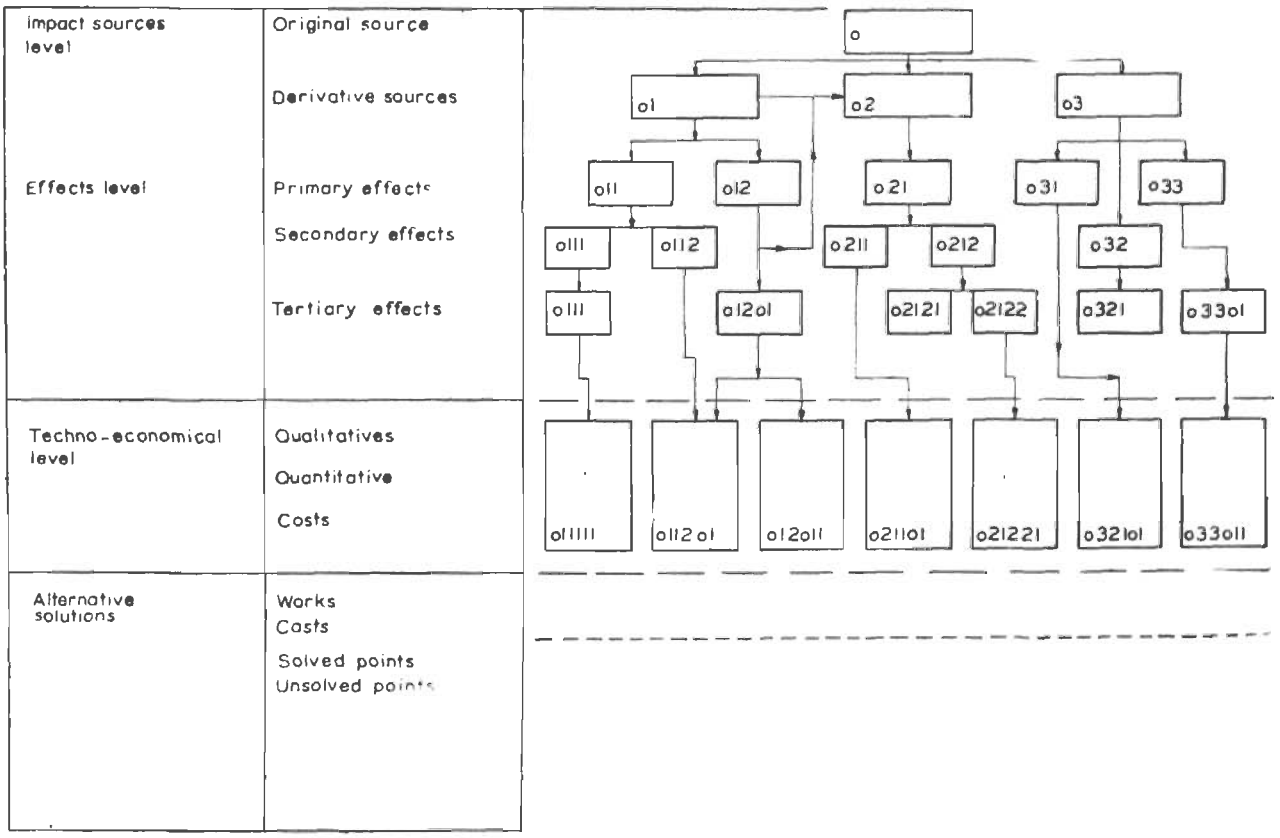

FIGURE 4 : The graph of ecological effects.

disturbances level ; the initial or *O* disturbance (in this case, the diversion) and the derivated disturbances (in the present case : 01, the levels decrease; 02, the salt concentration increase ; 03 the sediment transport unbalance). It follows the propagation or effects levels and there are four of them in this case (coded *o j k l m n*, *j, k,l,m,n*= 1,2,3...). The last is the appraisable effects level expressed qualitatively, quantitatively, and/or in monetary form (losses, annual expenses, investments). All these are logically connected with vectors indicating the sense from the source to the effect.

The adopted code gives indications about the complexity of the ecological processes, about links and sources of every effect. The more advanced the knowledge of the ecosystem, the more complex is the graph.

Nevertheless, such a graph cannot express the environment impact explicitly and an ecological matrix was used for this purpose.

The ecological matrix is structured on lines and columns (Figure 5). On the columns there are the "*n*" disturbing actions or factors (diversion, water intakes, wastewaters, etc.). In the studied case $n = 11$ such factors. On the lines there are all "*p*" the environmental factors (physical, biological, social) disturbed by the scheme (i.e., by the previous *n* factors). In our case, $p = 32$ disturbed factors.

There are the following distinctions between this matrix and other ones :

—the disturbed factors became disturbing factors (i.e., from the lines to the columns) as the vectors from the graph indicate ;

—each significant intersection is marked by two marks, from 0 to 5: one for the intensity of the disturbance (*I*), the second for the propagation area (*A*). The code for both is indicated in Table I.

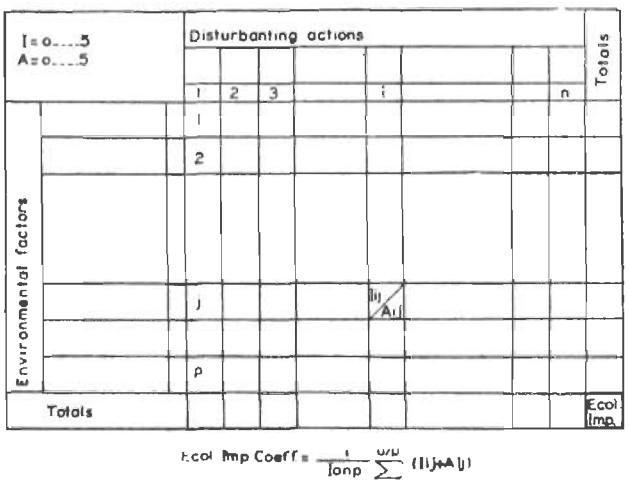

FIGURE 5 : The ecological matrix.

TABLE I

Code	Intensity of disturbance (*I*)	Area of propagation (*A*) (% from study area)
0	none	0
1	minimal	local
2	moderate	25
3	important	50
4	strong	75
5	exceptional	100

The expression:

$$C_{imp} = \frac{1}{10\,n\,p} \sum (I_{jk} + A_{jk}) \; (j = 1...n,\; k = 1...p) \qquad ...(3)$$

represents a first approximation of the environmental impact coefficient.

In our case, for a first alternative scheme, $C_{imp} = 0{,}32$.

It is very easy to formulate some objections against this matrix, first of all that the marks are subjective and conventional. But :

—there is a great number of marks, and it is a good chance for compensating some errors; in the studied case there are $32 \times 11 = 352$ intersections, but only 99 are significative;

—the conventional character of marks cannot give cost evaluation, but a possibility to compare different alternative solutions ; e.g., when for the first solution $C_{imp} = 0{,}32$, for the best one, $C_{imp} = 0{,}14$.

It is very important that the matrix gives not only a general impact coefficient, but also partial coefficients, on lines and on columns. The first ones indicate the degree of perturbation of each factor ; the latter, the role of each disturbing action within the general environmental impact. These partial coefficients give indications for priorities. In our case the most affected factors were : the bed morphology (0,45), the water quality (0,40) and the ground water flow (0,45); the most aggressive actions were : the diversion itself (0,36), the water-level change (0,46), etc. All these results give useful indications for the evaluation of the possible damages as well as for some works to be done for preventing or compensating the environmental impact.

In the studied case some 12 effects were evaluated in monetary expression.

From the components of the list there can be mentioned:

—alternative solutions for the water supply for some 100,000 people, using now ground water sources;

—supplementary water treatment stations, to compensate the decrease of self purification, and the increase in concentrations ;

—cost of soil treatment on about 12,000 ha, endangered by salination ;

—reconstruction of existing water intakes in the actual river valley.

A part of these effects can be estimated, others cannot, e.g. :

—the total degradation of the existing forest (on some 7 percent of the territory surface) can influence the local climate ;

—the rapid change necessary in agrotechnical technology will change the life conditions for all the people living in the zone.

But even the environmental effects of the first category were so considerable (about 15 percent from the total evaluated cost of the scheme) that alternative solutions were projected. The majority of the environmental effects have been prevented or compensated ($C_{imp} = 0,14$) in the best solution.

Conclusions

To evaluate the environmental impact of a river scheme a graph and an ecological matrix were used ; these engineering tools permit to use non-homogeneous informations and results of special studies, to conceive a river scheme, taking into account the ecological factors, as well.

References

(1) BATTELLE, Columbus Laboratories : Environmental Evaluation System, January 1972.

(2) RAZVAN, E. : Ecological Aspects of Water Resources (in Romanian), "Hidrotehnica" No. 6, 1974, Bucharest.

Water Pollution Control during Dam and Tunnel Construction

JOHN C. PETERS
Environmental Specialist
Office of Design and Construction Engineering and Research Center
U.S. Bureau of Reclamation, Denver, Colorado, U.S.A.

SYNOPSIS

To be in compliance with recently enacted environmental laws, Federal agencies must examine the full scope of their activities and evaluate the environmental impacts resulting from their program missions. Without proper treatment, the environmental impacts resulting from dam and tunnel construction can significantly affect the quality of water of a watercourse receiving construction wastewater. On Bureau of Reclamation projects, three basic water treatment techniques have been used successfully to treat construction wastewater ; namely, sedimentation, flocculation, and filtration. Analyses of the techniques used and the factors considered before selecting a particular water treatment method are presented.

Introduction

In the past 5 years, the U.S. Congress has passed significant environmental legislation whose overall thrust is the protection of the environment including physical, biological, and social-cultural environmental components. These laws include :

(1) National Environmental Policy Act of 1969, 42 U.S.C. Sec. 4332(2)(C), 4344(5) (1970)

(2) Clean Air Act, as amended, 42 U.S.C. Sec. 1957 et seq. (1970)

(3) Federal Water Pollution Control Act Amendments of 1972, October 18, 1972, P.L. 92-500, 86 Stat. 816

(4) Solid Waste Disposal Act, as amended, 42 U.S.C Sec. et seq. (1970)

(5) Federal Environmental Pesticide Control Act of 1972, October 21, 1972, P.L. 92-516, 86 Stat. 973

(6) Noise Control Act of 1972, October 27, 1972, P.L. 92-574, 86 Stat. 1234.

This legislation constituted a mandate for Federal agencies to examine the full scope of their activities including planning, design, construction, and operations, and to rigorously and objectively evaluate the environmental impacts resulting from their programs. This legislation has placed an additional responsibility on Federal agencies to see that environmental aspects are considered while carrying out their program missions.

For those Federal agencies responsible for water resource development, the most salient environmental laws are : (1) the National Environmental Policy Act, hereafter referred to as NEPA, and (2) the Federal Water Pollution Control Act Amendments of 1972, hereafter referred to as the Federal Water Act Amendments. NEPA requires the preparation of an environmental impact statement before a major Federal action affecting the environment such as a dam construction contract can be awarded. Citizens have an opportunity to challenge a Federal agency's appraisal of the consequences of its actions, through the Federal courts. The Federal Water Act Amendments require a permit to discharge wastes from point sources such as discharges from tunnel or dam construction activities.

Before dam construction activities can take place

for a Federal project, a rather exhaustive analysis of the environmental impacts of the water project must be made through the environmental statement process by the agency itself. In addition, the agency's analysis of the impacts must be scrutinized and reviewed with comments solicited from other Federal, State, and local agencies, and the private sector. Under the Federal Water Act Amendments, a National Pollution Discharge Elimination System permit, hereafter referred to as an NPDES permit, must be obtained to discharge wastes from a point source into any receiving water body.

The environmental impacts of dam and tunnel construction are mostly direct and short-term. A direct impact means there is an immediate response to an action. Rock is blasted in a tunnel—noise and dust are the results of the blasting action. A dam foundation is excavated in a flood plain—muddy wastewater is pumped out of the foundation. Typically, there is an immediate cause and effect relationship from a direct impact. Construction impacts are short-term, rarely continuing for more than 5 years. For the most part, the direct, short-term environmental impacts of the construction process are not difficult to analyse and assess. Good estimates can be made of the significance of the impact prior to construction. During the construction process, monitoring of impacts is required as a condition of an NPDES permit.

This paper considers the environmental impacts associated with dam and tunnel construction, the environmental laws that affect the design and construction process, and the mitigation measures used by the Bureau of Reclamation to reduce impact during construction of a dam or tunnel.

Environmental Laws and Construction Activities

Before proceeding with a construction contract, it is necessary to understand the relationship between environmental legislation and construction activities. NEPA and the Federal Water Act Amendments must be prudently followed and all legal requirements must be met. The following is a discussion of the interrelationships between environmental legislation and construction activities.

NEPA

The environmental statement is a full disclosure document available for Governmental agency and public review, pointing out the environmental impacts resulting from a proposed program or action. It must list all the beneficial and adverse impacts resulting from both the project and alternatives to the project. The discussion of mitigations for construction activities must be more than just guidelines or suggestions which are not implemented. The statement must spell out what is going to be done to soften or reduce the impacts associated with the project, who is going to do it, how it is going to be funded, and when it is going to be done. The direct, short-term impacts associated with construction activities must be fully discussed in the environmental statement. The construction mitigation measures must be written into contract specifications and undertaken during the construction period. It is essential that what is said in the impact statement is, in fact, carried out during the construction process. The environmental statement commits an agency to a course of action during construction.

Federal Water Act Amendments

The Federal Water Act Amendments require an NPDES permit to discharge wastes from a point source into a receiving water. According to the regulations promulgated to carry out the Act, a point source is defined as "any discernible, confined and discrete conveyance including but not limited to a pipe, ditch, channel, tunnel, conduit, well, discrete fissure, container, rolling stock, concentrated animal-feeding operation, or vessel or other floating craft from which pollutants are or may be discharged." An NPDES permit may be obtained by a Federal construction agency from the Environmental Protection Agency who administers this water pollution control law. Upon application for an NPDES permit, the Environmental Protection Agency publishes in the local newspapers a notice of an application for a permit to discharge wastes. This gives the public sector an opportunity to request a public hearing and formally comment on the conditions of the permit regarding the treatment of wastewater. An NPDES permit is issued specifying the amount of wastes that can be discharged into a water body. Contract specifications must provide the prospective bidders information on water quality standards for a particular water body impacted by dam or tunnel construction. Specifications may define methods that are acceptable to the Government to treat wastewater to meet existing water quality standards. Records must be kept on the wastewater discharge and regularly transmitted to the Environmental Protection Agency.

Both laws require citizen involvement and mandate full disclosure of the impacts associated with the construction process. The agency must meet the challenge of this legislation and provide for water pollution control that maintains environmental quality during construction.

Water Pollution Control Methods

In the construction of the dam or tunnel, the most significant water pollution problem is the treatment of turbid waters that result from construction activities. The excavation of a foundation for a dam, the discharge of tunnel water, the processing of aggregate, and the batching of concrete all result in turbid or sediment-laden wastewater. This untreated wastewater discharged into a watercourse can affect a municipal drinking water supply, disrupt irrigation activities, and impact commercial or sport fisheries. It can affect recreational activities such as fishing or boating. To adequately treat turbid wastewater resulting from construction activities on Bureau of Reclamation projects, three basic water treatment techniques have been used thus far : sedimentation, flocculation, and filtration.

Sedimentation

Sedimentation is an operation by which the action of turbulent flow is reduced in magnitude until suspended particles settle out by gravitational pull and are not resuspended by scour. A series of settling ponds have been successfully used to settle out suspended particles from water. Precipitating agents such as alum may be introduced to speed up settling of suspended particles. Chemical precipitation is an action where substances suspended and/or colloidal particles are settled out of a sediment-water mixture induced by coagulation from a precipitating agent. The settled substances are known as sludge and must be periodically removed from the ponds for disposal. Settling ponds have been used on the following Bureau projects: Currant Creek Dam, Bonneville Unit, Central Utah Project, Utah, and Nambe Falls Dam, Pojoaque Unit, San Juan-Chama Project, New Mexico. A layout for the Currant Creek Dam settling ponds to induce sedimentation is shown in Figure 1.

Flocculation

Flocculation is an operation designed to force agitation in a fluid and induce coagulation. In this technique, very small suspended particles collide and conglomerate into heavier particles or flocs and settle out. Floc growth generally depends on two factors : (1) intermolecular chemical forces, and (2) physical action induced by agitation. Mixing processes are employed to disperse chemical precipitating agents in fluids and enhance flocculation. Flocculation is directly proportional to the velocity gradients established in the water being treated. The stirring action derived from the flocculating mechanism is responsible for these gradients and, therefore, fundamental to the process. The number of contacts between particles in a unit time has been shown to vary with the number and size of particles.

Typically, the process begins by dissolving a precipitating agent in a rapid mix operation. Initial collisions between colloidal particles occur from Brownian motion and in contacts brought about due to differences in settling velocities in heavier and lighter particles. A period of gentle agitation or turbulent mixing is, therefore, necessary to produce rapid floc growth and is important in the design of the system. The Clarfloculator is a commercial clarifier that employs flocculation and sedimentation. It has been used on the following Bureau of Reclamation projects : Crystal Dam, Curecanti Unit, Colorado River Storage Project, Colorado; Teton Dam, Teton Basin Project, Idaho; Auburn Dam, Central Valley Project, California ; and Pueblo Dam, Fryingpan-Arkansas Project, Colorado. A layout for the Pueblo Dam water treatment system is shown in Figure 2. Primary treatment often occurs in a settling pond or series of settling ponds before final treatment is performed in a clarifier.

Filtration

Filtration is an operation to separate suspended matter from water by passing it through porous material. Filter materials used commonly include sand, anthracite, diatomaceous earth, or a finely woven media. These materials are used either singly or in combination

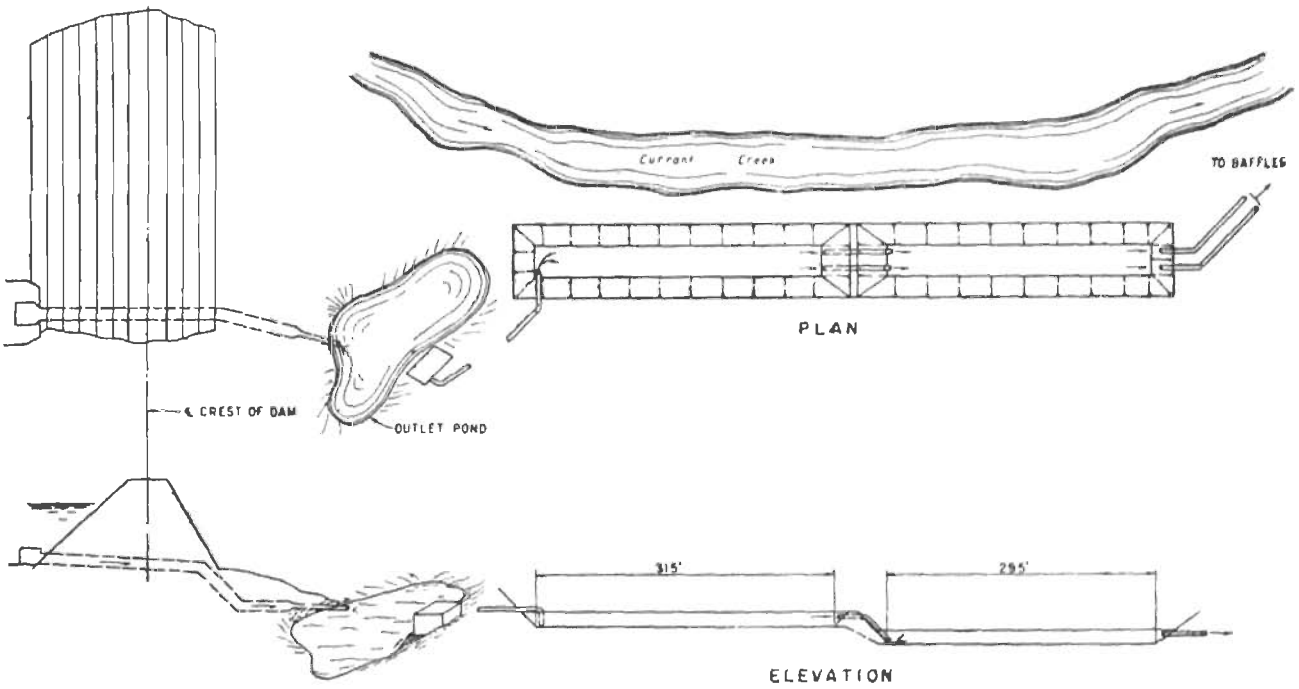

FIGURE 1 : Layout of Currant Creek Dam—water treatment system.

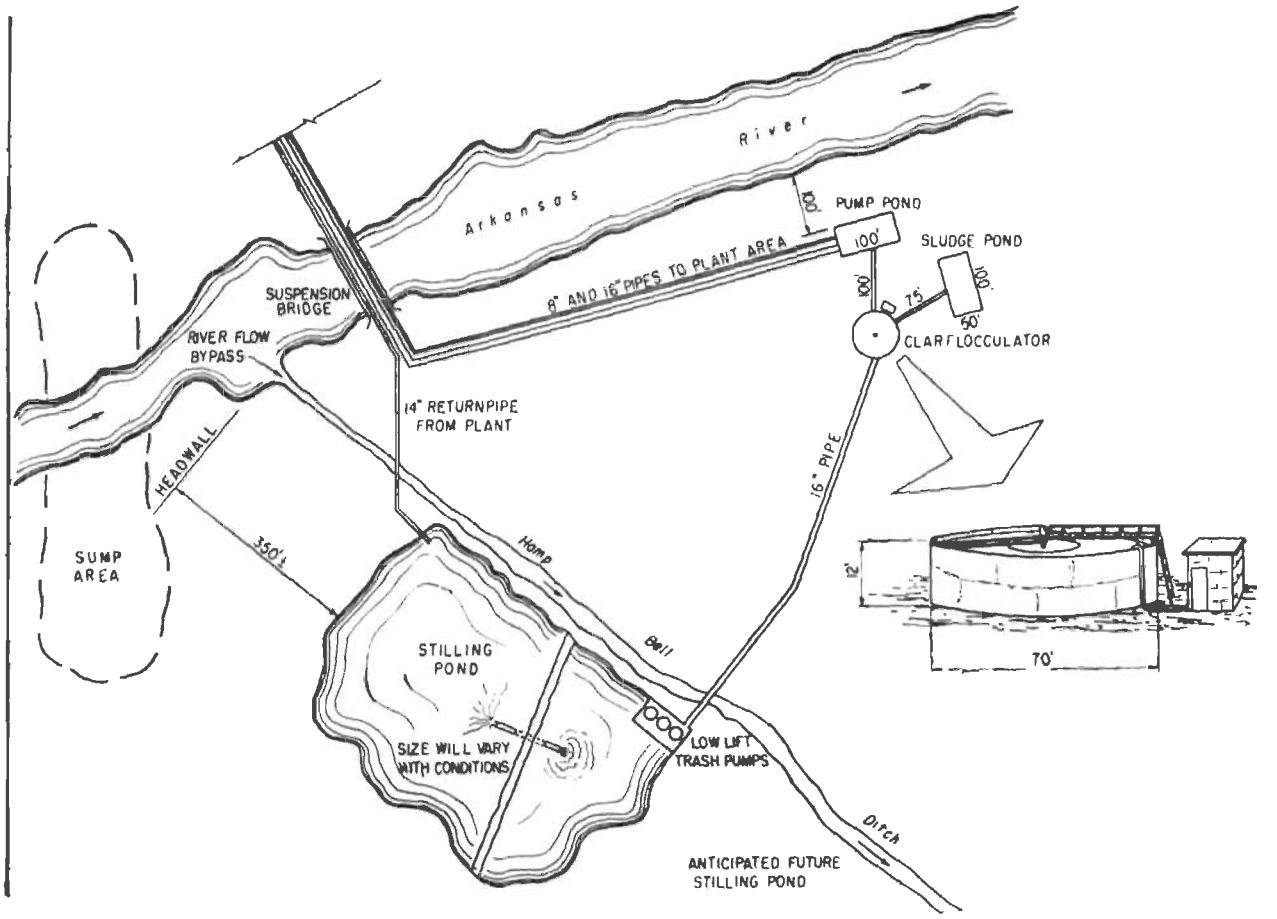

FIGURE 2 : Layout of Pueblo Dam –water treatment system.

as a multi-media filter. Filters may be either the gravity type or the pressure type. Pressure filters have media and underdrains installed in a closed steel tank. Water is pumped through the filter under pressure and the media washed by reversing flow through the bed, flushing out impurities. The filtration operation involves straining by interfacial contact combining to transfer suspended matter on to grains of sand, coal, or other granular materials. The accumulated sediment is flushed from the filter media singly or in combination by water and air mechanical rakes. A rapid pressure dual filter using anthracite and sand as media is being used on the Cunningham Tunnel, Fryingpan-Arkansas Project, Colorado, and a layout of this filter is shown in Figure 3. The wash water is the by-product of the water filtration and must be disposed of properly.

Other potential water pollutants such as refuse, garbage, sewage, debris, oil and other petroleum products, mineral salts, industrial chemicals, etc., must be controlled during construction. Oils, petroleum wastes, and chemicals cannot be drained randomly on to the soil, but must be confined in sealed containers and removed to disposal sites off the job. Debris and refuse must be removed and buried in designated solid waste disposal areas. Sanitary wastes must be treated and disposed of in accordance with state and local regulations.

If large quantities of oil are stored on a project construction site, oil spill prevention, control, and countermeasure plans, hereafter referred to as SPCC plans, must be prepared and fully implemented. Under the Federal Water Act Amendments, a SPCC plan must be maintained at each facility. The oil spill potential during construction must be analyzed, a listing of containment or diversionary structures installed, and spill contingency plans developed to control and remove any harmful quantity of oil discharges.

The Federal Water Act Amendments mandate that pollution caused by runoff during construction, as well as other non-point sources (mining, logging, agriculture, etc.), be controlled in addition to the control of point sources. Construction of temporary service roads and removal of borrow material are activities that typically result in pollution from non-point sources. The location of temporary service roads is often more important than control measures to reduce erosion such as matting

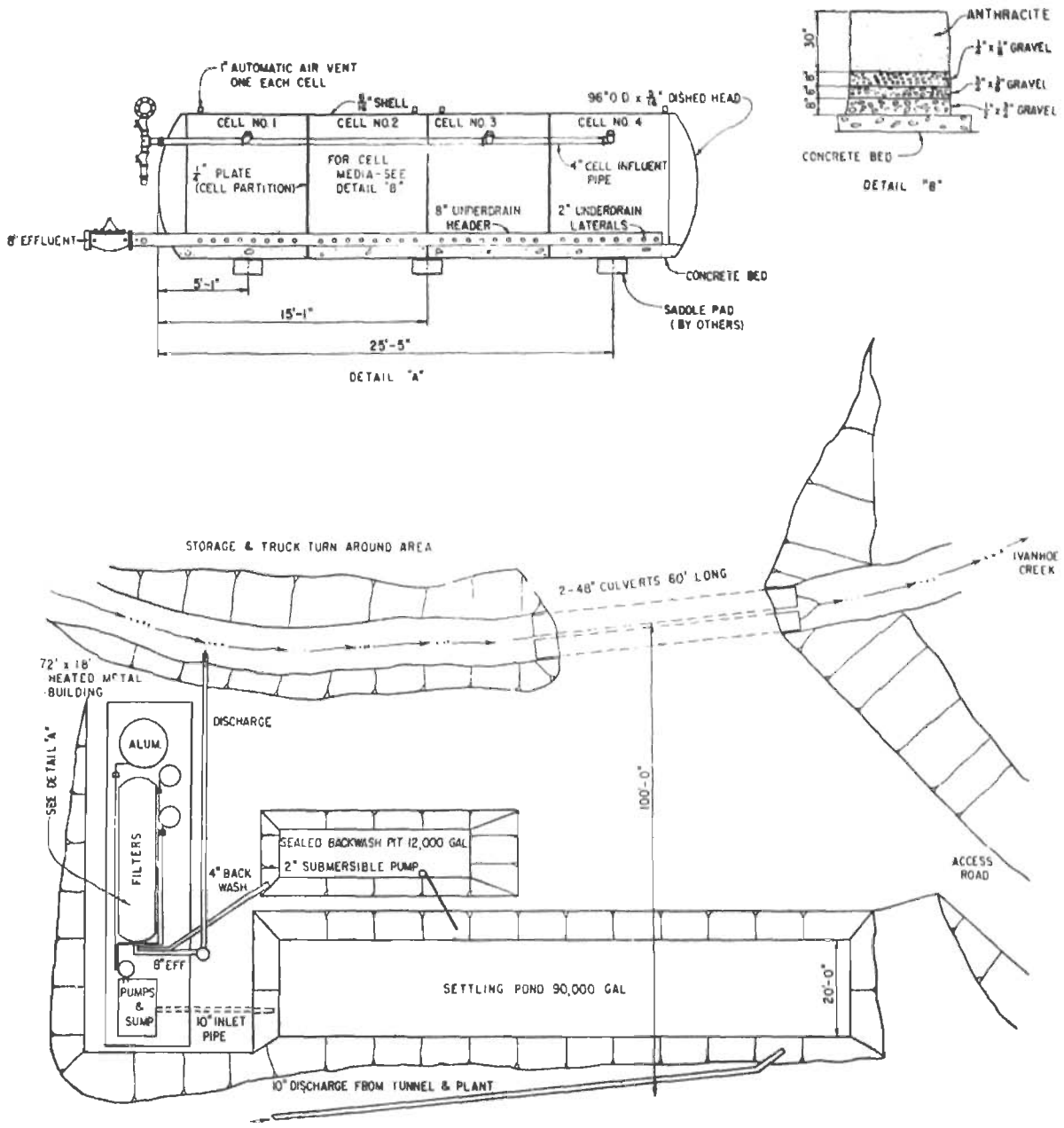

FIGURE 3 : Layout of Cunningham Tunnel—water treatment system.

or seeding. Temporary roads would be located with a minimum of steep cut and fill slopes. Typically, material sources are located in the reservoir pool to eliminate unsightly permanent landscape scars. Borrow areas collect water when they encroach upon the flood plain water-table. Large earthmoving equipment causes turbidity when moving through ground or runoff water which accumulates in the borrow areas. This turbid water moves downslope using natural runoff drainage channels before discharging into the watercourse. Low permeable check dams, such as shown in Figure 4, act as a settling pond and allow discharge of relatively clean water to the river.

Discussion

A wide range of factors must be considered before selecting a particular water treatment method. Some of these factors are technical, others are legal, while still others are institutional. Nevertheless, contract

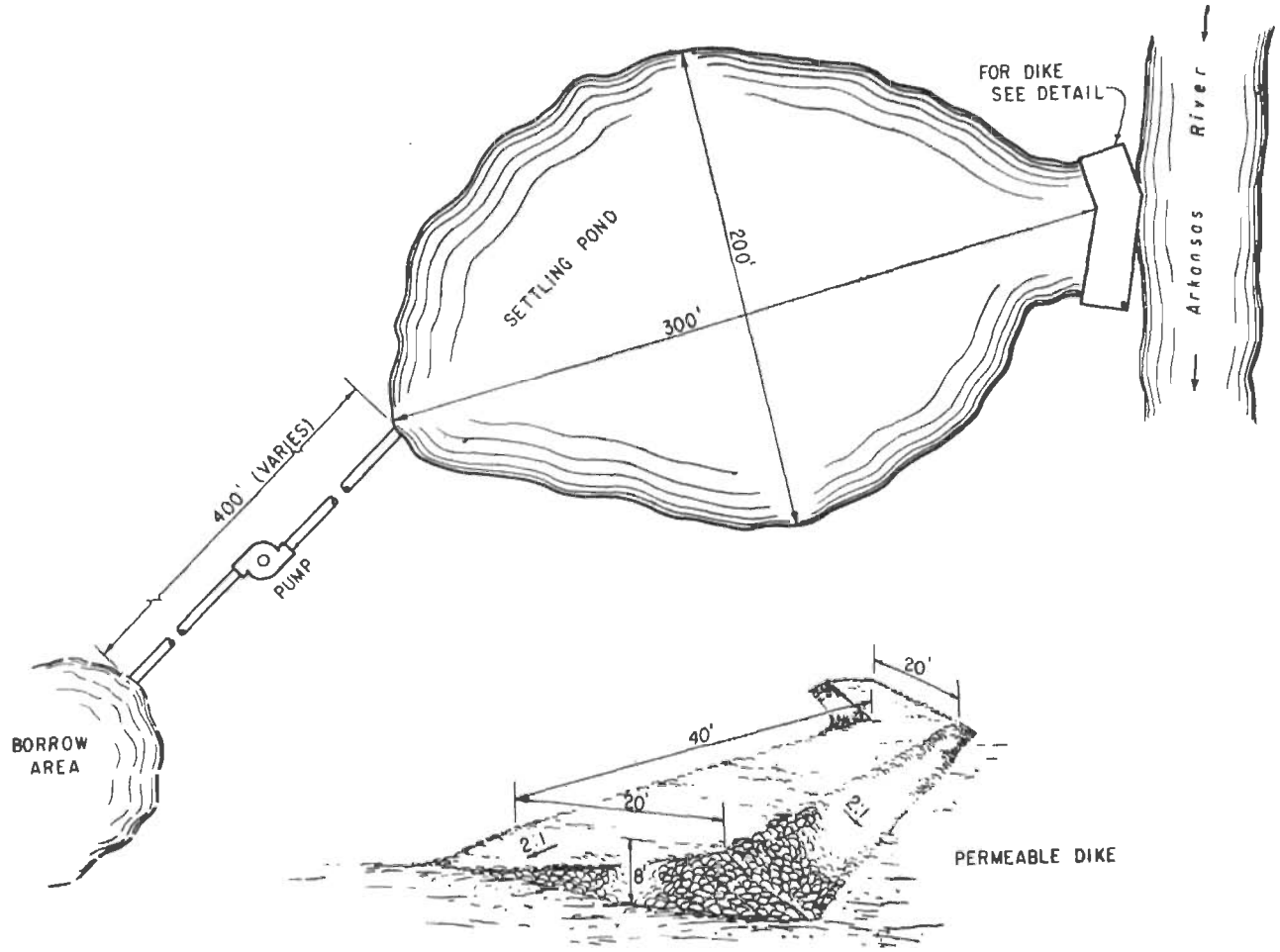

FIGURE 2 : Layout for permeable dike settling pond.

specifications should meet technical, legal, and institutional needs without complicated administrative burdens. Perhaps the most important technical factors are to accurately estimate : (1) the volume of wastewater and (2) the concentration of the pollutant requiring treatment. Generally speaking, the options available for selecting treatment methods are much greater when small volumes of water require treatment. Any of the three methods described earlier could be used to effectively treat wastewater discharges ranging between 1 and 2 cu ft/sec. However, when large volumes of wastewater (up to 7 and 8 cu ft/sec) require treatment, the Clarflocculator seems to be most effective when discharges are pretreated in settling ponds.

The type of dam to be constructed is another factor that must be considered before selecting a wastewater treatment technique. Concrete dams require more wastewater treatment than earthfill dams. Water is required to wash aggregate and batch and cure concrete. Typically, wastewater from these operations is highly polluted and has a high *pH*.

Tunnel construction must be considered differently than dam construction because of the year-round nature of tunnel construction. A water treatment system must be designed to meet a wide range of climatic conditions on a year-round basis. At high elevations in temperate latitude, the treatment plant must be contained in a heated building in the winter to operate properly. Freezing and thawing will cause significant maintenance problems when settling ponds are used at high elevations. If a tunnelling machine is used, large quantities of lubricating oil will be discharged along with the turbid tunnel water.

Most treatment methods require the use of chemical precipitating agents to speed up the sedimentation process. These precipitating agents must be selected so that they do not contaminate drinking water supplies or affect aquatic life. Use only non-toxic chemicals that are listed as safe by the Environmental Protection Agency. Wastewater from concrete dam construction is usually extremely basic with a *pH* greater than 10.5. Concentrated sulphuric or hydrochloric acid is used to

buffer this wastewater close to neutral. Concentrated acids and other industrial chemicals must be stored and used to prevent contamination of the watercourse. The use of any hazardous material for any construction purpose must be carefully managed.

The physical location of a dam or tunnel can influence the methods available for water treatment. For example, in a canyon it might be physically impossible to locate a series of sediment ponds to treat wastewater. There simply might not be sufficient space available for the number and size of ponds needed to treat wastewater. In relatively wide, undeveloped flood plain, the choices are nearly unlimited. The proximity to a town can influence the type of treatment selected. For example, if a municipal water supply was located in close proximity to the construction site, an additional safety factor should be required so that the water treatment system can operate under extreme conditions. The immediate topographic relief features should be considered too. It may be impossible to locate a series of settling ponds in a mountainous area without considerable permanent scarring. A treatment system might be selected because of its compact size.

Monitoring wastewater discharge is a requirement of an NPDES permit. Instruments should be used that monitor water quality parameters instantaneously such as a recording turbidimeter. Most permits are issued and discharges allowed based on State classification for existing water use. A water supply or high-quality trout stream will require more stringent water treatment and a smaller concentration of pollution discharged than waters designated for lesser uses. The selection of treatment devices and instruments to monitor the wastewater discharge should reflect the use and value of the water based on the State classification system.

The maintenance and care of equipment is important. After start-up and establishment of operating procedures, clarifiers and dual-media filters require only routine inspection by an operator. Alarms can be installed and automatic shutoff devices used if the equipment fails to operate properly. Generally, settling ponds require considerably more time and labor to keep them operating properly than filters or clarifiers. In all three methods, sludge or wastewater must be removed periodically. It is important to locate waste areas for sludge and wastewater so that they do not result in water pollution.

Bureau specifications are written with two or more acceptable Governmental methods for wastewater treatment with a provision for accepting a contractor's treatment method. Bidders are required to bid on a line item basis for water treatment. Recently, contractors working through consultants have submitted treatment techniques other than Governmental methods listed in the specifications. After review by the contracting officer, the contractor's method is either accepted or rejected. Whether a contractor selects a Government method or adapts one of his own, he is required to present a detailed layout describing his water treatment facility before being allowed to proceed with construction.

Conclusions

Environmental legislation (i.e., NEPA and the Federal Water Act Amendments) requires effective water treatment during dam and tunnel construction. Full disclosure of the water pollution impacts expected to occur during construction must be objectively and rigorously analyzed in the environmental statement. Measures to mitigate water pollution during construction must be enumerated. These mitigation measures represent a commitment to carry out water treatment to minimize pollution from point and non-point sources.

Contract specifications must be written so that water treatment can be implemented in compliance with the law. The specifications must translate water treatment commitments presented in the project environmental statement and implement treatment techniques which meet the Federal Water Act Amendments. Three techniques—sedimentation, flocculation, and filtration—have been successfully used to treat construction wastewater. These techniques represent standard water treatment methods, but have been adapted to meet construction requirements.

Each project must be analyzed in terms of its legal, technical, and institutional needs and water treatment techniques for construction must be consistent with site specific requirements.

The Ecological Effects of Thermal Discharge from Power Plants

R. V. HARMSWORTH
Limnetics, Inc.
6132 W. Fond du Lac Avenue, Milwaukee
Wisconsin, U.S.A.

C. H. WAHTOLA, JR.
Limnetics, Inc.
6132 W. Fond du Lac Avenue, Milwaukee
Wisconsin, U.S.A.

SYNOPSIS

This paper reviews the ecological investigations undertaken at the Point Beach Nuclear Power Plant on Lake Michigan, Wisconsin, U.S.A. The ecological studies included thermal plume measurements on a biweekly basis and biological measurements on a monthly basis. The biological studies included the measurement of fish, plankton and benthic macroinvertebrate populations in the plume areas and reference areas outside of the plume. Analysis of variance between the plume and non-plume areas showed that there were no consistent significant differences that could be attributed to the thermal discharge.

Introduction

Throughout the history of civilization, water has been a major element in the development of population areas. Initially, water resources were used for transportation and agriculture, and later used in the production of energy. The problems facing civilization today are in many ways similar to those of the past, and water is an integral part of the solution to these problems. In underdeveloped countries, one key to development is the proper and wise use and development of water resources, while in more developed countries, the protection of the water quality is an integral part in the further development of such countries. The United States has been blessed with abundant resources in terms of its major river systems and large lakes such as the Great Lakes that it shares with Canada.

Lapp (1974) in his paper "The Challenge of the Energy Dilemma," has projected an annual energy consumption growth rate of approximately 3 percent per annum from 1950 to the year 2000 ; however, in general, there is a trend toward the use of electrical energy and the projected growth rate of electrical energy until the year 2000 is 7 percent per annum. The increasing use of electrical energy will place a greater demand upon water resources and, consequently, the effects of power generation upon water resources in terms of water quality and the effect of generating stations upon biological parameters is of extreme importance. Figure 1 shows the estimated water use by steam electric generating stations in the United States. From Figure 1 it can be seen that, in 1950, approximately 22 percent of the total water used was used by steam electric utilities, and this percentage increased to 40 percent in 1975. However, it is a misnomer to state that electric utilities use water. The uses are generally non-consumptive ; however, with the advent of new rules and regulations, the consumptive use in terms of evaporation from cooling towers may well begin to climb significantly. This paper seeks to examine the effects of once-through cooling at the Point Beach Nuclear Plant, situated at Two Rivers, Wisconsin, on Lake Michigan. Figure 2 is a map of the United States showing the location of Wisconsin on Lake Michigan. Central Wisconsin is located on longitude 90 and latitude 44. The summers are warm with upper temperatures in the 90°F range, and the winters are cold with temperatures as low as 20°F below zero. Lake Michigan, which borders the eastern side of

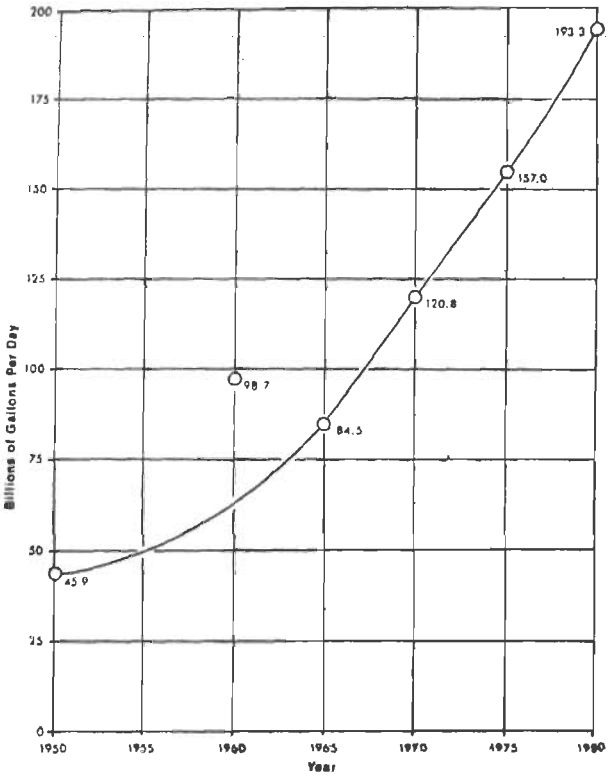

FIGURE 1 : Estimated water use by Steam Electric Utilities in the U.S.A. (Data from statistical abstracts of the U.S.A., 1972).

Wisconsin, is approximately three hundred miles long and a hundred miles wide, with an area of approximately 54,000 square miles. The deepest point in Lake Michigan is 924 ft. Lake Michigan is generally described as a dimictic lake with strong thermal stratification during the summer months and weak thermal stratification during the winter months. Biologically, Lake Michigan was formerly an obligotrophic lake, exhibiting relatively low algal productivity. However, in recent years, the southern basin of the lake has become more eutrophic and the northern basin is showing signs of becoming more eutrophic than in the past. This is undoubtedly due to the formerly heavy influx of sewage from the major towns in the areas and also extensive agricultural runoff.

The Point Beach Nuclear Plant, a pressurized moderated light water and cooled system located near Two Rivers, Wisconsin is an 1,100 megawatt plant, consisting of two 550 megawatt units.

This report presents the findings of the first year of an extensive environmental study conducted on the ecological effects of thermal discharges into Lake Michigan from the Point Beach Nuclear Plant. The report documents the result of the investigations performed during the period October 1972 to November 1973. The environmental studies have continued since that time and will continue in the future in compliance with the Nuclear Regulating Agency's (formerly the AEC) technical specifications for the plant. This investigation was commissioned by the Wisconsin Electric Power Company, Milwaukee, Wisconsin, in

FIGURE 2 : Location of the Point Beach Nuclear Plant.

June 1972, in response to the requirement established by the Wisconsin Department of Natural Resources and the NRA. The purpose of the study was to determine whether or not there were any significant ecological effects of the warm water discharge from the plant on Lake Michigan. The volume of the discharge at the Point Beach Nuclear Plant is approximately 885 cfs and the $\triangle T$ is approximately 10°C in the summer and 20°C in the winter. With such a large discharge, it would appear that some effects may occur. Also from observations of the plume, one can see immediately at certain times of the year that fish gather in the plume and consequently this leads one to believe that there may be certain behavioral reactions due to the plume and perhaps some more subtle ecological effects. The study consisted of the following major elements :

(1) Physical Studies
(2) Meteorology
(3) Plume Modelling
(4) Geology
(5) Water Chemistry
(6) Bacteriology
(7) Phytoplankton
(8) Periphyton
(9) Aquatic Macrophytes
(10) Primary Productivity
(11) Zooplankton
(12) Benthic Macroinvertebrates
(13) Psammon
(14) Fisheries.

With such a large number of elements of the ecosystem to study, it was imperative that a strong experimental design be formulated. There are three philosophical approaches to such a study :

(1) The first approach is to analyze the ecosystem in the experimental area, i.e., the plume, and compare this with the reference area which is unaffected by the plume.

(2) To introduce certain species into the plume and test their viability, i.e., an in situ bioassay experiment.

(3) Condenser passage experiments, in which the effects of entrained organisms are measured before and after the condensers.

In the surveys at the Point Beach Nuclear Plant, all three methods were utilized to a greater or lesser extent. However, the primary method for determining whether or not there were ecological effects at the Point Beach Nuclear Power Plant were by use of an experimental and a reference area. At this plant, the similarity between the experimental area and the reference area was not assured ; therefore, two reference areas were used. A series of sampling stations were selected along the lines of the two plumes at the plant and also on a line transact from the reference areas. These stations were selected primarily as a result of depth and expected temperature distribution (Figure 3). Sampling was undertaken on a monthly basis throughout the study period and the statistical analyses performed on the various groups of organisms and physio-chemical parameters collected at each sampling area were tested for differences using analysis of variance. Comparisons between the reference areas and the plume and between the north and south reference areas were made using Tukey's Test for pair wise comparisons, Scheffe's multiple comparisons test or Student-Neumann-Keuls multiple comparison test; utilizing these statistics, it was possible to determine whether or not there were significant differences existing between the populations of organisms at the reference areas and the plume or between the reference areas. In addition to the tests between reference areas and plume, similar statistical tests were run on analyses of organisms entering the plant condensers and leaving the discharge. These experiments centered primarily around destruction of zooplankton and the changes in primary productivity of algal populations resulting from passage through the condensers. Also, experiments were undertaken by caging fish in the plume area and the reference area, i.e., an in situ bioassay experiment which was run over a 96-hour period in order to determine whether or not there was increased mortality of fish in the plume due to the elevated temperatures.

Physical Studies

The physical studies undertaken at the plant consisted primarily of bimonthly measurements of the plume distribution at one metre intervals of depth. Examples of characteristic plumes measured during each season are shown in Figures 4 through 9. The plumes were measured to within one to two degrees centigrade above lake receiving water temperatures, although this was not always possible due to the variation in natural lake temperatures. The extreme envelope of all surface plumes, mapped to the second closed isoline, covered a total integrated area of 1.29 square miles and the farthest distance measured from the outfall to the second closed isoline was 2.13 miles. The largest single plume measured to the second closed isoline covered an area of 0.86 square mile to the second closed isoline. (The second closed isoline approximates two degrees centigrade above lake receiving water temperature). In general, thermal plumes were larger during the spring and fall than during winter and summer. During the winter period, the phenomenon of the sinking plume was observed. This occurs because in Lake Michigan the winter temperature approaches 0°C and consequently, because of the temperature-density relationships of water, the densest water, at 4°C is at the bottom of the lake and the lighter water at 0°C is at the surface. When the thermal plume enters the lake, the plume initially floats

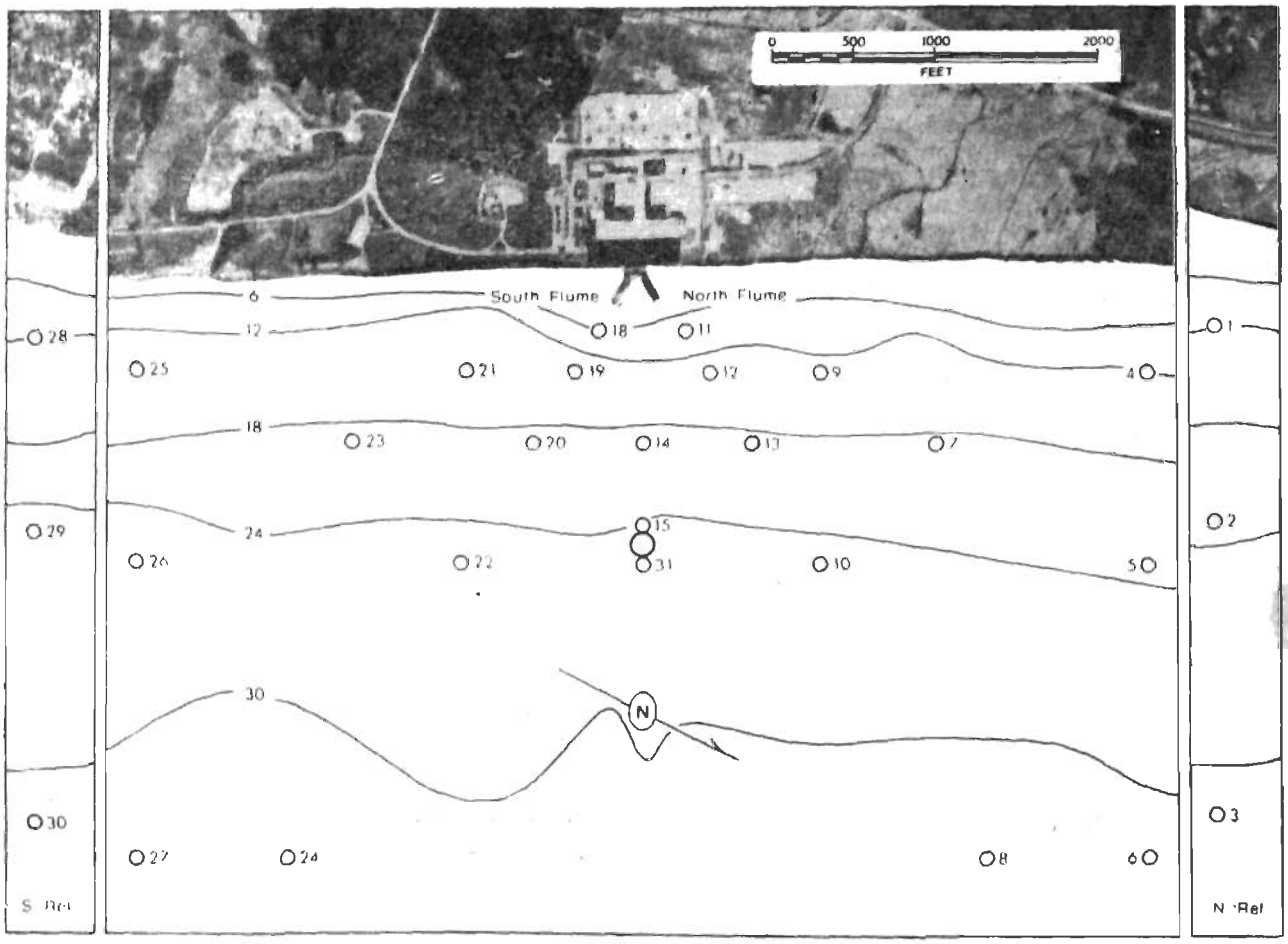

FIGURE 3: Diagrammatic sketch illustrating the sampling stations at the Point Beach Nuclear Plant.

on the surface because the water is lighter ; however, as mixing and entrainment occur, the water cools to 4°C which is the temperature of maximum density, and consequently falls to the bottom of the lake. This is the so-called sinking plume phenomenon. The average plume discharge velocity was 1.8 ft/sec and the plume velocity decayed as a non-linear function of distance down range. The plume currents decreased to natural lake current levels within approximately 2,000 ft. The point temperature relationships within the plume are a complex function with many variables ; however, drogue measurements showed that the maximum observed current/temperature relationship was approximately five hours in order for the water to cool to one to two degrees above receiving water temperature. Most of the heat from the thermal plume was dissipated outside of the approximately 1°C excess isotherm. In general, the total plant rejected heat within the confines of the one degree centigrade excess isotherm was less than 10 percent. A large portion of the plant rejected heat is transported laterally beyond the boundary of the 1°C excess isotherm by advection and mixed within the lake mass by diffusion processes that subsequently dissipates the heat into the atmosphere.

Water Chemistry

In general one would not expect the water chemistry parameters to vary as a result of either increased temperature or passage through condensers and indeed there are few, if any, meaningful changes as a result of condenser passage. The average annual means for the various water chemistry parameters were measured during the survey. There were some indications in the results that the levels of copper and zinc may at certain times have been greater in the discharge than at the intake at the plant ; however, these results are not entirely conclusive. The copper and zinc elevations may have been due to leaching from the condenser tubing which was made of admirality brass, a zinc-copper alloy. Turbidity appeared to increase as a result of condenser water passage which may have been a complex function of the stratum from which the water was being taken and discharged at a different level.

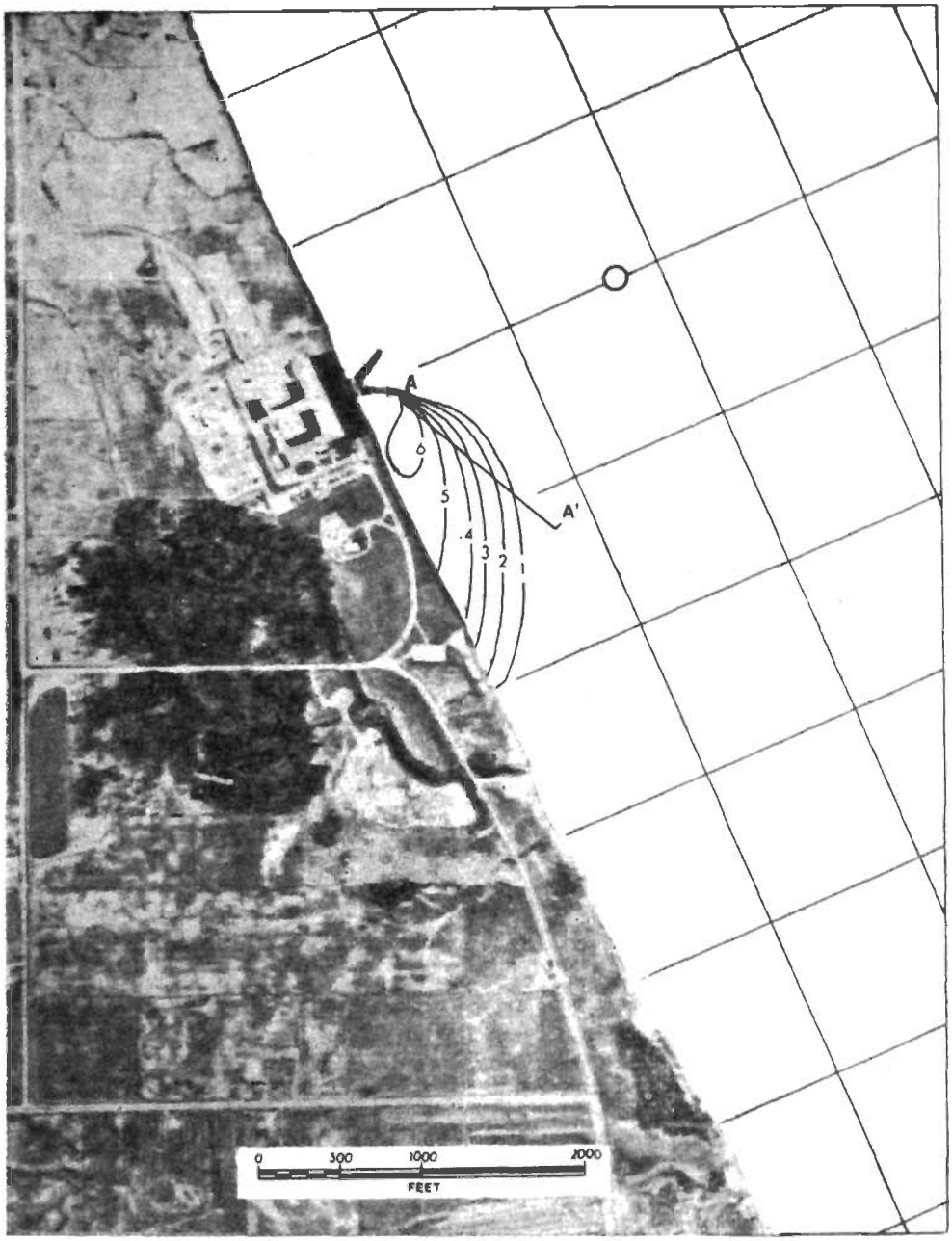

FIGURE 4 : Surface thermal plume map of the Point Beach Nuclear Plant, 15 December 1972. Temperature contours are in ° C and the offshore grid is 1,000 ft².

The primary changes in the water chemistry due to the elevated temperatures across the condensers were seen in the gas solubility relationships. When the temperature of water is raised, the solubility of gases decreases with a consequent increase in the percentage of saturation. This can have significant effects on fish due to the so-called "gas-bubble disease" which in the extreme case is characterized by "Popeye". This is, in fact, not a disease but a physiological state or condition unrelated to any disease-inducing organism and is similar to bends that occur when divers surface without adequate decompression.

Figure 10 shows the results of the super saturation dissolved gases tests taken at the plant, and it will be noted that the oxygen is super saturated in the area of the discharge. Published information includes the review by Rucker (1972), and indicates that values of under 118 percent gas saturation would be sufficient after a variable period of time to induce gas-bubble disease. During

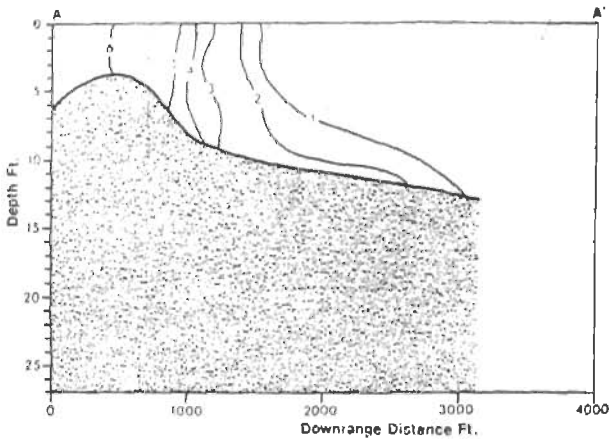

FIGURE 5: Cross-sectional profile of the thermal plume at Point Beach Nuclear Plant, 15 December 1972.

the present survey there were no observed cases of gas-bubble disease at the Point Beach Nuclear Plant. Gas-bubble disease does not occur at all power plants but only in a few specified cases. This appears to be due to the pumping mechanism and consequent entrapment of air which is then pumped under pressure creating super saturated water coming out of the plant. This would appear to be an area that the engineer should concern himself with.

Phytoplankton

General phytoplankton population trends were similar for both reference areas and plumes. Occasionally, statistically significant differences were calculated between the three areas, but these differences appeared unrelated to the thermal discharge.

The phytoplankton population shows two major pulses which is typical for Lake Michigan, one in the spring and one in the fall. These algal populations show a relationship with nitrate, ortho and total phosphorus, and silica concentrations in the lake with the major population peak related to decreasing and low levels of phosphorus and silica (Figures 11 & 12).

The dominant phytoplankton at Point Beach were the diatoms followed by the blue-green algae, chrysophytes, and green algae (Figure 13). Figure 14 shows the mean total numbers of the phytoplankton community collected at the reference areas and in the plume. This figure illustrates the similarities between the three areas. Although there were occasionally significant differences between the plume and one or the other of the reference areas, these differences were not consistent throughout the year and, consequently, it is believed that these differences were due more to random variation than to any effects induced by the power plant. Indeed, with such a large reservoir of plankton in Lake Michigan and the dynamic state with the water being continuously drawn in and pushed out from the plant, there is little reason to believe that the phytoplankton populations in terms of their numbers would be affected.

Because it is not possible to determine accurately any physical damage caused to the phytoplankton during passage through the condensers, a more pertinent test of condenser effects was developed by analyzing the primary productivity before and after passage through the condensers. The primary productivity, therefore, acts as a physiological measure of the effect. Four types of experiments were undertaken. Samples of the water were taken and inoculated with 14-Carbon in order to determine the productivity. The samples were taken and incubated as follows:

(1) Intake samples were incubated at the intake; this test gives "the reference or natural condition."

(2) The second test involved incubating the plume water within the plume in order to determine the effect on the plankton after passage through the condenser.

(3) The third test involved taking intake water and incubating it in the plume to distinguish between the effects of temperature and condenser passage.

(4) The fourth test involved incubating plume water at the intake to determine the effects of condenser passage alone without a long-term increase in temperature.

The results of these experiments taken during May, August and November of 1973 are shown in Figure 15.

Using the first test intake water incubated in the intake as a reference point, it can be seen that there are increases in the productivity of the plankton when the plume water is incubated in the plume and, therefore, this leads one to the elementary conclusion that an increase in temperature increases the photosynthetic rate ; however, this appears to be most strongly increased during the month of May.

The next experiment incubating the intake water in the plume showed that for two occasions the productivity was rather similar to the reference points ; however, during May the intake incubated in the plume was specifically higher than the intake in the intake. This fact cannot be explained entirely in terms of temperature, because of the essentially similar results between the intake and the plume and the intake and the intake, during August and November. The reason for this large increase in May is not known at this time, but may be a result of sampling variation.

The final test incubating plume water in the intake shows that the productivity of the samples is very close to the productivity of the reference samples, thereby determining the potential impact due to condenser

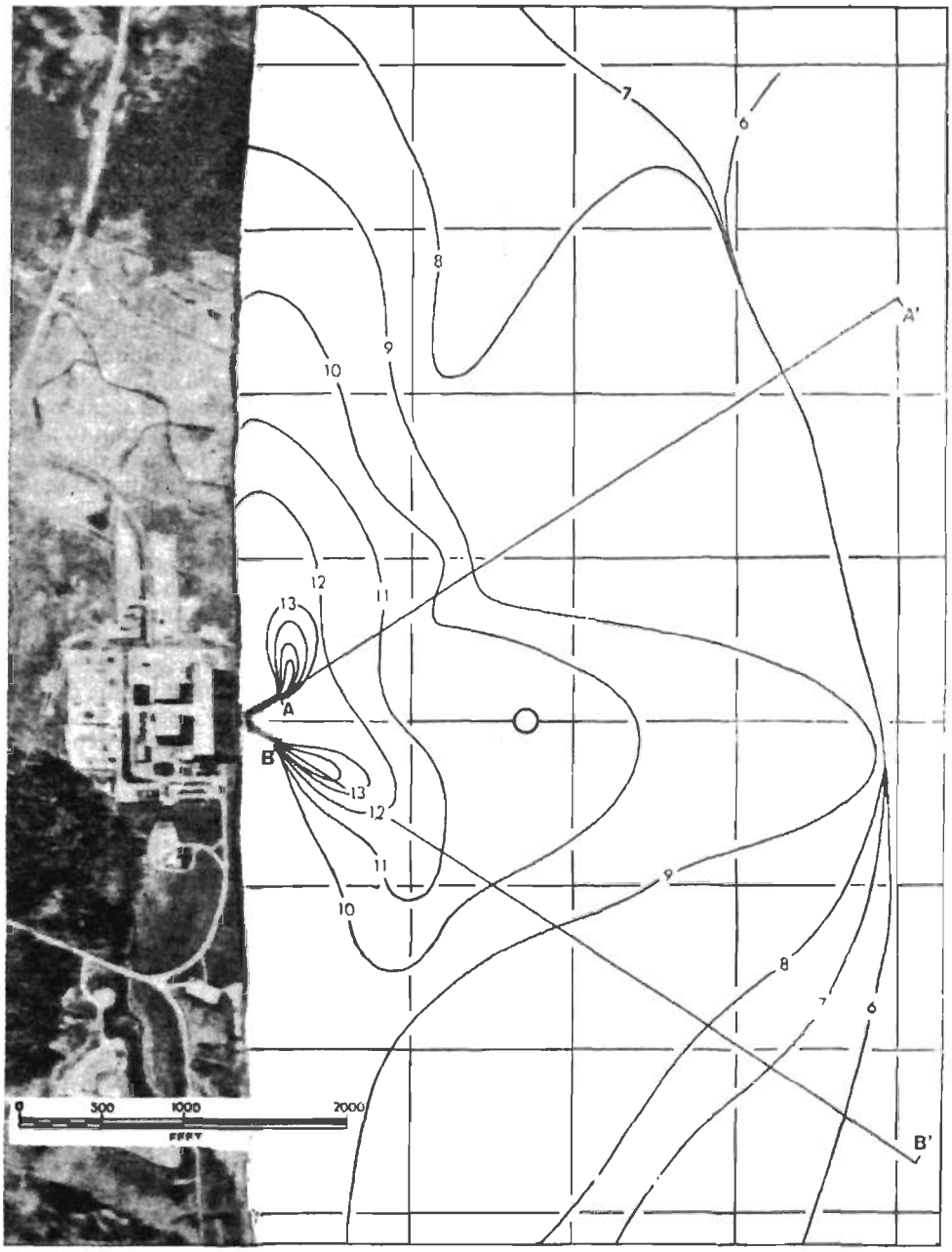

FIGURE 6 : Surface thermal plume map at the Point Beach Nuclear Plant, 23 April 1973. *Temperature contours are in °C and the offshore grid is 1,000 ft².*

passage. It must, therefore, be concluded that condenser passage alone probably does not greatly influence the plankton populations.

An additional type of test was undertaken to determine the time-temperature effects of phytoplankton during their passage through the plume. The productivity rates of phytoplankton were compared using the following three tests :

Light/dark chambers of phytoplankton were floated in the plume until they reached ambient temperature and these were compared with productivity rates of phytoplankton at the intake and incubated at natural lake temperatures. The third test was designed to determine residual or long-term effects due to condenser passage and effects generated by the plume. Light/dark chambers of phytoplankton filled with plume water were floated in the plume for two hours until they had reached ambient temperatures. They were then transported to the intake

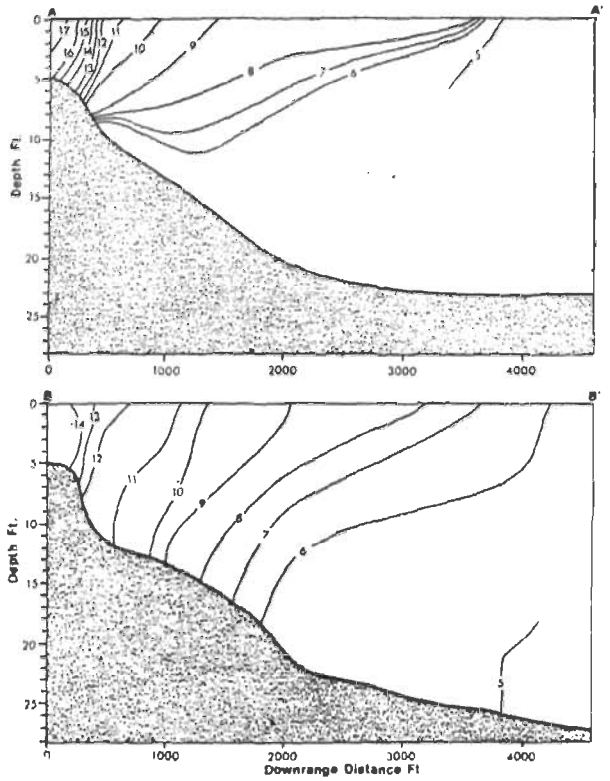

FIGURE 7 : Cross-sectional profile of the thermal plume at the Point Beach Nuclear Plant, 23 April 1973.

structure and incubated for a further two hours to reacclimate to the natural conditions. Photosynthetic rates were then measured. Statistical analyses undertaken on these tests show that there were no significant differences between the three tests during the months of July and November with one exception. For the month of November, differences were found and the floated phytoplankton that drifted in the plume was higher than the reference plankton and also the reacclimated plankton which was floated in the plume and then held at reference temperatures.

The experiment showed that during July, there was no significant difference between natural, floated, or reacclimated phytoplankton populations. However, during November, natural versus floated and floated versus reacclimated phytoplankton productivity result rates were different than floated rates but the same as natural rates. A recovery from the effects of condenser passage had occurred.

It must be concluded, therefore, that the effects of condenser passage on phytoplankton populations may occur ; however, these effects appear to be minimal and certainly by the time the temperature in the cooling water discharge had reached ambient temperature, there did not appear to be any residual effects from the condenser passage on the phytoplankton populations.

Zooplankton

Two types of studies were conducted on the zooplankton. The first, a survey of the reference areas and the plume area. The second consisted of condenser passage experiments. Figure 16 shows the total numbers of zooplankton during the year, and shows that there was an increase in populations through the spring and early summer reaching a population maxima during late summer and early autumn and thereafter declining. Statistical analyses of the results show that there was a significant difference between the south reference area and the plume and north reference area, although no significant difference was found between the plume and the north reference area. This point is significant in that had only one reference area been chosen, there would have been a strong inclination to attribute the cause of the difference to the thermal discharge ; however, the difference appears to be due to the fact that the south reference area is biologically different from the plume and the north reference area and, therefore, cannot be considered as a good reference area. Comparisons between the plume and the north reference area indicate that, in terms of total numbers, there appears to be no significant difference during the months surveyed between the plume and the north reference area and, therefore, possibly little if any effect on the plankton populations.

Various condenser passage experiments were undertaken on the zooplankton to determine whether or not mortality increased in the plankton as a result of passage. Unlike the phytoplankton, mortality can be determined in the zooplankton relatively easily by direct observation. Table I shows the monthly percent mortality of total zooplankton at the intake and at the discharge. It can be seen in general from this figure that there is a slightly higher mortality at the discharge than in the intake. The average net mortality of total zooplankton excluding rotifers after condenser passage was 6 percent, and the range was 0-14 percent. One condenser passage experiment that was undertaken while the plant was not operating, and, therefore, the mechanical effects alone were evaluated without introduction of heat, showed that there was an approximate 10 percent net mortality from mechanical stress alone.

Benthic Macroinvertebrates

The benthic or bottom living organisms in Lake Michigan consist primarily of four major groups : The Amphipods, the Oligochaeta, Chironomidae, and Sphaeriidae. These organisms are an important link in the aquatic food chain. Members of the benthic community living on the bottom substrates consume organic material from decaying phytoplankton and animals which settle to the bottom and in turn they act as an important food source for many species of juvenile and adult fish. The analysis of differences between various areas in the benthic macroinvertebrates is complicated by the different substrates found in the sampling areas. In the north reference area, substrates consisted primarily

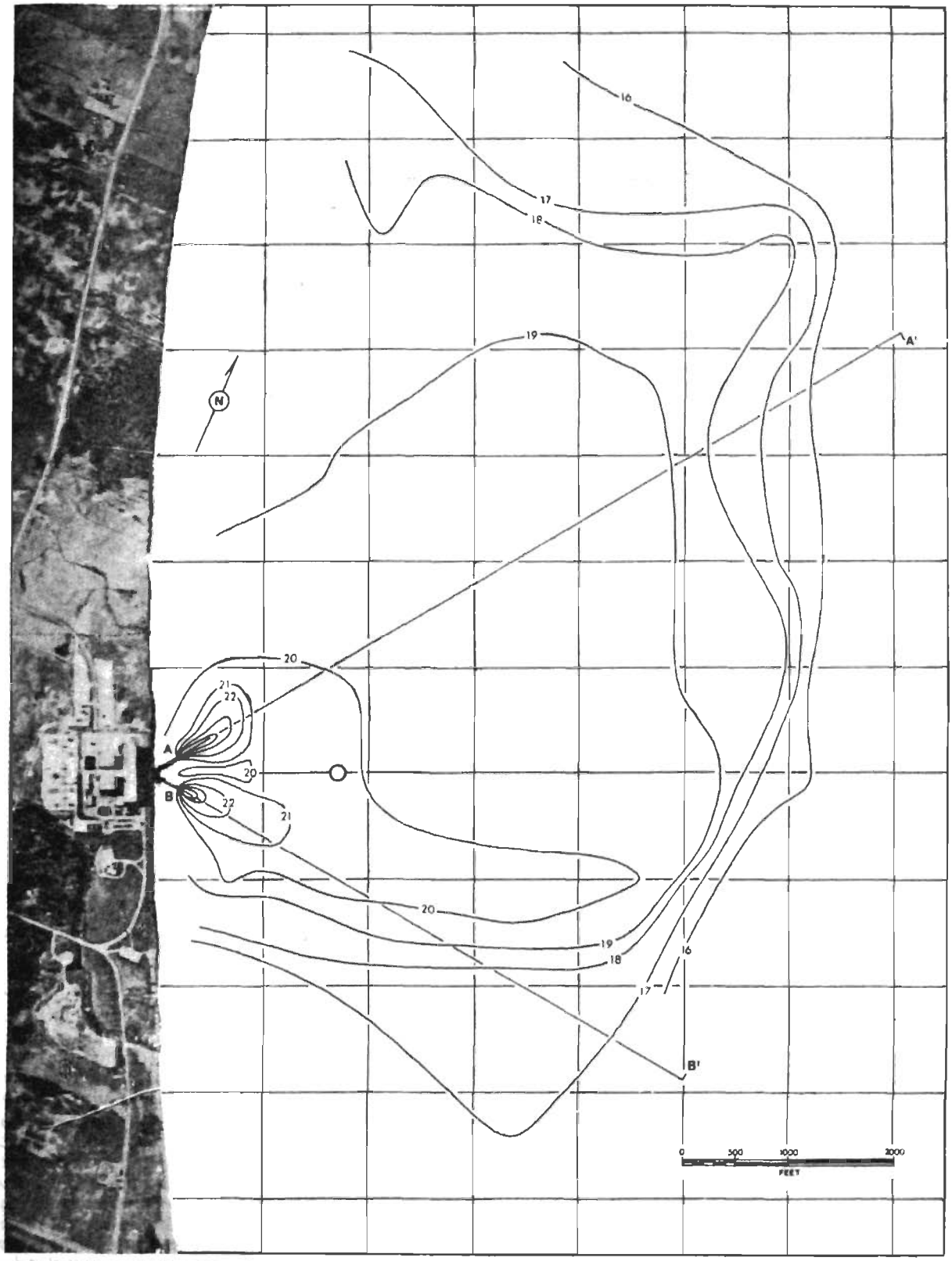

FIGURE 8 : Surface thermal plume map of the Point Beach Nuclear Plant, 8 October 1973. Temperature contours are in °C and the offshore grid is 1,000 ft².

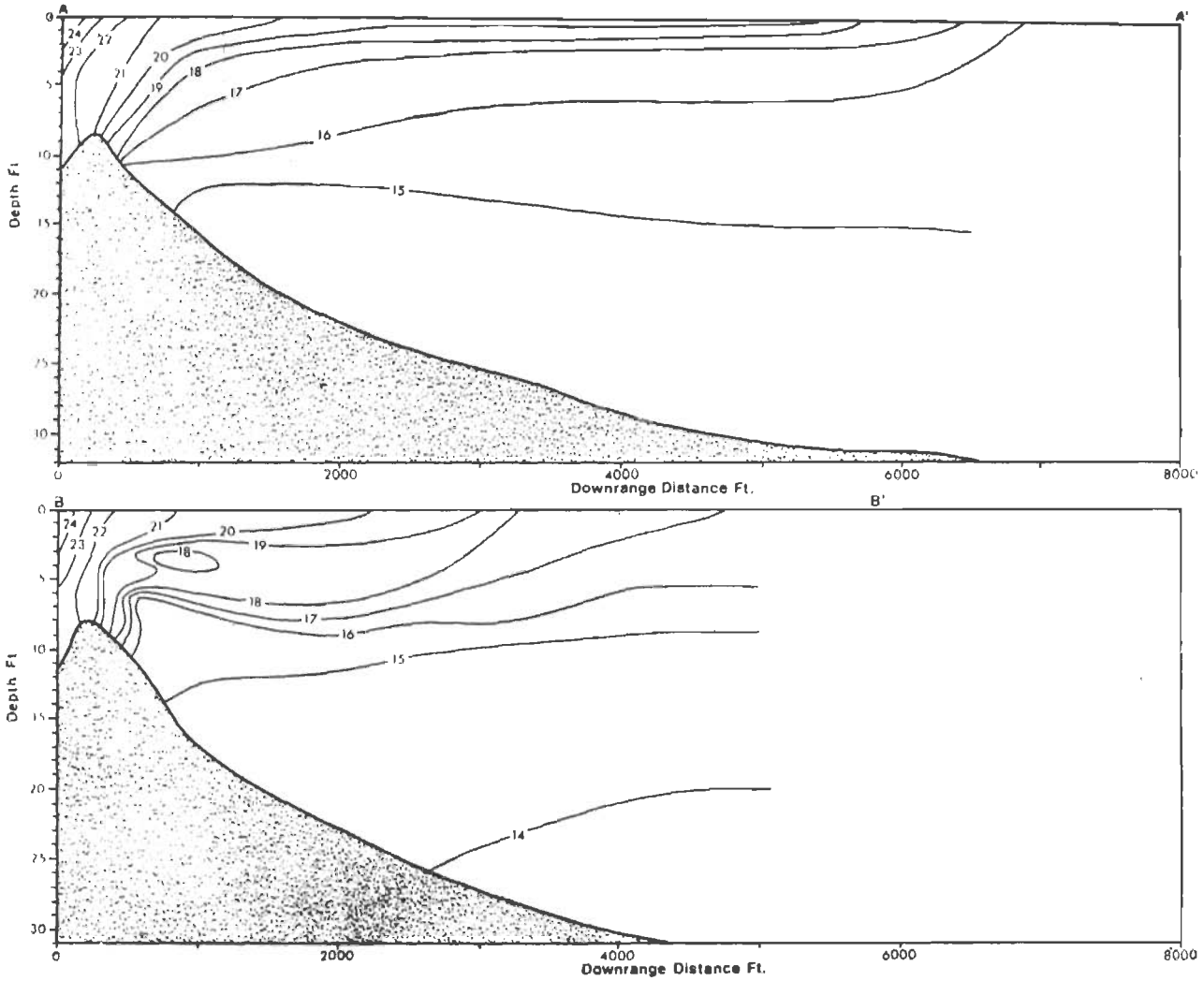

FIGURE 9 : Cross-sectional profile of the thermal plume at the Point Beach Nuclear Plant, 8 October 1973.

of clays, the south reference area primarily of sands, and the plume area a mixture of sands, clays and silts. Significant correlations were found between the various groups and the substrate types. Among the amphipods, the dominant form *Pontoporeia affinis* showed a distinct preference for sandy substrates in the shallower areas. The oligochaetes, dominated by *Uncinais uncinata*, *Stylodrilus heringianus*, *Potomothrix moldaviensis*, were collected primarily in sand, while others such as *Limnodrilus hoffmeisteri* and *Peloscolex superiorensis* occurred primarily in silt. The chironomids were found primarily in sandy areas, while the sphaerid clams were most abundant in sandy or loamy sediments.

Due to the complicated complex nature of the sediment arrangement around the plant, direct determination of the effects of the thermal discharge, if any, were not entirely possible. However, the evidence would indicate that there were no significant effects due to the thermal discharge, and if in fact any effects do occur, they are certainly of a localized nature. Except for the near field which is scoured due to the velocity of the discharge, a viable benthic population exists in the discharge area, which would indicate that certainly there would be no major effect of the discharge on the benthic community. Moreover, the thermal discharge during the summer tends to rise and float on the surface, whereas the benthic organisms live in the bottom waters and consequently very little effect would be expected. However, during the winter time when the thermal plume sinks, one might expect some changes in the populations. The benthic community is small during the winter period when all biological activity is low and also the sinking plume is at 4°C which cannot be considered an unnatural condition because most benthic organisms in these climates exist at 4° C, the temperature of maximum water density in most lakes.

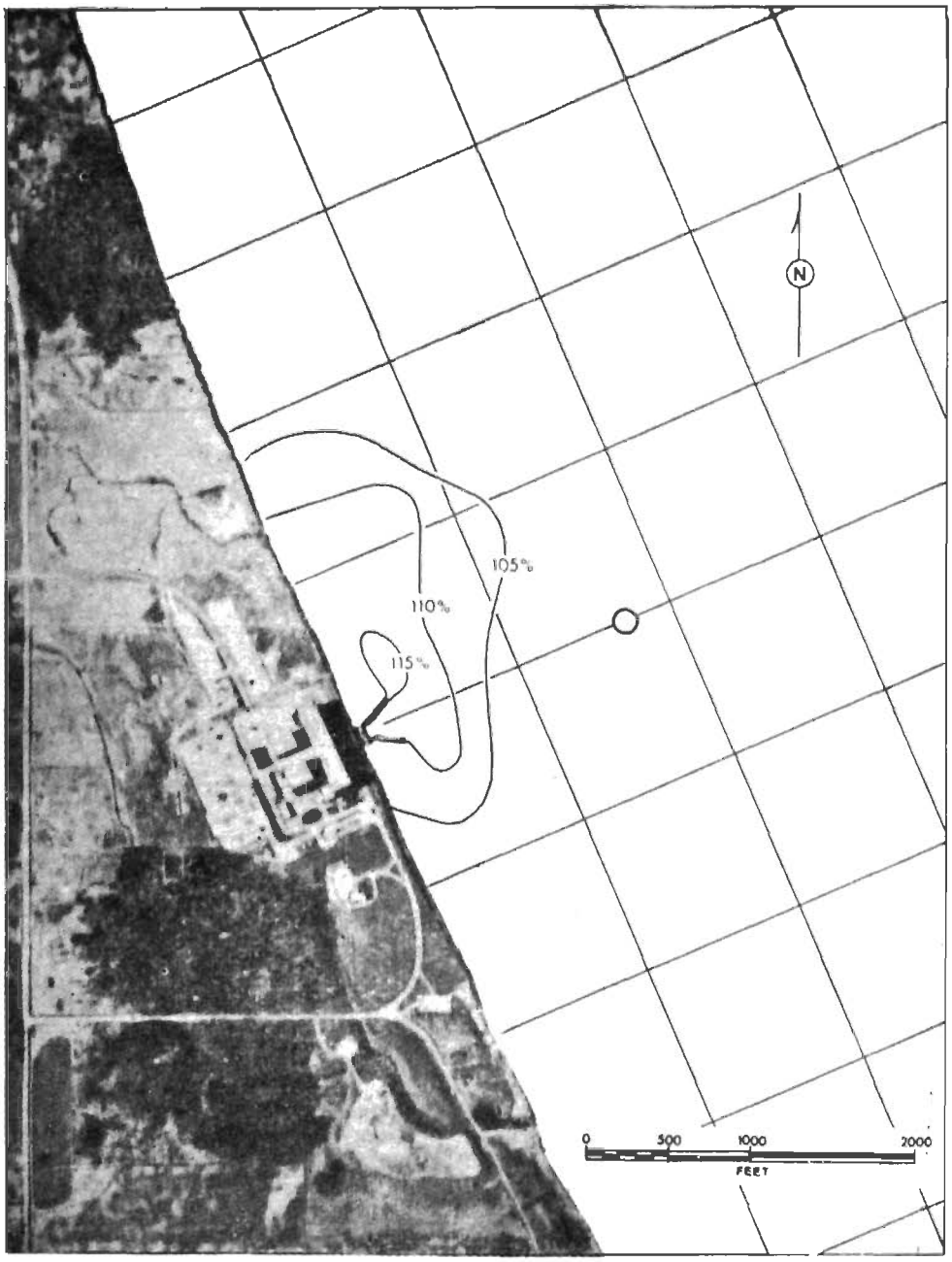

FIGURE 10 : Saturation of total dissolved gases calculated from dissolved oxygen data for the surface, 23 April 1973.

Fish

Twenty-seven species of fish were found in the vicinity of the Point Beach Nuclear Plant during the survey. These fishes were obtained using a variety of collection techniques, but primarily from gill nets and trawls and some of the juveniles were caught using tow nets. Of the fish captured throughout the year, over 70 percent were smelt and alewives, and sport fish represented 15 percent. In general, the populations had average or better than average condition factors when compared to values for fishes of the other great lakes. While age and growth studies based upon scale analyses showed that the fish in the vicinity of the plant had growth rates similar to other fishes in the Great Lakes, on a species by species basis, statistical analyses of the catches indicated that there were no consistent significant differences between the fish population parameters

TABLE I

Percent mortality of zooplankton (excluding rotifers and nauplii) after condenser passage.

Percent Mortality	14 Feb. 1973 Unit # 1	14 Feb. 1973 Unit # 2	9 March 1973 Unit # 1	28 March 1973 Unit # 1	19 April 1973 Unit # 1	4 May 1973 Unit # 1	13 June 1973 Unit # 1	11 July 1973 Unit # 1	7 August 1973 Unit # 1	24 Sept. 1973 Unit # 1	18 October 1973 Unit # 1
Total Dead	10	1	14	0	0	14	0	14	0	3	10
Copepoda	10	1	14	0	0	11	0	29	32	0	24
Cladocera	—	—	0	—	—	—	5	0	0	8	0
Calanoida	43	0	0	25	0	2	21	26	0	16	34
Cyclopoida	9	0	0	0	0	92	0	12	—	0	14
Harpacticoida	0	0	92	100	—	0	—	100	—	—	—

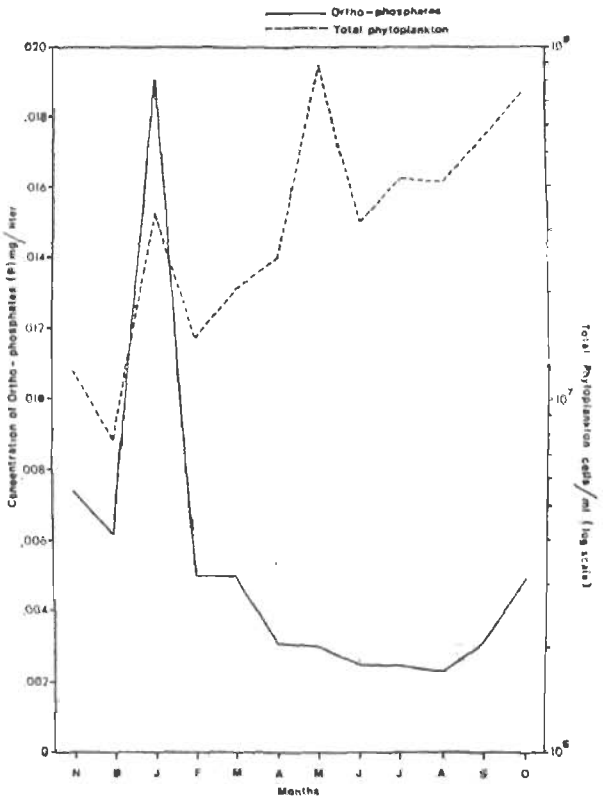

FIGURE 11 : Relationship between orthophosphate and total phytoplankron numbers at the Point Beach Nuclear Plant, November 1972 to October 1973.

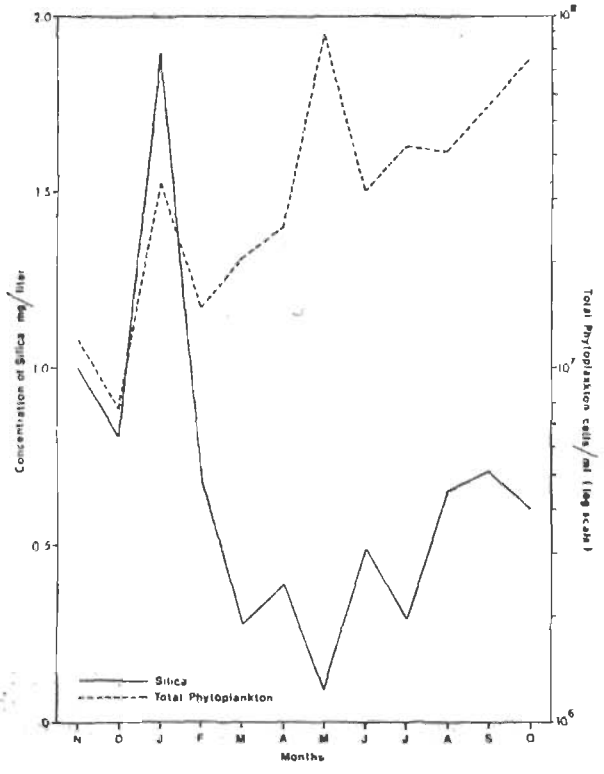

FIGURE 12 : Relationship between silica and total phytoplankton numbers at the Point Beach Nuclear Plant, November 1972 to October 1973.

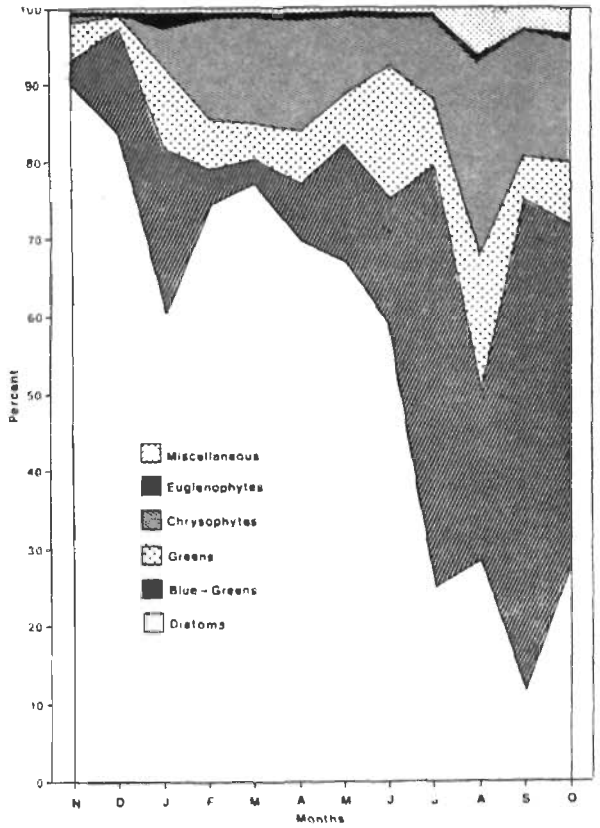

FIGURE 13 : Phytoplankton composition at the Point Beach Nuclear Plant, November 1972 to October 1973.

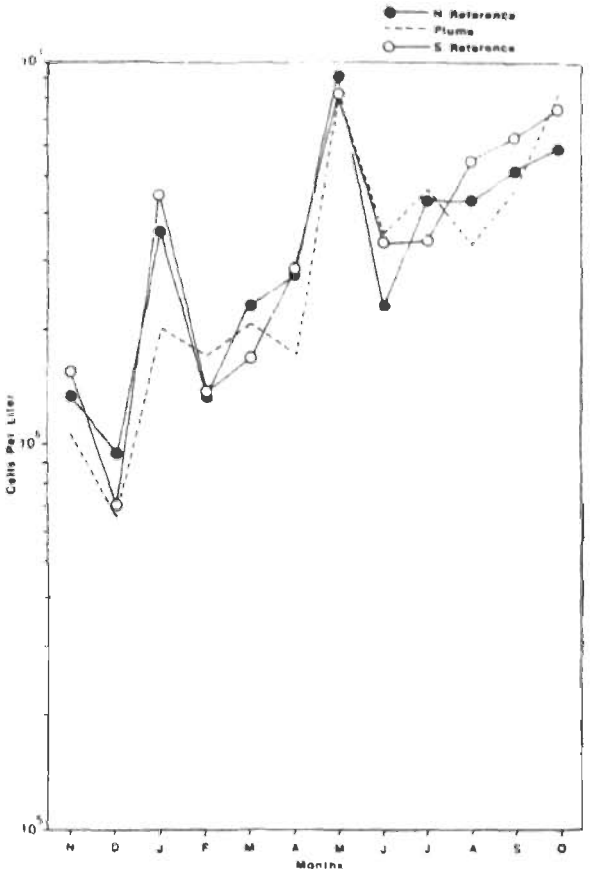

FIGURE 14 : Mean total numbers of phytoplankton at the Point Beach Nuclear Plant, November 1972 to October 1973.

measured in the plume and the reference areas. Although on occasion there were some instances of differences, these were not considered important because they were not consistent. Certain species of fish were undoubtedly attracted to the plume on certain occasions. During winter operating conditions, rainbow trout was the only species consistently found more often in the plume than in either reference area. During the spring and summer, brown trout were consistently attracted to the plume and periodically during the summer large numbers of alewives were attracted to the plume. However, there were no detectable effects of the plume on the basic migratory patterns of any fish species except for the brown trout and rainbow trout. This is most important since many fishes such as the coho migrate along the inshore zone at certain times of the year. During the autumn and onset of winter, all species migrate from the inshore zone to the open lake and, therefore, winter effects of the thermal plume on fish populations are negligible. In the summer, there is a shift in the age structure in the fish populations in the inshore zone from adults in the early summer to juveniles in later summer, which is a reflection of breeding habits of certain fish.

During the period May-October 1973, studies were undertaken on the numbers and types of fish that were taken up in the intake waters and impinged on the screens. During this period, over 300,000 fishes were impinged on the intake screens, with a 95 percent confidence interval of 140,000-450,000. Of the impinged fish, approximately 268,000 were alewives, 30,000 were smelt and 51 were salmonids. However, because the survey took place during the summer months, these figures represent the summer condition. During the winter period, these estimates would be considerably lower, because of the migration of the fish from the inshore zone.

A series of experiments was undertaken in order to determine whether or not fish spending any time in the plume would be stressed beyond normal stress. In order to undertake this experiment, cages were constructed and rainbow trout placed in these cages. The cages were located at the north reference area and at the two discharge plumes.

Five parameters were selected to test the physiological condition of the fish within the plume and without the plumes. These parameters were hematocrit (packed cell volume) total solids and plasma chloride which were utilized to summarize the status of the osmotic balance in the fish. The final two parameters

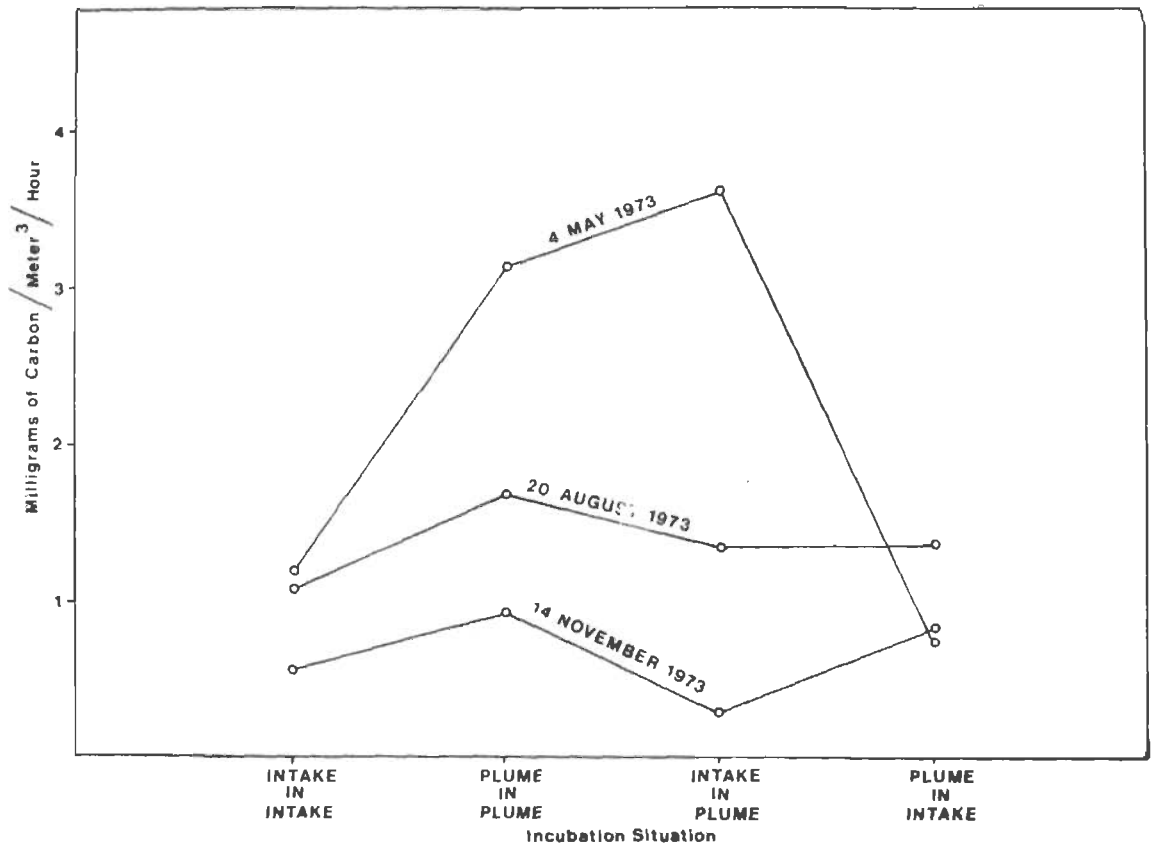

FIGURE 15 : Mean primary productivity of phytoplankton after condenser passage compared with reference phytoplankton.

were plasma glucose and liver glycogen, which were used to evaluate carbohydrate metabolism in relationship to energy metabolism.

Four cages were used in each experiment, each contained 25 six to seven-inch rainbow trout. Experiments were undertaken during July, August and November of 1963 and the experiments were conducted for four-day periods.

During the experiments, mortality of fish was noted only in the plume fish. Mortalities were not encountered in significant numbers during the first two experiments, however, more plume fish died during the November experiment. At no time did the mortality over the 96-hour period reach LD50.

During all of the experiments, stress was detected in plume fish as measured by the various physiological parameters. However, the reference area fish were also stressed as compared to the literature for similarly treated laboratory fish. In general the hematocrit values were higher in the plume than in the reference areas, while the total solids values showed no significant differences between the plume and reference areas. The plasma glucose levels were significantly higher in the plume fish than in the reference area fish indicating higher metabolism. Stressed fish tended to have higher hematocrit, total solids and plasma glucose levels and lower plasma chloride levels.

There was special concern for the effect of condenser passage upon fish egg entrainment ; therefore, an experiment was run in order to determine whether or not there would be any significant effect upon the mortality of fish eggs after passage through the condensers. During May 1973, over 1,000,000 white sucker eggs were obtained from a Wisconsin Department of Natural Resources hatchery and taken to the Point Beach Nuclear Plant. In a series of experiments, the eggs were released in the intake well in front of the fish screens. Three minutes after the eggs were released, which is the travel time through the condensers, nets were placed at the end of the plume for two minutes. The nets were then raised from the water and the captured eggs emptied into the plastic pails, whereupon they were transferred to a plastic bag and immersed in water of the same temperature that they originally were acclimated and transferred to the fish hatchery. In general, the eggs that had undergone condenser passage had a higher survival rate than those eggs that had not undergone condenser passage. Also, the eggs that had

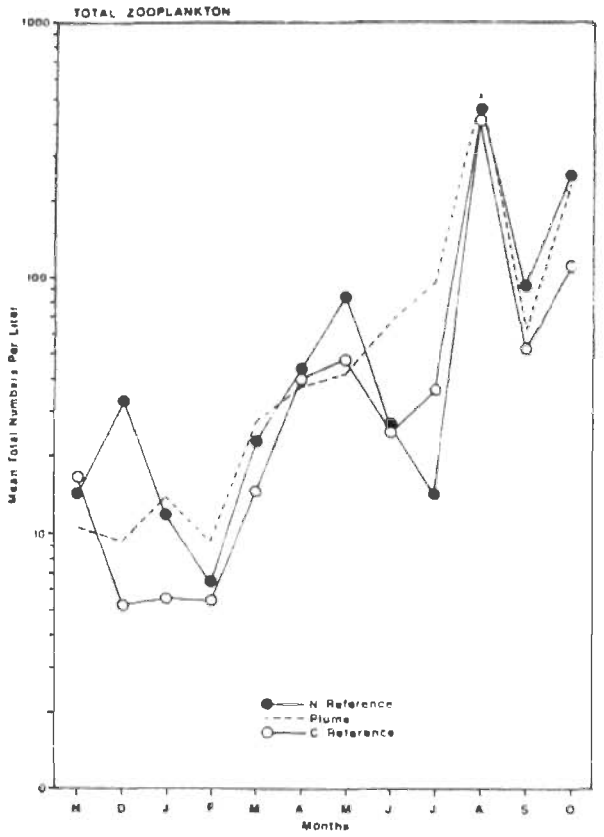

FIGURE 16 : Mean total numbers of Zooplankton at the Point Beach Nuclear Plant, November 1972 to October 1973.

undergone condenser passage hatched approximately four days before the eggs in the other experimental groups. It should be noted that the eggs used in the experiment were eyed stage eggs which is a hardy stage of egg development. It is doubtful that eggs in different stages would have survived the transportation to the power plant and/or passage through the condensers.

A further ecological problem encountered with power plants is that occasionally the plants undergo a relatively rapid shutdown, and consequently cold shock can occur. On 18 May 1973, a rapid shutdown in order to test various aspects of the reactor safety systems was scheduled and during this time various specimens were obtained in order to test the cold shock under real conditions. The slimy sculpin *Cottus cognatus* and the coho salmon *Oncorhynchus Kisutch* were quite abundant in the area around Point Beach and some were caught and placed in the north plume and south plume and in a reference area. The background temperature of the lake was 8.8°C, while the north plume averaged 16.6°C and the south plume averaged 16.0°C. The reactor discharging to the south plume was tripped and the temperature dropped from 16.6°C to 8.8°C in a period of 7.5 minutes, subjecting the fish in the cages in the south plume to a 7.8°C cold shock. The fish in all areas, the north plume which stayed constant, the south plume which was subjected to cold shock and the reference area, all had 100 percent survival of the coho and slimy sculpin.

Conclusions

The primary conclusion of the study was that although some statistically significant differences occurred between the plume area and the reference area, there were no major ecological effects of the thermal discharge from the Point Beach Nuclear Plant on Lake Michigan. Undoubtedly some effects of the thermal discharge on the local ecology of the Point Beach area occurred, although these effects are of such minor significance that they are probably within the natural variation of the ecosystem. The alternatives to once-through cooling in all probability have at least, if not more, effect on the ecosystem than once-through cooling. Moreover, the alternatives are unduly burdensome from the economic standpoint and such costs running into millions of dollars, are totally unjustified in comparison with the unknown, if any, ecological benefits.

This study can probably be generalized for any power generating facility on a large body of water in a temperate zone. However, because of the complexity of ecosystems, case by case evaluations should be made before power plant construction is undertaken so that the ecological significance of proposed action may be weighed against the economic and engineering feasibility of such construction.

Acknowledgements

This research was sponsored by the Wisconsin Electric Power Company and the Wisconsin Michigan Power Company. The authors wish to thank Mr. S. Burstein, Executive Vice-President and Dr. F. Boucher, and the staff of the Wisconsin Electric Power Company for their cooperation during the conduct of the study. The authors also wish to thank the many personnel at Limnetics, Inc. who participated in this study.

References

(1) LAPP, R. E. (1974) : "The Challenge of the Energy Dilemma." Proc. Symp. Energy Production and Thermal Effects, Limnetics, Inc., Milwaukee, Wisconsin, pp. 75-80.

(2) RUCKER, R. R. (1970) : "Gas-bubble Disease of Salmonids : A Critical Review." U. S. Bureau of Sport Fisheries and Wildlife Technical Paper No. 58, p. 11.

(3) U. S. Bureau of the Census, Statistical Abstracts of the United States, 1972 (93rd Edition) Washington, D. C., 1972, Library of Congress Card No. 4-18089.

Environmental Impact of Water Resources Utilization

ANAND PRAKASH
Water Resources Engineer
Sargent and Lundy Engineers, Chicago, Illinois, U.S.A.

SYNOPSIS

One of the increasingly important utilization of water resources is to sustain the cooling lakes and heat sinks of nuclear power plants. A typical 1000-MW reactor consumes about 163 million gallons of water per year and discharges about 50 million gallons of treated or untreated blowdown water back to the source. A mathematical model to analyze the environmental impact of such blowdown water released from an atomic reactor to an open body of water is described. A practical approach is developed to evaluate the effect of three-dimensional dispersion with radioactive decay and adsorption on the concentration of effluents spilled into a stream either instantaneously or for a finite time interval, due to normal blowdown or accidental leaks in the radwaste system of a nuclear plant. Methods to estimate the longitudinal and transverse dispersion coefficients are also discussed. The approach is useful for analyzing the environment related aspects of a nuclear power plant.

Introduction

With the accelerated emphasis on the development of nuclear, hydro-electric, thermal, geothermal and other forms of energy as alternatives to petroleum, water demands for different processes in the power industry have tremendously increased. Quantitative estimates of these demands indicate that a 1000-MW light-water reactor of a nuclear power plant, consumes about 163 million gallons (617 thousand m^3) of water per year, operating at 80 percent load factor. A coal gasification plant producing pipeline gas at 250 million standard cu ft (7 million m^3) per day consumes about 10,000 acre-ft (12 million m^3) to 45,000 acre-ft (55 million m^3) of water per year. Coal liquefaction requires about 0.2 acre-ft (247 m^3) to 1.3 acre-ft (1,600 m^3) per year per bpd (barrels per day) of synthetic oil produced. By 1965, increasing water withdrawals for power generation through thermal electric plants alone had surpassed the total irrigation withdrawals in U.S., being about 0.5 gallons (0.0019 m^3) per kWhr for fossil fueled, 0.8 gallons (0.00304 m^3) per kWhr for nuclear and 1.8 gallons (0.00684 m^3) per kWhr for geothermal plants([1]). The steady rise maintained by these demands over the past two decades or so has added new dimensions to the problem of water resource allocation and utilization.

Whereas, a major portion of the total water demand for the expanding energy development is consumptive, a certain part of it inevitably returns back to the adjoining surface and ground water bodies as blowdown discharge, with its quality considerably deteriorated and has its undesirable impact on the surrounding environment. This impact is of great concern, if the power plant happens to be nuclear, where, the water resource utilization is to sustain the cooling lakes and ultimate heat sinks for safe operation and shutdown of the reactor and the environmental impact pertains to the untreated or partially treated blowdown discharge continuously released into a natural stream or artificially created body of water ; or to the accidental spill of radioactive effluents into a nearby stream either instantaneously or for a finite time interval due to unforeseen damage to the radwaste system of the plant building. Following an accident, radioactive effluents leak into the ground water environ, undergo convective-dispersion through the commonly saturated soil matrix surrounding the plant building and finally join the nearest stream or lake. Convective-dispersion in saturated soils is discussed elsewhere([2])([3]). The objective of this paper is to discuss the impact of the above pollutant injection on the surface water environment involving the dilution, convection, dispersion, adsorption and radioactive decay

of the various isotopes present in the effluents, during their passage from the point of release into the stream to the nearest downstream surface water intake.

Mathematical Development

The convective-dispersion equation for the movement of a radioactive tracer in an open channel carrying organic or inorganic solids in suspension is given by(2) :

$$(c+nF)_t = \frac{1}{\sqrt{g}}\left[\frac{\sqrt{g}}{h_i^2}, D_{ij} \,.\, C_{,i}\right]_{,i} - \frac{V_i}{h_i^2}.C_{,i} - \lambda(c+nF) \qquad \ldots(1)$$

where, the subscript t denotes the time derivative,

$,i$ denotes covariant derivative

g is the absolute value of the determinant of the metric tensor g_{ij}

h_i are the scale factors for coordinate transformation

c = concentration of the tracer in water, i.e., quantity of the tracer per unit volume of water

V_i = i component of the velocity

F = quantity of the tracer adsorbed to the suspended matter per unit volume of solid phase

$$n = \frac{\text{volume of suspended solids}}{\text{volume of water}}$$

t_h = time necessary to reduce the concentration of a given radioactive isotope to half of its initial value by radioactive decay(4)

$$t_h = \frac{ln\, 2}{\lambda}$$

λ = radioactive decay constan

D_{ij} = dispersion tensor

For open channel flow in the cartesian system of coordinates,

$$D_{ij} = \begin{bmatrix} D_x & 0 & 0 \\ 0 & D_y & 0 \\ 0 & 0 & D_z \end{bmatrix}$$

and Equation (1) may be simplified as :

$$(c+nF)_t = \frac{\partial}{\partial x}\left(D_x \frac{\partial c}{\partial x}\right) + \frac{\partial}{\partial y}\left(D_y \frac{\partial c}{\partial y}\right) + \frac{\partial}{\partial z}\left(D_z \frac{\partial c}{\partial z}\right) - u\frac{\partial c}{\partial x} - v\frac{\partial c}{\partial y} - w\frac{\partial c}{\partial z} - \lambda(c+nF) \qquad \ldots(2)$$

where, u, v and w are the components of velocity in the x, y and z directions respectively.

Assuming equilibrium isotherm(5) for the adsorbed component such that,

$$F = a_I c \qquad \ldots(3)$$

where, a_I is a constant of proportionality, Equation (2) takes the following form :

$$(1+na_I).C_t = \frac{\partial}{\partial x}\left(D_x \frac{\partial c}{\partial x}\right) + \frac{\partial}{\partial y}\left(D_y \frac{\partial c}{\partial y}\right) + \frac{\partial}{\partial z}\left(D_z \frac{\partial c}{\partial z}\right) - u\frac{\partial c}{\partial x} - v\frac{\partial c}{\partial y} - w\frac{\partial c}{\partial z} - \lambda c(1+na_I) \qquad \ldots(4)$$

Setting, $1+na_I = R_d$ where, R_d may be called a retardation factor by virtue of its property to retard the appearance of the tracer plume, Equation (2) may be written as :

$$C_t = \frac{\partial}{\partial x}\left(\frac{D_x}{R_d} \cdot \frac{\partial c}{\partial x}\right) + \frac{\partial}{\partial y}\left(\frac{D_y}{R_d} \cdot \frac{\partial c}{\partial y}\right) + \frac{\partial}{\partial z}\left(\frac{D_z}{R_d} \cdot \frac{\partial c}{\partial z}\right) - \frac{u}{R_d} \cdot \frac{\partial c}{\partial x} - \frac{v}{R_d} \cdot \frac{\partial c}{\partial y} - \frac{w}{R_d} \cdot \frac{\partial c}{\partial z} - \lambda c \qquad \ldots(5)$$

Assuming R_d to be a constant factor and denoting,

$$D_x^* = \frac{D_x}{R_d},\ D_y^* = \frac{D_y}{R_d},\ D_z^* = \frac{D_z}{R_d},\ u^* = \frac{u}{R_d},$$

$$v^* = \frac{v}{R_d},\ w^* = \frac{w}{R_d},$$

$$C_t = D_x^* \frac{\partial^2 c}{\partial x^2} + D_y^* \frac{\partial^2 c}{\partial y^2} + D_z^* \frac{\partial^2 c}{\partial z^2} - u^* \frac{\partial c}{\partial x} - v^* \frac{\partial c}{\partial y} - w^* \frac{\partial c}{\partial z} - \lambda c \qquad \ldots(6)$$

where, the asterisks may now be dropped for convenience of representation.

Equation (6) is to be solved in the spatial domain,

$$-\infty < x < \infty,\ -\infty < y < \infty,\ -\infty < z < \infty,$$

with the following initial and boundary conditions :

(*i*) $c(x, y, z, 0) = f(x, y, z) = Q\,\delta(x)\,\delta(y)\,\delta(z)$, $t = 0$

(*ii*) $c(\pm\infty, \pm\infty, \pm\infty, t) = 0 \qquad \forall\ t > 0$

Using Fourier Transforms(6) and the product law(7), the solution is :

$$c(x, y, z, t) = \frac{Q}{4\pi t\sqrt{4\pi D_x D_y D_z t}} \cdot \exp\left[-\frac{(x-ut)^2}{4D_x t} - \frac{(y-vt)^2}{4D_y t} - \frac{(z-wt)^2}{4D_z t} - \lambda t\right] \qquad \ldots(7)$$

where,

Q = Strength of the point source in curies, and

δ = Dirac delta function.

Basic assumptions implied in the above solution are :

(*i*) u, v and w are the three average components of velocities at any cross-section,

(*ii*) the dispersion coefficients D_x, D_y and D_z are constants, and

(*iii*) mixing of the solute with water is uniform and brings about no density change.

When one attempts to apply Equation (7) to an open channel of finite width B and finite depth D in which a tracer quantity Q is injected at the origin 0 ($x = 0$, $y = 0$, $z = 0$), at time $t = 0$ as shown in Figure 1 (*a*) & (*b*), the infinite spatial domain in the y and z directions becomes finite and restricted and the boundary conditions are modified as follows :

$$(i)\ \frac{\partial c}{\partial z} = 0, \quad \frac{\partial c}{\partial t} \neq 0, \quad z = g$$

$$(ii)\ \frac{\partial c}{\partial z} = 0, \quad \frac{\partial c}{\partial t} \neq 0, \quad z = -h$$

$$(iii)\ \frac{\partial c}{\partial y} = 0, \quad \frac{\partial c}{\partial t} \neq 0, \quad y = b$$

$$(iv)\ \frac{\partial c}{\partial y} = 0, \quad \frac{\partial c}{\partial t} \neq 0, \quad y = -a$$

This problem may be resolved by taking recourse to the method of images([8])([9]). The first few images are illustrated in Figure 2. There will be an infinite set of such images in either direction for a source located at the origin. The combined effect of all these images may be introduced into Equation (7) as follows :

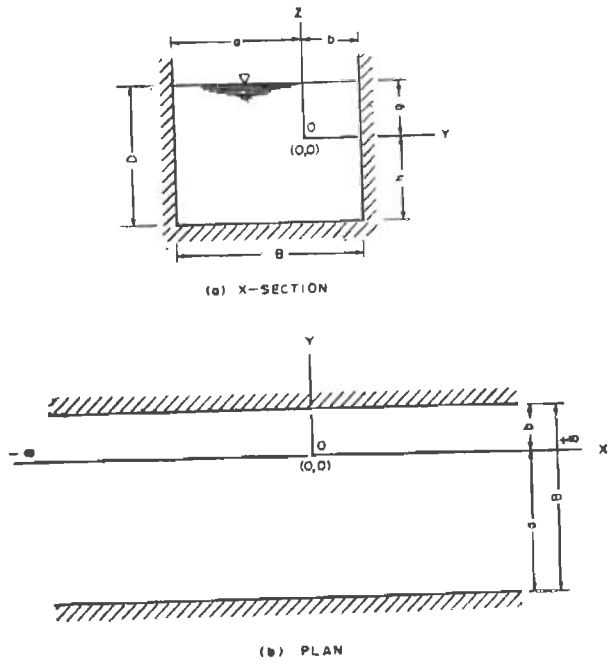

FIGURE 1.

$$c(x, y, z, t) = \frac{Q}{4\pi t \sqrt{4\pi D_x D_y D_z t}} \exp\left\{-\lambda t - \frac{(x-ut)^2}{4D_x t}\right\} \cdot \left[\sum_{m=0}^{\infty}\sum_{n=0}^{\infty} \exp\left\{-\frac{(y_n-vt)^2}{4D_y t} - \frac{(z_m-wt)^2}{4D_z t}\right\}\right.$$

$$+ \sum_{m=0}^{\infty}\sum_{n=1}^{\infty} \exp\left\{-\frac{(y_n'-vt)^2}{4D_y t} - \frac{(z_m-wt)^2}{4D_z t}\right\}$$

$$+ \sum_{m=1}^{\infty}\sum_{n=0}^{\infty} \exp\left\{-\frac{(y_n-vt)^2}{4D_y t} - \frac{(z_m'-wt)^2}{4D_z t}\right\}$$

$$\left. + \sum_{m=1}^{\infty}\sum_{n=1}^{\infty} \exp\left\{-\frac{(y_n'-vt)^2}{4D_y t} - \frac{(z_m'-wt)^2}{4D_z t}\right\}\right] \qquad \ldots(8)$$

where,

$$y_n = \frac{1+(-1)^n}{2}\{y+n(a+b)\} + \frac{1-(-1)^n}{2}\{(2b-y)+(n-1)(a+b)\}$$

$$y_n' = \frac{1+(-1)^n}{2}\{-y+n(a+b)\} + \frac{1-(-1)^n}{2}\{(2a+y)+(n-1)(a+b)\}$$

$$z_m = \frac{1+(-1)^m}{2}\{z+m(g+h)\} + \frac{1-(-1)^m}{2}\{(2g-z)+(m-1)(g+h)\}$$

$$z_m' = \frac{1+(-1)^m}{2}\{-z+m(g+h)\} + \frac{1-(-1)^m}{2}\{(2h+z)+(m-1)(g+h)\}$$

It may be easily seen that the contribution of the images to c (x, y, z, t) progressively decreases as their distance from the domain of interest increases, so that for a desired degree of accuracy, consideration of images beyond a certain number becomes unnecessary. For most practical situations, it may be sufficient to go up to $n = 4$ and $m = 4$. Even for this limited number of images, it is an arduous task to make hand computations of c (x, y, z, t) for various combinations of x, y, z and t values. However, it is a simple matter to write a computer program for carrying out these computations and even to plot equi-concentration contours for different patterns of pollutant injection. An algorithm to check the contribution of each succeeding image against the desired

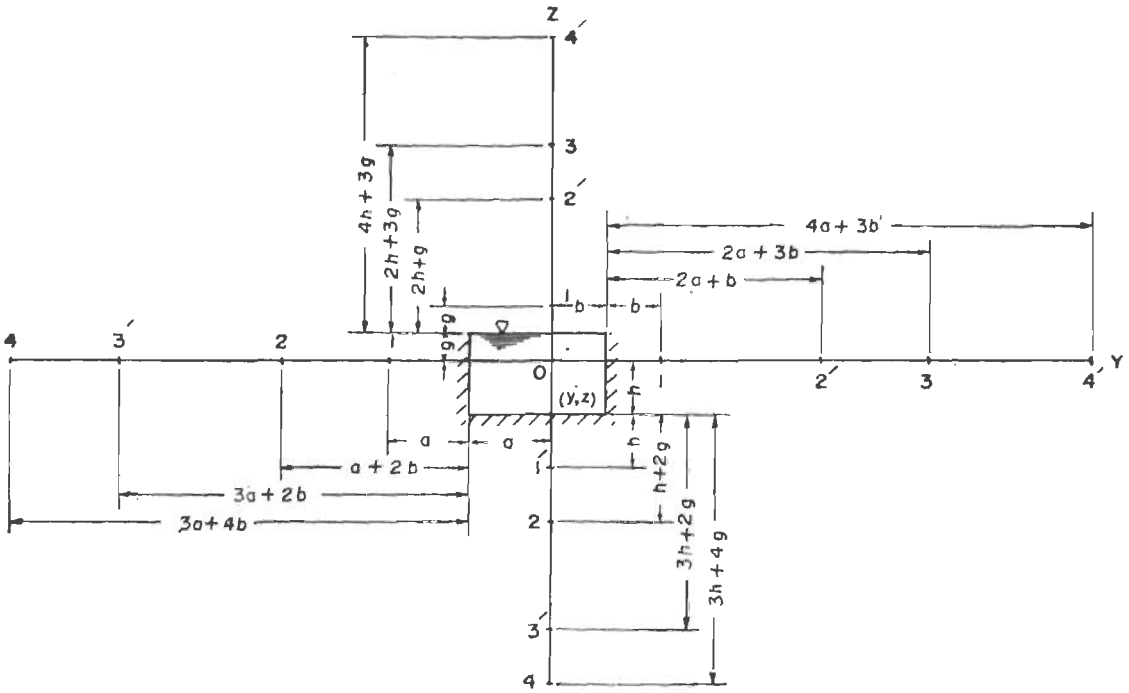

FIGURE 2.

accuracy and to stop computations as soon as the prescribed accuracy is obtained, may be introduced in this program without any difficulty.

It may be noted that Equation (8) is quite general and may be simplified for different situations as follows :

(*i*) For situations where the adsorption component is negligible, $R_d = 1$,

(*ii*) For non-radioactive tracers, $\lambda = 0$,

(*iii*) For infinitely wide bodies of water with the source located at the center, $n = 0$,

(*iv*) For infinitely deep bodies of water with the source located at mid-depth, $m = 0$,

(*v*) For two-dimensional dispersion, $m = 0$;
$[\exp\{-(z-wt)^2/4D_z t\}]/\sqrt{4\pi D_z t} = 1$

(*vi*) For one dimensional dispersion, $m = 0$, $n = 0$ and

$$[\exp\{-(z-wt)^2/4D_z t\}]/\sqrt{4\pi D_z t} = 1;$$

$$[\exp\{-(y-vt)^2/4D_y t\}]/\sqrt{4\pi D_y t} = 1$$

(*vii*) For steady state dispersion in uniform flow with a continuous source at the origin, where,
$C_i = 0$, $v = 0$, $w = 0$ and $D_x = 0$,
the equation reduces to,

$$D_y \frac{\partial^2 c}{\partial y^2} + D_z \frac{\partial^2 c}{\partial z^2} - u \frac{\partial c}{\partial x} = 0$$

and the elementary solution is,

$$c(x, y, z) = \frac{Qu}{4\pi x\sqrt{D_y D_z}} \exp\left(-\frac{uy^2}{4D_y x} - \frac{uz^2}{4D_z x}\right)$$

The contribution of images, if required, may be taken into account as in Equation (8).

The propagation of concentration in the space and time domains expressed by Equation (8) is in response to an instantaneous input of concentration. Distribution of concentration due to a continuous input is discussed elsewhere[10]. For most practical situations pertinent to the objective of this paper, the pollutant injection is for a finite time only. To predict the propagation of concentration induced by such inputs, Equation (8) has to be integrated over time[5]. Thus for finite time injection over a period τ in such a way that $Q\,dt'$ is the quantity of tracer injected over an elementary time period dt', at $x = 0$, $y = 0$, $z = 0$ and $t = t'$, the propagation of concentration is given by the following equation,

$$c(x, y, z, t) = \int_0^{\tau=t} \frac{Q}{8\pi\tau\sqrt{\pi D_x D_y D_z \tau}} \exp\left[-\lambda\tau - \frac{(x-u\tau)^2}{4D_x\tau} - \sum_{m=0}^{\infty}\sum_{n=0}^{\infty}\left\{\frac{(y_n-v\tau)^2}{4D_y\tau} + \frac{(z_m-w\tau)^2}{4D_z\tau}\right\} - \sum_{m=1}^{\infty}\sum_{n=1}^{\infty}\left\{\frac{(y'_n-v\tau)^2}{4D_y\tau} + \frac{(z'_m-w\tau)^2}{4D_z\tau}\right\}\right] d\tau \quad \ldots(9)$$

where, $\tau = t - t'$

For the case where the injection time is t_0 and the duration of propagation time for instantaneous injection is t_L, the duration of the output will be,

$$t_c = t_0 + t_L$$

Using the theory of linear and time-invariant systems[11], it could be assumed, without affecting the results in the domain of interest t_c, that the whole phenomenon is periodic with a period T, subject to the condition that T is equal to or greater than t_c. The resulting concentration distribution may then be expressed in the form of the convolution integral,

$$c(x, y, z, t \pm kT) = \int_{t-t_L}^{t} Q(\tau \pm kT).\, h(t-\tau)\, d\tau \quad \ldots(10)$$

where,

$h(t)$ is a symbolic representation of the impulse response function on the right-hand side of Equation (8).

k is an integer

$Q(t \pm kT) = 0$ for $t_0 < t < T$, and

$t \geqslant t_c = t_0 + t_L$

Simplified Approach

For practical problems, it is expedient to work in terms of discretised time increments to evaluate the convolution integral of Equation (10), such that,

$$\left.\begin{aligned} t_0 &= K\,\triangle t \\ t_L &= N\,\triangle t \\ t &= M\,\triangle t \end{aligned}\right\} \quad \ldots(11)$$

where, K, N and M are integers and $\triangle t$ is a small time increment, which for convenience may be chosen as one unit of time.

$\triangle t$ could be chosen as small as one pleases so that pollutant injection at a uniform rate over the time increment $\triangle t$ may simulate instantaneous injection. The resultant concentration at any time t, due to finite time injection over a period t_0 may then be obtained by summing up the contributions of K instantaneous injections, with each succeeding contribution lagged by the time increment $\triangle t$ from the preceding. Thus, denoting the resultant concentration due to finite time injection at time t by $cc(t)$.

$$cc(t) = \sum_{i=0}^{M-1} c(t - i\triangle t) \qquad 0 < t < t_0 \quad \ldots(12)$$

Similar expressions may be written for the time ranges,

$$t_0 \leqslant t \leqslant t_L \quad \text{and} \quad t_L < t < t_c$$

These operations for the entire range of time $0 < t < t_c$ may be conveniently performed on a computer. A brief outline of the algorithm is presented below and the results are illustrated in Figure 3 :

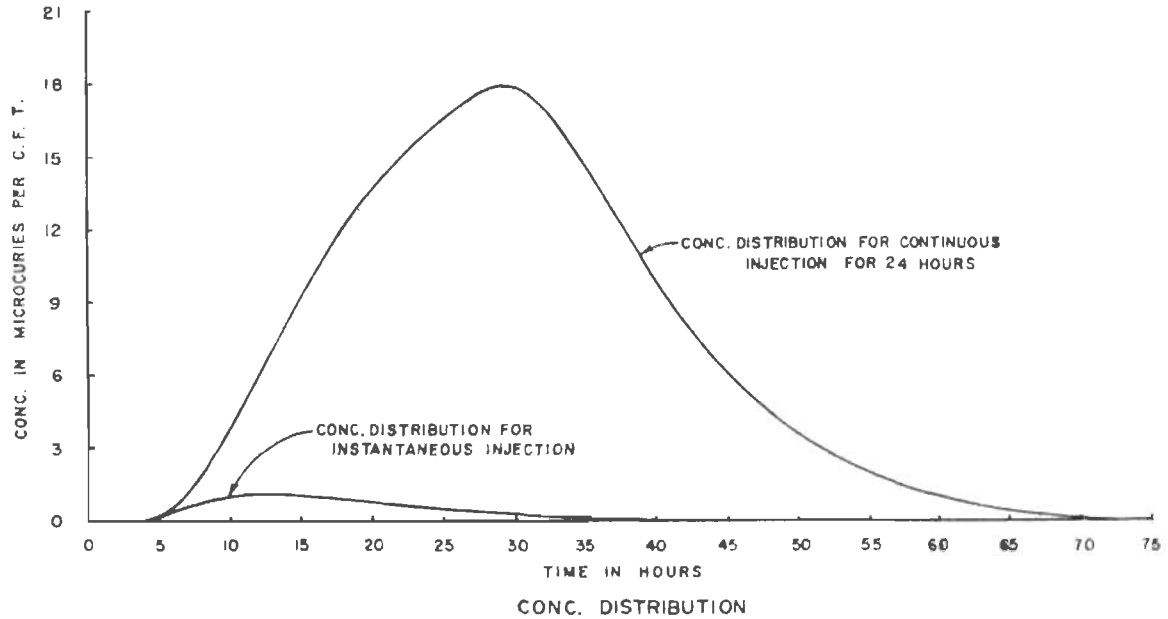

CONC. DISTRIBUTION

FIGURE 3.

$$
\left.\begin{aligned}
&\Delta t = 1\\
&cc(1) = c\ (1)\\
&cc(M) = cc(M-1)+c(M),\ 0<t\leqslant t_0,\ M\leqslant K,\ K<N\\
&cc(M) = cc(M-1)+c(M)-c(M-K),\ t_0<t<t_L,\ M>K,\ M\leqslant N,\ K<N\\
&cc(M) = cc(M-1)-c(M-K),\ t_L<t<\infty,\ M>N,\ K<N
\end{aligned}\right\} \quad ...(13)
$$

Similar algorithms may be easily written for the case $K > N$.

Dispersion Coefficients

An important difficulty often encountered in performing analyses pertaining to the environmental impact of radioactive effluents released into an open channel, accidentally or otherwise, is to estimate the practical values of D_x, D_y and D_z. Bansal[12] presents a summary of the various parametric relationships developed by different investigators for the determination of the longitudinal dispersion coefficient in open channel flow. Based on observations in a number of streams in the United States, he presents the following empirical expressions for the dispersion coefficients D_x, D_y and D_z :

$$
\left.\begin{aligned}
&\log\left(K_0\,\frac{V_s}{V}\cdot\frac{D_x}{u_* D}\right) = 6.467-0.714\log\left(\frac{\rho u_* D}{\mu}\right) \quad ...(i)\\
&\log\left(\frac{D_y}{u_* D}\right) = -2.698+1.498\log\left(\frac{B}{D}\right) \quad ...(ii)\\
&\log\left(\frac{D_z}{\nu}\right) = -8.08+1.89\log\left(\frac{\rho u_* D}{\mu}\right) \quad ...(iii)
\end{aligned}\right\} \quad ...(14)
$$

where, K_0 is a regional dispersion factor, V_s, the effective mean velocity of flow at the sampling station, V, the average velocity of flow in the reach, u_*, the overall bed shear velocity, ρ, the mass density of water, μ, the dynamic viscosity, and ν, the kinematic viscosity of water.

Whereas, his expressions for D_y and D_z could be used for predictive purposes, the one for D_x cannot be used like that, as it involves the adjustment factor k_0 which is not known apriori. For practical applications of the mathematical model developed in this paper, Equations (14) (*ii*) & (14) (*iii*) are used for computing D_y and D_z. For D_x, the expression developed by Fisher[13] following Taylor's theory of diffusion by continuous movements[14] is adopted. It can be shown[13] that,

$$D_x = \bar{u}'^2\, T \quad ...(15)$$

where, u' = spatial variation of u from the cross-sectional mean,

$T = 0.30\,\dfrac{l^2}{Ru_*}$ = Lagrangian time scale,

l = characteristic length of the channel (defined approximately as the distance on the surface from the point of maximum velocity to the most distant bank),

R = hydraulic mean radius.

The only parameter that occurs in Fisher's expression and is difficult to estimate in a field problem, is $\bar{u}'^2$. Normally, velocity measurements over different segments of a cross-section in a channel are not available for the extreme discharge conditions which are critical for analyzing the environmental impact of effluents released into a stream. However, one or two sets of velocity measurements for representative low and high flow conditions may often be available or may always be made for any specific project. With such velocity data, a curvilinear regression is run to obtain a polynomial expression in y for the segmental velocity. This polynomial is then used to estimate segmental velocities for given cross-sectional geometry and water surface elevation. Once segmental velocities u_i are obtained, $\bar{u}'^2$ is computed without much computational effort. The regression scheme used[15] utilizes the least square technique to obtain a system of simultaneous equations in terms of the coefficients in the polynomial,

$$u = a + b_1 y + b_2 y^2 + b_3 y^3 + \ldots \quad ...(16)$$

The above system of algebraic equations is solved by matrix inversion, in preference to the classical Gauss elimination as the former simultaneously yields the variances of the coefficients also.

The above approximation derives its logic from the fact that most of the regime equations[16] (Kennedy, Lindley, Lacey, Bose, Malhotra, White and Inglis) attempted to relate the velocity with the water depth or hydraulic mean depth of the channel, slope and channel roughness. The curvilinear regression implies invariance of the channel roughness and slope. If judgement of the designer indicates that the channel roughness corresponding to the discharge being analyzed is different from that for the observed discharge, the ratio of the two roughnesses is read in as input and is used to suitably modify the computed velocities. The effect of variation in energy slope is adjusted by multiplying the computed segmental velocities by the ratio of the measured or Manning's average channel velocity for the condition being analyzed with the one actually measured to serve as the base input for the curvilinear regression.

Application of the Model

To illustrate the use of the methodology developed herein, one dimensional analysis of the convective-dispersion of a radioactive tracer injected into the Ohio River at the rate of 1,670 curies/hour for a period of 24 hours, has been carried out over a distance of 644,160 ft (196,468.8 m). The results of this analysis are plotted in Figure 3.

Conclusion

A mathematical model is developed which describes the three-dimensional convective-dispersion of radioactive tracers instantaneously introduced at a point in an open channel, carrying water laden with adsorbent suspended sediment particles. The finite natural boundaries on the banks, bed and water surface of the channel are taken care of by the method of images. Using the convolution integral, the results of the instantaneous injection phenomenon are extended to a finite time injection case. The integration is performed by discretization in small time increments $\triangle t$ and summing up the results of a number of injections over the elementary time intervals, each lagged by $\triangle t$ from the preceding one. The coefficient of dispersion D_x is computed by the relation proposed by Fisher([13]). In the absence of actual measurements, the segmental velocities required for using Fisher's approach, are estimated by performing a curvilinear regression on available data for normal discharge conditions. The effect of channel roughness and energy slope is introduced in the above estimate by judgement of the channel geometry and by comparison of the average velocities for the actually measured case and for the case being analyzed. The transverse dispersion coefficients D_y and D_z are estimated from Bansal's([12]) empirical relationships. The approach developed herein is useful in analyzing the environmental aspects of accidental or normal effluent releases from a nuclear power plant.

Acknowledgements

The assistance and cooperation received from the Library and Computer Facility of Sargent and Lundy Engineers, Chicago and the confidence gained by applying the proposed methodology in the hydrologic analyses of some of the nuclear projects designed by them, generated the necessary impulse for the completion of this paper. The motivation and inspiration provided by that organization and its staff is thankfully acknowledged.

References

(1) DAVIS, G. H. and L. A. WOOD : "Water Demands for Expanding Energy Development." United States Geological Survey Circular 703, 1974, pp. 1-14.

(2) PRAKASH, A. : "Galerkin Simulation of Hydrodynamic Dispersion." Ph. D. Dissertation, Colorado State University, Fort Collins, 1974, p. 182.

(3) NALLUSWAMI, M.; R.A. LANGENBAUGH and D. K. SUNADA : "Finite Element Method for the Hydrodynamic Equation with Mixed Partial Derivatives." Water Resources Research, Vol. 8, No. 5, Oct. 1972, pp. 1247-1250.

(4) BROWN, R. H.; A. A. KONOPLYANTSEV; J. INESON and V. S. KOVALEVSKY : "Nuclear Techniques in Ground Water Hydrology." Chapter 10, Ground Water Studies, Supplement No. 1, April 1973, UNESCO, Paris, 1972, 10.4 p. 2.

(5) BEAR, J. : "Dynamics of Fluids in Porous Media." American Elsevier, Environmental Science Series, 1972, p. 764.

(6) CARSLAW, H. S. and JAEGER, J. C. : "Conduction of Heat in Solids." 2nd Ed., Oxford University Press, Oxford, England, 1959.

(7) GLOVER R. E. : "Dispersion of Dissolved or Suspended Materials in Flowing Streams." U. S. Geological Survey Professional Paper 433-B, 1964, p. 32.

(8) McWHORTER, D. B. ; D. K. SUNADA; A. PRAKASH and W.W. BURT : "Analytical Model of Stream-Aquifer System with Pumping and Recharge." Completion Report Submitted to Colorado State Engineer's Office, Denver, Colorado, AER72-73DBMc-DKS-AP-WWB2, Colorado State University, Fort Collins, Colorado, Oct. 18, 1972, p. 29.

(9) WALTON, W. C. : "Ground Water Resource Evaluation." McGraw-Hill Book Company, New York, 1970, p. 664.

(10) OGATA, A. and R. B. BANKS : "A Solution of the Differential Equation of Longitudinal Dispersion in Porous Medium." Professional Paper 411-A, U. S. Geological Survey, 1961, p. 7.

(11) DOOGE, J.C.I. : "Linear Theory of Hydrologic Systems." Tech. Bull. No. 1468, A. R. S., U. S. Department of Agriculture, 1973, p. 327.

(12) BANSAL, M. K. : "Dispersion in Natural Streams." Jnl. of the Hydr. Div., A. S. C. E., HY 11, Nov. 1971, pp. 1867-1886.

(13) FISHER, H. B. : "Longitudinal Dispersion in Laboratory and Natural Streams." Report No. KH-R-12, California Institute of Technology, Pasadena, California, June 1966.

(14) TAYLOR, G. I. : "Diffusion by Continuous Movements." Proc. London Math. Soc., Series 2, 20 (1921), pp. 196-212.

(15) CARNAHAN, BRICE ; H. A. LUTHER and JAMES O. WILKES : "Applied Numerical Methods." John Wiley & Sons, Inc., New York, 1969, p. 604.

(16) CHOW, V. T. : "Handbook of Applied Hydrology." McGraw-Hill Book Company, New York, 1964, pp. 7-27.

Hydrodynamic Aspects in Environmental and Ecological Enhancement

DANIEL M. DUBOIS
University of Liège, Institute of Mathematics
Avenue des Tilleuls, 15, B-4000 LIEGE (Belgium).

SYNOPSIS

The solution of the technical and many environmental problems requires application of mathematical and experimental techniques as tools which have been conceived and developed by fluid mechanicians and hydraulic engineers.

The emphasis which in recent years has been placed on environmental reclamation and enhancement has led to accelerated development of these tools.

It is necessary to focus upon the interface where the technique of fluid mechanics and mathematically based engineering are brought to bear upon environmental problems of the water resources.

This paper deals with hydrodynamics aspects in environmental and ecological enhancement and is more concerned with physical and mathematical modelling of interaction of fluid flow with biological and chemical processes. Two important aspects are presented. On one hand, the fluctuations which are connected to the diversity and the stability of ecological systems. On the other hand, the spatial structuration of interacting populations in relation with such mechanical properties as movement of water and turbulent diffusion. Several cases are simulated on computer and compared with mathematical results.

Introduction

The law of mass conservation for biological and chemical processes in a flow of water may be written

$$\partial/\partial t \int_V C_i dV = -\int_S C_i \underline{V}_i \cdot d\underline{S} + \int_V f_i \, dV \qquad \ldots(1)$$

where, C_i $(i = 1, \ldots, n)$ is the specific concentration of species i, $\partial/\partial t \int_V C_i dV$ the rate of time variation of concentration of species i in the volume V, $-\int_S C_i \underline{V}_i . d\underline{S}$ the surface flux of species i and $\int_V f_i \, dV$ the creation or destruction of species i due to chemical or biological interactions.

By used of Gauss theorem, Equation (1) becomes

$$\int_V [\partial C_i/\partial t + \nabla . (C_i \underline{V}_i) - f_i \, dV] = 0 \qquad \ldots(2a)$$

or

$$\partial C_i/\partial t + \nabla . (C_i \underline{V}_i) = f_i \qquad \ldots(2b)$$

A bulk velocity is defined by

$$\underline{V} = \sum_{i=1}^{n} C_i \underline{V}_i \Big/ \sum_{i=1}^{n} C_i \qquad \ldots(3)$$

With Equation (3), Equation (2*b*) is written

$$\partial C_i/\partial t + \nabla . (\underline{V} C_i) = f_i + \nabla . [(\underline{V} - \underline{V}_i) C_i] \qquad \ldots(4)$$

where, the last term is mainly due to molecular diffusion, sedimentation and migration. The molecular diffusion is often approached by Fick law, i.e.,

$$(\underline{V} - \underline{V}_i) C_i = D_{im} \nabla C_i \qquad \ldots(5)$$

where, D_{im} is the coefficient of diffusion.

When only horizontal distributions of concentrations are considered, a weighted average $\gamma(z)$ over depth z of

concentrations and velocities is made as follows

$$C_i = H^{-1} \int_{-h}^{\zeta} C_i(z)\,\gamma(z)\,dz \qquad \ldots(6)$$

$$\underline{U}\,C_i = H^{-1} \int_{-h}^{\zeta} \underline{V}(z)\,C_i(z)\,\gamma(z)\,dz \qquad \ldots(7)$$

In substituting Equations (5), (6) & (7) into Equation (4) we obtain

$$\partial C_i/\partial t + \nabla . (\underline{U}\,C_i) = F_i + \nabla . (D_{im} \nabla C_i) \qquad \ldots(8)$$

where, F_i is the weighted average over depth of the interaction function f_i.

In a closed environment like an artificial basin, a natural or artificial lake, the surface flux term drops and Equation (1) is then written

$$\partial/\partial t \int_V C_i\,dV = \int_V f_i\,dV \qquad \ldots(9)$$

In general, the interaction function f_i is expressed as a function of concentrations C_i, i.e.,

$$f_i = f_i(C_1, \ldots, C_n) \qquad \ldots(10)$$

When only the behaviour of mean concentrations is studied Equation (9), with Equation (10), becomes

$$\partial < C_i > /\partial t = < f_i(C_1, \ldots, C_n) > \qquad \ldots(11)$$

and, in this case, the mean interaction function cannot be expressed as a function of mean concentrations, i.e.,

$$< f_i(C_1, \ldots, C_n) > \neq f_i(< C_1 >, \ldots, < C_n >) \qquad \ldots(12)$$

because of the non-linear properties of ecological interactions. This remark is in narrow relation with criticisms which were made about Lotka([1]) and Volterra([2]) equations. Indeed, with Margalef([3]), we think that it is not stated if reference is made to a single point of space or to an indefinite expression of space in which case one assumes that any event has the same probability of interacting with any event everywhere, which is obviously false. Ecosystems deal often with several time and length scales corresponding each to particular physical phenomena. By example, concepts like ecological niche, territoriality and patchiness play an important role and are not exhibited with equations like Equation (11) which is only concerned with time variations of processes. To escape these difficulties, ecological systems may be described by an ensemble of subsystems with inputs and outputs. This approach is called the theory of "boxes" and is applicable only when the time behaviour of an ecosystem can be described by an ensemble of mean values of concentrations in each box. The purpose of this paper is to show that the approach by the theory of "boxes" is no more available when strong spatial heterogeneities of concentrations must be exhibited because of non-linear properties of living systems.

Moreover, the spatial structuration of living systems is directly related with their stability. Indeed, fluctuations perturbing a system can be amplified by non-linear interactions leading this system to another state. In the following section we deal with the concept of stability from a rather general point of view. After that, the practical case of prey-predator ecological populations will be analysed and numerical simulations will exhibit spatial structuration, i.e., patchiness, of these plankton populations in the Southern Bight of the North Sea.

The Concept of Stability for Ecosystems

Stability is a controversial term([3]). Generally, it is used as the property of a system to return to a state similar to a previous one, if it is led away from it by some agent or force (pollution by example) external to the system as described or not induced from its model.

Stability makes sense only in relation to the character that is considered : species composition, energy flow, etc., and the different kinds of stability are not necessarily coincident.

A most general concept of stability is implicit in the set of equations that are used to describe a system. If the composition of the ecosystem is represented by a point in a multivariant space the dimensions standing for the variables of state, numbers of individuals of such and such species, and so on, it could be assumed that a field of forces exists driving any point along optimal paths and towards some steady final state. This state should be implicit in the set of equations purporting to describe the system.

The activity of the effect of the forces driving the system or redressing it after a perturbation can be supposed to be proportional to the distance between the point representing the present state of the system and the point representing the final or asymptotic state, that stands for the reference value. This definition of the stability is similar to the concept of stability in the sense of Lyapunov([4])([5]). In Lyapunov theory, the distance between the present state and a reference state is given by the metric distance.

Moreover, it seems intuitive to relate the concept of stability to the diversity.

Margalef has introduced the Shannon-Weaver entropy H of the information content of a collection of species as an index of diversity. This index is the mean of the logarithm of the proportions p_i of individuals of each species i of an ecosystem and is given by

$$H = -\sum_{i=1}^{n} p_i \ln p_i \qquad \ldots(13)$$

This formula is identical to the definition of entropy in statistical mechanics. Moreover, the entropy constitutes a criterion of stability for closed systems of particles around an equilibrium state, i.e., the Boltzmann H-theorem which stands that at equilibrium, the entropy is maximum. When the system is slightly perturbed from its equilibrium state, entropy decreases of a quantity $\Delta H > 0$. In these conditions, entropy is a Lyapunov

function and the criterion of stability is identical to the concept of diversity (entropy). But these conclusions are only available for closed systems and we know that ecological systems are open systems far from equilibrium and are maintained at a steady state through an input of energy flow. This steady state is no more characterized by a maximum of the entropy. Nevertheless, a Lyapunov function can be deduced from the entropy formula in calculating the second variation of entropy around the steady state [e.g., Glansdorff and Prigogine(6)].

Recently, it was suggested to write the index of diversity [Equation (13)] under the following form(7)

$$H = \sum_{i=1}^{n} (-p_i \ln \bar{p}_i + \bar{p}_i - p_i) - D_0 \geqslant 0 \quad \ldots(14)$$

where, the set $\{\bar{p}_i\}$ represents the proportions of each population at a reference state. The function D_0 is written

$$D_0 = \sum_{i=1}^{n} (p_i \ln p_i/\bar{p}_i + \bar{p}_i - p_i) \geqslant 0 \quad \ldots(15)$$

Another function $D_0^{(2)}$ was also deduced from the H-function defined at the reference state, i.e., H_0

$$H_0 = -\sum_{i=1}^{n} \bar{p}_i \ln \bar{p}_i$$

$$= \sum_{i=1}^{n} (-\bar{p}_i \ln p_i + p_i - \bar{p}_i) - D_1^{(2)} \geqslant 0 \quad \ldots(16)$$

where,

$$D_0^{(2)} = \sum_{i=1}^{n} (\bar{p}_i \ln \bar{p}_i/p_i + p_i - \bar{p}_i) \geqslant 0 \quad \ldots(17)$$

Moreover, for systems slightly perturbed from the steady state, $p_i/\bar{p}_i \sim 1$, and Equations (15) & (17) become

$$D_0 \sim D_0^{(2)} \sim D_0^{*} = \sum_{i=1}^{n} (p_i - \bar{p}_i)^2/2\bar{p}_i \quad \ldots(18)$$

Thus, for small fluctuations around the steady state, D_0-functions look like a weighted variance and constitute a measure of the metric distance between the present state of the system $\{p_i\}$ and the reference state $\{\bar{p}_i\}$. We have suggested to call such Lyapunov functions, an index of fluctuations.

In conclusion, the indexes of diversity and stability are different concepts but they are narrowly related through a generalized H-theorem.

It is evident that this theory of stability is applicable for equations which deal only with time variations.

For space and time behaviour, the concept of stability must be generalized to include space variable. In considering the volume Ω of a system, we can define(5) a functional $V = \int_\Omega L \, d\Omega$ where, L is a positive definite function of concentrations. The system is stable if $dV/dt < 0$. As an example, for a population N described by the linear equation

$$\partial N/\partial t = \sum_{i,j=1}^{n} (\partial/\partial x_i) [a_{ij}(X, t) \, \partial N/\partial n_j]$$

$$+ \sum_{i=1}^{n} a_i \, \partial N/\partial x_i + a(X, t)N \quad \ldots(19)$$

with

$$X \equiv (x_1, \ldots, x_n) \quad \ldots(20)$$

a simple functional is given by

$$V = \int_\Omega N^2 d\Omega \quad \ldots(21)$$

The time derivative of V is

$$dV/dt = 2\int_\Omega U \Big[\sum_{i,j=1}^{n} (\partial/\partial x_i) [a_{ij}(X, t) \, \partial N/\partial x_j]$$

$$+ \sum_{i=1}^{n} a_i \, \partial N/\partial x_i + a(X, t)N \Big] d\Omega \quad \ldots(22)$$

If the following condition holds

$$\sum_{i,j=1}^{n} a_{ij}(X, t) \, \xi_i \xi_j \geqslant \alpha(t) \sum_{i=1}^{n} \xi_i^2 \quad \ldots(23)$$

we can write

$$dV/dt \leqslant -2\alpha(t) \int_\Omega \Big[\sum_{i=1}^{n} (\partial N/\partial x_i)^2 \Big] d\Omega + \int_\Omega a \, N^2 \, d\Omega \quad \ldots(24)$$

If $a(X, t)$ is non-positive, then $dV/dt < 0$ and the trivial solution is stable. It is well seen that the inhomogeneity $[(\partial N/\partial x_i)^2]$ of the population is a stabilizator.

For non linear systems, like prey-predator interaction, a generalization of the index of fluctuations

$$V = \int_\Omega D_0^{(2)} \, d\Omega \quad \ldots(25)$$

can be used as a criterion of stability for space and time evolution of populations.

Let us now consider the practical problem of the horizontal repartition of prey-predator plankton populations in the sea.

Horizontal Structuration of Marine Populations

Starting from Equation (8) and making time average of concentrations and velocity over a few tidal periods, two prey-predator populations can be described by the two following equations ([8]) :

$$\partial N_1/\partial t + \nabla . (\underline{u}\, N_1) = k_1 N_1 - k_2 N_1 N_2 + \nabla . (\kappa \nabla N_1) \quad ...(26)$$

$$\partial N_2/\partial t + \nabla . (\underline{u}\, N_2) = -k_3 N_2 + k_2 N_1 N_2 + \nabla . (\kappa \nabla N_2) \quad ...(27)$$

where, $<C_1> = N_1$, $<C_2> = N_2$, $\underline{u} = <\underline{U}>$

(brackets represent time average), κ is the eddy diffusivity, k_1 and k_3 the rates of natality-mortality of prey and predator respectively and k_2 their rate of interaction. It is well-known that phytoplankton and herbivorous zooplankton (copepods) being in a prey-predator relationship in the sea exhibit spatial heterogeneity in spite of agitation of water due to lateral turbulence and currents ($\underline{u}$).

Let us first study stability properties of Equations (26) & (27) without the advective term [$\nabla . (\underline{u}\, N_i)$; $i = 1, 2$].

The non-zero stationary solution uniformly distributed in space is given by

$$N_{10} = k_3/k_2 \quad ...(28)$$

$$N_{20} = k_1/k_2 \quad ...(29)$$

Let us consider perturbations around this uniform state

$$N_1 = N_{10} + n_1 \quad ...(30)$$

$$N_2 = N_{20} + n_2 \quad ...(31)$$

The linearized equations for perturbations n_1 and n_2 are written

$$\partial n_1/\partial t = -k_3 n_2 + \nabla . (\kappa \nabla n_1) \quad ...(32)$$

$$\partial n_2/\partial t = k_1 n_1 + \nabla . (\kappa \nabla n_2) \quad ...(33)$$

In view of simplifying the analytical resolution of these equations, we assume that

$$k_1 = k_3 = \omega = \text{constant} \quad ...(34)$$

where, ω represents the frequency of oscillations of the linearized classical Lotka-Volterra equations.

Let us introduce a complex variable n, the real part of which is given by n_1 and the imaginary part by n_2, i. e.,

$$n = n_1 + i\, n_2 \quad ...(35)$$

From Equations (34) & (35), Equations (32) & (33) are written under the simple form

$$\partial n/\partial t = i\omega n + \nabla . (\kappa \nabla n) \quad ...(36)$$

With the following variable change

$$n = N \exp(i\, \omega\, t), \quad ...(37)$$

Equation (36) becomes

$$\partial N/\partial t = \nabla . (\kappa \nabla N) \quad ...(38)$$

which represents the classical equation for heat conduction except the fact that N is here a complex variable.

Equation (38) is a parabolic equation depending on position $\underline{r}$ and time t. For the resolution of these equations, initial conditions ($t = 0$) on populations, i.e., $N_1(\underline{r}, 0)$ and $N_2(\underline{r}, 0)$, and boundary conditions ($\underline{r} = \underline{R}$), i. e., $N_1(\underline{R}, t)$ and $N_2(\underline{R}, t)$ must be given.

Plankton populations live in some sea-water mass characterized by suitable values of such properties as temperature, salinity, dissolved oxygen and dissolved nutrients. In regions where the water is physiologically unsuitable for organisms, their concentrations drop to zero. These regions constitute natural boundaries. Other natural boundaries are given by coastal regions. In other words, the natural domain for the integration of equations is limited by regions where populations concentrations drop to zero.

Equation (38) can be easily resolved analytically in one dimension. Let $x = 0$, one side of the studied region and $x = L$ the other one. The natural boundary conditions are $N_1(0, t) = N_1(L, t) = N_2(0, t) = N_2(L, t) = 0$ and the initial conditions are given by $N_1(x, 0) = f_1(x)$, $N_2(x, 0) = f_2(x)$ where, $f_1(x)$ and $f_2(x)$ represent the initial spatial repartitions of prey and predator populations respectively. As the analytical resolution is rather long, let us give directly the final solution :

$$N_1(x, t) = N_{10}[1 - A(2/\sqrt{2}) \sin(\pi/4 + \phi)] - 4\pi$$

$$N_{10}\kappa(2/\sqrt{2}) \sum_{m=0}^{\infty} \left\{ \left[(2n+1) \exp[-\kappa(2m+1)^2 \right.\right.$$

$$\pi^2 t/L^2] \sin[(2m+1)\pi x/L] / [L^4\omega^2 +$$

$$\kappa^2\pi^4(2m+1)^4] \left\} \left\{ L^2 \omega \cos(\omega t - \pi/4) \right.\right.$$

$$\left. - \kappa(2m+1)^2\pi^2 \sin(\omega t + \pi/4 \right] \right\} +$$

$$(2/L) \sum_{m=1}^{\infty} \exp(-\kappa m^2\pi^2 t/L^2) \sin(m\pi x/L)$$

$$\int_0^L \left\{ [f_1(x') - N_{10}] \cos \omega t - [f_2(x') - N_{10}] \sin \omega t \right\}$$

$$\sin(m\pi x'/L) dx' \quad ...(39)$$

$$N_2(x, t) = N_{10}[1 - A(2/\sqrt{2}) \cos(\pi/4 + \phi)] - 4\pi$$

$$N_{10}\kappa(2/\sqrt{2}) \sum_{m=0}^{\infty} \left\{ \left[(2m+1) \exp[-\kappa(2m+1)^2 \right.\right.$$

$$\left. \pi^2 t/L^2] \sin[(2m+1)\pi x/L] / [L^4\omega^2 + \kappa^2\pi^4(2m+1)^4] \right\}$$

$$\left\{L^2\,\omega\,\sin(\omega t-\pi/4)-\kappa(2m+1)^2\,\pi^2\cos(\omega t-\pi/4)\right]\Big\}$$

$$+(2/L)\sum_{m=1}^{\infty}\exp(-\kappa m^2\pi^2 t/L^2)\sin(m\pi x/L)$$

$$\int_0^L\left\{[f_1(x')-N_{10}]\sin\omega t-[f_2(x')-N_{10}]\cos\omega t\right\}$$

$$\sin(m\pi x'/L)dx' \qquad \ldots(40)$$

where,

$$A = |\cosh[k(x-L/2)(1+i)]/\cosh[kL(1+i)/2]|, \qquad \ldots(41)$$

and

$$\phi = arg\left\{\cosh\left[k(x-L/2)(1+i)\right]\Big/\cosh\left[kL(1+i)/2\right]\right\} \qquad \ldots(42)$$

with

$$k = (\omega/2\kappa)^{1/2} \qquad \ldots(43)$$

The first term of $N_1(x, t)$ and $N_2(x, t)$ depends on functions A and ϕ which are independent of time t. It represents the stationary solution and exhibits a stable spatial structuration with a characteristics length given by $\lambda_c = 2\pi/k$ where, k depends on ω and κ [Equation (43)]. This length λ_c was already found[9] by an analysis of the stability of normal modes of Equations (32) & (33).

Indeed, a normal mode is written

$$N_j(x, t) = N_{j_0}+n_j\exp(\Omega t+i\,2\pi\,K\,x) \quad j = 1, 2 \qquad \ldots(44)$$

where, n_j, Ω, and K are constants. The dispersion relation can be expressed as

$$\Omega = -\kappa(2\pi\,K)^2+(-k_1\,k_3)^{1/2} \qquad \ldots(45)$$

A critical wave-number K_c is obtained when $\Omega = 0$, i.e.,

$$2\pi\,K_c = \pm[-k_1\,k_3/\kappa^2]^{1/4} \qquad \ldots(46)$$

which can be written under the following form

$$K_c = \pm(1+i)/\lambda_c \qquad \ldots(47)$$

with

$$\lambda_c = \pm 2\pi(2\kappa/\omega)^{1/2} \qquad \ldots(48)$$

From Equation (48), Equation (44) is written

$$N_j(x, t) = N_{j_0}+n_j\exp(\pm i\,2\pi\,x/\lambda_c\mp 2\pi\,x/\lambda_c) \qquad \ldots(49)$$

Moreover, Equation (49) is the general stationary solution for the following boundary conditions : $N_1(0, t) = N_2(0, t) = N_{10}-B$ (B is a constant), $N_1(x, t)$ and $N_2(x, t)$ being bounded for $x \to \infty$. Indeed, in this case, the stationary solutions of Equations (32) & (33) are written

$$N_1(x, t) = N_{10}-B\exp(-2\pi x/\lambda_c)[\cos(2\pi x/\lambda_c) - \sin(2\pi x/\lambda_c)] \qquad \ldots(50)$$

$$N_2(x, t) = N_{10}-B\exp(-2\pi x/\lambda_c)[\cos(2\pi x/\lambda_c) + \sin(2\pi x/\lambda_c)] \qquad \ldots(51)$$

From Equations (50) & (51), the spatial structuration is well exhibited from terms like $\cos(2\pi x/\lambda_c)$ and $\sin(2\pi x/\lambda_c)$. Moreover, this structuration appears only next to the origin of the x-axis. Indeed, for a value of $x = \lambda_c$, the argument of the exponential is -2π and $\exp(-2\pi) = 0.0019$. In other words, for $x > \lambda_c$, $N_1(x, t) = N_2(x, t) \sim N_{10}$, i.e., the two stationary solutions are constants and homogeneous. Thus, the stationary spatial structuration in the linearized equations is essentially due to the constraint of the boundary conditions. It may be noted that Equations (50) & (51) are good approximations of the first term of Equations (39) & (40) for $x \in (0, L/2)$ if $L/2 > \lambda_c$ and are also in good agreement with the stationary solution of the non-linear equations.

The transitory terms given in Equations (39) & (40) are represented by a summation on spatial modes characterized by the index m, i.e., terms like $\sin(m\pi x/L)$. The time evolution of the transitory solutions is given by both an oscillating function with the frequency ω, i.e., terms like $\sin(\omega t+\pi/4)$, and a damping function with a constant of relaxation $\tau_m \sim L^2/m^2\pi^2\kappa$ depending on the spatial mode m. As each value of m corresponds to a wavelength $\lambda_m \sim L/m$, the terms corresponding to small wavelengths are first damped : only large spatial scale inhomogeneities have a great lifetime : indeed

$$\tau_m \sim \lambda_m^2\Big/\pi^2\kappa.$$

Drastic differences of the space and time behaviour of prey-predator populations exist between linearized and non-linear equations. In the linearized equations, the characteristic frequency of ecological response is given by $\omega = (k_1\,k_3)^{1/2}$ mean while in the non-linear equations, a frequency spectrum is exhibited. Indeed, from Lotka-Volterra equations, a continuous spectrum of frequency $f(\omega)$ exists, each frequency depending on the distance of the prey-predator populations from the stationary state (N_{10}, N_{20}). More the system is far from the stationary state, more the period of fluctuations is large. Thus, the period corresponding to the linearized equations is a low bound and the corresponding frequency is an upper bound. This fact is of great importance for the time persistence of spatial heterogeneity, i.e., patchiness, of populations.

Numerical Simulation of Patchiness

The non-linear partial differential Equations (21) & (22) were integrated numerically on computer in view of simulating the spatial structuration of both phyto and zooplankton in the Southern Bight of the North Sea.

The residual currents (velocity u in Equations (21) & (22) were calculated as in Nihoul et al paper[10].

Figure 1 shows the heterogeneous stationary steady state of prey-predator plankton populations by numerical

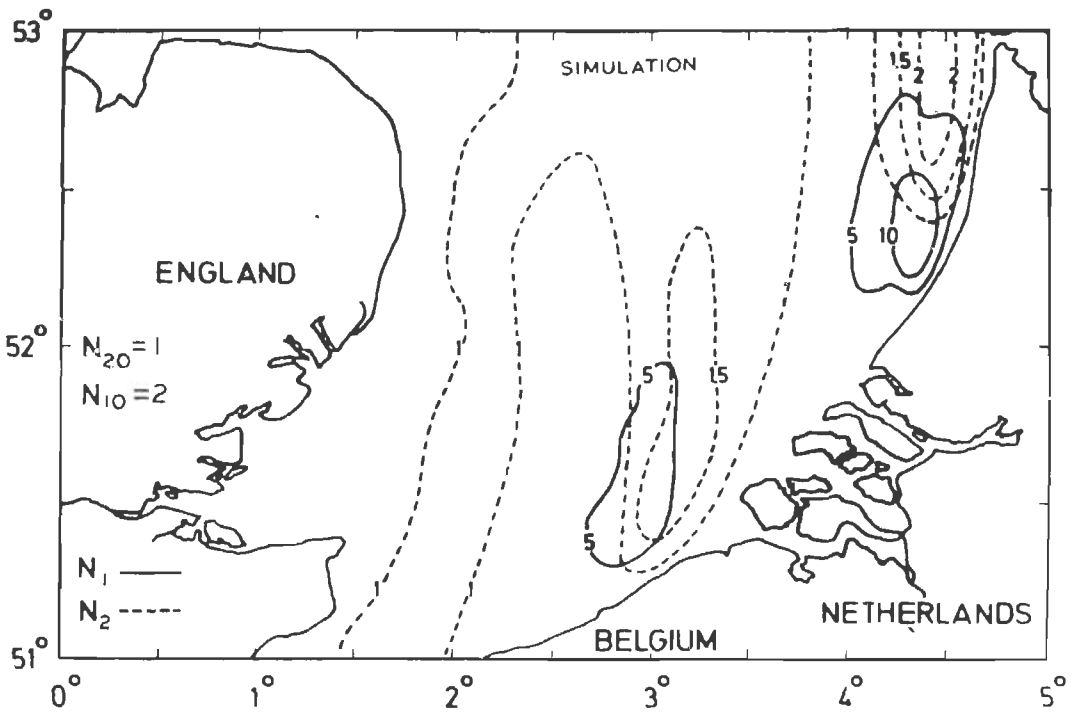

FIGURE 1 : Heterogeneous steady state of phyto (N_1) and zooplankton (N_2) populations in the Southern Bight of the North Sea by simulation of Equations (21) & (22). Notice two regions where natural accumulations of phyto and zooplankton populations occur.

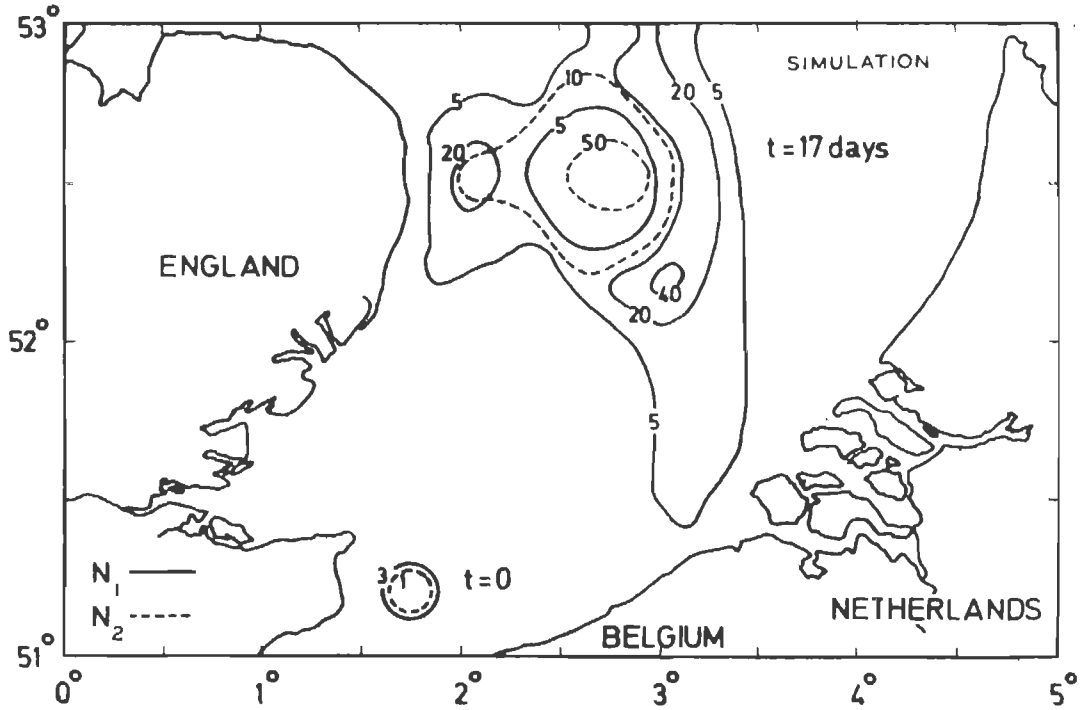

FIGURE 2 : Numerical simulation of the horizontal structuration of a patch of phyto (N_1) and zooplankton (N_2) populations in the Southern Bight of the North Sea. Notice the transformation of the disc structure ($t = 0$) to the ring structure ($t = 17$ days).

simulation of Equations (21) & (22). Concentrations of the two populations are maintained at N_{10} and N_{20} for both north and south boundaries. N_{10} and N_{20} are the same definitions as in Equations (28) & (29) and correspond to the homogeneous steady state of Equations (21) & (22) in neglecting advection.

An accumulation of plankton next to Belgium and The Netherlands is due to the gyre created by the tidal stress in the Westerschelde Estuary region. A second region of greater concentrations of plankton is also well exhibited. The particular properties of these two regions were already exhibited from experimental ecological data (see Ref. 10, Figure 9).

Figure 2 gives the spatial structuration of a patch of prey-predator plankton populations in the Southern Bight of the North Sea. The initial disc structure of the patch ($t = 0$) transforms to a series of patches surrounding an empty region at time $t = 17$ days.

From experimental data[11], the same succession of events was observed in following patches during a few weeks. During its drift in the Southern Bight, the horizontal structuration of a patch is given by a growing circular disc which loses its centre and breaks into segments. Due to advection, the highest densities lie in a series of areas surrounding the empty region.

For the two Figures 1 & 2, the numerical parameters were taken as follows : $\sigma = (k_1/k_3)^{1/2} = 2.24$ and $\omega = (k_1 k_3)^{1/2} = 0.134$ day^{-1}.

Conclusion

This paper deals with physical and mathematical modelling of interactions of fluid flow with ecological processes.

General considerations about the concept of stability for ecosystems were made in relation with the concept of diversity. The spatial distribution of populations is directly related with their stability. The mechanism of structuration is initiated by fluctuations which are afterwards amplified by the non-linear ecological interactions.

A non-linear model of the horizontal distributions of prey-predator plankton populations (taking into account advection, due to residual currents, and eddy diffusivity) was presented. The ecological interactions were assumed of the Lotka-Volterra type. The space and time evolution of plankton distributions was simulated on computer in the Southern Bight of the North Sea using this non-linear model. The results are in agreement with experimental data.

Prediction of the behaviour of ecological systems in their water environment is so made by using mathematical models. This paper shows that the solution of environmental problems requires application of mathematical techniques as tools. In environmental and ecological enhancement, mathematical modelling leads to a better understanding of nature and will help to solve the problem of food resources for human needs in the following decades.

Acknowledgement

This study was part of the Belgian National Program on Physical and Biological Environment. The author is grateful to the Ministry for Science Policy for the support of this research.

References

(1) LOTKA, A. J. (1925) : "Elements of Physical Biology." William and Wilkins, Baltimore.

(2) VOLTERRA, V. (1931) : "Leçons sur la théorie mathématique de la lutte pour la vie." Gauthier Villars, Paris.

(3) MARGALEF, R. (1973) : "Some Critical Remarks on the Usual Approaches to Ecological Modelling." In Investigation Pesquera, Vol. 37 (3), pp. 621-640.

(4) LA SALLE and LEFSCHETZ (1961) : "Stability by Lyapunov's Direct Method with Applications." Academic Press.

(5) ZUBOV, V. I. (1964) : "Methods of A. M. Lyapunov and their Application." Noordhoff – Groningen—The Netherlands.

(6) GLANSDORFF, P. and PRIGOGINE, I. (1971) : "Structure, Stability and Fluctuations." Wiley-Interscience.

(7) DUBOIS, D. M. (1973) : "Aspect mathématique de l'invariant en cybernétique : applications en écologie et en biologie." Cybernética (Namur), *16*, 161.

(8) DUBOIS, D. M. (1975) : "A Model of Patchiness for Prey-predator Plankton Populations." Internat. J. of Ecol. Mod. and Eng., *1*.

(9) DUBOIS, D. M. (1974) : "The Influence of the Quality of Water in Ecological Systems." I.F.I.P. Working Conference on Modelling and Simulation of Water Resources Systems Ghent, Publ. by North-Holland, Amsterdam, ed. by G. C. Vansteenkiste.

(10) NIHOUL, J. ; RONDAY, F. and PICHOT, G. (1975) : "Belgian Mathematical Model and Data Acquisition System for Monitoring, Prediction and Control of Marine Resources Quality." Second World Congress on Water Resources, New Delhi, India.

(11) WYATT, T. (1973) : The Biology of Oikopleura Dioica and Fritillaria Borealis in the Southern Bight." Marine Biology, *22*, 137.

Importance of Flushing Rate Calculations for Estimating Productivity of Tropical Reservoirs

A. M. BEETON
Senior Scientist
Center for Great Lakes Studies
The University of Wisconsin—Milwaukee
Milwaukee, Wisconsin, U.S.A.

SYNOPSIS

An approach is proposed whereby methods developed to determine flushing rates, lakeward transport, and volume of water moving lakeward can be used to estimate nutrient loading from bays to the open water of a reservoir. Some data from Volta Lake, Ghana and the Nam Ngum Reservoir, Laos are presented to indicate the importance of studying the exchange between bays and the open waters of reservoirs.

Introduction

The productivity of a natural lake is directly related to the productivity of the drainage basin and continual inputs of nutrients to the aquatic system. Any changes in the productivity of the aquatic system reflect some alteration in the nutrient influx. The nutrient poor lateritic soils of the tropics would not be expected to provide for high nutrient inputs either from tributaries or direct runoff. Consequently, lakes lying in a drainage basin with such nutrient poor soils would be expected to be less productive than lakes lying in nutrient rich soils. Of course, the morphometry of the basin is also important, since shallow lakes have a faster and greater recycling of nutrients than deep lakes, because the productive euphotic zone is more closely associated with the sediments and any release of nutrients.

The same principles must apply to man-made lakes, although these relationships are usually obscured initially by disruption of the riverine ecosystem due to impoundment. It appears that conditions may stabilize in temperate reservoirs in about 15 years. Stabilization probably occurs much quicker in tropical reservoirs. The initial productivity of a man-made lake is closely tide to the productivity of the flooded terrestrial environment and whether or not vegetation was cleared prior to flooding. All of the flooded organic matter may not be cycled through a food chain useful to man, however, especially if the lake is deep, stratifies, and anaerobic conditions develop in the bottom waters. Flooded trees and other vegetation will provide extensive areas for aufwuchs as well as hiding places for fish (es). The decaying forest litter and shrubs provide most of the initial nutrients, since the true biomass decays very slowly. As the flooded vegetation decays this source of nutrients becomes exhausted and surface area for aufwuchs decreases. Consequently, macrophytes in the shallow waters and plankton in the open, deep waters will become increasingly important in the productivity of the system as it stabilizes.

The productivity of the open waters of large, deep reservoirs is tied to inputs from the near-shore shallow waters, since recycling of nutrients in the open waters is impeded by stratification, loss of nutrients through the outflow, and by settling out of particulate matter from the euphotic zone. To maintain productivity in the open waters there must be a continual input of nutrients, but the quantity and nature of the inputs are determined by conditions in the shallow waters, since the major inputs from tributaries and non-point sources (surface runoff) are into the shallow environments.

Flushing rates are an important aspect to consider in dealing with productivity of small bodies of water[11]. In large aquatic systems the bays, harbors and shallow

near-shore environments differ greatly and pronounced differences exist between near-shore and open-water conditions(4). This situation can be even more pronounced in large reservoirs, especially those that are dendritic with many arms.

This paper was written to direct attention to the importance of studying the productivity of the major arms of a reservoir and determining contributions of this productivity to that of the open waters. In order to do this, estimates must be made of the flushing rates of the arms and the magnitude of exchange between these arms and open water.

Examples from Volta Lake, Ghana and Nam Ngum Reservoir, Laos

Data available for Volta Lake support the idea that the arms and shallow waters are more productive than the deep, open waters. Lawson, et al (1969)(6) reported on an increasing gradient of blue-green algae into the Afram arm in 1966. Other data such as that reported by Viner (1969)(10) show that diatoms were important in the open water, but blue-greens were dominant in the shallow waters.

The zooplankton data for Volta Lake certainly indicate the importance of the arms as possible "nursery" areas for planktonic Crustacea. Proszynska (1969)(9) observed abrupt changes in zooplankton numbers and a lack of larval stages in the open waters in 1965 and suggested that zooplankton may develop elsewhere to be carried into the open waters. She studied planktonic Crustacea of the Afram Confluence in 1966 and found that Crustacea were present all year, including abundant larval stages(8). Consequently, she concluded that these observations confirmed the suggestion that Crustacea occurring periodically in the open water originated in the Afram Confluence. The importance of shallow areas as "nursery" areas of zooplankton was recognized in 1929 for Lake Erie(3).

Limnological conditions progressively change from the shallower water among submerged trees out into the open waters of the Nam Ngum Reservoir (Figure 1). Dissolved-oxygen concentrations increased from 0.9 mg/l in the shallow water to 1.9 mg/l in the open water. Total alkalinity increased from 50 mg/l to 55 mg/l.

Abundant growths of aquatic macrophytes, *Pistia*, *Azolla*, and *Salvinia*, were found only in the bay of the Huai Nam Yen. Evidently nutrient loading from the Huai Nam Yen was such as to form the growth of these macrophytes and certainly have important implications for productivity of the reservoir, since these plants are those which have caused serious problems in other tropical lakes.

Very productive beds of *Hydrilla* grow in the shallow water of the Nam Ngum Reservoir. For example, dissolved-oxygen concentrations increased from 12.3 to 16.9 mg/l in a *Hydrilla* bed, near the dam, between

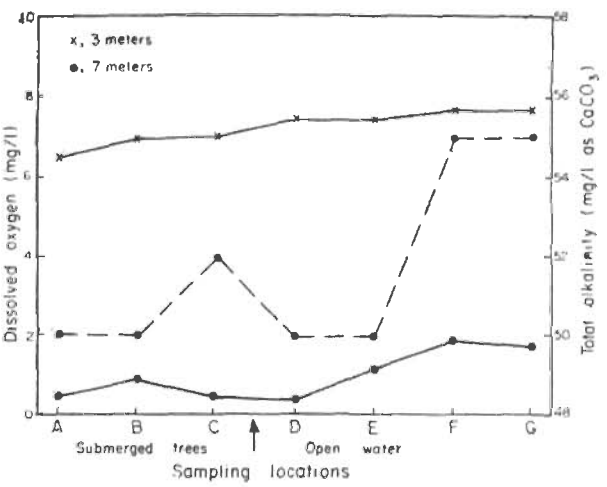

FIGURE 1: Dissolved oxygen (solid line) and total alkalinity (broken line) at depths of 3 and 7 m at sampling locations on a transect starting among submerged trees and extending into open water of the Nam Ngum Reservoir, Laos, 11 November 1974 (Sampling locations about 75 m apart).

9 : 15 and 11:00 on 7 November 1974. Dissolved-oxygen content increased less than 1 mg/l in the open water adjacent to the *Hydrilla*. Such a high level of production in the shallow, near-shore areas must affect the open waters by removing nutrients from the waters and/or producing organic matter eventually carried into the open waters.

Determination of Flushing Rates

Ketchum (1950)(5) used salinity, or lack of it, to identify fresh water and determine flushing rates and exchange between estuaries and the ocean. In an estuary salt concentrations progressively increase from the river mouth toward the open ocean. Salt concentrations are greatest, however, in most rivers and become diluted lakeward due to entrainment of lake water. Some conservative chemicals, eg sodium or chloride, can be used as a tracer to identify river water. Beeton, Smith, and Hooper (1967) used sodium as a tracer to determine flushing rates and exchange of Saginaw Bay, Lake Huron. Conductivity proved to be a more convenient tracer in a study of Green Bay, Lake Michigan(7). Conductivity cannot be used in many situations where calcium bicarbonate is the dominant factor determining conductivity. For example, the photosynthetic activity of massive growths of aquatic macrophytes in Lake Skadar, Yugoslavia, can reduce the conductivity of the water from *circa* μmhos to 100 μmhos in a matter of hours(2).

The methods developed and used successfully in Saginaw Bay can be used in tropical reservoirs. Needed are data on the flow of the river or rivers, average concentration of some conservative chemical in the river water, distribution of this chemical in the bay, average

concentrations of the chemical in the open waters of the lake, and a bathymetric chart of the bay. This assumes, of course, that concentrations of the chemical used as tracer are greater in the inflowing water than in the receiving waters. The distribution of the chemical in the bay can be obtained by synoptic survey, where enough samples are taken in one day to allow plotting the contoured distribution of the chemical.

Assuming that the river water is the main source of the tracer, the proportion of the river water in the bay, a water column, or some section of the bay can be determined by calculating the volume of lake water (v_h) and river water (v_r) in the particular area. This is determined from the relationship,

$$v_r s_r + v_h s_h = (v_r v_h) s_o$$

where, s_r is the concentration of tracer in river water, s_h the concentration in lake water and s_o the observed concentration in the area. The river water fraction (F_r) is determined by,

$$F_r = \frac{V_r}{V_r + V_h}$$

Flushing rate (F_l) is the time required for a one-day accumulation of river water (D) to move through the bay.

$$F_l = (F_r V) \frac{1}{D}$$

The total volume of the bay or section of bay is V.

The rate at which the river water moves through the bay is the lakeward transport (T_1),

$$T_1 = \frac{D}{(F_r)(A_{xs})}$$

where, A_{xs} is the cross-sectional area of some section of the bay.

The total volume (V_l) of river and entrained water moving lakeward is,

$$V_l = T_1 \cdot A_{xs}$$

By knowing the average concentration of the tracer in V_l, at the cross-section of the bay mouth, the mass transport (loading rate) of this material to the open lake can be calculated.

If similar information is obtained for nutrients, e.g., total phosphorus concentrations for the synoptic survey, then the loading rate of total phosphorus from the bay to the open lake can be determined. The distribution of this non-conservative property will differ from that of the conservative tracer primarily because of biological uptake and loss to sediments. Calculation of the loading rate at the bay mouth should also give an estimate of the loss of the nutrient to the bay system. The Saginaw Bay results indicated an appreciable decrease in phosphorus in the river water fraction as it moved through the bay([1]). If data are obtained on chlorophyll distribution it should be possible to make calculations of what fraction of the bay productivity is carried out into the open lake.

References

(1) BEETON, A.M. ; SMITH, S.H. and F.H. HOOPER (1967) : "Physical Limnology of Saginaw Bay, Lake Huron." Great Lakes Fish. Comm., Tech. Rept. No. 12, p. 56.

(2) BEETON, A.M. ; CLAFLIN, L.W. and R.J. RISTIC (1973) : "Aspects of the Physical Limnology of Skadar Lake." Report submitted to Smithsonian Institution.

(3) FISH, C.J. (1960) : "Limnological Survey of Eastern and Central Lake Erie, 1928-29." U.S. Fish. Wildl., Spec. Sci. Rept.—Fish No. 334, p. 198.

(4) HOLLAND, R.E. and A.M. BEETON (1972) : "Significance to Eutrophication of Spatial Differences in Nutrients and Diatoms in Lake Michigan." Limnol. Oceanogr., 17 : 88-96.

(5) KETCHUM, B.H. (1950) : "Hydrographic Factors involved in the Dispersion of Pollutants introduced into Tidal Waters." J. Boston Soc. Civil Engr., 37 : 296-314.

(6) LAWSON, G.W. ; PETR, T. ; BISWAS, S. ; BISWAS, E.R.I. and J.D REYNOLDS (1969) : "Hydrobiological Work of the Volta Basin Research Project 1963-1968." Bull. del I.F.A.N. Tome XXXI, Ser. A., No. 3, 965-1003.

(7) MODLIN, R.F. and A.M. BEETON (1970) : "Dispersal of Fox River Water in Green Bay, Lake Michigan." Proc. 13th Conf. Great Lakes Res. Internat. Assoc. Great Lakes Res., 468-476.

(8) PROSZYNSKA, M. (1967) : "A Quantitative Study of the Cladocera and Copepoda in the Afram Confluence area of the Volta Lake." Type-written Report to Volta Lake Research Project.

(9) PROSZYNSKA, M. (1969) : "A Preliminary Report on the Quantitative Study of the Cladocera and Copepoda in the Volta Lake 1964-1965." In : Obeng, L. edition, Man-Made Lakes, The Accra Symposium, p. 127-132.

(10) VINER, A.B. (1969) : "Observation of the Hydrobiology of the Volta Lake April 1965-April 1966." In : Obeng, L. (editor), Man-Made Lakes, The Accra Symposium, p. 133-143.

(11) VOLLENWEIDER, R.A. and P.J. DILLON. (1974) : "The Application of the Phosphorus Loading Concept to Eutrophication Research." Nat. Res. Council, Canada, Environmental Scientist Publ. No. 13690, p. 42.

Eutrophication Studies in a Planned Community

CALVIN H. WARD
Professor of Environmental Science and Biology

JOE M. KING
Research Associate
Environmental Science

Rice University, Houston, Texas, U.S.A.

SYNOPSIS

Woodlands, a planned new community located north of Houston, Texas, is being utilized as a study area for investigating the impact of increasing urbanization on the water resources of a particular drainage system. Two small recreational lakes in Woodlands, which will receive treated stormwater, untreated stormwater, and treated sewage effluent, are serving as natural biological reactors for comparing the water qualities before and after community development. Collection sites were established along a stream which courses through Woodlands in order to assess the eutrophication potential of runoff water from the Woodlands watershed. Chemical analyses of water samples are revealing the quantities of potential nutrients which are present in these ecosystems and controlled nutrient limitation studies are being used to ascertain the limiting nutrient requirements of the indigenous aquatic flora. Detailed knowledge of the water quality and the nutrient requirements of aquatic plants present in Woodlands should permit the formulation of strategies for Woodlands water management. These strategies will then be directed toward maintaining a desired water quality in a large recreational lake which is being constructed in Woodlands.

To date, these studies have revealed that there has been an overall increase in the nutrient content of Woodlands water as urbanization progressed in this area. Surface runoff from lawns and a golf course have been recognized as potential sources of nutrients for the Woodlands lakes. Nutrient limitation studies have shown that increased amounts of nitrogen and phosphorus in water from Woodlands will substantially stimulate the growth of algae. Phosphorus seems to be the limiting factor for algal growth in the lakes in Woodlands and in low-flow water from the stream. However, during periods of high stream flow, as in stormevents, nitrogen is the limiting element for algal growth. This information has been utilized in developing a tentative program for maintaining a water quality which will preserve the aesthetic and recreational values of the Woodlands lakes. Continuation of these studies during further community development will allow for modifications and refinements in these strategies.

Introduction

Eutrophication may be broadly defined as nutrient enrichment that results in high biological productivity and a decreased volume within an ecosystem. In undisturbed lakes, eutrophication is a natural "aging" process and eventually culminates in the disappearance of the lake itself. However, the addition of excessive quantities of nitrogen and phosphorus to aquatic ecosystems often accelerates eutrophication and leads to deteriorations in the aesthetic, recreational and water quality values of the ecosystems. Accordingly, values of lake properties may depreciate and increased burdens may be imposed on water systems due to additional costs incurred in the treatment of the water.

Sewage effluent is often a prime contributor of nitrogen and phosphorus to waterways. Also, significant

quantities of these elements may be transported to aquatic ecosystems from watersheds. If the watershed is used for urban purposes, the role of surface runoff becomes ecologically more critical since urbanization increases the amount of nitrogen and phosphorus discharge to surface waters[2][5][7][8][10]. However, there seems to be conflicting opinions on the stimulatory effects of urban runoff on algal growth[1][3][6].

Woodlands, a planned new community located north of Houston, Texas, is an ideal location for investigating the impact of urbanization on the water resources of a particular drainage system. Since two small recreational lakes in Woodlands will receive treated and untreated stormwater and sewage effluent, they are being used as natural reactors for comparing the water qualities before and after community development. Likewise, Panther Branch, which drains the major portion of Woodlands, is being investigated in order to determine the eutrophication potentials of low-flow water and stormwater runoff as urbanization increases in Woodlands. Chemical analyses are being utilized to ascertain the quantities of nutrients which are present in these aquatic ecosystems. Controlled nutrient limitation studies are being used in order to obtain information on the limiting nutrient requirements of the indigenous aquatic flora. Thus, accurate description of expected water quality, combined with detailed knowledge of the nutrient requirements of indigenous aquatic plants, should permit the formulation of strategies for Woodlands water management. These strategies may then be employed in controlling eutrophication in a larger recreational lake which is being constructed in Woodlands.

Methods

Description of Study Area

Woodlands is located in a pine-hardwood forest approximately 35 miles north of Houston, Texas. The Woodlands encompasses 17,776 acres and will be developed over a twenty-year period, beginning September 1972. Approximately 80 percent of the development is drained by Panther Branch, a tributary of Spring Creek.

Panther Branch is approximately 14 miles in length and has a total drainage area of 36.2 miles. Several collection sites were established along the course of Panther Branch and two sites were maintained on Spring Creek. Low-flow water samples were routinely collected at these sites and were subjected to chemical, biological and nutrient limitation studies. Stormwater runoff samples were collected from Panther Branch during the course of several stormevents and were subjected to similar studies.

Water samples were also collected from one of the small recreational lakes (Lake B) in Woodlands. Lake B has an area of 3.3 acres, an average depth of 6 ft, and contains approximately 20 acre-ft of water. During the initial phases of this investigation, surface runoff was the major source of water for this lake. However, in February 1975, a constant water-level will be maintained in the lake by the continuous addition of treated sewage effluent.

Analytical Procedures

Instantaneous discharge for Panther Branch and Spring Creek were determined at U. S. G. S. gauging stations located on these streams. Chemical analyses were conducted with a Technicon Autoanalyzer[9] and temperature was determined with a standard mercury thermometer. The Winkler method[9] was used to ascertain dissolved oxygen concentrations and *pH* was determined with a portable *pH* meter. Methods used in the batch culture bioassays were similar to those described by the Joint Industry/Government Task Force on Eutrophication[4]. Optical density, at 650 nm, was used as an index for algal growth and the results are presented as the average optical densities of triplicate samples, after 21 days incubation. In these studies, *Selenastrum capricornutum* was used as the test organism.

Results and Discussion

Extensive biological and chemical investigations have been conducted on the aquatic ecosystems in the Woodlands. These investigations have resulted in a volume of data which is too large to be presented in its entirety. Therefore, only those segments of data from the first year of study which exemplify certain points and are most pertinent to water management strategies will be presented in this report.

Lake B

During the first year of investigation the concentrations of nitrogen and phosphorus varied considerably in Lake B (Figure 1). Surface runoff was the only source of water for this lake and nutrient additions to the lake were dependent upon this factor. However, during the initial phases of study (November-May) spillway construction was still in progress and the lake experienced extreme fluctuations in water volume. These fluctuations, combined with surface runoff, were probably responsible for the initial variations in the concentrations of nutrients within the lake. Upon completion of construction (May 1974), the lake was filled rapidly and extreme fluctuations in water-level ceased. However, peaks in nitrogen and phosphorus concentrations were noted in April 1974. At this time the golf course in the vicinity of the lake and the lawns surrounding the lakes were established and had received periodic applications of fertilizer. Thus, nitrogen and phosphorus were transported to the lake by surface runoff from these areas. The peak in NH_4—N (September 1974) was probably caused by a coloring agent which was added to the water for public relations purposes.

Nutrient limitation studies with water collected from

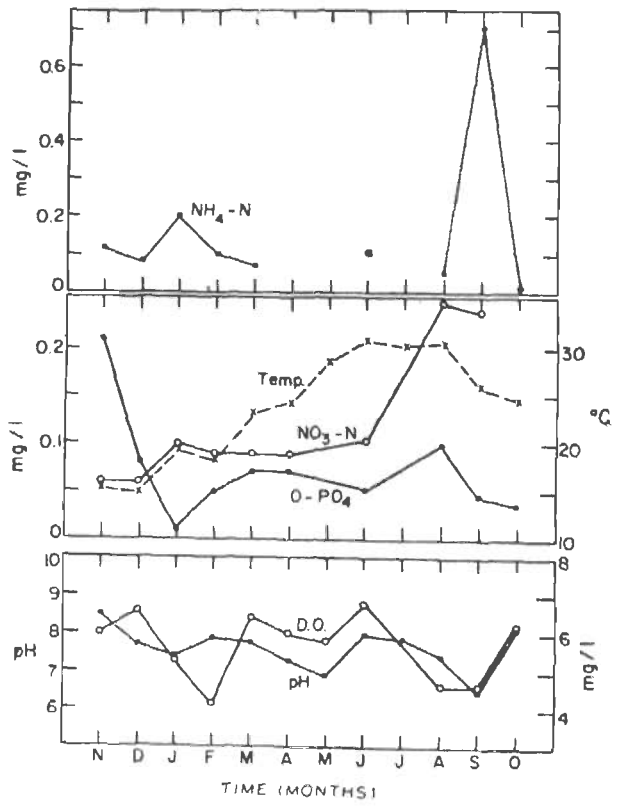

FIGURE 1 : Seasonal variations in the water quality of Lake B.

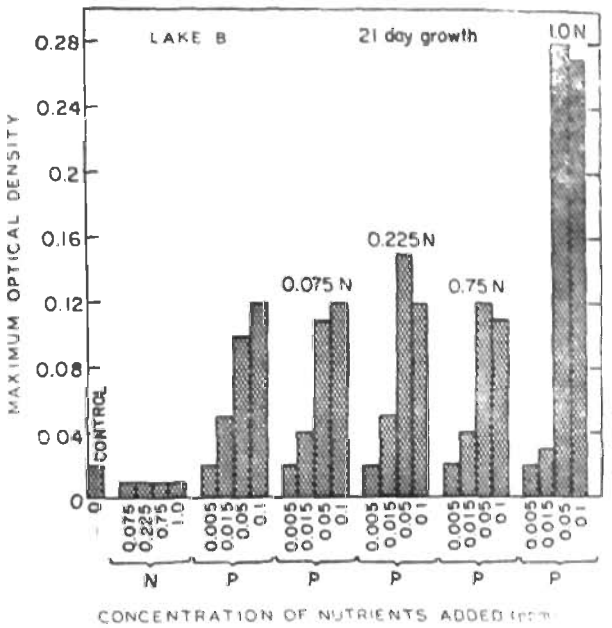

FIGURE 2 : Optical densities of *Selenastrum capricornutum* after 21 days incubation in various treatments of Lake B water.

Lake B revealed that algal growth was not stimulated by the addition of nitrogen to the water (Figure 2). However, phosphorus spikes did stimulate algal growth, thus indicating that phosphorus was the limiting nutrient for algal growth in Lake B. The relatively high levels of growth with combined spikes, especially at concentrations of 1.0 ppm N and 0.05 ppm P, also indicated that algal growth in Lake B water could be increased substantially by additions of these elements and that other nutrients were not particularly limiting for the growth of algae.

Panther Branch

Concentrations of NO_3—N and O—PO_4 (Figure 3) were lower in the upper region of Panther Branch (P—10) than in the portions of the stream (P—30, P—40) below the major part of the Woodlands. This increase in the concentrations of nutrients was due in part to irrigation runoff from the Woodlands golf course. Also, sewage effluent was being introduced into Panther Branch in the vicinity of P—30. The relatively higher nutrient concentrations in Spring Creek (S—10) are the result of sewage effluent which enters the creek from Spring, Texas.

Nutrient limitation studies on low-flow water collected from Panther Branch revealed that algal growth was stimulated by both phosphorus spikes and combined nutrient spikes (Figure 4). Additions of nitrogen did not stimulate algal growth in samples collected from Panther Branch, except at site P—20. Samples collected from Spring Creek had a greater capacity to support the growth of algae than those collected in Panther Branch. During periods of low-flow in Panther Branch phosphorus seemed to be the growth limiting factor. However, nutrient limitation studies with composites of stormwater runoff samples from Panther Branch (Figure 5) showed that algal growth was stimulated by nitrogen spikes or combined spikes and not by additions of phosphorus to the water.

Possible Management Program and Conclusions

The baseline data obtained from the first year's study of Woodlands will be helpful in formulating strategies for managing the water resources of this development. Nutrient limitation studies have shown that increased amounts of nitrogen and phosphorus in water from Woodlands will stimulate the growth of algae. Thus, it will be improtant that advanced wastewater treatment techniques be utilized if the lakes are used to reclaim sewage effluent. During periods of low-flow, when phosphorus would be expected to accumulate in lakes, it may become desirable to use phosphorus precipitating chemicals to lower the phosphorus level below the critical point when phosphorus concentrations approach those known to cause blooms under laboratory conditions. Dilution of the effluent with well water before entry into the lakes could also be used to maintain a desired water quality within the lakes. During periods of high flow, advanced treatment could possibly be suspended, since nitrogen would limit the growth of

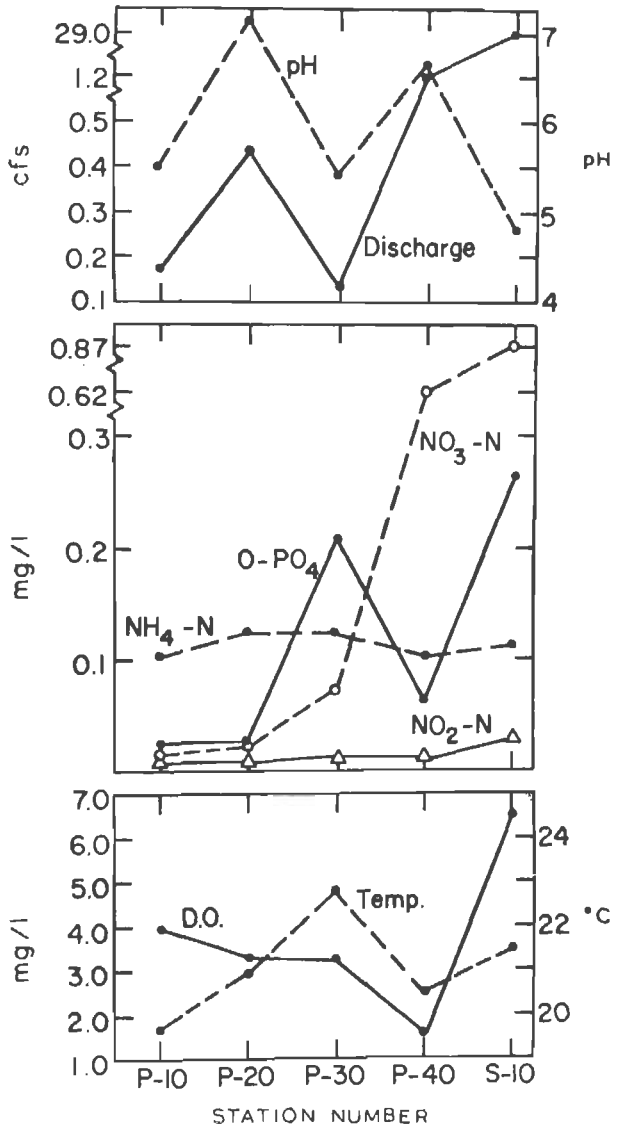

FIGURE 3 : Water quality at various stations on Panther Branch and Spring Creek.

algae. Such a strategy could result in substantial savings in the water treatment program at Woodlands.

In urban areas the first rains and runoff usually contain significant quantities of dissolved solids including troublesome amounts of nitrogen and phosphorus. Thus, it might be advantageous to collect the first stormwater runoff and treat it with the sewage. After the first flush, stormwater could then be directed through the lakes to achieve mixing and washout of accumulated bottom sediments. This procedure could be most useful in mitigating the effects of surface runoff from the golf course and lawns in Woodlands. The impact of surface runoff on the lakes could also be alleviated by limiting or prohibiting homeowner and golf course use of nitrate-nitrogen fertilizers. Instead,

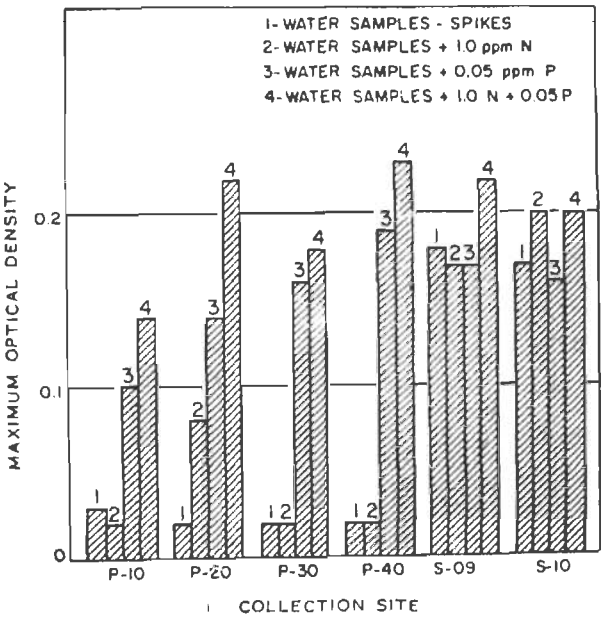

FIGURE 4 : Optical densities of *Selenastrum capricornutum* after 21 days incubation in water collected from various sites on Panther Branch and Spring Creek.

ammonia or urea fertilizers could be substituted for use in increasing lawn fertility. Another source of both nitrogen and phosphorus could be eliminated by reducing the amount of lawn clippings and tree litter which could be transported to the lakes by surface runoff.

Soil renovation of wastewater might be practical under some circumstances. It may be that the large recreational lake should be designed so that ground water serves as the primary source of recharge. Stormwater and sewage effluent could be percolated through and renovated by a spreading basin before going to the lake as ground water.

The above represent only a few possible strategies which could be utilized in maintaining a desired water quality in the lakes of Woodlands. They may be neither necessary nor financially justifiable unless there is strong evidence that one or more will help control eutrophication. Even so, the design of a lake management program which will maintain the aesthetic and recreational values of the lakes in Woodlands can only be achieved through detailed study of the biological and chemical components of the aquatic ecosystems.

Admittedly, there is much controversy over which nutrient is the most limiting for plant growth in aquatic ecosystems. The roles of nitrogen and phosphorus in limiting or enhancing algal growth have been investigated for many years. Recently, however, more attention has been given to carbon as a possible limiting nutrient. This controversy regarding limiting nutrients continues to rage and the fact is that nutrient limitations probably vary from one ecosystem to another and are dependent upon a certain set of physio-chemical conditions

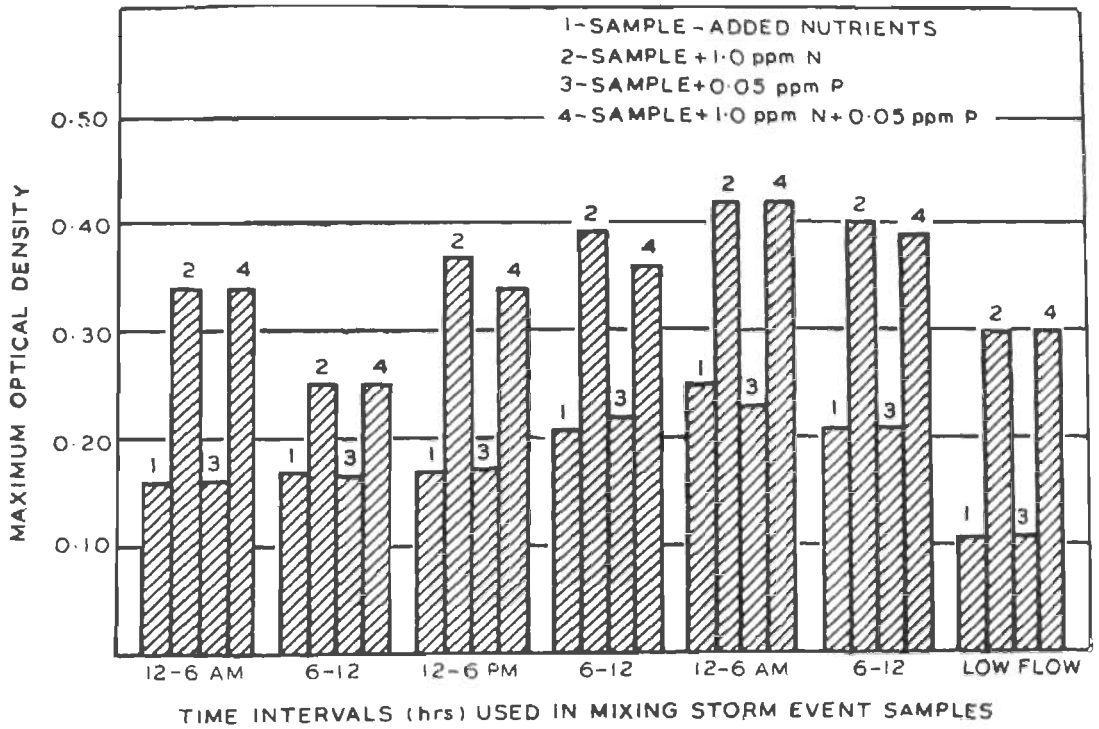

FIGURE 5 : Optical density of *Selenastrum capricornutum* after 21 days incubation in six-hour mixtures of Woodlands stormwater runoff.

which are present within a particular ecosystem. Thus, our data may only apply to lakes in eastern Texas, but hopefully this information will be applicable to similar systems throughout the southern piney-woods region of the United States.

Acknowledgements

This research was supported by Grant No. 802433 awarded to the Department of Environmental Science and Engineering, Rice University, by the United States Environmental Protection Agency. The technical assistance of Mrs. Gail A. T. Fortenberry is gratefully acknowledged. Also, the help of Mrs. Wanda Lloyd in preparing the manuscript is appreciated.

Literature Cited

(1) EMERY, R. M. ; MOON, C. E. and WELCH, E. B. : "Enriching Effects of Urban Runoff on the Productivity of a Mesotrophic Lake." Water Research, Vol. 7, 1973, pp. 1505-1516.

(2) FEDERAL WATER POLLUTION AUTHORITY : "Water Pollution Aspects of Urban Runoff." Pub. WP 20-15, 1969.

3) GOLDMAN, C.R. and ARMSTRONG, R. : "Primary Productivity Studies in Lake Tahoe California." Verh. Int. Verein. Limnol., Vol. 17, 1969, pp. 49-71.

(4) Joint Industry/Government Task Force on Eutrophication : "Provisional Algal Assay Procedure." P. O. Box 3011, Grand Central Station, N. Y., 10017, 1969, pp. 62.

(5) KEUP, L. E. : "Phosphorus in Flowing Waters." Water Research, Vol. 2, 1968. pp. 373-386.

(6) SHANNON, E. E. and BREZONIK, P. L. : "Eutrophication Analysis : A Multivariate Approach." J. Sanit. Engng. Div. Am. Soc. Civ. Engrs., Vol. 98, 1972, pp. 37-57.

(7) STEWART, W. D. P. : "Nitrogen Input into Aquatic Ecosystems." Algae, Man and the Environment, Syracuse Univ. Press, N. Y., 1968, pp. 554.

(8) SYLVESTER, R.O : "Nutrient Content of Drainage Water from Forested, Urban and Agricultural Areas." Algae and Metropolitan Wastes, USPHS, Trans. of 1960 Sem. Taft Sanitary Engng. Center, Pub. No. SECTR W61-3, 1961, pp. 80-87.

(9) United States Environmental Protection Agency : "Methods for Chemical Analysis of Water and Waste." Superintendent of Documents. U.S. Government Printing Office, Washington, D. C., 1971, pp. 312.

(10) WIEBEL, S.R. ; ANDERSON, R.J. and WOODWARD, R. L. ; "Urban Land Runoff as a Factor in Stream Pollution." J. Wat. Pollut. Control Fed., Vol. 36, 1964, pp. 914-924.

Coastal Zone Climatological Studies of the Laurentian Great Lakes

C. R. MURTHY
Research Scientist
Lakes Research Division, Canada Centre for Inland Waters
867 Lakeshore Road
Burlington, Ontario, L7R 4A6, Canada.

J. O. BLANTON
Physical Oceanographer
Division of Biomedical and Environmental Research
U.S. Atomic Energy Commission
Washington, D.C. 20545, U.S.A.

SYNOPSIS

Since coastal zones of the world are increasingly used for recreation and resource development, we at the Canada Centre for Inland Waters have conducted studies specifically designed to characterize, in a climatological sense, the water movements occurring in the coastal zone of the Laurentian Great Lakes. We have seen an array of complexities in coastal currents that vary in magnitude from place to place and from time to time. Nevertheless, there occur certain regimes that appear to repeat themselves with some frequency at any given location. By determining the frequency of occurrence of the various regimes, we can make a climatology of the coastal zone water movements that are particularly relevant to problems of siting power plants, waste water effluent lines, and water intakes. Some years of study are required before a climatology for a coastal region can be realistic for design purposes.

We have succeeded in identifying the following three regimes that make up the elements of a climatology for coastal circulation :

(1) Periods of stagnation or low currents.

(2) Periods of shore-parallel currents lasting 24 hours or longer.

(3) Current reversals occurring between periods of shore-parallel currents.

Data are presented in the paper that describe these three regimes and the physical processes that are relevant in the use of coastal water resources for various human needs.

1. Introduction

We have witnessed in the past decade the emphasis of many oceanographic and limnological studies shift to areas closer to the shore since most of the water exchange for human use takes place within a narrow zone loosely defined as the "coastal zone". The precise definition is rather difficult and in whatever way one defines "coastal zone", it is bound to be arbitrary to the other. Regardless of the definition used, it is clear that the coastal zone is a complex environment where interrelated biological, chemical, geological and physical processes are occurring along the interfaces of water, air and land.

Coastal areas are increasingly used for recreation and resource development. Human activities are bound to intensify with increasing urbanization and heavy concentration of population along the coastal regions of the world oceans and the Laurentian Great Lakes. Such continued pressure for utilization is bound to have deleterious effects on the coastal zone environments. The ecology of the coastal zone environment is strongly influenced by the water movements, thermal structure and the environment's capacity to disperse pollutants discharged into the coastal zone. An understanding of these processes is a basic prerequisite to effective conservation of the coastal zone environments.

We have carried out at the Canada Centre for Inland

Waters (CCIW) a series of field experiments in various coastal areas of Lake Ontario. These studies were specifically designed to study the climatology and coastal zone processes thought to be of particular relevance for such practical problems as thermonuclear power plant siting, discharge of sewage and industrial effluents, and the location of water intakes for drawing water for various human activities.

This paper will examine some of the basic coastal processes based on detailed experimental programs during 1968-1974 in Lake Ontario. While the observed characteristics of the coastal processes cannot be completely explained by available theoretical knowledge, we are attempting here to present these processes as we have observed them in a climatological sense with the above practical problems in mind.

2. Coastal Zone Water Movements

The current regimes in the Laurentian Great Lakes and the oceans exhibit special characteristics near the coastal boundaries. Meandering currents far removed from boundaries are restricted to move primarily along the boundaries once they approach close to the shore. This process of adjustment to the presence of the shore is illustrated in Figure 1. Shown here are current meter data obtained simultaneously from three locations, each at a different distance from the coastal boundary. The data displayed in Figure 1 are hourly averages of the current vector, with the tail of each consecutive vector placed appropriately oriented at the head of the preceding one. This type of data display is often called a progressive vector diagram (PVD) and simply represents the current flow past a point as it changes in time. Most important here is the changing pattern of the flow as distance from shore decreases. About 16 km, the current vector rotates completely each 17 hours with an irregular ill-defined displacement. Closer to shore (11 km offshore), the oscillatory motion is still present, but the net flow assumes an orientation closely parallel to shore. At only 6 km offshore, the rotary motion has disappeared for all practical purposes with well-defined shore parallel flow.

Currents in the open lakes and oceans often have nearly rotary motion, particularly after storms. These currents, called inertial currents, result from a balance between local particle acceleration and Coriolis force due to the rotation of the earth. The period T of such oscillations is given by $T = 2\pi/f$, where f is the rotational frequency of the earth defined by $f = 2\Omega \sin\phi$; Ω is the angular speed of rotation of the earth and ϕ is the latitude. At the latitude of the Laurentian Great Lakes, T is close to 17 hours. At locations such as Southern India, T is close to 60 hours. Physically, what it means is that the current vector rotates by 360° every inertial period. In addition to inertial currents, tidal currents with periodicity of 12 or 25 hours are quite common in the oceans although they are not dominant in the Great Lakes. However, in the coastal zones, these rotary currents must be modified since particle velocities perpendicular to the coast must vanish there. Consequently, there is an adjustment zone, typically 5 to 10 km wide, where rather high currents are forced to flow more or less parallel to the local shoreline. This zone

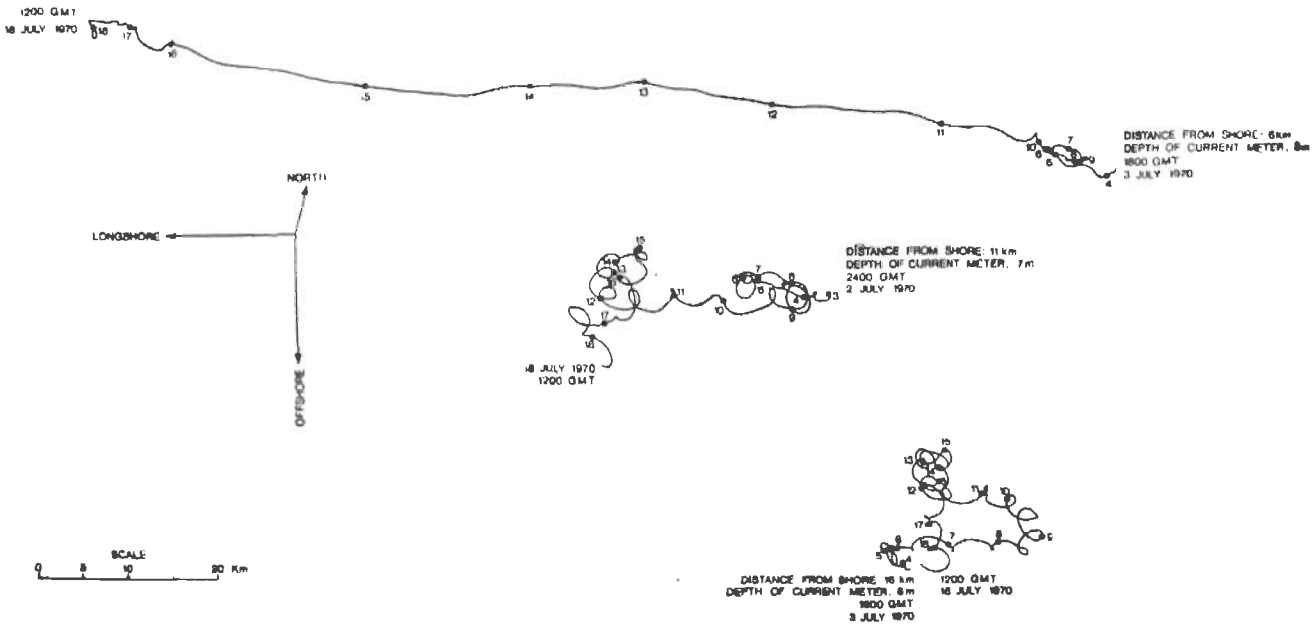

FIGURE 1 : Progressive vector diagrams from current meter data obtained off Oshawa, Lake Ontario, 3-18 July 1970.

has been described in the literature as one where "Coastal Jets" may be observed(1). Csanady(2) has also referred to this zone as a "Coastal Boundary Layer."

To develop a climatology of the water movements in the adjustment zone, hereafter referred to as the coastal zone, we have conducted extensive programs of current measurements, thermal structure and dispersion experiments in several locations of Lake Ontario. Figure 2 shows the geographic distribution of nearshore programs carried out during 1968-1974 by CCIW.

Coastal currents are usually measured by two well-known techniques : Lagrangian and Eulerian. Lagrangian techniques observe with current following devices the distance a "parcel" of water moves in a given time. Eulerian techniques, on the other hand, observe flow of water past a fixed point with current meters. One can expect some differences between the two techniques, particularly when there may be velocity gradients in a region where the two techniques are used simultaneously. A theoretical discussion by Longuet-Higgins(3) discusses the differences in water mass transport that may result. Our experiments in the coastal zone of Lake Ontario indicate that the differences between the two techniques are negligibly small(4) over time scales of interest in the coastal zone. Only when observation duration exceeds about 17 hours (the inertial period for Lake Ontario) do our experiments indicate that some discrepancy may result between the two techniques(5)(6).

Coastal dispersal processes were studied by the familiar Lagrangian technique of introducing fluorescent dye tracer into the coastal zone and by observing the growth and dilution of the resulting dye plume. A continuous dye plume is a better experimental target to study mixing and dispersal phenomenon in the coastal zone than is an instantaneous dye patch(7)(8).

3. Experimental Design and Data Collection

The coastal zone studies conducted at CCIW placed emphasis on physical processes operating in the nearshore area. These processes were interpreted through experiments in the diffusion of dye and through obtaining long time-series of current and temperature data at fixed locations. The former technique collects data over a period of one or two months. Since these two techniques cover such different time-scales, a separate discussion is desirable on the diffusion experiments and the experiments using a number of moored current meters and temperature sensors.

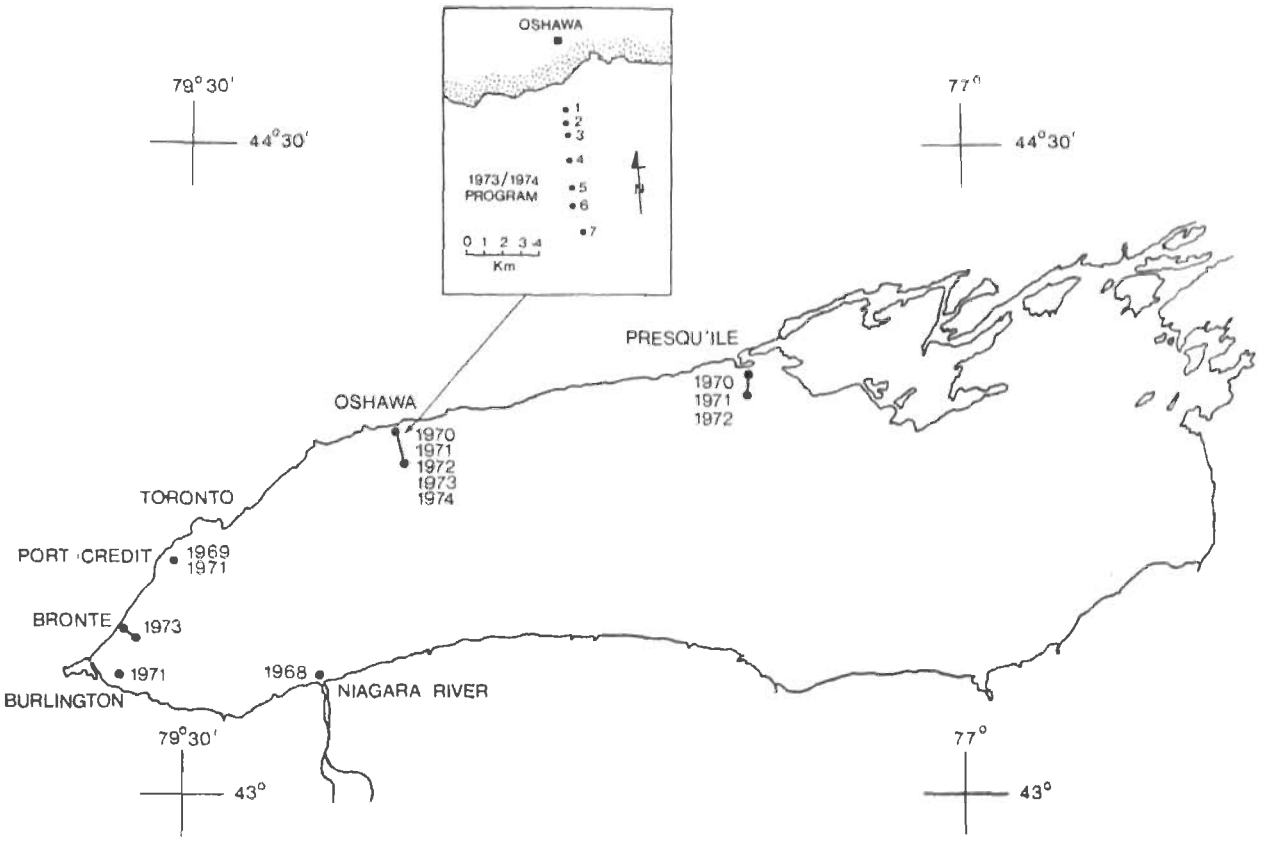

FIGURE 2 : Map of Lake Ontario showing the locations of nearshore programs during 1968-74. The inset illustrates the lay-out of current meters for a typical program.

The time-series of current and temperature data were obtained from self-contained instrument packages that automatically measure current speed and direction as well as temperature. Although the instruments record temperature and currents at 10 or 20-minute intervals, we have used hourly mean values since we are primarily interested in climatological studies. The data are collected at fixed depths and different distances offshore using a series of taut-line moorings, an example of which is shown in Figure 3. Our basic array design was to set out a series of current meters so that some resolution; across the coastal zone was obtained at a fixed depth below the water surface as well as a fixed depth above the bottom. (Typical numbers of moorings used in Lake Ontario are illustrated in the inset of Figure 2).

In our diffusion experiments, we made observations of a fluorescent dye tracer introduced into the receiving waters. We have used rhodamine-B dye as the tracer because it can be easily detected in small concentrations (as low as 1 part in 10" parts of water) by means of optical fluorometers. The dye is injected in a continuous stream into the water by means of the system shown in Figure 4. Essentially, the system simulates, a typical outfall by pumping the dye solution, pre-adjusted to the *in situ* density of the receiving waters, through a 11-nozzle diffuser. The nozzles are spaced 1 metre apart. The diffuser is suspended at the desired depth in a taut-line mooring (Figure 4) and is free to rotate and align itself in the direction of current flow by means of a large tail fin.

A line-source dye plume of approximately 10 m length is soon formed due to the prevailing coastal currents. The depth of dye injection may be varied 3 m from the free surface down to 3 m of the lake bottom in approximately 20 m deep water. The submerged dye plume is surveyed with fluorometers by towing sampling systems behind instrumented launches. Details of the operation of the complete system have been reported by Murthy([8])([9]).

A typical experiment consists of releasing dye in the early morning hours so that a well-developed dye plume is formed within a couple of hours due to the prevailing coastal currents. Close to the diffuser, the dye plume is generally narrow and slender. However, at some distance from the source the dye plume spreads due to lateral and vertical mixing. Lateral meandering due to large-scale turbulent eddies becomes particularly important as revealed by time-sequence synoptic aerial

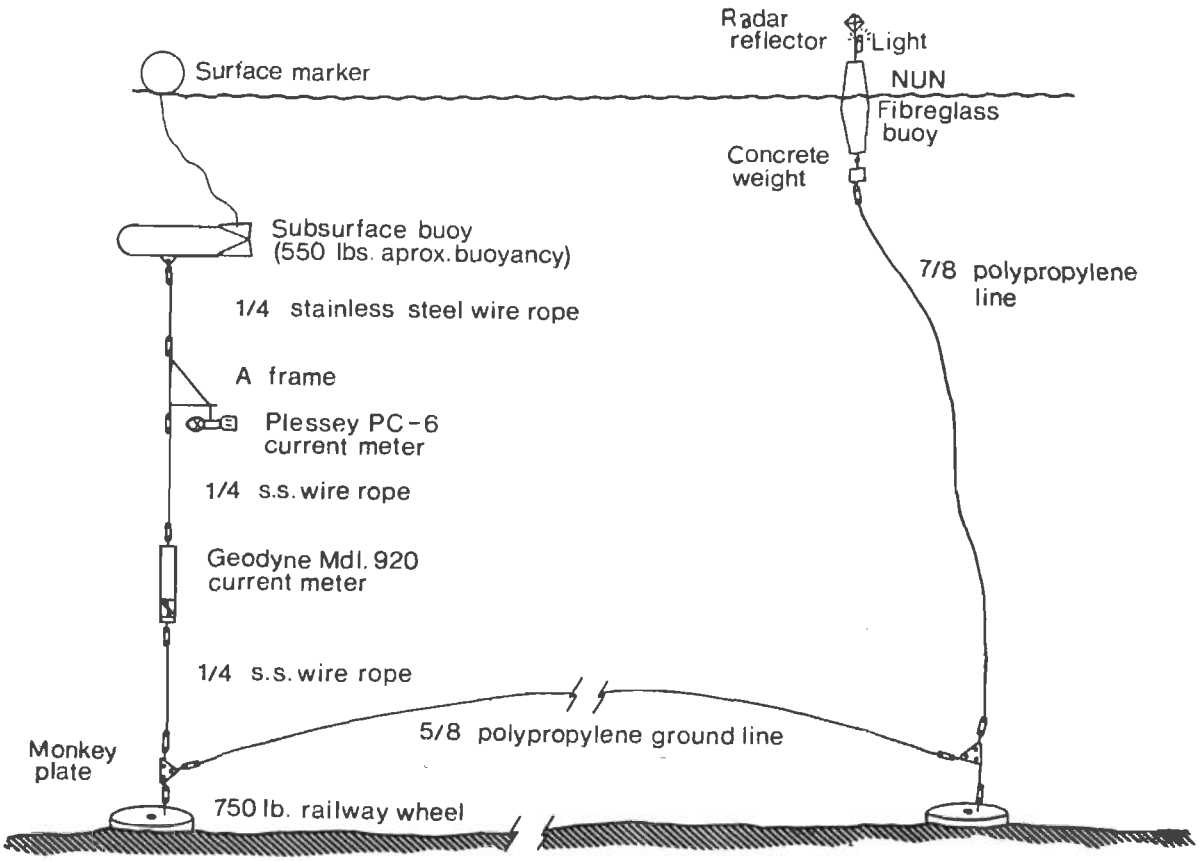

FIGURE 3 : An example of a taut-line mooring of recording current meters.

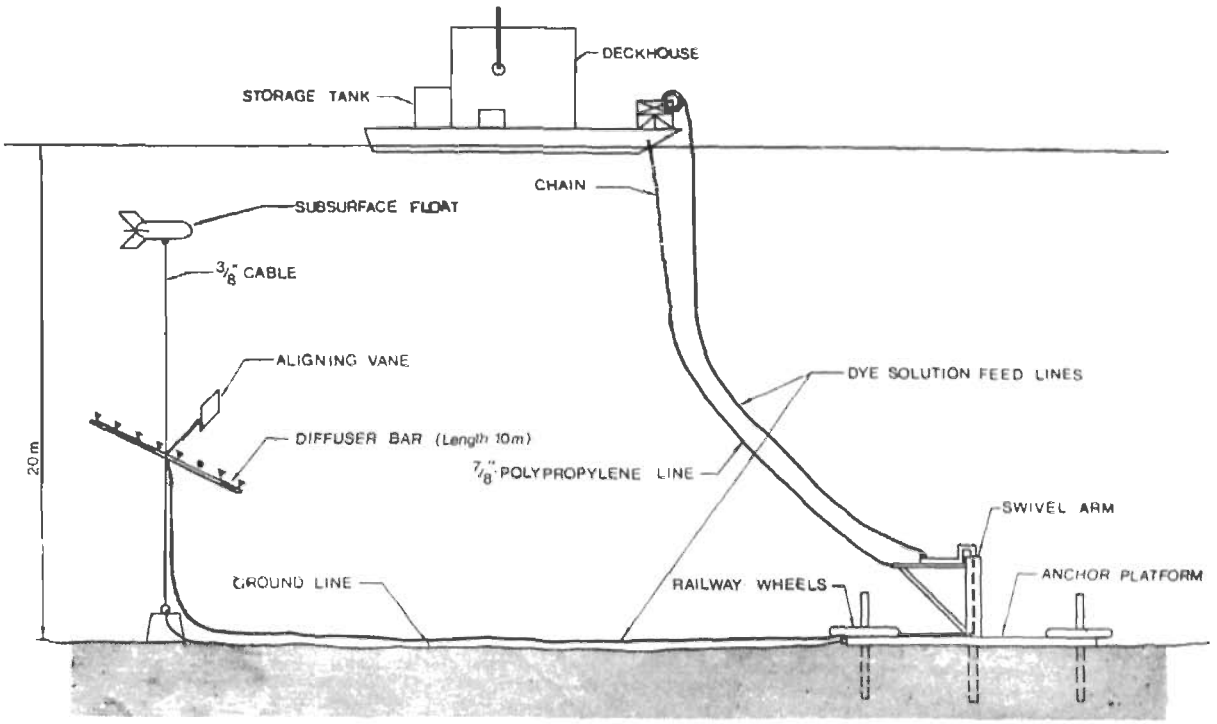

FIGURE 4 : Fluorescent dye release system to simulate outfall conditions.

photographs. Figure 5 shows a mosaic of the dye plumes prepared from time-sequence air photos. Note in Figure 5 that the lateral meandering of the dye plume was quite pronounced beyond about 1,000 m from the dye source.

Sampling by means of the fluorometers was conducted systematically at several regularly spaced cross-sections. The first cross-section was chosen as close as possible to the dye source (usually 200-300 m). Two anchored marker flags were dropped across the dye plume such that the line joining them is approximately perpendicular to the plume centre-line. The dye plume was sampled several times using the flags as reference markers. Upon completion of one cross-section, the instrumented launch was moved further downstream and the procedure was repeated. Under fair weather conditions, we were able to sample four to six regularly spaced cross-sections during an experiment making 15-20 crossings of the plume in each cross-section.

4. Coastal Zone Climatology

The complexities of water transport and dispersal processes in the coastal zone are well recognized[5][10][2][8]. However, from a series of experiments of the type described earlier, we will attempt to describe certain characteristics of the coastal currents that are consistently observed in several locations. In this section, we will illustrate these characteristics from results of several series of experiments with the sole objective of developing a classification of typical coastal zone regimes that have practical implications.

We illustrate first the observed complexities from a series of experiments carried out during 1971 at two locations : Hamilton, and Port Credit in Lake Ontario (see Figure 2). These experiments were carried out simultaneously and consisted of measuring coastal currents and temperature structure. We used Lagrangian current drifters at several depths to measure mean current velocities over a 6 to 8-hour period. A convenient way of presenting this data is a current hodograph. Mean current hodographs for this series of experiments are displayed in Figures 6 (*a*), (*b*) & (*c*).

Immediately apparent from a study of Figure 6 is that currents on the same day at the two locations can often be quite different. For example, on 29 April, current directions were similar but speeds were almost 3 times faster at Hamilton. On the following day, speeds were similar but directions were different by almost 90 degrees. For other examples of contrast, compare data for these two locations in July and October [Figures 6 (*b*) & (*c*)].

Not only are there differences between the two locations, but there are seasonal differences at the same location Note that speeds are usually greater in summer and autumn, a fact observed by many investigations of currents in the Great Lakes[5]. Another difference

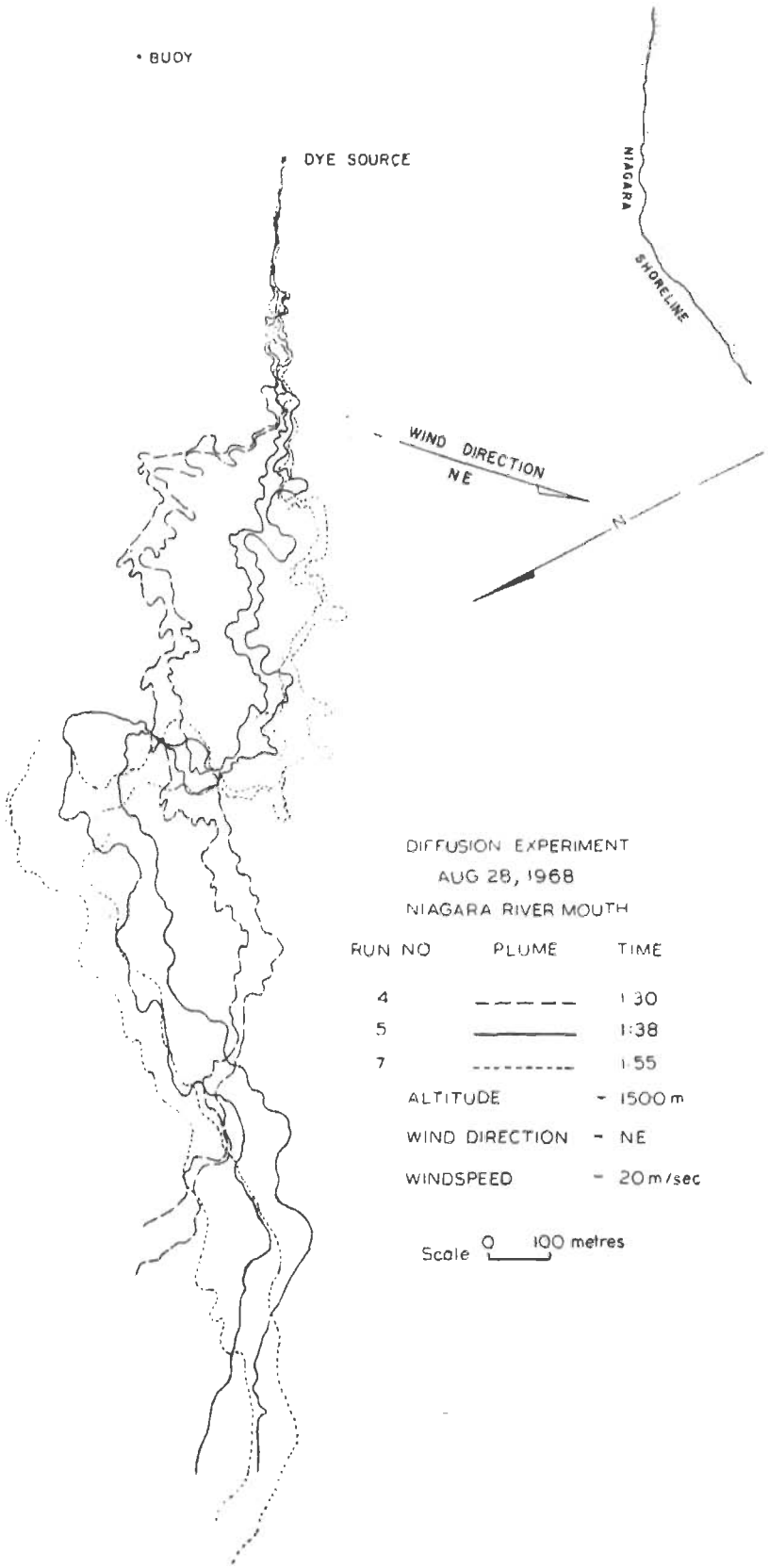

FIGURE 5 : Dye-plume behaviour in coastal currents from a typical diffusion experiment. Note the lateral meandering around 1,000 metres from the dye source.

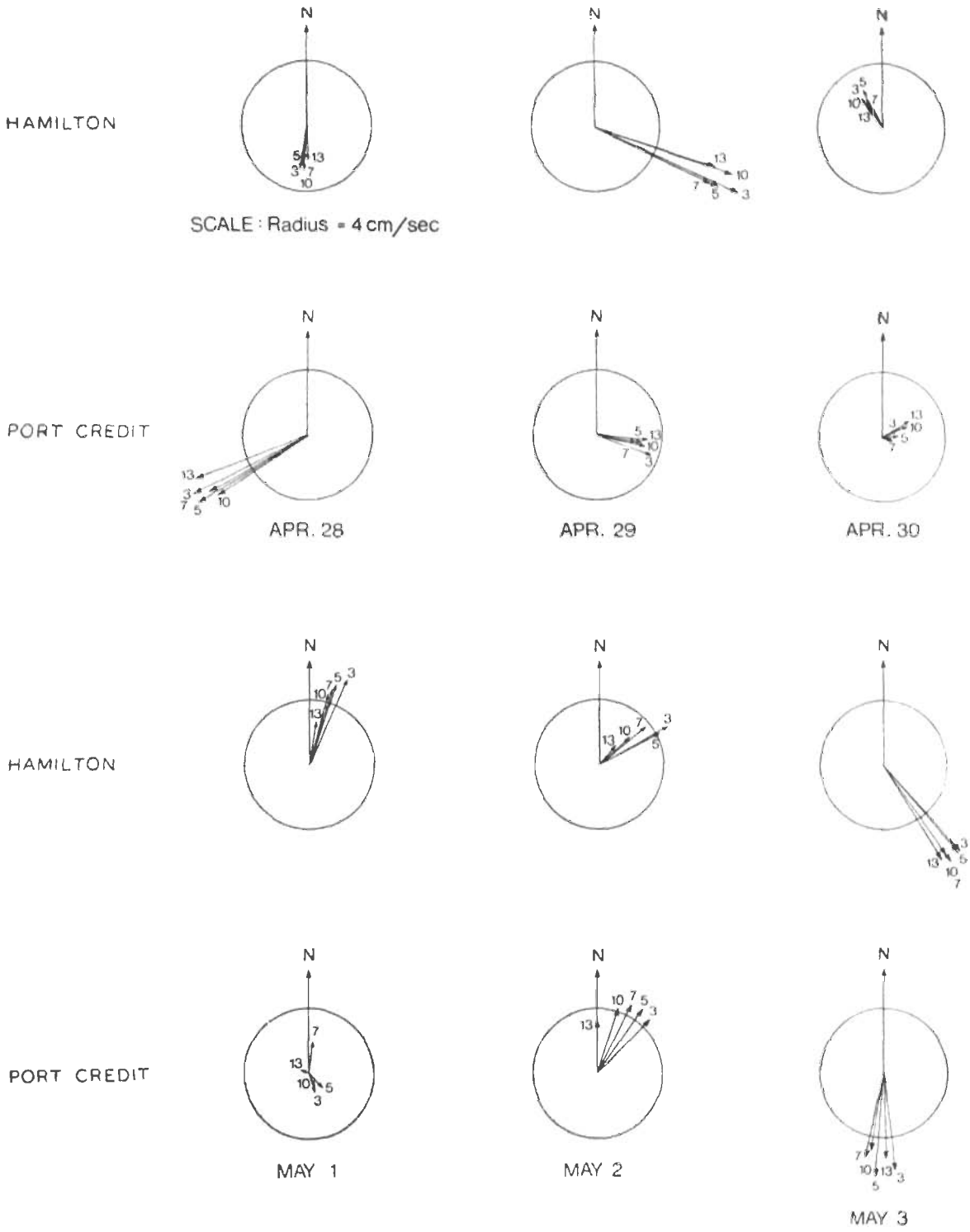

FIGURE 6 (a) : Comparison of coastal currents at two locations measured simultaneously—Port Credit and Hamilton Lake Ontario during April-May 1971. Numbers indicate depths of measurements in metres.

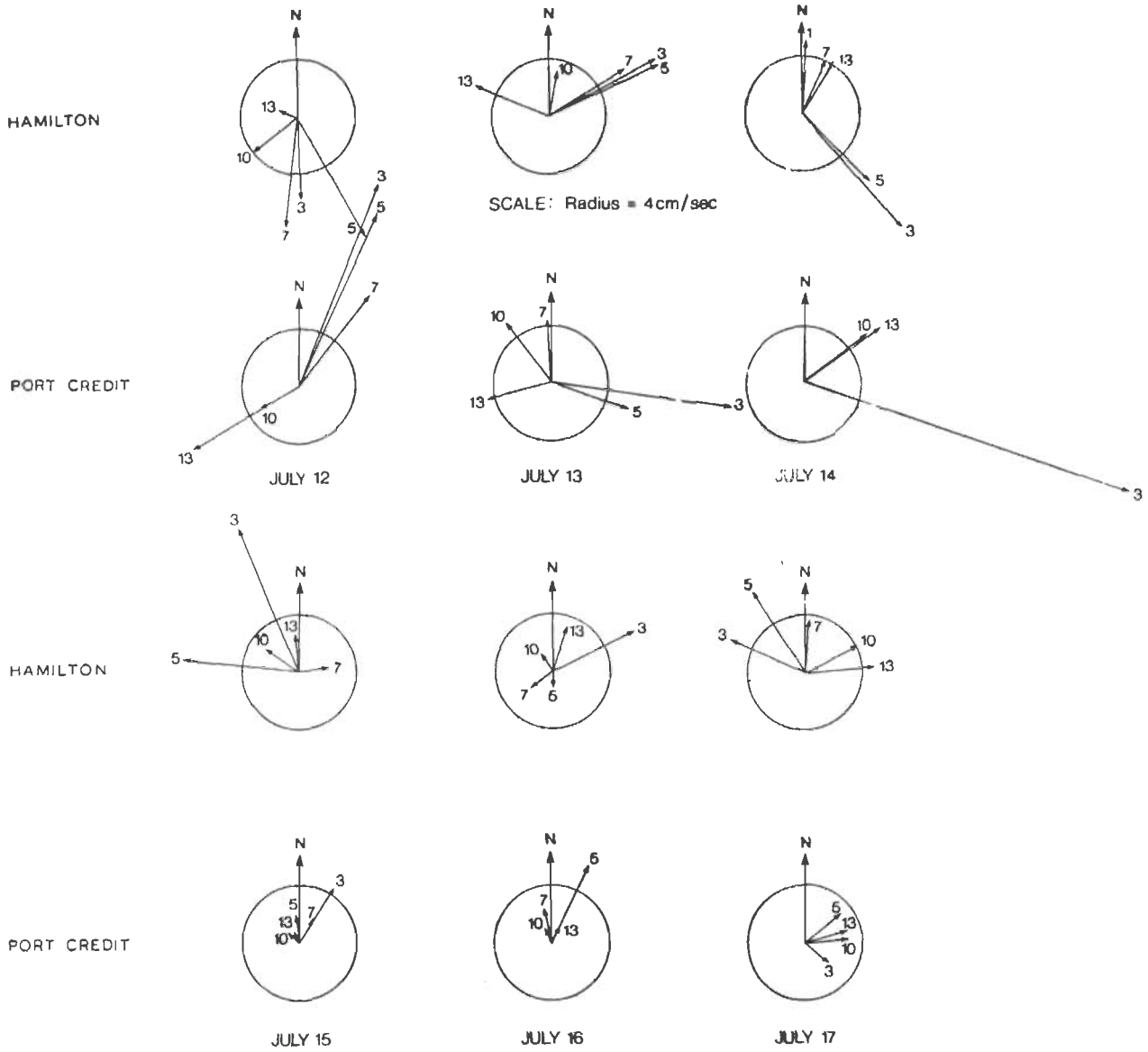

FIGURE 6 (b) : Same as Figure 6 (a) except for July 1971.

between spring and summer is that the waters are thermally stratified during summer and early autumn. Stratification has the effect of altering the vertical changes in currents. For example, lake water in spring is vertically homogeneous, with the result that the currents at different depths flow usually within 45° of the same direction. This is particularly true when currents are strong, although deviations from this general pattern can occur on the same day. Contrast the vertical variations in currents in spring with those in summer [Figure 6 (*b*)], when there is usually a strong vertical variation in temperature. There are many days when the deeper currents flow in opposite directions from those nearer the surface. Note for example data obtained between 12 July and 17 July.

In addition to the above complexities, we have observed days of extremely low current flow, almost stagnant, that can persist for several days. April 30 at Hamilton [Figure 6 (*a*)] was just such a period. We have reproduced the tracks of the current following devices (drogues) during that day (Figure 7). Clearly, pollutants discharged in such an environment will form a stagnant pool in a manner analogous to the drogues. Note that on 1 May at Hamilton, the currents accelerated greatly. Pollutants would be flushed out of the

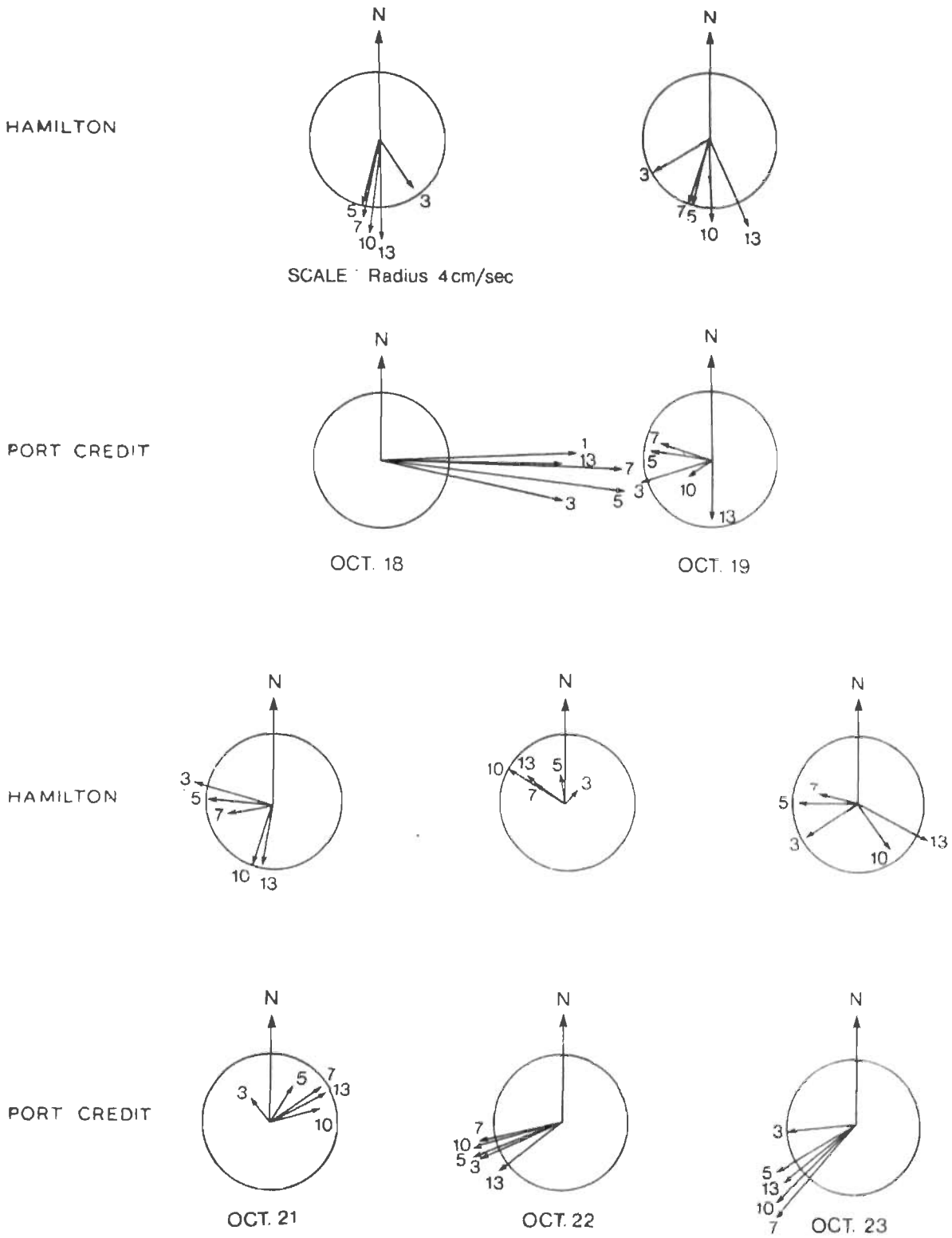

FIGURE 6 (c) : Same as Figure 6 (a) except for October 1971.

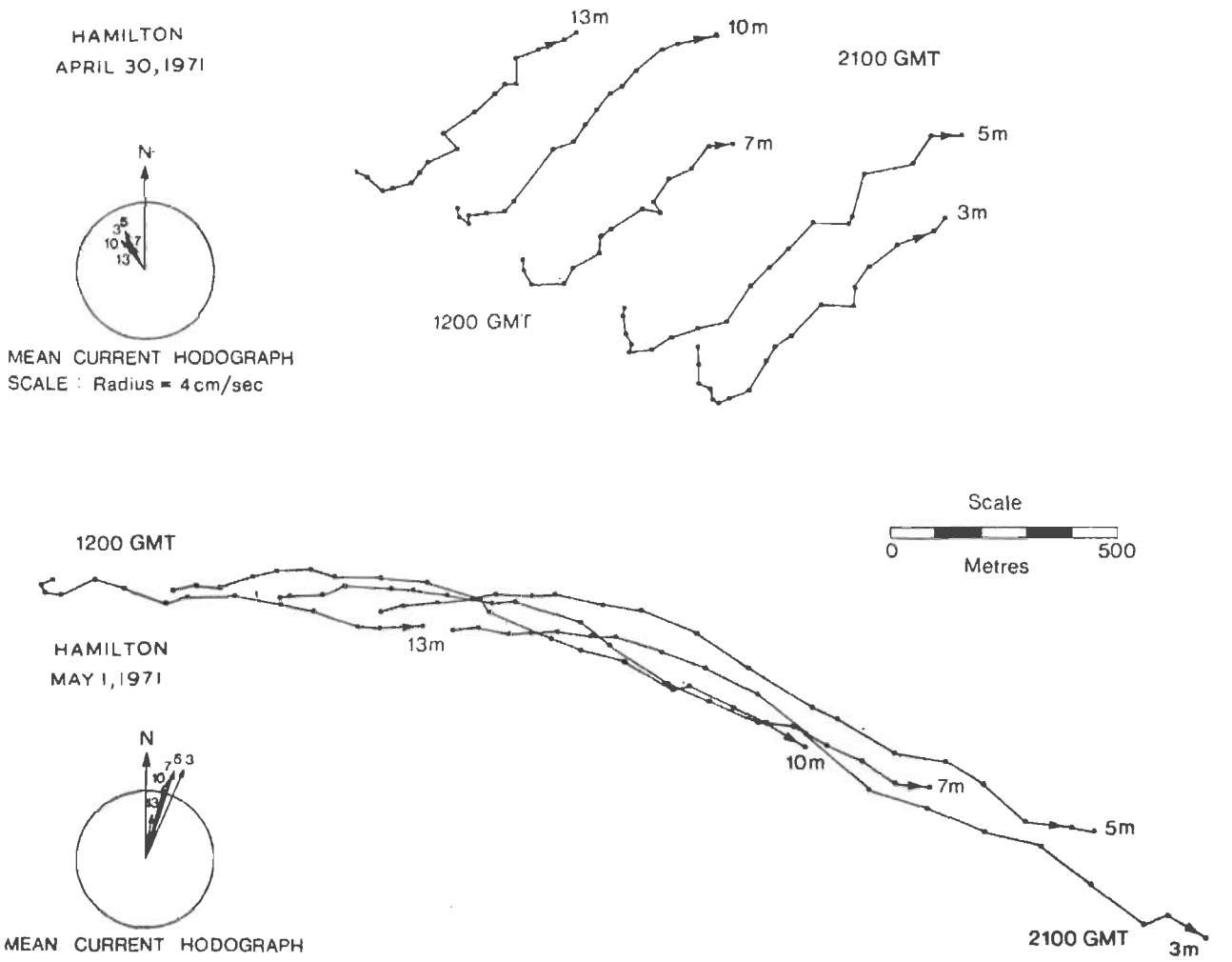

FIGURE 7 : A comparison of coastal currents at Hamilton, illustrating the change from a stagnant flow regime to a steady, strong shore-parallel current regime within 24 hours.

area on such a day. These complexities have been amplified by Murthy([8]) and will be discussed later. The stagnant flow periods may last for several hours up to several days, and they may be thought of as interludes between well-defined longshore flow episodes([5]).

Longshore currents are accompanied by upward and downward movements of water in the coastal zone([10]). When the water is thermally stratified the upward motions bring cold subsurface water into the coastal zone, whereas the downward motions bring warm surface water there. Upwelling and downwelling of water in the coastal zone is one of the more important processes affecting use of the water for human needs.

An experiment off Oshawa, Lake Ontario for 5 to 14 October 1970 contains an excellent example of an upwelling-downwelling cycle [Figures 8 (*a*) & (*b*)] and how this cycle influences the characteristics of currents in the coastal zone. Prior to 5 October, easterly flow had been established by winds blowing predominantly to the east and this flow persisted for several days. As a consequence, the cold stratified water upwelled into the coastal zone [Figure 9 (*a*)]. The 10°C isotherm was located up at the surface about 7 km offshore. On the 7th of October strong winds toward the west began to blow driving the warm surface waters inshore and to the west. By 12 October, the 10°C isotherm was depressed downward along the bottom [Figure 9 (*b*)]. The width of the coastal zone is about 10 km, and it is within this zone that water temperature fluctuates greatly.

Associated with the change-over from upwelling to downwelling are reversing currents. As the change-over is occurring, the water mass as indicated by its temperature undergoes a complete mass exchange. Note that by 9 October, the water mass in the coastal zone is completely mixed as indicated by its temperature [Figure 9 (*b*)].

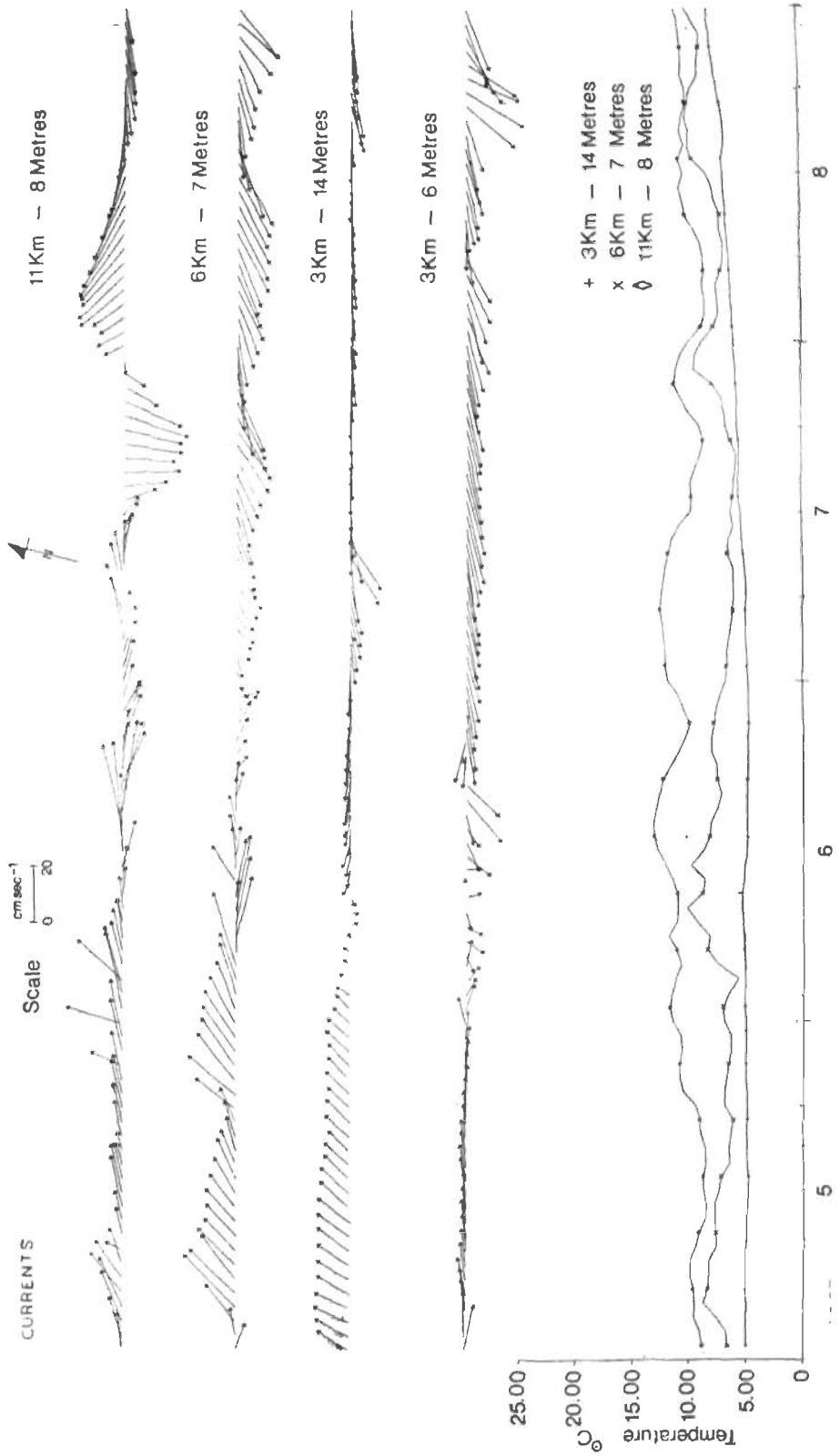

FIGURE 8 (a): Time-series of currents and temperature at 3 km (depth 6 m and 14 m) 6 km (depth 7 m), and 11 km (depth 8 m) from the shore off Oshawa, 5-8 October 1970.

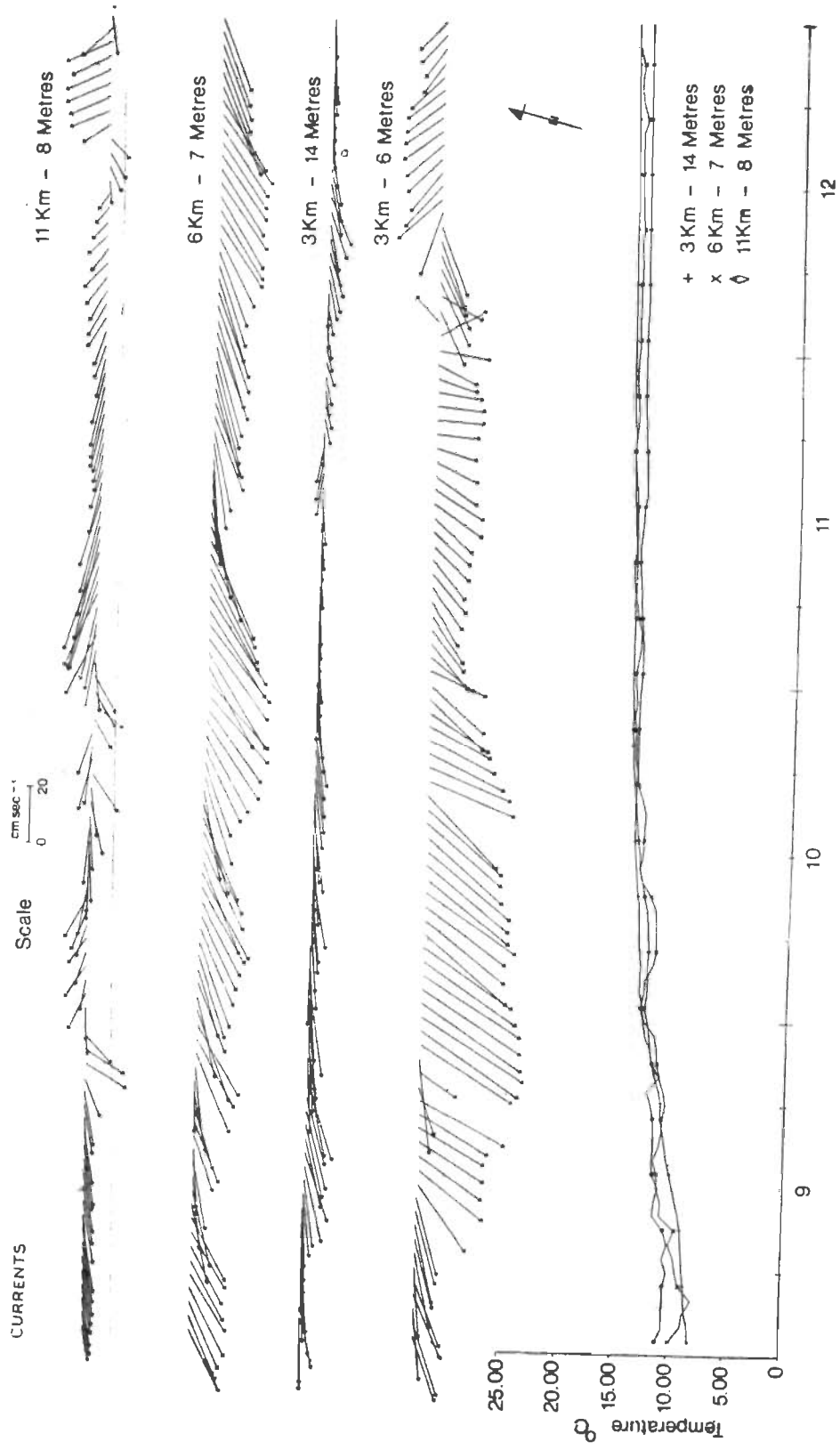

FIGURE 8 (b) : Same as Figure 8 (a) except for 8-12 October 1970.

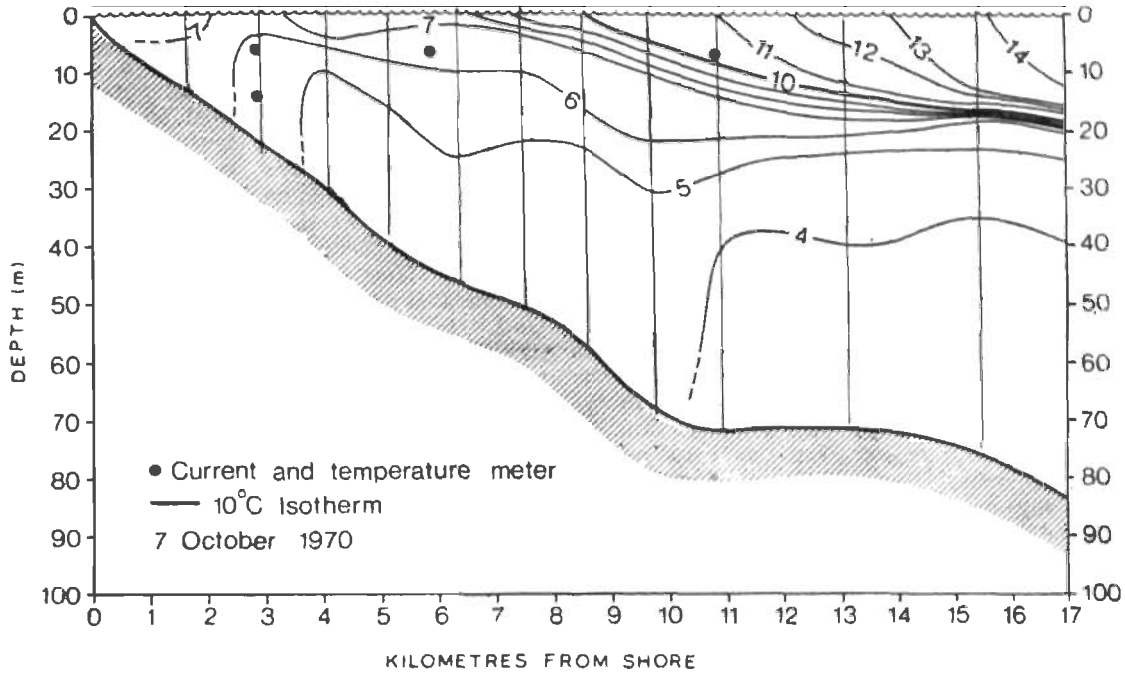

FIGURE 9 (a) : Thermal structure illustrating upwelling of coastal waters off Oshawa. Corresponding to data of Figures 8 (a) and 8 (b).

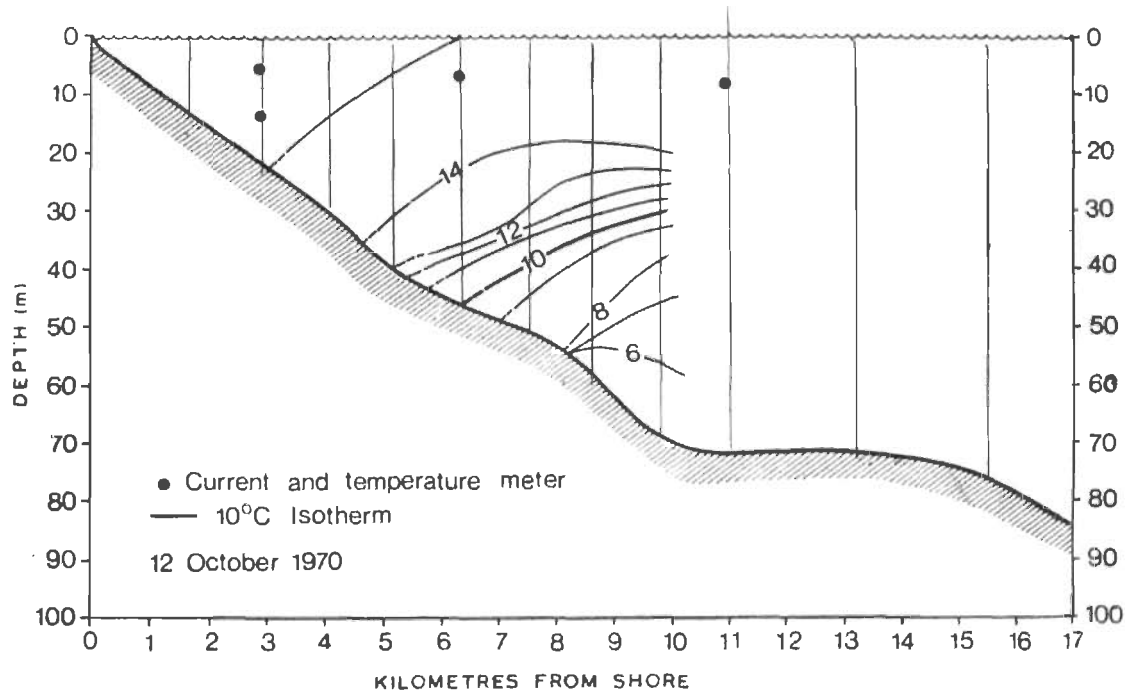

FIGURE 9 (b) : Thermal structure illustrating downwelling of coastal waters off Oshawa. Corresponding to data of Figures 8 (a) and 8 (b).

This mass exchange undoubtedly occurs even when the lake is homogeneous (when temperature can no longer be used as an indicator). Consider the near surface currents measured simultaneously during the upwelling/downwelling cycle discussed above at three locations in the coastal zone [Figures 8 (*a*) & (*b*)]. The currents 6 km offshore reversed later than those at 3 km offshore. It is often observed that sluggish currents at one location may be accompanied by fast currents only 3 km away. This situation induces large lateral shear in the coastal zone which causes rapid mixing of water in the coastal zone([6]).

Out of the array of complexities of coastal current and thermal structure that we see from place to place, from season to season and from year to year, there are certain regimes that can be identified that repeat themselves with some frequency. It is the determination of the frequencies of occurrence of the various regimes that make up a climatology. Several years of experimental data are required before a climatology for a certain coastal region becomes realistic. However, based on experimental studies in a number of locations of the Great Lakes, we have identified the following coastal regimes :

(1) Periods of stagnation or low currents ;

(2) Periods of shore-parallel currents lasting 24 hours or longer ;

(3) Current occurring between the periods of shore-parallel currents usually occurring between periods of upwelling and downwelling.

The practical implications of these regimes in so far as the dispersal capacity of pollutants in the coastal zone and utilization of coastal waters for various human and other needs will be discussed in the subsequent sections.

5. Coastal Dispersal Processes

Having discussed the complexities of the coastal flow regimes, let us now attempt to look at some of the implications of these flow regimes on the mixing and dispersal processes. These processes are of practical interest in the disposal of waste effluents and in the direct utilization of coastal waters for various human and other needs. Mixing and dispersal processes in the coastal zone are equally complex as evidenced from a number of experiments carried out in several locations. We will use some typical experiments to illustrate these complexities.

From a waste disposal point of view, the worst situations are the stagnant or very weak current periods during which the discharged effluents form stagnant pools with very little transport and mixing. With the likelihood of onshore transport, the deleterious effects of such episodes for recreation and other water uses could be disastrous. Figure 10 illustrates a typical situation of diffusion in the presence of weak coastal currents. The dye was released on 18 August and the plume developed in the general direction of the current. With the regular sampling at 500 and 1,000 m from the source, the maximum mean concentrations at the centre of the plume were 45 and 20 ppb. However, on the morning of the 19 August, a large pool of dye approximately 1 km wide and 3-4 km long remained in the vicinity of the dye source, slowly drifting in the direction of the current. The dye pool was mapped disclosing that concentrations in excess of 100 ppb were observed at distances of 1,000 m from the source. Fortunately, the prevailing currents on that day were offshore and freshened later in the day. Consequently, the accumulated dye pool was transported to offshore waters. Undoubtedly, such conditions are severe from the point of view of dispersing effluents in the nearshore zone. On the other hand, if the prevailing currents were onshore, the accumulated pool of dye may be transported toward the shore region and may remain trapped in the shore region. Figure 11 illustrates this situation from an experiment carried in the same location during 4-5 June. The persistent trapping of the effluents in the coastal zone has often been referred to as "coastal entrapment" phenomenon.

Following our flow climatological classification, the next regime of importance is periods of steady shore-parallel currents. Under such conditions any pollutant source located in the coastal zone would undoubtedly result in a regular effluent plume. The "mixing zone" (depending on the desired dilution) is the net result of the average current speed, persistency of current in a given direction and turbulent mixing. If currents are low and turbulent mixing is weak, there is a likelihood of fumigation of the nearshore zone over a 3-5 day period of persistency, which is the typical current reversal period. In our series of dye plume diffusion experiments in several locations we have encountered several occasions of steady and shore-parallel currents. Figure 12 shows the measured cross-plume mean concentration distribution of a typical experiment and it reasonably approximates a Gaussian distribution. For this reason, Gaussian diffusion models have been extensively used for quantitative modelling and dilution estimates of continuous effluent plumes([11]). These models have adequately demonstrated that one can make reasonable estimates of the so-called "mixing zone" around an effluent source, knowing the average current speed, persistency of current in a given direction and the available knowledge of turbulent diffusion. However, after a period of steady currents, one can encounter current shifts (or meandering currents). Under these conditions, what appeared to be a steady and regular plume shifts in the direction of the current shift with "accelerated diffusion" accompanied by rapid dilution. Figure 13 shows typical measured cross-plume mean concentration distributions from one such experiment, considerably departing from the Gaussian distribution. Although determination of the "mixing zone" is rather difficult under such complex cases, shifting currents have beneficial aspects from the point of minimizing the impact of contamination of the coastal zone through efficient dispersal of effluents. Figure 13 clearly illustrates

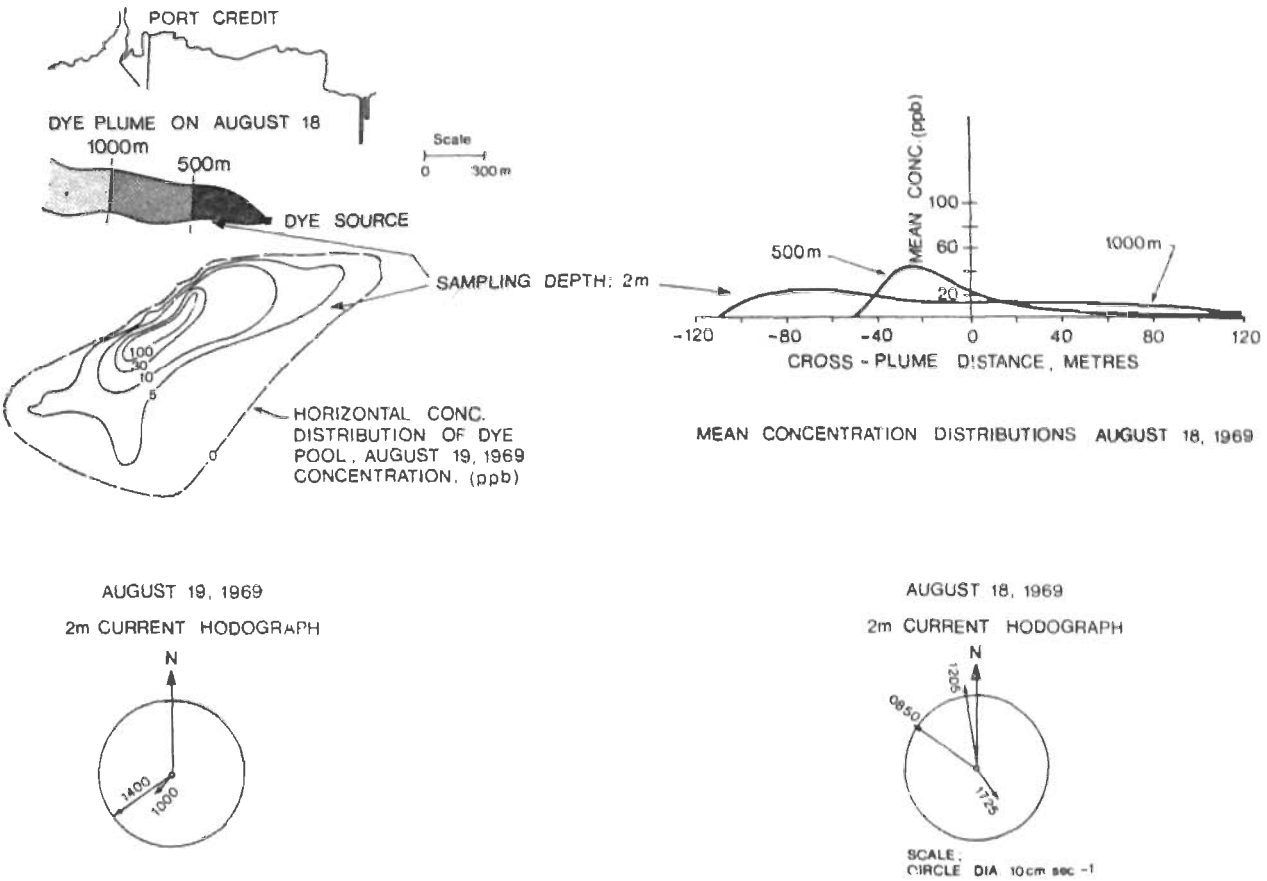

FIGURE 10 : Dispersal characteristics during steady currents followed by a stagnant flow regime.

the rapid dilution of the dye due to accelerated spread of the plume in the cross-plume direction.

Finally, the transition period between periods of shore-parallel currents are invariably accompanied by a complete reversal of direction of currents. As discussed earlier, these episodes are accompanied by upwelling and downwelling of coastal waters. During such episodes, entire coastal waters are renewed as a direct consequence of the mass exchange offshore[2][5]. The mixing and dispersal of effluents in such flow regimes is very efficient[11][8]. These periods are extremely favourable from the point of view of large-scale dumping of waste effluents (resulting from say dredge operations).

We have shown that several physical processes contribute to the mixing and dispersion of pollutants discharged into the coastal zone ; eddy diffusion due to turbulence, shear diffusion due to the interaction of current shears and turbulence and diffusion due to turbulence generated by breaking surface and internal waves. In reality, since it is difficult to separate out the processes, one attempts to quantify the overall effects on mixing and dispersion by defining certain dispersion parameters and their relationship to the observed environmental conditions. The data and results of field diffusion experiments conducted in widely varying environmental conditions have been extensively used to estimate diffusion parameters and their characteristics. It is not our intention to go into the discussion of these aspects here as they have been adequately reported in literature[12][13][14][15][16]. These diffusion characteristics have provided a basis for quantitative modelling of a number of coastal diffusion problems[17][11][18] and are currently being used extensively in CCIW modelling programs[19][20].

6. Discussion

While we recognize the complexities of the coastal processes, it may perhaps help in the appreciation of the above complex experimental data and results if we discuss some practical problems involving the direct use of coastal waters for human and other needs : For brevity, we will consider only some specific examples :

(*a*) *Recirculation* : This is particularly an important problem in thermonuclear power plant siting. The location of inlets and outlets for drawing water for condenser cooling and the discharge of hot waste water is quite critical in view of the bi-modal characteristics of the coastal currents.

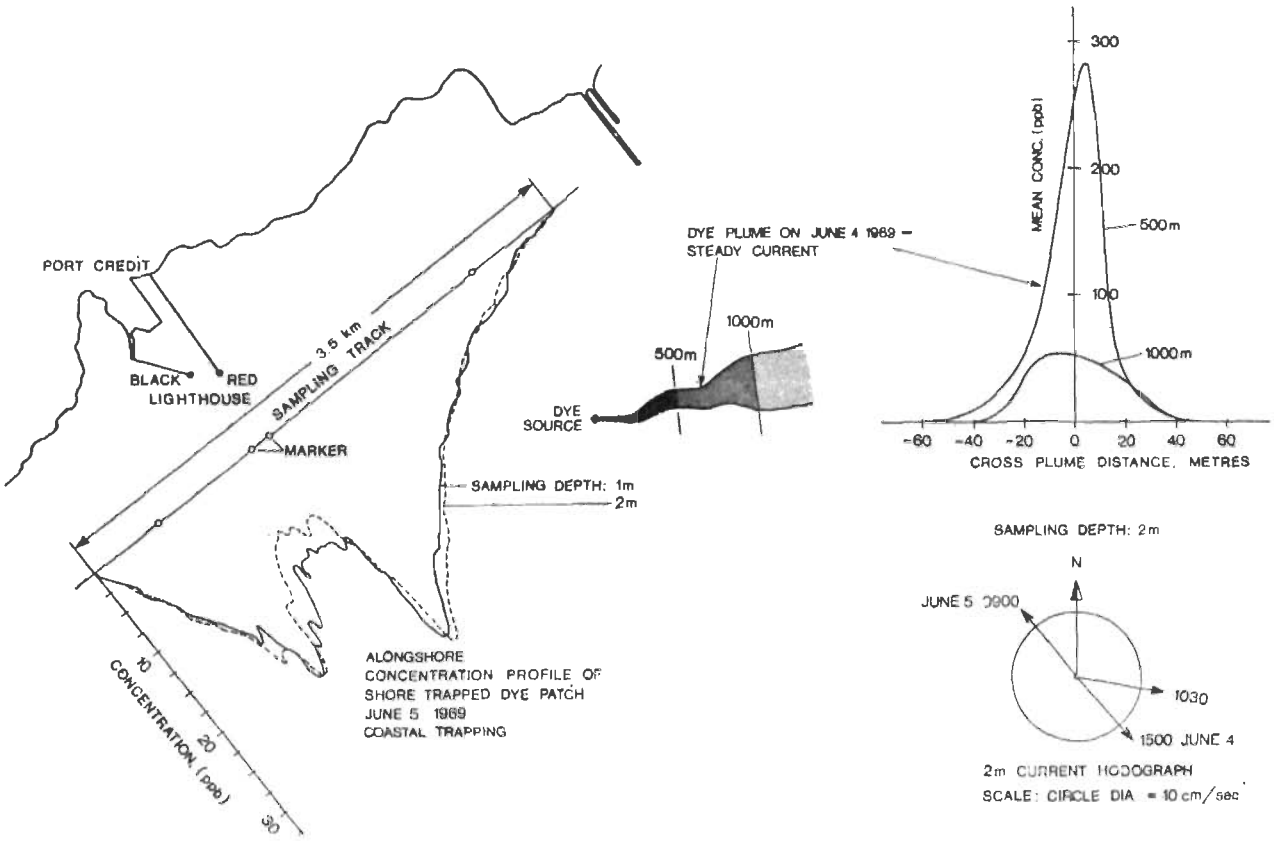

FIGURE 11 : Dispersal characteristics during steady currents followed by an onshore current shift illustrating coastal trapping of dye.

With periods of stagnation or very weak currents and frequent current reversals, recirculation of warm water into the inlets may result in considerable power reduction. Another similar problem of particular interest is the locations of sewage or other industrial waste effluent outlets and intakes for drawing water for drinking and other human needs. There are several engineering solutions to problems of this type. For example, one can locate the inlet in the hypolimnion for drawing water and discharge waste water in the epilimnion. While this may be a desirable solution for locations of inlets and outlets for thermonuclear power plants, it is certainly undesirable for the location of sewage effluent outlets. If not for any other reason, the discharge of sewage effluent or other waste waters in the surface layer of the coastal waters is undesirable aesthetically as well as recreationally. In this case the location of the sewage effluent outlet at deeper depth and the location of water intake in the surface layer may be desirable. However, the practical implication of this choice will be discussed briefly later. Other engineering solutions to this problem are locating two inlets on either side of the outlet and switching back and forth depending on the direction of coastal currents or possibly offsetting the locations of the inlets and outlets with depth and/or distance from the shore. Operationally such systems are no doubt complex and expensive but certainly not insurmountable technically.

(*b*) *Sewage Outfall Disposal* : Earlier in this discussion we mentioned the possibility of discharging sewage and other waste effluents at deeper depths to eliminate contamination of the surface layer waters (out of sight, out of mind). Such methods are widely used in oceanic coastal zones[21][22][23] by using offshore submarine outfalls placed at the ocean floor at some distance say 1-2 km from the shore. The underlying idea is to trap the effluents below the pycnocline and further mixing, dispersion and transport is controlled by the hypolimnion currents and their turbulent eddies. Such submarine outfalls are successfully in operation at several places (for example, Santa Monica, San Diego). In the Laurentian Great Lakes, however,

these methods may not be practicable due to frequent upwelling and downwelling of coastal waters. With the discharge below the thermocline, the effluents most probably are trapped below the thermocline, in the hypolimnion. The transport and dispersion processes are considerably weaker in the hypolimnion compared to the epilimnion[23][9][24]. With the possibility of occasional upwellings and shoreward transport, very high concentrations may be brought to the surface close to the coastal zone. Doubtless such conditions are unfavourable for waste disposal in the coastal zone, although there is a good possibility of dispersing effluents effectively due to intense vertical mixing usually associated with upwellings and downwellings. Just how frequently such shoreward transport and upwellings occur in different locations of the coastal zones and whether indeed such mixing is adequate under such conditions can only be assessed from detailed site specific climatological investigations of the type discussed earlier.

(c) *Large-Scale Dumping Operations*: To keep navigable channels open, dredging operation is a practical necessity. This is usually a large-scale operation involving several hundred tons

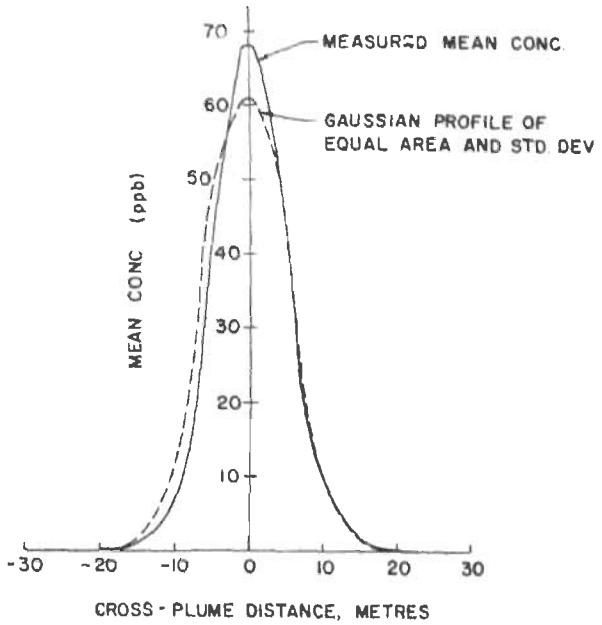

FIGURE 12 : Cross-plume distribution of dye concentration during steady currents compared with an equivalent Gaussian Profile. Concentrations were measured 500 m from the dye source : sampling depth : 2 m.

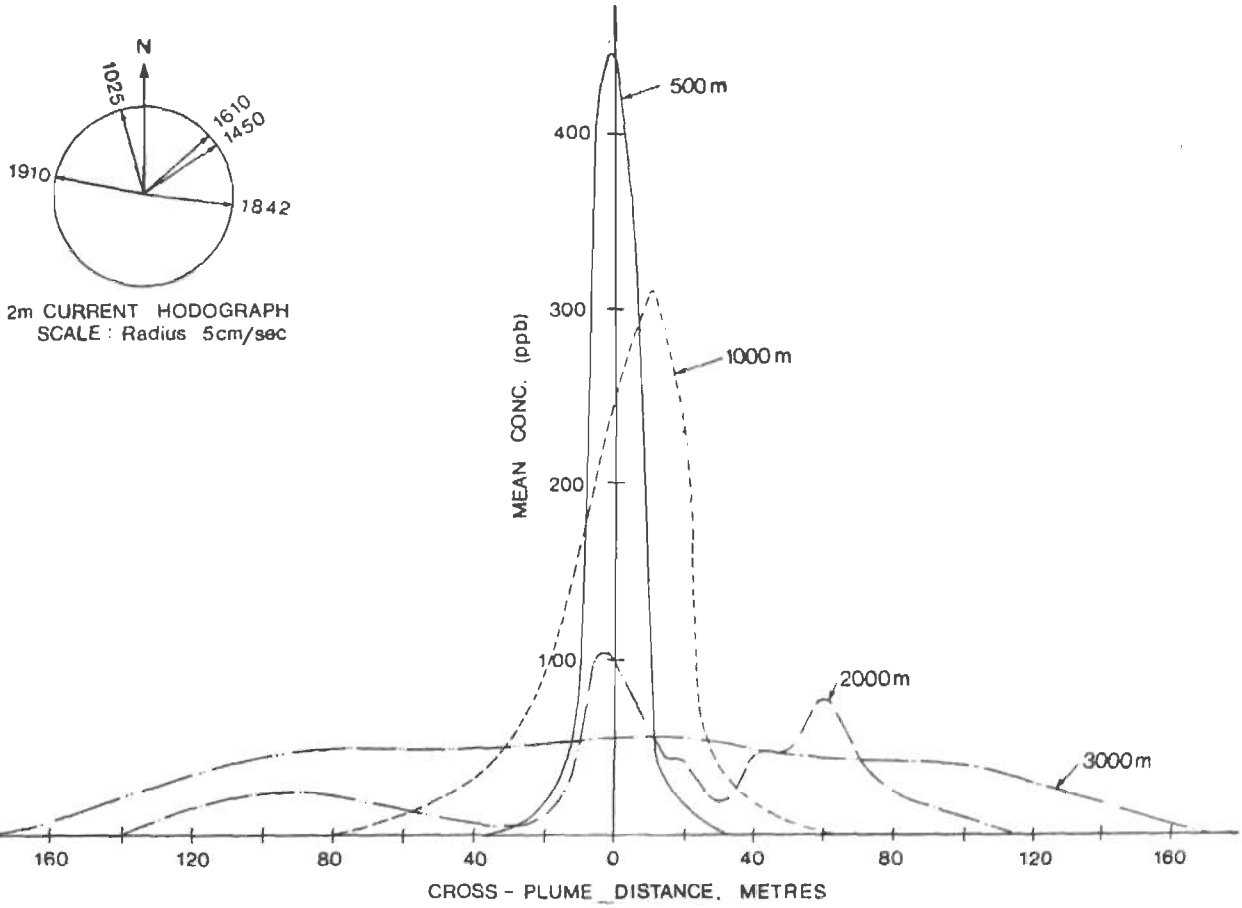

FIGURE 13 : Cross-plume distribution of dye concentration during shifting currents at 500 m, 1,000 m, 2,000 m and 3,000 m from the dye source : sampling depth : 2 m.

of dredge spoil and the efficient and safe disposal is a challenging practical problem. A frequently used method (among others, for example land disposal) is the large-scale dumping of dredged materials at some distance offshore. The transport and dispersion of dredge spoil is even more complicated due to the dynamic influence (negative buoyancy) on the receiving waters. While continuing studies to understand these phenomenon goes on, there is an urgent need for some efficient and safe disposal methods of these large-scale wastes. From our classification of coastal flow regimes, it is obvious, such large-scale dumping should take place during periods of current reversals for most efficient dispersal and offshore transport or at worst during periods of strong shore-parallel currents. In any case, there should be an embargo on large-scale dumping operations of any kind during stagnant or weak currents.

We have considered only some specific examples, which have direct bearing on waste management concepts in the coastal zones of Laurentian Great Lakes. There are a host of other problems which are equally important ; for example, shore erosion and sediment transport, installation of coastal structures of various kinds including the possibility of offshore nuclear power plants, and man-made modifications of the coastal zone for land reclamation and recreation. It is clear that solutions to problems of this type will only be possible from a thorough understanding of the coastal processes.

7. Conclusions

We believe that there are three interrelated objectives to be met before one can develop long-term concepts for management and conservation of the coastal zone environment, not only in the Laurentian Great Lakes, but in the world oceans. First, the complexities of the coastal zone environment must be reckoned with in the use of coastal water resources. Secondly, there is a need for ongoing research to understand the various manifestations of the coastal processes, if realistic predictions in the coastal zone are to become possible. Finally, practicing engineers, planners, and above all, the managers must begin to apply judiciously the vast amounts of results already available on coastal processes for the solution of practical problems.

8. References

(1) CHARNEY, J. G. : "The Generation of Oceanic Currents by Wind." J. Marine Res., Vol. 14, No. 4, 1955, pp. 477-498.

(2) CSANADY, G. T. : "The Coastal Boundary Layer in Lake Ontario, Part 1 : The Spring Regime." J. Phys. Oceanogr., Vol. 2, 1972, pp. 41-53.

(3) LONGUET-HIGGINS, M. S. : "On the Transport of Mass by Time-Varying Ocean Currents." Deep Sea Res., Vol. 16, 1969, pp. 431-447.

(4) MURTHY, C. R. : "A Comparison of Lagrangian and Eulerian Current Measurements in Coastal Waters of Lake Ontario." Proc. 16th Conf. Great Lakes Res., 1973, pp. 1034-1037.

(5) BLANTON, J. O. : "Some Characteristics of Nearshore Currents along the North Shore of Lake Ontario." J. Phys. Oceanogr., Vol. 4, 1974, pp. 415-424.

(6) BLANTON, J. O. and C. R. MURTHY : "Observations of Lateral Shear in the Nearshore Zone of a Great Lake." J. Phys. Oceanogr., Vol. 4, 1974, pp. 660-664.

(7) CSANADY, G. T. : "Dispersal of Foreign Matter by the Currents and Eddies of the Great Lakes." Pub. No. 15. Great Lakes Research Division, The University of Michigan, 1966, pp. 283-294.

(8) MURTHY, C. R. : "Complex Diffusion Processes in Coastal Currents of a Lake." J. Phys. Oceanogr., Vol. 2. 1972, pp. 80-90.

(9) MURTHY, C. R. : "Simulated Outfall Diffusion Experiments in Coastal Currents of a Lake." Water Research, Vol. 8, 1974, pp. 961-967.

(10) BLANTON, J. O. : "Nearshore Lake Currents Measured during Upwelling and Downwelling of the Thermocline in Lake Ontario." J. Phys. Oceanogr., Vol. 5, 1975, in press.

(11) CSANADY, G. T. : "Dispersal of Effluents in the Great Lakes." Water Research, Vol. 4, 1970, pp. 79-114.

(12) OKUBO, A. : "Oceanic Diffusion Diagrams." Deep Sea Research, Vol. 18, 1971, pp. 789-802.

(13) KULLENBERG, G. : "Apparent Horizontal Diffusion in Stratified Vertical Shear Flow." Tellus, Vol. 24, 1972, pp. 17-28.

(14) KULLENBERG, G. : "Vertical Diffusion in Shallow Waters." Tellus, Vol. 23, 1971, pp. 129-135.

(15) MURTHY, C. R. : "Horizontal Diffusion in Lake Currents." International Association of Hydrological Sciences, Pub. No. 109, 1973, pp. 327-334.

(16) MURTHY, C. R. : "Horizontal Diffusion Characteristics in Lake Ontario." 1975, Unpublished Manuscript.

(17) BROOKS, N. H. : "Diffusion of Sewage Effluent in an Ocean Current." Proc. 1st Conf. Waste Disposal in the Marine Environment, Pergamon Press, Oxford, 1960, pp. 246-267.

(18) SIMONS, T. J. : "Development of Numerical Models of Lake Ontario, Part 2." Proc. 15th Conf. Great Lakes Res., Internat. Assoc. Great Lakes Res., 1972, pp. 655-672.

(19) BOYCE, F. M. and P. F. HAMBLIN : "Models for the Transport of Soluble Materials in the Great Lakes." 1973, Unpublished Manuscript.

(20) LAM, D.C.L. and T.J. SIMONS : "Numerical Computations of Advective and Diffusive Transports of Chloride in Lake Erie for the year 1970." 1975, Unpublished Manuscript.

(21) RAWEN, A.M. ; F.R. BOWERMAN and N.H. BROOKS: "Diffusers for Disposal of Sewage in Sea Water." J. Sanitary Eng. Division, ASCE, Vol. 86, 1960, pp. 65-105.

(22) GUNNERSON, C. G. : "Sewage Disposal in Santa Monica Bay." Transactions, ASCE, Vol. 124, 1959, pp. 823-842.

(23) MURTHY, C. R. : "An Investigation of Diffusion Characteristics of the Hypolimnion of Lake Erie." Proc. 14th Conf. Great Lakes Res., Internat. Assoc. Great Lakes Res., 1971, pp. 799-804.

(24) KULLENBERG, G.; C.R. MURTHY and H. WESTERBERG : "An Experimental Study of the Diffusion Characteristics in the Thermocline and Hypolimnion Regions of Lake Ontario." Proc. 16th Conf. Great Lakes Res., Internat. Assoc. Great Lakes Res., 1973, pp. 774-790.

Monomixis in Kainji Lake, Nigeria

H. A. ADENIJI
Fisheries Limnologist
Kainji Lake Research Project, New Bussa, Nigeria.

SYNOPSIS

This paper gives an account of a year's study carried out on a small part of Kainji Lake which lacks an outlet. Earlier works on the mixing pattern of the lake are discussed. The factors studied such as temperature, pH, dissolved oxygen, dissolved hydrogen sulphide, and conductivity, including the methods of study are outlined. The results of this study elucidate the pattern of annual variation in surface temperature and stratification including vertical mixing. The annual vertical changes in pH, dissolved oxygen, and conductivity are also noted. The dissolved hydrogen sulphide in the hypolimnion during the early part of thermal and oxygen stratification are noted. This is followed by a discussion on the subject and the possible effects of stratification especially on this part of the lake, and on the Kainji Lake as a whole. It is concluded that the adverse effects of the long period of stratification in this small part of the lake may be negligible on the lake as a whole.

Introduction

Limnological studies of the Kainji Lake started in 1969. One aspect of the Limnological factors being studied is stratification and circulation([5]), used temperature—depth profile in his study and showed that stations located along the track of the old river in Kainji Lake showed an essential type of monomictic condition in which an extended period of partial mixing with complete withdrawal of the hypolimnion started in May and ended with thorough mixing and cooling at the onset of the dry season prior to the beginning of stratification in February(8), used deuterium in studying the mixing pattern in the lake. He concluded that for most part of the year the lake is well mixed but pronounced stratification was observed at the end of the black flood. This conclusion is similar to those of Ref. (5), because the sampling stations were located along the longitudinal axis of the old river in both studies. Adeniji, in his study of some aspects of the Limnology and the Fishery development of the lake showed that apart from the stratification and mixing conditions observed in the lake by Refs. (5) & (8), there was another type in which no significant stratification was observed throughout an annual cycle. This was observed in shallow areas where the lake water was more or less vertically mixed all the year round.

In the course of studying the Limnology of this lake it was observed that the west channel of the old river near the dam site did not have any outlet. The initiative was, therefore, taken in 1971 to study this part of the lake and observe the type of stratification and mixing conditions that were prevalent there. This paper is written on the results obtained from this study.

The Site Studied

The general description of Kainji Lake has been given by many authors such as Refs. (1), (3), (4) and (7). A map of the lake is shown in Figure 1 with the point of sampling marked '*A*'.

The site studied is located on the old river channel on the west side of the submerged Kainji Island, Figure 2. It is the deepest part of Kainji Lake with a depth of about 60 m at high water-level. At low water-level the depth drops to about 50 m. This west channel of the old river has no outlet from the lake contrary to the east channel which has the spillway outlets located directly on it at a depth of 15 m at high water-level. The

other outlets from the lake are those that pass through the turbines in the power house. These are located at points above the submerged Kainji Island at a depth of 30 m during high water-level. The surface area of this west channel at high water-level is about 0.6 sq km and the gross volume is about 0.007 cu km. The slope of this channel is very steep and the bottom is muddy with dark-greyish appearance.

Method

The site studied was sampled from station *A* on Figure 2 at five weeks' interval for a period of one year, October 1971 to October 1972. In March and April when stratification had set in, the station was sampled at two weeks' interval in order to observe the rate at which dissolved hydrogen sulphide was accumulating in the hypolimnion. The parameters studied were: temperature, *pH*, dissolved oxygen, dissolved hydrogen sulphide, and conductivity.

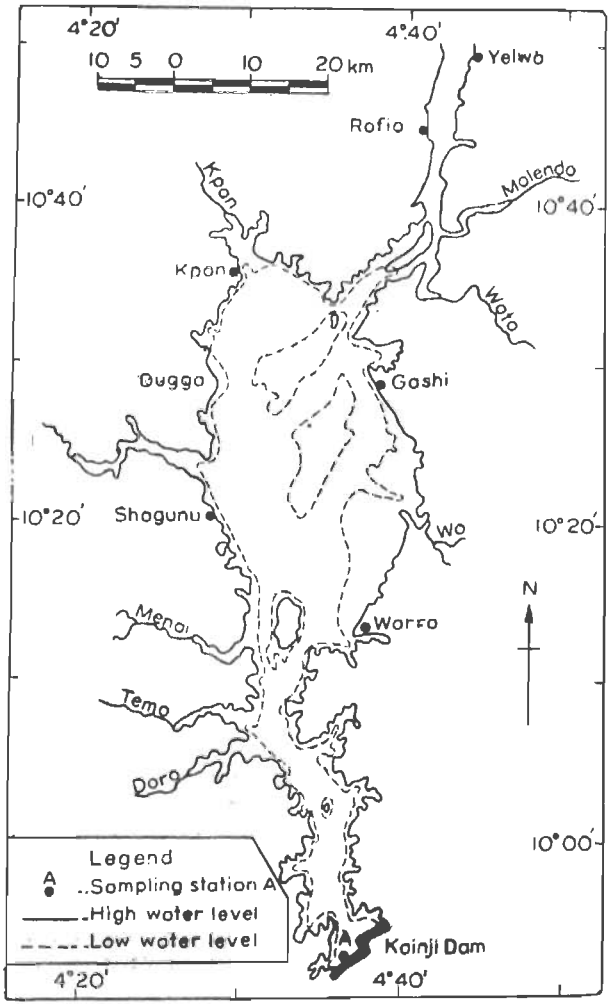

FIGURE 1 : Map of Kainji Lake.

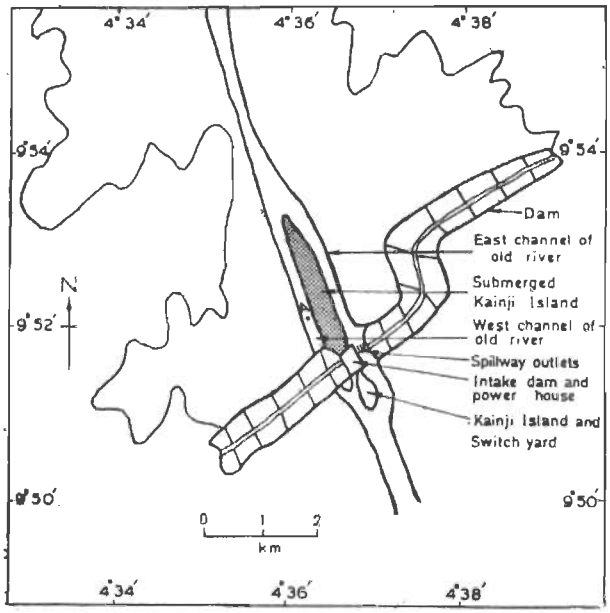

FIGURE 2 : Map of Kainji Lake near the dam site showing sampling station A.

Temperature

The surface water temperature of the lake was measured by using a standard thermometer, but the temperature profile from the surface to the bottom was recorded by using a bathythermograph. This instrument was checked for the variation between its reading and that of a standard thermometer at the beginning of every sampling trip. These differences were taken into consideration in estimating the temperature at each depth.

pH

The *pH* of the lake water was estimated by using a Lovibond comparator.

Dissolved Oxygen

The azide modification of the Winkler method was used in estimating the dissolved oxygen concentration of the lake water.

Dissolved Hydrogen Sulphide

This was estimated by using the lead acetate method for sulphide estimation as described in Ref. (2).

Conductivity

This was determined by using a Hach conductivity meter designed for field use. The meter was checked at regular intervals against a standard solution.

Water Samples

Water samples for the estimation of the above parameters were taken with a Van Dohn water sampler

from depths of 0.5 m, 5 m, and at 5 metres' intervals from the sampling point at each sampling trip. Water samples were, however, taken at shorter intervals for the estimation of these parameters when the needs arose.

Results

Temperature

It was observed from Figure 3 that the surface water temperature of the lake at the point of sampling dropped from October to January but increased from February to April. It then dropped again until September followed by a slight increase in October. The changes in the surface water temperature observed here are directly related to the seasonal changes in the year, Figure 3.

Figure 4 shows that thermal stratification was stable at this station from March until early December but by late December to the end of January the lake was homothermal. It also shows that a distinct thermocline was observed between 7 m and 21 m in April but this thermocline dropped to a depth of between 24 m and 27 m in June. The thermocline continued to drop very slowly thereafter reaching a depth of 37 m to 45 m by early December, just before homothermy set in. This drop in the thermocline layer resulted in an increase in the epilimnial layer and a decrease in the hypolimnial layer.

pH

Figure 5 shows that the surface water was having a *pH* which was near neutral in October but by December when there was vertical mixing the *pH* was neutral. From late January the *pH* increased to 7.6 and was at this level until late April when it started to fall, reaching a lower value of 7.1 by late July. It then increased to about 7.4 in September before it started to drop again.

Figure 5 also showed that the *pH* of the lake water followed the stratification and mixing pattern that was noticed from the temperature profile. The *pH* 6.8 isopleth possibly indicated the junction of the hypolimnion and the thermocline. This isopleth also dropped with the drop of the thermocline as thermal stratification continued. The lowest *pH* recorded in the hypolimnion was 6.4.

Dissolved Oxygen

Figure 6 shows the dissolved oxygen profile for the sampling station on the lake. The dissolved oxygen concentration was at its highest (10.2 mg/lit) near the surface in January towards the end of vertical mixing, but started to drop from March until October to a concentration of 6.9 mg/lit. It increased a bit in November to a concentration of 8.0 mg/lit before dropping

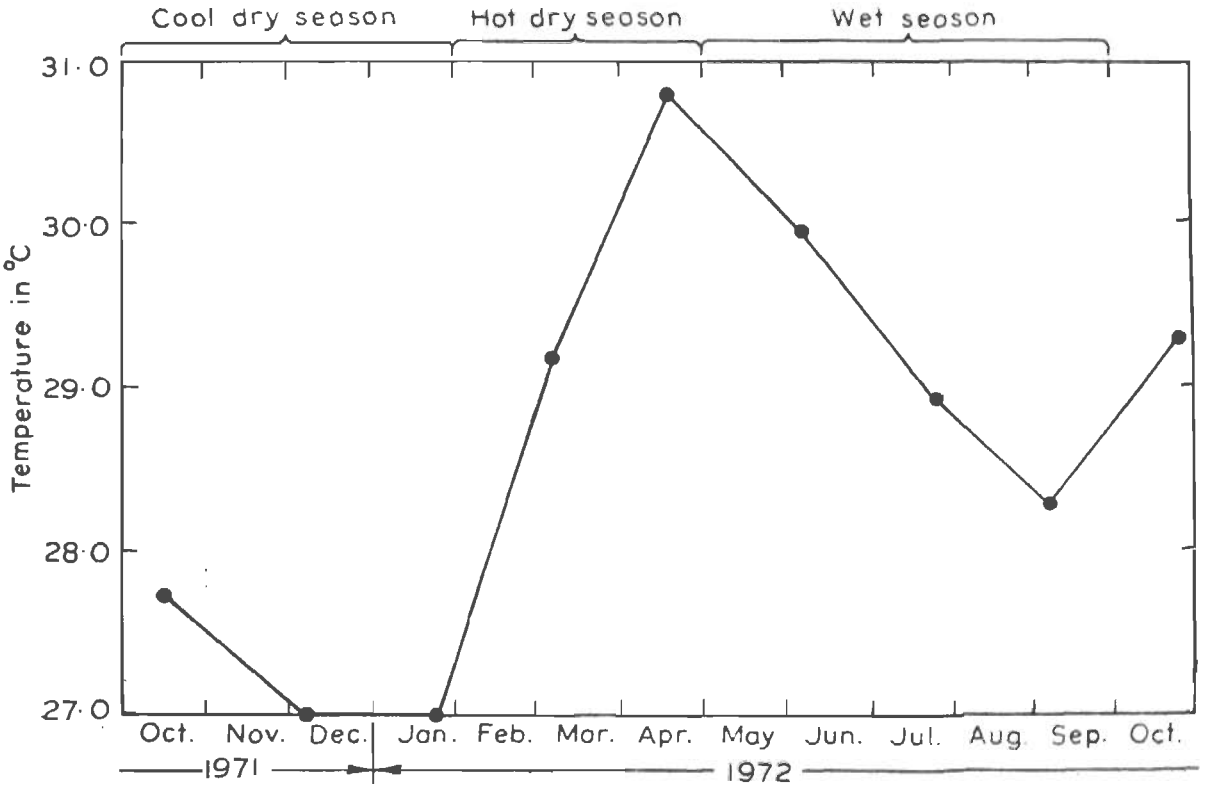

FIGURE 3 : Surface temperature in °C at sampling station A.

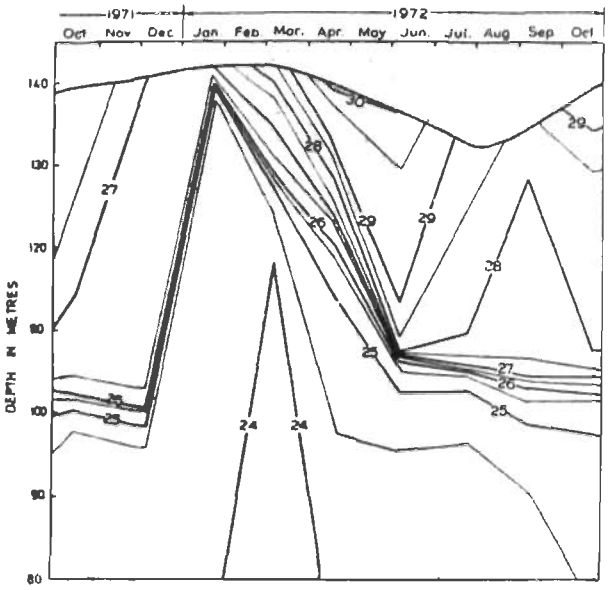

FIGURE 4 : Temperature isopleths in °C and lake level fluctuation (upper line) in metres above mean sea level at sampling station A.

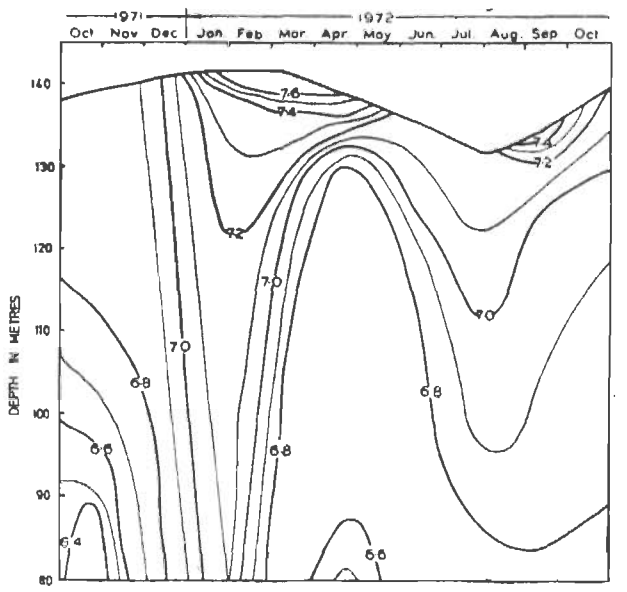

FIGURE 5 : pH isopleths and lake level fluctuation (upper line) in metres above mean sea level at sampling station A.

to its lowest value of 4.8 mg/lit in December at the beginning of vertical mixing. Figure 6 also confirms that there is dissolved oxygen stratification at this sampling station from March until early December. The deoxygenation isopleth which represents the top limit of the hypolimnion also dropped with the lowering of the thermocline during stratification. Homothermal

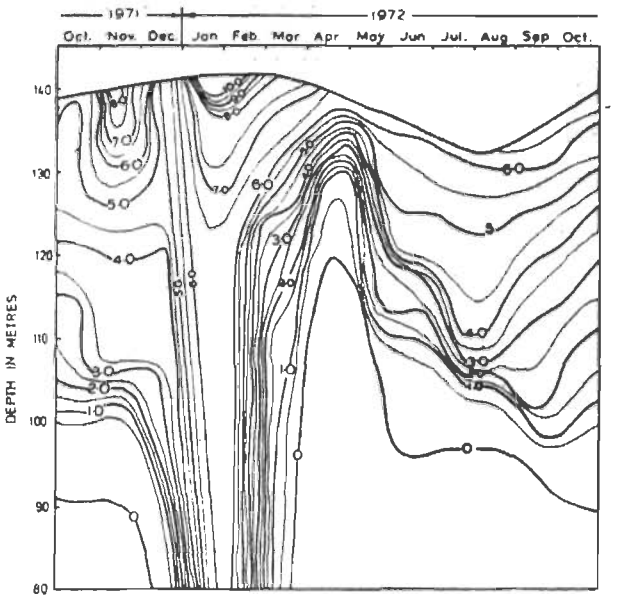

FIGURE 6 : Dissolved oxygen isopleths in mg/lit and lake level fluctuation (upper line) in metres above mean sea level at sampling station A.

condition which was observed in Figure 2 also corresponded with the period (December and January) when oxygen was well distributed to the bottom of the lake, thus destroying the deoxygenated hypolimnion.

Dissolved Hydrogen Sulphide

Table I shows that the dissolved hydrogen sulphide concentrations that were observed at this station were low. The highest concentration observed in the water above the mud was 0.13 mg/lit, but the mud-water samples showed a higher concentration of 3.0 mg/lit. It was also noticed that the dissolved hydrogen sulphide concentration increased with depth in the hypolimnion during the early part of stratification. The concentration at each depth was, however, fairly stable between mid March and late April. The slight increase in the dissolved hydrogen sulphide concentration at 50 m depth was noted.

TABLE I

Dissolved hydrogen sulphide concentration (mg/lit) in the deoxygenated hypolimnion of Kainji Lake.

Depth sampled	30 m	40 m	50 m	Bottom mud and water
13.3.1972	0.04	0.09	0.09	
30.3.1972	0.01		0.09	0.26
10.4.1972	0.03	0.07	0.09	
28.4.1972	0.03		0.13	3.00

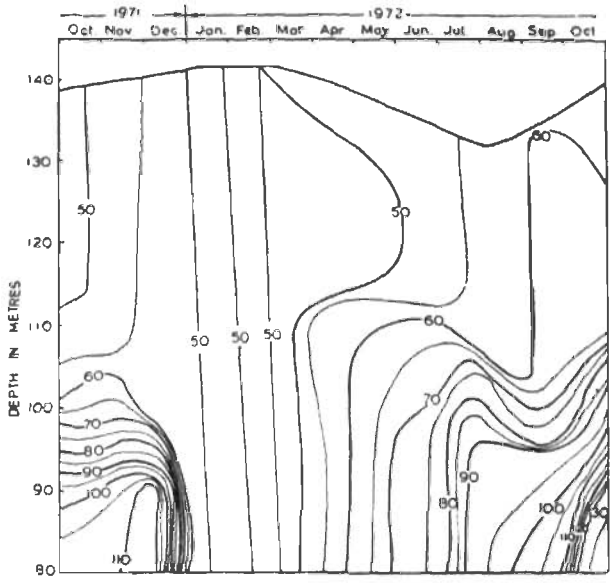

FIGURE 7 : Conductivity isopleths in μmhos/cm and lake level fluctuation (upper line) in metres above mean sea level at sampling station A.

Conductivity

The conductivity of the surface water increased gradually from 51 μmhos/cm in April to 63 μmhos/cm in October before it started to fall reaching its lowest level of 51 μmhos/cm in January, Figure 7. During December and January, when the lake was vertically mixed the conductivity of the lake water was more or less uniform vertically with depth. This uniform concentration continued until late February when thermal stratification started. By late April, the stratification in the conductivity of the lake water was clearly defined with concentrations of 50, 55, and 60 μmhos/cm in the epilimnion, thermocline, and hypolimnion respectively. As thermal stratification continued, a gradual increase in the conductivity of the hypolimnial water was noticed. This increased to about 135 μmhos/cm in late October. This concentration is about two times greater than the conductivity of the surface water at that time.

Discussion

The mixing pattern observed from this part of Kainji Lake agrees with the definition given in Ref. (6) for warm monomictic lakes which circulate only in winter above 4°C. Though winter season is not peculiar to tropical areas, it is noted that the vertical mixing in this part of Kainji Lake occurs only during the time that the temperature of the lake was at its lowest and simultaneously during the cool dry season of the year.

The long period (about ten months) of thermal stratification at this station is likely to lock up certain nutrients and dissolved substances in the hypolimnion during that period. This may be the result of the high conductivity measurements that were observed in the hypolimnion from August to December just before the vertical mixing.

It has been shown in Ref. (1) that the deoxygenated hypolimnion restricts the distribution of fish and zooplankton in this lake. This may also be true for this part of the lake especially during the ten months when the hypolimnion of this area is deoxygenated. This aspect and that of the effect of the high conductivity in the hypolimnion are subjects for future studies.

The warm monomictic condition which is peculiar to this part of the lake now brings the types of mixing conditions that have been observed in this lake to three. The other two are the uncertain type of monomictic condition observed in fairly deep parts of the lake by Refs. (1) & (5), and the other is the polymictic condition which was observed in the shallow areas of the lake by Ref. (1).

Conclusion

The type of stratification and mixing conditions observed in this part of Kainji Lake was shown and discussed. The mixing pattern here is definitely warm monomictic. Since the part of the lake affected by the long period of stratification and deoxygenation is small, it is believed that any adverse factor from this part of the lake will have a negligible impact on the lake as a whole.

Acknowledgement

The author is grateful to the Kainji Lake Research Project for providing the fund for this study which is a part of the assignment of the Limnology Programme. He also appreciates the cooperation of the staff of this programme, and the boat drivers in making this study a success.

References

(1) ADENIJI, H. A. : "Some Aspects of the Limnology and the Fishery Development of Kainji Lake, Nigeria." (in Press).

(2) BISWAS, S. : "Some Limnological Innovations." Volta Basin Research Project, Tech. Report XI 9, July 1967, pp. 1-6.

(3) EL-ZARKA, S. : "Kainji Lake, Nigeria." Geoph. Mono. Series 17, 1973, pp. 197-219.

(4) F. A. O. : "Pelagic Primary Production in Kainji Lake, based on the Work of S. G. Karlman." FI : SF/NIR. 24, Tech. Report No. 3, 1973, pp. 1-59.

(5) HENDERSON, F. : "Stratification and Circulation in Kainji Lake." Geoph. Mono. Series 17, 1973, pp. 489-494.

(6) HUTCHINSON, G. E. : "A Treatise on Limnology, Geography, Physics and Chemistry." J. Wiley, N. Y., Vol. 1, 1957, pp. 437-438.

(7) IMEVBORE, A. M. A. and ADEGOKE, O. S : "Lake Kainji—Lacustrine Studies." University of Ife Press, Vol. 1, 1971.

(8) ZIMMERMANN, U. et al : "Study of the Mixing Pattern of Kainji Lake using Stable Isotopes." (in Press).

Urban Development with Environmental Protection

WALTER FOX
Forester
U.S. Department of Agriculture-Forest Service
Atlanta, Georgia, U.S.A.

SYNOPSIS

Many metropolitan counties across the United States are experiencing rapid urban development—both industrial and residential. The structural and esthetic quality of these developments vary widely, but they generally share a common denominator—environmental degradation. What was once a pleasing productive landscape becomes cursed with dying trees, eroded hills, and sediment laden streams devoid of life. Unchecked accelerated surface water runoff scours streambanks, washes out roads and bridges, fills downstream reservoirs with sediment and causes flooding.

Cohn Communities and Irwin/Probst Associates (DeKalb County, Georgia), because of their environmental awareness, consulted with Lowe Engineers of Atlanta, Georgia, and the Soil Conservation Service, U.S. Department of Agriculture, to obtain assistance in planning runoff retention basins, sediment traps, recreation lakes and facilities, and vegetative measures in order to protect and enhance the environment of the 543 acres (219.75 ha) Mainstreet Development.

The environmental planning and construction of the urban Mainstreet Development in south-eastern United States led to the first and only National Merit Award presented to an urban land developer by the Soil Conservation Society of America(1).

Introduction

DeKalb County, Georgia, in south-eastern United States of America, receives about 50 in. (1,270 mm) of uniformly distributed precipitation annually. On a quantity basis, this amount of precipitation likely will be adequate to meet the domestic and industrial demands for at least the next 50 years. Water quality, however, leaves much to be desired.

The development of land into residential or industrial use causes drastic changes in land cover, soil conditions, land slopes and drainage patterns. These, coupled with the effects of earth moving operations too often result in excessive erosion and degrading of water quality.

The Developers of Mainstreet, Cohn Communities and Irwin/Probst Associates decided in 1972 to incorporate environmental protection in the planning and development of Mainstreet. This 543 acres (219.75 ha) development is planned to include, 575 single family homes, 700 condominiums and/or apartments, a 9-acre (3.6 ha) office complex, 11-acre (4.5 ha) site for a school, and the 70-acre (28.3 ha) flood plain for flood damage resistant recreation facilities.

The Soil Conservation Service of the U.S. Department of Agriculture, at the request of the Developers, prepared a map illustrating soil suitability groups with their potentials. Basic SCS soil survey data of an earlier date was used to help identify soils. Based on soil analysis, recommendations for species of vegetation and fertilizer rates were selected to obtain rapid stabilization of soil exposed during the construction process.

Lowe Engineers of Atlanta, Georgia, designed runoff detention reservoirs which fulfil the DeKalb County requirements for discharges of *no more* than the undeveloped rate as based on a 10-year storm. The Soil

An entrance to Mainstreet. "... a total way of life. Various housing concepts, shopping areas, office parks, leisure time facilities, and schools, all within a controlled environment where there's an emphasis on the natural beauty and integrity of the land"(2).

Conservation Service assisted the Developers with locating and designing sediment traps in order to prevent on-site and off-site damage. The development of the 70-acre (28.3-ha) flood plain for recreation is an adventure in innovation since this normally unusable urban land is put to productive use. The scope of this paper is concerned with the use of the land involved and not with the type of architecture, even though these designs fit and are part of the environmental concept for Mainstreet.

Planning and Development

The environmental awareness of the Mainstreet Developers stimulated the effort to provide the best possible project consistent with local governmental requirements, environmental and ecological factors, esthetics, and cost.

The Soil Conservation Service, U.S. Department of Agriculture, developed soils data which identified soil characteristics and described the problems and limitations which would be associated with each soil. In addition, soils engineering data was developed which identified such factors as depth to hard rock and depth to seasonal high water tables. These data were used by engineers of the Soil Conservation Service, Lowe Engineers, and Mainstreet to—

—determine the limitations of areas for residential and commercial sites, picnic grounds, playgrounds, trafficways, and other recreational use.

—locate roads, utilities and similar developments to conform to the most desirable soil conditions and topography, thus reducing installation and maintenance costs.

—identify areas which present drainage, flooding and severe erosion problems.

—locate suitable sites for detention and retention ponds and sediment traps which have native construction material available.

—establish priorities for development of facilities based on relative costs of environmental protection.

Mainstreet is being constructed under the local governmental requirement which dictates that the rate of runoff (based on the 10-year flood frequency) from a developed tract of land does not exceed the runoff from the tract before it is developed. The requirement does permit compensatory detention, i.e., one detention structure may detain a proportionately larger volume to compensate for unabated runoff from other areas. This allows greater flexibility in sizing and hence

locating each detention structure. Two detention structures, one on each tributary to Barbashela Creek, were designed to serve the development. One detention pond (Figure 1, No. 3) temporarily detains flood flows by controlling the outflow with two pipes which allow normal flows to pass unrestricted. This latter detention area retains all the original vegetation of trees and shrubs, and thus stays as a part of the natural landscape. One structure (Figure 1, No. 2A) serves both detention and retention purposes.

The body of water shown in Figure 2 was designed originally to be strictly a runoff detention lake of 4.5 acres (1.82 ha) with a depth of 4 ft (1.2 m). The Developer re-designed and enlarged the structure to provide a 10-acre (4 ha) lake with a depth of 6 ft (1.8 m). The lake still retains the required runoff detention control and becomes useful to serve future development as a recreation facility (Figure 1, No. 2A). The added size and depth will sustain small boating and fishing use as well as providing a pleasing view from adjacent housing. This lake will also serve to trap and store sediment when development begins.

DeKalb County requires only temporary erosion and/or sediment control. However, the Developers' planning and construction provided for many permanent control features. One of these was the installation of sediment traps (Figure 1, No. 10).

The small 0.25 acre (0.01 ha) body of water shown in Figure 3 was constructed as a sediment trap (Figure 1, No. 10 adjacent to No. 5) on Barbashela Creek which flows from north to south. A small dam made of native rock, with an outlet device, helps control high water flows in the creek and provides for drawdown for sediment removal. It is also maintained as an esthetic feature in the development. The upstream sediment trap (Figure 1, No. 10) serves only to control sediment. Both these traps help control sediment moving downstream from other developing areas outside the Mainstreet portion of the watershed. The sediment control feature of these two traps helps reduce channel scouring downstream.

Access into and throughout Mainstreet is based on cost, soil suitability, safety and esthetics. Road construction such as this must necessarily serve the facilities in an efficient manner. Figure 4 illustrates the access design principles by—

—road location which follows natural land form on stable soil with minimum cuts and fills and also provides adequate secondary access to residential developments.

—increasing esthetic appeal with gentle curves through the forested terrain.

—providing road curvature which promotes slower vehicle speeds.

—establishing a vegetative cover as soon as final shaping is completed.

Exposed soil on road cuts and fills as well as on other disturbed areas is revegetated as soon as practical by use of a hydro-seeder. The per acre (0.4 ha) vegetative mixture is 50 lb (22.68 kg) of Fescue grass (*Festuca Elatior L.*) and 50 lb (22.68 kg) of Rye grass (*Lolium Perenne L., L. Multiflorum Lam.*). Based on soil fertility analysis, 1,000 lb (453.6 kg) of 6-12-12 (Nitrogen-Phosphorus-Potassium) fertilizer and 2,000 lb (907.2 kg) of lime is added per acre (0.4 ha).

The major water and sediment control structures were supplemented by a system of secondary control measures, one of which is shown in Figure 5. Here, a natural drainage was lined with rock in order to slow down movement of water from the hill upstream. Otherwise, the volume and velocity of water moving along the drain would degrade the channel, cause the culvert to be washed out with the resulting deposition of eroded material in downstream impoundments. A heavy straw mulch on exposed soil adjacent to the drain holds the soil in place until the grass cover is established. Straw mulch, grass seed, and fertilizer are applied to exposed soil around the houses and condominiums as soon as exterior construction activities are completed.

Another secondary control measure is shown in the foreground of Figure 6. A small sediment trap was installed at the edge of this lake (Figure 1, No. 2B) in a natural waterway draining an area in which intensive construction activities were underway. The purpose of this trap is to keep upstream sediment out of the lake. This lake of 5 acres (2 ha) existed prior to development and was used as a cattle watering facility. The Developers then planned the lake for recreation use and built the Mainstreet Clubhouse on the shore. Part of the Clubhouse can be seen in the upper left corner of Figure 6. The Clubhouse complex (Figure 1, No. 7) includes a swimming pool and tennis courts and is constructed to blend with the natural land form. Additional recreational use of the lake includes fishing and small boating.

Planning the proper use of a flood plain in any metropolitan area is difficult at best, and the Barbashela Creek flood plain (Figure 1, No. 11) is no different. Past use and misuse of upstream lands caused acceleration of erosion. This resulted in excessive deposition of sediment in the flood plain which in turn caused changes in vegetative cover and degrading of what was once a natural ecosystem. The increased water runoff, heavily laden with sediment, from upstream land also caused stream channel changes which gradually destroyed natural drainage characteristics and created a swampy condition.

In order to utilize the 70 acres (28.3 ha) Barbashela Creek flood plain, considerable stream channel relocation (Figure 8) was required. In addition, needed control of accelerated overland flow from hillsides adjacent to the flood plain is controlled by diversion terraces and grassed waterways which carry the water to the Creek. Uncontrolled movement of water could damage recreation facilities and cause erosion. Figure 7

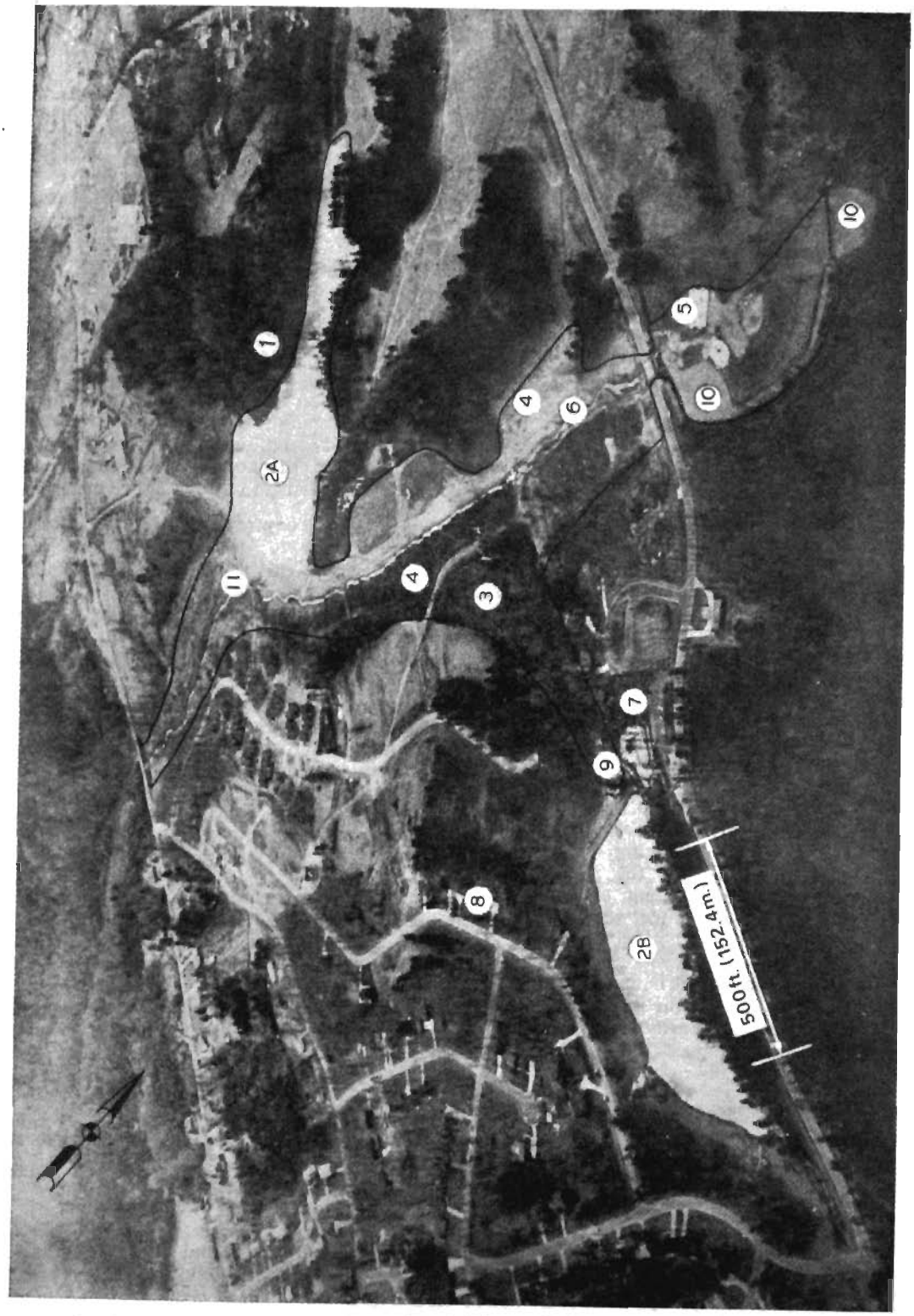

FIGURE 1 : Mainstreet Development Site (Aerial Photograph—Oblique).

LEGEND

1. Condominiums Planned. 2A. Detention Basin and Recreation Lake. 2B. Recreation Lake. 3 Detention Basin. 4. Recreation Use : Picnic Area ; Football, Baseball, Soccer and Rugby Fields ; Tennis Courts ; Bicycle and Nature Trails. 5. Basketball Court and Playground. 6. Barbashela Creek. 7. Clubhouse and Tennis Courts. 8. Single Family Dwellings. 9. Swimming Pool. 10. Sediment Traps. 11. Flood Plain (100-year).

FIGURE 2 : Detention and Retention Lake.

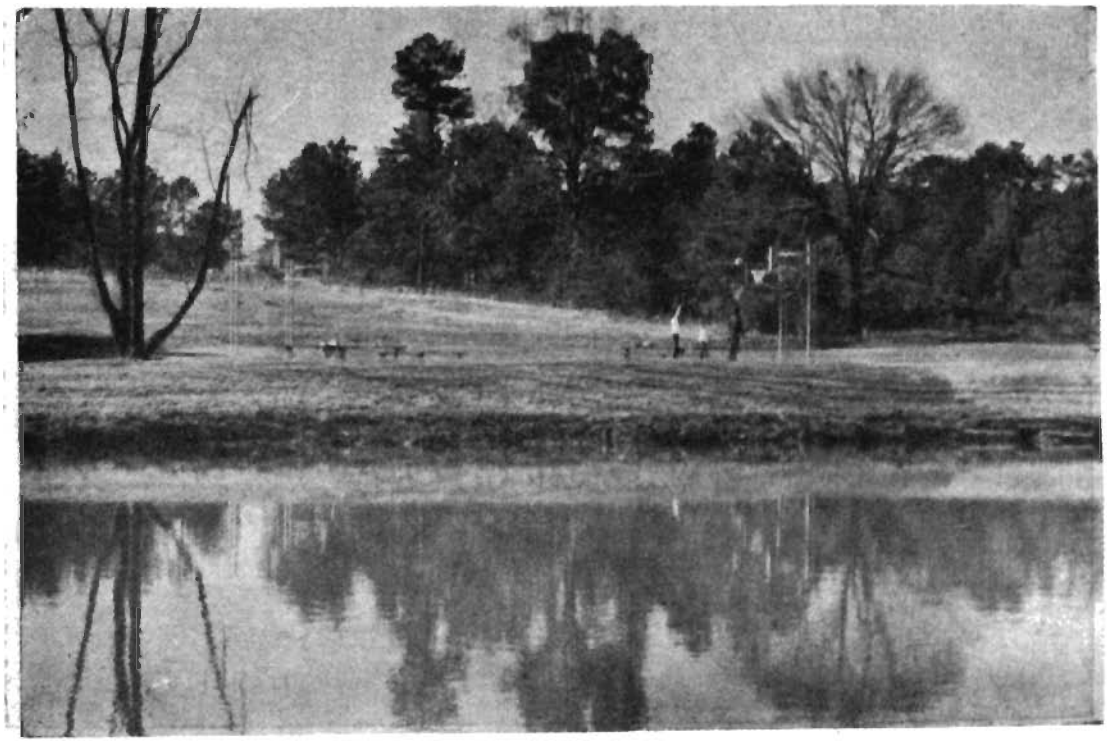

FIGURE 3 : Sediment Trap and Recreation Facility.

FIGURE 4 : Completed Road Construction.

FIGURE 5 : Water Control Installation.

FIGURE 6 : Recreation Lake.

FIGURE 7 : Flood Plain Water Management.

shows a terrace constructed to divert hillside overland water flow around the basketball court and playground (Figure 1, No. 5) which are in the flood plain.

Barbashela Creek relocation through the flood plain was done with the objective of keeping as much of the natural channel as possible with its existing vegetation and curvature. Grade changes were avoided in order not to increase flow velocities by constructing curves where necessary. Figure 8 shows a section of artificial and natural channel. Rock rip-rap was used to stabilize stream banks wherever soil was exposed.

Extensive filling and grading was required to make the flood plain usable for recreation. Existing trees were left insofar as possible to enhance esthetics and to provide needed shade where desirable. The picnic area shown in Figure 8 well illustrates flood plain use. Also shown in Figure 8 is an individual walking on one of several asphalt paved trails which are in the flood plain. These trails are useful as bicycle, hiking and nature trails. Other recreation features (Figure 1, No. 4) in the flood plain include fields for football, baseball, soccer and rugby. Space is available for additional recreation facilities. All the recreation facilities in the flood plain can withstand flood flows since the only damages would be the cost of sediment removal from tables, trails and other artificially covered surfaces.

Intensive urban development can severely deplete an area of its natural values including topsoil, vegetation and land form. The single family dwelling shown in Figure 9 is typical of the total environmental consideration given each lot by the Developer :

—The dwelling is constructed to fit the land form thereby reducing soil exposure.

—Trees are left for shade which reduces dwelling heating costs ; for holding soil in place ; for retaining esthetic values ; and for screening to reduce noise levels.

—A retaining wall of wood is used to maintain a more stable slope when final grading dictates slope changes.

—Native rock is used as landscaping material.

—A grass cover is promptly developed by using proper species, fertilizer and mulch.

The planning and development of Mainstreet is directly related to protecting and enhancing man's environment, both on-site and downstream. If the specific erosion control and sediment trapping measures taken by the Developers in addition to sediment storage in the detention structures had not been provided, off-site sediment movement would be increased by 600-700 percent.

This section fully describes the planning and construction schemes which led to the first and only (through 1975) National Merit Award presented to an urban land developer by the Soil Conservation Society of America—a private international organization dedicated to "advance the science and art of good land use(1)."

The next section discusses the problems that develop when environmental protection is ignored.

The Need for Planning

Comprehensive planning and management of urban soil and water resources are essential to the enhancement of the quality of the urban environment and the health of the Nation. The urbanite is dependent on these resources to provide adequate, attractive, and satisfying places to live, work, and play.

The unplanned, erratic, and irresponsible development of urban areas creates complex and difficult problems for the developer, adjacent and downstream landowners, urban authorities, utility companies, and others. These problems manifest themselves as erosion, sedimentation, sediment pollution, and flooding which result in damage to homes, commercial buildings, roads, utilities, streams, lakes and other improvements(2).

More specifically, environmental off-site damage from urban erosion causes :

Sediment on Streets and Highways

—creates dangerous traffic conditions (wet or dry).

—increases air pollutants (dust) and reduces visibility.

—plugs culverts.

—smothers roadside vegetation.

—increases water pollution by introducing solids, nutrients and pathogenic organisms when washed into storm sewers.

—reduces visibility.

Sediment in Navigation Channels

—blocks ship movement.

Sediment in Reservoirs

—reduces reservoir water holding capacity.

—smothers aquatic habitat.

—reduces light penetration which decreases the amount of desirable aquatic food production.

—reduces fish populations.

—restricts recreation use.

—harms esthetics.

—nutrients accompanying sediment accelerates eutrophication.

FIGURE 8 : Flood Plain Use and Channel Relocation.

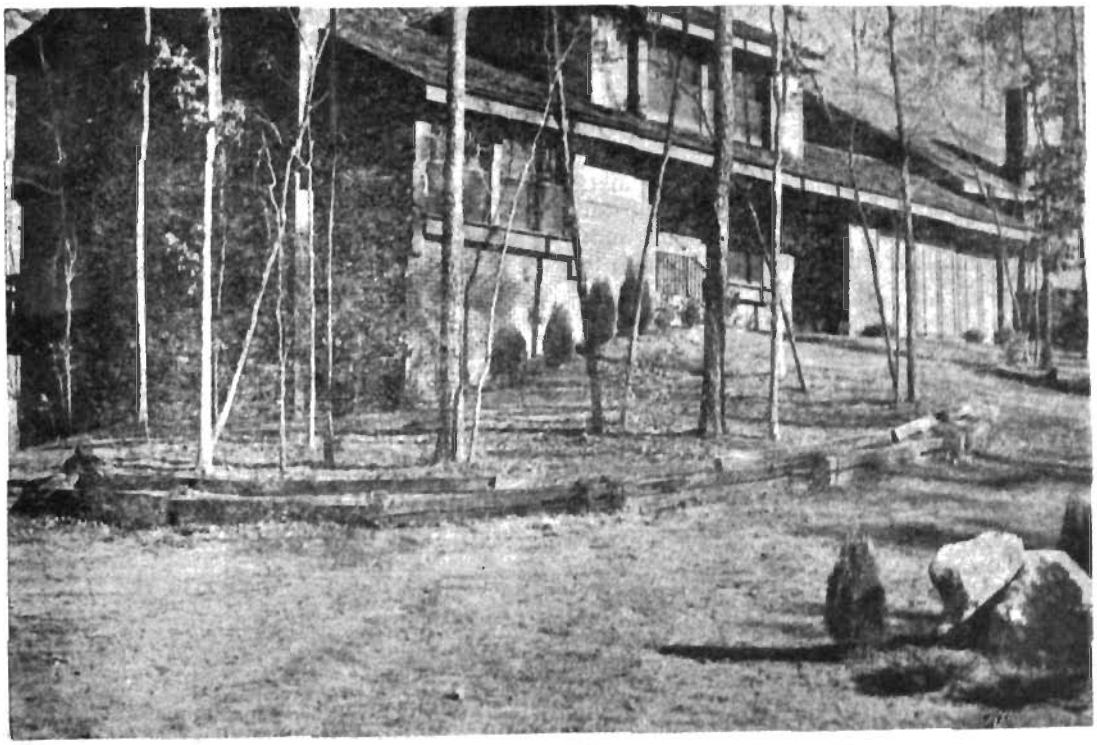

FIGURE 9 : Single Family Dwelling.

Sediment in Water Supplies

—increases treatment costs for flocculation, filtration and chlorination (human use).

—increases treatment costs for animal consumption.

—clogs intake pipes.

Sediment in Stream Channels

—smothers streamside vegetation from flood deposition.

—smothers aquatic habitat.

—reduces fish population.

—erodes streambanks.

—smothers aquatic habitat when transported to tidal water or estuaries.

—harms esthetics.

—promotes channel erosion in some instances and channel deposition in others.

—increases flood frequency.

Environmental on-site damage from urban erosion causes :

Esthetic Deterioration

—A well vegetated landscape provides a beautiful contrast as compared to the ugliness of a barren eroding landscape.

Productivity Loss

—Erosion depletes soil productivity by removing the most productive part of the soil (a chemical composition study of a soil similar to that in DeKalb County showed concentrations of organic matter and nitrogen nine times as great as the sub-soil ; phosphorus seven times as great ; calcium twenty-nine ; potassium four times ; and magnesium the same).

Hydrologic Disturbance

—The erosion process seals the larger soil voids, thus decreasing infiltration and permeability. This results in increased surface runoff and reduced percolation to recharge ground water.

Structural Damage

—Gully erosion can weaken and collapse walks, roads and walls.

The first step toward avoiding these problems is judicious land use planning which assesses the influence of all resources and environmental factors, including those pertaining to soils, geology, hydrology, recreation, residential and commercial amenity values and transportation route needs.

"The need for action in these areas is urgent." This statement was made by the President of the United States on 20 January 1972 as part of his State of the Union address (Protecting the Environment). Emphasis by the President on this phase of the environment stimulated many local governments and organizations to take the planning steps which lead toward a better way of life for urbanites.

Conclusion

The development of Mainstreet, as a total way of life for urbanites, was brought about by the environmental consciousness of Cohn Communities and Irwin/Probst Associates. These Developers obtained professional advice early in the project planning stage in order to protect and enhance the environment of the 543 acres (219.75 ha) development.

Planning and construction met local governmental requirements for runoff detention, and, in addition, provided water retention for recreation. Development of the deteriorated flood plain for recreation re-established a more natural water movement regime in addition to making unusable land productive. The development scheme was based on soil capability and utilized natural land forms and drainage features. Erosion control to protect on and off-site ecological values led to intensive soil stabilization measures following soil disturbance. Sediment traps were designed to protect downstream facilities and ecosystems. Use of native construction material enhanced the esthetic values.

Mainstreet is recognized throughout the United States for high quality environmental planning and construction. They lead the way and provide an example for other urban land developers around the world.

Acknowledgements

(1) Ground photography by Joseph H. Summerlin, Jr., 4196 Lehigh Blvd., Decatur, Georgia 30034, U.S.A., all rights reserved.

(2) Aerial photography by Lowe Engineers, Inc., 1920 Monroe Drive, N. E., Atlanta, Georgia 30324, U.S.A., all rights reserved.

(3) Typing assistance by Cohn Communities, Inc., 4321 Memorial Drive, Decatur, Georgia 30032, U.S.A.

(4) Technical assistance by the U. S. Department of Agriculture—Soil Conservation Service, Decatur, Georgia 30030, and Lowe Engineers, Inc.

References

(1) SOIL CONSERVATION SOCIETY OF AMERICA OBJECTIVE : "The Objectives of this Society shall be the development and advancement of the science and art of good land use and management and the promotion of the

conservation of soil, water, air, and related renewable natural resources, including; without limitation, trees, grass, fish, wildlife, and all forms of beneficial plant and animal life, and for these purposes to employ education of the people and other appropriate means, to the end that mankind may have the use and enjoyment of these resources forever."

Address : 7515 Ankeny Road, Ankeny, Iowa. 50021. U.S.A.

(2) COHN COMMUNITIES AND IRWIN/PROBST ASSOCIATES : Mainstreet Development Theme.

(3) U. S. DEPARTMENT OF AGRICULTURE-SOIL CONSERVATION SERVICE, ATHENS, GEORGIA, U.S.A. : "Handbook for Control of Soil Erosion and Sediment in Areas Undergoing Urban Development." 1972, page 2-1.

Belgian Mathematical Model and Data Acquisition System for Monitoring, Prediction and Control of Marine Resources Quality

JACQUES C. J. NIHOUL
Professor of Mechanics

FRANÇOIS C. RONDAY
Assistant

GEORGES PICHOT
Assistant

Institut de Mathématique Université de Liège, Liège, Belgium.

SYNOPSIS

The paper is a synopsis of the mathematical model and data acquisition system which have been the framework of the theoretical and experimental research conducted during the period January 1971—December 1974 in the scope of the Belgian National Program on the Environment sponsored by the Ministry for Science Policy.

Examples of exploitation of the model are given with particular emphasis on tide and storm surge simulation, determination of residual currents, dispersion of pollutants and simulation of ecosystems dynamics.

1. Demarcation of the System

Support

The support of the model is the Southern Bight of the North Sea and the Scheldt Estuary.

The hydrodynamical part of the model is extended to the whole North Sea whenever necessary to provide appropriate Northern boundary conditions for the Southern Bight.

Scope

The primary objective of the model is the study of the space and time characteristics of water motion, surface elevation, temperature, salinity, turbidity, oxygen, nutrients, trace metals, chlorinated hydrocarbons and living species.*

Reduction of Scope—Compartments

Attention is restricted to the most important compartments :

(*i*) dissolved substances,
(*ii*) suspensions,
(*iii*) plankton—phytoplankton, zooplankton,
(*iv*) fish—pelagic, benthic,
(*v*) shellfish and molluscs,
(*vi*) bottom sediments,
(*vii*) macro—and meio-benthos,
(*viii*) bacteria—faecal, marine heterotrophic, benthic.

The state variables include the specific mass** of each compartment and the aggregate concentrations of the selected chemicals in compartments (*i*) to (*vi*).

Selected nutrients : *P*, *N*, *Si*.

Selected heavy metals : *Zn*, *Cd*, *Pb*, *Cu*, *Fe*, *Mn*, *Mg*.

* Petroleum products are examined in a separate program.
** Mass per unit volume.

Selected chlorinated hydrocarbons : *pp' DDT, DDD, DDE*, aldrine, dialdrine, endrine, lindrane, heptachlore, epoxid heptachlore, *PCB*.

The specific masses of compartments (*i*) and (*ii*) may be called "salinity" and "turbidity" respectively ; the distinction between salinity and turbidity being, in a sense, arbitrary as the experimentalist will call *dissolved* everything which goes through a filter of pre-decided fineness. This must be borne in mind also while interpreting the budgets of nutrients and pollutants in the two compartments.

Reduction of Support—Space Averaging

All over the support except in the Scheldt Estuary the turbulent mixing ensures a uniform density.

While separate three-dimensional and combined depth-averaged and width-averaged two-dimensional models are being developed for the Scheldt Estuary, the model for the Southern Bight is further simplified by assuming constant mass density and considering only average properties over the total depth.

The mechanical variables are then reduced to the two horizontal components of the depth-averaged velocity vector and the surface elevation.

For the study of specific chemical and ecological interactions, the support may be divided in a limited number of boxes where similar conditions prevail. In a first approach, one may study the dynamics of the aggregate properties of the box obtained by further integrating (averaging) over the horizontal dimensions of the box. Box models of this sort have been developed and tested against the experimental observations made in the Ostend "*Bassin de chasse*", a closed sea basin at the coast which has been extensively studied in the past.

2. State Variables and Control Parameters

The state variables are defined by the scope of the system as stated above.

As a result of turbulence and other erratic or rapidly oscillating motions of the sea, each variable shows fluctuations around a mean value. Only these mean values are significant for the model.

The evolution equations are written for the mean variables and only the general effect of the fluctuations (through non-linear terms in the basic equations) is taken into account.

The mean variable, i.e., the smooth running functions of space and time, obtained by filtering out the fluctuations are denoted by special symbols. A bar over the symbol indicates the average over depth of the mean variable.

In addition to the mechanical variables and temperature, the other state variables represent essentially specific masses or concentrations. (The specific biomass of phytoplankton, the specific mass of copper in solution, suspension or plankton, etc.). These "concentration" variables are noted ρ_α (smooth running part r_α). For convenience ρ_α (r_α) will be referred to as the specific mass of "constituent α" ; the word constituent being used in a conventional sense as it may denote a whole aggregate (all dissolved substances...) or the aggregate content of a compartment in a specific chemical (concentration of mercury in pelagic fish...).

The mean (smooth running) variables are noted as follows :

		Depth-averaged
Velocity vector	$\underset{\sim}{u}$ (three-dimensional)	$\underset{\sim}{\bar{u}}$ (two-dimensional)
Flow rate vector		$\underset{\sim}{U} = H\,\underset{\sim}{\bar{u}}$
Surface elevation		ζ
Total height of water (where, h is the depth)		$H = h+\zeta$
Temperature	θ	$\bar{\theta}$
Specific mass of α	r_α	$\bar{r}_\alpha$

In addition to the state variables, different kinds of parameters appear inevitably in the mathematical description of the system. These may be called *control parameters* as they influence the evolution of the system (hence appear in the evolution equations) but are not predicted by the model itself (no specific evolution equation is written for them).

The chemical reaction rates may be regarded as control parameters hopefully determined by chemical kinetics, i.e., by laboratory experiments or by some fundamental molecular theory conducted in parallel with the model but not part of it.

The dynamics of *translocations* (transfer of a chemical element from one compartment to another) must be given appropriate mathematical form. This cannot be done in general without introducing several control parameters the value of which can only be ascertained experimentally.

To ascertain the value of the control parameters and determine the laws of interaction, complementary variables are measured or calculated. These include, for instance, transparency of water, primary production, diversity and stability indexes, antibiotic effects, etc.

3. Evolution Equations

The assumption of uniform sea water density which is justified by experiment (apart from the Scheldt Estuary where slightly different models are being developed) allows a decoupling between the mechanical variables and the others. The hydrodynamic equations can be solved independently of the other evolution equations and the

values of the flow velocity determined by the former substituted in the latter which in turn can be solved knowing the interactions between the constituents.

The *hydrodynamic models* which one can develop in this way differ whether one is interested in unsteady sea motions produced by tides and storm surges or in the residual—"steady"—circulation which results from the average of the actual flow over a time sufficiently long to cancel out tidal oscillations and transitory wind currents.

The evolution equations for the state variables r_α are coupled through the terms expressing the interactions of the constituent α with other constituents β, γ, ... They also depend on the water motion determined by the hydrodynamic models.

In a first approach, it is rewarding to separate the two effects and study first the dispersion (by currents, sedimentation and turbulence) of a "passive" constituent, i.e., one which does not have significant interactions with others. Then, to investigate the interactions (e.g., the path of a pollutant in the food chain), one can develop *box models* concerned with mean concentrations over some reasonably homogeneous regions of space. Box models are not affected by the detailed hydrodynamics of the sea, only its effects on inputs and outputs at the box's frontiers remain to be known.

Although *passive dispersion models* can only give conservative estimates of the distribution of chemicals and species in the sea and *box models* can only give an average knowledge of the interactions, they provide nevertheless a first valuable insight into the mechanisms of the marine system.

Of course, the model can combine dispersion and interactions and provide the detailed prediction of the state of the system at all points and time.

However, the gigantic amount of computer work which is required to solve large systems of coupled partial differential equations commends that the full scale simulation be restricted to dramatic cases where estimates are insufficient or to special problems (like the dumpings) where, in the area of interest, only a limited number of constituents are involved in a significant way.

The general dispersion-interaction model is described in (1) and subsequent papers (2). Different simplified forms of this model, pertinent to special studies, are given in the following and illustrated by examples of application.

4. Tide and Storm Surges Model

(*i*) *State Variables*

Mean depth-averaged horizontal velocity vector $\underset{\sim}{\bar{u}}$

Water height H

(The surface elevation ζ is given by $H = h + \zeta$ where, h is the water depth).

(*ii*) *External Forces per Unit Mass of Sea Water*

Tide-generating force $\underset{\sim}{\xi}$

Gradient of atmospheric pressure $\nabla\left(\frac{Pa}{\rho}\right)$

Wind stress $\underset{\sim}{\tau_s}$

Relation of wind stress to wind velocity $\underset{\sim}{v}$ at the reference height

$$\underset{\sim}{\tau_s} = \frac{C}{H}\,\underset{\sim}{v}\,\|\,\underset{\sim}{v}\,\|$$

(*iii*) *Evolution Equations*

$$\frac{\partial H}{\partial t} + \nabla \cdot (H\,\underset{\sim}{\bar{u}}) = 0$$

$$\frac{\partial \underset{\sim}{\bar{u}}}{\partial t} + \underset{\sim}{u} \cdot \nabla \underset{\sim}{u} + f\,\underset{\sim}{e_3} \Lambda\, \underset{\sim}{u} = \underset{\sim}{\xi} - \nabla\left(\frac{Pa}{\rho} + g\zeta\right) + a\,\nabla^2 \underset{\sim}{u} - \frac{D}{H}\,\underset{\sim}{u}\,\|\,\underset{\sim}{u}\,\| + \frac{C}{H}\,\underset{\sim}{v}\,\|\,\underset{\sim}{v}\,\|$$

where, the $\underset{\sim}{e_1}$ and $\underset{\sim}{e_2}$ axes are horizontal, the $\underset{\sim}{e_3}$-axis vertical and where,

$$\nabla = \underset{\sim}{e_1}\,\frac{\partial}{\partial x_1} + \underset{\sim}{e_2}\,\frac{\partial}{\partial x_2}$$

(*iv*) *Control Parameters*

f : Coriolis parameter (twice the vertical component of the angular velocity of the earth)

ρ : specific mass of the sea water

a : horizontal effective viscosity

D : bottom friction coefficient

C : atmospheric drag coefficient

h : depth.

(*v*) *Interpretation of the Evolution Equations*

The time variation of the velocity vector $\underset{\sim}{\bar{u}}$ is the result of :

α : advection $\underset{\sim}{\bar{u}} \cdot \nabla \underset{\sim}{\bar{u}}$

β : rotation $f\,\underset{\sim}{e_3} \Lambda\, \underset{\sim}{\bar{u}}$ produced by the Coriolis effect in axes fixed on the rotating earth

γ : mixing by shear effect and turbulence $a\,\nabla^2 \underset{\sim}{u}$

δ : friction on the bottom $-\frac{D}{H}\,\underset{\sim}{\bar{u}}\,\|\,\underset{\sim}{\bar{u}}\,\|$

ϵ : acceleration by agents of three different types

ε.1 : the wind stress on the sea surface $\frac{C}{H}\,\underset{\sim}{v}\,\|\,\underset{\sim}{v}\,\|$ related to the wind velocity $\underset{\sim}{v}$ at some reference height

ε.2 : the gradient of the atmospheric pressure and of the surface elevation

$$-\nabla\left(\frac{Pa}{\rho}+g\zeta\right)$$

ε.3 : the external force $\underset{\sim}{\xi}$. The type of external force one has in mind here is essentially the tide-generating force which is generally assumed to derive from a potential. (i.e., $\nabla\ \Lambda\ \underset{\sim}{\xi}=0$). $\underset{\sim}{\xi}$ can then be combined with the pressure and surface elevation gradients.

5. Model of Residual Circulation

(i) State Variables

Stream function ψ

The two components of the residual flow rate vector $\underset{\sim}{U}_0$ are given by

$$U_{0,1}=-\frac{\partial\psi}{\partial x_2}$$

$$U_{0,2}=\frac{\partial\psi}{\partial x_1}.$$

(ii) External Forces per Unit Mass of Sea Water

Residual stress $\underset{\sim}{\theta}$

$$\underset{\sim}{\theta}=(\underset{\sim}{\tau_s})_0+(\underset{\sim}{\tau_t})_0$$

where, $(\underset{\sim}{\tau_s})_0$ is the residual wind stress and $(\underset{\sim}{\tau_t})_0$ the residual tidal stress(2)

$$(\underset{\sim}{\tau_t})_0=-[g\zeta_1\ \nabla\zeta_1+\nabla\cdot(H^{-1}\underset{\sim\sim}{UU})]_0$$

where, ζ_1 denotes the surface elevation produced by tides and transitory wind forces.

(iii) Steady State Residual Equation

$$\kappa\nabla^2\psi-\frac{\partial\psi}{\partial x_1}\left(f\frac{\partial h}{\partial x_2}+\frac{2\kappa}{h}\frac{\partial h}{\partial x_1}\right)+\frac{\partial\psi}{\partial x_2}\left(f\frac{\partial h}{\partial x_1}-\frac{2\kappa}{h}\frac{\partial h}{\partial x_2}\right)=h\,\omega_3+\frac{\partial h}{\partial x_2}\theta_1-\frac{\partial h}{\partial x_1}\theta_2$$

where, θ_1 and θ_2 are the two horizontal components of $\underset{\sim}{\theta}$ and where, ω_3 is the vertical component of $\nabla\ \Lambda\ \underset{\sim}{\theta}$.

(iv) Control Parameters

κ : bottom friction coefficient for residual flow

f : Coriolis parameter

h : depth.

(v) Interpretation of the Residual Circulation Equation

The space distribution of the stream function ψ is the result of

α : combination of bottom slope and Coriolis effects

$$f\left(\frac{\partial\psi}{\partial x_2}\frac{\partial h}{\partial x_1}-\frac{\partial\psi}{\partial x_1}\frac{\partial h}{\partial x_2}\right)$$

β : combination of bottom slope and bottom friction effects

$$-\frac{2\kappa}{h}\left(\frac{\partial\psi}{\partial x_1}\frac{\partial h}{\partial x_1}+\frac{\partial\psi}{\partial x_2}\frac{\partial h}{\partial x_2}\right)$$

γ : combination of bottom slope and residual stress effects

$$\theta_1\frac{\partial h}{\partial x_2}-\theta_2\frac{\partial h}{\partial x_1}$$

δ : residual stress forcing $h\,\omega_3$.

6. Passive Dispersion Models

(i) State Variables

Depth-averaged concentration of any passive constituent α or depth-averaged temperature ($\bar{c}=\bar{r}_\alpha$ or $\bar{c}=\bar{\theta}$) — $\bar{c}$

Depth-averaged horizontal velocity vector (given by separate hydrodynamic model) — $\underset{\sim}{\bar{u}}$

Water height (given by separate hydrodynamic model) — H

(ii) Inputs-Outputs

Total input in a water column of unit base (including volume sources, surface and bottom fluxes. If these result in a net output, Λ is negative). — $H\Lambda$

(iii) Evolution Equation(3)

$$\frac{\partial\bar{c}}{\partial t}+\underset{\sim}{\bar{u}}.\nabla\bar{c}+H^{-1}\nabla.\left(\gamma_2\frac{H\sigma_3}{\bar{u}}\bar{c}\,\underset{\sim}{\bar{u}}\right)=\Lambda+H^{-1}\nabla.\left[\gamma_1\frac{H^2}{\bar{u}}\underset{\sim}{\bar{u}}(\underset{\sim}{\bar{u}}.\nabla\bar{c})\right]+\nabla.\tilde{\kappa}\,\nabla\bar{c}$$

(iv) Control Parameters

σ_3 : migration (sedimentation or ascension) velocity $\sigma_3=0$ for temperature and neutrally buoyant constituents

$\tilde{\kappa}$: horizontal eddy diffusivity

γ_1,γ_2 : shear effects coefficients(2)(3)(4)(5).

(v) *Interpretation of the Evolution Equation*

The evolution in time of the depth-averaged variable $\bar{c}$ is the result of

α : advection by the depth-averaged velocity $\bar{u} \cdot \nabla \bar{c}$

β : shear effect correction to the advection taking into account that, as a result of migration, the maximum of $\bar{c}$ may occur in a region of the water column where the actual horizontal velocity is significantly different from $\bar{u}$[2][3]

$$H^{-1} \nabla . \left(\gamma_2 \frac{H \sigma_3}{\bar{u}} \bar{c} \, \bar{u} \right)$$

γ : shear effect dispersion[2][3][4][5]

$$H^{-1} \nabla . \left[\gamma_1 \frac{H^2}{\bar{u}} \bar{u} (\bar{u} . \nabla \bar{c}) \right]$$

δ : turbulent dispersion $\nabla . \bar{\kappa} \nabla \bar{c}$

ε : external inputs (or outputs) Λ

7. Niche Interactions Model

(i) *State Variables*

Averages over the whole niche's space of all interacting chemical and ecological state variables r_α or θ s_α

(ii) *Inputs-Outputs*

Total input (output if negative) in the niche (including volume sources and fluxes or flows in and out of the niche at the boundaries) S_α

(iii) *Evolution Equations*

$$\frac{ds_\alpha}{dt} = S_\alpha + I_\alpha (t, s_1, s_2, \ldots, s_n)$$

I_α represents the rate of production (or destruction) of s_α by chemical, biochemical or ecological interactions. In general I_α is a function of time and all interacting variables s_β. I_α depends on the particular interactions involved. In many cases, it can be simply approximated by combinations (in sums and products) of simple laws such that

(a)	k_α	(constant)
(b)	$k_{\alpha\beta} s_\beta$	(linear)
(c)	$k_{\alpha\beta\gamma} s_\beta s_\gamma$	(bilinear)
(d)	$k_1 s_\alpha - k_2 s^2_\alpha$	(logistic)
(e)	$k_1 \frac{s_\beta}{k_2 + s_\beta}$	(Michaeles-Mentem-Monod)

where, the k_α , $k_{\alpha\beta}$, $k_{\alpha\beta\gamma}$ are functions of time and control parameters.

(iv) *Control Parameters*

Several control parameters influence the interaction laws and appear in particular in the expression of the coefficients k_α , $k_{\alpha\beta}$, ... In some cases, it is simpler to consider these coefficients as resulting control parameters to be determined experimentally.

(v) *Interpretation of the Evolution Equation*

The niche-averaged value of the state variables r_α or θ changes in time as a result of

α : input or outputs in or out of the niche S_α

β : chemical, biochemical or ecological interactions. I_α

8. Examples of Applications

8.1 *Tides and Storm Surges Model*

The current regime in the North Sea is mostly tidal. The most important partial tide is the lunar semi-diurnal tide. Coastal tidal data are well-known and come from the Table des Constantes Harmoniques de Monaco.

Currents and sea elevations are not purely harmonical function of time due to non-linear terms in the equations of motion. These non-linearities appear in shallow area ; the Belgian, Dutch, German, Danish coast are characterized by shallow waters. In order to compare the amplitude and phase of the M_2 tide at coastal stations a Fourier analysis of the sea level is carried out. The comparison between observed and calculated amplitudes and phases is given (Figure 1) for coastal stations. The agreement is fairly good ; most of the points are distributed near the ideal line at 45 degrees. Some discrepancies appear along the British coast for the amplitude due to very sharp depth variations. Near Lowestoft (Suffolk) some differences exist for the phase of the tide because this region is submitted to the influences of the North Atlantic and Dover Strait tidal forces. A slight error in the estimation of sea levels along open sea boundaries strongly modifies the phase of the tide in these regions. The approximation of the coast-line by a rectangular grid introduces also errors : the wave phase is thus very sensitive to the position of the numerical grid.

Figures 2 & 3 show the cotidal and corange lines[6]. The agreement is satisfactory. Due to the small number and low quality of sea level measurements in the inner part of the North Sea one can assume that our model gives better results than those provided by Proudman and Doodson[7].

Tidal currents measured and calculated are also compared ; the agreement is good.

8.2 *Residual Circulation Model*

The general circulation in oceans is mostly wind-driven. One can explain with such a theory the existence

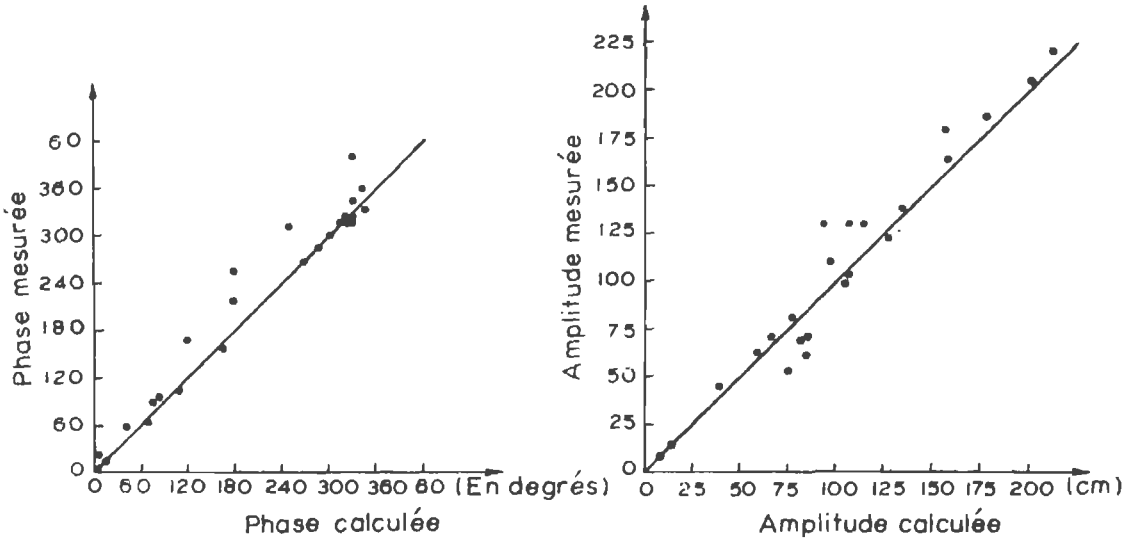

FIGURE 1 : Correlation between calculated and observed phase and amplitude of the M_2-tide.

of the well-known currents (Gulf Stream, Equatorial, Counter equatorial currents, etc.). The long-term circulation in the North Sea is influenced by the North Atlantic current which enters the North Sea through the Straits of Dover and through the Channel between the Orcades and Shetland Isles. The influence of the Baltic sea is weak but provides water with a low content of salt ($<34‰$). From oceanographic measurements (T, S, O_2) it is possible to determine the general distribution of the different water masses([8])([9]) (see Figure 4).

In winter the North Sea water has no haline and no thermal stratifications except in the Norwegian Channel and near the coast line. The barotropic model can be used. In summer the haline stratification remains weak but a thermal stratification exists in the northern and central part of the basin. The barotropic model may give approximate results during that period of time.

Figure 5 shows the residual circulation calculated without explicitly introducing the tidal stress. The wide stream coming from the North Channel flows down the British coast as far as East Anglia. The intensity of the stream is decreasing southerly ; there is only one swirl near the Scottish coast line. A small part of the North Atlantic water enters the Skaggerrak. The Dover Strait stream is broadening out after some kilometres and the width of this stream remains constant until the Skaggerrak. The circulation is very simple but it is impossible with this model to explain the swirl in the German Bight, the swirl around the Dogger Bank and the swirl near the Belgian coast. The model which takes into account the tidal stress is the only one able to reproduce the actual residual circulation (Figure 6). The general pattern remains but important modifications appear in different regions. Along the British coast and in the German Bight some swirls exist and are observed for a long time([10]). Figure 6 exhibits also an other vortex around the Dogger Bank ; Ramster([11]) proves its existence with sea-bed drifters. Other swirls exist in the central part of the North Sea where the residual current was very weak in the former model (Figure 5). The model reveals also a swirl and a south-westerly current near the Belgian coast([12]).

8.3 *Passive Dispersion Model*

The model has been applied to the determination of the dispersion pattern subsequent to a dye release or a dumping.

Figure 7 illustrates the influence of the shear effect on the anisotropy of the patch of dye.

Figure 8 shows a comparison between the observed and predicted shape of patch of rhodamine B, sixty-eight hours after release. The theoretical curve is calculated using a simplified version of the model which fits the best ellipse to the tidal velocity vector diagram.

8.4 *Box Interactions Model*

An extensive survey of chemical and ecological variables in the Eastern part of the Southern Bight was made during the years 1971, 1972, 1973 and 1974 in the scope of the Belgian National Program on the Environment, Sea Project. On the basis of these informations, the survey region was divided into three zones where different conditions prevail (Figure 9).

One can see that the different zones correspond to different residual circulation regimes.

(*i*) Zone 1, off the Belgian coast corresponds to the residual gyre. Water from the Scheldt Estuary is to a large extent entrained in the gyre before it can escape to the North. An

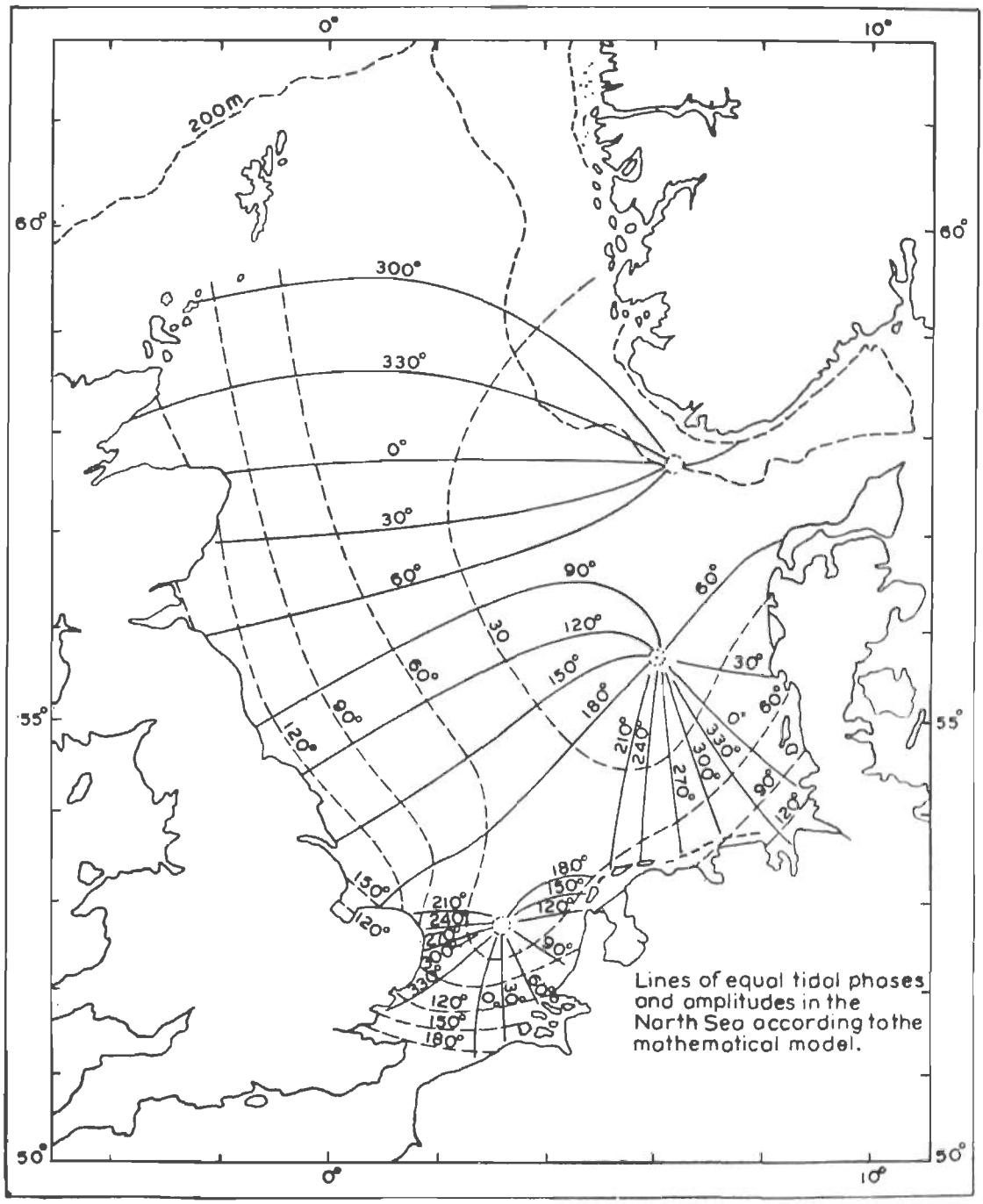
0°
10°
200m
60°
55°
50°
300°
330°
0°
30°
60°
90°
120°
150°
180°
210°
240°
270°
300°
330°
Lines of equal tidal phases and amplitudes in the North Sea according to the mathematical model.

FIGURE 2.

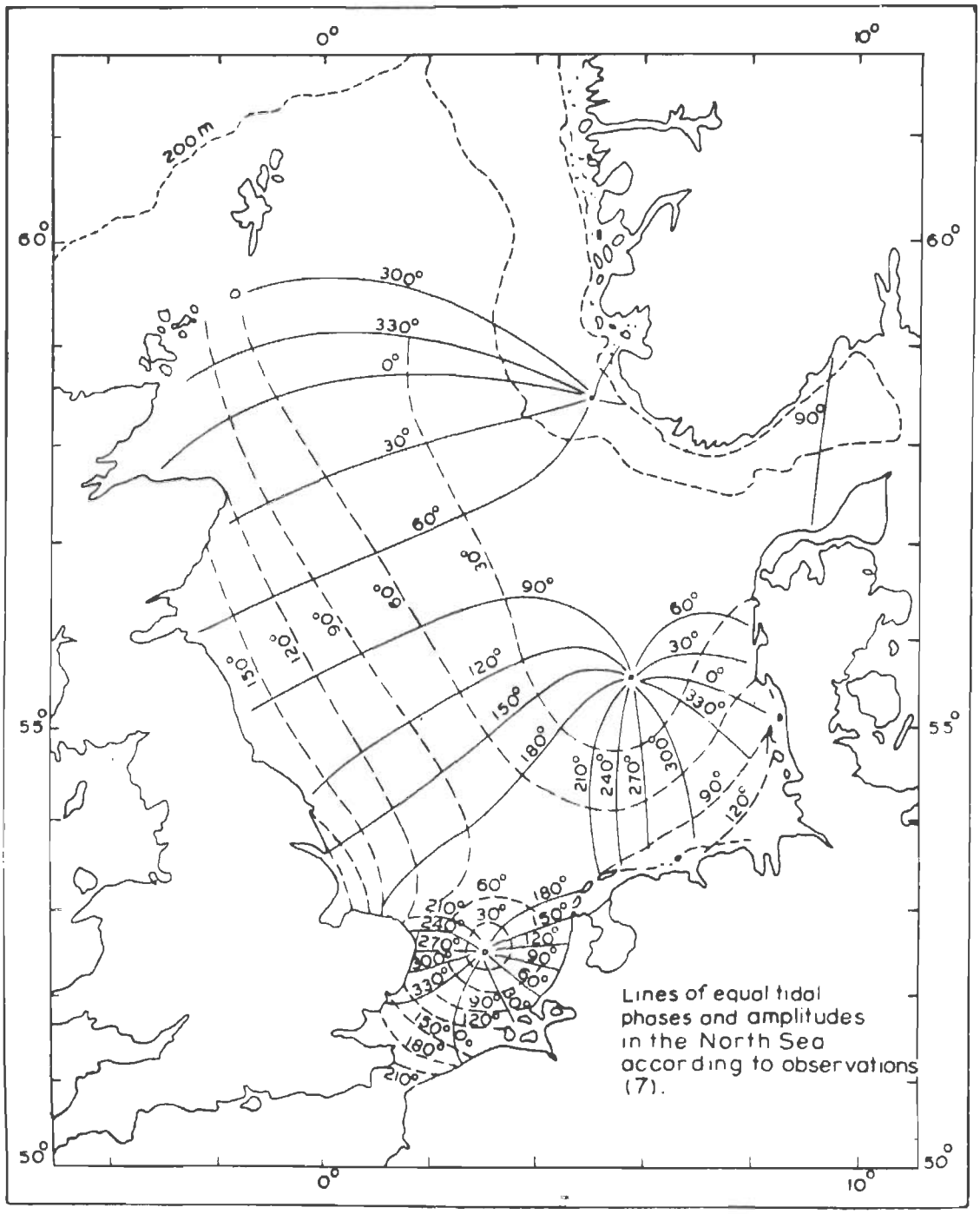
0°
10°
60°
55°
50°
200 m
Lines of equal tidal phases and amplitudes in the North Sea according to observations (7).

FIGURE 3.

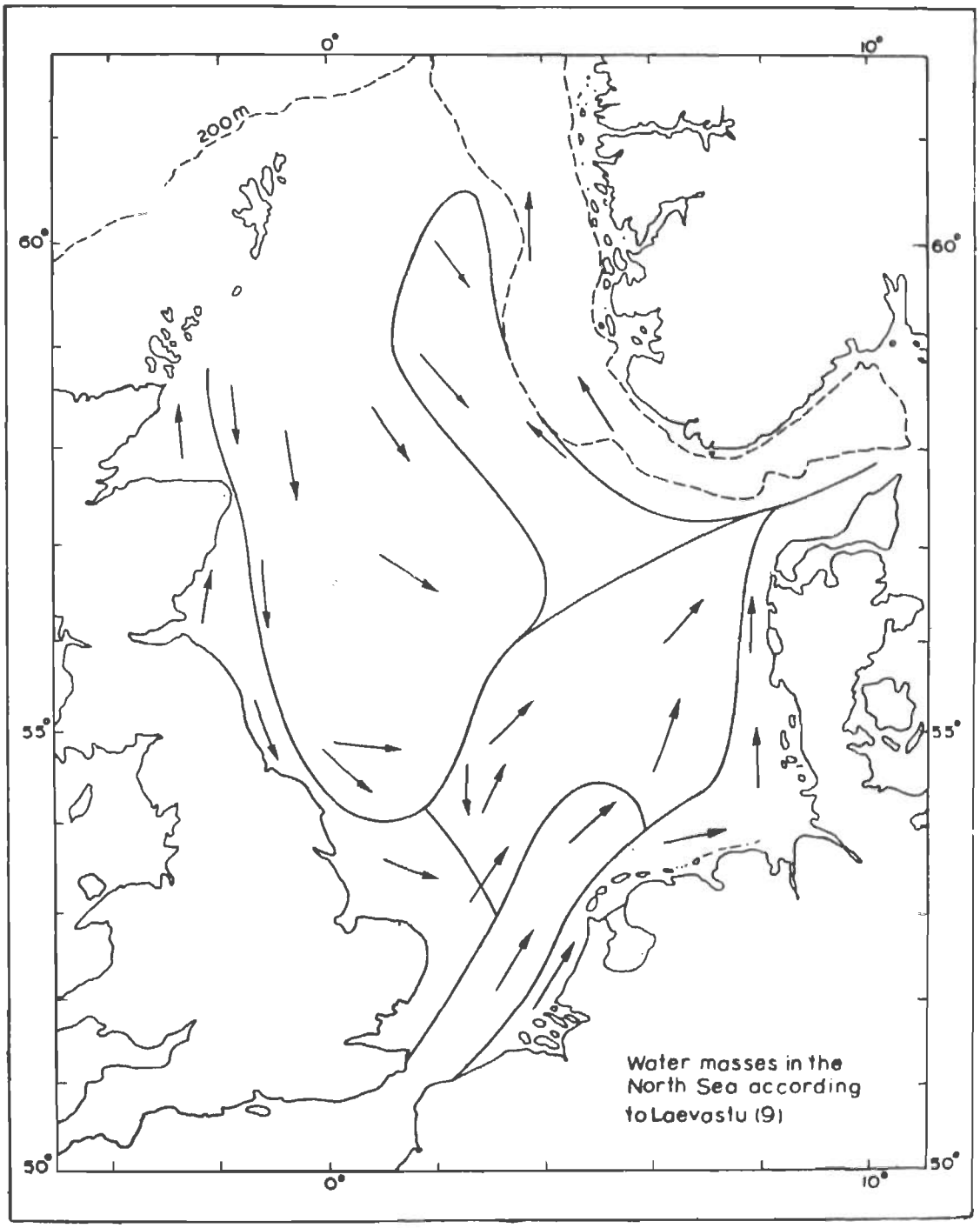
0°
10°
200m
60°
55°
50°
Water masses in the
North Sea according
to Laevastu (9)

FIGURE 4.

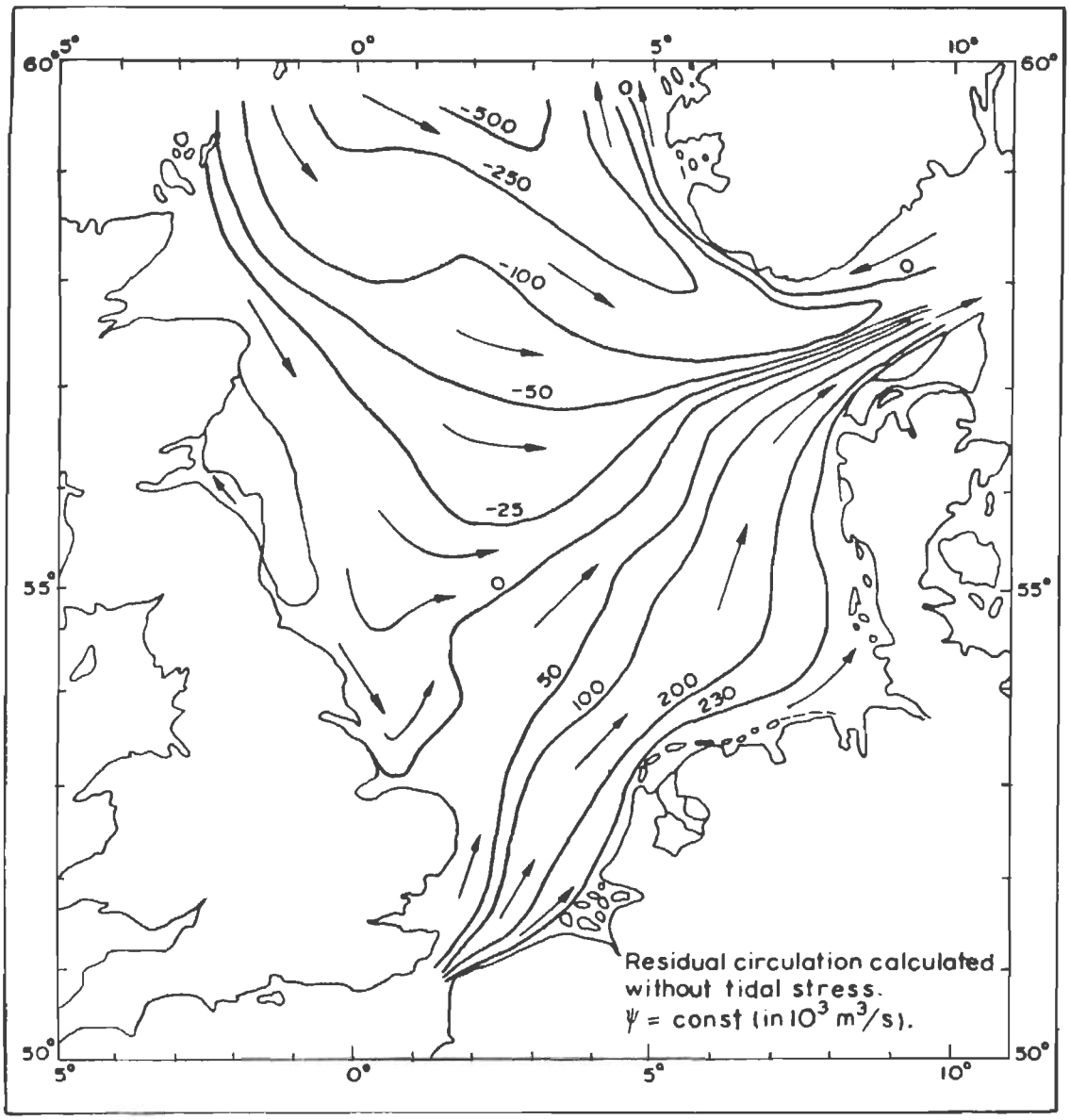

FIGURE 5.

island of high turbidity ($> 10^{-2}$ kg m^{-3}) is observed in the region where closed stream lines are predicted by the model. Bottom sediments in zone 1 are characterized by large areas of mud which can be explained by the tendency to form—as shown by the residual current model—an outer lagoon "in which increased suspended matter arrival tends to be preserved by the current pattern, is flocculated and aggregated by biological activity and preserved from net erosion by weakened wave activity"([14]).

(*ii*) Zone 2 corresponds to fairly parallel stream lines showing off the north-bound flow of the branch of the Gulf Stream which penetrates the North Sea through the Straits of Dover. The turbidity in zone 2 is considerably lower and no systematic silt deposition occurs.

(*iii*) Zone 3 corresponds to water masses under direct influence of the Meuse-Rhine estuary. The rivers' outfall is in a sense prolonged into the sea by a residual flow parallel to the Dutch coast, to the North.

The lagoon conditions which result from the residual circulation in zone 1 is responsible for striking differences between the dynamics of the ecosystems in that region and in zone 2.

The high turbidity of the water in zone 1 causes light

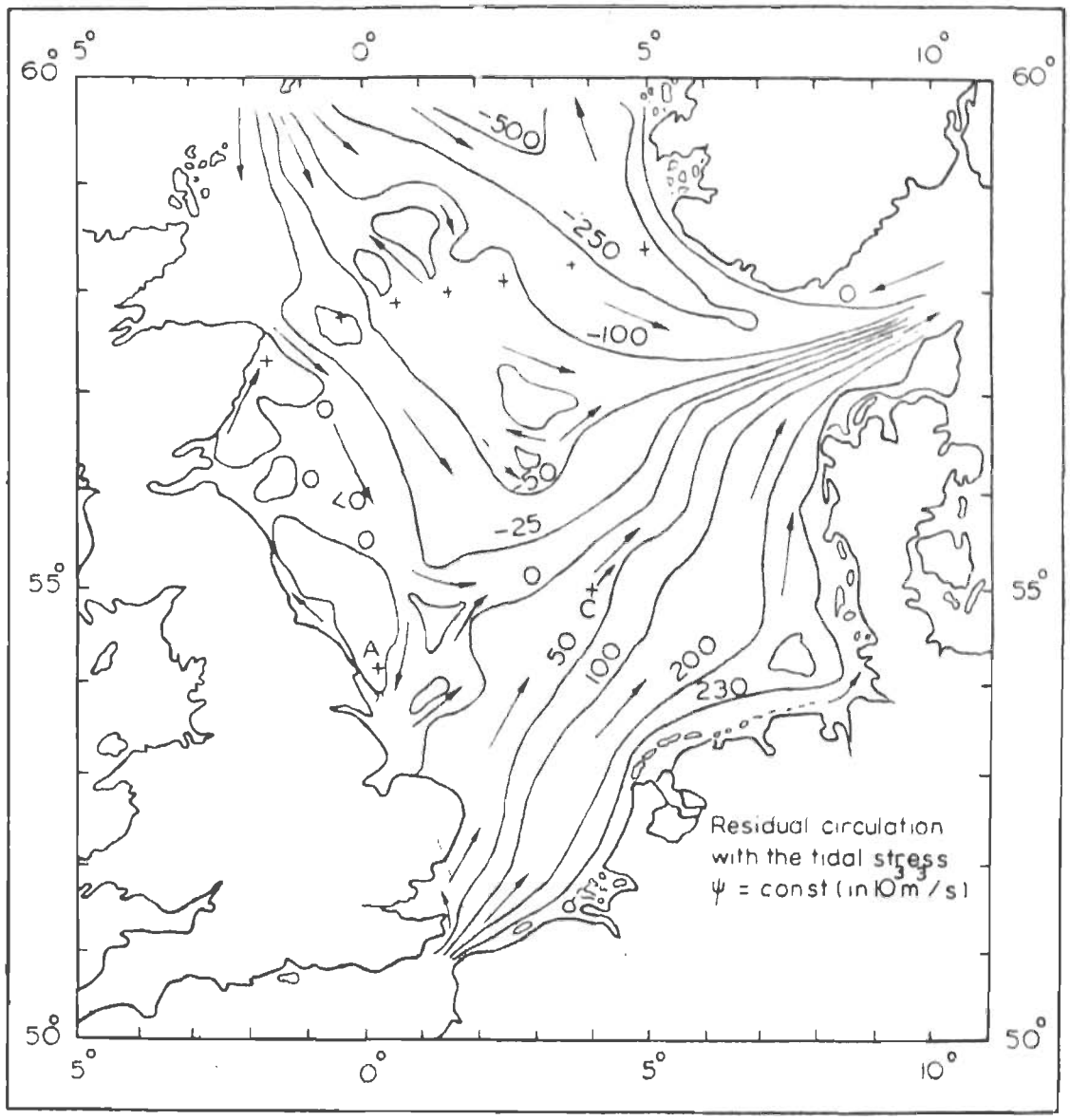

FIGURE 6.

extinction and reduces primary productivity. The dominance of microplankton in that region (as compared to nannoplankton in zone 2) with a higher half saturation constant could affect productivity in the same way. Taking into account, also, that the depth is smaller in the coastal region, one should expect the integrated production (over depth) to be considerably smaller in zone 1. Observations reveal, however, that—although there are differences in the annual variations—the yearly average is about the same in the two regions (~ 18 g N/m² year)([14]).

This result is obviously related to the much higher nutrient concentration and the much larger specific phytoplankton biomass (measured by chlorophyll *a*) observed in zone 1 where lagoon conditions prevail (Figure 10).

Additional information is provided by the ratio phaeophytin *a*/chlorophyll *a* which is systematically larger than one in zone 1 and smaller that one in zone 2; indicating that, in zone 1, most of the phytoplankton cells are dead cells. Zooplankton grazing, on the other hand, is more important in zone 2 than in zone 1, where planktonic and benthic heterotrophic bacteria seem to play the essential role.

A picture thus emerges of a fairly well balanced

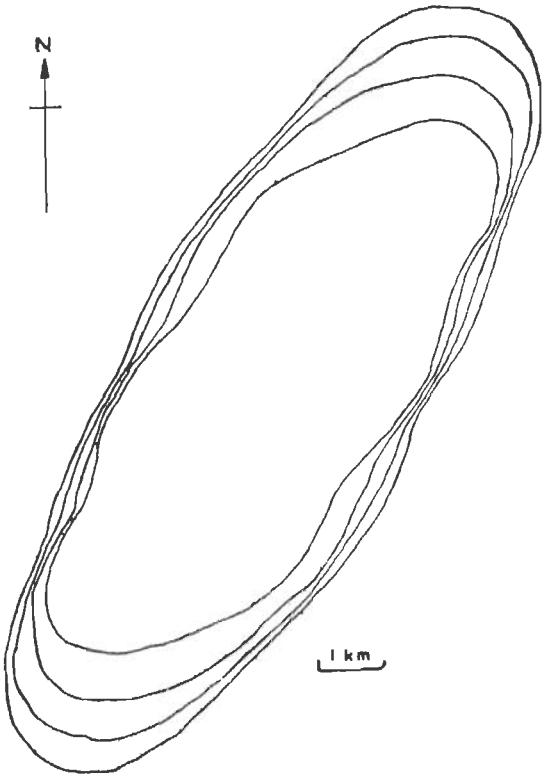

FIGURE 7 : Simulation of a dye-release experiment in the North Sea. Position : 51° 20′ N, 1° 34′ E ; Curves : 1/50 of initial central concentration 48 h-72 h-96 h-108 h after release.

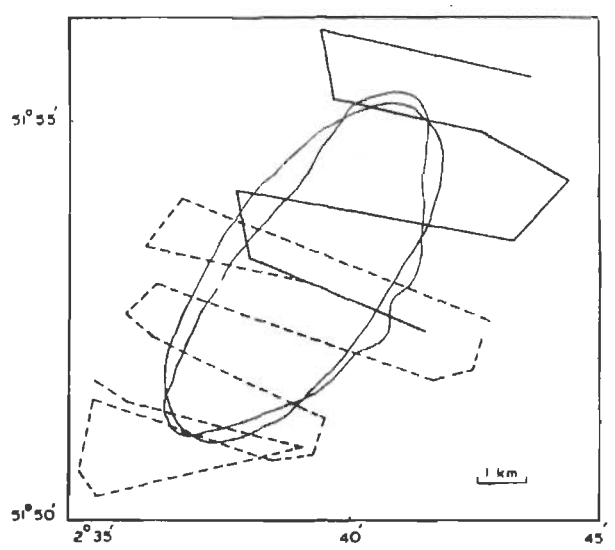

FIGURE 8 : Comparison between observed and predicted shape of a patch of rhodamine B 68 hours after release. The experimental curve is the irregular curve drawn by Talbot [18] [The broken plecewise straight lines are the ship's trajectories]. The theoretical curve is the regular ellipse predicted by the simplified model[5].

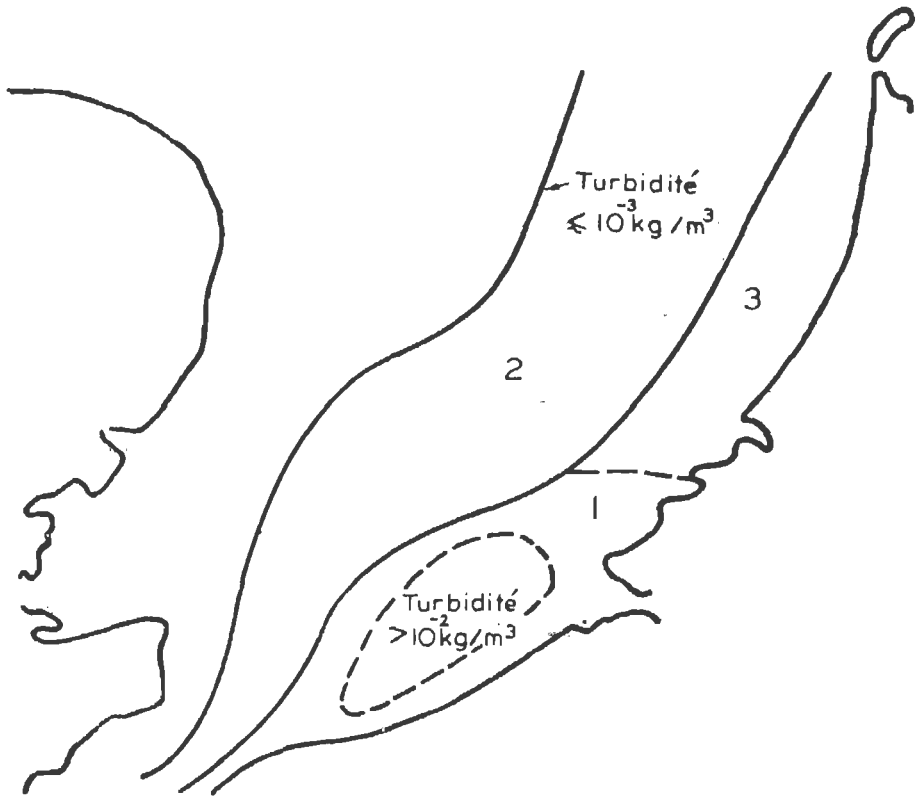

FIGURE 9 : Three Zones in the Southern Bight where a different pattern of residual circulation is predicted by the model and which also appear from the observations as three distinct boxes.

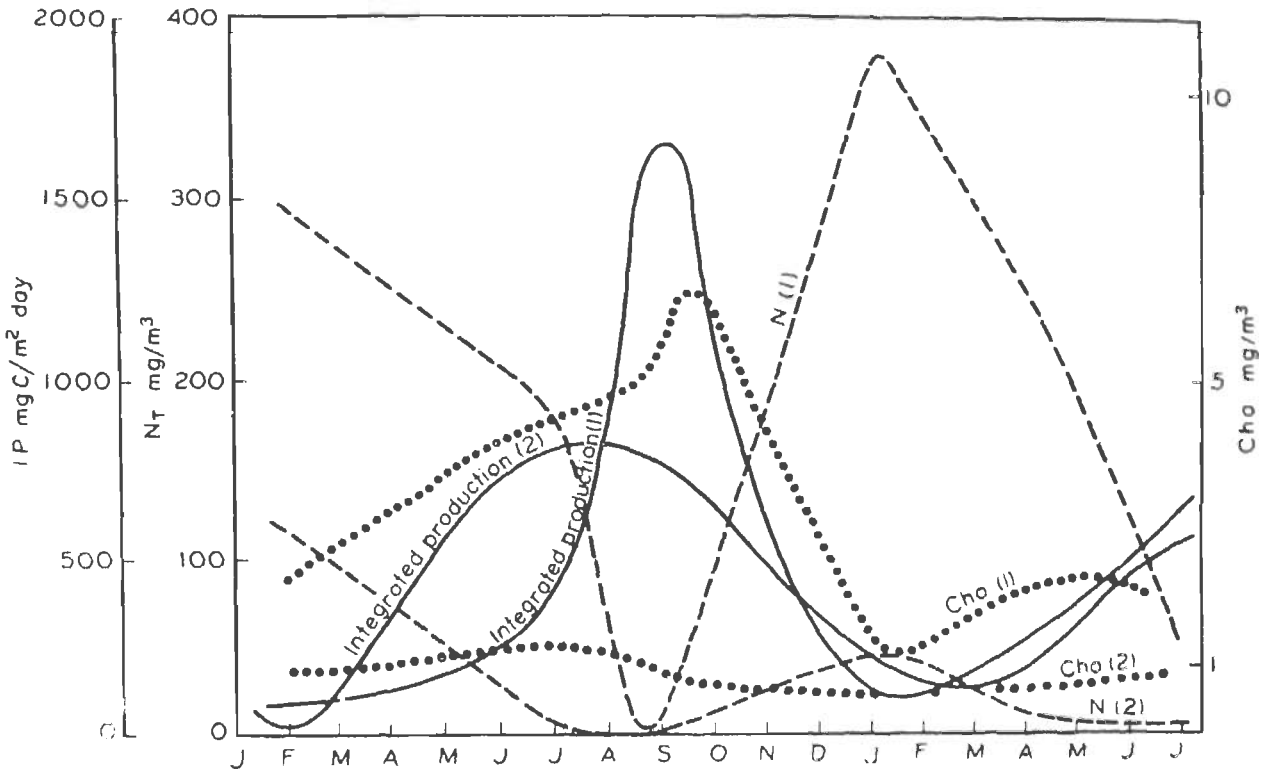

FIGURE 10.

ecosystem in zone 2 and a rather unhealthy one in zone 1 where intensive phytoplankton production occurs but not, as it should, to provide first level food in the food chain. The phytoplankton crop is harvested only to a small extent. Most of it is left to rot and most of the recycling of nutrients occurs at the dead phytoplankton level under the action of bacteria.

The dynamics of the ecosystems thus reflects the residual circulation patterns and the outer lagoon situation created by the residual gyre in zone 1.

9. Acknowledgement

This study was conducted in the scope of the Belgian National Environment Program, Sea Project. The authors are indebted to the Ministry for Science Policy for the support of their research.

10. References

(1) NIHOUL, J.C.J. (1973. a) : Mem. Soc. Sc. Lg, 4, 115.

(2) NIHOUL, J.C.J. (1974) : "Modelling of Marine Systems." Elsevier Publ., Amsterdam.

(3) NIHOUL, J.C.J. (1973. b) : Proc. Second IUTAM-IUGG Symposium on Turbulent Diffusion in Environmental Pollution, Charlottesville, U.S.A., 1973.

(4) NIHOUL, J.C.J. (1971) : Proc. North Sea Science Conf., Aviemore, Scotland, 1, 89.

(5) NIHOUL, J.C.J. (1972) : Bull. Soc. Sc. Lg, 10, 521.

(6) RONDAY, F.C. (1975) : "Modèle de circulation en Mer du Nord." Ph. D. Dissertation, Liège University.

(7) PROUDMAN, J. and DOODSON, A.T. (1924) : "The Principal Constituents of the Tide of the North Sea." Phil. Trans. Roy. Soc. London, A224, 185-219.

(8) BÖHNECKE, G. (1922) : Salzgehalt und Strömungen der Nordsee." Veröff. Inst. Meeresk. Univ. Berl., Neue Folge A., Geog.—Naturwiss. Reihe N° 10, 1-34.

(9) LAEVASTU, T. (1963) : "Serial Atlas of the Marine Environment." Folio 4, 2 Charts, published by Amer. Geogr. Sc.

(10) HILL, H.W. (1973) : "Currents and Water Masses." in North Sea Science, Edited by E. Goldberg, MIT University Press, 17-42.

(11) RAMSTER, J.W. (1965) : "Studies with the Woodhead Seabed Drifter in the Southern North Sea." Lab. Leafl. Fish. Lab. Lowestoft (N.S.) N° 6, 1-4.

(12) NIHOUL, J.C.J. and RONDAY, F.C. (1975) : Tellus 27, 5.

(13) TALBOT, J.W. (1970) : Proc. F.A.O. Technical Conf. on Marine Pollution, Rome, 1970.

(14) MATH. MODELSEA (1974) : "Mathematical Models of Continental Seas." Dynamic Processes in the Southern Bight, Hydrography Committee, C.M. 1974-C : 1.

APPENDIX

Data Acquisition and Processing

1. *Ships Survey*

The Belgian Navy provided five ships whose characteristics and activities are summarized in Table a. I. The main cruises consisted in the study

—of 25 points distributed on rectangular or radial networks and surveyed regularly, at least every season. Particularly, the important cruise of September-October 1973 was one of our contributions to the JONSDAP 73 (Joint North Sea Data Acquisition Program) exercise in collaboration with the United Kingdom and The Netherlands.

—of some characteristic points of open sea and coastal waters, considered as fixed stations and continuously surveyed during a week, in 1973.

—of 1200 points for a unic sedimentological survey.

2. *Currentmeter Stations*

Our Plessey MO21, NBA DNC2A and VACM-AMF currentmeters were only received in August 1973 and used for the first time during Jonsdap 73.

Figure 11 shows the deployment of automatic stations during this exercise. Our program assured two stations at 51° 14′ N 2° 28′ E and 51° 31′ N 2° 25′ E and contributed to the rigs of instruments intercalibration and of spatial coherency check with the KNMI (De Bilt).

3. *Automatic Oceanographic and Meteorological Data Stations*

Because the model requires continuous knowledge of the boundary conditions, the acquisition of automatic and meteorological data stations was decided.

The buoys were required to be big and robust enough to carry safely a great amount of all kinds of sensors, to be easily noticeable by ships and to survive long periods of unattended operation in all seasons. The French Sysna buoy appeared to be the best compromise between our program's requirements and its financial possibilities (Figure 12, Table a. II).

The electronics was designed and developed by ourselves. It is quite sophisticated so that it can receive and treat nearly any form of sensor signal, operate a certain level of pre-processing (numerical integration, vectorial projections, sums, etc.) and monitor the buoy itself (energy levels, movements, safety, etc.).

Because of the general use of "COSMOS" type integrated circuits in the "Data Acquisition System", its power drain has been kept very low and is of the order of 3 watts. The used voltages are + 24 volts and—18 volts for the D.A.S. and + 24 volts for the radio transmitter, the sensors and the light.

Two AEROWATT type 24FP7 wind generators are the buoy's main energy source. Under normal conditions, the battery buffered output of only one of them is sufficient to maintain the whole buoy system including the powerful flashing light in operation.

The inconvenience of wind generators is their irregular output. This is why they are buffered by 24 Volts 195 A hours lead acid batteries. This set gives the buoy system an endurance of 7 days at full performance in the complete absence of wind by total generator breakdown.

A small set of dry Mallory Duracell alkaline manganese batteries provides a negative 18 volts, 20 A hours power supply for operational amplifier and various other circuits requiring a negative polarisation. As a simplification this negative voltage will be provided in the future directly from the mains 24 volts by a solid-state AC-DC converter.

4. *The Data Acquisition System (D.A.S.)*

The basic unit consists of a signal scanner and an AC to DC converter for analog inputs, and of a code adaptor and a digital multiplexer for the digital inputs. Auxiliary

TABLE a. I

Name of the ship	Type	Length (m)	Crew	Scientists	Number of effective working days at sea			Total
					1971	1972	1973	
Mechelen	M.S.C.	44	28	11	74	76	78	228
Zenobe Gramme	Ketch	28	13	3	26	32	42	100
Hasselt or Herstal or Kortrijk	M.S.I.	34	12	1	37	125	80	242
Total					137	233	200	570

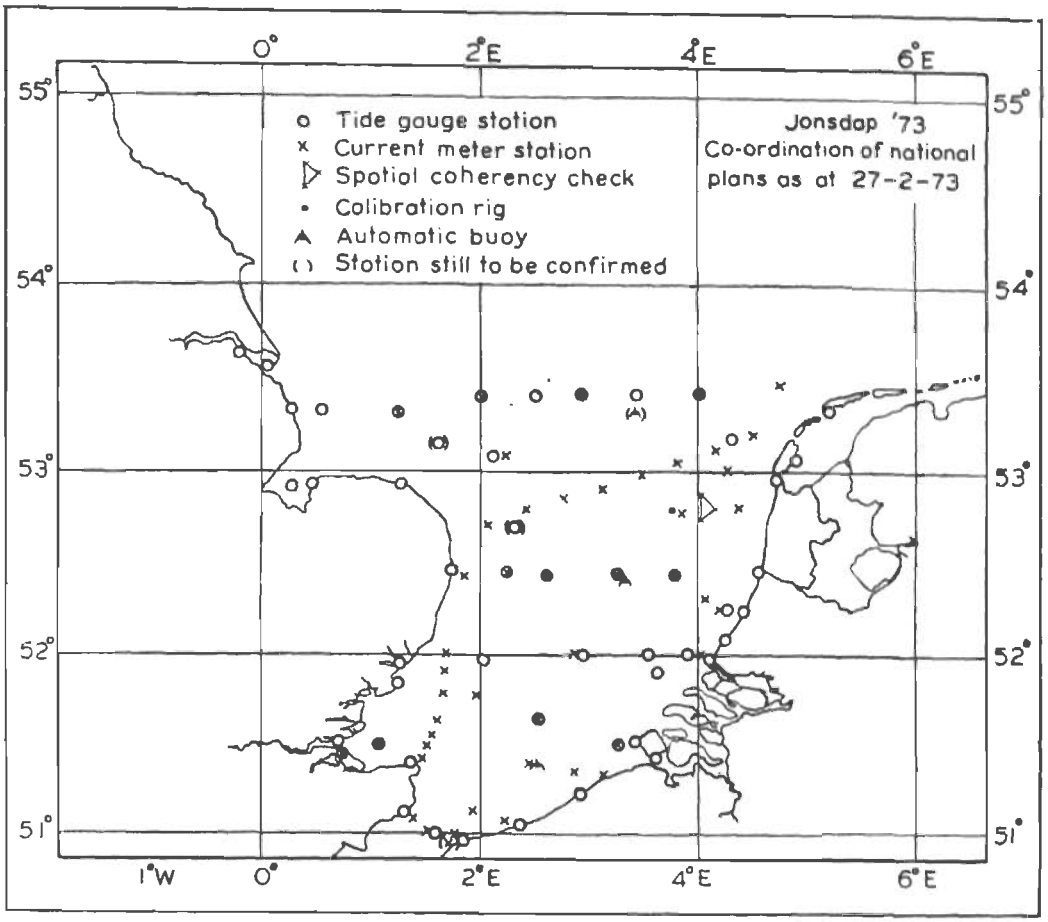

FIGURE 11.

TABLE a. II

The SYSNA Buoy.

MECHANICAL CHARACTERISTICS	
Overall diameter of the float	3,021 mm
Height of the float (including small ballast tail)	2,180 mm
Maximum height inside	1,580 mm
Mast length	8,100 mm
Mast diameter	150 mm
Displacement	2,000 kg
Float volume	10 m^3
Stability	2 t.m
Rolling period	2.8 s
Heave period	1 s
Spare buoyancy (with 1 ton of batteries and equipment)	7 tons
MATERIALS USED	
Buoys : AG4MC aluminium alloy, specially resistant to marine corrosion.	
Tubes : AG3. Cast parts : AS 13 74. Guys and guy fixings : stainless steel 316 (18/12 Mo).	

circuits adapt a wide range of input signals, numerically integrate certain parameters, record the time of the measurements, etc. The general use of "COSMOS" integrated circuits lead to high reliability and very reduced power requirements.

5. *Data Transmission*

The data are transmitted to Ostend by a 10 watt completely transistorized FM transceiver operating in the lower VHF band (Mobilophone CMT Phillips). A complete transmitter-receiver is used as well on the buoy as at the receiving station for two main reasons :

—equipment standardization and interchangeability ;

—possibility of bi-directional radio link for future remote control and selective interrogation.

The essential characteristics are :

Dimensions	: 70 × 235 × 235 mm ;
Weight	: 3 kg ;
Power requirements	: 24 V DC (21.1 to 31.7 V) transmission 2 A (48 W), receiving 0.12 A ;
Transmitting frequency	: 31.850 MHz ;

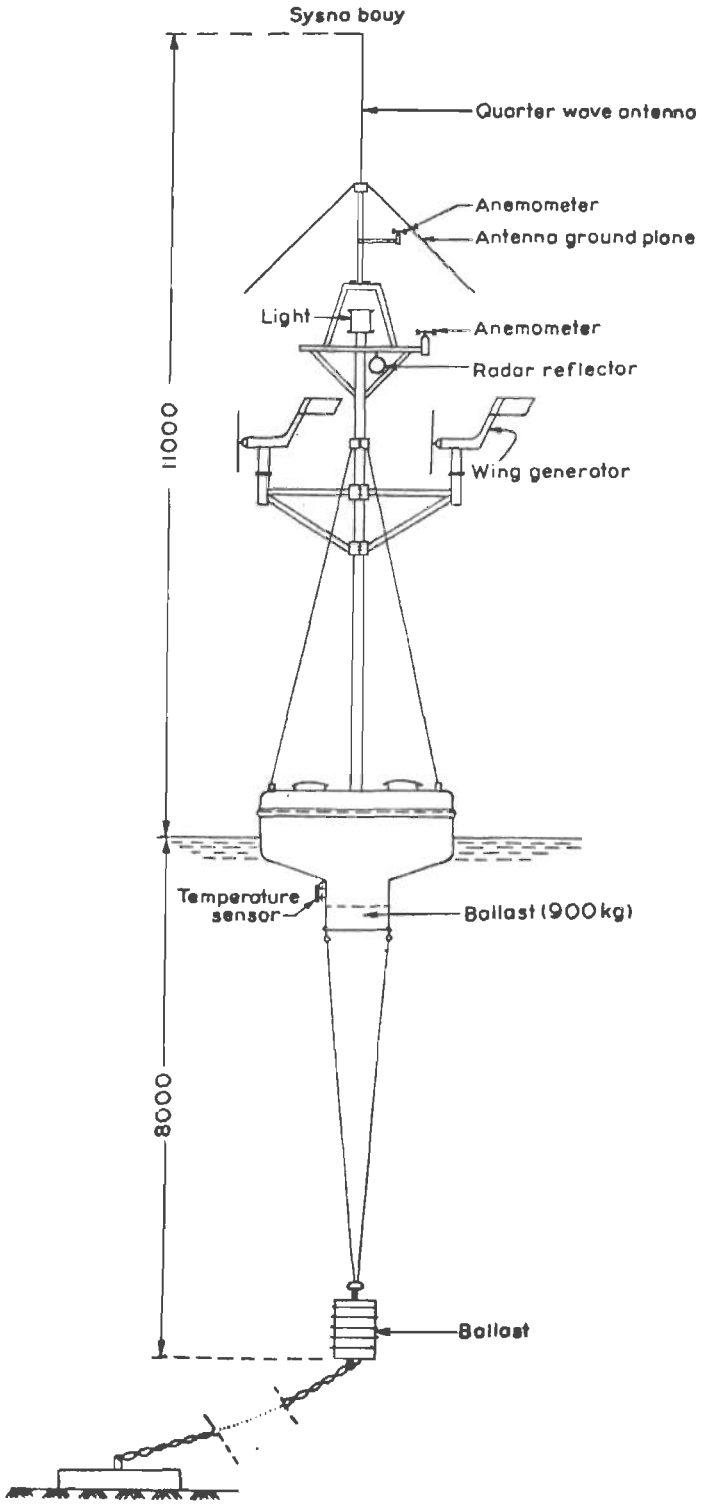
Sysno bouy
Quarter wave antenna
Anemometer
Antenna ground plane
Light
Anemometer
Radar reflector
Wing generator
11000
Temperature sensor
Ballast (900 kg)
8000
Ballast

FIGURE 12.

RF output power	: 10 watts ;
Modulation	: Phase modulation ;
Encoding	: P.C.M. applied to 2500 Hz subcarrier ;
Antenna	: Quarter wave fibreglass whip and ground plane elements ;
Range	: 80 km minimum.

6. *Sensors*

For the moment, the buoy is only equipped with some sensors which are known as the most reliable at sea. They measure wind speed, wind direction, barometric pressure, waves (Datawell heave sensor), air temperature and water temperature. The two latter ones are built and calibrated by ourselves.

Other sensors, and sometimes the most interesting ones, are still in an experimental phase, not yet miniaturised, cumbersome and energy greedy. Their long-term fiability is not warranted in reason of corrosion, fouling and shocks.

Sensors for direct and reflected light, *pH*, dissolved oxygen, heavy metals by accumulating, phytoplankton activity by autoradiography are at present in research and development.

7. *The Data Processing Computer*

A data processing computer is installed in Ostend and linked to the receiving radio station. It is a Hewlett Packard Type 2100 computer with a 32 words of 16 bits core memory. The various peripherals and input-output devices such as fixed and removable disc, magnetic tapes, teleprinter, fast tape puncher and reader, Tektronix CRT video display, 30 cm and 80 cm Calcomp plotters, Tally line printer, etc., make this relatively small computer specially suitable for receiving large amounts of data in all kinds and to output them after processing in any desired format.

The principal processing phases are :

—transcoding of the received binary data,

—putting in order the digits, the numbers and then the measuring cycles,

—dispatching of the data arriving from different stations,

—synchronisation and introduction or correction of the time scale,

—translation of the received numbers into proper parameters, by means of the calibration equations,

—control of the data : listing, display on video tube, automatic plots, statistical methods,

—editing, after manual or automatic error detection,

—concentration of the data : weighted averages, numerical filters,

—statistics, correlations, power spectra,...

It is very important that most of these operations can be carried out "on line" and the remaining ones as soon as possible after reception of the data in order to detect any instrumental malfunction immediately and to make them available for a direct, easy and efficient use in our mathematical models.

Use of the Computer to Control Land Subsidence

GIUSEPPE GAMBOLATI
IBM Scientific Center
S. Polo 1364, Venice, Italy.

SYNOPSIS

One consequence of growing concern over subsurface fluid pumping is the unrecoverable soil compaction and the related land subsidence. The mechanism of subsidence is an interaction between the stress field and the flow field operating within the geologic system. Withdrawals of fluid cause a decrease of the pore pressure head and hence an increase in the intergranular stress under whose influence formations compact and ground surface subsides. The use of high-speed digital computers appears quite promising in its ability to handle large systems and to predict the impact on the environment of an intensive exploitation of the subsurface resources. The numerical models described in this paper simulate and predict land sinking due to fluid withdrawals in natural two or three-dimensional basins and reservoirs. After calibrating the models against the available records, we can apply them at any stage of the system development to assess the convenience of alternative pumping schedules in relation to the irreversible modifications that land subsidence produces in the environment.

Introduction

In recent years a growing attention has been directed toward a group of environmental problems including regional land subsidence as a very important one. The worldwide exploitation of subsurface resources is creating many areas where the consequent land sinking will become soon a matter of concern for the inhabitants and the local authorities. The settlements of coastal regions are particularly dangerous because of the risk that stretches of land, once permanently above sea level, are entirely submerged or flooded periodically during the high tides. Among the major causes of surface lowering induced by human activities are the extensive artificial withdrawals of fluid from beneath the soil surface.

Major subsidence of several oil-gas fields has been reported in the literature (1). We can recall Wilmington oil field in the harbor area of Los Angeles and Long Beach, California (more than 8 m from 1937 to 1962), the oil fields on the shore of Lake Maracaibo in Venezuela (3.4 m from 1926 to 1954), Goose Creek oil field in Texas (almost 1 m from 1918 to 1925). Gas fields at Niigata, Japan, and in the Po Delta, Italy, experienced rapid subsidence in the late fifties. Lately subsidence is expected to develop in the Groningen gas field, The Netherlands(2).

Significant surface lowering due to ground water pumping has been observed in San Joaquin Valley, California (8 m from 1935 to 1966), in Mexico City (8 m from 1936 to 1968), in Santa Clara Valley (4 m from 1920 to 1967), California, in Tokyo and Osaka (3-4 m from 1928 to 1965), Japan.

A very recent case of particular interest is Venice (3). There the quantities of water extracted have been less than those that caused considerable sinking in the cited areas. The lowering, though modest, is nevertheless a matter of concern because it compounds the effect of the exceptionally high tides in the city during winter.

Many other gas-oil fields or hydrologic basins above sea level and not subject to inundation probably have shown subsidence, but with no marked deleterious consequence, therefore, they have not been publicized.

The mechanism that relates subsidence to withdrawal is that of subsurface compaction caused by changes in the fluid flow field operating within the geologic system. The artificial pumpings modify the balanced natural

conditions by causing a decrease of the pore pressure head and therefore, an increase of the effective intergranular stress. This is so because the fluid can no longer support as large a percentage of the load of the overlying formations, and more of this load must now be borne by the grain-to-grain contacts of the geologic material itself. Under the influence of the increase in effective stress the water or oil bearing strata compact and the land surface subsides.

Regardless of the nature of the fluid removed (gas, oil or water) the principles underlying the physical occurrence are the same. However, the geological setting can be different according to whether a gas-oil reservoir or a hydrologic basin is being analyzed. This accounts for the different models which are applied in either case.

If representative values of the soil and formation properties are available, we will be able to analyze these complex natural systems. One of the most powerful and effective methods of analysis involves the use of mathematical and numerical prediction models based on the equation of subsurface flow combined with the equations of the elastic equilibrium and solved numerically with the aid of a digital computer. With such models it is possible to determine the changes in the flow field due to well pumping and the compaction of the various formations in relation to both depth and time.

The models can be applied to predict the effects owing to different pumping schedules and to assess the suitability of alternative actions and the consequences of various proposed designs. Models can also provide guidance in the building of monitoring systems and even in the preparation of appropriate legislation and regulatory codes.

The present paper provides a critical survey of the numerical models suitable now-a-days to simulate and predict regional land subsidence due to subsurface fluid withdrawals. Particular emphasis is placed on the role that the digital computer can play in handling large and refined numerical models in relation to several influencing factors such as quality and quantity of available data, core storage requirement and processor time needed to perform an inevitably sizable number of long-term simulations. It will be shown that the most sophisticated techniques must often be dismissed in real subsidence calculations on the grounds that the scarcity of data together with the present computer limitations do not warrant their use.

Computer Models to Simulate Land Subsidence

It has long been understood that land subsidence is best analyzed with reference to the theory of consolidation, wherein it is recognized that consolidation represents the response of a compressible porous medium to changes in the fluid flow field operating within it. Till recently almost all mathematical models of land subsidence have been direct application of the Terzaghi consolidation theory (1, 4-6). This simplified theory has been adapted also to the computation of oil field compaction [e.g. (7)]. This approach, in the most sophisticated applications, involves analytical time-dependen t solutions to the boundary value problem based on the one-dimensional vertical equation of flow in which the piezometric declines are specified as boundary conditions. An excellent review of this approach as it applies to land subsidence is provided in (8). In a more recent review, presented at the Tokyo Symposium on Land Subsidence, Poland (9) refers to results based only on the classic one-dimensional theory, and he notes the need for more sophisticated mathematical or numerical models. In the entire symposium proceedings only one paper (10) presents an analysis based on a model of greater complexity.

A complete analysis of land subsidence requires the determination of the three-dimensional deformation field that accompanies the three-dimensional flow field. Schiffman et al (11) have classified consolidation theories into : 1) one-dimensional Terzaghi theory, 2) Pseudo three-dimensional consolidation theory based on the independent solution of the diffusion equation, and 3) complete three-dimensional consolidation theory based on the Biot equations.

In the remainder of this section we will develop the 2nd and 3rd approach as they apply to land subsidence and are used by the digital computer, starting with the latter and treating the second as a subset of the third. We will show that the 3rd approach must often be dismissed on the grounds of impracticability whereas the second offers at present the best trade off between data availability and computer limitations. We will also give indications as to how the working mathematical relations are modified according to whether a gas-oil reservoir or a hydrologic system is being simulated.

Coupled Models : General Three-dimensional Consolidation

The consolidation equations were first derived by Biot (12)(13) who stated the inter-relations existing in first approximation between the three-dimensional flow field of the fluid and the three-dimensional stress field of the medium. Neglecting the compressibility of the single grains usually much smaller than that of the rock bulk, Biot's theory relates the components of the rock matrix deformations u_i to the incremental "effective stresses" σ_{ik} acting upon the solid skeleton and the incremental pore pressure p. Including the equation of flow the results take the form of the following set of equations :

$$\frac{\partial \sigma_{1k}}{\partial x_1} + \frac{\partial \sigma_{2k}}{\partial x_2} + \frac{\partial \sigma_{3k}}{\partial x_3} = \frac{\partial p}{\partial x_k} \quad (K = 1, 2, 3) \quad \ldots(1)$$

$$\nabla \cdot \left[K_{ij} \left(\frac{\nabla \cdot p}{\gamma} + 1 \right) \right] = n\beta \frac{\partial p}{\partial t} + \frac{\partial \varepsilon}{\partial t}$$

where,

$$\sigma_{ik} = \sum_{jh} C_{ik,\,jh} \cdot \varepsilon_{jh} \quad \ldots(2)$$

In Equation (1) K_{ij}, γ, n, β and ε are respectively the hydraulic conductivity tensor, the specific weight of water, the medium porosity, the water compressibility and the volume strain. In Equation (2) $C_{ik,\,jh}$ are the components of the elasticity tensor : only 21 coefficients are distinct for real anisotropic media. The principal components of ε_{ij} are linked to the displacements u_i by :

$$\begin{cases} \varepsilon_{ii} = \dfrac{\partial u_i}{\partial x_i} \\ \varepsilon_{ij} = \varepsilon_{ji} = \dfrac{1}{2}\left(\dfrac{\partial u_i}{\partial x_j} + \dfrac{\partial u_j}{\partial x_i}\right) \quad i \neq j \end{cases} \qquad \ldots(3)$$

If we replace the σ_{ik} in Equation (1) by their values taken from Equation (2) keeping in mind Equation (3) for the strain components, we obtain a set of 4 equations in 4 unknowns : the incremental fluid pressure p and the three components of the displacement vector u_i. Solutions of the system will provide the distribution of u_i, in particular u_3 at the ground surface is the land subsidence.

At the theoretical level the Biot equations offer the most sophisticated approach to the prediction of land subsidence. Their Achilles heel is the large number of formation parameters needed: the 21 classical coefficients of anisotropic elasticity $C_{ik,\,jh}$, the six coefficients of anisotropic hydraulic conductivity K_{ij} and porosity n; 28 parameters in all. These parameters are needed for each formation in the case of non-homogeneous media. A second important drawback is the prohibitive amount of storage required to solve numerically Biot equations in natural three-dimensional compacting systems. Even if homogeneity and isotropy for both hydraulic and mechanical properties are assumed throughout the medium, as was done for instance in (14), the limitation still remains. The finite element solution supplied in (10) and (15) does not go far beyond the analytical formulation. The relevant applications are necessarily reduced to small and unrealistically simple configurations. The practical applicability of the Biot system of equations to regional land subsidence problems is at present unfeasible. A worthwhile alternative is provided by the approaches described below.

Decoupled Models : Three-dimensional Consolidation

We can partially remove ourselves from the horns of the previous dilemma by searching for the solution of the Equations (1) through two related steps. In the first step the equation of flow is solved independently of the remaining equations, thus providing the changes in the flow field. In the second step the outcome from the flow equation is used to compute the displacement distribution and ultimately the surface sinking. In other words the coupling between the flow field and the stress field is removed. To do so the necessary condition rests on a major assumption, namely, the volume strain ε in a point of the system depends only upon the pore pressure variation p in that point and not upon the pressure changes occurring in the surrounding medium.

An attempt to test the worth of this assumption has recently been contributed by Gambolati (16) who checked the validity of the diffusion equation in a semi-infinite mechanically homogeneous medium. The results show that the flow field and the stress field may be treated separately in the vast majority of artesian systems. The decoupling effect can produce appreciable deviations from the true solution only when the pumpage takes place in shallow units, particularly in water-table formations. However, in most free surface aquifers water is released mainly at the water-table and the transient flow is controlled by this moving material boundary rather than by the elastic aquifer compaction and fluid expansion. As a result the pore pressure distribution may again be provided independently of the calculation of the rock matrix displacements which can be made afterwards, once the time-dependent pressure head changes have been evaluated. According to this previously mentioned assumption we can write :

$$\varepsilon = \alpha \cdot p \qquad \ldots(4)$$

where, α is related to the elastic properties of the medium. Its value is :

$$\alpha = \frac{(1-2\nu)(1+\nu)}{E(1-\nu)} \qquad \ldots(5)$$

where, E and ν are the moduli of Young and Poisson respectively. Making use of Equation (4) the last relationship of the system (1) turns into the well-known parabolic differential equation whose solution is now more easily attainable than that of the complete Biot set of equations. The finite different scheme is the technique more frequently used [see for instance (17) & (18)] but recently the new powerful finite element method has been developing to an increasing degree even in the fluid flow field. The results, expressed in terms of time-dependent pressure distribution within the system, are then used as prescribed disturbing stresses in a three-dimensional calculation of the deformations. To this end the classical equations of elasticity (the first three of Equation (1) expressed in terms of displacements) are to be solved. This may be done numerically but in the case of homogeneous media one can resort to the concept of "strain nuclei". With such an approach the subsidence is evaluated by integrating the Green function u^*_i for the displacement field over the entire volume in which changes of p occurred. Geertsma (19) provided the vertical displacement u^*_3 due to a unit pressure change in a unit volume (tension center) of a semi-infinite homogeneous medium. Gambolati (20) extended the formulation so as to allow for a heterogeneous tension center in the homogeneous semi-infinite medium. The value of u^*_3 proves to be :

$$u^*_3 = A \cdot \left[\frac{h-z}{\rho^3} + \frac{z+3h-4\nu(z+h)}{\rho^{*3}} + \frac{6z(z+h)^2}{\rho^{*5}}\right] \qquad \ldots(6)$$

where, the meaning of the symbols is explained in Figure 1 and A is a coefficient depending upon the elastic properties of the nucleus and medium :

$$A = \frac{1+\nu_M}{\pi E_M} C_{bN}\left(\frac{2}{3} C_{bN} + \frac{1+\nu_M}{E_M}\right) \qquad ...(7)$$

In Equation (7) the subscripts M and N refer to medium and nucleus respectively and $c_b = 3(1-2\nu)/E$ is the compressibility of the rock bulk. Integration of Equation (6) yields the vertical displacement :

$$u_3(x_k) = \int_V p(x_l)\, u^*_3\ (x_l, x_k)\, dV(x_l) \qquad ...(8)$$

Relation (8) may advantageously be applied to provide the subsidence caused by oil production. In fact the relatively small dimension of the reservoir, its depth and geological setting (usually top and bottom impermeable, consolidated sediments, etc.,...) produce a three-dimensional displacement field and the effects at the land surface are substantially different from those observable in a hydrologic system where the subsidence is essentially equal to the basin compaction. The main limitation of Equation (8) lies in the requirement of homogeneity for the semi-infinite medium.

This approach has been recently used to predict the sinking of the Groningen area, The Netherlands, where a gas field is being developed (21). Integral (8) is evaluated numerically over an arbitrary-shaped reservoir. It is replaced by a finite sum of the discrete contributions from the small elements $\triangle V$ into which the reservoir is subdivided. Thus we obtain at the ground surface :

$$u_3(x, y, 0) = 4A(1-\nu_M) \sum_{n=1}^{N} p_n z_n \triangle V_n / [(x-x_n)^2 + (y-y_n)^2 + z_n^2]^{3/2} \qquad ...(9)$$

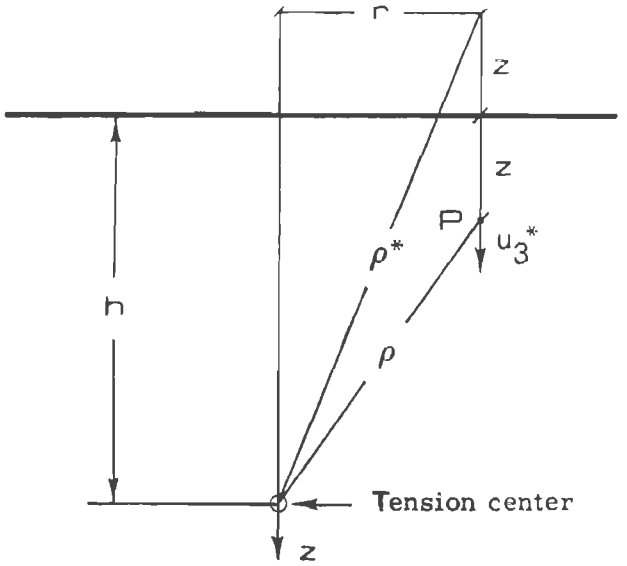

FIGURE 1 : Scheme of the semi-infinite medium with the tension center.

where, x_n, y_n and z_n are the coordinates of the n^{th} reservoir element in which the pore pressure is decreased by p_n.

It should be recalled that integral (8) is mathematically correct for any shape of V when the reservoir has the same elastic properties as the surrounding medium. If the tension center is heterogeneous with the rest of the medium the integration can be performed only if the shape of V approaches a sphere, i.e., when the differences between its dimensions along 3 arbitrary axes are not much pronounced.

The applicability of the above approach fails if appreciable contrasts in the parameters of the overlying and underlying rocks occur. One can resort to a finite element analysis but of course the extent of the system analyzed will be perforce limited.

Decoupled Models : One-dimensional Consolidation

Natural hydrologic basins usually consist of unconsolidated sedimentary soils. In layered sediments it is customary to discard the horizontal components of displacement in that they are assumed to be small in comparison with the vertical deformation. Flow is still considered to be three-dimensional. Since the consolidation is exclusively vertical, relation (4) is consistent with the approximation involved in the unidimensional compaction. Coefficient α in this case is the vertical compressibility of a sample of soil prevented from expanding laterally. The diffusion equation :

$$\nabla.(K_{ij}\nabla.\phi) = \gamma(\alpha + n\beta)\frac{\partial \phi}{\partial t} \qquad ...(10)$$

is solved numerically in a multi-aquifer-aquitard system under specified boundary conditions (natural conditions of the system), and imposing a prescribed discharge from the artificial wells [in (10) ϕ is the hydraulic head].

Any approach based on the diffusion equation will necessarily be a two-step procedure involving : (*a*) a hydrologic model to calculate the time dependent hydraulic head field, (*b*) a one-dimensional subsidence calculation based on these results.

In the latter step the one-dimensional form of Equation (10) :

$$\frac{\partial}{\partial x_3}\left(K_{x_3}\frac{\partial \phi}{\partial x_3}\right) = \gamma(\alpha + n\beta)\frac{\partial \phi}{\partial t} \qquad ...(11)$$

is solved numerically in multilayer aquitards in which the drawdowns of the adjacent aquifers estimated at the end of the first step, are specified as boundary conditions. The primary reason for a numerical solution is to allow prediction of rebound under possible pumping reductions. In this respect one must note that the compressibility α of each aquitard is in general a nonlinear and irreversible function of the effective intergranular stress. Often the nonlinearity is negligible if changes of effective stress are not very large but the

irreversibility must usually be taken into consideration. This creates in the simplest cases the need for two values of α for each layer : α_1 for compaction and α_2 for expansion. The latter is usually a tenth (or even less) of the former.

If an inversion of sign for $\partial\phi/\partial t$ occurs (shutdown of some wells or reduction of the withdrawal rate), Equation (11) must be treated as a nonlinear equation. Implicit schemes, such as the Crank-Nicholson or Wilson and Clough scheme, are strongly recommended. Generally they require also that iterations are performed within each time step during which changes of sign in the time derivative have taken place in some nodes, until a stationary distribution of compressibilities in the network is achieved.

The time dependent compaction η_i in the aquitard i is given by :

$$\eta_i(t) = \sum_{j=1}^{J} \gamma \alpha_j \, \Delta z_j \, \Delta \phi_j(t)$$

where, J is the number of nodal spacings of the aquitard. The compaction of the aquifers, although small, must also be considered and this can be done directly from the results of the hydrologic model.

For an aquifer :

$$\eta_i(t) = \gamma \alpha_i b_i \, \Delta \phi_i(t)$$

b_i being the aquifer thickness. The time-dependent subsidence is thus given by :

$$\eta(t) = \sum_{i=1}^{I} \eta_i(t)$$

where, I is the number of formations into which the hydrologic system has been idealized.

As far as the hydrologic model is concerned, there are at least three possibilities : 1) a full three-dimensional analysis, 2) a quasi-three-dimensional analysis (22), and 3) an analysis in a two-dimensional vertical cross-section in cartesian or radial coordinates. The first possibility must often be dismissed in complex natural basins on the grounds that there are serious computer limitations, in terms of both time and storage, to a full three-dimensional synthesis at this time. The-quasi-three-dimensional model is one of a class of models that links together a set of horizontal aquifer models by means of the leakage terms through the intervening aquitards. The fundamental assumption of this approach is that flow is horizontal in the aquifers and vertical in the aquitards. Neuman and Witherspoon (23) have stated that this assumption is satisfactory as long as the permeability contrasts are greater than 2 orders of magnitude. The quasi-three-dimensional model of Pinder and Bredehoeft (22) belongs to this class of models, with leakage from the aquitards given by a flux calculation based on an analytical solution for flow in the aquitards. The subsidence is the sum of the compaction of the aquitards and its time-dependent value is provided automatically during each time step of the simulation.

The primary purpose of a bi-dimensional flow model (either in radial or cartesian coordinates) is to obtain head drawdowns in the aquifers. These values are then inserted as boundary conditions in a refined one-dimensional vertical subsidence model that makes use of the local detailed data by considering the actual multilayer configurations within the aquitards. The model is first calibrated against the past history of available records (observed drawdowns and measured subsidence) by adjusting the regional formation parameters (permeability and compressibility) within their range of variation as provided by the laboratory test analyses. The model is then used as a predictive tool under a variety of possible pumping schedules.

Model Calibration and Operational Flow Diagram

In the previous section we did not investigate any possibility of using calibrations based on the search for rigorous inverse solutions since we are well aware that in most practical cases the sparse data condition precludes the adoption of inverse solutions and forces us to fall back on the more traditional direct trial and error procedure. With this approach, as with the more sophisticated methods, the calibration is inherently nonunique. There may be more than one feasible parameter distribution that leads to a satisfactory match between observed and simulated piezometric declines and subsidence rates. The subjective choice of a particular calibration must be made in the light of hydrogeologic reasoning : it is probably more art than science. But it is in this respect that the computer plays its essential role : enabling the scientist to make a sizable number of runs under different conditions and in a reasonable time, thus helping intuition find its way toward a more reliable interpretation of the apparently multi-faced reality. Once the calibration is made, the major effort is over. Predictions require now only a small fraction of the work done to bring the model into line with the past history of the observed records. From a variety of possible pumping schedules we can get the necessary picture of the consequences that the human activity is able to induce on the environment : hence the perspective of a better solution to this so complex problem.

We can summarize the operations to be performed in order to obtain an effective tool for predicting regional land subsidence in a flow chart as follows (Figure 2 refers to the case previously analysed wherein the final outcome is attained through a two step procedure involving two separate models).

Conclusion

In the present paper we have briefly summarized the

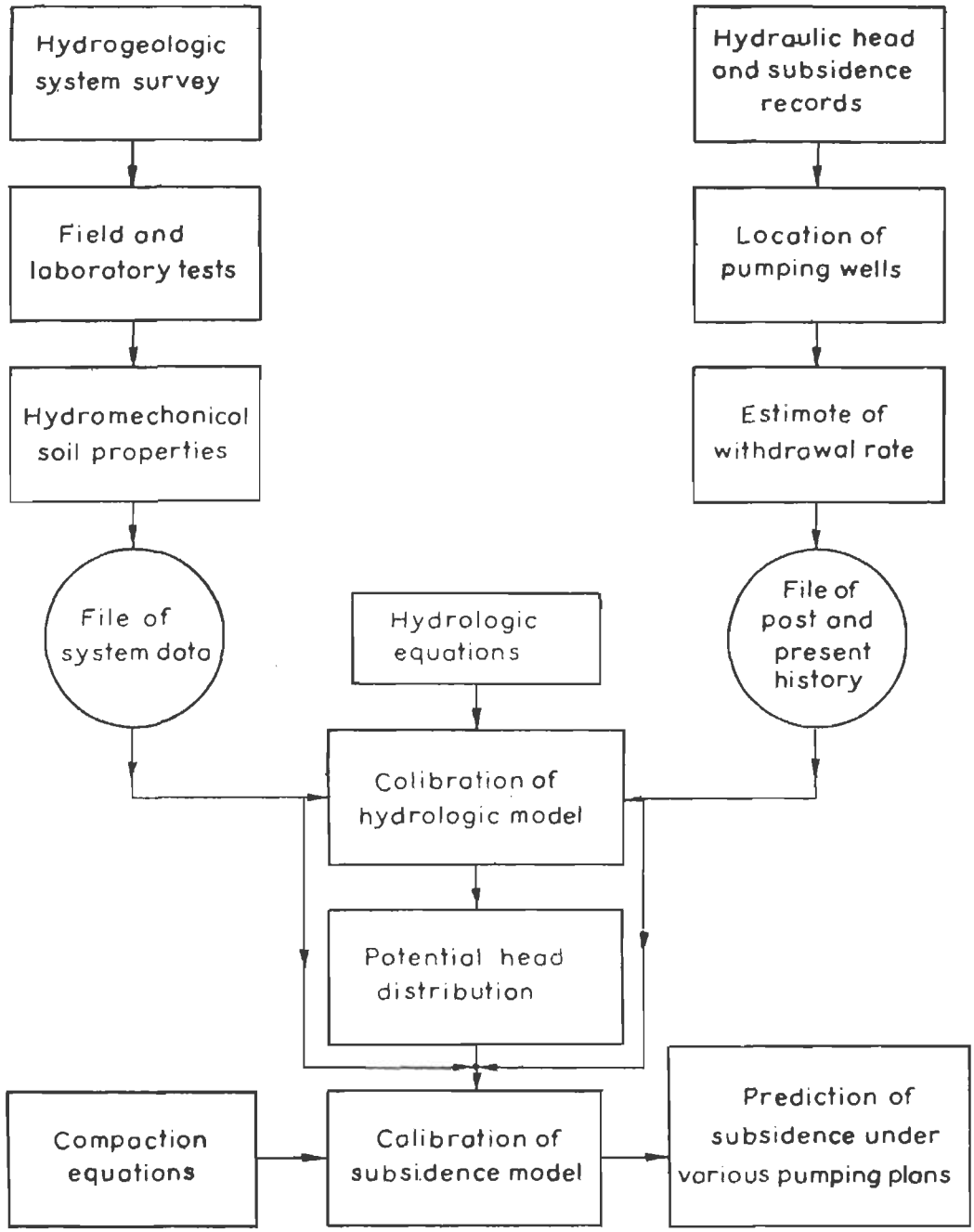

FIGURE 2 : Flow chart showing the logical sequence of the operations to be performed in an overall model simulating and predicting regional land subsidence.

computer models feasible to-date in order to simulate and predict regional land subsidence due to subsurface fluid withdrawals. The most sophisticated approach requires the solution of the coupled problem which involves the simultaneous inter-relation between the flow field and the stress field.

There are two main reasons discouraging any approach based on such a model :

(*a*) the general sparseness of available regional data which makes the usefulness of refinements of the theory beyond a certain limit strongly questionable.

(*b*) The present computer limitations which force one to simulate small and unrealistically simple geologic configurations.

Worthwhile alternatives are provided by the decoupling of the overall set of consolidation equations which can be solved independently either for the pore pressure head distribution or for the soil displacement field. There are practical and theoretical evidences that justify in most cases this simplified approach. The final solution is thus achieved through two related steps :

(1) An hydrologic model based on the customary diffusion equation supplies the time-dependent potential head distribution within the geologic system.

(2) A subsidence model based either on three-dimensional or one-dimensional consolidation uses the outcome from the hydrologic model and computes the surface sinking.

When subsidence caused by oil or gas production is analyzed, due to the particular geologic setting of the reservoir, the rock matrix stress field is in general three-dimensional. The same holds for the displacement field. Soil deformations may be calculated by making use of the strain nuclei approach if the necessary conditions underlying it are satisfied, as was done for instance in (2) & (19). If the conditions are not satisfied, the general equations of elastic equilibrium in three-dimensions may be solved with a numerical technique, but again we can meet the obstacle of point (*b*) above. In sedimentary soils, horizontal rock displacements are negligible when compared to vertical deformations. As a result the problem becomes appreciably simpler. The subsidence is estimated with a vertical one-dimensional model [as was done for instance in (24) & (25)]. The calculation must obviously be repeated as many times as the number of locations where the surface sinking evaluation is required.

Owing to the general lack of data, long calibration procedures are usually needed before a certain degree of confidence may be placed on the reliability of the results. The use of high speed digital computers appears therefore quite promising in its ability to carry out long-term simulations in relatively short times and to repeat tirelessly a large number of experiments.

Acknowledgement

The author is indebted to R.A. Freeze from whom he learned the importance of flow analysis in real subsidence problem and with whom he shared the fascinating experience of simulating and predicting the subsidence of Venice.

References

(1) J.F. POLAND and G.H. DAVIS : "Land Subsidence due to Withdrawal of Fluids." Rev. Eng. Geol., Vol. 2, 1969, pp. 187-269.

(2) NEDERLANDSE AARDOLIE MAATSCHAPPIJ B.V. ed. : "The Analysis of Surface Subsidence from Gas Production in the Groningen Area, The Netherlands." Verhandelingen Kon. Ned. Geol. Mijn. Gen. Vol. 28, 1973, pp. 109.

(3) M. CAPUTO; G. FOLLONI; A. GUBELLINI; L. PIERI and M. UNGUENDOLI : "Survey and Geometric Analysis of the Phenomenon of Subsidence in the Region of Venice and its Hinterland." TR. No. 9, CNR, Laboratorio per lo studio della dinamica delle grandi masse, Venice, 1971, pp. 20.

(4) J. H. GREEN : "The Effect of Artesian-pressure Decline on Confined Aquifer Systems and its Relation to Land Subsidence." Paper 1779-T, U.S. Geol. Survey, 1964, pp. 11.

(5) B.E. LOFGREN and R.L. KLAUSING : "Land Subsidence due to Ground Water Withdrawal, Tulare-Wasco area, California." Paper 437-B, U. S. Geol. Survey, 1969, pp. 101.

(6) G. GAMBOLATI : "Estimate of Subsidence in Venice Using a One-dimensional Model of the Subsoil." IBM J. Res. Develop., Vol. 16, No. 2, 1972, 130-137.

(7) D.R. ALLEN : "The Mechanics of Compaction and Rebound, Wilmington Oil Field, Long Beach, California." Tec. Rep. of the Dep. of Oil Properties, City of Long Beach, California, 1969, pp. 47.

(8) P.A. DOMENICO and M.D. MIFFLIN : "Water from Low-permeability Sediments and Land Subsidence." Water Resour. Res., Vol. 1, No. 4, 1965, 563-576

(9) J.F. POLAND : "Status of Present Knowledge and Needs for Additional Research on Compaction of Aquifer Systems, in Land Subsidence." *Proceedings of the IASH*, Tokyo, Vol. 1, 1969, 11-21.

(10) R.S. SANDHU and E.L. WILSON : "Finite Element Analysis of Land Subsidence, in Land Subsidence." *Proceedings of the IASH*, Tokyo, Vol. 2, 1969, 393-400.

(11) R.L. SCHIFFMAN ; A.T.F. CHEN and J.C. JORDAN : "An Analysis of Consolidation Theories." J. Soil Mech. Found. Div. ASCE, Vol. 65, No. SM 1, 1969, 285-312.

(12) M.A. BIOT : "General Theory of Three-dimensional Consolidation." J. Appl. Phys., Vol 12, No. 2, 1941, 155-164

(13) M. A. BIOT : "Theory of Elasticity and Consolidation for a Porous Anisotropic Solid." J. Appl. Phys., Vol. 26, No. 2, 1955, 182-185.

(14) A. VERRUIJT : "Elastic Storage of Aquifers, in Flow through Porous Media." R.J.M. DeWiest ed., Academic, New York, 1969, 331-376.

(15) J. GHABOUSSI and E.L. WILSON : "Flow of Compressible Fluid in Porous Elastic Media." Int. J. Num. Meths. Eng., Vol. 5, No. 3, 1973, 419-442.

(16) G. GAMBOLATI : "Second-order Theory of Flow in Three-dimensional Deforming Media." Water Resour. Res. Vol. 10, No. 6, 1974,...—...

(17) R.A. FREEZE : "Theoretical Analysis of Regional Ground Water Flow." Scient. Series No. 3, Inland Waters Branch, Ottawa, 1969, pp. 147.

(18) I. REMSON; G.M. HORNBERGER and F.J. MOLZ : "Numerical Methods in Subsurface Hydrology." Wiley-Interscience, New York, 1971, pp. 389.

(19) J. GEERTSMA : "Problems of Rock Mechanics in Petroleum Production Engineering." *Proceedings 1st Cong. Int. Soc. Rock Mechan.*, Lisbon, 1966, 585-594.

(20) G. GAMBOLATI : "A Three-dimensional Model to Compute Land Subsidence." IASH Bulletin, Vol. 17, No. 22, 1972, 219-226.

(21) J. GEERTSMA and G. VAN OPSTAL : "A Numerical Technique for Predicting Subsidence above Compacting Reservoirs." Based on the Nucleous of Strain Concept, Issue (2), 1973, 43-62.

(22) G.F. PINDER and J.D. BREDEHOEFT : "Application of the Digital Computer for Aquifer Evaluation." Water Resour. Res., Vol. 4, No. 5, 1968, 1069-1093.

(23) S.P. NEUMAN and P.A. WITHERSPOON : "Applicability of Current Theories of Flow in Leaky Aquifers." Water Resour. Res., Vol. 5, No. 4, 1969, 817-829.

(24) G. GAMBOLATI and R.A. FREEZE : "Mathematical Simulation of the Subsidence of Venice. 1. Theory." Water Resour. Res., Vol. 9, No. 3, 1973, 721-733.

(25) G. GAMBOLATI ; P. GATTO and R.A. FREEZE : "Mathematical Simulation of the Subsidence of Venice. 2. Results." Water Resour. Res., Vol. 10, No. 3, 1974, 563-577.

AUTHORS' PHOTOGRAPHS

AUTHORS

Wiroj Sangvaree
Thailand

V. C. Kulandaiswamy
India

Renata J. Kiczko
Poland

G. L. Grigolia
U.S.S.R.

T. Babu Rao
India

Zbigniew W.
Kundzewicz
Poland

A. N. Kilasonia
U.S.S.R.

Witold G. Strupczewski
Poland

Jaroslaw
J. Napiórkowski
Poland

G. G. Svanidze
U.S.S.R.

S. Ramaseshan
India

M. Krishnaswami
India

H. Eggers
Federal Republic of Germany

Vijay P. Singh
U.S.A.

H. D. Sharma
India

D. Koberg
Federal Republic of Germany

W. Trevor Dickinson
Canada

I. Kontur
Hungary

M. B. Szalay
Hungary

J. K. White
Britain

Thaipuck Thammongkol
Thailand

Paul MacRoberts
U.S.A.

A. W. Jayawardena
Britain

E. Mosonyi
Federal Republic of Germany

S. Chander
India

G. Jagmohan Das
India

E. J. Plate
West Germany

A. Popov
Bulgaria

S. C. Padhi
India

Prathet Sutabutr
Thailand

D. L. Vischer
Switzerland

Y. K. Murthy
India

L. Kotov
Bulgaria

M. Spreafico
Switzerland

P. Ramakrishna Rao
India

G. Krafti
Bulgaria

S. P. Chee
Canada

G. A. Schultz
West Germany

A. L. Velikanov
U.S.S.R.

D. N. Korobova
U.S.S.R.

V. N. Diwanji
India

M. P. S. Ramani
India

R. D. Hey
Britain

V. Ramanathan
India

Jagdish Bahadur
India

C. V. Gole
India

Umesh Chandra
India

Sun-Fu Shih
U.S.A.

P. C. Saxena
India

K. Balu
India

Jagat N. Sharma
U.S.A.

C. P. Venkatraman
India

A. C. Payatakes
U.S.A.

S. J. Gillam Smith
Britain

Robert Y. S. Lai
U.S.A.

L. Carballada
Canada

D. W. Moody
U.S.A.

R. G. Cembrowicz
West Germany

S. K. Sharma
India

D. M. Preble
U.S.A.

H. O. Anwar
Britain

S. C. Sharma
India

G. Ozoray
Canada

A. S. Ramamurthy
Canada

Valentina Voljin
Romania

K. V. Ramana Murthy
India

E. Zamfir
Romania

Mihaela Blidaru
Romania

V. R. Pantulu
Thailand

S. H. C. de Silva
Sri Lanka

Ernest H. Răzvan
Romania

John C. Peters
U.S.A.

R. V. Harmsworth
U.S.A.

C. H. Wahtola, Jr.
U.S.A.

Anand Prakash
U.S.A.

Daniel M. Dubois
Belgium

A. M. Beeton
U.S.A.

Calvin H. Ward
U.S.A.

Joe M. King
U.S.A.

C. R. Murthy
Canada

J. O. Blanton
U.S.A.

H. A. Adeniji
Nigeria

Jacques C. J. Nihoul
Belgium

Georges Pichot
Belgium

Walter Fox
U.S.A.

François C. Ronday
Belgium

Giuseppe Gambolati
Italy

IWRA EXECUTIVE BOARD
AND
GEOGRAPHICAL AREA COMMITTEES

G.K.V.K. Library

U. A. S. BANGALORE
UNIVERSITY LIBRARY

14SEP1979

ACC. NO. 83482

CL. NO. .....

IWRA EXECUTIVE BOARD

OFFICERS

President

Dr. Ven Te Chow
Professor of Hydraulic Engineering
University of Illinois at Urbana-Champaign
Urbana, Illinois, U.S.A.

Vice-Presidents

Dr. José M. M. Mendiluce
Director
Centro de Estudios Hidrograficos
Madrid, Spain.

Mr. Farid N. Mikhail
United Nations Expert
Cairo, Egypt.

Dr. K. L. Rao
Member of Parliament
New Delhi, India.

Prof. José Leite de Souza
Diretor
Instituto de Pesquisas Hidráulicas
Universidade Federal do Rio Grande do Sul
Porto Alegre, Brazil.

Secretary General

Dr. Gabor M. Karadi
Professor of Civil Engineering
University of Wisconsin, Milwaukee
Wisconsin, U.S.A.

Treasurer

Dr. Roy A. Williams
Head, Materials Laboratory
Newport News Shipbuilding Company
New Port News, Virginia, U.S.A.

BOARD MEMBERS

Dr. Ellis L. Armstrong
Vice-President
URS Systems Corporation
San Mateo
California, U.S.A.

Dr. Léopold Escande
President
Institute Nationale Polytechnique de Toulouse
Toulouse, France.

Prof. Dr. E. Mosonyi
Direktor der Versuchsanatalt für
Wasserbau und Kulturtechnik und des
Theodor-Rehbock-Flussbaulaboratoriums
Universität Karlsruhe
Karlsruhe, Federal Republic of Germany.

Prof. Dr. Techn. Helmut Simmler
Direktor
Institut für Wasserwirtschaft und
Konstruktiven Wasserbau
Technische Hochschule
Graz, Austria.

Dr. Iraj Vahidi
Minister of Energy
Tehran, Iran.

Prof. Dr. Dimo Velev
Secretary
Department of Technical Sciences
Director, Institute of Water Problems
Bulgarian Academy of Sciences
Sofia, Bulgaria.

Mr. J. Gavin Warnock
Vice-President
Acres Consulting Services Ltd.
Toronto, Ontario, Canada.

CHAIRMEN OF COMMITTEES

Coordination of Geographical Area Committees

Dr. Leopold A. Heindl
Executive Secretary
United States National Committee for
the International Hydrological Decade
Washington, D.C., U.S.A.

International Cooperation

Dr. Sandor C. Csallany
Professor of Hydrology
Western Kentucky University
Bowling Green, Kentucky, U.S.A.

Membership

Dr. William S. Butcher
Director
Office of Water Research and Technology
U.S. Department of the Interior
Washington, D.C., U.S.A.

Publications

Dr. Raymond J. Krizek
Professor of Civil Engineering
Northwestern University
Evanston, Illinois, U.S.A.

Technical Programmes

Dr. Herbert C. Preul
Professor of Civil and Sanitary Engineering
University of Cincinnati
Cincinnati, Ohio, U.S.A.

GEOGRAPHICAL AREA COMMITTEES FOR IWRA

Brazil

Mr. Renato João Baptista Della Togna
Chairman
Brazilian Committee for IWRA
Departamento de Aguas e Energia Elétrica
Secretaria dos Servicos e Obras Publicas
Rua do Riachuelo No. 115, 4º Ander
São Paulo.

Mr. Rubem La Laina Porto
Executive Secretary
Brazilian Committee for IWRA
Departamento de Aguas e Energia Elétrica
Secretaria dos Servicos e Obras Publicas
Rua do Riachuelo No. 115, 4º Ander
São Paulo.

Canada

Dr. Asit K. Biswas
Chairman
Canadian Committee for IWRA
Inland Waters Directorate
Environment Canada
Ottawa, Ontario K1A OH3.

Mr. Peter J. Reynolds
Executive Secretary
Canadian Committee for IWRA
Inland Waters Directorate
Environment Canada
Ottawa, Ontario K1A OH3.

India

Mr. Y. K. Murthy
Chairman
Indian Committee for IWRA
Chairman
Central Water Commission and
Ex-Officio Secretary to Government of India
New Delhi.

Mr. C. V. J. Varma
Executive Secretary
Indian Committee for IWRA
Central Board of Irrigation and Power
Kasturba Gandhi Marg
New Delhi.

Indonesia

Mrs. Srimoerni Doelhomid
Chairman
Indonesia Committee for IWRA
Indonesian Institute of Sciences
Jl, Bank V/8, P.O. Box 78 kby
Kebayoram-Jakarta Selatan.

Mr. Sunarjono Danudjo
Executive Secretary
Indonesia Committee for IWRA
Indonesian Institute of Sciences
Jl, Bank V/8, P.O. Box 78 kby
Kebayoram-Jakarta Selatan.

Japan

Dr. Koichi Aki
Chairman
Japanese Committee for IWRA
Professor, Faculty of Engineering
Kanto Gukuin University
Yokohama.

Mr. Toshio Iizuka
Executive Secretary
Japanese Committee for IWRA
River Planning Division, River Bureau
Ministry of Construction, Japanese Government
Kasumigaski, Tokyo 100.

Spain

Mr. Eugenio Vallarino
Chairman
Spanish Committee for IWRA
Centro de Estudios Hidrograficos
Paseo Bajo de la Virgin del Puerto, 3
Madrid 5.

Mr. José Maria Pliego
Executive Secretary
Spanish Committee for IWRA
Centro de Estudios Hidrograficos
Paseo Bajo de la Virgin del Puerto, 3
Madrid 5.

U.S.A.

Dr. Abel Wolman
President
U.S. Committee for IWRA
Professor Emeritus of Sanitary Engineering
Johns Hopkins University
Baltimore, Maryland.

Dr. Marcel Bitoun
Vice-President
U.S. Committee for IWRA
Vice-President
Harza Engineering Company
Chicago, Illinois.

Mr. Thaddeus W. Mermel
Vice-President
U.S. Committee for IWRA
Assistant to the Commissioner
U.S. Bureau of Reclamation
Washington, D.C.

Mr. Brian J. Gallagher
Executive Secretary
U.S. Committee for IWRA
Limnetics, Inc. 6132 W. Fond
du Lac Avenue, Milwaukee
Wisconsin.

19 NOV 1979
Released On

UNIV. OF AGRIL. SCIENCES
UNIVERSITY LIBRARY, BANGALORE-560024

This book should be returned on or before the date mentioned below; or else the Borrower will be liable for overdue charges as per rules from the DUE DATE.

Cl. No. 383.9106 Ac. No. 83482
W.C.W.R

READING ROOM

G.K.V.K. Library

U.A.S. UNIVERSITY LIBRARY BANGALORE G.K.V.K. CAMPUS

UAS LIBRARY GKVK
83482

Cl. No.....
Author W.C.W.R
83482

Printed at The Central Electric Press, 80-D, Kamla Nagar, Delhi-110007